NUCLEAR SCIENCE ABSTRACTS

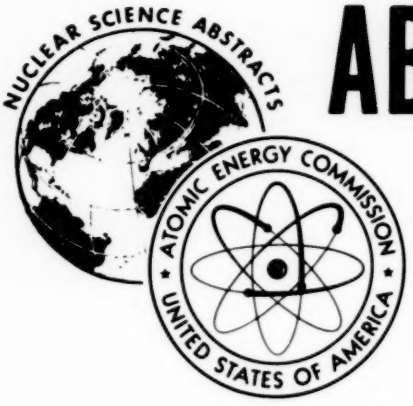

Volume 25 Number 5

Abstracts 8193-10420

March 15, 1971

UNITED STATES ATOMIC ENERGY COMMISSION
Division of Technical Information

REPORT COLLECTIONS IN THE UNITED STATES

The libraries listed below purchase and maintain microfiche collections of USAEC and foreign reports that are abstracted in *NSA*. Their collections also include *NSA* and its indexes, AEC's Technical Progress Reviews, AEC-sponsored translations, conference proceedings published by AEC, and various bibliographic tools. Most of these libraries have microfiche reader-printers or other photocopy facilities with which to reproduce enlarged copies from microfiche. Charges for reproduction services vary.

ALABAMA
Auburn, Auburn University
ALASKA
College, University of Alaska
ARIZONA
Tucson, University of Arizona
ARKANSAS
Fayetteville, University of Arkansas
CALIFORNIA
Davis, University of California
Los Angeles, University of California
COLORADO
Boulder, University of Colorado
DISTRICT OF COLUMBIA
Washington, Library of Congress (by deposit)
FLORIDA
Gainesville, University of Florida
GEORGIA
Atlanta, Georgia Institute of Technology
HAWAII
Honolulu, University of Hawaii
IDAHO
Pocatello, Idaho State University
ILLINOIS
Evanston, Northwestern University
Urbana, University of Illinois
INDIANA
Lafayette, Purdue University
IOWA
Ames, Iowa State University
KANSAS
Manhattan, Kansas State University
KENTUCKY
Lexington, University of Kentucky
Louisville, University of Louisville
LOUISIANA
Baton Rouge, Louisiana State University
New Orleans, Tulane University
MARYLAND
Baltimore, Johns Hopkins University
College Park, University of Maryland
MASSACHUSETTS
Cambridge, Massachusetts Institute of Technology
MICHIGAN
Ann Arbor, University of Michigan
MISSISSIPPI
State College, Mississippi State University
MISSOURI
Kansas City, Linda Hall Library
NEVADA
Las Vegas, University of Nevada
Reno, University of Nevada
NEW JERSEY
Princeton, Princeton University
NEW MEXICO
Albuquerque, University of New Mexico
NEW YORK
Albany, New York State Library
Buffalo, State University of New York at Buffalo
Ithaca, Cornell University
New York, Columbia University
Rochester, University of Rochester
Syracuse, Syracuse University
Troy, Rensselaer Polytechnic Institute
NORTH CAROLINA
Raleigh, North Carolina State University
OHIO
Cincinnati, University of Cincinnati
Columbus, Ohio State University
Toledo, University of Toledo
OKLAHOMA
Norman, University of Oklahoma
PENNSYLVANIA
Philadelphia, University of Pennsylvania
Pittsburgh, Carnegie Library
University Park, Pennsylvania State University
PUERTO RICO
San Juan, University of Puerto Rico
SOUTH CAROLINA
Columbia, University of South Carolina
TENNESSEE
Knoxville, University of Tennessee
Nashville, Joint University Libraries
Oak Ridge, Oak Ridge Associated Universities
TEXAS
Austin, University of Texas
College Station, Texas A & M University
Houston, Rice University
UTAH
Salt Lake City, University of Utah
VIRGINIA
Blacksburg, Virginia Polytechnic Institute
Charlottesville, University of Virginia
WASHINGTON
Pullman, Washington State University
Seattle, University of Washington
WEST VIRGINIA
Morgantown, West Virginia University
WISCONSIN
Madison, University of Wisconsin
WYOMING
Laramie, University of Wyoming

The following governmental and international organizations offer for sale USAEC reports abstracted in *Nuclear Science Abstracts*:

National Technical Information Services, U. S. Department of Commerce
Springfield, Virginia 22151
International Atomic Energy Agency, Vienna, Austria
National Lending Library, Boston Spa, England

XUM

Volume 25, Number 5, March 15, 1971

NUCLEAR SCIENCE ABSTRACTS

A semimonthly publication of the USAEC Division of Technical Information, Edward J. Brunenkant, Director, Published by the USAEC Division of Technical Information Extension, Robert L. Shannon, Extension Manager.

Nuclear Science Abstracts provides the only comprehensive abstracting and indexing coverage of international nuclear science literature. *Nuclear Science Abstracts* covers scientific and technical reports of the U. S. Atomic Energy Commission and its contractors, other U. S. Government agencies, other governments, universities, and industrial and research organizations. In addition, books, conference proceedings, individual conference papers, patents, and journal literature on a worldwide basis are abstracted and indexed. Each issue of *Nuclear Science Abstracts* includes four indexes: subject, personal author, corporate author, and report number.

The following organizations scan and abstract the nuclear science literature in their respective countries:

Atomic Energy of Canada Limited
Australian Atomic Energy Commission
Danish Atomic Energy Commission
Finnish Atomic Energy Commission
French Atomic Energy Commission
Japan Atomic Energy Bureau–Atomic Energy Research Institute
Institutt for Atomenergi (Norway)
Aktiebolaget Atomenergi (Sweden)
United Kingdom Atomic Energy Authority

Numerous organizations, societies, and publishers throughout the world provide *Nuclear Science Abstracts* with advance page-proof copy of their publications, e.g., in the United States the American Institute of Physics provides page-proof copy of its publications.

A list of the journals scanned regularly and the abbreviations used appears in Issue 1 (January 15) of each volume of *Nuclear Science Abstracts* and is supplemented in Issues 7, 13, and 19. Issue 1 of each volume also describes the scope and arrangement of the subject matter covered in *Nuclear Science Abstracts*. The subject matter covered is also described in TID-4552, *Subject Scope of Nuclear Science Abstracts*, available free from the USAEC Division of Technical Information Extension, P.O. Box 62, Oak Ridge, Tennessee 37830. An outline of the subject categories appears in the Contents of each issue.

AVAILABILITY OF PUBLICATIONS ABSTRACTED

Public availability of all U. S. Atomic Energy Commission reports is indicated in the report number indexes. The availability of other reports, when known, is also indicated. The availability of some unnumbered reports is given in the abstract.

Dissertations abstracted in *Dissertation Abstracts* and included in *Nuclear Science Abstracts* are available from University Microfilms, Inc., 315 N. First Street, Ann Arbor, Michigan 48103.

Information on the availability of the published literature and unpublished conference papers abstracted in *Nuclear Science Abstracts* can be obtained from the USAEC Division of Technical Information Extension, P.O. Box 62, Oak Ridge, Tennessee 37830.

HOW TO OBTAIN NUCLEAR SCIENCE ABSTRACTS

Nuclear Science Abstracts is available to the public on a subscription basis from the Superintendent of Documents, U. S. Government Printing Office, Washington, D. C. 20402.

For the 24 regular issues, the yearly rate is $42.00 for domestic subscribers and $52.50 for foreign subscribers. A single issue costs $1.75, domestic rates, or $2.19, foreign rates. Domestic rates apply to the United States, Canada, Mexico, and Central and South American countries except Argentina, Brazil, Guyana, French Guiana, Surinam, and British Honduras.

For a yearly subscription to the cumulative indexes, the rates are $38.00 for domestic subscribers and $47.50 for foreign subscribers.

The following cumulative indexes are available:

From Johnson Reprint Corporation, 111 Fifth Avenue, New York, N. Y. 10003:
Vols. 1–4, Subjects and Authors (1948–1950), $30.00.

From Superintendent of Documents, U. S. Government Printing Office, Washington, D. C. 20402:

Vols. 5–10, Subjects and Authors (1951–1956), $5.25.

Vols. 11–15, Subjects (1957–1961), $19.00.
Vols. 11–15, Personal Authors (1957–1961), $14.25.
Vols. 11–15, Corporate Authors (1957–1961), $2.50.

Vols. 16–20, Subjects (1962–1966), $36.00.
Vols. 16–20, Personal Authors (1962–1966), $22.50.
Vols. 16–20, Corporate Authors (1962–1966), $3.75.

Vol. 21, Subjects and Authors (1967), $16.00.
Vol. 22, Subjects and Authors (1968), $26.00.
Vol. 23, Subjects and Authors (1969), $25.75.
Vol. 24, Subjects and Authors (1970), $22.50.

Cumulative Report Number Index, Vols. 1-15 Revised, $4.00.
Cumulative Report Number Index, Vols. 16-20 Revised, $5.50.
Cumulative Report Number Index, Vols. 21-24, $4.25.

Nuclear Science Abstracts is available on an exchange basis to universities, research institutions, industrial firms, and publishers of scientific information. Government agencies may obtain *NSA* free of charge. Inquiries should be directed to the USAEC Division of Technical Information Extension, P. O. Box 62, Oak Ridge, Tennessee 37830.

INDEXES TO NSA

Comprehensive indexes appear in each issue and are cumulated quarterly and annually. Multivolume cumulations have been issued as indicated above.

All documents abstracted are indexed by subjects and personal authors. Report literature is indexed also by corporate author and report number. Each of these indexes in every issue is preceded by an introduction explaining in detail the organization of the index and the principles by which it is compiled. The reader is referred to these explanations for information not found in the brief summary below.

Personal Authors

Each author's name is indexed in the form appearing on the document abstracted:

ISHIHARA, T., Accumulation of fallout ^{137}Cs in newborn infants, 23:50538
ISHIHARA, Toyokuki, Shielding effect of paraffin, water, soil, concrete, Fe, and Pb for high-energy neutrons, 23:51748

Subjects

The subject index consisting of specific materials, objects, and processes is arranged alphabetically. Modifying phrases specific to these subjects in turn are arranged alphabetically under the subjects.

MELPHALAN
  effects on proliferation of cultured antigen-stimulated spleen cells from mice, dose-response curve for, 23:50820
MEMBRANE FILTERS
  design for removal of cell-free Streptococcus faecalus from bacteria cultures in fermentation tank, 23:49996 (UCRL-18667, pp 322-9)
MENDELEVIUM
  separation from einsteinium and fermium by electrolysis, 23:49772 (UCRL-18667, pp 277-312)
  separation from sodium acetate solutions by solvent extraction using sodium amalgam, 23:49772 (UCRL-18667, pp 277-312)
  stability of divalent state of, 23:49772 (UCRL-18667, pp 277-312)

Corporate Authors

Technical report literature is indexed from the name of the organization or institution responsible for the issuance of the report.

51093 (LA-4164) FABRICATION OF BORON CARBIDE RINGS AND DISKS. Sheinberg, H.; Herrera, T.; Kostacopoulos, J. (**Los Alamos Scientific Lab., N. Mex.**). Apr. 25, 1969. Contract W-7405-eng-36. 11p. Dep. CFSTI.

is indexed as:

LOS ALAMOS SCIENTIFIC LAB., N. MEX.
  Fabrication of boron carbide rings and disks, 23:51093 (LA-4164)

Report Numbers

Technical report literature is also indexed by report numbers. This index includes information on where individual reports may be obtained. While not reports, patents and conference papers are indexed here as a matter of convenience.

JPRS-	**(Non-AEC)**	
46949	23-51587	CFSTI
48330	23-52305	CFSTI
48331	23-52451	CFSTI
48481	23-50889	CFSTI
48743	23-51034	CFSTI
49028	23-51706	CFSTI (U. S. Sales Only)
JUL-	**(German)**	
571-RG	23-52269	Dep
578-PP	23-51624	Dep. CFSTI (U. S. Sales Only)
581-FN	23-51079	Dep. CFSTI (U. S. Sales Only)
584-RG	23-52313	Dep
586-FN	23-51035	Dep. CFSTI (U. S. Sales Only)
K-		
1777	23-50987	Dep. CFSTI
1778	23-50988	Dep. CFSTI
KFK-	**(German)**	
743	23-52461	Dep
743	23-52447	For translation see EURFNR-613
781/I	23-52462	Dep
824	23-52397	Dep. CFSTI (U. S. Sales Only)

XUM

TABLE OF CONTENTS

Volume 25, Number 5, March 15, 1971

Category	Page
CHEMISTRY	781
Analytical Chemistry	781
Chemical and Spectral Procedures	781
Isotope Dilution Procedures	783
Radiometric and Radiochemical Procedures	783
Activation Procedures	783
Inorganic, Organic, and Physical Chemistry	785
Chemical Properties	785
Isotope Effects and Exchange	786
Physical Chemistry	788
Radiation and Nuclear Chemistry	789
Radiation Effects	789
Radiation Processes	789
Radiolysis	790
Radioisotope Production	793
Recoil Production and Reactions	793
Radiochemistry	794
Separation Processes	794
EARTH SCIENCES	798
Geology and Hydrology	798
Meteorology	799
Mineralogy and Exploration	800
Oceanography	801
Seismology	801
ENGINEERING	802
Nuclear Explosions	802
Facilities and Equipment	802
Heat Transfer and Fluid Flow	804
Isotope Technology	805
Materials Testing	807
Protective Structures	808
Radioactive Material Handling	808
Vacuum Engineering	810
INSTRUMENTATION	811
Radiation Detection Instruments	811
General Detectors and Monitors	811
Nuclear Spectroscopic Instrumentation	816
High Energy Physics Instrumentation	817
Radiation Dosimeters	819
Radiometric Instruments	819
Miscellaneous Instruments and Components	819
Radiation Effects on Instruments and Instrument Components	820
LIFE SCIENCES	821
Biochemistry, Physiology, and Molecular Biology	821
Basic Processes	821
Metabolism, Physiology, and Toxicology	821
Radiation Effects	823
Immunology	825
Ecology	826
Genetics and Cytogenetics	827
Health Physics and Safety	830
Radioactive Contamination and Decontamination	830
Dosimetry and Monitoring	831
Radiation Protection	833
Safety Procedures	834

Category	Page
LIFE SCIENCES (Cont'd.)	
Legal Aspects	834
Medicine	835
Protective Substances	835
Radiation Sickness and Injuries	836
Radiodiagnosis	836
Radiotherapy	838
Blast and Thermal Effects	839
Radiation Effects on Animals	839
Invertebrates	840
Vertebrates	841
Man	845
Radiation Effects on Plants	845
Radiation Effects on Microorganisms	847
Radiosterilization and Radiopreservation	848
METALS, CERAMICS, AND OTHER MATERIALS	850
Metals and Alloys	850
Corrosion and Erosion	850
Preparation and Fabrication	851
Properties Evaluations	853
Structure and Phase Studies	856
Radiation Effects	856
Ceramics and Cermets	858
Corrosion and Erosion	858
Preparation and Fabrication	858
Properties Evaluations	860
Structure and Phase Studies	862
Radiation Effects	863
Plastics and Other Materials	864
PHYSICS (GENERAL)	866
Astrophysics and Cosmology	866
Cosmic Ray Exposure Ages	866
Stars	866
Quasi-Stellar, Radio, and X-Ray Sources	875
Solar Phenomena	878
Galaxies	881
Cosmology	883
Planetary Phenomena	884
Atomic and Molecular Physics	884
Atomic, Electron, Ion, and Molecular Beams and Their Reactions	884
Atomic and Molecular Properties	885
Positronium, Muonium, and Mesic Atoms and Molecules	886
Collision Phenomena	886
Atomic Theory	891
Cosmic Radiation	892
Direct Energy Conversion	893
Fluid Physics	894
Geophysics (Upper Atmosphere)	895
Low-Temperature Physics and Cryogenic Equipment	902
Superfluidity	902
Superconductivity	903
Equipment and Devices	906
Plasma and Thermonuclear Physics	906
Confinement and Heating	906
Diagnostics	907

TABLE OF CONTENTS (continued)

Category	Page
PHYSICS (GENERAL) (Cont'd.)	
Kinetics (General)	909
Kinetics (Experimental)	911
Kinetics (Theoretical)	912
Production	914
Stability	914
Thermonuclear Processes	916
Wave Phenomena	916
Shielding	918
Solid-State Physics	919
Radiation Effects	919
Physical Properties	922
Moessbauer Effects and NMR	924
Theory	924
Theoretical Physics	924
PHYSICS (HIGH-ENERGY)	927
Particle Interactions and Properties (Experimental)	927
Electromagnetic	927
Weak	927
Strong (Baryon-Induced)	928
Strong (Meson-Induced)	929
Particle Interactions and Properties (Theoretical)	932
General	932
Electromagnetic	933
Weak	936
Strong (General)	937
Strong (Baryon No. = 0)	938
Strong (Baryon No. = 1)	940
Strong (Baryon No. ≥ 2)	941
Particle Invariance Principles and Symmetries	943
General	943
Applications (Electromagnetic and Weak)	943
Applications (Strong)	943
Field Theories	944
General	944
Quantum Field Theory	944
Gravitation and General Relativity	947
Scattering Theory	948
Particle Accelerators	950
PHYSICS (NUCLEAR)	954
Neutron Interactions with Matter	954

Category	Page
PHYSICS (NUCLEAR) (Cont'd.)	
Nuclear Properties and Reactions, $A \leq 5$	956
Nuclear Properties and Reactions, $6 \leq A \leq 19$	957
Nuclear Properties and Reactions, $20 \leq A \leq 89$	960
Nuclear Properties and Reactions, $A \geq 90$	962
Nuclear Theory	965
REACTOR TECHNOLOGY	969
Commercial Power Reactors	969
Operation and Economics	971
Safety and Siting	972
Power Reactor Development	973
Kinetics and Dynamics	974
Control Systems	976
Shielding	976
Cooling Systems	977
Fuels	978
Auxiliary and Emergency Systems	980
Operation and Economics	980
Safety and Siting	981
Power Conversion Systems	982
Research and Test Reactors	982
Rocket and Space Reactors	985
Process Heat and Desalination Reactors	986
Marine and Portable Power Reactors	986
Reactor Theory	987
Kinetics	987
Dynamics	989
Experimental Applications	989
Reactor Components, Fuels, and Accessories	989
GENERAL	991
CORPORATE AUTHOR INDEX	INDEX-1
PERSONAL AUTHOR INDEX	INDEX-11
SUBJECT INDEX	INDEX-55
REPORT NUMBER INDEX	INDEX-140

XUM

STAFF OF NUCLEAR SCIENCE ABSTRACTS

John W. Norris
Managing Editor

Donald D. Davis
Assistant Managing Editor

David E. Bost
Production Manager

Sidney F. Lanier
Subject Heading Specialist

J. Paul Meredith
Descriptive Cataloging Specialist

Frederick E. Marsh, Jr.
Computer Index Coordinator

Clara L. Fox
Corporate Author Specialist

Helen W. White
Report Number Specialist

Section Editors

Everett J. Hoffman
Chemistry

Robert C. Kelly
Engineering; Earth Sciences; Metals, Ceramics, and Other Materials

Lee M. Thompson
General Physics

Charles E. Stuber
High Energy Physics; Instrumentation

Helen G. Donald
Life Sciences

Lawrence T. Whitehead
Nuclear Physics

James M. Jacobs
Reactor Technology

Evaluators

Thomas S. Chapman
Rose V. Jermain
John H. Mitchell
Mary H. Newman
Polly C. Summers

Abstractors

F. S. Armstrong*
Ellis R. Bedford
Mary M. Brown
Jane G. Buchanan
D. Lamar Cason
Gloria M. Caton
David C. Cunningham
James R. Dulaney
Helga B. Gerstner
Mary C. Grissom
Phyllis C. Hansen
Carolyn D. Houston
Elaine E. Huber
Rose V. Jermain
W. Hugh Kinser, Jr.
Lisbeth C. Lieberman
Betty L. McDowell
Patricia B. McEwen
Fay M. Martin
William D. Matheny
Dora H. Moneyhun
Jean F. Peckham
Henry D. Raleigh
Mona H. Raridon
Julia S. Redford
Jessie W. Rushing
Robert W. Rutkowski
Francis L. Sachs
Lila B. Smith
Anne G. Ward
Helen L. Ward
Milton O. Whitson
Juanita Wilson

*Atomic Energy of Canada, Ltd.

Charles R. Bruce
Publishing Coordinator

Communication concerning the editorial policy and content of *Nuclear Science Abstracts* should be addressed to the Managing Editor, *Nuclear Science Abstracts*, USAEC Division of Technical Information Extension, P. O. Box 62, Oak Ridge, Tennessee 37830.

Use of funds for printing this publication approved by the Director of the Bureau of the Budget, June 26, 1969.

Volume 25, Number 5 March 15, 1971

NUCLEAR SCIENCE ABSTRACTS

CHEMISTRY

Analytical Chemistry

Refer also to abstracts 8385, 8830, and 8831.

8193 (UCRL-20132) COMPUTER BASED LABORATORY-WIDE DATA ACQUISITION, ANALYSIS, AND RETRIEVAL SYSTEM. Despotakis, J. A.; Fink, R. L.; Itzkowitz, M. S.; Klein, M. P. (California Univ., Berkeley. Lawrence Radiation Lab.). 7 Oct 1970. Contract W-7405-eng-48. 9p. Dep. NTIS.

From Conference on Chemistry and Spectroscopy, San Francisco, Calif.

A system was designed to provide service to all analytical instruments in the laboratory. A Sigma-2 computer with 32K of core, a 1.5 Mbyte disc, 2 Magtape units, card reader and line printer comprise the center of the system. A PDP-8L with 8K of core and fast paper tape punch and reader provides output to plotter and I/O to the 17 control teletypes and storage scopes distributed through the lab. Data transmission between the individual instruments and computer is digital at a 500-KHz word rate and fully duplexed. Up to 54 instruments may be connected with 8 operating simultaneously-expandable to 32-in foreground while processing and manipulation of previously acquired data occurs in background. Long-term data storage and retrieval are design goals, as is remote batch terminal operation. (auth)

Chemical and Spectral Procedures

8194 (AECL-3743) CHOICE OF BATH MATERIALS FOR THE INERT GAS FUSION METHOD FOR THE DETERMINATION OF OXYGEN IN METALS. Ashley, R. W.; Longhurst, T. H. (Atomic Energy of Canada Ltd., Chalk River (Ontario). Chalk River Nuclear Labs.). Nov 1970. 16p. Dep. NTIS (U. S. Sales Only). AECL $0.50.

Some factors governing the choice of bath metals and operating conditions for the fusion method for the determination of oxygen in metals were investigated. The main conclusion reached is that precipitation of carbon must be avoided. A decrease in the solubility of carbon in the melt can occur through temperature reduction during operation or change in composition when samples are added. The performance of several melts is described. (auth)

8195 (AERE-R-6491) CHEMICAL DETERMINATION OF NITROGEN IN THE NITRIDES OF BORON, TITANIUM, ZIRCONIUM, CHROMIUM, MOLYBDENUM, NIOBIUM, TANTALUM, AND VANADIUM. Healy, C.; Parker, A. (Atomic Energy Research Establishment, Harwell (England)). Sep 1970. 14p. Dep. NTIS (U.S. Sales Only). UK 2s.6d.

The application of the Dumas and Kjeldahl methods, together with alkaline fusion and acid dissolution under pressure, to the determination of nitrogen in some nitrides is described. The accuracy and precision of the methods are given as are the limitations found when applying these techniques to certain of the nitrides investigated. (auth) (UK)

8196 (BARC-504) SPECTROGRAPHIC DETERMINATION OF RUTHENIUM IN SILICIOUS MATERIALS USED IN RADIOACTIVE WASTE DISPOSAL: AN A.C. SPARK METHOD. Murthy, P. Sreerama; Kamat, M. J. (Bhabha Atomic Research Centre, Bombay (India)). 1970. 7p. Dep. NTIS (U. S. Sales Only).

A spectrographic method is described to determine ruthenium in siliceous materials coated with iron oxide, using ac spark excitation. Two 5-mg portions of the sample are deposited on two flat top 1/4-in. dia graphite electrodes (U.C.C. type 107) and sparked for 40 seconds. The spectra are photographed on an Ebert 3.4-meter plane grating spectrograph using a 30,000 lines per inch grating in the first order in the region 3500 to 4125 Å. The concentration range of Ru covered is 0.1 to 5.0%. Palladium is used as the internal standard element. The coefficient of variation of the method is 8%. (auth)

8197 (BARC-510) IN-LINE ANALYTICAL METHODS FOR FUEL REPROCESSING STREAMS. PART I. DIRECT CALORIMETRY FOR URANIUM AND FREE ACID. Bhargava, V. K.; Chandrasekharan, E. S.; Iyer, R. H.; Rao, V. K.; Ramanish, M. V.; Srinivasan, N. (Bhabha Atomic Research Centre, Bombay (India)). 1970. 44p. Dep. NTIS (U.S. Sales Only).

A detailed investigation of a nondestructive, direct colorimetric method for uranium was carried out with a view to adapting this method for the in-line analysis of uranium in a fuel reprocessing plant by making use of the yellow color of the uranyl ion (absorption maxima at 404, 416, and 426 nm). Determination of uranium in the aqueous and organic phases (30% TBP in Shell sol-T) was carried out up to 30 g/l. The method can easily be extended to much higher uranium concentrations by using differential colorimetry. Effects of interfering metallic corrosion and fission products such as Fe(II), Ni(II), Co(II), Mn(II), Fe(III), Ru(III), Rh(III), Ce(IV), and Cr(VI), etc., were studied and it was established that except for Cr(VI), none of the other ions affects the uranium estimation. The optical density of uranyl nitrate solutions varied linearly with nitric acid concentration in the range 0.5 to 4.5M. This observation was made use of in the development of a method for the determination of free HNO_3 and HCl with an accuracy of ±0.1M. (auth)

8198 (BNL-50271) DETERMINATION OF SILVER, CADMIUM, INDIUM, TIN, AND ANTIMONY IN SODIUM SOLUBILITY STUDIES. Tassinari, S. J.; Auerbach, C. (comps.) (Brookhaven National Lab., Upton, N. Y.). Jun 1970. 15p. Dep. NTIS.

Procedures are described for the determination of silver, cadmium, indium, tin, and antimony when present individually in combination with sodium. The work was performed in support of a study of dilute binary sodium alloys. The matrix is dissolved in ethanol; the solute metal is filtered off and determined by conventional methods. Titration of the NaOH resulting from the dissolution yields the total weight of sodium. (auth)

8199 (BNWL-CC-2502) EVALUATION OF HYDROXYLAMINE NITRATE MONITORING SYSTEMS. Dierks, R. D. (Battelle-Northwest, Richland, Wash. Pacific Northwest Lab.). 20 Apr 1970. 19p. Dep. NTIS.

Electrodeless electric conductivity, pH, oxidation-reduction potential (ORP), ultraviolet absorption, and chemical indicator techniques were investigated as possible methods for indicating the composition of the effluent stream from an ion exchange column producing hydroxylamine nitrate from hydroxylamine sulfate. While pH measurements were more sensitive to changes during the rinsing cycle than electrodeless conductivity measurements and clearly showed the gradual removal of acidic materials during the rinsing cycle, the lack of detail during the elution cycle limited the investigation of pH to the preliminary measurements. Preliminary ORP and pH measurements were not sufficiently different to warrant further investigation of ORP techniques. Ultraviolet absorption measurements were not sufficiently informative to warrant anything other than preliminary measurements. Electrodeless conductivity measurements were made in more detail and offer the following advantages: sensitivity to changes equal to that of

pH measurements, except in the very low concentration ranges; sensitivity to changes during product elution period greater than those of pH measurement; no contact is required with the process stream, minimizing sealing designs and process leakage; no periodic standardization procedures are required that introduce foreign materials into the process system; and there are no electrodes that require periodic replacement. The sensor is an all solid state, rugged device. Chemical indication using potassium permanganate as an indicator was clearly the most accurate method of indicating low concentrations of hydroxylamine, particularly at the product cut-off point. However, the complexity of the system, the somewhat subjective judgment of color intensity required for indicator interpretation, the tendency of the equipment to plug with manganese dioxide and the hazard associated with the proximity of large amounts of permanganate and hydroxylamine, limited the investigation of this technique. (auth)

8200 (LA-4537) CONTROLLED-POTENTIAL COULOMETRIC AND POTENTIOMETRIC TITRATIONS OF URANIUM AND PLUTONIUM IN CERAMIC-TYPE MATERIALS. Waterbury, Glenn R.; Nelson, Gilbert B.; Bergstresser, Karl S.; Metz, Charles F. (Los Alamos Scientific Lab., N. Mex.). Oct 1970. Contract W-7405-eng-36. 19p. Dep. NTIS.

Accurate and precise measurements of the plutonium and uranium contents of mixed oxide, mixed carbide, and mixed nitride materials are now possible by methods developed for this purpose or by previously existing methods. Chemical separation of the elements before analysis is not necessary. Under optimum conditions for repeated analyses of $(U_xPu_y)O_2$, $(U_xPu_y)C$, and solutions containing high-purity uranium and plutonium, the relative standard deviation and the bias range from 0.03 to 0.14%. For analysis of sintered uranium-plutonium nitrides, the relative standard deviations did not exceed 0.3%. The effects of certain impurities and techniques for eliminating carbonaceous decomposition products were investigated. (auth)

8201 (LFEN-NI.-36-a) STUDY OF DETERMINATION OF FLUORINE IN URANIUM CONCENTRATES: OUTLINE OF THE VOLUMETRIC METHOD. Silva, A. Jr. (Junta de Energia Nuclear, Sacavem (Portugal). Laboratorio de Fisica e Engenharia Nucleares). 1968. 20p. (In Portuguese). Dep. NTIS (U. S. Sales Only).

A critical study was made of the various methods used for separation and determination of fluorine. In particular the method of separating fluorine by passing it through supersaturated water vapor and its subsequent titration with thorium nitrate in the presence of alizarin was studied. Tests were made to determine the limitations and errors of the method. Various modifications to improve its exactitude and precision were introduced. The method was applied to uranium concentrates. (tr-auth)

8202 (RCN-126) ACCURATE AND PRECISE TITRIMETRIC ANALYSIS OF URANIUM IN NUCLEAR FUELS. Tolk, A.; Lingerak, W. A.; Verheul-Klompmaker, T. A. (Reactor Centrum Nederland, Petten). Sep 1970. 11p. Dep. NTIS (U.S. Sales Only).

For the accurate and precise titrimetric determination of uranium in nuclear fuels, the material is dissolved in orthophosphoric and nitric acids. The nitric acid is fumed off, and the U(VI) present is analyzed reductometrically in a CO_2 atmosphere with iron (II) ammonium sulfate. For U_3O_8 test sample aliquots of 800 and 80 mg, coefficients of variation of 0.012 and 0.11%, respectively, were measured. (auth)

8203 (RCN-127) DETERMINATION OF OXYGEN-TO-URANIUM RATIO IN HYPERSTOICHIOMETRIC URANIUM DIOXIDE. Tolk, A.; Lingerak, W. A. (Reactor Centrum Nederland, Petten). Sep 1970. 14p. Dep. NTIS (U.S. Sales Only).

The following chemical procedure is preferred for the determination of the O/U ratio in hyperstoichiometric uranium dioxide. The sample is dissolved in concentrated phosphoric acid without change in uranium valence. Then the amount of U(VI) present in the solution is titrated with an Fe(II) standard solution in phosphoric acid. The titrimetric end-point is detected following the dead-stop-end-point procedure. When special precautions are taken, the O/U value can be determined with an accuracy and precision of ±0.0001 O/U units when 500-mg sample aliquots are used. (auth)

8204 (RCN-128) DETERMINATION OF OXYGEN-TO-URANIUM RATIO IN HYPOSTOICHIOMETRIC URANIUM DIOXIDE. Tolk, A.; Lingerak, W. A.; Boerger, D. (Reactor Centrum Nederland, Petten). Sep 1970. 10p. Dep. NTIS (U. S. Sales Only).

A method in which the sample is dissolved in concentrated phosphoric acid is used for the determination of the O/U ratio in hypostoichiometric uranium dioxide UO_{2-y}. During dissolution the following overall reaction occurs: $UO_{2-y} \xrightarrow{H^+} U(IV) + (2-y)\,H_2O + y\,H_2^{\uparrow}$. The amount of released hydrogen is measured by gas chromatography. In a new version of this method the sample is dissolved in phosphoric acid at 250 to 275° C in a closed vessel for a maximum of 60 hours. The hydrogen is then swept away from the solution in one stroke by a helium stream and analyzed in the original way. For test samples of metallic uranium the amount of released hydrogen measured was 99 to 100 % of the theoretical value. (auth)

8205 GAS DETERMINATION IN METALS. I. DETERMINATION OF NITROGEN BY VACUUM MELT EXTRACTION. Stahlberg, Rudi; Foerster, Walter (Zentralinstitut fuer Festkoerperphysik und Werkstofforschung, Berlin. Institutsteil fuer Metallische Spezialwerkstoffe, Dresden). Neue Huette; 15: 423-6(Jul 1970). (In German).

Improvements in the reproducibility and accuracy of the determination of nitrogen were achieved by increasing the extraction temperature or by changing the method of analysis. Use of the method for analysis of steel and special materials was tested. (M.C.G.)

8206 MICRODETERMINATION OF MOLYBDENUM BY ANODIC STRIPPING AT CONSTANT CURRENT USING THE HANGING MERCURY DROP ELECTRODE. Lagrange, Philippe; Schwing, Jean-Paul (Institut de Chimie, Strasbourg). Anal. Chem.; 42: 1844-5(Dec 1970).

A method is reported for the microdetermination of molybdenum based on the accumulation of $MoO_2 \cdot 2H_2O$ on the mercury drop, through cathodic reduction, followed by anodic stripping at constant current. The relative precision of the method is ±1.7% for 10^{-4} M solutions and ±5% for 5×10^{-6} M solutions. (D.H.M.)

8207 QUATERNARY OXIDE SYSTEMS AS HOSTS FOR X-RAY EXCITED OPTICAL FLUORESCENCE DETECTION OF RARE EARTHS IN NUCLEAR MATERIALS AT THE PART PER GIGA (PART PER 10^9) LEVEL. D'Silva, Arthur P.; DeKalb, Edward L.; Fassel, Velmer A. (Ames Lab., Iowa). Anal. Chem.; 42: 1846-7(Dec 1970).

The determination of ultra trace amounts of rare earths in uranium and zirconium is being studied. The oxides of U and Zr may be incorporated into ternary oxide hosts in which optical fluorescence of the rare earths is supported at the fractional ppM level. A system of quaternary oxide phosphor materials was developed, which provides even greater powers of detection. The preparation, spectral characteristics, and some analytical potentialities of these compounds are discussed. The compositions that gave best results were $2Li_2O \cdot SrO \cdot UO_2 \cdot 2WO_3$ and $Na_2O \cdot 2SrO \cdot 2ZrO_2 \cdot 3WO_3$. (M.C.G.)

8208 SPARK SOURCE MASS SPECTROMETRIC SURVEY ANALYSIS OF AIR POLLUTION PARTICULATES. Brown, R.; Vossen, P. G. T. (AEI Scientific Apparatus Ltd., Manchester, Eng.). Anal. Chem.; 42: 1820-2(Dec 1970).

Twenty-eight elements (including Mo, Sr, and Zr) were determined in air pollution particles by spark mass spectrography. Concentrations of the various elements were determined by measuring the height of a peak of an isotope of each element and the peak due to the m/e 107 isotope of silver, the internal standard. The preliminary work reported shows the feasibility of analysis of pollution particulates, and the relative ease of sample preparation and production of spectra. (D.H.M.)

8209 DETERMINATION OF RUTHENIUM BY ATOMIC ABSORPTION SPECTROPHOTOMETRY. Rowston, W. B.; Ottaway, J. M. (Univ. of Strathclyde, Glasgow). Anal. Lett.; 3: 411-17 (Aug 1970).

The use of a mixture of copper and cadmium sulfates to remove the widespread interferences found in the determination of ruthenium by atomic absorption spectrophotometry in an air-acetylene flame is discussed, and a procedure for the determination of 5 to 100 ppM of ruthenium is recommended. (auth)

8210 DIRECT DETERMINATION OF MOLYBDENUM IN HIGH ALLOY STEEL BY THE SPECTROPHOTOMETRIC METHOD. Sakaki, Takashi (Japan Special Steel Co., Ltd., Tokyo). J. Jap. Inst. Metals; 34: 1034-40(Oct 1970). (In Japanese).

A spectrophotometric method with thiomalic acid for the determination of molybdenum was investigated and applied to the direct determination of molybdenum in high alloy steel. The molybdenum thiomalic acid complex is formed quantitatively in a sulfuric acid-sodium acetate solution medium of pH 3.0 to 4.5. The absorption maximum of this complex is at a wavelength of 365 nm. Hydrochloric, nitric, and perchloric acids do not interfere with the formation of a molybdenum thiomalic acid complex, but phosphoric, tartaric, citric, and oxalic acids interfere. The presence of sulfuric acid increases slightly the absorbance for the determination of molyb-

XUM

denum, but its effect appears constant in the range from 1 to 5 ml as sulfuric acid (1 + 1). The presence of copper, iron(II), and tungsten increases the absorbance for the determination of molybdenum, and the presence of niobium, tantalum, titanium, and zirconium decreases. However, the effect of the copper can be masked by using thiourea, the effect of the iron(II) appears constant in the range from 10 to 20 mg, and the effect of the tungsten can be eliminated by measuring the absorbance at the wavelength of 400 nm. The effect of the niobium, tantalum, titanium, and zirconium can be masked by using sodium fluoride. The sample was fumed with sulfuric acid containing ammonium sulfate for dissolving completely the precipitated niobium, tantalum, and tungsten after the sample was dissolved in aqua regia containing ammonium bifluoride, and the sample solution was prepared by adding sodium fluoride for preventing the hydrolysis of the niobium, tantalum, and tungsten in the sample solution. As a result of the experiment, a method was established in which 0.5 to 20% of molybdenum in high alloy steel can be measured precisely without difficulty. The molybdenum contents in actual samples were measured by this method with satisfactory results. (auth)

8211 VOLTAMMETRIC STUDY OF MOLYBDENUM REDUCTION. Apte, V. P.; Dhaneshwar, R. G. (Bhabha Atomic Research Centre, Trombay, India). Indian J. Chem.; 7: 416-18 (Apr 1969).

The electrode system DME/Mo is recommended for studying molybdenum reduction. Three well-defined waves were obtained for molybdate reduction on dc polarograph in sulfuric acid medium as against a single well-defined wave using DME/SCE. Compared to DME/SCE system, DME/Mo system gives better results as far as number of reduction waves of Mo, their forms, reversibility and current-concentration linearity are concerned. (auth)

8212 BROMOPYROGALLOL RED AS A COLORIMETRIC REAGENT. IV. PHOTOMETRIC DETERMINATION OF MOLYBDENUM. Honsa, I.; Suk, V. (Charles Univ., Prague). Collect. Czech. Chem. Commun.; 35: 1283-7(Apr 1970). (In German).

On the basis of the experimental results of the reaction of hexavalent Mo with Bromopyrogallol Red in the presence of gelatin, a photometric method was proposed for Mo determination in the concentration range from 0.05 to 1 μg Mo/ml. The error calculated from the results of 10 determinations in the interval 2σ (probability 95%) was at most 13.5% in the range from 0.05 to 0.29, 8.5% in the range from 0.29 to 0.48, and 4.6% in the range from 0.48 to 1.00 μg Mo/ml. The sensitivity of the photometric method (for A = 0.001) was 2.4×10^{-3} μg Mo/ml. The method is simple since high sensitivity is obtained with extraction of the colored complex. (tr-auth)

Isotope Dilution Procedures

Refer also to abstract 8340.

Radiometric and Radiochemical Procedures

Refer also to abstracts 8447, 8465, 8466, and 8587.

8213 LIQUID SCINTILLATION COUNTING OF ^{113m}In CONVERSION ELECTRONS IN THE PRESENCE OF ^{3}H AND ^{14}C. Sisson, Warden B.; Oldendorf, William H.; Cassen, Benedict (Veterans Administration Center, Los Angeles. Univ. of California, Los Angeles). J. Nucl. Med.; 11: 749-52(Dec 1970).

Counting by liquid scintillation spectrometry of the internal conversion electrons of ^{113m}In is described. The counting efficiency for ^{113m}In liquid scintillation spectrometry approximates that found when counting the gamma emissions of ^{113m}In in a 3 × 3-in. (7.62 cm × 7.62 cm) NaI(Tl) well crystal. This method can be used in biological tissues which also contain both ^{3}H and ^{14}C, and it provides a convenient means of residual blood correction. The high-energy ^{113m}In conversion electrons are counted in the external standard pulse-height window set too high to record ^{14}C or ^{3}H emissions. The 395-keV gamma rays of ^{113m}In, produced at 65% efficiency, are not efficiently recorded in the liquid scintillation system; it is the internal conversion electrons (365 to 392 keV, 35%) which are counted effectively. After the ^{113m}In is counted and has decayed ($T_{\frac{1}{2}}$, 100 min), the ^{3}H and ^{14}C content is counted routinely. Correction of the ^{113m}In efficiency for quench is described. The technique requires no change of pulse-height setting from that used in routine ^{3}H and ^{14}C spectrometry by the external standard method. (auth)

8214 METHOD OF ISOLATION OF ^{95}Zr–^{95}Nb FROM A SOLUTION OF FISSION PRODUCTS BY EXTRACTION WITH DI-(n-OCTYL)PHOSPHORIC ACID AND USE OF ^{95}Zr FOR DETERMINING THE PERCENT BURN-UP OF NUCLEAR FUEL. Krtil, J.; Moravec, A. (Inst. of Nuclear Research, Prague). Coll. Czech. Chem. Commun.; 35: 2915-24(Oct 1970).

A fast selective extraction method was developed for isolating ^{95}Zr (^{95}Nb) from a solution of fission products. The pair of radionuclides ^{95}Zr–^{95}Nb is extracted quantitatively from 6M HNO_3 and 0.5M HF with a solution of di-(n-octyl) phosphate in toluene. The activity of ^{95}Zr was determined by measuring the γ-activity of the extract with the aid of a semiconductor detector. The method was tested on the isolation of ^{95}Zr from a mixture of fission products and used for determining the absolute activity of ^{95}Zr and of the percent burnup of irradiated samples of uranium. (auth)

8215 PROCESS AND DEVICE TO DETERMINE THE PERCENTAGE OF FISSILE MATERIAL IN SAMPLES OF FUEL OR OF NUCLEAR REACTOR FUEL ELEMENTS. (to Kernforschungsanlage, Julich GmbH). French Patent 1,570,956. 5 May 1969. Priority date 22 Jun 1967, Germany. (In French).

The sample of fuel or fuel element in which the content of fissile material is to be measured is first subjected to irradiation and the decrease in activity for a predetermined time is compared with the decrease in activity during the same time for a sample having a known content of fissile material. Two scintillation counters are used on which is mounted an electronic system for integral measurement of the activity of the fission products and automatic data processing. (P.C.H.)

Activation Procedures

Refer also to abstracts 8537, 8579, 8583, 8588, and 10040.

8216 (AERE-R-5363) PHOTON ACTIVATION ANALYSIS USING THE ELECTRON LINEAR ACCELERATOR AT HARWELL. Baker, C. A.; Pratchett, A. G.; Williams, D. R. (Atomic Energy Research Establishment, Harwell (England)). May 1967. 26p. Dep. NTIS (U. S. Sales Only).

The practical details of photon activation analysis are described with particular reference to the determination of carbon in metals and ceramics and oxygen in metals at the microgram level. (auth) (UK)

8217 (MLM-1772) INVESTIGATIONS INTO THE DETERMINATION OF MERCURY IN COPPER. Gillette, R. K. (Mound Lab., Miamisburg, Ohio). 21 Dec 1970. Contract AT(33-1)-Gen-53. 12p. Dep. NTIS.

The determination of parts per billion quantities of mercury in high-purity, oxygen-free high-conductivity (OFHC) copper was investigated by thermal neutron activation analysis. Radiochemical separations of mercury by anion exchange chromatography from a hydrochloric acid system and by solvent extraction with triisooctyl thiophosphate were considered along with a nondestructive determination. Linear regression analysis and a statistical evaluation of the standards were applied to the results. Satisfactory results are reported for the nondestructive neutron activation analysis procedure. (auth)

8218 (NP-18592) ACTIVATION ANALYSIS OF OXYGEN WITH THE AID OF TRITIUM. De Goeij, Jeroen Joannes Maria (Technische Hogeschool, Delft (Netherlands)). 1970. 153p. (In Dutch). Dep. NTIS (U. S. Sales Only).

Thesis.

A method for determination of oxygen by indirect neutron activation is described. The sample is mixed with ^{6}Li, which produces tritons by neutron capture. Subsequently the tritons interact with ^{16}O giving radioactive ^{16}F. Physical factors that may influence the accuracy and sensitivity of the triton activation of oxygen are considered. The practical aspects and usefulness of triton activation are discussed. (M.C.G.)

8219 (PH-3) DETERMINATION OF URANIUM CONTENT IN GEOLOGICAL SAMPLES BY NEUTRON ACTIVATION. Ahmed, M. R.; Abdulla, A. A.; Al-shahiry, G. Y. (Atomic Energy Commission, Baghdad (Iraq). Nuclear Research Inst.). Sep 1970. 10p. Dep. NTIS (U. S. Sales Only).

Samples were irradiated in the IRT-2000 research reactor. The decay rate of ^{239}Np → ^{239}Pu was measured and compared with a standard of known uranium content. Two techniques were applied; in the first method a Ge(Li) γ spectrometer of high resolution was used to measure the γ spectrum from this decay. In the second, scintillation counters were placed in coincidence for detecting two-step cascade γ from the same decay. The results from both techniques were in satisfactory agreement. (auth)

8220 (Y-1744) AUTOMATIC SAMPLE CHANGER FOR THE BERYLLIUM ANALYZER. Kienberger, C. A.; Caylor, J. D. (Union Carbide Corp., Oak Ridge, Tenn. Y-12 Plant). 11 Jan 1971. Contract W-7405-eng-26. 15p. Dep. NTIS.

An automatic sample changer with a sequential panel was de-

signed and built to operate the beryllium analyzer. The changer handles up to 45 samples and automatically changes the sample, operates the counting equipment, and records the counts. It is estimated that in the determination of beryllium, an activation and counting time of about five minutes per aliquant is saved. The analytical results obtained from its use are not significantly different from those obtained from the manually operated beryllium analyzer. (auth)

8221 USE OF SELECTIVE ION EXCHANGE PAPER IN X-RAY SPECTROGRAPHY AND NEUTRON ACTIVATION. APPLICATION TO THE DETERMINATION OF GOLD. Green, Thomas E.; Law, Stephen L.; Campbell, William J. (College Park Metallurgy Research Center, Md.). Anal. Chem.; 42: 1749-53(Dec 1970).

Ion exchange resin-loaded paper disks containing a highly selective ion exchange resin serve as an excellent medium for separating and collecting trace quantities of elements in an optimum form for x-ray spectrographic and neutron activation determination. A new collection procedure provides a simple means for preconcentrating the trace elements from large samples. A radioactive tracer added to the original sample is used as the collection monitor. Use of a cyclotron-produced radiotracer permits the application of this procedure to neutron activation determination. The determination of gold in the ppM range by x-ray spectrography and in the ppB range by neutron activation is given as an example. (auth)

8222 STRONTIUM AND MANGANESE CONCENTRATIONS IN MANDIBULAR RAT INCISORS FOLLOWING INTRAPERITONEAL INJECTIONS. Rasmussen, Erik Gerhard. Tandlaegebladet; 74: 696-702(1970). (In Danish).

The concentration of strontium and manganese in mandibular rat incisors was determined following intraperitoneal injections of $Sr(NO_3)_2$ and $MnCl_2$. Six samples from the middle third of the mandibular incisors of four rats were analysed. Animal A received one injection and was killed one day after the injection. Rats B and C got five injections, B was killed one day after the last injection, C was killed 8 days following the last injection. Rat D (control) got no injection. The samples were irradiated by an integrated thermal neutron flux of either 5.0×10^{16} neutrons/cm^2 or 7.2×10^{16} neutrons/cm^2. The radionuclides ^{87m}Sr (peak γ emission: 0.39 MeV) and ^{56}Mn (peak γ emission: 0.85 MeV) were measured using a 4 × 5 in. NaI(Tl) scintillation well detector and a 400-channel T.M.C. analyzer following radiochemical separation. The concentrations of strontium and manganese increased in tooth samples from rats B and C. The elements were not preferentially localized in odontoblasts or the periodontal membrane. (auth) (Denmark)

8223 DETERMINATION OF TRACE ELEMENTS IN GLASS BY ACTIVATION ANALYSIS USING HYDRATED ANTIMONY PENTOXIDE FOR SODIUM REMOVAL. Gills, Thomas E.; Marlow, William F.; Thompson, Barbara A. (National Bureau of Standards, Washington, D. C.). Anal. Chem.; 42: 1831-3(Dec 1970).

A procedure is reported for the determination of elements at the ppM and ppB level in glass by neutron activation after sodium removal using hydrated antimony pentoxide columns. Results are reported for manganese, gold, gallium, lanthanum, antimony, and copper. (D.H.M.)

8224 RAPID NEUTRON ACTIVATION METHOD FOR ALUMINUM DETERMINATION IN Al COORDINATION COMPOUNDS. Riekstinva, D. V.; Vevere, I. Z. (Inst. of Physics, Riga). Latv. PSR Zinat. Akad. Vestis, Fiz. Teh. Zinat. Ser.; No. 4, 125-6(1970). (In Russian).

The samples and the standards in polyethylene bags were subjected to irradiation for 30 sec. in a reactor neutron flux of 5×10^{12} n/cm^2 sec. After a 6.5 to 10-min. storage the activity was measured by means of a 256-channel γ spectrometer. The sensitivity of determining Al reached 2×10^{-6} g, and the reproducibility was 3%. The results of the investigation were found to be in a good agreement with the data of analyses obtained by chemical methods. (auth)

8225 DETERMINATION OF BERYLLIUM BY (γ,n) REACTION IN LINAC. Abbosov, O.; Abrams, I. A.; Kodiri, S.; Pelekis, L. L.; Starchik, L. P. (Inst. of Physics, Riga). Latv. PSR Zinat. Akad. Vestis, Fiz. Teh. Zinat. Ser.; No. 4, 27-30(1970). (In Russian).

A method for determination of beryllium using the (γ,n) reaction with linac is described. Dysprosium was used as a detector. The sensitivity of the method was determined. (auth)

8226 APPLICATION OF CADMIUM FILTER IN ACTIVATION ANALYSIS WITH REACTOR NEUTRONS. Damburg, N. A.; Pelekis, L. L. (Inst. of Physics, Riga). Latv. PSR Zinat. Akad. Vestis, Fiz. Teh. Zinat. Ser.; No. 4, 19-26(1970). (In Russian).

The cadmium ratios for 42 isotopes were measured at a Cd filter thickness of 0.5 mm. The flux depression near the filter, the slowing down of epicadmium neutrons in various substances and the increase of the thermal neutron flux due to the epithermal neutrons slowing down in solutions are considered. (auth)

8227 NEUTRON ACTIVATION ANALYSIS PROGRAM OF THE FOOD AND DRUG ADMINISTRATION. Tanner, James T.; Lambert, J. P. F.; Simpson, R. E. (Food and Drug Administration, Washington, D. C.). J. Ass. Offic. Anal. Chem.; 53: 1140-4(Nov 1970).

Activation analysis is a rapid and sensitive method of trace element analysis applicable to a large variety of samples. For the most part the method is nondestructive; however, for highest sensitivity, chemical separations are usually required. For about 4 years the Food and Drug Administration, utilizing the Naval Research Laboratory reactor, has applied neutron activation to various samples of foods, drugs, and biological materials. Elements such as vanadium, selenium, and mercury were determined at the nanogram level with little interference from the matrix. Possibly more important than interest in specific element determinations themselves is utilization of the elements or element profiles as indices of required information. Thus, in several forensic applications the authenticity of drugs and food items was evaluated through the characteristic gamma spectral "signatures." Through neutron activation the distribution of mycotoxin contamination in batches of foodstuffs was simulated to establish homogeneity of sample preparations. Some earlier examples of the applications of neutron activation analysis made in FDA and summaries of recent work are presented. (auth)

8228 DETERMINATION OF VANADIUM BY NEUTRON ACTIVATION ANALYSIS AT NANOGRAM LEVELS TO FORMULATE A LOW-VANADIUM DIET. Lambert, J. P. F.; Simpson, R. E.; Mohr, H. E.; Hopkins, L. L. Jr. (Food and Drug Administration, Washington, D. C.). J. Ass. Offic. Anal. Chem.; 53: 1145-50(Nov 1970).

Neutron activation analysis for vanadium is very sensitive if it is combined with a rapid and efficient chemical separation. A post-irradiation solvent extraction with N-phenylbenzohydroxamic acid reagent was evaluated by adding known amounts of vanadium to water. When 3.2 to 80 ng were added, the recovery ranged from 97 to 104%. The counting error at the 95% confidence level varied from 10% for 3.2 ng to less than 2% for 80 ng. The time of separation, interferences, and chemical yield, which influence sensitivity, are discussed. From data obtained in an animal diet survey, a low-vanadium diet with 14 ppB of vanadium was formulated. (auth)

8229 STUDY OF TRACE METALS IN FINGERNAILS AND HAIR USING NEUTRON ACTIVATION ANALYSIS. Mahler, Delmar J.; Scott, Arthur F.; Walsh, John R.; Haynie, Gordon (Veterans Administration Hospital, Portland, Oreg. Reed Coll., Portland, Oreg.). J. Nucl. Med.; 11: 739-42(Dec 1970).

The concentration of manganese, copper, gold, zinc, and sodium in fingernails and hair has been measured by means of neutron activation analysis and γ spectrometry. The results obtained for patients on hemodialysis indicated lower copper, sodium, and gold but increased manganese and zinc levels in fingernails as compared with controls. Hair samples showed minimal differences. Data are presented that indicate a possible effect of environment on trace metal deposition. (auth)

8230 ACTIVATION METHODS FOR DETERMINING THE CONTENT OF Ta AND Cs IN ROCKS. Lobanov, E. M.; Nurmatov, D. (Inst. of Physics, Tashkent). Dokl. Akad. Nauk Uzb. SSR; No. 3, 17-19(1970). (In Russian).

Radiochemical activation analysis was used to determine the content of Ta in mixed mineral oxides and rocks and Cs in seawater, algae, and carbon after concentration to 10^{-5} to 10^{-8} g. ^{182}Ta and ^{134}Cs were produced by thermal neutron irradiation with ^{182m}Ta lifetime $T_{\frac{1}{2}} = 16.6$ min and ^{134}Cs = 2.2 years. Results of the quantitative activation determination of Ta and Cs in rocks are tabulated. (R.V.J.)

8231 NEUTRON ACTIVATION ANALYSIS OF INORGANIC CONSTITUENTS OF AIRBORNE PARTICULATES. Pillay, K. K. S.; Thomas, C. C. Jr.; Hyche, C. M. (Western New York Nuclear Research Center, Inc., Buffalo). Nucl. Technol.; 10: 224-31(Feb 1971).

The applications of neutron activation analysis for the routine monitoring of airborne inorganic pollutants were investigated. The use of several filter media were studied and two suitable filter materials (Millipore EHW PO4700 and Dexter × 1215) were chosen for this investigation. An air sampling procedure was used to obtain several representative samples during the period of monitor-

XUM

ing. A non-isolative neutron activation analysis procedure involving multiple neutron irradiation and high resolution gamma-ray spectrometry was used to determine the concentrations of sixteen elements found in the airborne particulates in samples collected over a one-year period from the Buffalo, New York area. Differences from previous studies are due to higher filter efficiency and the particular local industrial workup. The findings indicate that in the analysis of the elemental composition of air pollutants, neutron activation techniques can compete well with other analytical methods. (auth)

8232 METHOD FOR DETERMINING THE CONTENT OF CEMENT IN CONCRETE. Frevert, Erich; Muhlberger, Friedrich (to Osterreichische Studiengesellschaft fuer Atomenergie GmbH). British Patent 1,213,961. 25 Nov 1970. Priority date 5 Mar 1968, Austria.

A method for determination of the cement content in concrete comprises dispersing an element (indium) or a compound of the element, activating the element by thermal neutrons, and measuring the activity of the ^{114}In and ^{116}In to determine the value of the cement content. A flux monitor (preferably Er) is irradiated at the same time as the concrete, and the ratio of the counting rates of the element, In, and the flux monitor, Er, are measured to indicate the cement content. (B.L.M.)

8233 NEUTRON ACTIVATION ANALYSIS OF TRACE IMPURITIES IN TITANIUM AND TITANIUM DIOXIDE. Neirinckx, Rudi Dominique. Ghent; State Univ. of Ghent (1969). (In Dutch). Thesis.

Titanium metal and titanium sponge, titanium dioxide powder and titanium dioxide single crystals were analyzed by neutron activation and high resolution γ spectrometry. Since the (n,γ) reaction on the titanium matrix yields only one radioactive isotope, ^{51}Ti, which has a short half-life only the determination of those elements, yielding short-lived isotopes, upon irradiation is affected by the matrix. The (n,p) reaction on the stable titanium isotopes yields the long-lived ^{46}Sc, ^{47}Sc, and ^{48}Sc isotopes, which constitute the matrix activity in the case of the determination of the elements, yielding long-lived isotopes. Various factors, such as preseparations, high blank values, and sample dissolution, influence this method for determination of impurities in Ti. All these factors lead to different analytical procedures for the determination of long-lived and short-lived isotopes in Ti metal and sponge, TiO_2 powder and TiO_2 single crystals. The procedure for TiO_2 powder is more complex than that for Ti metal and TiO_2 single crystals, which is due to the dominant activity, caused by the high concentration of Sb and Na. For the other procedures a fast chemical intervention suffices. For the isotopes with half-lives 15 min $< T_{\frac{1}{2}} <$ 3 hr, a non-destructive and two different destructive procedures were applied. For the short-lived isotopes ($T_{\frac{1}{2}}$ <15 min) a non-destructive and three different preseparation techniques were applied. Aluminum and V were analyzed and especially the preseparation, based upon scavenging of lead tetravanadate with lead fluoride allows sensitive analyses of V. A total of thirty metallic elements were treated in at least one of the analytical procedures. These are Ag, Al, As, Au, Ba, Ca, Ce, Co, Cr, Cu, Eu, Fe, Ga, Hf, In, K, La, Mn, Mo, Na, Ni, Sb, Sm, Sn, Ta, Th, U, V, W, and Zn. The sensitivity for the destructive analysis is normally 50 times higher than for the non-destructive analyses, on condition that the nuclides do not have to be measured in a group that contains a dominant activity caused by an accompanying impurity. The matrix only interferes in the determination of Ca and Sc. An accurate analysis of these elements would require a preseparation technique, unless an irradiation under and without cadmium shielding is applied. (Diss. Abstr. Int., B)

8234 AUTORADIOGRAPHY OF NEUTRON-ACTIVATED ROCK SLABS. Bjoerlykke, K.; Brunfelt, A. O. (Univ., Oslo). Chem. Geol.; 6: 233-7(Oct 1970).

Autoradiographs in macro-scale of rocks are produced after subjecting polished rock slabs to thermal neutron activation. The obtained picture shows the distribution of induced activity in the rock slab. One to five days after irradiation most of the exposure of the film is due to ^{24}Na formed by (n,γ) reaction from natural sodium (^{23}Na). After about one week the picture is dominated by elements with long-lived radionuclides. Iron and cobalt and certain trace elements will produce staining depending on the composition of the rock. (auth)

8235 TRACK AUTORADIOGRAPHY FOR THE STUDY OF THE MICRODISTRIBUTION OF CERTAIN ELEMENTS IN METALS. Krishtal, M. A.; Ivanov, L. I.; Grinberg, E. M. At. Energ. (USSR); 29: 127-8(Aug 1970). (In Russian).

The determination of boron in austenitic steels was studied by etching α particles obtained from the reaction of boron with thermal neutrons on polymer detectors. The experiments to select detector material and to optimize the radiation source involved the use of methyl isobutyl ketone films on the polished surface of the alloy. After air drying, the specimens were irradiated in the thermal column of the reactor at a flux of $\sim 7 \times 10^7$ n · cm^{-2} sec^{-1}. The film was then etched in a 56% aqueous KOH solution. The method made it possible to obtain a reliable picture of the microdistribution and the local concentration of boron in metals and alloys; it may also serve to study the diffusion mechanism in alloys. (TTT)

Inorganic, Organic, and Physical Chemistry

Refer also to abstracts 8830 and 8831.

Chemical Properties

Refer also to abstracts 8199, 8325, 8384, and 8922.

8236 (ARH-SA-72) PYROCHEMICAL PROCESS FOR THE REDUCTION OF PLUTONIUM DIOXIDE TO METAL. Felt, R. E. (Atlantic Richfield Hanford Co., Richland, Wash.). 15 May 1970. Contract AT(45-1)-2130. 18p. (CONF-701103-6). Dep. NTIS.

From 63rd National Meeting of the American Institute of Chemical Engineers, Chicago, Ill.

A pyrochemical process was developed for reducing plutonium dioxide directly to metal with calcium and a salt flux. Direct oxide reduction eliminates several intermediate processing steps that generate waste streams requiring further processing. Waste recovery is nearly eliminated by this method of producing plutonium metal. The process was demonstrated by producing 2000 grams of plutonium metal. Further equipment development is required to make the process operational. (auth)

8237 (KFK-1210) COMPLEX FORMATION OF TETRAVALENT ACTINIDES WITH PYRIDINE- AND α-AMINOPOLYCARBOXYLIC ACIDS. Paul, M. Th. (Kernforschungszentrum, Karlsruhe (West Germany). Institut fuer Radiochemie). Jun 1970. 45p. (In German). Dep. NTIS (U. S. Sales Only).

The complexation of Th(IV), U(IV), and Np(IV) with two pyridinacetic acids and five aminopolyacetic acids were studied by using a potentiometric and an absorption spectrometric method (Ionic strength μ = 1.0 Na, $HClO_4$, T = 25.0°C). The stability constants were calculated for these complexes. Also a mixed complex of Np(IV) was found. The hydrolytic constants of U(IV) and Np(IV) were obtained by using absorption spectrometric technique. (auth)

8238 (LF-tr-41, pp 3-5) PHYSICAL AND CHEMICAL PROPERTIES OF ^{239}Pu. Translated from Problemy Toksikologii Plutoniya, Atomizdat, Moscow, 1969.

The nuclear properties of ^{239}Pu and the chemical properties of plutonium are discussed. The chemical properties of some plutonium compounds are listed. (M.C.G.)

8239 (MLM-1744) DISPROPORTIONATION OF TETRAVALENT AND PENTAVALENT PLUTONIUM IONS IN THE PRESENCE OF HEXAVALENT PLUTONIUM. Silver, G. L. (Mound Lab., Miamisburg, Ohio). 22 Dec 1970. Contract AT(33-1)-Gen-53. 47p. Dep. NTIS.

The concept that the disproportionation reactions of tetravalent and pentavalent plutonium ions are special cases of the general plutonium equilibrium problem is illustrated with the estimation of the distribution of plutonium valence states when tetravalent and pentavalent plutonium ions are allowed to disproportionate in the presence of excess hexavalent plutonium. Sources of errors in disproportionation stoichiometry coefficients are described, and a table of relative errors is presented. A computer program suitable for estimating plutonium valence state distributions for any initial plutonium oxidation number is included. Application of the program to the study of the autoreduction of solutions of hexavalent ^{238}Pu and ^{239}Pu is suggested. (auth)

8240 KINETIC INVESTIGATION OF METAL ION HYDROLYSIS AND INDICATOR REACTIONS USING A SQUARE WAVE DISSOCIATION FIELD EFFECT APPARATUS. Cole, David LeRoy. Salt Lake City; Univ. of Utah (1970). 118p. University Microfilms Order No. 70-11,937.

Thesis.

A square wave dissociation field effect relaxation method apparatus was designed and built. The operating procedures for this apparatus, as well as the theory of operation and a description of individual components, have been provided. With this equipment a series of metal ion hydrolysis reactions of differing ionic charge

were studied. The metal ions were uranyl, scandium(III), and thorium(IV). The microsecond-time scale relaxation times measured for the uranyl system were assigned to the first monomeric hydrolysis equilibrium:

$$UO_2^{+2} + H_2O \underset{k_{-1}}{\overset{k_1}{\rightleftharpoons}} UO_2OH^+ + H^+.$$

The rate constants for this system were calculated to be $k_1 = 1.73 \times 10^4$ sec^{-1} and $k_{-1} = 1.65 \times 10^{10}$ M^{-1} sec^{-1}. Relaxation times were measured by both the electric field-jump and the temperature-jump relaxations methods for the scandium(III) system. The temperature-jump relaxations were assigned to the dimer equilibrium,

$$2ScOH^{+2} \underset{k_{-2}}{\overset{k_2}{\rightleftharpoons}} Sc_2(OH)_2^{+4},$$

with calculated rate constants of $k_2 = 8.5 \times 10^5$ M^{-1} sec^{-1} and $k_{-2} = 1.1 \times 10^3$ sec^{-1}. The electric field-jump relaxations were assigned to the first monomeric hydrolysis equilibrium,

$$Sc^{+3} + H_2O \underset{k_{-1}}{\overset{k_1}{\rightleftharpoons}} ScOH^{+2} + H^+,$$

with calculated rate constants of $k_1 = 1.7 \times 10^5$ sec^{-1} and $k_{-1} = 1.0 \times 10^{10}$ M^{-1} sec^{-1}. Relaxation times for the thorium(IV) system were assigned to the first monomeric hydrolysis equilibrium,

$$Th^{+4} + H_2O \underset{k_{-1}}{\overset{k_1}{\rightleftharpoons}} ThOH^{+3} + H^+,$$

and the rate constants calculated to be $k_1 = 1.4 \times 10^5$ sec^{-1} and $k_{-1} = 4.3 \times 10^8$ M^{-1} sec^{-1}. The specific rates of recombination for the above three monomeric hydrolysis equilibria were compared to systems of similar charge type and to theoretical values calculated from the Debye equation,

$$k_R = \frac{4\pi N_O Z_A Z_B e^2 (D_A + D_B)}{10^3 \epsilon kT \left[\exp\frac{Z_A Z_B e^2}{\epsilon kTa} - 1\right]}$$

for diffusion controlled reactions. A modification of the apparatus was designed and built. This modification allowed the kinetics of systems to be followed spectrophotometrically. This apparatus was used to study the acid-base kinetics of methyl red. (Diss. Abstr. Int., B)

Isotope Effects and Exchange

Refer also to abstracts 8318, 8320, 8329, 8335, and 8422.

8241 (CU-755-7, Sect. 3) STUDY OF THE EXCHANGE EQUILIBRIA BETWEEN METHYLACETYLENE-d AND WATER BY MASS SPECTROMETRY. Smith, Jessie Gregory (Columbia Univ., New York. Dept. of Chemistry). 104p.

Part I of Ph. D. Dissertation.

The single-stage separation factor, α, was measured for the base-catalyzed exchange of deuterium between water and methylacetylene as a function of temperature. Values of α were determined from mass spectrophotometric analyses. At any one temperature α was found to be dependent on the initial concentration of D in the H_2O. This result is discussed in terms of instrumental memory effects and a deviation of the equilibrium constant for the disproportionation reaction of water from 4.0. The observed results for the values of α were significantly larger than reported theoretical values. Procedures developed for the analysis of deuterated methylacetylene are discussed in terms of the use of this reaction for analysis of deuterium content of water. Some results are presented for analyses of water containing between 1 and 80 at. % D. The range of sample sizes and concentrations for which this procedure is applicable are given. (auth)

8242 STEREOCHEMISTRY OF THE σ-COMPLEX INTERMEDIATE IN STERICALLY HINDERED ELECTROPHILIC AROMATIC SUBSTITUTIONS. Snyckers, F.; Zollinger, H. (Eidgenoessische Technische Hochschule, Zurich). Helv. Chim. Acta; 53: 1294-1305(1970).

The kinetics of the diazo coupling reactions of diazotized sulfanilic acid with 9 derivatives of 2-naphthol, each containing a substituent in the 8-position, were measured. The reactions proceed by general base catalysis. The rate constants (k_1) for the formation of the steady-state intermediate in the presence of varying concentrations of a base (pyridine) were evaluated from rate measurements. Similarly the ratios k_2/k_1 (where k_2 is the rate constant for proton transfer from the steady-state intermediate to the base, and k_{-1} is the rate constant for the dissociation of the intermediate) were determined. The dependence of log k_1 on σ_m^+ and of the ratio k_2/k_{-1} on a steric parameter R^f (defined in this paper) is interpreted as evidence for the steady-state intermediate existing as a benzodienone σ-complex with the sp^3-bound hydrogen in a pseudo-equatorial position and the electrophile pseudo-axial. A sterically caused destabilisation of the intermediate can be excluded. The steric influence on the ratio k_2/k_{-1} is therefore due to the steric influence on k_2 only. Diazo coupling of 8-(2'-pyridyl)-2-naphthol is subject to intramolecular base catalysis, as demonstrated by kinetic hydrogen isotope effects. (auth)

8243 ISOTOPE EFFECTS IN CHEMICAL PROCESSES. 153rd Meeting of the American Chemical Society, Miami Beach, Fla., April 11, 1967. Gould, Robert F. (ed.). Advan. Chem. Ser.; No. 89, 1-278(1969). (CONF-670460).

Thirteen papers presented at the conference are included and an abstract was prepared for each. (M.C.G.)

For abstracts of individual papers see: 8244–8247, and 8328–8336.

8244 ISOTOPIC EXCHANGE BETWEEN HYDROGEN AND LIQUID AMMONIA CATALYZED BY ALKALI AMIDES. Delmas, Robert; Courvoisier, Pierre; Ravoire, Jean (CEN de Saclay, Gif-sur-Yvette, France). Advan. Chem. Ser.; No. 89, 25-39 (1969).

From Conference on Isotope Effects in Chemical Processes, Miami Beach, Fla. See CONF-670460.

The catalytic action of alkali amides on the isotopic exchange between hydrogen and liquid ammonia was reinvestigated. A kinetic study and a careful calculation of the dissociation coefficients of the amides of sodium, potassium, and cesium were made. If the results are interpreted according to the theory of the acid–base catalysis given by Bell, the conclusion is that only the free amide ion acts as a catalytic species. The kinetic data are in agreement with an associative mechanism. (auth)

8245 ANALYSIS OF ISOTOPE-EFFECT CALCULATIONS ILLUSTRATED WITH EXCHANGE EQUILIBRIA AMONG OXYNITROGEN COMPOUNDS. Monse, E. U. (Rutgers–The State Univ., Newark, N. J.); Spindel, W.; Stern, Marvin J. Advan. Chem. Ser.; No. 89, 148-84(1969).

From Conference on Isotope Effects in Chemical Processes, Miami Beach, Fla. See CONF-670460.

The applicability of several approximation methods to the prediction and/or temperature extrapolation of isotopic partition-function ratios for, and equilibrium constants for isotope exchange among, some simple ^{15}N- and ^{18}O-substituted oxynitrogen compounds is evaluated. It is shown that some of the approximation methods investigated can lead to reasonable estimates of room-temperature-region values of the isotopic partition-function ratios. However, attempted application of these methods to the prediction of the (near-unity) equilibrium constants, at room temperature, usually produced rather poor results, owing, for the most part, to the prevalence of "anomalies" in the "exact" temperature dependences. The characteristic frequency of the simple gamma-bar-method equation for either a partition-function ratio or an isotope-exchange equilibrium constant is discussed in terms of the contributing isotope-dependent vibrational frequencies. (auth)

8246 CORRECTION TO THE EFFECT OF ANHARMONICITY ON ISOTOPIC EXCHANGE EQUILIBRIA. Wolfsberg, Max (Brookhaven National Lab., Upton, N. Y. State Univ. of New York, Stony Brook). Advan. Chem. Ser.; No. 89, 185-91 (1969).

From Conference on Isotope Effects in Chemical Processes, Miami Beach, Fla. See CONF-670460.

It is demonstrated that the formula for the vibrational energy states of a diatomic molecule should be written as $E_n/hc = G_0 + \omega_e(n + \frac{1}{2}) - \omega_e x_e(n + \frac{1}{2})^2$ with non-zero G_0. G_0 values are evaluated for some diatomic hydrides and the effect of G_0 on the theoretical calculation of isotopic exchange equilibrium constants is shown. (auth)

8247 ELECTROMIGRATION IN METALS, SALTS, AND AQUEOUS SOLUTIONS. Klemm, A.; Heinzinger, K. (Max Planck-Institut fuer Chemie, Mainz). Advan. Chem. Ser.; No. 89, 248-63(1969).

From Conference on Isotope Effects in Chemical Processes, Miami Beach, Fla. See CONF-670460.

The progress achieved in the field of isotope electromigration in metals, salts, and aqueous solutions since the meeting on isotope separation in Paris in 1963 is reported. It is shown that the temperature dependence of the isotope effect in liquid metals leads to the conclusion that it is a result of classical atom–atom interactions. Isotope effects in molten salts are smaller than in classical ionic gases. A three stage model is proposed for an explanation of the temperature dependences of the isotope effects

XUM

in molten salts. The available data of the relative difference in mobilities of isotopes in aqueous solutions are summarized. (auth)

8248 EFFECT ON TRINITROPHENYLATION OF MYOSIN ON THE ISOTOPIC EXCHANGE REACTION OF OXYGEN IN THE SYSTEM MYOSIN ATP–$H_2{}^{18}O$. Kuleva, N. V.; Karandashov, E. A.; Panteleeva, N. S. (Leningrad State Univ.). Biokhimiya; 35: 42-7 (Jan-Feb 1970). (In Russian).

The ^{18}O exchange reaction, catalyzed by myosin in the presence of Mg^{2+} and $H_2{}^{18}O$ during ATP hydrolysis, was shown to be inhibited by 40 to 70% on treatment of myosin by 2,4,6-trinitrobenzenesulfonate, a specific reagent for free protein NH_2 groups. Under the same conditions ATP-ase activity of myosin was increased. The trinitrobenzenesulfonate action on the isotopic exchange and ATP activity is similar to the action of actin. (auth)

8249 KINETIC ISOTOPE EFFECTS IN THE QUENCHING OF $O_2(b^1\Sigma_g^+)$ BY SOME DEUTERATED COMPOUNDS. Stuhl, F.; Niki, H. (Ford Motor Co., Dearborn, Mich.). Chem. Phys. Lett.; 7: 473-4(15 Nov 1970).

Absolute rate constants for the quenching of metastable $O_2(b^1\Sigma_g^+)$ molecules by acetylene-d_2, ethylene-d_4, propylene-d_6, H_2O,D_2O, H_2, HD, and D_2 were determined at 300°K. The $O_2(b^1\Sigma_g^+)$ molecules were generated by vacuum uv flash photolysis of O_2 and were monitored by $O_2(b^1\Sigma_g^+ \rightarrow X^3\Sigma_g^-)$ emission at 7620Å. The isotope ratios of the rate constants for the hydrogenated and the fully deuterated compounds range from 1.4 for H_2O/D_2O to 50 for H_2/D_2. (auth)

8250 FAR INFRARED SPECTRA OF HCl AND DCl IN A NITROGEN MATRIX. Katz, B.; Ron, A. (Technion-Israel Inst. of Tech., Haifa). Chem. Phys. Lett.; 7: 357-9(1 Nov 1970).

The spectra of HCl and DCl molecules trapped in a nitrogen matrix were studied in the 100 to 250 cm^{-1} spectral region. Two absorptions were observed for each species: at 154 and 207 cm^{-1} for HCl and at 132 and 162 cm^{-1} for DCl. These absorptions showed monomeric behavior. They are assigned to libration-translation motions of the isolated HX molecule in the nitrogen matrix. (auth)

8251 IONIZATION AND DISSOCIATION ENERGIES OF HF AND DF AND THEIR BEARING ON $D_0^0(F_2)$. Brundle, C. R. (Bell Telephone Labs., Inc., Murray Hill, N. J.). Chem. Phys. Lett.; 7: 317-22(1 Nov 1970).

The high-resolution photoelectron spectra of HF and DF were recorded. Ionization potentials to the $^2\Pi$ and $^2\Sigma^+$ states of the ion are given, together with an estimate for the dissociation limit in the $^2\Sigma^+$ state. The data are compared to previous results and it is suggested that a recent mass-spectrometric determination of $D_0^0(HF)$ and $D_0^0(F_2)$ may be in error. (auth)

8252 ELECTRON SPIN RESONANCE STUDIES ON NEUTRAL AROMATIC HYDROCARBON RADICALS. SUBSTITUENT AND ISOTOPE EFFECTS. Dalton, D. R.; Liebman, A. (Temple Univ., Philadelphia). Tetrahedron; 26: 3265-70(Jul 1970).

The neutral, ^{13}C bearing, radicals diphenylmethyl and 9-fluorenyl were generated in solution and the hyperfine coupling between ^{13}C and the free electron obtained. On the basis of this information, the nonplanarity assigned to these radicals is seen to lie not in the hybridization of $C_{central}$, which is sp^2, but rather in the "propellor" type disposition of the phenyl rings. Some substituted neutral diphenylmethyl radicals have also been examined and no simple correlation between the usual σ substituent parameters and the hyperfine (a_H) splitting constants of the hydrogen at $C_{central}$ is apparent. (auth) (UK)

8253 STUDIES IN CARBANION CHEMISTRY. Roitman, James Nathaniel. Los Angeles; Univ. of California (1969). 209p. University Microfilms Order No. 70-12,018.

Thesis.

The base-catalyzed hydrogen isotope exchange reaction of an optically active carbon acid can generate three products in addition to the starting substrate. Each of these may be associated formally with a stereospecific process: isotopic exchange with retention, isotopic exchange with inversion, and inversion without isotopic exchange (isoinversion). Although the rate constants for isotope exchange and racemization can in some instances provide unequivocal information about the course of isotopic exchange for an optically active carbon acid, more detailed information can be obtained by a method of partial exchange and racemization, followed by reresolution and subsequent isotopic analysis. The reresolution technique was applied to two carbon acid systems: (+)-2-methyl-2,3-dihydrobenzo[b]thiophene-1,1-dioxide (I-h) and its corresponding 2-deuterio derivative (I-d) and p-biphenylylphenylmethoxymethane (II-h) and its corresponding deuterio analog (II-d). In methanol with potassium methoxide, I-d underwent exchange with net inversion of configuration, the first such unequivocal example. There was also a considerable contribution from isoinversion, which may be explained by the ability of sulfone oxygens to provide hydrogen bonding sites. Very low primary kinetic isotope effects for racemization of I in methanol were observed and are attributed to a preequilibrium before the rate determining step. An optically active derivative of (+)-I, (+)-4,6-dinitro-2-methyl-2,3-dihydrobenzo[b]thiophene-1,1-dioxide (III-h) and its 2-deuterio analog (III-d) were prepared by nitration of (+)-I-h and (+)-I-d. Reactions of (+)-III-d with amine bases caused racemization and chemical decomposition of the substrates, but no exchange. The discovery of the cation-complexing behavior of a series of cyclic polyethers prompted investigation of the effect one of these might have on the retention mechanism of carbanions generated by two different routes. The base-catalyzed exchange of (–)-II-d in t-butyl alcohol with equimolar amounts of potassium t-butoxide and 2,5,8,15,18,21-hexaoxatricyclo[20.4.0.0^{9,14}]hexacosane (XV) proceeded at a much faster rate and with no stereospecificity, whereas exchange occurred with high retention in the absence of XV. The hydrazine p-toluenesulfonamide derivative (XX) of 1,1,1-triphenylethane was prepared and decomposed in base to see if the 1,1,1-triphenylethyl carbanion underwent phenyl migration before capturing a proton from the medium. In no case was any 1,1,2-triphenylethane detected; proton capture was much faster than rearrangement. (Diss. Abstr. Int., B)

8254 α- AND β-DEUTERIUM ISOTOPE EFFECTS ON THE SOLVOLYSIS OF NORBORNYL BROSYLATES. Conkling, John Alexander. Baltimore; Johns Hopkins Univ. (1969). 211p. University Microfilms Order No. 70-11,781.

Thesis.

Secondary deuterium isotope effect studies of the solvolysis of norbornyl derivatives were undertaken in an attempt to determine whether an intermediate carbonium ion or its counterpart, a pair of rapidly equilibrating classical ions, better accounts for the exo-brosylate solvolysis results. New synthetic procedures were developed to prepare stereospecifically-labeled substrates, in which the position of deuterium substitution was rigorously established. For alpha-deuterated exo-norbornyl brosylate the same low k_H/k_D of 1.12 was observed in both acetic acid and 80% aqueous ethanol. Alpha-deuterated endo-norbornyl brosylate exhibited a k_H/k_D of 1.19 for ethanolysis, in good agreement with other data and consistent with solvolysis isotope effects of model classical compounds. For exo-brosylate solvolysis, an extraordinary nonequivalence of isotope effects for deuterium at the 3-exo and 3-endo positions was noted. The beta-isotope effects on solvolysis of the corresponding endo-brosylates were of magnitudes similar to those of model compounds. These observed isotope effects are in good agreement with classical ionization for endo-norbornyl brosylates. However, classical ionization cannot satisfactorily explain the results for solvolysis of the deuterated exo-norbornyl brosylates. The exo-brosylate results are explainable in terms of a transition state leading to the nonclassical carbonium ion. (Diss. Abstr. Int., B)

8255 FAST GAS-PHASE ISOTOPIC EXCHANGE REACTIONS IN NITROGEN OXIDES. Wong, Kam-yuen. Toronto; Univ. of Toronto (1969).

Thesis.

The kinetics of the very fast oxygen self exchange reaction $N^{16}O_2 + N^{18}O_2 \rightleftharpoons 2N^{16}O^{18}O$ was studied in a fast flow gas phase tubular reactor designed and constructed in the ion source of a mass spectrometer. The reaction is second order and has a rate constant of $(3.0 \pm 0.1) \times 10^8$ l mole^{-1} sec^{-1} at room temperature. It occurs homogeneously in the gas phase and has no measurable temperature dependence between 23 and 82°C. Since the most reasonable mechanism of exchange consistent with experimental observations is the formation of the bridged $N_2O_4^*$ excited intermediate, the existence of the bridged structure as a transient species in the gas phase is established, and the possibility of having it as the stable structure of N_2O_4 cannot be entirely excluded. Other exchange studies in the system $NO + NO_2 + {}^{18}O_2$ showed that any dissociative mechanism leading to rapid self exchange in NO_2 is implausible. The exchange rate constant is smaller than the second order recombination rate constant of NO_2 to form N_2O_4. The rate constant of the even faster nitrogen atom exchange reaction between ^{14}NO and $^{15}NO_2$ was found to be $(4.9 \pm 0.8) \times 10^7$ l mole^{-1} sec^{-1} at room temperature. Conditions were found under which the tubular flow reactor would operate properly. An innovation in the present design was the method used in maintaining a constant flow of the expensive labelled gas through the reactor. A mathematical analysis of the effects of diffusion was made and equations were developed to correct for back diffusion. (auth) (Diss. Abstr., Int., B)

8256 REACTIVE SCATTERING OF HYDROGEN AND DEUTERIUM ATOMS FROM HALOGEN MOLECULES. Grosser, J.; Haberland, H. (Univ., Freiburg i. B.). Chem. Phys. Lett.; 7: 442-4(15 Nov 1970).

Angular distributions for the reaction products from the reactions of H and D atoms with Cl_2 and Br_2 molecules are reported. Within experimental error the angular distributions do not vary on changing from H to D atoms. Most of the hydrogen halide molecules recoil backwards with respect to the incoming hydrogen beam. The peak of the angular distribution occurs at larger angles for chlorine than for bromine. The results are in agreement with trajectory calculations of Polanyi et al. (auth)

8257 ISOTOPIC EFFECT AND TEMPERATURE DEPENDENCE OF THE ESR SPECTRUM OF THE METHYL RADICAL. Riveros, Jose Manuel (Univ., Sao Paulo, Brazil). An. Acad. Brasil. Cienc.; 42: 181-4(Jun 1970).

The idea that a vibrational effect could be responsible for the temperature dependence and the isotope effect of the methyl radical is considered. The isotope effect is predicted to hold for all the temperatures calculated, although this effect tends to decrease slowly with temperature. The model yields a correct explanation for the isotope effect observed in the ESR spectra of methyl radicals. (M.C.G.)

8258 APPLICATION OF MICROWAVE SPECTROSCOPY TO THE SELF-EXCHANGE OF DEUTERIUM IN PROPYLENE-3-d_1 CATALYZED BY GROUP VIII METALS. Ueda, Tomiko; Hirota, Kozo (Inst. of Physical and Chemical Research, Yamato, Japan). J. Phys. Chem.; 74: 4216-21(26 Nov 1970).

The self-exchange of deuterium in propylene-3-d_1 was investigated on nickel, nickel–alumina, palladium, platinum, and rhodium catalysts in the absence of water, and on nickel in the presence of water. The reaction products, the isotopic isomers of mono- and dideuterated propylene, were determined quantitatively by the microwave spectroscopy. At the initial stage transfer of deuterium from the methyl to the methine position was much slower than that to the methylene position in all the catalysts, and both absolute rates decreased in the presence of water-on-nickel catalyst. From these results, it was concluded that the self-exchange occurs through the three adsorbed intermediates, π-allyl, n-propyl, and isopropyl adsorbed species. Isopropyl intermediate is more important than n-propyl intermediate in the self-exchange mechanism. (auth)

Physical Chemistry

Refer also to abstracts 8234, 8321, 10195, and 10294.

8259 (ANL-Trans-869) DETERMINATION OF THE BOILING POINT OF ASTATOBENZENE. Kuzin, V. I.; Nefedov, V. D.; Norseev, Yu. V.; Toropova, M. A.; Khalkin, V. A. Translated by Gerda Siegel (Argonne National Lab., Ill.), from Radiokhimiya; 12: 414(1970). 3p. Dep. NTIS.

A method based on a relation between the retention time of a substance on a chromatographic column and its boiling point was used for the measurement of the boiling point of astatobenzene. Starting with the dependence of the boiling point of various halogen derivatives of benzene on the logarithm of the retention time on the column, the boiling point of astatobenzene was found to be 222 ± 3°C at atmospheric pressure. (P.C.H.)

8260 (COO-1149-180) LOW TEMPERATURE CHEMICAL THERMODYNAMICS PROJECT. Technical Progress Report No. 18, November 1969–November 1970. Westrum, Edgar F. Jr. (Michigan Univ., Ann Arbor. Dept. of Chemistry). 1 Nov 1970. Contract AT(11-1)-1149. 31p. Dep. NTIS.

Studies on chemical thermodynamics and solid-state behavior of matter over the low-temperature region were continued. Studies on actinide compounds, lanthanide compounds, organic crystals, and selected inorganic compounds are briefly reported. (M.C.G.)

8261 (RISO-224) PROPERTIES OF HELIUM: DENSITY, SPECIFIC HEATS, VISCOSITY, AND THERMAL CONDUCTIVITY AT PRESSURES FROM 1 TO 100 bar AND FROM ROOM TEMPERATURE TO ABOUT 1800K. Petersen, Helge (Danish Atomic Energy Commission, Risoe. Research Establishment). Sep 1970. 42p. Dep. NTIS (U.S. Sales Only).

An estimation of the properties of helium was carried out on the basis of a literature survey. The ranges of pressure and temperature chosen are applicable to helium-cooled atomic reactor design. A brief outline of the theory for the properties is incorporated, and comparisons of the recommended data with the data calculated from intermolecular potential functions are presented. (31 references) (auth)

8262 (UCRL-50903) ANHARMONIC LATTICE DYNAMICAL PROPERTIES OF SOLID NEON, ARGON, KRYPTON, AND XENON. Jelinek, George E.; Karo, Arnold M. (California Univ., Livermore. Lawrence Radiation Lab.). 10 Jul 1970. 57p. Dep. NTIS.

The thermodynamic properties of solid neon, argon, krypton, and xenon are calculated. Using the Born and Huang method of homogeneous deformations, terms cubic and quartic have been included in the lattice Hamiltonian to yield the free energy to the second order in the strain. The static lattice contribution to the fourth order has also been included. The computations were performed for simple two-body central force potentials (containing no arbitrarily adjustable parameters) dynamically fitted to the sublimation energy at zero temperature and zero pressure and to the lattice constant. Although good agreement is obtained for the thermal properties of Ar, Kr, and Xe for temperatures up to 60% of the melting point, root-mean-square displacements greater than 4% of the nearest-neighbor distance at temperatures lower than 40% of the melting temperature represent the limit of applicability of the perturbation expansion. (auth)

8263 INFRARED SPECTRA AND MOLECULAR PROPERTIES OF TETRAHYDROBORATES OF METALS OF THE $M(BH_4)_4$ TYPE. Volkov, V. V.; Myakishev, K. G.; Grankina, Z. A. (Inst. of Inorganic Chemistry, Novosibirsk, USSR). Zh. Neorg. Khim.; 15: 2861-2(Oct 1970). (In Russian).

Infrared spectra of the valence oscillations of $NaBH_4$, $Zr(BH_4)_4$, $U(BH_4)_4$, and $Th(BH_4)_4$ were studied. A differential-thermographic method was used for determining phase transformations and temperatures of disintegration of uranium and thorium tetrahydroborates. Thermograms in the temperature range from –180 to 55°C for specimens of $U(BH_4)_4$ did not reveal any thermal effects. Thermograms for $Th(BH_4)_4$ in the temperature range from –180 to 250°C showed one exothermal effect at 158°C, which corresponds to the irreversible disintegration of the substance. Thus, it was confirmed that at the temperatures studied tetrahydroborates do not undergo phase transformations. (R.V.J.)

8264 EXPERIMENTAL STUDY OF THE LIQUID-VAPOR EQUILIBRIUM OF A URANIUM HEXAFLUORIDE–MOLYBDENUM HEXAFLUORIDE BINARY MIXTURE UNDER A PRESSURE OF 2,600 TORR. Reynes, Jean; Carles, Maurice; Aubert, Jacques (CEA, Saclay, France). J. Chim. Phys.; 67: 1526-9(Sep 1970). (In French).

The liquid–vapor equilibrium of a UF_6–MoF_6 mixture was studied under a constant pressure of 2,600 torr. The device used is made of monel. Homogeneity in both phases was obtained by stirring and bubbling in the solution. The composition of mixtures was determined by means of an infrared spectrophotometer. The analyzing cell, made of monel, is provided with two silver chloride windows. The two hexafluorides are completely miscible. The dew and boiling isobar values do not show any extremum. The solutions are almost ideal solutions and the calculated activity coefficients vary only very slightly from unity. (France)

8265 EXPERIMENTAL STUDY OF THE LIQUID-VAPOR EQUILIBRIUM OF A URANIUM HEXAFLUORIDE–TUNGSTEN HEXAFLUORIDE BINARY MIXTURE UNDER A PRESSURE OF 2,600 TORR. Reynes, Jean; Carles, Maurice; Aubert, Jacques (CEA, Saclay, France). J. Chim. Phys.; 67: 1530-3(Sep 1970). (In French).

The UF_6–WF_6 equilibrium was studied under a constant pressure of 2,600 torr. The device used is made of monel. The composition of liquid and gaseous phases was determined by using an infrared spectrophotometer; the analyzing cell is provided with two silver chloride windows. The two hexafluorides are completely miscible. The system does not show any azeotropic mixture and the deviation from Raoult's Law is a positive one. (auth) (France)

8266 GRAVIMETRIC ADSORPTION STUDIES OF THORIUM OXIDE. V. WATER ADSORPTION BETWEEN 25 AND 500°. Grammage, R. B.; Fuller, E. L. Jr.; Holmes, H. F. (Oak Ridge National Lab., Tenn.). J. Phys. Chem.; 74: 4276-80(26 Nov 1970).

Reversible and irreversible adsorptions of water vapor on thorium oxide surfaces were studied gravimetrically between 25 and 500°C. On an oxide with fine pores the water that became irreversibly bound between these two temperatures was equivalent in weight to 40 hydroxyls/100 Å^2, an amount far in excess of the 12.8 hydroxyls/100 Å^2 required to completely hydroxylate the 100 face. The excess is attributed to molecular water strongly associated with the surface hydroxyls. Between 300 and 500°C the irreversible adsorption involves only surface hydroxyls (mass equivalent) and poses no kinetic barrier to obtaining equilibrium isotherms. The irreversible binding of molecular water below 300°C is so kinetically complicated and slow that there is considerable difficulty in establishing the equilibrium isotherms. Measurements were also made on a nonporous sample of thorium oxide. The irreversible adsorption of 36 hydroxyls/100 Å^2 (mass equivalent) is close to that observed with the porous sample. The capacity of the open surface for reversible adsorption is considerably lower than that of the finely porous oxide, so much so that above 350°C it was

XUM

not detectable. Reversible adsorption on the porous oxide could be measured at temperature up to, and including, 500°C. (auth)

8267 POSSIBILITY OF LUMINESCENCE OF U^{4+}_{aq} ION. Baran, Václav; Tympl, Milan. Z. Anorg. Allg. Chem.; 375: 103-6 (Jul 1970).

Uranium(IV) solutions are violet in color under certain conditions. Direct experiments excluded the possibility that its origin is luminescence of U^{4+}_{aq} ions. The unusual color behavior of the systems follows most likely from peculiarities of color perception of the human eye, in combination with specific properties of the U^{4+}_{aq} ion absorption spectrum. (auth)

8268 CONFORMATION OF RADIOPROTECTANT COMPOUNDS. CRYSTAL STRUCTURES OF 2-MERCAPTOETHYLAMINE HYDROCHLORIDE AND 3-MERCAPTOPROPYLAMINE HYDROCHLORIDE. Jandacek, R. J.; Swartz, H. M. (Walter Reed Army Inst. of Research, Washington, D. C.). Radiat. Res.; 44: 523-30(Nov 1970).

The crystal structures of 2-mercaptoethylamine hydrochloride and 3-mercaptopropylamine hydrochloride were determined in a study of the conformation of radioprotectant compounds. 2-Mercaptoethylamine is in a gauche conformation in the hydrochloride crystal and sulfur–nitrogen interaction is present, but the conformation of 3-mercaptopropylamine in the hydrochloride crystal shows no sulfur–nitrogen interaction. (auth)

Radiation and Nuclear Chemistry

Radiation Effects

8269 POSITRON ANNIHILATION IN IRRADIATED ACETYL METHIONINE. Hadley, J. H. Jr.; Hsu, F. H. (Georgia State Univ., Atlanta). Chem. Phys. Lett.; 7: 465-8(15 Nov 1970).

The effects of x radiation on positron annihilation in acetylmethionine were measured. Correlation of the results with ESR data indicates that the intensity of the τ_2 component depends on the type of free radicals present. (auth)

8270 INFLUENCE OF IONIZING RADIATION ON THE STRUCTURE AND PROPERTIES OF MODIFIED KAPRON FIBERS. Spitzyn, V. I.; Goryaev, V. M.; Plavnik, G. M. (and others); (Inst. of Chemical Physics, Moscow. Scientific-Research Inst. of The Tire Industry, Moscow). Khim. Vys. Energ.; 4: 372-3(Jul-Aug 1970). (In Russian).

The effects of 1-MeV electrons on the structure and mechanical properties of Kapron fibers modified by radioinduced grafting of vinyl monomers or by introducing various aromatic additions (α-naphthol, pyrogallol, and phenothiazine) were analyzed. The strength of the fibers was most sensitive to radiation effect. The strength of the fiber decreased about 40% during irradiation at 10 to 15 Mrad. Modification of the surface by graft polymerization of vinyl monomers or introduction of aromatic compounds increased the radiation resistance of the fiber but reduced the structural sensitivity of the fibers to ionizing radiation. (R.V.J.)

8271 RADIATION-INITIATED HOMOGENEOUS GRAFTING OF STYRENE TO BENZYLCELLULOSE. Betty, Robert Warren. Toronto; Univ. of Toronto (1968).

Thesis.

Graft copolymers of benzyl cellulose and styrene were prepared by direct irradiation of benzyl cellulose–styrene solutions with ^{60}Co γ radiation. The solutions remained homogeneous throughout the grafting procedure and the formation of graft copolymer was dose dependent up to 4.0 MR. The existence of a true graft copolymer was proven by the solubility behavior, intrinsic viscosity, number average molecular weight, and density gradient sedimentation of the products of the grafting procedure. The graft copolymer consisted of both branched and linear structures and supported one grafted polystyrene chain for every 140 to 1020 benzylated anhydroglucose units. The average molecular weight and molecular weight distribution of the grafted polystyrene side chains was the same as those of the homopolymer formed simultaneously during the grafting procedure. Column elution fractionation of the gross products of the grafting procedure failed to isolate the benzyl cellulose–styrene copolymer, which was eluted with ungrafted benzyl cellulose. (Diss. Abstr. Int., B)

8272 NATURE OF BLEACHED COLOR CENTERS IN IRRADIATED ALKALINE ICE. Nazhat, N. B.; Weiss, J. J. (Univ. of Newcastle upon Tyne, Eng.). J. Phys. Chem.; 74: 4298-9(26 Nov 1970).

Gamma irradiation of 1M alkaline ices (NaOH, KOH, and CsOH) leads to formation of color centers that can be bleached by visible light. ESR studies on the bleached color centers showed that the spectra were different from those of the trapped electron before bleaching. Interactions of the electron in the ice matrix are discussed. (D.P.O.)

8273 INTERPRETATION OF THE OPTICAL DENSITY-DOSE RELATIONSHIP IN IRRADIATED CLEAR POLYMETHYL METHACRYLATE. Chadwick, K. H. (Inst. for Application of Atomic Science in Agriculture, Wageningen, Netherlands). Radiat. Res.; 44: 282-95(Nov 1970).

A model was proposed describing the radiation-induced processes that lead to the change in optical density in clear poly(methyl methacrylate). The two part model was used to analyze the measured optical density-dose relationship. The major part of the optical density change was ascribed to a radical production and annihilation process, and the coefficient for radical annihilation deduced in the analysis was compared with values in the literature for other organic materials. The minor, but more stable, part of the optical density change was ascribed to a dissociation type of process. (auth)

8274 RADIOLUMINESCENCE OF ORGANIC SUBSTANCES. VIII. THE DEPENDENCE OF THE EFFECTIVENESS OF EXCITATION OF ALCOHOL SOLUTIONS BY α- AND β-PARTICLES ON THE MOLECULAR WEIGHT OF THE LUMINESCING ADDITIVE. Spurny, F.; Kilin, S. F.; Rozman, L. M. Opt. Spectrosc. (USSR) (Engl. Transl.);28: 506-9(May 1970).

Translated from Opt. Spektrosk.; 28: 934-40(May 1970).

The radio- and photoluminescence of solutions of p-xylene, anisole, β-naphthol, biphenyl, phenylindole, diphenyloxadiazole, and triphenyloxazole in methyl and butyl alcohols were investigated. The absolute values of the yields of the additive in the first singlet ("fluorescent") state–$g(S_1)$ were obtained under α and β excitation. It was shown that the duration of the luminescence under β excitation was less than the duration of the fluorescence of the additive. (auth)

8275 EFFECT OF γ IRRADIATION ON DIELECTRIC CONSTANTS OF KH_2PO_4. Tokumaru, Yukuya; Abe, Ryuji (Nagoya Univ., Japan). Jap. J. Appl. Phys.; 9: 1548-9(Dec 1970).

The effects of γ radiation on the dielectric constant of KH_2PO_4 monocrystals at 70 to 150°K were investigated. Both the real and imaginary parts of the complex dielectric constant decreased with increasing dosage, until they nearly saturated at about 3×10^5 rad. Recovery was observed on heating to about 175°K. (M.C.G.)

Radiation Processes

Refer also to abstract 9552.

8276 (JAERI-Memo–4147) STUDY ON THE RADIATION-INDUCED CHAIN CROSSLINKING AND CROSSLINKING POLYMERIZATION. Kagiya, Tsutomu; Mitsui, Hiroshi; Hagiwara, Miyuki; Hosoi, Fumio; Yamaji, Katsuhiro (Japan Atomic Energy Research Inst., Tokyo). Sep 1970. 118p. (In Japanese). Dep. NTIS (U. S. Sales Only).

In the basic studies on the γ-induced polymerization of ethylene, it was found that the crosslinking of polyethylene is accelerated by acetylene. On the basis of this result, the effects of acetylene on the γ-induced crosslinking of polyethylene were investigated from the viewpoint of the changes in the solubility and structure of polymer, and of the amount of hydrogen formation. As a result, a chain mechanism of radiation-induced crosslinking of polyethylene was proposed. From the results of studies on energetics of this mechanism, the γ-induced chain crosslinking of polyethylene was studied in the presence of the gaseous mixtures of monomers containing fluorine and acetylene. In addition, the results applied the mechanism to the chain crosslinking polymerization of methyl methacrylate are also reported. (auth) (Japan)

8277 (NSJ-tr–160) ESR STUDY OF RADIATION-INDUCED GRAFT-POLYMERIZATION OF METHYL METHACRYLATE ON FLAKY GLASS. Kanazawa, Yoshiko; Higashide, Fukuji, Translated from Kobunshi Kagaku; 26: 582-6(Aug 1969). 9p. Dep. NTIS (U. S. Sales Only).

The mechanism of graft-polymerization of methyl methacrylate (MMA) on γ-irradiated flaky aluminosilicate glass and the effect of the radiation-induced defect in the glass on the graft polymerization using the preirradiation method was studied. The characteristic six line ESR signal due to the radiation-induced defect in the glass disappeared when MMA monomer was added at room temperature to the irradiated glass which was previously treated with $K_2Cr_2O_7$–H_2SO_4 solution. After a few hours a different signal composed of nine hyperfine components with a separation of 11.5 gauss began to appear, which is attributed to the growing radical of PMMA, $R\text{-}CH_2\text{-}C(CH_3)(COOCH_3)$. The intensity of the nine line signal was observed to increase with time and reached to a maximum after 50 to 60 hours. The polymer radical was

very stable and has survived keeping its maximum concentration even after five months or longer. The presence of graft polymer was confirmed by the ir spectrum. (auth)

8278 PROCESS FOR PREPARING POLYMERIZED AMINOPLAST SURFACE COATINGS USING IONIZING RADIATION. Ravve, Abraham (to Continental Can Co., Inc.). U. S. Patent 3,535,148. 20 Oct 1970. Filed 7 Aug 1968.

A process for coating an article comprises applying to the surface of the article to be coated a thin film of a polymerizable etherified aminoplast prepared by the reaction of a monohydric alcohol with a condensate of an ethylenically unsaturated amide, a polyfunctional amine, and an aldehyde, such as formaldehyde, and exposing the film-containing surface to a source of ionizing radiation for a time sufficient to effect polymerization of the aminoplast film. (Offic. Gaz.)

8279 RADIATION-THERMAL ISOMERIZATION OF ALKYL BROMIDES. Pozdeev, V. V.; Fomina, N. V.; Kocheshkov, K. A. (Inst. of Physical Chemistry, Moscow). Khim. Vys. Energ.; 4: 379-80(Jul-Aug 1970). (In Russian).

The effects of radiation and temperature on isomerization of alkyl halides were studied using specimens of n-alkyl bromide irradiated for 24 hr with doses of 125 rad/sec of ^{60}Co γ rays at 150 to 240°C. Tabulated data showed that the radiothermal isomerization of butyl bromide into sec-butyl bromide begins at 150°C without any interference from side reactions. Experiments confirmed the efficiency of the radiothermal method for production of sec-butyl bromide from n-alkyl bromides. (R.V.J.)

8280 RADIATION-INDUCED BINDING OF PHENYLALANINE AND OH SUBSTITUTED DERIVATIVES. Okuda, Atsuyuki; Yamamoto, Osamu (Hiroshima Univ.). Proc. Res. Inst. Nucl. Med. Biol; No. 11, 35-41(1970). (In Japanese).

Radioinduced binding of phenylalanine and its derivatives substituted with OH group(s) was studied. Acid, neutral, and alkaline solutions of phenylalanine, tyrosine, and dihydroxyphenylalanine mixed with serum albumin were irradiated with ^{60}Co gamma rays. The binding yield was measured by determining the radioactivity of ^{14}C-amino acid bound with serum albumin. No marked difference in radioinduced binding among three kinds of amino acids was observed in neutral solution. However, there was no difference for dihydroxyphenylalanine, some difference for tyrosine, and a remarkable difference for phenylalanine in the binding in acid solution compared to that in neutral solution. Comparison in alkaline solution could not be made because dihydroxyphenylalanine was very unstable. On the other hand, the binding yields of each solution were compared under various atmospheres. In the presence of O_2, the binding yield markedly decreased for all amino acids in acid and neutral solutions. In neutral solution, the yield was decreased by the presence of MeOH and KCNS, which are reagents scavenging the OH free radical, but it was increased by the presence of N_2O, which is a reagent scavenging e^-_{aq}. The greater the number of OH substituents, the smaller was the decrease caused by MeOH and KCNS and the increase by N_2O. The effects of MeOH, KCNS, and N_2O suggest that the OH free radical plays an important role in binding. Disappearance of hydrogen atom on the ring of phenylalanine was also confirmed. These facts suggest radical formation by the abstraction of hydrogen atom from the aromatic ring by the OH free radical. (auth)

8281 ROLE OF CHARGED PARTICLES AND EXCITED MOLECULES DURING RADIATION OXIDATION OF n-HEPTANE BY MOLECULAR OXYGEN. Muratbekov, M. B.; Saraeva, V. V. (Moscow State Univ.). Khim. Vys. Energ.; 4: 365-7(Jul-Aug 1970). (In Russian).

In order to determine the mechanism of radioinduced oxidation at low temperatures, studies were made of the effects of nitrous oxide and oxygen at various concentrations on the yield of the γ radiolysis products of heptane at 0°C and doses of 1.2×10^{16} eV/ml. sec. Data obtained revealed that oxygen in the heptane–N_2O (0.3M)–O_2(0.02M) mixture did not inhibit heptyl radical formation processes. With an increase in oxygen concentration from 0.002 to 0.22M, the yield of heptyl radicals diminished, which confirms oxygen participation in reactions with electrons. Radiation yields of hydrogen in heptane–N_2O(0.3M)–O_2(0.02M) and heptane–N_2O (0.3M) equal 2.3 ± 0.2 and 2.6 ± 0.2, respectively. Thus, oxygen inhibits hydrogen yields by interacting only with the secondary excited molecules. A new active particle, which is capable of destroying N_2O, appears. In the absence of N_2O a new active particle forms one heptyl radical. (R.V.J.)

8282 POWDER POLYETHYLENE ADSORBENT. (to Japan Atomic Energy Research Inst.). British Patent 1,213,873. 25 Nov 1970. Priority date 2 Mar 1967, Japan.

Polyethylene powder having a specific surface area of not less than 22 m^2/g for adsorbing vapors of organic solvent and volatile radioactive substances can be modified by radioinduced crosslinking, by graft polymerization of an olefinically unsaturated compound onto it, or by coating the surface of the particles with a polymer material. The modified powder polyethylene is packed in a column through which the vapors to be adsorbed are passed. (B.L.M.)

8283 STUDY OF THE PROPERTIES OF THE GELS PRODUCED BY RETICULATION OF DILUTE AQUEOUS SOLUTIONS OF POLY(ETHYLENE OXIDE) IN A ^{60}Co GAMMA RADIATION FIELD. Van Brederode, Robert Adrian. Ithaca, N. Y.; Cornell Univ. (1969). 86p. University Microfilms Order No. 70-5812. Thesis.

Dilute aqueous gels of poly(ethylene oxide), PEO, were prepared by γ irradiation of a degassed solution of PEO samples, which ranged in molecular weight from 3×10^5 to 4×10^6. By means of a torsion pendulum designed for the measurement of the storage and loss moduli of weak gels, the formation of a gel may be studied by following its mechanical properties. The dose to gel PEO increases with polymer concentration indicating that the mechanism of radical formation on the polymer is indirect; however, the % of crosslinks induced indirectly decreases from 30% at 0.5 wt % PEO to 18% at 1.0 wt. %. The dose to gel is defined from the experimental curves of gel modulus versus dose received where the modulus for incipient gelation can be calculated theoretically. Beyond the gel dose, the storage modulus rises as the gel tightens and attains a plateau where the number of crosslinks remains constant. This plateau modulus is found to depend on the concentration of polymer raised to the 2.25 power and on the initial molecular weight of the polymer raised to the 0.3 power. It is not found to vary with initial molecular weight distribution nor with the dose rate, but it decreases with an increase in the irradiation temperature and with increased oxygen presence in the cover gas. The storage modulus, in addition to indicating the number of crosslinks produced by the radiation, also, includes an effect of hydrophobic bonding. The result is that the modulus rises faster with temperature than would be expected from the kinetic equation of rubber elasticity. The number of crosslinks added per 100 eV, "G," is about the same below and above the dose to gel and is calculated to be 1.4 below the gel point based on the energy absorbed both directly and indirectly by the polymer. The log decrement, λ, decreases rapidly with dose beyond the dose to gel and reaches an asymptotic value of 0.02 to 0.05. Higher initial molecular weight polymer reaches lower values of the asymptote for a given concentration while at a given molecular weight. As the concentration is increased, the log decrement levels off at a lower value. The log decrement is found to increase when the gel is irradiated at elevated temperatures, but there is no observable effect of oxygen concentration or the dose rate on the value that λ reaches. (Diss. Abstr. Int., B)

Radiolysis

8284 (ANL-Trans-870) THE REACTION WITH BENZENE OF ^{125}I AND ^{211}At FORMED FROM THE NOBLE GASES DURING K-CAPTURE. Nefedov, V. D.; Toropova, M. A.; Khalkin, V. A.; Norseev, Yu. V.; Kuzin, V. I. Translated by Gerda Siegel (Argonne National Lab., Ill.), from Radiokhimiya; 12: 194-5(1970). 4p. Dep. NTIS.

An abstract of this paper, prepared from the original language, appeared as NSA 24: 38946.

8285 (RPI-3821-5) STUDY OF THE PULSE RADIOLYSIS OF GASES. Annual Technical Progress Report. Harteck, P.; Dondes, S. (Rensselaer Polytechnic Inst., Troy, N. Y.). Nov 1970. Contract AT(30-1)-3821. 26p. Dep. NTIS.

Primary emphasis in the past year was on modification of the pulsed source of radiation and in the detection system. Initial experimentation was begun on techniques for design of experiments on studies for pulse radiolysis systems. (M.C.G.)

8286 FORMATION AND KINETICS OF ACCUMULATION OF NO_2 RADICALS IN γ-IRRADIATED BARIUM SULFATE CONTAINING NITRITE ION IMPURITIES. Spitsyn, Vikt. I.; Ershov, B. G.; Barsova, L. I.; Popova, G. Yu. (Inst. of Physical Chemistry, Moscow). Izv. Akad. Nauk SSSR, Ser. Khim.; No. 8, 1691-7(Aug 1970). (In Russian).

On irradiation of polycrystalline $BaSO_4$ with occluded nitrite ions, NO_2^- radicals were formed along with SO_4^- and SO_3^-. The kinetics of accumulation of NO_2 radicals in relation to the concentration of nitrite ions was investigated. A mechanism for formation of paramagnetic centers, considering the transfer of radiation energy in barium sulfate crystals, is proposed. (tr-auth)

8287 KINETICS OF THERMAL AND PHOTOSTIMULATED EXTINCTIONS OF TRAPPED ELECTRON IN γ-IRRADIATED

VITREOUS ALKALINE ICE. Makarov, I. E.; Ershov, B. G.; Pikaev, A. K. (Inst. of Physical Chemistry, Moscow). Izv. Akad. Nauk SSSR, Ser. Khim.; No. 8, 1697-1702(Aug 1970). (In Russian).

The kinetics of thermal and photostimulated extinction of trapped electrons and O^- ions in γ-irradiated vitreous alkaline ice at 77°K was studied. Thermal extinction occurs by second-order reactions and photostimulated disappearances are first order. Rate constants were measured. (M.C.G.)

8288 SPATIAL DISTRIBUTION OF RADICAL DURING γ IRRADIATION OF METHANOL AT 77°K. Raitsimring, A. M.; Pomytkin, A. P.; Tsvetkov, Yu. D. (Inst. of Chemical Kinetics and Combustion, Novosibirsk, USSR). Khim. Vys. Energ.; 4: 369-70(Jul-Aug 1970). (In Russian).

Spatial distribution of radical products from the radiolysis of methanol in the solid state was studied. Electron spin echo and EPR methods were used in studies of vitreous specimens of methanol irradiated with γ rays at 0.02 to 1.5 Mrad doses at 77°K. Graphical data are given on the rate of relaxation as a function of time of γ irradiation, before and after irradiation by uv radiation, and as a function of the mean concentration before the irradiation. (R.V.J.)

8289 STUDY OF THE PRODUCTS OF ANTHRACENE TRANSFORMATION UNDER (n,γ) IRRADIATION. Zedelashvili, E. N.; Shanshiashvili, M. I. (Inst. of Physical and Organic Chemistry, Tbilisi, USSR). Soobshch. Akad. Nauk Gruz. SSR; 59: 577-80 (Sep 1970). (In Russian).

With a view to establishing the chemical nature of the final products of radiolysis, the (n,γ) radiation-chemical transformation of crystalline anthracene (in the presence of oxygen) was investigated. The data indicate that during the radiation-chemical transformation of anthracene, formation of anthraquinone is the main process. At the same time, a mechanism resembling that of the radiation-chemical transformation of naphthalene is observable in anthracene. It consists of opening the aromatic ring. (auth)

8290 MASS-SPECTROMETRIC INVESTIGATION OF LOW-TEMPERATURE RADIOLYSIS OF ORGANIC SULFIDES. Dapkviashvili, A. G.; Panchvidze, M. V.; Khidesheli, G. I.; Nanobashvili, H. M. (Inst. of Inorganic Chemistry and Electrochemistry, Tbilisi, USSR). Soobshch. Akad. Nauk Gruz. SSR; 59: 851-84(Sep 1970). (In Russian).

Low-temperature radiolysis of aliphatic sulfides was studied by mass spectrometry. The molecular hydrogen yield from radiolysis was determined. Values of yields increased with increasing the molecular weight of sulfides. Correlation between the yields of radicals and molecular hydrogen is shown. $G(H_2) \simeq \frac{1}{2} G_R$ for all sulfides. (auth)

8291 SALT EFFECTS DURING PULSE RADIOLYSIS OF NEUTRAL WATER AND ALKALI SOLUTIONS. Brusentseva, S. A. (Inst. of Electrochemistry, Moscow). Khim. Vys. Energ.; 4: 377-8(Jul-Aug 1970). (In Russian).

The influence of the ionic force, μ, on the absolute magnitude of the rate constant k_0 of hydrated electron disappearance in water at various pH values was studied with doses of 2 to 3 × 10^{17} eV/cm^3 and pH values from 7.0 to 12.7 in hydrogen-saturated solutions. Tabulated data showed that the effective charges of the reacting particle for pH values of 12.7, 12.0, and 11.4 were 0.85, 0.65, and 0.60, respectively, which confirmed that the disappearance of optical absorption was the result of the interaction of two negatively charged particles compounded by complex side processes. (R.V.J.)

8292 PROCESS FOR ACCUMULATING THERMAL ENERGY OR ENERGY PRODUCED BY A RADIOACTIVE RADIATION OR BY THE ACTION OF NEUTRONS. (to Kernforschunganlage, Julich GmbH). French Patent 1,572,234. 19 May 1969. Priority date 17 Feb 1967, Germany. (In French).

A method is described for accumulating thermal energy, energy produced by a radioactive radiation, or by neutrons—especially the energy produced by a nuclear reactor. The procedure consists of transmitting to a decomposable substance, such as ethane or propane, under the action of these types of energy the quantity of energy accumulated, which is necessary for eventual decomposition in the presence of a known catalyst to assist the decomposition. After this the constituents obtained are stored and/or after lowering the temperature, they are transported in a mixture, eventually with the addition of other substances, to the apparatus used or they are recombined in the presence of a catalyzer. (P.C.H.)

8293 NOTES ON THE PROPERTIES OF INTERMEDIATE PARTICLES DURING RADIOLYSIS OF AQUEOUS OXYGEN SOLUTIONS. Byakov, V. M.; Kalyazin, E. P. (Inst. of Theoretical and Experimental Physics, Moscow. Moscow State Univ.). Khim. Vys. Energ.; 4: 373-4(Jul-Aug 1970). (In Russian).

It was previously found that the recombination diffusion model of radiolysis is capable of describing the yield from radiolysis of water as a function of the concentration of dissolved substances. Studies were made of the hypothesis stating that the initially produced excited $H_2O^*_{aq}$ molecules, formed on the ionizing particle track are electrically neutral excited states of H_2O, participate in the acid-basic reaction with surrounding water molecules described by $H_2O^* + H_2O \rightleftharpoons H_3O^+ - OH^-_{aq}{}^*$. (R.V.J.).

8294 ION-MOLECULE REACTIONS IN GASEOUS HYDROCARBON-SILANE MIXTURES. Beggs, David Phillip. University Park, Pa.; Pennsylvania State Univ. (1969). 133p. University Microfilms Order No. 70-13,798.

Thesis.

To gain a better understanding of the reactions occurring in the radiolysis of gaseous hydrocarbon-silane systems, the ionic reactions taking place in mixtures of silane with four representative hydrocarbons were studied in a mass spectrometer source. The cross-reactions (reaction between ions of one compound and the molecules of the other compound) and their rates of reaction were determined. Observance of these reactions in a mass spectrometer source at pressures of 10^{-2} torr enabled the establishment of upper limits to the standard heats of formation of the products. In mixtures of acetylene and silane, $C_2H_2^+$ and SiH_3^+ were the only ions observed to undergo cross-reactions. The silylene ion reacted with acetylene to produce the condensation type products $SiCH_3^+$ and $SiC_2H_3^+$. The acetylene ion reacted with silane to produce a H_2^- transfer reaction as well as condensation type products such as $SiCH_3^+$ and $SiC_2H_X^+$ where x may be 1 to 5. The principal reactions are the H_2^- transfer reaction and the formation of $SiCH_3^+$ from the SiH_3^+ precursor. Studies of ethylene-silane mixtures showed this system to undergo reactions similar to those in acetylene-silane mixtures. $C_2H_3^+$, $C_2H_5^+$, and SiH_3^+ participated in cross-reactions to produce condensation type products, and silane transferred a H_2^- to both $C_2H_3^+$ and $C_2H_5^+$ to produce SiH_5^+. An analysis of deuterated sample mixtures demonstrated that the reactions in both the acetylene-silane and ethylene-silane mixtures proceeded mainly via an intimate long-lived intermediate complex. This complex is suggested to be of a cyclic nature with sufficient vibrational energy to equalize the probability of an H-loss. Three reactant ions were found in mixtures of methane and silane, SiH_3^+, CH_3^+ and CH_5^+. The methyl and silylene ions, by reacting with silane and methane respectively, formed condensation type product ions of the form $SiCH_3^+$, analogous to their counterparts in pure methane. While CH_5^+ reacted with silane to form condensation-type product ions, it also participated in a tertiary reaction producing SiH_5^+. Besides establishing the stability of SiH_5^+, its observance also enabled an upper limit to the proton affinity of silane to be defined. Analyses of deuterated sample mixtures showed that the intermediate complex prefers a Si-H bond fracture to a C-H fracture indicating lower relative bond dissociation energies of Si-H bonds. Only condensation type cross-reactions were observed in benzene-silane mixtures and the products observed (SiC_6H_x, x = 5 to 9) were all attributed to the ionic precursor $(C_6H_6)^+$. Deuterated sample mixtures indicated a greater probability for an H-loss from the silicon rather than from the aromatic ring, demonstrating Si is not assimilated into the ring as is C under similar circumstances. In nonaromatic mixtures, it was found that the ionic reactants participating in cross-reaction could be predicted from their analogous behavior in pure systems. The observance of fast H_2^- transfer reactions and the formation of some condensation-type products was found to be helpful in explaining the effects of the addition of C_2H_4 or C_2H_2 to the radiolysis of monosilane. (Diss. Abstr. Int., B)

8295 CONFIRMATION OF THE PRESENCE OF MONOMOLECULAR REACTIONS DURING THE RADIOLYSIS OF AQUEOUS OXYGEN SOLUTIONS. Kabakchi, S. A.; Shubin, V. N. (Inst. of Electrochemistry, Moscow). Khim. Vys. Energ.; 4: 375(Jul-Aug 1970). (In Russian).

A previous analysis of the steady concentrations of hydrogen peroxide, hydrogen, and oxygen as functions of the dose in the γ radiolysis of aqueous solutions of oxygen suggested that the value of the steady concentrations conformed with the $I^{1/2}$ law in the dose range 1 × 10^{15} to 6.3 × 10^{16} eV/ml./sec and oxygen concentrations of 1.5 × 10^{-5} to 1.3 × 10^{-3}M. Measuring the hydrogen peroxide concentrations in the dose range from 2.7 × 10^{14} to 6.3 × 10^{16} eV/ml./sec confirmed the hypothesis on the monomolecular processes in the radiolysis of aqueous O_2 solutions. (R.V.J.)

8296 INFLUENCE OF RADIATION DOSE AND METHOD OF SPECIMEN PREPARATION ON THE KINETICS OF RADICAL ACCUMULATION IN ANILINE. Tolkachev, V. A.; Sokolov, I. B. (Inst. of Chemical Kinetics and Combustion, Novosibirsk, USSR). Khim. Vys. Energ.; 4: 367-8(Jul-Aug 1970). (In Russian).

Experiments with purified specimens of aniline irradiated in ampules with a ^{60}Co γ source at 77°K (at doses of 0.05 Mrad/min) and in an electron accelerator at 83 and 120°K (with a pulse dose of 2×10^4 Mrad/min) and electron energy ~3 MeV showed that the accumulation of free radicals during γ irradiation was identical in specimens prepared two different ways. In the case of electron irradiation in the presence of air, the yield of radicals was higher than in the case of γ irradiation. Changes in the temperature range from 77°K to 120°K at doses exceeding 70 Mrad resulted in changes in the processes determining destruction of radicals. Absolute values of yields of radiolytic radicals were 0.05 for the first specimen and 0.1 for the second. (R.V.J.)

8297 DETERMINATION OF RADIATION YIELD OF NITRITE IONS DURING IRRADIATION OF SODIUM NITRATE SOLUTIONS WITH SMALL DOSES. Podzorova, E. A.; Orekhov, V. D.; Vereshchinskii, I. V.; Kabakchi, A. M. (Inst. of Physical Chemistry, Moscow). Khim. Vys. Energ.; 4: 370-2(Jul-Aug 1970). (In Russian).

The yield of nitrite ions during radiolysis at doses below 1×10^{17} eV/ml was studied using an improved colorimetric method based on the extraction of an azo dye that did not mix with the aqueous phase. The specimens were irradiated with ^{60}Co γ rays at doses of 8×10^{12} and 3×10^{14} eV/ml/sec. The efficiency of the extraction method for determining the concentration of nitrite ions in the radiolysis of acid nitrate solutions was confirmed. (R.V.J.)

8298 EFFECT OF CHARGED GROUPS ON THE INDIRECT ACTION IN FROZEN AQUEOUS SOLUTIONS. Sanner, Tore (Norsk Hydro's Inst. for Cancer Research, Oslo). Radiat. Res.; 44: 313-22(Nov 1970).

Electron spin resonance studies have been carried out on frozen aqueous suspensions of different derivatives of crosslinked dextran (Sephadex, Carboxymethyl-Sephadex, and Diethylaminoethyl-Sephadex). The samples were irradiated in vacuum at 77°K with x rays to a dose of 0.5 Mrad and the measurements were carried out at 77°K immediately after irradiation and after subsequent heat treatments. The total number of radicals stabilized in the suspensions after irradiation at 77°K was significantly higher than expected on the basis of the yields for the components. The qualitative spectra indicated that the "excess radicals" stabilized in the suspensions were mainly solute radicals. The results obtained upon heat treatment of the samples indicated that the water radicals stabilized at 77°K reacted only to a very small extent with the solute molecules. The number of "excess radicals" formed was found to depend on the electric charge of the macromolecules. Thus, many more radicals were stabilized in suspensions of the positively charged DEAE-Sephadex than in those containing negatively charged CM-Sephadex, uncharged DEAE-Sephadex, or ordinary Sephadex. The data indicate that the high yield of solute radicals observed in frozen suspensions is caused primarily by interaction of water radicals formed in the bound water with the solute. The possibility is considered that "excited water" may also contribute to the formation of solute radicals. (auth)

8299 RADIATION CHEMISTRY OF PHOSPHINE–AMMONIA MIXTURES IN GAS PHASE. Buchanan, James W.; Hanrahan, Robert J. (Univ. of Florida, Gainesville). Radiat. Res.; 44: 296-304(Nov 1970). (ORO–3106-27). Contract AT(40-1)-3106.

Irradiation of gaseous mixtures of ammonia and phosphine with ^{60}Co gamma rays yields hydrogen, red phosphorus, and nitrogen. Attempts to find other products have been unsuccessful. Hydrogen yields are larger than predicted from the assumption of an "ideal" mixture, in which the ammonia and phosphine decompose proportionately to the dose each absorbs, but nitrogen yields show a striking depression. This occurs even in mixtures with less than 0.1 mole percent phosphine. Phosphine appears to be acting as an efficient radical scavenger, via reactions such as $NH_2\cdot + PH_3 \rightarrow NH_3 + PH_2\cdot$ and $H\cdot + PH_3 \rightarrow H_2PH_2\cdot$. The phosphino radical reacts further to yield (finally) phosphorus and hydrogen. By comparing the radiolytic decomposition of ammonia in a mixture containing a few mole percent phosphine and in the pure state, it can be shown that roughly one phosphine is removed for each ammonia that is prevented from decomposing in the mixture. This "protective" effect occurs at least partly via radical scavenging reactions. (auth)

8300 RADIATION CHEMISTRY OF ALCOHOLS. XV. γ RADIOLYSIS OF ETHYLENE GLYCOL IN AQUEOUS SOLUTIONS. von Sonntag, C.; Thoms, E. (Kernforschungszentrum, Karlsruhe, Ger.). Z. Naturforsch.; 25b: 1405-7(Dec 1970). (In German).

In the γ-radiolysis of aqueous N_2O-saturated solutions of ethylene glycol (0.1 M) the following products (G-values at 20°C) were found: succinaldehyde (1.73), glycolaldehyde (1.05), acetaldehyde (1.2), 3,4-dihydroxybutanal (0.22), and erythritol (0.15). Radicals from water radiolysis (H· and ·OH) attack ethylene glycol and yield $\cdot CHOH-CH_2OH$ radicals. These radicals readily split off water yielding $\cdot CH_2-CHO$ radicals. All products can be explained by disproportionation or dimerization of these two radicals. Material balance of products formed with respect to the primary yields ·H and ·OH radicals from water radiolysis was obtained. In contrast to the yields of the other products the acetaldehyde yield depends strongly on ethylene glycol concentration and temperature. (auth)

8301 RADIOLYSIS OF 1 M AQUEOUS ETHANOL SOLUTIONS OF POTASSIUM NITRATE. Baquey, Ch.; Roux, J. C.; Sutton, J. (Centre d'Etudes Nucleaires de Bordeaux-Gradignan, Le-Haut-Vigneau, France). J. Phys. Chem.; 74: 4210-16(26 Nov 1970).

Deaerated solutions containing 1 M ethanol and different concentrations of nitrate ion have been irradiated with ^{60}Co γ radiation and the following products analyzed: hydrogen, nitrite ion, acetaldehyde, 2,3-butanediol, hydrogen peroxide, methane, ethane, and ethylene. The formation of an apparently "molecular" yield of acetaldehyde with $G = 1.3 \pm 0.15$ has been demonstrated and its origin explained in terms of the capture of radical pairs close to their site of production. The nitrite yields in the range $[NO_3^-] = 10^{-3}$ to 5×10^{-3} M lead to a value for the free ion solvated electron yield $G^{-}_{e_{s(f.i.)}} = 2.55 \pm 0.10$ and the data at high nitrate concentrations indicate that in 1 M aqueous ethanol G(total ionization) ≥ 4.15 and $G(-H_2O) = 4.6 \pm 0.4$. (auth)

8302 RADIOLYSIS REACTIONS OF COLLOIDAL SILVER AND SILVER BROMIDE. Johnston, F. J.; Mehrotra, K. N.; Huh, Yeon (Univ. of Georgia, Athens). Radiat. Res.; 44: 323-37(Nov 1970).

Colloidal silver is produced when aqueous silver solutions containing gelatine absorb ionizing radiation. The reduction is accelerated in the presence of organic solutes. The colloidal silver is solubilized when irradiated in the presence of added nitrate. Colloidal silver bromide is relatively stable toward ionizing radiation but undergoes reduction to colloidal silver when organic solutes are added prior to irradiation. Reduction rates were measured for systems having known average initial particle sizes and concentrations. (auth)

8303 USE OF PHOSPHINE AS A FREE RADICAL SCAVENGER IN THE RADIOLYSIS OF METHYL IODIDE VAPOR. Buchanan, James W.; Hanrahan, Robert J. (Univ. of Florida, Gainesville). Contract AT(40-1)-3106). Radiat. Res.; 44: 305-12(Nov 1970). (ORO–3106-28).

A limited study has been made of the gamma radiolysis of methyl iodide vapor and mixtures of phosphine and methyl iodide in the gas phase. Analyses of methane and hydrogen yields from irradiation of the pure vapor at 270 torr show that both are proportional to absorbed dose from 1×10^{20} to 4×10^{20} eV, with $G(CH_4) = 2.3$ and $G(H_2) = 0.6$. Both yields show a dependence on methyl iodide pressure. $G(CH_4)$ increases with pressure above 200 Torr, but $G(H_2)$ falls off. The mechanism for methane production is presumed to involve hot methyl radicals. Hydrogen production may be via a molecular elimination or hot atom process. Those mixtures containing a few mole percent phosphine show a greatly enhanced methane yield. A maximum $G(CH_4)$ of 12.6 occurs in a mixture containing 3.5 mole % phosphine and in which 99% of the radiation dose is absorbed by methyl iodide. This yield probably approximates the G for methyl radical production in pure methyl iodide vapor. In mixtures with greater phosphine concentrations the methane yield falls off sharply, perhaps due to an energy transfer process. (auth)

8304 CHEMICAL CONSEQUENCES OF THE AUGER EFFECT: IODINE YIELD FROM IODOAMINO ACIDS AS A FUNCTION OF X-RAY DOSE AND ENERGY. Diefallah, El-Hussieny M.; Stelter, Lothar; Diehn, Bodo (Univ. of Toledo). Radiat. Res.; 44: 273-81(Nov 1970).

Absorption of x-radiation in the iodothyronines results mainly in deiodination. G-values and dose effect curves were determined from 0.5 to 3.0 Mrads total absorbed dose for 3,5-diiodo-DL-thyronine, 3,5,3'-triiodo-DL-thyronine, and thyroxine. Radiation sensitivity increases with decreasing number of iodine atoms per molecule. Calculations based on I_2 yield measurements, as a function of maximum x-ray energy, indicate (after correction for radiation dose) that resonance absorption has a distinct effect upon the ensuing chemical transformation. This effect is stronger than would be predicted from published values of the K-to-L-shell Auger yields in iodine. (auth)

8305 γ-RADIOLYSIS OF 2-DEOXY-D-RIBOSE IN AQUEOUS SOLUTION. Hartmann, V. (Kernforschungszentrum, Karlsruhe, Ger.); von Sonntag, C.; Schulte-Frohlinde, D. Z. Naturforsch.; 25b: 1394-1404(Dec 1970). (In German).

In the γ-radiolysis of N_2O-saturated aqueous solutions of 2-deoxy-D-ribose (8×10^{-3} mol/l) the following products (G-values)

XUM

are formed: 2-deoxy-D-erythro-pentonic acid (and its γ-lactone) (2.5), 2,5-dideoxy-D-erythro-pentonic acid (0.63), 2-hydroxy-oxa-cyclohexanone-(4) (1.15), 2-hydroxy-oxa-cyclohexanone-(5) (1.0), 3-hydroxyglutaraldehyde (0.55), further, α-hydroxycarbonyl compounds (0.2), and possibly malonaldehyde (≪0.1). The formation of the products can be explained by the attack of water radicals (·OH and ·H) on the 2-deoxy-D-ribose to give primarily 2-deoxyribosyl radicals. These radicals may disproportionate directly, rearrange, or eliminate water analogous to those from ethylene glycol. The main product stems from a disproportionation reaction of primary 2-deoxyribosyl radicals. The mechanism is discussed. (auth)

8306 PULSE RADIOLYSIS STUDY OF THE TRANSITORY SPECIES Au II. Baxendale, J. H. (Univ. of Manchester, Eng.); Koulkes-Pujo, Anne-Marie. J. Chim. Phys.; 67: 1602-7(Sep 1970). (In French).

Pulse radiolysis measurements on auric chloride solutions indicate the formation of Au(II). The yield of formation in $HClO_4$ (10^{-2} M) + CH_3OH(0.25 M) medium is 3.1, in good agreement with the calculated value, assuming that Au(II) disappears by disproportionation. The rate constant of this reaction varies from 0.025 to $1.4 \times 10^9 M^{-1}S^{-1}$, in accordance with the ionic form of Au II. (France)

8307 EFFECT OF GAMMA IRRADIATION ON THE VERY DILUTE SOLUTION OF COLLAGEN IN THE ATMOSPHERE OF AIR AND NITROGEN. Kohno, Kaku (Japan Leather Co., Tokyo); Nishihara, Tomio; Fukada, Eiichi. Jap. J. Appl. Phys.; 9: 1431-6 (Dec 1970).

Low dosage gamma irradiations of very dilute solutions of collagen were investigated. Acid-soluble collagen extracted from calf skin was fully purified and dissolved in a 0.05% aqueous solution of acetic acid at a concentration of 0.021%. Gamma irradiation at a dose rate of 4×10^2 r/min was carried out in an atmosphere of air or nitrogen. Irradiation in air up to 3×10^4 r produced about a 70% decrease of intrinsic viscosity, about a 20% decrease in optical rotation and average molecular length estimated from flow birefringence, and noticeable lowering of denaturation temperature. The results suggest the occurrence of scission reactions in polypeptide chains in the triple helix of collagen molecule. On the other hand, irradiation in nitrogen up to 3×10^3 r caused about a 20% decrease of optical rotation, about a 20% increase of average molecular length, and a remarkable increase of intrinsic viscosity. Gelation takes place at about 5×10^3 r. The results indicate the predominance of crosslink reactions during irradiation in nitrogen. (auth)

Radioisotope Production

8308 OPTIMUM NEUTRON IRRADIATION CONDITIONS FOR RADIOISOTOPE PRODUCTION. Terent'ev, V. P.; Zharkov, V. A.; Fradkin, G. M.; Chavychalova, T. P. At. Energ. (USSR); 29: 260-4(Oct 1970). (In Russian).

Optimum irradiation conditions were found for production of isotopes generated by neutron capture followed by intermediate nucleus decay. The generated isotope minimum cost and maximum yield per unit of the initial material were chosen as the optimization criteria. Optimum irradiation time on which depends chemical processing losses and different operation costs were determined. The optimum flux-time function and corresponding irradiation time were found also. (auth)

8309 PRODUCTION OF A PHARMACEUTICALLY ACCEPTABLE SALINE SOLUTION CONTAINING RADIOACTIVE GAS AND USE THEREOF. Tilbury, Roy Sidney; Kramer, Henry Herman (to Union Carbide Corp.). British Patent 1,210,938. 4 Nov 1970. Filed 31 Jan 1968.

A process is described for preparing saline solutions for use in radiopharmaceutical diagnostic applications, and which when administered from the same vial contain essentially the same concentrations of radioactive gas, which may be ^{133}Xe or ^{85}Kr. The process involves the following steps: (a) admitting the radioactive gas into a sterile closed and evacuated vessel; (b) condensing the gas in the presence of sufficient NaCl to given an isotonic solution; (c) adding degassed and pharmaceutically acceptable water to entirely fill the vessel and give an isotonic solution containing dissolved radioactive gas; (d) adding insoluble silicone oil to displace the solution and dispensing the solution into sealable sterile unit cartridges so that no air space remains. Alternatively, step (b) may be omitted and saline solution substituted for water in step (c). Details are given for the preparation, dispensation and administration of the solution. (auth) (UK)

Recoil Production and Reactions

8310 (ORO-3898-2) REACTIONS OF HIGH ENERGY RADIOACTIVE ATOMS RESULTING FROM NUCLEAR TRANSFORMATIONS IN THE SYSTEMS OF SILICON-CONTAINING COMPOUNDS. Progress Report, February 1970–January 1971. Tang, Yi-Noo (Texas Agricultural and Mechanical Univ., College Station. Dept. of Chemistry). 1 Nov 1970. Contract AT(40-1)-3898. 60p. Dep. NTIS.

Reactions of high-energy chlorine atoms, formed by the nuclear reaction $^{37}Cl(n,\gamma)^{38}Cl$, with silicon-containing compounds were studied. The reactions of tritium from the reaction $^3He(n,p)^3H$ with silanes were also investigated along with reactions of ^{31}Si from the $^{31}P(n,p)^{31}Si$ reaction. (M.C.G.)

8311 HOT-ATOM CHEMISTRY OF LOW-ENERGY CARBON IONS IN BENZENE. Pohlit, Helmut Martin. Berkeley, Calif.; Univ. of California (1969). 248p. University Microfilms Order No. 70-13,138.

Thesis.

A 10-kV ion accelerator is described with which $^{14}C^+$-beams of 1 to 2μA intensity and variable energies between 3 eV and 15,000 eV (at ca. 3 eV energy spread) are obtained. At energies above ca. 100 eV the hot-atom chemistry of nucleogenic carbon isotopes can be simulated with this equipment. Below 100 eV, the dependence of the product yields on the kinetic energy can give valuable information about the mechanisms and kinetics underlying the product formation. Methods, and their limitations, employable in this area of chemical experimentation are discussed. The formation of products from fast ^{14}C ions and atoms in solid benzene (–196°) were investigated. The yields of the seven major products (benzene, toluene, cycloheptatriene, phenylacetylene, biphenyl, diphenylmethane, and phenylcycloheptatriene) were determined as a function of the beam energy. The yields of toluene, cycloheptatriene, and phenylacetylene strongly decreased as the beam energy decreased below 100 eV, while those of all other compounds remained constant. The energy-independent yields indicated that the corresponding products are formed from carbon atoms with less than 3 eV energy. At least 15% of the initially fast carbon ions ended up in this form. The energy-dependent, i.e., decreasing yields of toluene and cycloheptatriene, were interpreted as being due to the decreased chance of hydrogen pick-up to form the precursors CH_2, as the beam energy decreases below 100 eV. A similar conclusion was drawn for the assumed precursor C_2H_x for phenylacetylene. This indicated that pick-up of hydrogen or carbon extends up to 50 eV or more. At least 6% of the (high-energy) carbon ions react in the form of CH_2 and 3% in the form of C_2H_x. One additional major product (benzaldehyde-"U–2") contains oxygen, posing a problem which occurs uniquely in this particular accelerator technique, namely possible contamination of the chemical system during the "irradiation." "U–2"'s abnormal yield dependence on various experimental parameters (e.g., the yield increases threefold as the beam energy is lowered from 15,000 to 100 eV) is discussed in this context. A partial degradation of cycloheptatriene shows a large extent of isomerization, indicating that the reacting CH_2 carries high internal and/or kinetic energy into the product. (Diss. Abstr. Int., B)

8312 REACTIONS OF SULFUR ATOMS PRODUCED BY THE $^{35}Cl(n,p)^{35}S$ PROCESS IN POTASSIUM CHLORIDE AND BY PHOTOLYSIS OF CARBONYL SULFIDE. Giulianelli, James Louis. Madison, Wis.; Univ. of Wisconsin (1969). 203p. University Microfilms Order No. 70-3541.

Thesis.

The purposes of this investigation were to test the hypothesis that neutral ^{35}S atoms, formed by the $^{35}Cl(n,p)^{35}S$ process, are among the ^{35}S species that react when neutron-irradiated KCl is dissolved in water and to study the chemical properties of sulfur atoms. The study of the ^{35}S atoms from irradiated KCl was carried out with the aid of S atom scavengers in the aqueous solutions used for dissolving the KCl. The further studies of S atoms were made by the photolysis of OCS in aqueous solution and in solid 3-methylpentane. It was shown that vacuum-sublimed, neutron-irradiated KCl (treated with γ radiation prior to neutron irradiation) yields ca. 20% $^{35}S_i$ upon dissolution, as evidenced by ca. 20% recovery of the total ^{35}S as $^{35}S_2O_3^{2-}$ or as $^{35}SCN^-$ when dissolution is in 0.3M aqueous NaOH containing SO_3^{2-} or CN^-, respectively. In the absence of scavengers, $^{35}S_i$ was oxidized by water or by oxidants released into solution when the neutron-irradiated KCl dissolved. Allyl alcohol (0.1 mole fraction) or S^{2-} in the dissolving solution also prevent oxidation of $^{35}S_i$. Evidence that a considerable fraction of the total ^{35}S in irradiated KCl is present as some other (non-$^{35}S_i$) metastable sulfur species, and speculations concerning its identity and the mechanism by which additives prevent its oxidation, are presented. After dissolution at 0 to 5°C in aqueous NaOH containing 4.3×10^{-2}M SO_3^{2-}, the distribution of ^{35}S was: 57.3% S^{2-}, 23.7% $S_2O_3^{2-}$, 15.2% SO_3^{2-}, and 3.8% SO_4^{2-}. In contrast, when the irradiated KCl was dissolved in aqueous NaOH without other anions, the distribution of ^{35}S was: 11.0% S^{2-}, 1.2% $S_2O_3^{2-}$, 1.8% SO_3^{2-}, and 85.9% SO_4^{2-}; and

when all four sulfur-containing anions were present in the dissolving solution, the distribution of ^{35}S was 91.0% S^{2-}, 2.0% $S_2O_3^{2-}$, 4.1% SO_3^{2-}, and 2.9% SO_4^{2-}. Distributions similar to the latter were found when S^{2-} was the only carrier anion present at the time of dissolution. When the crystals were dissolved in 4×10^{-2}M or 4×10^{-4}M CN^- solutions, ca. 58% $^{35}S^{2-}$ and 25% $^{35}SCN^-$ resulted. Exchange of ^{35}S between any of the sulfur-containing anions employed was shown to be negligible under the conditions of the experiments. Carbonyl sulfide (^{35}S) with a specific activity of 1,300 mCi/mM was synthesized. When this gas was dissolved in water (pH 4) and photolyzed ($\lambda > 200$ nm), sulfite and sulfate were produced with a quantum yield of ca. 0.5. The production of S atoms by photolysis of OCS in aqueous solution was evidenced by turbidity (presumably due to polymeric sulfur) that developed even when a dilute OCS solution (4×10^{-5}M) was photolyzed, and by the lack of this turbidity in a photolyzed OCS solution that contained some allyl alcohol. In exploratory experiments in a specially designed photolysis cell in which OCS was photolyzed in a 3-methylpentane matrix at 77°K, the sec-3MP radical esr signal and a signal assigned to a thiyl radical were observed. This suggests the possibility of hydrogen abstraction from the matrix hydrocarbon by "hot" S atoms. (Diss. Abstr. Int., B)

8313 CHEMICAL EFFECTS OF NUCLEAR TRANSFORMATIONS IN SOLIDS: A CONTRIBUTION TO SOLID STATE PHYSICS. I. Mueller, Horst (Univ., Freiburg i. B.). Atomkernenergie; 16: 237-42(1970). (In German).

The physical fate of atoms with kinetic energy can be investigated besides using purely physical methods by producing radioactive recoil atoms in nuclear reactions. By utilizing suitable chemical compounds new radioactively labeled species may be synthesized the sort and amount of which allow conclusions concerning physical processes in solids. (auth)

8314 CHEMICAL EFFECTS OF NUCLEAR TRANSFORMATIONS IN SOLIDS: CONTRIBUTION TO SOLID STATE PHYSICS. II. Mueller, Horst (Univ., Freiburg i. B.). Atomkernenergie; 16: 323-6(1970). (In German).

The physical fate of atoms with kinetic energy was investigated by producing radioactive recoil atoms in nuclear reactions. The initial kinetic energy may be varied in some limits by the releasing nuclear reaction. The experiments supply some qualitative and some quantitative results about displacement energies, replacement reactions, recoil ranges, and size and structure of reaction zones and confirm to some extent in a direct illustrative manner physical models of solid state damage. (auth)

Radiochemistry

Refer also to abstracts 8313, 8314, and 8574.

Separation Processes

Refer also to abstracts 8197, 8199, 8214, 8247, 8422, 8423, 8445, 8830, 8831, 8963, 10210, and 10211.

8315 (AAEC/TM-562) HEAVY WATER PRODUCTION: A REVIEW OF PROCESSES. Levins, D. M. (Australian Atomic Energy Commission Research Establishment, Lucas Heights). Sep 1970. 62p. Dep. NTIS (U.S. Sales Only).

Methods of heavy water production are examined in detail. Processes based on chemical exchange, distillation, electrolytic, and chromatographic methods are discussed. In the immediate future most of the world output of heavy water will be produced by hydrogen sulfide-water exchange (the GS process). Recent advances in process development make the ammonia-hydrogen route an attractive alternative since the enrichment obtainable in each stage is greater while the energy consumption is less. A variation of the ammonia-hydrogen scheme involving the use of amines as additives to, or substitutes for, ammonia also appears promising. The greatest obstacle to the development of either the ammonia-hydrogen or amine-hydrogen schemes on a large scale is the limitation on the supply of hydrogen. Ammonia synthesis gas is currently the most plentiful supply available but 1500 tonnes/day of ammonia capacity is needed for each 100 tonnes of heavy water produced annually. Unlimited production could be achieved using an equilibration stage in which hydrogen depleted in deuterium is exchanged with water at high temperature. The economics of this scheme depend on the development of a satisfactory catalyst for water/hydrogen equilibration. Distillation of water, methane, and hydrogen has been proposed as an economic route to heavy water production but design studies and experimental data need to be clarified. Processes based on chromatography or selective adsorption need to be re-examined. (auth)

8316 (BNWL-CC-1939) INTEGRATED LMFBR AQUEOUS FUEL REPROCESSING CONCEPTS. Richardson, Gerald L.; Schulz, Wallace W. (Battelle-Northwest, Richland, Wash. Pacific Northwest Lab.). 7 Jan 1969. Contract AT(45-1)-1830. 31p. Dep. NTIS.

Three conceptual solvent extraction schemes for integrated recovery of plutonium, uranium, and selected by-products from nitric acid solutions of irradiated LMFBR fuels are described and compared. These schemes range in complexity from a slightly modified version of the present-day Purex process to an advanced scheme designed for recovery and fractionation of fission product rare earths as well as of uranium, neptunium, plutonium, americium, and curium values. The former type of process can be readily incorporated into existing or scheduled LWR reprocessing plants, while the more ambitious processes appear more suitable to plants especially built for handling LMFBR fuels. In this latter category is included an amine extraction process designed to fractionate a crude plutonium (or plutonium-neptunium product) from short-cooled LMFBR fuels. This process does not have the flexibility afforded by the Purex (TBP) or DBBP (dibutyl butylphosphonate) processes, but this disadvantage may be offset in part by the greater stability of amine solvents. Anion exchange processes are also briefly discussed, both as adjuncts to the amine extraction process and as the primary decontamination process. Plutonium processing capacity and radiation stability of the resin appear to limit the utility of such processes. Precipitation processes were eliminated after a cursory examination because of the severe criticality limitations imposed by heterogeneous plutonium slurries. The integrated aqueous processing schemes considered are based on existing technology and reasonable extrapolations. (auth)

8317 (CU-755-7) SEPARATION OF ISOTOPES. Annual Progress Report. (Columbia Univ., New York. Dept. of Chemistry). 1 Sep 1970. Contract AT(30-1)-755. 268p. Dep. NTIS.

The report contains seven sections. Separate abstracts were prepared for five of them. The sections omitted include a summary and a reprint on preparation of 99.5% ^{15}N already published elsewhere. (B.L.M.)

For abstracts of individual sections see: 8241, 8318-8319, 8320, and 8422.

8318 (CU-755-7, Sect. 2) PREPARATION OF HIGH-CONCENTRATIONS OF ^{13}C BY CHEMICAL EXCHANGE BETWEEN AMINE CARBAMATES AND CARBON DIOXIDE IN A SOLVENT CARRIER SYSTEM. Ghate, Madhav R.; Taylor, T. I. (Columbia Univ., New York. Dept. of Chemistry). 31p.

From the results of studies on di-n-butylamine (DNBA) and triethylamine (TEA) for concentration of ^{13}C by exchange between amine carbamates and CO_2 previously reported and from further results reported in this paper, the equipment necessary to produce 90% ^{13}C was redesigned and tested in-line as sections of the cascade. The redesigned apparatus is described in detail. The effects of flow rates were investigated in some detail. The results of test runs on individual sections of the cascade and on test runs with three sections of the cascade are reported. (B.L.M.)

8319 (CU-755-7, Sect. 4) STUDY OF THE SEPARATION OF THE ISOTOPIC ISOMERS OF NO BY LOW-TEMPERATURE GAS CHROMATOGRAPHY. Smith, Jessie Gregory (Columbia Univ., New York. Dept. of Chemistry). 88p.

Part II of Ph. D. Dissertation.

In a study of the possible use of gas chromatography for separating and analyzing isotopic isomers of NO, silica gel, glass beads, molecular sieve 5A, and porous glass were investigated in adsorption columns, while Chromosorb W with 2-methylpentane and porous glass with silicone oil were investigated in partition columns. Forward and rear sections of eluted NO peaks from various columns were collected and analyzed mass spectrometrically to determine the degree of isotopic fractionation. In all cases, both ^{15}N and ^{18}O were found to be concentrated in the rear sections. The degree of isotopic fractionation was found to increase as the column temperatures were lowered. However, the isotopic isomers of NO were not resolved for any of the conditions studied. The most favorable results were obtained for Chromosorb W with 2-methylpentane in an 18-ft column. At temperatures near liquid N_2, concentrations of ^{15}N and ^{18}O in the rear sections were nearly twice as large as in the forward sections. The number of theoretical plates for this column was about 3500. Longer columns (50ft) packed with the adsorbents gave smaller isotopic fractionations. Additionally, it was found that a portion of the NO was irreversibly adsorbed on the molecular sieve 5A and porous glass columns after they had been activated at 325°C. The results for the various columns are discussed in terms of the possible formation of NO dimers in the liquid phase as opposed to adsorbed dimers. (auth)

XUM

8320 (CU-755-7, Sect. 6) A. HOLD-UP OF AMINES AND AMINE CARBAMATES ON COLUMN PACKINGS. DENSITY, SURFACE TENSION AND VISCOSITY OF THE LIQUID PHASES. Schenk, L. U. (Columbia Univ., New York. Dept. of Chemistry). 16p.

Measurements were made in the hold-up of liquids in the packed column used for the concentration of ^{13}C in the chemical exchange system of amine carbamates and CO_2 in order to analyze the equilibrium data for the system. Measurements were made both with the pure amines and with 1 and 2M solutions of dibutylamine in triethylamine both with and without a counterflow of CO_2. An increase in hold-up was noted with an increase in density; however, the hold-up increase was less at higher flow rates that at lower flow rates. (B.L.M.)

8321 (IN-1363) SILVER ZEOLITE: IODINE ADSORPTION STUDIES. (Project Report for July 1-December 31, 1969). Pence, Dallas T.; Maeck, William J. (Idaho Nuclear Corp., Idaho Falls). Nov 1970. Contract AT(10-1)-1230. 39p. Dep. NTIS.

A program is in progress to evaluate the use of metal-exchanged zeolites for the adsorption of airborne iodine species in reactor containment cleanup systems and in the treatment of nuclear fuel processing plant off-gas streams. The test apparatus used for evaluating these materials and its operation are described. The following properties of silver zeolite, type X, are discussed: preparation from the sodium form; adsorption efficiency for methyl iodide at various face velocities, relative humidities, and temperatures; methyl iodide loading capacity, desorption characteristics, and stability. Comparison data for chemically impregnated charcoal are given. The effect of various gaseous pollutants on the elemental iodine adsorption efficiency of silver zeolite is also presented. (auth)

8322 (IN-1423) DEVELOPMENT OF A FLUIDIZED-BED BURNER FOR PROCESSING ROVER FUEL. Borduin, L. C.; Kilian, D. C.; Roeh, A. P. (Idaho Nuclear Corp., Idaho Falls). Nov 1970. Contract AT(10-1)-1230. 38p. Dep. NTIS.

Development of a fluidized-bed combustion process for recovering uranium from spent graphite-matrix nuclear rocket (Rover) fuels is described. The graphite matrix is removed by combustion in a bed of inert alumina particles fluidized by oxygen; the uranium and other metals in the fuel are converted to their oxides. Uranium oxide, U_3O_8, and other metallic oxides are removed from the burner by elutriation and enter the dissolution phase of the headend process. (auth)

8323 (IN-1439) PARTICLE SIZE CONTROL BY JET GRINDING IN A FLUIDIZED-BED DENITRATOR. Hogg, G. W. (Idaho Nuclear Corp., Idaho Falls). Nov 1970. Contract AT(10-1)-1230. 26p. Dep. NTIS.

The application of jet grinders to the control of particle size in a fluidized-bed denitrator was evaluated. Correlations showing the effect of jet velocity, particle size, attrition index, jet location and orientation, and impact plates in reducing mean particle size were developed from experimental data. A jet grinder was used to control particle size in a pilot-plant denitrator. (auth)

8324 (ORNL-tr-2406) REPROCESSING OF THORIUM-CONTAINING NUCLEAR FUELS. First Semi-Annual Activity Report, 1970. (Kernforschungsanlage, Juelich (West Germany). Institut fuer Chemische Technologie). Translated for Oak Ridge National Lab., Tenn., from German report. 72p. Dep. NTIS.

In Thorex flowsheet studies, the fixed bed-fluidized bed furnace intended for hot-cell tests was completed, installed, and tested in cold experiments. While the temperature regulating system operated satisfactorily, difficulties occurred in metering and bed height regulation. Malfunctions in the milling installation for SiC-coated particles also could be eliminated. Orienting tests on the post-combustion of SiC-coated particles proceeded smoothly. Studies on the dissolution rate of oxide particles indicate a dependence on crystal size. The protactinium adsorption equipment was improved. Loading of the Vycor glass attained 0.04 mg Pa/g of glass. The scientific and technological studies on individual process steps of the KFA-TBP 23/25 process were completed. The final chemical flowsheets are available for the head-end as well as the first extraction cycle. As a part of the cold testing of the process, a total of 3 kg nuclear oxide fuel was reprocessed; no process malfunctions occurred. Engineering work on the experimental hot-cell equipment was also completed. After the individual components are finished, the complete system will be installed in the hot cells during the second half of 1970. In the Chlorinex process, the milling plant consisting of hammer mill, beater-disk mill, and ventilating system was completed. The chlorination reactor was also completed and subjected to a 600 h continuous test. More than 7 kg of particles were chlorinated. As a part of off-gas treatment, the removal of silicon tetrachloride by oxidation was successfully investigated. Laboratory experiments concerning the treatment of high-level wastes, particularly roll drying and melting of silicate glasses, were started. More than 700 analyses were made for the 6 reprocessing runs based on the THOREX flowsheet and performed in the first half of 1970. The reasons for the discrepancies of the mass balances of protactinium and thorium described in the 1969 semi-annual report were investigated. Improved analytical methods were then developed for both elements. Semiconductor detectors are now used for the determination of fission product activities. The γ-spectrometry facilities in the hot cells were improved. The analytical methods developed for the isolation of nuclides ^{237}Np, ^{238}Pu, ^{239}Pu, and ^{240}Pu were tested in the hot cells with the process streams of the THOREX process. Main attention was given to investigating the behavior of these nuclides during reprocessing according to the THOREX flowsheet. Start-up of the JUPITER pilot plant for reprocessing of thorium-containing fuel elements with a capacity of 2 kg heavy metal/day is planned by the end of 1973. After formulation of a flowsheet, the design drawings for transport and discharging of fuel element containers as well as for transporting, storage, and activity measurements of the fuel elements were started. In addition, the material balances for the pilot plant were largely completed. The combustion-head-end process with a throughput of 20 kg heavy metal/day is being studied. After formulation of a utilization plan of the chemistry cells under construction, several modifications were necessary. (M.C.G.)

8325 (SU-326-P-28-X-2) NITRIDE FORMING REACTIONS IN LIQUID URANIUM ALLOYS AND THEIR APPLICATIONS TO THE REPROCESSING OF SPENT NUCLEAR FUELS. Annual Progress Report, June 1, 1969-March 1, 1970. Parlee, Norman A. D. (Stanford Univ., Calif. Dept. of Mineral Engineering). Mar 1970. Contract AT(04-3)-326. 13p. Dep. NTIS.

The equilibrium thermodynamics and reaction kinetics of the UN and U_2N_3 forming reactions in liquid U-Sn alloys are being studied. Studies elucidated equilibrium constants of the reactions, activity coefficients, interaction coefficients and free energy of dilution of U in liquid Sn. Application of the nitride precipitation study to metallurgical separations involved in nuclear fuel reprocessing was studied theoretically. (M.C.G.)

8326 WATER AND THE NUCLEAR INDUSTRY. Rodier, J. Meded. Vlaam. Chem. Ver.; 32: 26-44(Jan-Feb 1970). (In French).

The uses, sources of contamination, and methods for decontamination of water in nuclear industry are discussed. The uses include reactor cooling, electric power stations, treatment of fuels, biological protection, and decontamination of fabrics. The quality of water is adapted to each particular case: industrial water, demineralized water, and crude filtered water. The principal methods for decontamination of water include: chemical treatment, evaporation, and ion exchange. The factors of decontamination and the different treatments are variable. In the European countries, the present level of radioactivity in water remains largely inferior to the maximum admissible concentrations for the population. (P.C.H.)

8327 TWO YEARS OF OPERATION OF EUROCHEMIC. Detilleux, E.; Cao, S.; Cabella, A. Neue Tech., B; 11: 15-19 (1969). (In French).

The facilities are designed for the treatment of either natural or slightly enriched uranium fuels coming from power and most research reactors, or fuels of highly enriched uranium used in some research reactors. Technical details are given on the chemistry of decladding and dissolution operations and the treatment of highly enriched fuels. Equipment performance is discussed, including three incidents involving evaporator leaks. (J.G.B.)

8328 ISOTOPE SEPARATION PRACTICE. Bigeleisen, Jacob (Brookhaven National Lab., Upton, N. Y.). Advan. Chem. Ser.; No. 89, 1-24(1969).

From Conference on Isotope Effects in Chemical Processes, Miami Beach, Fla. See CONF-670460.

A survey is presented of isotope separation processes. A distinction is made between processes suitable for laboratory-scale isotope separation and large-scale processes. Examples of laboratory scale separation by electromagnetic separation, thermal diffusion, distillation, and chemical exchange are discussed. Large-scale processes must be designed and operated in accord with cascade principles. These are discussed and illustrated by their implications to the production of heavy water by various processes. The cost of reflux operations in distillation and exchange processes is stressed. Thermal reflux can be achieved in chemical exchange systems by the dual temperature and exchange distillation processes. (auth)

8329 CHEMICAL FRACTIONATION OF BORON ISOTOPES. Palko, A. A.; Drury, J. S. (Oak Ridge National Lab., Tenn.). Advan. Chem. Ser.; No. 89, 40-56(1969).

From Conference on Isotope Effects in Chemical Processes, Miami Beach, Fla. See CONF-670460.

Studies on the chemical fractionation of boron isotopes between BF_3 and its molecular addition compounds resulted in the development of a separation process superior to methods previously employed. The work also led to a theoretical explanation of the exchange reaction, which accounted for the anomalous concentration of ^{10}B in the molecular addition compound, and the observed variations of the isotopic equilibrium constants as a function of different donors. The model predicted maximum isotopic equilibrium constants for the exchange reaction, which were consistent with the experimental data. It also predicted the behavior of the other boron halides. (auth)

8330 ENRICHMENT OF LITHIUM ISOTOPES BY EXTRACTION CHROMATOGRAPHY. Lee, D. A. (Oak Ridge National Lab., Tenn.). Advan. Chem. Ser.; No. 89, 57-64(1969).

From Conference on Isotope Effects in Chemical Processes, Miami Beach, Fla. See CONF-670460.

Lithium isotopes were fractionated by extraction chromatography. The chemical exchange reaction used was aqueous lithium hydroxide equilibrated with lithium dibenzoylmethane–trioctylphosphine oxide in dodecane. Granulated Teflon supported a dodecane solution of dibenzoylmethane–trioctylphosphine oxide in dodecane as the stationary phase. The mobile phase was an aqueous solution of lithium hydroxide. The single stage separation factor was 1.003, as determined by frontal analysis at "breakthrough." ^6Li concentrated in the aqueous phase. Separation of lithium isotopes by extraction chromatography was compared with separations made by ion exchange resin chromatography. The nature of the isotopic species involved determined the magnitude of the separation factor. (auth)

8331 PHOTOCHEMICAL SEPARATION OF THE CARBON ISOTOPES. Liuti, G.; Dondes, S.; Harteck, P. (Rensselaer Polytechnic Inst., Troy, N. Y.). Advan. Chem. Ser.; No. 89, 65-72(1969).

From Conference on Isotope Effects in Chemical Processes, Miami Beach, Fla. See CONF-670460.

The photolysis of CO using the 2062.4 Å line of iodine produces a ^{13}C enrichment in the reaction product, C_3O_2, and an ^{18}O enrichment in the reaction product, CO_2. The reaction mechanism is as follows: $^{13}CO^* + CO \rightarrow CO_2 + {}^{13}C$; $^{13}CO^* + {}^{12}CO \rightarrow {}^{13}CO_2 + {}^{12}C$; $^{12}C^{18}O^* + CO \rightarrow {}^{12}C{}^{16}O{}^{18}O + {}^{12}C$; $^{13}C + {}^{12}CO + M \rightarrow {}^{13}C = {}^{12}C = O$; $^{13}C = {}^{12}C = O + CO + M \rightarrow O = {}^{12}C = {}^{13}C = {}^{12}C = O + M$. The distribution of the ^{13}C in C_3O_2 and CO_2 shows that the reaction between $^{13}CO^*$ and CO forms ^{13}C and CO_2. (auth)

8332 ISOTOPE AND ORTHO-PARA SEPARATIONS OF THE MOLECULAR HYDROGENS BY ADSORPTION AT LOW TEMPERATURES. Haubach, W. J.; Radhakrishna, P.; Katorski, A.; Wang, R.; White, David (Univ. of Pennsylvania, Philadelphia). Advan. Chem. Ser.; No. 89, 73-98(1969).

From Conference on Isotope Effects in Chemical Processes, Miami Beach, Fla. See CONF-670460.

The theory of isotope and ortho-para separation of diatomic molecules, by preferential adsorption at low temperatures, is reviewed, and a comparison between theory and experiment is made for the isotopic molecular hydrogens. In the plane surface approximation for a molecule-surface interaction coupling the angular motions with the center of mass vibrations normal to the surface, good agreement is found between the measured and calculated separation factors. It is, however, not possible (solely on the basis of the experimental separation factors) to establish the exact form of the potential of interaction. The influence of surface heterogeneity on the separations is discussed and in both cases (spin and isotopic) reasonable agreement between theory and experiment is obtained for monolayers on a heterogeneous surface. (auth)

8333 ISOTOPE SEPARATION BY GAS CHROMATOGRAPHY. Van Hook, W. Alexander (Univ. of Tennessee, Knoxville). Advan. Chem. Ser.; No. 89, 99-118(1969).

From Conference on Isotope Effects in Chemical Processes, Miami Beach, Fla. See CONF-670460.

Gas chromatographic techniques for separating isotopically substituted stable molecules are discussed as is the theory of the separations. The discussion focuses on both gas–liquid and gas–solid chromatographic separations of small hydrocarbons substituted with hydrogen and deuterium or tritium, but one $^{12}C-{}^{13}C$ separation is cited. The available data agree with the predictions of the statistical theory of isotope effects in condensed phases. Other systems of interest are also mentioned. (auth)

8334 PREPARATION OF 99.5 PERCENT ^{15}N BY CHEMICAL EXCHANGE BETWEEN OXIDES OF NITROGEN IN A SOLVENT CARRIER SYSTEM. Jeevanadam, M.; Taylor, T. I. (Columbia Univ., New York). Advan. Chem. Ser.; No. 89, 119-47(1969).

From Conference on Isotope Effects in Chemical Processes, Miami Beach, Fla. See CONF-670460.

Solvents such as CCl_4 and n-heptane increased the single stage enrichment factor, α, for the distribution of ^{15}N between the gas and liquid phase for the $NO-N_2O_3$ exchange system. A further increase resulted when donor molecules such as 1,4-dioxane were present in the solution. It was shown that the changes in composition of the phases could account for the increases in α. The use of solvents as carriers in exchange columns for the $NO-N_2O_3$ system resulted in marked increases in the overall separations for ^{15}N. Besides their effect on α, solvents improved the interphase exchange rate and decreased the hold-up of exchangeable material. A cascade of two columns was constructed and 99.5% ^{15}N was produced to test the reflux process for the solvent carrier systems. (auth)

8335 THEORETICAL ANALYSIS OF CHEMICAL ISOTOPE FRACTIONATION BY ORTHOGONAL POLYNOMIAL METHODS. Ishida, Takanobu (Yeshiva Univ., New York); Spindel, W.; Bigeleisen, Jacob. Advan. Chem. Ser.; No. 89, 192-247(1969).

From Conference on Isotope Effects in Chemical Processes, Miami Beach, Fla. See CONF-670460.

The reduced partition functions of isotopic molecules determine the isotope separation factors in all equilibrium and many non-equilibrium processes. Power series expansion of the function in terms of even powers of the molecular vibrations has given explicit relationships between the separation factor and molecular structure and molecular forces. A significant extension to the Bernoulli expansion, developed previously, which has the restriction $u = h\nu/kT < 2\pi$, is developed through truncated series, derived from the hypergeometric function. The finite expansion can be written in the Bernoulli form with determinable modulating coefficients for each term. They are convergent for all values of u and yield better approximations to the reduced partition function than the Bernoulli expansion. The utility of the present method is illustrated through calculations on numerous molecular systems. (auth)

8336 THERMOTRANSPORT IN MONATOMIC AND IONIC LIQUIDS. Lodding, A. (Chalmers Univ. of Tech., Goteborg). Advan. Chem. Ser.; No. 89, 264-74(1969).

From Conference on Isotope Effects in Chemical Processes, Miami Beach, Fla. See CONF-670460.

The phenomenon of thermotransport in simple liquids is described in a generalized treatment that does not require the adoption of any particular existing model of liquid diffusion. The results of recent isotope experiments in liquid metals are used as illustrations of applicability. The treatment is extended to liquid salts, where electrotransport mobility data under favorable conditions may facilitate the interpretation of thermotransport experiments. The experimental results in the few liquid salt systems, where thermo- as well as electrotransport of isotopes was measured, are discussed in terms of the above treatment. (auth)

8337 BACTERIA-AIDED WATER LEACHING OF URANIUM ORES. Aslam, K. M.; Aslam, M. (Directorate of Nuclear Minerals, Lahore). Nucleus (Karachi); 7: 28-36(Jan-Apr 1970).

The present status of the method for enrichment of uranium ores by the bacteria-aided water leaching that makes the recovery of U_3O_8 commercially feasible is reviewed. The bacterial species concerned is Ferrobacillus ferrooxidans whose presence was confirmed in the research laboratories of Rio Algom Mines Ltd. While the method is in the development stage, it promises to be a commercially feasible proposition, since by using a semicontinuous bench-scale countercurrent decantation system (CCD) in which bacteria were employed to aid in the oxidizing conditions in the leach solution, uranium extraction of over 90% with an acid consumption of about 25 lb. H_2SO_4/ton at 30°C was effected. The method holds considerable promise for Pakistan. (auth)

8338 PROCESSES FOR SIMULTANEOUSLY PURIFYING AND CONCENTRATING PLUTONIUM SOLUTIONS. Boudry, Jean Claude; Chambon, Marcel; Faugeras, Pierre; Lheureux, Colette; Talmont, Xavier L. R. (to Commissariat a l'Energie Atomique). U. S. Patent 3,533,757. 13 Oct 1970. Priority date 9 Jun 1964, France.

A method of purifying a mother liquor of Pu comprises extracting a mixture of the mother liquor of Pu and an aqueous extract containing Pu in a countercurrent extraction process with an organic phase containing tributylphosphate. The organic phase containing the Pu is then extracted in a countercurrent extraction process with a solution of HNO_3 and then with a diluted

XUM

sulfo-nitric acid solution, and a portion of the aqueous extract containing the Pu is then recycled. (Offic. Gaz.)

8339 METHOD FOR FRACTIONATION OF CARBON ISOTOPES. Palko, Aloysius A. (to United States Atomic Energy Commission). U. S. Patent 3,535,079. 20 Oct 1970. Filed 8 Mar 1968.

A two-phase chemical exchange process for the fractionation of C isotopes is provided by contacting an aqueous solution of cuprous chloride and ammonium chloride–carbon monoxide complex with carbon monoxide to exchange ^{13}C in the gas phase with ^{12}C in the liquid phase and thereafter thermally dissociating the complex to yield carbon monoxide enriched with ^{13}C. (Official Gazette)

8340 DESIGN AND PROJECT OF RADIOACTIVE TREATMENT AND DISPOSAL SYSTEM IN LARGE CAPACITY BWR NUCLEAR POWER STATION. Shimozato, Atou; Takeshima, Masaki; Osano, Katsuharu (Hitachi Ltd., Ibaraki, Japan). Hitachi Hyoron; 52: 308-14(Apr 1970). (In Japanese).

An essential feature for the safe and smooth operation of a large-capacity BWR nuclear power station is an efficient means of handling all the radioactive wastes produced during operation, so as to release them to the environment at the rate well below the maximum permissible limit. The storage method for gas removal from the steam system by the air ejector on a main condenser has been developed. This system consists of a recombiner, a compressor, one-day holdup tanks and a filter, allowing the decay of activated gases to reduce the radioactivity to acceptable level. The liquid waste disposal system removes insoluble particles and soluble impurities, assures the radioisotopic and chemical purity of the liquid before recirculating in the process or release, and stores concentrated salt solution. The solid wastes, such as filter sludge and contaminated resin, are collected in storage tanks, cemented or stuffed in drum cans, and thrown away. When the layout for radioactive waste treatment and disposal system is planned, the radioactivity level of each constituent and the radiation dose to which workers are exposed should be taken into account. The equipment for Xe and Kr gas holdup, the calcination of concentrated liquid waste, the burning up of filter sludge, and an activated charcoal filter have been under development. (Japan)

8341 SORPTION OF STRONTIUM AND CALCIUM CATIONS ON THE KU-2 TYPE CATION EXCHANGE RESIN. Rauzen, F. V.; Trushkov, N. P. At. Energ. (USSR); 29: 103-6(Aug 1970). (In Russian).

The purification of low-activity waters containing ^{90}Sr with a maximum permissible concentration of 10^{-10} Ci/l requires determination of the optimum adsorption conditions for removing this isotope from solutions containing calcium ions. Experiments were carried out to take advantage of the known selectivity of the KU cation exchange resin with respect to strontium. A solution containing 3 mg. equiv/l of $CaCl_2$ and $SrCl_2$, tagged by ^{45}Ca and ^{90}Sr, respectively was filtered through the resin at the rate of 0.5 $cm^3/cm^2/min$. The results indicated that the resin may be used for purifying low-activity waters until the appearance of calcium cations in the field rate corresponding to a purification of $C/C_0 > 0.01$. If 0.95-mm-diameter grains are used, the filtration rate should be faster than 0.15 $cm^3/cm^2/min$, making sure that the resin and the water are in contact for a period of less than 10 minutes. The yield may be increased by using a higher column and increasing the flow rate through it. A smaller grain size helps to increase the efficiency, i.e., to decrease the minimum time of contact, thus increasing the amount of purified filtrate per cycle. (TTT)

8342 PILOT PLANT FOR PREPARATION OF URANIUM HEXAFLUORIDE BY DRY TREATMENT OF NUCLEAR COMPOUNDS. Harnie, R. Ind. Chim. Belge; 35: 878-90(Oct 1970). (In Flemish).

By nonaqueous reprocessing of reactor fuels, various methods for recovering U in the form of UF_6 can be used. The technological problems in these various processes are being studied. An installation for continuous fuel cycle processes is being built. (M.C.G.)

8343 PROCESS FOR SEPARATING ISOTOPIC COMPOUNDS BY ABSORPTION. Espagno, Lucien; Blanc, Claude; Huynh, Chanh Trung (to Societe Nationale des Petroles d'Aquitaine). U. S. Patent 3,533,220. 13 Oct 1970. Priority date 15 Feb 1966, France.

A method for enriching or separating at least one isotopic compound comprises at least one step in which relatively small quantities of the isotopic mixture in the gaseous state are periodically injected into a continually circulating gaseous carrier. The gaseous carrier along with the mixture circulates in an enclosure containing a porous absorbing medium that is inert to the carrier gas. The appearance of the isotopic mixture or one of its components at the exit of the enclosure is detected by a mass spectrometer, and this detection is used to control the collection of successive fractions of the isotopic mixture in different containers. (B.L.M.)

8344 METHOD OF DECONTAMINATING RADIOACTIVE EFFLUENTS. Berton, Yves; Chauvet, Pierre (to Commissariat a l'Energie Atomique). British Patent 1,211,816. 11 Nov 1970. Priority date 9 Jul 1968, France.

A method for decontamination of liquid radioactive effluents obtained by chemical decanning of irradiated fuel elements comprises forming, successively and without separation, the following precipitates: ferrous sulfide or hydroxide (elimination of Ru), barium sulfate, adjusting pH to ~8.5 (elimination of Sr, Zr, and Ce), and transition element ferrocyanide, such as Co or Ni ferrocyanide (elimination of Cs). The pH is between 7 and 9 at the end of the treatment, and the combined precipitates are removed leaving the bulk of the magnesium in solution. (B.L.M.)

EARTH SCIENCES

Geology and Hydrology

Refer also to abstracts 8385, 8570, and 8593.

8345 (BNWL-SA-3494) MATHEMATICAL SIMULATION OF GROUNDWATER TRANSPORT OF RADIONUCLIDES AT HANFORD. Cearlock, D. B.; Routson, R. C.; Bryan, C. A. (Battelle-Northwest, Richland, Wash. Pacific Northwest Lab.). 27 Aug 1970. Contract AT(45-1)-1830. 24p. (CONF-700827-1). Dep. NTIS.

From 18th Annual Specialty Conference, Minneapolis, Minn.

A method for predicting the distribution and movement of radioisotopes in heterogeneous subsurface environments is being developed to improve understanding of the radiological effects of environmental waste disposal practices at Hanford. The transport equation used to predict the time-dependent, concentration distribution in saturated and unsaturated soils is discussed. Experiments performed to determine the effects of concentration of solution macroions on radioisotope adsorption, particularly Sr adsorption, and to obtain ion exchange data are described. Data on the energy potential of water in the Hanford soil were obtained to study the deep percolation of rainfall. The tritium content of deep well waters was measured to study the characteristics of the confined aquifer, the interrelations between the surface and confined aquifers, and the effects of Hanford operations on the water quality in the confined aquifer. Finally a method for developing a computer program for visually displaying the ground water contours and flow paths for the measured aquifer conditions is described. (L.C.L.)

8346 (CU-2493-11) GEOCHEMICAL STUDIES OF CONTINENTAL WATERS. Annual Report and Renewal Proposal. Broecker, Wallace S.; Thurber, David L. (Columbia Univ., Palisades, N. Y. Lamont-Doherty Geological Observatory). Oct 1970. Contract AT(30-1)-2493. 282p. Dep. NTIS.

Geochemical studies of continental waters are presented in six appendixes. A separate abstract was prepared for each. (L.C.L.)

For abstracts of individual sections see: 8347–8352.

8347 (CU-2493-11, App.1) TRITIUM IN CRATER LAKE, OREGON. Simpson, H. James (Columbia Univ., Palisades, N. Y. Lamont-Doherty Geological Observatory). 39p.

From Geochemical studies on continental waters.

The transfer of tritium from the atmosphere to the ocean and to continental water bodies by vapor exchange, as well as by precipitation, is well documented. Vapor exchange has been suggested as the dominant mechanism for transfer of tritium to small continental lakes. Evidence is presented to suggest that input by precipitation can explain most of the tritium content of Crater Lake, Oregon. The hydrology of Crater Lake makes it ideal for this study since less than ½ of 1% of the lake volume is lost by seepage each year and there is no surface outflow. Very little tritium can be lost from the lake by vapor exchange because of the dilution of the surface concentration by vertical mixing. If Crater Lake has retained nearly all its input tritium, and less than half of this input was supplied by vapor exchange as suggested by budget calculations, then deep lakes, with small drainage basins can provide good estimates of the total tritium rainout. (auth)

8348 (CU-2493-11, App.2) CLOSED BASIN LAKES AS A TOOL IN GEOCHEMISTRY. CHAPTER II. CHEMISTRY AND HYDROLOGY OF THE DILUTE LAKES. Simpson, Harry James Jr. (Columbia Univ., Palisades, N. Y. Lamont-Doherty Geological Observatory). 66p.

From Geochemical studies on continental waters.

The chemistry and hydrology of dilute lakes are examined by discussing sources of dissolved ionic species in Crater Lake and Lake Tahoe. The hydrology of Crater Lake, its water level variations, and temperature profiles are presented. Sampling and analysis methods used for determining the chemical content of Crater Lake sediments and water, of spring waters from the surrounding area, and of local rainwater are discussed, and the results tabulated. This information is combined to produce a model chemical budget of Crater Lake. The hydrology of Lake Tahoe is examined. Previously published data on the chemical composition of Lake Tahoe are presented and compared with Crater Lake. (L.C.L.)

8349 (CU-2493-11, App.3) CLOSED BASIN LAKES AS A TOOL IN GEOCHEMISTRY. CHAPTER III. CHEMISTRY AND HYDROLOGY OF THE SALINE LAKES. Simpson, Harry James Jr. (Columbia Univ., Palisades, N. Y. Lamont-Doherty Geological Observatory). 122p.

From Geochemical studies on continental waters.

The chemistry and hydrology of saline lakes were studied using data for water and sediment samples from several high-alkalinity closed basin lakes, principally from Mono Lake, Calif. New data for pore waters were obtained. The sampling and analysis methods used are discussed. The cation contents of major closed basin lakes and seas are compared. Mechanisms operating in the ocean to remove alkalinity are compared with those in a closed basin lake. (L.C.L.)

8350 (CU-2493-11, App.4) GEOCHEMICAL STUDIES ON CRANBERRY AND STERLING LAKES. Mathieu, G.; Broecker, W. S. (Columbia Univ., Palisades, N. Y. Lamont-Doherty Geological Observatory). 25p.

From Geochemical studies on continental waters.

A method for measuring the rate of groundwater flow into a lake using natural Rn as a tracer is described. Factors that influence the Rn content of a shallow lake were evaluated during a study of Cranberry Lake, N. Y. conducted during Aug. 1969 to Aug. 1970. These factors include rainfall, ice cover, Rn content of stream feeding lake, horizontal mixing, and Rn diffusion from sediments. Water samples from both Cranberry Lake and nearby Sterling Lake were analyzed for ionic balance. Measured data are presented for the Rn concentration in Cranberry Lake at surface, 2m and 4m depths; surface and deep level measurements of O content, partial CO_2 pressure, and temperature; and for the O and Rn content, and temperature of Sterling Lake as a function of depth. (L.C.L.)

8351 (CU-2493-11, App.5) PROJECT ROSS. Broecker, W. S. (Columbia Univ., Palisades, N. Y. Lamont-Doherty Geological Observatory). 42p.

From Geochemical studies on continental waters.

A program of geochemical studies for determining the factors that control the chemistry of waters and the processes responsible for the cycling and transport of pollutants in water systems is discussed. Some data related to water pollution in urban environments were obtained from New Jersey and New York state suburban areas near New York City. (L.C.L.)

8352 (CU-2493-11, App.6) DETERMINATION OF MIXING AND GAS EXCHANGE RATES USING NATURAL AND ARTIFICIALLY INTRODUCED RADON AT THE EXPERIMENTAL LAKES AREA, WESTERN ONTARIO. Emerson, Steve; Brunskill, Gregg; Broecker, Wallace S.; Peng, T.-H. (Columbia Univ., Palisades, N. Y. Lamont-Doherty Geological Observatory). 39p.

From Geochemical studies on continental waters.

Two experiments performed at the Experimental Lakes Area in western Ontario are described. The first measured the distribution of natural ^{222}Rn in groundwater, streams, and lakes. In the second, a small lake was spiked with ^{226}Ra in order to study gas exchange rates and vertical mixing processes. The results of ^{222}Rn measurements are tabulated. Depth profiles of ^{222}Rn content and temperature in two lakes before and after spiking are presented. Data for the gas exchange and vertical mixing studies are incomplete. (L.C.L.)

8353 (HASL-237, pp I.11-26) ACCUMULATED FALLOUT ^{90}Sr IN THE ROCKY FLATS AREA. Hardy, E.; Krey, P.; Feiner, M. (New York Operations Office (AEC), N. Y. Health and Safety Lab.).

From Fallout program.

Soil samples collected in the vicinity of Rocky Flats, Colorado in February 1970 were analyzed for fallout strontium-90 to ascertain how precisely one can determine the cumulative deposit for a particular locality. Depth profiles indicate that the 20 cm sampling depth used was adequate for those sites on Rocky Flats but many of the samples taken beyond this area were not deep enough to include all of the strontium-90. Based on 13 samples in the Rocky Flats area, it was determined that 64 ± 8 millicuries of strontium-90 has deposited as a result of atmospheric nuclear testing. (auth)

8354 (HMI-B-86) ESTIMATION OF THE SURFACE WATER'S CONTAMINATION BY THE NEAR FALLOUT BY NUCLEAR EXPLOSIONS. Jacobi, W.; Stolterfoht, N. (Hahn-Meitner-Institut fuer Kernforschung, Berlin (West Germany)). Aug 1969. 42p. (In German). Dep. NTIS (U. S. Sales Only).

A method is described for estimating the contamination of river water by the near fallout of a megaton nuclear bomb which

explodes close to the ground. The fallout model of Miller and measurements of the distant fallout after nuclear test explosions are taken as basis. The results are discussed with respect to the treatment of river water for providing drinking water for the population. The contamination of the drinking water is expected to be negligible if the relation of the bomb's fission power to the draining area of the river is smaller than 10^{-4} megaton/km^2. (auth)

8355 (USGS-474-88) BIBLIOGRAPHY OF PUBLISHED REPORTS BY U. S. GEOLOGICAL SURVEY PERSONNEL ON THE GEOLOGY AND HYDROLOGY OF THE NEVADA TEST SITE, 1957–1969. (Geological Survey, Denver, Colo.). 1970. Contract AT(29-2)-474. 67p. (NTS-220). Dep. NTIS.

Listings are presented of 277 published reports on the geology and hydrology of the Nevada Test Site by U. S. Geological Survey scientists. Reports on related subjects, knowledge of which has been gained through investigations made at the Nevada Test Site, are also listed. The time span of interest is 1957 to 1969, with a few reports that have been published in the early months of 1970 included. The list is in alphabetic order by senior author's surname. A cross index of all junior authors is interalphabetized with the senior author listing. The letters OTS or CFSTI following a bibliographic entry indicate that the report may be purchased from the National Technical Information Service, Department of Commerce, Springfield, Virginia 22151. A second section of the bibliography is a generalized index, which includes topical categories and geographic areas integrated into alphabetical order. Two index maps show the area of the Nevada Test Site as it is divided into 7½-minute quadrangles and numbered test areas are included along with a third index map which outlines major topographic features. (auth)

8356 (USGS-474-92) U20e POSTSHOT FRACTURES, JORUM EVENT. Special Studies-84. Snyder, R. P. (Geological Survey, Denver, Colo.). 1970. Contract AT(29-2)-474. 10p. Dep. NTIS.

Surface fractures caused by the U20e (Jorum) event of September 16, 1969, were mapped by members of the U. S. Geological Survey, at the Nevada Test Site. Faults were activated or reactivated as far as 4 miles from GZ. Four major fault zones are reported on and movement along these faults is shown. (auth)

8357 (USGS-474-96) REVISED LITHOLOGIC LOG OF PAHUTE MESA EXPLORATORY DRILL HOLE NO. 1, NEVADA TEST SITE. Jenkins, Evan C. (Geological Survey, Denver, Colo.). 1970. Contract AT(29-2)-474. 8p. Dep. NTIS.

Poor correlations to Pahute Mesa No. 1 from other drill holes prompted a reexamination of the drill hole throughout the depth interval of 1,140 to 2,890 feet. Two additional Area 20 rhyolitic lava flow units were found. (auth)

8358 NUCLEAR RESONANCE WELL LOGGING METHOD AND APPARATUS. Schwede, Harold F. (to Schlumberger Well Surveying Corp.). U. S. Patent 3,528,000. 8 Sep 1970 Filed 5 Mar 1954.

Methods and equipment for well logging are described which can be used to obtain quantitative data concerning the earth formations traversed by a well or borehole. The logging is based on nuclear magnetic resonance techniques. (J.R.D.)

8359 METHOD AND APPARATUS FOR NEUTRON LIFETIME WELL LOGGING USING DUAL DISCRIMINATION WITHIN ONE OF TWO INTERVALS. Youmans, Arthur H.; Hopkinson, Eric C. (to Dresser Industries, Inc.). U.S. Patent 3,532,885. 6 Oct 1970. Filed 31 May 1967.

Pulse height discrimination is used to provide a plurality of ranges within one measurement taken during the logging of the decline of the thermal neutron population to provide spectral information. (auth)

8360 METHOD FOR SEPARATING THE γ RADIATION DOSE RATE OF ARTIFICIAL AND NATURAL RADIOACTIVE ISOTOPES IN THE GROUND. Vorob'ev, V. A.; Kogan, R. M.; Nazarov, I. M.; Fridman, Sh. D. At. Energ. (USSR); 29: 133-5(Aug 1970). (In Russian).

The artificial radioactivity of the surface of the Earth from fallout is of the same order of magnitude as the γ radiation of naturally radioactive elements. The two types of γ radiation have been determined separately by a spectral method; however, it is technically simpler to take advantage of the differences in the angular distribution of the γ quanta in the soil. The depthwise distribution of natural radioactive elements is fairly uniform, while the artificial ones are either only at the surface or is a thin upper layer, decreasing exponentially with the depth. Monte Carlo calculations indicated an angular correlation for the γ quanta emitted by ^{137}Cs and ^{60}Cs, while the uranium, thorium, and potassium content was found to be independent of the angle. Measurements by isotopic and collimated detectors may also be used to differentiate between dose rates attributable to natural and artificial radioisotopes. The statistical error in these determinations, considering the global contamination and a measurement period of 10 minutes, amounts to about 3%. (TTT)

8361 TRANSPORT OF RADIOISOTOPES BY FINE PARTICULATE MATTER IN AQUIFERS. Champlin, Jerry B. Francis, Atlanta; Georgia Inst. of Tech. (1970). 199p. University Microfilms Order No. 70-19,265.

Thesis.

The information required to explain the long-range movement of radioactive fission products from waste pits, fallout, and underground nuclear explosions, as well as that of other environmental pollutants was sought. Both theoretical and experimental investigations of the various phenomena that pertain to ion transport or retention by soils are included. The theoretical section delves into the interactions between solids in water that result from thermal forces, electrostatic charges, and van der Waals forces. The particle range considered is that of the large colloid to the finest silt. Sources of energy sufficient to cause breakage of adsorption bonds and the importance of the concept of additive bonding in the water are discussed. The important relationship between suspended particles and the "massive" granules making up the model aquifer is explored at some depth. In the experimental section, factors which influence either retention of radioactivity by the sand bed or transport of the activity through such a bed by micro-particles are considered. Correlation is sought between the phenomena observed experimentally and that predicted in the theoretical section. Casimir's correction to the theoretical van der Waals interactions is proposed to account for major changes in the particle retention ability of the sand bed when dispersants are included in the influent water. The future potential of such research, as well as some of the practical aspects of the results reported here is discussed. (auth) (Diss. Abstr. Int., B)

Meteorology

Refer also to abstracts 8340, 8452, 8629, 8658, 8659, and 8668.

8362 (AD-707427) CLOUD CHEMISTRY OF FALLOUT FORMATION. Final Report. Norman, John H.; Winchell, Perrin (Gulf General Atomic, Inc., San Diego, Calif.). 15 Feb 1970. Contract DAHC20-69-C-0138. 65p. (GA-9945). NTIS.

In initial studies of short-lived fission products for use in fallout fractionation models, several known isotopes have been recognized. The observed gamma ray intensities of recognized energies from the double-tape recoil-range measuring system are consistent with expected recoil range variations. It is planned to satisfy a requirement for more intense gamma spectra by moving the recoil fission product source close to the reactor. The interaction between condensation phenomena, gas, and condensed-phase diffusion of fission products during fallout formation has been investigated analytically. Regions of importance of each of these phenomena have been discussed. Further tests of the application of the compensation law to condensed-state diffusion data have been carried out. The compensation law applied well to all silicate systems except those loaded by fission-product recoil. The thermodynamics of GeO_2(g) have been measured. Attempts to define the stabilities of AsO_2(g) and SnO_2(g) have failed because of low stability of these species. Gaseous release of iodine from TeO_2 particles has been shown to be controlled by diffusion in the TeO_2. Rates of diffusion have been determined. These data indicate that the volatility of iodine from fallout particles could be very high. Leaching studies of recoil loaded fission products are consistent with release of these fission products to the aqueous leaching solution being diffusion controlled. These measurements point out the importance of the distributions of fission products in fallout particles to their biological activities. (USGRDR)

8363 (AECL-3731) USE OF ^{41}Ar TO STUDY THE DISPERSION OF EFFLUENT FROM STACKS. Barry, P. J. (Atomic Energy of Canada Ltd., Chalk River (Ontario). Chalk River Nuclear Labs.). Sep 1970. 21p. (CONF-701023-2). Dep. NTIS (U. S. Sales Only). AECL $0.50.

From Symposium on the Use of Nuclear Techniques in the Measurement and Control of Environmental Pollution, Salzburg, Austria.

Since 1963 the concentration of ^{41}Ar emitted from the reactor stack at CRNL has been measured continuously at ground level at several sites. The field concentrations have been normalized to a unit emission rate by dividing by the rate of emission at the stack which is also measured continuously. The normalized field concentration is a measure of the turbulent diffusivity of the atmosphere between the stack and the sampling site. The techniques and equipment used are described and a summary of the most important findings is included. A simple model of turbulent

atmospheric diffusivity is described which is applicable to some of the problems of air pollution control. The model requires knowledge of two probability distribution parameters—the long term average diffusivity and the frequency of wind in the direction of the point of interest. (auth)

8364 (AERE-R-6556) RADIOACTIVE FALLOUT IN AIR AND RAIN: RESULTS TO THE MIDDLE OF 1970. Cambray, R. S.; Fisher, E. M. R.; Brooks, W. L.; Peirson, D. H. (Atomic Energy Research Establishment, Harwell (England)). Nov 1970. 53p. Dep. NTIS (U. S. Sales Only). UK 8s.

Samples of atmospheric dust and rainwater were collected from the U.K. and elsewhere. Results are presented of analyses of these samples for various fission products and certain other radionuclides. The concentrations of the long-lived fission products ^{137}Cs and ^{90}Sr in air in the U. K. were, in the first half of 1970, about 20% greater than for the first half of 1969; the deposition and concentration in rainwater were also somewhat greater than in 1969. The Chinese explosion of 29th September 1969 contributed about 70% of the long-lived activity in the summer of 1970, which continued at about one-tenth of the levels reached in 1963-64. There has been little change in the rates of deposition of ^{137}Cs and ^{90}Sr since 1966. During 1969 the deposition continued to be slightly less than the loss by radioactive decay of that already deposited. An estimate is made of the worldwide deposition of ^{90}Sr in rain to the end of 1969. Measurements in air in the southern hemisphere show that, in mid-1970, about 80% of the long-lived activity was contributed by the French tests held in the South Pacific in 1968. In 1969 the annual deposition of ^{90}Sr in the southern hemisphere exceeded that in the north for the first time; the cumulative deposit in the south at the end of 1969 was however less than one-third of that in the northern hemisphere. Long-term estimates are made of washout factor and the velocity of dry deposition. Measurements of short-lived fission products from the Chinese explosion of 29th September 1969 and the French tests of May-July 1970 are given in an appendix. (auth) (UK)

8365 (COO-1199-19) STUDY OF RAINOUT OF RADIOACTIVITY IN ILLINOIS. Ninth Progress Report, November 1970. Semonin, Richard G. (Illinois State Water Survey, Urbana). Contract AT(11-1)-1199. 40p. Dep. NTIS.

The Illinois Tracer Experiment (Project Itrex) was conducted during May and June of 1970 to study rainout of radioactivity. The field experiments involved putting indium and/or lithium, contained in aircraft-borne flares, into prescribed parts of thunderstorm clouds, collecting rainwater samples from those clouds at stations over a 1600 sq mi area, and analyzing the storm rainwater for the tracers. The equipment and methods used are described. Data on the cloud core parameters and preliminary data on patterns of thunderstorm deposition of Li, Na, and K introduced into the clouds are presented. Laboratory studies were conducted to determine the scavenging of atmospheric particles by rain. The equipment and method for measuring the collection efficiency of a single drop of rain are described. Measured data on the scavenging efficiency for 1-μm spores of uncharged raindrops in the size range of 0.25 to 4.0 mm dia and of drops of 0.40, 2.8, and 3.7 mm dia with electric charges from 0 to 8×10^{-11} C. The results show that the smallest drops have the greatest scavenging efficiency, and that, for a given size drop, the scavenging efficiency increases with increased electrical charge. (L.C.L.)

8366 (DOCKET-50201-56) WEST VALLEY REPROCESSING PLANT. Quarterly Report, July 1-September 30, 1970, Revision. (Nuclear Fuel Services, Inc., West Valley, N. Y.). 14 Dec 1970. 3p. Dep. NTIS.

A table on ^{85}Kr release in the 18th Quarterly Report was in error and a revision is presented. (M.C.G.)

8367 (HASL-237) FALLOUT PROGRAM. Quarterly Summary Report, June 1-September 1, 1970. Hardy, Edward P. Jr. (New York Operations Office (AEC), N. Y. Health and Safety Lab.). 1 Oct 1970. 117p. Dep. CFSTI.

Eight reports of current data, covering June to Sept. 1970, from the HASL Fallout Program are presented. A separate abstract was prepared for each of six. Two were previously abstracted in NSA as 24: 39495 and 24: 41862. (L.C.L.)

For abstracts of individual sections see: 8353, 8368-8370, 8658, and 8659.

8368 (HASL-237, pp I.27-37) ^{90}Sr DEPOSITION IN THE ATLANTIC OCEAN. [PART] III. Volchok, H. L. (New York Operations Office (AEC), N. Y. Health and Safety Lab.).

From Fallout program.

^{90}Sr analyses have been routinely performed on precipitation samples collected at the four U. S. Atlantic Ocean weather observation stations. Comparing the resultant data with similar collections on land, indicates no systematic differences in either the concentration of this radionuclide in precipitation, or in the seasonal fluctuations of the fallout. (auth)

8369 (HASL-237, pp I.38-62) COMPARISONS OF OBSERVED CONCENTRATIONS OF NUCLIDES IN THE STRATOSPHERE WITH PREDICTIONS BY THE STREAK MODEL. Deland, R. J. (New York Univ., N. Y.).

From Fallout program.

The "Streak" model, developed for explaining and predicting fallout concentrations and distributions in the stratosphere, was used to calculate the stratospheric distribution of radioisotopes from French and Chinese atmospheric nuclear tests conducted during 1967 and 1968. Measured data on the ^{90}Sr inventories from each of these three explosions are compared with the calculated data. It is shown that the computed decrease of stratospheric inventories is quite realistic and that the main variable which causes discrepancies between the calculated and measured data is the altitude of injection. (L.C.L.)

8370 (HASL-237, pp III.18-23) PROTECTIVE SERVICE, SITE SURVEY AND METEOROLOGY SECTION QUARTERLY REPORT. (European Atomic Energy Community, Ispra (Italy). Joint Nuclear Research Center).

From Fallout program.

The results of March to July 1970 fallout monitoring at the Ispra site near Milan, Italy are presented. The measured data included: fallout deposition; gross beta activity, ^{137}Cs, ^{238}Pu, ^{239}Pu, ^{89}Sr, and ^{90}Sr in the atmosphere; and the ^{90}Sr content of milk. (L.C.L.)

8371 (SZS-14/70, pp 1-10) INFLUENCE OF SHORT-TERM ACTIVITY RELEASES INTO THE ATMOSPHERE ON THE ANNUAL RADIATION BURDEN IN THE ENVIRONMENT OF NUCLEAR POWER PLANTS. Eichhorn, H. (Staatliche Zentrale fuer Strahlenschutz, Berlin (East Germany)). (In German).

An evaluation of the influence of short-term radioactive releases on the radiation burden in the environment of nuclear power plants was made by calculating the meteorological distribution conditions for a certain site. As an example, a maximum release of a five-day limit during 10 hours was investigated. It was concluded that in the case of total exploitation of the atmospheric dilution, maximum releases may always lead to an exceeding of the permissible annual radiation burden when in the environment of a nuclear power plant areas of maximum annual radiation burden are concerned. (auth)

8372 ATTITUDE DISTRIBUTION OF ^{238}U, ^{232}Th, AND ^{239}Pu IN ATMOSPHERIC FALLOUT. Styro, B. I.; Shpirkauskaite, N. K.; Kuptsov, V. M. At. Energ. (USSR); 29: 135-6(Aug 1970). (In Russian).

The starting elements of the natural radioactive series ^{238}U, ^{235}U, and ^{232}Th are dispersed everywhere in the Earth; the continual wind erosion carries them with dust particles into the atmosphere which also contains artificial radioisotopes from nuclear testing. The distribution of such long-lived α-emitters in various layers of the air was studied on the basis of fallout specimens collected near the ground. The collectors, consisting of 0.11 m^2 vessels, were placed at 6 levels of the Vilna, Lithuania, television tower, at altitudes of 30, 90, 103, 140, 160, and 200 m. During 1966 to 1968 the measurements were carried out for 5 months during the winter and 7 months during the summer. The uranium isotopes were extracted with diethyl ether, determining the yield on the basis of ^{238}Pu; the thorium isotopes were also extracted and were separated on Dowex 2×10 resin. The ^{238}U and ^{232}Th fallout during the summer was due to wind erosion of the soil. The largest amount was noted at the 30-m level. The presence of ^{239}Pu points to the availability of artificial radioactive materials. The fallout density was found to decrease up to 100 m, remaining constant in the 100 to 160 m layer and starting to increase beyond ~160 m. The observed increase of α active isotopes in the upper layer during the winter may be due to air currents from the Atlantic Ocean. Summertime conversion is responsible for the accumulation of the isotopes. (TTT)

Mineralogy and Exploration

Refer also to abstracts 8393, 10214, and 10328.

8373 WORLD URANIUM PICTURE. Nininger, Robert D. (Atomic Energy Commission, Washington, D. C.). pp 45-52 of Mining Year Book 1970. Denver; Colorado Mining Association (1970).

From 73rd National Western Mining Conference and Exhibition, Denver, Colo. See CONF-700216.

It is noted that in the noncommunist world about 86% of the

known low-cost uranium reserves are controlled by Canada, South Africa, United States, and France. Data on these reserves are discussed for the individual countries. (J.R.D.)

8374 SOME FINANCING APPROACHES FOR SMALL URANIUM OPERATORS. Aley, Maxwell. pp 61-4 of Mining Year Book 1970. Denver; Colorado Mining Association (1970).

In financing exploration it is noted that a well-prepared brochure is very important for information and selling purposes. Information and discussions are also included on partnerships, farm out arrangements, joint operating agreements, private placement of securities, and obtaining funds from venture capital companies. (J.R.D.)

8375 PHOTOGEOLOGY USES IN EXPLORATION OF URANIFEROUS DEPOSITS. Benavente, Carmen Marin (Junta de Energia Nuclear, Madrid). Energ. Nucl. (Madrid); 13: 527-37 (Nov-Dec 1969). (In Spanish).

The geological fundamentals of the photointerpretation are reported. The efficiency and the yield which can be obtained from the application of the photogeological techniques in lithological, tectonic, structural, and geomorphological studies, found in the exploration and investigation of uraniferous deposits, are analyzed. (tr-auth)

8376 URANIUM MINERALIZATION AND ALTERATION, ORPHAN MINE, GRAND CANYON, ARIZONA. Gornitz, Vivien; Kerr, Paul F. (Columbia Univ., New York). Econ. Geol.; 65: 751-68(Nov 1970).

The Orphan Mine uranium orebody occurs in a nearly circular, vertical pipe structure, which ranges from about 150 to 500 feet in diameter. The pipe extends downward from the lower part of the Coconino Sandstone into the Supai Formation and may continue down into the Redwall Limestone. The pipe fill consists of downward displaced massive Coconino Sandstone, angular siltstone, shale and limestone breccia from the Supai and Hermit Formations. There is no intrusive material within the pipe, and therefore, a direct igneous origin is unlikely. The pipe probably formed by solution collapse initiated in the underlying Redwall Limestone. Uranium ore is concentrated in places along the pipe border (Annular Ring) and is distributed in irregular masses within the pipe. Uraninite and pyrite at the center of the pipe grade into a complex mixture of chalcocite, tennantite, chalcopyrite, galena and uraninite at the margins. Elements such as Mo, Co, Ni, As, Mn, and V appear in minor amounts, but Th and the rare earth group have not been detected. Effects of alteration include bleaching of normally red Supai Sandstone near the contact and within the pipe, carbonatization and development of hematitic haloes around uraninite. Significant argillic alteration has not been observed. Temperatures of ore deposition, as suggested by fluid-inclusion thermometry of calcite (60 to 110°C) were somewhat higher than the temperature estimated (58 ± 5°C) from the burial of sediments and the geothermal gradient. A minimum age of about 141 million years has been furnished by U/Pb dating. Sulfur isotope ratios show enrichment in ^{32}S over ^{34}S. The pipe structure and mineral distribution suggest a hydrothermal origin, but a direct unmixed magmatic source is improbable. The ore solutions may have originated in a distant hydrothermal source and in moving upward mingled with groundwater. (auth)

8377 SIMILARITIES, DIFFERENCES, AND SOME GENETIC PROBLEMS OF THE WYOMING AND COLORADO PLATEAU TYPES OF URANIUM DEPOSITS IN SANDSTONE. Fischer, R. P. (Geological Survey, Denver). Econ. Geol.; 65: 778-84(Nov 1970).

Uranium deposits of the Wyoming roll type and the Colorado Plateau peneconcordant type are the principal domestic resources of uranium. Both types occur in lenticular sandstone beds of continental origin, have a similar suite of elements and minerals, are associated with mildly altered rock, and are thought to have formed by reduction precipitation from ground waters before significant regional deformation. They differ in several respects. The Wyoming deposits are in unlithified sandstone that is highly arkosic, whereas the Colorado Plateau deposits are in lithified sandstone that is only slightly to moderately arkosic. Uranium is the only ore metal in the Wyoming deposits, whereas vanadium or copper is more abundant than uranium in some of the Plateau deposits. The Wyoming deposits are elongate crescent-shaped bodies that extend vertically through, or partly through, a sandstone unit and which are scattered, like widely spaced beads on a string, along miles-long interfaces between oxidized (altered) and unoxidized sandstone, whereas the Plateau deposits are thin tabular layers that are nearly concordant to bedding and which occur as discrete bodies, like raisins in raisin bread, enveloped in rock altered by reduction. The Wyoming-ore rolls and interfaces were dynamic, having been pushed downdip by downward-moving oxygen-bearing water that passed through the interfaces and deposited the ore minerals on the reducing side, whereas the Plateau deposits seemingly formed as static bodies, localized by intensive reducing "patches" in a mildly reducing environment. These differences focus attention on genetic problems relating to the Eh of the ore-bearing and altering solutions, the shape and localization of deposits, and the source of the uranium. (auth)

8378 REMOTE SENSING IN EXPLORATION FOR MINERAL DEPOSITS. Lyon, R. J. P. (Stanford Univ., Calif.); Lee, Keenan. Econ. Geol.; 65: 785-800(Nov 1970).

Remote sensing, a new term for an old practice of airborne exploration, has become a "cure-all" for the search for new mineral deposits. Those aspects of the technology which can be of use to the exploration geologist are evaluated, and the various sensors are placed in a priority listing for several types of geological targets. A point of significance to be clearly understood is that the "skin" (or penetration) depth of most sensors is shallow. Remote sensing really offers a chance to rapidly survey large areas, in seeking the diagnostic surface phenomena from more deeply hidden ore deposits. (auth)

8379 URANINITE-BEARING CONTACT METAMORPHIC DEPOSITS, HEATHS PEAK, CARBON COUNTY, WYOMING. Harshman, E. N.; Bell, Kenneth G. (Geological Survey, Denver). Econ. Geol.; 65: 849-55(Nov 1970).

Deposits that contain uraninite and sulfide minerals at Heaths Peak, Carbon County, Wyo., display a zoned distribution of metals from the edge of granite into adjacent metamorphic rocks. The metallic minerals—uraninite, molybdenite, pyrite, chalcopyrite, galena, pyrrhotite, and marcasite—are concentrated on the undersides of metamorphosed roof pendants. At the Little Man mine, deposition was related to a small cupola projecting into the central part of an elongated pendant. The host rocks and the deposits are of Precambrian age. (auth)

Oceanography

Refer also to abstract 8386.

8380 COMMENTS ON THE PAPER BY T. L. KU, Y. H. LI, G. G. MATHIEU, AND H. K. WONG, RADIUM IN THE INDIAN–ANTARCTIC OCEAN SOUTH OF AUSTRALIA. Edmond, John M. (Univ. of California, San Diego, La Jolla). J. Geophys. Res.; 75: 6878-83(20 Nov 1970).

The depletion of Ra in surface waters of the Indian–Antarctic Ocean south of Australia was studied. The hypothesis is presented that the Antarctic Ocean is unique oceanographically in that the effects of carbonate and silicate on radium transport can be clearly differentiated, and that calcium silicate is the radium carrier. Experimental data on silicate concentration, alkalinity, temperature, and ^{226}Ra content in these ocean waters are presented. (L.C.L.)

8381 RADIOCARBON IN THE SOUTHERN OCEANS. Fairhall, A. W.; Ostenson, Alan T.; Yang, I. C.; Young, A. W. (Univ. of Washington, Seattle). Antarctic J. U. S.; 5: 190-1(Sep–Oct 1970).

The ^{14}C content of waters of the Southern Oceans (approximately 40°S) was measured to depths of 4000 m during research cruises in 1968 and 1969. The ^{14}C profile data obtained are compared with data from the Northeast Pacific. Both data show a maximum ^{14}C content at the surface level, a noticeable decrease in ^{14}C with depth to levels between 1000 to 2000 m, and little depth effect thereafter. (L.C.L.)

Seismology

Refer also to abstracts 8356 and 10017.

8382 (UCRL-50939) COMPUTER CODE FOR THE ANALYSIS OF DIGITIZED SEISMIC SIGNALS. Howard, Barry C. (California Univ., Livermore. Lawrence Radiation Lab.). 10 Oct 1970. 46p. Dep. NTIS.

The ADSS code, a multipurpose tool for the reduction of digitized seismic signal data, is presented. The 48 major functions of the code, subroutines identified and called by number, are described. A sample application of the program to digitized seismic data is included. (auth)

XUM

ENGINEERING

Nuclear Explosions

Refer also to abstracts 8354, 8441, 8626, 8627, and 8962.

8383 (AD-706767) HYDRO SHOCK EXPERIMENT. Final Report, February-October 1969. Miller, Edwin; Cushing, Vincent J. (Engineering Physics Co., Rockville, Md.). Jan 1970. Contract N00014-69-C-0238. 17p. NTIS.

A number of small scaled explosions were carried out. The source of the explosion is an exploding wire, energized by rapid discharge from an electrical capacitor. The explosions are nuclear-like in that there are substantially no combustion products. In order to approximate a point-source explosion, the exploding wire consisted of No. 40 Nichrome wire with lengths ranging from 2.3 mm to 4.5 mm. Burst points ranged from a depth of 63.5 mm beneath the water surface to an altitude of 100 mm. Bubble growth and progress of shock fronts in the air and in the water were followed through a schlieren optical system by means of very high speed photography. Pressure-time information, in the water only, was provided by piezoelectric gages. Surface waves were followed by means of high speed photography. (USGRDR) (auth)

8384 (PNE-G-68) CHEMISTRY OF THE GASBUGGY CHIMNEY. Duff, R. E.; Schalit, L. M. (Applied Nuclear Co., La Jolla, Calif.). Nov 1970. 37p. Dep. NTIS.

A model was developed to explain the composition of gas withdrawn from the Gasbuggy chimney following an underground nuclear explosion to stimulate the recovery of natural gas. The model assumes that homogeneous, gas phase reactions occurred during cavity formation among the species formed from the volatile fraction of 1550 tons of formation per kiloton of explosive yield. After chimney collapse, heterogeneous reactions between this gas mixture and natural formation gases occurred which significantly altered the composition. Two criteria are given for choosing the shot points for future explosions: the rock should be free of solid carbon and relatively rich in carbonates. The application of these criteria is expected to reduce significantly the radioactive burden of T and ^{14}C found in the hydrocarbons subsequently produced. (auth)

8385 (PNE-G-69) PETROGRAPHIC ANALYSIS, GASBUGGY NO. 1 AND GASBUGGY NO. 3. Pawlowicz, Richard (El Paso Natural Gas Co., Farmington, N. Mex.). Aug 1970. 76p. Dep. NTIS.

Petrographic descriptions of 107 thin sections from Gasbuggy No. 1 and Gasbuggy No. 3 were made during the summer of 1970. Forty-eight of the sections were from GB-1 and covered a depth from 3493.8 to 4279.8 ft. The remaining 59 sections were from GB-3 and covered a depth from 3850 to 4590 ft. A general description, approximate mineral percentages, and amount of fracturing are included for each section. It is concluded that no definite evidence of effects on Gasbuggy rocks, caused by the nuclear device, can be observed through normal petrographic analysis. (L.C.L.)

8386 (UCRL-50940) WATER WAVES PRODUCED BY CRATERING EXPLOSIONS IN SHALLOW WATER. Garcia, W. J. Jr. (California Univ., Livermore. Lawrence Radiation Lab.). 20 Oct 1970. 7p. Dep. NTIS.

In the course of developing the capability of predicting the characteristics of water waves generated by explosions detonated beneath the ocean floor in shallow water, the pertinent data from past experiments were analyzed using dimensional analysis as a framework. Data were examined from one series of high explosive cratering experiments detonated beneath the floor in shallow water, and from two series of high explosive experiments and one nuclear explosive experiment detonated above the floor in shallow water. The data indicate that the maximum radius of the water column produced by the explosion is proportional to the cube root of the ratio of explosive yield to ambient pressure at the point of detonation. Further, the data show that the maximum radius of the column of water is proportional to the square root of the product of wave height and distance from the source. The conclusions of this scheme of analysis are being tested with hydrodynamic computer code calculations. (auth)

8387 (UCRL-71868) TRANSIENT FLOW IN A GAS RESERVOIR STIMULATED BY A NUCLEAR EXPLOSION: PROJECT GASBUGGY. Sherwood, A. E. (California Univ., Livermore. Lawrence Radiation Lab.). 30 Jul 1969. 47p. Dep. NTIS.

A simplified model is proposed for transient flow in an underground natural gas reservoir containing a gas well created by a nuclear explosion. The usual assumptions of radial flow with an effective well radius are made, but the effect of a large wellbore storage volume is accounted for. A solution is given to a linearized version of the gas flow equations which reduces to simple and useful forms for small or large time. Model parameters are determined using well pressure-time data from the Gasbuggy experiment, and good agreement is obtained between calculations and measurements for nearly one year following detonation. Calculations are also made and compared with measurements of transient pressure in a nearby monitor well and the change in ^{85}Kr concentration in the nuclear well. (auth)

8388 TECHNOLOGY OF NUCLEAR EXPLOSIONS FOR PEACEFUL USES. Kruger, Paul (Stanford Univ., Calif.). Energ. Nucl. (Madrid); 13: 539-67(Nov-Dec 1969). (In Spanish).

The Plowshare Program, the USAEC program for the development of nuclear explosions for peaceful uses, is described in detail. The characteristics of the nuclear explosion itself are first described. The technological properties of such explosions are considered in some detail. The safety considerations of nuclear explosions for peaceful uses are emphasized. Possible applications, such as the cutting of a new canal across the Isthmus of Panama, gas and petroleum production stimulation, deepening of sea harbors, etc., are discussed. (J.S.R.)

Facilities and Equipment

Refer also to abstracts 8432, 8458, 8460, 8914, 9261, 9377, and 9394-9397.

8389 (AERE-M-1990) HIGH TEMPERATURE FURNACE FOR COMPATIBILITY STUDIES. Evans, J. P. (Atomic Energy Research Establishment, Harwell (England)). Dec 1967. 8p. Dep. NTIS (U. S. Sales Only).

An apparatus is described for carrying out compatibility tests at temperatures up to 2000°C in an atmosphere of argon. A dead-weight loading system ensures continuous contact between the components. (auth) (UK)

8390 (AERE-R-5502) SODIUM PURIFICATION AND GENERAL HANDLING FACILITY. Thompson, R.; Evetts, M. A.; Mott, B. W. (Atomic Energy Research Establishment, Harwell (England)). Jul 1967. 10p. Dep. NTIS (U. S. Sales Only).

An account is given of the design and performance of a molecular sodium still, together with a vacuum/glove box for general handling of the purified metal. Analysis of sodium both before and after distillation was made and the results are reported. It is concluded that in general the system worked well but for the production of material of greater purity, particularly with respect to carbon, some modifications to the vacuum systems are required. (auth) (UK)

8391 (EUR-4537) DESIGN AND CONSTRUCTION OF A PROGRAMMER FOR AN ELECTRON BEAM WELDING MACHINE. Herzberger, P. (European Atomic Energy Community, Ispra (Italy). Joint Nuclear Research Center). 1970. 44p. (In French). Dep. NTIS (U. S. Sales Only). EUR FF 6,65.

A programmer for the control and automatization of the welding processes for an electron beam welder is described. The linear velocity of the cylindric samples to be welded is measured. Digital indications of the welding parameters are also obtained.

8392 (GA-9994) NONLINEAR QUASI-STATIC ANALYSIS OF TWO-DIMENSIONAL CONCRETE STRUCTURES. PART I: THEORY. PART II: COMPUTER PROGRAM MANUAL. Rashid, Y. R. (Gulf General Atomic, Inc., San Diego, Calif.). 23 Mar 1970. Contract W-7405-eng-26; Subcontract 2848. 131p. Dep. NTIS.

For Oak Ridge National Lab., Tenn.

A description is presented of the quasi-static nonlinear analysis of concrete structures with particular emphasis on two-dimensional (plane and axisymmetric) structures, such as prestressed concrete pressure vessels. In this analysis, the specific creep of concrete as an age and temperature dependent function, concrete failure under combined stresses, and transient temperature and mechanical loadings are considered. By permitting the pressure to increase monotonically, instantaneously, or as a function of time, ultimate load analyses of prestressed concrete pressure vessels are carried out. The input procedure of the computer program SAFE-CRACK is also described. The program is written in the

XUM

FORTRAN-V language and is compiled for the UNIVAC 1108 computer. It applies the nonlinear analysis to plane and axisymmetric structures and has a capacity of 300 nodal points, 675 elements and 70 time steps. (auth)

8393 (NVO-410-6) MODEL 102 AIR SAMPLER. Kight, Harry K. (Reynolds Electrical and Engineering Co., Inc., Mercury, Nev. Radiological Sciences Dept.). Jun 1969. Contract AT(26-1)-410. 8p. Dep. NTIS.

An effluent sampling device was developed and used successfully to document radioactive effluent release associated with nuclear experiments conducted at the Nevada Test Site. The requirement for effluent sampling in extremely remote areas and rough terrain where commercial power is not available and the high costs associated with maintenance and placement of bulky trailer-mounted equipment previously used, necessitated development of the Model 102. The Model 102 is a self-contained, compact air sampler which utilizes a Roots, Model A. B. 22, blower, driven directly by a Tecumseh, Model HH60, one-cylinder gasoline engine. These components and associated hardware are mounted on a tubular steel frame of all welded construction. Maintenance, calibration and field placement of these units can be accomplished in a few hours by trained personnel. Use of the Model 102 in the effluent sampling program has resulted in significant cost savings and improved efficiency. (auth)

8394 (NYO-3930-7) LIQUID METAL BEARINGS TECHNOLOGY FOR LARGE, HIGH TEMPERATURE SODIUM ROTATING MACHINERY. Progress Report, November 1, 1969-April 31, 1970. (Mechanical Technology Inc., Latham, N.Y.). Contract AT(30-1)-3930. 32p. (MTI-70-TR-61). Dep. NTIS.

Progress in developing the design data and instrumentation needed for reliable design, optimization, and experimental evaluation of sodium-lubricated bearings for high capacity sodium pumps as well as other auxiliaries of the sodium circulation systems for sodium-cooled, fast breeder reactors is discussed. The two main objectives of the program are: extension of turbulent flow bearing theory to incorporate fluid inertia effects, followed by preparation and testing of accurate bearing design data and procedures applicable to the large, highly turbulent sodium-lubricated bearings; and development of accurate and reliable instrumentation with which proximity and film pressure measurements may be made directly in the high temperature sodium environment. The following activities are reported: completion of the analysis and preparation of a computer program for large externally-pressurized bearings; long-term testing of the proximity and film pressure probes in Na at 1150°F; installation of the large tapered metal bearing test rig; and screening and corrosion testing of selected bearing surface materials in 1150°F Na. (L.C.L.)

8395 (ORNL-TM-3077) EXAMINATION OF NICKEL HEAT PIPES CONTAINING POTASSIUM. DeVan, J. H.; Jansen, D. H. (Oak Ridge National Lab., Tenn.). Dec 1970. Contract W-7405-eng-26. 62p. Dep. NTIS.

Three heat pipes constructed of pure nickel that contained potassium as a working fluid were examined after operation at 600°C for 6000 to 10,000 hr. These heat pipes had been designed and operated by the Electronic Components Division of the Radio Corporation of America and were shipped intact to ORNL for metallurgical analyses. No deterioration of the pipes was indicated during operation, and visual examination confirmed that no serious corrosion occurred under the test conditions. Metallographic examination did reveal local areas of the evaporator in which the capillary wick and adjacent pipe wall had been attacked and the attendant formation of a black oxide scale, which appeared to be a double oxide of the type $Ni_xO_yK_z$. Metallographic examination of the condenser area revealed no metallurgical changes other than grain growth. After the test, the potassium contained 50 to 120 ppM O and less than 50 ppM metal impurities. (auth)

8396 (TID-4100(Suppl.61)) ENGINEERING MATERIALS LIST. Smith, Richard J.; Sachs, Francis L.; Clark, Willie E. (eds.) Division of Technical Information Extension (AEC), Oak Ridge, Tenn.). Dec 1970. 66p. DTIE Free.

Twenty-two packages of engineering drawings and specifications are presented. Packages of drawings are included on a plutonium buy back facility, Mark II UV photometer, dual channel log count rate meter, UF_6 sampling and shipping facility, prototype mockup converter (PMC-3) for SNAP-23A, experimental mockup converter (EMC-3) for SNAP-23A, SNAP-21 thermoelectric power system, average radius integrator, PDP-8 interface to IBM controller 2701, leak tester, contour measuring apparatus, Brookhaven portable cesium development irradiator (BPCDI), shock-absorbing caster wheel, encoder, Polly II bubble chamber film processor, photoelectron spectrometer, filter fire test, criticality alarm system, Compton scattering monochromator, lidar system, laser camera Mark II, and one-megajoule inductive energy storage system. A subject index is included. (L.C.L.)

8397 (UCRL-72509) DIGITAL DATA ACQUISITION SYSTEM FOR DISPLACEMENT MEASUREMENT. Hall, Donald F. (California Univ., Livermore. Lawrence Radiation Lab.). Jun 1970. 6p. Dep. NTIS.

This system records time-multiplexed data from many displacement transducers, saving much coaxial cable. Each transducer may be sampled at a programmable rate up to every 10 μsec, for 33 msec, and can resolve a 0.010-inch displacement. The 50-volt transducer output provides an excellent signal-to-noise ratio. The data are recorded in digital form on a disc recorder. (auth)

8398 (Y-1750) COMPENSATING TOOL-PATH DATA IN NUMERICAL CONTROL MACHINE TAPES. Bookhart, T. W.; Easterday, R. J. (Union Carbide Corp., Oak Ridge, Tenn. Y-12 Plant). 7 Dec 1970. Contract W-7405-eng-26. 17p. Dep. NTIS.

A computer routine for making adjustments to two-dimensional tool path data has been incorporated into the APT system as a prepostprocessor. The routine reads the cutter location tape (CL TAPE), makes specified adjustments to the cutter center data, and creates a new CL TAPE for use by the machine postprocessor. (auth)

8399 AUXILIARY EQUIPMENT FOR A NUCLEAR POWER GENERATION TURBINE. Aoyama, Hideyuki (Tokyo Shibaura Electric Co. Ltd., Kawasaki, Japan). Karyoku Hatsuden; 20: 1267-73(Dec 1969). (In Japanese).

Auxiliary equipment for a turbine was constructed for the Tsuruga atomic power station of JAPC. The power station will begin commercial power generation early in 1970. Auxiliary equipment for the turbine is described, with emphasis on the particular auxiliary equipment such as the steam condenser which has anti-earthquake design, provision for elimination of gases from the condensed water, a zigzag passage into the condenser water pool, installed tubes, and tubular plates fabricated by welding. The air ejector is operated by remote switching and automatic adjustment. The feed water heater is described as regards the materials used and construction. (Japan)

8400 ELECTROMAGNETIC FLOW RATE MEASUREMENT DEVICE BRANCHED OFF A PIPE CONTAINING A FLOW OF FLUID. Delisle, Jean-Paul; Lacroix, Andre; Lions, Noel (to Commissariat a l'Energie Atomique). French Patent 1,589,456. 31 Mar 1970. Filed 23 Jul 1968. (In French).

An electromagnetic flow rate measurement device branched off a pipe containing a fluid flow is described. It includes an electromagnetic flowmeter fitted outside the pipe, together with a narrow tube serving to supply the flowmeter with fluid tapped from the pipe and to operate it. The electromagnetic flowmeter is housed in a borated steel envelope containing an argon atmosphere. When the apparatus is destined to supply the flow of the fluid in the pipe on which it is mounted, the tube serving to operate the flowmeter is made up of two sections with one end connected to the flowmeter inlet or outlet and the other ending by a section with a terminal opening turned towards the incoming flow of fluid in the pipe. An interesting application of this device is the flow rate measurement in the pipes of liquid sodium cooled reactor circuits. (France)

8401 AUTOCLAVE VALVE. Vrillon, Bernard (to Commissariat a l'Energie Atomique). French Patent 1,589,447. 31 Mar 1970. Filed 5 Jun 1968. (In French).

An autoclave valve closing the end of the vertical channels of a nuclear reactor is described. The set of fuel elements of the reactor channels rests on the valve through a dummy cartridge. The displacement of the outer end of a lever pivoting around an axis outside the reactor channel is controlled by any suitable means. To the inner end of the lever was fixed a clapper shaped in such a way as to provide continuity of the channel wall in the open position, and measures were provided to prevent the complete opening of the clapper before the dummy cartridge is lifted by a handling machine. Consideration is given to cases where the controls of the lever end displacement are screw-nut or wheel-worm screw systems and cases where they are placed inside or outside the reactor coolant medium. (France)

8402 ARRANGEMENT FOR MOUNTING A FILAMENT THROUGH A WALL. (to Commissariat a l'Energie Atomique). British Patent 1,209,932. 21 Oct 1970. Priority date 27 Sep 1966, France.

An arrangement for mounting a filament such as a sensing

device through a reactor pressure vessel wall is described. The arrangement incorporates a plurality of plastic disks which conform to the aperture and effect a tight seal around the filament while it is extended into the pressure vessel. The disks are so constructed that they provide a hermetic seal upon withdrawal of the filament. (J.R.D.)

8403 ASSEMBLY FOR TIGHTLY CLOSING AN APERTURE. Benzel, Martin (to H. Krantz Verwaltungs GmbH). British Patent 1,208,673. 14 Oct 1970. Priority date 28 Jan 1967, Germany.

The assembly includes a pivotably mounted flap having a groove along its edges which incorporates an inflatable elastic sealing member. Sealing is effected by positioning the flap across the aperture and inflating the sealing member. The assembly is useful for temporary closing of ventilation ducts in radiochemical laboratories or fallout shelters. It is also useful for sealing doors and windows. (J.R.D.)

8404 NOZZLES FOR MIXING A LIQUID AND A GAS TO PRODUCE A DISPERSION OF DROPLETS IN THE GAS. (to Atomic Energy of Canada Ltd.). British Patent 1,214,372. 2 Dec 1970. Priority date 22 Apr 1967, Canada.

The design and operation of a mixing nozzle for producing a dispersion of water droplets in gas flow are described. (L.C.L.)

Heat Transfer and Fluid Flow

Refer also to abstracts 8387, 8395, 8400, 8404, 8961, 10194, and 10203.

8405 (BNL-13957) AN EXPERIMENTAL INVESTIGATION OF TWO-PHASE PRESSURE DROP FOR POTASSIUM WITH AND WITHOUT NET VAPORIZATION. Chen, John C.; Kalish, Sheldon (Brookhaven National Lab., Upton, N. Y.). [1969]. 11p. (CONF-700828-1). Dep. NTIS.

From 4th International Heat Transfer Conference, Paris, France.

Pressure drops were measured for two-phase upward flow of potassium in vertical tubes. Data were obtained for both adiabatic and diabatic conditions, over a range of flow rates, absolute pressures, vapor qualities, and heat fluxes. The results were found to be well correlated by the simple annular-flow model, using an empirical equation for estimation of void fractions. (auth)

8406 (CEA-CONF-1649) HEAT EXCHANGE FOR TWO-PHASE FLOW IN HORIZONTAL AND VERTICAL TUBES. Ricque, R.; Roumy, R. (Commissariat a l'Energie Atomique, Grenoble (France). Centre d'Etudes Nucleaires). [1970]. 11p. (In French). (CONF-700805-4). Dep. NTIS (U. S. Sales Only).

From 4th International Heat Transfer Conference, Versailles, France.

Experimental results for heat transfer with two-phase fluid flow in heated tubes were obtained using Freon-12 and are presented. After preliminary studies with vertical tubes to determine the importance of the effects of bends in the tubing, it was possible to precisely define burnout conditions for dispersed flow in a horizontal tube section preceding a tubing bend. (tr-auth)

8407 (CLM-R-106) VORTEX: A 2-DIMENSIONAL HYDRODYNAMICS SIMULATION CODE. Christiansen, J. P. (United Kingdom Atomic Energy Authority, Abingdon (England). Culham Lab.). Jul 1970. 41p. Dep. NTIS (U.S. Sales Only). UK 5s 6d.

Program VORTEX is a computer code which simulates the behavior of an incompressible, inviscid homogeneous fluid in two dimensions by following the motion of a large number of point vortices. The theory behind the program and the program itself are described. (auth)

8408 (CONF-660675-1) CORRELATION FOR BURNOUT PREDICTIONS IN VERTICAL ROD BUNDLES. Becker, Kurt M. (Aktiebolaget Atomenergi, [Studsvik] (Sweden)). 1966. 72p. (S-349). Dep. NTIS (U.S. Sales Only).

From Symposium on Boiling Crisis in Two-Phase Flow Systems, Ispra, Italy.

A correlation for predicting the burnout conditions for flow of boiling water in vertical rod bundles is presented. The correlation is based on the Becker round duct correlation and was written in the form: $x_{BO} = 0.68 \cdot \eta \cdot \eta_1 \cdot x_{RD}$, where x_{RD} is the burnout steam quality in a round tube at corresponding flow conditions, η is the ratio of heated to total perimeter and η_1 is a correction factor, which is a function of q/A only. It was demonstrated that this equation combined with the heat balance equation $q/A = [G/(4L/D_H)] [\Delta h_{sub} + x_{BO} h_{fg}]$ predicts the burnout heat fluxes for 352 measurements obtained within a scatter of ±7.5% and with an RMS error of 3.8%. The correlation shows that the burnout conditions in wide ranges of variables are independent of the inlet sub-cooling and the heated length, and that the effects of mass velocity and pressure are the same in rod bundles and in round tubes. It was also demonstrated that the effects of a radial heat flux variation within the rod bundle can be handled by the correlation by modifying the η-value for the bundle. The rod bundle data obtained by other investigators were also analyzed in terms of the measured and predicted burnout heat fluxes. It was found that a very good agreement existed between the present correlation and the measurements. (auth)

8409 (RD/B/N-1755) NOTE ON THE METHOD OF SUPERPOSITION OF TEMPERATURE DISTRIBUTIONS IN FORCED CONVECTION HEAT TRANSFER EXPERIMENTS. Elston, M. J. H. (Central Electricity Generating Board, Berkeley (England). Berkeley Nuclear Labs.). Jul 1970. 43p. Dep. NTIS (U. S. Sales Only).

The method of superposition was investigated for the general case of a steady flow, forced convection heat transfer system, consisting of gas-cooled electrically heated elements in a duct. In a theoretical development, the non-linear equations governing the temperature distribution are linearised by taking the limit of zero heat generation rate. Isothermal dimensionless temperatures defined in this process are shown to be valid throughout the system, including heated material regions, providing the coolant remains at low Mach number and is remote from its critical point. It is further shown that, provided ambient conditions remain constant, small deviations from ideally constant inlet conditions and adiabatic system boundary conditions do not lead to systematic errors in the superposition process. An experimental investigation using two A. G. R. clusters of fuel elements, one tested in atmospheric air and the other in pressurised CO_2 reveal systematic differences of up to 2% between superposed and measured temperatures for heated pins. However, this is less than the uncertainty in the experimentally obtained isothermal dimensionless temperatures and the method of superposition is therefore taken to be confirmed to within the accuracy of these experiments. (auth) (UK)

8410 USE OF FREON 12 TO MODEL FORCED CONVECTION BURNOUT IN WATER: THE RESTRICTION ON THE SIZE OF THE MODEL. Stevens, G. F.; Macbeth, R. V. (Atomic Energy Establishment, Winfrith, Eng.). J. Brit. Nucl. Energy Soc.; 9: 249-57(Oct 1970).

From initial experimental work it appeared that in modeling forced convection burnout there was little restriction on the size of the model, provided dimensional similarity was maintained. Test results on uniformly heated round tubes showed that burnout in water was accurately modeled by Freon 12, even though the Freon 12 test section varied from twice the size to one quarter the size of the water test section. Since these early tests, more experimental results for annuli and multi-rod clusters with both uniform and nonuniform axial heat flux profiles were produced at Winfrith. These results showed that with the more complex geometries a restriction on physical size does appear to exist. All the relevant experimental facts are presented and the conclusion is reached that for universal application of the Freon modeling technique, the burnout test section in the Freon experiment must not be much smaller in size than the water channel under study. (auth) (UK)

8411 TWO PHASE FLOW IN THE BLEED PIPING OF A NUCLEAR TURBINE. Saito, Ryozo (Hitachi Ltd., Tokyo). Karyoku Hatsuden; 21: 9-12(Jan 1970). (In Japanese).

The bleed piping of a nuclear turbine inherently involves the problem of steam-water mixture flow. Since this unstable phenomenon of two-phase flow may act as a power source for the forced oscillation of the system, the design of bleed piping should be such that the unstable flow in which pulsation occurs is avoided. To gain a basic understanding of the phenomena in the piping, a series of experiments was carried out with a nearly full size model in which the test section was supported horizontally and vertically. Under turbine operation conditions, using 6B pipes, the observation of steam-water mixture flow brought out useful results. It was concluded that when the pressure in the pipe is higher, stable flow is more easily obtainable at low velocity. Although the velocity of the fluid may be increased in order to get stable flow, the upper limit is restricted by increased erosion. The examination of the liquid film reveals that the increase in steam velocity decreases the thickness of liquid film, while the increasing liquid quantity increases it. (Japan)

8412 TEPLOFIZICHESKIE SVOISTVA ORGANICHESKIKH TEPLONOSITELEI. (Thermophysical Properties of Organic Coolants). Vukalovich, M. P.; Babikov, Yu. M.; Rasskazov, D. S. Moscow; Atomizdat (1970). 240p.

XUM

The thermophysical properties of organic liquids used as coolants in nuclear installations are discussed. Experimental data are presented on density, equilibrium phases, thermal capacity, viscosity, thermal conductivity, and surface tension of the most commonly used heat transfer media. Experimental methods for investigating the stability and thermal properties of liquids are described. Tables are presented of recommended values of the thermophysical properties of coolants as functions of temperature and concentration of products of decomposition resulting from pyrolysis and radiolysis. The accuracy of the tabulated data is evaluated. (406 references) (tr-auth)

8413 APPROXIMATE SOLUTION AND MEASUREMENT OF THE STEADY TEMPERATURE DISTRIBUTION IN A FINITE REGION WITH MANY CIRCULAR HOLES. Takeuti, Yoitiro (Shizuoka Univ., Hamamatsu, Japan); Sumi, Naobumi; Nada, Hideyuki. Nippon Kikai Gakkai Rombunshu; 36: 258-65(Feb 1970). (In Japanese).

The heat transfer in a reactor or in an electronic circuit component is concerned with internal heat generation in a finite region with many circular holes. Analytical approximate solution was obtained for circular and square regions, the outer boundary of the region was assumed to be thermally insulated. The Poisson equation was solved with a suitable boundary condition by means of series expansion. The infinite series was approximated by finite terms, and the coefficients were determined from the valves assigned to boundary points. In order to confirm the accuracy, a simulation experiment was performed using ac and dc methods. The result of the measurement is in good agreement with the calculation. The case in which heat was not generated was also treated both theoretically and experimentally, in order to see the accuracy of the present method. (Japan)

8414 NATURAL CIRCULATION STABILITY OF HEAT TRANSFER AGENT IN ONE-LOOP SYSTEM. Znyshev, V. V.; Sabaev, E. F. (Gorky State Univ., USSR). Izv. Vyssh. Ucheb. Zaved., Radiofiz.; 13: 1178-87(1970). (In Russian).

The stationary mode stability in a heating system which is a loop with a heat-transfer agent circulating due to heterogeneous distribution of the agent's specific weight over the loop length was studied. Heat-exchange dynamics in the loop are described by a set of equations with deviating arguments. Sufficient conditions for total stability and inequalities for determining the equilibrium state were obtained. (auth)

8415 EXPERIMENTAL DEMONSTRATION OF INERT GAS EFFECTS UPON THE INCIPIENT POOL BOILING OF SODIUM. Singer, Ralph M. (Argonne National Lab., Ill.). Nucl. Sci. Eng.; 42: 427-8(Dec 1970).

A series of tests were conducted to determine the effects of inert gas partial pressure variations on the heat flux measurements in incipient boiling of Na. Results of the tests show that loss of inert gas from surface cavities in alkali metals can mask other phenomena such as incipient-boiling superheat. It is noted that experimenters should avoid or at least be aware of uncontrolled variations in inert gas pressure in surface cavities when studies of parameters other than incipient boiling are in progress. (J.R.D.)

8416 HEAT TRANSFER IN SMOOTH TUBES, BETWEEN PARALLEL PLATES, IN ANNULI, AND TUBE BUNDLES WITH EXPONENTIAL HEAT FLUX DISTRIBUTIONS IN FORCED LAMINAR OR TURBULENT FLOW. Graeber, H. (EURATOM–CEN, Saclay, France). Int. J. Heat Mass Transfer; 13: 1645-1703(Nov 1970). (In German).

By introducing an additional parameter F_ϑ, the processes for calculating heat transfer are extended to the heat flux distributions which give a heat transfer coefficient independent of position downstream of the thermal and hydraulic stabilization regions. This condition is satisfied for laminar and turbulent flow with a linear pressure drop when the heat flux distribution follows an exponential law $q_w = \exp(mx)$, as with heat exchangers. The influence of the exponent m on the heat transfer is described by the differential quotient $d\vartheta_w/d\vartheta_0 = F_\vartheta$, defined by the temperature gradients $d\vartheta_w/dx$ along the wall transmitting the heat and $d\vartheta_0/dx$ in the fluid at the point where the temperature gradient normal to the wall reduces to zero. For the annular space, the equations for explicit calculation of the temperature field will be given, as well as the Nusselt number in laminar flow and constant heat flux, the heat transfer taking place on one wall or both. In turbulent flow, the laws of distribution of eddy diffusivity for momentum in a tube, established by H. Reichardt, adapted for the annular space and the tube bundle, give the velocity field and the coefficient of friction and thus permit solution of the heat transfer equations. The results of the numerical calculation carried out with an IBM-7094 computer are given in the tables and diagrams for an extended range of the various parameters and compared with the experimental results: distribution of velocity, temperature and heat flux density normal to the wall, Nusselt number and mean temperature. A simple process to determine the lower limit of the thermal entry length is described. (auth)

8417 AXIAL DISTRIBUTION OF BULK TEMPERATURE AND VOID FRACTION IN A HEATED CHANNEL WITH INLET SUBCOOLING. Ahmad, S. Y. (Atomic Energy of Canada Ltd., Chalk River, Ont.). J. Heat Transfer; 92: 595-609(Nov 1970).

A theoretical model is developed to determine the axial temperature distribution of subcooled liquid. It is a simple function of a heat transfer and a condensation parameter. The proposed model satisfactorily correlates the measured bulk temperature profiles. The corresponding void fraction is computed by using a new empirical slip correlation, valid in both subcooled and bulk boiling regions. The resulting axial void profile has been compared (over the entire heated length) with steam and water data from six different sources, covering a wide range of pressure, mass flux, surface heat flux, inlet subcooling and channel geometry. The method gives satisfactory agreement with experimental data. (auth)

8418 DEPARTURE FROM NUCLEATE BOILING IN ROD BUNDLES DURING PRESSURE BLOWDOWN. Cermak, J. O. (Westinghouse Electric Corp., Pittsburgh); Farman, R. F.; Tong, L. S.; (and others). J. Heat Transfer; 92: 621-7(Nov 1970).

Tests were performed in a high pressure heat transfer loop to determine the behavior of transient departure from nucleate boiling (DNB) during pressure blowdown in rod bundles. Water flowed along a 21-rod, 5-ft-long electrically heated rod bundle with a radially nonuniform heat flux distribution. Both steady-state and transient DNB tests were conducted over the following range of operating parameters: pressure of 750 to 1500 psia; inlet temperature of 480 to 540°F; mass velocity of 1×10^6 to 3×10^6 lb/hr ft^2; and grid configurations of 2. The data were analyzed using calculated subchannel local velocity and enthalpy as a function of time with proper allowance for the mixing and cross flow within the bundle. Results show that the inception of transient DNB during pressure blowdown can be predicted on the basis of steady-state data. (auth)

8419 EFFECT OF BUBBLE STABILIZATION ON POOL BOILING HEAT TRANSFER. Fuls, G. M. (Westinghouse Electric Corp., Pittsburgh); Geiger, G. E. J. Heat Transfer; 92: 635-40(Nov 1970).

It is an established phenomenon that bubbles can be stabilized in a vertically vibrating liquid column. The effect of bubble stabilization on the rate of pool boiling heat transfer is experimentally investigated. With the liquid and heating surface vibrating as a unit, the data indicates a decrease of up to 12 percent in the temperature difference necessary for a given heat flux within the range of frequencies from 200 to 300 cps. The experimental results and comparison with results of previous investigators show that the effect is unique and not due simply to the vibrations per se. (auth)

8420 QUASI-DEVELOPED TURBULENT PIPE FLOW WITH HEAT TRANSFER. McEligot, D. M.; Smith, S. B.; Bankston, C. A. J. Heat Transfer; 92: 641-50(Nov 1970).

Available literature on wall friction and heat transfer for gas flow strongly heated in the downstream region of tubes shows disagreement between analysis and experiments. Possible explanations are examined quantitatively, then the governing equations are treated in more complete form than in previous analyses. The results compare favorably with existing experiments for nonreacting, high-Reynolds-number, turbulent flow of a gas with negligible natural convection and with a constant wall heat flux imposed. (auth)

Isotope Technology

Refer also to abstracts 8315, 8328, 8363, 8537, 8711, 8736, 8850, 9537, and 9595.

8421 (AERE-M–1594) INTERIM REPORT ON THE FIRST BRITISH RADIOACTIVE ISOTOPE POWERED THERMOELECTRIC GENERATORS R.I.P.P.L.E. I AND II. Dunn, P. D.; Yeats, F. W. (Atomic Energy Research Establishment, Harwell (England)). May 1965. 11p. Dep. NTIS (U. S. Sales Only).

The original design figure of 30 milliwatts at a useful voltage was achieved. While the power output from the RIPPLE generator is very low, the design concepts used can be readily incorporated into larger powered generators. The difficulties encountered in conserving the heat, and the problem of inverting low voltages improved as the size of the generator increased

XUM

and a considerably higher overall efficiency than that achieved in these generators is possible. The use of thermoelectric material capable of operating at higher temperatures will also improve the overall efficiencies. The lead telluride family of materials is a possibility. Inversion efficiencies of twice that achieved on RIPPLE are possible in the power output range 0.5 to 3 W(e). With development the expected limits for overall efficiency (for the complete generator and output power >1 W(e)) are 4% for the Bi_2Te_3 type material (<250°) 6% for the PbTe type (<550°C) and 8% for the GeSi material (<1000°C). (auth) (UK)

8422 (CU-755-7, Sect. 5) EFFECT OF CHEMICAL EXCHANGE BETWEEN D_2 AND HBr ON THE THERMAL DIFFUSION SEPARATION OF D AND H IN A TRENNSCHAUKEL. Mathur, B. P. (Columbia Univ., New York. Dept. of Chemistry). 22p.

The trennschaukel used to study the exchange between D_2 and HBr is described in detail. Test runs of the apparatus were made using Ne–Ar and H_2–D_2 mixtures. These results are tabulated and show good reproducibility. An equation is given for calculating the thermal diffusion factors. The D_2–HBr mixtures presented serious problems, and all ultimate samples for mass spectral analysis were in the form of H_2, HD, and D_2 mixtures. For the uncatalyzed exchange the D was found to concentrate in the hot region, but the presence of Pt as a catalyst caused D to concentrate in the cold region. Even though chemical exchange results in a reduction of the concentration of D in the hot region, it was not a sufficient effect to cause the D to be preferentially transferred to the cold region. (B.L.M.)

8423 (MLM-1439(Rev.)) THERMAL DIFFUSION COLUMN COEFFICIENTS FOR THE SEPARATION OF N_2^{14}–$N^{14}N^{15}$ AND O_2^{16}–$O^{16}O^{18}$. Kaminski, K. J.; Rutherford, W. M.; Willis, M. S. (Mound Lab., Miamisburg, Ohio). 23 Dec 1970. Contract AT(33-1)-Gen-53. 127p. Dep. NTIS.

The thermal diffusion column coefficients H', K'_c, and K_d of the Jones and Furry theory were compared to coefficients obtained from experiments dealing with the separation of the N_2^{14}–$N^{14}N^{15}$ and the O_2^{16}–$O^{16}O^{18}$ systems. The thermal diffusion column transport equation was developed from general kinetic theory expressions which describe the mass flux resulting from concentration and temperature gradients. This equation contains collections of integrals which are represented by the column coefficients H', K'_c, and K_d. In order to evaluate the column coefficients from theory, the temperature dependence of the viscosity, thermal conductivity, diffusivity, and thermal diffusion factor must be known. A complete set of smoothed experimental transport properties for N_2 and O_2 between 200 and 1100°K was obtained from the literature. Column coefficients for the experimental conditions were evaluated on the basis of these properties. The thermal diffusion column coefficients were determined from separation experiments performed under both static and flowing conditions at hot wall temperatures of 500 and 800°C. The column, which was 24 ft (7.2 m) long, had an inside (cold wall) diameter of 0.750 in. (18.95 mm). The hot wall was a 0.063 in. nichrome wire. Detailed drawings of the column and accessory equipment along with operating procedures are presented. The results indicate that the Jones and Furry column theory adequately describes the separation of the O_2^{16}–$O^{16}O^{18}$ and the N_2^{14}–$N^{14}N^{15}$ systems in the thermal diffusion column. The ratios of the experimentally determined column coefficients to those calculated theoretically were 0.974 ± 0.047, 0.954 ± 0.134, and 1.07 ± 0.056, for H', K'_c, and K_d. The deviations between experiment and theory were, in general, within the combined limits of the estimated experimental error and the estimated error in the theoretical calculations. (auth)

8424 (MLM-1768) STABLE GASEOUS ISOTOPE SEPARATION AND PURIFICATION: JULY–SEPTEMBER 1970. (Mound Lab., Miamisburg, Ohio). 11 Dec 1970. Contract AT-33-1-GEN-53. 35p. Dep. NTIS.

Developments are reported for studies on carbon isotope separation; separation of stable isotopes of argon, krypton, neon, and xenon; and thermal diffusion research. (R.C.K.)

8425 (NP-18563) INFORMATION BULLETIN ON ISOTOPIC GENERATORS. Number 10, November 1970. (European Nuclear Energy Agency, Paris (France)). Commissariat a l'Energie Atomique, Saclay (France). Centre d'Etudes Nucleaires). 55p. Dep. NTIS (U. S. Sales Only).

The development by the C.E.A. of sealed ^{238}Pu sources for implantable cardiac pacemakers is reviewed. The safety requirements for such sources and methods for testing the chemical, mechanical, radiological, and thermal safety of isotopic batteries are discussed. (L.C.L.)

8426 (NSJ-tr-155) CHOICE OF ACTIVABLE TRACER FOR SPRAYING AGRICULTURAL INSECTICIDES BY HELICOPTER. Bando, Shoji; Tominaga, Hiroshi; Kawakami, Yutaka; Senoo, Muneaki. Translated from Radioisotopes (Tokyo); 18: 488-93(Nov 1969). 13p. Dep. NTIS (U. S. Sales Only).

The fundamental studies were made on the selection of activable tracers which can be used for examining the distribution of agricultural insecticide sprayed by helicopter. Considering the conditions that the samples are organic substances, sufficiently strong radioactivity should be produced in a short irradiation-time, and the half life of the activity is desired to be longer than two hours for the sake of convenience of activity measurement, manganese, gold and europium were selected as typical tracers. Other conditions required for the field experiments were checked on these elements. Minimum detectable limits of each tracer were estimated from both the activity produced by each tracer and the background due to interference components in the sample. As a result, europium tracer was found to be the best in sensitivity (minimum detectable limit was 1.5×10^{-10} g Eu/5 cm^2 filter paper) and also in cost, if the sampling was carried out using filter paper and a thin scintillator was used to measure low energy photons. Therefore, it was concluded that europium would be the most suitable tracer for the determination of distribution of insecticide sprayed by helicopter. (auth)

8427 (ORNL-4639) ORNL ISOTOPIC POWER FUELS QUARTERLY REPORT FOR PERIOD ENDING SEPTEMBER 30, 1970. Lamb, Eugene (Oak Ridge National Lab., Tenn.). Dec 1970. Contract W-7405-eng-26. 28p. Dep. NTIS.

The solubility and leach rates of $^{244}Cm_2O_3$ are being studied because of their importance in preventing release of radioactivity in the event of exposure of a ^{244}Cm isotopic power fuel to the earth's environment. Dense pellets of $^{244}Cm_2O_3$ were exposed to water for four weeks in preliminary experiments. There was no apparent damage and it is believed that the rate of dissolution (by hydration) will be controlled. A means of releasing helium produced by decay in $^{244}Cm_2O_3$ with a minimum loss of $^{244}Cm_2O_3$ is being studied. A study of alpha-particle damage in cermets is being made to define the effect of some of these variables on the volume % of the metal affected. A study of the effect of varying the radiation dose rate on the diffusion parameter of helium in $^{244}Cm_2O_3$ has been completed. A 2200-W heat source using $^{244}Cm_2O_3$ as the fuel form is being designed as an alternative heat source for the generator being designed by General Electric. Eighteen $^{170}Tm_2O_3$ pellets have been selected for the compatibility study. An oxidation-resistant strong cladding alloy has been prepared that has a melting point greater than 2000°C. (auth)

8428 (ORNL-IIC-30(Pt.3)) SELECTED ABSTRACTS OF WORLD LITERATURE ON PRODUCTION AND INDUSTRIAL USES OF RADIOISOTOPES (FROM NSA JULY–SEPTEMBER 1970). Gerrard, Martha; Baker, P. S. (Oak Ridge National Lab., Tenn.). Dec 1970. Contract W-7405-eng-26. 49p. Dep. NTIS.

Approximately 430 abstracts of domestic and foreign publications on production and use of radioisotopes and radiation, selected from the July–September 1970 issues of Nuclear Science Abstracts, are presented. (auth)

8429 (ORNL-tr-2400) TECHNOLOGY OF ISOTOPE PRODUCTION. PART I. IRRADIATION TECHNOLOGY. Knoll, Peter (Zentralinstitut fuer Kernphysik, Rossendorf bei Dresden (East Germany)). Translated by J. J. Pinajian (Oak Ridge National Lab., Tenn.), from report ZFK-RCH-1. 86p. Dep. NTIS.

Isotope technology development in the German Democratic Republic is reviewed. Discussions are included on production equipment and programs, scheduling, production control, target standardization, target can design, and target requirements. Isotope data tables are also included. (J.R.D.)

8430 FRENCH NUCLEAR-POWERED PACEMAKER PROGRAM. Alais, M.; Berger, R.; Boucher, J. D.; (and others) Nucl. News; 13: 42-6(Dec 1970).

The French program for developing a ^{238}Pu-fueled cardiac pacemaker is reviewed. The design, fabrication, operating characteristics, and testing of the components are described. Laboratory experiments with implantation in dogs and clinical uses in humans are discussed including the measured dose rates to the bearers. The two year study resulted in the following conclusions: the radiation dose rates received by the bearer of this type of nuclear-powered cardiac pacemaker and by the general population seem to be below regularly admitted levels; the pacemaker design assures a high degree of nuclear safety; international regulation for clinical use of nuclear-powered pacemakers is making good progress; the reliability of the pacemaker is great; and the bearer of such a pacemaker will be able to live a normal life for at least 10 years without any surgical intervention. (L.C.L.)

8431 URANIUM ENRICHMENT IN THE U. K. Geoghegan, G. R. H.; Kehoe, R. B. Atom(London); No. 169, 224-30(Nov 1970).

XUM

The development of diffusion and centrifuge plants is discussed. Preliminary studies of centrifuge plants had indicated that costs would be prohibitive, but fresh studies in 1967 and 1968 showed that compared with diffusion plants larger centrifuge plants than those previously considered had lower specific capital costs. Improved detail design and a close investigation of manufacturing methods for centrifuges showed that they could be substantially cheapened and that machine life was greater than had previously been assumed. A full comparison study of diffusion and centrifuge plants is given. A tri-national organisation, which is now being set up, consisting of the U. K., the Netherlands and the German Federal Republic and comprising separate companies for the development, construction and operation of centrifuge plants is described. With this organisation it is hoped to combine the best features of machine and plant design, to lower costs for each country and to secure a large share of the European market. It is felt that the centrifuge process offers the greatest potential for a local and viable source of enrichment for the European nuclear power industry. (UK)

8432 NEW ASPECTS IN THE FIELD OF GAMMA IRRADIATION PLANTS. Christen, H. Sulzer Tech. Rev.; 52: No. 1, 59-63(1970).

Applications of gamma irradiation including the radiosterilization of equipment, foodstuffs, and pharmaceutical products, and the production of new combinations of materials such as concretes and plastics (concrete polymer) and plastics and wood are discussed. Gamma irradiation facilities are described, and irradiation costs in large and small facilities are compared. (L.C.L.)

8433 CLOSED SYSTEM GENERATION AND CONTAINERIZATION OF RADIOISOTOPES. Shumate, Donald J. (to Mallinckrodt Chemical Works). U. S. Patent 3,535,085. 20 Oct 1970. Filed 7 Aug 1967.

A generator and process are described for obtaining a sterile daughter radioisotope solution from a parent radioisotope. The generator includes a center chamber containing the parent radioisotope, an upper chamber closed by a rubber stopper for injection of a sterile eluant, and a lower chamber closed by a rubber stopper for receiving the eluate solution from the center chamber. A fritted glass filter separates the center and lower chambers. The sterile eluate containing the dissolved daughter radioisotope is drawn from the lower chamber into an evacuated sterile vial via a tube fitted at each end with a tubular needle, the vial being closed by a rubber stopper. (auth)

8434 USE OF THE ^{125m}Te ISOTOPE AS A SOURCE OF X-RAY RADIATION. Smirnov, V. N.; Ushkova, M. I.; Novikov, A. M. This paper was summarized in At. Energ. (USSR); 25: 424-5(Nov 1968) as paper No. 240. (In Russian).

Radioactive preparations of metallic Te having an activity of about 100 mCi from ^{125m}Te were investigated. It was found that the radiation from this isomer with an energy of 110 keV can be used to excite the fluorescent spectra of elements Z = 70 to 90. The 110-keV radiation can also be used in absorption radiography of Pb, Bi, Hg, and W. The line with the energy of 27.5-keV can be used for absorption radiography of elements Z = 40 to 48. (J.R.D.)

8435 CREATION OF AN INSTALLATION FOR THE ENRICHMENT OF URANIUM IN THE EUROPEAN COMMUNITY. Baruffa, A. Neue Tech., B; 10: 237-41(1968). (In French).

The creation in the European Community of a facility for uranium enrichment involves an examination of commercial, political, and technical problems of considerable difficulty. These considerations include: the enrichment requirements and capabilities of the western world, particularly those of the Community and the availability of enriched uranium supplies from the UK or USA; the technical and industrial aspects; economic aspects; and a comparison of currently used enrichment processes, i.e., gaseous diffusion, ultracentrifugation, and the gas nozzle process. (E.J.H.)

8436 IMPLANTABLE CIRCULATORY SUPPORT SYSTEM. Lance, Joseph R.; Disney, Richard K.; Selz, Allen; Tauson, Peter O. (to United States Atomic Energy Commission). U. S. Patent 3,534,409. 20 Oct 1970. Filed 10 Jun 1968.

An implantable circulatory support system incorporating a steam power conversion loop utilizing an isotopic heat source, a steam engine and a hydraulic power transmission loop for utilizing engine shaft power to operate a replacement blood pump is described. Heat is rejected to the blood of the donee while the power transmission loop provides water make up for the conversion loop. (Offic. Gaz.)

8437 USE OF TRITIUM TARGETS FOR BETA-IRRADIATION EXPERIMENTS. Radzievskii, G. B. (Inst. of Biophysics, Moscow). Instrum. Exp. Tech. (USSR) (Engl. Transl.); No. 1, 75-6 (Jan-Feb 1970).

Translated from Prib. Tekh. Eksp.; No. 1, 70-1(Jan-Feb 1970).

The distribution of the energy absorbed in light materials in contact with the active surface of a tritium target was measured. A plane-parallel ionization chamber in which the air pressure could be varied was used for the measurements. The dose distributions above the targets turned out to be close to exponential: $P(x) = P(0)e^{-\alpha x}$, where P is the dose rate, and α (for water) = 1.50 μ^{-1}. From this result, the form of the function describing the dose distribution around a point tritium target can be found: $\psi(r) = 1.27\ \alpha^2 E e^{-\alpha r}/r$, where E (keV) is the average energy of the β-spectrum, r is in microns, and ψ is in rad/sec · disintegration. (auth)

8438 EFFECT OF FLOW PATTERN IN GASEOUS DIFFUSION PROCESS. Higashi, Kunio; Doi, Hideo; Saito, Toru (Kyoto Univ.). Nippon Genshiryoku Gakkaishi; 12: 649-54(Nov 1970). (In Japanese).

In the process of uranium enrichment by gaseous diffusion, the scale of operation of the plant e.g., barrier area and power consumption, is highly dependent on the single stage separation factor. The effect of the flow pattern on the separation factor is worth thorough investigation, because it may contribute to reducing the plant size by one-half. The flow patterns of perfect mixing and cross-flow are analyzed. The results should serve in estimating quantitatively any intermediate flow pattern between these two extreme cases. Various flow patterns were realized by connecting in series 1 ~ 10 pieces of barrier made of sintered nickel. Good separation was obtained with cross-flow, as verified by experiments in isotope separation made on nitrogen gas. The applicability of the analysis to the estimation of intermediate flow patterns was demonstrated. Cases of counter-current flow and parallel flow can be dealt with similarly to cross-flow. (auth)

Materials Testing

Refer also to abstracts 8389, 8392, 8871, 8881, and 8883.

8439 (ORNL-4600, pp 153-6) NONDESTRUCTIVE TESTING TECHNIQUES FOR LMFBR. (Oak Ridge National Lab., Tenn.).

From Fuels and materials development program.

Efforts devoted to development of new methods, techniques, and equipment for nondestructively evaluating materials are reported for liquid-metal-cooled fast breeder reactors (LMFBR) with emphasis on measuring cold work in stainless steel tubing. An eddy-current instrument is being developed to measure both size and depth of defects and have constructed new modular circuits for the instrument. Ultrasonic schlieren techniques are being compared with both delta and conventional ultrasonic techniques for the examination of flaws in welds of both Al and stainless steel. Construction and assembly of components is continuing on the high-sensitivity impedance bridge to be used in the measurement of changes in magnetic permeability related to cold work in stainless steel tubing. Studies were initiated with the electron microscope on samples that contain various degrees of cold work to relate microstructural changes to the results of nondestructive tests. (auth)

8440 (ORNL-4600, pp 266-70) NONDESTRUCTIVE TESTING. (Oak Ridge National Lab., Tenn.).

From Fuels and materials development program.

A matrix method using Green's functions was developed; it improves methods of calculating solutions to problems of electromagnetic induction. Computer programs were used to design an eddy-current coil with superior accuracy for the measurement of electrical conductivity. Results of studies on frequency analysis of ultrasonic signals emphasized characterization of hidden flaws. Analytical expressions developed during the period were confirmed experimentally for the determination of both angular orientation and diameter of reflectors using analysis of the frequency spectrum. Fluorescent x rays excited in U by radiation from a Pm source were used to measure changes in Al thickness placed on the U. Preliminary development of techniques for using a closed-circuit television system as part of a high-speed, high-resolution densitometer is reported. (auth)

8441 (SC-RR-70-600) ACCEPTABLE IMPERFECTIONS IN IMPULSIVE LOADS FOR SIMULATION TESTS ON CIRCULAR CYLINDRICAL SHELLS. Julian, Carl L. (Sandia Labs., Albuquerque, N. Mex.). Sep 1970. 72p. Dep. NTIS.

The membrane strain in a thin elastic shell that is subjected to simultaneously applied impulsive loads is considered. The shell is infinitely long, cylindrical, and circular in cross section. The shell is made of a single isotropic, homogeneous, uniformly thick material. It is concluded that if an adjustable but imperfect load

is used to approximate an ideal load, then a good strategy is to match locally the surface integrals of the distributed impulse functions. This strategy is guessed to be applicable to more general shells. The present work partially justifies the technique for spacing explosive rods over foam. (auth)

8442 TECHNIQUE FOR OBTAINING NEUTRON RADIOGRAPHS IN THE RESONANCE REGION. Forman, L.; Benton, C. U.; Garrett, D. A.; Schelberg, A. D. (Los Alamos Scientific Lab., N. Mex.). Rev. Sci. Instrum.; 41: 1900-1(Dec 1970).

The transmission of neutrons through a resonance sample can show wide variations dependent upon neutron energy. A technique for obtaining an image from transmitted neutrons in a desired energy interval is described. The technique employs time-of-flight methods to define neutron energies of interest. Moderated neutrons from the Sandia Pulsed Reactor Facility were transmitted through a sample onto a neutron sensitive lithium-6 loaded glass fluor. Fluor light was then focused onto the photocathode of an image intensifier television camera tube. This tube contains a channel plate electron multiplier assembly coupled to an EBIC storage target. It has sufficient gain to observe single photoelectrons. The tube was gated to record an image during a time interval corresponding to the neutron energy interval of interest. (W.H.K.)

8443 NONDESTRUCTIVE TESTING: NEW RADIOGRAPHIC PROCESS. Wright, D. L. Metals Aust.; 2: 180-1(Jul 1970).

A direct viewing x-radiographic process is described which operates on-stream following the welding operation. An x-ray image intensifier (up to X8000) is used enabling the detection of small defects. The system comprises a Mueller 150 kV constant potential x-ray unit with fine focus beryllium window tube and a Philips 6-in. image intensifier coupled with a Plumbicon C.C.T.V. chain with 11-in. monitor. (Australia)

Protective Structures

Refer also to abstract 8403.

8444 (ORNL-HUD-17) TUNNELING: AN ANNOTATED BIBLIOGRAPHY WITH PERMUTED-TITLE AND KEY-WORD INDEX. Cristy, G. A.; Brooks, C. B. (Oak Ridge National Lab., Tenn.). Dec 1970. Contract W-7405-eng-26. 269p. Dep. NTIS.

A bibliography is presented of approximately 1200 references published from 1955 to 1970 on tunneling, particularly small dia tunneling in urban areas to provide for the underground installation of utilities. The bibliographic information includes the title, key words, authors, corporate affiliation of the principal author, reference, and the abstract. Indexes are provided for the corporate author, personal author, and key words. (L.C.L.)

Radioactive Material Handling

Refer also to abstracts 8196, 8345, 8577, and 10131.

8445 (AERE-R-5104) PROCESSING IN LIMITED GEOMETRY. PART XVI. THE HYDRAULIC LIFTING OF SOLIDS FROM A CONTINUOUS DISSOLVER FOR NUCLEAR FUEL. Laaner, G. S.; Carley-Macauly, K. W.; Moulton, R. J. (Atomic Energy Research Establishment, Harwell (England)). Feb 1966. 36p. Dep. NTIS (U. S. Sales Only).

Work relating to the continuous leaching of sheared fuel elements or similar material in a vertical tube dissolver is described. In such a dissolver, the problem arises of continuously removing the undissolved pieces of fuel can from the base of the dissolver tube. This may be achieved by using an hydraulic lift device to carry the cans to above the free liquid surface, while the actual disengagement at the dissolver tube base is controlled by a pulsing action. Two hydraulic lift devices, an air-lift and a pulsed ladder were tested using water as the working fluid, to lift solids and lengths of sheared tube up to 0.5 in diameter and 0.5 in long. Data are presented on the lift requirements as pulse magnitude or air flow for different solids, and on the control of lifting rates in the air lift by using a pulsed box. The possibility of washing cans during transport was also investigated. Reliability of operation is discussed in relation to the dimensions of the equipment. It is concluded that for the application to fuel dissolution, the advantages of the pulsed ladder are insufficient to justify its greater structural complexity compared to the air-lift device, which itself worked well with a variety of solids. (auth) (UK)

8446 (ANL-7672) ENGINEERING DEVELOPMENT OF FLUID-BED FLUORIDE VOLATILITY PROCESSES. PART 16. A SAFETY MANUAL FOR THE ENGINEERING-SCALE ALPHA FACILITY. Kullen, B. J.; Murphy, W. A.; Carls, E. L.; Levitz, N. M.; Vogel, G. J.; Kinzler, R. V. (Argonne National Lab., Ill.). Apr 1970. Contract W-31-109-eng-38. 91p. Dep. NTIS.

Safety procedures and warning and protective devices used in the operation of a plutonium-processing facility are described. Hazards protected against are release of radioactive or other noxious materials, fires, criticality, failure of electric power, process abnormalities, and explosion hazards. Also considered are safe procedures for routine operations, such as processing operations, material transfer into and out of gloveboxes, and waste disposal. (auth)

8447 (BHO-65-1) ENRICHED URANIUM ACTIVE ASSAY PROGRAM. First Quarterly Progress Report, April-June 1970. Schamberger, R. D. (United Nuclear Corp., Elmsford, N. Y. Research and Engineering Center). 8 Sep 1970. Contract AT (30-1)-65. 16p. (UNC-5266). Dep. NTIS.

Descriptions are presented of a nondestructive assay system for U to be used in a scrap recovery plant. Design of the system as it is expected to be when in operation, the manner in which it will be calibrated and used, and an indication of the current status of the work are outlined. (J.R.D.)

8448 (BNWL-SA-3336) TOTAL QUALITY CONTROL CONCEPT FOR MATERIAL BALANCE MEASUREMENTS. Wirfs, L. F. (Battelle-Northwest, Richland, Wash. Pacific Northwest Lab.). 18 May 1970. Contract AT(45-1)-1830. 18p. (CONF-700541-2). Dept. NTIS.

From 11th Annual Meeting of the Institute of Nuclear Materials Management, Gatlinburg, Tenn.

The safeguards effectiveness of material balance accounting systems must ultimately be based upon the capabilities of material unaccounted for (MUF) to detect material shortages. Because errors in material measurements directly affect these detection capabilities, the control of measurement errors is an important function of the material balance effort for safeguards. A total systems approach to quality control lends itself well to the control of measurement errors in material balance accounting. An integrated concept of quality planning, organization, motivation, and control for nuclear material measurements is described. (auth)

8449 (CONF-691008-18) A DESCRIPTION OF HOT FACILITIES AT THE PAKISTAN INSTITUTE OF NUCLEAR SCIENCE AND TECHNOLOGY, PAKISTAN. Shaikh, Mohammad U.; Mubarak, Mohammad A. (Pakistan Inst. of Nuclear Science and Technology, Nilore). [1969]. 24p. (SM-125/60). Dep. NTIS (U. S. Sales Only).

From Symposium on Radiation Safety Problems in the Design and Operation of "Hot" Facilities, Saclay, France.

A brief description of the hot facilities at the Pakistan Institute of Nuclear Science and Technology is presented. These facilities include a 5-MW swimming pool type reactor, nuclear chemistry, and nuclear materials laboratories. The facilities provided in the nuclear chemistry laboratory comprise a general purpose hot cell, situated in the basement intended for experiments involving high levels of radioactivity and for training purposes in remote handling operations; production plants for ^{35}S, ^{131}I, ^{32}P, and a 1000 Ci general purpose production unit for Cr, Au, Fe, Zn, Ir, Na, K, and all unprocessed isotopes; an irradiation facility containing a 30,000 Ci ^{60}Co source and research laboratories mainly on the development of methods and procedures for isotope production. The nuclear materials laboratory will have a pilot scale fuel reprocessing facility based on the Purex Method; hot metallographic laboratories; mixed oxide powder and pellet preparation and cold metallographic laboratory and uranium laboratories where UO_2 powder fabrication, powder properties measurement, mechanical testing, heat treatment and metallographic examination will be carried out. The general arrangement of the laboratories, philosophy of containment and function of change rooms, description and location of protective equipment and alarms, geographic characteristics of the site, and collection and disposal of radioactive wastes are described. (auth)

8450 (IN-1449) RELEASE OF RADIOIODINE FROM OPEN POOLS. Yuill, W. A.; Baston, V. F.; Cordes, O. L. (Idaho Nuclear Corp., Idaho Falls). Dec 1970. Contract AT(10-1)-1230. 14p. Dep. NTIS.

An analytical approach based on mass transfer relationships is presented for calculating radioiodine evolution from open waste storage pools. The analytical relationships are checked by comparing iodine water-gas phase partition coefficients that were calculated through use of the mass transfer relationships and data taken from the literature with observed coefficients also taken from the literature. Calculations, based on these relationships, indicate radioactive iodine release from open waste storage pools,

XUM

under certain conditions, can be a potential problem unless proper precautions are taken. The usefulness of these analytical relationships for more general gaseous releases is demonstrated in applications to gas evolution from waste storage facilities. (auth)

8451 (ORNL-TM-2971) DESIGN AND SAFETY CONSIDERATIONS OF SHIPPING SOLIDIFIED HIGH-LEVEL RADIOACTIVE WASTES. Perona, J. J.; Dillon, R. S.; Blomeke, J. O. (Oak Ridge National Lab., Tenn.). Dec 1970. Contract W-7405-eng-26. 28p. Dep. NTIS.

The high-level waste from processing a ton of spent fuel that has been irradiated to about 30,000 Mwd/ton may contain from 20 to 30 g of ^{244}Cm. The neutron flux from spontaneous fission of this isotope is such as to require that a hydrogenous material be included in the shielding of casks to be used for shipment of the solidified wastes. Design calculations were made for a nominal 100-ton cask, which has an internal cavity about 5 ft in diameter and can carry thirty-six 6-in.-diam cans, nine 12-in.-diam cans, or four 24-in.-diam cans. The gamma shield is 24 cm of lead, 40 cm of iron, or 13.5 cm of uranium. Water containing 1% borate was selected for the hydrogenous shield, and thicknesses of 11.5 cm are required on the outside of the lead and uranium shields, and 5 cm on the outside of the iron shields to reduce the neutron dose to 5 mrem/hr at 8.5 ft from the center of the casks. The outer surface temperature of the cask is limited to about 380°F by the maximum allowable pressure in the neutron shield. Circular steel fins ½ in. thick and spaced 4 in. apart in lengths of 18 in. for lead and uranium casks and 12 in. for iron casks can dissipate 240,000 to 300,000 Btu/hr, which would allow solidified wastes from reprocessing light water reactor fuels to be shipped as early as 2 to 3 years after the fuel had been removed from the reactor. A precise calculation of the probability of the release of activity by a shipping accident must await the compilation of accident severity statistics. Until then we can only point out that the probability of a single accident for the estimated number of shipments which will occur in the year 2000 is 1/77, assuming the accident frequency rate for passenger trains. The probability cannot be estimated that an accident, if it occurs, would be sufficiently severe to breech a cask passing the impact, puncture, fire, and submersion tests that are specified in current regulations. (auth)

8452 (ORNL-TM-3187) SOME TECHNIQUES FOR ESTIMATING THE RESULTS OF THE EMISSION OF RADIOACTIVE EFFLUENT FROM ORNL STACKS. Binford, F. T.; Hamrick, T. P.; Cope, Beth H. (Oak Ridge National Lab., Tenn.). 1 Oct 1970. Contract W-7405-eng-26. 171p. Dep. NTIS.

Methods for calculating the maximum permissible release rates from the 5 reactor stacks at ORNL are presented. Previously used estimation methods are discussed. The presently recommended methods assume either a constant unit release with space- and time-variable meteorological conditions or an inadvertent activity release of such short duration that the meteorological conditions would be constant. The computer program, STAREL, used to calculate ground-level radioactivities resulting from various stack releases, is presented. Calculated and measured data on ^{131}I concentrations at ground level are compared. (L.C.L.)

8453 (ORNL-TM-3209) GLOVE BOX VACUUM SYSTEM FOR RADIOISOTOPIC TARGETS. Gibson, J. R. (Oak Ridge National Lab., Tenn.). Jan 1971. Contract W-7405-eng-26. 11p. Dep. NTIS.

Several vacuum systems are being used for the fabrication of accelerator and reactor targets from radioisotopes of some of the heavy elements. These vacuum systems are enclosed in glove boxes to provide containment for the alpha-particle emitting radioisotopic elements being handled. The requirements for the variety of highly specialized target forms which the systems attempt to satisfy are discussed. Included are the several methods such as electron-bombardment heating, levitation melting, and reduction-distillation used to process the radioisotopic materials as well as the construction and operating features of the containing glove boxes and the oil diffusion vacuum systems. The operation and maintenance problems which have developed over the nearly three year period of use of the systems are also discussed. (auth)

8454 (SZS-14/70, pp 11-21) CLASSIFICATION OF THE NEW NUCLEAR FUEL ELEMENTS FOR WATER-MODERATED REACTORS WITH REGARD TO THE REGULATIONS FOR THE TRANSPORT OF RADIOACTIVE MATERIALS. Albrecht, L. (Staatliche Zentrale fuer Strahlenschutz, Berlin (East Germany)). (In German).

Existing regulations and data on nuclear fuel elements for water-moderated reactors derived from the literature are reviewed and the classification of these elements is discussed with regard to the packaging of radioactive materials. Nuclear fuels consisting of freshly produced uranium, reprocessed uranium or uranium-plutonium mixtures are taken into consideration. Problems of criticality safety are mentioned. (auth)

8455 (TID-25576) DISPOSAL OF SOLID RADIOACTIVE WASTES IN BEDDED SALT DEPOSITS. (National Academy of Sciences-National Research Council, Washington, D. C. Committee on Radioactive Waste Management). Nov 1970. 28p. Dep. GPO $0.35.

The Committee on Radioactive Waste Management (CRWM) of the National Academy of Sciences-National Research Council has examined the technical feasibility of the burial of solid radioactive wastes in bedded salt deposits. This method of waste management was originally suggested in 1957 and has been under continuous study and development since that time. In June 1970, the AEC announced its intention to initiate a demonstration project to provide technical data and experience on operational methods and costs of long-term storage of solidified wastes from the processing of spent nuclear power fuels. A site near Lyons, Kansas, was selected tentatively as the location of the demonstration project for a salt mine repository. To assist in evaluating the AEC plans, the CRWM convened a Panel on Disposal in Salt Mines. Recommendations of the panel resulted in the following Committee conclusions: the use of bedded salt for the disposal of radioactive wastes is satisfactory and is the safest choice now available, provided the wastes are in an appropriate form and the salt beds meet the necessary design and geological criteria; and the site near Lyons, Kansas, selected by the AEC is satisfactory, subject to the development of certain additional confirmatory data and evaluation. Initial disposal will be for low-level solid waste material contaminated with plutonium and other long-lived transuranium nuclides. Subsequent disposal will include highly radioactive, high temperature, solidified wastes. (auth)

8456 DEVICE FOR THE PACKING OF RADIOACTIVE MATERIAL. Capet, Henri (to Commissariat a l'Energie Atomique). French Patent 1,569,898. 6 Jun 1969. Filed 12 Apr 1968. (In French).

The design of a container for radioactive materials, particularly irradiated fuels, is described. The various parts of the container taken separately or in combination include: a leak-tight interior vessel to contain the material; a buffer heat evacuator; a protective shield; thermal insulation; a housing for mechanical protection; an opening for air in the lower part of the arrangement; and an outlet for warm air in the upper part of the arrangement. (P.C.H.)

8457 MELTER PUMP (29 Oct 1969) (Engineering Materials). (Brookhaven National Lab., Upton, N. Y.). (CAPE-2040). 7 drawings.

The Archimedes screw-type lift pump is used in a phosphate-glass process to transfer waste concentrates from the evaporator to the melter. The pump, which is installed by remote handling tools, delivers 6.6 l/hr and remains free of deposits. The screw is encased in a Type 304-L stainless-steel pipe. The stainless steel conveyor screw is cut with a pitch of ½ in. Clearance between the screw and the housing is 0.010 in. (For details see TID-4100 Suppl. 62) (see also 24: 45620) (F.S.)

8458 IMPROVEMENTS IN AND RELATING TO PROTECTIVE CLOSURES. Brisac, Michel; Vertut, Jean (to Commissariat a l'Energie Atomique). British Patent 1,211,528. 11 Nov 1970. Priority date 22 May 1968, France.

A slideable duct closure mechanism is described. The closure members are shaped to conform to the shape of the duct so that when the closure member is in the open position it effects an extension of the duct. The protective closure may in this way be extended into enclosures containing dangerous materials such as radioactive products. (J.R.D.)

8459 EMPIRICAL MODEL FOR SAFE PIPE INTERSECTIONS CONTAINING FISSILE SOLUTION. Dickinson, Deanne; Schuski, C. L. (Dow Chemical Co., Golden, Colo.). Nucl. Technol.; 10: 179-87(Feb 1971).

An empirical model is presented for calculating safe nuclear criticality parameters for systems of intersecting pipes containing enriched uranyl nitrate solution. The model, which applies to systems consisting of a main pipe (the central column) from which smaller pipes (arms) branch off, uses as a criticality parameter the area of intersection of the arms with the column. Maximum safe values for both the central column diameter and the area of intersection of the arms with the column are provided for conditions of minimal, nominal, or full reflection. The model, an extension of an earlier one, is based on Monte Carlo calculations as well as on experimental data. A review of the experimental and calculational data is included. (auth)

XUM

8460 WINCHES USED FOR THE HANDLING OF NUCLEAR MATERIALS. Martin, Jean (Groupement Atomique Alsacienne Atlantique, Le Plessis-Robinson, France). Ind. At.; 14: No. 7-8, 45-53(Jul-Aug 1970). (In French).

This article is the continuation of a previously published paper and was already abstracted. (Ind. At. 1970 v 14/5-6, p. 47-52). See Nuclear Science Abstracts 24: 48252. (France)

Vacuum Engineering

8461 APPLICATIONS OF VACUUM TECHNOLOGY IN NUCLEAR INSTALLATIONS. Gegusch, M.; Schimmel, W. (Staatliche Zentrale fuer Strahlenschutz, Berlin). Exp. Tech. Phys.; 18: 89-95(1970). (In German).

Vacuum techniques and their use in production of fuel cans to prevent release of fission products to the environment are discussed. Uses of vacuum techniques include: production of reactor-grade zirconium, production of fuel pellets, electron-beam welding of fuel rods, and leak detection on helium-filled fuel elements. (M.C.G.)

8462 SOME PROBLEMS WITH EVAPORATION IN THE UHV. Meister, W. (Arbeitsstelle fuer Molekularelektronik, Dresden). Exp. Tech. Phys.; 18: 141-51(1970). (In German).

Methods of operation of an all-metal ultrahigh-vacuum vaporization installation are described. Construction and characteristics of the UHV installation are discussed along with operation for vapor sources and substrate heating. Residual gas analysis with a mass filter and the gas inlet system are considered. (M.C.G.)

XUM

INSTRUMENTATION

Radiation Detection Instruments

Refer also to abstract 8447.

General Detectors and Monitors

Refer also to abstracts 8666, 8727, 9910, and 10181.

8463 (BLG-447) THE FABRICATION OF Ge(Li) DETECTORS. Fettweis, P. (Centre d'Etude de l'Energie Nucleaire, Brussels (Belgium)). Sep 1970. 27p. Dep. NTIS (U. S. Sales Only).

The fabrication of lithium-drifted germanium detectors for use in gamma-ray spectroscopy is described. The performances of the different types such as planar and one and two open-ended coaxial detectors are briefly discussed in view of their applications in straight spectroscopy and timing circuits. (auth)

8464 (BMBW-FBK-70-15) SMALL ROD-SHAPED SILICON-DETECTORS FOR MEDICAL AND BIOLOGICAL APPLICATIONS. Jaentsch, O.; Glasow, P.; Grosse, W. (Siemens A. G., Erlangen (West Germany)). Aug 1970. 57p. (In German). Dep. NTIS (U. S. Sales Only).

It is shown that diffused Si-detectors for medical and biological applications can be manufactured only with high expense. Their spectrum is continuous even for monoenergetic radiation. This can be explained theoretically by using a RC-delay-line as equivalent circuit of the detector. (auth)

8465 (BNWL-SA-1514) SOLID STATE X-RAY-ALPHA COINCIDENCE COUNTER. Swinth, K. L. (Battelle-Northwest, Richland, Wash. Pacific Northwest Lab.). [1970]. Contract AT(45-1)-1830. 21p. (CONF-701109-5). Dep. NTIS.

From IEEE Nuclear Science Symposium, New York, N. Y.

A system using solid-state detectors has been developed for the laboratory measurement of x-ray/alpha ratios of transuranic elements. In order to maintain high efficiency and accuracy at low levels of activity, a coincidence system with high geometrical efficiency was built. The system uses a coaxial geometry with the alpha detector sandwiched between the source and X-ray detector. A 3 mm × 110 mm^2 lithium-drifted-silicon detector cooled to liquid nitrogen temperature is used for X-ray detection. The alpha detector is a 40 micron by 100 mm^2 totally depleted surface barrier detector. Sources are either 0.635 or 1.58 cm diameter electrodeposited on stainless steel and are placed on a rotatable disc 1.1 cm from the X-ray detector and 0.21 cm from the alpha detector. The X-ray detector has a resolution of 0.95 keV FWHM for the 26.4 keV gamma of ^{241}Am and an average efficiency of 6.5% for the X-rays of ^{241}Am (0.635 cm). The alpha detector resolution is 70 keV FWHM and its efficiency is 31% for alphas from ^{241}Am. The system uses standard coincidence techniques gating the analyzer on the various alpha energy peaks. Dual parameter analysis is also used, but does not yield additional information. Data are presented for the various plutonium isotopes, ^{242}Cm, ^{244}Cm, and ^{237}Np to demonstrate the versatility of this technique. Besides measuring X/α ratios, it is possible to measure isotopic composition of materials with this system when the individual alpha peaks are not resolved. (W.H.K.)

8466 (BNWL-SA-3624) A COUNTER FOR THE DIRECT MEASUREMENT OF ^{55}Fe IN BLOOD AND OTHER LIQUID SAMPLES. Palmer, H. E. (Battelle-Northwest, Richland, Wash. Pacific Northwest Lab.); Cook, J. D. (Washington Univ., Seattle. Dept. of Medicine). 3 Nov 1970. Contract AT(45-1)-1830. 11p. (CONF-701109-4). Dep. NTIS.

From IEEE Nuclear Science Symposium, New York, N. Y.

Iron-55 can be accurately determined directly in blood or other liquid samples by placing the sample in a long length of fine-bore thin-walled polyethylene tubing which is located between two large-area, low background proportional counters. This method reduces the required analysis time from days to minutes with only a slight reduction in sensitivity. (auth)

8467 (BRH/NERHL-70-4) CALIBRATION AND INITIAL FIELD TESTING OF ^{85}Kr DETECTORS FOR ENVIRONMENTAL MONITORING. Smith, D. G.; Cochran, J. A.; Shleien, B. (Bureau of Radiological Health, Winchester, Mass. Northeastern Radiological Health Lab.). Nov 1970. 37p. NTIS.

In order to measure ^{85}Kr in the environment around nuclear fuel reprocessing facilities, several types of commercially available detectors were calibrated in the laboratory and then field tested. Among the detectors evaluated were several sizes of flow-through ionization chambers (with vibrating-reed electrometers), thin-walled cylindrical GM tubes, single and double thin-window GM tubes, and β scintillation detectors. A laboratory facility for calibrating all types of external β detectors against standardized ionization chambers has been developed. Following calibration all suitable instruments were field tested in the environs of an operating nuclear fuel reprocessing plant to ascertain their limits of sensitivity, reliability, and applicability. The most sensitive detector tested, a double window pancake-type GM tube, had a maximum sensitivity under field conditions of 1.2×10^{-8} μCi/cc. However, its window was extremely fragile. A more rugged cylindrical probe GM tube had a sensitivity of 2.4×10^{-8} μCi/cc. All successfully tested instruments are discussed with respect to appropriate environmental monitoring applications. (auth)

8468 (CEAL-1054) SIMPLE THRESHOLD AND DELAY CIRCUIT FOR MULTI-WIRE PROPORTIONAL CHAMBERS. Rubbia, Carlo (Cambridge Electron Accelerator, Mass.). 5 Oct 1970. Contract AT(30-1)-2076. 10p. Dep. NTIS.

A one-shot device with input threshold of about one millivolt has been constructed and tested. The circuit, built around one quarter of the inexpensive MC-1020 integrated circuit, delivers standard squared pulses of predetermined duration. By differentiation a delayed pulse can be generated. The circuit is sufficiently sensitive to be driven directly by the chamber in which traces of Freon 13 are added, thus eliminating the need for an amplifier. (auth)

8469 (JUL-CONF-4) SYMPOSIUM ON POSITION-SENSITIVE DETECTORS IN NUCLEAR PHYSICS. Organized by Institute for Nuclear Physics of Juelich Nuclear Research Facility, 8-9 July 1969, Juelich, Germany. Martin, Siegfried; Mayer-Coericke, Claus (eds.) (Kernforschungsanlage, Juelich (West Germany)). Mar 1970. 178p. (In German and English). (CONF-690722).

Separate abstracts were prepared for the 11 papers presented. (W.H.K.)

For abstracts of individual papers see: 8470-8480.

8470 (JUL-CONF-4, pp 1-10) POSITION-SENSITIVE COUNTERS. Sistemich, K. (Kernforschungsanlage, Juelich (West Germany). Institut fuer Festkoerper- und Neutronenphysik). (In German).

From Symposium on position-sensitive detectors in nuclear physics.

Studies were made on the development of position-sensitive counters by the use of high-ohm material for the counter wire or counter mantle. The functioning of such a counter is first described. Experiments with high-ohm counter wires and high-ohm counter mantles are reported. Measurements showed that in counters with high-ohm wires the position resolution is limited by the effect of the electronics and by the bunching of the beam of α particles in the filling gas and in the foil covering the inlet window. Two of the three counters with high-ohm mantles gave results as satisfactory as the counter with high-ohm wire. A counter filled with 100 torr argon and 12 torr alcohol was provided with vacromium wire. The pulses from this counter could be used for position determination. (J.S.R.)

8471 (JUL-CONF-4, pp 11-21) ANALOG-DIVISION STAGE FOR USE WITH POSITION-SENSITIVE DETECTORS. Kuhlmann, W. (Kernforschungsanlage, Juelich (West Germany). Institut fuer Kernphysik). (In German).

From Symposium on position-sensitive detectors in nuclear physics.

Two methods for the design and construction of analog division circuits, one using special properties of the construction elements with the division being chronologically directly carried out and the second using passive standard construction elements with the introduction of an amplitude-time or time-amplitude transformation, are discussed. (J.S.R.)

8472 (JUL-CONF-4, pp 22-9) DESCRIPTION OF A POSITION-SENSITIVE PROPORTIONAL COUNTER FOR THE MEASUREMENT OF BETA SPECTRA IN A SPECTROGRAPH. Eichner, H. (Cologne Univ. (West Germany). Institut fuer Kernphysik). (In German).

From Symposium on position-sensitive detectors in nuclear physics.

The possibility of using a counter for the resolution of β spectra in a semicircular focussing permanent magnet β spectrograph was investigated. A position-sensitive proportional counter is described. The continuous β spectra of ^{60}Co, ^{90}Sr, ^{90}Y, and ^{137}Cs

were measured with this counter. The results show good agreement with the theoretical distributions. The response of the counter to γ radiation was disadvantageous since it lengthened the measurement time. Considerable difficulties were caused by the sensitivity of the wire to mechanical oscillation and the large pressure difference on the counter window, both of which reduce the reliability of the counter. The poor position resolution limits its application possibilities. (tr-auth)

8473 (JUL-CONF-4, pp 30-47) POSITION RESOLVING DETECTOR BANK FOR NEUTRON SCATTERING EXPERIMENTS. Abend, K. (Kernforschungsanlage, Juelich (West Germany). Zentrallabor fuer Elektronik). (In German).

From Symposium on position-sensitive detectors in nuclear physics.

A position resolving detector bank with an active counting surface of about $\frac{1}{2}$ m^2 and a position resolution of 1.5 cm in one direction and 5 cm in the other was developed. The considerations which led to the selection of this type detector bank are briefly discussed and the detector bank is described. The characteristics of the detector bank — pulse-time behavior, position resolution, electronic noise, linearity, effect of upper level discriminators, position resolution of the complete bank, linearity of the position resolution, and position resolution in the formation of the signal ratios U1/U2 and U1/(U1 + U2) — are given graphically. (J.S.R.)

8474 (JUL-CONF-4, pp 48-58) USE OF POSITION-FIXING SEMICONDUCTOR COUNTERS IN MAGNETIC SPECTROGRAPHS. Puehlhofer, F. (Marburg Univ. (West Germany). Physikalisches Institut). (In German).

From Symposium on position-sensitive detectors in nuclear physics.

The methods used in the application of position-fixing silicon counters in the focal plane of broad band spectrographs for the detection of charged particles as p, d, or α from nuclear reactions are reported. The principle of position-determining boundary layer counters is briefly summarized. The electronics necessary in the use of semiconductor detectors are discussed. Examples of typical measurements are given. (tr-auth)

8475 (JUL-CONF-4, pp 59-70) POSITION-SENSITIVE DETECTORS FOR THE SIMULTANEOUS DETERMINATION OF SEVERAL PARAMETERS OF A PARTICLE. Klein, S. S. (Technische Hogeschool, Eindhoven (Netherlands)).

From Symposium on position-sensitive detectors in nuclear physics.

Possible uses of position-sensitive detectors (PSD) are briefly discussed. A single PSD can be used for angular cross section measurements and can be used in large solid angle low-yield experiments such as correlation and polarization measurements. Two PSD's can operate in the E-dE mode, and also, two PSD's can be used for detecting several particles in nuclear reaction studies. Advantages and disadvantages of PSD's are outlined. (W.H.K.)

8476 (JUL-CONF-4, pp 71-120) SURVEY OF APPLICATIONS OF SPARK CHAMBERS AND MULTIWIRE PROPORTIONAL COUNTERS IN MAGNETIC SPECTROGRAPHS. Specht, J. H. (Munich Univ. (West Germany)).

From Symposium on position-sensitive detectors in nuclear physics.

Position-sensitive spark chambers and multiwire proportional detectors for use with broad range magnetic spectrographs are described. Sonic, current ratio, ferrite core, and magnetostriction readout techniques are described and compared. Spatial resolution and maximum trigger rates (including resolving time, recovery time, and readout time) are discussed for the various detectors. Example data are given. (W.H.K.)

8477 (JUL-CONF-4, pp 121-40) MULTIWIRE PROPORTIONAL DETECTORS, PARTICULARLY FOR THE DETECTION OF LOW-ENERGY PARTICLES. Epple, E. (Stuttgart Univ. (West Germany). Institut fuer Gasentladungstechnik und Photoelektronik). (In German).

From Symposium on position-sensitive detectors in nuclear physics.

A review is given of the work done at Stuttgart University on the properties of multiwire proportional detectors, especially in the detection of low-energy particles. The detector geometry, field configuration, and position resolution are first considered. The factors considered in the selection of the gas and the effect of the gas on the pulse amplitude are discussed. The dependence of the pulse spectrum on the input position of α particles is shown. The peculiarities of proportional counters with undivided cathodes are described. Results obtained in neutron detection and x-ray detection are illustrated. (J.S.R.)

8478 (JUL-CONF-4, pp 141-7) REPORT ON THE PLANNING AND CONSTRUCTION OF A MULTIWIRE SPARK AND/OR PROPORTIONAL CHAMBERS FOR THE BONN SPLIT-POLE MAGNETIC SPECTROGRAPH. Bachner, D.; Blumenberg, F. E. (Bonn Univ. (West Germany). Institut fuer Strahlen und Kernphysik). (In German).

From Symposium on position-sensitive detectors in nuclear physics.

A device was designed and constructed for particle detection in the focal plane of the Bonn split-pole magnetic spectrograph. The device permits on-line evaluation of the measurements without abandoning the advantages of the split-pole. Both spark and proportional multiwire counters can be used. Block diagrams are given of the selection techniques and of the selection and particle discrimination. A flow diagram of the principal control unit is also given. (J.S.R.)

8479 (JUL-CONF-4, pp 148-64) REPORT ON THE CONSTRUCTION OF A MULTIWIRE PROPORTIONAL CHAMBER. Becker, H.; Wiedner, C. A. (Max-Planck-Institut fuer Kernphysik, Heidelberg (West Germany)). (In German).

From Symposium on position-sensitive detectors in nuclear physics.

A QDDD-type spectrograph designed to have electron data selection so that the experiment could be controlled from the data obtained was constructed at the Max Planck Institut fuer Kernphysik at Heidelberg. The special requirements placed on such a selection system were outlined. The construction of a multiwire proportional chamber that would fulfill these requirements is described and the characteristics of the proportional chamber with respect to energy resolution and position resolution were determined. The time behavior of the chamber was also determined. The incorporation of the chamber into the selection system is described. (J.S.R.)

8480 (JUL-CONF-4, pp 165-71) THE PRESENT USES AND FURTHER DEVELOPMENT OF WIRE SPARK CHAMBERS AT THE INSTITUTE FOR EXPERIMENTAL NUCLEAR PHYSICS, KARLSRUHE. Schmidt-Parzefall, W. (Kernforschungszentrum, Karlsruhe (West Germany). Institut fuer Experimentelle Kernphysik). (In German).

From Symposium on position-sensitive detectors in nuclear physics.

The wire spark chambers developed at Karlsruhe coupled the high voltage pulse to the chamber and used ferrite core accumulators for data selection. The high voltage coupling and the arrangement of the ferrite core are shown schematically. The characteristics of these wire spark chambers are discussed. Examples are given of their use. (J.S.R.)

8481 (KFK-1233) MEASUREMENT OF NEUTRON SPECTRA IN THE ENERGY RANGE FROM 1 eV to 10 keV WITH THE HELP OF SANDWICH TECHNIQUES. Mueller, Manfred (Kernforschungszentrum, Karlsruhe (West Germany). Institut fuer Angewandte Reaktorphysik). Jul 1970. 103p. (In German). Dep. NTIS (U. S. Sales Only).

Thesis. Submitted to Technische Hochschule, Karlsruhe, Ger.

Twenty-one different resonance absorbers were investigated theoretically and experimentally in order to check their suitability as sandwich detectors for the determination of neutron spectra in fast reactors below the energy of 10 keV. The obtainable accuracy of the measured results of all detectors was found to be influenced strongly by the hardness of the neutron spectrum. By means of the absolute cross sections of gold (Au) and manganese (Mn) the results could be given absolutely. The accuracy of the measurements was 10 to 20% for spectra similar to those in a fast steam-cooled breeder reactor and 20 to 40% for spectra similar to those in a fast sodium-cooled breeder reactor. 32 references. (auth)

8482 (NYO-2740-7, pp 112-53) RADIOLOGICAL PHYSICS: III. ANCILLARY PROBLEMS. (Columbia Univ., New York. Radiological Research Lab.).

From annual report on research project.

Studies on multiple Coulomb scattering in tissue-equivalent gas, the development of dosimetry instrumentation, and research on electron transport in tissue-equivalent gas mixtures are described. Development and research at the Radiological Research Accelerator Facility which employs a Van de Graaff accelerator are outlined. (W.H.K.)

8483 (PH-1) VERSATILE AND MODULAR DATA ACQUISITION SYSTEM USEFUL IN NUCLEAR EXPERIMENTS. Al-Quraishi, N. H.; Al-Kaysi, B.; Ohannesian, O. A.; Younan, I. S. (Atomic Energy Commission, Baghdad (Iraq). Nuclear Research Inst.). Sep 1970. 10p. Dep. NTIS (U. S. Sales Only).

A versatile and modular acquisition system useful in recording data from nuclear experiments is described. The overall system allows complete intercompatibility between its various subsystem modules. The functional specifications of the system are outlined. The operational characteristics of some selected

XUM

circuits are reported. The design and development work is still in progress. (auth)

8484 PROCESS FOR THE MANUFACTURING OF VERY HIGH QUALITY RADIATION DETECTORS. Kalbitzer, S. French Patent 1,570,841. 5 May 1969. Priority date 13 Jun 1967, Germany. (In French).

A procedure is described for the fabrication of Si or Ge radiation detectors by ion implantation in the range of 1 to 10 keV using two or more chemical elements simultaneously or successively and carrying out the thermal treatment at 300 to 400°C. (P.C.H.)

8485 EFFECT OF ELECTRON BOMBARDMENT ON LUMINESCENCE OF ZnS–Cu PHOSPHOR. Kolomoitsev, F. I.; Belov, D. G.; Kondrashov, A. P. Zh. Prikl. Spektrosk.; 12: 353-5(Feb 1970). (In Russian).

Luminescence excitation of a ZnS(Cu) phosphor by an electron beam is investigated. Experimental results on the luminescence characteristics of an electroluminiphor EL-510 upon separate and combined excitation by a sinusoidal voltage and an electron beam are given. The nonadditivity of the luminescence intensity relative to the excitation parameters was determined. The data were analyzed and the results explained on the basis of minority charge carrier injection through p-n transitions on ZnS–Cu_2S boundaries and reverse polarization formation. (tr-auth)

8486 CRITICALITY DETECTION SYSTEM FOR A FUEL REPROCESSING PLANT. Mitchell, B. (English Electric Co., Ltd., Whetstone, Eng.). J. Brit. Nucl. Energy Soc.; 9: 223-6 (Oct 1970).

A criticality system is described which was designed for use in a plant for processing irradiated fuel. The method adopted, which employs a mean current fission chamber, offers the facilities for detecting neutron bursts of less than one millisecond duration, and can produce an alarm within 200 ms. The approach was to produce as fail-safe a solution as possible, and the equipment used to achieve this is outlined. (auth) (UK)

8487 MONITORS AND DETECTORS FOR RADIOLOGICAL PROTECTION. Heys, H. Electron. Eng.; 42: No. 513, 80-3 (Nov 1970).

Personal dosemeters, ambient contamination monitors and semiconductor probes for radiation detection during radiotherapy are surveyed. All these devices have been designed by AERE Harwell and developed in association with commercial instrument companies. (auth) (UK)

8488 ELECTRONICS FOR NUCLEAR PARTICLE ANALYSIS. Herbst, L. J. (ed.). Harwell Post Graduate Series. London; Oxford University Press (1970). 383p. 110s.

The subject is dealt with under the following chapter headings: system requirements for nuclear particle analysis, pulse shaping, bipolar and field-effect transistors, the transistor as a circuit element, basic circuit techniques, nuclear pulse amplifiers, low-noise head amplifiers, pulse amplitude discriminators, counting circuits, coincidence and time-spectrometer circuits, multi-channel pulse data analysis, logic and logic circuitry, the use of digital computers in experiments, practical design aspects of electronic equipment, and reliability. (UK)

8489 ENCAPSULATION OF HELICAL CHANNEL MULTIPLIERS FOR SPACE FLIGHT APPLICATIONS. Carruthers, George R. (Naval Research Lab., Washington, D. C.). Rev. Sci. Instrum.; 41: 1882-3(Dec 1970).

A method for encapsulating helical channel multipliers for space flight applications to prevent breakage due to shock, vibration, and temperature variations and to prevent high voltage breakdown in the vicinity of the multiplier is described. This encapsulation will withstand thermal cycling in the range of 100 to −10°C. (W.H.K.)

8490 ABSOLUTE EFFICIENCY MEASUREMENTS FOR CHANNEL ELECTRON MULTIPLIERS UTILIZING A UNIQUE ELECTRON SOURCE. Paschmann, G. (Max-Planck-Institut fuer Physik und Astrophysik, Garching, Ger. Max-Planck-Institut fuer Extraterrestrische Physik, Garching, Ger.); Shelley, E. G.; Chappell, C. R.; Sharp, R. D.; Smith, L. F. Rev. Sci. Instrum.; 41: 1706-11(Dec 1970).

A unique low energy (0 to 50 keV) electron accelerator has been developed which provides a broad, parallel, low intensity electron beam with excellent long term stability. The beam intensity is approximately 10^6 electrons · cm^{-2} · sec^{-1} and the long term stability is better than 2%/day. A prototype of this accelerator is described and the results of its application to instrument calibration and channel electron multiplier (CEM) efficiency measurements are presented. The absolute electron detection efficiency for CEM's was found to vary from approximately 90% at 1 keV to 73% at 14 keV with a probable error of ±10%. The large disagreement among the various published measurements of CEM detection efficiency is discussed. (auth)

8491 HIGH-RESOLUTION NUCLEAR RADIATION DETECTORS FROM EPITAXIAL n-GaAs. Eberhardt, J. E.; Ryan, R. D.; Tavendale, A. J. (Australian Atomic Energy Commission, Sutherland). Appl. Phys. Lett.; 17: 427-9(15 Nov 1970).

Surface barrier p-n junction diodes, made from high-purity n-GaAs grown by liquid-phase epitaxy, were operated as α-particle and low-energy γ-ray detectors over the range 77 to 373°K. Resolutions observed were 1.2 and 2.95 keV (FWHM) at 130 and 295°K, respectively, for 122-keV γ rays and 30 keV for 5.47-MeV α particles. The energy per electron-hole pair for α particles is 4.51 eV and the Fano factor for γ rays is ≤0.24 at 130°K. (auth)

8492 MEASUREMENT OF LET SPECTRA USING A SPHERICAL TISSUE-EQUIVALENT PROPORTIONAL COUNTER. Wilson, K. S. J. (Royal Postgraduate Medical School, London); Field, S. B. Phys. Med. Biol.; 15: 657-66(Oct 1970).

The initial tests and calibrations of a spherical tissue-equivalent proportional counter system designed by Rossi are described. The instrument was used to obtain LET spectra for (d,n), (p,n) and (α,n) neutron beams from a cyclotron, 14.6 MeV neutrons from a (d,t) generator, and the scattered radiation at a 7 GeV proton synchrotron, with sphere diameters in the range equivalent to 0.4 to 1.0 μm of tissue. A LET spectrum for cyclotron (d,n) neutrons at 10 cm depth in a paraffin phantom was also measured, the only significant change being an increase in the γ-ray component. Very good agreement was obtained in the two cases compared with theoretical spectra calculated by Bewley. (auth) (UK)

8493 NUCLEAR PROBE USING A SINGLE CABLE. Maillot, Jean-Paul (to Le Materiel Telephonique). French Patent 1,589,905. 6 Apr 1970. Filed 24 Oct 1968. (In French).

A remote nuclear radiation measurement device is described. The low tension feed and the counting circuit are connected by a coaxial cable to the probe containing the detector. Only the central conductor plays an active role; the external conductor accounts for the mass of the device. One of the polarities of the power supply is connected to the input of the central conductor by a resistance equal to the characteristic impedance of the cable. At the end of the cable is the probe which consists of a low–high tension converter; an amplifier-phase inverter which processes pulses originating from the detector element; and a pulse shaping stage and an electronic switch operating from pulses received from the previous stage, mounted in cascade. (France)

8494 RATIONAL SELECTION OF PARAMETERS IN RATEMETER CONTROLLED RECTILINEAR SCANNING (WITH SPECIAL REFERENCE TO COLOUR PRESENTATION). Keyes, W. I.; Gillespie, P. J. (Radiotherapy Centre, Belfast). Int. J. Appl. Radiat. Isotop.; 21: 649-55(Nov 1970).

The inter-relationships of the various parameters in ratemeter-controlled rectilinear scanning were examined, with particular reference to immediate color presentation of data. A scheme of dependences is suggested and from this, criteria established to enable the optimum line spacing, scan speed, time constant and number of colours in the display system, to be determined before the scan is commenced. The experimental evidence, obtained to justify the various criteria, is presented and discussed. It is concluded that this could form the basis for a standardized approach to rectilinear scanning. (auth) (UK)

8495 MEASUREMENT OF FAST NEUTRON FLUX DENSITIES ABOVE 0.5 MeV BY A SIMPLE MODERATION METHOD. Bruninx, E. (Philips Research Labs., Eindhoven, Netherlands). Int. J. Appl. Radiat. Isotop.; 21: 657-66(Nov 1970).

The method used the activation of indium by thermal neutrons resulting from the moderation of fast neutrons in a paraffin-wax sphere shielded by cadmium foil. The absolute response of this detector is given as a function of the average neutron energy. A simple method is used to correct for the presence of low-energy scattered neutrons. The technique was tested in practice for measurement of the neutron flux density produced by 18-MeV and 26-MeV deuterons incident on a thick beryllium target. (auth) (UK)

8496 CONTRAST PERCEPTION IN IMAGING SYSTEMS. Rao, G. U. V. (Johns Hopkins Univ., Baltimore. Johns Hopkins Hospital, Baltimore). Int. J. Appl. Radiat. Isotop.; 21: 571-80 (Oct 1970).

In all imaging systems, four basic factors govern the perception of detail: (1) the magnitude of the input contrast in the object being imaged, (2) the fidelity with which this contrast is displayed in the image, (3) the statistical uncertainty associated with the contrast thus displayed, and (4) the observer's visual performance. An expression is given for a measure of the signal-to-noise ratio of the system which takes into account all the basic nonsubjective parameters that govern contrast perception. Hence the term contrast perceptibility function is proposed for its variation with spatial frequency. The interpretation of the equation was confirmed experimentally. (UK)

8497 GAMMA RAY CAMERA. Lloret, Polen. Sci. Progr. Decouverte; No. 3425, 16-23(Sep 1970). (In French).

The operating principles of a gamma ray camera are recalled and the Anger camera is described. The use of the image intensifying tube (Esicon) of the C.E.A. is examined. This tube is intended to rapidly yield gamma ray photographs. (France)

8498 IONIZING RADIATION DETECTOR WITH A THIN WINDOW. Cacheux, J. A.; Meuleman, J. (to Radiotechnique Coprim RTC). French Patent 1,576,367. 23 Jun 1969. Filed 15 Dec 1967. (In French).

A thin-window silicon surface-barrier detector is described. The detector is composed of an n–i–p junction. The crystal is placed in the middle of an insulating ring on which are fixed a conducting plate and a ring. (J.G.B.)

8499 SATELLITE-BORNE INSTRUMENT FOR THE MEASUREMENT OF SOFT SOLAR X RAYS. Brinkman, A. C.; Imhof, J. P. (Univ. of Utrecht). ELDO/ESRO Sci. Tech. Rev.; 2: No. 1, 85-158(1970).

An instrument designed to measure soft solar x rays, for operation in the ESRO-II satellite, is described. Two nearly identical proportional counters are used as detectors for x rays in the wavelength region between 44 and 55 Å. This wavelength region is mainly determined by the transmission characteristics of the detector window material (mylar). Photons from other-wavelength regions in which the window is also transparent, are discriminated against by electronic pulse-height discrimination. The gain of the detector is checked in flight indirectly, with the aid of a reference proportional counter. The gas pressure and gas composition of the reference counter and the x-ray counter are identical; furthermore, the counters are fed from the same supply. Calibration curves for the output of the reference counter are given. The time resolution of each detector is 16 seconds. In addition to measurements of the solar x-ray flux, background measurements are made. Each detector is followed by its own amplifier and there is one common discriminator and memory. The memory is a binary counter-shift register combination. Logic circuits, which are triggered by the telemetry address pulse and photodiode pulses, determine the periods over which data can be accumulated. One voltage converter supplies the necessary high voltage (1700 V) for both counters. A description is given of the tests carried out to calibrate the instrument and to ensure reliable operation under space environment conditions. Those parts of the test equipment that have been designed specially to test the instrument are also described. (auth)

8500 STATE OF INSTRUMENTATION IN NUCLEAR MEDICINE. von Harsdorf, J. (Siemens AG, Erlangen, Ger.). Kerntechnik; 12: 429-35(Oct 1970). (In German and English).

A survey of instrumentation for radiodiagnosis is given. Uptake systems, radioisotope scanners, and gamma cameras are discussed. (W.H.K.)

8501 SELF-AUDITING MULTICHANNEL NEUTRON MONITOR. Splichal, W. F. Jr. (E. I. du Pont de Nemours and Co., Aiken, S. C.). Nucl. Technol.; 10: 221-3(Feb 1971).

A neutron monitor was designed with the unique feature of continuously self-auditing circuits. The monitor has four simultaneously operable channels; each alarms at a preset neutron level. Neutrons are detected by polyethylene-moderated BF_3 tubes connected to the monitor by coaxial cables as long as 100 ft. Detector preamplifiers are not necessary and the detectors are unaffected by gamma fields up to 500 R/hour. (auth)

8502 RELATIVE PHOTOPEAK EFFICIENCIES AND PHOTOFRACTIONS OF A 2″ × 2″ CsI(Tl) CRYSTAL. Irfan, M.; Prasad, R. D. G. (Memorial Univ. of Newfoundland, St. John's). Nucl. Instrum. Methods; 88: 165-76(1970).

Relative photopeak efficiencies of a 2″ × 2″ CsI(Tl) crystal for various crystal-to-source distances and in the energy range 0.279 to 3.25 MeV have been experimentally measured in terms of the corresponding photopeak efficiencies of a 3″ × 3″ NaI(Tl) crystal. Photofractions of the 2″ × 2″ CsI(Tl) crystal have been evaluated using Heath's values of photofractions of a 3″ × 3″ NaI(Tl) crystal and by using the "scaling relations" to calculate the absolute detection efficiencies of the 2″ × 2″ CsI(Tl) crystal. Our evaluated photofractions are somewhat lower than the theoretical photofractions given by Miller and Snow. Other comparisons have also been included in the discussion. (auth)

8503 LINEAR RATEMETER WITH NOISE SUPPRESSION. Berg, Chr. (Institut fuer Angewandte Physik, Hanover). Nucl. Instrum. Methods; 88: 325-6(1970). (In German).

A simple ratemeter is described with the special features, that the pulse-height is considered and that the detector noise can be suppressed. (auth)

8504 COMPARISON OF SCINTILLATOR SOLVENTS FOR PULSE SHAPE DISCRIMINATION. Czirr, J. B. (Univ. of California, Livermore). Nucl. Instrum. Methods; 88: 321(1970).

The relative pulse-shape-discrimination capability of five liquid scintillators has been measured. The results indicate that the best discrimination is obtainable from benzene-based scintillators. (auth)

8505 ENERGY DEPENDENCE OF PROPORTIONAL COUNTER PULSE-HEIGHT RESOLUTION IN THE RANGE 5 TO 23 keV. Shaikh, F. (Univ. of Sussex, Brighton, Eng.); Byrne, J.; Kyles, J. Nucl. Instrum. Methods; 88: 317-19(1970).

The pulse-height resolution of an argon–methane proportional counter has been found to vary in inverse proportion to the square root of the particle energy at pressures less than one atmosphere but deviations from this behavior are observed at higher pressures. (auth)

8506 PULSE SHAPE DISCRIMINATION: AN INVESTIGATION OF n-γ DISCRIMINATION WITH RESPECT TO SIZE OF LIQUID SCINTILLATOR. Kalyna, J.; Taylor, I. J. (Columbia Univ., New York). Nucl. Instrum. Methods; 88: 277-87(1970).

Neutron and gamma ray discrimination for liquid organic scintillators of 4″ to 8″ in dia. has been studied with a "true zero crossover" type pulse shape discriminator. The effectiveness of various configurations of scintillators, light pipers and 5″ dia. photomultipliers in n-γ discrimination for neutrons of 100 keV to 3 MeV has been investigated and data are presented. The poor performance of psd systems with 8″ dia. scintillators has been examined with reference to self absorption effects, increased optical path lengths and transit time spreads and photocathode sensitivity of photomultipliers. Variations in the transit time and sensitivity across a 5″ photomultiplier were studied with a light emitting diode. A technique for optimizing the performance of photomultipliers to obtain more efficient pulse shape discrimination is discussed and results are presented after such optimization. (auth)

8507 HIGH SPEED PULSE SHAPE DISCRIMINATOR. Taylor, I. J.; Kalyna, J. (Columbia Univ., New York). Nucl. Instrum. Methods; 88: 267-75(1970).

A high speed pulse shape discriminator utilizing the true zero crossover technique is described. Tunnel diodes are used in leading edge "anti-walk" timing and for zero crossover detection. The circuit has been used for n-γ discrimination applications with liquid scintillators and is demonstrated at rates above 8×10^4 cps. The circuit's performance in a typical application is shown in results from a neutron time-of-flight experiment using a pulsed beam of neutrons from the $^7Li(p,n)^7Be$ reaction and where the peak to background ratio of the neutron time-of-flight spectrum is improved by a factor of more than 40. The circuit is also applied to low energy n-γ discrimination in a measurement of the low energy response for the NE213 liquid organic scintillator. Results are presented which relate gamma ray energies to neutron energies of equivalent pulse heights in the range 100 keV to 2.0 MeV neutrons. (auth)

8508 POLARIZATION SENSITIVITY OF A RECTANGULAR LITHIUM DRIFTED SILICON DETECTOR. Logan, B. A.; Fairweather, I. L.; Gauthier, R. (Univ. of Ottawa). Nucl. Instrum. Methods; 88: 257-9(1970).

The polarization sensitivity of a rectangular silicon detector has been investigated with linearly polarized 121 keV photons. It is shown that the detector can determine the polarization plane of low energy polarized photons. (auth)

8509 CORRECTIONS FOR DISTORTION EFFECTS IN FAST NEUTRON FLUX MEASUREMENTS WITH A STILBENE-SCINTILLATOR. Bormann, M.; Kuehl, R.; Schaefer, K.; Seebeck, U. (Univ., Hamburg). Nucl. Instrum. Methods; 88: 245-9(1970).

If the method of recoil detection in organic scintillators shall be used for measuring the flux of fast neutrons with good accuracy, corrections have to be applied for accounting for various effects distorting the recoil spectrum. This problem is investigated ex-

XUM

perimentally as well as theoretically for a 1'' dia. × 1'' stilbene scintillator for neutrons in the energy region 2.6 to 14.1 MeV. A Monte Carlo method is used for calculating the distortion of the recoil proton spectrum by multiple neutron scattering, edge-effects and nonlinear response of the scintillator. Theoretical and experimental corrections to be applied to the integral recoil proton spectrum used for the flux measurement are given. An accuracy of better than 4% for the flux determination is claimed. (auth)

8510 NEW END-WINDOW VARIABLE GEOMETRY X-RAY PROPORTIONAL COUNTER. Cairns, J. A.; Desborough, C. L.; Holloway, D. F. (Atomic Energy Research Establishment, Harwell, Eng.). Nucl. Instrum. Methods; 88: 239-44(1970).

The new detector described, of the end-window type, is readily accessible to X-ray sources in a confined environment, and thus offers very favorable X-ray collection geometry. It exhibits extremely good resolution, particularly in the vital soft-to-ultrasoft X-ray region. The anode wire is held in a novel compact unit, which may be interchanged with ease. Other features include a built-in head amplifier and a simple assembly which allows windows to be replaced and fitted in a gas-tight seal. The variable geometry feature of the instrument arises as a result of the incorporation of a calibrated dial, by means of which the anode-to-window distance may be varied during operation. This allows the effective gas path length to be optimized, so that X-rays of a particular energy may be detected in a more selective manner. (auth)

8511 RESPONSE OF A MINERAL-OIL BASED LIQUID SCINTILLATOR TO HEAVILY IONIZING PARTICLES. Webb, R. C.; Hauser, M. G.; Mischke, R. E. (Princeton Univ., N. J.). Nucl. Instrum. Methods; 88: 227-32(1970).

The response of a mineral-oil based liquid scintillator to heavily ionizing particles has been determined by measuring the light produced by stopping protons and deuterons. The results are expressed in terms of a saturation parameter which is found to have a value similar to that obtained in a variety of organic scintillators. (auth)

8512 CALIBRATION OF A LARGE NEUTRON COUNTER USING THE PION NUCLEON CHARGE EXCHANGE REACTION. Chen, K. W.; Crean, P. A.; Dakin, J. T.; Hauser, M. G. (Princeton Univ., N. J.). Contract AT(30-1)-4159. Nucl. Instrum. Methods; 88: 219-25(1970).

The efficiency of several large liquid scintillation counters for detection of 110 MeV neutrons has been measured in a tagged neutron beam utilizing the reaction $\pi^- + p \rightarrow n + \pi^0$. These measured values have been combined with calculations based on known n-p and n-C scattering cross sections to obtain the neutron detection efficiency of these counters from 40 to 400 MeV. (auth)

8513 APPARATUS FOR THE INVESTIGATION OF NEUTRON INDUCED α-ACTIVITIES IN THE ORDER OF SECONDS. Scobel, W. (Univ., Hamburg). Nucl. Instrum. Methods; 88: 213-18(1970). (In German).

The mechanical design of an apparatus for the investigation of neutron induced α-activities with halflives in the order of seconds is presented. The equipment consists of a gridded back-to-back ionization chamber and a chopper. Its response under operation conditions is described. The apparatus is tested with the measurement of the α-spectrum from the $^8Li(\beta)^8Be^*(2\alpha)$ decay. Finally an expression for the counter efficiency is derived. (auth)

8514 INTERNAL SOURCE SCINTILLATION SPECTROMETER. Goedbloed, W.; Goverse, S. C.; Gerner, C. P.; Brinkman, A.; Blok, J. (Vrije Univ., Amsterdam). Nucl. Instrum. Methods; 88: 197-204(1970).

NaI(Tl), CsI(Tl) and CsI(Na) have been used as host crystals for radioactive atoms. These so-called source crystals were grown from the melt and used for measurements on electron capture ratios. In order to envelop these source crystals various crystal assemblies have been constructed and compared with regard to their light-yields. Test measurements have been performed on the electron capture decay of ^{109}Cd. The capture ratios have been measured using either an extrapolation method or a 4π method, while both made use of NaI(Tl) as well as CsI(Na) source crystals. The results of all these measurements are consistent with one another. Source crystals with inhomogeneous source distributions have been measured in 4π geometry, the results of these measurements demonstrate the reliability of this method. (auth)

8515 AUTOMATIC LIFE TIME CORRECTION IN MULTICHANNEL COUNTING OF SHORT-LIVED NUCLIDES. Goerner, W.; Hoehnel, G. (Zentralinstitut fuer Kernforschung, Rossendorf, Ger.). Nucl. Instrum. Methods; 88: 193-5(1970).

An automatic correction of dead time and decay in counting short-lived nuclides is proposed, where the life time frequency of the analyzer is made decaying with the half-life of interest. The paper deals with the methodical problems, the technical realization and the results of the method. (auth)

8516 PULSE SHAPE DISCRIMINATION IN PROPORTIONAL COUNTERS: THEORY OF ELECTRONIC SYSTEM. Mathieson, E.; Harris, T. J. (Univ. of Leicester, Eng.). Nucl. Instrum. Methods; 88: 181-92(1970).

The effects on a proportional counter pulse of double RC differentiation, single RC integration and noisy amplification have been examined theoretically to obtain formulae and data relevant to pulse shape discrimination systems. Theoretical formulae for waveforms have been developed and evaluated. An optimum set of circuit time constants have been determined, and a limit of discrimination set by electronic noise has been calculated. (auth)

8517 SOME FURTHER INVESTIGATIONS OF TIMING WITH SURFACE BARRIER DETECTORS. Emmerich, W.-D. (Univ., Erlangen-Nuernberg, Ger.); Hofmann, A.; Philipp, G.; (and others). Nucl. Instrum. Methods; 88: 327-9(1970).

The timing resolution using surface barrier detectors was studied using leading edge and constant fraction triggering of the detector charge and current pulses. The best result was 1.3 ns (fwhm). (auth)

8518 CERTAIN MISUNDERSTANDING CONCERNING COUNTING PHOTON COINCIDENCES. Aleksandrov, E. B. Opt. Spectrosc. (USSR) (Engl. Transl.); 28: 541-3(May 1970).

Translated from Opt. Spektrosk.; 28: 1000-4(May 1970).

A graphical examination of the nature of experiments on the recording of photon coincidences in spatially coherent light beams has been conducted. It is shown that for the study of the statistics of emission from non-laser sources, a variant of Mandel's method with one photodetector is practically useless. In connection with this, a conclusion is drawn concerning an inaccuracy in the literature, where this variant was employed. (auth)

8519 FAST CURRENT PREAMPLIFIER FOR OPERATION IN AN ELECTRONIC NEUTRON COLLIMATION SYSTEM. Andreev, E. A.; Sit'ko, S. P.; Shevchenko, V. A. (Kiev State Univ.). Instrum. Exp. Tech. (USSR) (Engl. Transl.); No. 1, 147-8(Jan-Feb 1970).

Translated from Prib. Tekh. Eksp.; No. 1, 132-3(Jan-Feb 1970).

A fast current preamplifier for a surface-barrier semiconductor detector is described. The preamplifier is based on GT311 and GT313 high-frequency transistors and is used to obtain a coincidence (referred to associated $^3He_2$ particles) in an electronic system for collimating neutrons from D–D reactions with a resolution time of several nanoseconds. The gain of the preamplifier is approximately 500, and pulse rise time at the output is less than 15 nsec. Current amplification makes it possible to obtain an eight-fold increase in the signals from the $^3He_2$ particles over noise, which represents an improvement over a charge-sensitive tube circuit. (auth)

8520 PORTABLE INTERNALLY LOADED COUNTER FOR MEASURING LOW LEVELS OF GAS ACTIVITY. Beskorskii, A. I.; Elakov, L. S.; Goikhberg, E. Ya.; Borisov, I. Ya. Instrum. Exp. Tech. (USSR) (Engl. Transl.); No. 1, 68-9(Jan-Feb 1970).

Translated from Prib. Tekh. Eksp.; No. 1, 64-5(Jan-Feb 1970).

The design and method of connection are described and the basic electrical parameters are given for a compact portable beta-radiation counter which can be loaded internally and which has a useful volume of 1 liter. The smallest measurable activity the counter can measure is $5 \cdot 10^{-12}$ curie/liter. (auth)

8521 MINIATURE END WINDOW COUNTER FOR SOFT BETA-RADIATION. Beskorskii, A. I.; Pervyshev, E. V.; Malduev, V. L.; Chechetina, N. A. Instrum. Exp. Tech. (USSR) (Engl. Transl.); No. 1, 70-1(Jan-Feb 1970).

Translated from Prib. Tekh. Eksp.; No. 1, 66-7(Jan-Feb 1970).

A miniature end window β-counter, which is convenient for counting β rays in a γ-background and can be operated in a vacuum, is described. The dimensions and thickness of the mica window of the counter are considerably smaller than in similar commercial models. The construction and the parameters of the miniature counter for soft β-radiation are given. (auth)

8522 SENSITIVITY OF SPHERICAL NEUTRON DETECTORS IN THE ENERGY RANGE FROM THERMAL TO 10 MeV. Andreeva, L. S.; Keirim-Markus, I. B.; Uspenskii, L. N.; Filyushkin, I. V.; Chernov, E. N. (Inst. of Biophysics, Moscow). Instrum. Exp. Tech. (USSR) (Engl. Transl.); No. 1, 77-80(Jan-Feb 1970).

Translated from Prib. Tekh. Eksp.; No. 1, 72-5(Jan-Feb 1970).

Experimental data are reported on the sensitivity of thermal-neutron detectors with spherical polyethylene moderators $\rho = 0.94$ g/cm^3 of various sizes (from 4.86 to 24.1 g/cm^2) in the neu-

tron-energy range from thermal to 10 MeV. The low-energy measurements were carried out by a time-of-flight method on a fast pulsed reactor, while those in the high-energy range were carried out on a Van de Graaf accelerator. Optimum moderator dimensions were chosen on the basis of these measurements for an all-wave radiometer and a neutron rem-meter. (auth)

8523 COUNTING CHARACTERISTICS OF SEMICONDUCTOR DETECTORS. Pronkin, N. S. Instrum. Exp. Tech. (USSR) (Engl. Transl.); No. 1, 81-4(Jan-Feb 1970).

Translated from Prib. Tekh. Eksp.; No. 1, 75-8(Jan-Feb 1970).

The counting characteristics of semiconductor detectors are discussed. It is shown that they have a plateau of minimum slope when the parameters of the electronic circuit and the operating conditions of the detector are chosen properly. A p-i-n Si(Li) detector is studied. (auth)

8524 RECORDING OF 10 TO 100 keV ELECTRONS WITH SURFACE-BARRIER SILICON COUNTERS. Maksimenko, B. P. Instrum. Exp. Tech. (USSR) (Engl. Transl.); No. 1, 85-6(Jan-Feb 1970).

Translated from Prib. Tekh. Eksp.; No. 1, 78-80(Jan-Feb 1970).

A linear relationship between the amplitude of pulses of surface-barrier silicon counters (t = +18°C) and the energy of electrons in the range 10 to 100 keV is obtained. The total width of the peak at half maximum is $\Delta E \simeq 4.7$ keV for energies from 15 to 40 keV and it increases to ~6 keV at 100 keV. (auth)

8525 EFFICIENT SEPARATION OF NEUTRONS AND GAMMA RAYS WITH A STILBENE CRYSTAL. Omel'yanenko, A. A. (Joint Inst. for Nuclear Research, Dubna, USSR). Instrum. Exp. Tech. (USSR) (Engl. Transl.); No. 1, 87-9(Jan-Feb 1970).

Translated from Prib. Tekh. Eksp.; No. 1, 80-2(Jan-Feb 1970).

An apparatus is described for neutron detection with efficient separation of γ rays. The apparatus consists of a scintillation counter (stilbene, FEU-13 phototube), a circuit which separates the pulses from neutrons (due to recoil protons) and γ rays, and solid-state spectrometric and logic units. The dynamic range of the neutron detection is 40 : 1. The efficiency of the separation of neutrons from γ rays is nearly 100% when only neutrons in the presence of γ rays are detected, or only γ rays in the presence of neutrons. The γ rejection factor is 10^3. The energy threshold for separation in this apparatus is no worse than 300 keV (for α-particles) with a resolving time no worse than 0.5 μsec. (auth)

8526 MECHANICAL QUENCHING OF THE LIGHT OF LIQUID SCINTILLATORS. Zemskova, I. I.; Zhil'tsova, L. Ya.; Matveeva, E. N.; Tyminskii, V. G. (Joint Inst. for Nuclear Research, Dubna, USSR). Instrum. Exp. Tech. (USSR) (Engl. Transl.); No. 1, 90-1(Jan-Feb 1970).

Translated from Prib. Tekh. Eksp.; No. 1, 83-4(Jan-Feb 1970).

A study of the quenching of the light flashes from toluene-base liquid scintillators with iron and copper powder is reported. It is shown that a comparison of the light from a standard liquid scintillator with that from a contaminated liquid scintillator permits determination of the quenching agent in it within $\sim 10^{-5}$ g. (auth)

8527 LIQUID SCINTILLATORS FOR LARGE SCINTILLATOR DETECTORS. Voevodskii, A. V.; Dadykin, V. L.; Ryazhskaya, O. G. (Inst. of Physics, Moscow). Instrum. Exp. Tech. (USSR) (Engl. Transl.); No. 1, 92-4(Jan-Feb 1970).

Translated from Prib. Tekh. Eksp.; No. 1, 85-7(Jan-Feb 1970).

The characteristics of new liquid scintillators based on inexpensive petroleum products are reported. These scintillators are highly transparent, have light outputs close to those of standard plastic scintillators, and can be produced in the laboratory. (auth)

8528 EFFECT OF NATURAL LIGHTING ON PLASTIC SCINTILLATORS. Golutvina, I. G.; Zhil'tsova, L. Ya.; Matveeva, E. N.; (and others). (Joint Inst. for Nuclear Research, Dubna, USSR). Instrum. Exp. Tech. (USSR) (Engl. Transl.); No. 1, 95-6 (Jan-Feb 1970).

Translated from Prib. Tekh. Eksp.; No. 1, 88-9(Jan-Feb 1970).

A study of the effects of 10 yr of natural lighting on the light output and scintillation time of polystyrene-base plastic scintillators is reported. Although such lighting does not affect the scintillation time, there is a maximum decrease in the light output (by 50%) in the surface layers of the sample. (auth)

8529 PROPERTIES OF ^{6}LiI(Eu) CRYSTALS AT LOW TEMPERATURES. Pavlovskaya, T. F.; Lyalin, E. O.; Borob'ev, Yu. A. Instrum. Exp. Tech. (USSR) (Engl. Transl.); No. 1, 97-8 (Jan-Feb 1970).

Translated from Prib. Tekh. Eksp.; No. 1, 90-1(Jan-Feb 1970).

A study of the scintillation and spectrometric properties of europium-activated lithium iodide crystals cooled to −150°C is reported. Temperature dependences of the light output and resolution of the crystals are reported for excitation by ^{137}Cs γ-rays and by thermal and fast monochromatic neutrons. The scintillation time constant was measured at −150°C. (auth)

8530 ELECTRONIC APPARATUS FOR RAPIDLY IDENTIFYING CHARGED PARTICLES. Dolya, G. P.; Tutubalin, A. I. (Physical-Technical Inst., Kiev). Instrum. Exp. Tech. (USSR) (Engl. Transl.); No. 1, 123-6(Jan-Feb 1970).

Translated from Prib. Tekh. Eksp.; No. 1, 112-15(Jan-Feb 1970).

The main circuit of an electronic device for shaping the function $F \sim \log_{1.5}[(E + E_0 + k\Delta E/\Delta x)\Delta E/\Delta x]$ is presented together with its amplitude characteristics. The energy dependence of the function F is determined for α-particles in the energy range 5 to 24 MeV and for protons in the range 1 to 14.7 MeV. The particles are recorded by means of a telescope comprising two proportional and one scintillation counter. It is shown that the use of the telescope together with the electronic device facilitates the rapid distinction of α-particles from a background of other charged particles in the energy range indicated. (auth)

Nuclear Spectroscopic Instrumentation

Refer also to abstract 10017.

8531 (MLM−1773) A PEAK STRIPPING PROGRAM FOR THE NUCLEAR DATA 50/50 ANALYZER SYSTEM. Haas, F. X. (Mound Lab., Miamisburg, Ohio). 21 Dec 1970. Contract AT(33-1)-Gen-53. 19p. Dep. NTIS.

Two computer subroutines have been written for the PDP-8L computer for the purpose of analyzing spectra displayed by a Nuclear Data 50/50 Analyzer System. The program is being used to operate on gamma-ray spectra obtained with a Ge(Li) spectrometer, but could easily be used for any spectrum accumulated in the analyzer. The Peak Strip routine gives the peak centroid, energy and area for an intensified peak. The Peak Normalize subroutine includes the printout of the peak centroid, peak energy, the count rate in counts per second, its statistical error, the relative intensity of the peak relative to some stored intensity and the statistical error in the relative intensity calculation. (auth)

8532 (UCRL−72481) PREAMPLIFIER NOISE EFFECTS ON SPECTROMETER ENERGY RESOLUTION. Armantrout, G. A. (California Univ., Livermore. Lawrence Radiation Lab.). 23 Oct 1970. 8p. (CONF-701109−1). Dep. NTIS.

From IEEE Nuclear Science Symposium, New York, N. Y.

Determining the detector contribution or the total system resolution of a Ge(Li) detector by quadrature subtraction or addition of electronic noise introduces serious error due to the non-Gaussian effects of carrier trapping. The contributions of electronic noise and detector spread to the total system resolution are found by computer spectrum simulation to be greater than expected. The conclusions are substantiated by agreement with experimental measurements. (auth)

8533 DYNAMICAL BEHAVIOR OF A CHOPPER-ROTATING CRYSTAL SYSTEM IN A NEUTRON TIME-OF-FLIGHT EXPERIMENT. Eder, O. J. (Physics Inst., Seibersdorf, Austria). Rev. Sci. Instrum.; 41: 1877-9(Dec 1970).

The installation of a phased chopper in front of a rotating crystal time-of-flight experiment is described. The results of the dynamics of the system, the background improvement, and the luminosity of the chopper rotating crystal spectrometer are presented. It is found that the significant background is reduced by a factor of 10, while the luminosity is decreased by about 10% only. (auth)

8534 SPECTROMETER WINDOWS. (to Office National d'Etudes et de Recherche Aerospatiales). French Patent 1,589,495. 31 Mar 1970. Filed 1 Oct 1968. (In French).

A plane circular element, which can be used as an entrance or an exit window for spectrometric or spectrographic apparatus, is described. The surface is divided into two multiple zone regions which behave differently with respect to the incident radiation. The zone contours are spiral shaped and form a non repetitive pattern in at least one direction. The total surface areas of the two regions are sensibly equal. These windows may be used at the entrance and exit of the same spectrometer; one or both of them may be given a periodic motion, thus modulating the radiant flux. (France)

8535 CALIBRATION OF A HIGH-SENSITIVITY GAMMA SPECTROMETER. Szende, Gabriella. Magy. Kem. Foly.; 76: 385-9(Aug 1970). (In Hungarian).

A low-background NaI(Tl) detector is described which is suitable for the qualitative and quantitative determination of gamma emit-

XUM

ting isotopes with low specific activity, in large volumes of material. The gamma spectrometer was calibrated utilizing the radiations from ^{123}Te, ^{131}I, ^{137}Cs, ^{65}Zn and ^{40}K for various source-detector geometries. The photopeak efficiencies, the contribution factors and the minimum detectable amounts are presented in tabulated form. (auth)

8536 SIMPLE TOTAL-REFLECTING LOW-ENERGY NEUTRON SPECTROMETER. Fiala, Werner; Wheeler, Carlos V. (Univ. of Puerto Rico, Mayaguez). Nucl. Technol.; 10: 215-20 (Feb 1971).

An instrument proposed as a total-reflecting low-energy neutron spectrometer was designed, constructed and tested at the Puerto Rico Nuclear Center. The spectrometer consists of a collimator and mirror assembly with standard counting equipment. The tests consisted of measurements of the spectra of three slightly different core conditions at a radial beam hole of the Swimming Pool Reactor of the PRNC. The data obtained indicate that the instrument is very sensitive and surprisingly able to detect changes in the neutron spectra due to small changes in the reactor core configuration. (auth)

8537 CONSTRUCTION MATERIALS FOR NEUTRON CAPTURE-GAMMA-RAY MEASUREMENT ASSEMBLY USING ^{252}Cf. Senftle, F. E. (Geological Survey, Washington, D. C.); Evans, A. G.; Duffey, D.; Wiggins, P. F. Nucl. Technol.; 10: 204-10 (Feb 1971).

To measure the neutron capture gamma ray spectrum of a sample using neutrons from a multimicrogram ^{252}Cf source, the Ge(Li) detector must be in a position to "see" the source. Thus, the encapsulation, moderating and shielding materials all become potential sources of spectral interference. An interference parameter is calculated for a number of elements generally found in the associated source and detector hardware. Using this parameter, other construction materials can also be chosen to minimize spectral interference in measuring neutron capture gamma ray spectra. (auth)

8538 DEVELOPMENTS IN APPLIED SPECTROSCOPY. VOLUME 7A. Selected Papers from the Seventh National Meeting of the Society for Applied Spectroscopy (Nineteenth Annual Mid-America Spectroscopy Symposium) Held in Chicago, Illinois, May 13–17, 1968. Grove, E. L.; Perkins, Alfred J. (eds.).

Publication of the Chicago Section of the Society for Applied Spectroscopy. New York; Plenum Publishing Corporation (1969). 348p. $15.00. (CONF-680560).

A separate abstract was prepared for one of the 42 papers presented. The remaining 41 papers were not within the scope of NSA. (W.H.K.)

For abstract of the individual paper see: 8539.

8539 NUCLEAR APPLICATIONS OF LIQUID SCINTILLATION SYSTEMS. Horrocks, Donald L. (Argonne National Lab., Ill.). Develop. Appl. Spectrosc.; 7A: 303-25(1969).

From 7th National Meeting on Society for Applied Spectroscopy, Chicago, Ill. See CONF-680560.

The use of liquid scintillation systems to study such nuclear properties as disintegration rates and energy spectra and for making particle determinations is discussed. The use of pulse-shape discrimination as a method for counting particles with a high specific ionization over a background of particles with low specific ionization is described. (30 references) (auth)

8540 IMPROVEMENT OF CHARACTERISTICS OF A DOUBLE-DIODE RESTORER OF BASE LEVEL. Ivanov, V. B.; Reshetov, N. N. Instrum. Exp. Tech. (USSR) (Engl. Transl.); No. 1, 120-2(Jan-Feb 1970).

Translated from Prib. Tekh. Eksp.; No. 1, 110-12(Jan-Feb 1970).

A method is described for improving the characteristics of a restorer of base level for a precision γ-spectrometer. The circuit for the restorer and the results of tests are presented. (auth)

8541 SEMICONDUCTOR GAMMA SPECTROMETER. Negrei, S. A.; Firsov, E. I. (Inst. of Physics, Minsk). Instrum. Exp. Tech. (USSR) (Engl. Transl.); No. 1, 45-7(Jan-Feb 1970).

Translated from Prib. Tekh. Eksp.; No. 1, 44-6(Jan-Feb 1970).

A gamma spectrometer is described having a Ge(Li) detector 2.7 cm^3 in volume with a resolution of 0.5% for ^{60}Co gamma radiation. The technique for preparing planar detectors is described. (auth)

8542 PULSE GENERATOR FOR STABILIZING A SPECTROMETER CIRCUIT. Marchenkov, V. V.; Nekhai, A. P. (Physical-Technical Inst., Leningrad). Instrum. Exp. Tech. (USSR) (Engl. Transl.); No. 1, 135-6(Jan-Feb 1970).

Translated from Prib. Tekh. Eksp.; No 1, 123-4(Jan-Feb 1970).

A reference-pulse generator intended for stabilizing a spectrometer circuit is described. The generator produces pulses close in shape to the signals at the detector output. The stability of the amplitude is not worse than 2 to 3 · 10^{-5}/°C; the range of overlapping energies (when operating with Ge(Li) detectors) is from 0.1 to 8 MeV with discrete switching of 25% of the preceding value. The maximum amplitude of the output signals is 0.75 V and the polarity of the pulses is positive. (auth)

High Energy Physics Instrumentation

8543 (DESY–70/60) STORING TRACKS IN STREAMER CHAMBERS. Eckardt, V. (Deutsches Elektronen-Synchrotron, Hamburg (West Germany)). Nov 1970. 13p. Dep. NTIS (U. S. Sales Only).

It is shown that a streamer chamber has storage capabilities for particle tracks when two high voltage pulses are applied to the chamber in succession. The first -"storage"- pulse produces invisible avalanches containing metastable states with a decay time of about 10^{-3} seconds. The second -"record"- pulse is the usual high voltage pulse for streamer photography. At a memory time for free electrons of less than 10^{-6} seconds (this is also the time resolution of the chamber) a storage time of a few 10^{-3} seconds is shown to be possible without loss in the accuracy of track location. (auth)

8544 (JINR–P1-5361) MAGNETIC SPARK CHAMBER SPECTROMETER FOR THE $K_L^0 - K_S^0$ REGENERATION INVESTIGATIONS AT HIGH ENERGIES. Basiladze, S. G.; Bespalova, T. V.; Birulev, V. K.; (and others) (Joint Inst. for Nuclear Research, Dubna (USSR)). 1970. 24p. (In Russian). Dep. NTIS (U. S. Sales Only).

The on-line spectrometer which consists of a magnet and magnetostrictive spark chambers triggered by a system of counters is described. The spectrometer has the invariant mass resolution of ±4 MeV, the space resolution of ±0.3 mm and the angular one ±0.4 mrad. (auth)

8545 (JINR–P13-5377) PULSE SHAPER WITH THE ZERO TIME OF REGENERATION FOR THE APPARATUS BLOCKING AT THE LARGE LOADING. Ondrish, L.; Mukhin, S. V.; Rikhvitskii, S. V.; Semenyushkin, I. N.; Khorvat, P.; Khrenov, A. N. (Joint Inst. for Nuclear Research, Dubna (USSR). Lab. of High Energy). 1970. 12p. (In Russian). Dep. NTIS (U. S. Sales Only).

A pulse shaper with zero regeneration time is described and the results of its test are presented. The amplitude and duration of the trigger pulses are not less than 0.3 V at 50 ohm and 10 ns respectively. The output pulse duration is fixed— 150, 350, 800, 1600 μs, the amplitude being 1 V at 50 ohm. The polarities of the trigger and output pulses are negative. The shaper was used in the blocking schemes for elimination of the pulse pile-up at the large loading. (auth)

8546 (LYCEN–6847) FABRICATION AND UTILIZATION OF LITHIUM-DRIFTED SILICON DETECTORS. Mackowski, J. M. (Lyon Univ. (France). Institut de Physique Nucleaire). Nov 1969. 23p. (In French). Dep. NTIS (U. S. Sales Only).

The discussion of lithium-drifted silicon detectors covers the principles of the method and theory of ion migration or drift, and fabrication tests and methods including lithium diffusion, measurement of the diffusion depth and the resistivity, choice of structure, test of the N/P junction, migration, and assembling. The characteristics and uses of these detectors are also considered. (J.F.P.)

8547 (PURC-4159-13) PERFORMANCE OF A LARGE-VOLUME TWO-PHOTOTUBE NEUTRON DETECTOR. Technical Report No. 4. Dakin, J. T.; Hauser, M. G.; Kreisler, M. N.; Mischke, R. E. (Princeton Univ., N. J. Dept. of Physics). 2 Dec 1970. Contract AT(30-1)-4159. 21p. Dep. NTIS.

This report describes the construction and performance of a $4 \times 1 \times 1/2$ ft liquid-scintillation counter having 5 in. diam phototubes at each end. An array of these detectors was developed to detect neutrons in $\pi^- + p \rightarrow n +$ (neutral missing mass) interactions for an experiment studying decays of the ω (783 MeV) and η' (958 MeV) mesons. When used for detection of 50 to 300 MeV neutrons, the system had a time-of-flight resolution of 2 nsec (FWHM), position resolution varying between 2 and 8 in. depending on the amount of scintillation light, and detection efficiency of 14% when operated at a light threshold of about 8 MeV electron energy. (auth)

8548 (UCRL–20126) FINDING EVENTS IN A SEA OF BUBBLES. White, Howard S. (California Univ., Berkeley. Lawrence Radiation Lab.). Oct 1970. Contract W-7405-eng-48. 26p. (CONF-701015–1). Dep. NTIS.

From Symposium on Future Extraction and Selection in Pattern Recognition, Argonne, Ill.

DAPR is a digital automatic pattern recognition system, designed to find and measure events in bubble chamber film without manual intervention. It is able to measure film which has come directly from the photographic development process, and to produce on magnetic tape a digital abstraction of the information contained in the film, from which a subsequent selection of desired events takes place by means of a digital scanning process. The DAPR system at Lawrence Radiation Laboratory, Berkeley, achieved production status earlier this year, and already has abstracted more than fifty thousand bubble chamber picture sets. Although development continues in some areas of the programs, DAPR measurements are being used by physics experimenters in the analysis of their data. It is expected that DAPR will process an increasing fraction of the data as the measurement of current experiments is completed, and that of new experiments is begun. (auth)

8549 (UR-875-324) SOME REMARKS CONCERNING THE PRECISION OF 1 TO 2 METER BUBBLE CHAMBERS. Slattery, P. (Rochester Univ., N. Y. Dept. of Physics and Astronomy). [1970]. 41p. (CONF-700623-2). Dep. NTIS.

The precision of 1- to 2-meter bubble chambers is discussed based on observations of the characteristics of the bubble chambers at SLAC, BNL, and ANL. Effects of Coulomb scattering on particle track resolution, actual resolution, particle track distortions, and kinematic fitting are discussed. Also a Monte Carlo study of the transverse momentum resolution, effective mass resolution, and missing mass resolution is discussed. (W.H.K.)

8550 USE OF ^{3}He COUNTERS IN THE ANTINEUTRINO EXPERIMENTS. Bogatyrev, V. K. Yadern. Fiz.; 12: 753-6 (Oct 1970). (In Russian).

A possibility of getting very low inherent background in the neutron counters is noted. This allows one to fulfill a number of experiments with antineutrinos: to measure the cross sections of deuterons, to test the neutrino oscillation theory, to measure the background from explosures of collapsing stars, to determine the total quantity of uranium on the earth. It is pointed out that measuring the time correlation between the Weber detector of gravitation waves and the antineutrino detector one is able to obtain the lower bound for the neutrino mass at a level of 1 eV. Observing the explosure of a collapsing star with three detectors one is able to determine the location of the star. (auth)

8551 SOME CHARACTERISTICS AND CAPABILITIES OF A DISCHARGE-CONDENSATION CHAMBER. Mandzhavidze, Z. Sh.; Roinishvili, V. N.; Dzhavrishvili, A. K. (Inst. of Physics, Tbilisi, USSR). Instrum. Exp. Tech. (USSR) (Engl. Transl.); No. 1, 48-52 (Jan-Feb 1970).

Translated from Prib. Tekh. Eksp.; No. 1, 46-51(Jan-Feb 1970).

A discharge-condensation chamber—a new particle detector similar to the cloud chamber—is described, and its characteristic features are reported. The chamber has a high time resolution and a long memory time for events. Other features of the chamber are isotropy, good spatial resolution, high track brightness, and suitability for use in working media of most gases, including He and H_2. (auth)

8552 WIRE SPARK CHAMBER SYSTEM WITH MAGNETOSTRICTIVE INFORMATION RETRIEVAL. Bekrenev, V. S.; Gordeev, V. A.; Kruglov, S. P.; Shchetkovskii, A. I. (Inst. of Engineering Physics, Leningrad). Instrum. Exp. Tech. (USSR) (Engl. Transl.); No. 1, 53-5(Jan-Feb 1970).

Translated from Prib. Tekh. Eksp.; No. 1, 52-4(Jan-Feb 1970).

A system of standard wire spark chambers with magnetostrictive information retrieval, operating on a coupling line with automatic information storage and processing center, has been developed. The time characteristics of the chambers and the accuracy of localization of the cosmic particle tracks were investigated experimentally. The efficiency of the chambers is >98% at an oscillator voltage of >4.5 kV, the storage time at a sweep voltage of 70 V is 2 μsec for He and 1 μsec for Ne. The dead time of the chambers is 20 and 40 μsec, respectively. The accuracy of location of the particle tracks is σ = 0.52 mm. (auth)

8553 SHOWER SPARK CHAMBERS FOR DETECTING PARTICLES MOVING AT SMALL ANGLES WITH RESPECT TO THE BEAM BEING STOPPED. Kryshkin, V. I.; Rybakova, N. A.; Sterligov, A. G.; Usov, Yu. P. (Tomsk Polytechnical Inst., USSR). Instrum. Exp. Tech. (USSR) (Engl. Transl.); No. 1, 56-9(Jan-Feb 1970).

Translated from Prib. Tekh. Eksp.; No. 1, 54-7(Jan-Feb 1970).

An apparatus with shower spark chambers is described for detecting particles moving from an internal synchrotron target at small angles with respect to the beam being stopped. The chambers and scintillation detectors have apertures for the beam. The apparatus has been used to measure the lifetime of the neutral pion and to study the angular distribution of electron-position pairs on the 1.5-GeV synchrotron. (auth)

8554 MEASURING DEVICES FOR PROCESSING PHOTOGRAPHS OF BUBBLE CHAMBERS (REVIEW). Mikheev, V. P.; Rozov, B. S. (Moscow Engineering Physics Inst.). Instrum. Exp. Tech. (USSR) (Engl. Transl.); No. 1, 1-17(Jan-Feb 1970).

Translated from Prib. Tekh. Eksp.; No. 1, 7-24(Jan-Feb 1970).

The characteristic features of devices for measuring the coordinates of tracks on photographs from bubble chambers are examined. Organization of data processing, scanning devices, measuring devices, instruments for rough measurements, ordinary measuring devices, instruments with local scanning, the HPD (Hough-Powell Device), the Spiral Reader (SR), cathode-ray tube systems, and laser beam scanning of film (SWEEPNIK) are discussed. A classification of instruments based on the method of determining coordinates is presented. (38 references) (W.H.K.)

8555 70-kOe PULSE MAGNET. Makar'in, V. K. (Inst. of Atomic Energy, Moscow). Instrum. Exp. Tech. (USSR) (Engl. Transl.); No. 1, 232-4(Jan-Feb 1970).

Translated from Prib. Tekh. Eksp.; No. 1, 201-3(Jan-Feb 1970).

A description is given of a pulse magnet designed for operation with a bubble chamber associated with a high-energy accelerator. A pulse magnetic field with an intensity of 70 kOe is obtained in a volume of 25 liters. Formulas are given for calculating the magnitude of the magnetic field and the time interval during which the intensity of the magnetic field remains constant with a given accuracy. The agreement between calculated and experimental magnitudes is good. (auth)

8556 COSMIC-RAY MU-MESON INTENSITY METER. Dragun, G. S. (Inst. of Physics, Moscow). Instrum. Exp. Tech. (USSR) (Engl. Transl.); No. 1, 127-9(Jan-Feb 1970).

Translated from Prib. Tekh. Eksp.; No. 1, 116-18(Jan-Feb 1970).

The circuit and construction of a meter for measuring the intensity of μ-mesons (m.i.m.) based on two scintillation counters situated one over the other are described. The area of the scintillator in each counter is 0.25 m^2. The m.i.m. is intended for measuring the flux of cosmic-ray μ-mesons under the ground at depths corresponding to a water equivalent of 500 m. At sea level the m.i.m. records 1710 ± 41 particles/min. (auth)

8557 EFFICIENCY OF A SPARK CHAMBER AT THE LOWER LIMIT OF IONIZATION. Sborshchikov, V. G.; Mikheev, S. P. (Inst. of Physics, Moscow). Instrum. Exp. Tech. (USSR) (Engl. Transl.); No. 1, 60-2(Jan-Feb 1970).

Translated from Prib. Tekh. Eksp.; No. 1, 58-9(Jan-Feb 1970).

A method is described for obtaining and measuring a small number of free electrons in a spark chamber. The measured efficiency for the detection of a single electron in a spark chamber is no less than 70%. (auth)

8558 USE OF THE MAXIMUM-PROBABILITY METHOD TO DETERMINE THE KINEMATIC PARAMETERS OF TRACKS. Ososkov, G. A.; Shlyapnikov, P. V. (Joint Inst. for Nuclear Research, Dubna, USSR). Instrum. Exp. Tech. (USSR) (Engl. Transl.); No. 1, 63-4(Jan-Feb 1970).

Translated from Prib. Tekh. Eksp.; No. 1, 60-1(Jan-Feb 1970).

It is shown that evaluations of kinematic parameters of bubble chamber tracks by the method of least squares and by the method of maximum probability are essentially the same, despite the strong dependence of the multiple-scattering matrix on the particle momentum. (auth)

8559 DISTRIBUTION OF THE RANDOM DISPLACEMENT OF TRACK POINTS DUE TO COULOMB MULTIPLE SCATTERING. Manyukov, B. A.; Shlyapnikov, P. V. (Joint Inst. for Nuclear Research, Dubna, USSR). Instrum. Exp. Tech. (USSR) (Engl. Transl.); No. 1, 65-7(Jan-Feb 1970).

Translated from Prib. Tekh. Eksp.; No. 1, 61-3(Jan-Feb 1970).

A multidimensional distribution function is obtained for the random displacement of a track point due to multiple scattering; this procedure is based on representing multiple scattering as a random Markov process. It is shown that the covariation matrix in the distribution coincides with the previously introduced multiple-scattering matrix. (auth)

8560 COMMUNCIATION SYSTEM BETWEEN A SCINTILLATION HODOSCOPE AND MINSK-22 COMPUTER. Belotsvetov, A. E.; Belyaevskii, L. V.; Derevshchikov, A. A. (and others) (Inst. of High-Energy Physics, Serpukhov, USSR). Instrum. Exp. Tech. (USSR) (Engl. Transl.); No. 1, 99-100(Jan-Feb 1970).

Translated from Prib. Tekh. Eksp.; No. 1, 92-3(Jan-Feb 1970).

A communication system between a scintillation hodoscope and

XUM

Minsk-22 computer is described. A system of programs is described for setting up the hodoscope communication system. (auth)

8561 CALCULATION OF THE MOMENTUM VECTOR IN A MAGNETIC TRACK SPECTROMETER. Tarasov, E. K.; Kishkurno, V. V. (Inst. of Theoretical and Experimental Physics, Moscow). Instrum. Exp. Tech. (USSR) (Engl. Transl.); No. 1, 42-4(Jan-Feb 1970).

Translated from Prib. Tekh. Eksp.; No. 1, 42-4(Jan-Feb 1970).

A method is proposed for directly calculating the momentum vector p at the measured points of the track of a charged particle moving in the magnetic field of a track apparatus (magnetic spectrometer with spark chambers). Depending on the accuracy required, the results of the p calculation can be used to solve the physical problem either directly or after refinement by an iterative method. (auth)

Radiation Dosimeters

Refer also to abstracts 8482, 8487, 8672, 8676, and 9574.

8562 (CERN-DI/HP-29) APPROACH TO A REM DOSIMETER USING IONIZATION CHAMBERS. Sullivan, A. H. (European Organization for Nuclear Research, Geneva (Switzerland)). 8 Jan 1964. 11p. (CONF-640109-1). Dep. NTIS (U. S. Sales Only).

From Symposium on Neutron Dosimetry for Radiological Purposes, London, England.

The columnar recombination in an ionization chamber is a function of the specific ionization of the ion columns produced by the radiation and hence of the L.E.T. and Q.F. An ionization chamber has been designed to make use of this effect so that it has a response proportional to the average Q.F. of radiation. The proposed dosimeter consists of a low-pressure tissue equivalent ionization chamber to measure rad dose-rate, coupled to the chamber to estimate the Q.F. A simple difference circuit enables rem dose-rate to be read directly. The performance and limitations of such a dosimeter are discussed. (auth)

8563 (NYO-2740-7, pp 52-110) RADIOLOGICAL PHYSICS: II. MEASUREMENTS OF MICROSCOPIC DISTRIBUTION OF RADIATION ENERGY. (Columbia Univ., New York. Radiological Research Lab.).

From annual report on research project.

The development of wall-less proportional counters is discussed; developments in the theory of microdosimetry are described; and a study on the measurement of the dose distribution for californium-252 is outlined. Also, an attempt to measure the wall effect in the tissue-equivalent proportional counter is outlined, and an experimental and theoretical investigation of the counting rate vs gas density in a cylindrical wall-less proportional counter are reviewed. (W.H.K.)

8564 ERRORS IN FERROUS SULPHATE DOSIMETRY. Broszkiewicz, R. K.; Bulhak, Z. (Inst. of Nuclear Research, Warsaw). Phys. Med. Biol.; 15: 549-56(Jul 1970).

A statistical analysis is made of 83 values of the Fe^{3+} extinction coefficient in direct uv spectrophotometry. Six of these coefficients were obtained by varying the source of standard ferric solution. The results show that errors in Fricke dosimetry arise from the preparation of the reference Fe^{3+} solution as well as in the spectrophotometer. The effect of NaCl on the extinction coefficient is shown to be negligible in 0.8 N but not in 0.1 N H_2SO_4 solution. A recommended procedure of establishing the Fe^{3+} extinction coefficient is proposed. (auth)

8565 SEMICONDUCTOR DOSIMETER HAVING LOW TEMPERATURE DIFFUSED JUNCTION. Kramer, Gordon. U. S. Patent 3,527,946. 8 Sep 1970. Filed 13 Jun 1966.

A fast-neutron radiation dosimeter comprising a semiconductor having a low temperature diffused p-n junction comprising silicon with a dopant of lithium diffused therein is described. Total dosage is indicated by measuring the short circuit current obtained in the presence of light (photovoltaic effect). (auth)

8566 STORED-CHARGE EFFECTS ON ELECTRON DOSE-DEPTH PROFILES IN INSULATORS. Harrah, L. A. (Sandia Labs., Albuquerque, N. Mex.). Appl. Phys. Lett.; 17: 421-3 (15 Nov 1970).

The dose-depth profiles for electrons extracted from a pulsed electron beam machine were studied, using a castable radiation-sensitive plastic. These profiles exhibit a pronounced range shortening at charge fluences greater than 0.5 μ C/cm^2 which reaches a limiting value, corresponding to a limiting internal field, at fluences greater than 1 μ C/cm^2. This behavior is interpreted in terms of charge buildup and relaxation by radiation-induced conductivity in the host material, poly(vinyl toluene). Positive charge-trapping additives reduce this conductivity and allow the internal field to build up at lower charge fluences. The ratio of radiation-induced conductivity to dose rate derived from these measurements 1.6×10^{-18} sec/Ω-cm rad compares favorably with the value found at low dose by direct measurement of 3.0×10^{-18} sec/Ω-cm rad. (auth)

8567 MIXED RADIATION DOSIMETRY WITH LiF (TLD-100). Busuoli, G. (CNEN, Bologna); Cavallini, A.; Fasso, A.; Rimondi, O. Phys. Med. Biol.; 15: 673-81(Oct 1970).

The LiF dosemeter presents two main glow peaks, one at 210°C and the other at a temperature between 250 and 300°C. It is shown that the two-peak ratio depends on the type of incident radiation. This characteristic makes is possible to use LiF to measure doses in mixed fields (slow neutrons and electromagnetic radiations). The method is reliable for personal dosimetry. (auth) (UK)

8568 CALIBRATION OF CLEAR PERSPEX HX FOR RADIATION DOSIMETRY. Simmons, J. A. Phys. Med. Biol.; 15: 748-50(Oct 1970).

Measurements are described on the calibration of clear Perspex HX for use as a radiation dosemeter which gave results at variance with those of Berry and Marshall (Phys. Med. Biol. 14: 585 1969). The Perspex was obtained from the U. K. Panel on Gamma and Electron Irradiation together with the calibration. After irradiation with x-rays, the Perspex gave a 10% high reading in comparison with an ionization chamber. The source of discrepancy was thoroughly investigated from which it appeared that this lay with the Perspex calibration and it is therefore suggested that if better than 10% accuracy is required, users must be prepared to carry out their own calibration. In reply to the letter above it is stated that the original work was the cumulative effort of five independent laboratories and the agreement between these was of the order of a few percent. In an attempt to explain the discrepancy it is mentioned that the time between irradiation and readout in the measurements of Simmons was 24 hours while the original delay time was 4 days to obviate any errors arising from optical density build-up and fading changes. It is also pointed out that post-irradiation exposure of Perspex HX to sunlight can cause large increases in radiation-induced optical density. (UK)

8569 THERMOELASTIC DOSIMETRY OF RELATIVISTIC ELECTRON BEAMS. Perry, F. C. (Sandia Labs., Albuquerque, N. Mex.). Appl. Phys. Lett.; 17: 408-11(1 Nov 1970).

A technique is described of obtaining directly the energy absorption profile of a solid heated by pulses of intense radiation. The appropriate thermoelastic equations were solved for two cases of particular interest, instantaneous deposition and energy absorbed at a constant rate. The dynamic response of aluminum and copper to electrons of average energy 1.5 MeV was measured by means of a laser interferometer, and the resulting energy profiles were compared with profiles obtained using a thin-film dosimetry technique. The resulting quantitative agreement with the thermoelastic theory is discussed. (auth)

Radiometric Instruments

8570 NEUTRON METHOD OF SOIL MOISTURE MEASUREMENT INDEPENDENT OF DRY DENSITY. Couchat, Philippe (CEA, Cadarache, France). Compt. Rend., Ser. D; 271: 1264-7(12 Oct 1970). (In French).

To obtain a neutron measurement of soil moisture, a principle of slow neutron detection at two energy levels is proposed. The constants by which the moisture can be calculated from the counting values are given for six soils. In cases where the water content used is the total water content, these constants depend only on the absorbing capacity of the soils. (France)

Miscellaneous Instruments and Components

Refer also to abstracts 8193, 8220, 8397, 9301, 10018, 10255, 10267, 10271, 10323, 10324, and 10326.

8571 (AAEC/TM-568) ON-LINE COMPUTER SYSTEM FOR A MASS SPECTROMETER. Tighe, L. E. (Australian Atomic Energy Commission Research Establishment, Lucas Heights). Oct 1970. 23p. Dep. NTIS (U. S. Sales Only).

Surface ionization mass spectrometers are commonly used to provide accurate isotopic abundance measurements of solid

samples. The method of mass scan control is described, together with the data logging system. Included as well are a description of the relevant parts in the PDP-8/L program, instructions for communication with the computer by the operator, and the computer interface circuit diagrams. (Australia)

8572 (HMI-B-96) A MODULAR PROGRAM SYSTEM FOR EXPERIMENTAL PROGRAMING FOR THE PDP-9. Degenhardt, K. H.; Frevert, L.; Woletz, W. (Hahn-Meitner-Institut fuer Kernforschung, Berlin (West Germany)). Jul 1970. 82p. (In German). Dep. NTIS (U. S. Sales Only).

A programming system for nuclear physics experiments controlled by a digital computer is described. Programs are generated by a preassembler program which takes macro instructions and prefabricated subroutine calls out of a library and places parameters into them which the user has been asked for. Each type of macro instruction is represented by a special flow chart symbol. Thus programs can be generated in dialog by using flow charts only. (auth)

8573 (KFK-1241) CAMAC: A SYSTEM OF COMPUTER-CONTROLLED ELECTRONICS. PRINCIPLE AND USE. Tradowsky, K. (Kernforschungszentrum, Karlsruhe (West Germany). Labor fuer Elektronik und Messtechnik). Jul 1970. 32p. (In German). Dep. NTIS (U. S. Sales Only).

The CAMAC system creates a strong connection between a computer and measuring and control techniques. A specified 24-bit dataway with command and function codes ensures the development of compatible modules. So this modular system is very flexible and has a great reliability. The CAMAC system is not restricted to the instrumentation of nuclear physics experiments and the like. It is also applicable to measurement and control systems and process control. A computer increases the features of the CAMAC system enormously but it may also be used with any digital controller. The CAMAC system of computer-controlled electronics is described in summary. It is pointed out that CAMAC has correlations with the software. By means of some finished or projected equipment assemblies the state-of-art of the system is shown. (auth)

8574 (PRNC-140) ANNUAL REPORT, 1969. (Puerto Rico Nuclear Center, Mayaguez). Contract AT(40-1)-1833. 157p. Dep. CFSTI.

Research and development progress in nuclear science, nuclear engineering, physical sciences, clinical radioisotope applications, radiotherapy and cancer, tropical agro-sciences, medical sciences and radiobiology, reactors, health physics, and radioecology is outlined. The international exhibits program is described, and papers, publications, and seminars are listed. (W.H.K.)

8575 DIGITAL rf PULSE BURST GENERATOR FOR NMR RELAXATION EXPERIMENTS. Radeka, V. (Brookhaven National Lab., Upton, N. Y.).; Chase, R. L.; Petrinovic, M.; Glasel, J. A. Rev. Sci. Instrum.; 41: 1766-70(Dec 1970).

A pulse burst generator designed to provide coherent rf pulse sequences with lengths applicable to NMR relaxation experiments is described. The burst generator is based on a principle which provides an inherently high on/off ratio. The frequency of interest is generated by mixing two higher frequencies. Bursts of arbitrary length are generated by gating these two higher frequencies so that in the off intervals there is no signal at the frequency of interest in the entire generator system. Burst lengths are determined digitally to within one cycle by a preset counter. A number of different burst lengths can be selected by several sets of switches to generate a Carr-Purcell sequence of bursts. Bursts with 90° rf phase shift can be generated in this sequence as is required for the Meiboom-Gill method. Phase and frequency relations in the generator are determined digitally, so that no tuning adjustments are required for operation of the generator over the whole frequency range. The described generator employs MECL II integrated circuits which restrict the highest output frequency of the generator to about 10 MHz. (auth)

8576 MINIMUM IMAGE SIZE IN A PARALLEL PLATE ELECTROSTATIC SPECTROGRAPH. Proca, G. A.; Green, T. S. (European Space Research Inst., Frascati, Italy). Rev. Sci. Instrum.; 41: 1778-83(Dec 1970).

Previous analysis of the focusing properties of a parallel plate electrostatic spectrograph has shown that second order focusing can be achieved. It is demonstrated that as a corollary, there exists an optimum focal line in which the angular aberrations are reduced to one quarter of their values on the normal focal line, as is the case in optical systems. Results of computations of the line shapes are also presented. (auth)

8577 RADIATION SEALED X-RAY DIFFRACTION CAMERA. Bataller, Simone; Nemoz, Alain (to Commissariat a l'Energie Atomique). French Patent 1,589,405. 31 Mar 1970. Filed 3 Apr 1968. (In French).

A cylindrical x-ray diffraction camera for the analysis of radioactive powder samples is described. The various sealings are mounted between the observation holes and the interior of the camera, between the camera and the collimator tube, at the level of the rotating specimen holder, at the lid level, at the level of the exterior specimen alignment mechanism, and the film tension adjustment screw. The various devices used are described and the nature of joints, varnishes, and greases used to ensure radiation sealing are specified. (France)

8578 MASS SPECTROMETER WITH ENERGY DISPERSION. Graefen, W.; Ewald, H. (Justus-Liebig-Univ., Giessen, Ger.). Nucl. Instrum. Methods; 88: 295-308(1970). (In German).

For special mass spectrometers consisting of three sector fields the ion optical properties are derived in a second order approximation with the use of the matrix method. All fringing field effects are included in the calculations. The field arrangements are chosen in such a manner that stigmatic focusing is achieved on the image surface. Similar to the parabola spectrograph the instruments produce an energy dispersion in the direction of the mass lines. The transfer matrix product of the whole field combination is derived using (27×27)-matrices which combine the radial and axial transfer matrices of the single fields. In this product also a matrix is used which allows the connection of the first two fields which have a common mean plane of deflection. Another matrix renders the connection of the second and the third field the mean planes of deflection of which are vertical to each other. Numerical results are given for the geometrical dimensions and the image aberrations of one example of these field arrangements. (auth)

8579 COMPLEMENTARY TO 14-MeV NEUTRON GENERATOR: AUTOMATIC SYSTEM FOR THE CONTROL OF THE SHORT-LIVED ISOTOPE ANALYSIS EQUIPMENT. Adamek, A.; Severa, F. (Inst. of Physics, Bratislava). Czech. J. Phys.; 20: 1209-13(1970).

A description of the system for both remote and automatic control of the entire process of the sample irradiation, transfer, and counting is given. The system, which is most frequently referred to as a sequence programmer, has been found suitable for the control of the short-lived isotope analysis equipment. (auth)

8580 CURRENT GENERATOR FOR STUDYING SUPERCONDUCTIVITY BY AN IMPULSE METHOD. Frantsevich, V. M.; Klyushnikov, O. I.; Romanov, E. P. (Inst. of Physics of Metals, Sverdlovsk, USSR). Instrum. Exp. Tech. (USSR) (Engl. Transl.); No. 1, 141-2(Jan-Feb 1970).

Translated from Prib. Tekh. Eksp.; No. 1, 127-8(Jan-Feb 1970).

A saw-tooth waveshape impulse current generator for studies of superconductivity is described. Current impulses of 70 A with durations of 50, 100, and 150 μsec are generated on a load of 0.1 Ω. (auth)

Radiation Effects on Instruments and Instrument Components

8581 (LYCEN-6933) TRANSIENT EFFECTS OF RADIATION ON DIODES AND BIPOLAR TRANSISTORS. Gaillard, Remi (Lyon Univ. (France). Institut de Physique Nucleaire). Jul 1969. 107p. (In French). Dep. NTIS (U. S. Sales Only).

Thesis.

After a review of the interaction mechanisms of nuclear particles with solids, the creation of electron-hole pairs and the relation with the absorbed energy are discussed. Photocurrents in junctions in various technologies are studied. Mechanisms for amplification of photocurrents in transistors and calculations of storage time under radiation are considered. Finally, measurements of physical parameters and the transient response of bipolar transistors are described. (J.F.P.)

8582 DEGRADATION OF THE LUMINESCENCE OF PLASTIC POLYSTRENE SCINTILLATORS. Zhiltsova, L. Ya.; Matveeva, E. N.; Stoletova, I. M.; Shafranov, M. D. Opt. Spectrosc. (USSR) (Engl. Transl.); 28: 510-11(May 1970).

Translated from Opt. Spektrosk.; 28: 941-2(May 1970).

A study was conducted of the changes in the luminescence intensity (degradation) of plastic scintillators as a function of the time of uv irradiation (2540 Å) in the absorption bands of the activators. The luminescence spectra of samples of different compositions were investigated before and after irradiation. It was established that the degradation rate of the scintillating materials depends on the molecular structure. (auth)

XUM

LIFE SCIENCES

Biochemistry, Physiology, and Molecular Biology

Refer also to abstract 8268.

Basic Processes

Refer also to abstracts 8662 and 8724.

8583 (STI/PUB-252) NUCLEAR TECHNIQUES FOR STUDYING PESTICIDE RESIDUE PROBLEMS. Panel Proceedings Series. Proceedings of a Panel held in Vienna, 16-20 December 1968. (International Atomic Energy Agency, Vienna (Austria)). 1970. 89p. (CONF-681228). IAEA $3.00.

Abstracts were prepared for two of eight papers. The titles of the papers not abstracted were Insecticide Residues in Cocoa, Malathion Residues and Their Fate in Cereals, Metabolism of ^{14}C-Labeled Organochlorine Insecticides, Organo-mercurials as an Environmental Problem, International Co-operation on the Problems of Pesticide Residues in Food, and The Activities of FAO/WHO on Pesticide Residues in Food. (E.E.H.)

For abstracts of individual papers see: 8588 and 8600.

8584 (SZS-15/70) QUANTITATIVE ALPHA-AUTORADIOGRAPHY: A DOCUMENTATION. Kraus, W.; Friemert, R. (Staatliche Zentrale fuer Strahlenschutz, Berlin (East Germany)). Jun 1970. 21p. (In German). Dep. NTIS (U. S. Sales Only).

A documentation compiling 130 articles on problems of quantitative autoradiography published up to 1969 is presented. Based on characteristic examples taken from the literature, the most important aspects of the subject are summarized in a brief discussion. (auth)

8585 NORMAL PLASMA CORTISOL VALUES DETERMINED BY A DOUBLE ISOTOPE DERIVATIVE TECHNIQUE. Hippe, E.; Buus, O.; Blichert-Toft, M.; Jensen, H. Kaalund. Ugeskr. Laeger; 132: 219-21(1970). (In Danish).

The normal plasma cortisol values between 8 and 9 a.m. were determined on 2 × 2 ml plasma employing a double isotope derivative technique. In order to correct for the loss during the analysis procedure, a known quantity of cortisol labeled with tritium was added from the commencement. The cortisol was then esterified with ^{35}S-pipsan. Isolation was undertaken by partition between two fluid phases and thin-layer and paper chromatography. Investigation of 155 normal individuals aged 14 to 94 yr revealed the normal limits to be 6.5 to 30.0 μg/100 ml with an average value of 15.1 μg/100 ml ± 5.4 (S.D.). Neither sex nor age variations were encountered. (auth) (Denmark)

8586 USE OF ^{133}Xe FOR STUDIES ON EFFECTS OF INSULIN AND GLUCOSE ON BLOOD FLOW IN RESTING MUSCLE. II. Graban, Wieslaw. Pol. Przegl. Radiol. Med. Nukl.; 34: 127-41 (Jan-Feb 1970). (In Polish).

The influence of various combinations of glucose and insulin on blood flow in resting muscles was studied using ^{133}Xe as a tracer. A marked increase in blood flow was observed following small doses of glucose. An increase of the blood adrenalin level is suggested as a cause of this phenomenon. This is associated with an increased insulin concentration and increased osmotic tension in the intercellular space during the course of glucose administration. (auth)

8587 DETERMINATION OF CONTAINED-MILK VOLUME OF THE MAMMARY GLAND OF THE GOAT BY ^{141}Ce AND ^{14}C-PEG-4000. Snipes, M. B.; Lengemann, F. W. (Cornell Univ., Ithaca, N. Y.). Contract AT(30-1)-4039. J. Dairy Sci.; 53: 1596-1602(Nov 1970).

Cerium-141 and ^{14}C-polyethylene glycol, molecular weight 4,000, were used in an isotope dilution technique to determine the volume of milk in the mammary gland of the goat. Procedures included introduction of label into the mammary gland by way of the teat meatus and an intravenous injection of 2 IU of oxytocin followed by hand manipulation of the udder to facilitate uniform mixing of cistern, duct, and that portion of the alveolar milk let down in response to the oxytocin. Assay of any size milk sample taken after this procedure allows approximation of the mammary gland-contained milk volume at the time of the oxytocin dose. Results were consistently the same for both ^{141}Ce and ^{14}C-polyethylene glycol, allowing the option of using either label in the technique. Recovery of both labels was essentially 100% 3 days after dosing the udder, and no ^{141}Ce was detected in blood or urine within 24 hours. Label was distributed uniformly among serial samples of the milk readily collectable after the mixing procedure, representing 87.9% of the computed total milk volume. A portion of the residual milk recovered with a second dose of oxytocin showed ^{141}Ce and ^{14}C-polyethylene glycol amounts similar to those of the milk already collected. (auth)

8588 DETERMINATION OF MERCURY AND BROMINE IN FLOUR. Merten, D.; Tugsavul, A. (International Atomic Energy Agency, Vienna). pp 39-41 of Nuclear Techniques for Studying Pesticide Residue Problems. Vienna; International Atomic Energy Agency (1970).

From Panel on Nuclear Techniques for Studying Pesticide Residue Problems, Vienna, Austria. See STI/PUB-252; CONF-681228.

A study was made on the presence of bromine and mercury in flour using a neutron activation technique. Due to the widespread use of organic compounds of these elements in industry, agriculture, and the food industry, they are common contaminants of food products. In cooperation with a number of institutes, four comparisons were made to investigate the accuracy of results in particular types of analysis. The results were presented graphically. (E.E.H.)

8589 DIURNAL VARIATION IN THE LABELING INDEX OF MOUSE EPIDERMIS: A DOUBLE ISOTOPE AUTORADIOGRAPHIC DEMONSTRATION OF CHANGING FLOW RATES. Grube, D. D.; Auerbach, H.; Brues, A. M. (Argonne National Lab., Ill.). Cell Tissue Kinet.; 3: 363-73(Oct 1970).

A diurnal rhythmicity in the labeling index was observed in the epidermis of hairless mice, injected with either ^{14}C- or ^{3}H-thymidine, at different times during a 24 hr period. A modified autoradiographic technique, using ^{14}C- and ^{3}H-thymidine and two overlying emulsion layers, makes it possible to clearly differentiate synthesizing cells that were singly labeled with either carbon-14 or tritium, and cells labeled with both isotopes. At various times during a 24 hr period, hairless mice were injected with thymidine-2-^{14}C and colcemid, followed at 2 or 3 hr by a second injection of ^{3}H-thymidine. The labeling indices were calculated for the ^{14}C- and ^{3}H-thymidine injection times. These labeling indices were consistent with the control, single isotope, labeling indices and exhibited the same diurnal rhythm. Cells singly labeled with ^{3}H- or ^{14}C-thymidine either started or completed DNA synthesis during the interval between the two injections. Flow rates into and out of DNA synthesis, throughout the 24 hr period, can be calculated from these singly labeled cells. The flow rates varied rhythmically throughout the day and paralleled changes in the labeling indices. The influx and efflux flow rates, at all times measured, were not equal. The influx flow rate was reflected in the efflux rate at a time later equal to the duration of S. By means of these flow rates, the percent of cells in DNA synthesis was calculated for each hour during a 24 hr period. The resulting labeling index curve matched the observed 24 hr diurnal rhythm in labeling indices. By extension of these flow rates through mitosis, the resulting mitotic index curve was comparable to the reported 24 hr diurnal rhythm in mitotic indices. (auth)

Metabolism, Physiology, and Toxicology

Refer also to abstracts 8669 and 8755.

8590 (CEA-CONF-1658) EXPERIMENTAL RESEARCH ON THE TREATMENT OF CONTAMINATION BY TRANSPLUTONIUM ELEMENTS. Lafuma, J.; Nenot, J. C.; Morin, M. (Commissariat a l'Energie Atomique, Fontenay-aux-Roses (France). Centre d'Etudes Nucleaires). 1970. 8p. (In French). (CONF-700930-1). Dep. NTIS (U. S. Sales Only).

From Seminar on Radiation Protection Problems Relating to Transuranium Elements, Karlsruhe, Germany.

Saline solutions of ^{239}Pu, ^{238}Pu, ^{241}Am and ^{242}Cm were administered by intramuscular injection and by inhalation in the form of aerosols to Sprague Dawley rats (SPF) for therapeutic research purposes. The diffusion in the organism of quantities injected intramuscularly was studied as a function of time, together with the activity distribution in the skeleton, urinary system, liver and feces. A fraction of ^{241}Am and a still larger fraction of ^{238}Pu remained in the blood and the muscles. Next was studied the metabolism of the inhaled activity fraction, which was insolubilized in the air cells of the lungs and eliminated in the bones and urinary system. The greater solubilization of Am and Cm was observed, and also the elimination of Pu from the lung by the trachea and the feces. Therapeutic studies were

carried out in two directions: general decontamination and decontamination of the skeleton. Treatments were performed with sodium DTPA at pH 5, administered either by intramuscular injection or by inhalation of aerosols. The results showed the effectiveness of the treatment in the prevention of bone accumulations. (auth)

8591 (CEA-CONF-1677) CLEARANCE OF RADIOISOTOPES FROM LUNGS OF RATS. Nenot, J. C. (Commissariat a l'Energie Atomique, Fontenay-aux-Roses (France). Centre d'Etudes Nucleaires). 1970. 7p. (In French). (CONF-700931-1). Dep. NTIS (U. S. Sales Only).

From 3rd International Symposium on Inhaled Particles, London, England.

The influence of exposure to radiation on lung clearance in rats was studied: either external exposure at L.D. 50 or internal exposure with ^{239}Pu aerosols at different concentrations. Three levels of alveolar contamination by α emitters were studied (1, 0.1 and 0.007 μCi.g of lung). Lung clearance was tested 10 days after exposure, with insoluble ^{59}Fe oxide particles given to the animals by inhalation. External exposure did not modify either the retention or clearance rate, whereas internal exposure to α particles significantly modified clearance kinetics. (France)

8592 (COO-1339-43) ANIMAL METABOLIC STUDIES OF STRONTIUM AND CALCIUM WITH SPECIFIC REFERENCE TO FALLOUT RADIONUCLIDES. Progress Report No. 7, August 16, 1969-August 15, 1970. (Illinois Univ., Urbana. Dept. of Veterinary Physiology and Pharmacology). Contract AT(11-1)-1339. 21p. Dep. NTIS.

Kinetics of ^{47}Ca metabolism were investigated in eight cows during successive periods of gestation, parturition, and lactation. It was found that the turnover of the exchangeable calcium pool was markedly increased only at parturition and the onset of lactation, but not during pregnancy itself. The turnover remained at a high level only during moderate to heavy lactation, subsequently declining as milk production decreased. The non-pregnant, non-lactating cow demonstrated relatively constant values for the exchangeable calcium pool. Studies on effects of dietary calcium and phosphorus intake on kinetics of the exchangeable calcium pool in goats showed that only goats ingesting the high calcium ration were in positive calcium balance, whereas all goats were in positive phosphorus balance. Data from the ^{47}Ca kinetic studies demonstrated that the turnover rate of all goats decreased during the second trial period. For studies on the role of estrogens in the etiology of parturient hypocalcemia in dairy cows, a method for radioimmunoassay of estrogen in plasma using ^{3}H-estradiol was developed. Preliminary studies on the effects of estrogens on rats showed that 17 B estradiol resulted in a stimulated ^{47}Ca and ^{85}Sr transfer in the females only. Studies on retention of strontium in swine were initiated. (H.L.W.)

8593 (COO-1733-11) ^{210}Po IN SOILS AND PLANTS. Hansen, Wayne R. (Colorado State Univ., Fort Collins. Dept. of Radiology and Radiation Biology). Jun 1970. Contract AT(11-1)-1733. 142p. Dep. NTIS.

Polonium-210 used as a radionuclide fuel for SNAP electrical generators may present a long term hazard if accidental release of the isotope were to contaminate agricultural soils. Absorption of $^{210}PoO_2$ in soils studied by bulk determination of distribution coefficients (K_d) indicated retention in the top soil samples was correlated with silt content. An empirical equation describing agricultural top soil absorption was derived as $\ln K_d = 3.2 + 0.046$ (percent silt). The distribution coefficients of the combined data for the A, B, and C horizons combined were correlated with soil pH and silt content and could be described by the derived empirical equation $\ln K_d = -1.3 + 0.034$ (percent silt) + 0.88 (pH). Polonium oxide was eluted through soil columns and successfully tested these distribution coefficients. Greater than 98% of the $^{210}PoO_2$ was retained by the first 2 cm of soil with K_d's greater than 100. Top soil samples with K_d's less than 100 indicated $^{210}PoO_2$ would be retained by the lower soil horizons. Hazards to water supplies by movement of ^{210}Po through soil would be minimal. Chemical species of ^{210}Po in soil solution examined by electrophoresis and dialysis experiments indicated both positive and negative species existed. Dialysis experiments indicated approximately 34% of the ^{210}Po in soil solution passed through a semi-permeable membrane. Plant uptake of $^{210}PoO_2$ added to three different soils was measured and expressed as a transfer coefficient, U, where U = (^{210}Po/g dry plant tissue)/(^{210}Po/g dry soil). Transfer coefficients of 11 different fruit, grain, leafy, and root crops ranged from 10^{-2} to 10^{-4}. The transfer coefficients remained constant for the majority of plant tissues examined, although the distribution coefficients differed for the three soils used. Calculations using the transfer coefficients for estimating dietary intake of ^{210}Po from vegetables indicate a potential long-term ingestion hazard to the population. Protein hydrolyzates of wheat and spinach were separated by paper chromatography to investigate possible organic forms of polonium in plants. One possible organic form of polonium was observed. Measurements of naturally occurring ^{210}Po in the soil samples indicated a range of 0.22 to 3.47 pCi/g in top soils. Polonium-210 measured in the vegetation used for controls in the greenhouse experiments indicated the primary source of the isotope was the fallout of airborne ^{210}Po and its radioactive precursors. (auth)

8594 (LF-tr-41) PROBLEMS OF PLUTONIUM TOXICOLOGY. Buldakov, L. A.; Lyubchanskii, E. R.; Moskalev, Yu. I.; Nifatov, A. P. Translated by A. A. Horvath (Lovelace Foundation, Albuquerque, N. Mex.), from Problemy Toksikologii Plutoniya, Atomizdat, Moscow, 1969. 225p. Dep. NTIS.

Separate abstracts were prepared for four parts of the report. An introduction which deals with various aspects of plutonium toxicology and extensive bibliographies is also included. (H.L.W.)

For abstracts of individual sections see: 8238, 8595, 8596, and 8674.

8595 (LF-tr-41, pp 7-125) DISTRIBUTION OF ^{239}Pu IN THE BODY AFTER VARIOUS ROUTES OF ADMINISTRATION. Translated from Problemy Toksikologii Plutoniya, Atomizdat, Moscow, 1969.

A review of the literature is presented on the distribution of ^{239}Pu in the body after the following routes of administration: intravenous, intraperitoneal, subcutaneous, and intramuscular injection, application to the skin, inhalation, and ingestion. Effects of the following factors on the fate of intravenously injected ^{239}Pu are reviewed: type of compound injected, dose, species of animal, and age. A table is presented to show results of studies on relative concentrations in various organs and tissues. Studies on relative tissue distribution as a function of route of administration showed that a considerable fraction remained at the site of application and in lymph nodes following peroral, subcutaneous, intramuscular, topical, and inhalation administration. Studies on microdistribution of ^{239}Pu in the body emphasized localization in the lungs, skeleton, liver, and skin. The mechanism of plutonium binding in the liver and skeleton is reviewed; binding with nucleic acids and proteins is emphasized. (239 references) (H.L.W.)

8596 (LF-tr-41, pp 127-97) BIOLOGICAL EFFECTS OF PLUTONIUM FOLLOWING VARIOUS ROUTES OF ADMINISTRATION. Translated from Problemy Toksikologii Plutoniya, Atomizdat, Moscow, 1969.

The effects of the following routes of administration of ^{239}Pu on tissue distribution, life span, hematopoietic system, biochemistry of tissues, and pathology are reviewed: intravenous, intraperitoneal, inhalation, intratracheal, peroral, cutaneous, and subcutaneous. Studies on toxicity of plutonium as related to the route of administration are reviewed and tables are presented to show the maximum safe dose and dose rates to the skeleton after various routes of administration. Studies on comparison of the biological effects of ^{239}Pu with effects of other radioisotopes are reviewed using life span, carcinogenic effects, and hematological changes as criteria. Isotopes studied were ^{144}Ce, ^{210}Po, ^{226}Ra, ^{90}Sr, ^{232}U, and ^{233}U. (181 references) (H.L.W.)

8597 ACCUMULATION OF ^{85}Sr IN VARIOUS TYPES OF BONE NEOPLASMS. Wojciechowski, J.; Komitowski, D.; Patryn, A. Pol. Przegl. Radiol. Med. Nukl.; 34: 143-50(Jan-Feb 1970). (In Polish).

Strontium-85 was administered to patients suspected of having neoplastic growths. Marked accumulation of the isotope was observed in sarcomas with osteoblastic activity; accumulation in benign and osteolytic neoplasms was lower. Microscopic examination revealed the highest osteoblastic activity in tumors localized in the marrow cavity, while muscle-infiltrating tumors demonstrated lower osteoblastic activity and lower radioactivity. (auth)

8598 TEMPERATURE EFFECTS ON THE SORPTION OF RADIONUCLIDES BY FRESHWATER ALGAE. Harvey, R. S. (E. I. du Pont de Nemours and Co., Aiken, S. C.). Health Phys.; 19: 293-7(Aug 1970).

Water temperatures of 23, 26, 29, and 32°C had no significant effect on the sorption of ^{137}Cs, ^{85}Sr, ^{65}Zn, ^{59}Fe, ^{57}Co, and ^{54}Mn by the filamentous green alga Stigeoclonium lubricum. Radionuclide concentrations in the unicellular diatom Navicula semimulum were 2 to 5 times higher at 32°C than those obtained at lower temperatures. Water temperatures of 25, 30, 35, and 40°C had no significant effect on the sorption of ^{137}Cs, ^{85}Sr, ^{65}Zn and ^{59}Fe by the filamentous blue-green alga Plectonema boryanum. However, ^{57}Co concentrations in P. boryanum decreased with temperature, and ^{54}Mn concentrations increased from 25 to 35°C.

XUM

Growth rates of N. seminulum and P. boryanum were inhibited at 32 and 25°C, respectively. Growth of S. lubricum was not influenced by the temperatures tested. (auth) (UK)

8599 ACCUMULATION OF TECHNETIUM ^{99m}Tc IN RAT THYROID. Kapitola, J.; Schuellerova, M. (Charles Univ., Prague). Endocrinol. Exp.; 3: No. 1, 17-21(1969).

The uptake of ^{99m}Tc by thyroid in rats was compared to that of ^{131}I under adequate conditions. Technetium-99m was found in the thyroid immediately after the intravenous injection, the highest radioactivity being found after 15 min. Following methylthiouracil (MTU) feeding (0.2% MTU in the diet for 7 days) the maximum ^{131}I uptake was found 5 min after the intravenous injection of ^{131}I and it decreased more rapidly than the content of ^{99m}Tc. After feeding dessicated thyroid (0.1% dessicated thyroid in the diet for 7 days), the accumulation of ^{99m}Tc (30 min after its administration) was decreased to about 10% of control values. All these changes were similar to those observed with ^{131}I. (NSA of Czech.)

8600 TOXICITY OF PESTICIDES LABELLED WITH RADIONUCLIDES. Wortley, G. (Joint FAO/IAEA Division of Atomic Energy in Food and Agriculture, Vienna). pp 57-65 of Nuclear Techniques for Studying Pesticide Residue Problems. Vienna; International Atomic Energy Agency (1970).

From Panel on Nuclear Techniques for Studying Pesticide Residue Problems, Vienna, Austria. See STI/PUB-252; CONF-681228.

Calculations were made for the assessment of potential radiation hazards resulting from the ingestion of food containing residues from field experiments with radio-labeled pesticides. The radioactivity of food containing residues of maximum commercially available specific activity at concentrations given by the FAO/WHO tolerances was compared with the maximum permissible (ICRP) concentrations of radionuclides in water. Safety factors were given for dieldrin (^{14}C), DDT (^{36}Cl), lindane (^{14}C), ethylene dibromide (^{82}Br), malathion (^{32}P, ^{35}S, ^{14}C, ^{3}H) and phenyl mercuric acetate (^{203}Hg). (auth)

8601 EFFECTS OF ALTERED EXTERNAL CALCIUM CONCENTRATIONS ON FLUXES OF ^{45}Ca IN RAT MYOMETRIUM. Krejci, I.; Daniel, E. E. (Univ. of Alberta, Edmonton). Amer. J. Physiol.; 219: 263-9(Jul 1970).

The dependence on external Ca of ^{45}Ca efflux from estrogen-dominated rat uterine horns was studied. Efflux of tracer is diminished by lowering the external Ca. Efflux in low external Ca is increased by 2 mM EDTA and by 3 mM tetracaine, as well as by Ca, Sr, and Ba ions. Evidence was found that ^{45}Ca influx had two components: one saturable at low external Ca concentration, and one which increased with external Ca concentration. No evidence was obtained that tracer entered a compartment during uptake from low-Ca concentrations different from that during uptake from normal Ca concentrations. Calcium-45 uptake from low-Ca solutions (0.05 M) was inhibited by tetracaine, EDTA, calcium, and barium ions. Therefore the same substances that restore ^{45}Ca efflux into low-Ca solutions also inhibit ^{45}Ca influx from low-Ca solutions. The effects of EDTA and tetracaine on efflux and influx of ^{45}Ca were not consistent with a simple exchange-diffusion model. High K (44 mM), adrenaline (1 μg/ml), and oxytocin (30 mU/ml) did not significantly alter ^{45}Ca uptake from 0.05 M calcium solution. These results may be explained if there is back influx of tracer during efflux studies from a region of incomplete mixing of emergent tracer. Such back influx might occur via an uptake mechanism separate from the efflux mechanism and separate from the efflux mechanism and saturable at low external Ca concentrations. (auth)

8602 EFFECT OF CCCP AND UO_2^{++} ON ION FLUXES IN ROOTS. Weigl, Josef (Technische Hochschule, Darmstadt, Ger.). Planta; 91: 270-3(1970). (In German).

The efflux of Rb^+ from preloaded corn roots across the plasmalemma of root cortex cells was stimulated by addition of 5×10^{-4} M UO_2^{++}, whereas the flux of Rb^+ into the xylem was inhibited by addition of 5×10^{-4} M UO_2^{++}. Efflux of Cl^- across the plasmalemma was stimulated by 10^{-5} M CCCP, the flux of Cl^- via the xylem was inhibited by 10^{-5} M CCCP. The problem of interpreting efflux experiments with roots is stated and discussed. (auth)

8603 UPTAKE OF ^{32}P BY DIFFERENT KINDS OF ECTOTROPHIC MYCORRHIZA OF PINUS. Mejstrik, V. (Lincoln Coll., Canterbury, New Zealand). New Phytol.; 69: 295-8(1970).

The rates of uptake of phosphate by two different kinds of mycorrhiza of Pinus radiata (Fa and Ca) were both greater than that of uninfected roots at all temperatures studied. Over periods of 160 minutes the optimum temperature for both mycorrhizal and uninfected roots was about 25°C, but the uptake rate of type Fa fell off more steeply above this optimum than that of Ca over the same time-period. Uninfected roots showed, at all temperatures, a more rapid rate of absorption over the first 60 minutes of the experimental period than later. (auth)

Radiation Effects

Refer also to abstracts 8280, 8666, 8758, 8816, and 8823.

8604 (COO-690-41) FRACTIONATION AND ANALYSIS OF GAMMA IRRADIATED LYSOZYME. Marciani, Dante Juan (Colorado Univ., Boulder. Dept. of Chemistry). 1970. Contract AT(11-1)-690. 168p. Dep. NTIS.

Thesis.

The chemical and conformational properties of whole and fractionated lysozyme irradiated in the dry solid state by Cesium-137 gamma rays have been studied by a variety of procedures. The results have been used to extend our understanding of the basic mechanisms by which enzymes are inactivated by radiation. Irradiated lysozyme (26 Mrad) was fractionated by salting out with 0.1 N acetic acid-1 M NaCl. The salt insoluble fraction, F-I, accounts for 39% of the irradiated lysozyme, and the salt soluble fraction, F-II, the remainder. Chromatography of F-I on Bio-Gel P-60 shows components with hydrodynamic volumes up to 10 times the volume corresponding to native lysozyme. Sodium dodecyl sulfate polyacrylamide gel electrophoresis indicates the presence of 13% of polymers which are formed by integral numbers of lysozyme monomers. The relationship between the amount of polymer and degree of polymerization is exponential, indicating a random process of polymerization. Reduction of irradiated lysozyme with 2-mercaptoethanol and alkylation with iodoacetamide show that polymers are formed by intermolecular disulfide bonds. Polyacrylamide gel electrophoresis of F-I in urea reveals the presence of different monomeric forms which differ from native lysozyme and from each other in charge, size and/or shape. Difference spectra of F-I in 0.1 N versus 1 N acetic acid show that most of the increase in hydrodynamic volume is due to the unfolding of damaged molecules. Difference spectra of F-I components versus native lysozyme do not show significant destruction of tyrosyl residues but indicate that tryptophyl residues are destroyed by γ rays. The specific lytic activity of F-1 on cells of Micrococcus lysodeikticus was 10% of the activity of native lysozyme. The destruction of enzyme activity can be a result of the conformational damage and of the destruction of tryptophyl residues that play an important role in the binding of the substrate to the active site of lysozyme. Chromatography on Bio-Rex 70 of whole irradiated lysozyme shows that a large part of F-II molecules are damaged since only 28% of the whole irradiated lysozyme elutes in a position comparable to native lysozyme, whereas the F-II fraction accounts for 61% of the whole irradiated lysozyme. Heavily damaged molecules of irradiated lysozyme tend to aggregate, especially at high ionic strength or high pH values. Spectrographic studies of irradiated lysozyme show that tryptophyl groups are removed from contact with the solvent, supporting the suggestion that at high ionic strength or pH, aggregation involves some of the exposed tryptophyl residues. (auth)

8605 (ORO-2832-85) RADIATION AND BIOPHYSICAL STUDIES ON VIRUSES AND CELLS. Progress Report, October 16, 1969-October 15, 1970. Shalek, Robert J. (Anderson (M. D.) Hospital and Tumor Inst., Houston, Tex.). Contract AT(40-1)-2832. 111p. Dep. NTIS.

Progress during the reporting period on the various projects relating to the central purpose of the research is briefly summarized. In structural studies of mitotic mammalian chromosomes, it was found that suitable concentrations of monovalent and divalent salts produced a partial unraveling such that chromosome extensions of hundreds of micrometers were induced. Thermal denaturation studies on the specificity of the association of histones with DNA indicated a more complicated interaction than was previously reported. Double strand scission studies on γ-irradiated mammalian DNA revealed that a structure exists in association with the DNA that is at least one order of magnitude more radiosensitive than DNA double strand scission. Speculation concerning the nature of this structure is that it is a disulfide bonded protein. Post-irradiation shifts toward a higher molecular weight (observed in about 40% of the DNA studies) indicate the presence of a strand rejoining type of mechanism for repair in mammalian cells. However, no firm conclusion regarding the presence of this mechanism could be made. Using sedimentation analysis and thermal denaturation techniques, it was concluded that in the case of isolated mammalian DNA that the mechanism causing strand breakage under the influence of γ irradiation is nearly all indirect and that double strand scission occurs as a result of the close proximity of single strand breaks on opposite strands. Sedimentation studies on γ-irradiated nucleohistones showed that all of the histone fractions tested conferred substan-

tial protection to the DNA against both single and double strand breakage. It is also reported that complementary studies on radioinduced single strand scissions and repair of cellular DNA at Dr. R. M. Humphrey's laboratory support the tentative conclusion reached in the double strand scission studies at this laboratory regarding the existence of a strand rejoining type of mechanism for repair in mammalian cells. (E.R.B.)

8606 (ORO-3630-10) PHOTOREPAIR OF UV DAMAGE TO DNA: PURIFICATION AND PROPERTIES OF THE DNA-PYRIMIDINE DIMER PHOTOMONOMERASE-THE DNA-PHOTOREACTIVATING ENZYME. Progress Report. Werbin, Harold (Texas Univ., Dallas). 2 Jan 1971. Contract AT(40-1)-3630 19p. Dep. NTIS.

Progress is reported on the purification and properties of the DNA-Pyrimidine dimer photomonomerase (DPDP) from the blue-green alga, Anacystis nidulans. Because of the difficulties of growing large quantities of algae required, Baker's yeast was used as a source of the enzyme. A procedure was developed using affinity chromatography on uv-irradiated DNA noncovalently bound to cellulose, and a 70,000 fold purification of the enzyme was obtained. Examination of this preparation by ultraviolet and fluorescence spectrometry disclosed that the enzyme was associated with a chromophore having spectroscopic properties indicative of its involvement in photoreactivation. (H.L.W.)

8607 (ORO-3882-3) MECHANISM OF RADIATION EFFECTS ON THE TRANSPORT AND BIOELECTRIC PROPERTIES OF RAT INTESTINE. Progress Report. McKenney, Joel R. (Medical Coll. of Georgia, Augusta. Dept. of Physiology). 24 Sep 1970. Contract AT(40-1)-3882. 12p. Dep. CFSTI.

The following observations were made and data collected during the current reporting period. A quantitative relationship was observed between the relative unidirectional fluxes of Na^+, Cl^-, and water across isolated rat ileum. Bile diversion studies in isolated rat intestine revealed a five-fold increase in the mucosal to serosal flux of glucose across the intestine. Data were collected on the sequence of changes in the glucose and salt transport properties and the fine structure of the mucosa of isolated rat intestine following a 1200 R x-ray exposure. In a study of the combined effects of chronic bile diversion and 1200 R x irradiation on glucose and salt transport and fine structure of isolated rat intestine, a quantitative relationship was observed between the unidirectional fluxes of Na^+, Cl^-, and glucose and the transmural voltage difference across jejunum and ileum following irradiation. (E.R.B.)

8608 ADAPTATION OF HEMOPOIETIC SYSTEMS TO ENVIRONMENTAL CONDITIONS. Lamerton, L. F. (Inst. of Cancer Research, Sutton, Eng.). Blut; 9: 132-7(1970).

From 13th International Congress of Hematology, Munich, Germany. See CONF-700820.

The ability of the hematopoietic system to maintain a normal blood picture under changing environmental conditions such as reduced oxygen pressure and continuous irradiation is emphasized. It is pointed out that the main effect of ionizing radiation is on the dividing cells of any population. It was found that dose rates of 100 rads/day led to the depletion of dividing cells and early collapse of bone marrow function in rats. However, at lower dose rates the bone marrow was able to adapt to the cell depletion and set up a new steady state so that the rate of erythrocyte production was maintained for a long period of time. Studies using ^{55}Fe and autoradiography for determining radiation effects on multiplication of red cells are reviewed. A review of transplantation experiments indicated that under continuous irradiation the stem cell numbers in rats fall to about 10% of their normal value; at the same time, however, the rate of cell proliferation is greatly increased. Results of experiments showed that the adaptive process is shared between the stem cell compartment and the compartment of maturing but dividing cells. Studies on duration of the cell cycle showed that in rats continuously irradiated at 50 rads/day the cycle of red cells was reduced from 30 to 12 hrs. (H.L.W.)

8609 ACTION OF IONIZING RADIATIONS ON THE EYE. Haye, C. (Fondation Curie, Paris). Arch. Ophtalmol.; 30: 249-53(1970). (In French).

Many publications have appeared on the action of ionizing radiations on the eye and concerning the various elements of the ocular system. The crystalline lens has been studied by means of different radiations and it has been observed that neutrons are often more effective than gamma rays in producing opacities of this lens. Changes in the mass of the crystalline lens were also observed, together with histological lesions and a reduction in the cytoplasmic ribonucleic acid. Ionizing radiations lead to modifications in the metabolic processes of the retina as is shown by the electroretinogram. Lesions of the retinal cell population and ultrastructural changes affecting the outer membrane of the retina were also observed. The atomic flash produces retinal burns and lesions which may cause the crystalline lens to become completely opaque. Radiation diseases can lead to histological and histochemical changes in all the eye layers, with deteriorations of the cones and rods in particular and to vascular lesions, while beta radiation affects the synthesis of DNA. Irradiation of the eye poses problems of crystalline lens protection. (auth)

8610 CHANGES IN THE DNA TEMPLATE AFTER X-RAY IRRADIATION IN VITRO. Russev, G. K.; Djirkolova, T.; Bogdanova, N. (High Military Medical Inst., Sofia). Compt. Rend. Acad. Bulg. Sci.; 23: 439-42(1970).

DNA was isolated from calf thymus and a 1% solution in 0.01 M NaCl was given 1800 and 100,000 R doses of x radiation. Various mixtures of nucleosides and nucleotide phosphates were added to DNA solutions. Activities of DNA and RNA polymerases were assayed using ^{14}C-DNA triphosphate. Results showed that irradiation increased the activity of RNA polymerase but not that of DNA polymerase. When the medium contained deoxycytidine, incorporation of ^{14}C-labeled thymidine triphosphate was diminished. When the medium contained thymidine, the changed DNA transcription gave an RNA product with more adenosine but not with guanosine. It is thought that radiation intensifies the process of exchange of DNA bases with nucleosides of the environment. (H.L.W.)

8611 RADIATION AND CARCINOGENESIS. FROM THE REPAIR OF DAMAGE IN DNA OF MAMMALIAN CELLS INDUCED BY RADIATION. Horikawa, Masakatsu (Kanazawa Univ., Japan); Suzuki, Fumio; Nikaido, Osamu; Sugahara, Tsutomu. Tanpakushitsu Kakusan Koso; 15: 485-94(Apr 1970). (In Japanese).

Carcinogenesis resulting from the damage of DNA and its repair in the cultured mammalian cells from the effects of uv and x rays, and chemical carcinogens (4-nitroquinoline 1-oxide and its derivatives is discussed. The pyrimidine dimer formed inside cellular DNA by uv rays inhibits or retards DNA synthesis, and removal of this dimer depends on the mechanism of dark repair and photoreactivation. Single strand breaks of DNA molecules by x irradiation can be repaired but not double strand breaks. 4-Nitroquinoline 1-oxide (4-NQO) and its derivatives induce single and double strand breaks, and this single strand break can be repaired relatively easily in the case of x irradiation. With respect to enzymes taking part in the repair process of DNA damage, animals cells seem to have a fundamental mechanism for repairing DNA damaged by radiation or chemical carcinogens, or under natural conditions to a certain extent. It is thought that if the damage is beyond this repair ability, cell death will result, while misrepair in this process results in carcinogenesis (or mutation). Experiments on in vitro carcinogenesis were carried out. The theory of mutation, viewed as one of the carcinogenic mechanisms of radiation, was derived from the ability of radiation to produce mutations and was used to explain carcinogenesis by irradiation from mutation of somatic cells. (Japan)

8612 EFFECT OF K_3-VITAMIN AND MONOIODOACETIC ACID ON SERUM COERULOPLASMIN ACTIVITY. Tomas, E. (Inst. of Inframicrobiology, Bucharest). Atomkernenergie; 16: 79-81(1970).

Both x irradiation and the administration of K_3 vitamin and monoiodoacetic acid cause an initial decrease in the serum coeruloplasmin activity. X rays and monoiodoacetic acid appear to act by the same mechanism in which an increase in citric acid concentration inhibits the enzymic reaction. K_3 vitamin, however, produces the same inhibitory effect by competition with the substratum. It is possible to explain some of the characteristics of acute x irradiation in terms of the changes in coeruloplasmin activity that can be observed after both irradiation and the administration of radiomimetics. Thus by studying a system of circulatory redox enzymes it is possible to observe biochemical similarities between irradiation and radiomimetics. (auth)

8613 INTERMOLECULAR TRANSFER OF RADIATION ENERGY AT 77°K. AN ESR STUDY OF IRRADIATED MIXTURES OF MACROMOLECULES AND OXIDIZED PENICILLAMINE. Sanner, Tore (Norwegian Radium Hospital, Oslo). Radiat. Res.; 44: 13-23(Oct 1970).

The relative importance of intermolecular transfer of radiation energy occurring at 77°K and upon subsequent heat-treatment was studied. In these studies, x-irradiated cross-linked dextran, Sephadex, and some of its derivatives were used as macromolecules. Sephadex was chosen since this compound was studied to a considerable extent by the ESR technique in previous investigations. (auth)

8614 RADIATION RESPONSES OF FERN SPORES DURING THEIR FIRST CELL-CYLCE. Howard, Alma; Haigh, Mary V.

XUM

(Christie Hospital, Manchester, Eng.). Int. J. Radiat. Biol.; 18: 147-58(1970).

Spores of the Royal fern, Osmunda regalis, were irradiated at different times after water uptake and before their first mitosis. ^{3}H-thymidine labelling showed that light-grown cells synthesized DNA between 10 and 22 hours after water uptake, and half of these reached mitosis between 24 and 30 hours. Dark-grown cells did not synthesize DNA nor divide until given light. Sensitivity to killing by x-rays determined by D_0 values of survival curves increased by a factor of 4.5 throughout interphase in light-grown cells but leveled off after 6 hours in dark-grown cells. The suggested correlation between increasing sensitivity and DNA synthesis was thus in the direction opposite to that seen in many other cell types. We conclude that a basic connection between radiation sensitivity and DNA synthesis is contra-indicated. The sparing effect of splitting the radiation dose into two equal fractions was approximately equal throughout interphase and was similar in light- and dark-grown cells. We conclude that this effect was independent of DNA synthesis. Survival was increased when mitosis was delayed by maintaining the cells in the dark for a period after irradiation. We interpret this as indicating rescue from potentially lethal damage. (auth) (UK)

Immunology

Refer also to abstracts 8762 and 8769.

8615 HEMATOLOGY 1970. Plenary Sessions. Scientific Contributions of the XIII. International Congress of Hematology, Munich, August 24–28, 1970. Blut Zeitschrift fuer die Gesamte Blutforschung, Band 9. Munich; J. F. Lehmanns Verlag (1970). 176p. (In several languages). (CONF-700820).

Fifteen articles are included; separate abstracts were prepared for three. The remaining 12 articles contain information on: molecular hematology; treatment of leukemia; physiology and pathology of intravascular coagulation; hematological ecology; and paraproteinemias. (H.L.W.)

For abstracts of individual papers see: 8608, 8616, and 8617.

8616 HOST AND GRAFT FACTORS IN THE HOMING OF HAEMATOPOIETIC CELLS. Hasek, M.; Nouza, K. (Inst. of Experimental Biology and Genetics, Prague). Blut; 9: 79-85 (1970).

From 13th International Congress of Hematology, Munich, Germany. See CONF-700820.

A review of experimental studies on hematopoietic tissue grafts is presented. In a discussion of recipient's factors the following topics are considered: natural chimaeras; artificial parabiosis in avian embryos; and transplantation of hematopoietic cells into adult organisms following whole-body irradiation or administration of immunosuppressive drugs. A discussion of factors influencing graft-versus-host reactions includes species of animal, age, radiation dose, genetic relation of recipient and donor, and origin of transplanted cells. A review of critical factors in the homing of transplanted cells includes age, sex of host and donor, genetic factors, and role of the thymus. A review of non-immune interactions includes a discussion on parental strain tumors and allogeneic inhibition. (H.L.W.)

8617 BONE MARROW CHIMERAS IN MAN AND ANIMALS. Thomas, E. D.; Storb, R.; Epstein, R. B. (Univ. of Washington, Seattle. Public Health Service Hospital, Seattle). Blut; 9: 86-95 (1970).

From 13th International Congress of Hematology, Munich, Germany. See CONF-700820.

A review of laboratory studies of allogenic marrow grafts in dogs and monkeys that may be applicable to man is presented. The use of whole-body radiation and immunosuppressive drugs for preparing the recipient of a marrow graft is described. Studies on histocompatibility typing in dogs and monkeys are discussed. Techniques of leukoagglutination and cytotoxicity testing are discussed for organ grafting in man. A technique for marrow grafting involving multiple aspirations from the sternum, iliac crests, and other bones is described. A method for preserving human bone marrow by freezing in glycerol or dimethyl sulfoxide is discussed. It was found that canine bone marrow preserved at low temperatures in glycerol or dimethyl sulfoxide for a long period of time was still effective when reinfused into the donor following lethal whole-body radiation. A review of secondary syndromes following marrow grafting is presented; it is pointed out that the principal changes are disturbances in the skin, the intestine, the liver, and the lymphoid tissue. Long-term survival of human and animal chimeras is discussed. It was found that blood transfusions given before marrow grafting diminished the chance for long-term survival. (H.L.W.)

8618 MATERNAL MODIFICATION OF TISSUE ANTIGENICITY AND THE HISTOCOMPATIBILITY-2(H-2) LOCUS. Uphoff, Delta E. (National Cancer Inst., Bethesda, Md.). J. Nat. Cancer Inst.; 45: 1035-7(Nov 1970).

Differences in time of onset and severity of the secondary disease syndrome produced by the graft-versus-host reaction occurred in lethally irradiated reciprocal hybrid mice inoculated with bone marrow from parental strains of different H-2 genotypes. A less severe graft-versus-host reaction occurred when the marrow donor strain was syngeneic with the maternal strain of the hybrid. Differences in the survival pattern after inoculation of marrow from either parental strain were attributed to the quantitative difference in antigenicity control by the H-2 locus. The difference in the survival pattern between lethally irradiated reciprocal hybrid recipients inoculated with marrow of the same parental strain was attributed to reduced antigenicity as a result of a maternal modification of expression of paternally derived tissue antigens occurring during fetal development. (auth)

8619 SECONDARY DISEASE MORTALITY IN RAT-MOUSE RADIATION CHIMERAS. Congdon, C. C.; Mitchell, T. J.; Gardiner, D. A.; Kastenbaum, M. A.; Toya, R. E. (Oak Ridge National Lab., Tenn.). J. Nat. Cancer Inst.; 45: 1055-64(Nov 1970).

Two statistical experimental designs were used to investigate factors involved in 90-day mortality from secondary disease in lethally irradiated mice treated with rat bone marrow. Secondary disease is a graft-versus-host syndrome that has a mortality of about 65 to 95% in this transplant situation. When the factors, such as age-of-donor-cells, day-of-cell-injection, dose-of-marrow-cells, sex, and environment, were examined for their main effects and interactions, some combinations of these factors were found to give about 25% 90-day mortality. The experiments indicate that the lowest mortality can be achieved with an injection of 40 million or more cells 1 day after irradiation and an ultraclean environment of unlimited filter-top caging. (auth)

8620 BONE MARROW RESTORATION OF TRANSPLANTATION IMMUNITY IN THE LEOPARD FROG RANA PIPIENS. Cooper, Edwin L.; Schaefer, D. William (Univ. of California, Los Angeles). Proc. Soc. Exp. Biol. Med.; 135: 406-11(Nov 1970).

The effects of ^{60}Co γ irradiation at 5000 R on the survival of skin allografts in adult Rana pipiens (leopard frog) were observed with the changes in the peripheral blood at 25 ± 1°. Graft survival was assessed by estimating the survival of melanocytes. Autografts healed and survived permanently. In nonirradiated control animals, median survival time (MST) of allografts was 14.25 days ± 1.5. In the group receiving total-body irradiation no graft rejection was observed at the time the frogs died, at the earliest on the 7th day postgrafting and the latest on the 20th day. By contrast, skin allografts in the partially irradiated and shielded group were rejected almost as rapidly (within 2 days), as those observed in unirradiated controls. The mean percent of lymphocytes in the peripheral blood declined sharply, but less in the partially shielded group. Little change was noted in the percentage of basophils, eosinophils, or monocytes but neutrophils seemed to increase. Bone marrow was sufficient to maintain the alloimmune mechanism and life itself. (auth)

8621 BIOSYNTHESIS STIMULATION OF GAMMA-M AND GAMMA-G ANTIBODIES IN IRRADIATED ORGANISM. Prokopenko, L. G. (Kursk Medical Inst., USSR). Byull. Eksp. Biol. Med.; 69: No. 5, 74-6(May 1970). (In Russian).

The introduction to x-irradiated (1000 R) and immunized (500 million Escherichia coli microbes) rabbits of 5 mg of homologous serum gamma-globulin stimulated the production of gamma-M and accelerated the appearance of gamma-G antibodies. An increase of immunized antigen dose up to 3 billion stimulated the synthesis of gamma-M, but did not influence the production of gamma-G antibodies. (auth)

8622 ALLOGRAFT SURVIVAL IN NONSUSCEPTIBLE C57BL/6J MICE HOSTS. TEMPORAL RELATIONSHIP BETWEEN WHOLE-BODY X IRRADIATION AND THE IMMUNE RESPONSE. Halkett, James A. E. (Boston Veterans Administration Hospital. Boston Univ.). Radiology; 96: 645-8(Sep 1970).

Survival of a transplantable AKR leukemia used as an allograft model was studied in x-irradiated nonsusceptible C57BL/6J hosts. X-irradiated mice died of leukemia, but postirradiated mice did not, as confirmed by transfer of homogenized spleens from irradiated allogenic hosts to AKR mice syngeneic with the leukemic cells. More leukemic cells developed in preirradiated host spleens, suggesting that a concentration-dependent control mechanism regulating allograft proliferation in normal mice may be damaged by preirradiation. (auth)

Ecology

Refer also to abstracts 8592, 8593, 8661, 8667, 8670, 8673, 8675, 8698, 8750, 8760, and 10159.

8623 (BNWL-SA-3419) STUDIES OF INHALED RADON DAUGHTERS, URANIUM ORE DUST, DIESEL EXHAUST, AND CIGARETTE SMOKE IN DOGS AND HAMSTERS. Stuart, Bruce O.; Willard, Donald H.; Howard, Edwin B. (Battelle-Northwest, Richland, Wash. Pacific Northwest Lab.). [1970]. Contract AT(45-1)-1830. 24p. (CONF-700931-3). Dep. NTIS.

From 3rd International Symposium on Inhaled Particles, London, England.

The incidence of lung cancer in uranium ore miners on the Colorado Plateau has risen to six times that of non-miners. Although the primary carcinogenic agent is generally accepted to be the inhaled short-lived radioactive decay products of radon, the miners are routinely exposed to several other hazardous airborne contaminants, including ore dust and diesel engine exhaust fumes. In addition, 97% of those uranium miners who have developed lung cancer have histories of cigarette smoking. A program involving inhalation exposures of experimental animals was undertaken to determine the relative effectiveness of the principal mine air contaminants in the production of pulmonary fibrosis, emphysema, or neoplastic changes. Six groups of 100 hamsters each are being exposed in life-span studies for 6 hours daily to radon daughters, ore dust, and/or diesel exhaust fumes. The possible synergistic action of radon daughters and cigarette smoking in the development of lung cancer in uranium miners is being studied using beagle dogs. Three groups of 20 dogs each are receiving daily exposures to 4 hours of 600 Working Levels of radon daughters plus ore dust, exposure to cigarette smoking over 16 hour periods, 7 days per week, and exposure to both radon daughters and cigarette smoking; nine dogs serve as controls for hematology, physical examination and radiographic examination. Two dogs in each group receive lung washings for lung exfoliative cytology studies. The current results of these long-term multiple exposure studies with experimental animals are discussed. (auth)

8624 (EUR-4509) RADIOACTIVE CONTAMINATION OF FOODSTUFFS IN THE COUNTRIES OF THE COMMUNITY IN 1968. (European Communities, Luxembourg. Commission). 1970. 66p. (In several languages). Dep. NTIS (U. S. Sales Only). EUR DM 6,20.

Data are presented on the radioactive contamination of foodstuffs in the Community countries in 1968. The data relate to the radionuclides ^{90}Sr and ^{137}Cs. Tables and graphs illustrate the pattern followed in the course of the year. The average milk contamination for the Community is compared with that of the United States, Canada, and the United Kingdom. An estimate is given of the strontium-90 intake by man. For 1968 this intake averages 3,986 pCi of strontium-90, which corresponds to 15.0 pCi/gCa in the diet. (auth)

8625 (NP-18429) UPTAKE OF MERCURY (^{203}Hg) BY TAPES DECUSSATUS L. Unlu, M. Yasar (Cekmece Nuclear Research Center, Istanbul (Turkey)). 1970. 27p. (In Turkish). Dep. CFSTI (U. S. Sales Only).

In order to investigate the potential contamination of the seas with mercury, the metabolism of ^{203}Hg in Tapes decussatus was examined. The study indicated that ^{203}Hg, used as chloride, is rapidly accumulated by Tapes decussatus: the weight concentration in the animals was ten times higher within an hour than in the environment. The accumulation is slower if the animals are in contact with the radioactive environment for a long period of time. The interior organs were found to contain more than half, and the muscles less than 2% of the total amount of ^{203}Hg accumulated in the animals in 14 days. The removal rate did not depend on the duration of the contact but was strongly affected by the manner of uptake. The highest retention was observed in animals which have been injected with ^{203}Hg in the muscles. Only about 25% of the injected radioactivity was lost in 2 months, -most of it during the first 6 days. The biological half-life of animals which accumulated the mercury through the food or the sea water was about 10 and about 5 days, respectively. (TTT)

8626 ECOLOGICAL MODELS APPLIED TO RADIONUCLIDE TRANSFER IN TROPICAL ECOSYSTEMS. Raines, G. E.; Bloom, S. G.; Levin, A. A. (Battelle Memorial Inst., Columbus, Ohio). Bioscience; 19: 1086-91(Dec 1969).

Estimates were made of the potential internal intake of various radionuclides by indigenous populations assumed to be living in or near areas contaminated by fallout from nuclear excavation of a canal. This was achieved by utilizing ecological models to predict the redistribution and accumulation of these radionuclides in various components of the biota, thus yielding estimates of radiocontamination of various foodstuffs. Simplified dose estimates were performed to ascertain the relative significance of different radionuclides. A mathematical model designed to simulate the entire process of radionuclide redistribution is discussed and general equations for radionuclide transport models are presented. It was assumed that the transport of radionuclides through food webs can be described by mathematical models consisting of first-order, ordinary differential equations. (auth)

8627 USE OF STABLE ELEMENT DISTRIBUTION PATTERNS FOR PREDICTING DISTRIBUTION OF RADIONUCLIDES IN MARINE ORGANISMS. Ting, Robert Y. (Puerto Rico Nuclear Center, Mayaguez). Bioscience; 19: 1082-5(Dec 1969).

Nuclear explosives, used for excavating an Atlantic-Pacific sea-level canal, would introduce radionuclides into terrestrial and aquatic environments. For predicting hazards from radioactive fallout and contamination in marine and estuarine environments the specific activity approach was used. The concentrations of several biologically important stable elements (Zn, Fe, Mn, Ca, Sr, Sc, C, H, and N) were determined in fish and invertebrates from Panamanian and Colombian waters. These measurements, in conjunction with the specific activity predictions, were then used to predict the amounts of radionuclides that would be present in food items. The amounts of ^{32}P, ^{45}Ca, ^{46}Sc, ^{54}Mn, ^{55}Fe, ^{59}Fe, ^{65}Zn, and ^{89}Sr, predicted for 250 g of different marine foods, were compared with the daily intake allowed in members of the general population in which it is possible to identify the population group expected to receive the highest dose. In general, food of marine origin in areas contaminated by fallout would provide smaller amounts of radionuclides per unit weight than would most foods of terrestrial origin harvested from areas of equal contamination. In areas of fallout, the accumulation of radionuclides from surface contamination of the individuals, and the items they handle or contact, would be expected to be greater than the accumulation of radionuclides from marine foods. (auth)

8628 EFFECTS OF IONIZING RADIATION ON NATURAL AND LABORATORY POPULATIONS OF MANITOBA TOADS, BUFO HEMIOPHRYS. Tester, John R.; Ewert, Michael A.; Siniff, Donald B. (Univ. of Minnesota, Minneapolis). Radiat. Res.; 44: 379-89(Nov 1970).

The $LD_{50(30)}$ and $LD_{50(60)}$ for adult male Bufo hemiophrys exposed to whole-body cesium-137 radiation in the laboratory was 2200 and 2000 R, respectively. Survival of toads exposed to 1500 R was higher in the group that hibernated for 6 mo than for those that were kept active. An entire natural population of 264 adults and and 850 juveniles was irradiated with 1500 R at the time of emergence from the overwintering site. This irradiation had little detectable behavioral effect on breeding activity, summer feeding, or any aspect of overwintering. The only effect of the irradiation detected was a marked reduction in survival in all sex and age categories of the population emerging from overwintering sites one year following irradiation. (auth)

8629 RADIOIODINE LEVELS IN THE U.S. PUBLIC HEALTH SERVICE PASTEURIZED MILK NETWORK FROM 1963-1968 AND THEIR RELATIONSHIP TO POSSIBLE SOURCES. Machta, Lester; Telegadas, Kosta (Environmental Science Service Administration, Silver Spring, Md.). Health Phys.; 19: 469-85(Oct 1970).

Meteorological analysis of the paths of nuclear clouds was used to assign the source of ^{131}I in the milk samples collected in the U.S. Public Health Service Pasteurized Milk Network (PMN). Most of the instances of elevated values between April 1963 and December 1968 are attributed to six atmospheric nuclear explosions in western China. Only one of five cratering events at the Nevada Test Site caused elevated values in the PMN milk. Two periods with relatively low concentrations of radioiodine in milk possess no apparent explanation. By selecting periods with no atmospheric or cratering events, it is argued that at most small amounts of radioiodine in the PMN can be attributed to accidental releases from underground nuclear tests in the United States during the period of analysis. Radioiodine from accidental releases, reactor tests, and cratering events has been detected in a local raw milk network surrounding the Nevada Test Site. (auth) (UK)

8630 RADIOEKOLOGICHESKIE ISSLEDOVANIYA SREDIZEMNOGO MORYA. (Radioecological Studies of the Mediterranean Sea). Polikarpov, G. G.; Zaitsev, Yu. P.; Kulebakina, L. G.; Timoshchuk, V. I.; Tsytsugina, V. G.; Rozhanskaya, L. I.; Risik, N. S.; Strogonov, A. A.; Zesenko, A. Ya. Kiev; Izdatel'stvo Naukova Dumka (1970). 231p.

Twenty-three articles are included that discuss the radioecology of the Mediterranean Sea. The radioecological instruments and methods used for the radiometric analysis of samples of animals and plants are described. The methods used for radioecological experiments; methods for determining radioactive and stable Sr

in sea organisms and water; and methods for determining ^{238}U, Zn, and Mn are described in the first part of the book. The second part deals mainly with results obtained during a number of studies. Chromosome number, mitotic activity, and the natural mutation rate in embryonic cells of certain fish species, the uptake of radionuclides by the living organisms of the sea, mechanisms for radionuclide transport, and effects of sedimentation on ^{137}Cs transport are covered in five articles. The uptake of radionuclides by the plants of the Mediterranean Sea, the uptake of ^{90}Sr by algae as a factor of water salinity; the concentration of ^{90}Sr on the surface of the sea, content of Sr in the Adriatic Sea, and the content of ^{238}U in the sea water and plants are discussed in several articles. Ecological processes and their role in the protection of live organisms in sea water against radiation injury are also discussed. (R.V.J.)

8631 URANIUM LEVEL IN FOODSTUFFS. Rezanov, I. I. Vop. Pitan.; 28: 87-8(Mar-Apr 1969). (In Russian).

Fourteen classes of foodstuffs in Russia were investigated for their uranium level. Quantities of the order of 10^{-3} to 10^{-6}% were found. From animal products the highest concentration of uranium (4.3×10^{-7}%) was noted in goose eggs. (tr-auth)

Genetics and Cytogenetics

Refer also to abstracts 8666, 8702, 8705, 8756, 8788, 8797, 8799, 8800, and 8818.

8632 (EUR-4526) WORK OF THE EURATOM STUDY GROUP ON RADIATION AND HUMAN CYTOGENETICS OF THE UNIVERSITY OF PAVIA. Final Report, 1 April 1963-31 March 1968. (Pavia Univ. (Italy)). 1970. 20p. (In Italian). Dep. NTIS (U. S. Sales Only). EUR Lit. 500,-.

Results of research on the following projects are reported: in vitro cultures of somatic cells for the study of cell markers; cellular effects of actinomycin; continuous irradiation of cells in vitro; human cytogenetics; replication of chromosome DNA by means of marked precursors; chromosome variability in tumor cell populations; duplication of chromosome DNA in tumor cells; effects of actinomycin on nucleus and chromosomes; demonstration of metachromatic granulation in the cytoplasm of fibroblasts cultivated in vitro of subjects with Morquio's of Hurler's syndrome; effects of continuous low-dose irradiation with tritiated water on average number of cells in a colony; computer analysis of human karyotype; and descriptions of chromosome anomalies with analyses of meiotic chromosomes. A study of Drosophila melanogaster chromosomes revealed a correspondence between the genetic localization of heterochromatin and late duplication of DNA in chromosome segments. It was shown in various mammals that the Y chromosome of the spermatogonia exhibits asynchromic duplication. The karyotype variability was studied in cell populations of ovarian carcinomas; the same tumors were studied after cytostatic treatment and their selective effect was demonstrated. The duplication of chromosome DNA of tumor cells shows that their reproductive capacity is slower than that of cells normally present in the same cell specimen. (auth)

8633 (NP-18483) GENETIC INVESTIGATION OF RADIATION-SENSITIVE MUTANT OF ESCHERICHIA COLI. Mattern, Ina Elisabeth (Leiden Rijksuniversiteit (Netherlands)). 1969. 99p. (In Dutch). Dep. NTIS (U. S. Sales Only).

Thesis.

A survey is presented of photoproducts induced by ultraviolet irradiation of DNA, of repair processes for uv damage, such as photoreactivation, excision repair, and recombination repair, and of the properties of the various classes of radiosensitive mutants. A discussion is given of the localization of a number of mutations leading to radiosensitivity in Escherichia coli B and E. coli K12 by transduction with phages P1 and 363. Ultraviolet induction of prophage λ is achieved at a lower dose in all mutants than in the wild type; in addition, the vegetative multiplication of the prophage is more radiosensitive in each of these mutants than in the wild type. The induction of the prophage by thymine starvation, however, is not influenced by any of the uvr genes; these genes appear to act specifically on uv mediated induction and not on the induction process per se. The isolation and classification of 90 radiosensitive mutants derived from KMBL 97, KMBL 146, and W 602 are described and the genetic constitution of three Hcr^+ type mutants was further investigated. Conjugation of an HfrH donor strain with the wild type strain KMBL 146 produced uv-sensitive recombinants. (H.L.W.)

8634 (ORO-4024-1) THE EFFECT OF RADIATION-SENSITIVE MUTATIONS AND RADIATION ON RECOMBINATION IN PARTIALLY DIPLOID DERIVATIVES OF ESCHERICHIA COLI. Progress Report. (Texas Univ., Houston. Graduate School of Biomedical Sciences). 15 Sep 1970. Contract AT(40-1)-4024. 5p. Dep. CFSTI.

Recombination was studied in diploids which carried two copies of the histidine operon with various mutational compositions. The purpose of the study was to introduce mutations effecting the dark repair system into partially diploid strains which contain mutations that are being converted or lost in the reciprocal products during recombinational events and to determine the effect of these ultraviolet-sensitive mutations on the frequency of gene conversion. Partially diploid derivatives containing the uvrA mutation were constructed and their genotypes are tabulated. A table is presented to show analysis of recombinants resulting from a limited number of spontaneous events occurring in the uvrA mutation. (H.L.W.)

8635 (STI/DOC-10/119) MANUAL ON MUTATION BREEDING. (International Atomic Energy Agency, Vienna (Austria)). Sep 1970. 242p. IAEA $6.00.

The value of mutations in plant breeding and the advantages of using radiation for inducing mutations are emphasized. Other topics discussed are chemical mutagens; mutagen effects observable in the first generation; the nature of mutations; mutations in characters with continuous variation; factors influencing the mutant spectrum and the quality of mutants; particular problems of mutation breeding; mutation breeding of vegetatively propagated plants; improvement of crop plant characters by mutation breeding; and utilization of mutational events for solving other plant breeding problems. A bibliography of approximately one thousand references is included. (H.L.W.)

8636 (SU-326-P-7-X-22) REPAIR REPLICATION: ITS ROLE IN GENETIC STABILITY. Hanawalt, Philip C. (Stanford Univ., Calif. Dept. of Biological Sciences). [1970]. Contract AT(04-3)-326. 23p. (CONF-700823-1). Dep. NTIS.

From 1st International Symposium on Genetics of Industrial Microorganisms, Prague, Czechoslovakia.

A model is described for the enzymatic process of excision repair of damaged DNA in Escherichia coli. It is thought the same enzyme is also responsible for the second step which involves an incision in the damaged DNA strand. Endonuclease activity specific for pyrmidine dimers was isolated from Micrococcus lysodeikticus and from E. coli infected with phage T4. Other enzymes involved in excision repair are DNA polymerase, exonuclease, and polynucleotide ligase. Studies on repair replication in E. coli included combined labeling of replicating DNA with a density label and a radioactive label; repair replication in uv sensitive mutants of E. coli; and determination of quantity of repair replication using chromatographic analysis. Repair replication studies were also conducted on mycoplasmas, T4 bacteriophage, Tetrahymena pyriformis, and human fibroblasts from Xeroderma pigmentosum patients. The role of excision repair in mutagenesis is discussed. (H.L.W.)

8637 EFFECT OF CAFFEINE ON MUTATION AND RECOMBINATION. Loprieno, N.; Schupbach, M. (Consiglio Nazionale della Ricerche, Pisa, Italy. Univ., Pisa, Italy). Newslett. Environ. Mutagen Soc.; No. 3, 17(Jun 1970).

The influence of caffeine on mutation and recombination was investigated in the yeast, Schizosaccharomyces pombe. Mutations were assessed with a forward mutation system from wild type to purple phenotype (ad-6 and ad-7 loci); recombination was analyzed in the cross his-2-245 x his-7-366 where the markers are located on the mating-type chromosome. Tabulated results show that caffeine reduced survival and mutation after uv treatment, partly reduced mutation induced by N-methyl-N'-nitro-N-nitrosoguanidine, and reduced the percentage of intergenic recombination about 60%. The data confirmed findings obtained in bacteria and show that part of the DNA damage induced by MNNG is subjected to the same recombinational-repair mechanism hypothesized for uv. Spontaneous mutation was not affected by caffeine. (auth)

8638 APPEARANCE OF GENETIC MUTATIONS IN THE CELL CULTURES OF MAMMALS AS AFFECTED BY VARIOUS FACTORS. Shapiro, N. I.; Petrova, O. N.; Khalizev, A. E. (Kurchatov Inst. of Atomic Energy, Moscow). Genetika; 6: No. 4, 138-50(Apr 1970). (In Russian).

The mode of appearance of mutations manifested by the resistance to an analog of purine bases-6-mercaptopurine-(15 and 30 μg/ml) in the cell cultures of the chinese hamster subjected to the action of x irradiation (350 R), 5-bromodeoxyuridine (15 μg/ml) and N-nitrosomethylurea (0.1 mg/ml) was investigated. A high efficiency of mutagenic action of 5-bromodeoxyuridine and N-nitrosomethylurea was demonstrated. The values of induction induced by these agents amounted to $11.1 \cdot 10^{-3}$ and $0.7 \cdot 10^{-3}$, respectively, i.e., they were about twice as high as for the rate of spontaneous mutations ($1.5 \cdot 10^{-6}$). A retardation of the

phenotypical manifestation of the mutations induced by x irradiation and N-nitrosomethylurea was found. The duration of this retardation did not exceed the two cell generation. The dependence of the demonstrated number of mutations induced by N-nitrosomethylurea on the number of cell generations passed to the time of the establishment of selective conditions. The highest number of 6-mercaptopurine-induced mutations was registered after 2 to 7 cell generations. The number of registered mutations decreased with the number of cell generations. (auth)

8639 INDUCTION OF SEGMENT EXTENSION AND CHROMATID STRUCTURAL CHANGES IN VICIA FABA CHROMOSOMES AFTER TREATMENT WITH 5-AZACYTIDINE AND 5-AZADEOXYCYTIDINE. Fucik, Vladimir (Inst. of Organic Chemistry and Biochemistry, Prague); Michaelis, Arnd; Rieger, Rigomar. Mutat. Res.; 9: 599-606(Jun 1970).

When root tips of Vicia faba were treated with 5-azacytidine (5-ACR) or 5-azadeoxycytidine (5-ACD) local uncoiling (segment extension) of specific chromosome segments and chromatid aberrations was produced. The peak of cells with segment extension was observed 2 to 8 hrs after treatment (non-delayed effect); cells with chromatid aberrations appeared after recovery times of more than 20 hrs (delayed effect). Colchicine labelling of cells after 5-ACR treatment showed that chromatid aberrations were present in 4n cells, i.e., they became induced during the interphase preceding the second mitosis. Post treatment with 5-ACR after x irradiation increased the frequency of x ray-induced chromatid aberrations, and pretreatment was without influence on the aberration yield induced by x rays alone. The preliminary conclusion drawn from the experimental results is that segment extension is due to the inhibition of RNA and concomitantly, protein synthesis or the failure of complex formation between DNA and specific proteins. The incorporation of the analogues into DNA is presumed to be responsible for the induction of chromatid aberrations. (auth)

8640 ULTRAVIOLET-LIGHT SENSITIVE MUTANTS OF ASPERGILLUS NIDULANS. Wright, P. J.; Pateman, J. A. (Flinders Univ., Bedford Park, Australia). Mutat. Res.; 9: 579-87 (Jun 1970).

Fourteen mutants of Aspergillus nidulans were isolated that were more sensitive to the lethal effects of uv light than wild type strains. Haploidization analysis of six mutants showed that four are on linkage group IV, one on V, and the other on II or VIII. The sensitivity of six mutants to nitrous acid was tested and it was found that it was parallel to uv sensitivity. No effects on the frequency of meiotic intergenic recombination were found in crosses heterozygous for seven of the mutants. One of these mutants was tested in a homozygous cross and again no effects were observed. The mutations were inherited as single mendelian genes and the survival of diploid conidia after uv irradiation suggested that they were also recessive. Five mutants had an effect on ascospore development. Viable ascospores were recovered from crosses on these mutant strains in reduced numbers. (P.B.M.)

8641 RELATIVE FREQUENCY OF CHLOROPHYLL TO MORPHOLOGICAL AND STERILITY MUTATIONS INDUCED IN DURUM WHEAT BY RADIATIONS AND CHEMICALS. Bozzini, A.; Scarascia-Mugnozza, G. T. (National Centre for Nuclear Energy, Rome). Mutat. Res.; 9: 589-97(Jun 1970).

The relative efficiency of x rays, fast neutrons (Nf), thermal neutrons (Nth), ethyl methanesulphonate (EMS), and diethyl sulphate (DES) in inducing chlorophyll and morphological mutations in Triticum durum cultivars Cappelli and Aziziah was investigated. Comparison of the relative efficiency following the different mutagenic treatments was made on the basis of M_1 plant fertility and frequency of mutations in M_2. An estimate of the mutagenic efficiency gives the following sequence: for chlorophyll mutations DES ≤ X-rays < Nf ≤ EMS ≤ Nth; for morphological mutations: X-rays < DES < EMS ≤ Nth ≤ Nf. Significant correlation coefficients were found between chlorophyll and morphological mutation frequencies ascertained respectively in greenhouse and field analyses, that confirm the validity of chlorophyll mutation data as an index of mutagenic efficiency. Very high ratios of morphological/chlorophyll mutations (ranging from 1.7 to 4.2) were found in the treated material. This finding could possibly be related to the polyploid structure of durum wheat, in which the presence of homologous chromosomes duplicates the genes controlling chlorophyll synthesis and at the same time probably preserves a significant fraction of structural chromosome modifications induced by the treatment. The polyploid structure of T. durum is also probably the most important factor accounting for the high frequency of mutations ascertained by visual selection in the treated material (up to 70% on a spike progeny basis). (auth)

8642 INFLUENCE OF COMBINED ACTION OF CHEMICAL MUTAGENS AND DIFFERENT DOSES OF ULTRA-VIOLET RAYS ON THE AUXOTROPHIC MUTATION IN ESCHERICHIA COLI B. Panfilova, Z. I. (Inst. of Cytology and Genetics, Novosibirsk, USSR). Genetika; 6: No. 8, 164-9(Aug 1970). (In Russian).

It is established that the irradiation of bacteria previously treated with formaldehyde by a dose of uv rays of 100 erg/mm² extends the auxotrophic mutation spectrum. The irradiation of bacteria by a dose of uv rays of 200 erg/mm² results in a further extension of the auxotrophic mutation spectrum. Thus, while formaldehyde (FA) alone induces, in the main, mutants deficient in phenylalanine or alanine and leucine, after irradiation at a dose of 100 erg/mm², besides mutants induced by formaldehyde, there appear mutants deficient in arginine or ornithine, tryptophane, cystine-thiosulfate-methionine, and glutamic acid. Treatment with formaldehyde and subsequent uv irradiation at a dose of 200 erg/mm² resulted in the appearance of the above-mentioned mutants and additional mutants, requiring alanine, adenine or guanine, threonine, ornithine, and isoleucine. The results of the combined treatment of Escherichia coli B with nitrosomethylurethan (NMU) and uv rays showed that, though NMU itself represents a mutagen inducing a wide mutation spectrum, the irradiation of the culture with uv rays after addition of NMU resulted in a further extension of the auxotrophic mutation spectrum. The data obtained are discussed in connection with the possibility of involving in the mutation process new loci using the denaturizing action of uv rays and the increased sensitivity of denatured DNA to some chemical mutagens. (auth)

8643 A NEW SECONDARY B_β MUTATION IN SCHIZOPHYLLUM REVEALING FUNCTIONAL DIFFERENCES IN WILD B_β ALLELES. Raudaskoski, Marjatta (Turku Univ., Finland). Hereditas; 64: 259-66(1970).

A new type of secondary mutation at the Bβ incompatibility locus of Schizophyllum commune is reported. The secondary mutation Bβ7 (1−4) was induced by x rays from the primary mutant allele Bβ7(1). The mutant Bβ7(1−4) allele showed an exceptional pattern of interactions with wild Bβ alleles, that normally behave as though they are completely equivalent and uniform in their mating interactions with other wild alleles and with mutant alleles of the locus. The new Bβ mutation is compatible with three wild Bβ alleles and incompatible with four wild Bβ alleles. (auth) (Sweden)

8644 RADIATION-INDUCED DIVISION AND MITOTIC DELAY STUDIES IN GREEN ALGA (OEDOGONIUM CARDIACUM). Pujara, C. M.; Horsley, R. J.; Banerjee, S. N. (Ontario Cancer Treatment and Research Foundation, Hamilton). Radiat. Res., 44: 413-20(Nov 1970).

Studies on radiation induced division and mitotic delay were made on Oedogonium cardiacum cells at different stages during the first cell cycle. The results obtained indicate that division and mitotic delay vary with the age of the cells at the time of irradiation. Further, both division and mitotic delay are maximum for cells irradiated in G_2, moderate for cells irradiated in S, and a minimum for cells irradiated in G_1. The division delay, measured by cell counting, increases linearly with dose after approximately 500 rads for cells in G_1, S, and G_2 and is 0.10, 0.19, and 0.33 min/rad, while mitotic delay, measured by the appearance of mitotic figures, is a linear function of dose for cells in G_1, S, and G_2 and is 0.10, 0.24, and 0.33 min/rad respectively. (auth)

8645 INVESTIGATION INTO THE EXPRESSION OF THE REX MUTANT IN THE HOUSE MOUSE: ITS EFFECTS ON HAIR GROWTH. Korolenko, Frances Jane. Providence; Brown Univ. (1969). 88p. University Microfilms Order No. 70-8746.

Thesis.

An investigation was undertaken to explain the morphological effects of the Rex gene. The coat of the Rex mouse consists of hair containing crookedness, waviness, and an irregularly spaced narrowness of the shafts. Dorsal skin and individual follicles were examined in histological sections and in whole mounts during anagen stages of the hair growth cycle. Histological sections of Rex skin, 7-hr post-partum to 55-hr post-partum, suggested a slower initiation and/or slower and asynchronous growth of the follicles and hair in comparison with equivalently timed non-mutant skin. Skin changes, normally accompanying stages of the hair growth cycle, were not evident in the mutant. Whole mounts and microdissected follicles also suggested an asynchrony in the growth of the hair. Whole mounts of skin examined twelve days after plucking with Aeroplast contained excessively long and curled follicles. It was suggested from the findings in this study that the three distinct phenomena seen in the hair of the mutant were produced by different events. Waviness of the hair shaft may be produced from the long, eccentrically twisted follicles. Crookedness may be the product of crooked follicles produced by an asynchronous development of skin, follicle, and hair. Irregular narrowness of the hair shafts may be due to an uncontrolled variation in the distribution of cells between the hair shaft and the internal root sheath. This would account for the lack of normal zigzags in the

XUM

coat of the Rex mouse. Alterations of the extremely well-regulated hair growth in non-mutants by x irradiation, chemicals, and Aeroplast were, in most cases, unsuccessful. All abnormalities found in the Rex mutant thus seem to be secondary effects of the gene. Further investigation is necessary before the primary target of the gene can be identified. (Diss. Abstr.)

8646 FACTORS INFLUENCING THE EXPRESSION OF ANOPHTHALMIA IN THE MOUSE. Osmolski, Thaddeus Vincent. Providence; Brown Univ. (1969). 60p. University Microfilms Order No. 70-8774.

Thesis.

The failure of the optic vesicle to invaginate in anophthalmic mutant mice was explored using descriptive and experimental methods. Measurements of the distance between the optic vesicle and the overlying ectoderm showed no differences between the anophthalmic and control groups during the critical time. The vesicles of both groups react in an identical manner to several histochemical procedures. The optic vesicles of embryos of the anophthalmic strain were found to be smaller than those in the embryos of the control strain at this critical time. This sole difference is due to cell proliferation. Inhibition of vesicle growth at the critical time was produced by exposure to x rays and by colchicine. A high percentage of treated embryos mimicked embryos of the anophthalmic strain with respect to eye development. One teratogen, cortisone, was used in conjunction with embryos of the anophthalmic strain in order to correct for the genetically programmed delay in optic vesicle growth during the critical period. It was concluded that the action of the hormone provides an acceleration of optic vesicle growth at this time which places the development of the vesicle in phase with that of the overlying ectoderm. Interaction of the two tissues then occurs and normal eye development proceeds. It was concluded that the optic vesicle must exceed a certain threshold size during this critical period in order to interact with the overlying ectoderm. If this size is not achieved at this particular time, whether in response to the mutant allele or to teratogens, there is no interaction between these two tissues, and anophthalmia is produced. (Diss. Abstr.)

8647 UNSCHEDULED DNA SYNTHESIS AT LOW X-RAY DOSES. Spiegler, P.; Norman, A. (Univ. of Southern California, Los Angeles. Univ. of California School of Medicine, Los Angeles). Mutat. Res.; 10: 379-87(Oct 1970).

Studies on the kinetics of unscheduled DNA synthesis in human lymphocytes following high radiation doses were extended to the dose range of 600 to 2400 rad. As in the case of the high doses, the data can be modeled in terms of a single enzyme system. There are, however, differences; at high doses the ratio of radioinduced substrate (lesions) to enzyme is much greater than 1 and a Michaelis Menten plot of the data is possible. Below 1000 rad, this ratio appears to be less than 1 and consequently the Michaelis Menten plot breaks down. In the dose range of 600 to 2400 rad, the data are represented in terms of a dose dependent rate constant. The rate constant increases as the dose decreases from 2400 to about 1000 rad and then reaches a constant value of 3 h^{-1} which corresponds to a half-life of about 14 min. Under the assumption of a single enzyme system, the high dose data and low dose data can be used together to obtain an estimate of the average number of enzymes per lymphocyte. A value of 10 to 20 thousand enzyme units per cell is obtained. This is equivalent to 1 enzyme unit per 2 to $4 \cdot 10^9$ dalton of DNA. At low doses, the amount of exogenous thymidine (TdR) incorporated as a result of radioinduced unscheduled DNA synthesis amounts to 6 molecules of TdR/rad/cell at saturated concentration of exogenous TdR (about 5 μM). Coupled with the enzyme model, this amounts to approximately 10 to 20 lesions per rad or that 1 or 2 nucleotides are incorporated per lesion. (auth)

8648 MUTAGENIC EFFECT OF ^{90}Sr IN BARLEY. Lindgren, D.; Eriksson, G.; Ehrenberg, L. (Royal Coll. of Forestry, Stockholm. Univ. of Stockholm). Mutat. Res.; 10: 335-51(Oct 1970).

The mutation frequency in the pollen character waxy was investigated in barley plants cultivated on soil contaminated with ^{90}Sr. Doses in the range of human safety interest were mutagenic. The mutation frequency per dose unit was higher in the lowest dose region than at moderate doses. In a comparison with ^{90}Sr β-radiation originating outside the plants no indication of any transmutation effects of ^{90}Sr was found. The doses were estimated by LiF thermoluminescence dosimetry and by theoretical calculations. Theoretical dose distributions in ^{90}Sr contaminated cylinders were calculated. (auth)

8649 ANALYSIS OF PHOTOENZYMATIC REPAIR OF UV LESIONS IN DNA BY SINGLE LIGHT FLASHES. VIII. INHIBITION OF PHOTOENZYMATIC REPAIR OF UV LESIONS IN E. COLI DNA BY CAFFEINE. Harm, Walter (Univ. of Texas, Dallas). Mutat. Res.; 10: 319-33(Oct 1970).

The rate of photoenzymatic repair (PER) obtained with continuous illumination of uv-irradiated Escherichia coli B_{s-1} cells is much decreased in the presence of 16 mg/ml caffeine. This inhibitory effect is usually not observed in B/r cells. It occurs in T1 phage infecting either B_{s-1} or B/r, indicating that its absence in B/r cells has not a trivial explanation such as destruction or decreased uptake of the inhibitor. Experimental evidence is presented that caffeine interferes strongly with the formation of enzyme–substrate (ES) complexes, presumably by binding to DNA at, or close to, the repairable photoproducts. This results in a lower equilibrium of complex formation in the dark. A single caffeine molecule can block the formation of a complex; this effect is fully reversible when the caffeine is diluted out. Caffeine does not interfere with the photolysis of existing ES complexes. Failure to observe, under usual conditions, caffeine inhibition of PER in irradiated B/r cells is explained by the large number of uv lesions in these cells, compared to much smaller numbers in B_{s-1} cells or in phage infecting either type of cell. Due to this high number, complex formation in B/r cells is so rapid that—in spite of the showdown by caffeine—most of the PRE is tied up in ES complexes in the steady state during continuous illumination at moderate intensity. Only at very high light intensity, where the steady-state concentration of complexes is lower, is the caffeine inhibition observed. Correspondingly, illumination of irradiated B_{s-1} cells at very low light intensity results in decreased caffeine inhibition of PER. (auth)

8650 ANALYSIS OF PHOTOENZYMATIC REPAIR OF UV LESIONS IN DNA BY SINGLE LIGHT FLASHES. VII. PHOTOLYSIS OF ENZYME–SUBSTRATE COMPLEXES IN VITRO. Harm, Helga; Rupert, Claud S. (Univ. of Texas, Dallas). Mutat. Res.; 10: 307-18(Oct 1970).

The extent of complexing of the repairable ultraviolet lesions in Haemophilus influenzae transforming DNA with yeast photoreactivating enzyme in the dark can be determined by applying intense light flashes, which cause repair of essentially all lesions complexed. With full complexing of repairable lesions the kinetics of photoreactivation by steady illumination reflect only the photochemical reaction occurring in the enzyme–substrate complex. Complexes are heterogeneous with respect to their rates of photolysis, described by the first-order rate constant k_3. At early stages of repair $k_3 = k_p I$, where I is the light intensity and k_p is the photolysis constant. The measured value of k_p permits calculation of the product $\epsilon\Phi$, where ϵ is the molar extinction coefficient for the complex, and Φ is the quantum yield for photolysis, giving an absolute action spectrum. In the region of most effective wavelengths (355–385 nm), $\epsilon > 10^4$ liter $\cdot$ $mole^{-1} \cdot cm^{-1}$, and $\Phi > 0.1$, with the possibility that $\Phi \approx I.k_p$ is independent of temperature and ionic strength over a range producing large effects on the rate of complex formation, but does increase with pH over the range 6.7–7.4. For the slower repair of a minority of lesions the measured value of k_p depends somewhat on intensity and continuity of illumination, suggesting some differences not yet understood. At the usual illumination intensities used for photoreactivation k_3 is greater than k_2, the rate constant for dark dissociation of complexes. (auth)

8651 ANALYSIS OF PHOTOENZYMATIC REPAIR OF UV LESIONS IN DNA BY SINGLE LIGHT FLASHES. VI. RATE CONSTANTS FOR ENZYME–SUBSTRATE BINDING IN VITRO BETWEEN YEAST PHOTOREACTIVATING ENZYME AND ULTRAVIOLET LESIONS IN HAEMOPHILUS TRANSFORMING DNA. Harm, Helga; Rupert, Claud S. (Univ. of Texas, Dallas). Mutat. Res.; 10: 291-306(Oct 1970).

Rate constants k_1 for formation, and k_2 for dissociation of the enzyme–substrate complexes of yeast photoreactivating enzyme and uv lesions in Haemophilus influenzae transforming DNA, were measured as functions of temperature, pH, and ionic strength in vitro. The measurements employed intense light flashes which cause repair of essentially all lesions complexed, to determine the number of complexes existing at any moment. Absolute concentrations of substrate were referred to the known numbers of pyrimidine dimers in irradiated DNA, while enzyme concentrations were determined by titration against substrate in a concentration range where the binding was essentially complete. The results reported permit a choice of optimum conditions for photoreactivation under various conditions of illumination. UV lesions are heterogeneous with respect to both formation and dissociation of complexes, and the values determined for the constants are weighted averages. The two rate constants depend on temperature as described by the Arrhenius expression with activation energies of about 9.3 and 5.5 kcal $\cdot$ $mole^{-1}$, respectively. This particular difference between the two activation energies indicates that the binding energy in the complex is small. Both constants increase with pH over the range 6.0 to 7.7, but their ratio, which governs the equilibrium complexing in the dark, is higher at the lower pH. k_1

depends critically on the salt concentration, the position of the sharp maximum varying with the particular ions present, while k_2 increases generally with salt concentration over the range studied. Simple empirical expressions were found which quantitatively describe the behavior of both constants as a function of ionic strength. (auth)

8652 ANALYSIS OF PHOTOENZYMATIC REPAIR OF UV LESIONS IN DNA BY SINGLE LIGHT FLASHES. V. DETERMINATION OF THE REACTION-RATE CONSTANTS IN E. COLI CELLS. Harm, Walter (Univ. of Texas, Dallas). Mutat. Res.; 10: 277-90(Oct 1970).

It was shown earlier that the use of intense light flashes permits analyzing in greater detail the reaction involved in photoenzymatic repair (PER). This paper describes experiments in which the reaction-rate constants for the formation of enzyme–substrate complexes (k_1) and dark dissociation of the complexes (k_2), and the photolytic constant (k_p) for the light-dependent repair step were determined in Escherichia coli B_{s-1}. All three reactions are heterogeneous with respect to these constants. Presumably this reflects the diversity of pyrimidine dimers in irradiated DNA, all of which serve as substrate for photoreactivating enzyme (PRE). (P.B.M.)

8653 INFLUENCE OF HOST-CELL REACTIVATION AND UV DOSE ON FORMATION OF PURE AND MIXED CLONES OF c MUTANTS IN PHAGE KAPPA. Kaplan, R. W.; Stoye, Hilde (Univ., Frankfurt am Main). Mutat. Res.; 10: 257-67(Oct 1970).

When free phage kappa was irradiated with uv and plated with host strains HY or hcr 42, respectively, most plaques due to c mutations contained solely or predominantly the mutant type. Both wild and c type from the infrequent mixed (mosaic) plaques were stable; inherited instability was very rare. The relative rarity of mosaics with <50% c type was neither caused by selection within a host cell or plaque nor by a frequent very low burst size. The two different uv doses used did not lead to significant differences in the percentage of mosaics among all mutant plaques, using either host strain. Nevertheless, recessive lesions within the DNA strand opposite to the premutated one could be the cause of c-clone purity. An explanation is proposed of the effects of UV dose as well as repair, assuming a premutation to consist of 2 different hit products in opposite DNA strands. (P.B.M.)

8654 KILLING AND MUTAGENIC ACTION IN E. COLI ASSOCIATED WITH THE AUGER EFFECT DURING ^{125}I DECAY. Ahnstroem, G.; Ehrenberg, L.; Hussain, S.; Natarajan, A. T. (Univ. of Stockholm). Mutat. Res.; 10: 247-50(Sep 1970).

The decay of radioactive nuclides incorporated in the DNA of living cells may lead to effects with a certain specificity, due to their localization in the molecule and the decay scheme. In the case where the decaying atom occupies a vital position in the gene material, considerable damage might be due to such events as the chemical change in transmutation, to collisions of the recoiling daughter atom or to multiple ionization, although from a dosimetrical point of view these events carry but a minor fraction of the average radiation dose absorbed by the cell or cell nucleus. One important aspect of the biological effects of incorporated radioisotopes is the dose dissipated locally within small volumes around the site of disintegration. With the Auger effect a number of low-energy events leads to a highly localized energy dissipation, which, besides the multiply ionized[11,12,16,17] daughter atom, may be responsible for special biological effects. The present investigation concerns the consequences of decay of ^{125}I incorporated into DNA. One aim of the project was to investigate whether a possible radiobiological role of multiple ionization might be discerned by means of qualitative criteria for radiation action. This paper deals with the killing and mutagenic action due to [^{125}I]-IUdR incorporated in the DNA of Escherichia coli. (P.B.M.)

8655 FURTHER OBSERVATIONS ON EMBRYO-ENDOSPERM RELATIONS IN IRRADIATED WATER SOAKED SEEDS OF DURUM WHEAT. Floris, C.; Meletti, P.; d'Amato, F. (Univ., Pisa, Italy). Mutat. Res.; 10: 253-5(Sep 1970).

Seeds of the durum wheat cultivar Cappelli were soaked in petri dishes, filled with deionized water (100 seeds, 50 ml water per dish), for 24 h at 20° in the dark. Some of the seeds were irradiated with 500 or 1000 R of x rays delivered at 180 kV, 6 mA, 200 R/min without an extra filter. Soon after irradiation, embryos were excised from irradiated and unirradiated seeds with an appropriate gauge which allowed the excision of endosperm-free undamaged embryos with scutellum. The following transplants were made: $EM_{(i)}/EN_{(i)}$, $EM_{(i)}/EN_{(u)}$ and $EM_{(u)}/EN_{(u)}$. For seedling-growth studies, the transplants were sown in sand at 2.5 cm depth in wooden boxes in a dark room at a constant temperature of 20°; 7 days later, the seedlings were removed from the sand and measured. For mutagenic studies, the transplants were sown in a layer of sand overlying a layer of soil in small sphagnum pots (jiffy-pots), one per pot, and grown in the greenhouse up to the 3-leaf stage, at which time they were transplanted to a field. At maturity the plants were harvested and in the next autumn were scored for chlorophyll mutations on a plant and spike progeny basis, so that possibly occurring heterozygotes, which might alter mutation rates, could be discarded. (P.B.M.)

8656 NEW VARIETIES OF MALTING BARLEY PRODUCED BY RADIATION BREEDING. Hirai, Shin; Osada, Tadanori; Hasegawa, Koichi; Hiraki, Makoto (Kirin Brewery Co. Ltd., Takasaki, Japan). Rep. Res. Lab. Kirin Brewery Co., Ltd.; No. 12, 69-77(1969).

Kirin Choku No. 1, cultivated widely as a malting barley in Japan, has some defects as a variety for commercial cultivation. This variety has tendency to lodge because of its long culm, and matures fairly late. In 1956, experiments were begun to induce mutations by radiation to improve it without changing the malting quality of the variety. Two short culm mutants, Gamma No. 4 and 33γ15, were obtained from the progenies of γ-irradiated seeds (Kirin Choku No. 1) in 1958 and also an early ripening mutant, 34γ127, from the progeny of seeds in 1959. Gamma No. 4, a short culm mutant was crossed in 1962 with 34γ127, the early ripening mutant, to obtain a variety having both these favorable characters. One double recessive line, 37FC1-1, was selected from the progeny of this cross. This line has a 20 cm shorter culm and ripened 4 to 5 days earlier than the parental variety, Kirin Choku No. 1. This selected line was named Gamma No. 8 and was released for commercial cultivation. The grain yield and malting quality of Gamma No. 8 were almost the same as those of the parent. (auth) (Japan)

Health Physics and Safety

Refer also to abstract 8827.

Radioactive Contamination and Decontamination

Refer also to abstracts 8326, 8594, 8595, 8624, 8625, 8629, 8630, and 8681.

8657 (CEA-R-4008) ACCIDENTAL RELEASE OF ^{131}I AT THE UP 2 PLANT ON OCTOBER 2nd AND 3rd 1968. Scheidhauer, Jean; Cassabois, Georges; Gandon, Remi (Commissariat a l'Energie Atomique, La Hague (France)). Sep 1970. 45p. (In French). Dep. NTIS (U. S. Sales Only).

The description of an accidental release of ^{131}I at La Hague reprocessing plant (UP 2) is made. Safety measures taken are reported. An account is given of the results found in the control of the released quantities and of the contamination in grass and milk. A discussion on the low values found for the activity is presented. (France)

8658 (HASL-237, pp II.1-16) HASL FALLOUT PROGRAM DATA. (New York Operations Office (AEC), N. Y. Health and Safety Lab.).

From Fallout program.

The results of HASL fallout monitoring programs are presented. The following data are tabulated: ^{238}Pu deposition at various world sites caused by the disintegration of a SNAP-9A power source in April 1964; the ^{238}Pu, ^{239}Pu, and ^{90}Sr content of atmospheric precipitation at eight world sites from 1966 to 1970; the ^{90}Sr content of human diets in New York City and San Francisco from April to July 1970; and the daily intake of ^{90}Sr by humans in Chicago, New York City, and San Francisco from 1960 to 1970. (L.C.L.)

8659 (HASL-237, pp III.14-17) ^{137}Cs IN VARIOUS CHICAGO FOODS (COLLECTION MONTH, JULY 1970). Brar, S. S.; Nelson, D. M. (Argonne National Lab., Ill.).

From Fallout program.

Since April, 1961, the ^{137}Cs and potassium content of the Chicago portion of Tri-City Diet Sampling Program has been determined in bulk food samples by gamma ray spectrometry using a 4'' × 4'' NaI(Tl) crystal. The individual food components were counted for a minimum of 100 minutes, and from these measurements composite daily and yearly food intakes were obtained. Cesium-137 activity in food, now, is an order of magnitude lower than it was a few years ago; consequently, a new procedure for these measurements has been adopted in order to improve accuracy. The same variety of foods (all fresh vegetables, all fresh fruits, etc.) is composited before measurement, and the samples are counted a minimum of 400 minutes. The results for the July, 1970, quarter are tabulated. (auth)

8660 (HMI-B-87) CONTAMINATION OF THE RIVER WATER BY THE FALLOUT AFTER EXTREME REACTOR ACCIDENTS. Jacobi, W.; Stolterfoht, N. (Hahn-Meitner-Institut

XUM

fuer Kernforschung, Berlin (West Germany)). Oct 1969. 61p. (In German). Dep. NTIS (U. S. Sales Only).

The contamination of river water by direct fallout on the water surface and by fallout on the draining area of the river after a reactor accident is discussed. An estimation of the time dependent activity and the time integration over the concentration of biologically important fission products in the river is given. As a result, it was found that even in the case of an extreme reactor accident the contamination of the river water is minimal and the population using prepared river water as drinking water is exposed to danger only if extreme meteorological conditions coincide with the accident. The most critical fission products are ^{131}I and ^{90}Sr. (auth)

8661 (JAERI-4052) NUCLEAR ACCIDENTS IN NUCLEAR INSTALLATIONS. Survey Report. Onishi, Takeshi; Minami, Kentaro; Yamagishi, Hideo; Sato, Nobuyuki; Murata, Mikio (Japan Atomic Energy Research Inst., Tokai. Tokai Research Establishment). Nov 1969. 203p. (In Japanese). Dep. NTIS (U. S. Sales Only).

In order to plan radiation safety procedures effectively, a literature survey was made on the various accidents that occurred in nuclear installations throughout the world. General and useful comments were derived from accidental experiences. Two-hundred and eighty-five accidents were reviewed from the standpoint of their causes and their consequences. Emphasis is placed on the latter, and descriptions are also made of the steps and measures that were taken after the accidents, including the recommendations. (auth)

8662 (UCRL-Trans-10488) ^{137}Cs-DECONTAMINATION WITH COLLOIDALLY SOLUBLE PRUSSIAN BLUE IN RATS. Mueller, W. H. Translated by J. D. Loydall for Univ. of California Lawrence Radiation Lab., Livermore, from Strahlentherapie; 137: 705-7(1969). 9p. Dep. NTIS.

The effectiveness of Prussian blue for the removal of ^{137}Cs from rats was tested. The effect of the chemical form of the Prussian blue on its Cs decontamination effects was also investigated. It was found that colloidally soluble Prussian blue was the most effective for the removal of ^{137}Cs. Methods for the preparation of three chemical forms of Prussian blue and results of tracer studies on their metabolism and toxicity studies in rats are included. (C.H.)

8663 FAST DRYING SHIPPABLE PROTECTIVE COVER FOR RADIOACTIVE DECONTAMINATION. Bernaola, O. A. (Univ. de Oriente, Cumana, Venezuela); Filevich, A. Health Phys.; 19: 685-6(Nov 1970).

A strippable plastic film was developed that can be sprayed on large surfaces for decontamination purposes. In contrast to similar previous methods, the film has a hardening time of approximately 3 min and results in a very high decontamination factor with only one application. The basic composition of the film is vinyl acetate-vinyl chloride copolymer that is easily processed at room temperature. The most favorable prospect of this product is in the prevention of surface contamination (on the order of 0% ± 1%) from many types of contaminating substances. (auth) (UK)

8664 PROCESS FOR DECONTAMINATING RADIOACTIVE ARTICLES. (to Ugine Kuhlmann). British Patent 1,208,480. 14 Oct 1970. Priority date 17 Aug 1967, France.

A process for decontaminating radioactive articles comprises washing the articles in a solution that is a substantially neutral sodium salt of an α-amino(alkanephosphonic) acid and a biodegradable surface active agent in deionized water. A high molecular weight alcohol with a straight oxyethylated chain is a suitable surface active agent. The washing effluents are purified by precipitation of insoluble calcium salts and/or treatment with zeolites. (B.L.M.)

8665 INVESTIGATIONS REGARDING THE RADIOACTIVITY OF HONEY. Barabas, B.; Lupsan, V.; Butiu, Doina; Balogh, L. Rev. Med. (Tirgu-Mures); 15: 214-19(1969). (In Rumanian).

The total β and γ activity of samples of honey as well as the radium afferent α activity was determined. By means of the potassium content of honey, the afferent activity of ^{40}K was calculated. The natural activity was compared to the artificial activity of honey, and a value about 10 times higher was found for the artificial activity as compared to the natural activity. The total β activity of the samples varied between 24.3 and 749.3 pCi/kg honey, respectively 95.6 to 308 pCi/g ash. The afferent activity of ^{90}Sr was about 10% of the total artifical activity. The α activity of the samples was about 0.1 mCi or less, depending on the sensitivity of the method. The results obtained were also examined for alimentary hygiene and the administration of honey as a medicine for children was considered. (auth)

Dosimetry and Monitoring

Refer also to abstracts 8393, 8437, 8452, 8467, 8492, 8563, 8574, 8596, 8729, 8730, 8734, 8735, and 8761.

8666 (AECL-3728) BIOLOGY AND HEALTH PHYSICS DIVISION PROGRESS REPORT, APRIL 1 to JUNE 30, 1970. (Atomic Energy of Canada Ltd., Chalk River (Ontario). Chalk River Nuclear Labs.). 52p. (PR-B-86). Dep. NTIS (U. S. Sales Only). AECL $1.50.

The research and routine monitoring activities of the Biology and Health Physics Division of AECL for the period of April 1 to June 30, 1970 are summarized. The various branches within the division and their major areas of study include: Biology Branch; biochemical and molecular studies, and developmental and population genetics studies; Environmental Research Branch; biological and physical studies, meteorological studies, chemical studies, and soil studies and radiochemical analysis. Health Physics Branch; dosimetry, detector, and monitoring instrumentation studies. The economic importance to AECL of the seasonal and geographic variations in the deuterium content of Canadian waters is discussed by the division director. (E.R.B.)

8667 (BNWL-SA-3233) EVENTUAL WHOLE BODY EXPOSURE RATE FROM ^{85}Kr RELEASED TO THE ATMOSPHERE. Hendrickson, M. M. (Battelle-Northwest, Richland, Wash. Pacific Northwest Lab.). 13 Jul 1970. Contract AT(45-1)-1830. 16p. (CONF-700810-52). Dep. NTIS.

From Symposium on Environmental Aspects of Nuclear Power Stations, New York, N. Y.

The whole-body exposure rate for man was calculated for immersion in ^{85}Kr dispersed in the atmosphere. Both γ rays and Bremsstrahlung were accounted for. Immersion exposure for one year to a semi-infinite cloud of ^{85}Kr with an activity concentration of 3×10^{-7} $\mu Ci/cm^3$ would result in a calculated dose of 7 millirem to the whole-body and 300 m rem to the skin (7 mg/cm^2 depth). In numerous instances the above concentration has been equated to a whole-body exposure rate of 500 millirem per year when in fact this is the exposure rate to the surface of the body. Using currently popular estimates of the growth of nuclear power production, release of ^{85}Kr into the atmosphere could conceivably cause a total body dose (or genetically significant dose) of about 0.03 millirem in the year 2000. (C.H.)

8668 (BNWL-SA-3424) REASONS FOR DIFFERENCES IN CALCULATED ESTIMATES OF THE "CLOUD DOSE". Hendrickson, M. M.; Strenge, D. L. (Battelle-Northwest, Richland, Wash. Pacific Northwest Lab.). [1969] Contract AT(45-1)-1830. 13p. (CONF-701106-2). Dep. NTIS.

From Symposium of the Health Physics Society, Idaho Falls, Idaho.

Many factors have been identified which cause differences in calculated estimates of the cloud dose. The factors include calculational models and methods, differences in input data to the calculations and the definition of "cloud dose" or "immersion dose" itself. Differences in estimates may be as high as a factor of 100,000, depending on assumptions made. As new data from safety tests are applied and as new models are developed for inclusion in consequences calculations (e.g. models for aerosol behavior or dose rate buildup in air) it will be necessary to explain each calculation step precisely. Otherwise differences may be increased rather than diminished. It is essential that those engaged in the estimation of the potential radiological consequences of accidents be aware of the factors which are causing differences. The factors are described and some examples are given illustrating their impact on dose calculations. (auth)

8669 (COO-2088-1) ARGONNE RADIUM STUDIES. Evaluation of Clinical Effect Versus Dose in Radium Dial Painters. Final Report. Miller, Charles E.; Finkel, Asher J.; Hasterlik, Robert J. (Loyola Univ., Maywood, Ill. Stritch School of Medicine). [1969]. Contract AT(11-1)-2088. 99p. Dep. NTIS.

The total accumulated radiation dose and dose rate at various times following the ingestion of ^{226}Ra by radium dial painters were calculated using computer methods based on decay scheme data for ^{226}Ra. The data were correlated with results of radiographic examinations of the skeleton for bone lesions. Methods for the calculation of the content of ^{222}Rn, ^{214}Pb, and ^{214}Bi in the body at various times following the ingestion of ^{226}Ra, and the radiation dose delivered therefrom, are discussed. Data are included on the number of bone neoplasms and bone fractures in relation to the absorbed radiation dose and dose rate to the skeleton. An attempt was made to relate the radiation dose to the reproductive capacity of women dial painters but no conclusive data were obtained. (C.H.)

8670 (HASL-237(App.)) HEALTH AND SAFETY LABORATORY FALLOUT PROGRAM QUARTERLY SUMMARY REPORT,

JUNE 1, 1970–SEPTEMBER 1, 1970. (New York Operations Office (AEC), N. Y. Health and Safety Lab.). 1 Oct 1970. 400p. Dep. CFSTI.

The appendix to the Health and Safety Laboratory Fallout Report for June to September, 1970 presents, in tabular form, data from monitoring activities around the world. These data include: monthly deposition of ^{89}Sr and ^{90}Sr at world land sites, radiostrontium deposition at Atlantic Ocean weather stations, radionuclides in surface air over selected terrestrial and marine sites, and radiostrontium in milk and tap water in New York. Tables containing the conversion factors used in presenting the data and half-life values for the radionuclides of interest in the program are included. (E.R.B.)

8671 (ICRU-16) LINEAR ENERGY TRANSFER. (International Commission on Radiation Units and Measurements, Washington, D. C.). 15 Jun 1970. 51p. ICRU Publications, Washington, D. C.

A Task Group of the International Commission on Radiation Units and Measurements (ICRU) revised the previous (1962) definition of linear energy transfer (LET). This 1968 definition states: The linear energy transfer or restricted linear collision stopping power (L_Δ) of charged particles in a medium is the quotient of dE by dl, where dl is the distance traversed by the particle and dE is the mean energy-loss due to collisions with energy transfers less than some specified value Δ. $L_\Delta = (dE/dl)_\Delta$. The definition specifies an energy cut-off and not a range cut-off with the maximum energy transfer (Q_{max}) governed by the type and velocity of the incident particle. The concepts on which the definition is based are discussed in detail. Data on interactions of radiations with matter are reviewed, calculations of distributions of absorbed dose in LET are included, and applications of LET calculations in the estimation of dose equivalent for radiation protection and in fundamental studies of observed relations between radiation effects, such as the relative biological effectiveness (RBE) of various radiations, are discussed. The limitations of the LET concept and other methods of specifying radiation quality are also discussed. Data relevant to calculations and uses of LET are appended. (150 references.) (C.H.)

8672 (ICRU–17) RADIATION DOSIMETRY: X RAYS GENERATED AT POTENTIALS OF 5 TO 150 kV. (International Commission on Radiation Units and Measurements, Washington, D. C.). 15 Jun 1970. 39p. ICRU Publications, Washington, D. C. $2.50.

The special problems that arise during the measurement of x rays generated at potentials of 5 to 150 kV are discussed. The relationships between radiation quantities and units, measurement of energy fluence, the spectral distribution of photons, other specifications of radiation quality, and methods for measuring exposure dose and absorbed dose are discussed. X ray interaction coefficients for this energy range are tabulated for a number of elements and materials. The performance of chemical detectors, ionization chambers, and solid state devices for measurements over this energy range is discussed. It is pointed out that the exposure standard for x rays at this energy range is the free-air ionization chamber. The use of low-energy x-ray exposure standards for calibration of instrument calibration is discussed. (140 references) (C.H.)

8673 (JAERI-Memo–4098) HEALTH PHYSICS AND SAFETY AT OARAI RESEARCH ESTABLISHMENT, APRIL 1969–MARCH 1970. (Japan Atomic Energy Research Inst., Tokyo). Jul 1970. 81p. (In Japanese). Dep. NTIS (U. S. Sales Only).

The activities of the Section of Health Physics and Safety, Oarai Research Establishment, Japan, for the period from April 1969 to March 1970 are summarized. Training programs for the handling of accidents, area monitoring, environmental monitoring, personnel monitoring, and the maintenance and calibration of monitoring instruments are reported. (auth)

8674 (LF-tr–41, pp 199-220) BASIS FOR SETTING THE MAXIMUM PERMISSIBLE LIMITS OF ^{239}Pu IN THE HUMAN BODY, AIR, AND WATER. Translated from Problemy Toksikologii Plutoniya, Atomizdat, Moscow, 1969.

A review is presented of the maximum permissible dose to the human body and the maximum permissible concentration in air of the bone-seeking radioisotopes, ^{227}Ac, ^{241}Am, ^{144}Ce, ^{237}Np, ^{239}Pu, ^{226}Ra, ^{90}Sr, and ^{232}Th. Recommendations of the ICRP for the maximum permissible dose of ^{239}Pu to workers in the plutonium industry are discussed. Recommendations were based on comparison with the maximum permissible dose of ^{226}Ra. Equations for deriving the maximum permissible dose of ^{226}Ra and ^{239}Pu based on toxicity data are presented. Methods for calculating the potential osteosarcomagenic effects of ^{239}Pu in man are described. Equations for the determination of the maximum permissible of ^{239}Pu in air and water are presented, and parameters used by the ICRP are discussed. It is emphasized that recent information on the biological effects of plutonium under natural conditions of entry into the body, dealing with the kinetics of metabolism and microdistribution, points to the necessity for a revision of the current values of the maximum permissible dose and maximum permissible concentration. (H.L.W.)

8675 (NP–18529) ANNUAL REPORT FOR THE YEAR 1969. (National Radiation Lab., Christchurch (New Zealand)). 41p. (NRL-AR-20). Dep. NTIS (U. S. Sales Only).

The radiation protection program of the National Radiation Laboratory, New Zealand, is outlined and activities during 1969 are reported. The Laboratory is responsible for the administration of radiation protection legislation governing all users of radiation, provides assistance in the field of radiation physics, and maintains standards for the calibration of x ray sources and other radiation sources. A film badge dosimetry service is provided for monitoring all personnel occupationally exposed to radiation. Training courses are given to groups of professional and technical workers in New Zealand and assistance is being given to Thailand in setting up a National Radiation Protection Service. The Laboratory is responsible for monitoring fallout in New Zealand and adjacent Pacific Ocean locations. Data are included from measurements of total β activity in air filter samples and rainwater samples collected during 1968, measurements of ^{89}Sr and ^{90}Sr in rainwater samples collected during the first three months of 1969, and the content of ^{137}Cs and ^{90}Sr in milk during 1968. (C.H.)

8676 (NYO–2740-7) ANNUAL REPORT ON RESEARCH PROJECT. (Columbia Univ., New York. Radiological Research Lab.). 1 Jul 1970. Contract AT(30-1)-2740. 263p. Dep. CFSTI.

Separate abstracts were prepared for the five sections included. (W.H.K.)

For abstracts of individual sections see: 8482, 8563, 8677, 8756, and 8757.

8677 (NYO-2740-7, pp 5-51) RADIOLOGICAL PHYSICS: I. DOSIMETRY. (Columbia Univ., New York. Radiological Research Lab.).

From annual report on research project.

Research projects in dosimetry conducted by the Radiological Physics group are presented. The following areas of dosimetry are discussed: gas multiplication chambers for radiation measurements; dosimetry studies for a fast neutron therapy beam; dosimetry of monoenergetic neutrons; calibration of a 10 Ci Pu-Be neutron source; neutron energy response of an air-filled parallel plate cavity; and specialized neutron dosimetry at the Radiological Research Accelerator Facility (including dosimetry of monoenergetic neutrons for Tradescantia, Drosophila, and mice). (E.R.B.)

8678 (ORNL-tr–2403) RECOMMENDATIONS CONCERNING THE MAXIMUM PERMISSIBLE TRITIUM OXIDE CONCENTRATIONS IN THE ATMOSPHERE OF INDUSTRIAL PREMISES. Moskalev, Yu. I.; Shtukkenberg, Yu. M.; Zhuravlev, V. F. Translated for Oak Ridge National Lab., Tenn., from Gig. Tr. Prof. Zabol.; 13: 39-43(1969). 7p. Dep. NTIS.

Data on the periods of half-life of tritium oxide passed from the human organism and some information as to its comparative biological effectiveness are presented. Some rated figures as to the access of tritium oxide into the human organism are listed. A new level of the maximum permissible concentrations of tritium oxide in the atmosphere of industrial premises, in the moisture of expired air, and in the urine is recommended. (auth)

8679 (SZS–6/70, pp 9-18) THE NEED FOR MEASURING THE RADIATION BURDEN OF THE BLADDER AND RECTUM WITH THE "GAMMAMETER" IN GYNECOLOGICAL CONTACT THERAPY TO AVOID RADIATION DAMAGE. Glaser, F. H. (Staatliche Zentrale fuer Strahlenschutz, Berlin (East Germany)). (In German). Dep. CFSTI (U. S. Sales Only).

The difference between the measured and the evaluated radiation burden of the bladder and rectum was determined with 700 intracavitary treatments of gynecologic carcinomas performed during a 3-yr period. The results show that the less the applied activity, the larger the difference and that the measurement of dose rates may lead to a shortening of the treatment. Thus unnecessary radiation burdens of bladder and rectum are avoided. (auth)

8680 RELATIONSHIP OF ^{210}Pb AND SHORT LIVED ^{222}Rn DAUGHTER PRODUCTS. Fisher, H. L. (Bureau of Radiological Health, Bethesda, Md.). Health Phys.; 19: 697-8(Nov 1970).

Corrections for recent misuses of a conversion factor needed in a model put forward by Fisher (NSA 23: 26788) for estimating

inhalation exposure to ^{222}Rn and daughter products from the accumulated ^{210}Pb body burden are given. The effect of the violation of the assumption that there was no significant ^{210}Pb contributions from sources other than ^{222}Rn daughters on the model, and the results are considered. (UK)

8681 DERIVATION OF WORKING LIMITS FOR CONTINUOUS RELEASE RATES OF ^{129}I TO ATMOSPHERE. Bryant, Pamela M. (United Kingdom Atomic Energy Authority, Harwell, Eng.). Health Phys.; 19: 611-16(Nov 1970).

Working limits for continuous release rates of ^{129}I to atmosphere are derived by the specific activity method and, with appropriate modification, by the direct foliar contamination method used for ^{131}I involving the grass-cow-milk-infant critical pathway. Limitations of the methods are discussed. It is concluded that derived working limits calculated by the specific activity method are appropriate for design purposes in connection with planned continuous release rates of ^{129}I. As an illustrative example, the derived working limit is 270 mCi/day for a chimney of effective height 60 m, assumed to be the only source of ^{129}I in the area and situated at 400 to 500 m from the nearest pasture. In some environmental situations, e.g., near the sea, the derived working limit might be up to ten times greater than this due to a high average stable iodine (^{127}I) concentration in the atmosphere. (auth) (UK)

8682 DOSIMETRY OF PROTON RADIATION FIELDS IN SPACE WITH NUCLEAR EMULSIONS. Schaefer, H. J. (Naval Aerospace Medical Inst., Pensacola, Fla.); Sullivan, J. J.; Richmond, R. G. Health Phys.; 19: 663-70(Nov 1970).

The bulk of the astronauts' radiation exposure in space is due to trapped protons in the South Atlantic Anomaly or, on a deep space mission, in the radiation belt itself. The energy spectrum of the proton flux in both cases is a broad continuum from zero to several hundred MeV, with low energy protons and protons ending in tissue carrying a substantial fraction of the total dose. As demonstrated with the emulsion data of the Earth-orbital mission Apollo VII, a method using grain counting of tracks traversing the emulsion combined with a count of those ending in it (zero energy) provides sustained accuracy over the entire energy range. Within certain limits, the counts of ending protons at various locations in the space vehicle are proportional to the corresponding total doses. Highly structured directional patterns that are generally characteristic for the low energy particles were analyzed in detail from the unmanned Apollo VI mission during which a total proton dose of 1.56 rad was observed within the vehicle. The fact that low energy protons with their comparatively high LET contribute substantially to the total dose is reflected in large microdosimetric fluctuations of the absorbed energy in tissue, with Bragg peaks of ending tracks occurring only in a few percent of the total cell population even at dose levels of 50 to 100 rad. (auth) (UK)

8683 COMPUTER CALCULATION OF RADIATION ATTENUATION AROUND A MEDICAL CURIETRON-TYPE RADIOACTIVE PROBE. Costa, A.; Dutreix, Andree (Institut Gustave Roussy, Villejuif, France). J. Biol. Med. Nucl.; 5: No. 20, 22-6(May-Jun 1970). (In French).

The Curietherapy Service of the Gustave Roussy Institute uses an apparatus commercialized under the name Curietron, by the A.G.S. Company. This unit allows permanent storage of miniaturized ^{137}Cs sources and their automatic transfer by remote control in a radium holder. The design of the Curietron and the choice of ^{137}Cs comply with the IAEA rules on the safety and protection of hospital staff. A programme of dose calculation for a computer, in FORTRAN IV, was established to determine the form of the isodose around a rectilinear probe, taking into account the presence of metal bearings between the grains of ^{137}Cs. (France)

8684 COMPUTER DOSIMETRY OF THE RADIOIRIDIUM CASTINGS. Sinistrero, G.; Ragni, G.; Benedetto, A. (Turin Univ.). J. Radiol. Electrol., Med. Nucl.; 51: 399-402(Jun-Jul 1970). (In French).

The castings used were 0.5 and 1 cm thick and rectangular shaped; the isodoses were studied in two planes: a plane parallel to the longest side and a plane parallel to the shortest side. Percentage depth dose and isodose curves were calculated at quarter millimeter intervals; along each isodose curve values were calculated every millimeter. It appeared that under such conditions the superficial dose tended to be small. It was thus possible to use spheres of higher activities (between 2 and 3 miCi/sphere). The wires were first used for the castings and then for implantations when their activities had decreased. These castings were used to treat basal cell epitheliomas, which were not very thick but were very extensive (more than 4 cm in diameter), intermediate metaplastic epitheliomas, and also a few differentiated squamous cell epitheliomas located in regions with curved or irregular surfaces covering bony or cartilaginous planes (alae nasi, auricle, etc.). (France)

8685 DOSE AND LET DISTRIBUTIONS IN SMALL-ANIMAL SIZED CYLINDERS FOR A FISSION NEUTRON SPECTRUM. Willhoit, Donald G.; Jones, Troyce D. (Oak Ridge National Lab., Tenn.). Radiat. Res.; 44: 263-72(Nov 1970).

Monte Carlo sampling techniques were used to produce neutron histories in tissue geometries corresponding in size to the mouse, rat, and guinea pig. Dose and LET distributions were evaluated for 60,000 to 80,000 normally incident neutrons having an energy distribution corresponding to that of the Health Physics Research Reactor (HPRR) spectrum. For these geometries, 99% of the dose delivered by recoil nuclei was from elastic scattering with H, O, C, and N. The dose averaged over the volume of each animal was 94, 84, and 78% of kerma for tissue for free space (2.2×10^{-7} erg g^{-1} neutron^{-1} cm^2) for the mouse, rat, and guinea pig, respectively. For these geometries, unilateral exposure results in maximum to minimum dose ratios greater than 1.30, which according to the ICRU recommendations are classified as nonuniform irradiation condition. These data indicate that rotation of the animals in the field would result in a uniform (variation less than 15%) irradiation condition. The distribution of dose as a function of LET was not markedly dependent on depth in the animal geometries. The dose median LET was estimated to be about 50 keV/μ for these geometries for the HPRR neutron spectrum. (auth)

8686 GAMMA-RAY DOSE DISTRIBUTIONS IN EXTERNALLY IRRADIATED CYLINDERS. Hubbard, Lincoln B. (Oak Ridge National Lab., Tenn. Knoxville Coll., Tenn.). Radiat. Res.; 44: 4-12 (Oct 1970).

An approximate model was presented for the irradiation of uniform cylinders by external, broad-beam γ rays. In the model, the point doses for unilateral and bilateral irradiations were simple expressions of elementary functions. The range from maximum to minimum dose values was shown to be about half as great for bilateral irradiation as compared with unilateral irradiation. Thus, if the unilateral irradiation was considered nonuniform, then the bilateral irradiation was at best moderately uniform. The dose distributions for unilateral and bilateral irradiations have very different properties. These distributions were discussed, and their effects on experimental design were noted. The surface average, volume average, and midline dose were compared for these irradiations. (auth)

8687 TECHNIQUES FOR MEASURING GAMMA RADIOACTIVITY IN THE HUMAN BODY. Clemente, Gianfelice (CNEN, Rome). G. Fis. Sanit. Prot. Radiaz.; 12: 200-13(Jul-Sep 1968). (In Italian). (RT/PROT-(69)6).

All the principal geometries used for external scintillation detector measurements of γ activity in the human body were examined critically. For all geometries the principal advantages and disadvantages were analyzed as a function of the type of measurement made. Applications of partial-body and whole-body scanning and other external measurements for radiation protection programs and medical studies are considered. The best working conditions are outlined. (tr-auth)

Radiation Protection

Refer also to abstracts 8755, 8793, and 9540.

8688 (SZS-6/70) METHODS OF APPLICATION OF GAMMA EMITTERS IN CONTACT THERAPY WITH REGARD TO RADIATION PROTECTION. THE NEED FOR MEASURING THE RADIATION BURDEN OF THE BLADDER AND RECTUM WITH THE "GAMMAMETER" IN GYNECOLOGICAL CONTACT THERAPY TO AVOID RADIATION DAMAGE. METHODS OF APPLICATION OF GAMMA EMITTERS, ESPECIALLY RADIO-GOLD-SEEDS IN CONTACT THERAPY WITH SPECIAL REGARD TO RADIATION PROTECTION. THE SITUATION AND THE TREND OF CONTACT THERAPY IN THE TREATMENT OF GYNECOLOGIC CARCINOMAS. Moebius, W.; Glaser, F. H.; Dietze, R.; Grossmann, H. (Staatliches Zentrale fuer Strahlenschutz, Berlin (East Germany)). Mar 1970. 35p. (In German). Dep. NTIS (U. S. Sales Only).

Separate abstracts were prepared for the four sections of this report. (E.R.B.)

For abstracts of individual sections see: 8679, 8689, 8729, and 8730.

8689 (SZS-6/70, pp 19-27) METHODS OF APPLICATION OF GAMMA EMITTERS, ESPECIALLY RADIO-GOLD-SEEDS IN CONTACT THERAPY WITH SPECIAL REGARD TO RADIATION PROTECTION. Dietze, R. (Staatliche Zentrale fuer Strahlen-

XUM

schutz, Berlin (East Germany)). (In German). Dep. CFSTI (U. S. Sales Only).

The sphere of indication and the mode of application are outlined. The radiation protection measures are based on the principle of performing the preparation and the application in different rooms and the transport of radionuclides with a shielded car driven by a motor and manageable from each room. Furthermore, a special application table is used. Measurements have shown that the radiation burden of the gonads is tolerable for all persons concerned, and of the whole body and the hands is highest for assistants. (auth)

8690 PRACTICAL RADIATION. METHODS FOR PROTECTION AND THEIR FACTORS. Fitzgerald, Gordon M. ADM (Rev. Asoc. Dent. Mex.); 26: 567-72(Nov-Dec 1969). (In Spanish).

The precautions and procedures to be followed in radiation protection during the taking of radiographs by assistants of dentists and radiologists are outlined. The rationale for these procedures is discussed, and the obligation of the dentist and radiologist to fully inform his assistants of the radiation hazard is emphasized. (J.S.R.)

8691 RADIATION-PROTECTIVE CLOTHING. Scott, A. N. B. (Atomic Energy Research Establishment, Harwell, Eng.). Proc. Roy. Soc. Med.; 63: 1015-16(Oct 1970).

The hazards arising from the handling of radioactive materials fall into two main groups. There is the external hazard of penetrating radiation which can only be dealt with by the use of shielding, remote handling techniques, or by limiting the time of operation. The other group arises from the dangers of inhalation or ingestion of radioactive or toxic materials. Adequate protection can be given against this latter hazard by the provision of adequate protective clothing, and a suit designed within the United Kingdom Atomic Energy Authority for this purpose is described. This comprises a one-piece garment of two-ply laminated 0.012 in. (0.30 mm) translucent PVC with integral PVC feet over which short boots are worn. The helmet is of 0.020 in. (0.50 mm) PVC, the front two-thirds of which is transparent; it is welded to the neck of the suit. The dolman sleeves end in detachable, corrugated polythene wrist cuffs which serve as securing rings for a wide range of gloves. The entry, at the back of the suit, is closed by a lock-fold comprising two zip fasteners (inner and outer) and held in position by a splash guard secured at its lower edge with buttons which are themselves protected. Air is supplied via a single air-line and led by a duct to a perforated false-top air distributor in the headpiece; a plastic foam cartridge silencer is fitted in the duct. The air is distributed initially to the breathing zone and then circulated within the garment prior to removal from the suit extremities via four ducts which terminate in a manifold at the back of the suit; from the manifold, the air is exhausted from the suit through four outlets, all of which can take a variety of filters and two of which can take non-return valves as an alternative to filters. The ducts and the manifold are kept open by spacer material. The supporting belt for an air-line and outlet arrangements is of 0.065 in. (1.65 mm) polythene and is situated inside the suit and its weight is borne by a sleeve attached to the inner surface of the suit. The emergency breathing tube terminates in a filter at the back of the suit. Splash cuffs and guards are fitted to the sleeves and legs of the suit, to the filters, and to the valves. A sealed gland is fitted adjacent to the air-entry point to permit the entry of intercom wires if required. The weight of the suit is about 7.75 lb (3.5 kg). For hanging the suit, a moulded eyelet is welded on each shoulder. This suit is generally worn with a disposable PVC oversuit for ease of decontamination and the operator may require on occasion additional protective garments such as leaded or flameproof aprons. This means that he must be lightly clad within the suit if strenous work is to be performed. (auth)

Safety Procedures

Refer also to abstracts 10090, 10132, and 10160.

8692 (GAT-627) HEALTH AND SAFETY ACTIVITIES REPORT FOR 1969. (Goodyear Atomic Corp., Piketon, Ohio). 3 Sep 1970. Contract AT(33-2)-1. 48p. Dep. NTIS.

The health and safety activities at Goodyear Atomic Corporation are divided between two major specialized groups — the Medical Subdivision and the Safety Department. Some of the activities of these groups are peculiar to atomic energy gaseous diffusion operations; other activities are typical of those found in most large industrial organizations. This report covers the significant activities of the various groups and their resultant statistics compiled during 1969. It is the aim of the Medical Subdivision to maintain a program of continuing surveillance over possible health hazards, to cooperate in the elimination of such hazards, and to provide occupational medical services. Major functions of the Safety Department include: hazard control, inspections, and code application. More explicitly, functions performed by both health and safety groups include: medical examinations, fitting and repairing safety glasses, urinalyses, first aid and medical care, noise level surveys, equipment inspections, accident investigations, radiation control, and environmental testing. Many of these services are performed on a routine basis, while others are scheduled as needed. The success or failure of any health and safety program is measured by the degree to which undesirable incidents pertaining to health, property damage, and personal injuries are limited. The Goodyear program appears to be serving the best interests of Goodyear personnel, the neighboring communities, and the Atomic Energy Commission. (auth)

8693 (JAERI-5025) ACTIVITIES IN THE DIVISION OF HEALTH PHYSICS AND SAFETY, APRIL 1, 1969-MARCH 31, 1970. (Japan Atomic Energy Research Inst., Tokyo). Jun 1970. 111p. (In Japanese). Dep. NTIS (U. S. Sales Only).

Following a brief review of the various sections operating within the division, the routine monitoring and maintenance activities of the division are presented. These activities include; accident prevention measures, safety countermeasures, results of external and internal personnel monitoring, monitoring data for nuclear facilities, results of environmental monitoring, maintenance and calibration of monitors and surveymeters, and routine radioactive waste treatment and decontamination. In the area of radiation and operational safety techniques, divisional activities included; development of safety control systems, design and testing of new internal and external personnel monitoring instrumentation, operational testing of particle filters and failed-fuel detectors in nuclear facilities, design and improvement of environmental monitoring instruments; characterization of α particle and tritium monitoring instruments, and improved radioactive waste treatment and decontamination facilities. Research activities in the division included the following areas; radiation dosimetry, body radioactivity, aerosol technology, environmental radiation and contamination, and treatment of liquid radioactive waste. (E.R.B.)

8694 EVALUATING HEALTH HAZARDS FROM MILITARY LASERS. Sliney, David H. (Army Environmental Hygiene Agency, Edgewood Arsenal, Md.). J. Amer. Med. Ass.; 214: 1047-54 (9 Nov 1970).

Potential health hazards associated with the use of laser beams were evaluated. Several safety guidelines were prepared for laser radiation control based on the potential hazards to the retina of the eye during research, development, and testing of laser beam equipment. Safe exposure levels were estimated but are not to be considered as fine lines between safe and hazardous intensities. Location of personnel outside beam paths, protective eye wear, and communication between laser operators and personnel in the target area were effective for protection of personnel against laser radiation injuries. (E.E.H.)

8695 PROBLEMS OF CONTROL OF CONTAMINATED AIR IN A REACTOR FUEL ELEMENT FABRICATION PLANT. Cortissone, C. (CNEN, Saluggia, Italy); Ilari, O.; Lembo, G.; Prodi, V.; Melandri, C. G. Fis. Sanit. Prot. Radiaz.; 12: No. 2, 80-97(Apr-Jun 1968). (In Italian). (RT/PROT-(69)14).

The control of air contamination during normal and high risk plant operation was examined for the evaluation of the mean contamination level of the work area. The importance of the granulometry of aerosols is indicated, and the methods used for the measurement of air and surface contamination are described. The analysis of individual operations of correction of the pellets and extrusion for air contamination is described. The spatial and time studies of the general contamination of the environs are outlined. The results from the physical control, biological controls, and individual dosimeters are compared. (J.S.R.)

8696 INCIDENTS DURING RADIOISOTOPE TRANSPORT AND DOSES TO INDIVIDUALS. Com. Naz. Energ. Nucl., Notiz.; 16: No. 3, 69-71(Mar 1970). (In Italian).

The basic criteria on which the radiation levels established for individuals accidentally exposed during accidents involving the shipment of radioisotopes are reviewed. The criteria have international implications. A recent action of the CNEN seeking to establish rotating work periods for Italian health physicists in order to furnish technical assistance for incidents during transport, in cases of the lack of locally competent authority, is given as illustration of the international framework needed. (tr-auth)

Legal Aspects

Refer also to abstracts 8717 and 8824.

XUM

8697 AEC WORKMEN COMPENSATION STANDARDS. Eason, Charles F. (Atomic Energy Commission, Washington, D. C.). J. Occup. Med.; 12: 410-15(Oct 1970).

State workmen's compensation laws and rules of evidence in the USA are reviewed from the standpoint of compensation for injuries received during occupation exposure to ionizing radiations. It is pointed out that in 1970 there were an estimated 600,000 radiation workers, including those working with radium, x radiation, and other sources of ionizing radiation and that this number is expected to double by 1980. A review of 300 claims for radiation injury filed to date shows that 230 cases were decided on their merits and decisions favorable to the plaintiff occurred where there was proof or evidence of traumatic injury resulting from a single excessive exposure (awards made in 75% of cases); and in malpractice cases (awards made in 74% of cases). In one-third of the delayed injury cases no radiation records were introduced in evidence. The difficulties in establishing a causation or contributing relationship between radiation and injury in any individual case involving long-delayed effects are emphasized. It is pointed out that some 10 states require that claims for workmen's compensation must be filed within a relatively short period (6 mo. to one year) following injury and that 10 to 20 years or more can elapse before an injurious exposure to ionizing radiation may manifest itself. The AEC program for the compensation of radiation workers for injury is discussed and the status of Federal legislation covering workmen's compensation is reviewed. (C.H.)

8698 DEVELOPMENT OF UNIFORM STANDARDS FOR INTERNAL RADIATION PROTECTION. Com. Naz. Energ. Nucl., Notiz.; 16: No. 3, 72-3(Mar 1970). (In Italian).

The need for the development of uniform standards for internal radiation protection is discussed. The Italian standards for maximum permissible concentration (MPC) of radioisotopes in man are summarized and compared with international standards. (J.S.R.)

Medicine

Refer also to abstract 8574.

8699 POTENTIATION OF PRIMARY VIRUS INFECTION BY RADIOMIMETIC DRUGS. Robinson, T. W. E. Brit. J. Dermatol.; 82: 311-13(Mar 1970).

The clinical and experimental evidence for the potentiation of primary viral infections by immunosuppressive agents (i.e., x rays, cytostatic drugs, and steroids) was reviewed. Experimental evidence concerning the role of cyclophosphamide in the potentiation of encephalomyocarditis virus and Sendai virus infections in animals is discussed in detail. The role of interferon in viral infection and oncogenesis is also mentioned. (E.R.B.)

Protective Substances

Refer also to abstracts 8268, 8637, and 8786.

8700 BODY TEMPERATURE AS AN INDICATOR OF THE RADIOPROTECTIVE EFFECT OF SODIUM FLUOROACETATE IN MICE. Sikulova, J.; Novak, L. (Inst. of Biophysics, Brno). Int. J. Radiat. Biol.; 17: 587-90(1970).

Sodium fluoroacetate was given intraperitoneally in doses of 5 mg/kg live weight. Body temperature was measured with a thermistor in the rectum before injection, and then immediately before irradiation. Within 3 hours of injection, the temperature of individual animals had dropped by 3–10°C. (A body temperature of less than 25°C was not found.) The decrease was independent of its initial values and limited by the temperatures of the environment. Irradiation was with doses of 700–1000 R, (180 kV, 15 mA, 0.5 mm Al, 0.5 mm Cu, dose rate 43 R/min), and there was a significantly higher percentage of survival in animals which reached the lower limits of body temperature. (UK)

8701 STUDIES OF THE TOXICITY AND RADIOSENSITIZING ACTIVITY OF TRIACETONEAMINE-N-OXYL IN MICE. Hewitt, H. B.; Blake, E. R. (Mount Vernon Hosp., Eng.). Brit. J. Radiol.; 43: 91-6(Feb 1970).

Leukaemic CBA mice were injected intravenously with 6.8 mg of triacetoneamine-N-oxyl (TAN) three minutes before killing and exposure to single doses of x rays in the range 1,000 to 3,000 R. Immediately after exposure, leukaemia cells were extracted from the infiltrated livers of the mice and assayed for determination of the fraction of cells surviving. In controlled studies there was no evidence that pretreatment of the mice with TAN had increased the sensitivity of the leukaemia cells. Mice receiving repeated intraperitoneal sublethal doses of TAN displayed considerably increased tolerance of the drug when the interval between doses was 90 minutes or longer, indicating that the drug is excreted or destroyed at a moderately fast rate in vivo. The radiosensitizing capacity of TAN for anoxic bacteria was not measurably reduced after incubation of the drug for one hour with a dense suspension of metabolizing tumor cells. Erythrocytes were used to show that TAN passes through the cell membrane and that its sensitizing action on anoxic bacteria is not degraded in the presence of a high concentration of haemoglobin. (auth) (UK)

8702 PHOTOSENSITISING EFFECT OF 8-METHOXYPSORALEN ON THE INACTIVATION AND MUTATION OF ASPERGILLUS CONIDIA BY NEAR ULTRAVIOLET LIGHT. Alderson, T.; Scott, B. R. (Medical Research Council, Harwell, Eng.). Mutat. Res.; 9: 569-78(Jun 1970).

A methionine dependent ($meth_1$) strain of Aspergillus nidulans was used to study the inactivating and mutagenic effects of 8-methoxypsoralen (8-MOP) plus near uv light (NUV). The presence of the $meth_1$ locus allows reversion to methionine independence to be detected after forward mutation at any of several (at least 5) independent suppressor gene loci, and revertants can be divided by phenotype into 3 distinct classes corresponding to mutation at particular groups of suppressor loci. Treatments of conidia with either 8-MOP, NUV, visible light (VL), 8-MOP plus VL, or NUV followed by 8-MOP, show no inactivating or mutagenic effect, whereas a treatment with NUV in the presence of 8-MOP produces inactivation and mutation under similar conditions. The prior treatment of conidia with 8-MOP before exposure to NUV produces a more rapid inactivating effect, and a greater mutagenic effect, than a treatment with 8-MOP followed by immediate exposure to NUV, presumably because the prior treatment allows the 8-MOP to reach a higher initial concentration in the conidia before exposure to NUV. The results suggest that the optimum effect of 8-MOP is attained by about 5 min treatment with 8-MOP before exposure to NUV. The similar frequencies of mutation for the 3 $meth_1$ suppressor classes over varying times of exposure to 8-MOP and NUV indicate that the various suppressor loci are equally mutable by the treatment, in contrast to that found for spontaneous mutation, and for previously reported treatments with chemical mutagens. The frequency of $meth_1$ suppressor mutations induced by 8-MOP prior to NUV is about 12 times greater than a corresponding treatment with diethyl sulphate at approximately the same level of conidial survival. (auth)

8703 THE EFFECT OF SYNKAVIT ON THE TERATOGENIC ACTIVITY OF X RADIATION: A PRELIMINARY REPORT. Packer, A. D.; Fozzard, J. A. F.; Woollam, D. H. M. (Univ. of Cambridge, Eng.). Brit. J. Radiol.; 43: 36-9(Jan 1970).

Four groups of pregnant mice were treated on day 12 of gestation. Group A received intraperitoneal (IP) distilled water and 300 R, B received aqueous IP Synkavit (100 mg/kg) and 300 R, C received IP distilled water and sham irradiation, and D received IP Synkavit and sham irradiation. Foetuses were examined, mainly for limb anomalies, on day 20. Groups C and D showed no significant anomaly rate. Group B foetuses, when compared with Group A showed a significant increase in the complete absence of ossification of one or more long bones, fusion of long bones in forelimbs, haemorrhagic blebs present or hindfeet; no significant differences were found in anomalies of digits or metacarpals (-tarsals) in the forefeet or hindfeet in these two groups. The findings indicate that Synkavit has a potentiating effect on the teratogenic action of x radiation, at least in relation to certain skeletal anomalies. (auth) (UK)

8704 OXYGEN ENHANCEMENT RATIO FOR PROTRACTED IRRADIATION WITH ^{252}Cf. Fairchild, R. G.; Drew, R. M.; Atkins, H. L. (Brookhaven National Lab., Upton, N. Y.). Radiology; 96: 661-5(Sep 1970).

Oxygen enhancement ratios were measured for protracted irradiation of HeLa cells using ^{252}Cf neutron sources. Values of 1.3 were found, which are lower than those usually obtained for acute neutron irradiation. The poor survival of unirradiated anoxic control cells indicates the possibility that low values obtained under protracted irradiation may be a result of the combination of anoxia and irradiation. (C.H.)

8705 EFFECT OF 1-METHYL-3-NITRO-1-NITROSOGUANIDINE ON THE X-RAY-INDUCED CHROMOSOMAL LESIONS IN VICIA FABA. Kaul, B. L. (Regional Research Lab., Jammu, India). Naturwissenschaften; 57: 455-6(Sep 1970).

In the present experiment, nitrosoguanidine (NG) was given either immediately before or immediately following x irradiation to determine its effects on the restitution of chromosome breaks produced by the x rays. Secondary roots of Vicia faba grown in running tap water were used in the study. The data showed that when NG was given prior to irradiation, the yield of total abnormalities did not increase, but when NG was given immediately following irradiation the yield increased significantly. The in-

crease was mainly due to single-hit events like chromatid breaks, while there was actually a reduction in double-hit events. The ratio of single-hit to double-hit events rose from 2.7 to 4.3. Breaks, that would have been restored to the original shape and gone unnoticed or restituted in a different order to give translocations, remained as breaks, resulting in an increase in the number. It was concluded that the presence of NG during the post-irradiation recovery phase inhibits the recovery system of chromosomal lesions in the cell, probably by interfering with the synthesis and replication of DNA needed for restitution. This would lend support to the idea that a lesion in the chromosome may be a lesion in the DNA molecule that forms its backbone and for the repair of which, DNA synthesis is essential. (E.E.H.)

8706 RECOVERY FROM RADIATION INJURY WITH AND WITHOUT BONE MARROW TRANSPLANTATION: EFFECTS OF SPLENECTOMY. Smith, L. H.; McKinley, T. W. Jr. (Oak Ridge National Lab., Tenn.). Radiat. Res.; 44: 248-61(Oct 1970).

The importance of the spleen to recovery of lethally x-irradiated mice injected with syngeneic bone marrow was evaluated. When splenectomy was performed 2 days before irradiation, injection of marrow resulted in 30-day survival, which was the same as that of intact mice. However, when splenectomy was performed 2 or 3 days after exposure and marrow injection, survival was decreased, probably because the fraction of marrow committed to the spleen was removed. Results of ferrokinetic studies (^{59}Fe) showed that early regenerative erythropoiesis in lethally irradiated mice injected with marrow is reduced in animals splenectomized before irradiation, but only when the marrow cell dose is limiting. Even at a limiting cell dose, erythropoiesis is eventually restored to that of intact mice. Thus the spleen appears to contribute to early restitution of a hemopoietic compartment least critical to survival of the animal, and whatever contribution the spleen makes to survival is compensated by other tissues when the spleen is absent. Interpretation of splenic contribution to hemopoietic regeneration and survival is complicated by the fact that splenectomy performed 2 days before irradiation increases the $LD_{50/30}$ about 65 R. This kind of protective effect, however, is also manifested by uninephrectomy but not by partial hepatectomy or uniorchidectomy. The data shed no light on the basis for this kind of radioprotection. (auth)

8707 EFFECTS OF ACRIDINE ORANGE ON THE BIOLOGICAL ACTION OF GAMMA-RAY. Nishiwaki, Y.; Matsui, H.; Goto, H. (Tokyo Inst. of Tech.). Bull. Tokyo Inst. Technol. (Engl. Ed.); No. 96, 23-6(Mar 1970).

A series of experiments were performed to study the effects of acridine orange on the γ ray inactivation of transforming DNA (Bacillus subtilis, strain 168), coliphages (T3) and bacteria (Escherichia coli K12 Hfr H). Solutions of acridine orange at various levels of concentration were applied prior to irradiation. Irradiation was carried out with ^{137}Cs γ rays at a dose rate of approximately 40 Kr/hr. In the experiment with DNA, no effect was observed on the inactivation of the genetic capacity of the arginine marker when the concentration of solution was lower than 10 μg per ml of acridine orange. A protective action of the dye was noted at 20 μg per ml, and at 50 μg per ml the transforming processes were affected although the protective effect was still maintained. The presence of the dye proved to be effective in protecting the bacteriophage T3 of Escherichia coli K12 c600 from γ ray inactivation. No significant effect was observed in the inactivation of a bacterial strain, Escherichia coli K12 Hfr. H. (Japan)

Radiation Sickness and Injuries

8708 RADIOTHERAPEUTIC CARDIOMYOPATHY. PATHOGENIC MECHANISM BY AUTO-ANTIBODY. Giard, P.; Crinquette, J. (Hopital de la Charlite, Lille). Sem. Hop. Paris; 46: 923-8(20 Mar 1970). (In French).

A case showing the existence of post-radiotherapy myocardial disease is reported. A physiopathologic explanation is proposed in which immune processes might be produced, justifying the use of cortisone in treatment. The probably high frequency of pericarditis with effusion and coronary atheroma after radiotherapy is discussed. (CEA, France) (auth)

Radiodiagnosis

Refer also to abstracts 8494, 8496, 8497, 8500, and 8687.

8709 (DP-1229) DEUTERATION IN SLOW NEUTRON RADIOGRAPHY OF BIOLOGICAL MEDIA. Parks, P. B.; Reichard, S. M.; Brown, M. (Du Pont de Nemours (E.I.) and Co., Aiken, S. C. Savannah River Lab.). Jul 1970. Contract AT(07-2)-1. 21p. Dep. CFSTI.

Contrasts in slow neutron radiography of biological media can be improved by replacing hydrogen with deuterium in various tissues. Muscle and bone exposed to D_2O readily exchange hydrogen for deuterium. If fully deuterated, their linear attenuation coefficients are reduced from approximately 3.4 and 2.3 cm^{-1} to 0.5 and 0.5 cm^{-1}, respectively. Fatty tissues, however, have little tendency to deuterate, and the linear attenuation coefficients remain approximately 3.5 cm^{-1}. Slow neutron radiographs of deuterated-biological specimens show the fat distribution with contrasts exceeding those of conventional roentgenography. Calculations show that with a 50 to 70% hydrogen-deuterium exchange, slow neutron radiography of specimens as thick as the adult human arm or leg could be done without excessive radiation dose. However, clinical application of this technique cannot be recommended at this time because of the toxic effects of D_2O. (auth)

8710 (NP-18560) ISOTOPE ENCEPHALOGRAPHY. DIAGNOSIS OF INTRACRANIAL FOCAL LESIONS WITH THE AID OF RADIOACTIVE SUBSTANCES. Van Eck, J. H. M. (Groningen Rijksuniversiteit (Netherlands)). 1968. 262p. (In Dutch). Dep. NTIS (U. S. Sales Only).

The history of the development of radioisotope scanning techniques for the differential diagnosis of brain lesions is reviewed. The labeled compounds and counting techniques that have been employed are evaluated and results obtained are compared with results obtained using electroencephalography. Results of brain scans using ^{131}I-labeled human serum albumin, ^{203}Hg-neohydrin, or ^{99m}Tc-pertechnetate in a series of 750 patients are reviewed and evaluated. Brief case histories are included for 46 patients to illustrate the value of radioisotope scanning in the solution of diagnostic problems. It is concluded that the technique should be carried out by a team of investigators and the results interpreted in conjunction with the clinical history, a careful neurological examination, and results of other ancillary examinations. (575 references) (C.H.)

8711 (NYO-3937-2) POSITRON SCANNING WITH COMPUTER INTERFACE. Technical Progress Report, January 1-October 31, 1970. (Massachusetts General Hospital, Boston). 10 Nov 1970. Contract AT(30-1)-3937. 20p. Dep. NTIS.

The development of techniques and equipment for use in studies of pulmonary physiology and blood flow in other organs using positron cameras for scanning the short-lived cyclotron-produced radioisotopes ^{11}C, ^{13}N, and ^{15}O is reported. Emphasis was placed on the use of ^{15}O in the form of O_2, CO, and CO_2. A positron camera using two detector banks, each containing 127 crystals and 72 photomultiplier tubes, was developed for obtaining rapid sequential images. A computer data analysis system was developed for use with a hybrid scanner for brain tumor localization. The cyclotron production of ^{15}O by the ^{14}N(d,n)^{15}O reaction, ^{13}N by the ^{12}C(d,n)^{13}N reaction, and ^{11}C by the ^{10}B(d,n)^{11}C reaction is reported. Methods for the incorporation of ^{15}O in CO_2, CO, H_2O, and erythrocytes are described. (C.H.)

8712 (ORNL-TM-2091(Suppl.1)) ^{99m}Tc IN MEDICINE: A SUPPLEMENTARY BIBLIOGRAPHY. Stemple, Ruth M. (comp.) (Oak Ridge National Lab., Tenn.). Oct 1970. Contract W-7405-eng-26. 25p. Dep. NTIS.

A list is presented of approximately 450 references to recent publications on uses of metastable ^{99}Tc for scanning various organs for the diagnosis of various disease conditions. (C.H.)

8713 (UCLA-12-798) EFFECTS OF CORONARY ARTERIAL INJECTION OF RADIOALBUMIN MACROAGGREGATES ON CORONARY HEMODYNAMICS AND MYOCARDIAL FUNCTION. Poe, Norman D. (California Univ., Los Angeles. Lab. of Nuclear Medicine and Radiation Biology). [1970]. Contract AT(04-1)-Gen-12. 41p. Dep. NTIS.

The effects of intracoronary arterial injections of ^{131}I-labeled albumin macroaggregates on coronary hemodynamics and myocardial function were studied in normal, anesthetized dogs to evaluate the possible use of scanning for determination of regional myocardial blood flow. Slow injections of macroaggregates containing less than 0.05 mg albumin with no particles greater than 60 to 70 microns in maximum diameter can usually be given directly into the left anterior descending coronary artery with no significant changes in coronary flow, myocardial contractility, arterial pressure or the electrocardiogram. As the mass of albumin and/or particle size are progressively increased, a sequence of functional changes evolves. Coronary flow is reduced followed immediately by transient hyperemia. Contractility falls. Only after marked flow and contractile changes have been produced do abnormalities in arterial pressure and the EKG develop. The course of events is similar to that resulting from progressive coronary arterial occlusion. It is concluded that carefully pre-

XUM

pared radioactive particles, in amounts sufficient for external scintillation scanning, can be injected into the coronary arteries without detectable alterations in function, and that the technique is suitable for acute and chronic determinations of regional myocardial perfusion both experimentally and clinically. The functional effects in the presence of coronary or myocardial disease are yet to be determined. (auth)

8714 PLACE OF CEREBRAL GAMMAGRAPHY IN THE DIAGNOSIS OF CEREBRAL ABSCESS. Akerman, M. (Hopital Foch, Suresnes, France); Langie, St. Ann. Radiol.; 12: R915-27(1969). (In French).

The value of cerebral gammagraphy in the diagnosis of cerebral abscess is discussed. In 19 cases of abscess explored surgically, the expanding lesion was accurately localized. In three instances, gammagraphy demonstrated multiple lesions. Repeated investigation in some cases led to the detection of abscess during the course of meningo-encephalitis. The importance of repeat examinations when there is suspicion of cerebral abscess is stressed, particularly in children with congenital heart disease. False positive results may occur in cases of osteomyelitis or following surgery on the inner ear. The extra-cerebral nature of these lesions is recognized by their particular localization. A diagnosis of abscess is not possible on gammagraphic findings alone. Certain features of the scan together with the clinical findings may support the diagnosis of an abscess. (auth)

8715 BIPHASIC SCAN IN CIRRHOTIC LIVER DISTURBANCES BASED ON VARIOUS PHYSIOLOGICAL PRINCIPALS. Locher, J. Th.; Elke, M. (Univ., Basel). Schweiz. Med. Wochensch.; 100: 1599-1603(19 Sep 1970). (In German).

A two-step scan is described for use in advanced cirrhosis of the liver, in which routine scans may prove ineffectual. The chief reasons for inaccuracy of the routine scan are low local blood flow and insufficiency of the reticuloendothelial system. Since increased dosage of the same radiocolloid does not improve diagnostic potential, a change in the physiologic principle of the scanning method is suggested. Instead of the ^{131}I-labeled Rose-Bengal usually administered it is proposed that in these cases ^{75}Se-selenomethionine should be used that is quickly absorbed by the polygonal liver cells. It does however remain longer in the cells, as it is an amino acid. Reasonably good scanning is possible by this method even in cases of severely damaged liver function. The two cases reported show that even in emergency situations this technique permits rapid and safe evaluation of upper abdominal masses. Moreover, a more dynamic understanding of the lesions is possible by the use of two- or multi-step scanning involving several different radiopharmaceuticals. Additional evidence of functional failure of a single cell-system is a better diagnostic result than the mere description of local defects of colloid phagocytosis. (auth)

8716 DEVELOPMENT AND APPLICATIONS OF QUANTITATIVE AND COMPUTER-ANALYZED COUNTING AND SCANNING. Laughlin, J. S.; Ritter, F. W.; Dwyer, A. J.; Mayer, K.; Greenberg, E. J.; Dimich, A. B.; Hasan, S.; Rothschild, E.; Myers, W. P. L. (Sloan-Kettering Inst. for Cancer Research, New York. Memorial Hospital for Cancer and Allied Diseases, New York). Contracts AT(30-1)-910; NCI-CA-08748. Cancer; 25: 395-405 (Feb 1970).

The development of a system of quantitative and computer-analyzed counting and scanning is described and applied to both metabolic nuclide studies as well as to diagnosis. The evolution to this quantitative method was from earlier and similar procedures developed for the description and analysis of radiation dose distribution. A variety of advantages associated with this approach is enumerated and examples are given for different body functions. (auth)

8717 USE OF RADIOISOTOPES IN HUMAN EXPERIMENTATION. Stanbury, John B. (Massachusetts Inst. of Tech., Cambridge). J. Nucl. Med.; 11: 586-91(Oct 1970).

Radiation protection committees charged with setting safety standards for the use of radioisotopes in human experimentation have had the difficult task of balancing the needs of investigators against the conjectural risks of radiation injuries. The biological effects of ionizing radiations are reviewed briefly and the genetic risks and risks from radioinduced leukemia or thyroid neoplasms as a function of radiation dose are discussed. It is concluded that there is no reason for apprehension about either genetic or somatic effects following exposure of man to the few rads of whole-body radiation resulting from the diagnostic use of radioisotopes, with the exception of the first few years of life or the pregnant female. Proposed guidelines for the use of radioisotopes in clinical studies on man are presented. (55 references.) (C.H.)

8718 RADIONUCLIDE ANGIOGRAM AND SCAN FINDINGS IN A CASE OF HERPES SIMPLEX ENCEPHALITIS. Mishkin, Fred S. (Indiana Univ., Indianapolis). J. Nucl. Med.; 11: 608-9 (Oct 1970).

A frequent cause of encephalitis in man, herpesvirus hominis, often proves fatal. However, prompt institution of a course of the antimetabolite, idoxuridine, appears promising so that establishing the diagnosis early assumes new importance. Since the scan is often used as a screening procedure in disorders of the brain, knowledge of the effects of herpesvirus encephalitis on the appearance of the brain scan may aid in prompt diagnosis. The case history and ^{99m}Tc-pertechnetate finding are reported for one case. The findings on the routine brain scan clearly demonstrated the localized site of involvement confined to the temporal lobe. This correlates nicely with the known pathologic feature of preferential involvement of the temporal lobes by herpesvirus hominis. It was concluded that these findings on the brain scan and the increased vascularity in the abnormal area indicated by radionuclide angiography, when correlated with the clinical findings of encephalitis, should lead one to strongly consider herpesvirus hominis as the offending agent. (C.H.)

8719 MULTIPLE ECHINOCOCCUS GRANULOSUS CYSTS OF LIVER. Reifsnyder, David N. N. Y. State J. Med.; 70: 2722-5 (1 Nov 1970).

A patient was presented who harbored five primary Echinococcus granulosus cysts of the liver. Four of the cysts were calcified, another was noncalcified and was detected preoperatively using radioactive gold scanning. The Echinococcus skin test and indirect hemagglutination titer for Echinococcus showed positive findings. The not infrequent occurrence of multiple Echinococcus granulosus cysts of the liver was emphasized, and the usefulness of radioisotopic scanning of the liver in detecting noncalcified cysts was underscored. (auth)

8720 DIAGNOSTIC USE OF ^{85}Sr IN THE PREOPERATIVE EVALUATION OF NON-UNION. Segmueller, G.; Cech, O.; Bekier, A. (Kantonsspital, St. Gallen, Switzerland). Acta Orthop. Scand.; 41: 150-60(1970).

A clinical investigation was conducted on the use of ^{85}Sr for preoperative evaluation of non-union in bone fractures. In different types of non-union, remarkable differences in ^{85}Sr uptake were recorded, demonstrating the range of differences in tracer uptake at the fracture site. It was concluded that external ^{85}Sr counting techniques were a valuable parameter in the preoperative evaluation of the functional state of pseudarthrosis. By means of early photoscanning and/or early external counting techniques as well as late external counting of ^{85}Sr with the aid of a scintillation detector, a parameter of local mineral metabolism for the evaluation of local osteogenetic capacity of non-union of long bones was obtained. (E.E.H.)

8721 LUNG SCINTIPHOTOGRAPHY WITH ^{113m}In $Fe(OH)_3$ AGGREGATES. Tori, G.; Cabassa, N.; Marabini, A.; Franchi, R. (Bologna Univ. City Hospital, Verona, Italy). Radiol. Clin. Biol.; 39: 476-84(1970).

The ready availability of short-lived radionuclides for clinical use and the development of the Anger-type scintillation camera have improved even more the lung scanning procedure. Lung scintiphotos were performed with the MAA–^{131}I or with ^{99m}Tc albumin macroaggregates. It is the purpose of this report to present our experience of lung scintiphotography using as radioactive agent the ^{113m}In-tagged iron hydroxide. (auth)

8722 CLINICAL VALUE OF LIVER FUNCTION APPRAISAL BY MEANS OF ^{131}I-ROSE BENGAL. III. COMPARISON OF THE RESULTS OF ^{131}I-ROSE BENGAL TEST AND BSP TEST. Dobrzanski, Z.; Toth, Z. (Postgraduate Medical Training Inst., Warsaw). Pol. Med. J.; 9: 599-603(1970).

A comparison was made of the results of the ^{131}I-rose bengal test versus the bromosulphtalein test, in 100 subjects, including ten healthy persons and 90 patients with various liver diseases. The results of both tests were found to be markedly consistent. The half-time of ^{131}I-rose bengal excretion by the liver was proved to be the most sensitive index of hepatic parenchymal injury. The half-time of blood clearance of ^{131}I-rose bengal and the BSP test came next. The ^{131}I-rose bengal test is superior to the BSP test because of its simpler technique and practicability even in severe hyperbilirubinemia. (auth)

8723 ^{99m}Tc SCANNING OF THE STOMACH. Mikolajkow, A. (Postgraduate Medical Education Center, Warsaw). Pol. Med. J.; 9: 559-65(1970).

After intravenous injection, ^{99m}Tc was accumulated in the cells of the gastric mucosa and then it was secreted with gastric juice. Owing to the favorable physical properties of ^{99m}Tc, satisfactory gastric scans were obtained. Gastric cancers appeared as areas

of lower density on scans, while inflammatory lesions or ulcers were not visualized by this technique. The method of preparation of ^{99m}Tc and scanning was described. The results of several gastric scans were presented. The effects of various factors on the scan and the information provided by this method were discussed. (auth)

8724 PLASMATIC CONCENTRATIONS OF TRITIATED DESACETYL-LANATOSIDE C AFTER INTRAVENOUS AND INTRAMUSCULAR INJECTIONS IN CARDIOPATHIC SUBJECTS. Foresti, A.; Damascelli, B.; Formentini, A.; Riva, D. (Univ., Milan). Atti Soc. Ital. Cardiol.; 2: 211-13(1968). (In Italian).

The plasma concentrations of tritiated desacetyl-lanatoside C after intravenous and intramuscular injection in cardiopathic patients were determined. The amount of the drug in the blood at various times after injection is reported and compared with similar curves obtained from the injection of the drug into healthy persons. The shape of the curves with intravenous injection is similar for healthy persons and cardiopathic patients, but the retention is higher in the cardiopathic patient. Intramuscular injection produces a completely different type of curve. The reasons for this difference are discussed. (J.S.R.)

8725 DIGITAL COMPUTER DATA ACQUISITION, DISPLAY, AND ANALYSIS SYSTEM FOR THE GAMMA CAMERA. Bruno, Fred P.; Brookeman, Valerie A.; Williams, Clyde M. (Veterans Administration Hospital, Gainesville, Fla. Univ. of Florida, Gainesville). Radiology; 96: 658-61(Sep 1970).

A digital computer data acquisition, display, and analysis system for use with a scintillation camera is described. The system makes possible quantitative analysis of a scan image now represented by a 50 × 50 matrix. The low cost of the small general-purpose computer employed in this system makes it a practical consideration for the average nuclear medicine laboratory. (auth)

8726 GAMMA-RAY SPECTROMETRIC METHOD USING A LITHIUM-DRIFTED SILICON DETECTOR TO DETERMINE THE ANTIMONY DEPOSITS IN THE LUNG IN VIVO. Bloch, Peter (Univ. of Pennsylvania, Philadelphia). Radiology; 96: 657-8 (Sep 1970).

The quantity of antimony present in antimony pneumoconiosis may be determined using γ-ray spectrophotometry by measuring the fractional transmission of ^{125}I photons of two different energies through the lung, one being slightly less and the other slightly greater than the K-shell binding energy of antimony. (auth)

8727 COMPUTER PROCESSING OF IMAGES IN NUCLEAR MEDICINE. Kuhl, David E. (Univ. of Pennsylvania, Philadelphia). Nucl. News; 13: 47-8(Dec 1970).

The development and use of the Mark III scanner, a self-sufficient unit for multiple view and section scanning of the brain, are discussed. The scanner has four detectors that view different aspects of the brain simultaneously. A small self-contained computer controls display, processing, and all automatic operations. The instrument is also capable, at the discretion of the physician, of transverse sectional scanning i.e., production of a cross-section picture. The main advantages of the Mark III scanning system are: minimum options in technician operation to assure simplicity and reliability; and maximum options for physician option to assure completeness of examination. (E.R.B.)

Radiotherapy

Refer also to abstracts 8309, 8487, 8679, 8683, 8684, 8688, 8689, 8759, 8791, and 8792.

8728 (STI/PUB-251) DIRECTORY OF HIGH-ENERGY RADIOTHERAPY CENTRES. 1970 Edition. (International Atomic Energy Agency, Vienna (Austria)). 1970. 235p. IAEA $5.00.

A list is presented of 1670 high-energy radiotherapy installations in use throughout the world during 1970. Data are included on the type of installation, therapist, physicist, and other pertinent information. (C.H.)

8729 (SZS-6/70, pp 1-8) METHODS OF APPLICATION OF GAMMA EMITTERS IN CONTACT THERAPY WITH REGARD TO RADIATION PROTECTION. Moebius, W. (Staatliche Zentrale fuer Strahlenschutz, Berlin (East Germany)). (In German). Dep. CFSTI (U. S. Sales Only).

The important role of intracavitary therapy in the treatment of female genital carcinomas is pointed out. It is necessary to make an isodose atlas and to know the peritherapeutic radiation burden of the patient and the medical personnel. The most appropriate form of therapy is the use of radium cells welded into standard containers and avoiding inflexible systems such as a colpostat. Thus, constant radiation intensity, safe use, and minimum radiation burden of all persons concerned are attained. (auth)

8730 (SZS-6/70, pp 28-35) THE SITUATION AND THE TREND OF CONTACT THERAPY IN THE TREATMENT OF GYNECOLOGIC CARCINOMAS. Grossmann, H. (Staatliche Zentrale fuer Strahlenschutz, Berlin (East Germany)). (In German). Dep. CFSTI (U. S. Sales Only).

For some female genital carcinomas, intracavitary therapy is not replaceable by another form of therapy. Therefore the equipment of installations performing intracavitary treatments should be at an optimum, particularly as this is not very expensive. It is recommended to replace radium by ^{137}Cs in ready-made applicators and to use ^{60}Co only when there are special demands on dose rate and dimension, respectively. The development of applicators showing heavily deformed isodose curves is demanded. (auth)

8731 RADIOACTIVE SCLERAL SHELLS IN THE TREATMENT OF CONJUNCTIVAL TUMORS. Miller, David; Carroll, John M.; Holmberg, Adolph; Schulz, Milford D.; Wipfelder, Rosemarie (Massachusetts General Hospital, Boston). Amer. J. Ophthalmol.; 70: 783-6(Nov 1970).

A technique for uniformly irradiating superficial conjunctival neoplasms using individually constructed ^{32}P applicators is described. These applicators are essentially lead scleral shells, onto which are placed a beta radiation emitting source, which appose the area of tumor. Such an applicator attacks the area of tumor, yet protects the normal portions of the globe from irradiation. Two cases of conjunctival tumors treated in such a manner are described. (auth)

8732 VARIOUS RADIOBIOLOGICAL CONSIDERATIONS ON THERAPEUTIC CASTRATION OF WOMEN. Marin Gorriz, D. Francisco. An. Real Acad. Nac. Med. (Madrid); 85: 51-89(1968). (In Spanish).

The results of the x-ray sterilization of 185 women for metropathia hemorrhagica, myoma, endometriosis, and nipple neoplasia were reported from a radiobiological viewpoint. In all cases of nipple neoplasia the ovaries were removed two years after the sterilization to eliminate a possible estrogen activity of the ovary, to detect the metastasis to the ovary of the mammary neoplasia, and to eliminate the possible carcinogenic effects on the ovaries as a result of the irradiation. Microscopic studies of the ovaries revealed that all were normal and therefore conclusions could be made of the effects of radiation on the normal ovary. The procedure used was outlined. The radioinduced sterilization produced no case of cancer in 26 patients. It is possible that the appearance of ovarian cancer is caused by a hypophysic effect to suppress the ovarian function. The administration of corticoids and androgen inhibits the symptoms of the menopause. The average dose capable of producing definitive sterilization was 872.5 rad/ovary in patients up to thirty years; 719.2 rad in patients between thirty and forty; and 451.8 rad for those from forty to sixty years of age. (J.S.R.)

8733 ASSESSMENT AND TREATMENT OF ENDOCRINE EXOPHTHALMOS. Cant. J. Stanley (Univ. of Glasgow). Proc. Roy. Soc. Med.; 63: 783-6(Aug 1970).

It was shown that intraorbital injections of triamcinolone acetonide produced a significant improvement in the symptoms and signs of chronic dysthyroid orbital infiltration in man. It was also shown that total thyroid ablation with ^{131}I had no effect on established exophthalmos. (F.M.M.)

8734 PHYSICAL AND DOSIMETRIC ASPECTS OF THE RADIOTHERAPY OF MALIGNANT LYMPHOMAS. II. THE INVERTED-Y TECHNIQUE. Page, Vera; Gardner, Angela; Karzmark, C. J. (Stanford Univ., Calif.). Radiology; 96: 619-26(Sep 1970).

The routine dosimetry and field-shaping methods in use at the Stanford University Medical Center for the treatment of lymphoma patients with the inverted-Y technique using 6-MeV x rays are described and discussed. Gonad and kidney doses, field-matching, and penumbra were investigated to find optimum conditions for treatment. (auth)

8735 PHYSICAL AND DOSIMETRIC ASPECTS OF THE RADIOTHERAPY OF MALIGNANT LYMPHOMAS. I. THE MANTLE TECHNIQUE. Page, Vera; Gardner, Angela; Karzmark, C. J. (Stanford Univ., Calif.). Radiology; 96: 609-18(Sep 1970).

In routine dosimetry and lung-shielding systems for treatment of lymphoma patients with the mantle technique, the dosimetry of 6-MeV x rays is dependent on use of tabulated factors and is based on physical measurements of source-skin distance values and patient thicknesses at five anatomical sites. No calculations are required for individual patients. The method is efficient and rapid

XUM

and yields acceptable uniformity of dose. Less staff time is involved than for more complex dosimetry systems or for the fabrication of individual compensating filters. The skin and shielded lung doses received by the patients were also investigated, and possible improvements are discussed. (auth)

8736 AFTERLOADING VAGINAL IRRADIATORS. Delclos, Luis; Fletcher, Gilbert H.; Suit, Herman D.; Sampiere, Vincent; Moore, Bailey (Univ. of Texas, Houston). Radiology; 96: 666-7(Sep 1970).

A set of vaginal cylinders of variable diameter (2 to 5 cm) and of adaptable length were constructed for use during ^{226}Ra implant therapy of cancers of the uterus. With these almost any vagina may be fitted at the time of surgery, and exposure to personnel is eliminated. Lead may be incorporated in the cylinders to partially shield either the vagina or the rectum. (C.H.)

8737 TECHNIQUE FOR AFTERLOADING IMPLANTS USING RADIOACTIVE IRIDIUM WIRE [SUMMARY]. Gambel, D. (Essex County Hospital, Colchester, Eng.). Proc. Roy. Soc. Med.; 63: 1034(Oct 1970).

The advantages of ^{192}Ir for γ implant therapy include the fact that it can be loaded into narrow plastic tubing, it is obtainable in wire of various diameters, it can be shaped and used unsupported in tissues such as the bladder or tongue, and it can be obtained in a wide range of specific activities to suit many different applications. The only real disadvantage is its short half-life of 74 days. A procedure is described for the afterloading plastic tubing implants with ^{192}Ir wire. (C.H.)

8738 USE OF HIGH ACTIVITY ^{60}Co SOURCES FOR INTRACAVITY AND SURFACE MOLD THERAPY. Joslin, C. A. F.; Smith, C. W. (Velindre Hospital, Whitchurch, Wales). Proc. Roy. Soc. Med.; 63: 1029-34(Oct 1970).

The use of low activity radium and other radioactive isotopes for the treatment of uterine and superficial skin cancer is associated with problems of radiation protection. The recent introduction of high activity ^{60}Co sources has enabled treatment times to be reduced to minutes. In this procedure the sources must be afterloaded into the treatment applicator by remote control. It also becomes necessary to carry out treatment within a radiation-protected room. The radiation exposure dose received by staff can be greatly reduced by these methods. The clinical advantages of this form of therapy include: a reduction of treatment time from days or hours to minutes; fractionation of the dose on a daily basis; combined external beam therapy may be given; and the treatment may be extended over several weeks, depending upon tissue response. (C.H.)

8739 SOME COMPLICATIONS IN HIGH ENERGY THERAPY. Rodriguez de Quesada, Blas; Rodriguez de Quesada, Angel. Acta Iber. Radiol.-Cancerol.; 23: 23-8(Jan-Mar 1968). (In Spanish).

High energy therapy places more stringent requirements on the knowledge of the isodose and the exact distribution and control of the dose administered, as more serious problems and complications can arise than in low energy therapy. The cutaneous tolerance to high energy therapy is advantageous, but delayed reactions in the interstitial tissue, which play an important role in the progressive resorption of the tumor and in the regeneration of the destroyed tissue, must be considered. The site of the interstitial tissue damage can affect the decision on the advisability of the use of high energy therapy. The injuries caused to the digestive tract are discussed. The advantages of high energy therapy, in spite of these and other complications, are emphasized. The special problems presented by cardiac patients are considered. (J.S.R.)

8740 CONFORMATION THERAPY TECHNIQUE ON 6 MeV LINEAR ACCELERATOR IN THE TREATMENT OF THE CARCINOMA OF THE CERVIX UTERI. CLINICAL APPLICATION. Kitagawa, Toshio; Mori, Tomoyuki; Yamashita, Nobuo; Kakehi, Masae; Chihara, Tsutomu (Aichi Cancer Center, Nagoya, Japan). Gan No Rinsho; 15: 1052-5(Dec 1969). (In Japanese).

In order to reexamine the value of external irradiation for Stage II and III uterine cervical carcinoma cases (squamous cell carcinoma), examinations were made on 114 cases handled during the past 3 yr (1967 to 1970) at the Aichi Cancer Center Hospital. Selective irradiation with Lineac (linear accelerator) was given to 54 cases and results of treatment were compared with cases given counter dual irradiation with cobalt γ rays and Lineac. Dose to primary focus differed with each case but the total irradiation dose was in the range of 6000 to 7500 rads. Clinical observations were made on the following changes during 18 mos from the end of irradiation: systemic condition, local changes, metastasis, variation of biochemical serum test values, diarrhea during and after irradiation, tissue necrosis, and bladder damage. The survival rate 18 mos following irradiation was 55% in the group given counter dual irradiation with cobalt γ rays (A), 75% in that of counter dual irradiation with Lineac (B), and 87% in that given selective irradiation with Lineac (C). The cases found with remaining focus in the primary tumor after external irradiation and which required irradiation of the pelvic cavity with radium were 40% in A, 25% in B, and 24% in C. Diarrhea during irradiation was thought to be inevitable in the irradiation of the whole pelvic cavity but it was believed that this diarrhea was due to the irradiation of the colon. By shielding the colon from the irradiation field, diarrhea cases were reduced to 89% in A, 80% in B, and 29.6% in C. (Japan)

Blast and Thermal Effects

8741 (ABCC-TR-0-69) BIBLIOGRAPHY OF PUBLISHED PAPERS OF THE ATOMIC BOMB CASUALTY COMMISSION. (Atomic Bomb Casualty Commission, Hiroshima, Nagasaki (Japan)). 1969. Contract AT(30-1)-72. 7p. (In English and Japanese). Dep. NTIS.

A list of 48 papers published during 1969 that discuss the medical status of atomic bomb survivors of Hiroshima and Nagasaki and their offspring is presented. Emphasis is placed on cytogenetic studies on survivors and their offspring and the occurrence of malignant neoplasms and leukemia in survivors. (C.H.)

Radiation Effects on Animals

Refer also to abstracts 8605, 8632, and 8638.

8742 APPLICATION OF INFORMATION THEORY TO THE STUDY OF THE STIMULATING EFFECTS OF IONIZING RADIATION, THERMAL ENERGY, AND OTHER ENVIRONMENTAL FACTORS: PRELIMINARY IDEAS FOR A THEORY OF ORGANIZATION. Atlan, Henri (Ames Research Center, Moffet Field, Calif.). J. Theor. Biol., 21: 45-70(Oct 1968).

The stimulating effects of low doses of ionizing radiation or of factors of the normal environment that are detrimental at high levels were compared with the stimulating effects of thermal energy and of the passage of time. In attempts to extend the information theory of Yockey to the domain of low doses of ionizing radiation and other physical agents, and to account also for their stimulating effect, an organization theory was proposed that explains the existence of optimum doses of environmental factors, all of which may be summarized in the existence of an optimum age, following an ascendant phase (development), and preceding a descending phase (aging). This goal is achieved without recourse to any features other than the way in which such an organization must react to external factors. In turn, these factors always remain the same, e.g., generators of noise and errors. The ensuing need for a change of alphabet, with an increase in the number of letters, and the relation to such a change actually observed in all living organisms, were viewed as interesting experimental arguments in favor of the validity of this theory. (BBB)

8743 AUTORADIOGRAPHIC INVESTIGATION OF THE DURATION OF THE MITOTIC CYCLE IN THE NORMAL AND IRRADIATED CELLS OF THE HUMAN DIPLOID STRAIN WI-38. Gibadulin, R. A.; Kuznetsova, L. V.; Chervonskaya, N. V. (Moscow Research Inst. of Virus Preparations). Byull. Eksp. Biol. Med.; 59: No. 4, 100-3(Apr 1970). (In Russian).

Radioautography and the method of labeled mitosis curve was used to investigate the duration of the mitotic cycle in the normal and irradiated cells of the human diploid strain WI-38. It is shown that in these cells the mitotic cycle lasts 22 hrs with the duration of the postsynthetic period (G_2) being equal to 5 to 7 hrs, the period of DNA synthesis (S), 8½ hrs, and the presynthetic period (G_1), 6½ to 8½ hrs. X-irradiation at a dose of 50 R results in prolongation of the mitotic cycle in irradiated cells to 39 to 46 hrs at the cost of prolongation of all interphase periods. This involves a more than double prolongation of the G_1 period (up to 16 to 25 hrs). The period of DNA synthesis increases to 14 hrs and the g_2 period, to 7 to 9 hrs. (auth)

8744 PARTIAL CELL IRRADIATION BY ULTRAVIOLET AND VISIBLE LIGHT: CONVENTIONAL AND LASER SOURCES. Moreno, Giuliana; Lutz, Marc; Bessis, Marcel (Hopital de Bicetre, Kremlin-Bicetre, France). Int. Rev. Exp. Pathol., 7: 99-137(1969).

The following aspects of the effects of localized irradiation of cellular structures with microbeams of uv and visible photons, including laser microbeams, are reviewed. The following topics are included: general aspects of nonionizing microirradiation, instrumentation, and techniques of microirradiation (uv dosimetry, flux measurements at the target area, laser instrumentation, and preparation of biological specimens for microirradia-

tion); techniques for evaluation of micropuncture effects (light and electron microscope studies); morphological effects following microirradiation of cell organelles; biochemical behavior of cells after microirradiation (synthesis of nucleic acids, proteins, and enzymes); use of microirradiation in the study of cellular functions (embryogenesis, regeneration phenomena in unicellular organisms, cell division, and muscular contraction); and studies in molecular arrangement (DNA in chromosomes of living cells). Photodestruction or photoalteration of cellular structures can be induced by numerous simultaneous mechanisms. The two principal mechanisms are photochemical action [primary (photolysis) or secondary (photoactivation followed by chemical reactions of activated molecules). This action may be predominant with sufficiently energetic photons (uv) or, possibly, with photons in very high density; supravital stains may act as intermediaries for energy transfer from photons to sensitive biological sites (sensitized photooxidation)] and thermal action, which is the principal result of photoenergy absorbed by a liquid medium. This action increases as a function of the wavelength employed. (BBB)

8745 RELATIVE BIOLOGICAL EFFECTIVENESS OF THE $^{10}B(n,\alpha)^{7}Li$ REACTION IN HeLa CELLS. Davis, Michael A. (Harvard Univ., Boston); Little, John B.; Ayyangar, K. M. M. S.; Reddy, A. R. Contract AT(30-1)-3937. Radiat. Res.; 43: 534-53 (Sep 1970).

The effects of the $^{10}B(n,\alpha)^{7}Li$ reaction in HeLa S3 cells were compared to those of 250 kVp x rays by studying the colony-forming ability of irradiated cells. The beam at the medical therapy portal of the M. I. T. Nuclear Reactor was used as the neutron source. This reactor beam is composed of γ rays, fast neutrons, and thermal neutrons; dosimetric studies showed that 50% of the dose arose from the γ component and 50% from the mixed neutron component. In 26 experiments, cells were exposed to the reactor beam in the presence of various concentrations of 92% enriched ^{10}B-boric acid. A computer program was developed to convert the exposure time to the beam into total absorbed dose in the HeLa cells. The dose-survival curves from neutron irradiations at ^{10}B concentrations of 0, 2, 5, 10, and 20 μg g cells gave D_0 values of 47, 45, 42, 41, and 39 rads, respectively, and corresponding RBE values of 2.83, 2.96, 3.17, 3.24, and 3.41. The RBE for the ionizing particles liberated from the $^{10}B(n,\alpha)^{7}Li$ reaction can be estimated from these RBE values and from the knowledge of the relative contribution of both beam dose and ^{10}B capture dose to the total dose. The calculated RBE for the alpha particle and lithium recoil released from the $^{10}B(n,\alpha)^{7}Li$ reaction was 3.7 for reproductive failure. (auth)

8746 CHEMICAL CARCINOGENESIS IN VITRO. Kuroki, Toshio (Tohoku Univ., Sendai). Tanpakushitsu Kakusan Koso; 15: 117-34(Feb 1970). (In Japanese).

Experiments were conducted on incorporation of a carcinogen into the cell, its binding with high molecular substance, its effect on cell functions, and the significance of such changes on carcinogenesis. Incorporation of a chemical carcinogen was tested with 4-nitroquinoline labeled in its benzene ring with ^{14}C, i.e., 4-nitroquinoline [5,6,7,8,9,10-^{14}C] 1-oxide (^{14}C-NQO). The first step in the incorporation of ^{14}C-NQO into HE cells began in the cytoplasm, especially in the ribosomes. This incorporation was affected by the synthesis of high molecular weight substances and the physiological condition of the cells. The incorporated compound binds with the protein, RNA, and DNA in the cell, in that order. The carcinogen that binds with the high molecular weight substance interferes with DNA synthesis but not with its decomposition. Inhibition of RNA synthesis was thought to be due to the lowered template activity of DNA or the polymerase activity on RNA. Studies on repair activities rely cheifly on x ray or uv irradiation, and the action of 4-NQO was considered to be similar to that of x rays in severing the single- and double-strained DNA molecule. Progression of malignancy, in vitro, was examined with regard to colony-forming ability in soft agar and dependence on sialic acid. There seemed to be a correlation between colony formation and tumor formation since the colonies appeared only during the latent period or following the appearance of proliferating nodules. Sialic acid dependency increased with carcinogenesis. (Japan)

8747 EFFECTS OF TEMPERATURE ON THE DOSE-RESPONSE CURVE OF HeLa S3 CELLS IRRADIATED WITH X RAYS. Masuda, Kouji (Kyushu Univ., Fukuoka). Nippon Igaku Hoshasen Gakkai Zasshi; 29: 1332-4(Jan 1970). (In Japanese).

The effects of temperature during irradiation on the surviving fraction of HeLa S3 cells were studied. Methods of culture and handling of the cells were essentially the same as that described by Puck and his colleagues. An adequate number of cells were transplanted to the media in glass dishes in order to yield about the same number of survivors at each dose level. After incubation at 37°C at a high humidity for 4 to 5 hrs to allow the cells to attach themselves to the bottom of the dish, the cells were irradiated. The plates were kept at 10, 23, 26, and 37°C for 5 min prior to, during, and for 2 min after irradiation. Culture was continued following irradiation for 14 days at 37°C in an incubator with a humidified atmosphere of 5% CO_2. The cells were then fixed and stained with crystal violet. Colonies containing more than 50 normal cells were counted and regarded as reproductively intact. X-ray exposure was made at 250 kVp with HVL of 1.45 mm Cu and dose rate of 62 rads/min. Decreased radiosensitivity of cells was observed when irradiated at a low temperature. This was in agreement with the results reported by Belli and Bonte, using x rays and HeLa cells. (Japan)

8748 ANALYSIS OF DOSE-RATE DEPENDENCE OF RADIATION INJURY. Fang, P. H. (Electronics Research Center, Cambridge, Mass.). Radiat. Res.; 44: 1-3(Oct 1970).

Some inconsistencies were found in the analysis of the dose-rate dependence of radiation injuries by treating the dose rate as a function of the radiation time. What was suggested instead was an analysis by treating the total dose to reach a critical mortality as a function of the dose rate. (auth)

Invertebrates

8749 (NSJ-tr-156) DEPENDENCY OF INHIBITION OF IMAGO FORMATION IN SARCOPHAGA PUPAE UPON DOSE-RATE. Sakka, Masatoshi. Translated from Nippon Igaku Hoshasen Gakkai Zasshi; 28: 1176-9(Nov 1968). 9p. Dep. NTIS (U. S. Sales Only).

Pupae of Sarcophaga peregrine, Robineau-Desvoidy, 1 ± 0.5 day of age, were irradiated by beta rays with different intensities. The source was a round applicator which had 200 mCi of ^{90}Sr in 2 cm^2 with a surface exposure of 5350 rep per minute and the variation of intensity was produced by distance. The highest intensity was given at a distance of 15 mm and the lowest at 370 mm, the relative intensity was 1 and 1.94×10^{-3}, respectively. Dose in pupal tissues was calculated by well known formulae. Dose-response relations for four different intensities were plotted on a probability paper and analysed by probit method. The degree of inhibition of imago formation responded linearly to doses (intensity × exposure time) on the coordinate in spite of the difference by a factor of 500 in exposure rate. Dependency of response upon dose rate is probably explained by the fact that at the lowest exposure rate in the present experiments (2.58×10^{7} beta particles for unit area per minute at a distance of 370 mm) the dose rate in pupal tissue is too high for recovery to occur. (auth)

8750 (ORNL-4612) EFFECTS OF CHRONIC IRRADIATION AND TEMPERATURE ON POPULATIONS OF THE AQUATIC SNAIL PHYSA HETEROSTROPHA. Cooley, J. L.; Nelson, D. L. (Oak Ridge National Lab., Tenn.). Nov 1970. Contract W-7405-eng-26. 71p. Dep. NTIS.

Thesis. Submitted by J. L. Cooley to Univ. of Tennessee, Knoxville.

Three separate, but related, studies were conducted to determine the effects of chronic irradiation and temperature on laboratory and natural populations of the aquatic snail Physa heterostropha. In the laboratory, at 25 C, dose rates of chronic gamma irradiation of 1, 2, 5, 10, and 25 rads/hr caused a significant decrease in the fecundity of snails. A dose rate of 25 rads/hr caused extinction of a population in one generation; 10 rads/hr, in one or two generations. Dose rates of 1, 2, and 5 rads/hr did not lead to an immediate extinction; the reduction in fecundity increased with increasing dose rate. The percentage of eggs hatching was decreased by all dose rates except 1 rad/hr. Dose rates of 10 and 25 rads/hr significantly increased growth. The life span of adult snails was shortened significantly by all dose rates except 1 rad/hr. Laboratory populations were exposed to dose rates of 1, 2, and 5 rads/hr at 15 C. Only a dose rate of 5 rads/hr significantly decreased fecundity. Hatching of eggs was significantly decreased by dose rates of 2 and 5 rads/hr. The effects of chronic irradiation on snail populations were determined to be greater at the higher temperature of 25 C. A temperature of 25 C, as compared with 15 C, caused a significant increase in the fecundity of laboratory populations. Temperature elevation did not have an effect on the hatching of eggs. The elevated temperature was judged to be non-detrimental to snail populations for the conditions of this laboratory study. A natural study population of Physa living in an area where it is exposed to chronic environmental radiation of 0.65 rad/day was studied. An acute gamma radiation study indicated that this population has not developed resistance to radiation. A $LD_{50(30)}$ dose of 47,000 rads was determined. When compared to a control population, the frequency of capsule production in the population exposed to chronic environmental radiation was reduced. A corresponding reduction in egg production was not

XUM

caused by an increased number of eggs per capsule. It was suggested that the compensation for the reduced capsule production by increased number of eggs per capsule was brought about by natural selection. (auth)

8751 CHRONOLOGY OF THE REGENERATION OF CELLS IN MITOSIS INDUCED BY LARGE DOSES OF X RADIATION (20,000 TO 100,000 R). Olivo, O. M.; Valentini, A. F. (Univ., Bologna). Boll. Soc. Ital. Biol. Sper.; 45: 790-4(30 Jun 1969). (In Italian).

The chronology of the degeneration of cultured chicken fibroblast cells during mitosis induced by 20,000 and 100,000 R doses of x radiation was defined within the experimental limits of the study. The results obtained for both irradiation doses are shown graphically and indicate that the death during mitosis or the profound morphological alteration which indicates regression occurs 100% in all the phases within one hour. After 15 min the degeneration of the mitoses is increasing percentage in the order: metaphase, prophase, telophase, anaphase. A partial progression of the mitotic processes can occur in all the phases and probably from the preprophase. (J.S.R.)

8752 MITOSIS IN IN VITRO CULTURED FIBROBLASTS FOLLOWING X IRRADIATION WITH 20,000 R. Valentini, A. F.; Olivo, O. M. (Univ., Bologna). Boll. Soc. Ital. Biol. Sper.; 45: 787-9(30 Jun 1969). (In Italian).

The effects of 20,000 R x ray doses on mitosis of in vitro cultured fibroblasts of chicken are compared quantitatively and qualitatively with the effects caused by 100,000 R. No significant difference was found in the number of mitosis five minutes after irradiation at both the high and low dose. After 15 and 30 min., however, the reduction in the number of mitoses is significantly higher with the lower dose. The most apparent alterations are the agglutinations of chromosomes in homogeneous masses, resulting in unequal divisions of the chromatin between the daughter nuclei. No morphological differences were observed in the 100,000 R irradiated fibroblasts. After one hour all the residual mitoses are very abnormal. The lower dose has a steadily decreasing effect on the number of mitosis and reaches a minimum at three hours, but then increases slightly again. The higher dose has no effect on mitosis after six hours. The 100,000 R dose slows down or inhibits cellular migration, but the 20,000 R dose appears to have no effect on this activity. (J.S.R.)

8753 ACTION OF X-RAYS ON THE MORPHOGENESIS OF BUDS IN SALMACINA INCRUSTANS (CLAP). Cresp, Jean (Univ. Marseille). Compt. Rend., Ser. D; 270: 2547-9(25 May 1970). (In French).

Irradiation acts before or after the beginning of the morphogenetic phenomena of budding in Salmacina incrustans by changing their normal course. It enables their various aspects to be dissociated: cephalic epimorphosis, pygidial, epimorphosis, and thoracic morphallaxy. (auth) (France)

8754 MEIOSIS IN THE GRASSHOPPER: CHIASMA FREQUENCY AFTER ELEVATED TEMPERATURE AND X-RAYS. Church, K.; Wimber, D. E. (Univ. of Oregon, Eugene). Can. J. Genet. Cytol.; 11: 209-16(Mar 1969).

Grasshoppers were given an acute dose of x rays, injected with ^{3}H-thymidine and thereafter maintained at 42°C. Autoradiographic analysis of testicular tubules taken at daily intervals after injection gave meiotic stage durations. The mean chiasma frequency was reduced 4 days after the grasshoppers were placed at 42°, in both x-rayed and non-irradiated animals, and remained low in the non-irradiated animals throughout the experiment. In the x-rayed animals the chiasma frequency rose to control levels on the 6th day and dropped again thereafter. Analysis of the data indicates a period ending approximately at zygotene during which chiasma frequency can be reduced by high temperature. The chiasma frequency can be increased by irradiating leptotene-zygotene. The end of the heat and x-ray sensitive stages are temporally distinct. Univalents were never produced by the heat treatment. Changes in chiasma frequency are restricted to the four pairs of larger chromosomes where multiple chiasmata are commonly found. Hence, the presence or absence of chiasmata shows a complex interaction with the physical environment. (auth) (UK)

Vertebrates

Refer also to abstracts 8607, 8608, 8612, 8615–8622, 8628, 8645, 8646, 8676, 8700, 8701, 8703, 8706, 8713, 8719, 8723, and 8806.

8755 (JPRS-51660) BIOMEDICAL PROBLEMS OF SPACE FLIGHT. Grigor'ev, Yu. G.; Khazen, I. M.; Kosmolinskii, F. P.; Yablochkin, V. D.; Belitskaya, R. A.; Evsyukov, E. P.; Ushanov, A. I. Translation of papers from Materialy III Nauchnoy Konferentsii Molodykh Spetsialistov, Moscow, 1969. 321p. NTIS.

Brief summaries are presented of results of studies on dogs, rats, and plants of radiation effects related to biomedical problems of space flight. Data are included on the effects of chronic or fractionated dose whole-body exposure to various dose levels of γ radiation on the leukocyte count in peripheral blood, and on the induction of chromosome aberrations in bone marrow cells in dogs; the effectiveness of shielding of various body parts on the protection of hematopoietic tissues in dogs against acute proton irradiation; the effects of chronic exposure of dogs over a two-year period to low-dose γ radiation on conditioned reflex activity and reproductive capacity; the combined effects of reduced muscular activity and fractionated dose γ irradiation on hematopoiesis and the excretion of calcium and chlorides in the urine of rats; the effects of γ and proton irradiation on the survival of cabbage and radish plants; and the effects of α irradiation on survival and mutation rate of Chlorella. Other papers discuss the effects of space flight environmental factors other than radiation on the physiological and psychological responses of animals and man. (C.H.)

8756 (NYO-2740-7, pp 154-217) BIOPHYSICS. (Columbia Univ., New York. Radiological Research Lab.).

From annual report on research project.

The following studies were conducted by the biophysics section during the reporting period: theoretical radiobiology (a simple relation between RBE and dose of low energy fast neutrons for diverse biological effects); RBE studies with monoenergetic neutrons (opacification studies in mouse lens); genetic effects of neutrons and x rays in Drosophila melanogaster; and RBE's of 0.43 MeV and low energy neutrons on somatic aberrations and cell number in Tradescantia stamen hairs. (E.R.B.)

8757 (NYO-2740-7, pp 218-56) RADIOBIOLOGY. (Columbia Univ., New York. Radiological Research Lab.).

From annual report on research project.

The following studies were conducted by the radiobiology section during the reporting period: the effects of gestational age on x-radiosensitivity of developing retinal tissues in fetuses of monkeys; the OER and RBE of ^{252}Cf mixed γ rays and neutrons at low dose rates in comparison to radium rays as measured in cultured cells of Vicia faba and Chinese hamsters; and the response of cultured Chinese hamster cells in synchronous division to ^{60}Co γ rays, x rays, and mixed neutrons and γ rays from ^{252}Cf under aerated and hypoxic conditions. (E.R.B.)

8758 (UCB-34-P-82-10) ELECTROPHYSIOLOGICAL AND BIOCHEMICAL STUDIES OF THE EFFECTS OF RADIATION ON BRAIN ACTIVITY AND DEVELOPMENT. Comprehensive Progress Report. (California Univ., Berkeley). 31 Jul 1970. Contract AT(04-3)-34. 25p. Dep. CFSTI.

Investigations conducted during the past ten years are summarized. Studies on the effects of radiation on gross CNS excitability in adult rats showed that single doses of whole-body x radiation ranging from 15 to 500 R increased brain excitability as reflected in lowered seizure threshold and facilitated tonic convulsions. Correlative studies using high-energy proton irradiation of the head in high doses showed that convulsibility was decreased at this dose level in contrast to the increase observed following exposure to low doses. Studies were conducted on effects of x radiation on electrical activity in selected brain areas of adult rats; it was found that the excitability of neural systems was generally enhanced and that the time course of neural response was increased. Studies on neurochemical effects of x radiation in adult rats included changes in electrolyte distribution and rates of aerobic and anaerobic metabolism. Effects of x radiation on the functional maturation of the central nervous system were studied by administering radiation to specific brain areas in developing animals at selected ages throughout the period of postnatal brain maturation. Effects of x radiation on the biochemical maturation of the central nervous system were studied with emphasis on electrolyte distribution, myelin formation, lipid and cerebroside content of cortical and subcortical areas, and cholinergic transmission. (H.L.W.)

8759 STUDIES OF THE CELLULAR RADIOSENSITIVITY OF TRANSPLANTS OF MURINE EPENDYMOMAS IRRADIATED IN VIVO. Stratton, K.; Anderson, A. (Massachusetts General Hospital, Boston. Harvard Medical School, Boston). Int. J. Radiat. Biol.; 18: 1-23(1970).

Cell-survival curves for in vivo tumor irradiation were obtained for two subcutaneously transplantable murine ependymomas, using end-point dilution assays in isologous hosts. No significant transplantation immunity could be detected in either tumor system, but both exhibited a "Révész effect." The TD_{50} for No. 15 tumor was about 300 unirradiated cells in the initial assays, but in a later series this was reduced to 20. The TD_{50} of tumor No. 48 was about 100 cells. The survival curves gave D_0 = 260 rads

XUM

for tumor No. 15, and D_0 = 288 rads for tumor No. 48, suggesting that a large fraction of the viable tumor cells were hypoxic in vivo. For unirradiated tumors, doubling-times of 21 hr for No. 48 were estimated both for the latency data and from caliper measurements of small tumors. After high radiation doses (3500 rads), these values were increased to as long as 5 days, although such long doubling-times were not always maintained as the tumors increased in size. (auth) (UK)

8760 SHORT-TERM EFFECTS OF ACUTE SUBLETHAL GAMMA RADIATION ON POPULATIONS OF THE OLD-FIELD MOUSE, PEROMYSCUS POLIONOTUS. Sealander, John A. (Univ. of Arkansas, Fayetteville). Health Phys.; 19: 299-306 (Aug 1970).

Three experimental populations of 20, 20 and 22 old-field mice (Peromyscus polionotus) were introduced into outdoor enclosures of approximately two acres in July and August, 1968. Before release into the enclosures, half of each population was given an acute, sublethal dose of gamma irradiation (500 R of ^{60}Co). The nonirradiated members of the populations served as controls. Mice in different introduced populations were allowed to interact freely under natural field conditions for nine days in one experiment and fourteen days in another. After these periods of interaction the populations were removed by live-trapping and were analyzed for gross body composition, organ weights and blood morphology. There were no significant differences in gross body composition between irradiated and nonirradiated mice in two introduced populations after nine days of interaction. Weights of liver, spleen, paired kidneys, paired adrenals, heart and lung were measured in a third population along with reticulocyte number and relative numbers of leucocytes. There were no significant differences in either absolute or relative organ weights of irradiated and nonirradiated mice in this population, but the variances of relative weights were greater in irradiated mice, significantly so for lung. Relative numbers of lymphocytes were significantly lower and those of monocytes significantly higher in irradiated mice as compared with controls. Relative neutrophil numbers were higher and reticulocyte numbers were lower in irradiated as compared with nonirradiated mice, but the differences were not significant. (auth) (UK)

8761 TOXIC EFFECT OF THERMAL NEUTRONS ON THE RABBIT ELECTRORETINOGRAM. Krohn, David L.; Jacobson, Jerry H.; Najac, Harold W.; Newton, Mary C. Barsa; Robertson, James S. (New York Eye and Ear Infirmary, N. Y.). Amer. J. Ophthalmol.; 70: 814-21(Nov 1970).

The electroretinogram was used to assess the relative destructive effect of thermal neutrons and x-rays on the rabbit retina. Some of the dosimetry problems in comparing these radiations are considered. Although the relative effects at 24 hours post-exposure were particularly examined, observations were made at various other selected intervals. The relative biological effectiveness of thermal neutrons under the limited circumstances of the experiment is in the order of 0.9 for loss of b-wave in 50% of tested animals. Doses of thermal neutrons (with accompanying gamma radiation) of less than 10^{13} nvt have little or no acute retinal destructive effect. (auth)

8762 MORPHOLOGICAL ASPECTS OF THE EFFECT OF IONIZING RADIATION ON ANTIBODY FORMATION. Lebedev, K. A. Usp. Sovrem. Biol., 67: 68-78(Jan-Feb 1969). (In Russian).

Literature data on the radiosensitivity of different types of immune-competent lymphoid tissues were compiled and critically analyzed. Questions on the different radiosensitivities of the tissues, existing in different stages of differentiation, were discussed in detail; the effect of radiation on the differentiation and proliferation of lymphoid tissues was also considered. (tr-auth)

8763 DOSIMETRIC EVALUATION OF RADIATION EFFECTS IN RATS CREATED BY AIR CONTAINING THORON AND THE INFLUENCE OF INHALATION ON PHYSIOLOGICAL REGENERATION OF KIDNEYS. Tadzhikov, M. M.; Sharilov, F. Kh. Dokl. Akad. Nauk Tadzh. SSR; 13: No. 6, 57-60(1970). (In Russian).

Effects of whole-body radiation and effects induced by inhaling air containing 2.5×10^{-5} Ci/l of thoron on mitotic activity of kidney cells of mice were studied. Techniques are described and results are tabulated. (R.V.J.)

8764 MORPHO-FUNCTIONAL STUDY OF HYPOTHALAMIC NEUROSECRETION. VI. THE EFFECT OF LOCALLY ADMINISTRATED X-IRRADIATION IN RANA TEMPORARIA AND RANA ESCULENTA. Dubis, Krystyna; Srebro, Z. (Medical Academy, Krakow). Folia Biol. (Krakow); 18: 247-52(1970).

The preoptico-neurohypophysial neurosecretory system of Rana temporaria and Rana esculenta was examined following x irradiation of the head region. Conspicuous changes were observed 7 days after doses of 2000 R and 3000 R. These were: depletion of the preoptic nucleus of neurosecretory material and considerable shrinkage of neurosecretory cells. Nuclear volume of the neurosecretory cells was decreased by over 30% in comparison with nonirradiated animals, this difference being statistically highly significant. High mortality was observed in Rana temporaria after 3000 R. (auth)

8765 FACTORS INFLUENCING HAEMATOPOIETIC SPLEEN COLONY FORMATION IN WHOLE-BODY IRRADIATED MICE. I. EFFECTS OF DEXAMETHASONE. Caniggia, A.; Gennari, C.; Bencini, M.; Cesari, L.; Borrello, G. (Univ., Siena, Italy). Boll. Soc. Ital. Biol. Sper.; 46: 86-8(31 Jan 1970). (In Italian).

The effects of dexamethasone on the formation of endogenous splenic colonies were studied in mice exposed to whole-body sublethal ^{60}Co irradiation in a single exposure. In the animals pretreated with dexamethasone the number of endogenous splenic colonies is reduced by about a half with respect to the controls. It appears possible to attribute the phenomenon to a direct effect of dimensional contraction of the splenic hematopoietic proliferative compartment independently of the subsequent irradiation. (J.S.R.)

8766 CERTAIN PECULIARITIES OF HEMATOLOGIC CHANGES IN THE CRUSH SYNDROME IN IRRADIATED ANIMALS. Ul'yanov, M. I. Eksp. Khir. Anesteziol.; 14: 58-61(Mar-Apr 1969). (In Russian).

In order to examine the effect of radiation injuries combined with other actions on the organism, the functional state of the blood was studied in relation to trauma in 12 irradiated and 20 unirradiated dogs. The animals were fastened to a stand and their rear end was placed under pressure by a 500-kg weight for 6 hours, without using anesthetic or narcotic agents. A dose 400 R of x radiation was used for the exposure. Arterial blood pressure and respiration rate of the animals were recorded kymographically. It was found that hematologic changes occur during various stages of the trauma syndrome, reflecting the overall reactivity, the defensive, and adaptive compensatory mechanism of the organism. No definite changes were observed in the white blood cells of the irradiated dogs at the start of the crushing; the reactive shifts in the hemogram were noted toward the end of the crushing period; the leukocytes number in the tail increased by 72.7% with respect to the original value following compression. The radiation-induced changes of the blood are of interest for the hematologic diagnosis of radiation and combined injuries and for therapeutic interventions aimed at the normalization of the blood activity. (TTT)

8767 FACTORS INFLUENCING HAEMATOPOIETIC SPLEEN COLONY FORMATION IN WHOLE-BODY IRRADIATED MICE. II. EFFECTS OF STRESS BY COLD AND ACTH. Cittadini, G.; Mancini, G. (Univ., Siena, Italy). Boll. Soc. Ital. Biol. Sper.; 46: 88-91(31 Jan 1970). (In Italian).

The effects on the formation of endogenous splenic colonies of the sudden exposure to cold and of the administration of ACTH in mice exposed to 800 and 900 rad ^{60}Co whole-body irradiation were studied. The results showed that sudden exposure to cold had no effect on the controls, but the animals exposed to 800 and 900 rads had a sharp reduction in the endogenous splenic colonies. The administration of ACTH had no effect on the controls, but there was a marked decrease of the endogenous splenic colonies in the irradiated animals. The effects of sudden exposure to cold and the administration of ACTH are qualitatively equal to that observed after the administration of dexamethasone. (J.S.R.)

8768 RADIOSENSITIVITY OF MICE EXPOSED TO VARIOUS TEMPERATURES AND LOW-DOSE RATE RADIATION. Levan, H.; Haas, R. E.; Stefani, S.; Reyes, E. (Veterans Admistration Hospital, Hines, Ill. Chicago Medical School. Univ. of Illinois, Chicago). Amer. J. Physiol.; 219: 1033-5(Oct 1970).

The effect of three ranges of temperature, 4, 16, and 26 C on the radiosensitivity of CF_1 male mice exposed to low-dose rate (0.2 R/min) γ radiation is reported. The animals were maintained in each temperature before, during, and following lethal radiation exposure (1,000 to 1,500 R). The results show that radiation mortality is significantly delayed and reduced in mice kept in low environmental temperature. (auth)

8769 SELECTION OF A SINGLE ANTIBODY-FORMING CELL CLONE AND ITS PROPAGATION IN SYNGENEIC MICE. Askonas, B. A.; Williamson, A. R.; Wright, B. E. G. (National Inst. for Medical Research, London). Proc. Nat. Acad. Sci. U. S. A.; 67: 1398-1403(Nov 1970).

A single antibody-forming cell clone was selected from primed mice by sequential transfer of limited numbers of spleen cells into irradiated syngeneic mice. The original spleen cell donors were immunized with dinitrophenylated bovine gamma globulin. Specific antibody molecules in sera of recipient mice were separated by isoelectric focusing on polyacrylamide gels and visualized by ^{131}I-hapten binding and autoradiography. This method provided a

XUM

marker for antibody-forming cells derived from a single cell clone. This report describes the history of one clone of cells (E9) producing IgG antibody to dinitrophenyl. Clone E9 is long-lived and was maintained for five transplant generations (over 6 months) by serial transfer of spleen cells into irradiated syngeneic mice. Clone E9 has the following properties: Antibody production strictly depends on antigen, presented either in vivo or in vitro; induction of E9 anti-dinitrophenyl shows specificity for the carrier protein; antibody is produced in amounts (2–3 mg/ml serum) comparable with myeloma-protein production by murine plasmacytomas; in the absence of antigen, memory cells have a lifetime exceeding 28 days. (auth)

8770 UV-IRRADIATION INDUCED CHANGES IN THE UPTAKE OF ACRIDINE ORANGE IN LIVING MOUSE FIBROBLASTS IN VITRO. Hagenas, Lars; Killander, Dick; Rigler, Rudolf (Inst. for Medical Cell Research and Genetics, Stockholm. Medical Nobel Inst., Stockholm. Karolinska Inst., Stockholm). Exp. Cell Res.; 62: 118-24(Sep 1970).

Earlier microspectrofluorimetric investigations showed that the capacity of nuclear chromatin in binding acridine orange (AO) was correlated to the functional state of the cells. The variation in the degree of AO binding was shown to reflect structural changes in the deoxyribonucleoprotein (DNP) complex which might be of importance for the regulation of genome activity. These studies were exclusively performed on cells after fixation. The purpose of the present work was to evaluate the possibility of characterizing the nucleoprotein complex in individual living cells with the AO technique. The uv irradiation used for excitation of fluorescence was found to strongly influence the uptake of AO in living mouse fibroblasts. An increased cellular uptake of AO was found during continuous irradiation. This seemed to be a direct irradiation effect rather than a photodynamic effect of AO. Most of the intracellular AO was bound to nucleoproteins. The augmented AO binding might be due to increased permeability of cell membranes induced by irradiation and/or to labilization of the nucleoprotein complex resulting in liberation of AO binding sites. (auth)

8771 EFFECT OF BRAIN STEM IRRADIATION ON DESCENDING SYSTEMS TO THE SPINAL CORD. Olson, Karin E.; Barnes, Charles D. (Indiana Univ., Bloomington). Radiat. Res.; 44: 404-12(Nov 1970).

Brain stem and cerebellar irradiation was found to affect brain stem conditioned lumbar cord flexor and extensor monosynaptic reflexes. The preconditioning extensor and flexor monosynaptic reflexes were either both inhibited or both facilitated. The conditioned reflex was affected conversely; i.e., the flexor tended to be facilitated while the extensor was inhibited. Radiation appeared to affect a balance of brain stem level interaction on the descending systems to the spinal cord. The cerebellum seems to take part in the mediation of this balance since decrebellates did not show an effect of radiation. (auth)

8772 MECHANISM OF WOUND HEALING IN IRRADIATED MOUSE SKIN. Gonsalves, Neil Ignatius. Providence, Brown Univ. (1969). 62p. University Microfilms Order No. 70-8719. Thesis.

Certain parameters of wound healing were investigated in skin irradiated at various times relative to wounding. Groups of C57 Black mice were exposed to single doses of 1000 R or 3500 R Kvp x-irradiation on a 9 × 7 mm area between the scapulae. Wounds were made in the irradiated field by a biopsy punch. At various times after wounding, a minimum of two animals were sacrificed and the wound tissues used for histological examination and the counting of epidermal mitosis. All observations ended on the 21st day after wounding. Increased inflammation of the wound area and delayed dermal regeneration occurred in all irradiated groups. These reactions were more pronounced in specimens that were x-rayed and wounded on the same day, and in this group the specimens that received the higher dose gave a more pronounced reaction. Irradiation caused delayed contraction in all groups. The activation of surrounding hair follicles, a process that usually accompanies wounding in mouse skin, occurred earlier, over a shorter elapsed time, and over a greater area of skin, in animals irradiated 30 or 90 days prior to wounding than in the controls or in those irradiated and wounded simultaneously. Epidermal mitotic activity in wounds made at the time of irradiation was initially depressed but recovered by the second postoperative day and was sustained in an oscillatory manner until healing was completed. Wounds in specimens irradiated 30 and 90 days prior gave an unexpected result. These specimens responded with an immediate burst of mitotic activity without the usual 24 hr lag that was seen in controls. A substantial number of cells appeared to die after division. Mitotic activity was sustained in an oscillatory manner until healing was completed. It is suggested that radiation administered at the time of wounding serves as an additional insult to the tissue, and in effect enlarges the original wound resulting in delayed healing. The unusual mitotic response (including that of the hair follicle) to the wounding stimulus in preirradiated specimens appears to be due to an altered control mechanism in these cells. It is proposed that the normal homeostatic mechanism that controls mitotic activity is mediated by an inhibitor susbtance produced by the cells. When inhibitor level drops below threshold level, mitotic activity begins. This mechanism is apparently radiation sensitive, and radiation serves as an agent for selecting a population of cells in which the mechanism is altered. The alteration may remain hidden over an extended period of time unless some stimulus such as wounding provokes a mitotic response. (Diss. Abstr.)

8773 CLINICAL AND GROSS PATHOLOGICAL FINDINGS IN SWINE RELATIVE TO LATE EFFECTS OF MIXED GAMMA-NEUTRON AND X-IRRADIATION. Brown, Daniel G.; Johnson, Donald F. (Univ. of Tennessee, Oak Ridge). Contract AT(40-1)-Gen-242. Radiat. Res.; 44: 498-511(Nov 1970).

Late effects of mixed gamma, neutron, and x radiation were studied in swine from 2 yrs postirradiation throughout the remainder of their life span. Clinical changes were similar in the irradiated and controls except for unilateral atrophy of the musculature in some of the irradiated individuals surviving doses of bomb radiation above 250 rads. The major causes of death were chronic diseases. Thus the usual clinical syndrome was loss in body weight, debilitation, bacterial infection, and the usual blood changes associated with infections. Pathological lesions presumably attributable to effects of ionizing radiation were: asymmetrical conformation with diminution in the respective sizes of the musculature and underlying bone in the pelvic region, usually in one pelvic limb; genital neoplasia, commonly manifested as leiomyomas of the broad ligaments and uteri; hepatomas; and annular, sclerosing adenocarcinomas usually present as strictures in the posterior one-third of the small intestines. Mean postirradiation survival times for the irradiated swine, all doses combined, were: 8.3 yrs (males) and 7 yrs (females); and for the controls, 9 years (males) and 7.9 years (females). The mortality rate was higher in the irradiated animals through approximately 7 years postirradiation. Regression of survival time on dose for the combined data of both sexes indicated life shortening was approximately 3% per 100 rads. (auth)

8774 HEMATOPOIETIC RECOVERY IN IRRADIATED DOGS. Baum, S. J.; Wyant, D. E. (Armed Forces Radiobiology Research Inst., Bethesda, Md.). Radiat. Res.; 44: 531-44(Nov 1970).

Hematological recovery in dogs exposed once or repeatedly to either 150 rads of x rays or 150 rads of mixed gamma–neutron radiation was measured. Comparisons were made among animals exposed to each radiation quality and to different numbers of repeated exposures. Prior to the first radiation exposure and on 19 days during a 30 day postirradiation study, ^{59}Fe uptake and other hematological values were obtained from all dogs. The dogs showed an oscillatory erythropoietic recovery response during the 30 days postirradiation. Near complete recovery on days 5 and 11 was followed by cellular decreases reaching low values about days 6 and 18. In general, for a given dose the effects of x rays were significantly greater than those of the mixed gamma–neutron radiation. This was particularly pronounced in the number of lethalities with repeated radiation doses. Previously irradiated dogs did not respond as well to a subsequent exposure of equal magnitude after a 3-mon rest period. This clearly implied residual injury in stem cells from the prior radiation exposure. The oscillatory recovery responses observed in the dogs of the present study may be basic response patterns in mammals, since they were detected previously in rodents. Presumably, these hematological response mechanisms have their origin in the inherent negative feedback systems of hematopoiesis. (auth)

8775 EFFECT OF ERYTHROPOIETIN IN COMBINATION WITH RADIOPROTECTIVE AGENTS ON ERYTHROPOIETIC RECOVERY AND SURVIVAL IN IRRADIATED MICE. Vittorio, P. V.; Amey, E. A. (National Research Council of Canada, Ottawa). Radiat. Res.; 44: 434-45(Nov 1970).

The present study shows the effect of erythropoietin administered one hour post-irradiation on the erythropoietic recovery and survival of gamma-irradiated mice pretreated with a number of radioprotective agents and radioprotective mixtures. Both polycythemic and normal mice were used in these studies. Erythropoietin administered one hour post-irradiation to AET-protected mice produced more rapid erythropoietic recovery (as measured by blood and spleen ^{59}Fe uptake) and better survival than in AET-protected mice which were not treated with erythropoietin. Doses of erythropoietin ranging from one to twenty units produced an equivalent effect. The erythropoietic recovery pattern of AET-protected mice given erythropoietin post-irradiation was studied to determine the effect of time (1 to 10 days) and increasing radiation exposure dose (700 to 1000 rads) on erythropoietic recovery

XUM

using the radioiron technique. The possibility of further increasing erythropoietic recovery and survival in mice after irradiation by using the erythropoietin post-irradiation treatment in combination with other radioprotective agents or mixtures was investigated. The results show that erythropoietin treatment post-irradiation increased erythropoietic recovery in AET-protected mice exposed to radiation doses of up to 1000 rads. If the radioprotective agent or mixture increased erythropoietic recovery and survival, the erythropoietin post-irradiation treatment would further increase both these factors. (auth)

8776 STRAIN AND SUBSTRAIN DIFFERENCES IN THE RECOVERY OF THYMUS FUNCTION AFTER WHOLE-BODY X-IRRADIATION OF MICE. Takada, Yumiko; Takada, Akikazu; Ambrus, Julian L. (Roswell Park Memorial Inst., Springville, N. Y. State Univ. of New York, Buffalo). Proc. Soc. Exp. Biol. Med.; 135: 473-7(Nov 1970).

Adult mice of various strains, either sham-thymectomized or thymectomized, were irradiated. Sheep red blood cells (SRBC) were injected on day 15, and sera were taken on day 22. Sham-thymectomized ICR/Ha produced an almost normal level of hemolysin. C57 BL/6, DBA/2, BDF_1, and CBA, however, could not produce the normal level, but generated decreased amounts of hemolysin even if the thymus was present. There was a difference between the rates of recovery of functions in the irradiated thymus in two substrains of CBA, CBA/St, and CBA/H. (auth)

8777 ESTIMATION OF SURVIVAL CURVE PARAMETERS FOR THE CELLS OF ORGANIZED TISSUES IN VIVO FROM SPLIT DOSE DATA. Lange, C. S. (Christie Hospital and Holt Radium Inst., Manchester, Eng.). Radiat. Res.; 44: 390-403(Nov 1970).

A split dose method was presented for the determination of the extrapolation number (with confidence limits) of the second dose survival curve following a given first or conditioning dose of radiation. Application of this method to published data (for mouse dermal and jejunal mucosal epithelia), where the slopes of the first and second dose curves were accurately measured but the extrapolation numbers were unknown, has yielded well determined values of the extrapolation number of the second dose survival curve. The case where direct measurement of the survival curve slopes is not possible was also considered, and as an illustration the method was applied to planarian stem cells. (auth)

8778 ULTRASTRUCTURE OF THE LUNG OF MICE EXPOSED TO A SUPRA-LETHAL DOSE OF IONIZING RADIATION ON THE THORAX. Maisin, J. R. (CEN/SCK, Mol, Belgium). Radiat. Res.; 44: 545-64(Nov 1970).

Mice were exposed to 2000 R of x rays to the whole chest or to the right hemithorax. At various periods, from 0 to 15 mon after exposure, the changes in the ultrastructure of the lung were studied. The lesions are initially limited to certain foci (early phase). At 3 hrs after exposure, all types of lung cells present changes in their ultrastructure, and the interstitial tissue is dissociated by edema. Six hrs after exposure, the lesions are more marked than after 3 hours. Between 2 to 7 mon after irradiation (intermediate phase), most of the mice irradiated at the entire thorax died and the ultrastructure of the lung is characterized by a marked accumulation of myelin-like figures, cell debris and fibrin-like material in the lumen of the alveoli; a large increase in size and number of granular pneumocytes, severe lesions in the capillaries, and an increase in number of macrophages, neutrophilic leucocytes, and plasmocytes. On the contrary, collagen fibers and elastic fibers are only slightly more abundant at this time than normally. The lungs of mice surviving the intermediate or proliferative phase display an extensive sclerosis and hyalinization of the alveolar septa associated with lesions in the capillaries (chronic phase). (auth)

8779 BEHAVIOR OF SOME GLYCOLYTIC ENZYME ACTIVITIES IN RABBITS AFTER PAN-IRRADIATION. Del Vecchio, E.; Rossi, A.; Sessa, G.; Verrengia, F. (Univ., Naples). Folia Med. (Naples), 50: 804-9(Nov. 1967). (In Italian).

The activities of some glycolytic enzymes (aldolase, lactic dehydrogenase, and glucose-6-phosphate-dehydrogenase) in rabbits submitted to irradiation with sublethal doses were studied. No significant changes compared to the controls were found. It was concluded that these enzymes were not modified by the action of the ionizing radiations in sublethal doses. (auth)

8780 HISTOPATHOLOGIC STUDIES ON BIOLOGICAL EFFECTS OF 15 MeV ELECTRON BEAMS OF BETATRON TO LYMPHOID TISSUES OF MICE (SPLEEN, LYMPH NODES, AND THYMUS). Mukai, Yoshihiro (Osaka City Univ.). Osaka Shiritsu Daigaku Igaku Zasshi; 18: 433-56(Dec 1969). (In Japanese).

A comparative study was made of the biological effectiveness of 15 MeV electron beams and 200 kV x-rays on lymphoid tissue in mice. Whole-body irradiation by electron beams and x-rays was delivered in doses of 50, 100, 200, and 500 R and the subsequent histocytological changes of the spleen, lymph nodes, and thymus were observed. In the white pulp of the spleen and in the lymph nodes, degenerative changes of the nucleus and inhibition of mitosis were observed 1 hr after electron beam irradiation, followed by necrosis of lymphocytes in 3 to 6 hrs (stage of destruction). Disposal of nuclear debris by macrophages took place 6 to 24 hr after irradiation. Atrophy of lymphoid tissue continued for 3 to 7 days, depending on irradiation dose, before the regeneration process began. The thymus presented lesions almost identical to those of the spleen and lymph nodes. No essential difference was observed between the histological changes due to irradiation by 15 MeV electron beams and 200 kV x-rays. However, 15 MeV electron beams proved to be less destructive to lymphoid tissue compared to 200 kV x-rays and regeneration began sooner. As indicated by inhibition of mitosis in thymic lymphocytes, the biological effectiveness of 15 MeV electron beams was set at approximately 70% of that for 200 kV x-rays. (TSS) (Japan)

8781 COURSE OF PULMONARY ASCARIASIS IN AN IRRADIATED ORGANISM. II. INFLUENCE ON TISSUE CHANGES ON THE OCCURRENCE OF BACTERIA IN ORGANS. Radvan, Rostislav; Moravek, Frantisek. Sb. Ved. Pr. Lek. Fak. Karlovy Univ. Hradci Kralove, Suppl.; 12: 533-43(1969). (In Czech).

Experiments were conducted to determine the effects of simultaneous x irradiation and irruption of Ascaris suum larvae in white mice. Histological changes in the liver and lungs and the spread of microbes into the organs of the mice were studied. Simultaneous irruption of Ascaris suum larvae and x irradiation in mice were found to have additive effects. (E.E.H.)

8782 EFFECT OF ERYTHEMIC ULTRAVIOLET IRRADIATION ON THE OSMOTIC RESISTANCE OF ERYTHOCYTES AND LYSOZYME CONTENT IN THE BLOOD SERUM. Baronenko, V. A.; Iskrzhitskaya, A. I. Vop. Kuorotol., Fizioter. Lech. Fiz. Kul't.; 33: 448-50(Sep-Oct 1968). (In Russian).

Adult rabbits were exposed to erythemia-inducing doses of uv irradiation to determine the effect on the osmotic resistance of erythrocytes and lysozyme content in the blood serum. The osmotic resistance and lysozyme content were determined before irradiation and 24 and 48 hrs after irradiation. The results are tabulated and show that the irradiated animals can be divided into two groups on the basis of the character of the changes of the index of non-specific resistance after irradiation. The animals in which the index increased were designated positive and those in which it decreased were designated negative. In the positive animals the osmotic resistance first decreased and then increased. In the negative animals the pattern was reversed. The changes of the osmotic resistance of the erythrocytes appeared to a greater degree than changes in the lysozyme content of blood serum in both groups of animals. (J.S.R.)

8783 METABOLIC AND HEMODYNAMIC DISTURBANCES IN THE LIVER SUBDUED TO EXTRACORPOREAL PERFUSION. Olszewski, W.; Polanski, J.; Bulien, D.; Nielubowicz, J. (Center of Experimental and Clinical Medicine, Warsaw). Pol. Med. J.; 9: 690-6(1970).

A study of arterial hypotension and metabolic acidosis of blood during in vitro perfusion of swine livers was made. Various rates of flow and pressure, pH measurements, distribution of flow using ^{133}Xe, and the function of liver cells using ^{131}I-labeled Rose Bengal were investigated. Results indicated that blood flowing from the liver under low pressure and volume results in metabolic acidosis of the blood. Distribution of the blood under normal pressure was not uniform. The peripheral portions of the liver became ischemic and were a source of acid products of carbohydrate metabolism. Successful perfusion of liver, in vitro, requires a steady, high flow and a uniform distribution of blood. (E.E.H.)

8784 PROTEINS OF THE BRAIN AND BLOOD SERUM OF ANIMALS SUBJECTED TO THE EFFECT OF MICROWAVES. Grigor'yan, D. G. Vop. Kurortol., Fizioter. Lech. Fiz. Kul't.; 34: 510-3(Nov-Dec 1969). (In Russian).

The content of albumin in the blood serum was reduced and the content of α- and β-globulin was increased by the effects of microwaves with output current density of 0.006 and 0.04 w/cm^2 administered over the lumbar region of rabbits. The effect of the microwaves increased the content of sulfur compounds in the brain and of β-globulin albumin fractions of the brain serums; the content of γ-globulin fractions was reduced only during the action of microwaves in non-thermal doses. The content of albumin fractions in the white substance of the brain of rabbits was changed little, and in the hypothalamus changes independent of the intensity of the microwaves were not noticed. (tr-auth)

8785 AGE SENSITIVITY OF EPITHELIAL CELLS OF MOUSE SMALL INTESTINE. Gillette, Edward L.; Withers, H. Rodney; Tannock, Ian F. (Univ. of Texas, Houston). Radiology; 96: 639-43(Sep 1970).

XUM

Variations in radiosensitivity during phases of cell cycle of jejunal crypt stem cells of mice were determined. Hydroxyurea blocked DNA synthesis and synchronized cells in crypts of mouse small intestine. Assays of number of regenerating crypts after exposing gut to 1150 rads γ radiation at varying intervals following hydroxyurea injection suggested cells were more resistant in late S-phase of cell cycle. Sensitivity to radiation apparently increased as cells passed through S-phase for first time after hydroxyurea treatment. Redistributing age density and changing population radiosensitivity should be considered in radiotherapy if gut is exposed after hydroxyurea treatment. (auth)

8786 SOME CHANGES IN THE GINGIVAL CONNECTIVE TISSUE IN ACUTE RADIATION SICKNESS. Slateva, M.; Datschew, B.; Svrakoff, D. (Wissenschaftliche Forschungsinstitut fuer Stomatologie, Sofia. Hohen Medizinische Instituts, Sofia). Deut. Stomatol.; 19: 896-903(Dec 1969). (In German).

White rats were irradiated at 700 R. Besides a control group, there was a group that received cortisone and another group that was treated with anabolic steroids. It was found that in cases of acute radiation syndrome there was an impairment of the barrier function of the connective tissue associated with quantitative and chemical changes of the elements of the intercellular substance and of certain cell constituents. Treatment of the irradiated mals with hydrocortisone did not lead to a change of the pathological picture that is connected with its inhibitory effect on the connective tissue. Though Deca Durabolin (anabolic steroid) does not inhibit the formation of intercellular substance, it cannot be assumed that it displays a marked protective action against x rays. (auth)

8787 ULTRASTRUCTURAL STUDY OF CONTROL AND ACUTE, WHOLE BODY GAMMA-IRRADIATED MEDULLA OBLONGATA TISSUE. Dodson, Ronald Franklin. College Station, Tex.; Texas A and M Univ. (1969). 403p. University Microfilms Order No. 70-11,534.

Thesis.

Investigations of the ultrastructure in the medulla oblongata of non-irradiated and acute, whole-body γ-irradiated rats were carried out. The irradiated groups received 1000, 2000, 5000, and 10,000 R respectively. Control micrographs revealed an ultrastructural morphology similar to that reported in cerebellar and cerebral studies, with one major exception. In the s-collidine buffered, perfused animals, an unreported structure termed concentric membrane body was shown. This entity consisted of a tight packed membranous complex that had an internal periodicity of approximately 50 Å. These structures were often observed to be associated with synaptic membrane complexes. In the irradiated groups, neurological ultrastructural alterations were proportional to irradiation dosage. Cytoplasmic vacuolization, mitochondrial damage, and myelin sheath abnormalities were observed. Even in the lowest dosages, concentric membrane bodies were observed forming membranous swirls, and apparently are indicators of immediate irradiation sensitivity within the tissue. Of particular importance was the observation that in no dosage level was capillary bed damage seen. In the limited views of the blood compartment, as seen in the medullary capillaries, several abnormal cells were noted. These observations indicated that capillary damage was not a major direct result of irradiation, but rather an indirect effect. (Diss. Abstr.)

Man

Refer also to abstracts 8600, 8611, 8647, 8661, 8669, 8697, 8704, 8722, 8732, 8739, and 8741.

8788 (LIB/Trans-296) TIME WISE BEHAVIOUR OF IRRADIATION INDUCED CHROMOSOME ABERRATIONS IN HUMANS. Schmid, E.; Bauchinger, M. Translated by J. B. Hopkinson (Australian Atomic Energy Commission Research Establishment, Lucas Heights), from Mutat. Res.; 8: 599-611(Nov-Dec 1969). 18p. Dep. NTIS (U. S. Sales Only).

An abstract of this article, prepared from the original, appeared as NSA 24: 14608(1970). (Australia)

8789 (NYO-4034-2) [STUDY OF THE IN VITRO EFFECTS OF IONIZING RADIATION ON GERMINAL EPITHELIUM OF HUMAN TESTIS AND ON STEROID BIOSYNTHESIS OF LEYDIG CELLS: UTILIZING TISSUE CULTURE METHODS]. Progress Report. (Albert Einstein Medical Center, Philadelphia, Pa.). [1970]. Contract AT(30-1)-4034. 28p. Dep. NTIS.

Testicular material from four patients was used for experiments on effects of in vitro x irradiation on the count of germinal cells. Cultures were exposed to doses of 225 to 2500 R. Histological sections of cultured fragments of irradiated and control cultures were prepared. Spermatogonia and Sertoli cells were counted; the tabulated results show that there was an abnormality in the spermatogenic process. Studies on effects of in vitro irradiation on the uptake of ^{3}H-thymidine by spermatogonia showed that radiation interfered markedly with the ability of the cells to incorporate thymidine label. Radioautography was used for a comparative study of the pattern of ^{3}H-thymidine labeling in the rat and human seminiferous tubules. It was found that dark type A spermatogonia invariably failed to incorporate tritiated thymidine in tubules incubated with the precursor for up to 5 hrs; during the same length of time the pale type A spermatogonia were heavily labeled. DNA synthesis of the pale type A spermatogonia and spermatocytes was impaired by radiation. (H.L.W.)

8790 MICROWAVES IN THE KITCHEN. Sher, Lawrence, D. (Univ. of Pennsylvania, Philadelphia). Arch. Environ. Health; 21: 702-3(Dec 1970).

Data on the biological effects of microwaves on small animals and plants as a function of energy are reviewed. It is concluded that the slight risks to man of microwave cooking should be weighed against those risks which are well known and accepted for other forms of cooking. (C.H.)

8791 PATHOLOGY OF RADIATION FIBROSIS OF THE LUNG. Nagahara, Sadao (Shinshu Univ., Nagano, Japan). Shinshu Igaku Zasshi; 18: 181-9(Oct 1969). (In Japanese).

With the advance of large-dose radiotherapy of malignant tumors, damage of adjacent healthy tissue is increasing. "Radiation fibrosis of the lung" was examined in human autopsy cases and animal experiments. Patho-histological observations in human body were divided into exudation period and fibrosis period of lung tissues. Exudation reaction is the result of direct damage to the lung from irradiation. The pathological changes begin from alveolar septum and spread to the alveolus. Intra-alveolar exudation is found in the lungs after continuous irradiation. Fibrosis is not the direct effect of radiation but is the final result of exudative change, and is often seen in the chronic stage after irradiation of the lung. In animal experiment, intra-alveolar fibrosis occurs in the alveolar cavity, and calcification is seen as an organic pathway of the exudative fluid, but this was not observed in any of human autopsy cases. From the study of inductive pathology, the presence of radiation pneumonia in lung tissues other than the irradiated portion can be explained from the immunomechanism theory. Secondary infections accompanying pulmonary blood circulation obstruction and bronchial epithelial degeneration also augment lung fibrosis. Allergic changes due to destruction of lung tissue by irradiation complicates pathological changes of the lung. Lung fibrosis increases with time following radiotherapy. (Japan)

8792 FUNCTIONAL CHANGES IN THE VESTIBULOCOCHLEAR ANALYSOR DUE TO IRRADIATION. Kasparek, L.; Zamecnik, J. (Inst. of Postgradual Medicine, Prague. Oncological Inst., Prague). Cesk. Otolaryngol.; 18: 12-18(Feb 1969). (In Czech).

Six subjects irradiated for cancer in the otorhinolaryngeal area were examined. Tests of the cochlear analysor showed a slight improvement due to a release of tubular occlusion and the direct radiation effect upon the sensory cell. Sensitivity of the vestibular analysor was temporarily lowered. Late postirradiation changes of the vestibulocochlear analysor functions were not observed. (NSA of Czech.)

8793 RADIATION-INDUCED EYE LESIONS. Heydenreich, A. Arbeitsmed.-Sozialmed.-Arbeitshyg.; 4: 280-4(Nov 1969). (In German).

Eye lesions caused by infrared and uv radiation, microwave radiation (radar and diathermic waves), laser beams, and ionizing radiation are reviewed with indications of appropriate protective measures. (Occup. Safety and Health Abstr.)

Radiation Effects on Plants

Refer also to abstracts 8600, 8635, 8639-8641, 8644, 8648, 8655, 8656, 8702, 8705, 8755, 8757, 8790, 8813, and 8818.

8794 (NSJ-tr-158) INFLUENCE OF GAMMA-IRRADIATION ON THE POLLEN FORMATION OF THE MORACEAE. Tojyo, Isao. Translated from Sanshi Kenkyu; No. 70, 22-3(Jan 1969). 18p. Dep. NTIS (U. S. Sales Only).

Gamma-radiation (2.5 to 10.0 kr) was applied to the sprouts of Moraceae developed in winter, and the effects on the growth of flower buds, pollen grains, and formation of pollen tetrads were investigated. After cutting and starting at 3 to 5°C twigs of each Morus alba Linn. (2x) and Kobuso No. 21 (2x), winter buds of the twigs were turned to the gamma source at 11.0 cm for irradiation at 5 kr/h dose rate at 17.5°C. Growth of the flower buds decreased as the dose increased. At the 2.5 to 7.5 kr irradiation, almost all flower buds were stripped and the anthers were dehisced, but

at 10.0 kr, insufficient growth of most flower buds, few dehiscence of anthers, and no perfect pollen were observed. When the dose was large, pollen sizes were variable, and many inferior pollens were produced. Many pollens were observed to have more than three germ spores. The formation of abnormal pollen was caused by abnormal karyokinesis of mother cells of the pollen and abnormal pollen tetrad formation, caused by the irradiation. With increase of the dose, abnormalities such as early separation of chromosomes, delayed mitosis, nucleoli formation, formation of non-reduced gametophytes, abnormal arrangement of nuclear plates, disorder of chromosome separation, double nucleus formation, chromosome bridges, macropollen mother cells, 1 to 3 spores with abnormal pollen tetrad, pollen tetrads containing abnormal microspores, and 5 to 15 spores of macro pollen tetrad were observed frequently. (auth)

8795 EFFECT OF HYPOXIA ON RECOVERY FROM SUBLETHAL DAMAGE IN CHLAMYDOMONAS. Bryant, P. E. (Hammersmith Hospital, London). Int. J. Radiat. Biol.; 17: 533-9(1970).

Experiments with Chlamydomonas reinhardii showed that the sparing effect of fractionation was unaffected by the absence of oxygen during irradiation, provided that oxygen was present during the fractionation interval. When oxygen was excluded from the system during the interval between doses, recovery was reduced or absent. If air was admitted to the irradiated system after a two-hour period of hypoxia, cells recovered promptly. The extent of the sparing effect was dependent on the concentration of oxygen present during the fractionation interval. The concentrations of oxygen which reduced recovery were in the range which reduced the rate of respiration of the cells. These results suggest that the recovery process in Chlamydomonas requires energy which is supplied in the cell by aerobic respiration. (auth) (UK)

8796 EFFECTS OF SIMULATED RADIOACTIVE FALLOUT BUILDUP AND DECAY ON SURVIVAL AND YIELD OF LETTUCE, MAIZE, RADISH, SQUASH, AND TOMATO. Sparrow, A. H.; Floyd, Brenda; Bottino, P. J. (Brookhaven National Lab., Upton, N. Y.). Radiat. Bot.; 10: 445-55(Sep 1970).

Experiments were designed to determine the relative effectiveness of similar total exposures of ^{137}Cs γ radiation given as either 16-hr or 36-hr treatments at constant exposure rates (CR) compared with 36-hr fallout decay simulation (FDS) or 36-hr buildup and fallout decay simulation (Bu + FDS) treatments with variable exposure rates. Seedlings of maize and squash were given FDS, 16-hr CR, and 36-hr CR treatments and seedlings of radish and lettuce were given Bu + FDS, FDS, and 16-hr CR treatments. Tomato seedlings were given a 16-hr CR exposure only. Comparisons among the various treatments were made with survival and yield as the end points studied and reported. (UK) (TSS)

8797 RECOVERY PHENOMENA IN YEAST SACCHAROMYCES CEREVISIAE. II. LIQUID HOLDING RECOVERY OF VIABILITY AND MITOTIC RECOMBINATION IN YEAST. Arman, I. P.; Kuznetsova, O. B.; Olteanu, V. (Kurchatov Inst. of Atomic Energy, Moscow). Genetika; 6: No. 4, 170-8(Apr 1970). (In Russian).

Liquid holding recovery (LHR) was studied on uv-sensitive diploid strains of Saccharomyces cerevisiae (homozygous for uvs_1 and uvs_2 loci). uvs_2-mutant cells defective for dark repair (DR) were able to recover from uv-inactivation in LH-condition (storage for 24 hr in phosphate buffer at 30°C), thus proving the DR-independence of the LHR. In LH-conditions, the maximal decrease of uv-induced mitotic recombination frequency was found in uvs_1 mutant, as compared to the normal diploid strain. The yield of mitotic recombinants can be decreased by delayed plating after treatment with γ rays and nitrous acid but not with nitrosoguanidine. (auth)

8798 PHYSIOLOGICAL AND GENETIC STUDIES OF X-RAY RESISTANCE IN BUDDING YEAST CELLS. Perper, Timothy Pelle. New York; City Univ. of New York (1970). 98p. University Microfilms Order No. 70-12,658.

Thesis.

In diploid Saccharomyces cerevisiae, budding cells were resistant to x-ray induced inactivation, mitotic recombination, respiratory deficiency, lag, and colony morphology alterations in experiments using single cells, log phase, and synchronized cultures. Resistance to non-lethal damage was greater than resistance to lethal damage. Post-irradiation growth on minimal or on galactose-containing media elicited more repair of potentially lethal damage in budding cells than in interdivisional cells, in both haploid and diploid strains. These media failed to reverse non-lethal damage. Diploid budding cells sensitive to both lethal and non-lethal damage were prepared from an aged, small-cell interdivisional population refrigerated overnight in water. Post-irradiation medium shifts elicited considerably more repair of potentially lethal damage in these budding cells than in equally sensitive interdivisional cells, but such shifts were without reparative effect on non-lethal damage. The results suggested that budding cell resistance to x-ray induced lethal and non-lethal damage involve different mechanisms, resistance to inactivation depending on repair. (Diss. Abstr.)

8799 STUDIES ON THE EFFECTS OF IONIZING RADIATION ON SOME WESTERN CONIFEROUS SPECIES. El-Lakany, Mohamed Hosny Hassan. Vancouver, B. C.; Univ. of British Columbia (1969).

Thesis.

The radiosensitivity of Pseudotsuga menziesii (Mirb.) Franco, Douglas-fir, from two different provenances representing the coastal and interior regions in British Columbia, Picea sitchensis (Bong.) Carr., Sitka spruce, and Tsuga heterophylla (Raf.) Sarg., Western hemlock was investigated and correlated with some cytogenetical and biochemical characteristics. Induction of mutations and radiostimulation of seed germination and seedling growth were also sought. Filled seeds of the above mentioned species were given five different dosages of γ irradiation from ^{60}Co source control, 500, 2,000, 5,000, and 10,000 R. Stratification for 14 days at 0°–2°C as post-irradiation treatment was tested. Germination values were evaluated and germinants were transplanted. Survival and growth under controlled environmental conditions were recorded for 182 days. The species exhibited differential responses to seed irradiation. All showed drastic reduction in germination and survival at the higher dosages, (5,000 to 10,000 R). There was some stimulation of Interior Douglas-fir seed germination and seedling survival at 500 and 2,000 R irradiation dosages over the control. The same exposures stimulated the height growth of Coastal Douglas-Fir. Stratification after irradiation reduced seed germination and seedling growth and survival in all the species. The tolerance to γ irradiation decreased in the following order: Interior Douglas-fir, Coastal Douglas-fir, Western hemlock and Sitka spruce. Sitka spruce had a significantly larger nuclear volume than Western hemlock and Douglas-fir. No correlation was found between nuclear volume, or interphase chromosome volume, and LD_{50} (germination). The amount of DNA per cell and per chromosome differed significantly among the three species with Sitka spruce having the highest DNA content followed by Western hemlock, Coastal Douglas-fir and Interior Douglas-fir. Significant negative correlations were found between DNA content per cell and per chromosome, and LD_{50} (germination). This indicated that DNA content plays a more important role than nuclear volume in determining the radiosensitivity of the species. The differences in radiosensitivity, nuclear volume and DNA content between the Coastal and Interior forms of Douglas-fir are discussed in relation to their ecogeographic distribution and taxonomy. Chromosome breaks, micro-nuclei, and chromosome erosion were detected in irradiated seeds of Douglas-fir. Intraspecific hybridization was carried out in Douglas-fir using γ-irradiated pollen grains. Pollen irradiation up to 5,000 R increased the number of filled seeds/cone. Seedlings from pollen irradiated at 500 R, exhibited some increase in height growth. Similar effects were obtained for pollen germination in vitro. The possibilities of utilizing seed and pollen irradiation in forest tree improvement are discussed and recommendations are made for future mutation breeding work. (Diss. Abstr.)

8800 RELATIVE BIOLOGICAL EFFECTIVENESS OF HEAVY IONS IN PRODUCING MUTATIONS, TUMORS, AND GROWTH INHIBITION IN THE CRUCIFER PLANT, ARABIDOPSIS. Hirono, Y.; Smith, H. H.; Lyman, J. T.; Thompson, K. H.; Baum, J. W. (Brookhaven National Lab., Upton, N. Y. Univ. of California, Berkeley). Radiat. Res.; 44: 204-23(Oct 1970).

Investigations were carried out to determine the relative biological effectiveness (RBE), in a higher plant, of radiations that give ionizing tracks of widely different average linear energy transfer (LET) in exposed tissues. The radiations consisted of ions of different mass accelerated in the HILAC (heavy-ion linear accelerator) and x rays. Arabidopsis thaliana, a cruciferous angiosperm, was well adapted for such studies: The seeds were unusually small and the embryo meristem so situated that accurate dosimetry of radiations of shallow penetration could be achieved. Mutants of chlorophyll b-deficient phenotype were available which, in heterozygotes grown from irradiated seed, produce gene-specific, dose-dependent, yellow-green sectors in the plant. The plants grew rapidly and well on culture media in test tubes under controlled conditions and gave uniform, reproducible results. In addition to inhibiting normal development, radiation caused tumors in Arabidopsis at frequencies dependent on dose and radiation quality. Utilizing these advantages, experiments were conducted to investigate quantitatively the effect of several heavy ionizing particles and 250 kVp x-rays on plant growth inhibition, tumor formation, and somatic mutation. (auth)

XUM

8801 RBE OF FAST NEUTRONS IN GROWTH INHIBITION: EVIDENCE FOR A COMPONENT REQUIRING CELL DIVISION. Haber, Alan H.; Triplett, Larry L.; Haywood, Fred F.; Ward, Donald R. (Oak Ridge National Lab., Tenn.). Radiat. Res.; 44: 446-55(Nov 1970).

The RBE of fast neutrons was studied on four responses of the first leaf of irradiated wheat seedlings. The RBE was 6 to 7 for reduction of the ultimate extent of growth accompanied by and requiring many cell divisions. The RBE was 2 to 3 for reduction of short-term growth after seedling irradiations which permitted limited growth with relatively few cell divisions. The RBE was also 2 to 3 for reduction of the ultimate extent of growth after seedling irradiation of gamma plantlets (seedlings germinating and growing without any cell divisions due to heavy gamma irradiation of the dry grains). We conclude that for growth inhibition the RBE has a nonmitotic component (i.e., a component not requiring cell divisions) with a value of 2 to 3 and a mitotic component (i.e., a component requiring cell divisions) with a value greater than 6 to 7. In the system containing postirradiation cell divisions, the nonmitotic component (RBE = 2 to 3) combines with mitotic component (RBE > 6 to 7) to give an overall RBE of 6 to 7. A fourth system involves tissue death in the absence of both cell division and cell growth. This RBE is 2½ to 3. These findings might explain previous generalizations concerning the dependence of RBE on dose or on biological criteria of damage. (auth)

8802 HISTOLOGICAL IDENTIFICATION OF IRRADIATED POTATOES. Penner, H. (Bundesforschungsanstalt fuer Lebensmittelfrischhaltung, Karlsruhe, Ger.). Z. Lebensm.-Untersuch. Forsch.; 144: 99-101(Oct 1970). (In German).

The prospect of commercial irradiation of potatoes makes it necessary to develop methods which enable the responsible government agencies to identify irradiated potatoes. It is possible to use the well known inhibition of wound periderm formation by irradiation for such an identification. (auth)

Radiation Effects on Microorganisms

Refer also to abstracts 8636, 8642, 8649–8654, 8701, and 8707.

8803 (TID-25468) PLANETARY QUARANTINE PROGRAM. Seventeenth Quarterly Report of Progress for Period Ending June 30, 1970. (Sandia Labs., Albuquerque, N. Mex.). Jun 1970. 75p. Dep. CFSTI.

Experimental activities in thermoradiation sterilization this quarter included: thermoradiation sterilization of Bacillus subtilis var. niger spores at 60°C with simultaneous γ radiation at 8 Krads/hr. The D value for this combined environment was found to be 6 hrs; exposure of spores embedded in methylmethacrylate to thermoradiation environments at 105°C and varying dose rates. A synergism apparently comparable percentage-wise to that found for surface contamination was observed; and studies by other organizations at Sandia to investigate any deleterious effects of thermoradiation on typical electronic devices and materials and to determine the feasibility of building a relatively inexpensive thermoradiation chamber large enough to handle a Viking spacecraft. The thermoradiation inactivation model was used to generate a family of curves relating B. subtilis var. niger inactivation rates to temperature at given dose rates. It is shown how these curves may be used in planning sterilization cycles. An attempt was made to simulate the behavior of embedded spores in thermoradiation environments by using small sealed aluminum containers. When the containers were sealed, results approximating those obtained from spores embedded in methylmethacrylate were obtained. In continuing to study the mechanisms for bacterial spore inactivation in thermoradiation (and other) environments, it was found that there might be a link between the resistance of bacterial spores to alcohols and their resistance to heat. If such a link is found, it offers a chemical means of investigating spore inactivation and variations in spore resistance. Two humidity control systems were designed, built, and tested that are capable of controlling relative humidity to ±1% at ambient temperature and delivering this air to a temperature chamber. One system is relatively portable but requires some periodic manual control. The other system is slightly unwieldy but requires no manual control. A document describing the use of the basic bioburden model for bioburden estimation, and prediction and derivations of some sampling requirements was drafted. In addition to this, computations involving variable fallout rates and removal factors were begun, and the instrumentation to estimate a critical model parameter (numbers of organisms per viable particle) was developed and preliminary experimentation for model verification was begun. A very general and versatile computerized identification system was designed, programmed, and tested against the Public Health Service (PHS) Apollo data. This system has as inputs all information relating to tests, their interpretations, and possible organism categories. Consequently, it is easily modified to keep pace with the PHS improvements in their identification scheme. At the request of the AEC, the status of Federal Standard 209a concerning clean room and work station requirements, controlled environment was reviewed. It was decided that no revision was currently needed. (E.R.B.)

8804 (TID-25556) INOCULATED PACK STUDIES ON LOW-DOSE IRRADIATED MARINE PRODUCTS: SHRIMP. Final Report. Ward, B. Q. (Miami Univ., Fla. Rosenstiel School of Marine and Atmospheric Sciences). Dec 1970. Contract AT (40-1)-3698. 43p. Dep. NTIS.

Packs of fresh shrimp inoculated with 0, 10^2, 10^4, or 10^6 spores of Clostridium botulinum type E (Beluga strain) per gram of shrimp, and subsequently γ irradiated at levels of 0, 100, or 200 K-rad, were incubated at temperatures of 38, 42, 50, or 70°F. The day of total consumer rejection, as determined by an informal panel of non-experts, was noted for each permutation, and total plate counts were determined for each on the day of rejection. The time required for the development of toxicity in each permutation, and the type of botulism involved, were determined by mouse protection testing. (auth)

8805 INACTIVATION OF THE SCRAPIE AGENT BY NEAR MONOCHROMATIC ULTRAVIOLET LIGHT. Latarjet, R. (Radium Inst., Paris); Muel, B.; Haig, D. A.; Clarke, M. C.; Alper, T. Nature (London); 227: 1341-3(26 Sep 1970).

Studies with ionizing and uv radiation led to the question as to whether the scrapie agent depends on replication of a nucleic acid moiety for proliferation, which occurred also when the titre of the injected material had been reduced by irradiation in vitro. The dose of ionizing radiation required to give an average of one inactivating event per infective unit was much larger, and the inferred "target volume" (molecular weight about 1.5×10^5) therefore much smaller, than for any virus. If the "target" were nucleic acid this molecular weight could be too low to allow sufficient coding information replication. With uv irradiation at 254 nm, detectable inactivation required doses very large compared with those that inactivated even the most "resistant" entities whose functions depended on the integrity of nucleic acid, suggesting that the agent might be comparatively transparent to uv of wavelength in the "germicidal" region in which nucleic acids most strongly absorb. A comparison is described of the effectiveness of bands centered at 237, 250, and 280 nm, using doses large enough to give considerably more inactivation than previously possible. Light at 254 nm from a germicidal lamp was also used. Mice were employed in the experiments. Data for inactivation of the agent by uv irradiation at various wavelengths are tabulated. Amongst the findings were the following: inactivation curves were exponential; the efficiency of inactivation at 250 and 280 nm was the same; and inactivation at 237 nm was about six times as effective as with higher wavelengths. The difference in response of the scrapie agent compared with other systems which rely on nucleic acid for their function, including viruses, was striking. Caution in interpretation of the results is, however, emphasized, on account of the effect of energy transfer processes, or interactions between parts of a complex. However, bearing in mind these reservations, it could seem reasonable to postulate that the chromophase responsible for the uv inactivation of the scrapie agent could be other than a part of a nucleic acid molecule or a nucleoprotein complex. (UK)

8806 EFFECT OF U.V.-IRRADIATED VESICULAR STOMATITIS VIRUS ON NUCLEIC ACID SYNTHESIS IN CHICK EMBRYO CELLS. Yaoi, Y.; Mitsui, H.; Amano, M. (National Cancer Center Research Inst., Tokyo). J. Gen. Virol.; 8: 165-72(Sep 1970).

When monolayer cultures of chick embryo cells were infected with the New Jersey serotype of vesicular stomatitis virus at high input multiplicities, the synthesis of cellular RNA was rapidly inhibited. The stimulation of cellular DNA synthesis observed in control cells following medium replacement was also inhibited in the infected cells. These activities of vesicular stomatitis virus on the synthesis of cellular nucleic acids were quite resistant to uv irradiation, although no virus RNA synthesis was detected in the cells infected with uv irradiated vesicular stomatitis virus. No stimulation of degradation of cellular nucleic acids was observed in cells treated with irradiated vesicular stomatitis virus. (auth) (UK)

8807 EFFECT OF SODIUM FLUORESCEIN AND PLATING MEDIUM ON RECOVERY OF IRRADIATED ESCHERICHIA COLI AND SERRATIA MARCESCENS FROM AEROSOLS. Dorsey, Emerson L.; Berendt, Richard F.; Neff, Everett L. Jr. (Aerobiology and Evaluation Labs., Frederick, Md.). Appl. Microbiol.; 20: 834-8(Nov 1970).

Irradiation of aerosols of either Escherichia coli or Serratia marcescens with simulated solar (xenon) radiation caused a significant decrease in viability. When sodium fluorescein was employed to determine the physical loss of organisms from the aerosol, an additional adverse effect upon survival was noted. The decay curves indicated that at least two mechanisms of inactivation were operative, one due to aerosolization, the other to irradiation. After collection from aerosols, both species of microorganisms grew better on blood agar base than on Casitone agar, but this finding did not appear to be related to the effect of irradiation. (auth)

8808 ACTION OF ATOMIC HYDROGEN, HYDRATED ELECTRONS, AND IONIZING RADIATION ON BACTERIOPHAGE T_7 IN AQUEOUS SOLUTION. Dewey, D. L.; Stein, Gabriel (Mount Vernon Hospital, Middlesex, Eng.). Contract AT(30-1)-3242. Radiat. Res.; 44: 345-58(Nov 1970).

Coliphage T_7 in aqueous suspension were inactivated by hydrogen atoms produced in an electrodeless discharge, by hydrated electrons produced from ferrocyanide ions, by uv light, and by various mixtures of radicals produced by the γ radiolysis of water. The contribution of each type of radical was determined by comparing the known G values for radical production under defined conditions of γ radiolysis of water. It was concluded that hydrogen atoms inactivate phage with high efficiency and that hydrated electrons inactivate phage with a lower efficiency, but also sensitize the survivors to hydrogen peroxide. O_2^- radicals do not inactivate the phage. OH radicals react with phage, but do not inactivate or sensitize them. (auth)

8809 BACTERIA AS SPECIFIC BINDING AGENTS FOR AN ISOTOPIC ASSAY OF SERUM FOLATE. McCall, Mary S.; White, Jerry D.; Frenkel, Eugene P. (Veterans Administration Hospital, Dallas. Univ. of Texas, Dallas). Proc. Soc. Exp. Biol. Med.; 134: 536-8(Jun 1970).

Saturation analysis or competitive inhibition utilizing bacteria Lactobacillus casei as the specific binder permitted the measurement of serum folate. Unlike conventional microbiologic techniques, organism growth rate was not determined. This new radiomicrobiologic approach quantitated serum folate by competitive binding of tritiated folic acid during the early lag phase of bacterial growth. (auth)

8810 NITROUS OXIDE AS A SENSITIZER OF BACTERIAL SPORES TO X-RAYS. Powers, E. L.; Cross, Marian (Univ. of Texas, Austin). Contract AT(40-1)-3408. Int. J. Radiat. Biol.; 17: 501-14(1970).

In N_2O-saturated water, spores of Bacillus megaterium exhibit sensitivity to x-rays that is higher than that in N_2-saturated water, but lower than that in O_2-saturated water. O_2-N_2O mixtures show O_2 sensitivity. Ethyl alcohol present simultaneously at 0.8 Molar prevents the N_2O sensitization completely. These results can be interpreted as due to an increase in ·OH radical yield by N_2O; and removal of ·OH by ethanol. In dilute solutions of ethanol only partial reversal (or competition) of the N_2O effect is observed. This effect is concentration-independent over a wide range of dilute concentrations. An apparent exhaustion of the alcohol is observed at higher doses, producing a two-component survival curve, each component being exponential. The break-points are dose-dependent, with only one being expected on the basis of measured yields in chemical systems; and the slope beyond the break-point is always that of O_2-saturated suspensions. The last results can be interpreted as indicating two actions of N_2O, only one of which is prevented in dilute solutions of alcohol, and the operation of O_2 or an O_2-mimicking system after exhaustion of the alcohol. (auth) (UK)

8811 DECREASE IN ANOXIC SENSITIVITY, AND RESULTANT INCREASE IN OXYGEN ENHANCEMENT RATIO, WITH DECREASE IN ENERGY OF FAST ELECTRONS. Forage, A. J.; Alper, Tikvah (Hammersmith Hospital, London). Int. J. Radiat. Biol.; 17: 527-32(1970).

When bacteria are exposed to ionizing radiation of low LET while lying on a surface, oxygen enhancement ratios are higher than when they are in suspension; but the effect is not observed with uv-sensitive or repair-deficient strains, which normally have OER's of 2 or less. This phenomenon is associated with maximum electron energies of a few hundred keV, with which oxygen enhancement ratios are of the order of 4, or more, compared with values of about 3 for suspensions. With considerably higher maximum electron energies the effect is not observed, and with energies of 5 to 7 MeV the ratios are probably less for bacteria on a surface than in suspension. (auth) (UK)

8812 GLUCOSE-INDUCED RESISTANCE TO GAMMA-RAYS IN ESCHERICHIA COLI. Friesen, B. S.; Iyer, P. S.; Baptist, J. E.; Meyn, R.; Rodgers, Jean-Marie (Univ. of Kansas, Lawrence). Contract AT(11-1)-1686. Int. J. Radiat. Biol.; 18: 159-72(1970). (COO-1686-11).

Some strains of Escherichia coli, when grown to stationary phase in nutrient broth which has been enriched with glucose, become more resistant to radiation (glucose-induced resistance, GIR) than when grown in nutrient broth without glucose. Various repair-deficient strains of E. coli were examined for GIR. GIR was present in cells which were rec^+ and lon^+ and absent in cells which were either rec^- or lon^-. Host-cell reactivation in these cells and the effects of caffeine, acriflavine, and ultra-violet light exposure on the sensitivity to gamma-rays of cells grown in glucose-enriched nutrient broth are all consistent with the hypothesis that, at low gamma-ray doses, glucose enhances the type of recovery controlled by the rec^+ loci. (auth) (UK)

Radiosterilization and Radiopreservation

Refer also to abstract 8803.

8813 (NP-18236) A CASE STUDY IN TECHNOLOGICAL INNOVATION: FOOD IRRADIATION. Weiss, Harald H. (Harvard Univ., Boston, Mass.). 10 May 1967. 80p. CFSTI.

The state of the art of food irradiation is reviewed and six areas of potential application are described. These include sterilization, pasteurization, disinfection, disinfestation, sprout inhibition and delayed ripening, and product improvement. The history of food irradiation up to May 1967 is discussed and valiant efforts by the Atomic Energy Commission, the U. S. Army, and the U. S. Congress are identified. Nine forces opposing commercialization i.e., unresolved technical difficulties; health dangers, real and imagined; treatment by the press; warnings by the academic community; attitude of the Food and Drug Administration; magnitude and direction of the Government effort; competing processes and comparative economics; consumer reaction; and active sources of resistance are identified. Four attempts at commercialization are described. These include the irradiation of dehydrated vegetables, the irradiation of seeds by several companies, the irradiation of beef, and the irradiation of potatoes. (74 references) (auth)

8814 (STI/DOC-10/114) TRAINING MANUAL ON FOOD IRRADIATION TECHNOLOGY AND TECHNIQUES. (International Atomic Energy Agency, Vienna (Austria)). 1970. 134p. IAEA $4.00.

The lecture material contained in the manual is presented under the following headings. Radioisotopes and Radiation; Radiation Detection and Measurement; Health Physics; Radiation Chemistry; Effects of Radiation on Living Organisms; Preservation of Foods; Radiation Preservation of Foods; Packaging; Wholesomeness of Irradiated Foods; Government Regulation of Irradiated Foods; Food Irradiation Facilities; and Commercial Considerations of Food Irradiation. The second part of the manual contains 13 laboratory experiments. A glossary of frequently used terms and lists of publications of organizations and books on food irradiation are also included. (E.R.B.)

8815 INHIBITION OF THE GERMINATION IN GAMMA IRRADIATED ONIONS. Mumtaz, Ali; Farooqui, W. A.; Sattar, A.; Muhammad, Amir (Atomic Energy Centre, Lahore). Food Irradiat.; 10: 10-14(Apr-Jun 1970). (In French).

Punjab Red onions were irradiated with doses up to 10 Krad. Observations were made on germination, weight loss, and rot during storage. The onion odor was analyzed. Germination may be controlled with doses up to 8 Krad without observing any detrimental effects on the onion flavor or odor. (France)

8816 EFFECT OF GAMMA RADIATION ON VITAMIN CONTENT OF ENRICHED FLOUR. Chappel, C. I. (Bio Research Labs. Ltd., Quebec); Macqueen, K. F. Food Irradiat; 10: 7-9 (Apr-Jun 1970). (In French).

The effect of gamma radiation doses of 75, 100 and 150 Krad on the thiamine, riboflavin, and niacin contents of two different samples of enriched flour was studied. No effect was observed on the thiamine or riboflavin contents, neither immediately after being irradiated, nor after a three month storage period. A decrease in the niacin content was observed after the flour was irradiated, in particular with 100 and 150 Krad doses. Flour irradiated with doses up to 75 Krad exhibited no special problems. (France)

8817 GAMMA IRRADIATION OF TABLE GRAPE VARIETY HOANES. Belli Donini, M. L.; Pansolli, P. (Comitato Nazionale per l'Energia Nucleare, Casaccia, Italy). Food Irradiat.; 10: 14-20(Apr-Jun 1970). (In French).

A total radiation dose of 200 Krad increases the preservation

time by 2 to 3 weeks. Standard grapes may be kept up to 40 days, whereas the irradiated grapes can be kept another 12 to 18 days more, depending upon whether the crop was harvested at a degree of rtpeness less than 45% or greater than 50%. Biochemical studies on the amounts of pectic substances and the pectin-esterase activity confirm the effect of these substances on the fruit ripening process. The total percentage of reducing sugars was not significantly modified by irradiation. (France)

8818 NUCLEAR TECHNIQUES FOR INCREASED FOOD PRODUCTION. Freedom from Hunger Campaign, Basic Study No. 22. New York; Unipub, Inc. (1969). 90p. $1.25.

Activities of the Joint FAO/IAEA Division of Atomic Energy in Food and Agriculture in agricultural research and food production are surveyed. Areas of research include mutation induction, insect control, radio-attenuated animal vaccines, food irradiation, fertilizer and plant nutrient studies, animal nutrition, irrigation, and nuclear desalination of water. (H.L.W.)

8819 RADIATION PRESERVATION OF CHAPATIES (INDIAN) UNLEAVENED BREAD). Savagaon, K. A.; Dharkar, S. D.; Sreenivasan, A. (Bhabha Atomic Research Center, Bombay). Food Technol.; 24: 1158-60(Oct 1970).

Chapaties—Indian unleavened bread—could be stabilized against mold spoilage by a radiation dose of 1 Mrad for more than six months and were highly acceptable organoleptically for at least two months. No added advantage accrued by use of any antioxidant which afforded a certain degree of protection against radiation to molds. (auth)

8820 DEHYDRO-IRRADIATION PROCESS FOR TROPICAL SHRIMPS. Gore, M. S.; Sawant, P. L.; Kumta, U. S.; Sreenivasan, A. (Bhabha Atomic Research Centre, Bombay). Food Technol.; 24: 163-8(Oct 1970).

Shelf stability of shrimps depends on the moisture content. Semi-dried shrimps (40% moisture) take less time for dehydration, but are prone to mold and bacterial spoilage. Single treatments of sorbic acid dip or blanching prior to dehydration or post-dehydration irradiation with tolerance dose of 0.25 Mrad provide limited extension in shelf-life. An integrated process consiting of dip for 60 min in 0.5% sorbic acid, blanching in 10% NaCl solution at 80°C for 5 min, dehydration to 40% moisture and irradiation with 0.25 Mrad stabilizes the product for room temperature storage (25 to 30°C). Such products, containing 25 mg % of sorbic acid and 3.25 g % of NaCl, remain free from mold and bacterial spoilage for 4 months at room temperature. Optimum conditions of process variables, including packaging requirements, have been described for the dehydro-irradiation process for tropical shrimps. (auth)

8821 IRRADIATING MUSHROOMS AND THEIR GROWING SOIL. Casalina, Samuel L. U. S. Patent 3,527,645. 8 Sep 1970. Filed 21 Sep 1966.

Prolonging the market life of raw mushrooms by irradiating them with between 25 and 125 krad of an ionizing radiation at a dose rate in excess of 25 krad per minute is discussed. Still greater improvement is achieved by maintaining the temperature between 33° and 55°F during irradiation. (Office Gaz.)

8822 EFFECTS OF GAMMA RADIATION ON THE REPRODUCTION AND LONGEVITY OF THE STABLE FLY, STOMOXYS CALCITRANS (L.). Offori, Evans Dunstan. Fargo, N. D.; North Dakota State Univ. (1969). 94p. University Microfilms Order No. 70-11,517.

Thesis.

The purpose of this study was to obtain information on induced sterility and other aspects of the biology of stable flies. Male and female stable flies, Stomoxys calcitrans (L), were irradiated as adults 30 ± 6 hr after emergence and as pupae 24 to 18 hr before eclosion. Cytological study of the testes revealed that when a dose of 5 krad was applied to pupae or adults, all spermatogenic activity ceased within ten days after treatment, thus rendering the male completely sterile. The mating performance of sterilized males was studied and hatchability of eggs from females indicated that radiosterilized males compete favorably with untreated males. Females were more sensitive to radiation than males and egg production was dependent upon both the age at irradiation and the dose administered. The effect of the sterilizing doses on the ovarian growth and cytopathology of the ovary was studied with a view to elucidating the morphological and cytological basis of sterility in females. Examination showed that a dose of 2 krad given to pupae and adults retarded ovarian growth considerably within five days after treatment. This dose did not stop development of the more mature oocytes, although it did cause gross abnormalities in younger follicles. With a dose of 3 krad, degeneration and atrophy of the egg follicles was so complete as to halt egg production in females treated as adults or pupae. When late pupae were given high doses of radiation (10 krad and above), the proportion of adults emerging over a 48-hr period decreased with dosage. Mortality studies made of irradiated and control flies showed that the sterilizing dose produced no significant shortening of lifespan in treated insects when compared with the longevity of the control insects. (Diss. Abstr.)

8823 USE OF IONIZING RADIATION FOR THE HYDROLYSIS OF PECTINS AND THE EFFECT ON THE PROPERTIES OF THE EXTRACTED PECTINS. Kassem, Abdel-Hamid A. Gainesville, Fla.; Univ. of Florida (1969). 126p. University Microfilms Order No. 70-11,742.

Thesis.

Exposure of dry and wet residue from Valencia oranges to radiation doses of 0 to 1000 krad with 100 krad increments increased the percentage yield of pectins, and decreased the jelly grade and jelly units of the extracted pectins. The methoxyl contents of the pectins from the residue decreased with irradiation. Solutions made from the extracted pectins had a lower relative viscosity than solutions made from pectins extracted from non-irradiated residue. (Diss. Abstr.)

8824 WHOLESOMENESS OF IRRADIATED FOOD WITH SPECIAL REFERENCE TO WHEAT, POTATOES, AND ONIONS. Report of a Joint FAO/IAEA/WHO Expert Committee, Geneva, 8-12 April 1969. World Health Organ., Tech. Rep. Ser.; No. 451, 1-44(1970).

The irradiation of food offers an attractive method of preventing spoilage and reducing contamination with pathogenic organisms. At the same time it is a method that presents certain hazards if proper precautions are not taken. The general principles that should govern the production and use of irradiated food and the legislation needed to safeguard consumer and producer were discussed in 1964 by a Joint FAO/IAEA/WHO Expert Committee. One of the most difficult problems is the assessment of the safety of irradiated food from the point of view of the possible formation of toxic products, microbiological hazards, and nutritional inadequacy. The investigations needed for this purpose and the procedures for evaluation of the experimental data were reviewed by another Joint FAO/IAEA/WHO Expert Committee in 1969. These procedures were then applied by the Committee to the evaluation of γ irradiated wheat, potatoes, and onions. On the basis of studies undertaken so far, the Committee did not find any evidence that, under the conditions specified, either irradiated wheat or irradiated potatoes were harmful. However, certain additional information was considered essential. In the meantime, temporary acceptance of these two irradiated foods was recommended. Inadequate data were available to permit an assessment of irradiated onions. Other recommendations refer to the choice of animal species, the numbers of animals and the diets to be used, and reproduction studies. Guidance is given on the lines that should be followed in future research. In addition, the Committee recommended that appropriate studies on mutagenicity should be undertaken for the evaluation of the wholesomeness of irradiated foods. (auth)

8825 ESR STUDY OF BONE TISSUE STERILIZED BY γ IRRADIATION. Stachowicz, Waclaw (Inst. of Nuclear Research, Warsaw); Ostrowski, Kazimierz; Dziedzic-Goclawska, Anna; Komender, Andrzej. Nukleonika; 15: 131-43(1970).

Powdered samples of lyophilized human bone, deproteinized bone, demineralized bone, synthetic hydroxyapatite, and collagen were subjected to 3.3 Mrads of ^{60}Co γ radiation in air and in vacuo at room temperature. The ESR spectra of irradiated samples were recorded. On the basis of the results obtained it was concluded that in irradiated bone, two types of paramagnetic species are involved: those revealing an asymmetric singlet and attributed to the structural defects of crystalline hydroxyapatite, and those derived from bone collagen (symmetric doublet). The spin intensities of ESR signals in all investigated specimens were determined and compared. There was no indication of the spin transfer process between both types of paramagnetic species in γ-irradiated bone at room temperature. The asymmetric signal that exhibits unusual stability is proposed as a kind of physical label in biological studies of bone. (auth)

8826 RADIO-STERILIZATION OF A HYDROCORTISONE ACETATE- AND CHLORAMPHENICOL-CONTAINING OPHTHALMIC OINTMENT. 1. STUDY OF HYDROCORTISONE ACETATE AND CHLORAMPHENICOL. Hangay, Gyoergy. Acta Pharm. Hung.; 40: 17-24(Jan 1970). (In Hungarian).

Experimental data on the radiosensitivity of hydrocortisone acetate and chloramphenicol are presented. Samples were irradiated with 2.5, 5.0, and in some cases 10.0 Mrad doses, respectively. These were investigated by several physical, chemical, and biological tests; the individual parameters were compared with that of nonirradiated samples. Results are analyzed from the point of view of sterilizability of the substances and their applicability in ophthalmic ointments. (auth)

XUM

METALS, CERAMICS, AND OTHER MATERIALS

Metals and Alloys

Refer also to abstract 8439.

8827 (ANL-7691) GUIDELINES FOR SODIUM FIRE PREVENTION, DETECTION, AND CONTROL: REPORT OF THE AD HOC COMMITTEE ON SODIUM FIRES. Cissel, D. W.; Coleman, L. F.; Pancner, F. O.; Smith, F. A.; Tevebaugh, A. D. (Argonne National Lab., Ill.). Jun 1970. Contract W-31-109-eng-38. 166p. Dep. NTIS.

The problems of sodium-fire prevention, detection, and fighting are discussed, and recommendations are presented. Some pertinent literature articles are reproduced and included. (auth)

8828 (BNWL-SA-3426) MATERIALS FOR NUCLEAR REACTORS. Bush, S. H. (Battelle-Northwest, Richland, Wash. Pacific Northwest Lab.). 30 Jun 1970. 30p. (CONF-700934-1). Dep. NTIS.

From 2nd International Conference on the Science of Materials, Tremezzo, Italy.

In a system as complex as a nuclear reactor, it is difficult to present more than a cursory discussion of the materials that make up the core region. An overview of the principal reactor materials and some of the associated problems during reactor operation is presented. (auth)

8829 (ORNL-4600) FUELS AND MATERIALS DEVELOPMENT PROGRAM. Quarterly Progress Report for Period Ending June 30, 1970. Patriarca, P. (comp.); Rucker, D. J. (ed.) (Oak Ridge National Lab., Tenn.). Nov 1970. Contract W-7405-eng-26. 296p. Dep. NTIS.

Research progress is reported in twenty-six sections. A separate abstract was prepared for each section. (J.R.D.)

For abstracts of individual sections see: 8439, 8440, 8835–8838, 8847–8854, 8869, 8870, 8909–8912, and 8952–8957.

8830 PLUTONIUM-DOKUMENTATION. Referate-Zietschrift mit Anhang Transplutonium-Elemente. Oktober 1970. Band 4, Heft 10. 231 Referate (Register-Nr.3379-3841) 55 Referate (Register-Nr.479 T-533 T). (Plutonium-Documentation. Abstract Journal with Appendix on Transplutonium Elements. October 1970. Vol. 4, No. 10. 231 Abstracts (Register No. 3379-3841) 55 Abstracts (Register No. 479 T-533 T)). Karlsruhe, Ger.; Gesellschaft fuer Kernforschung m.b.H. (1970). 132p. (In German and English).

8831 PLUTONIUM-DOKUMENTATION. Referate-Zeitschrift mit Anhang Transplutonium-Elemente. 3. Vierteljahresregister 1970. Band 4, Heft 7-9. (Plutonium-Documentation. Vol. 4, No. 7-9, 1970). Karlsruhe, Ger.; Gesellschaft fuer Kernforschung m.b.H. (1970). 64p. (In German and English).

Corrosion and Erosion

Refer also to abstracts 8389 and 8395.

8832 (AEC-tr-7204) EFFECTS OF HALIDES ON ANODIC POLARIZATION OF ZIRCONIUM IN AMMONIUM NITRATE SOLUTION. Morozumi, Taksashi; Moriya, Makoto; Ohashi, Hiroshi. Translated from Boshoku Gijutsu; 18: No. 3, 104-9(1969). 13p. Dep. NTIS.

Various ammonium halide salts were added to an aqueous solution whose principal electrolyte was NH_4NO_3, and the effects of these additions on the anodic polarization characteristics of electropolished zv at constant potential and constant current were measured. It was found that when the solution contained only NH_4NO_3, the logarithmic law applied to the formation of a thin passive film in transient polarization at constant potential and constant current. The addition of a halide, such as Cl^-, Br^-, or I^-, resulted in an initial stage very similar to that with NH_4NO_3 itself, but the passive surface was broken and pitting began to take place on the specimen surface once the induction step had stopped. NH_4NO_3 usually tends to act toward suppressing this destruction of the passive state, but the degree of this effect differs with the halide. Fluoride at rather low concentration destroys the passive state and initiates an oscillatory phenomenon. The entire Zr surface was corroded or dissolved in the presence of fluoride. (auth)

8833 (AERE-M-1854) PRELIMINARY CORROSION TESTS ON SOME STEAM TREATED ZIRCONIUM ALLOYS. Walters, G. P. (Atomic Energy Research Establishment, Harwell (England)). Mar 1967. 4p. Dep. NTIS (U. S. Sales Only).

Corrosion tests at 300 and 600°C were carried out on zirconium, Zircaloy-2, Zr-1%Se and Zr-1%Ge. All specimens steam treated at 300°C, up to 300 hr, had adequate corrosion resistance. However, at 600°C none of the materials tested were satisfactory; severe surface and internal oxidation occurred. (auth) (UK)

8834 (COO-2069-6) A STUDY OF THE MECHANISMS OF STRESS CORROSION CRACKING IN THE IRON-NICKEL-CHROMIUM ALLOY SYSTEM IN CHLORIDE ENVIRONMENTS. Quarterly Report, December 1, 1969–March 31, 1970. Staehle, R. W. (Ohio State Univ. Research Foundation, Columbus). 24 Jun 1970. Contract AT(11-1)-2069. 62p. Dep. NTIS.

Results of studies are reported on work using circulating autoclaves, weight loss in boiling $MgCl_2$ solutions, transient dissolution, morphology of sensitized stainless steel, and work on the partial current dissolution of Fe-Cr-Ni alloys. Results of autoclave studies show that the performance of the higher nickel alloys continued to improve as the $Cl^- + O_2$ is lowered into the 1 to 5 ppM range. At 10 ppM Cl^- + 10 ppM O_2 Incoloy 800 cracks easily; at concentrations below this cracking is progressively less likely. Weight loss data for 51 alloys exposed up to 154°C were carried out for six months. In general, the Fe-Cr-Ni base alloys exhibit weight loss behavior typical of film covered materials where the exponent of time in $\Delta\omega = at^n$ is in the range of 0.05 to 0.40. Only the alloys containing the platinum element exhibit higher exponents. Grains from sensitized stainless steels were examined in the scanning electron microscope after they had been removed by chemical attack. The results defined the general distribution of chromium-depleted regions. Work on the time-dependence of reactions for film growth in acid and neutral solution demonstrated that certain portions of the kinetic behavior follow well-known inverse logarithm behavior. Results of the studies on Fe-Ni electrodes show that the specific rate constants for Fe and Ni dissolution in a given alloy are the same, providing the alloys are dissolving in the activated region of potentials where Tafel behavior applies. (auth)

8835 (ORNL-4600, pp 57-64) EFFECT OF POWER CYCLING ON LMFBR FUEL-CLADDING BEHAVIOR. (Oak Ridge National Lab., Tenn.).

From Fuels and materials development program.

Results of investigations of the effects of power cycling on fuel behavior and the mechanical interaction of fuel and cladding for a liquid-metal-cooled fast breeder reactor (LMFBR) are reported. The initial objectives of the study are to compare the mechanical interaction of mixed oxide fuel and cladding during thermal cycling conditions typical of those to be expected in an LMFBR. The first two capsules for power cycling in-reactor are planned as prototype fuel pins for the Fast-Flux Test Facility Reactor to operate in the poolside facility of the Oak Ridge Research Reactor in such a fashion as to measure in-reactor, the axial extension of the fuel column and cladding and the internal gas pressure of the fuel pin during operation. The design effort on the first capsule (MINT-1) is progressing satisfactorily. The capsule design is now being detailed. (auth)

8836 (ORNL-4600, pp 157-66) SODIUM CORROSION STUDIES. (Oak Ridge National Lab., Tenn.).

From Fuels and materials development program.

The partitioning of O between V alloys and Na at 600°C was investigated. The addition of Mo to V lowered the concentration of O entering into solid solution during equilibration with Na. Vanadium alloys that contained Zr additions were internally oxidized by O in Na. The effect of N contamination on the creep properties of unalloyed V was determined at 600°C. Interaction of N with V at N_2 pressures to 3.4×10^{-6} torr lowers the creep strength; however, on the basis of time required to produce a given strain, V was strongest at a N_2 pressure of 1.5×10^{-6} torr. A bimetallic thermal-convection loop composed of V and Type 321 stainless steel was examined following operation with Na for 3000 hr at a maximum temperature of 700°C. Insert specimens of V increased in C, N, and O; however, the amount picked up at 700°C was less than that for an earlier loop with Type 304 stainless steel rather than Type 321 stainless steel. The tensile properties of the hottest V inserts were not noticeably changed by the test exposure. The effect of Na leakage on the oxidation of Type 304L stainless steel was studied in a N_2 + 1% O_2 mixture that contained 100 ppM H_2O. Sodium was passed through a defect in a stainless steel tube at 760°C and into a contiguous thermal insulation layer which also was at 760°C. Unlike earlier tests in which the tube was heated but not the insulation, there was no

XUM

plugging of Na in the defect; the Na was quickly absorbed by the insulation with negligible oxidation of the stainless steel. (auth)

8837 (ORNL-4600, pp 216-22) CORROSION STUDIES OF ADVANCED REFRACTORY METALS. (Oak Ridge National Lab., Tenn.).

From Fuels and materials development program.

Testing of a forced-circulation loop of T-111 with Li at high temperature was completed. The loop operated for 3000 hr at a maximum temperature of 1370°C. A vent line that failed after 1735 hr was successfully repaired. Additional thermocouples were attached to the loop during this repair, and a very accurate measurement of the temperature distribution and Li flow rate during subsequent operation was obtained. Results of failed vent line analyses indicated that the failure was not produced by any effect of the Li. Rather, it appears to have been caused by traces of Ni that had contaminated the failed area before or during fabrication of the loop. (auth)

8838 (ORNL-4600, pp 282-6) ADVANCED MATERIALS FOR STEAM GENERATORS. (Oak Ridge National Lab., Tenn.).

From Fuels and materials development program.

A comparison of the general corrosion at 650°C of weldments of alloys for steam generators with results for unwelded specimens exposed at 620°C showed that in spite of the temperature difference the weldments are less susceptible to corrosion. Although the steam used in unwelded specimen exposure contained 20 ppM O and 2.5 ppM H, compared with undetectable levels in the weldments tests, the lower corrosion of the weldments is attributed to differences in surface condition. Studies designed to show differences in corrosion at 595 and 650°C of root passes (the ones exposed to the steam side of heat exchangers) of weldments as a function of differing composition and surface condition revealed large differences in amounts of corrosion. At the extremes, the corrosion rates of type 304 stainless steel welded with type 308 stainless steel and Incoloy 800 welded with Inconel 82 with the as-welded finish were two orders of magnitude higher than those of Hastelloy X joined to Incoloy 800 with Inconel 82 with the as-welded, ground, sandblasted, and electropolished finishes. (auth)

8839 (ORNL-TM-3188) PROGRESS IN ZIRCALOY CLADDING FAILURE MODES RESEARCH. Rittenhouse, P. L. (Oak Ridge National Lab., Tenn.). Dec 1970. Contract W-7405-eng-26. 34p. Dep. NTIS.

Recent results obtained in studies of cladding failure behavior (deformation, rupture, and embrittlement), the resulting blockage of the core coolant channels, and the effect of blockage on emergency cooling are described. Continuing programs in these areas of research are outlined. Recommendations are given for the extension of some existing programs and the initiation of new work. (auth)

8840 (RFP-1575) EXPLOSIVE NATURE OF URANIUM-BASE NIOBIUM ALLOYS AFTER IMMERSION IN NITRIC ACID. Jackson, Ross J.; Johns, Wilbur L. (Dow Chemical Co., Golden, Colo. Rocky Flats Div.). 8 Dec 1970. Contract AT(29-1)-1106. 5p. Dep. NTIS.

The explosive behavior of uranium-base niobium alloys after immersion in nitric acid is characterized. The explosive behavior is related to a finely divided, two-phase microstructure, and to a high carbon content. In the first case, the nitric acid selectively attacks the alpha-uranium phase leaving behind a finely divided niobium-rich gamma phase which can oxidize with explosive violence. In the second case, niobium carbide inclusions accumulate at the surface and are likewise subject to rapid oxidation. The most violent explosions occur with slow-cooled, slab-cast, high-carbon alloys having a casting scale of UO and UO_2. Nitric acid dissolves the UO and UO_2 casting scale and leaves behind a reactive surface layer of finely divided γ-U, Nb_2C, NbC, and $UO_2(NO_3)_2 \cdot 6H_2O$. When this wet or dry layer is sparked or struck, a violent decomposition occurs which rapidly produces large quantities of gases and heat, and leaves behind a residue of UO_2 on the surface of the metal. (auth)

8841 ROLE OF CONTAMINATION IN THE KINETICS OF OXIDATION NUCLEATION OF TUNGSTEN AND MOLYBDENUM. Hoover, Scott. Chicago; Illinois Inst. of Tech. (1970). 162p. University Microfilms Order No. 70-12,473.

Thesis.

The field emission microscope was used to study the influence of foreign gases on the initial oxidation stages of molybdenum and tungsten. The technique was based on the known field enhancement effect exhibited by oxide microcrystals, allowing detection following their nucleation. Reactions were studied in pure oxygen and in oxygen mixtures, at oxygen partial pressures of from 1.0×10^{-7} to 1.0×10^{-5} torr. Partial pressures of contaminating gases were within the same range. Substrate temperatures of molybdenum ranged from 380 to 755°C, and for tungsten, from 670 to 980°C. Effects of the presence of carbon monoxide were investigated with molybdenum, and of carbon monoxide, nitrogen, carbon dioxide, and methane with tungsten. For equal partial pressures of oxygen, an increase in the incubation time for the formation of oxide microcrystals on molybdenum was found to be associated with added partial pressures of carbon monoxide. Of the four foreign gases investigated with tungsten, all affected the oxidation kinetics, and all affected morphologies of the oxidized substrate. The nucleation of oxide microcrystals within preferred regions of the substrate was altered by contaminating gases in that incubation times for the appearance of the first microcrystals were increased or decreased depending on temperature, pressure and crystallography. While initial oxidation of molybdenum yielded highly discrete emission spot patterns (indicative of resolvable oxide microcrystals), both in pure oxygen and in oxygen-carbon monoxide mixtures, less emission anisotropy accompanied the initial oxidation stages of tungsten in pure oxygen. This was interpreted as being due to a lack of whisker-like growth, and possibly also to a higher surface concentration of oxide crystallites, rendering the latter less resolvable. With added low partial pressures of foreign gases, tungsten oxidation patterns exhibited more discrete local emission spots. This was believed to result from the deactivation of certain crystallographic sites or regions, which in turn promoted a greater separation between emitting crystallites that could now be resolved by the microscope. At the higher partial pressures of CO, the discrete emission now diminished which was attributed to further deactivation of the remaining active nucleation sites. The kinetic results tend to support the applicability of the heterogeneous nucleation approach to the initial stages of oxidation. (Diss. Abstr. Int., B)

8842 EFFECT OF TREATMENT OF STEEL WITH TRYLON B ON ITS HYDROGEN ABSORPTION. Margulova, T. Kh.; Gerasimov, V. V.; Lipanina, A. A. At. Energ. (USSR); 29: 209-10(Aug 1970). (In Russian).

Pearlitic steels are susceptible to hydrogen absorption which affects their mechanical properties. Results of previous studies indicated that the oxide film formed as a result of treatment with Trylon prevents the penetration of oxygen into the material; investigations were therefore conducted to examine the possibility of protecting steel against hydrogenation by the same technique. Steels used for the manufacture of steam pipes and reactor vessels were used for the study, carried out by electrolytic hydrogenation in a 5% sulfuric acid solution at a current density of 0.15 A/cm^2. The samples were treated before the hydrogenation with 500 mg/kg Trylon B solution at a pressure of 100 atm and 290°C for 6 hours, keeping them under similar conditions for another 12 hours. Some of the samples were kept in the condensate at 200 atm and 350°C for 500 hours. Mechanical tests after the treatment revealed that hydrogenation affects only slightly the strength of the steel but it changes greatly its plastic properties. The oxide film formed by the pure condensate did not protect the specimens against hydrogenation; this resulted in a practically complete loss of plasticity. The oxide film resulting from treatment with Trylon B had a strong protective action as indicated by the greatly decreased loss of plasticity. In both cases the hydrogen penetrated only between the magnetite crystals but the more closely-packed, smaller, irregular magnetite crystals created by the treatment with Trylon B reduced the gaps between the crystals and decreased the hydrogen concentration. Thus, treatment with complexions improved the properties of steel exposed to hydrogen. (TTT)

8843 OBSERVATIONS OF NEEDLE CRYSTALS OF TUNGSTEN OXIDE BY FIELD EMISSION AND ELECTRON MICROSCOPY. Okuyama, Fumio (Nagoya Inst. of Tech., Japan). J. Appl. Phys.; 42: 256-9(Jan 1971).

The needle crystals of tungsten oxide grown on the tungsten substrate from vapor phase were studied by field emission and electron microscopy. The observed FEM patterns of the needles were quite similar to the pattern of the oxidized W emitter and mostly had twofold symmetry. Less frequently, the FEM patterns having nearly threefold and fourfold symmetries could be observed. From the comparison of the electron micrographs as well as the FEM patterns of a needle and an oxidized W emitter, evidence was obtained that the surface of the oxidized emitter tip had been covered with thin layer of a crystallized tungsten oxide. (auth)

Preparation and Fabrication

Refer also to abstracts 8236, 8390, 8391, 8461, and 8917.

8844 (AERE-M-1561) HOMOGENISING THE STRUCTURES AND MECHANICAL PROPERTIES OF WELDED ZIRCALOY 2

TUBES. Davies, J. M.; Steer, C. (Atomic Energy Research Establishment, Harwell (England)). Sep 1965. 31p. Dep. NTIS (U. S. Sales Only).

Variations in the structures and mechanical properties of the parent material, the welds and the heat affected zones in butt welded Zircaloy-2 tubes are examined. A technique combining planetary swaging and heat treatment to homogenise the material is described. The results of metallography, hardness testing, and hydraulic pressure burst testing indicate that excellent homogenisation is achieved using this technique. (auth) (UK)

8845 (AERE-R-5483) AN INVESTIGATION INTO THE METALLOGRAPHIC EXAMINATION OF SODIUM. Taylor, A.; Mott, B. W. (Atomic Energy Research Establishment, Harwell (England)). May 1967. 16p. Dep. NTIS (U. S. Sales Only).

The results are described of various preliminary experiments to establish a technique for the metallographic examination of sodium with particular reference to the slicing of sections by means of a microtome mounted in a dry-box and operated under purified argon. It is concluded that the microtome method of preparation of surfaces offers the best solution but it is essential to use a blade with a cutting edge of the highest possible quality to reduce the number and depth of the grooves produced. The cut surface must be kept in an atmosphere containing less than 2 ppM of moisture or oxygen to avoid rapid oxidation, and a suitable chamber for this and for viewing the specimen under a microscope through an optical glass window is described. Possible ways in which the technique might be improved are discussed. It appears however that only marginal improvements can be achieved unless expensive dry-box equipment can be provided for carrying out both the preparation and examination of specimens in highly purified atmospheres. (auth) (UK)

8846 (KFK-1252) UAl_3-Al AS DISPERSION FUEL FOR HIGH-FLUX REACTORS. Nazare, S.; Ondracek, G.; Thuemmler, F. (Kernforschungszentrum, Karlsruhe (West Germany). Institut fuer Material- und Festkoerperforschung). Aug 1970. 83p. (In German). Dep. NTIS (U. S. Sales Only).

The interaction between the phases and the properties of UAl_3-Al dispersions is reviewed. The preparation of single-phase UAl_3 and fabrication of fuel dispersions with Al (28.43 vol % UAl_3-50 wt % UAl_3) are described. Hot rolling (picture frame technique) of Al-clad fuel element plates of this dispersion is also described. Metallographic and x-ray methods are used to control the quality of such fuel plates. The reaction between UAl_3 and Al occurs at 450°C and leads to the formation of UAl_4. The kinetics of this reaction have been studied qualitatively with a hot stage microscope and quantitatively with a dilatometer as well as quantitative metallography. The activation energy of the reaction is about 60 kcal/mol. The course of the reaction can be described in an intermediate range with models (Jander, Carter). Addition of ternary elements such as Si (3 wt %) can suppress the reaction. Some properties of such dispersions (thermal expansion, thermal and electrical conductivity, Young's modulus, and 0.2% proof stress and tensile strength) have been measured as a function of the UAl_3-concentration. The influence of the reaction on properties has been investigated. The 0.2% proof stress and tensile strength of Al-clad fuel plates (~28 vol % UAl_3) have been obtained as a function of the temperature. The results are discussed in the light of existing theories. (auth)

8847 (ORNL-4600, pp 126-30) FABRICATION DEVELOPMENT FOR LMFBR STAINLESS STEEL TUBING. (Oak Ridge National Lab., Tenn.).

From Fuels and materials development program.

An investigation of the use of artificial defects to simulate natural defects in tubing is continuing. Additional specimens have been prepared for testing mechanical properties at elevated temperatures. Modifications to the planetary swager were completed. By combining the more conventional process of mandrel drawing with planetary swaging, the possibility of improved quality and properties for type 316 stainless steel tubing is being investigated. It appears that tubes manufactured by this combined process are about 10% stronger but less ductile than tubes produced by mandrel drawing alone. Increasing the rotational speed of the swager head and bench speed increased the strengths with no significant changes in ductility. (auth)

8848 (ORNL-4600, pp 131-41) WELDING DEVELOPMENT FOR LMFBR VESSELS AND COMPONENTS. (Oak Ridge National Lab., Tenn.).

From Fuels and materials development program.

Submerged-arc weldments were prepared in 1-in.-thick Type 304 stainless steel with a variety of commercial fluxes and a range of energy input conditions. Tests of mechanical properties showed these welds to be consistently weaker but much more ductile than similar shielded metal-arc welds. Composite (fusion-line) specimens showed lower strength in the base metal but ruptured in the stronger weld metal due to the early initiation and short duration of third-stage creep in the weld metal. Welds made with various energy inputs showed more substantial variations in mechanical properties after longer test times. Corrosion studies by means of the Strauss Test on heat-treated weldment specimens are being performed in conjunction with extensive metallographic heat-treatment studies. An irradiation program involving 226 weldment specimens was designed; all specimens were machined, and installation into the irradiation assembly was begun. Metallographic studies have continued, emphasizing the effect of the amount and morphology of the delta-ferrite phase on subsequent metallurgical reactions and mechanical properties at elevated temperatures. (auth)

8849 (ORNL-4600, pp 142-6) SHIELDED METAL-ARC WELDING FOR LMFBR COMPONENTS. (Oak Ridge National Lab., Tenn.).

From Fuels and materials development program.

Results of prior investigations indicated that the decreasing ductility with increasing time to rupture at 650°C exhibited by the standard lime-TiO_2-coated electrode was due primarily to formation of sigma phase at the phase boundaries. However, results of new creep-rupture tests at 593°C indicate that the loss in ductility is still severe after 1000 hr at the testing temperature. This may imply that precipitation of carbides causes some of the phase-boundary instability. Three experimental batches of lime-coated electrodes were added to the program. These new batches contain additions of ferro-titanium, ferro-titanium plus B, and ferro-titanium plus B and P. These additions significantly increase rupture life and rupture ductility. Results of further tests at 650°C indicate that additions of C increase the strength somewhat while only slightly improving the ductility. However, additions of B and P, as indicated above, tend to increase the rupture time and ductility more than C. (auth)

8850 (ORNL-4600, pp 181-5) CLADDING MATERIALS FOR SPACE ISOTOPIC HEAT SOURCES. (Oak Ridge National Lab., Tenn.).

From Fuels and materials development program.

Efforts to develop alloys with optimum strength and resistance to oxidation for use as cladding materials for space isotopic heat sources were continued. Partial replacement of Cr with Ti in the ordered Pt_3Cr alloy increased hardness and critical temperature for ordering. Additions of Hf to form ordered Pt_3Hf in Pt-Mo and Pt-W solid-solution alloys are also being investigated to improve strength and retard grain growth at high temperatures. The weight losses of alloys Pt_3Cr and Pt-0.6% W-1% Hf in air oxidation tests at 1000°C approximated that of pure Pt while $Pt_3(Cr_{0.84},W_{0.16})$ gained weight at the same low rate. (auth)

8851 (ORNL-4600, pp 186-97) PHYSICAL AND MECHANICAL METALLURGY OF REFRACTORY ALLOYS. (Oak Ridge National Lab., Tenn.).

From Fuels and materials development program.

The existence of a stable miscibility gap in the Ta-Zr system was confirmed by x-ray studies of a Ta-43.5 wt % Zr alloy. The diamond pyramid hardness (DPH) of this alloy decreases from about 500 to about 300 DPH after aging for 4×10^3 min at 850°C. The precipitation of uniform Hf-rich particles in Ta-Hf alloys is attributed to the possible existence of a metastable miscibility gap with a critical temperature of about 1400°C. The oxidation rate of Ta-65 wt % Hf at 1000°C in air is comparable to the rates of the complex Hf-Ta base alloys developed by the Illinois Institute of Technology Research Institute, Chicago. Crack-free zones observed at the surfaces of ruptured creep specimens of alloy C-129Y are attributed to interstitial contamination. Measurements of the width of these zones agree with the diffusion rates of interstitials in Nb. The compatibility of Ta and Pt with various metals at 1200°C was studied to find a suitable transition barrier between tubular welds of these metals. The thermal conductivity of Ta, estimated from experimentally derived low-temperature phonon conductivity and Lorenz function values, is within 3% of the recommended values to 3000°K. (auth)

8852 (ORNL-4600, pp 198-209) TUNGSTEN METALLURGY. (Oak Ridge National Lab., Tenn.).

From Fuels and materials development program.

In development of chemical vapor deposition large sheet deposits of W with a low F impurity content were produced by cooling the deposition chamber. Preliminary experiments were performed on the deposition of W with a {110} orientation from WCl_6. A study of the effect of gas composition on formation of nodules and porosity in W-5% Re deposits showed that the best deposits are produced at a stoichiometric mixture of H_2, WF_6, and ReF_6. Bend tests of chemically vapor deposited W specimens joined by gas W-arc welding showed that 0.050-in.-thick material had a

XUM

ductile-to-brittle transition temperature greater than 550°C whereas 0.030-in.-thick material bent at 450°C. Data on the secondary creep rate at 1200 to 2200°C for arc-melted W, W–5% Re, W–26% Re, W–25% Re–30% Mo and chemically vapor deposited W are presented. Data for arc-melted W agreed with data from three other sources. The creep rate varied with the hyperbolic sine of the stress. The creep strength of W–25% Re in an atmosphere of 10^{-6} torr O_2 was greater than in a vacuum of 10^{-8} torr. This effect is opposite to that observed in unalloyed W. (auth)

8853 (ORNL–4600, pp 249) TECHNICAL ASSISTANCE IN PROCUREMENT OF FUEL ELEMENTS. (Oak Ridge National Lab., Tenn.).

From Fuels and materials development program.

Various possibilities are being examined to explain why some fuel plates have small holes or cracks in the cladding that expose the fuel composite to the reactor coolant. (auth)

8854 (ORNL–4600, pp 252-65) JOINING RESEARCH ON NUCLEAR MATERIALS. (Oak Ridge National Lab., Tenn.).

From Fuels and materials development program.

Elevated-temperature (650°C) tensile data obtained for welds on Incoloy 800 base metal showed that the Inconel 82T commercial filler metal has the best strength and ductility properties. The welds made from filler metals prepared from an electroslag-remelted commercial heat of Incoloy 800 and the experimental heat that contained P had strengths comparable to that of the Inconel 82T welds. The ductility of the Inconel 82T filler metal at 650°C was considerably better than that of either of the other two filler metals. Studies of the ductility of Inconel 600 at intermediate temperatures were initiated. Preliminary data indicate that this alloy loses ductility in the 600°C temperature range. A ternary composition, Ni–15.5% Cr–8% Fe, did not recover its ductility at 900°C. The quantitative television microscope is being used to determine the correlation between the Magne-gage readings currently being used to measure qualitatively the amount of ferrite in the microstructure of the experimental stainless steel alloys. The investigation of the interrelationship between ferrite and martensite on the properties of stainless steel weldments is continuing. Martensite was produced by cold rolling. Its presence is verified by the Magne gage. Metallographic studies by means of bright-field optical microscopy did not satisfactorily differentiate the martensite and slip and mechanical twins. Some success was obtained with phase-contrast microscopy. The use of a magnetic-particle etching technique that appears to permit the identification of the martensite is being investigated. (auth)

8855 PLASMA SPRAYING OF TUNGSTEN. Glaetzle, R.; Benesovsky, F. (Metallwerk Plansee AG, Reutte, Austria). Metall; 24: 823-9(Aug 1970). (In German).

Deposition of surface layers of tungsten by plasma spraying is discussed. The influence of the most important spraying variables such as electric power, gas flow, spraying distance, amount of powder, and powder grain size on the thickness and texture of the sprayed layer was investigated. (M.C.G.)

8856 COLOMBIUM ALLOY. (to Union Carbide Corp.). French Patent 1,573,413. 27 May 1969. Filed 1 Jul 1968. (In French).

The development of an alloy composed of 5% V, 1% Zr, 0.005 to 0.4% C and not less that 92% Nb by weight with important nuclear applications is described. The alloy has good corrosion resistance in hot water, water vapor, and other analogous media that exist in thermal reactors. Data on neutron absorption, in barns, are given. (P.C.H.)

8857 BEHAVIOR OF CANS AND CENTERING DEVICES. Weisz, M.; Millet, P. (CEA, Saclay, France). Bull. Inform. Sci. Tech. (Paris); No. 148: 33-54(May 1970). (In French).

The recent work carried out on cans, centering devices and plugs is presented. It is possible to stop the diffusion of plutonium by placing a graphite or aluminum barrier between the fuel and the can. The ductility of the Mg-Zr alloys is good in spite of structural modifications occuring during the operation. By blocking the centering device in the jacket it is shown that the device has a good fatigue resistance. The problem of the creep resistance of the plug is solved by using Mg–Mn or sintered Mg–Zr alloys. (auth) (France)

8858 PRODUCTION OF THIN METALLIC SINGLE CRYSTALS. Gregory, W. D.; Superata, Michael A. (Georgetown Univ., Washington, D. C.). J. Cryst. Growth; 7: 5-8(Jul–Aug 1970).

A technique is described for obtaining thin metallic single crystals for use in a variety of measurements. The method has been used successfully to make gallium and indium single crystal plates as thin as 25 μm. (auth)

8859 DROPS OF OXIDES ON TUNGSTEN OXIDE NEEDLES AND NUCLEI OF DENDRITIC CRYSTALS. Hashimoto, Hatsujriro (Kyoto Technical Univ.); Kumao, Akihiro; Eto, Terukazu; Fujiwara, Kishio. J. Cryst. Growth; 7: 113-16(Jul–Aug 1970).

The formation of small crystals in drops of tungsten oxides from which needle crystals are grown is reported. Electron microscopy was used in the study. (auth)

8860 ALUMINUM PRODUCTS STRENGTHENED BY DISPERSION. (to Atomenergikommissionen). French Patent 1,573,897. 2 Jun 1969. Filed 16 Jan 1968. (In French).

A method for producing aluminum products of high ductility is described. Powdered Al is mixed with powdered ZrO_2, HfO_2, CeO_2, PrO_2, TiO_2, UO_2, or SiO_2. The mixture is compacted and heated. During the superficial reduction of the oxides by the Al, an intermediate layer is formed that binds the oxide particles to those of Al. The product obtained has a satisfactory mechanical resistance at high temperatures. (J.G.B.)

Properties Evaluations

Refer also to abstracts 8427, 9580, 9589, and 10197.

8861 (AD–709580) FATIGUE BEHAVIOR OF MOLYBDENUM. Stephens, R. I.; Dubensky, R. G.; Frauen, L. L.; Wrenn, R. L. (Iowa Univ., Iowa City. Dept. of Mechanical Engineering). May 1970. 27p. NTIS.

Contract DAAF03-69-C-0014.

The objective of the research was to further elucidate the fatigue behavior of commercially pure arc-cast polycrystalline molybdenum; in particular, to investigate the possible relationship between the French damage line and cyclic dependent yield behavior, and to determine coaxing phenomena as a function of grain size. Although the French damage line and the cyclic yield point removal line appear macroscopically similar, the mechanisms proposed for these two phenomena are quite different. The removal of the upper yield point under cyclic stress conditions is explained in terms of localized cumulative multiplication of mobile dislocations, whereas the French damage line is explained in terms of the initiation and propagation of microcracks. Molybdenum, vacuum annealed at 2150, 2600, and 3000°F with resulting ASTM grain sizes of 7 to 8, 4 to 5 and 2 to 3 respectively, was subjected to various coaxing patterns. Using a cycle ratio summation as a criteria, no definite coaxing response pattern occurred for all three molybdenum grain sizes. Cycle ratio summations n/N ranged from .004 to 808. Thus, molybdenum did respond to coaxing under certain applied stress and cycle increment conditions. (auth) (USGRDR)

8862 (AD–709957) THERMODYNAMICS OF VANADIUM ALLOYS. PART I. MASS SPECTROMETRIC DETERMINATION OF THERMODYNAMIC PROPERTIES OF VANADIUM–TITANIUM ALLOYS. Final Report, January 1969–April 1970. Rolinski, Ednund J. (Air Force Materials Lab., Wright–Patterson AFB, Ohio); Hoch, M.; Oblinger, C. J. (Cincinnati Univ., Ohio). Jun 1970. Contract F33615-67-C-1565. 51p. (AFML-TR–70-119(Pt.1)). NTIS.

The Knudsen effusion method was combined with a mass spectrometer sensing technique in order to measure thermodynamic quantities of solid solution alloys of V–Ti in the bcc(beta) phase. The technique makes use of the regular solution model in order to treat the vaporization data in terms of ion current ratios obtained from the mass spectrometer. The internal consistency between the data was demonstrated by calculating the relative electron impact ionization cross sections and found to agree with previously reported calculated results. The pairwise interaction parameter for the V–Ti binary alloys was found to be 1.82 plus or minus 0.13 kcal/g-atom for the experimental temperature range of 1500 to 1725°C and for .10 < N sub Ti < .90 at. %. The experimental result on the pairwise interaction parameter agrees with the theoretically calculated value. (auth) (USGRDR)

8863 (BMI–1891) PROGRESS ON LMFBR CLADDING, STRUCTURAL, AND COMPONENT MATERIALS STUDIES DURING JULY THROUGH SEPTEMBER 1970. Quarterly Report. Keller, Donald L. (Battelle Memorial Inst., Columbus, Ohio). Oct 1970. Contract W-7405-eng-92. 12p. Dep. NTIS.

Research and development progress is reported in two sections, a separate abstract was prepared for each section. (J.R.D.)

For abstracts of individual sections see: 8864 and 8895.

8864 (BMI–1891, Sect.A) DEVELOPMENT OF MECHANICAL-PROPERTY DESIGN DATA FOR REACTOR MATERIALS. (Battelle Memorial Inst., Columbus, Ohio.). 8p.

Low-cycle strain-controlled fatigue tests were conducted on solution-annealed Incoloy 800 specimens at 1000, 1200, and 1400°F. Eight of the specimens were tested under strain-controlled cycling with hold times at the tensile strain limit only, and one was tested at 1000°F with a 10-min hold time at the compressive strain limit only. Specimens tested with only tension hold times exhibited significantly lower fatigue lives than specimens tested with no hold times. (auth)

8865 (CEA-R-4066) DETERMINATION OF SMALL SOLUBILITIES BY MEASUREMENT OF CHEMICAL DIFFUSION COEFFICIENTS: APPLICATION TO THE NICKEL-URANIUM SYSTEM. Zanghi, Jean-Pierre (Commissariat a l'Energie Atomique, Fontenay-aux-Roses (France). Centre d'Etudes Nucleaires). Oct 1970. 79p. (In French). Dep. NTIS (U. S. Sales Only).

Thesis. Submitted to Univ. of Paris, Faculte des Sciences, Orsay, France.

The solubility $S_{(o)}$ of uranium in nickel was determined by diffusion technique in a polyphased system, on welded couples made of pure nickel and of a two-phase nickel-uranium alloy (saturated matrix of nickel and UNi_5 precipitates). The two following equations were obtained: $\epsilon = 2\gamma\sqrt{Dt}$ and $(S_o/C_o - S_o) = \sqrt{\pi}\gamma(I + \text{erf}\ \gamma) \exp \gamma^2 = f(\gamma)\sqrt{\pi}$ in which epsilon is the displacement of the boundary between the one-phased and the two-phased zones, γ is a constant, D is the chemical diffusion coefficient of uranium in nickel, t is the annealing time and C_o is the uranium concentration in the nickel-uranium alloy. Epsilon was measured with welded couples, D was determined using the thin layer method, $f(\gamma)$ was tabulated, so that $S_{(o)}$ could be derived from the two equations. D is expressed in the form of $D = 1\ cm^2 \cdot s^{-1} \exp(-56400/RT)$. S_o varies from 0.18 up to 0.35 atom per cent U between 975 and 1075°C. The enthalpy and entropy associated with the dissolution are respectively 20 kcal/mole and 3.6 cal $°K^{-1}$ mole. (auth) (France)

8866 (GEAP-10205) STATUS OF PIPE RUPTURE STUDY AT GENERAL ELECTRIC COMPANY. PART III. Vandenberg, S. R. (General Electric Co., San Jose, Calif. Atomic Power Equipment Dept.). Jun 1970. Contract AT(04-3)-189. 72p. Dep. NTIS.

The Pipe Rupture Study is designed to extend the understanding of failure-causing mechanisms, and to provide improved capability for evaluating reactor piping systems to minimize the probability of failures. A review to determine the effort most needed to improve nuclear system piping analytical and experimental efforts is presented. The accomplishments of a broad program in fatigue studies through both bench-scale and large-component tests, at-reactor tests of the effect of primary coolant environment on the fatigue behavior of piping steels, fracture mechanics, solution of problems in stress analysis, and failure probability study of actual reactor piping systems are summarized. (auth)

8867 (NLCO-1060) ELEVATED-TEMPERATURE TENSILE TESTS OF CAST URANIUM-BASE DILUTE QUINARY ALLOYS. Randall, P. O.; DuVall, R. E. (National Lead Co. of Ohio, Cincinnati). Nov 1970. Contract AT(30-1)-1156. 9p. Dep. NTIS.

Cast uranium-base alloys containing additions of 1000 ppM or less of carbon, iron, silicon, and aluminum were tensile-tested at temperatures of 885, 1025, and 1150°F. An alloy containing 1000 ppM C, 1000 ppM Fe, 1000 ppM Si, and 1000 ppM Al exhibited the best combination of low-temperature strength with high-temperature ductility. (auth)

8868 (NSJ-tr-159) FATIGUE STRENGTH OF NUCLEAR PRESSURE VESSEL MATERIAL ASTM A 302 B STEEL AND ITS WELDED JOINTS. Sakabe, Kiyozo; Tsukada, Hisashi. Translated from Nippon Seiko Giho; No. 25, 2938-46(Feb 1969). 24p. Dep. NTIS (U. S. Sales Only).

An abstract of this paper, prepared from the original language, appeared as NSA 23: 32032.

8869 (ORNL-4600, pp 147-52) PROPERTIES OF FERRITIC STEEL WELDS. (Oak Ridge National Lab., Tenn.).

From Fuels and materials development program.

A program is described in which the weldabilities of four types of ferritic steel for liquid-metal-cooled steam generators are compared. The materials include plain-C steels (for background data), 2.25% Cr-1% Mo low-alloy steel, low-C (0.02% C) 2.25% Cr-1% Mo steel, and stabilized 2.25% Cr-1% Mo steel. The overall weldability of these materials will be assessed by use of such weldability tests as the VARESTRAINT, Lehigh restraint, TIGA-MAJIG, and Duffer's Gleeble tests. A thorough search into the weldability of these steels has included correspondence and discussion with various domestic and foreign organizations and firms. Conflicting reports have been received concerning the weldability of the stabilized 2.25% Cr-1% Mo steels. Specimens for Lehigh restraint tests were machined from the standard 2.25% Cr-1% Mo steel plate and were ordered from SAE 1010 steel plate. A Jominy test was run on the stabilized material, and specimens for Duffer's Gleeble and TIGAMAJIG weldability tests were also made from this material. Great care was taken to assure identical microstructures in the as-received material and the prepared specimens. (auth)

8870 (ORNL-4600, pp 271-81) IMPROVEMENT OF HASTELLOY N AND RELATED COMPOSITIONS. (Oak Ridge National Lab., Tenn.).

From Fuels and materials development program.

The mechanical properties of several heats of modified Hastelloy N were evaluated after irradiation at 760°C to a thermal fluence of 3×10^{22} neutrons/cm^2. Alloys were studied containing additions of Ti, Hf, and Nb, both singly and in combination; those containing at least 0.5% Hf seemed to have the highest ductilities. These additions had very little effect on the creep strength except that one alloy that contained 3% Ti was very strong but had low ductility. Some small commercial heats of these alloys were procured for study. Transmission electron microscopy revealed several differences in the microstructures of the commercial alloys and those of our laboratory melts. (auth)

8871 (ORNL-TM-3244) STRESSES IN OUT-OF-ROUND PIPE DUE TO INTERNAL PRESSURE. PHASE REPORT NO. 115-8. Rodabaugh, E. C. (Battelle Memorial Inst., Columbus, Ohio). Jan 1971. Contract W-7405-eng-26. 70p. Dep. NTIS.

For Oak Ridge National Lab., Tenn.

A nonlinear strength of materials formulation was developed for the elastic bending stresses caused by internal pressure in an out-of-round pipe. The formulation is based on the assumptions that thin-walled shell theory is valid and that deviations from a circular cross-sectional shape are small in comparison with the average radius of the pipe. For the general solution, both the initial cross-section and the deformed shape are represented by Fourier sine-cosine series. Elliptical cross-sections and cross-sections which have either flat spots or peaks are treated as special cases of the general nonlinear solution. The results obtained using the analytical method are compared with experimental results with good agreement. Comparisons are also made with published linear analyses for the elliptical cross-sections and for the cross-sections with a peak. The nonlinear analysis gives generally lower maximum stress values. Stress indices and proposed design rules were developed for use in the nuclear piping codes and standards. For piping which meets certain minimum dimensional tolerance requirements, use of these rules eliminates the need for detailed inspection or special design stress evaluations as required by USAS B31.7-1969. (auth)

8872 (WCAP-7579) HEAVY SECTION STEEL TECHNOLOGY PROGRAM. TECHNICAL REPORT NO. 11. NOTCH PREPARATION IN COMPACT TENSION SPECIMENS. Mager, T. R. (Westinghouse Electric Corp., Pittsburgh, Pa. PWR Systems Div.). Nov 1970. Contract W-7405-eng-26; Sub-contract 3196. 31p. Dep. NTIS.

For Oak Ridge National Lab., Tenn.

The effects of fatigue precrack stress level, corrosive environment, and brittle crack initiation were evaluated on the fracture toughness, K_{Ic}, of A533 Grade B Class 1 Steel (HSST Plate 02). Fatigue precracking was done at two different temperatures and two different stress intensity levels. Results indicated that notch preparation is an important factor in fracture toughness testing. In addition, it was shown that use of an electron beam starter weld would be feasible as a means to initiate a flaw for simulated pressure vessel service tests. (auth)

8873 PRODUCTION AND PROPERTIES OF DISPERSION HARDENED Cu. PART II. Ruehle, M. (Metallgesellschaft AG, Frankfurt am Main. Vereinigte Deutsche Metallwerke AG, Frankfurt am Main). Metall; 24: 852-7(Aug 1970). (In German).

Properties of dispersion-hardened copper, with Al_2O_3, BeO, SiO_2, MgO, W, and ThO_2 as the dispersed phases, are discussed. Recovery and recrystallization, short-time hardness, creep behavior, stability, and uses are discussed. (53 references). (M.C.G.)

8874 HIGH-TEMPERATURE EMBRITTLEMENT OF THE BINARY Mg-Zr ALLOY BY HYDROGENATION. Dabosi, F. (CEA, Saclay, France); Millet, P.; Viatte, M.; Pegoud, J. Mem. Sci. Rev. Met.; 67: 507-18(Jul-Aug 1970). (In French).

Hydrogenation of $MgZr_{0.5}$ alloys led to the precipitation of zirconium in the form of hydride. At high temperatures a hardening of the matrix connected with this precipitation was observed, together with an improved ductility due to limitation of grain growth, the joints being strongly held by the precipitates. The development of these properties, revealed by ex-

XUM

trusion tests under traction, was analyzed as a function of various values of the grain size-insoluble Zr content couple. The influence of each of these two factors on the ductility to rupture was studied and it was shown that the embrittlement effect, bound up with the precipitation of hydride, was all the more pronounced as the grain size was large. The embrittlement observed was due to the formation and development of cavities in the zones deprived of precipitates, zones which appeared on either side of grain boundaries normal to the axis of application of the tensile stress. (auth) (France)

8875 SOLUBILITY OF $M_{23}C_6$ IN TYPE 316 STAINLESS STEEL. Deighton, M. (Fulmer Research Inst., Ltd., Stoke Poges, Eng.). J. Iron Steel Inst. (London); 1012-14(Nov 1970).

The solubility of $M_{23}C_6$ in type 316 steel containing 16.9% Cr, 14% Ni, 2.7% Mo, and 50 to 2000 ppM carbon was determined because of interest in this steel as a canning material in gas cooled nuclear reactors, by electron metallography of aged specimens. Over the range of temperature 750 to 1100°C, the solubility of the carbide, which is probably $(Fe, Cr, Mo)_{23}C_6$, is defined by the equation: log [C, ppM] = 7.771 − (6272/T°K) with a heat of solution of 170 ± 25 kcal/mole. Small amounts of χ-phase were found at temperatures below 900 to 1000°C as the carbon increased from 50 to 1000 ppM. The carbide solubility line did not appear to be affected by the presence of these small amounts of χ-phase. (auth) (UK)

8876 X-RAY DETERMINATION OF LATTICE PARAMETERS AND THERMAL EXPANSION COEFFICIENTS OF ALUMINUM, SILVER, AND MOLYBDENUM AT CRYOGENIC TEMPERATURES. Woodard, Claude Lowell. Rolla, Mo.; Univ. of Missouri (1969). 142p. University Microfilms Order No. 70-11,768.

Thesis.

A multiple exposure back reflection diffraction camera was designed to mount on the vacuum jacket of a pressurized helium gas Cryomite. With this design it was possible to obtain six diffraction exposures on a single film at any temperature in the range of 180 to 25°K. Temperatures within this range were reached in short intervals and exposure periods were less than 30 minutes in a 2.875 inch diameter camera. Some of the advantages of this design are: direct measurements, multiple exposures on a single film, short exposures, direct compensation of film length changes due to evacuation or processing of the film, and easy determination of transformation changes. Different specimen mounting methods did not influence a detectable change in the lattice parameters on a 99.99+% silver sample with a particle size of 5 to 25 micron. The lattice parameters of aluminum determined by x-ray diffraction in the temperature range of 40 to 120°K were lower while lattice parameters of silver in the temperature range of 40 to 180°K were higher than values calculated from interferometric expansivities. Molybdenum lattice parameters determined by interferometric and x-ray diffraction methods agree well in the temperature range of 100 to 180°K, while lattice parameters calculated from interferometric methods below 100°K are lower than those determined by x-ray diffraction. The linear thermal coefficients of expansion are given for: aluminum at 40 to 160°K; silver at 50 to 160°K; and molybdenum at 30 to 170°K. (Diss. Abstr. Int., B)

8877 GROWTH OF STRUCTURE COMPONENTS IN WC−TaC−Co ALLOYS OF K10 TYPE. Grewe, H.; Walter, P. Metall; 24: 734-43(Jul 1970). (In German).

The growth of the structure components and the changes in tensile properties dependent on this growth were studied for WC−TaC−Co alloys with TaC of different initial particle sizes. Metallographic, magnetophysical, and mechanical tests, as well as diffusion experiments, were carried out. Growth of a cobalt inner layer caused changes in the properties. (M.C.G.)

8878 TOTAL HEMISPHERICAL EMITTANCE OF RHENIUM IN THE TEMPERATURE RANGE FROM 1200 TO 2800°K. Peletskii, V. E.; Druzhinin, V. P. (Inst. of High Temperature, Moscow). High Temp. (USSR). (Engl. Transl.); 7: 331-2(Mar-Apr 1969).

Translated from Teplofiz. Vys Temp.; 7: 364-5(Mar-Apr 1969).

The emittance of a Re monocrystal was measured in a calorimetric device, using black-body temperature measurements. The smoothed emittance curve varied from 0.184 at 1200°K to 0.325 at 2800°K, with an accuracy of <±5%. The results are compared with literature data. (D.L.C.)

8879 SOLID CADMIUM EMBRITTLEMENT: TITANIUM ALLOYS. Fager, D. N.; Spurr, W. F. (Boeing Co., Seattle). Corrosion; 26: 409-19(Oct 1970).

The phenomenon, solid cadmium embrittlement, was identified and studied in the titanium alloys Ti−6Al−4V and Ti−8Al−1Mo−1V using cadmium coated tensile specimens and residual stress specimens. The conditions necessary for this phenomenon were found to be tensile stress and intimate contact between the cadmium and titanium. Intimate contact was provided by pressing the cadmium into the titanium surface such that the titanium surface was plastically deformed or by exposing the cadmium plated titanium in a vacuum. Brittle cracking was observed at all exposure temperatures from above the melting point of cadmium down to room temperature. Crack propagation rates increased with increasing temperature, but decreased with time even though the net stress increased. This dependence of the crack propagation rate on temperature and time was found to be consistent with a cadmium surface diffusion controlled crack propagation rate. The failure mode was found to be the same as for mercury embrittlement of Ti−8Al−1Mo−1V, i.e., both intergranular and transgranular cleavage. The cleavage plane was found to be on or near the (0001) plane. (auth)

8880 EFFECTS OF INTERSTITIAL IMPURITIES ON THE YIELDING BEHAVIOUR OF NIOBIUM SINGLE CRYSTALS. Kim, H. C.; Pratt, P. L. (Imperial Coll. of Science and Tech., London). Phys. Status Solidi; 41: 797-805(1 Oct 1970).

The effect of the overall impurity content on the yielding behavior of niobium single crystals has been investigated in tension between 77 and 473 °K. In the ⟨110⟩ orientation, the amount of yield drop depends on the impurity level of the crystal, and the temperature dependence of the yield stress was decreased significantly for both ⟨110⟩ and ⟨100⟩ orientations for purer crystals. Current theories of solution and lattice hardening were applied to try to account for the observed temperature dependence of the yield stress. Gilman's reaction rate theory is found to be the best explanation for the observed yielding behavior. The twinning stress of ⟨110⟩ oriented single crystals in compression showed no systematic variation with impurity content when tested at 20.4 °K. (auth)

8881 LOW−TEMPERATURE TENSILE DEVICE FOR TESTS ON MONO- AND POLYCRYSTALLINE MICROSAMPLES. Fries, J. F.; Cizeron, G. (CEN, Saclay, France). Metaux (Corros.-Ind.); No. 539-540, 226-79(Jul-Aug 1970). (In French).

A low-temperature tensile device was designed to determine the mechanical properties of metals and alloys at temperatures below room temperature. Tests between 20 and 293°K in a gaseous atmosphere were carried out with the set-up described, which is simple and economical and can be easily converted into a compression system. Results obtained at various temperatures for Nb, Mo, Zr, stainless steels and U are presented. (auth) (France)

8882 CORRELATION BETWEEN STRUCTURE AND ELECTRIC CONDUCTIVITY OF In−Sn, In−Zn, AND In−Pb ALLOYS IN LIQUID STATE. Dutchak, Ya. I. (Lvov State Univ.). Izv. Vyssh. Ucheb. Zaved., Fiz.; No. 9, 152-5(1970). (In Russian).

The structure of liquid In−Sn, In−Zn, and In−Pb alloys was studied by means of x-ray analysis using a scintillation counter with an NaI(Tl) crystal. Coordinate numbers and interatomic space in the liquid alloys were tabulated. Data obtained were correlated with the electric conductivity which was measured by the rotating magnetic field method. The measurements were carried out in a vacuum ($\sim 10^{-4}$ torr) or in an argon atmosphere. The results showed a good congruence between the measured and calculated electric conductance values. (R.V.J.)

8883 DEVELOPMENT OF A DEVICE FOR MEASURING CIRCUMFERENTIAL MECHANICAL PROPERTIES OF CLADDING TUBES. Nagasaki, Ryukichi (Japan Atomic Energy Research Inst., Tokyo); Kawasaki, Satoru; Fukaya, Kiyoshi; Inoue, Mamoru; Yamasaki, Tatsuo. Nippon Genshiryoku Gakkaishi; 12: 642-8 (Nov 1970). (In Japanese).

A method of measuring the mechanical strength in the circumferential direction of cladding tubes for fast breeder reactors was developed. Circumferential yield stress, ultimate tensile strength, and elongation were obtained by analyzing the stress-strain curve. The proposed device is simple in operation, and lends itself to application in remotely controlled systems. Another advantage is that the specimens used in the device are very small, so that the method could prove useful for studying the radiation effects on cladding materials. (auth)

8884 MECHANISMS OF PLASTIC DEFORMATION IN A NICKEL−CHROMIUM−NIOBIUM ALLOY PRECIPITATION HARDENED AT 700°C. Royer, A.; Gantois, M. (Ecole Nationale Superieure de la Metallurgie et de l'Industrie des Mines, Nancy). Scr. Met.; 4: 651-6(Aug 1970). (In French).

An electron microscope study of precipitation mechanisms, morphology, and crystallographic structure of precipitates in alloys containing 80 at. % Ni, 12 at. % Cr, and 8 at. % Nb or Ta, was carried out. At the beginning of tempering (less than 100 hr at 700°C), the precipitate Ni_3Nb had a tetragonal structure. It was in the form of thin platelets parallel to the [001] plane and of 25 Å thickness after 20 hr of tempering. Prolonged tempering caused the tetragonal precipitate to redissolve and form an ortho-

rhombic phase, identical to the equilibrium phase Ni_3Nb, of the binary alloy. At the beginning of tempering in the presence of a tetragonal precipitate, deformation is caused by slipping and shearing of the precipitates by complete dislocation of the Burger's vectors. Electron microscopy made it possible to demonstrate the stacking faults resulting from this dissociation. The method of deformation by slipping is preferred. When the lamellae of the orthorhombic precipitate appears and replaces the tetragonal precipitate (140 hr at 700°C), plastic deformation proceeds by slipping of the orthorhombic precipitate even at liquid nitrogen temperature. Formation of bicrystals was observed in the lamellae of the orthorhombic Ni_3Nb phase. Frequently a twinned single crystal system was visible. (R.C.K.)

Structure and Phase Studies

Refer also to abstracts 8927, 9576, and 9588.

8885 (ANL-Trans-867) STUDY OF THE TANTALUM-HYDROGEN SYSTEM: EQUILIBRIUM DIAGRAM AND ELECTRONIC STRUCTURE. Ducastelle, F.; Caudron, R.; Costa, P. Translated for Argonne National Lab., Ill., from J. Phys. Chem. Solids; 31: 1247-56(1970). 13p. Dep. NTIS.

An abstract of this paper, prepared from the original language, appeared as NSA 24: 36934.

8886 TERNARY SYSTEMS Gd-(Y, Tb, Dy, Ho, Er, Sc)-Al IN THE REGION TO 25 AT. % RARE-EARTH METALS. Zalutska, O. I.; Kontsevoi, V. G.; Karamyshev, M. I.; Ryabov, V. R.; Zalutskii, I. I. (Lvov State Univ., Kiev. Electrolytic Inst., Kiev). Dopov. Akad, Nauk Ukr. RSR, Ser. A; No. 8, 751-3(Sep 1970). (In Ukrainian).

The Al-rich alloys of ternary systems Gd-{Y, Tb, Dy, Ho, Er, Sc}-Al were investigated by means of the x-ray powder method. The isothermic section (at 500°C) of the region $Al-GdAl_3-RAl_3$ was determined for each system. The crystal structures of the ternary compounds (Gd, R) Al_3 were intermediate (in respect to the content of hexagonal and cubic layers) between the structures of the binary compounds $GdAl_3$ and RAl_3. (auth)

8887 ERBIUM-COPPER SYSTEM. Buschow, K. H. J. Philips Res. Rep.; 25: 227-30(Aug 1970).

The system erbium-copper was investigated by means of x-ray diffraction, thermal analysis, and metallography. A phase diagram is presented. Five intermediate phases were observed. Lattice constants are given for ErCu, $ErCu_2$ and $ErCu_5$. (auth)

8888 CONCERNING AN ORDERED SOLID SOLUTION OF BERYLLIUM IN U_3Si_5. de Tournemine, R.; Molho, S. (Centre d'Etudes Nucleaires, Grenoble, France). J. Nucl. Mater.; 37: 345-6(Dec 1970). (In French).

By chemical and electron microprobe analyses of the uranium-silicon-beryllium system, it was possible to isolate a phase with a formula approximating $USi_{1+x}Be_{1-y}$ ($x - y \leq 0$; $0 \leq x \leq 0.20$; and $y \leq 0.10$). X-ray diffraction analysis of a polycrystalline sample of this phase (referred to as USiBe for convenience) shows a spectrum identical to that for the compound U_3Si_5. The parameters are: for U_3Si_5, $a = 3.843$ Å and $c = 4.069$ Å; and for USiBe $a_0 = 3.866 \pm 0.001$ Å and $c_0 = 4.011 \pm 0.001$ Å. Analysis always gave a sum for Si + Be very near to 2. The structure corresponds to an ordered solid solution of a formula close to that of USiBe in the region of the solid solution of beryllium in U_3Si_5. It was not possible to determine a critical temperature for the order-disorder transition by thermal analysis or by measurement of electric resistivity, but there is evidence that it is above 800°C. (R.C.K.)

8889 PHASE DIAGRAM OF THE CHROMIUM-TERBIUM SYSTEM. Svechnikov, V. N.; Kobzenko, G. F.; Ivanchenko, V. G. (Inst. of Physics of Metals, Kiev). Dopov. Akad. Nauk Ukr. RSR, Ser. A; No. 8, 758-60(Sep 1970). (In Ukrainian).

On the basis of data of thermal, metallographic, x-ray diffraction, and durometric analyses, a phase diagram is plotted under conditions close to equilibrium ones. (auth)

8890 INVESTIGATION OF Nb-Fe-Al AND Nb-Co-Al SYSTEMS. Burnashova, V. V.; Ryabov, V. R.; Markiv, V. Ya. (Lvov State Univ., Kiev. Electrolytic Inst., Kiev). Dopov. Akad. Nauk Ukr. RSR, Ser. A; No. 8, 747-50(Sep 1970). (In Ukrainian).

The Nb-Fe-Al and Nb-Co-Al systems were investigated by means of x-ray diffraction and microscopic analyses. The phase equilibria were determined at 800°C. The formation of the ternary μ^1-phases, the homogeneity regions of which were extended along lines of constant Nb-content ~50 to 52 at. % from ~3 to 26 at. % Al (Nb-Fe-Al system) and ~54 at. % from 20 to 24 at. % Al (Nb-Co-Al system), was characteristic of both systems. The binary λ_1- and μ-phases of Nb-Fe and Nb-Co systems dissolved considerable amount of aluminum. The homogeneity regions of λ_1-phases are extended along lines of constant Nb-content (33.3 and 36.5 at. %) from zero to 56 and 55 at. % Al, respectively; μ phases dissolve ~26 (Nb-Fe-Al) and ~32 (Nb-Co-Al) at. % Al. In the crystallochemical relation the Nb-Fe-Al and Nb-Co-Al systems are related to the Nb-Ni-Al system. (auth)

8891 CRYSTALLINE STRUCTURES OF THE INTERMETALLIC COMPOUND $(Gd_{0.2}Fe_{0.8})Fe_5$. Givord, Francoise; Lemaire, R. (CNRS, Grenoble, France). J. Less-Common Metals; 21: 463-8(1970). (In French).

The crystal structure of $GdFe_{8.5}$ was studied by x-ray diffraction after thermal treatment. The high-frequency induction method was used for levitation melting of the elements at approximately 1700°C thereby avoiding contamination of the sample by a crucible. Rapid tempering stopped the various paratectic reactions and made it possible to obtain the expected intermetallic compound. Annealings under vacuum at 900 and 1050°C were carried out for a week. The tempered compound $GdFe_{8.5}$ was found to be isomorphous with Th_2Ni_{17} with a hexagonal structure. The compound $GdFe_{8.5}$ annealed at 1050°C was isomorphous with Th_2Zn_{17} and was of rhombohedral structure. The x-ray diffraction negative of the sample annealed at 900°C was analogous to those of the preceding samples. The stability of the crystalline structures was found to depend principally on geometrical considerations. It was found that with rare earths of small atomic radios, it was not possible to stabilize the rhombohedral phase because certain distances between Fe atoms would be too short; the hexagonal phase could be prepared by tempering from the liquid. (R.C.K.)

8892 CONTINUOUS SERIES OF METASTABLE HEXAGONAL CLOSE-PACKED SOLID SOLUTIONS IN THE ERBIUM-ZIRCONIUM SYSTEM. Wang, R. (Univ. of Southern California, Los Angeles). Appl. Phys. Lett.; 17: 460-2(15 Nov 1970).

The complete mutual solid solubility of hcp forms of erbium and zirconium was observed by x-ray diffraction for specimens rapidly quenched from the liquid state to room temperature. The lattice-parameter measurements show negative deviations from the linearity as expressed by Vegard's law, with maximum deviations $\Delta V/V$ of $\lesssim 2\%$ at approximately 41 at. % Zr and 2.3% at 70 at. % Zr. The axial ratio c/a remains as a linear relationship between those of two elements. The formation of the metastable solid solutions can be explained by classical rules. (auth)

8893 CRYSTAL STRUCTURE OF Th_2Co_7. Buschow, K. H. J. (Philips Research Labs., Eindhoven, Netherlands). Acta Crystallogr., Sect. B; 26: 1389-92(1970).

The intermetallic compound formerly designated as $ThCo_3$ has been identified as Th_2Co_7. This compound occurs in two allotropic forms: α-Th_2Co_7 is hexagonal (Ce_2Ni_7 type); β-Th_2Co_7 is rhombohedral (Gd_2Co_7 type). Both forms usually occur together. There is some indication of a martensitic type of transformation between the α and β forms. The influence of a varying Co concentration is discussed. Lattice parameters are presented for isostructural rare-earth compounds of the type R_2Co_7. (auth)

8894 METALLOVEDENIE I TERMICHESKAYA OBRABOTKA METALLOV. (Metallurgy and the Hot Working of Metals). Lakhtin, Yu. M. Moscow; Izdatel'stvo Metallurgiya (1969). 448p.

Information is included on the crystalline structure of metals, processes and mechanisms of crystallization, recrystallization, and plastic deformation. Results of alloy phase diagram studies are also presented for binary and ternary systems. Attention is directed to the theory and technology of thermal and chemical-thermal treatment of steel. Descriptions are included concerning production of construction, instrument, stainless and heat-resistant steels. Data are also included on Ti-, Cu-, Al-, and Mg-base alloys. (tr-auth)

Radiation Effects

Refer also to abstracts 8956, 9542, 9564, and 9571.

8895 (BMI-1891, Sect.B) STUDIES OF THE EFFECTS OF IRRADIATION ON CLADDING AND STRUCTURAL ALLOYS. (Battelle Memorial Inst., Columbus, Ohio). 11p.

The stainless steel specimens being irradiated in the EBR-II intended for examination to correlate irradiation damage effects with those determined for specimens exposed in the ETR, were discharged and are to be returned to the Battelle Hot-Cell facility. Irradiation was initiated in the EBR-II of nickel single crystals and of stainless steel specimens with grains of controlled orientation and with shock-hardened structures to investigate the effect of microstructure on irradiation-induced embrittlement and void formation. In continuing studies to establish optimum shocking conditions, the effect of explosive pressure and of shocking by

contact explosives or by means of a flyer plate was investigated. While yield and ultimate strengths increase with increasing shocking pressures up to 320 kbar, the ductility goes through an intermediate maximum. Contact shocking appears to produce accelerated changes for equivalent calculated shocking pressures. Studies to evaluate associated microstructures are planned. A variety of creep-rupture results have been obtained on ferritic 2¼ Cr-1 Mo alloy materials containing 0.012 and 0.042 wt % carbon. Larson-Miller plots of stress-rupture data for these and commercial materials indicate a sequential reduction in rupture life with decrease in carbon content for applied stresses below about 15,000 psi. At higher stresses, although still below the yield strength, the low-carbon alloys apparently undergo strain hardening; resultant increases in rupture life produce a sharp break in the Larson-Miller plot for these alloys. Significantly, this abrupt change associated with strain hardening has generally not been shown in other studies of low-carbon alloy material. It has generally been interpreted as indicating a strengthening of low-carbon alloys relative to higher-carbon commercial alloys at lower testing temperatures. It was found possible to describe the minimum creep rates of the 0.012 and 0.042 wt % carbon alloys, respectively, by the equations $\dot{\epsilon} = 5.76 \times 10^{14}\ \sigma^{5.0} \exp(-54,960/RT)$, and $\dot{\epsilon} = 7.45 \times 10^{13}\ \sigma^{5.0} \exp(-54,960/RT)$, for temperatures in degrees Rankine. The creep constants indicate that the creep strength of the 0.042 wt % carbon material is greater than that of the 0.012 wt % carbon alloy. (auth)

8896 (BNWL-tr-57) CERTAIN PROPERTIES OF FUEL BEHAVIOR OF CAN AND STRUCTURAL MATERIALS IN FAST REACTOR CONDITIONS AND FUEL ELEMENT TESTING PROGRAM IN BOR-60 REACTOR. Prochorov, V. I.; Lebedev, I. G.; Krassnoyarov, N. V. Translation of Russian report. 14p. Dep. NTIS.

Variations in fuel performance related to testing conditions are discussed emphasizing fast reactor fuels. In discussions of fuel testing it is noted that fast reactor conditions can be realized in thermal reactors. Methods of testing fuel can materials are discussed and plans for testing in the BOR-60 reactor are reviewed. (J.R.D.)

8897 (ORNL-TM-3169) EFFECT OF FAST NEUTRON IRRADIATION ON THE CREEP-RUPTURE PROPERTIES OF TYPE 304 STAINLESS STEEL AT 600°C. Bloom, E. E.; Stiegler, J. O. (Oak Ridge National Lab., Tenn.). Jan 1971. Contract W-7405-eng-26. 23p. Dep. NTIS.

The creep-rupture properties of Type 304 stainless steel have been determined at 600°C after irradiation at temperatures in the range 370 to 600°C to fast-neutron fluences of 1×10^{21} to 6.7×10^{22} neutrons/cm^2 (>0.1 MeV). The microstructures were characterized by electron microscopy. Irradiation at 370 to 470°C caused a decrease in ductility and rupture life which became larger with increasing fast neutron fluence. The irradiated specimens fractured along the grain boundaries with no evidence of deformation within the matrix. A specimen irradiated at 410°C to 6.7×10^{22} neutrons/cm^2 (>0.1 MeV) ruptured in 0.5 hr with 0.1% elongation as compared with the unirradiated rupture life of 185 hr and elongation of 19.7%. Specimens irradiated at 600°C to fluences from 2.5 to 3.5×10^{22} neutrons/cm^2 (>0.1 MeV) exhibited decreased ductilities and creep rates and essentially the same rupture lives as unirradiated specimens. The increased tendency for grain-boundary fracture, and thus reduced ductility and rupture life, appears to result from the effects of the irradiation-produced voids and dislocations upon the deformation processes which would be operative in an unirradiated specimen. The voids and dislocations prevent dislocation motion within the matrix. Regions along grain boundaries are denuded of these defects and grain-boundary sliding occurs, leading to stress concentrations and the initiation of grain-boundary cracks. The presence of helium at the boundaries may increase the rate of crack propagation. (auth)

8898 (SRARI-P-85) AN ANALYSIS OF THE VARIATION OF THE DEFORMATION PROCESSES OF CONSTRUCTION MATERIALS AFTER REACTOR IRRADIATION. PART I. Balashov, V. D.; Votinov, S. N. (Scientific Research Atomic Reactor Inst., Melekess (USSR)). 1970. 30p. (In Russian). Dep. NTIS (U. S. Sales Only).

The comparison of strain mechanisms of unirradiated and neutron irradiated fcc and bcc construction materials has been carried out. Serrated strain, rate dependence, and high temperature annealing effects were investigated. The role of radiation defects in low- and high-temperature radiation embrittlement phenomena is explained. (auth)

8899 (ZJE-89) RADIATION STABILITY OF STEELS FOR PRESSURE VESSELS OF CZECHOSLOVAK NUCLEAR REACTORS. Brumovsky, M. (Skoda Concern, Pilsen (Czechoslovakia). Nuclear Power Plants Div.). 1970. 16p. Dep. NTIS (U. S. Sales Only).

The choice of materials, change of material properties due to radiation, and the operational and safety aspects of nuclear reactor pressure vessels are discussed. The chemical composition and mechanical properties data of steel for the Czechoslovak reactor pressure vessel are included. (auth)

8900 (ZJE-90) NEUTRON IRRADIATION INDUCED CHANGES IN MECHANICAL PROPERTIES OF THE PRESSURE VESSEL STEEL FOR A-1 NUCLEAR POWER PLANT. Brumovsky, M. (Skoda Concern, Pilsen (Czechoslovakia). Nuclear Power Plants Div.). 1970. 30p. Dep. NTIS (U.S. Sales Only).

Results of irradiation studies on ČSN 13030.9 modified steel for the pressure vessel of the A-1 reactor are summarized. Changes in mechanical properties determined by static tensile, static bend, impact notch, and hardness tests, and in stress relaxation are emphasized. Besides these properties factors influencing radiation damage such as irradiation temperature, killing elements, heat treatment, artificial strain aging, and post-irradiation annealing are discussed. (auth)

8901 (ZJE-91) NEUTRON IRRADIATION INDUCED CHANGES IN MECHANICAL PROPERTIES OF BASE MATERIAL AND WELDING JOINTS OF A-1 PRESSURE VESSEL STEEL. Brumovsky, M. (Skoda Concern, Pilsen (Czechoslovakia). Nuclear Power Plants Div.). 1970. 30p. Dep. NTIS (U.S. Sales Only).

Results of radiation stability studies on base materials and joints welded by manual arc, electroslag and semiautomatic in CO_2 atmosphere, of the A-1 reactor pressure vessel steel are summarized. Results of static tensile and impact tests show that all these three types of joints are similar from the point of view of radiation damage, no different sensitivity of any particular part of the joint to radiation damage has been observed. The sensitivity of heat affected zones to the radiation damage is lower than that of other parts of welded joints. It is shown that (without the influence of neutron spectrum) this material under working conditions of the pressure vessel of A-1 is capable of safe operation in pressure vessels up to the dose of 3.10^{18} n/cm^2 which is the dose received during 25 years of service. (auth)

8902 STUDY OF NEUTRON DAMAGE IN Be-DOPED COPPER. Ipohorski, M.; Brown, L.M. (Cambridge Univ., Eng.). Phil. Mag.; 22: 931-44(Nov 1970).

The experiments of McIntyre on the nature of the defects induced by fast neutrons in copper were repeated, and confirmed. It is shown that the addition of a small amount of beryllium to the copper does not affect the visible loop density, although beryllium is known to trap interstitials. It is concluded that the interstitial loops cannot be nucleated by the random collisions of free interstitials, but that some other process such as prismatic punching in the thermal spike must be responsible for their creation. (auth) (UK)

8903 POTENTIAL DANGER OF EMBRITTLEMENT FOR STRUCTURES OF STEEL 22K TYPE. Dovzhenko, A. S. At. Energ. (USSR); 29: 255-60(Oct 1970). (In Russian).

The problems of the service safety of reactor structures subjected to a brittle fracture are given. A brief survey of testing of thick plates and standard specimens fabricated of Type 22K steel is given; a relationship between stresses, temperature and flaw sizes in brittle fracture of ferritic-perlitic steels is shown. The effects of neutron irradiation on the brittle fracture transition temperature are given. The minimum zero ductility temperature at which the ultimate stress is approximated to the yield point ($\sigma/\sigma_T = 1$) for integral neutron irradiation in case of a summary dosage of 10^{19} n/cm^2 for a ferritic-perlitic steel is −18°C without irradiation and −220 to +125°C with irradiation. The irradiation temperatures 260°, 300°, 340° and 400°C are characterized by displacement of the zero ductility temperature to 110, 75, 35 and 10°C respectively. For stresses, equal to $0.5\sigma_T$, the temperature for non-propagation of cracks is approximately displaced by 25°C from the minimum zero ductility temperature for given conditions of irradiation up to the temperature of 6, 150, 135, 100, 60 and 35°C respectively. (auth)

8904 CONTRACTION OF β AND δ PHASES OF PLUTONIUM UNDER THE EFFECT OF SELF-IRRADIATION AT 4.2°K. Jacquemin, J.; Lallement, R. (CEN, Fontenay aux Roses, France). Phys. Lett.; 33A: 384-5(30 Nov 1970).

Correlations among measurements of variations in length and resistance as a function of time of self-irradiation at 4.2°K lead one to think that the β and δ phases of plutonium must contract under the effect of damages caused by the irradiation. This contraction is shown experimentally to be important for the δ phase. (tr-auth)

XUM

8905 CORRELATION OF HYDROGEN EVOLUTION WITH SURFACE BLISTERING IN PROTON-IRRADIATED ALUMINUM. Daniels, Raymond D. (Univ. of Oklahoma, Norman). J. Appl. Phys.; 42: 417-19(Jan 1971).

The outgassing behavior of aluminum samples irradiated with 100-keV protons was studied during annealing to determine the relationship between hydrogen evolution and observations on blister formation during annealing. The outgassing process appears to be diffusion-controlled and competes with the process of blister formation for the available hydrogen. (auth)

Ceramics and Cermets

Refer also to abstracts 8828–8831.

Corrosion and Erosion

Refer also to abstract 10201.

8906 (AERE-R-4857) SIMULTANEOUS REACTION, DIFFUSION AND BULK FLOW IN TUBULAR SPECIMENS OF GRAPHITE. V. THE USE OF THE MATHEMATICAL MODEL IN AN EXAMINATION OF THE INHIBITION OF GRAPHITE OXIDATION WITH PHOSPHORUS OXYCHLORIDE. Hawtin, P., Gibson, J. A. (Atomic Energy Research Establishment, Harwell (England)). Mar 1965. 29p. Dep. NTIS (U. S. Sales Only).

The effect of the addition of phosphorus oxychloride vapour to the oxidising gas, on the observed oxidation rate of large specimens of graphite was studied using tubular samples 12″ long, 6″ O.D. with a bore of 1.16″ which were oxidised in the temperature region 450° to 510°C. The addition of phosphorus oxychloride ($POCl_3$) vapour to the oxidising gas reduced the rate of oxygen attack on the graphite, but the full inhibiting effect of the $POCl_3$ was delayed for many hours after its first injection. The final inhibition effect is best quantified as an inhibition factor (R) defined as: R = (unihibited reaction rate/corresponding inhibited rate). R varied markedly with the initial uninhibited reaction rate and in the present study values of R between 11.1 (corresponding to an uninhibited rate of 1.9×10^{-5} g/g.h at 480°C) and 29.1 (corresponding to 13.4×10^{-5} g/g.h at 510°C) were recorded. A small amount of evidence was obtained to show that $POCl_3$ reduces the energy of activation for the oxidation of graphite. In reactions between porous solids and gases at elevated temperatures the full chemical rate is often masked by the presence of in-pore mass transport resistance. A previously derived mathematical theory enables these effects to be quantitatively estimated and accordingly this theory was used to analyse the results in the present studies. Good agreement between the observed results and those predicted from the theory was obtained both for the uninhibited and the inhibited reactions. (auth) (UK)

8907 (CEA-Bib-183) OXIDATION OF URANIUM CARBIDES IN GASEOUS ENVIRONMENTS. Matcheret, Georges (Commissariat a l'Energie Atomique, Fontenay-aux-Roses (France). Centre d'Etudes Nucleaires). Nov 1970. 19p. (In French). Dep. NTIS (U. S. Sales Only).

The reaction mechanisms and the oxidation kinetics of uranium carbides in various gaseous environments, namely oxygen, water vapor, carbon dioxide and carbon monoxide are described. (auth) (France)

Preparation and Fabrication

Refer also to abstracts 8323 and 10334.

8908 (BARC-507) STUDIES ON SINTERING OF UO_2: RELATION BETWEEN ELECTRICAL CONDUCTIVITY AND MICROSTRUCTURE OF SINTERED UO_2. Rao, S. V. K.; Agnihotri, P. K.; Anandan, N. S.; Prasad, G. Eswara; Moorthy, V. K. (Bhabha Atomic Research Centre, Bombay (India)). 1970. 16p. Dep. NTIS (U. S. Sales Only).

In an earlier investigation, it was reported that the electrical conductivity of sintered compacts of urania powders depended on the calcination temperature and the sintering treatments. In the current investigation, the conductivity of the samples sintered at temperatures 1100 to 1700°C was studied. Attempts were made to correlate the change in the conductivity with the microstructure of the samples. The details of the microstructure were studied by electron microscopy. (auth)

8909 (ORNL-4600, pp 3-40) DEVELOPMENT OF FAST-REACTOR OXIDE FUELS. (Oak Ridge National Lab., Tenn.).

From Fuels and materials development program.

A total of 1.2 kg of Pu sol and 4.5 kg of 93% enriched U sol was prepared to meet the requirements of the oxide fuels program. About 1 kg of dense $(^{239}U_{0.8}, Pu_{0.2})O_2$ microspheres was also prepared. About 1.5 kg of $(^{235}U_{0.75}, Pu_{0.25})O_2$ microspheres 350 to 595 μm in diameter and about 0.2 kg of additional microspheres less than 44 μm in diameter were prepared for fuel development studies. All of the fuel has been prepared for the fuel pins for the 37-pin subassembly for the series II irradiation tests in the Experimental Breeder Reactor-II (EBR-II). Nine of these fuel pins were loaded with Sphere-Pac microspheres and two were loaded with pellets. Nine of these fuel pins were tagged with Xe. A great effort was made to statistically characterize analytical data on $(U,Pu)O_2$ fuel before irradiation, including methods for determining Pu content of $(U,Pu)O_2$ microspheres by γ-ray spectroscopy and α-ray autoradiography and variations in analyses for the ratio of O : metal in $(U,Pu)O_2$. In addition to this effort both light and replica electron microscopy and α-ray autoradiography were used to characterize the microstructure of sol-gel $(U_{0.8}, Pu_{0.2})O_2$ fabricated for the instrumented tests in the Engineering Test Reactor (ETR). All of these show the fuel to be of excellent and consistent quality. A sol-gel Sphere-Pac capsule that contains $(U,Pu)O_2$ attained a calculated burnup of 9.7 fissions per initial actinide metal atom (FIMA) in the ETR, and the irradiation of the capsules is continuing at a peak heat rate of 15 kW/ft to a burnup of 10 at. %. The postirradiation examination of two capsules that contain UO_2 and $(U,Pu)O_2$ Sphere-Pac fuels that have been irradiated to a peak burnup of 6.5% FIMA was completed during the quarter. The third instrumented capsule irradiated in the Oak Ridge Research Reactor (ORR), which contains one Sphere-Pac fuel pin and one sol-gel pellet fuel pin of the same composition and smear density, was removed from the reactor after operating successfully. This experiment, which provided direct comparison of pellet and Sphere-Pac fuels to central fuel temperatures near 2000°C, indicated, again, that Sphere-Pac and pellet fuels have essentially the same effective thermal conductance during irradiation at low burnup. Two instrumented capsules were constructed to investigate fuel swelling and chemical interaction of fuel and cladding and to compare Sphere-Pac and pellet fuels under peak conditions for a liquid-metal-cooled fast breeder reactor (LMFBR). These capsules were inserted into the ETR. Destructive examination of six fuel pins containing Sphere-Pac and pellet fuels that were subjected to power transients in TREAT was continued. Metallography results indicate extensive restructuring of the fuel and the presence of large gas bubbles formed from the release of adsorbed gases from the molten fuel during the power transient. Encapsulated Sphere-Pac $(U,Pu)O_2$ fuel pins were removed from EBR-II subassembly X050 after having attained the calculated peak burnup of 6.2% FIMA. Two of these pins are to be returned to ORNL after neutron radiographs have been made, and three others have been scheduled to be reinserted in a new subassembly for continued irradiation to a peak burnup of 11.8% FIMA. This additional burnup has been approved so that the three encapsulated pins can serve as lead experiments for the unencapsulated tests for the series II irradiation tests. (auth)

8910 (ORNL-4600, pp 41-56) DEVELOPMENT OF ADVANCED LMFBR FUELS. (Oak Ridge National Lab., Tenn.).

From Fuels and materials development program.

Ten fuel pins consisting of cold-pressed-and-sintered (U,Pu)N pellets clad with Type 316 stainless steel were fabricated for irradiation testing in the Engineering Test Reactor. These pins have a 0.010-in. radial gap filled with NaK-19 (Na–19% K) between the fuel and cladding to simulate Na bonding. Arc-melted, nominally U–20% Pu alloy, fully enriched in ^{235}U, was ordered. The Pu content was lowered to about 18% to reduce pyrophoricity which is probably due to the presence of the ζ phase. The use of phosphoric acid to dissolve UN before quantitative analysis for N_2 improved precision and eliminated the loss of N_2 that occurred previously. This method is now to be applied to the analysis of mixed nitrides. The lattice constants of (U,Pu)N solid solutions were found to deviate significantly from Vegard's law. (auth)

8911 (ORNL-4600, pp 65-80) LMFBR FUEL ELEMENT DESIGN AND MODEL DEVELOPMENT. (Oak Ridge National Lab., Tenn.).

From Fuels and materials development program.

The variation of grain size with radial position was determined for a Sphere-Pac $(U,Pu)O_2$ fuel pin after thermal-reactor irradiation at a linear heat rate of 10.5 kW/ft to a burnup of 0.5% fissions per initial actinide metal atom (FIMA). The activation energy for grain growth in the irradiated $(U,Pu)O_2$ was less than that for out-of-reactor grain growth in UO_2 and ThO_2. Electron microprobe analysis was used to determine the distribution of Pu across a transverse section of a Sphere-Pac $(U,Pu)O_2$ pin irradiated in the Engineering Test Reactor at a linear heat rate of 13.6 kW/ft to a burnup of 0.7% FIMA. A radial scan made simultaneously for Pu and U in the region of columnar grains adjacent to the

central void showed that the Pu content decreased and the U content increased with decreasing fuel temperatures. Observations of high Pu content near the central void and low Pu content in vapor-deposited fuel support the theory of transport down the temperature gradient of a gas phase rich in U. The computer subroutine used in the FMØDEL computer code for mechanical analysis of cladding was separated from that code and extensively modified so that it can handle power-cycling conditions and calculate ratchetting of plastic strains during power cycling. A simple problem formulated to test the code confirmed that the subroutine functions properly. The integrated model for cladding performance is being altered to convert it for use with power cycling. Compilation of available data on the physical and tensile properties of type 316 stainless steel was continued along with discrete-element analysis of the créep of stainless steel tubing for use in liquid-metal-cooled fast breeder reactors. (auth)

8912 (ORNL-4600, pp 167-74) DEVELOPMENT OF FAST-REACTOR NEUTRON-ABSORBER MATERIALS. (Oak Ridge National Lab., Tenn.).

From Fuels and materials development program.

Transmission electron microscopy techniques were developed for B_4C with the use of an ion-bombardment milling machine. Transmission electron photomicrographs indicate that B_4C is capable of twinning and also show the crystallographic orientation of the voids within the grains. Additional specimens are undergoing thermal irradiation at 500°C and will be removed at an estimated 3.1×10^{21} depletions/cm^3 (15% burnup of ^{10}B). Fabrication of Ta disks containing B_4C as a dispersoid was unsuccessful because of extensive reaction between the materials at the fabrication temperatures. Powder samples of commercial-grade TaB and TaB_2 are now being characterized. X-ray diffraction results indicate that TaB_2 is single phase whereas TaB contains Ta_3B_2 and Ta in addition to TaB. (auth)

8913 (ORNL-tr-2365) PREPARATION OF URANIUM MONONITRIDE PELLETS OF DIFFERING DENSITIES BY COLD PRESSING AND SINTERING. Siebmanns, W. (Kernforschungszentrum, Karlsruhe (West Germany). Institut fuer Material- und Festkoerperforschung). Translated by R. Gregg Mansfield (Oak Ridge National Lab., Tenn.), from report KFK-1049. 17p. Dep. NTIS.

This paper was abstracted from the original language and appeared in NSA as 24: 10143.

8914 FABRICATION OF CERAMIC MATERIALS BY MELTING IN AN OVERPRESSURE ELECTRIC ARC FURNACE. Thuemmler, F.; Wedemeyer, H.; Politis, C. (Gesellschaft fuer Kernforschung mbH, Karlsruhe, Ger.). Sci. Ceram.; 5: 409-22 (1970).

From 5th International Conference on Science of Ceramics, Ronneby Brunn, Sweden. See CONF-690432.

An arc furnace was developed in which it is possible to work under a gas pressure of up to 20 atm. The application ranges from the preparation of very pure laboratory specimens to that of massive fused ceramic bodies. By using a high pressure of inert gas it is possible to produce melts of mixtures of materials of different melting points, such as UO_2 and Cu; and under high N_2 pressure it is possible to convert high melting point metals directly into nitrides, even though these may have high decomposition pressures, such as UN. The coarse grained fused bodies, produced by the consumable electrode technique, are suitable for the production of powders for vibration compaction of fuel rods. Compounds such as UN, U(N,C) and U(O,C) were successfully melted using this technique. If the distance between the electrode and the melt is kept constant when melting U electrodes under 15 to 20 atm N_2 pressure the UN produced contains no free U, and small amounts of a higher nitride can be removed by additional annealing. Very pure U(N,C) was obtained by melting together massive pieces of UN and UC using a permanent electrode under 3 to 5 atm N_2 pressure. Melting UO_2 with UC, using a C electrode under 3 to 5 atm of Ar pressure, gave massive U(O,C) with U metal as a grain boundary impurity; by adding appropriate quantities of C to the melt charge, however, formation of U metal was avoided. ThN prepared by these techniques contained minor amounts of higher nitride. (UK)

8915 IMPORTANCE OF SOL-GEL PROCESSES FOR CERAMIC NUCLEAR FUELS. Hermans, M. E. A. (RCN-KEMA Reactor Development Group, Arnhem, Netherlands). Sci. Ceram.; 5: 523-38(1970).

From 5th International Conference on Science of Ceramics, Ronneby Brunn, Sweden. See CONF-690432.

It is stated that although sol-gel processes are widely recognized for their ability to produce high density microspheres of well defined properties in a rather simple way, new route for the production of high density ceramic materials might with advantage be found. The sintering properties of ceramic materials are considered, together with the most important technical factors for nuclear fuel production methods. Any method yielding a solid of small crystallite size dispersed in a liquid or gas should be considered as a potential technique for ceramic processing, and the main feature of sol-gel processes would then be the possibility of using specific shaping techniques, such as the production of spheres, thin layers. Sintering temperatures might be decreased by the addition of some sol or gel- like material of the same composition, to fill intergranular pores. At higher ratios of liquid to solid phase extrusion becomes technically attractive. The excellent reproducibility of sol-gel material and its large shrinkage on sintering make it well suited to the production of porous ceramic fuel parts. Another application is the use of sol-gel material as an intergranular filler in a packing of sintered molecules. The extremely small crystallite size in sol-gel materials results in high chemical reactivity, and by co-precipitation or mixing of suitable sols compound formation can be effected at very low temperatures. It is concluded that although sol-gel processes have opened up a new field for the production of nuclear fuels, they have stressed the importance of studying alternative routes; the potential of wet processes was further demonstrated. (UK)

8916 APPARATUS FOR AND METHOD OF PREPARING MICROSPHERES. Ashby, George Elliott; Flack, Herbert Paul; Katz, Herbert Marvin (to W. R. Grace and Co.). British Patent 1,213,426. 25 Nov 1970. Priority date 11 Apr 1968, United States.

An apparatus is described for preparing microspheres from sols or solutions comprising a column having at its lower end an extraction solvent inlet and at its upper end a solvent outlet. A means is provided for creating a nonturbulent zone and a tube is provided for injection of sols or solutions in the nonturbulent zone. An aquasol of a metal oxide is injected into the nonturbulent zone containing water extraction solvent according to one design. The aquasol droplets fall through the water extraction solvent forming particles. The method may be used for actinide oxides and lanthanide oxides. (J.R.D.)

8917 COVERING GRAPHITE WITH NIOBIUM FROM A VAPOR-GAS MIXTURE. Nikitin, K. A.; Krukovskii, V. K. (Inst. of High Temperature, Moscow). High Temp. (USSR) (Engl. Transl.); 7: 314-17(Mar-Apr 1969).

Translated from Teplofiz. Vys. Temp.; 7: 349-53(Mar-Apr 1969).

The theoretical extent of the reduction of niobium from niobium pentachloride and the optimum conditions for the reaction have been determined. A mechanism for niobium deposition on graphite from the vapor-gas mixture is suggested on the basis of the heterogeneity of the process. Laws describing the nonuniformity of the covering thickness over the sample are found, and an equation is presented for estimating the extent of this nonuniformity. (auth)

8918 STABILIZED ZIRCONIA. (to Cie Francaise de Raffinage). French Patent 1,569,636. 28 Apr 1969. Filed 20 Dec 1967. (In French).

A method is described for the preparation of zirconium dioxide stabilized in the cubic phase by a mixture of lime and at least one rare earth oxide of atomic number not less than 59. (P.C.H.)

8919 BORON CARBIDE AGGLOMERATE. Maire, J.; Slonina, J.-P.; Sherer, A. (to Le Carbone Lorraine). French Patent 1,568,883. 21 Apr 1968. Filed 9 Feb 1968. (In French).

A method is described for the fabrication of agglomerates of boron carbide, B_4C, using a phenolic resin to bond the mixture of desired consistency. The various steps involve compression or machining in the crude form prior to polymerization of the resin, polymerization by heat, carbonization, and impregnation. The agglomerates of B_4C are used as neutron moderators. (P.C.H.)

8920 FORMATION, MICROSTRUCTURE, AND PROPERTIES OF BARIUM ZIRCONIUM SULFIDE CERAMICS. Nitta, Tsuneharu; Nagase, Kaneomi; Hayakawa, Shigeru (Matsushita Electric Industrial Co., Ltd., Osaka). J. Amer. Ceram. Soc.; 53: 601-4(Nov 1970).

The preparation, microstructure, and properties of $BaZrS_3$ ceramics are described. The compound was prepared by heating either an equimolar mixture of BaS and ZrS_2 or $BaZrO_3$ alone in CS_2 gas. The reaction of the $BaZrO_3$-CS_2 system was extremely rapid, as would be expected in an autocatalytic reaction caused by very strong reduction by CS_2. Well-sintered bodies were obtained only by the $BaZrO_3$-CS_2 reaction. The time dependence of grain growth was affected considerably when reac-

tion and sintering occurred above 1250°C. Nonuniform grain growth which occurs when an excess of Ba is present can be interpreted in terms of secondary recrystallization resulting from segregation of BaS at the grain boundary during sintering The $BaZrS_3$ ceramic was stable in air up to 550°C and was oxidized above that temperature. (auth)

8921 PROCESS FOR THE PRODUCTION OF STABLE HYPOSTOICHIOMETRIC OXIDIC NUCLEAR FUEL AND PRODUCTS OBTAINED BY SUCH PROCESS. (to SADEM, SA). French Patent 1,571,230. 5 May 1969. Priority date 3 Jul 1967, Germany. (In French).

A method is described for the production of stable hypostoichiometric oxidic nuclear fuels, such as uranium oxide, thorium oxide, plutonium oxide and their mixtures. By stabilizing the hypostoichiometric phase with low additions of Cr, Mo, W, or Re, the desired behavior during operation is obtained. (P.C.H.)

8922 PRODUCTION OF SPHERICAL OXIDIC OR CARBIDIC PARTICLES FROM HEAVY METAL SALT SOLUTIONS. Hackstein, Karl-Gerhard; Fleischhauer, Gerhard; Nowak, Jurgen (to NUKEM-Nuklear-Chemie und-Metallurgie Gesellschaft mbH. Kernforschungsanlage). U. S. Patent 3,535,264. 20 Oct 1970. Priority date 6 Jul 1966, Germany.

A process is described for the production of high density oxide or carbide particles from metal salt solutions, preferably, those of uranyl and/or thorium salts, which form solid compounds when introduced into aqueous alkaline precipitating baths. The aqueous salt solution is emulsified with an oil, and if desired, with addition of a binding agent. The emulsion is introduced in droplet form into an aqueous alkaline precipitation bath to produce solid spheres that are dried and sintered to produce the desired dense particles. When carbide particles are desired, finely divided C is also suspended in the emulsion so that carbide particles are formed during sintering. (Offic. Gaz.)

8923 FORMATION OF INTIMATE OXIDE–CARBON MIXTURES OF FUEL MATERIALS AS AN INTERMEDIATE FOR CARBIDE AND NITRIDE FUELS. Coppinger, E. A.; Johnson, B. M. (Battelle-Northwest, Richland, Wash.). Nucl. Technol.; 10: 232-41(Feb 1971).

A process for preparing an intimate mixture of uranium (or mixed uranium–plutonium) oxide and carbon was investigated. The objective was to obtain a starting material for carbide or nitride fuel material by a carbothermic reaction between carbon, uranium (plutonium) oxide, and nitrogen. These materials are attractive as nuclear fuel materials because of their high thermal conductivity and fissile material density but suffer from the high cost of production. The process studied, which involves the rapid calcination of a mixture of uranium nitrate and sugar, would potentially lower the cost because it would avoid forming the metal, and it would eliminate the necessity of several steps heretofore required to thoroughly mix reactants for a carbothermic reaction. (auth)

Properties Evaluations

Refer also to abstracts 8427, 8877, 9577, 9586, 9592, 10288, and 10323.

8924 (DP-Report–437) CORRELATION BETWEEN THE EFFECTIVE DIFFUSION COEFFICIENT AND THE POROUS STRUCTURE IN NUCLEAR GRAPHITE. Project DRAGON. Beyer, H. D.; Hugo, P. (Atomic Energy Establishment, Winfrith (England)). Jun 1966. 20p. (CONF-660318–11). Dep. NTIS.

From Dragon Contractors Research and Development Symposium, Harwell, England.

A new method for the experimental determination of effective diffusion coefficients in porous graphites is described. For the measurements the self-diffusion or ortho- and parahydrogen is used; the partial pressure difference in the porous sample is maintained by the conversion of para- to orthohydrogen. Experiments were carried out with nuclear graphites Type G5 and HX12 at different degree of burn-off. The effective diffusion coefficient of hydrogen was measured as a function of pressure at different temperatures. A pore model containing two parameters (tortuosity factor x and shape factor α) is assumed, to correlate the diffusion coefficients with the pore size distribution of the graphite. From the experimental values the two parameters x and α are calculated as a function of burn-off. (auth)

8925 (EUR–4501) CRUSHING BEHAVIOUR OF PYROCARBON COATED FUEL PARTICLES. Drago, A.; Huber, W. (European Atomic Energy Community, Petten (Netherlands). Joint Nuclear Research Center). 1970. 22p. Dep. NTIS (U. S. Sales Only). EUR FF 4.45.

The importance of the optical analysis of the mode of crushing of stressed coated particles, for the characterization of mechanical behavior of the coating, is examined. Experimental results are presented and discussed. (auth)

8926 (GEAP–12133) A THERMODYNAMIC DATA PROGRAM INVOLVING PLUTONIA AND URANIA AT HIGH TEMPERATURES. Quarterly Report No. 12, May 1–July 31, 1970. Aitken, E. A.; Evans, S. K. (General Electric Co., Pleasanton, Calif. Nucleonics Lab.). Oct 1970. Contract AT(04-3)-189. 12p. Dep. NTIS.

Results of experiments directed toward understanding plutonium segregation in urania-plutonia solid solutions and in fast reactor environments through a knowledge of its thermodynamic behavior are reported. The progress of several experiments which have a bearing on plutonium segregation is described. (J.R.D.)

8927 (ORNL–4503(Vol.2)) THORIUM CERAMICS DATA MANUAL. VOLUME II. NITRIDES. Peterson, Sigfred; Curtis, C. E. (Oak Ridge National Lab., Tenn.). [1970]. 13p. Dep. NTIS.

Chemical, mechanical and physical properties of thorium nitrides, alone and in combination with other nitrides and other thorium compounds, are collected from the literature through January 1970 (35 references). The thorium-nitrogen phase equilibrium is reviewed. (auth)

8928 (UCRL-Trans-10505) SINTERING AND STRUCTURE OF TiC–Ni–Mo COMPACTS. Fukatsu, T.; Yamaya, S. Translated by T. Nakagawa for Univ. of California, Lawrence Radiation Lab., Livermore, from Funtai Oyobi Funmatsuyakin; 10: No. 4, 167-71(1963). 15p. Dep. NTIS.

The sintering process of the TiC–10% Ni–10% Mo composition was investigated to study the influence of the addition of Mo on the structure and properties of TiC-based cermets for cutting tools. During solid-state sintering Mo changes into Mo_2C at 800 to 1000°C, the Mo_2C diffusing in TiC and forming a new phase around the TiC particles. The new phase is intermediate in hardness between TiC and Ni, but has the same crystal structure as TiC, and it is therefore regarded as a TiC–Mo_2C solid solution. The development of this phase depends on the sintering conditions, especially temperature, and is remarkable above 1400°C. However, sintered compacts containing such solid solution are unsuitable for cutting tool materials, because of the low wear and chipping resistance of this phase. (auth)

8929 STUDY OF THE EVAPORATION RATES OF THE CARBIDES OF TITANIUM, ZIRCONIUM, HAFNIUM, NIOBIUM, AND TANTALUM AT HIGH TEMPERATURES. Fesenko, V. V.; Bolgar, A. S. (Inst. for Problems in Materials Science, Kiev). High Temp. (USSR) (Engl. Transl.); 7: 226-31(Mar-Apr 1969).

Translated from Teplofiz. Vys. Temp.; 7: 244-51(Mar-Apr 1969).

Langmuir's method has been used to investigate the evaporation rates of the carbides of titanium, zirconium, hafnium, niobium, and tantalum in the temperature range 2800-3400°K. It is shown that during evaporation the compositions of the carbides of titanium, zirconium, and hafnium do not vary and lie close to the stoichiometric composition, whereas the carbides of niobium and tantalum lose carbon preferentially and then evaporate congruently at compositions close to the lower limit of the homogeneity range ($NbC_{0.77}$, $TaC_{0.71}$). The evaporation coefficients of the carbides investigated were determined on the assumption that they dissociate during evaporation. An equation for the congruent evaporation of the materials concerned was derived from the data obtained. It is shown that the results can be explained by the difference in the energy of the Me–Me and Me–C bonds in the carbide lattices. (auth)

8930 INTEGRAL NORMAL EMISSIVITY OF CARBIDES OF TANTALUM AND HAFNIUM OVER THE TEMPERATURE RANGE 1300 TO 3000°K. Sheindlin, A. E.; Petrov, V. A.; Vinnikova, A. N.; Nikolaeva, V. A. (Inst of High Temperature, Moscow). High Temp. (USSR) (Engl. Transl.); 7: 236-8(Mar-Apr 1969).

Translated from Teplofiz. Vys. Temp.; 7: 257-9(Mar-Apr 1969).

The integral emissivity of tantalum and hafnium carbides is determined by a radiation method in vacuum over the temperature range 1300 to 3000°K. The characteristics of the samples are presented. The experimental results are compared with the results of other authors. (auth)

8931 INTEGRATED HEMISPHERICAL EMISSIVITY OF ZIRCONIUM CARBIDE. Petrov, V. A.; Chekhovskii, V. Ya.; Dymov, B. K.; Kilin, V. S. (Inst. of High Temperature, Moscow). High Temp. (USSR) (Engl. Transl.); 7: 239-42(Mar-Apr 1969).

Translated from Teplofiz. Vys. Temp.; 7: 260-4(Mar-Apr 1969).

XUM

Experimental results are presented of measurements of the integrated hemispherical emissivity of pyrolytic zirconium carbide in the temperature range 1200 to 2900°K. Separate experiments were performed to measure the change in the integrated hemispherical emissivity as the specimens were first heated. The results obtained are compared with data in the literature which were obtained by the powder-metallurgy method. (auth)

8932 THERMAL CONDUCTIVITY OF CERAMIC SOLID SOLUTIONS. Murabayashi, Masayuki (Tokyo Univ.). J. Nucl. Sci. Technol. (Tokyo); 7: 559-68(Nov 1970).

The thermal conductivity of ThO_2-UO_2 and ThO_2-CeO_2 systems was measured by laser flash method, and the results are discussed with the aid of the relaxation-time theory. Two parameters characteristic to systems of the same base—the ratio α of scattering rates between N- and U-scatterings and the strain parameter ϵ—were determined experimentally from the measured thermal conductivity of the ThO_2-UO_2 system at 25°C. Using these parameters, the thermal conductivities of ThO_2-UO_2 system at 100 and 500°C and that of ThO_2-CeO_2 at 25°C were calculated. The results obtained agree very well with the experimental values. In the ThO_2-UO_2 system, the predominant contribution to the scattering cross section of phonons is the strain factor, while in the ThO_2-CeO_2 system, the contribution from the mass factor increases, which makes the thermal resistivity of the ThO_2-CeO_2 system higher than that of the ThO_2-UO_2. (auth)

8933 SCIENCE OF CERAMICS. VOLUME 5. Proceedings of the Fifth International Conference Held at Ronneby Brunn, Sweden, 20-23 April 1969. Brosset, C.; Knopp, E. (eds.). Goteborg; Swedish Institute for Silicate Research (1970). 588p. £5.8.9. (CONF-690432).

Twenty-seven papers were presented, of which separate abstracts are included for eight papers. Discussions are included. (UK)

For abstracts of individual papers see: 8914, 8915, 8934–8937, 8945, and 8959.

8934 ANION AND CATION DIFFUSION IN SOME TRANSITION METAL OXIDES. Lacombe, P. (Ecole des Mines, Paris. Faculte des Sciences, Orsay, France). Sci. Ceram.; 5: 111-50 (1970).

From 5th International Conference on Science of Ceramics, Ronneby Brunn, Sweden. See CONF-690432.

Various transition metal oxides (FeO, MnO, ZrO_2, TiO_2, UO_2) were investigated with regard to electrical conductivity and cation diffusion coefficients. Experiments were also made on transport number by diffusion at high temperatures under an electric field. By comparing values of diffusion coefficients as measured by radiotracer technique with values calculated from measurements of transport number, it was possible to determine the predominant mechanism of diffusion (anionic or cationic). The nature of the defects in these oxides can be specified as a function of the deviation from stoichiometry; the chemical and physical properties are directly related to the nature of the defects. Some examples are discussed. (auth) (UK)

8935 KINETICS AND MECHANISM OF SOLID STATE REACTIONS IN THE SYSTEMS OF REFRACTORY OXIDES. Glushkova, V. B.; Koehler, E. K.; Scherbakova, L. G. (Inst. of Silicate Chemistry, Leningrad). Sci. Ceram.; 5: 219-42(1970).

From 5th International Conference on Science of Ceramics Ronneby Brunn, Sweden. See CONF-690432.

The kinetics of the reactions leading to the formation of rare-earth zirconates and hafnates and to ZrO_2 and HfO_2 based solid solutions of the rare earths, and the mechanism of these reactions, are still not clearly understood. The mechanism of interaction between the components was investigated by preparing the rare-earth zirconates and the ZrO_2-based solid solutions. The compositions investigated were prepared by different methods, namely: by thermal decomposition of zirconium nitrate and rare earth nitrate mixtures; by coprecipitation of the polymeric hydroxides and subsequent crystallization of the final product; by heating mixtures of zirconium and rare earth oxide hydrates; and by heating mixtures of ZrO_2 and rare earth oxides. The first two methods gave an intermediate product, the metastable cubic solid solutions. The progressive development of phases formed as a result of interaction of hafnium dioxide with the rare earth oxides and yttrium oxide was also investigated. The second method produced the metastable low temperature cubic (CaF_2-type) solid solution. The kinetics of formation of lanthanum zirconate, neodymium hafnate, and ZrO_2-based solid solutions with additions of rare-earth oxides were investigated. The kinetic data were processed in accordance with Jander's equation and the generalized equation of Erofeev. Activation energies for the reactions studied were calculated. (auth) (UK)

8936 HIGH TEMPERATURE CERAMIC CONDUCTORS AND INSULATORS. Millet, J.; Guillou, M.; Busson, N.; Asquiedge, M.; Jacquin, M. (Electricite de France, Paris). Sci. Ceram.; 5: 423-40(1970).

From 5th International Conference on Science of Ceramics, Ronneby Brunn, Sweden. See CONF-690432.

The development of MHD processes for energy conversion has led to a search for new ceramics with special electrical properties, and the materials must be capable of operation in the presence of high temperature gas (2700°C) containing potassium salts. This surface temperature can reach 2000°C and they must act as electrical conductors or insulators at above 1000°C; they must also be able to withstand thermal shock. Research was concentrated mainly on binary oxides with ZrO_2, the second oxide being CaO, Y_2O_3 or a rare earth oxide. An important factor is the nature of electrically charged particles in the oxide, and oxides which conduct electronically are less affected by the passage of current than those showing ionic conduction; the latter may be electrolysed. Resistance to corrosion due to condensation of potassium salts is related to the nature of the porosity of the ceramic, and to the acid/base properties of the oxides; also to the presence of impurities which collect at grain boundaries. It was possible to select materials of the electronic conduction type by using the rare earth oxides in which the cation can exist in two oxidation states. Ceramics containing 75% ZrO_2 and 25% CeO_2 were found the most suitable. Very pure MgO was found very suitable as a high temperature insulating material. A ceramic insulator can maintain its properties only if it has low porosity and does not contain fine pores through which the molten salts can move easily. (UK)

8937 FABRICATION AND PROPERTIES OF HIGH STRENGTH OXIDES AND OXIDE COMPOSITES. Matkin, D. I. (Atomic Energy Research Establishment, Harwell, Eng.). Sci. Ceram.; 5: 441-72(1970).

From 5th International Conference on Science of Ceramics, Ronneby Brunn, Sweden. See CONF-690432.

The influence of microstructure on the mechanical properties of oxide ceramics is reviewed, and since the microstructure is determined by the method of fabrication, an assessment is made of techniques for the fabrication of oxides with the required microstructure, such as high density and fine grain size. The importance of the initial powder characteristics is emphasized. The brittle behavior of ceramics is also examined and current studies on the toughness of ceramic composites are discussed. The cases of Al_2O_3, MgO, and BeO are considered. (UK)

8938 HIGH-TEMPERATURE X-RAY STUDIES OF WIDELY NONSTOICHIOMETRIC REGIONS IN THE PRASEODYMIUM OXIDE–OXYGEN SYSTEM AND STRUCTURE AND THERMAL STABILITY OF THE RARE EARTH CARBONATES AND FORMATES. Turcotte, Rheal Peter. Tempe, Ariz.; Arizona State Univ. (1970). 161p. University Microfilms Order No. 70-11,898.

Thesis.

Powder x-ray diffraction methods were used in elucidating certain structural properties of the praseodymium oxides and the rare earth carbonates and formates, mostly at high temperature in controlled atmospheres. Thermogravimetric analysis (TGA) was also used. The PrO–O system was examined in the nonstoichiometric regions: sigma ($1.5 < O/M < 1.714$), alpha ($1.75 < O/M < 1.85$), and the pseudo-phase regions for $O/M \sim 1.80$ and 1.72. The high-temperature x-ray study in the sigma region defined a metastable phase diagram showing two biphasic regions in the nonstoichiometric field. The two-phased, bcc region was shown to be formed in cooling at a temperature of ~380°, while the (σ-ι) region extended over the entire temperature range of stability for the ι phase ($PrO_{1.714}$). The stable phase relations were shown to be essentially as given by earlier workers with the A-form sesquioxide and ι-phase defining a two-phased region for $t < 910°$. The alpha-phase investigation supported detailed tensimetric experiments which showed that this nonstoichiometric phase consisted of four modifications, seen as discontinuities in a plot of chemical potential versus temperature. The x-ray data included precision lattice parameter measurements and a qualitative line-broadening study. An analysis of the combined information led to a plausible description of the alpha phase as composed of domains of the ordered phases with coherence maintained in the metal sublattice. The pseudo-phase regions at compositions near $PrO_{1.72}$ and $PrO_{1.80}$, so-called because of their bivariant behavior, are entered either from the alpha phase or from more oxidized, ordered phases (in the $PrO_{1.80}$ case). Of primary significance, in a study of these, was the observance of distortion

from cubic symmetry and the appearance of weak superstructure in the x-ray patterns of the alpha phase preceding conversion to the 1.80 pseudo-phase. Thus, a progression from very short-range order to medium-range, to long-range order is seen in going from alpha at high temperatures, to the ordered phases at lower temperatures. A description of the 1.80 pseudo-phase as composed of microdomains of ordered and partially ordered types can account for the observed behavior. The rare earth dioxymonocarbonates were investigated by x-ray-diffraction, tensimetric, and infrared methods. The intermediate, $Ln_2O_3 \cdot yCO_2$ reported by others as a decomposition product was shown to be a mixture of Ln_2CO_5 II and Ln_2O_3 and the structures for the polymorphic forms (I tetragonal, IA-monoclinic, II-hexagonal) were further elucidated by thermal expansion measurements and by the infrared absorption spectra. The preparation and investigation by x-ray and TGA methods of the rare earth formates gave an extensive, preliminary description of the hydrated and anhydrous forms and their decomposition products. The initial preparation by direct reaction of the oxide and formic acid gave an anhydrous formate of rhombohedral symmetry for the light rare earths or one of two dihydrated structures for the heavy members. Of eight structure types found, powder-diffraction data were obtained for seven, and three patterns were indexed. The remaining diffraction patterns were not able to be indexed on orthorhombic or higher symmetry. (Diss. Abstr. Int., B)

8939 HEAT CAPACITY AND THERMODYNAMIC PROPERTIES OF α-BERYLLIUM NITRIDE, Be_3N_2, FROM 20 TO 315 K. Furukawa, George T.; Reilly, Martin L. (National Bureau of Standards, Washington, D. C.). J. Res. Nat. Bur. Stand.; 74A: 617-29(Sep-Oct 1970).

The heat capacity of α-beryllium nitride, Be_3N_2, was determined from 20 to 315°K and the thermodynamic properties calculated from 0 to 315°K. The entropy at 298.15°K was found to be 34.4 ± 0.3 J/K · mol (8.23 ± 0.08 cal/K · mol). The precision using a calorimeter of a new design is shown to be ±0.01 percent over most of the temperature range of the measurements. (auth)

8940 CRACK FORMATION NITRIDED COMPONENTS OF X6CrMo4. Kurz, Rudolf; Nissl, Adolf; Lissy, Margit (Siemens-AG, Berlin). Prakt. Metallog.; 7: 634-6(Nov 1970). (In German and English).

An analysis of failure causes in nitrided $X6CrMo_4$ components is presented. The analysis is illustrated by microphotographs. (J.R.D.)

8941 THERMODYNAMIC PROPERTIES OF THE ACTINIDE NITRIDES. Tagawa, Hiroaki (Japan Atomic Energy Research Inst., Tokyo). Nippon Genshiryoku Gakkaishi; 12: 658-65(Nov 1970). (In Japanese).

The present state of knowledge of the thermodynamic properties of the actinide nitrides is reviewed. Few thermodynamic data are available for these nitrides except for the case of UN. The thermal functions for uranium nitrides are derived, and those for ThN and PuN are estimated. (auth)

8942 EXPERIMENTAL STUDY OF THE THERMAL CONDUCTIVITY OF HIGH-POROSITY GRAPHITIC CARBON. Bel'skaya, E. A.; Tarabanov, A. S. (High Temperatures Inst., Moscow). Heat Transfer - Sov. Res.; 2: No. 5, 136-43(Sep 1970).

An experimental study was carried out of the thermal conductivity of graphitic carbons in the 19–80% porosity range. The thermal conductivity was measured by using a steady radiant heat flux from an internal bar-type heater. The studies were carried out in the temperature range of 500 to 2200°K. The experimental data in the above temperature range in the 19–50% porosity range are satisfactorily described by the equation $\lambda = \lambda_0 (1 - p)$. For higher porosities, the experimental points deviate somewhat from this relationship in the direction of decreasing λ. (auth)

Structure and Phase Studies

Refer also to abstracts 8263 and 9577.

8943 (KFK-1235) ON THE SYSTEM $UO_2-UO_3-LaO_{1.5}$. Diehl, Hans Guenther (Kernforschungszentrum, Karlsruhe (West Germany). Institut fuer Radiochemie). Jul 1970. 74p. (In German). Dep. NTIS (U. S. Sales Only).

Single-phase regions found in the system $UO_2-UO_3-LaO_{1.5}$ at 1250°C include $\beta-U_3O_8$ in which no solubility for $LaO_{1.5}$ could be observed and a fluorite phase in which increasing lanthanum content the transition from $(U,La)O_{2+x}$ (additive substitution) to $(U,La)O_{2-x}$ (subtractive substitution) via $(U,La)O_{2.00}$ was observed. A rhombohedral phase II was also found which extends from 71.5 to 76.5 mole % $LaO_{1.5}$ (U^{6+}) and shows little phase width. A rhombohedral phase I occurs exactly stoichiometrically at the limiting compositions $UO_2 \cdot 6LaO_{1.5}$ and $UO_3 \cdot 6LaO_{1.5}$. Between these compositions a maximum of phase width is observed for U^{5+}. In the quasi-binary system $UO_{2+x}-LaO_{1.5}$ (1 atm O_2) the rhombohedral phase II transforms to a fluorite phase above 1310°C. A third rhombohedral phase occurs at 55–66.7 mole % $LaO_{1.5}$ below 1220°C. The relation O:Me is 2.00 all over the phase range. The medium valence ($\overline{W}$) of uranium is rather independent of the annealing temperature, it increases with increasing content of lanthanum and keeps constant at contents of lanthanum higher than 66.7 mole %, the valence of uranium then being 6.00. The greater the content of lanthanum oxide is in the mixed oxides, the less completely uranium is reduced by hydrogen. IR-spectra of the different phase ranges exclude a UO_2^{2+}-grouping in the lattice. For the composition $(U_{0.5}La_{0.5})O_{2+x}$ a minimum of the lattice parameters was found for x = O depending on the stoichiometry of the compounds. (auth)

8944 (KFK-1236) RELATIONS BETWEEN STEREOMETRIC MICROSTRUCTURE AND PROPERTIES OF CERMETS AND POROUS MATERIALS. Nazare, S.; Ondracek, G.; Thuemmler, F. (Kernforschungszentrum, Karlsruhe (West Germany). Institut fuer Material- und Festkoerperforschung). Jul 1970. 15p. (CONF-700709-1). Dep. NTIS (U. S. Sales Only).

From International Powder Metallurgy Conference, New York, N. Y.

The characteristic parameters of a dispersed phase in a matrix of another phase may strongly influence the properties of a two-phase material. This is especially true for cermets, which consist of a phase having often very different properties, because one phase is a ceramic, the other is a metal. In this sense, porous specimens, as achieved generally with powder metallurgical methods, are a special case of cermets. This is why the effects of several parameters of a dispersed phase in a matrix on some properties shall be considered here in a more general manner. At first theoretical considerations are discussed for the concentration function of the electrical conductivity of cermets. Some other properties like permeability and thermal conductivity are also mentioned. The limiting cases of the equations enable us to consider the influence of pores in single phase material as well as particle shape, distribution and size of the dispersed phase on cermet properties. These considerations from a theoretical point of view are then compared with experimental results available. Conclusions are drawn about the relationship between the stereometric microstructure of cermets and porous materials and the properties mentioned. (auth)

8945 HIGH TEMPERATURE OXYGEN EQUILIBRIUM IN THE PLUTONIUM–OXYGEN SYSTEM. Riley, B. (Westinghouse Electric Co., Cheswick, Pa.). Sci. Ceram.; 5: 83-109 (1970).

From 5th International Conference on Science of Ceramics, Ronneby Brunn, Sweden. See CONF-690432.

The oxygen equilibrium dissociation pressures over PuO_2 up to its melting point were measured using a unique high temperature oxidation furnace. PuO_2 melts at 2400 ± 20°C under ~½ atmosphere of oxygen. PuO_2 has a fcc fluorite structure with a_0 = 5.395 to 5.400 Å over the composition range $PuO_{2.007}$ to $PuO_{1.98}$. PuO_2 readily loses oxygen when heated in vacuum, reducing or inert atmospheres to form a series of reduced oxides, having room temperature structures of firstly a two-phase fcc–bcc structure, and finally hexagonal $PuO_{1.5}$. The composition of the bbc phase above 600°C was determined on quenched samples by comparison of x-ray line intensities and O/Pu ratio and approximates to the composition $PuO_{1.62\pm0.01}$. This phase is similar to a modified C-type rare earth sesquioxide (M_2O_3) of varying lattice parameter between 10.950 and 11.100 Å. It melts at 2200 ± 20°C under an oxygen dissociation pressure within the range 10^{-15} to 10^{-10} atm O_2. Further loss of oxygen from the $PuO_{1.62}$ results in the formation of hexagonal $PuO_{1.5}$, an A-type rare earth sesquioxide (La_2O_3) of lattice constant a_0 = 3.848 Å, c_0 = 5.950 Å, melting at 2075 ± 5°C under a partial oxygen pressure of between 10^{-15} and 10^{-20} atm O_2. Between the compositions bcc $PuO_{1.62}$ and hexagonal $PuO_{1.5}$ a eutectic exists, melting at 1970 ± 5°C and of composition $PuO_{1.55\pm0.01}$. No evidence was found of a PuO phase even on prolonged heating, or of metallic Pu at high temperatures. PuO_2 was heated and quenched from temperatures up to 1700°C under 10 atm O_2 without any significant change in lattice parameter or increase in O/Pu ratio. The fcc room temperature structure extends over the composition range $PuO_{1.96}$ to $PuO_{2.007}$. The high and low temperature phase diagrams in the Pu–O system are compared in the light of recent data. (auth) (UK)

8946 CONTRIBUTION TO THE STUDY OF THE FORMATION AND NATURE OF TWIN CRYSTALS IN U_3Si. Lombard, L.; Pelissier, J.; Silvestre, G.; Zberea, I. (CEN, Grenoble, France). J. Nucl. Mater.; 37: 121-4(Oct 1970). (In French).

XUM

The compound U_3Si was studied to determine the relation between the formation of bicrystals and the tetragonal cubic transformation. The crystallographic plane of the bicrystal was studied by electron diffraction microscopy. It was found that U_3Si, formed by thermal treatment between 600 and 700°C, did not show bicrystals. In the products formed above 700°C, examination after cooling showed that bicrystal formation appeared and increased with temperature. For temperatures of 765°C and above, the density of bicrystals remained at a maximum and constant. Furthermore, it was observed that bicrystal formation obtained in the course of the formation of U_3Si or by subsequent treatment, persisted in spite of holding it at constant temperature for a long period of time at a temperature below 700°C. (R.C.K.)

8947 CONCERNING AN ORDERED SOLID SOLUTION OF BERYLLIUM IN U_3Si_5. De Tournemine, R.; Molho, S. (Centre d'Etudes Nucleaires Grenoble, France). J. Nucl. Mater.; 37: 255-6(Nov 1970). (In French).

A study was made of the ternary U–Si–Be in which it was possible to isolate a phase with an approximate formula $USi_{1+x}Be_{1-y}$ ($x - y \leq 0$; $0 \leq x \leq 0.20$ and $y \geq 0.10$) determined by chemical analysis and electron microprobe analysis. It was found that the x-ray diffraction spectrum of USiBe was identical to that of U_3Si_5 which has a hexagonal structure of the same type as AlB_2. The parameters for U_3Si_5 are: $a = 3.843$ Å and $c = 4.069$ Å and for USiBe: $a_0 = 3.866 \pm 0.001$ Å and $c_0 = 4.011 \pm 0.001$ Å Evidence was found that the compound has a formula very close to $USi_{1.1}Be_{0.9}$. (R.C.K.)

8948 NEW TERNARY COMPOUNDS WITH THE STRUCTURE OF $YCrB_4$ TYPE. Kuz'ma, Yu. B. (Lvov State Univ., Kiev). Dopov. Akad. Nauk Ukr. RSR, Ser. A; No. 8, 756-8(Sep 1970). (In Ukrainian).

The compounds RVB_4 and $RMnB_4$ (R–Y, Gd, Tb, Dy, Ho, Er) with the orthorhombic structure of the $YCrB_4$ type were found by means of x-ray diffraction. Lattice constants are given. (auth)

8949 CHARACTERIZATION OF ALKOXY-DERIVED YTTRIA-STABILIZED HAFNIA. Brown, L. M. (Univ. of Cincinnati); Mazdiyasni, K. S. J. Amer. Ceram. Soc.; 53: 590-4(Nov 1970).

High-purity submicron $HfO_2 \cdot Y_2O_3$ powders were prepared by the simultaneous hydrolytic decomposition of hafnium and yttrium alkoxides. Compositions of 1 to 7 mole % Y_2O_3 in HfO_2 were studied by high-temperature x-ray diffraction, electron microscopy, BET surface area measurements, emission spectrographic analysis, TGA, and DTA. X-ray diffraction and atomic absorption were used to determine the Y_2O_3 concentration. Hot-pressing or cold-pressing and sintering of the powders resulted in nearly theoretically dense bodies with uniform microstructure containing grains 1 to 5 μm in size. Surface reflection ir spectra were obtained for monoclinic, tetragonal, and cubic specimens. Fully cubic HfO_2 with 7 mole % Y_2O_3 additions was obtained at a relatively low temperature. The hot-pressed specimens, initially slightly oxygen-deficient or gray HfO_{2-x}, were reoxidized at 1000°C with no deleterious effects; thin sections were translucent to incident light. (auth)

8950 ELECTRON-DIFFRACTION INVESTIGATION OF THE PHASE TRANSITION IN THIN FILMS OF TANTALUM OXIDES HAVING A PEROVSKITE-LIKE STRUCTURE. Khitrova, V. I.; Pinsker, Z. G. (Inst. of Crystallography, Moscow). Sov. Phys.-Cryst. (Engl. Transl.); 15: 455-60(Nov-Dec 1970).

Translated from Kristallografiya; 15: 540-6(May-Jun 1970).

The electron diffraction structural analysis method was used to investigate that phase from a number of cubic tantalum oxides with the perovskite-like structure, the identity parameter of the cell of which a = 7.75 Å. The analysis of the structure was performed from the profiles of the three-dimensional series of the Fourier potentials. The phase is totally preserved in the structure of the cubic cell made only of the tantalum atoms which, however, have different probabilities of occupancy of its points as compared to isotypic structures; the coordination of the Ta atoms was changed due to the substantial change in the coordinates of the oxygen atoms, and —all in all —the structure does not have a cubic symmetry and is described by the space group Pmmm. The coordinates of the atoms are given. The structure must be considered as being an intermediate one during the phase transition to another structure with a lower symmetry. (auth)

Radiation Effects

Refer also to abstracts 8896, 9551, 10125, and 10213.

8951 (GEAP-10217) ZIRCALOY-CLAD UO_2 FUEL ROD EVALUATION PROGRAM. Quarterly Progress Report No. 11, May–July 1970. Megerth, F. H. (comp.) (General Electric Co., San Jose, Calif. Reactor Fuels and Reprocessing Dept.). Aug 1970. Contract AT(04-3)-189. 52p. Dep. NTIS.

The relative rod-average burnups of 41 rods were determined by gamma scanning with a germanium (lithium) detector system and counting the ^{137}Cs line. The minimum-to-maximum burnup ratio among these rods was 0.82. The axial gamma profiles of the 41 rods were of similar shape. The ratios of axial peak burnup to average burnup for the different rods ranged from 1.06 to 1.17. Some data on the distributions of ^{144}Ce, ^{106}Ru, and ^{95}Zr also were obtained by gamma scanning. Diameter profiles determined on six fuel rods before and after chemically removing the deposited crud indicated rod-average crud thicknesses that ranged from 0.0008 cm to 0.0017 cm and had an overall mean value of 0.0012 cm. The maximum circumferential-average crud thickness at any axial location of any rod was 0.0028 cm. When compared with pre-irradiation rod diameter measurements, the diameters after decrudding showed an overall average increase of 0.0025 cm and a maximum rod-average increase of 0.0046 cm. Some local increases in diameter up to approximately 0.010 cm were noted. All rods showed peaks in their diameter profiles at the VBWR spacer locations, and frequently peaks also were present at the SA-1 subassembly spacer locations. Some instances of diameter peaking at pellet-length intervals were noted. The difference in diameter between these peaks and the corresponding troughs was typically 0.0012 to 0.0019 cm and had a maximum value of about 0.0025 cm. The difference between the maximum diameter and the minimum diameter at a given point along the rod axis ($o.d._{max} - o.d._{min}$) was as large as 0.0075 or 0.010 cm at some locations of some rods. Decrudding resulted in decreases in $o.d._{max} - o.d._{min}$ in some cases and increases in others. A surface roughness, which varied in degree from rod to rod and with axial location and with radial orientation on a given rod, was observed after the six rods had been decrudded. Portions of the rod surfaces were primarily white or light gray after the decrudding operation, while other areas had a generally darker appearance, sometimes in combination with fine, white speckling. The darker areas had a brownish color. Four of the rods showed smooth, dark brown circumferential rings spaced at pellet-length intervals, and concentrations of small, blister-like protrusions arranged in a series of narrow parallel rings were noted on three rods. Marks where the SA-1 subassembly spacer springs had contacted the cladding surface were apparent on most of the rods. They did not appear to indicate cladding penetrations any deeper than those measured in the initial phase of the program (i.e., ~0.005 cm). Two rods contained small pit-like penetrations up to 0.010 or 0.012 cm deep. Neutron radiographs were taken of six rods in which possible cracks, small pit-like penetrations, small blisters, or discolored areas were noted during visual examination of the external surfaces. Nothing significant was detected on the neutrographs in these particular regions. The neutrograph of one rod, however, did show a ~0.1 cm-long, rather faint dark gray spot on the tube wall which might have been caused by a relatively high concentration of hydrogen. Further investigation of this region is planned. Nine of the fuel rods were punctured, and the contained free gases were collected. They have not yet been analyzed for composition or fission gas release. The gas contents ranged from 5.1 to 12.5 cm^3. By comparison, rods examined in the initial phase of the program contained 4.7 to 9.5 cm^3 of gas. The maximum fission gas release shown by any of these earlier rods was 0.9 percent. Seven cladding samples from some of the fuel rods that were removed from SA-1 in January 1967 were analyzed for tritium. The tritium contents ranged from approximately 5 to 58 ppB, equivalent to about 2 to 16 percent of the tritium generated during operation. The samples contained 500 to 920 μl/gm (45 to 82 ppM) total hydrogen and, in addition, 6 to 108 μl/gm CO, 3 to 26 μl/gm CO_2, 15 to 20 μl/gm nitrogen, up to 5 μl/gm oxygen, and up to 2 μl/gm CH_4. Krypton-85 analyses also were performed primarily to qualitatively determine the detectability of this isotope in cladding samples. (auth)

8952 (ORNL–4600, pp 81-125) MECHANICAL PROPERTIES OF ALLOYS IN REACTOR ENVIRONMENTS AND DEVELOPMENT OF LMFBR CLADDING AND STRUCTURAL MATERIALS. (Oak Ridge National Lab., Tenn.).

From Fuels and materials development program.

Specimens of Type 304 stainless steel were irradiated at 370 to 600°C to fast-neutron fluences of 2 to 6.7×10^{22} neutrons/cm^2. After irradiation at 370 to 470°C, their microstructures consisted of voids and faulted interstitial dislocation loops. The void concentration increased with increasing fluence at constant temperature. Specimens irradiated at 600°C contained a dislocation network, a few unfaulted dislocation loops, and voids. These changes in microstructure brought about large changes in the creep properties at 600°C. The fracture strain was reduced by all exposures. Nickel 270 was irradiated at 370 to

525°C to fast-neutron fluences up to 1.4×10^{20} neutrons/cm^2. A comparison with other studies showed that the void configuration was very dependent upon the source and condition of the material but that the macroscopic swelling was independent of such variables. These findings and observed inhomogeneous void distributions are the basis of a model in which the voids are nucleated by preexisting gas bubbles or He produced during irradiation. Specimens of Mo, Mo–0.5% Ti, and Mo–50% Re were irradiated at 425°C to a fast-neutron fluence of 1.5 to 3.5×10^{22} neutrons/cm^2. Tensile tests after irradiation showed that the ductility was reduced drastically for all alloys at test temperatures of 400 to 800°C. Results of previous irradiation experiments showed that Incoloy 800 had lower fracture strains when irradiated at 500°C than at higher temperatures. The possibility of a thermal instability was checked further by aging material that had been solution annealed and material that had received a further treatment at 800°C to agglomerate carbides. Creep tests at 650°C showed that aging strengthened both materials and that the ductility of the sample that had been solution annealed was reduced whereas that of the material annealed to agglomerate carbides was unaffected. (auth)

8953 (ORNL–4600, pp 177-80) DEVELOPMENT OF URANIUM MONONITRIDE FUELS. (Oak Ridge National Lab., Tenn.).

From Fuels and materials development program.

Postirradiation examination of the bottom pin of capsule UN-3 revealed incipient failure of the T-111 cladding. This pin was a duplicate of the middle pin in the same capsule that failed after 5800 hr at peak temperatures above 1400°C. (auth)

8954 (ORNL–4600, pp 210-15) FAST-NEUTRON IRRADIATION EFFECTS ON ELECTRICAL INSULATORS. (Oak Ridge National Lab., Tenn.).

From Fuels and materials development program.

Advanced materials (sapphire Al_2O_3, single-crystal MgO, and transparent, polycrystalline Y_2O_3) were irradiated at low temperature (below 150°C) in the Engineering Test Reactor (ETR) to fast fluences up to 2×10^{21} neutrons/cm^2 (>1 MeV). Metallographic examinations revealed no microfracturing. One MgO specimen and one Y_2O_3 specimen broke during irradiation, but all sapphire specimens survived without fracturing. Polycrystalline alumina expanded more in volume and sustained greater microstructural damage in irradiations in the Experimental Breeder Reactor-II (EBR-II) than in the ETR for comparable fast fluences with energies above 1 MeV. This is explained on the basis of differences in the neutron-energy spectra of the two reactors. (auth)

8955 (ORNL–4600, pp 225-34) FISSION-GAS RELEASE AND PHYSICAL PROPERTIES OF FUEL MATERIALS DURING IRRADIATION. (Oak Ridge National Lab., Tenn.).

From Fuels and materials development program.

The preliminary evaluation of data shows the thermal diffusivity to be a function of fission-rate density. The mathematical process of evaluating data is working well, and the method of measuring thermal diffusivity during irradiation by perturbation techniques has been established. The evaluation of the physical condition of mixed oxide fuel specimens by analysis of fission gas was confirmed by analysis after irradiation. (auth)

8956 (ORNL–4600, pp 235-48) DEVELOPMENT OF FUEL ELEMENT FABRICATION. (Oak Ridge National Lab., Tenn.).

From Fuels and materials development program.

Fabrication of the irradiation experiment to be inserted into the High Flux Isotope Reactor (HFIR) for the purpose of establishing the irradiation performance of Advanced Test Reactor (ATR) types of fuel at high burnup is continuing. Postirradiation examination of the HFIR fuel element 49–I is in progress with no evidence of any blisters of the fuel core. The use of Al_2O_3 particles in the filler side of the shaped HFIR core was successful in reducing fabrication blisters in a proof test run by the manufacturer of the fuel elements. Good correlation was obtained between the void volume generated in plates fabricated at ORNL and at Texas Instruments, Inc. Deformation behavior of shaped cores to be used for UAl_x cores is being studied. (auth)

8957 (ORNL–4600, pp 250-1) BEHAVIOR OF REFRACTORY MATERIALS UNDER IRRADIATION. (Oak Ridge National Lab., Tenn.).

From Fuels and materials development program.

The status of the work under this program, which was terminated on June 30, 1970, is summarized. (auth)

8958 (SRARI-P–73) MECHANISM OF GAS RELEASE FROM CERAMIC NUCLEAR FUELS. Davydov, E. F.; Zavidovski, V. Ya.; Syuzev, V. N.; Chushkin, Yu. V. (Scientific Research Atomic Reactor Inst., Melekess (USSR)). 1970. 28p. (In Russian). Dep. NTIS (U.S. Sales Only).

Based on the analysis of literature data and other investigations, a trap mechanism for gas release is proposed. On this basis the behavior of inert gases in nuclear fuels is explained. Special experiments at preset temperatures and burnups allowed establishment of the relation between the quantity of gas released during annealing and structural defects behavior. The hypothesis of two stages of gas release occurring during annealing is introduced. Feasible ways of controlling deleterious consequences from fission gas fragments are considered. (auth)

8959 EFFECT OF CYCLIC FAST NEUTRON IRRADIATION DAMAGE AND THERMAL TREATMENT ON MODULUS OF RUPTURE OF BeO. Buresch, F. E. (Max-Planck-Institut fuer Metallforschung, Stuttgart); Hecker, R.; Rixen, W. Sci. Ceram.; 5: 195-218(1970).

From 5th International Conference on Science of Ceramics, Ronneby Brunn, Sweden. See CONF-690432.

BeO has superior nuclear properties as a moderator compared with graphite and it also provides neutron multiplication due to the (n,2n)-reaction. This reaction produces He, which coagulates at high temperature and neutron doses. Internal stresses develop in polycrystalline BeO because of anisotropic thermal expansion after cooling from the sintering temperature. Fast neutrons produce interstitials through knock-on processes, and these diffuse at high temperatures into clusters after doses of about 10^{20} n_f cm^{-2}. These clusters are predominantly parallel to the hexagonal basal plane and therefore also contribute internal stresses. The change in the modulus of rupture of polycrystalline BeO produced by internal stresses due to the anisotropic thermal expansion and the irradiation induced clusters are computed as a function of the grain size, the porosity, the irradiation damage by fast neutrons, the temperature, and the content of He-bubbles, using the modified Griffith-Orowan equation. In the light of experimental results from the literature, the surface energy was treated as a function of grain size and of irradiation-induced internal stresses. The computations showed that the modulus of rupture diminished with grain growth and with increase in the internal stresses. The decrease was diminished with increase of porosity in the range 0 to 15%, on account of relaxation of internal stresses. (auth) (UK)

Plastics and Other Materials

Refer also to abstracts 8392 and 9552.

8960 (CEA-N–1355) CHARACTERISTICS OF ORDINARY CONCRETE RELATIVE TO RADIOPROTECTION CALCULATION. Le Dieu de Ville, Alain; Pepin, Pierre (Commissariat a l'Energie Atomique, Fontenay-aux-Roses (France). Centre d'Etudes Nucleaires). Oct 1970. 10p. (In French). Dep. NTIS (U. S. Sales Only).

The composition of ordinary concrete (water and impurity contents) obtained from experimental results (H transport cross sections and thermal diffusion length) is given. (auth) (France)

8961 (LA–4511) TEPLO: A HEAT CONDUCTION CODE FOR STUDYING THERMAL EXPLOSIONS IN LAMINAR COMPOSITES. Anderson, C. A. (Los Alamos Scientific Lab., N. Mex.). Aug 1970. Contract W-7405-eng-36. 44p. Dep. NTIS.

The Crank–Nicolson finite difference method is used to determine the one-dimensional heat flow in slab, cylindrical, and spherical geometry of reactive solids obeying zero-order kinetics and with temperature-dependent thermal properties. Temperature, flux, or convective boundary conditions can be handled by TEPLO, for which the initial conditions can be taken in exponential form. The method is valid for solids composed of up to 10 materials with different thermal properties. One phase change is permitted in each layer of the composite. The inherent stability of the Crank–Nicolson method and the incorporation of time-step adjustment in TEPLO significantly reduce the computing time for most problems with little loss in accuracy. The small number of data cards and the availability of several plotting options for LASL's CDC 6600 computers allow TEPLO to be readily used. Comparison of numerical solutions from TEPLO with exact solutions for conduction in composites and with solutions to previously studied thermal ignition problems indicate a good accuracy for TEPLO. (auth)

8962 (POR–4013) GROUTING AND MATERIALS CONTROL. Project Officers Report. Project 3.5 of OPERATION FLINT LOCK, SHOT PILE DRIVER. Hoff, G. C.; Stowe, R. L.; Burnett, W. L. (Army Engineer Waterways Experiment Station, Vicksburg, Miss.). 14 Mar 1969. 241p. (WT–4013). Dep. NTIS.

The Grouting and Materials Control Program was undertaken to provide laboratory and field data on all portland-cement-based packing material and instrument grouting used for the Piledriver Event. The program activities included: the selection of one type of backpacking concrete for use in the explosion; providing concrete mixing proportions for all tunnel liners requiring concrete backpacking; assisting the contractor in emplacing the backpacking concrete; inspection, sampling, and testing of all material during emplacement; evaluating the mechanical and physical properties of the granodiorite rock at the site; and development, emplacement, and postshot testing of an epoxy grout with characteristics similar to the surrounding granodiorite and to be used for embedding the instrumentation placed in the rock. The results of each activity are described in detail. (L.C.L.)

8963 BEHAVIOR OF SOME ION-EXCHANGERS, MADE IN ROMANIA, IN THE CONDITIONS OF URANIUM HYDROMETALLURGY. David, B. Rev. Minelor (Bucharest); 19: 150-3(Apr 1968).

Comparing AT-1, IRA-401 and W-SBU resins shows the superior U sorption capacity of AT-1 and the possibility of using it for U sorption from alkaline suspensions with best efficiency at pH = 10 to 10.2; maximum Na_2CO_3/Na HCO_3 content = 30/15 g/liter; resin/suspension ratio = 2/100; and of using VIONITAT-1 resin for sorption from sulfuric acid suspensions with best efficiency for pH = 1.5 to 2.0 and resin/suspension ratio = 6/100. (Fuel Abstr)

8964 LATTICE EXPANSION AND STRAIN IN ION-BOMBARDED GaAs AND Si. Whan, R. E.; Arnold, G. W. (Sandia Labs., Albuquerque, N. Mex.). Appl. Phys. Lett.; 17: 378-80 (1 Nov 1970).

Measurements of the surface topography of ion-bombarded GaAs and Si show a marked elevation of the irradiated portion of the surface relative to the surrounding unirradiated material. The average lattice atom displacement brought about by the expansion can cause anomalously high yields of displaced atoms as measured by backscattering of particles incident along channeling directions. (auth)

PHYSICS (GENERAL)

Astrophysics and Cosmology

Cosmic Ray Exposure Ages

8965 COMPOSITION OF STONY METEORITES. VI. a. THE Mg–Cr RELATIONSHIP IN SOME BASALTIC ACHONDRITES. APOLLO 11 SOIL AND APOLLO 12 ROCK 12038. b. THE Ba–RARE EARTH RELATIONSHIP IN STONY METEORITES AND APOLLO 11 ROCKS AND SOIL. Ahrens, L. H. (Univ. of Cape Town. Max-Planck-Institut fuer Kernphysik, Heidelberg). Earth Planet. Sci. Lett.; 9: 336-40(1 Nov 1970).

Several elements, mainly lithophile, were classified into three groups, according to tendencies and relationships in the basaltic achondrites: (i) Fe, Si, and Mn—concentrations uniform and equivalent, in eucrites and howardites; (ii) Ca, Al, Sc, Ti, Sr, Y, Zr, Nb, Ba, rare earths, Hf, Ta, Th, and U—concentrations in eucrites greater than in howardites; and (iii) Mg and Cr—concentrations in howardites greater than eucrites. In part (a), the Mg–Cr relationship is discussed, and in (b) the relationship between Ba and one rare earth, Nd. In both (a) and (b), the relationships are such that there appears to be a close connection between the composition of basaltic achondrites and the lunar surface. (auth)

8966 COMPOSITION OF STONY METEORITES. VII. SPECIAL SIGNIFICANCE OF EUCRITES STANNERN AND NUEVO LAREDO IN LUNAR-METEORITE COMPARATIVE STUDIES. Ahrens, L. H. (Univ. of Cape Town. Max-Planck-Institut fuer Kernphysik, Heidelberg). Earth Planet. Sci. Lett.; 9: 341-4(1 Nov 1970).

Several refractory elements (Sc, Sr, Ba, Ti, Y and rare earths, U, and Zr) which are strongly enriched in the lunar surface, are enriched in eucrites Nuevo Laredo and Stannern relative to other eucrites and the howardites. Thorium appears to be an exception. The degrees to which these elements enrich, between average eucrite and eucrites Stannern and Nuevo Laredo, vary considerably. For Sc and Sr, the degree of enrichment is small (~5 to 10%) whereas other elements (Zr, Ti, Ba, and particularly the rare earths, for example) are more strongly enriched (~25 to 100%). Nuevo Laredo and Stannern appear to contain either similar or equivalent amounts of the refractory elements considered. (auth)

8967 COMPOSITION OF STONY METEORITES. VIII. OBSERVATIONS ON FRACTIONATION BETWEEN THE L AND H CHONDRITES. Ahrens, L. H. (Univ. of Cape Town. Max-Planck-Institut fuer Kernphysik, Heidelberg). Earth Planet. Sci. Lett.; 9: 345-7(1 Nov 1970).

Quantitative concentration differences of the elements Fe, Si, Mg, Ca, Al, Ti, Mn, K, and P between the L- and H-group common chondrites are compared. The Fe difference (26%) is by far the largest. Phosphorus is positively correlated with Fe, indicating that P may have some siderophile character despite the fact that it occurs either as apatite or merrilite in the common chondrites. Phosphorus is distinctly enriched in the Fe-high enstatite chondrites. The degree of fractionation of most of the lithophile elements examined is 7 to 12%; fractionation of Ti appears to be a little less. A critical comparison of the Si–Mg relationship in the L and H groups of chondrites indicates that these two abundant lithophile elements are slightly fractionated between these two chondrite groups. (auth)

8968 COSMIC-RAY RECORD IN THE METALLIC PHASE OF CHONDRITES. Nyquist, Laurence Elwood. Minneapolis; Univ. of Minnesota (1969). 165p. University Microfilms Order No. 70-15,780.

Thesis.

The concentrations and isotopic compositions of the rare gases He, Ne, and Ar were measured mass spectrometrically in the separated metal phase as well as in bulk samples of fifteen ordinary chondrites. (TSS) (Diss. Abstr. Int., B.)

Stars

Refer also to abstracts 9186, 9187, and 9616.

8969 SCANNER ABUNDANCE STUDIES. II. LATE G AND K DWARFS IN THE SOLAR NEIGHBORHOOD. Taylor, Benjamin, J. (Univ. of California, Berkeley). Astrophys. J., Suppl. Ser.; 22: 177-248(Nov 1970).

A technique developed by Spinrad and Taylor for obtaining metal abundances of late-type stars, and used by them in an earlier investigation of evolved stars, was applied to field dwarfs in the solar vicinity and to the Hyades. The following major conclusions were reached: 1. Super-metal-rich dwarfs (i.e., dwarfs with higher metal content than the Hyades) are to be found in the solar neighborhood; this conclusion is in accord with previous investigations. The fractions of stars which are super-metal-rich in each metal range from 3% for Fe to 9% for Na; about 4% of the stars studied have mean metallicities greater than that of the Hyades. 2. The tight correlation between N, Na, and Fe abundances found by Spinrad and Taylor for evolved stars exists for dwarfs as well. Magnesium and Ca are also correlated with Fe, but with some intrinsic scatter. Alpha-rich stars of solar metallicity exist, but moderately iron-poor, α-poor stars apparently do not. 3. Dwarfs for which $e > 0.35$ and/or $|W| > 40$ km sec^{-1} and which have solar or higher metallicities exist, contrary to the results of Eggen, Lynden-Bell, and Sandage. Little certain correlation between kinematic properties and overall metal abundance is found in the sample studied. Alpha-rich stars generally (but not always) have high velocities; no other generalizations about them appear possible. 4. The abundance heterogeneity observed by Breger in the Hyades moving group probably exists in the 61 Cyg group as well. 5. Helium abundances ranging from fractions of 0 to 0.5 by weight may well be found among some stars in the solar neighborhood. (auth)

8970 PHOTOMETRY OF RR LYRAE VARIABLES IN THE GLOBULAR CLUSTER NGC 6171. Dickens, R. J. (Carnegie Institution of Washington, D. C. California Inst. of Tech., Pasadena). Astrophys. J., Suppl. Ser.; 22: 249-88(Nov 1970).

Photometry in U, B, and V is reported for twenty-one RR Lyrae variables in and near the metal-rich globular cluster NGC 6171. One of the variables is probably not a cluster member. The variations in light and color are discussed, and correlations between various parameters of these curves are found to be similar to those in the more metal-poor globular clusters M3 and ω Cen. The period-amplitude relation of NGC 6171 is shifted slightly toward shorter periods from that of the Oosterhoff group I cluster M3. Detailed comparisons are made with the results of nonlinear pulsation calculations by Christy. These show that the principal physical difference between variables in clusters of different metal abundance is their mean luminosity, which increases with decreasing metal abundance. The theory is successful in reproducing many of the observed characteristics of the variables and was therefore used to derive the following physical quantities for the variables in NGC 6171: $0.84 \leq M_v \leq 1.10$ mag, $0.40\,\mathcal{M}_\odot \leq \mathcal{M} \leq 0.51\,\mathcal{M}_\odot$, $0.33 \leq Y \leq 0.43$. Similar values for the mass $\mathcal{M}$ and helium content Y were derived for M3 and ω Cen. It is probable that a spread in mass of ~20% occurs among the variables in NGC 6171. (auth)

8971 DISTRIBUTION FUNCTIONS OF STAR CLUSTERS. Broderick, John. Waltham, Mass.; Brandeis Univ. (1970). 96p. University Microfilms Order No. 70-17,115.

Thesis.

A model globular cluster was constructed and studied from a point of view different than that usually used. The model is defined by an analytical surface density law found by King (1962) to be in good agreement with observed surface densities of star clusters. From this surface density law the phase space distribution function was sought. Since the distribution function corresponding to a given surface density was not unique, computing was limited to two distribution functions that may have physical significance. These were: the isotropic distribution function (IDF), which depends only on the magnitude of the velocities of the stars and thus is a function of energy only, and the distribution function that makes the entropy of the cluster a maximum. The IDF was found to depend exponentially on the energy for low energies and at high energies it goes linearly to a finite value at the cutoff energy. It was found that the coefficient in the exponential does not keep on increasing as the concentration of the cluster increases, which explains why the model fails to fit spherical galaxies. The abrupt cutoff at high energies would not be physically plausible were the cluster governed solely by an encounter equation; however, arguments in favor of such a cutoff are advanced, which are based on the long relaxation time compared with a cluster's circumgalactic orbital period, and on the change in the tidal escape energy as a cluster executes an elliptical circumgalactic orbit. An integral equation for the maximum entropy distribution function (MEDF) was obtained from a variational principle. From this it is shown that the truncated Maxwellian distribution is an MEDF, as is the distribution that is constant up to the escape energy and is zero thereafter. For the model used, the MEDF was computed by

XUM

constructing a set of perturbing distribution functions that do not contribute to the density. These were added to the IDF in such a way that the result was an MEDF for that set. Six such perturbing functions were constructed and three used in finding the MEDF. The result indicated that the MEDF increases as a function of the magnitude of the angular momentum, which was contrary to what one expects is the situation in a cluster. (Diss. Abstr. Int., B)

8972 MIXING BETWEEN STELLAR ENVELOPE AND CORE IN ADVANCED PHASES OF EVOLUTION. II. EVOLUTION OF STELLAR CORES OF INITIAL MASSES 10 AND $3M_{\odot}$. Sugimoto, Daiichiro (Nagoya Univ., Japan). Progr. Theor. Phys. (Kyoto); 44: 599-616(Sep 1970).

Evolution of stellar cores of initial masses 10 and 3 $M_{\odot}$ was studied from the helium-burning phase up to exhaustion of oxygen in the central region of the core. These cores were assumed to have been formed as a result of hydrogen burning of the stars of mass around 30 and 12 $M_{\odot}$. As discussed in Paper I of this series, a hydrogen-rich envelope with an extended surface convection zone is taken into account by replacing it with suitable boundary conditions at the outer edge of the core. For the core of initial mass 10 $M_{\odot}$ the convection in the envelope was found to become deeper and deeper after a stage near the onset of carbon burning. When there is no neutrino loss, about 4 $M_{\odot}$ of the material in the core has been mixed into the envelope before the exhaustion of oxygen. When there is neutrino loss due to the universal Fermi interaction, on the other hand, the amount of mixing is limited after the carbon burning phase, because the time-scale of evolution is too short compared with the time-scale of heat transfer. For the core of initial mass 3 $M_{\odot}$, the mixing begins after the oxygen-burning phase. Such a difference in mixing as well as difference in chemical evolution of the stars is discussed. (auth)

8973 EFFECT OF ELECTRON CAPTURE ON THE TEMPERATURE IN DENSE STARS. Nakazawa, Kiyoshi (Kyoto Univ.); Murai, Tadayuki; Hoshi, Reiun; Hayashi, Chushiro. Progr. Theor. Phys. (Kyoto); 44: 829-30(Sep 1970).

It has been shown previously that an iron star collapses after the photodisintegration of iron nuclei begins. The central density, as well as the degeneracy of electrons, becomes so great that electron capture by nuclei becomes important. The effect of electron capture on the change of the temperature in such a collapsing star was studied. (W.D.M.)

8974 CALCULATIONS OF COOLING RATES AND SPECTRAL EMISSION OF GASEOUS NEBULAE. Cox, Donald Peyton. San Diego, La Jolla, Calif.; Univ. of California (1970). 189p. University Microfilms Order No. 70-14,347.

Thesis.

A general method of computing hydrogenic recombination decrements in gaseous nebulae is described. The effects of any combination of partial Lyman-line leakage, Balmer-line self-absorption, and internal dust can be calculated from known case-A decrements. Sample calculations are made and their relevance to real nebulae is discussed. The results of calculations of the ionization equilibrium and radiative cooling rate of a high-temperature low-density plasma are presented. The elements H, He, C, N, O, Ne, Mg, Si, and S are considered, and the temperature range is taken to be 10^3 to 10^8 °K. Electron collisions are assumed to be the only ionizing agent. The dynamic and radiative properties are calculated for a steady-state shock wave traveling at about 100 km/sec into the interstellar medium. This is discussed as a possible explanation for the spectra of certain expanding shell-like filamentary nebulae, such as the Cygnus Loop, which may be very old supernova remnants. Guidelines are given for determining the shock velocity, the interstellar particle density, the helium abundance, and the ambient magnetic field strength from observable characteristics of any such flow. (Diss. Abstr. Int., B)

8975 MAGNETIC RESONANCE SPECTRUM OF VIBRATIONALLY EXCITED OH AND A PREDICTION OF THE RADIO-ASTRONOMY SPECTRUM. Churg, Antonie; Levy, Donald H. (Univ. of Chicago). Astrophys. J.; 162: L161-5(Dec 1970).

The magnetic resonance spectrum of the $^2\Pi_{\frac{1}{2}}$, $J = \frac{3}{2}$ rotational state of the $v = 1$ vibrational state of the OH radical was measured. The parameters derived from this spectrum were used to calculate the zero-field lambda-doubling transition frequencies which might be observed in the OH radio spectrum of infrared stars. (auth)

8976 DISTRIBUTION AND KINEMATICS OF THE LATE B-TYPE STARS. Hube, Douglas Peter. Toronto; Univ. of Toronto (1968).

Thesis.

One of the largest gaps in the knowledge of the velocities of the bright stars has been in the radial velocities of the stars with late B-type spectra. In 1963, Heard at the David Dunlap Observatory initiated a program for determining the radial velocities of all the B8 and B9 stars brighter than apparent visual magnitude 6.5m. In 1964 the writer measured the spectrograms that had already been obtained and, with the assistance of other observers, continued the observations, and measured, in all, about 1550 spectrograms of about 250 stars representing nearly all the B8 and B9 stars north of declination −30° that had not previously been adequately observed for radial velocity. The program was extended to the southern hemisphere where an additional 470 spectra were taken at the Radcliffe Observatory, Pretoria. Altogether new radial velocities for 343 stars were obtained and are listed. The radial velocities were combined with proper motions and UBV and H_{β} data to give space velocities, galactocentric coordinates, and ages. The distribution in space as a function of age indicates that the youngest B8–9 stars are members of Gould's Belt for which an age of 40 million years was found—in agreement with the kinematic age. The velocity distribution was compared with that found by Eggen for the A-type stars. There is little similarity between the velocity distributions of the two classes of stars, and reasons are given for believing that Eggen's "stellar groups" are not as well-defined as he has suggested. (TSS) (Diss. Abstr. Int. B)

8977 OBSERVATIONAL ASPECTS OF CEPHEID EVOLUTION. Havlen, Robert James. Tucson, Ariz.; Univ. of Arizona (1970). 204p. University Microfilms Order No. 70-13, 733.

Thesis.

Three galactic classical Cepheids (RS Pup, Su Cas, and SV Vul) were studied with respect to their relationship to the surrounding stars and interstellar material. The observations are interpreted within the existing framework of present theories of Cepheid evolution and of the origin of stars in groups. (TSS) (Diss. Abstr. Int., B.)

8978 DEVELOPMENT OF A STAR WITH 0.6 SUN MASS. Fritze, K. Monatsber. Deut. Akad. Wiss. Berlin; 12: 149-50 (1970). (In German).

The development sequence of a star of 0.6 $M_{\odot}$ was calculated. The chemical composition with a hydrogen content of $X = 0.602$ and a heavy element content $Z = 0.044$ corresponded to extreme population I. The calculations showed that, in cosmological time, no remarkable changes of the entropy of the star occurs. After 17×10^9 years the brightness increase is 0.4. Since simultaneously an increase of the effective temperature results, the deviation from the theoretical main sequence is only about 0.1. A change of the time scale because of the eventual intermixing effect is not to be expected, since the depth of the convection layer remains approximately constant and the region of modified hydrogen occurrence is not attained. (J.S.R.)

8979 ENCOUNTER PHENOMENA IN TRIPLE STARS. Harrington, Robert S. (Naval Observatory, Washington, D. C.). Astron. J.; 75: 1140-2(Dec 1970).

A series of numerical integrations was performed to study the encounter of a binary system with a third body. The model assumes coplanar orbits and point masses, with the third body encountering the binary on a parabolic orbit. Twenty-three special and 197 random orbits were considered. Capture is possible if the initial periastron distance of the parabolic orbit is less than 6 times the semimajor axis of the binary. The lifetimes of such systems may be very long, suggesting that a few of the observed wide multiple or trapezium systems may be transient capture phenomena. There is a slight suggestion that such an encounter may tend to increase the eccentricity of the orbit of the remaining binary. (auth)

8980 NEW AUTOMATIC METHOD FOR THE DETERMINATION OF ELEMENTS OF A CLOSE BINARY SYSTEM. Horak, Thomas B. (Univ. of South Florida, Tampa). Astron. J.; 75: 1116-22(Dec 1970).

An improvement of the iterative minimization method of calculating the elements in the ellipsoid–ellipsoid model is presented. For the sphere–sphere model it becomes possible to introduce a new procedure for finding a minimum of the minimized function. Knowledge of the initial elements is unnecessary. Probable errors of the limb-darkening coefficients and of the relative luminosities can be calculated. New elements of W Ursae Majoris in blue and yellow are given. The method has been checked using synthetic light curves of known elements. (auth)

8981 ROTATIONAL VELOCITIES IN THE ORION NEBULA CLUSTER. Abt, Helmut A. (Kitt Peak National Observatory, Tucson, Ariz.); Muncaster, George W.; Thompson, Laird A. Astron. J.; 75: 1095-7(Dec 1970).

Rotational velocities for 26 O6–A7 stars in the Orion Nebula

cluster show: (i) the unusually low mean rotational velocity for the early B stars that is a characteristic of the Orion association, (ii) higher rotational velocities for the middle and late B stars than in the association, and (iii) very high rotational velocities among A stars relative to similar field stars. It is not known whether the high rotational velocities are a peculiarity of the Orion stars or a characteristic of all B- and A-type stars that have recently arrived on the main sequence. (auth)

8982 CALIBRATION OF THE HYADES-PRAESEPE MAIN SEQUENCE BY A NEW TREATMENT OF THE STELLAR MOTIONS. Upton, Edward K. L. (Univ. of California, Los Angeles). Astron. J.; 75: 1097-1115(Dec 1970).

The distance of the Hyades cluster is determined by dividing its mean radial velocity by the fractional rate of change in angular diameter ($\dot{\theta}/\theta$). This method does not require the location of the convergent point. More importantly, $\dot{\theta}/\theta$ can be determined separately from the proper-motion gradients in right ascension and declination. The two values of $\dot{\theta}/\theta$ differ by only 6%, thus restricting the plausibility of systematic error in either proper-motion component. The detailed treatment makes allowance for the expected deviations from a strictly linear gradient arising from the large angular extent of the cluster. The effect of the spread in distance of individual stars is partly removed by determining relative distances for 70% of them, based on the color–magnitude diagram for Praesepe. Thus the shape of the main-sequence curve is taken from Praesepe, with only a zero point to be determined. The solution yields simultaneously this zero point and the mean distances of the two clusters. The mean proper-motion gradient, based on both μ_α and μ_δ, leads to distance moduli of 3.09 and 6.03 for the Hyades and Praesepe, ±0.04 (p.e.). These results are in good agreement with recent analyses by the convergent-point method. But the zero-age main sequence is found to be brighter by about 0.09m than in previous calibrations based on the Hyades. Most of the change in M_v is caused not by any change in the mean distance to the Hyades, but by a difference in the assumed effect of unresolved binaries on the main-sequence spread. The main-sequence luminosities found are in excellent agreement with a 1955 calibration by Eggen. A rediscussion of possible systematic errors indicates that their total effect on the M_v calibration is unlikely to exceed 0.05m. The total error in the present calibration, from all causes, is unlikely to exceed 0.10m. The discrepancy between the heliocentric and moving-cluster parallaxes for the Hyades is reexamined and found to be 0.0031″ ± 0.0015″ (p.e.). (auth)

8983 DVOINYE ZVEZDNYE SISTEMY S ATMOSFERNYM ZATMENIEM TIPA ζ VOZNICHEGO. (Binary Star Systems With Atmospheres of ζ Aurigae Eclipsing Type). Botsula, R. A. Moscow; Izdatel'stvo Nauka (1968). 104p.

The questions of structure and physics of external layers of the atmospheres of cold supergiants, two-component systems with eclipsing atmospheres, are considered. Results of observations and their explanation are presented. Different hypotheses of the physical state of the substances of the atmospheres are given. The specific methodology of investigation and the formulated problems of study are presented for stars of the ζ Aurigae type. The book is intended primarily for scientists working in the fields of stellar atmospheres, stellar spectroscopy, and variable stars, but may be used by teachers and students of higher courses. (132 references) (tr-auth)

8984 HEAVY ELEMENTS IN PECULIAR A STARS. Sargent, W. L. W.; Brubidge, G. R. (Univ. of California, San Diego). Comments Astrophys. Space Phys.; 11: 172-7(Sep-Oct 1970).

Two recent developments, one theoretical, and one observational, have served to crystallize the problems raised by the remarkable abundance anomalies in the peculiar A stars. The observations are briefly reviewed, and the various theoretical explanations are examined in the light of the new data. (W.D.M.)

8985 INSTABILITIES OF DIFFERENTIAL ROTATION. Spiegel, E. A.; Zahn, J.-P. (Columbia Univ., New York). Comments Astrophys. Space Phys.; 11: 178-83(Sep-Oct 1970).

In recent years the study of stellar models has become sufficiently refined that the effects of rotation must be included. For the calculation of a static model, one needs to know the distribution of angular velocity throughout the model. Of course, this distribution in principle should be calculated from initial conditions, but that is too formidable a task at the present level of the subject, even were the initial conditions known. The alternate procedure, now widely preferred, is to restrict the class of angular-velocity distributions considered by ruling out unstable configurations. This approach has focused attention on the theory of the instability of differential rotation and, accordingly, a brief account of the subject of rotational instabilities is given. (W.D.M.)

8986 SPECTROPHOTOMETRIC STUDY OF SOME STARS OF Of TYPE. Oganesyan, R. Kh. Dokl. Akad. Nauk Arm. SSR; 50: 139-43(1970). (In Russian).

Spectrophotometric studies were made of nine stars of the Of type. The studies were confined to the Of stars selected from the Hiltner and Johnson catalog and included only one normal star O9(HD 209481) and one super giant type O9(HD 209975). Tabulated gradients, parameters, and temperatures are given. The spectrophotometric gradients during the period of the observation varied only slightly. (R.V.J.)

8987 PROCESSES OF NUCLEOSYNTHESIS. Cameron, A. G. W. Comments Astrophys. Space Phys.; 2: 153-60(Jul-Aug 1970).

The classification of the processes of nucleosynthesis given by Burbidge, Burbidge, Fowler, and Hoyle (1957) is presented in a slightly modified form, and the present outlook regarding the stages of stellar evolution that appear to be responsible for specific processes is discussed. (W.D.M.)

8988 UBVr COLORS OF MAIN-SEQUENCE STARS. Boehm-Vitense, E. (Univ. of Washington, Seattle). Astron. Astrophys.; 8: 283-98(Oct 1970).

The UBVr colors of main-sequence stars with spectral types between AO and KO are computed, taking into account theoretical line blanketing. The observed colors require turbulent velocities between 2 and 4 km/sec, provided the solar microturbulence is 2 km/sec, as assumed here. For late A and F stars good agreement with observations is obtained if scaled solar "Bilderberg" models are used, showing that convection in these stars is more effective than indicated by the local mixing-length theory. The scarcity of stars with $0.2 < B-V < 0.4$ can be understood if convection sets in abruptly for $T_{eff} \leqq 8000°$. The relation between B–V and T_{eff} is derived for $B-V \leq 0.90$. (auth)

8989 CONVECTION IN A AND F STARS AND METALLICISM. Boehm-Vitense, E. (Univ. of Washington, Seattle). Astron. Astrophys.; 8: 299-306(Oct 1970).

Theoretical spectra of radiative and convective A and F stars with a given color B–V are compared. The H_γ lines are essentially the same. The Ca II K line is weakened in the convective star. Temperature inhomogeneities further weaken the K line. The possibility is discussed that the metallic-line stars may be the convective version of late A stars. (auth)

8990 STUDY OF SPECTROGRAMS OF CH CYGNI. (Nguyen-Doan (Observatoire de Lyon). Astron. Astrophys.; 8: 307-14(Oct 1970).

About twenty spectra of CH Cygni taken with a moderate dispersion since the outburst of 1967 were studied. The ultraviolet spectra taken in 1968 show that the emission lines visible in 1967 vanish, giving place to an absorption spectrum that is mainly composed of Ti II lines from multiplet 1 (ground state) to multiplet 8 and other low-excitation lines of Cr II, V II, ... The Fe II lines seem to be very weak. The calcium envelope was observed in the spectra taken in March 1969. In the green and red, the spectrum shows, beside the usual absorption lines of the M 6 star veiled from time to time by the hot continuum, the emission nebular lines of [O I], [S II] and chromospheric lines of Na I, He I, Fe II, and [Fe II]. On the whole, CH Cygni offers a stellar, chromospheric, and nebular spectrum with a rather low excitation potential, in contrast to other symbiotic stars and old novaes. (auth)

8991 EXTREME RED STARS IN CYGNUS. Ackermann, G. (Landessternwarte, Heidelberg). Astron. Astrophys.; 8: 315-34 (Oct 1970).

Results are presented of a photographic survey for infrared stars in several fields in Cyg and of photoelectric measurements on a sample of extremely red stars. About 400 new infrared stars were discovered. These stars are concentrated toward the galactic plane. The reddened stars are correlated with dark clouds (field 95–0) and with strong H II regions (field 78–0). Some infrared stars seem to be highly reddened O stars, and possibly the until-now-unknown excitation stars of some H II regions. (auth)

8992 EVOLUTIONARY STATUS OF STARS ABOVE THE HORIZONTAL BRANCH IN GLOBULAR CLUSTERS. Strom, S. E. (State Univ. of New York, Stony Brook. Smithsonian Astrophysical Observatory, Cambridge, Mass.); Strom, K. M.; Rood, R. T.; Iben, I. Jr. Astron. Astrophys.; 8: 243-50(Oct 1970).

Spectra of 13 stars falling above the horizontal branch in M2, M10, M13, M15, and NGC 6712 were obtained with the Carnegie image-tube spectrograph at Kitt Peak. At least 11, and probably all, of these stars are shown to be members on the basis of radial velocity measurements. Of this group, 3 stars are hot enough to show lines of He I, and to within the estimated errors, the abundance of helium is approximately the same as for Pop I B stars. These three stars are very luminous and probably burning helium

XUM

in a shell after a second ascent of the giant branch; that is, they are probably similar in evolutionary state to the cores of planetary nebulae. There is some evidence that in at least two of these stars (M10 I, 33 and Von Zeipel 1128 in M3) significant mixing between the surface and the interior has altered the surface composition. It is suggested that the remaining 8 stars have left the horizontal branch and are burning helium in one shell and hydrogen in another. These 8 stars are most likely the progeny of stars that occupied the very blue end of the horizontal branch. The latter are presumed to have lost a significant amount of mass. The evolutionary lifetimes of these stars above the horizontal branch are consistent with this suggestion for their origin. (auth)

8993 THREE COLOUR PHOTOMETRY OF THE GALACTIC STAR CLUSTERS NGC 7226, NGC 7245, IC 1442 AND Be 94. Yilmaz, Fatma (Univ., Basel). Astron. Astrophys.; 8: 213-22 (Oct 1970).

Three color photometry of these four clusters was carried out with 48" Palomar–Schmidt plates in the RGU system. The distances of the clusters were found as 2240, 1925, 1810, and 1610 pc, respectively. The first two clusters are of an advanced type with a red-giant sequence. The third and fourth are of an early type, b3 and b6, respectively. (auth)

8994 KINEMATIC STUDY OF IONIZED HYDROGEN IN NGC 4490–85. Boulesteix, J.; Dubout-Crillon, R.; Monnet, G. (Observatoire de Marseille). Astron. Astrophys.; 8: 204-12 (Oct 1970). (In French).

The galaxy NGC 4490 was observed in H α light through a narrow band interference filter. New very faint H II regions were detected showing, in particular, that a bridge of matter appears between the galaxy and its companion. The catalog of H II regions of Véron and Sauvayre (1965) was completed. Radial velocities were obtained by an interference method using a Perot–Fabry interferometer with a mean dispersion of 22 Å mm^{-1}. The rotation curve was plotted up to 2.4′ from the center. The center of symmetry is the center of NGC 4490, but the rotational velocities of the H II regions along the north–west major axis are abnormally low and confirm the asymmetric rotation curve of Bertola, who used spectra with the slit set along the major axis. The radial velocities of the H II regions of the bridge and of the companion show evidence of a recent ejection. The total mass of the galaxy was computed, and is discussed. An investigation of the M/L ratio as a function of the distance from the center showed that it increases slowly from the center up to 1.2′. The density as a function of the distance from the center was computed. (auth)

8995 COARSE ANALYSIS OF THE HELIUM-WEAK B STAR IOTA ORI B. Conti, P. S.; Loonen, J. P. (Univ. of Utrecht). Astron. Astrophys.; 8: 197-203(Oct 1970).

An abundance analysis of the helium-weak star ι Ori B was undertaken by means of a relative curve of growth analysis. The standard star was the B2V star HD 35912. Both stars have nearly identical Hγ profiles and Si II/Si III ionization equilibria. Equivalent width measures in both stars revealed the following anomalies in ι Ori B: He deficient by more than a factor ten; O slightly deficient; P and Ga are enormously enhanced. The elements C, N, Mg, Al, Si, S, and Fe are roughly normal in ι Ori B. It is not possible to explain the anomalies in this helium-weak star by nuclear processes and two other suggestions are offered. (auth)

8996 RADIO OBSERVATIONS OF PLANETARY NEBULAE AND POSSIBLE PLANETARY NEBULAE. Rubin, R. H. (Univ. of Illinois, Urbana). Astron. Astrophys.; 8: 171-80(Oct 1970).

Radio observations in the continuum at 2 cm were made of many objects classified by optical astronomy techniques as planetary nebulae or possible planetary nebulae. The primary purpose was to seek out significant radio emitters among those objects called planetaries that had not yet been looked at in the radio region. One object, K3–50, had been called a planetary nebula but current evidence indicates that it is likely a compact H II region. A goal of this work was to obtain statistics on what fraction of objects called planetary nebulae are K3–50-type objects and to aid in discriminating planetary nebulae from compact H II regions. Two of the objects observed (H2–3 and H2–6) appear to be similar to K3–50, while two other objects (M1–78 and A77) are found to have significant radio emission and are probably bonafide planetary nebulae. (auth)

8997 NUMERICAL STUDY OF GRAVITATIONAL STELLAR COLLAPSE. Wilson, James R. (Univ. of California, Livermore). Astrophys. J.; 163: 209-19(15 Jan 1971).

The dynamic gravitational collapse of stars of mass 1.25 to 10 $M_\odot$ was calculated in terms of general relativity. Neutrino flow was calculated in considerable detail to evaluate whether the energy flow of neutrinos can produce mass ejection. Most stars evidently eject no mass by the process of neutrino transport during their collapse even though they radiate about 10^{52} g of neutrinos. Only the low-mass star of 1.25 $M_\odot$ ejects material mass, in this case 1.1×10^{32} g. In this latter case neutrino flow is not important. (auth)

8998 NEUTRON-STAR FORMATION, THERMONUCLEAR SUPERNOVAE, AND HEAVY-ELEMENT REIMPLOSION. Colgate, Stirling A. (New Mexico Inst. of Mining and Tech., Socorro). Astrophys. J.; 163: 221-30(15 Jan 1971).

The reimplosion mass fraction of a presumed supernova explosion was calculated under the assumption of the dynamical formation of a remnant neutron star. It has been pointed out by Arnett and Truran that previous numerical calculations of supernovae based upon transport of heat by neutrinos and dynamical neutron-star formation predicted the ejection of inconsistently large ($\times 10^3$) amounts of neutron-rich matter. The present analytical calculations of the behavior of matter adjacent to the neutron star immediately after the explosion show that this matter cools so rapidly by neutrino emission that reimplosion occurs and a rarefaction wave progresses outward from the surface of the neutron star and reverses the radial trajectory of matter previously exploding. When the rarefaction overtakes exploding matter whose velocity is significantly greater than escape velocity, escape continues. For a rather wide range of explosion conditions (adiabat and surface velocity), an inner mass fraction of 50% of the initially expelled matter reimplodes and removes essentially all the neutron-rich matter from further observation. The subsequent continuing and small reimplosion luminosity was calculated; at late times (10^6 seconds) it is shown to be small, 2.2×10^{38} ergs sec^{-1}, and to have a decay time of 5×10^5 seconds. (auth)

8999 DUST–RADIATION INSTABILITY IN IONIZED NEBULAE. Nordsieck, Kenneth H. (Univ. of California, San Diego). Astrophys. J.; 163: 287-97(15 Jan 1971).

Inhomogeneities in planetary nebulae and H II regions may be formed by the pressure of trapped resonance-line radiation on dust grains. For a large range in physical conditions in such nebulae, the formation time of sizable regions of abnormal dust content is considerably less than the lifetime of the nebulae. The dust and gas, however, are only weakly coupled: the dust perturbation is always at least 10 times the ionized-gas perturbation. The resulting grain-enriched gas may later form into a star with peculiar abundance characteristics, if the region of perturbation is large enough to include a stellar mass of gas. A conventional linear perturbation approach is used to obtain the e-folding time of a dust-density perturbation from a set of differential equations describing the motion and interaction of the dust and gas fluids, the ionization balance of hydrogen, and the diffusion of La line radiation. Also, an estimate of the La density caused by cosmic-ray ionization and excitation of neutral hydrogen in interstellar clouds shows that the instability may be marginally active there for regions less than 1 pc in size (corresponding to included gas masses $M/M_\odot < 1$). (auth)

9000 SCANNER ABUNDANCE STUDIES. III. THE SUPER-METAL-RICH CLUSTER NGC 6791. Spinrad, Hyron; Taylor, Benjamin J. (Univ. of California, Berkeley). Astrophys. J.; 163: 303-7(15 Jan 1971).

From scanner observations of the old open cluster NGC 6791, obtained in a manner previously described by Spinrad and Taylor, it was found that $[M/H] = +0.75 \pm 0.2$ for its metal abundance with respect to the Sun. Despite its position 1 kpc above the galactic plane, this cluster therefore has the highest metal abundance known. The implications of this result are discussed. (auth)

9001 BRIGHTENING OF THE ULTRAVIOLET SPECTRUM OF THE CARBON STAR HD 59643. Greene, Arthur E.; Wing, Robert F. (Ohio State Univ., Columbus. Ohio Wesleyan Univ., Delaware). Astrophys. J.; 163: 309-12(15 Jan 1971).

The carbon star HD 59643 was observed at 66 Å mm^{-1} from 3840 to 7200 Å in 1970 February. Longward of 4000 Å the absorption spectrum matches previous descriptions, but weak hydrogen emission has now appeared. Below 4000 Å the spectrum appears continuous, broken only by asymmetrical emission lines of hydrogen. There is no trace of the H- and K-lines of Ca II which normally appear strongly in absorption when carbon stars are adequately exposed in the ultraviolet. The ultraviolet continuous emission must be of a transitory nature since it was not present when the star was observed by Wildt. Similar activity has been observed in the M star CH Cyg, but has not previously been reported in carbon stars. (auth)

9002 NARROW- AND BROAD-BAND PHOTOMETRY OF RED STARS. V. LUMINOSITIES AND TEMPERATURES FOR YOUNG DISK-POPULATION RED STARS OF HIGH LUMINOSITY.

Eggen, O. J. (Australian National Univ., Canberra). Astrophys. J.; 163: 313-31(15 Jan 1971).

Most of the known high-luminosity red stars, including long-period Cepheids, in the young disk-population groups, clusters, and associations in the Galaxy were observed in the (UBVRI) system. Also, a few Cepheids and supergiants in the Large Magellanic Cloud were included. No clues to possible differences between LMC and galactic stars were found. The simple relation between M(I) and M_{bol} and the available temperature calibration of (R – I) made it possible to construct a composite (M_{bol}, log T_e)-diagram for luminous stars in the young disk population. This diagram may be useful in the construction of stellar models and in the understanding of the evolutionary state of these stars. (auth)

9003 ROTATIONAL VELOCITIES IN SHORT-PERIOD A-TYPE BINARIES. Abt, Helmut A.; Hudson, Katherine I. (Kitt Peak National Observatory, Tucson, Ariz.). Astrophys. J.; 163: 333-6(15 Jan 1971).

Although a low rotational velocity is a necessary condition for a star to have a metallic-line (Am) spectrum, is it a sufficient condition? This study of rotational velocities of stars in binaries with periods less than 5 days shows that (1) most, but not all, late A-type stars rotate synchronously, and the remainder rotate too rapidly; (2) there is an overlap in equatorial rotational velocities of normal and Am stars which indicates that a given rotational velocity is sometimes insufficient to determine whether a star should have a normal or an abnormal spectrum. The additional distinguishing parameter does not appear to be the star's age, the angle at which the star is viewed, or previous history of mass exchange, although it could be a combination of these. (auth)

9004 ASYMMETRIES IN ENVELOPES OF WOLF–RAYET COMPONENTS OF CLOSE BINARIES. Limber, D. Nelson (Univ. of Virginia, Charlottesville). Astrophys. J.; 163: 337-44 (15 Jan 1971).

Idealized dynamical models, based upon different ad hoc WR-centered force laws for both the radiative and hydrodynamic forces, were used to study the effects of close companions in giving rise to geometrical and dynamical asymmetries in W–R envelopes. These effects were found to be significant for the envelopes of that important class of dynamical models that now appears most promising for describing the phenomenon: envelopes for which the outward velocities increase from photospheric values that are small to values at five or more W–R radii that are large, both relative to the absolute orbital speed of the W–R component. This same class of models appears to be consistent with the observations presently available insofar as these asymmetries are concerned and insofar as occultation effects are concerned. (auth)

9005 APSIDAL-MOTION TEST FOR LATE-TYPE STARS. Heasley, James N. Jr. (Yale Univ. Observatory, New Haven). Astrophys. J.; 163: 345-51(15 Jan 1971).

The application of the apsidal-motion test to late-type stars was investigated. The effect of varying the ratio of mixing length to pressure scale height, l/H_p, on the theoretical apsidal-motion coefficient, k_2, was studied for several 1 $M_\odot$ models on the main sequence; and the implications for post–main-sequence evolution were considered. Theoretical apsidal-motion coefficients were calculated for twelve subgiant models. Theoretical models computed by Mathis are used to rediscuss the empirical apsidal-motion coefficients for the subgiant components of six semi-detached binary systems. It is found that observational uncertainties in the ratio of stellar radius to semimajor axis of the orbit can increase these empirical coefficients by a factor of 2. Agreement between theory and observations remains poor, even when the uncertainties in the stellar radii are allowed for. Both the theoretical and empirical coefficients show a high degree of internal consistency, which suggests that a higher-order theory may be appropriate to determine the coefficients for subgiant models or that the internal structure of the secondary component has been changed due to mass loss. (auth)

9006 EVOLUTION OF GROWING STELLAR CORES AND PRESUPERNOVA MODELS. Barkat, Z. (California Inst. of Tech., Pasadena). Astrophys. J.; 163: 433-6(15 Jan 1971).

Recent evolutionary calculations are interpreted in terms of growing carbon cores. The convergence of evolutionary tracks in a specific but important range of parent masses ($4 \lesssim M/M_\odot \lesssim 8$) found by Paczyński is explained, and is shown to be quite general, therefore defining almost a unique presupernova model in the range. (auth)

9007 INVESTIGATION OF THE DYNAMICS OF TRIPLE SYSTEMS BY THE MONTE CARLO METHOD. III. THE CASE OF COMPONENTS WITH DIFFERENT MASSES. Anosova, Zh. P. (Leningrad State Univ.). Astrophysics (Engl. Transl.); 5: 84-4 (Spring 1969).

Translated from Astrofizika; 5: 161-7(1969).

The equations of motion for triple systems were integrated numerically on a computer for 300 different initial configurations. The components were initially at rest, and their masses were as follows: 1) $m_1 = 9$, $m_2 = 3$, $m_3 = 1$; 2) $m_1 = 3$, $m_2 = 3$, $m_3 = 1$; 3) $m_1 = 3$, $m_2 = 1$, $m_3 = 1$. In all cases, the motion of the components terminated in decay of the system. In each case, the decay occurred after a close triple approach of the components. The mean decay time is $\bar{T} = (27.8 \pm 3.5)\tau$, where τ is the mean time of motion of a component through the system. In the great majority of cases the triple system loses the component with the smallest mass. The spread in the masses of the components reduces the decay time by a factor of about three. (auth)

9008 SALMONA'S PAPER ON MODELS OF STATIC CONFIGURATIONS. Avakyan, R. M.; Mnatsakanyan, M. A. (Byurakan Astrophysical Observatory, USSR. Erevan State Univ.). Astrophysics (Engl. Transl.); 5: 85-6(Spring 1969).

Translated from Astrofizika; 5: 169-71(1969).

Salmona (1967) considered a model of a neutron star, using the field equations and the exterior solution obtained by Dicke and Brans. The results were not very different from the Einstein theory and, in principle, indicated that the generalized theory excludes the possibility of static bodies with masses substantially exceeding the solar mass. The aim of the present note is to remove the resulting contradiction with the work of Saakyan and Mnatsakanyan by indicating that the analysis given by Salmona is not correct. (W.D.M.)

9009 NONSTATIONARY RADIATION FIELDS IN INFINITE MEDIA. Nagirner, D. I. (Leningrad State Univ.). Astrophysics (Engl. Transl.); 5: 13-22(Spring 1969).

Translated from Astrofizika; 5: 31-53(1969).

Nonstationary resonance radiation fields in stationary infinite and semi-infinite media are discussed. It is assumed that single scattering occurs without frequency change or with complete frequency redistribution. Nonisotropic scattering and the fact that the velocity of light is finite are not taken into account, but absorption in the continuous spectrum is allowed for. Exact expressions are found for the resolvents of the basic integral equations, and for the intensity of the emerging radiation. The exact formulas are then used to establish the asymptotic properties which reflect the behavior of the radiation field in the line wings and the degree of excitation of atoms at large distances from the radiation sources and after long intervals of time after they cease to radiate. (auth)

9010 EMISSION OF NOVAS PRIOR TO LIGHT MAXIMUM. Leonov, V. V. (Leningrad State Univ.). Astrophysics (Engl. Transl.); 5: 23-8 (Spring 1969).

Translated from Astrofizika; 5: 55-66(1969).

The sources responsible for the radiation emitted by a nova prior to the light maximum are discussed. These are: the energy contained by the envelope, the emission of the star, and the energy originating during the collision between ejected stellar material and the main envelope. Theoretical light curves for CP Lac, v476 Cyg, and DQ Her are calculated and compared with observational data. (auth)

9011 GAS MOTION IN CLOSE BINARY SYSTEMS. Korovyakovskii, Yu. P. (Leningrad State Univ.). Astrophysics (Engl. Transl.); 5: 29-31(Spring 1969).

Translated from Astrofizika; 5: 67-73(1969).

The trajectories of gas jets in close binary systems are considered in the three-dimensional case, taking into account dynamic effects of gas pressure. The coordinates of the point of collision between the gas stream and the envelope of the main star are obtained. The relative velocity of the gas stream and of the envelope at the point of collision lie between 200 and 300 km/sec for model I and between 900 and 1000 km/sec for model II. (auth)

9012 CURVE OF GROWTH FOR AN EXPANDING ATMOSPHERE. Arakelyan, M. A. (Byurakan Astrophysical Observatory, USSR). Astrophysics (Engl. Transl.); 5: 32-5(Spring 1969).

Translated from Astrofizika; 5: 75-81(1969).

The curves of growth for an expanding atmosphere are calculated for the pure-absorption model. It is assumed that the rate of expansion of the envelope is constant, and that the continuous-spectrum intensity of the photosphere is a linear function of cos φ, where φ is the angular distance between the center and the limb. (auth)

9013 EXPANSION OF PLANETARY NEBULAS. Vityazev, V. V. (Leningrad State Univ.). Astrophysics (Engl. Transl.); 5: 36-42(Spring 1969).

XUM

Translated from Astrofizika; 5: 83-95(1969).

The relation between the rate of expansion and the radius of planetary nebulae is confirmed statistically with a satisfactory positive correlation coefficient. The expansion of nebulas is considered under the action of direct L_ν and diffuse L_α radiation. It is shown that L_α radiation plays an appreciable role in the dynamics of nebulas. Assuming that the envelope expands under the action of corpuscular pressure, an estimate is obtained for the rate of emission of matter from the nuclei of planetary nebulae ($\sim 10^{-8}$ $M_\odot$/year). (auth)

9014 SPECTROPHOTOMETRY OF F STARS. IV. LINE PROFILES IN THE SPECTRA OF σ BOO, ν HER, AND 41 CYG. Kipper, T. A. (Inst. of Physics and Astronomy, Tallin, USSR). Astrophysics (Engl. Transl.); 5: 60-6(Spring 1969).

Translated from Astrofizika; 5: 123-35(1969).

A program for calculating the line profiles of Hγ and K Ca II from atmospheric models is described. The program was used to calculate the line profiles for nine models of the atmosphere of F stars. The computed profiles are compared with observational data on the spectra of σ Boo, ν Her, and 41 Cyg. It is established that the Balmer lines are not very sensitive to changes in gravitational acceleration. The K Ca II line profiles are used to determine the amounts of calcium in the atmospheres of σ Boo, ν Her, and 41 Cyg. (auth)

9015 A SEARCH FOR OH 18-cm EMISSION IN THE CEPHEUS IV ASSOCIATION. Winnberg, A.; Lundahl, L. (Onsala Space Observatory, Goteborg). Astron. Astrophys.; 9: 321-4(Nov 1970).

The Cepheus IV area was searched with the Onsala 25.6-m radio telescope on all four OH ground-state lines and with both senses of circular polarization. No line signal stronger than 4 flux units was found after averaging over 10 kHz. The OH absorption lines at 1665 and 1667 MHz were measured with 5 kHz resolution against the continuum source W1 in the center of Ceph IV. The line intensity ratio was found to be compatible with thermodynamic equilibrium and small optical depth. An upper limit to the total mass of the OH clouds surrounding the H II region was estimated to be of the order of 10^{-2} solar masses. (auth)

9016 ON THE POPULATION OF THE 2 ^{3}S LEVEL OF He IN PLANETARY NEBULAE. van Rensbergen, Walter (Univ. of Utrecht. Univ. of Brussels); Wuyts, Jan. Astron. Astrophys.; 9: 325-7(Nov 1970).

Robbins (1968) has noticed a discrepancy between the theoretical and the observed population of the 2 ^{3}S level of He in nine planetary nebulae, the theoretical value of N (2 ^{3}S) being a factor of 5 to over 80 greater than the observed one. This discrepancy is mainly due to too small a value of the excitation rates of exchange collisions (2 ^{3}S − 2 ^{1}P), wrongly derived from the expression for the corresponding cross section as given by Burke et al. (1967). (auth)

9017 A STUDY OF THE Hβ PROFILES AND PULSATION OF THE ENVELOPE OF THE Be STAR HD 218393. Doazan, V.; Peton, A. (Observatoire, Paris. Observatoire, Meudon, France). Astron. Astrophys.; 9: 245-51(Nov 1970). (In French).

A study of the radial velocity curve for lines produced by the envelope of HD 218393 has shown: (1) the expansion is accelerated during all the period, but the acceleration decreases progressively from the maximum to the minimum of the radial velocity curve; (2) the acceleration of the deeper layers is greater than that of higher layers. One can conclude that the motion originates in parts of the envelope near the surface of the star. The structure of the Hβ profile is correlated with the phase of the radial velocity variation. (auth)

9018 INFRARED EMISSION FROM Be STARS. Woolf, N. J. (Univ. of Minnesota, Minneapolis); Stein, W. A.; Strittmatter, P. A. Astron. Astrophys.; 9: 252-8(Nov 1970).

Observations of Be stars at 3.4, 5, 8.5, and 11.5 μ are reported. Evidence for thermal free−free radiation superposed upon the stellar continuum was found in most of the stars in the sample. In 48 Per and κ Dra, however, a sharp increase in emission towards 11.5 μ was detected in March 1969. A similar feature has been noted in α Leo by previous investigators but the present observations indicate a purely stellar continuum. Physical conditions in the envelopes of Be stars are briefly discussed. (auth)

9019 ENVELOPE MODELS FOR A TYPE-STARS. THE DENSITY INVERSION ZONE WITH THE MIXING LENGTH THEORY. Latour, Jean (Observatoire, Nice). Astron. Astrophys.; 9: 277-87(Nov 1970).

A grid of models for envelopes of A-type stars, with $0.5 < \theta_e < 0.7$ and $2.0 < \log g_s < 4.44$ was computed. The T (τ) law of the atmosphere was that used by Mihalas. Convection was treated by the mixing length theory in which the Böhm and Stückl hypothesis is adopted. Different assumptions for the mixing length were also examined. All the models had a density inversion zone that starts in the atmosphere at an optical depth ranging from $\tau = 0.33$ or $\tau = 0.88$. This density inversion diminished when the effective temperature increased or the gravity decreased. The opacity was computed from Cox and Stewart's table using a smoothed interpolation procedure. (auth)

9020 OBSERVATIONS OF THE [S II] DOUBLET 6717 Å, 6731 Å IN ORION. Danks, A. C. (Univ. of Manchester, Eng.). Astron. Astrophys.; 9: 175-80(Nov 1970).

Observations of the variations of the intensity ratio of the 6717 Å/6731 Å doublet over the area of the bright central core of Orion are presented. The results show a systematic variation of the [S II] ratio with distance from the Trapezium. The variations in the ratio are interpreted as variations in the local electron density N_e. These are compared to the equivalent results from [O II]. (auth)

9021 AN OBLIQUE ROTATOR MODEL FOR THE MAGNETIC AND SPECTRUM VARIABLE HD 173650. Rice J. B. (Univ. of Western Ontario, London, Can.). Astron, Astrophys.; 9: 189-203(Nov 1970).

The star HD 173650 was investigated with respect to its light, line strength, and radial velocity variations to determine whether the oblique rotator is an adequate model for this typical magnetic and spectrum variable. It is shown that the light variation and line strength variations for all elements including Cr and Eu are in phase and the radial velocity curves for all species become most positive one quarter cycle following line strength maximum. It is also shown that Babcock's magnetic observations are in antiphase to the light variability. The curve of growth analysis suggests that the line-strength variation is primarily due in Cr and Fe, to an apparent change in microturbulent velocity and only secondarily to change in abundance with phase. The observation that the curve of light intensity variation has the same shape as the line strength variation, assists greatly in forming a general nonsymmetric oblique rotator model of the star by a method of harmonic analysis. This model of the star gives predictions of the line strength and radial velocity variations that are in good agreement with observation. The requirement that the inclination of the rotational axis be 65° or greater, as determined from the line profiles (V_e sin i), the period and the radius (determined from the photoelectric data), has been met. The solution indicates that there is an area of line strength maximum in the form of a wide irregular belt around the star. By placing a dipole field on the star so that the irregular belt is coincident with the magnetic equator and the positive pole is located at the northern area of minimum line strength, negative pole in the southern minimum, a predicted magnetic variation was obtained that fits the observations. Therefore, the model is satisfactory in that it fits all the observations and that the line and dipole field strength distributions bear some resemblance to one another as one might hope if the current belief in a relation between the magnetic field and spectroscopic anomalies is correct. (auth)

9022 THE OLD OPEN CLUSTER NGC 7142. van den Bergh, S.; Heeringa, R. (Univ. of Toronto). Astron. Astrophys.; 9: 209-15(Nov 1970).

The Hale 5.08-m and the Kitt Peak 2.15-m telescopes were used to obtain a color−magnitude diagram for the open cluster NGC 7142. The data indicated that this cluster is probably older than NGC 7789 but younger than M 67. The observations yield $(m-M)_V \cong 13.7$, $E_{B-V} = 0.41$ and $R = 3.2$ kpc. (auth)

9023 MASS LOSS RATES FOR VIBRATIONALLY UNSTABLE VERY MASSIVE MAIN-SEQUENCE STARS. Appenzeller, I. (Univ., Goettingen, Ger.). Astron. Astrophys.; 9: 216-20(Nov 1970).

The amount of pulsationally driven mass loss from vibrationally unstable zero-age main-sequence stars of $60 < M/M_\odot < 600$ is estimated. Using nonlinear pulsation calculations and an approximate procedure based on the linear pulsation theory, it is found that the mass loss increases strongly with increasing mass. For stars with $M > 300$ $M_\odot$ the mass loss turns out to be so violent that these stars lose most of their mass on a time scale that is much shorter than the phase of core hydrogen burning. The stars with $100 \lesssim M/M_\odot \lesssim 200$, on the other hand, probably can survive for a time interval comparable to their normal main-sequence lifetime without rapidly changing their mass. Stars with $M \lesssim 100$ $M_\odot$ were found to lose no or only very little mass. Thus, if their mass is not reduced by another mechanism, stars with $M \lesssim 100$ $M_\odot$ should evolve like ordinary stable stars. (auth)

9024 THE OPEN CLUSTER NGC 2236. Rahim, M. (Univ., Basel). Astron. Astrophys.; 9: 221-6(Nov 1970).

A three-color photometry in the RGU system leads to a distance of 3430 pc for the open cluster NGC 2236. (auth)

9025 SHORT PERIOD VARIABLE STARS. II. VARIATIONS IN THE SPECTRUM OF THE βCMa STAR HD 43818. Le Contel, J. M.; Sareyan, J. P.; Dantel, M. (Observatoire de Paris). Astron. Astrophys.; 8: 29-40(Sep 1970).

Spectral observations of HD 43818, a βCMa variable star discovered by Hill, were carried out. The line profiles and the radial velocities display large variations. The Van Hoof effect is present. The existence of components in the line profiles made it necessary to proceed to a thorough discussion of the radial velocity measurements, from the observed profiles. The line widths seem to be due more to an important velocity field than to a large "ν sini." Comparisons between the observations and those performed by several authors, on stars of the same group, lead to the conclusion that most of the observed features can be explained by the propagation of shock waves in the atmosphere of HD 43818. The same variations on the line profiles were also observed on the star HD 13745. (auth)

9026 DISTRIBUTION OF OB STARS IN THE SOUTHERN MILKY WAY. Lynga, G. (Lund Observatory, Sweden). Astron. Astrophys.; 8: 41-9(Sep 1970).

The distribution of 1477 OB stars in the galactic longitudes 283 to 332° was analyzed statistically. Twelve concentrations were found, most of which are OB associations. Relations between these and other objects are discussed. Systematic deviations of the OB stars from the galactic plane were investigated, using stars in intermediate latitudes. (auth)

9027 THERMAL BEHAVIOR OF ROTATING AND MAGNETIC STARS. Kippenhahn, R. (Universitaets-Sternwarte, Goettingen, Ger.). Astron. Astrophys.; 8: 50-6(Sep 1970).

Expressions are derived that govern the variation of the mean temperature in a rotating magnetic star during homologous changes and that determine the secular stability of central nuclear burning. It is shown that cooling during contraction of a star occurs for lower degrees of degeneracy than in the nonrotating case and that thermal runaways like the helium flash are favored by rotation. (auth)

9028 Hα/[N II] RATIO IN THE ORION NEBULA. Baudel, L. (Institut d'Astrophysique, Paris. Laboratoire d'Astronomie Spatial, Marseille). Astron. Astrophys.; 8: 65-72(Sep 1970). (In French).

With the wide-field multislit spectrograph used by Courtès et al. (1969), the Hα/[N II] ratio was obtained over the Orion Nebula (238 measures). The observations were made during the winter of 1965, at the 193-cm telescope of the Haute Provence Observatory. The results showed: (1) the Hα/[N II] ratio decreases smoothly from the center to the outer parts of the nebula (Hα/[N II] varies between 6 and 1.5), (2) the exciting star (θ^1 Ori) is not the center of symmetry. It is difficult, in the present state, to interpret the Hα/[N II] ratio in diffuse nebulae. The electron density model given by Osterbrock and Flather (1959) was adopted to study both electron temperature variations over the Orion Nebula and the relative abundance of nitrogen $Z = N(N)/N_e$. It was found that: (1) the electron temperature varies slowly inside the nebula; and (2) the value of $Z = N(N)/N_e$ is between 1.5×10^{-4} and 4×10^{-4} in complete agreement with those adopted by many theoretical workers. The electron temperature plays an important role in the interpretation of Hα/[N II]. So, the temperature from point to point in the Orion Nebula is measured by observing the width at half intensity of line profile. (auth)

9029 MASS LOSS FROM T TAURI STARS. Gahm, Goesta F. (Stockholm Observatory, Saltsjoebaden, Sweden). Astron. Astrophys.; 8: 73-5(Sep 1970).

Observations of variations in the widths of various emission lines in the spectrum of RW Aur are considered and the implications of Kuhi's model for the atmospheres of T Tauri stars are discussed. It was found that the mass loss rates, as derived by Kuhi, may be overestimated for T Tauri stars with strong emission line spectra. (auth)

9030 RAPID UNIFORM ROTATION ALONG THE MAIN SEQUENCE. II. Sackmann, I.-J. (Max-Planck-Institut fuer Physik und Astrophysik, Munich. Universitaets-Sternwarte, Goettingen, Ger.). Astron. Astrophys.; 8: 76-84(Sep 1970).

Sixty detailed uniformly rotating main-sequence models varying in rotation from zero to the critical values and ranging in mass from 20 to 0.8 $M_\odot$ were constructed. The variation of the rotation changes as one passes along the main-sequence was investigated. It was found that for a given ratio of the centrifugal force to the gravitational force, rotation produces larger changes for late-type stars than for early-type stars. The maximum change in the luminosity of a 10 and 1 $M_\odot$ critically rotating main-sequence star is 7% and 15%, respectively; corresponding changes in the polar radius are 3% and 6%, respectively. For masses above 1.5 $M_\odot$, rotation causes an increase in the central pressure for a star of a given mass, while for masses below 1.5 $M_\odot$ the opposite is true. This break in the effects of rotation shows up in all physical quantities of a star and is caused primarily by the cross-over from the carbon–nitrogen cycle to the proton–proton cycle. The central values of critically rotating main-sequence stars obey the same $T_c - \rho_c$ relation as nonrotating main-sequence stars. Slow as well as rapid uniform rotation has the same effect upon the central regions of a main-sequence star as lowering the mass of the star; for critical rotation, this mass-lowering effect of rotation is 2 and 4% at 10 and 1 $M_\odot$, respectively. A qualitative theory to explain all rotation effects found is given. (auth)

9031 MEMBERSHIP OF THE INTERMEDIATE-AGE OPEN CLUSTER NGC 2420. van Altena, W. F.; Jones, B. F. (Univ. of Chicago). Astron. Astrophys.; 8: 112-16(Sep 1970).

Probabilities of membership based on proper motions with an average accuracy of ±0.0007″/yr (m.e.) were determined for 85 stars in the region of the intermediate-age open cluster NGC 2420. The color–magnitude diagram for probable members shows a well-populated, nearly vertical giant branch which bends towards the red at the top, one horizontal branch star, and two "blue stragglers." There are approximately 17 cluster members brighter than $M_v \sim +1.5$. (auth)

9032 Hα-EMISSION OBJECTS IN TWO SELECTED REGIONS OF THE SOUTHERN MILKY WAY (CENTAURUS AND NORMA). Velghe, A. G.; Denoyelle, J.; De Kersgieter, A. (Royal Observatory, Brussels). Astron. Astrophys.; 8: 123-33(Sep 1970).

Positions and photometric data are presented for 45 objects in the region of Centaurus–Musca and for 24 objects in the region of Norma–Ara. The search for Hα-emission objects on objective-prism plates, taken with the ADH-telescope of the Boyden Observatory, was carried out independently by the three authors. The relation between the Hα-emission stars and galactic structure is discussed. (auth)

9033 APSIDAL MOTION IN CLOSE BINARIES WITH AND WITHOUT MASS EXCHANGE. Cisneros-Parra, J. U. (Universitaets-Sternwarte, Goettingen, Ger.). Astron. Astrophys.; 8: 141-7(Sep 1970).

Apsidal motion coefficients were calculated for homogeneous main-sequence models, both those in the middle of their main-sequence phase and those in different stages of mass exchange in several close binary systems. It is shown that the mass loss from a subgiant component can decrease the apsidal motion coefficient k_2 by a factor of 100, i.e., even below the values observed in semidetached binary systems. (auth)

9034 STUDY OF Be STARS: WIDTH OF EMISSION LINES. Doazan, V. (Observatoire de Paris). Astron. Astrophys.; 8: 148-58(Sep 1970). (In French).

The widths of the hydrogen emission lines of 26 Be stars belonging to classes V, IV and III (shells, V/R variables and rotationally instable stars) were measured. It is shown: (1) for 7 of these stars, the width of Hα does not obey the width wavelength proportionality relation for the emission lines; (2) for all the stars studied, the rotational velocities corresponding to the Hα emission line width are larger than that due to the rotation of the central star (v sin i). This is also the case for the Hβ line of 17 stars and for the Hγ line of 12 stars; and (3) no correlation exists between the widths of the Hα, Hβ, and Hγ emission lines and the velocity due to the rotation of the central stars (v sin i) when this velocity is less than 350 km/s. (auth)

9035 SHORT-PERIOD VARIABLE STARS. III. HIGH-RESOLUTION SPECTRA OF THE K LINE IN γ BOOTIS AND THREE OTHER A-TYPE STARS. Le Contel, J. M.; Praderie, F.; Bijaoui, A.; Dantel, M.; Sareyan, J. P. (Observatoire de Paris–Meudon, France). Astron. Astrophys.; 8: 159-67(Sep 1970).

Fine variations in the K-line profile of γ Boo (HD 127 762, A7 III), are presented from a series of high-resolution spectra (2.2 Å/mm) obtained with an electronic camera during one night. Differential radial velocities were measured on each profile. The velocity of the line axis, defined at half intensity, varies in a quasi-periodical way. Correlative variations with time of the equivalent width and the half-width are clearly shown. Two Am and one Ap star were also observed in the same line; no reversal could be detected. A photospheric model was derived for γ Boo. Two interpretations for the K-line profile are suggested: chromospheric temperature rise plus velocity field, or Hillendahl mechanism. (auth)

XUM

9036 P CYGNI AND THE STELLAR RING 274. Isserstedt, J. (Ruhr Univ., Bonn). Astron. Astrophys.; 8: 168-70(Sep 1970). (In German).

The reality of the stellar ring 274 is confirmed by 4 OB stars that are members of the ring. The colors and magnitudes of these young stars from the Hamburg–Cleveland Spectral Survey were measured in the UBV system by means of photographic photometry. The reddening is $E_{B-V} = 0.58$m; the distance modulus is 12.24 ± 0.54m. The distance r = 2.8 kpc corresponds to a minor diameter of the stellar ring $D_m = 6.4$ pc. This agrees with the observation that the minor ring diameters are constant. Near the center of the ring is the unique variable shell star P Cygni. Assuming this coincidence is not accidental the absolute magnitude and intrinsic color of P Cygni can be determined. Using geometric distance determination ($D_m = 7.1$ pc) the resulting values are: $M_V = -9.48$m; $(B-V)_0 = -0.16$m; $(U-B)_0 = -1.00$m. The colors correspond to a B star of the luminosity class Ia–0, but the luminosity is still higher. (auth)

9037 THE r-PROCESS IN A HYDRODYNAMICAL MODEL OF THE HELIUM FLASH. Molnar, Michael R. (Univ. of Wisconsin, Madison). Astrophys. J.; 163: 203-5(1 Jan 1971).

The explosive temperature rise in Edwards's hydrodynamical model of the helium flash produces an r-process. A neutron density of 10^{24} cm^{-3} is sustained for 4.1 sec from $^{18}O(a,n)^{21}Ne(a,n)^{24}Mg$. (auth)

9038 SUPERNOVA LIGHT CURVES AND PRESUPERNOVA MODELS. Arnett, W. David (Inst. of Theoretical Astronomy, Cambridge, Eng.). Astrophys. J.; 163: 11-16(1 Jan 1971).

Recent numerical models due to Grasberg and Nadezhin and to Morrison and Sartori of the light curves of supernovae of Types II and I were examined for their implications regarding presupernova evolution and the nature of the supernova process. In these models an extremely extended envelope (radius r ~ 10^{15} cm instead of r ~ 10^{13} considered by Colgate and White) for the supernova is required. Such a structure is suggested by theoretical investigations of advanced stages of stellar evolution. Some hitherto inexplicable properties of supernovae of Types I and II can be explained. It is predicted that presupernovae will be infrared sources of high luminosity, and that several may currently exist in the Galaxy. (auth)

9039 NONLINEAR PULSATIONS OF UNSTABLE MASSIVE MAIN-SEQUENCE STARS. I. SMALL-AMPLITUDE TESTS OF AN APPROXIMATION TECHNIQUE. Talbot, Raymond J. Jr. (Massachusetts Inst. of Tech., Cambridge). Astrophys. J.; 163: 17-27(1 Jan 1971).

Pulsationally unstable massive main-sequence stars have e-folding times greater than ~10^5 periods, a fact which makes impractical a straightforward numerical integration of the full nonlinear equations. As a first step in an investigation into the fate of these stars, a promising approximation technique was studied in detail. The technique involves the introduction of a second time scale by a multiplicative factor inserted in the thermal-energy equation. Results are presented for the evolution of a 100-$M_\odot$ star model onto the main sequence, including the evolution of its small-amplitude pulsations. Star models of 30 and 65 $M_\odot$ were also evolved onto the main sequence. The small-amplitude modes of these three masses are compared with the results of linear pulsational analysis, and the precision of the approximation is evaluated. The method is found to be a valid approximation for small-amplitude pulsations with long e-folding times, and with appropriate care it is applicable to large-amplitude motions. (auth)

9040 MASS ACCRETION AND PULSATIONAL STABILITY. Axel, Leon; Perkins, Francis (Princeton Univ. Observatory, N. J.). Astrophys. J.; 163: 29-35(1 Jan 1971).

The question of whether mass accretion on a star can cause pulsational instability by itself is considered. The principal result is a formula for the effect of accretion on the growth (or decay) rate of a radial pulsation mode. Application of this formula to a white dwarf undergoing mass accretion shows that the destabilizing effects of accretion are balanced (in order of magnitude) by acoustic energy loss through the hot corona. Although a quantitative answer to the stability question requires numerical calculations, it is argued that the net effect is stable. For rates of mass accretion ~10^{-7} $M_\odot$ year^{-1}, the decay rates compete with the destabilization resulting from nuclear burning for a thermal instability. Also, a useful "Schrödinger equation" representation of the adiabatic-pulsation equation is given. (auth)

9041 THE EARLY EVOLUTION OF POPULATION II STARS. II. Demarque, Pierre (Yale Univ. Observatory, New Haven); Mengel, John G.; Aizenman, Morris L. Astrophys. J.; 163: 37-49(1 Jan 1971).

Evolutionary tracks for Population II stars of low mass are presented. The chemical composition lies in the range $0.50 < X < 0.999$ and $10^{-5} < Z < 10^{-3}$. Isochrones suitable for comparison with color–magnitude diagrams of globular clusters were constructed. The results were compared with earlier work, in particular with models by Simoda and Iben and Iben and Rood. Discrepancies were everywhere less than 12%, except for the stellar radii, which were subject to larger uncertainties due to the hydrogen convection zones. The strong dependence on Z of the turnoff luminosity for very low Z found by Simoda and Iben was confirmed qualitatively. (auth)

9042 INVESTIGATION OF SIX O-TYPE SPECTRA. Peterson, Deane M.; Scholz, M. (Carnegie Institution of Washington, D. C.). Astrophys. J.; 163: 51-73(1 Jan 1971).

New observations of six O-type spectra (09.5 V–05) are reported. These spectra were studied by means of LTE model atmospheres, which include the continuous opacities of twelve heavy-element ions. Effective temperatures and surface gravities were estimated from ionization equilibria and Balmer-line wings. These temperatures, ranging from 36200° to 54000°K, were higher than those quoted by Morton. The Kepple–Griem theory for hydrogen-line broadening leads to log g ≃ 4.3 ~ 4.5. Appreciable departures from LTE occur as predicted by Mihalas and Auer. Most chemical elements had abundances close to solar values, but neon was overabundant. 15 Mon A (07) was deficient in carbon. (auth)

9043 STARS WITH STRONG CYANOGEN ABSORPTION. Schmitt, John L. (Univ. of Michigan, Ann Arbor). Astrophys. J.; 163: 75-94(1 Jan 1971).

An attempt was made to define the properties of G8–K4 giants with abnormally strong CN (Miss Roman's "4150 stars"). Slit spectrograms were obtained of stars that had been suspected to have strong CN on objective-prism plates or that were noted in the literature as having strong CN. A list of 146 stars with strong CN is given. Five groups (all G8–K2 stars, G8–K2 III–IV stars, G8–K2 stars with moderately strong CN, G8–K2 stars with quite strong CN, and K3–K4 stars) were formed from these stars, and for each group a statistical parallax and a mean visual absolute magnitude were calculated. Visual absolute magnitudes of +1.3 ± 0.4, +1.5 ± 0.6, +1.4 ± 0.5, +1.3 ± 0.5, and +1.0 ± 0.7 (m.e.), respectively were found for the above groups. The low absolute magnitude of the strong-CN giants places them, in the H–R diagram, near the loci for old open clusters. Spectroscopically they appear similar to the red giants in the old open clusters. Evidence indicates that they have masses near 1 $M_\odot$. Elemental abundances are discussed, but no conclusion is reached. (auth)

9044 FORMATION OF RESONANCE LINES IN EXTENDED AND EXPANDING ATMOSPHERES. Lucy, L. B. (Columbia Univ., N. Y.). Astrophys. J.; 163: 95-110(1 Jan 1971).

Approximate expressions are derived for the profiles of lines formed by coherent scattering in extended and expanding atmospheres with spherical symmetry. For an extended, static atmosphere, the derived expression gives a greater residual intensity at every point in the line than does the corresponding result for a plane-parallel atmosphere. For an expanding atmosphere, an expression for the resulting P Cygni profile is derived on the assumptions that the expansion velocity v(r) is a strictly increasing function of radius r, and that v is large compared with the thermal velocity of the scattering ions but small compared with the velocity of light. With these assumptions, the calculation of the residual intensity reduces to a quadrature through the expanding atmospheres of hot stars to obtain profiles for ultraviolet resonance lines. It is found that the rates of mass loss predicted by Lucy and Solomon give profiles in qualitative agreement with those observed in the far-ultraviolet spectra of early-type supergiants and of the Of star ζ Puppis. The theory is also applied to a model for the quasistellar object PHL 5200 to obtain a profile for the λ1548 resonance line of C IV. A comparison of this profile with the spectra published by Lynds suggests that the expanding envelope of PHL 5200 is not spherically symmetric. (auth)

9045 THE X- AND Y-FUNCTIONS OF CHANDRASEKHAR. Caldwell, James (Teesside Polytechnic, Middlesbrough, Eng.). Astrophys. J.; 163: 111-20(1 Jan 1971).

Chandrasekhar's X and Y functions are defined in terms of two coupled integral equations whose solutions for certain values of optical depth and albedo have already been found by means of iterative processes. A noniterative method of solving for the X and Y functions for all values of optical depth is described here. Tables of these functions and their moments are presented for values of the optical depth in the range 0.5–4.5 and albedo 1 with an assessment of their accuracy. (auth)

9046 CONTINUOUS SPECTRUM OF NEUTRAL HELIUM FROM GASEOUS NEBULAE. Kaler, J. B. (Univ. of Illinois,

Urbana); Lee, P.; Aller, L. H. Astrophys. J.; 163: 141-9(1 Jan 1971).

The continuous spectrum associated with the 2^3P term of neutral helium was detected in six planetary nebulae and the Orion Nebula. Although the errors are large, reasonable estimates were made of the strength of this continuum in most of these nebulae. On the average, the ratio of the flux density of the 2^3P continuum to the flux in the λ4471 line of He I were about twice as great as that predicted by recombination theory at the electron temperature measured from the forbidden lines. In addition, the ratio of the flux density of the 2^3P continuum to that of the Balmer continuum was generally significantly greater than is allowed on the basis of the measured helium-to-hydrogen ratio. (auth)

9047 OBSERVATION AND CLASSIFICATION OF THE NEBULA YM 29. Johnson, Hugh M. (Lockheed Missiles and Space Co., Palo Alto, Calif.); Rubin, Robert H. Astrophys. J.; 163: 151-3(1 Jan 1971).

YM 29 has been classified at different times as a galactic nebula, a planetary nebula, and a supernova remnant. New observations of the radiofrequency and optical spectra specify certain peculiarities of the object. The 6- and 20-cm flux density are low compared with the flux density of the red Palomar Sky Survey image but the radiofrequency spectrum could be nonthermal. Only [O II] λλ3726–3729 is present in the blue spectrum. (auth)

9048 MORPHOLOGICAL AND KINEMATICAL STUDY OF TWO PLANETARY NEBULAE. Hua, C. T.; Louise, R. (Observatoire, Marseille). Astron. Astrophys.; 9: 448-52(Dec 1970). (In French).

Using narrow band (Δλ = 10 Å) interference filters centered on Hα (λ = 6563 Å) and [N II](λ = 6584 Å) lines, several photographs were taken of two planetary nebulae: NGC 6720 and NGC 6853. The observations were made at the Newtonian focus of the 120-cm telescope of the Haute Provence Observatory with the classical "focal reducer" (Courtès, 1960). In addition to monochromatic photographs, two interferograms were obtained, one in Hα and one in [N II] light, of the Dumbbell nebula. These observations show: (1) the images in Hα light are smaller (10 to 20%) and less distinct than the [N II] ones, confirming the observations of Carranza et al. (1968) of the Helix nebula; (2) the ring of NGC 6720 probably does not have a toroidal form but is flat like the ring of Saturn; (3) the Dumbbell nebula is an expanding shell; the expansion velocity is about 31.5 km s^{-1}. (auth)

9049 LUMINOSITY DETERMINATION OF OB STARS BY Hβ INDICES. Haug, U. (Hamburg Observatory). Astron. Astrophys.; 9: 453-60(Dec 1970).

The distribution of Hβ indices is discussed for different groups of early type stars. O- and B0-type stars for which the relation between luminosity and Hβ index shows a dispersion of 0.7m have Hβ indices smaller than 2.63. The Hβ indices of Be stars are, in general, below 2.60. Luminosities may therefore be derived from Hβ indices with an accuracy of approximately 0.4m for stars with Hβ indices greater than approximately 2.63. In a sample of 100 stars taken from the catalogue of Klare and Szeidl (1966), 32 out of 77 OB stars have indices above this limit, while the rest and all OB^+ stars are below it. Changes in brightness and colors were found for several Be stars in the program. (auth)

9050 DISRUPTION OF STAR CLUSTERS THROUGH PASSING INTERSTELLAR CLOUDS INVESTIGATED BY NUMERICAL EXPERIMENTS. Bouvier, P.; Janin, G. (Geneva Observatory). Astron. Astrophys.; 9: 461-5(Dec 1970).

The stochastic tidal effect of interstellar clouds passing near a star cluster causes the latter to expand and disintegrate. The problem, already tackled by Spitzer (1958), was taken up anew with the help of numerical experiments performed on a model of the cluster and of the clouds. The results point out the importance of the interstellar passing clouds with respect to the disintegration of a small stellar cluster; in particular, a cluster of 25 stars should disrupt in less than half a billion years. The galactic tidal field was not included. (auth)

9051 ON THE PRESENCE OF METALLIC LINE STARS IN YOUNG CLUSTERS: M7 AND NGC 7160. Conti, Peter S.; van den Heuvel, E. P. J. (Astronomical Inst., Utrecht). Astron. Astrophys.; 9: 466-71(Dec 1970).

MK types and radial velocities are given for a number of A stars in the galactic clusters Messier 7 and NGC 7160. Two metallic-line A stars (Am) were identified in Messier 7 (age ~2.5×10^8 years) and one in NGC 7160 (age ~2×10^7 years). The membership of one of the Am stars in M 7 was not completely certain, but the other two Am stars appeared to be cluster members according to radial velocity and position in the color–magnitude diagrams of their respective clusters. These findings imply that Am stars may occur even in very young galactic clusters. An average cluster reddening $E_{B-V} = 0.40$m in NGC 7160 was derived from the MK classification of spectra of lower main-sequence stars and a cluster distance of 830 pc was found. Evidence is presented for the occurrence of differential reddening in this cluster. (auth)

9052 NEWTONIAN ELECTRODYNAMICS FROM GENERAL-RELATIVISTIC ARGUMENTS. Occhionero, Franco (Goddard Space Flight Center, New York). Astron. Astrophys.; 9: 472-4 (Dec 1970).

In general relativity, a vacuum is electrically polarized in the presence of a magnetic field whenever the mixed components of the metric tensor do not vanish (which occurs in astronomy around a massive rotating object because of the dragging of the inertial frame). This note illustrates the phenomenon by making use of the fact that it does not require curvature and, hence, may occur in a flat space–time: In fact, in corotating coordinates the vacuum around a rotating, magnetic, Newtonian star is electrically charged. By assuming near sphericity of the star and an external 2^n-pole poloidal magnetic field, it is easy to evaluate the electrostatic potential, which reflects the existence of the fictitious charge density with a nonharmonic term proportional to $(1/r)^n P_{n+1}(\cos\theta)$. This note also establishes a convenient formalism for the treatment of the general-relativistic aspects of the same problem. (auth)

9053 MEASURES OF DOUBLE STARS ON PARALLAX PLATES. Osborn, W. (Van Vleck Observatory, Middletown, Conn.). Astron. Astrophys.; 9: 475-7(Dec 1970).

Position angles and separations for 23 visual double stars as determined from parallax plates are presented. (auth)

9054 REDUCTION TO H-FUNCTIONS IN RADIATIVE TRANSFER WITH A GENERAL ANISOTROPIC PHASE FUNCTION. van de Hulst, H. C. (Sterrewacht, Leiden). Astron. Astrophys.; 9: 359-65(Dec 1970).

The solution of the diffusion problem in an unbounded homogeneous medium, containing the Kuščer polynomials, and the solution of the reflection function against a semi-infinite atmosphere, containing the Busbridge polynomials and the H-function, are reviewed. It is shown that the solution of the Milne problem and nonconservative scattering is expressible in the same polynomials, the characteristic root and the H-function. The derivation is simple with the help of a new integral containing a combination of these polynomials and the H-function. Some additional constants and the transition to conservative scattering are discussed. In spite of the simplification reached in this paper, the reduction to H-functions is not recommended as a practical method if the phase function contains Legendre polynomials of large order. (auth)

9055 SPECTRUM OF THE ANISOTROPIC TRANSFER EQUATION. van de Hulst, H. C. (Sterrewacht, Leiden). Astron. Astrophys.; 9: 366-73(Dec 1970).

The discrete values of k, for which the equation of transfer in a homogeneous medium with an arbitrary phase function has a solution proportional to $\exp(\pm k\tau)$, where τ is optical depth, are studied. Various forms of the characteristic equation, from which k can be solved, are given. The simple relation $g_n(k^{-1}) \to 0$ for $n \to \infty$, where $g_n(x)$ are the Kuščer polynomia, is recommended for practical computation. The relation by which the albedo for simple scattering, $\omega_0 = a$, depends on k when the form of the scattering pattern is given, is derived both for linearly anisotropic scattering (N = 1) and for the Henyey–Greenstein scattering functions. Knowledge of the multiple values of k for one a, which may be read from the graphs presented, is helpful in estimating the domain of practical validity of the diffusion approximation. (auth)

9056 SPECTROSCOPIC ANALYSIS OF THE SILICON STAR HD 34452. Tomley, Leslie J. (Univ. of Hawaii, Honolulu); Wallerstein, George; Wolff, Sidney Carne. Astron. Astrophys.; 9: 380-91(Dec 1970).

Model-atmosphere techniques were used in an analysis of the spectrum of HD 34452. Both the external evidence concerning the mass and radius and the spectroscopic evidence of the hydrogen line profiles and lines of Si III and Si II indicated that the atmosphere can be described by the basic parameters $\theta_{eff} = 0.28$, log g = 4.2. Helium and neon were found to be deficient while many other elements, including silicon, chlorine, titanium, chromium, iron strontium, and europium were greatly overabundant. The peculiar composition was compared with theoretical predictions regarding surface reactions due to magnetically accelerated protons and α-particles; nuclear reactions in the interior followed by mass loss, mixing, or mass-transfer; chemical effects

XUM

associated with star formation; and diffusive and radiative separation of elements. None of these theories can at present account for the surface composition of HD 34452. Two surprising points were noted. First, it appeared that almost all the peculiar stars of types B, A, and F, including the metallic line stars, have an excess of iron. Second, the elements of high abundance in HD 34452 could come from silicates and metallic oxides along with such common molecules as H_2, H_2O, and HCl, if these constituents formed the last material accreted during star formation onto a star with a stable atmosphere. (auth)

9057 TECHNETIUM STARS. Peery, Benjamin F. Jr. (Indiana Univ., Bloomington). Astrophys. J.; 163: L1-3(1 Jan 1971).

A list of stars with spectra showing absorption lines of Tc is presented. Characteristics of Tc stars are: types MS, S, and N; enhanced abundances of s-process elements near neutron magic number 50; variability (the observed nonvariable MS and S stars show no Tc). N-type irregular variables have Tc; the N semiregular variables do not. Long-period variables excepted, Tc stars are extreme Population I objects that have evolved rapidly. (auth)

Quasi-Stellar, Radio, and X-Ray Sources

Refer also to abstracts 8975, 8996, 9044, and 9132.

9058 SEARCH FOR STRONG RADIO SPECTRAL LINES IN THE RANGE 12.4 TO 15.1 AND 15.3 TO 17.3 GHz. Hvatum, Hein; Howard III, William E. (National Radio Astronomy Observatory, Green Bank, W. Va.). Astrophys. J.; 162: L167-8(Dec 1970).

Strong radio spectral lines were searched for in the radio sources Sgr A, Sgr B2, W49, and Cas A in the frequency range 12.4 to 15.1 GHz and in the sources W3, Ori A, VY CMa, Vir A, and 3C 273 in the frequency range 15.3 to 17.3 GHz. No strong spectral lines exceeding 440 flux units were detected with the NRAO 140-foot telescope in any of these sources. (auth)

9059 OBSERVATIONS OF PULSAR SPECTRA. Ewing, M. S.; Batchelor, R. A.; Friefeld, R. D.; Price, R. M.; Staelin, D. H. (Massachusetts Inst. of Tech., Cambridge). Astrophys. J.; 162: L169-72(Dec 1970).

Analysis of multichannel radio observations of pulsars demonstrated slow systematic drifting of spectral features of CP 0834, CP 1133, and CP 1919. An interpretation of the data with a simple interstellar-scintillation model determines transverse velocities of ~100 km s^{-1} for the pulsar with respect to the interstellar medium and Earth. Additionally, the widths of spectral features of CP 0328, CP 0834, and CP 1919 were found to scale approximately as the fourth power of frequency, in agreement with the model. (auth)

9060 DETECTION OF METHYL ALCOHOL IN SAGITTARIUS. Ball, John A. (Harvard Coll. Observatory, Cambridge, Mass.); Gottlieb, Carl A.; Lilley, A. E.; Radford, H. E. Astrophys. J.; 162: L203-10(Dec 1970).

Observations are reported of radio line emission at 834 MHz (36 cm), due to a K-type doubling transition in methyl alcohol, in the directions of Sgr A and Sgr B2. Line widths and Doppler velocities compare favorably with other molecular spectra observed toward the galactic-center region. (auth)

9061 LIMITS FOR OPTICAL COUNTERPARTS OF FIFTEEN RADIO PULSARS. Kristian, Jerome (Carnegie Institution of Washington, D. C. California Inst. of Tech., Pasadena). Astrophys. J.; 162: L173-5(Dec 1970).

Observed limits are given and converted to estimates of absolute intensity compared with the Crab pulsar. These range from 10^{-1} to 10^{-6} and are not compatible with the hypothesis that the visible pulsed radiation for all pulsars scales as Ω^4 and is normalized to the Crab. (auth)

9062 LOW-ENERGY GAMMA RAYS FROM NP 0532. Hillier, R. R.; Jackson, W. R.; Murray, A.; Redfern, R. M.; Sale, R. G. (Univ. of Bristol, Eng.). Astrophys. J.; 162: L177-80 (Dec 1970).

Pulsed γ rays with energies greater than 0.6 MeV were detected from NP 0532. The intensity of the pulsed radiation exceeds the intensity of the radiation from the nebula in this region of the spectrum. The interpulse is approximately 3 times as intense as the main pulse. (auth)

9063 GRAVITATIONAL RADIATION AND THE OBLIQUE ROTATOR MODEL. Chau, W. Y. (Queen's Univ., Kingston, Ont.). Nature (London); 228: 655-6(14 Nov 1970).

It is known that gravitational radiation can play an important part in the energetics of neutron stars, and its effects have been included in some recent investigations of pulsar models. Only the energy loss, however, was considered; the angular momentum loss was ignored. The problem for the case of an oblique rotator is considered here, and expressions for both types of loss are obtained. The conditions under which these become comparable with effects from the magnetic dipole mechanism were also investigated, and comparison was made with conclusions reported by others. The oblique rotator model is taken to be one in which pulsars are rotating neutron stars with a frozen-in magnetic field, the axis of which is included at an angle to the rotation axis. It is also assumed that the mass distribution is not spherically symmetric, and distortion is ascribed to a flattening of the star in the region of the magnetic poles, thus also being asymmetric with respect to the axis of rotation. This gives a time-dependent mass quadrupole moment that leads to gravitational radiation. The expressions obtained show clearly the effects of rotation and field strength on the relative importance of the gravitational and magnetic mechanisms. (UK)

9064 CORRELATED SUBPULSE STRUCTURE IN PSR 1237 + 25. Backer, D. C. (Cornell-Sydney Univ., Arecibo, Puerto Rico). Nature (London); 228: 752-5(21 Nov 1970).

It was observed that PSR 1237 + 25 has a short-period subpulse system in which subpulses march in a sense opposite to that found in other pulsars and a long-period system that is strongest in the midpulse region where the short-period system disappears. (auth) (UK)

9065 LUNAR OCCULTATION SATELLITE FOR HIGH-RESOLUTION STUDIES OF COSMIC X-RAY SOURCES. Collet, J.; Dilworth-Occhialini, C.; Pacault, R.; (and others) (ESRO, Neuilly-sur-Seine, France). Nature (London); 228: 756-7(21 Nov 1970).

A proposal for a European x-ray astronomy satellite employing a lunar-occultation technique for the more accurate observation of new and existing x-ray sources is discussed. (auth) (UK)

9066 OPTICAL OBJECTS IN THE FIELDS OF SOUTHERN HEMISPHERE RADIO SOURCES. II. Lue, Phillip K. (Yale Univ. Observatory, New Haven). Astron. J.; 75: 1164-70(Dec 1970).

Photographs of 52 radio fields are given. Positions of stars and galaxies in the area of positional uncertainty of the radio source were determined with an accuracy of 0.5 to 1.0 sec of arc. Descriptions of the fields are given for most sources. (auth)

9067 SUGGESTED IDENTIFICATION OF SOUTHERN HEMISPHERE RADIO SOURCES. I. Lue, Phillip K. (Yale Univ. Observatory, New Haven). Astron. J.; 75: 1161-4(Dec 1970).

From examining plates of the fields of 85 radio sources in the southern hemisphere, photographs of 41 radio fields are given and tentative identifications are suggested. Eighteen objects are proposed as quasi-stellar objects; 23 are radio galaxies. The method of identification is discussed, and optical position of the objects is measured with a probable error of one second of arc. Attention is called to Parkes 1031−40, 1830−39, and 2259−37, which may be QSO's and whose estimated magnitudes are brighter than 15.5m. (auth)

9068 RADIO EMISSION FROM SMALL GALACTIC NEBULAE. Terzian, Yervant (Cornell Univ., Ithaca, N. Y.). Astron. J.; 75: 1155-60(Dec 1970).

Ninety small galactic nebulosities (size $\lesssim 10'$) were observed with the 1000-ft radio telescope at the Arecibo Observatory at a frequency of 318 MHz. Thirty-seven of these regions showed radio emission. Positions, flux densities, possible identifications, and exciting stars are given for the detected sources. Several of the detected sources are probably compact H II regions. Some others appear to be more blue than red on the Palomar Plates. No OB-type stars were found within one degree for 30% of the detected nebulae. NGC 6888, which is excited by a Wolf−Rayet star, is found to be partially optically thick at 318 MHz. (auth)

9069 OPTICAL DEPTH AND EXCITATION TEMPERATURE OF GALACTIC HYDROGEN IN THE DIRECTION OF W49. Hughes, V. A.; Routledge, D. (Queen's Univ., Kingston, Ont.). Astron. J.; 75: 1148-54(Dec 1970).

Absorption profiles from the Maryland−Green Bank 21-cm Survey were used to study profiles of optical depth and excitation temperature in the direction of the two components of W49. The results were consistent with the model in which hydrogen is concentrated in clouds whose temperature is less than 80°K, embedded in a diffuse medium whose density is about 1 H atom cm^{-3} and whose temperature is about 1000°K. Evidence is presented for the existence of a local expanding ring structure of cold dense hydrogen. (auth)

9070 COHERENT MECHANISMS OF EMISSION AND THEIR APPLICATION TO PULSARS. I. INTRODUCTION. ANTENNA MECHANISMS OF EMISSION. Ginzburg, V. L.; Zheleznyakov, V. V. Comments Astrophys. Space Phys.; 11: 167-71(Sep-Oct 1970).

Examples are given which testify that any pronounced antenna mechanism is unrealistic for cosmic conditions. It is concluded that, under cosmic conditions, the maser coherent mechanisms rather than the antenna mechanisms are of significance. (W.D.M.)

9071 MOLECULES IN THE INTERSTELLAR MEDIUM. II. Synder, Lewis E. (Univ. of Virginia, Charlottesville); Buhl, David. Sky Telesc.; 40: 345-8(Dec 1970).

Recent discoveries of additional kinds of molecules and free radicals in interstellar space have opened up an exciting new field where radio astronomy and chemistry overlap, as described in Part I. In Part II, an attempt is made to look at some of the concepts that physicists and astronomers use to interpret the radio emission from interstellar molecules. (W.D.M.)

9072 PULSARS TODAY. II. Green, Louis C. (Strawbridge Observatory, Haverford, Pa.). Sky Telesc.; 40: 357-60 (Dec 1970).

Since the initial discovery of pulsars about 60 have been studied in more-or-less detail, and much information is available about the character of their radio signals. The discussion in Part I is continued by surveying some of these findings. Topics discussed include pulse characteristics, interstellar scintillation, and optical and x-ray bursts from NP 0532. (W.D.M.)

9073 POLARIZATION OF TYCHO'S SUPERNOVA REMNANT AT A WAVELENGTH OF 2.8 CENTIMETERS. Kundu, M. R.; Velusamy, T. (Univ. of Maryland, College Park). Astrophys. J.; 163: 231-4(15 Jan 1971).

The polarized-brightness distribution for Tycho's supernova remnant was obtained at a wavelength of 2.8 cm. The degree of linear polarization varied considerably over the source from 8% near the outer boundary to nearly zero at the center; the orientation of the electric vectors was circumferential. From a comparison of the 2.8-cm map with similar maps obtained at other wavelengths, the distributions of spectrum, rotation measure, and depolarization over the source were studied. (auth)

9074 INFERENCES FROM SPECTROPHOTOMETRY OF QUASI-STELLAR SOURCES. Bahcall, John N. (California Inst. of Tech., Pasadena); Oke, J. B. Astrophys. J.; 163: 235-8(15 Jan 1971).

Limits are placed on the amount of neutral and ionized hydrogen gas that can be in the vicinity of 4C 05.34 (and three other QSSs); these results place severe restraints on models of quasi-stellar radio sources in which the QSS phenomenon is supposed to occur within a galaxy. A limit on the electron temperature is also established ($1 \times 10^4 < T_e \leq 2 \times 10^{4\text{o}}$K). The relative abundance of C^{2+} to C^{3+} is determined approximately in five QSSs, and the ratio of helium to hydrogen is estimated for fourteen QSSs. (auth)

9075 QUARK FUSION IN QUASI-STELLAR OBJECTS. Bahcall, John N. (Inst. for Advanced Study, Princeton, N. J. California Inst. of Tech., Pasadena); Callan, C. G. Jr.; Dashen, Roger. Astrophys. J.; 163: 239-47(15 Jan 1971).

The rates of the most likely quark-fusion reactions are estimated. An approximate formula is derived for the efficiency ($\gtrsim$50%) of converting rest mass into photons by quark fusion. The temperature at which quarks might fuse is crudely estimated to be a few million degrees Kelvin. Several ways are discussed that quark-electron atoms could conceivably be detected in astronomical objects. (auth)

9076 SEARCH FOR EXTRATERRESTRIAL $H_2{}^{18}O$ EMISSION. Ball, J. A. (Harvard Coll. Observatory, Cambridge, Mass.); Gottlieb, C. A.; Radford, H. E. Astrophys. J.; 163: 429-30(15 Jan 1971).

A search for microwave emission from $H_2{}^{18}O$ at 5625 MHz, in objects with well-known $H_2{}^{16}O$ emission at 22.2 GHz, produced negative results. The upper limit is interpreted to mean either that the H_2O maser pumping mechanism is dependent on isotopic species or that the H_2O maser is not fully saturated at the two frequencies. (auth)

9077 OBSERVATIONS OF SEVEN COMPACT SOURCES IN H II REGIONS AT WAVELENGTHS OF 0.95, 1.65, AND 2.73 CENTIMETERS. Hobbs, R. W.; Johnston, K. J. (Naval Research Lab., Washington, D. C.). Astrophys. J.; 163: 299-302(15 Jan 1971).

Observations of seven compact sources in H II regions were made at 0.95, 1.65, and 2.73 cm with the Naval Research Laboratory's 85-foot reflector. Antenna temperatures and response widths were measured, and flux densities with respect to Jupiter are given. There was no significant increase in flux density at these frequencies for any of the sources observed. (auth)

9078 SLOW ROTATION OF RELATIVISTIC POLYTROPIC MODELS. Papoyan, V. V.; Sedrakyan, D. M.; Chubaryan, E. V. (Erevan State Univ. Byurakan Astrophysical Observatory, USSR). Astrophysics (Engl. Transl.); 5: 42-50(Spring 1969).

Translated from Astrofizika; 5: 97-111(1969).

Slow rotation of relativistic polytropic models was investigated. Only linear corrections in the angular velocity were taken into account. The distribution of the moment of inertia and the nondiagonal component of the metric was obtained for n = 1, 1.5, 2, 2.5, and 3. The case n = 3 was analyzed in detail in connection with the Hoyle–Fowler hypothesis. It is shown that two configurations correspond to the same number of baryons, and the transition from one to the other is accompanied by the release of energy of the order of 10^{58} to 10^{66} erg. Some of the radiated energy (about 30%) is used in increasing the rotational energy. The transition is accompanied by the ejection of matter from the equator of the star. This appears to be a satisfactory model of a quasar. (auth)

9079 LOCATION OF X-RAY SOURCES AND THE GALACTIC BACKGROUND. Ryter, Charles (CEN de Saclay, Gif-sur-Yvette, France). Astron. Astrophys.; 9: 288-97(Nov 1970).

The recently observed x-ray flux recieved from the galactic ridge in the 2- to 15-keV energy band is compared to the flux received from resolved sources. Assuming that the background is produced by unresolved sources and using a simple model for the distribution of sources in the Galaxy, it is shown that the weakness of the galactic background requires that most of the sources are actually resolved and are generally situated at large distances. However, a few sources have been identified with supernova remnants and lie within a few kpc from the Sun. Both facts lead to group x-ray sources in two categories: (i) x-ray emitting supernova remnants, estimated to be about one hundred in the whole Galaxy. Their luminosity is of the order $L \approx 3 \times 10^{36}$ erg/s in the 2 to 6 keV band, and they alone can account for a large fraction of the observed galactic background. (ii) Objects of another kind, probably all resembling Sco XR–1. They form a loose cluster around the galactic center and most of them are observed. Their luminosity amounts to some 8×10^{37} erg/s. In this context, the distance to Sco XR–1 is found to be about 1.2 kpc. (auth)

9080 SHAPES OF RECOMBINATION LINES AT λ3 cm IN M 42, M 17, AND IC 1795. Gordon, M. A.; Churchwell, E. (National Radio Astronomy Observatory, Green Bank, W. Va.). Astron. Astrophys.; 9: 307-11(Nov 1970).

High precision observations of 85 α (~λ3 cm) lines of hydrogen and helium permit the separation of thermal from turbulent line broadening for M42 and IC 1795. These sources give kinetic temperatures of approximately 12000°K—consistent with those derived from non-TE analyses of recombination line intensities. The hydrogen line of M17 is nongaussian, thereby suggesting the blending of two or more H II regions within the beamwidth. Its helium line width is approximately that of hydrogen, perhaps caused by blending with other lines. The IC 1795 spectra has an additional line in addition to those of hydrogen, helium and "carbon." The ratio of helium to hydrogen intensities is approximately 0.07 for M42 and IC 1795. (auth)

9081 ON THE AVERAGE GAUNT FACTOR FOR FREE–FREE EMISSION. Gayet, R. (Observatoire, Paris-Meudon). Astron. Astrophys.; 9: 312-17(Nov 1970).

The exact quantum expression for the bremsstrahlung of a free electron in the pure Coulomb field of a proton at nonrelativistic energies (Sommerfeld, 1951; Menzel and Pekeris, 1935) is averaged over a Maxwellian distribution to obtain the mean free–free Gaunt factor for electron temperatures ranging from 10°K to $10^{7\text{o}}$K and for frequencies ranging from 10^6 to 10^{13} Hz, which cover a wide domain of astrophysical interest. No shielding effect being taken into account, these calculations are only valid for frequencies well above the plasma frequency. The results are compared with those given by a classical expression (Oster, 1963) and by an approximate quantum expression (Menzel, 1969; Oster, 1963). Except at low temperatures where the exact Gaunt factor is shown to be close to unity, results are in essential agreement with Oster (1963) for $\nu \leq 10^{10}$ Hz. However for $\nu > 10^{11}$ Hz no approximate formula is found to be appropriate below $10^{5\text{o}}$K: the use of the exact result is thus necessary for calculations in the infrared region. (auth)

XUM

9082 FREE–FREE EMISSION AND ABSORPTION COEFFICIENTS IN THE RADIO FREQUENCY RANGE AT VERY LOW TEMPERATURES. Oster, Ludwig (Univ. of Colorado, Boulder). Astron. Astrophys.; 9: 318-20(Nov 1970).

The Gaunt factor for free–free radiation is computed for temperatures down to the 3°K level in the cm and dm range. (auth)

9083 FURTHER OBSERVATIONS OF SOME OH SOURCES IN CYGNUS. Winnberg, A. (Onsala Space Observatory, Goteborg). Astron. Astrophys.; 9: 259-68(Nov 1970).

Detailed observations were made of the OH 18-cm spectral lines of the four OH sources in Cygnus discovered by Elldér et al. (1969). It is suggested that these sources be called ON 1, ON 2, ON 3, and ON 4. The observations were made with the Onsala 25.6 m radio telescope equipped with a travelling wave maser (T_{sys} = 40°K) and a multichannel receiver. Complete spectra of the OH ground state lines were obtained with right and left circular polarization and 1 kHz resolution. Many of the line components were observed with 250 Hz resolution. Some of the components were found to be double, and in ON 1 a component with a linewidth of 600 Hz was observed. ON 1 and ON 2 show intensity variations since the end of 1968, when these sources were observed for the first time. Various interpretations and possible identifications of the sources are discussed and the importance of infrared observations is stressed. (auth)

9084 MINIMUM OBSERVABLE DIAMETER OF RADIO SOURCES. Harris, D. E.; Zeissig, G. A.; Lovelace, R. V. (Instituto Argentino de Radioastronomia, Villa Elisa. Arecibo Observatory, Puerto Rico). Astron. Astrophys.; 8: 98-104 (Sep 1970).

Failure to observe saturation of interplanetary scintillations predicted for extremely small angular diameter radio sources prompted an investigation of the minimum observable diameter to be expected due to interstellar scattering and synchrotron self-absorption. The relative importance of these two processes as a function of radio frequency is discussed, and it is noted that the diameter of a source will be strong function of frequency if the interstellar scattering dominates. (auth)

9085 POWER SPECTRUM OF ELECTROMAGNETIC RADIATION SCATTERED BY A RELATIVISTIC BEAM. Stewart, P. (Univ. of Manchester, Eng.). Astron. Astrophys.; 8: 57-64(Sep 1970).

The power spectrum of radiation scattered by a beam of relativistic particles is considered for the case of an incident electromagnetic field that propagates at right angles to the beam. Results apply to a general beam distribution; the case of a relativistic Maxwellian beam is computed in detail and graphical results given. The resulting spectral features of the reflected waves resemble the high-frequency radio spectra of quasars. (auth)

9086 OPTICAL MONITORING OF Sco X-1 FOR 1967-1969. Hiltner, W. A.; Mook, D. E. (Univ. of Chicago). Astron. Astrophys.; 8: 1-6(Sep 1970).

Light curves and brightness histograms of Sco X–1 are given for 1968 and 1969. The light curves confirm the irregular nature of the light variation. The histograms show a time evolution of the system on a time scale of months. (auth)

9087 SURFACE RECOMBINATION OF HYDROGEN MOLECULES. Hollenbach, David (Harvard Coll. Observatory, Cambridge, Mass.); Salpeter, E. E. Astrophys. J.; 163: 155-64(1 Jan 1971).

The problem of the formation of molecular hydrogen on the surfaces of dust grains was examined. A "recombination efficiency" $\gamma'(T)$ is discussed, the fraction of adsorbed atoms which form molecules before evaporating from a surface, as a function of the surface temperature T. For grains with a perfectly regular surface, γ' would be small at grain temperatures exceeding about 13°K. An irregular surface with some lattice-defect or impurity sites having enhanced adsorption energies for atomic hydrogen is considered. The main result is that even a small number of such sites can greatly extend the range of temperatures over which the efficiency of molecular formation is high. On realistic grains, $\gamma' \simeq 1$ for all $T < T_{tr}$, where T_{tr} is some critical value between 25 and 50°K. Since all dust grains in H I regions are likely to be cooler than T_{tr}, it is concluded that $\gamma' = 1$ for molecular formation on grains in H I regions. (auth)

9088 MOLECULAR HYDROGEN IN H I REGIONS. Hollenbach, David J. (Harvard Coll. Observatory, Cambridge, Mass.); Werner, Michael W.; Salpeter, Edwin E. Astrophys. J.; 163: 165-80(1 Jan 1971).

Density profiles of molecular hydrogen were calculated for interstellar clouds of various densities n and radii R, on the assumption of equilibrium conditions. Rates of molecular formation on the surface of dust grains were taken from the preceding paper; rates of molecular destruction by photons from diluted starlight near 1000 Å were calculated, and the effects of line absorption by the hydrogen molecules and general absorption by dust grains were included. The line absorption was more important qualitatively, but the grain absorption had a quantitative effect. Together they gave a resultant fractional abundance of molecular hydrogen $f\ (\equiv 2n_{H2}/[n_H + 2n_{H2}])$ inside a cloud which depends mainly on the combination $n^2\tau_v \exp(5\tau_v)$ (where τ_v is the optical depth to the cloud center due to grains) and is large when this product exceeds (200 cm^{-3})^2. The results were very insensitive to both the gas and the grain temperatures usually assumed for H I clouds. For "standard clouds" with $n \simeq 10\ cm^{-3}$ and $\tau_v \simeq 0.1$, the fractional abundance was $f \simeq 10^{-3}$. Denser and more opaque clouds (in particular, dark nebulae with more than 1 mag of visual extinction) should be mainly in the form of molecular hydrogen, which may account for as much as one-half of the mass of interstellar gas. (auth)

9089 ACCURATE TIMING OF LIGHT FLASHES FROM THE PULSAR IN THE CRAB NEBULA DURING THE 1969–1970 SEASON. Duthie, J. G.; Murdin, Paul (Univ. of Rochester, N. Y.). Astrophys. J.; 163: 1-10(1 Jan 1971).

The pulses of the pulsar in the Crab Nebula were timed at the 10-μsec level throughout the winter of 1969–1970. After adding the light equation between the observatory and the barycenter of the solar system a smooth ephemeris of the pulsar was formed. Residuals from the ephemeris do not show the oscillation previously reported to be occurring before the starquake in 1969 September. Among other explanations of this apparent conflict of evidence, it is suggested that the oscillations reveal instabilities of growing amplitude, resulting in the starquake, and that the pulsar has returned to a stable, nonoscillating configuration. The "braking index" confirms none of the simple models so far proposed for the loss of energy. (auth)

9090 RESULTS OF A SEARCH FOR OPTICAL PULSARS. Horowitz, P. (Harvard Univ., Cambridge, Mass.); Papaliolios, C.; Carleton, N. P. Astrophys. J.; 163: L5-10(1 Jan 1971).

Fourier and correlation techniques were used to search for optical pulsars at the sites of radio-frequency pulsars, x-ray sources, nova and supernova remnants, white dwarfs, infrared stars, planetary nebulae, radio sources, and some other peculiar nebulosities. To limits reaching visual magnitude 20, no pulsars were found over the range of periods searched, from 5 msec to several seconds. (auth)

9091 OBSERVATIONS OF INTERSTELLAR SCINTILLATIONS OF PULSAR SIGNALS AT 2388 MHz. Downs, G. S.; Reichley, P. E. (California Inst. of Tech., Pasadena). Astrophys. J.; 163: L11-16(1 Jan 1971).

The scintillation index and fading time were measured at 2388 MHz. These measurements, together with low-frequency measurements, were interpreted in terms of the extended-medium theory of Uscinski. Typically a scale size of electron irregularities of 4×10^{10} cm and an rms value of the electron density fluctuations of $2 \times 10^{-5}\ cm^{-3}$ were found. Failure to observe long-term variations suggests a second component of density fluctuations. (auth)

9092 SECULAR DECREASE OF THE OPTICAL AND X-RAY LUMINOSITY OF PULSARS. Pacini, F. (Cornell Univ., Ithaca, N. Y.). Astrophys. J.; 163: L17-19(1 Jan 1971).

If the optical and x-ray pulses of pulsars originate close to the velocity-of-light radius, then the emitted power should be roughly proportional to $(\text{period})^{-10}$. The predicted decrease of the optical luminosity of NP 0532 is about 1% every 2 years. The Vela pulsar PSR 0833 could have an apparent magnitude of ~25. (auth)

9093 SEARCH FOR THE $^2\Pi_{\frac{1}{2}}$, J = $\frac{1}{2}$ EXCITED STATE OF OH IN W3. Ball, John A. (Harvard Coll. Observatory, Cambridge, Mass.); Gottlieb, Carl A.; Meeks, M. L.; Radford, H. E. Astrophys. J.; 163: L33-4(1 Jan 1971).

Laboratory measurements were made of the four line rest frequencies of the $^2\Pi_{\frac{1}{2}}$, J = $\frac{1}{2}$ state of OH. The F = 2 → 2 frequency places the feature reported by Schwartz and Barrett at −17 km sec^{-1} instead of −43 km sec^{-1}. This feature was not detected in W3(OH), and it is concluded that its peak flux was less than 0.3 f.u. (5 σ) at the time of the measurements. (auth)

9094 DETECTION OF INTERSTELLAR CYANOACETYLENE. Turner, B. E. (National Radio Astronomy Observatory, Green Bank, W. Va.). Astrophys. J.; 163: L35-9(1 Jan 1971).

Microwave emission from cyanoacetylene (HC_3N) was detected in the galactic radio source Sgr B2. Two of the three quadrupole-

split transitions of the J = 0 → 1 transition were observed, the strongest with a strength of ~4 f.u. The emission is not linearly polarized. Within the frequency uncertainty of the transitions, the HC_3N lines in Sgr B2 have the same radial velocity, +62 km s^{-1}, as the formaldehyde absorption. No HC_3N was detected in sixteen other galactic sources in which the molecules OH, H_2CO, and HCN were detected. (auth)

Solar Phenomena

Refer also to abstracts 8499, 9257, 9300, 9309, 9310, 9333, 9454, and 9737.

9095 (CSIRO-Trans-10258) PHOTOSPHERIC AND CHROMOSPHERIC MAGNETIC FIELDS AND THE BRIGHTNESS OF FACULAE AND FLOCCULI. Tsap, T. T. Translated by G. Losonci from Izv. Krym. Astrofiz. Observ.; 39: 265-75(1969). 14p. Dep. NTIS (U.S. Sales Only).

An abstract of this article, prepared from the original appeared as NSA 24: 17531 (1970). (Australia)

9096 (CSIRO-Trans-10289) PHOTOSPHERIC MAGNETIC FIELDS AND FLOCCULI BRIGHTNESS. Tsap, T. T. Translated by G. Losonci from Izv. Krym. Astrofiz. Observ.; 34: 296-304(1965). 9p. Dep. NTIS (U.S. Sales Only).

An abstract of this article, prepared from the original, appeared as NSA 21: 16718 (1967). (Australia)

9097 (LA-4454(Vol.2)) VELA V AND VI SOLAR X-RAY ATLAS. II. SEPTEMBER 1, 1969-JANUARY 1, 1970. Blocker, N. K.; Fehlau, P. E.; Kunz, W. E.; Chambers, W. H.; Fuller, J. C.; Milkey, R. W. (Los Alamos Scientific Lab., N. Mex.). Oct 1970. Contract W-7405-eng-36. 124p. Dep. NTIS.

Data obtained from the solar radiation monitors on the Vela V Satellites are presented. Equivalent graybody flux in three bands (0.3 to 3, 1 to 8, and 1 to 16 Å) is plotted as a function of universal time, one day per page. Data from September 1, 1969, to January 1, 1970, are presented. (auth)

9098 (MPI-PAE/EXTRATERR-48) GAMMA RAY AND NEUTRON EMISSIONS FROM THE SUN. Chupp, E. L. (Max-Planck-Institut fuer Physik und Astrophysik, Munich (West Germany)). Sep 1970. 88p. Dep. NTIS (U. S. Sales Only).

The evidence for acceleration of charged particles in the solar atmosphere is reviewed from the point of view of production of gamma rays and neutrons at the Sun. The estimates of fluxes at the Earth of these components are also reviewed. The expected knowledge about the Sun to be derived from such observations is also discussed. Estimates and conditions for obtaining observable fluxes from Syrovatskii's dynamic dissipation model are also considered. The present status of experimental observations is reviewed, and suggestions for new experimental approaches are given. (auth)

9099 MAGNETIC AND SPECTRAL CHARACTERISTICS OF SMALL H-ALPHA SOLAR PLAGES. Schoolman, Stephen Allan. Boulder, Colo.; Univ. of Colorado (1969). 165p. University Microfilms Order No. 70-16,520.

Thesis.

Magnetic fields were measured in 18 small solar plages between June, 1966, and May, 1967. The 14 bipolar regions had the same magnetic orientation as sunspot groups of the current cycle. Of the four monopolar plages, two were remnants of old active regions. (TSS) (Diss. Abstr. Int., B)

9100 IDENTIFICATION OF MgO LINES IN THE SPECTRUM OF A LARGE SUNSPOT. Sotirovski, Pascal (Observatoire de Paris, Meudon, France). Compt. Rend., Ser. B; 271: 926-8 (28 Oct 1970). (In French).

The large sunspot observed near the center of the solar disk on June 22, 1959 was studied. Lines corresponding to the $^1\Sigma \rightarrow {}^1\Sigma$ transition of MgO are present in its spectrum. (France)

9101 SOLAR MAGNESIUM ISOTOPIC ABUNDANCE RATIOS. Branch, David Reed. College Park, Md.; Univ. of Maryland (1969). 59p. University Microfilms Order No. 70-15,392.

Thesis.

The magnesium isotopic abundance ratios in the Sun were estimated, using the magnesium hydride $A^2\Pi - X^2\Sigma$ (0,0) absorption band in sunspot spectra. It is probable that in the Sun the relative proportions of the three stable magnesium isotopes, ^{24}Mg, ^{25}Mg, and ^{26}Mg, differ from those of terrestrial and meteoritic magnesium. Examination of the wavelength region λλ4975 to 5211 Å in high-dispersion (7mm/Å) sunspot spectrograms revealed that, in addition to strong absorption lines of ^{24}MgH, features due to ^{25}MgH and ^{26}MgH could be identified. The wavelengths of these isotopic lines were found to be in excellent agreement with predicted positions, based upon calculations of vibrational and rotational isotopic wavelength shifts. A coarse analysis indicated that in the sunspot region, the magnesium isotopic ratios ^{24}Mg: ^{25}Mg: ^{26}Mg are nearer to 60:20:20 than to the terrestrial and meteoritic values of 79:10:11. Fine analysis, employing several different sunspot models, also yielded isotopic ratios of approximately 60:20:20. However, owing to uncertainties involving sunspot models, continuum location, line blending, and scattered photospheric light, the conclusion is limited to the statement that the heavy isotopes of magnesium appear to be enhanced by as much as a factor of two in the Sun, relative to the Earth. Further study based upon photoelectric spectrophotometry and improved sunspot models (when available) is warranted. A discrepancy exists between the magnesium hydride band strength as observed and as predicted by cool sunspot models. A model due to Zwaan (Recherches astr. Obs. Utrecht 17, part 4, 1965) overestimates the MgH band strength by a factor of approximately twenty-five. A hotter model provides better agreement with the observations. (Diss. Abstr. Int., B)

9102 PRELIMINARY POWER SPECTRA OF THE INTERPLANETARY PLASMA. Intriligator, D. S. (California Inst. of Tech., Pasadena); Wolfe, J. H. Astrophys. J.; 162: L187-90 (Dec 1970).

Spacecraft observations of the solar-wind plasma were used to estimate power spectra of the density of solar-wind protons. An average frequency dependence of $f^{-1.3}$ in the frequency range 10^{-4} to 10^{-3} Hz and a plasma-density correlation length of 10^6 km or more for the structure of turbulence were implied. Both estimates were consistent with results from direct observations of the interplanetary magnetic field and the solar-wind speed and also with data on interplanetary scintillations. (auth)

9103 RELATIVE ABUNDANCES AND ENERGY SPECTRA OF ^3He AND ^4He FROM SOLAR FLARES. Hsieh, K. C.; Simpson, J. A. (Univ. of Chicago). Astrophys. J.; 162: L191-6(Dec 1970).

The isotope ^3He from solar flares has been detected in interplanetary space with the charged-particle telescope on the IMP-IV satellite. The study included ^1H, ^3He, and ^4He nuclei in the energy range 10 to 100 MeV per nucleon from seven flares in 1967. The summed differential energy spectra obtained for ^4He and ^3He are $\propto E^{-3.0}$ and $\propto E^{-1.8}$, respectively. When one integrates over this energy range, the ratio $^3He/^4He = (2.1 \pm 0.4) \times 10^{-2}$. For the entire energy span it is estimated that this ratio becomes $\leq 2 \times 10^{-3}$, which is below the optically observed upper limits of chromospheric $^3He/^4He$ and in agreement with calculated values. The measurements support the view that flare abundances of the isotopes are samples of the chromospheric abundances, but significant production of ^3He in nuclear interactions cannot be excluded. (auth)

9104 SIX-MINUTE PERIODICITY DURING X-RAY FLARES. Glencross, W. M. (University Coll., London). Nature (London); 228: 654-5(14 Nov 1970).

Reference is made to observations of soft x-ray emission from the Sun made by the satellite OSO-IV launched on Oct. 18th, 1967. During a visible class IN flare the x radiation showed two peaks, with maxima 6 min apart. In flares of this type the initial event has been regarded as a precursor to the main event, but it is suggested that the precursor is really a part of the main flare activity, and that the initial development is relatively small compared with the second increase. A minor increase in x-ray flux appeared to occur about 6 min after the main increase. If the relative intensities of the two increases had been different, the first peak might have been regarded as a precursor. An examination was made of the time profiles of a number of flares showing more than one intensity peak, and the results are shown by histogram. There was strong evidence that the time separations between related peaks were multiples of about 6 min. Possible explanations of the periodicity are discussed. Because the 6-min period is not very different from the 300-sec oscillation observed at lower levels it may be that the longer period arises as a result of differences of height and magnetic field, in which case the flare increases would appear to be triggered by the arrival of energy in the solar atmosphere from the photosphere; this possibility is discussed. (UK)

9105 EFFECTS OF AN ANNULAR SOLAR ECLIPSE ON THE PHASE OF VLF TRANSMISSIONS. Hoy, R. D. (Australian National Univ., Canberra). J. Atmos. Terrest. Phys.; 32: 1835-9 (Nov 1970).

Effects of the annular solar eclipses of March 18 and September 11, 1969 on vlf transmissions were studied. Phase changes attributable to the March 18 eclipse were found corresponding to an increased time of propagation over the paths of 2.0 μsec from NWC (22.3 kHz) and 10 μsec from GBR (16.0 kHz). Similarities were

noted between the observed phase delays and calculated eclipse obscuration along the great circle paths. (auth) (UK)

9106 VELOCITY FIELDS IN MAGNETICALLY DISTURBED REGIONS OF THE Hα CHROMOSPHERE. Roberts, Phillip Howard Jr. Pasadena, Calif.; California Inst. of Tech. (1970). 148p. University Microfilms Order No. 70-14,849.

Thesis.

A cancellation machine was constructed to automatically produce the cancellation required by the method of Leighton in making Doppler movies. Various adaptations of the machine allow rapid data reduction to the 16-mm print required for cinema viewing. The preliminary data gathered in 1966 and 1967 were reduced. These data consist mostly of the Hα Doppler movie pairs, and some Zeeman movie pairs, of sunspot regions. A new calibration technique for inferring Doppler velocities from cancellation densities was developed. This technique extends the calibration to large Doppler shifts with no loss in accuracy. (TSS) (Diss. Abstr. Int., B)

9107 COMPOSITION AND DYNAMICS OF THE SOLAR WIND PLASMA. Hundhausen, A. J. (Los Alamos Scientific Lab., N. Mex.). Rev. Geophys. Space Phys.; 8: 729-811(Nov 1970).

Although the coronal origin of the interplanetary plasma implies some general connection between solar and solar wind properties, strong evidence for specific relationships has emerged only recently. Three such relationships are reviewed: their observational and theoretical foundations are discussed, as is their use in determining solar properties from solar wind observations. The first of these involves solar and interplanetary chemical compositions; emphasis is placed on the implied concentration of helium (and other elements heavier than hydrogen) in the corona. The second relationship involves the effects of coronal and interplanetary dynamical processes on the properties of the undisturbed solar wind. Arguments for and against the extension of the basic coronal heating process well out into interplanetary space are developed. The final relationship involves solar activity and properties of the disturbed solar wind. Attention is focused on interplanetary shock waves produced by solar flares and on implications for the coronal deposition of energy released in flares. (auth)

9108 LYMAN-α SCATTERING DURING THE SOLAR RADIATION PERIOD. Fahr, H. J.; Blum, P. W. (Institut fuer Astrophysik und Extraterrestrische Forschung, Bonn). Astron. Astrophys.; 8: 226-30(Oct 1970).

The solar Lyman-α radiation shows a typical 27-day variation of about 30%. On the assumption that Lyman-α scattering is due to the scattering of solar Lyman-α by interplanetary hydrogen, the variation of the scattered intensity was investigated theoretically. The dependence of the density of slow interstellar hydrogen in interplanetary space on solar euv radiation during the 27-day cycle was analyzed. It is shown that there exists a phase difference of about 6 days between the maximum of the solar euv radiation and the minimum of the hydrogen density. A correlation between solar Lyman-α and scattered Lyman-α results from the theory and yields a predicted phase delay of up to 3 days. The measurements of Meier and Mange seem to be an experimental verification of this theoretical approach. The apparent existence of such a 27-day variation of the Lyman-α background is a test for the still-controversial origin of this background and therefore, gives strong support to the assumption that Lyman-α scattering is at least partly due to interplanetary hydrogen. (auth)

9109 POLARIZATION OF CONTINUUM AT THE SOLAR LIMB. Debarbat, S.; Dumont, S.; Pecker, J.-C. (College de France, Paris). Astron. Astrophys.; 8: 231-42(Oct 1970). (In French).

The classical expressions for the source function lead to an estimate of the polarization rate at the solar limb at various wavelengths. Two methods were used; in both cases the computed polarization was compared to the observations by Dollfus and Leroy (1960). An attempt was made to justify the models introduced in the computation through an inversion of the expression of the polarization rate. For the models considered, the computed polarization is too weak by a factor 3 to 6. It seems necessary to take into account, as the main contributor to this factor, the effect of Fraunhofer lines. The comparison of the observed and computed polarization rates suggests, however, that another additional phenomenon should be invoked to explain the discrepancy. In order to improve the understanding of this question, the study of the effect of lines has to be pursued; but it will be necessary, as well, to obtain new observations in the visible and to extend them to other wavelengths, especially in the ultraviolet. (auth)

9110 FOUR NEW BOUND, LOW-LYING STATES OF CYANOGEN: $^4\Sigma^+$, $^4\Sigma^-$, $^4\Pi$, $^4\Delta$. Heil, Timothy G.; Schaefer III, Henry F. (Univ. of California, Berkeley). Astrophys. J.; 163: 425-7(15 Jan 1971).

Simple molecular-orbital theory predicts the existence of four low-lying, bound, quartet states of CN. Ab initio configuration-interaction calculations were carried out on these and other states of CN. The four states, $^4\Sigma^+$, $^4\Pi$, $^4\Delta$, and $^4\Sigma^-$, were calculated to lie at 4.02, 5.33, 5.91, and 6.67 eV. Only the $X\ ^2\Sigma^+$, $A\ ^2\Pi$, and $B\ ^2\Sigma^+$ states of CN appear to lie below these four new states. (auth)

9111 DIFFERENTIAL ROTATION: MERIDONAL VELOCITIES, AND POLE-EQUATOR DIFFERENCE IN TEMPERATURE OF A ROTATING CONVECTIVE SPHERICAL SHELL. Durney, B. (National Center for Atmospheric Research, Boulder, Colo.). Astrophys. J.; 163: 353-61(15 Jan 1971).

A rotating, convective, spherical layer of fluid is considered in the Boussinesq approximation. The coupled equations for the axisymmetric modes of the velocity and temperature fields are solved in the steady state with the low-order "Legendre components" of the fluctuating self-interactions (evaluated in the quasi-linear approximation) as the driving terms. It is found that (a) the angular velocity increases inward; (b) there is pole-equator differential rotation with equatorial acceleration; (c) beneath the surface the equator is hotter than the poles (at the surface the temperature is given as a boundary condition); (d) two types of meridional circulation are compatible with the observed differential rotation of the Sun. For example, in the northern hemisphere, in one case the flow comprises two cells in the radial direction, and in the other case each radial cell is divided latitudinally into two subcells. (auth)

9112 FORMATION OF GIANT CELLS AND SUPERGRANULES. Vickers, Glenn T. (National Center for Atmospheric Research, Boulder, Colo.). Astrophys. J.; 163: 363-74(15 Jan 1971).

The linear equations for time-independent convection in a plane-parallel layer of a perfect gas with the temperature profile given by Böhm were studied under the assumption of constant kinematic viscosity. These equations were solved by a shooting method to give the onset of steady convection. The solutions found corresponded to cells with a diameter of about 400,000 km and were identified as the giant cells. By calculating the eigenfunction of the most unstable mode, it was found that these giant cells carry energy downward in a layer with a depth of about 40,000 km at the top of the convection zone. It is thus expected that secondary cells will be generated in this layer. This idea is strengthened by a calculation of Rayleigh numbers. It was found that all cells extending from the upper boundary to a depth greater than about 5,000 km were unstable. The horizontal scales of cells extending from the upper boundary to depths between 5,000 and 40,000 km were found to lie in the range 10,000 to 90,000 km, and so the cells were identified as the supergranules. (auth)

9113 TEMPERATURE VARIATION AND THE SOLAR OBLATENESS. Ingersoll, Andrew P. (California Inst. of Tech., Pasadena); Spiegel, Edward A. Astrophys. J.; 163: 375-82(15 Jan 1971).

Dicke and Goldenberg's oblateness measurement may be explained by an equatorial temperature excess of 30°K, smoothly distributed in optical depths ≤0.01. The resulting brightness variation with solar latitude is concentrated close to the limb, and it is not possible, with data presently available, to distinguish such variation from true oblateness. (auth)

9114 ELECTRON TEMPERATURE IN THE TWO-COMPONENT SOLAR WIND. Cuperman, S.; Harten, A. (Tel-Aviv Univ., Israel). Astrophys. J.; 163: 383-92(15 Jan 1971).

A systematic investigation of possible modifications in the equations of the two-fluid model for the solar wind, in order to predict, in addition to the other characteristics, the electron temperature and electron heat flow observed at 1 A.U., was carried out numerically. The equations used allow for a modified rate of energy exchange between electrons and protons, as well as for modified electron and proton thermal conductivities. That is, these transport coefficients are allowed to include (besides collisional interactions) contributions from turbulent wave-particle interactions existing in the solar wind as well as effects due to inhibition across the interplanetary magnetic field. When the thermal equilibrium between electrons and protons is assumed to extend to a distance of 5 to 6 $R_\odot$ away from the Sun, it is found that the agreement between the theoretical predictions and observations at 1 A.U. can be achieved in either one of the following two ways: (i) by using an energy-exchange rate about 30 times larger than the collisional one in conjunction with an electron thermal conductivity about 4 times lower than the collisional one; this pro-

vides (at 1 A. U.) $n_E = 6.33$ cm^{-3}, $v_E = 256$ km sec^{-1}, $T_{eE} = 1.6 \times 10^{5}$°K, $T_{pE} = 0.43 \times 10^{5}$°K, and $-K_e(dT_e/dr)_E = 0.75 \times 10^{-2}$ ergs cm^{-2} sec^{-1}; (ii) by using a proton thermal conductivity about twice the collisional one in conjunction with an electron thermal conductivity about 5 times lower than the collisional one; this provides $n_E = 6$ cm^{-3}, $v_E = 270$ km sec^{-1}, $T_{eE} = 1.59 \times 10^{5}$°K, $T_{pE} = 0.43 \times 10^{5}$°K, and $-K_e(dT_e/dr)_E = 0.6 \times 10^{-2}$ ergs cm^{-2} sec^{-1}. It is suggested that additional measurements of the proton temperature at distances $r \gtrsim 1$ A.U. could help to determine the actual situation, which should probably be intermediate between the two possible ones described above. (auth)

9115 NATURE OF INTERPLANETARY GAS. Gidalevich, E. Ya.; Rodkina, T. E. Cosmic Res. (USSR) (Engl. Transl.); 7: 105-9(Jan-Feb 1969).

Translated from Kosm. Issled.; 7: 117-21(Jan-Feb 1969).

A stream of compressed gas is examined in the gravitational field of a point body whose gravitation potential significantly exceeds the potential of the gas proper. In the adiabatic approximation it is found that the enthalpy i of the gas is approximately equal to the gravitational potential φ of the body in the region where $\varphi \gg i_0$ (here i_0 is the enthalpy of the unperturbed gas). The gas density increases correspondingly in the adiabatic relationship. The problem is solved for the Sun and the interplanetary gas. The results are compared with the existing theory of solar wind. Conclusions are drawn concerning the nature and properties of the interplanetary gas. (tr-auth)

9116 COUPLING BETWEEN RADIATIVE TRANSFER AND THERMAL CONDUCTION IN THE CHROMOSPHERE. Frisch, H. (Meudon Observatory, France). Astron. Astrophys.; 9: 269-76 (Nov 1970).

The influence of the transfer of radiative energy on the temperature structure of a plane slab of finite thickness heated by thermal conduction was studied. The temperatures at the boundaries and the radiation entering the slab are given. In some cases, constant absorption coefficient per cm and coefficient of thermal conductivity proportional to the third power of the temperature, the problem can be solved analytically. When the absorption coefficient goes to zero or infinity, the temperature distribution in the slab becomes asymptotically identical to that of a slab heated by thermal conduction only. In intermediate cases the temperature inside the slab may become greatly inferior to that of the boundaries with very rapid variations in the vicinity of those boundaries. A generalization of the results to the case of a nonconstant absorption coefficient is outlined. (auth)

9117 EXPERIMENTAL OSCILLATOR STRENGTHS FOR Ni I LINES. Garz, T.; Heise, H.; Richter, J. (Univ., Kiel). Astron. Astrophys.; 9: 296-300(Nov 1970). (In German).

Relative oscillator strengths of 48 Ni I lines were determined from emission measurements with a high-current electrical arc burning in an argon atmosphere. Introducing a small admixture of nickel chloride into the center of the arc, spectra of nickel can be observed end-on without self-absorption and self-reversal of the lines. The oscillator strengths were obtained from the Ni I line intensities and the measured arc temperature. The question of LTE was investigated carefully. Using absolute oscillator strengths of two resonance lines that have been measured by Lawrence et al. (1965) with the atomic beam technique, the scale of relative f-values was converted to an absolute scale. The accuracy of the relative scale is in the range of 10 to 20%. To this value the experimental error of Lawrence et al. (20%) has to be added. (auth)

9118 INTERPRETATION OF THE EAST–WEST ASYMMETRY OF THE INITIAL APPEARANCE OF SUNSPOTS. Rix, H.; Roddier, F. (Faculte des Sciences, Nice). Astron. Astrophys.; 9: 301-6(Nov 1970).

The east–west asymmetry in the initial appearance of sunspots is explained, assuming that sunspots begin to form at a level deeper than optical depth unity and move towards the surface of the Sun, by the variation of the photospheric opacity with height combined with the variation of the heliocentric angle as the observation moves from the center to the limb. This contribution to the asymmetry is the same order of magnitude as the contribution from the classical "foreshortening effect." A conical model of a sunspot is used to include the contribution of these two effects. A comparison of the theory with the observed east–west asymmetry gives a mean ascension velocity of the sunspots of 3 m/s. This comparison gives further evidence that the evolution of some sunspots in interrupted. (auth)

9119 NUMERICAL EXPERIMENTS ON PHOTOSPHERIC LINE PROFILES. Boyer, R. (Observatorie de Meudon, France). Astron. Astrophys.; 8: 134-40(Sep 1970). (In French).

The aim of this work was to find what types of physical processes are able to change the shape and the asymmetry of metallic-line profiles belonging to the spectrum of the undisturbed photosphere. Two lines (Sr I 4607 and C I 10754 Å) observed with high resolution at the center of the solar disk were analyzed. By means of numerical experiments the correlation between a line profile and the following parameters was studied: microturbulence, mean arithmetical value of the upward and downward convective macroscopic velocities (related to temperature inhomogeneities), upper limit of the convection zone and the relative surfaces of hot ascending, mean, and cold descending elements belonging to the convection cell structure. The computations are based on the inhomogeneous Utrecht Reference Photosphere model. (W.D.M.)

9120 IDENTIFICATION OF SiH^+ IN THE SOLAR PHOTOSPHERIC SPECTRUM. Grevesse, N. (Univ., Liege); Sauval, A. J. Astron. Astrophys.; 9: 232-8(Nov 1970).

The first convincing identification of a molecular ion in a stellar atmosphere is presented: the absorption band spectrum of SiH^+ (transition A $^1\Pi - X\ ^1\Sigma^+$) in the solar photospheric spectrum. Values of the band oscillator strengths were deduced for two bands: $f_{00} = 0.0005$ and $f_{01} = 0.0004$. (auth)

9121 CORRELATION OF THE IMPULSIVE COMPONENT OF mm-BURSTS AND THE GRADUAL RISE OF SOFT X-RAY EMISSION. Feix, G. (Univ. of Missouri, Columbia). Astron. Astrophys.; 9: 239-44(Nov 1970).

From a survey of high-resolution measurements of the Sun at mm wavelengths it was found that the impulsive maximum occurs before the maximum of the associated soft x-ray burst. These observations appear to be consistent with well-known cm observations. It can be clearly seen from the mm observations that the impulsive radio component is being released explosively after a gradual heating of the flaring region. (auth)

9122 A PROPOSED METHOD FOR CALIBRATING MEASUREMENTS OF LINEARLY POLARIZED LIGHT FOR THE OBSERVATION AND ANALYSIS OF ZEEMAN EFFECTS IN SOLAR SPECTRAL LINES. Semel, M. (Observatoire, Meudon, France). Astron. Astrophys.; 9: 356-8(Dec 1970).

In the proposed method, the calibration depends only on the broadening mechanism of Fraunhofer lines. Because this mechanism is expected to be common to many lines, the use of several lines with different Landé factors may lead to reliable measurements of the magnetic field and to the determination of the broadening parameters. (auth)

9123 ELECTRON EXCITATION RATE OF THE GREEN CORONAL LINE 5303 A. Petrini, D. (Observatoire, Nice). Astron. Astrophys.; 9: 392-404(Dec 1970).

The collision strengths between levels of Fe^{+13} were calculated using the close coupling and the Coulomb–Born I methods. It is shown that the Coulomb–Born I approximation gives reliable results for highly ionized ions. The electron excitation coefficient rate α_e ($^2P^0_{\frac{3}{2}} \rightarrow {}^2P^0_{\frac{1}{2}}$) corresponding to the green coronal line was investigated in detail using the quantum defect method, which takes into account the excitation via autoionization levels of Fe^{+12}. The statistical equilibrium of the populations of Fe^{+13} levels was solved under coronal conditions, and the effective coefficient rate for the green line is given for a wide range of temperatures and densities. (auth)

9124 SPACE RADIOASTRONOMY OF SOLAR BURSTS AT ALL FREQUENCIES: THE STEREO-PROJECT. Steinberg, J.-L.; Caroubalos, C. (Observatoire, Meudon, France). Astron. Astrophys.; 9: 329-38(Dec 1970).

Most observed characteristics of Type III bursts are accounted for by the "plasma hypothesis" which implies that the radio energy is radiated from the coronal altitude where the local plasma frequency is close to the observing frequency and the index of refraction vanishes. Strong focusing is to be expected in the absence of scattering effects. Type I's are also assumed to be excited in a magnetoactive plasma near the level corresponding to the observing frequency, so that focusing effects might also be expected. It has also been suggested that Type III harmonics are radiated preferentially in the backward direction towards the Sun and that the mechanism of Type I's is directive in itself. It is first shown here that center-to-limb histograms of occurrence cannot provide reliable information on the directivity (or focusing) of short-lived solar events as soon as it is no longer assumed that the "polar diagram" axis is radial. The only way to provide evidence for or against directivity of solar bursts is to observe them simultaneously from the Earth and a remote space probe (stereo-type experiment). Some of the information one can expect from such an experiment is then analyzed, for instance from the measurement of the difference in travel time of radio waves from the solar source to the Earth and to the

spacecraft. It is shown that the position of an "apparent source" can be obtained from high-resolution ground-based observations and space observations. Using models of the radio corona, the positions of the apparent source that can be found sometimes below the photosphere are computed, thus providing direct evidence of refractive effects in the corona and an estimation of the index of refraction at the source. Finally, some of the problems encountered in designing stereo-type experiments are briefly reviewed, and other examples of problems in solar physics that could be investigated by such experiments are suggested. (auth)

Galaxies

9125 CLASSIFICATION OF THE FORMS OF CLUSTERS OF GALAXIES. Bautz, L. P. (Northwestern Univ., Evanston, Ill.); Morgan, W. W. Astrophys. J.; 162: L149-53(Dec 1970).

A classification of clusters of galaxies based on the relative contrast of the brightest member galaxy is described. Clusters containing a supergiant D galaxy define Type I; at the other extreme (Type III) are clusters which contain no members significantly brighter than the general bright population. A list of seventy-six clusters classified according to the present system is included. (auth)

9126 ISOLATED EXTRAGALACTIC H II REGIONS. Sargent, Wallace L. W.; Searle, Leonard (California Inst. of Tech., Pasadena. Carnegie Institution of Washington, D. C.). Astrophys. J.; 162: L155-60(Dec 1970).

Two isolated dwarf emission-line galaxies are shown to be observationally indistinguishable from giant H II regions in nearby galaxies. Either they are young systems or, more likely, the luminosity function of newly formed stars in them differs radically from that found in the Galaxy. (auth)

9127 CONJUGATE PHOTOELECTRON IMPACT IONIZATION. Shawhan, S. D.; Block, L. P.; Falthammar, C.-G. (Univ. of Iowa, Iowa City). J. Atmos. Terrest. Phys.; 32: 1885-1900 (Dec 1970).

The exchange of photoelectrons between ionospheres in a matter of minutes rather than at the slow ambipolar speed is discussed. It is shown that the electron density may be affected by secondary processes resulting from the conjugate photoelectron flux but not by the flux itself. The flux spectrum of conjugate photoelectrons throughout the day at the solstices for minimum solar activity is calculated for 55 N° geographic latitude over Europe, using a method previously employed by Nisbet. Summer escaping flux values range up to 9×10^{12} electrons m^{-2} sec^{-1} and winter values to 5×10^{12} electrons m^{-2} sec^{-1}. Compared at specific solar zenith angles the computed values are in good agreement with recent satellite measurements. Approximately half of this flux is lost by Coulomb collisions along the field line path. The resulting flux arriving at the local ionosphere produces ionization by inelastic collisions in the atmosphere. This additional ionization is about 3% of the ionization from local processes at summer noon and 48% at winter noon. During winter nighttime this conjugate photoelectron ionization can be significant for several hours. Although small in magnitude, this additional ionization should systematically modify the summer total electron content depending on geographic location. The large seasonal differences in the relative impact ionization may explain in part the F-layer seasonal anomaly. This source may be important for maintaining and causing enhancements in the winter night-time ionosphere. (auth) (UK)

9128 NEW OBSERVATIONS OF BLUE HARO GALAXIES. DuPuy, David L. (Univ. of Toronto. Kitt Peak National Observatory, Tucson, Ariz.). Astron. J.; 75: 1143-7(Dec 1970).

Redshifts are listed for 23 blue Haro galaxies and eight cluster members (located at 12h44m, +55°00′ and including Haro 32) obtained with the 84-inch reflector and Carnegie image intensifier at Kitt Peak. UBV data for these galaxies were obtained with the 36-inch reflectors of Kitt Peak. Application of the virial theorem to eight members of the H32 cluster yields an average mass per galaxy of 1.2×10^{10} $M_\odot$ and a mass-to-luminosity ratio of $(M/L)_V \leq 1$. The Haro galaxies appear to reveal excitation by hot stars, but they do not show the usual properties of irregular galaxies. (auth)

9129 ORIGIN OF MAGNETIC FIELDS. Parker, E. N. Comments Astrophys. Space Phys.; 2: 127-33(Jul-Aug 1970).

Effective turbulent diffusion appears to be essential for the origin of magnetic fields. If ϵ (universal number) is 0.01 to 1.0 then the magnetic fields observed in the Earth, Sun, and Galaxy appear to be a direct consequence of the observed fluid motions (nonuniform rotation and cyclonic turbulence). It is concluded that the question of turbulent diffusion needs careful study if there is to be a solid foundation for understanding the origin of the observed magnetic fields. (W.D.M.)

9130 NATURE OF GALACTIC NUCLEI. Burbidge, Geoffrey. Comments Astrophys. Space Phys.; 2: 144-52(Jul-Aug 1970).

That the nuclei of some galaxies and quasars are centers from which tremendous energy fluxes are emitted and large amounts of matter are ejected has been known for many years, but no generally acceptable explanations of these phenomena have been available. Recent observations, which may necessitate a new approach to the evolution of galactic nuclei are discussed, in which the very dense states may be the initial rather than the final phase. (W.D.M.)

9131 SURFACE BRIGHTNESS OBSERVATIONS OF DARK NEBULAE. Mattila, K. (Landessternwarte, Heidelberg). Astron. Astrophys.; 8: 273-82(Oct 1970).

Photoelectrical measurements of the surface brightness of the Southern Coalsack were carried out with a 50-cm telescope of the Heidelberg Observatory. The foreground components of the night-sky brightness (zodiacal light, airglow, atmospheric scattered light) were first subtracted from the measured values. Special attention was given to the light scattered by atmospheric dust and smoke. Then the light scattered in the Coalsack was separated from the Milky Way background brightness; its intensity reached the values of about 80, 50, and 60 S_{10}/deg^2 in V, B, and U, respectively, in the most opaque areas of the Coalsack. For the colors of the scattered light it was found that: B−V = 0.50m, U−B = −0.10m. In addition, measurements of the surface brightness of a dark nebula in Libra are reported. The intensity of the diffuse light in this nebula amounts to 26 and 14 S_{10}/deg^2 in V and B respectively, and it was found to be polarized; the polarization direction was perpendicular to the galactic equator. (auth)

9132 KINETIC TEMPERATURE OF COLD H I GALACTIC COMPONENTS. Schmidt-Kaler, Th.; Pospieszczyk, A. (Ruhr. Univ., Bochum, Ger.). Astron. Astrophys.; 8: 335-8(Oct 1970). (In German).

Flat "saturated" emission components of the 21-cm line of H I were studied from a survey of line profiles between longitudes 355 and 220°, obtained with the 25-m Stockert dish. Apparently flat profiles, resulting from the superposition of two gaussian profiles were eliminated, using the Parkes and the Maryland–Green Bank hydrogen line surveys with their greater angular resolution. The average kinetic temperature of the cold H I components inferred was 52°K. Some conclusions of this result are discussed. (auth)

9133 CONCERNING A PROPOSED TEST FOR THE EXPANSION OF CLUSTERS OF GALAXIES. Noerdlinger, Peter D. (Ames Research Center, Moffett Field, Calif.). Astrophys. J.; 163: 437-8(15 Jan 1971).

An expanding association of galaxies will exhibit smaller dispersion in the radial velocities of its members near its outer boundary only if the expansion is due to a force that has accelerated the galaxies outward. In other cases, the dispersion may be larger on the line of sight through the center. (auth)

9134 RATE OF STAR FORMATION IN M31. Hartwick, F.D.A. (Univ. of Victoria, B. C.). Astrophys. J.; 163: 431-2 (15 Jan 1971).

A correlation was made between the surface distribution of H II regions and the neutral hydrogen gas in M31. It was found that the density of H II regions is related to the gas density by the relation $\rho_{HII} \propto \rho_g^{1.50 \pm 0.12}$. (auth)

9135 GENERATION OF MAGNETIC FIELDS IN ASTROPHYSICAL BODIES. III. TURBULENT DIFFUSION OF FIELDS AND EFFICIENT DYNAMOS. Parker, E. N. (Univ. of Chicago). Astrophys. J.; 163: 279-85(15 Jan 1971).

It is shown by formal calculation that the probability distribution of magnetic field carried in a turbulent fluid varies with the time in a manner identical with the probability distribution of a scalar field carried in the same turbulence. Then if Kraichnan's results are used for the diffusion of scalar fields, the effective turbulent-diffusion coefficient η is $0.15\ u/k_0$, where u is the rms velocity of the turbulence and k_0 is the wavenumber of the large eddies. In the gaseous disk of the Galaxy this gives $\eta \approx 3 \times 10^{25}$ cm^2 sec^{-1}. It follows from this large value of η that the galactic field cannot be primordial, but is automatically generated by the nonuniform rotation and turbulence throughout the gaseous disk. (auth)

9136 GENERATION OF MAGNETIC FIELDS IN ASTROPHYSICAL BODIES. II. THE GALACTIC FIELD. Parker, E. N. (Univ. of Chicago). Astrophys. J.; 163: 255-78(15 Jan 1971).

The gaseous disk of the Galaxy is subject to nonuniform rotation and internal turbulence. The rotation causes the turbulence to be cyclonic. Formal solution of the dynamo equations in a slab of gas, representing the galactic disk, produced regenerative modes, in which the azimuthal field is an even function of the distance z from the central plane of the slab. Inclusion of the "eddy diffusivity" of the turbulence in the dissipation terms of the dynamo equations gives growth times of 10^8 years. Hence it is suggested that the magnetic field of the Galaxy is generated by the combination of nonuniform rotation and turbulence in the gaseous disk. The dynamo principle responsible for the magnetic field of Earth and of the Sun appears to be operative on a galactic scale, too. (auth)

9137 DIFFERENCES IN STELLAR CONTENT OF THE NUCLEI OF GALAXIES WITH MEASURED ROTATION CURVES. Saslaw, William C. (Univ. of California, Berkeley). Astrophys. J.; 163: 249-54(15 Jan 1971).

New observations show there is little correlation between the position of a galaxy on the dynamical $R-\omega$ sequence and the stellar content of its central regions. This suggests that different amounts of evolution from similar initial conditions are insufficient to account for the variety of dynamical and stellar properties among Sb and Sc galaxies. (auth)

9138 PREFERENCE OF TRAILING SPIRAL WAVES. Contopoulos, G. (Univ. of Chicago). Astrophys. J.; 163: 181-93 (1 Jan 1971).

A linear analysis gives the response of a disk galaxy to an imposed slightly growing spiral field near the inner Lindblad resonance. The response is trailing in both cases of a trailing or a leading imposed spiral field. (auth)

9139 FAINT OUTER REGIONS OF ELLIPTICAL GALAXIES. Arp, Halton (Carnegie Institution of Washington, D. C.); Bertola, Francesco. Astrophys. J.; 163: 195-201(1 Jan 1971).

Photographs to faint limiting magnitudes have enabled isophotes of five elliptical galaxies to be traced to greater distances than previously. The giant ellipticals NGC 383, NGC 541, NGC 1275, NGC 4261, and NGC 4486 were found to extend to diameters of several tenths of a megaparsec. Somewhat smaller ellipticals in these groups have similar gradients, but spirals are sharply bounded. The faint luminosity in the outer regions is interpreted as being due to stars, probably dwarf stars predominantly. Since the density of matter in these regions is so low, it is concluded the stars were more likely to have been ejected from the center than condensed in situ. The results further indicate that in many clusters the outer regions of galaxies adjoin and that to some extent the cluster galaxies are imbedded in a common medium. With masses of E galaxies generally increased by an order of magnitude, the Oort limit of matter observable in galaxies should be raised toward a higher mean density for the average of observable space. The luminosities, masses, and M/L ratios of the individual galaxies all increase when the usual computations are corrected for the presence of the outer regions. This correction then reduces the well-known discrepancy between M/L ratios for the average galaxy derived by applying the virial theorem to clusters of galaxies and the M/L ratios derived from individual galaxies from rotation curves or velocity dispersions. (auth)

9140 SPECTRAL OBSERVATIONS OF MARKARYAN GALAXIES WITH ULTRAVIOLET CONTINUUM. II. Weedman, D. W. (Texas Univ., Austin. Byurakan Astrophysical Observatory, USSR); Khachikyan, E. E. Astrophysics (Engl. Transl.); 5: 51-9(Spring 1969).

Translated from Astrofizika; 5: 113-22(1969).

Preliminary results are reported of spectroscopic observations of galaxies in the Markaryan list. Results for 17 of these galaxies were given in a previous paper (1968). The remaining 18 galaxies are now described. About 80% of the galaxies have emission lines in their spectra. Observations indicate the presence of hydrogen emission lines and of the forbidden lines of helium, oxygen, neon, sulfur, and other elements in the spectra of many of these galaxies. Two new Seyfert-type galaxies have been found. It follows that among the galaxies which were investigated there are four galaxies whose spectral characteristics show that they belong to the Seyfert type (Markaryan 9, 10, 34, and 42). For three of them (9, 10, and 34) the absolute magnitude and the redshift are greater than those for known Seyfert galaxies, and they are similar to quasars. Arguments in favor of cosmogonic activity in the nuclei of many of the Markaryan galaxies and their nonthermal emission are presented. Both the redshift and the absolute magnitude of the galaxies lie within very broad limits ($0.002 < z \leq 0.050$; $-22 < M < -13$). The spectra of the Markaryan galaxies exhibit a considerable variety. An attempt is made to classify them into four main groups. (auth)

9141 THE ANDROMEDA GALAXY M 31. I. A PRELIMINARY MODEL. Einasto, Ya. I. (Struve Astrophysical Observatory, Tartu-Tyravere, USSR). Astrophysics (Engl. Transl.); 5: 67-80(Spring 1969).

Translated from Astrofizika; 5: 137-59(1969).

Published photographic and photoelectric data on the luminosity distribution along the major and minor axes of M 31 were used to develop a four-component model of the galaxy. The masses of the components were determined from the angular velocity derived from optical and radio data, from stellar velocity dispersion, and from spectral determinations of the stellar composition of the center of the galaxy. It was found that the circular velocity reaches a maximum value of 380 km/sec at a distance of only 4' from the center, where the rotational velocity of stars in the spheroidal component in this region is only 125 km/sec. This large displacement of the velocity centroid is due to the large spread in the velocities and the large radial gradient of the density of the component. The dynamic mass–luminosity ratio of 17.3 is in good agreement with the spectroscopic result. The mass of M 31 was found to be 200×10^9 solar masses. The higher values found by other workers are, however, uncorrected for the finite size of the galaxy. The interstellar hydrogen shows local deviations from circular motion. (auth)

9142 PROBLEMS IN GALACTIC SPIRAL STRUCTURE: AN ACCOUNT OF A SPIRAL WORKSHOP. Simonson III, S. Christian (Univ. of Maryland, College Park). Astron. Astrophys.; 9: 163-74(Nov 1970).

A "Spiral Workshop" was held at the University of Maryland on February 16 and 17, 1970, to discuss problems of the spiral structure of the Galaxy arising from the I.A.U. Symposium No. 38 at Basel in August, 1969. After reviewing the methods of obtaining information about the spiral structure and assessing the current state of the observational data, the group discussed the principles and techniques by which the spiral structure may be determined. To illustrate the problems encountered in tracing spiral structure, the differences between the map by Kerr and the map by Weaver were examined. Some recent attempts at constructing maps were described that used the theory of spiral density waves to progress beyond simple rotation for the galactic velocity field. Other aspects of the theory of spiral density waves came under discussion. Taking note of the irregularities observed in the Galaxy and considering the present knowledge of the state of the interstellar medium, participants raised questions about the extent to which this theory could be applied under the conditions existing in the Galaxy. Theoretical problems were explored concerning mechanisms for originating the waves, instabilities to which they were subject, and the limitations of the theory in its present form. (auth)

9143 SOME APPLICATIONS OF AN IMAGE TUBE TO OBSERVATIONS OF FAINT EXTRAGALACTIC H II REGIONS. Deharveng, J. M.; Pellet, A. (Observatoire, Marseille). Astron. Astrophys.; 9: 181-8(Nov 1970).

Details are given on the use of an RCA C 33011 two-stage cascaded image tube for observation of extended and faint sources by photography with narrow-band interference filters, interferometry and spectrography. Emphasis is placed on preserving contrast and signal-to-noise ratio while minimizing the exposure time. These technics were applied to a study of ionized gas in galaxies in the Hα and [N II] lines. An evaluation of electron density was made over the strange arm of NGC 4258, and the Hα filamentary structure in M 82 which was found to extend up to 4.9 kpc from the center. Based on the Hα to [N II] ratio the electron temperature was estimated to be 7300°K in the extended region of emission in M 33. From this value and from the measured Hα surface brightness, an emission measure of 55 cm^{-6} pc was deduced. Similar physical conditions seem to exist in the disk of M 101. (auth)

9144 THE GALACTIC HALO IN THE DIRECTION TO THE NORTHERN GALACTIC POLE (SA 57). Becker, W. (Univ., Basel). Astron. Astrophys.; 9: 204-8(Nov 1970). (In German).

It is shown that it is possible to identify faint halo stars in a field of high galactic latitude by means of a two-color photometry (without U) if the brighter stars have been treated by a three-color photometry before. The method assumes a rather sharp limitation of the disc, beyond which there are only halo-objects. For SA 57 this limiting distance is determined by the disc stars, treated by a three color photometry. In the color–magnitude diagram it appears as a straight line confining disc stars to its right. The linear relation between color-index and absolute magnitude yields the latter for the halo stars. The density functions of SA 57 and 51 for the interval $4.0 \leq M\ (G) \leq 6.9$ are given. They are put together with the density functions of the three-color photometry. A strong flattening of the halo

XUM

is suggested. The flattening was proved by the density gradients calculated on the basis of much larger numbers of stars in the fields observed by use of the 48-inch Schmidt telescope. (auth)

9145 . GALACTIC ROTATION FROM H II REGIONS. Georgelin, Y. P.; Georgelin, Y. M. (Observatoire de Marseille). Astron. Astrophys.; 8: 117-22(Sep 1970). (In French).

A model of the galactic rotation curve was derived from radial velocities and spectrophotometric distances of H II regions; it was in very good agreement with the Schmidt curve. From H II regions the solar motion constants were found to be: $U_0 = -7.5 \pm 1$ km s^{-1} and $V_0 = +13.1 \pm 1.5$ km s^{-1}. The component V_0 was very similar to the value obtained from OB stars and Cepheids. No significant expansion term was found. It was determined that $A = 14.3$ km s^{-1} kpc^{-1} and $\alpha = -0.9$ km s^{-1} kpc^{-2}. The kinematic data deduced from the interstellar matter (ionized hydrogen) and from the young stars (OB and Cepheids) are identical, which can be interpreted as due to the predominance of gravitational forces. (auth)

9146 DISTRIBUTION OF ATOMIC HYDROGEN IN CARINA. Garzoli, Silvia L. (Instituto Argentino de Radioastronomia, Buenos Aires). Astron. Astrophys.; 8: 7-25(Sep 1970).

A survey of the distribution of the intensity of the 21-cm line of atomic hydrogen in the region $270° \leq l \leq 310°$, $-3° \leq b \leq 2°$, was made with the 30-meter radiotelescope and multichannel receiver of the Radio Astronomy Station of the Instituto Argentino de Radioastronomía and the Department of Terrestrial Magnetism of the Carnegie Institution of Washington. The analysis of the data included the identification of hydrogen concentrations and the study of their interconnection, which gives rise to the different structures that produce the spiral appearance of the Galaxy. Structures were found with radial velocities forbidden by Schmidt's mass model of the Galaxy; some estimates of the errors which may incur by the use of this model in determining distances are made. The distribution of local hydrogen and that of the hydrogen in the Carina and Sagittarius arms was studied. An attempt was made to fit these arms to those in the Eastern galactic hemisphere. Evidence was found that Carina does not go through the Sun but rather seems to join Sagittarius. The bending of the galactic plane towards the Magellanic Clouds was clearly detected. Concentrations as far as 1 kpc below $b = 0°$ were found. The results were compared with those of optical astronomy. Regions of low density of stars and of gas were found near the Carina edge which are real and not an effect of local obscuration; however, the stellar and gaseous "holes" are shifted in longitude. (auth)

9147 3C 390.3: AN N SYSTEM WITH TWO EMISSION REDSHIFTS. Burbidge, E. M.; Burbidge, G. R. (Univ. of California, San Diego). Astrophys. J.; 163: L21-4(1 Jan 1971).

It is shown that the N galaxy 3C 390.3 has two emission redshifts, 0.056 for the strong emission cores of the Balmer lines and for the forbidden lines, and 0.042 for a second set of emission peaks in the Balmer lines. It is suggested that the larger redshift is that of a central mass of gas excited by a powerful nonthermal source and that the smaller redshift arises in a mass of gas being ejected with a line-of-sight velocity component of about 4100 km sec^{-1}. Other emission-line objects in which similar phenomena are seen are briefly discussed. (auth)

9148 MAFFEI 1: A NEW MASSIVE MEMBER OF THE LOCAL GROUP. Spinrad, Hyron (Univ. of California, Berkeley); Sargent, W. L. W.; Oke, J. B.; (and others). Astrophys. J.; 163: L25-31(1 Jan 1971).

An extensive collection of observational data is presented which indicates that the recently discovered infrared object Maffei 1 is a highly reddened giant elliptical galaxy at a distance of about 1 Mpc, and thus is probably a new massive member of the Local Group. (auth)

9149 MASS DISTRIBUTION AND A STELLAR POPULATION MODEL IN THE SPIRAL GALAXY M 33. Boulesteix, J.; Monnet, G. (Observatoire, Marseille). Astron. Astrophys.; 9: 350-5 (Dec 1970). (In French).

The kinematical properties of the galaxy M33 are now well known, and the rotation curve obtained from interferometric optical studies and radio observations leads to a precise calculation of the mass density, total mass, and mass–luminosity ratio at every point. The method used here assumes that the equidensity surfaces are flattened and homothetic ellipsoids. From the study of M33, several results are obtained. The mass contained within 50′ from the center is between 1.5 and 2.10^{10} $M_\odot$. The mass luminosity ratio increases from 2.5 (at 5′ from the center) to about 20 (at 40′). M33 consists of an old population: H I mass is at most 10% of the total mass, and other mass is 95% of the old population and 5% of young population (eccentricity 0.01). It seems also that this ratio is larger in external regions. (auth)

9150 INFLUENCE OF THE ACCURACY OF STELLAR DISTANCES ON THE ESTIMATIONS OF KINEMATICAL PARAMETERS FROM RADIAL VELOCITIES. Creze, M. (Observatoire, Paris). Astron. Astrophys.; 9: 405-9(Dec 1970).

The inaccuracy of the stellar distances may falsify all the estimates of the parameters of solar motion and galactic rotation from radial velocities. It is shown that, if the distances are affected by random errors, the constant A is underestimated in any least-squares solution from radial velocities. The underestimation is considered to be at least 1 km s^{-1} kpc^{-1} for samples of early-type stars with spectroscopic parallaxes, which have an important weight in the value $A = 15$ km s^{-1} kpc^{-1}. (auth)

9151 ESTIMATION OF THE PARAMETERS OF GALACTIC ROTATION AND SOLAR MOTION WITH RESPECT TO POPULATION I CEPHEIDS. Creze, M. (Observatoire, Paris). Astron. Astrophys.; 9: 410-19(Dec 1970).

A number of kinematic studies from Population-I Cepheids were examined. The inaccuracy of the stellar distances is shown to be largely responsible for the discrepancies between the various estimates, as well as for anomalous variations of the residuals of the least-squares solutions. The validity of the linear expansion used for analyzing the radial velocities is discussed. Using both proper motions and radial velocities, new estimates of the parameters of solar motion and galactic rotation are proposed, which are corrected for the effects of distance errors: $A = 15.5 \pm 1.5$ km s^{-1} kpc^{-1}; $U_0 = -9.5 \pm 1.5$ km s^{-1}; $v_0 = 13.7 \pm 1.2$ km s^{-1}. (auth)

Cosmology

Refer also to abstracts 9614, 9877, and 9881.

9152 EQUIVALENCE PRINCIPLE AND GEODESIC DE BROGLIE WAVES. THE ROLE OF COSMOLOGICAL ZERO-POINT FLUCTUATION OF METRIC IN THE GENERATION OF MASS SPECTRUM AND IN THE SLOWED-DOWN EXPANSION OF THE UNIVERSE. Hokkyo, Noboru (Hitachi Central Research Lab., Ozenji, Japan). Progr. Theor. Phys. (Kyoto); 44: 801-7 (Sep 1970).

An idea is proposed to construct the geodesic structure of space–time from quantized world lines of long-lived massive elementary particles (Nambu particles). It is postulated that quantized orbits of Nambu particles are indistinguishable from one another in the gravitational field so that the principle of weak equivalence holds for Nambu particles. Assuming that the geodesic postulate (stating that a world line is a geodesic) is valid for quantized world lines of Nambu particles, one arrives at a picture of wavelike geodesic tubes of radius $\sim 10^{-33}$ cm and wavelength $\sim 10^{-13}$ cm that can interfere with themselves. It is suggested that the wavelike geodesic is a consequence of the cosmological zero-point fluctuation of the quantized metric and that the Nambu's mass spectrum is a manifestation of the quantized fluctuating metric. The fluctuating metric is, however, made to be undetectable by Nambu particles owing to the gravitational Bohm–Aharonov effect, which makes the wave-mechanical diffraction of quantized geodesic lines disappear in regions surrounding the quantized fluctuation. The undetectability is also explained in terms of local compensation of the gravitational potential associated with the fluctuating metric by the "rest energy of the wavelike goedesic." It is conjectured that the uncompensated gravitational interaction between vibrating geodesics is responsible for the slowed-down expansion of the Universe during the period corresponding to the redshift $z = 1.95$ of the absorption lines in quasar spectra. (auth)

9153 REVERSIBLE AND IRREVERSIBLE TRANSFORMATIONS IN BLACK-HOLE PHYSICS. Christodoulou, Demetrios (Princeton Univ., N. J.). Phys. Rev. Lett.; 25: 1596-7(30 Nov 1970).

The concepts of irreducible mass and of reversible and irreversible transformations in black holes are introduced, leading to the formula $E^2 = m_{ir}^2 + (L^2/4m_{ir}^2) + p^2$ for a black hole of linear momentum p and angular momentum L. (auth)

9154 EINSTEIN–BOHR BOX EXPERIMENT. Treder, H.-J. Monatsber, Deut. Akad. Wiss. Berlin; 12: 180-4(1970). (In German).

Einstein's paradox and Bohr's proposal for its solution are discussed critically. (J.S.R.)

9155 NONSPHERICAL GRAVITATIONAL COLLAPSE: DOES IT PRODUCE BLACK HOLES? Thorne, Kip S. (California Inst. of Tech., Pasadena). Comments Astrophys. Space Phys.; 11: 191-6(Sep-Oct 1970).

Indirect methods must be used to learn about highly deformed collapse. Some of the recent results obtained by indirect studies

are described, along with some of the conjectures suggested by those results. A brief review is given on the nature of a black hole and the associated concept of an event horizon. (W.D.M.)

9156 HOW NOW, NO COSMOLOGICAL HELIUM. Fowler, William A. Comments Astrophys. Space Phys.; 2: 134-7(Jul-Aug 1970).

An interesting aspect of the calculation made by Wagoner, Fowler, and Hoyle (Astrophys. J., 148: 3(1967)) is pointed out, which showed little or no helium resulted from "big-bang" nucleosynthesis if either neutrinos or antineutrinos were taken to be sufficiently degenerate. This is in contrast with the canonical Friedmann cosmology with nondegenerate neutrinos, which predicts a universal helium abundance, Y ~ 0.22 to 0.27 by mass. (W.D.M.)

9157 GRAVITATIONAL INSTABILITY OF A TWO-COMPONENT FLUID: MATTER AND RADIATION. Guyot, M. (Faculte des Sciences, Nice); Zeldovic, Ya. B. Astron. Astrophys.; 9: 227-31(Nov 1970).

The gravitational instability of a two-component fluid (radiation and zero pressure matter) in the expanding Universe was investigated. The case of an open Universe with comparable density of radiation and matter during the growth of perturbations was studied. The gravitational action of radiation on the universal expansion weakens the growth of perturbations. In a particular case, their increase from the moment of recombination up to the present day amounts to 8 instead of $\frac{3}{5}(Z_{re} + 1) = 800$ in a matter-dominated flat Universe, or $\frac{3}{5}\Omega_0 Z_{re} = 52$ in a matter-dominated open Universe with the same dimensionless density $\Omega_0 = 0.025$. (auth)

Planetary Phenomena

Refer also to abstracts 8965, 8966, 9129, and 9355.

9158 POLARIZATION OF THE DECAMETRIC RADIATION FROM JUPITER. Kennedy, David James. Gainesville, Fla.; Univ. of Florida (1969). 141p. University Microfilms Order No. 70-14, 889.

Thesis.

Measurements of the two circular polarization components of the decametric radiation from Jupiter were made at the University of Florida Radio Observatory and at an allied observatory of the University of Chile. Fixed-frequency observations were made at 10, 16, and 22 MHz, with 60,755 bursts analyzed for the years 1961–68. The time constant of the polarimeter systems used was approximately 0.1 sec. (TSS) (Diss. Abstr. Int., B)

9159 MOON: GLOBAL ELECTROMAGNETIC SOUNDING USING THE SOLAR WIND. Sonett, C. P.; Dyal, P. (Ames Research Center, Moffett Field, Calif.). Comments Astrophys. Space Phys.; 11: 184-90(Sep-Oct 1970).

The results discussed give an indication of the overall global electrical decay time of the Moon, as well as to suggest that a steep conductivity gradient exists in the outer layers. These very early results show that the eventual aim of electrical probing to the center of the Moon seems a well-founded possibility. (W.D.M.)

9160 OBSERVATIONS OF JUPITER AT 11.13 cm. Gerard, E. Astron. Astrophys.; 8: 181-8(Oct 1970).

The total flux density of Jupiter was measured at 2695 MHz from December 1967 to August 1968 using the Nançay radiotelescope; appreciable changes were observed (the most remarkable one near opposition during a sharp decrease of solar activity) and show a correlation with solar activity as measured by the 10.7-cm solar flux. Such a correlation was first suggested by Roberts and Huguenin (1963), however, present results contradict these authors' conclusion that only the polarized component varies. No variation was found within error limits in the "radio diameters" in both the vertical and horizontal polarizations. On the other hand the results support the suggestion by Komesaroff and McCulloch (1967) of a secular decrease of the linear polarization at 11 cm. The asymmetrical beaming of the nonthermal radiation with System III longitude (1957.0) appears to be partly due to a strengthening of the vertical flux density from $L_{III} = 90°$ to $L_{III} = 220°$ combined with a weakening of the horizontal flux density from $L_{III} = 110°$ to L_{III} 250°. A possible explanation is suggested in terms of a magnetic "anomaly" near $L_{III} = 160°$. (auth)

Atomic and Molecular Physics

Refer also to abstracts 9978 and 10015.

Atomic, Electron, Ion, and Molecular Beams and Their Reactions

Refer also to abstract 8569.

9161 (LA-tr-70-24) ENERGY DEPENDENCE OF THE MEAN ENERGY PER ION PAIR AT LOW ELECTRON ENERGIES. Booz, J.; Ebert, H. G. Translated for Los Alamos Scientific Lab., N. Mex., from Biophysik; 2: 226-32(1965). 10p. Dep. NTIS.

An abstract of this paper, prepared from the original language, appeared as NSA 19: 39375. (M.O.W.)

9162 (SC-RR-70-788) RANGE-ENERGY RELATIONS FOR HELIUM IONS AND PROTONS IN N_2, O_2, AND AIR (0.2 TO 2.0 MeV). Langley, Robert A. (Sandia Labs., Albuquerque, N. Mex.). Nov 1970. 22p. Dep. NTIS.

The ionization extrapolated ranges of H^+ and He^{2+} in N_2, O_2, and air were measured from 200 keV to 2.0 MeV with an accuracy of ±1%. A magnetically analyzed beam of ions was brought through a differential pumping system into a gas-stopping cell. A single-grid ionization chamber, movable parallel to the beam axis, was used to obtain the data necessary to plot a Bragg curve. The observed range-energy relations are compared with previous data where possible. (auth)

9163 MULTIPLE SCATTERING OF PROTONS AND NITROGEN IONS ON COPPER. Sakisaka, Masakatsu (Kyoto Univ.); Yamazaki, Tetsuo; Tekasaki, Minoru; Nakamoto, Shunsuke. J. Phys. Soc. Jap.; 29: 1551-6(Dec 1970).

Multiple scattering of protons (0.407, 0.851 and 1.45 MeV) and nitrogen ions (1.28 and 2.29 MeV) on copper was studied. The observed angular distributions are compared with Molière's theory and some deviations are found. However, these can be diminished by introducing the effective atomic number, Z_{eff}, of incident ions. The appropriate Z_{eff}'s are estimated as 0.87, 0.90 and 0.94 for the protons, respectively. The values 5.2 and 6.2 are obtained for the respective nitrogen ions. The effective atomic number is attributed to the electron screening of slow ions during the collision process. (auth)

9164 X-RAY PRODUCTION IN ION-ATOM COLLISIONS: THE INFLUENCE OF LEVEL MATCHING. Kavanagh, T. M.; (Univ. of California, Livermore); Cunningham, M. E.; Der, R. C.; (and others). Phys. Rev. Lett.; 25: 1473-5(23 Nov 1970).

Cross sections for L x-ray production in Cu were measured for collisions between Cu and a wide range of heavy ions and atoms for collision energies in the range 40 keV to 1.1 MeV. Two sets of experimental results are presented: one from bombardment of a Cu target by ions of various atomic numbers and one from bombardment of solid targets of various atomic numbers by Cu ions. In both cases, cross sections show a strong cyclic dependence on the Z of the collision partner. Comparison of the two sets of results indicates a lack of reciprocity in the roles of target and projectile. (A.G.W.)

9165 CALCULATION OF A PLANE ELECTRON BEAM IN INTERSECTED FIELDS BY MONTE CARLO METHOD. Romanov, P. V.; Roshal, A. S.; Galimullin, V. N. Izv. Vyssh. Ucheb. Zaved., Radiofiz.; 13: 1096-1105(1970). (In Russian).

A calculation (by Monte Carlo method) is given of nonlinear processes in a quasi-periodic electron beam propagating in an infinite plane gap between the cathode and anode structure. The method is very accurate and gives a quick solution. Some results of calculations are presented. (auth)

9166 RANGE-ENERGY RELATION IN HYDROGEN. Garbincius, P. H. (Manhattan Coll., Bronx, N. Y.); Hyman, L. G. Phys. Rev., A; 2: 1834-8(Nov 1970).

The mean excitation potential of liquid hydrogen was determined to be 20.4 ± 0.9 eV. This value was obtained from measurement in a hydrogen bubble chamber of (i) the range of monoenergetic muons and (ii) the range and momentum of protons that stop in the chamber. (auth)

9167 ELECTRON ENERGY LOSS SPECTRA OF GRAPHITE SINGLE CRYSTALS AND EVAPORATED CARBON FILMS IN THE RANGE 0.02 TO 0.4 eV. Geiger, J.; Katterwe, H.; Schroeder, B. (Technische Univ., Berlin). Z. Phys.; 241: 45-54(1971). (In German).

High-resolution electron energy-loss spectra of graphite and of evaporated carbon films were measured in the energy-loss range between 20 and 400 meV. The primary energy was 25 keV, the energy resolution between 4 and 7 meV. The energy-loss spectrum of graphite is characterized by a strong continuum due to the free charge carriers. Two weak and broad bands at 45 and 128 meV

XUM

superimposed on this continuum are probably due to electronic excitations. In the energy-loss spectrum of evaporated carbon films phonon creations predominate below 160 meV, where several well-separated peaks are observed. An energy loss at 370 meV is caused by a longitudinal band transition. (auth)

Atomic and Molecular Properties

Refer also to abstracts 9110, 9117, 9598, and 9832.

9168 (ORNL-4614) EIGENVALUES, RADIAL EXPECTATION VALUES, AND POTENTIALS FOR FREE ATOMS FROM Z = 2 TO 126 AS CALCULATED FROM RELATIVISTIC HARTREE-FOCK-SLATER ATOMIC WAVE FUNCTIONS. Carlson, T. A.; Lu, C. C.; Tucker, T. C.; Nestor, C. W. Jr.; Malik, F. B. (Oak Ridge National Lab., Tenn.). Dec 1970. Contract W-7405-eng-26. 267p. Dep. NTIS.

Relativistic Hartree-Fock-Slater wave functions have been calculated for all elements from Z = 2 to 126. From these wave functions, the eigenvalues and expectation values of r, $1/r$, $1/r^3$, r^2, and r^4 for each orbital, the total energy of the atom, and the total potential as a function of radius were obtained. The potential is broken down into contributions from the nucleus, the electrons, and exchange. The results are presented in tables. (auth)

9169 DETERMINATION OF THE ELECTRON BINDING ENERGY IN THE NEGATIVE ION He^- BY DETACHING THE ELECTRON WITH AN ELECTRIC FIELD. Oparin, V. A.; Il'in, R. N.; Serenkov, I. T.; Solov'ev, E. S.; Fedorenko, N. V. (Ioffe Inst. of Physics and Tech., Leningrad). JETP Lett. (USSR) (Engl. Transl.); 12: 162-5(5 Sep 1970).

Translated from Zh. Eksp. Teor. Fiz., Pis'ma Red.; 12: 237-42(5 Sep 1970).

A detailed study of the disintegration of the He^- ion in an electric field indicates that two Stark states of the ion $1s2s2p\ ^4P^0$ are present in the beam entering the field. The average binding energy of the electron of the He^- ion in the two states was found to be 0.076 ± 0.002 eV. (A.G.W.)

9170 POPULATION INVERSION IN He TRANSITIONS. Gatzke, J. Monatsber. Deut. Akad. Wiss. Berlin; 12: 171-3(1970). (In German).

In a helium discharge, the changes of the population density as a function of the principal quantum number were investigated in four transitions by measurement of atomic line absorption. The percent absorption values A for the four transitions are tabulated. Negative absorption values in transitions with medium principal quantum numbers are noteworthy. The occurrence of inversions in the level populations in He plasma is conceivable although exact calculations are not possible, principally because of the unsatisfactory knowledge of the collision cross section for the elementary processes. (J.S.R.)

9171 MEASUREMENT OF THE STARK BROADENING OF THE RESONANCE LINES OF NEUTRAL ARGON AND NEON. Moo-Young, G. A.; Greig, J. R.; Griem, Hans R. (Univ. of Maryland, College Park). Phys. Rev., A; 2: 1617-23(Nov 1970).

The product of the Stark width and the oscillator strength for the resonance lines of neutral argon and neon was measured from a comparison of the Stark-broadened emission profiles of these lines with those of Lyman α and Lyman β, all lines saturating at the blackbody level. The Stark-broadening (damping) constant for each of the lines is found from this product, using known values of their respective oscillator strengths. The lines investigated and their Stark widths for an electron density of 10^{16} cm^{-3} are Ar I 1048 Å, $(4.6 \pm 0.7) \times 10^{-4}$ Å; Ar I 1067 Å, $(5.1 \pm 0.7) \times 10^{-4}$ Å; Ne I 736 Å, $(1.2 \pm 0.5) \times 10^{-4}$ Å; Ne I 744 Å, $(1.3 \pm 1.0) \times 10^{-4}$ Å. Further, comparison of the experimental Stark profiles of the Lyman line indicates that their current theoretical line shapes agree with each other to better than ~±10%. The radiation source employed was an electromagnetically driven T tube filled with the appropriate gas mixtures of argon-hydrogen and neon-hydrogen. Electron densities and temperatures were determined from the measured half-widths of Hβ and the relative intensities of selected visible lines, respectively. (auth)

9172 EXCITATION TEMPERATURE FUNCTIONS OF SOME SPECTRUM LINES OF He, Ne, Ar, Kr, AND Xe. Petrakiev, Asparuch; Voeroes, Tibor (Univ., Sofia). Beitr. Plasmaphys.; 9: 285-91(1969).

The excitation temperature functions of 19 spectral lines of 5 rare gases (He, Ne, Ar, Kr, and Xe) were calculated according to the method given by Fowler and Milne. The results make it possible to determine the radial plasma temperature distribution in the range of temperatures of 1.4×10^4 °K to 14×10^4 °K. Some examples are given for the determination of the plasma temperature distribution in space and time by using the Ar excitation temperature functions calculated. (auth)

9173 ENERGIES OF 1snl($l \geq 3$) CONFIGURATIONS IN ^{4}He I AS CALCULATED FROM POLARIZATION THEORY. Martin, William C. (National Bureau of Standards, Washington, D. C.). J. Res. Nat. Bur. Stand.; 74A: 699-702(Sep-Oct 1970).

The calculated singlet-triplet mean energies are given for all ^{4}He I configurations having $3 \leq l \leq n-1$ from 4f to 8k. Since only Stark-shifted transitions have been observed for such configurations with $l \geq 4$, the calculated positions are the most accurate available. The polarization energy (to the quadrupole approximation) for two-electron ions may be evaluated for higher nl or Z from the simple formulas. The calculated and observed positions of the 1snf configurations in ^{4}HeI and ^{7}LiH agree within the experimental uncertainties. (auth)

9174 POLARIZABILITY OF H^-. Jaswal, S. S.; Heinisch, H. L. Jr. (Univ. of Nebraska, Lincoln). Phys. Rev., A; 2: 2162-4 (Nov 1970).

The electric dipole polarizability of H^- is calculated by the variational method. The computed values of the polarizability corresponding to the unperturbed wave functions of the form $(e^{-\alpha r_1-\beta r_2} + e^{-\beta r_1-\alpha r_2})$ and $(e^{-\alpha r_1-\beta r_2} + e^{-\beta r_1-\alpha r_2})(1 + \gamma r_{12})$ are 73.6 and 19.5 $Å^3$, respectively. (auth)

9175 PADE-TYPE VARIATIONAL WAVE FUNCTION FOR H_2^+. Rothstein, Stuart M. (Brock Univ., St. Catharines, Ont.). J. Chem. Phys.; 54: 817-19(15 Jan 1971).

A two-parameter rational function for the $1s\sigma$ ground state of H_2^+ is reported. Energies as a function of internuclear separation for optimized values of the two parameters are tabulated. The energies are lower than results of other calculations with which they are compared and are the lowest of any published values known to the authors. (A.G.W.)

9176 VAN DER WAALS CONSTANTS FOR TWO He ATOMS AND THREE He ATOMS BY THE COUPLED HARTREE-FOCK APPROXIMATION. Kaneko, Shobu (Univ. of Tennessee, Knoxville. Tokyo Univ.). Contract AT(40-1)-2598. J. Chem. Phys.; 54: 819-20(15 Jan 1971).

Values for the constants for two and three He atoms obtained by direct numerical solution of the coupled Hartree-Fock equations are $C_{HeHe} = 1.38$ a.u. and $\nu_{HeHeHe} = 1.33$ a.u. These values coincide with values obtained by Dalgarno and Victor (Proc. Phys. Soc. (London), 90: 605 (1967)) using a variational procedure and analytic continuation. (A.G.W.)

9177 He AND H^- 1^1S AND 2^3S STATES COMPUTED FROM FEYNMAN PATH INTEGRALS IN IMAGINARY TIME. Lawande, S. V.; Jensen, C. A.; Sahlin, H. L. (Univ. of California, Livermore. Univ. of California, Davis). J. Chem. Phys.; 54: 445-52(15 Jan 1971).

Feynman path integrals in imaginary time are developed for systems of identical particles exhibiting exchange statistics. The Metropolis-Teller Monte Carlo procedure is applied to the integrals appropriate to H^- and He 1^1S and 2^3S states. (auth)

9178 DICKINSON ENERGY OF H_2^+. Weinhold, Frank (Stanford Univ., Calif.). J. Chem. Phys.; 54: 530-2(15 Jan 1971).

Dickinson's function for H_2^+ is recalculated for the $1s\sigma_g$ and $2p\sigma_u$ states at nuclear separations up to 20 a.u. Although inadequate near the ground-state minimum, the Dickinson function is very good for larger separations and describes quite accurately the shallow potential minimum ($D_e \approx 0.015$ eV, $R_e \approx 12.6$ a.u.) in the "repulsive" $2p\sigma_u$ excited state. (auth)

9179 O(2,1) ALGEBRA AND THE HYDROGEN ATOM. Dmitriev, V. F.; Rumer, Yu. B. (Novosibirsk State Univ., USSR). Teor. Mat. Fiz.; 5: 276-80(Nov 1970). (In Russian).

It is shown that the nonrelativistic as well as the relativistic hydrogen-atom problem can be formulated in terms of the noncompact algebra O(2,1) generators. Allowed values of the energy (the Balmer's and Sommerfeld's formulas, respectively) are determined by means of adequate choice of the basis for the O(2,1) algebra generators. (auth)

9180 MANY-BODY PERTURBATION CALCULATION OF THE INDIRECT SPIN-SPIN COUPLING CONSTANT IN HD MOLECULE. Dutta, C. M.; Dutta, N. C.; Das, T. P. (Univ. of Utah, Salt Lake City). Phys. Rev. Lett.; 25: 1695-9(21 Dec 1970).

The linked-cluster many-body perturbation approach was applied to the study of the indirect nuclear spin-spin coupling constant J_{HD} in the HD molecule. The complete set of states used consisted of the bound and continuum states of the H_2^+ molecular ion with an internuclear separation appropriate to the H_2 molecule. The calculated value of J_{HD} is +42.57 Hz in good agreement with the most recent experimental value of +42.7 ± 0.7 Hz. (auth)

9181 STARK-MIXING SIGNALS IN THE n = 3 TERM OF SINGLY IONIZED HELIUM. Baumann, M.; Eibofner, A. (Univ., Tuebingen, Ger.). Phys. Lett.; 33A: 409-10(14 Dec 1970).

Three crossings of Zeeman sublevels of the 3S, 3P, and 3D states of He^+ were detected both by a magnetic- and an electric-field modulation method. The crossing-field strengths are in good agreement with the calculated values. From these measurements, a Lamb shift of 4184.3 ± 7 MHz was deduced. (auth)

9182 HIGH-RESOLUTION OBSERVATIONS OF THE He II n = 3 TO 5, 3204-A TRANSITION EXCITED IN A HOLLOW CATHODE. Berry, H. G. (Univ. of Wisconsin, Madison). J. Opt. Soc. Amer.; 61: 123(Jan 1971).

The positions of the fine-structure components of the hollow-cathode-excited 3204-Å line of He^+ were obtained to approximately ±0.02 cm^{-1}. Their separations agree with quantum-electrodynamic predictions. The intensity distribution is similar to that of the previously studied hollow-cathode-excited n = 3–4 transition, indicating that the same excitation process is responsible for its population distribution. The total half-widths were 0.250, 0.020 cm^{-1}. (A.G.W.)

9183 ATOMIC $2s_{\frac{1}{2}}-1s_{\frac{1}{2}}$ TRANSITION. Boehm, F. (California Inst. of Tech., Pasadena). Contract AT(04-3)-63. Phys. Lett.; 33A: 417-18(14 Dec 1970).

The relativistic $2s_{\frac{1}{2}}-1s_{\frac{1}{2}}$ x-ray transition was observed in Tm. Its strength was found to be $(0.29 \pm 0.015) \times 10^{-3}$, with respect to the $2p_{\frac{3}{2}}-1s_{\frac{1}{2}}$ transition, in good agreement with the relativistic M1 rate calculated by Rosner and Bhalla. (auth)

9184 SEMI-EMPIRICAL CROSS SECTIONS AND RATES FOR EXCITATION AND IONIZATION OF HYDROGEN BY ELECTRON IMPACT. Golden, Lawrence B.; Sampson, Douglas H. (Pennsylvania State Univ., University Park). Astrophys. J.; 163: 405-10(5 Jan 1971).

A slightly different proposal is offered as an alternative to a method given previously by Sampson and Golden for the calculation of semiempirical cross sections and rates for excitation and ionization of hydrogen by electron impact. Numerical results obtained with the new formula are in better agreement with the experimental data for the $(n = 1) \rightarrow (n' = 2)$ excitation cross section. The rates based on the new proposal are smaller for $n \rightarrow n + 1$ transitions and larger for most other excitation transitions and for ionization than those based on the previous proposal. (auth)

9185 PERTURBED GENERALIZED EIGENVALUE EQUATION FOR THE HELIUM ATOM. Laughlin, C.; Amos, A. T. (Univ. of Nottingham, Eng.). Int. J. Quant. Chem.; 4: 613-23 (Nov 1970).

The Schrödinger equation for helium is written as a generalized eigenvalue equation and this is solved perturbatively for the ground state. The zero-order equation is taken to be that of a "six-dimensional hydrogen atom" since, in generalized eigenvalue form, this has a discrete spectrum. Although the zero-order wave function is very poor and gives only 86% of the energy the perturbation procedure is able to improve this to 99% through third order. (auth)

9186 THE EMISSION SPECTRUM OF CN^+. Lutz, Barry L. (National Research Council of Canada, Ottawa). Astrophys. J.; 163: 131-40(1 Jan 1971).

The emission spectrum of CN^+ between 2000 and 3600 Å was reinvestigated, and two new systems were found. One system is shown to be due to $^1\Pi-{}^1\Pi$ type bands, and the other system is assigned to a $^1\Sigma-{}^1\Pi$ transition connecting the $f^1\Sigma$ state of CN^+ to the lower state of the $^1\Pi-{}^1\Pi$ bands. The analysis of these bands shows the lowest vibrational level of the lower $^1\Pi$ state, designated b $^1\Pi$, lies 8141.51 cm^{-1} above v = 0 of a $^1\Sigma$, and has the following molecular constants: $B_e' = 1.6767$ cm^{-1}, $\omega_e' = 1688.35$ cm^{-1}. The upper $^1\Pi$ state, designated d $^1\Pi$, has irregular vibrational intervals and rapidly decreasing B_v' values. No values of B_e and ω_e could be determined. The v = 0 level of d $^1\Pi$ lies 45686.00 cm^{-1} above v = 0 to a $^1\Sigma$ and has a B′ value of 1.6018 cm^{-1}. The electron configurations of the known CN^+ states are discussed, as is the uncertainty in identifying the ground state. (auth)

9187 MEASUREMENT OF THE BROADENING OF SILICON LINES BY ELECTRONS AND HYDROGEN ATOMS. Meyer, J.; Beck, R. J. (Univ. of British Columbia, Vancouver). Astron. Astrophys.; 8: 93-7(Sep 1970).

The shift and width of two astrophysically important silicon lines were investigated, using a pressurized hydrogen plasma jet. The influence of Stark-effect interactions with free electrons and of van der Waals interactions with hydrogen atoms on the lines was determined, and the results are compared with theoretical values. The deviations from theory are discussed separately for the case of Stark-effect interactions and for that of van der Waals interactions. (auth)

Positronium, Muonium, and Mesic Atoms and Molecules

Refer also to abstracts 8269, 9606, and 9791.

9188 LAMB SHIFT IN MUONIC HELIUM IONS. Campani, E. (Univ., Pisa, Italy. Istituto Nazionale di Fisica Nucleare, Pisa, Italy). Lett. Nuovo Cim.; 4: 982-4(21 Nov 1970).

Results of calculations of the Lamb shift in the charged systems $(^3He,\mu)^+$ and $(^4He,\mu)^+$ are tabulated. The following contributions to the 2S–2P energy difference were taken into consideration: (1) fine structure and, for $(^3He,\mu)^+$, also hyperfine structure, (2) electron vacuum polarization potential to order α and α^2, and (3) finite size of the nucleus. The implications of these results with regard to Lamb-shift measurements are noted briefly. (A.G.W.)

Collision Phenomena

9189 (BNWL-SA–3482) ELECTRON DISTRIBUTIONS FROM HYDROGEN FOR 0.6, 1.0, AND 1.5 MeV HYDROGEN IONS. Wilson, W. E.; Toburen, L. H. (Battelle-Northwest, Richland, Wash. Pacific Northwest Lab.). 7 Oct 1970. Contract AT(45-1)-1830. 14p. (CONF-701018–1). Dep. NTIS.

From 23rd Gaseous Electronics Conference, Hartford, Conn.

Energy and angular distributions of electrons ejected in collisions of H_2^+ on H_2 were measured for incident-ion energies of 0.6, 1.0, and 1.5 MeV. A peak in the electron yield at an electron energy very near to that of an electron with velocity equal to that of the incident H_2^+ ion was observed at all angles and at all incident-ion energies. The fraction of the total yield contained in the peak increased for higher ion energies, but the overall yield decreased with increased ion energy. Comparison of these results with similar results for the electron yields from equal-velocity protons incident upon H_2 supports the suggestion, discussed in more detail in BNWL-SA-3498, that the two protons and the electron in the H_2^+ ion act independently in collisions. (A.G.W.)

9190 (BNWL-SA–3498) ANGULAR AND ENERGY DISTRIBUTIONS OF ELECTRONS FROM HYDROGEN ION BREAKUP. Wilson, W. E.; Toburen, L. H. (Battelle Northwest, Richland, Wash. Pacific Northwest Lab.). 16 Nov 1970. Contract AT (45-1)-1830. 14p. (CONF-701111–3). Dep. NTIS.

From Electron and Atomic Physics Division Meeting, Seattle, Wash.

Electron yields from collisions of 600-keV H_2^+ ions with H_2 are compared with electron yields from collisions of 300-keV protons with H_2. The obvious difference is a peak in electron yield at an energy near the energy that a free electron would have if it had the velocity of the incident ion. This peak is independent of angle. It was also found that the yields for H_2^+ and protons are in the ratio of 2 to 1. It is suggested that these results are consistent with an interaction model that assumes that the two protons and the electron of the H_2^+ ion act independently in the collision and that the electron yield is produced by the two protons incident upon the H_2 target plus an equal-velocity electron elastically scattered from the H_2 target molecule. (A.G.W.)

9191 (BNWL-SA–3631) ABSOLUTE CROSS SECTIONS, DIFFERENTIAL IN ENERGY AND ANGLE, FOR EJECTION OF ELECTRONS FROM XENON BY FAST PROTONS. Toburen, L. H. (Battelle-Northwest, Richland, Wash. Pacific Northwest Lab.). 13 Nov 1970. Contract AT(45-1)-1830. 18p. (CONF-701111–1). Dep. NTIS.

From Electron and Atomic Physics Division Meeting, Seattle, Wash.

Energy and angular distributions of electrons ejected from collisions of 0.3- to 2.0-MeV protons with xenon were measured. Plots of electron energy distribution as a function of emission angle for proton energies of 0.3, 1.0, and 2.0 MeV are basically similar. They show a maximum in the cross section for electron energies of a few eV, a peak corresponding to N-00 Auger emission at ~32 eV, and a group of M-Auger lines at ~520 eV. The cross sections decrease sharply for electron energies greater than the kinematic maximum energy transfer in a proton–electron collision. Cross sections for electron ejection into large emission angles were found to be larger than corresponding cross sections for a hydrogen target. Total ionization cross sections obtained by integrating the doubly differential cross sections with respect to emission angle and electron energy agree quite well with previous measurements. (A.G.W.)

9192 (ORO-2591-51) FORMATION OF EXCITED HYDROGEN ATOMS BY CHARGE TRANSFER AND DISSOCIATION. Progress Report No. 6, December 1, 1969–November 30, 1970. Thomas, E. W.; Edwards, J. L.; Ford, J. C.; Fitzwilson, R. L. (Georgia Inst. of Tech., Atlanta. School of Physics). 30 Nov 1970. Contract AT(40-1)-2591. 29p. Dep. NTIS.

Results of measurements of total cross sections for formation of fast excited hydrogen atoms by charge exchange in proton collisions with Ar, He, H_2, and N_2 at incident-proton energies of 75 to 350 keV are reported briefly. The results indicate that the available theoretical predictions of charge-exchange cross sections are in serious error. An investigation of formation of metastable hydrogen atoms by similar processes as a function of projectile scattering angle is also described. Results for collisions of 10-keV protons with He are included as an example. More detailed reports have been or will be published. Work not yet completed and future plans are summarized. (A.G.W.)

9193 (ORO-2591-52) FORMATION OF METASTABLE HYDROGEN ATOMS BY CHARGE TRANSFER. Fitzwilson, R. L.; Thomas, E. W. (Georgia Inst. of Tech., Atlanta). [1970]. 19p. Dep. NTIS.

Measurements are presented of the total cross sections for formation of metastable hydrogen atoms by charge transfer as protons traverse targets of helium, argon, nitrogen, and oxygen. Projectile energies range from 4 to 26 keV. An H^+ beam was directed into a cell containing the target gas and emerged into an evacuated region where the metastable-state content was determined. The H(2s) flux was monitored by electric field mixing of this state with the 2p level and detection of the resulting Lyman-α photon. The relative variation of cross section with projectile energy for targets of He and Ar is in agreement with previous work. For oxygen the cross section increases with energy from 4 to 10 keV and remains constant from 10 to 26 keV; for nitrogen the cross section increases monotonically with increasing energy. (auth)

9194 (SC-RR-70-721) ATOMIC SUBSHELL PHOTOIONIZATION CROSS SECTIONS FOR $2 \leq Z \leq 54$. McGuire, E. J. (Sandia Labs., Albuquerque, N. Mex.). Nov 1970. 79p. Dep. NTIS.

The subshell photoionization cross sections used in determining total photoionization cross sections are tabulated, along with model parameters and one-electron eigenvalues. (auth)

9195 (SC-RR-70-773) THE DIFFERENTIAL IONIZATION CROSS SECTION IN THE BORN APPROXIMATION. McGuire, E. J. (Sandia Labs., Albuquerque, N. Mex.). Dec 1970. 22p. Dep. NTIS.

An expression for the ionization cross section differential in secondary electron energy and angle and projectile angle is described. The results are obtained for the Born approximation, without exchange, and for a one-electron system. (auth)

9196 LOW-ENERGY POSITRON–HELIUM SCATTERING. Husain, D. (Dacca Univ.); Rahman, M. Progr. Theor. Phys. (Kyoto); 44: 808-9(Sep 1970).

The effect of correlation within the He atom on elastic positron–helium scattering was studied by calculating the phase shifts with a good uncorrelated and a simple correlated wave function. The partial-wave phase shifts obtained using the correlated wave function are less than those obtained using the uncorrelated wave function and are thus in better agreement with experiment. (A.G.W.)

9197 SEMICLASSICAL TREATMENT OF COLLISION-INDUCED DISSOCIATION. Johnson, L. L.; Roberts, R. E. (Indiana Univ., Bloomington). Chem. Phys. Lett.; 7: 480-2(1 Dec 1970).

Transition probabilities for the collision-induced dissociation reaction $A + BC \rightarrow A + B + C$ are calculated for a harmonic oscillator model using a semiclassical approximation. One of the unique features of this investigation is the appearance of quantum oscillations in the dissociation probability as a function of collision energy. The number of oscillations is correlated with the number of bound states of the BC molecule. (auth)

9198 EXTENSION OF THE WKB METHOD TO WAVE FUNCTIONS AND TRANSITION PROBABILITY AMPLITUDES (S-MATRIX) FOR INELASTIC OR REACTIVE COLLISIONS. Marcus, R. A. (Univ. of Illinois, Urbana). Chem. Phys. Lett.; 7: 525-32(1 Dec 1970).

A WKB-type method is used to calculate the wave function and S matrix for these collisions directly, instead of applying WKB to the customary infinite set of coupled differential equations. Action-angle variables and exact or approximate classical trajectories are used. (auth)

9199 PHOTOELECTRON SPECTRUM OF H_2. Asbrink, L. (Royal Inst. of Tech., Stockholm). Chem. Phys. Lett.; 7: 549-52 (1 Dec 1970).

The photoelectron spectrum of H_2 was measured with high resolution. Some individual rotational lines are completely resolved and it has been possible to measure some ionization energies with an accuracy of the same order of magnitude as in the best spectroscopic measurements. The rotational and vibrational constants show agreement with theoretical values. (auth)

9200 PHOTOELECTRON SPECTRA OF GROUND-STATE ATOMIC HYDROGEN, NITROGEN, AND OXYGEN. Jonathan, N. (Univ. of Southampton, Eng.); Morris, A.; Smith, D. J.; Ross, K. J. Chem. Phys. Lett.; 7: 497-9(1 Dec 1970).

The detection of gas-phase atomic hydrogen, nitrogen, and oxygen by photoelectron spectroscopy, using He I 21.21-eV radiation, is reported for the first time. The use of the technique in gas phase kinetic studies is suggested. (auth)

9201 EXCHANGE EXCITATION OF 2s STATE OF HYDROGEN IN CLOSE COLLISIONS WITH PROTONS. Caussorgues, C.; McCarroll, R.; Piarcentini, R. D.; Salin, A. (Observatorie de Paris, Meudon, France). J. Phys., B (London); 3: L138-41(Nov 1970).

The probability of exciting the 2s state of hydrogen in an exchange collision between a proton and a hydrogen atom was measured by Bayfield (1970). Calculations are carried out which give some evidence on the mechanism responsible for the experimental observations. (auth) (UK)

9202 TOTAL ELASTIC SCATTERING AND SPIN-CHANGE CROSS SECTIONS FOR COLLISIONS BETWEEN ALKALI ATOMS. Dickinson, H. O.; Rudge, M. R. H. (Queen's Univ., Belfast). J. Phys., B (London); 3: 1448-74(Nov 1970).

Semitheoretical potential energy curves for the $x\ ^1\Sigma$ and $x\ ^3\Sigma$ states of the diatomic alkalis Na_2, K_2, Rb_2, Cs_2, and RbCs are presented and compared with other estimates. Using these potential-energy functions calculations of the total elastic and spin-change cross sections were made. The cross sections are compared with experimental data and with the results of other theoretical calculations. (auth) (UK)

9203 RESONANCE CHARGE TRANSFER BETWEEN PROTONS AND EXCITED HYDROGEN ATOMS. III. QUANTAL EIGHT-STATE APPROXIMATION. Malaviya, V. (Queen's Univ., Belfast). J. Phys., B (London); 3: 1492-1500(Nov 1970).

Cross sections for symmetrical resonance and asymmetrical resonance charge transfer occurring between protons and hydrogen atoms in the second quantum level were calculated in the quantal two-state and eight-state approximations using the impact parameter formulation. Momentum transfer was taken into account by the method suggested by Cheshire (1967). As one goes from the quantal two-state approximation to the eight-state approximation, there is a considerable change in the results, especially at low energies of impact. The cross sections obtained by the quantal eight-state approximation and those obtained by Bates and Reid (1969) using a classical approximation are in remarkably close accord. (auth) (UK)

9204 BORN WAVE CROSS SECTION CALCULATIONS FOR THE EXCITATION OF $He(1^1S)$ TO $He(N^1L)$ BY HELIUM, NEON, ARGON, AND KRYPTON. Levy II, H. (Smithsonian Astrophysical Observatory, Cambridge, Mass. Harvard Coll. Observatory, Cambridge, Mass.). J. Phys., B (London); 3: 1501-9(Nov 1970).

Excitation cross sections for the processes $He(1^1S) + B \rightarrow He(N^1L) + B(\Sigma)$ for N = 2, 3, 4, 5 and L = S, P, D, and for target atoms B of helium, neon, argon, and krypton are calculated over the incident energy range 1.0 keV to 6.4 MeV, in the first Born approximation with the added approximation of closure used to describe excitation of the target. Scaled cross sections are also calculated for neon, argon, and krypton target atoms over the incident energy range 1.60 to 400.0 keV by use of velocity-dependent scaling factors determined from electron-loss data for the collision of hydrogen atoms. The tentative nature of such an application of the scaling factors is emphasized. (auth) (UK)

9205 COMMENTS ON THE PHOTOIONIZATION OF HELIUM. Bell, K. L.; Kingston, A. E. (Queen's Univ., Belfast). J. Phys., B (London); 3: 1433-6(Nov 1970).

The continuous oscillator strength $df/d\epsilon$ for photoionization of atomic helium is evaluated in the dipole length and velocity formulations using a 50-parameter correlated ground-state wave function together with both Hartree–Fock and polarized-orbitals free-state representations. The results are compared with those obtained from 6-parameter and 20-parameter correlated ground-state wave functions. It is found that if a particular free-state

representation is taken and df/dε calculated using increasingly more accurate ground-state wave functions, then the dipole velocity results tend much more rapidly to a constant value than do those obtained from the dipole length formula. However, if a particular ground-state wave function is chosen and the two continuous oscillator strengths calculated are compared with the Hartree–Fock and polarized-orbital free-state representations, then, at low photon energies, there is much better agreement between the two dipole length values than there is between the dipole velocity results. (auth) (UK)

9206 INVESTIGATION OF PHOTON–PHOTON ANGULAR CORRELATIONS IN ATOMIC MERCURY. Popp, M.; Schaefer, G.; Bodenstedt, E. (Univ., Bonn). Z. Phys.; 240: 71-92(1970).

By application of the time differential coincidence technique developed in nuclear spectroscopy, for the first time the angular correlation of light quanta of atomic decays was observed. The experiments were carried out with the $7\,^3S_1 - 6\,^3P_1 - 6\,^1S_0$ cascade of mercury excited by electron impact at energies of 50 eV. The two transitions of 4358 and 2536 Å were selected by interference filters and detected by photomultipliers. Time differential coincidence spectra were measured at the two angular positions $\theta = 90°$ and $\theta = 180°$. It was found that the excitation of the $7\,^3S_1$ state by the electron beam leads to no alignment. Therefore the usual $\gamma-\gamma$ angular correlation theory is applicable. Perturbations occur by static interaction with external magnetic fields and by free hyperfine interaction in the odd isotopes of mercury. The interaction frequencies of the free hyperfine interaction are in all cases too high to be resolved. Measurements were performed using mercury of natural abundances, with and without external magnetic fields. First of all the spin rotation in the magnetic field of the earth (690 mG) was observed, giving for the g factor of the $6\,^3P_1$ state g(Hg, 6^3P_1) = 1.35 ± 0.10. This value is in agreement with the more precise values determined by other techniques. Shielding of the earth's field gave a nearly unattenuated angular correlation, with an integral attenuation factor of $G_2 = 0.98 \pm 0.06$. The value of the angular correlation coefficient $A_2 = -0.188 \pm 0.009$ is in good agreement with the expected average value for the natural isotope mixture $A_2^{\text{theor}} = -0.196$. A third measurement in an external magnetic field of 5.6 G showed several complete spin rotations. A nice fit was possible by using the superposition of all six participating cascades in the hyperfine level schemes of the different isotopes. The theoretical anisotropies, g_F values, and intensities were inserted according to natural isotope abundances. (auth)

9207 FINE-STRUCTURE TRANSITIONS IN SODIUM-RARE-GAS COLLISIONS. Masnou-Seeuws, F. (Observatoire de Paris, Meudon, France). J. Phys., B (London); 3: 1437-47(Nov 1970).

An impact-parameter treatment is used to obtain cross sections for reactions such as $Na(^2P_{\frac{1}{2}}) + He \rightarrow Na(^2P_{\frac{3}{2}}) + He$. The coupled equations with and without rotational coupling are numerically solved. The relation between this work and the Landau–Zener formula is discussed. It is shown that rotational coupling cannot be neglected even at low velocities. The effect of repulsive exchange interaction is shown to be much more important at temperatures exceeding 400 K than Van der Waals interaction for Na–He collisions. At 400 K, the cross sections are 78 Å^2 for Na–He, 68 Å^2 for Na–Ne, and 62 Å^2 for Na–Ar. (auth) (UK)

9208 ELECTRON SCATTERING BY ATOMIC HYDROGEN USING A PSEUDO-STATE EXPANSION. III. EXCITATION OF 2s AND 2p STATES AT INTERMEDIATE ENERGIES. Burke, P. C.; Webb, T. G. (Queen's Univ., Belfast). J. Phys., B (London); 3: L131-4(Nov 1970).

Calculations of the 1s–2s and 1s–2p excitation cross sections in e^-–H scattering are reported. The results agree qualitatively with experiment over an energy range from close to the ionization threshold to 54.4 eV. (auth) (UK)

9209 UNIQUE DEFINITION OF THE QUASI-STATIONARY STATE FOR RESONANT PROCESSES. Lippmann, Bernard A. (New York Univ., N. Y.); O'Malley, Thomas F. Phys. Rev., A; 2: 2115-24(Nov 1970).

The quasistationary-state formalism for describing all manner of resonant collision processes and the diabatic states of molecules is made unique by defining the hitherto arbitrary quasistationary-state energy uniquely. The unique quasistationary-state energy E_r (together with its wave function) is defined by a pair of eigenvalue equations, which require that it remain unshifted by coupling to the continuum. Two alternate and equivalent definitions are also given, and the results are generalized first to the many-resonance case and secondly in the unusual direction of negative energies, where the quasistationary state produces a resonance among the discrete set of Rydberg levels. This last generalization is necessary for the principal present application of the states, i.e., to the diabatic states mediating molecular transitions, since the energy of these diabatic states moves freely between the continuum and the negative-energy region of the Rydberg states. (auth)

9210 VIBRATIONAL EXCITATION BY ELECTRON IMPACT IN O_2. Spence, D.; Schulz, G. J. (Yale Univ., New Haven). Phys. Rev., A; 2: 1802-11(Nov 1970).

The trapped-electron method is applied to a study of vibrational excitation by low-energy (0- to 1-eV) electrons on O_2. It is found that the dominant feature of the vibrational cross section consists of spikes spaced about 0.11 eV apart. This spacing is characteristic of the spacing of the vibrational levels of the O_2^- system, which serves as a compound state and which is also measured in the present study. It is found that one of the levels of the compound system (O_2^-) is coincident with the v = 3 level of O_2. When the measured anharmonicity of the O_2^- system (3 ± 0.5 mV per level) is taken into account, the spacing of the lowest vibrational states ($\nu' = 0 \rightarrow \nu' = 1$) of O_2^- becomes 132 mV, provided that the Pack–Phelps value of 0.43 eV is used for the electron affinity of O_2. The spacing of the $\nu' = 0 \rightarrow \nu' = 1$ vibrational states obtained in the present experiment is in excellent agreement with the values obtained by Raman spectroscopy of alkali halide crystals in which O_2^- is trapped (135 mV). The magnitudes of the cross sections of the spikes, integrated over the electron energy distribution, are given and the branching ratio for the decay of O_2^- states is discussed. (auth)

9211 ON THE APPLICATION OF FADDEEV EQUATIONS AND THE COULOMB t MATRIX TO ASYMPTOTIC ELECTRON CAPTURE IN HYDROGEN. Carpenter, C. P.; Tuan, T. F. (Univ. of Cincinnati). Phys. Rev., A; 3: 1811-21(Nov 1970).

Faddeev equations together with the Coulomb t matrix were used to determine the asymptotic amplitude for electron capture from neutral hydrogen by fast protons. The results show that in the high-energy limit the capture cross section should go down as ν^{-11}, where ν is the velocity of the incident proton. The capture amplitude is identical to Drisko's second-Born-approximation calculation except for a complex energy-dependent phase factor, which ultimately approaches unity with sufficiently high incident energy. The major contribution to the three-body capture amplitude can be shown to come from the on-energy-shell two-body t matrix, in agreement with general theorems concerning scattering from complex systems. At high incident energies, the on-energy-shell contribution to the capture amplitude (not the cross section) will decrease as ν^{-5}, while the off-energy-shell continuum contribution will decrease as ν^{-6}. The contributions from the sum of the infinite number of two-body bound-state poles can be shown to converge, and the sum can be explicitly performed at high enough incident energies in all except the forward direction. The bound-state contributions to the capture amplitude go down as ν^{-11}, which is much less than the continuum contributions. (auth)

9212 Na–Cs DIFFERENTIAL SPIN-EXCHANGE SCATTERING. Chang, C. K.; Walker, R. H. (Univ. of Houston). Phys. Rev., A; 2: 1821-3(Nov 1970).

Unpolarized and spin-exchange differential scattering cross sections of Na–Cs are calculated the authors' phenomenological potentials for $r < 14$ a.u. and the difference potential of Dalgarno and Rudge for $r \geq 14$ a.u. The calculated results are in good agreement with the experimental results. (auth)

9213 OPTICAL SPECTRA OBSERVED DURING ION–MOLECULE COLLISIONS USING LOW-ENERGY N_2^+ AND Ar^+ BEAMS. Liu, Chelcie; Broida, H. P. (Univ. of California, Santa Barbara). Phys. Rev., A; 2: 1824-34(Nov 1970).

A survey has shown that light emission from low-energy (<1 keV) ion–molecule reactions is a common occurrence. Ar^+ and N_2^+ were used with target gases of Ar, H_2, CO, N_2, O_2, NO, N_2O, CO_2, CH_4, and C_2H_2; in addition, He, Ne, and Kr were used as N_2^+ targets. Electronically excited states were produced by charge transfer and ionization with simultaneous excitation, conversion of translational to electronic energy of the incident ion or target, and dissociation with simultaneous excitation. For several collision partners, more than one of these reactions was seen. In general, charge-transfer reactions had the largest cross sections, to 2×10^{-16} cm^2, for ion laboratory energies of several hundred eV. Cross sections for the strongest features in the other types of reactions were about (1 to 5) $\times 10^{-17}$ cm^2. (auth)

9214 INTERMEDIATE-ENERGY ELECTRON–ATOM SCATTERING. I. Mittleman, Marvin H. (City Coll., New York). Phys. Rev., A; 2: 1846-51(Nov 1970).

The problem of electron–atom scattering in the energy range where both high- and low-energy methods are unreliable is considered. A previously proposed equation is made tractable by a separable approximation on the electron–electron correlation function. This results in a pair of coupled equations in which all inelastic channels are lumped into one effective one. The equations

XUM

are then reduced to a tractable form by some drastic approximations and solved by an eikonal approximation. The results are good in a restricted angular range, and the restrictions are shown to be due to the "drastic approximations" and the eikonal approximation, neither of which is really necessary. (auth)

9215 SINGLE-ELECTRON CAPTURE BY C^{4+} IN HELIUM, NEON, AND ARGON BELOW 40 keV. Zwally, H. Jay; Koopman, David W. (Univ. of Maryland, College Park). Phys. Rev., A; 2: 1851-61(Nov 1970).

Total cross sections for single-electron capture by C^{4+} from the target gases He, Ne, and Ar were measured at laboratory energies between 400 eV and 40 keV. The fast-collision products that scattered less than 1° were charge analyzed after single collision in a gas cell. Experimental results are interpreted in terms of pseudocrossings of the adiabatic potential curves for the initial and final states. The cross sections for C^{4+} + He and C^{4+} + Ne are consistent with the second maximum predicted for distant pseudocrossings by a numerical solution of the two-state semiclassical approximation by Bates, Johnson, and Stewart. Electron capture with an Auger-type ionization of the target is exothermic for C^{4+} + Ne and C^{4+} + Ar and is considered as the explanation of the large (50 Å^2) and slowly varying cross section measured for C^{4+} + Ar. (auth)

9216 GENERALIZED VARIATIONAL BOUNDS ON THE POSITRON–HYDROGEN REACTION MATRIX. I. THE COUPLED-STATIC APPROXIMATION. Dirks, Johan F.; Hahn, Yukap (Univ. of Connecticut, Storrs). Phys. Rev., A; 2: 1861-72(Nov 1970).

The theory of generalized variational bounds is applied to two-channel collisions of positrons on hydrogen leading to positronium formation. The formalism is developed in detail for this problem, and the zero partial-wave solution is obtained in the coupled-static approximation. The nonlocal coupling kernels and the behavior of the wave functions are exhibited in detail. Eigenphase shifts and coupling parameters and the stripping and pickup cross sections, as well as the elastic amplitudes for positron–hydrogen and positronium–proton collisions, are studied as functions of scattering energies. The unitarity limits are exhibited, one of which is nearly saturated in the Ps–p channel. A useful iteration procedure for solving the coupled equations with large coupling kernels is developed. (auth)

9217 INELASTIC SCATTERING OF HIGH-ENERGY ELECTRONS FROM ATOMS: THE HELIUM ATOM. Schneider, Barry (General Telephone and Electronics Labs., Bayside, N. Y.). Phys. Rev., A; 2: 1873-8(Nov 1970).

A discussion of the inelastic scattering of high-energy electrons from atomic systems using linear-response theory is presented. Following Van Hove, an expression for the differential scattering cross section within the Born approximation is derived. The relationship of this expression to the linear-response function is demonstrated and a practical procedure for its computation using the so-called random phase approximation is given. Finally, explicit results for the excitation of the lowest singlet S and singlet P state of helium by 500-eV electrons are given. (auth)

9218 CHARGE-EXCHANGE COLLISIONS BETWEEN METASTABLE HYDROGEN ATOMS AND IODINE MOLECULES. Knutson, L. D. (Univ. of Wisconsin, Madison). Phys. Rev., A; 2: 1878-81(Nov 1970).

Beams of hydrogen atoms in the (2S) metastable state and ground state were passed through an iodine vapor target at energies between 0.2 and 2.5 keV. Measurements of the positive-ion current after the iodine target indicate that the cross section for ionization of the metastable atoms by iodine is much larger than the cross section for ionization of ground-state atoms, especially at the lower energies. The results indicate that this reaction can be effectively used for production of polarized protons in a Lamb-shift polarized-ion source. (auth)

9219 MULTIPLE IONIZATION OF IODINE IN 1.5- TO 12.0-MeV I^{n+}–Xe COLLISIONS. Kessel, Quentin C. (High Voltage Engineering Corp., Burlington, Mass.). Phys. Rev., A; 2: 1881-5(Nov 1970).

The results of an experiment measuring the charge states of 1.5-, 3.0-, 6.0-, and 12.0-MeV iodine ions scattered through angles between 2.5° and 8.0° by single collisions with xenon atoms are reported. The charge states measured range from 9 to 27, and the charge-state distributions showed average values from 11 to 23. The variation of these average values with the collision's distance of closest approach shows the influence of the M and L shells of the colliding ions. (auth)

9220 PRACTICAL APPROACH TO THE COUPLED EQUATIONS FOR SCATTERING AND REARRANGEMENT COLLISIONS. Chen, Joseph C. Y.; Chung, Kwong T. (Univ. of California, San Diego, La Jolla). Phys. Rev., A; 2: 1892-9(Nov 1970).

The coupled equations of collision theory are examined in the projection-operator formulation of Feshbach. It is shown that the separate treatments of the open and closed channels provide distinct numerical advantages over the conventional methods. As an illustrative example, the phase shift and resonances for the (e,H) system are calculated. (auth)

9221 ANGULAR DISTRIBUTION OF O^- FROM DISSOCIATIVE ELECTRON ATTACHMENT TO O_2. Van Brunt, R. J.; Kieffer, L. J. (Univ. of Colorado, Boulder). Phys. Rev., A; 2: 1899-1905(Nov 1970).

The angular distribution of O^- produced by electron bombardment of O_2 was measured in the electron energy range 5.75 to 8.40 eV. The results show a strong energy dependence and are consistent with the theory of O'Malley and Taylor if the final O_2^- repulsive resonance state is assumed to have the symmetry $^3\Pi_u$, and if only the first two allowed partial waves of the incident electron corresponding to L = 1 and L = 3 contribute. The results indicate that the L = 3 term becomes more important as energy increases and thereby demonstrate that the single-term approximation for the angular distribution does not apply for this process. (auth)

9222 ABSOLUTE MEASUREMENT OF DIFFERENTIAL CROSS SECTIONS FOR ELECTRON SCATTERING IN HELIUM. Chamberlain, G. E.; Mielczarek, S. R.; Kuyatt, C. E. (National Bureau of Standards, Washington, D. C.). Phys. Rev., A; 2: 1905-22(Nov 1970).

Absolute measurements of cross sections for electron scattering in helium at an angle of 5° were made for elastic scattering and excitation of the 2^1P and 2^1S states and for incident energies of 50 to 400 eV. Cross-section values of $\sigma(2^1P,5°)$ are found to be lower than theoretical Born values by (9.5 ± 5.4)% at 400 eV, (31.5 ± 4.6)% at 100 eV, and (62.5 ± 3.4)% at 50 eV. Deduced values of total 2^1P excitation cross sections (E ≥ 100 eV) are in agreement with other experimental values. The measurements for elastic scattering agree well with recent theoretical calculations. (auth)

9223 ALKALI–ALKALI DIFFERENTIAL SPIN-EXCHANGE SCATTERING. I. Pritchard, David E.; Carter, Gary M.; Chu, Frank Y.; Kleppner, Daniel (Massachusetts Inst. of Tech., Cambridge). Phys. Rev., A; 2: 1922-31(Nov 1970).

Measurements of differential elastic cross sections for various alkali–alkali pairs are presented, as well as the angular dependence of the probability of electron spin exchange in these collisions. The resolution is sufficient to reveal interference structure in the angular dependence of both quantities. The apparatus, which polarizes one incident beam and analyzes the polarization of the scattered atoms, is described, and the measurement and data-reduction procedures are discussed. Results are presented in the range 0.1 to 0.2 eV for the systems Na–Cs, Na–Rb, Na–K, K–Cs, and K–Rb. (auth)

9224 ALKALI–ALKALI DIFFERENTIAL SPIN-EXCHANGE SCATTERING. II. Pritchard, David E.; Chu, Frank Y. (Massachusetts Inst. of Tech., Cambridge). Phys. Rev., A; 2: 1932-48 (Nov 1970).

The data on differential spin-exchange scattering in collisions between alkali metal atoms presented in the preceding paper is analyzed. The data on the probability of exchange is analyzed to obtain the relative phase shift produced by the triplet and singlet potentials. A semiclassical impact approximation is developed and used to calculate this phase shift from theoretical calculations of the asymptotic behavior of the potentials. The results are consistent with the data only when the largest calculated value for the van der Waals potential is combined with the smallest calculated value of the difference potential. The rainbow structure in the spin-summed differential cross section was also analyzed to obtain information about the depth and shape of the minimum in the triplet potentials in various alkali–alkali systems. The result of this analysis is compared with results from other experiments on alkali–alkali systems. (auth)

9225 DIFFERENCES IN SINGLE, PLURAL, AND MULTIPLE SCATTERING OF ELECTRONS AND POSITRONS THROUGH INTERMEDIATE ANGLES. Erman, Peter (Research Inst. for Physics, Stockholm). Phys. Scr.; 1: 93-103(1970).

Experiments were done in which the elastic scattering of a divergent beam of electrons and positrons in foils of Al, Cu, Ag, and Pb was studied. The difference between the scattered fractions of the two types of particles was measured as a function of the particle energy in the range 100 to 1300 keV, for foil thicknesses of 0.2 to 10 mg/cm^2, and for incidence angles in the intervals 15° to

30° and 30° to 47°. The results are compared to available theoretical treatments and good agreement is found between experiments with thin scatterers and the Mott formula for single scattering, while difficulties occur in attempts to get a theoretical representation of the scattering in thicker foils. The latter fact may be understood from the incompletenesses in the theoretical treatments of plural and multiple scattering, in the first place the neglect of spin–orbit effects and the absence of a calculation of the real crooked paths of the particles. A theoretical fit to the measured differences in scattering was obtained by assuming a larger screening parameter for positrons than for electrons, but this assumption should only be considered as a mathematical way of obtaining a larger single-scattering cross section for electrons than for positrons as required by the Mott formula. (auth) (Sweden)

9226 DEPENDENCE OF VIBRATIONAL TRANSITION PROBABILITIES ON THE ORIENTATION ANGLE IN THE THREE-DIMENSIONAL BC + A COLLISION. Shin, H. K. (Univ. of Nevada, Reno). Chem. Phys. Lett.; 7: 436-8(15 Nov 1970).

The dependence of vibrational transition probabilities on molecular orientation in the three-dimensional BC + A collision at high velocities was investigated. For O_2 + Ar collisions calculation of the $0 \rightarrow 1$ vibrational transition probability shows that the collinear orientation is very inefficient for vibrational transitions above the collision velocity of about 10^6 cm/sec when the impact parameter is greater than the Lennard-Jones parameter (i.e., $b > \sigma$). When $b < \sigma$, it is also very inefficient for velocities lower than this value. At higher collision velocities, the perpendicular orientation with nonzero impact parameter becomes efficient for vibrational energy transfer. (auth)

9227 CLASSICAL S-MATRIX: A MORE DETAILED STUDY OF CLASSICALLY FORBIDDEN TRANSITIONS IN INELASTIC COLLISIONS. Miller, W. H. (Univ. of California, Berkeley). Chem. Pnys. Lett.; 7: 431-5(15 Nov 1970).

Procedures are investigated for describing classically forbidden collision processes within the framework of the classical limit of quantum mechanics. The goal is to use exact classical mechanics (numerically computed trajectories) to treat classically forbidden transitions in a complex collision (such as an atom plus diatom) in a manner analogous to the way it is used to treat barrier transmission by a single particle in one dimension (a classically forbidden process); in this latter example the transmission coefficient is $\exp(-2\theta)$, θ being the classical action integral through the barrier (a classically forbidden region). Numerical application of these procedures is made to the linear atom–diatom collision system (without reaction), and the resulting vibrational transition probabilities for the classically forbidden transitions are in as good agreement with the exact quantum mechanical values as are the transition probabilities for classically allowed transitions. It appears, therefore, that the dynamics of even these classically forbidden transitions is accurately described in this semiclassical framework. (auth)

9228 CLASSICAL AND SEMICLASSICAL LIMITS IN COLLISION THEORY. Levine, R. D.; Johnson, B. R. (Ohio State Univ., Columbus). Chem. Phys. Lett.; 7: 404-8(15 Nov 1970).

The classical scattering observable is obtained as $\exp(i\Delta)$ where Δ is the interaction. Elements of the scattering matrix in the semiclassical limit are then defined, using the correspondence procedure, as the Fourier components of the classical scattering observable. This procedure is equivalent to carrying out the exponential approximation to the lowest order in $\hbar$. A soluble model of vibrational excitation is considered as an example. (auth)

9229 CROSS SECTIONS FOR CHARGE TRANSFER DURING COLLISIONS BETWEEN H^+ AND Kr, Xe, NH_3, C_2H_2, C_6H_6. Le Doucen, Roger; Lenormand, Jean-Michel; Guidini, Joseph (Facultes des Sciences, Rennes, France. EURATOM–CEA, Fontenay-aux-Roses, France). Compt. Rend., Ser. B; 271: 777-80(12 Oct 1970). (In French).

The total cross sections for charge exchange were measured in the energy range 15 to 150 keV by the direct detection of the neutral particles formed. (tr-auth) (France)

9230 QUANTUM VIBRATIONAL TRANSITION PROBABILITIES IN ATOM–DIATOMIC MOLECULE COLLISIONS. V. EFFECTS OF MASS AND WELL DEPTH. Wilson, David J. (Vanderbilt Univ., Nashville). J. Chem. Phys.; 54: 540-4(15 Jan 1971).

The method of Cheung and Wilson is used to investigate the dependence of vibrational transition probabilities on atomic masses and on the well parameters of the intermolecular potential. The presence of a well in the intermolecular potential causes quite large changes in the transition probabilities, as do changes in the masses of the colliding particles. Difficulties in using this method on systems having certain unfavorable mass ratios had been noted earlier; a procedure is presented in which these difficulties are overcome. (auth)

9231 CLASSICAL THEORY OF SCATTERING: THREE-BODY PROBLEMS. Eu, Byung Chan (McGill Univ., Montreal). J. Chem. Phys.; 54: 559-65(15 Jan 1971).

The classical theory of scattering for a two-body problem by Prigogine and Henin, Résibois, and Miles and Dahler is extended to include a three-body system in which exchange reactions are allowed as well as excitations in the internal states. The results obtained are parallel to those in the quantum mechanical three-body theory of Faddeev and given in such a way that an introduction of approximation methods is possible without difficulty. (auth)

9232 POTENTIAL FOR THE INTERACTION OF ATOMS AND HEAVY POLAR MOLECULES IN THERMAL SCATTERING. van de Ree, J.; Okel, J.G.R. (Technische Hogeschool, Eindhoven, Netherlands). J. Chem. Phys.; 54: 589-97(15 Jan 1971).

The anisotropy of a molecule interacting with an atom in thermal collisions is given a more fundamental basis by separating the effects of the motion of the electrons through mutual induction and through the rotation of the nuclei to which they are connected. For heavy polar molecules with an asymmetric mass distribution the positions of the centers of dispersive and electrostatic interaction on the internuclear axis are different from the center of mass. Most of the anisotropy is accounted for by the dynamical effect of these displacements. Two models applicable in classical mechanics are proposed. The total scattering cross sections were evaluated for the partners TlF and Ar. The anisotropy parameter thus derived is in agreement with experiment. (auth)

9233 TRANSIENT ION CYCLOTRON RESONANCE METHOD FOR STUDYING ION–MOLECULE COLLISION AND CHARGE-TRANSFER RATES: N_2^+ AND CH_4^+. Dunbar, Robert C. (Stanford Univ., Calif.). J. Chem. Phys.; 54: 711-19(15 Jan 1971).

A heterodyne technique of ion cyclotron resonance (ICR) is described and shown to give spectra having the form of an exponentially damped sinusoidal curve. The rate of damping is related to the collision and charge-transfer rates in the ion–molecule system. The generalized ICR equations required to analyze the data are developed and solved and are shown to fit experimental spectra very closely. Results for N_2^+ in N_2 agree well with mobility data and with ICR linewidth studies and indicate substantial probability for charge transfer. Results for CH_4^+ in CH_4 are found to rule out any substantial charge-transfer cross section. (auth)

9234 FLUORESCENCE EFFICIENCIES OF NITROGEN EXCITED BY 1- TO 5-MeV POSITIVE IONS. Dunn, Jerry L.; Holland, Redus F. (Los Alamos Scientific Lab., N. Mex.). J. Chem. Phys.; 54: 470-8(15 Jan 1971).

Fluorescence efficiencies for excitation of nitrogen by 1- to 5-MeV positive ions were measured at pressures of 2 to 19 torr. Typically, N_2 pressure of 3.6 torr was required to stop a beam of 4-MeV Ne^+ in the 1.5-m-long collision chamber. Power output in the 3914-Å (0,0) N_2^+ first negative band was measured with a photometer, and low-pressure efficiencies were calculated from the collisional deactivation rate. For Ne^+, O^+, N^+, N_2^+, and O_2^+ ions with various initial velocities from 3.1 to 8.3×10^8 cm/sec, the low-pressure efficiencies were between 0.4% and 0.6%. For 2.0 and 3.4×10^8 cm/sec Kr^+, 3914-Å efficiencies were 0.27% and 0.35%, and for 1.38×10^9 cm/sec H^+, 0.67%. Spectra of the nitrogen emission in the 3400 to 7800-Å range were recorded. N_2^+ first negative and N_2 first and second positive bands were prominent, with most first negative in the $v' = 0$ vibrational sequence, and most second positive in the $v' = 0 - 2$ sequences. The spectra were corrected for collisional quenching and low-pressure efficiencies were determined relative to the 3914-Å band. For 4- to 5-MeV N^+, Ne^+, N_2^+, and Kr^+, total efficiencies for the second positive $v' = 0 - 2$ sequences were about 1.5 times the 3914-Å efficiencies. Efficiencies were determined for 10 first positive bands of the $v' = 2$ to 7 sequences excited by 4.75-MeV Ne^+; the (2,0) and (3,1) band efficiencies, for example, were about one-fourth the 3914-Å efficiency of 0.52%. The nitrogen fluorescence excited by the ions has a spectral intensity distribution similar to those observed by Hartman for 850-eV electrons in air and by Mitchell for 1.5-keV x rays in N_2. (auth)

9235 MEASUREMENT OF K-SHELL PHOTOELECTRIC CROSS SECTIONS IN URANIUM. Sahota, H. S. (Punjabi Univ., Patiala, India). Phys. Lett.; 33A: 430-1(14 Dec 1970).

The fluorescent K x-radiation production in γ-irradiated uranium at low energies is essentially through the photoelectric interaction. At higher energies the other competing processes also contribute considerably. (auth)

9236 COMMENT ON OSCILLATIONS IN THE CROSS SECTION OF Ar^+–Ar CHARGE TRANSFER. Johnson, R. E. (South-

XUM

ern Illinois Univ., Carbondale). Phys. Lett.; 33A: 452(14 Dec 1970).

It is pointed out that an approximate theory of charge-transfer predicts incorrectly oscillations in cross sections if extended beyond its region of validity. (auth)

9237 LOCAL EXCHANGE POTENTIAL IN THE THEORY OF ELECTRON SCATTERING ON ATOMS. Gurchumeliya, A. D. (Georgian Polytechnic Inst., Tbilisi, USSR). Soobshch, Akad. Nauk Gruz. SSR; 59: 565-8(Sep 1970). (In Russian).

The use of a local exchange potential in the nonrelativistic Hartree–Fock scheme for electron–atom scattering is discussed. The local potential depends on the energy of the incident electron. Calculations are carried out for elastic scattering of low-energy electrons from neon and argon. (auth)

9238 TRANSFER OF EXCITATION ENERGY IN ION–ATOM INTERACTION. Zapesochnyi, I. P.; Zavilopulo, A. N.; Shpenik, O. B. Opt. Spectrosc. (USSR) (Engl. Transl.); 28: 465-6(May 1970).

Translated from Opt. Spektrosk.; 28: 856-8(May 1970).

A description is given of an experimental apparatus used for the study of the excitation of atoms in collisions with slow ions. Results are obtained for the spectral zinc line at 4811 Å, which is excited by zinc ions in the energy range from threshold to 900 eV. In the energy dependence of the cross section of the excitation of this line, a significant maximum was detected at 20 eV, which is explained by the transfer of excitation energy from an excited zinc ion to a neutral zinc atom. (auth)

9239 RESONANCE PHOTOIONIZATION OF HELIUM AND HELIUM-LIKE IONS. Balashov, V. V.; Grishanova, S. I.; Kruglova, I. M.; Senashenko, V. S. Opt. Spectrosc. (USSR) (Engl. Transl.); 28: 466-71(May 1970).

Translated from Opt. Spektrosk.; 28: 859-68(May 1970).

Within the framework of the diagonalization method, the photoionization resonances of helium and of Li^+ and Be^{2+} ions are investigated in the range between the first and second ionization thresholds. The agreement between calculation and experiment is good. The relationship between the diagonalization method and other methods of describing resonances is discussed. (auth)

9240 SIMPLEST MODEL OF VIBRATIONAL EXCITATION OF DIATOMIC MOLECULES BY SLOW ELECTRONS. Soshnikov, V. N. Opt. Spectrosc. (USSR) (Engl. Transl.); 28: 475-8(May 1970).

Translated from Opt. Spektrosk.; 28: 877-82(May 1970).

In a continuation of the work of Herzenberg and Mandl (Proc. Roy. Soc. (London), A270: 48(1962)) on resonance excitation of the vibrations of diatomic molecules by slow electrons, a numerical calculation of two variations of the problem of the scattering of electrons by a spherical potential well with a depth depending on the vibrational coordinates of the molecule was carried out. Partial waves to $l = 4$ inclusive were used. Qualitative agreement with the primary attributes of the experimental cross sections was obtained; this supports the position that the observed resonance scattering can be considered as scattering by a one-electron potential. (auth)

9241 EXPERIMENTAL EVIDENCE FOR THE MECHANISM OF CHARGE TRANSFER INTO CONTINUUM STATES. Crooks, G. B.; Rudd, M. E. (Univ. of Nebraska, Lincoln). Phys. Rev. Lett.; 25: 1599-1601(7 Dec 1970).

A prominent peak was observed in the energy spectrum of electrons ejected in the forward direction from helium bombarded by protons ranging in energy from 100 to 300 keV. The peak occurs at an ejected-electron velocity equal to the velocity of the incident proton. The experimental results verify the existence of the mechanism of charge transfer into continuum states of the incident ion. (auth)

Atomic Theory

9242 CONFIGURATION INTERACTION COMBINED WITH A CORRELATION FACTOR FOR TWO-ELECTRON ATOMS. Grein, F.; Tseng, T. J. (Univ. of New Brunswick, Fredericton). Chem. Phys. Lett.; 7: 506-10(1 Dec 1970).

Variational calculations were performed on the ground state of He and O^{6+}. The configuration-interaction wave functions containing s, p, d, and f orbitals are multiplied by the correlation factor $(1 + \alpha r_{12})$. The best energies obtained are −2.90361 and −59.1562 a.u., respectively. The s and p improvements combined exceed the respective angular energy limits by 0.00006 a.u., based upon the angular energy analysis of Chandrasekhar's wave function by Green and coworkers. (auth)

9243 BASIS SETS OF GAUSSIAN AND SLATER-TYPE ATOMIC ORBITALS. Silver, D. M. (Centre Europeen de Calcul Atomique et Moleculaire, Orsay, France). Chem. Phys. Lett.; 7: 511-16(1 Dec 1970).

The concept of constructing molecular wave functions using basis sets whose members consist of both Slater-type and gaussian-type atomic orbitals is examined through pilot SCF calculations on some simple atoms. (auth)

9244 MASTER-EQUATION APPROACH TO SPONTANEOUS EMISSION. Agarwal, G. S. (Univ. of Rochester, N. Y.). Phys. Rev., A; 2: 2038-46(Nov 1970).

Spontaneous emission from a system of N identical two-level atoms is considered using a master equation recently derived by the author. The master equation describing the time evolution of the phase-space distribution function associated with the reduced density operator of the atomic system is obtained. This master equation, which is of the type of a Fokker–Planck equation, is used to derive the equation of motion for the mean values of various atomic operators characterizing the physical properties of the system. This leads to a hierarchy of equations, which is decoupled by making a suitable approximation. The intensity of the spontaneously emitted radiation is then calculated. Next, the spontaneous emission from geometrically small systems is considered. For this case, the master equation is solved exactly, and an exact expression for the radiation rate is obtained. The exact solution of the master equation is also used to calculate the normally ordered correlation functions for the electric field. Section V deals with the spontaneous emission from a system of harmonic oscillators, the size of the system being small compared to a wavelength. The master equation for this problem is also solved exactly, and it is shown that this system also leads to superradiant emission in some cases, e.g., if all the oscillators are excited initially to some coherent state $|z_0\rangle$. (auth)

9245 CONVERGENCE OF THE DENSITY GRADIENT EXPANSION FOR ATOMS. Brueckner, K. A.; Perez, J. D. (Univ. of California, San Diego, La Jolla). Phys. Rev., A; 2: 2161-2 (Nov 1970).

The inhomogeneity correction to the correlation energy of an electron gas is added to the Thomas–Fermi energy-density functional for atoms. The density is significantly modified only inside a radius of the order $Z^{-\frac{1}{3}} \times 10^{-5}$ Bohr radii. This does not reduce the density gradient sufficiently to make the expansion convergent. (auth)

9246 EXPERIMENTAL INVESTIGATION OF THE THEORETICAL EXPRESSIONS FOR THE RYDBERG CONSTANT. Zygan, H. (Farbenfabriken Bayer AG, Leverkusen, Ger.). Z. Naturforsch.; 25a: 1236-43(Aug-Sep 1970). (In German).

Calculations of the fundamental constants of nature from appropriate precision measurements lead to the conclusion that the values of the elementary charge, the electron mass, Planck's constant, and Avogadro's number, as well as the values of the Sommerfeld fine-structure constant α calculated from them, agree to about 0.2% if these values are calculated first from such precision measurements that make no use of the theory of one-electron atoms and a second time with the use of the measured value for the Rydberg constant. Between the measured Rydberg constant and the theoretical value, computed from the constants of nature without using atomic theory, there is a difference of over 0.4%. For the definitive experimental confirmation or denial of this discrepancy, a new method for the direct precision measurement of the elementary charge is presented. (tr-auth)

9247 HARTREE–FOCK PROBLEM. Musher, J. I. (Yeshiva Univ., New York). Chem. Phys. Lett.; 7: 397-403(15 Nov 1970).

The Hartree–Fock problem is investigated by examining the symmetry properties of the self-consistent-field (SCF) spin orbitals. These can be classified as closed-shell, open-shell, or general spin orbitals according to the commutation rules satisfied by their one-electron SCF hamiltonians. The effect of symmetry breaking in spin, angular-momentum, and space-group symmetry is considered schematically and the physical implications of such symmetry breaking are discussed. (auth)

9248 THE ENERGY LEVELS OF DOUBLE-WELL POTENTIALS. II. Froeman, Nanny; Myhrman, Ulla (Univ. of Uppsala). Ark, Fys.; 40: 497-508(Aug 1970).

The higher-order phase-integral approximations are expressed with the aid of new contour integrals, which for certain purposes are more convenient than those used in the previous paper. The approximate quantization condition obtained in a previous paper is illuminated further by an alternative derivation based on the analysis of the barrier transmission problem worked out in another paper. For a symmetric, but otherwise general, double

oscillator, expressions for the wave function on the whole real axis are given, except in the neighborhood of the transition points, in terms of the higher-order phase-integral approximations used. To illustrate the accuracy of the above-mentioned approximate quantization condition some energy levels for a special symmetric double oscillator are computed with the aid of the first-, third-, and fifth-order phase-integral approximations, and comparison is made with results of exact numerical computations made by other authors. (auth) (Sweden)

9249 APPLICATION OF TRUNCATED MULTIPOLAR EXPANSION PAIR FUNCTIONS IN ATOMIC STRUCTURE CALCULATIONS. Jankowski, K. (Simon Fraser Univ., Burnaby, B. C.). Can. J. Phys.; 48: 2707-13(15 Nov 1970).

A class of truncated multipolar expansion pair functions (TMEPF) for application in atomic structure calculations is defined, and their properties as well as their relationships to previously applied pair functions are discussed briefly. In order to get a better insight into the effectiveness of TMEPF's in representing the properties essential for correlated pair functions, a pilot calculation of the energy and expectation values of some operators for the ground state of H^-, He, and Li^+ is also presented. (auth) (Canada)

9250 CONVERGENCE OF THE SERIES EXPANSION SOLUTION TO THE THOMAS–FERMI–DIRAC EQUATION. Enstrom, James E. (Rand Corp., Santa Monica, Calif.). J. Chem. Phys.; 54: 820-2(15 Jan 1971).

A recursion relation was obtained for calculating successive coefficients for use in the series-expansion solution to the Thomas–Fermi–Dirac equation. The first few hundred coefficients were computed for selected Z values. A plot of the magnitude of the coefficient ratio $R_n \equiv |a_n/a_{n-1}$ shows that R_n increases monotonically from about 1.1 up to an asymptotic value that ranges between approximately 1.51 for Z = 6 and 1.49 for Z = 92. From this a radius of convergence for the series can be obtained. (A.G.W.)

9251 STUDIES IN THE SINGLE-CENTER METHOD. Anderson, Alfred B. (Johns Hopkins Univ., Baltimore). J. Chem. Phys.; 54: 806-9(15 Jan 1971).

The Coulson–Barnett expansion and a Taylor series in powers of $\cos\theta$ for the off-center hydrogen 1s function are examined. Energy converges as L^{-4} in the former case and L^{-5} in the latter, where L is the expansion length. Other rates are found. The single-center integral Hellmann–Feynman method is briefly discussed. Radial-angular separation using a function of correct asymptotic behavior is also considered. (auth)

9252 HARTREE–FOCK CALCULATIONS OF AUTOIONIZATION STATES. Perkins, J. F. (Army Missile Command, Redstone Arsenal, Ala.). Phys. Rev., A; 2: 1704-7(Nov 1970).

It is argued that Hartree–Fock (HF) and certain HF-like calculations provide upper bounds to energies of certain atomic autoionization states defined as eigenfunctions of Feshbach's QHQ. A detailed discussion and supporting calculations are given for the $2s^2\ ^1S$ state of He. The Q-space constraint can be satisfied by assignment of a suitable value to an orbital-expansion parameter. A slightly higher, and hence upper-bound, value of energy is obtained instead by maximizing energy with respect to this parameter. It is argued that a HF calculation can be reduced to such a parameter-maximization process, on the assumption that the solution is unique. Several autoionization states in two-electron atoms are discussed, and it is noted that the HF energy bounds are useful for some such states but are useless for others because of configuration mixing. The general approach is not inherently limited to two-electron atoms, and a similar argument is given for the lowest ^2S autoionization state of a three-electron atom. (auth)

Cosmic Radiation

Refer also to abstracts 8556, 9336, 9638, and 9872.

9253 (MPI-PAE/EXTRATERR-47) EXTENSIVE AIR SHOWERS. Truemper, J. (Max-Planck-Institut fuer Physik und Astrophysik, Munich (West Germany)). Sep 1970. 24p. (CONF-700708-2). Dep. NTIS (U. S. Sales Only).

From 6th Interamerican Seminar on Cosmic Rays, La Paz, Bolivia.

Topics discussed include air shower evidence of quarks, evidence of large transverse momenta in air shower cores, primary energy spectrum, chemical composition, arrival direction distribution, possible role of pulsars as cosmic-ray accelerators at air shower energies, apparent isotropy at 10^{18} eV, chemical composition of pulsar produced cosmic rays, and pulsed neutron sources. (W.D.M.)

9254 π^0 DECAY AND THE DIFFUSE γ-BACKGROUND RADIATION. Cavallo, Giacomo Giulio Francesco. San Diego, La Jolla, Calif.; Univ. of California (1970). 185p. University Microfilms Order No. 70-17,279.

Thesis.

In the last few years, some upper limits and positive results have been produced in direct observations of the diffuse γ-background, with photon energy larger than 50 MeV. The most detailed among these experiments is due to Clark, Garmire, and Kraushaar, who observed a line source along the galactic plane, and an isotropic background of intensity 1.1×10^{-4} (cm^2 sec sr)$^{-1}$. This work is concerned with the explanation of both results. In both cases one might think that the results are due to the superposition of discrete sources (galactic and metagalactic respectively). This plausible approach is discussed, and, although the results are not unsatisfactory, its weaknesses are pointed out. (TSS) (Diss. Abstr. Int., B).

9255 PARTICLE-TRACK IDENTIFICATION: APPLICATION OF A NEW TECHNIQUE TO APOLLO HELMETS. Fleischer, R. L.; Hart, H. R. Jr.; Giard, W. R. (General Electric Research and Development Center, Schenectady, N. Y.). Science; 170: 1189-91(11 Dec 1970).

The Apollo helmets are being used to record the dose of heavy particles to which astronauts are exposed on space missions. An improved method for examining and identifying the etched tracks of heavy charged particles consists of replicating tracks and measuring the etching rate as a function of position along the track. Tracks have been observed in Apollo helmets that correspond to ionized atoms heavier than iron. (auth)

9256 PULSARS AND VERY HIGH-ENERGY COSMIC-RAY ELECTRONS. Shen, C. S. (Purdue Univ., Lafayette, Ind.). Astrophys. J.; 162: L181-6(Dec 1970).

In the study of the propagation of cosmic-ray electrons, the use of a continuous-source distribution is not valid in the range of very high energies. The electron spectrum in that energy range depends on the age and distance of a few local sources. It is shown that if the far-infrared background discovered recently exists in the Galaxy, the very high-energy electrons observed at Earth probably all come from the source Vela X, and a cutoff energy at about 2×10^3 BeV is predicted. Implications on the propagation of cosmic rays in the Galaxy are discussed. (auth)

9257 GALACTIC ^{3}He ABOVE 10 MeV PER NUCLEON AND THE SOLAR CONTRIBUTIONS OF HYDROGEN AND HELIUM. Hsieh, K. C.; Simpson, J. A. (Univ. of Chicago). Astrophys. J.; 162: L197-201(Dec 1970).

The flux of ^{3}He between 10 and 30 MeV per nucleon was measured in interplanetary space for the first time. The ^{3}He spectrum between 10 and 100 MeV per nucleon is compared with the proton and ^{4}He spectra. The ^{3}He flux is of galactic origin and is used as a tracer to identify the galactic spectrum of ^{1}H and ^{4}He between 10 and 30 MeV per nucleon in the presence of a quasi-steady solar component whose proton spectrum has a slope of opposite sign in this energy range. During the quietest periods on the Sun in 1967, the Sun contributed approximately 70% of the observed proton flux at 10 MeV, 30% at 15 MeV, 15% at 20 MeV, and a negligible flux at higher energies. These values are consistent with those obtained by using galactic ^{2}H as a tracer. The ^{3}He and ^{4}He spectra above 10 MeV per nucleon also provide evidence that adiabatic deceleration is operative as a mechanism in cosmic-ray modulation and that the local interstellar spectrum flattens toward low energies. (auth)

9258 FLUCTUATION OF COSMIC-RAY ANISOTROPY AND THE DIMENSIONALITY OF PROPAGATION. Jones, Frank C. (Goddard Space Flight Center, Greenbelt, Md.). Phys. Rev. Lett.; 25: 1534-5(23 Nov 1970).

The relation between the dimensionality of the cosmic-ray propagation function and the statistical distribution of anisotropies is demonstrated and an argument is presented in favor of "essentially" one-dimensional propagation. This implies that a fluctuation explanation of low observed anisotropy cannot be ruled out, as was stated previously by other authors. (auth)

9259 INVESTIGATIONS OF COSMIC-RAY INTENSITY VARIATIONS IN ANTARCTICA. Pomerantz, Martin A.; Duggal, Shakti P. (Bartol Research Foundation, Swarthmore, Pa.). Antarctic J. U. S.; 5: 167-8(Sep-Oct 1970).

The ground-level event of Nov. 18, 1968 was abnormal in that none of the more energetic solar cosmic rays were observed at some high-latitude stations at any stage, and the anisotropy persisted at least until the cessation of the influx of particles having

XUM

energies sufficiently high to be observed with ground-level cosmic-ray detectors. Anisotropy continued for the total time indicating that little diffusive scattering occurred in the vicinity of the Earth. This behavior was unprecedented and unexpected since the event coincided with the maximum of the ongoing 11-year solar activity cycle, when the density of disordered magnetic fields in the interplanetary medium is high. This event is ideal for studies of the diurnal shift of arrival directions of solar particles arising from the deformed magnetosphere. Due to the large anisotropy, the energy spectrum of the solar particles cannot be determined with good precision from the latitudinal distribution of the enhancement, hence, the normalized nucleonic flux at six stations is plotted as a function of the finally determined angle between the asymptotic cone and the axis of symmetry. It is noted that the dispersion of the data from the line representing 100% anisotropy is minimal. (J.C.W.)

9260 SOLAR COSMIC-RAY OBSERVATIONS DURING 1969. Masley, A. J.; McDonough, J. W.; Satterblom, P. R. (McDonnell Douglas Astronautics Co., Santa Monica, Calif.). Antarctic J. U. S.; 5: 172-3(Sep-Oct 1970).

During 1969, twenty-one solar cosmic ray events were observed with riometer absorption greater than 0.4 db at 30 MHz, as compared to 20 events during 1968, and 16 during 1967. The two largest 1969 events occurred on April 11 and Nov. 2 and were apparently due to solar activity behind the east and west limbs, respectively. For about 5 hours after the onset of the June 7, 1969 event, significant anisotropies were observed as the satellite crossed a given polar cap. Variations pertaining to each polar cap are discussed. The profile during the Nov. 2, 1969 event was similar to that observed during the Nov. 18, 1968 event, and this feature may be characteristic of extreme west-limb events and their propagation path to Earth. (J.C.W.)

Direct Energy Conversion

Refer also to abstracts 9275 and 9439.

9261 PRODUCTION OF HIGH-TEMPERATURE COMBUSTION PRODUCTS FOR THERMOELECTRIC PLANTS WITH A MAGNETOHYDRODYNAMIC GENERATOR. Shumyatskii, B. Ya.; Khokhlova, L. K.; Sokol'skii, A. G.; Rogachev, A. P. (Inst. of High Temperature, Moscow). High Temp. (USSR) (Engl. Transl.); 7: 307-13(Mar- Apr 1969).

Translated from Teplofiz. Vys. Temp.; 7: 342-8(Mar-Apr 1969).

Methods are examined for obtaining high-temperature combustion products of methane by preheating the air, by enrichment of the air with oxygen, and by the use of preliminary thermochemical treatment of the fuel; these products are promising for industrial electric power plants with an open-cycle magnetohydrodynamic generator. An analysis is made of the possible high temperatures for the above methods with a given preheat temperature of the oxidizer, as well as the effect of various factors (preheating of the fuel, the coefficient of excess oxidizer, the pressure, and method of introducing an ionizing additive) on the combustion temperature. (auth)

9262 ANALYSIS OF OPTIMUM CHARGED-PARTICLE SIZE BASED ON THE CONVERSION EFFICIENCY OF ELECTROGASDYNAMIC GENERATORS. Biblarz, Oscar (Naval Postgraduate School, Monterey, Calif.). Energy Convers.; 10: 207-13(Nov 1970).

The feasibility of electrogasdynamic (EGD) generators can be described in terms of an efficiency that reflects a fundamental feature of the EGD process. The conversion efficiency is defined as the fraction of the total kinetic energy of the flow which is available for electrical conversion. This definition applies to any such generator in the sense that fluid dynamic losses and charge losses are not considered. This analysis is inherently microscopic in that it describes single-particle interactions rather than the complete continuum equations. A representative case is treated that has features of both the viscous and the collisionless case and, whenever appropriate, results in terms of the viscous limit are given. In order to formulate the fundamental efficiency, a thermodynamic argument is used to show that there is an energy degradation due to the need to ionize an otherwise neutral gas flow. An aerosol flow consisting of water droplets in air is considered for various particle sizes; such a treatment is representative of other aerosols. Two limitations appear from this analysis in terms of particle radius: a minimum flow velocity and a minimum value for the charged particle-to-neutral ratio. This ratio can be related to the injector size through the breakdown field strength of the carrier gas. These results may be helpful in elucidating the difficulties that can be encountered at the injector of an EGD system. (auth) (UK)

9263 EXPERIMENTAL STUDY OF THE POTENTIAL DISTRIBUTION BETWEEN THE ELECTRODES OF A FARADAY MHD TUBE SUPPLIED BY SUPERSONIC CURRENT OF IONIZED ARGON. Inglesakis, Georges; Bouesc, Jacky; Bournot, Philippe (Institut de Mecanique des Fluides, Marseille). Compt. Rend., Ser. B.; 271: 831-4(19Oct 1970). (In French).

The potential distribution between the electrodes of a magnetohydrodynamic Faraday tube situated at the extremity of the test tube of a combustion shock tube was measured. Argon was used as the test gas. Large potential gradients were observed in the electrode region within the boundary layer. For current densities between 50 and 100 A/cm^2 the potential drops at the cathode and the anode were observed to have constant values of approximately 30 and 20 volts, respectively. This fact indicates that an arc conduction region exists between the electrodes and the plasma. (auth)

9264 THEORETICAL CALCULATIONS ON THE NOBLE-GAS CLOSED MHD LOOP FIRED WITH FOSSIL FUELS AND FIRST EXPERIMENTAL RESULTS WITH THIS SCHEME. Azalbert, Jean-Paul; Scaricabarozzi, Ricardo; Vavasseur, Camille; Zettwoog, Pierre (Centre d'Etudes Nucleaires de Saclay, Gif-sur-Yvette, France). Energy Convers.; 10: 177-82(Nov 1970).

The feasibility of a gas closed loop MHD power station, fired with fossil fuels or better with cookery gases at low pressure is examined both from a technical and theoretical point of view. Computations of the performances and basic elements of the costs evaluation are given for some typical applications. Experiments performed with a pebble-bed heat exchanger fired with CH_4 and used for heating a 5 MW thermal power helium closed loop are related. A nearly zero contamination of the helium was found. It is suggested that this scheme would lead to a practical MHD achievement at the best cost and minimal chance of misadventure. (auth) (UK)

9265 OPTIMUM NUMBER OF THE LOAD CIRCUITS IN THE HALL-TYPE MHD GENERATOR. Celinski, Z. Arch. Elektrotech. (Warsaw); 19: 413-22(1970).

The two-terminal Hall generator is a relatively low-efficiency device when the gas parameters vary strongly along the channel. In such cases, more power may be extracted from the gas flow when the generator is connected in multi-terminal mode. The problem is generally formulated, and the power produced in the multi-terminal mode of operation is determined. Conclusions about the optimum circuit number and optimum division of the generator channel were drawn. The results are strongly influenced by the end effects. (auth)

9266 MAGNITNAYA GIDRODINAMIKA V SUDOVOI TEKHNIKE. (Magnetohydrodynamics in Marine Engineering). Vasil'ev, L. G.; Khozhainov, A. I. Leningrad; Sudostroenie (1967). 248p.

The state of development of magnetohydrodynamics and the equipment that operates on magnetohydrodynamic principles are described. Magnetohydrodynamic effects, which are dependent on the interaction of an incompressible conducting liquid with a transverse magnetic field, are considered. The elements of the theory, the fabrication and working characteristics of magnetic flowmeters, electromagnetic pumps, MHD generators, MHD ship engines, and MHD energy equipment for the transport of objects are included. (M.H.R.)

9267 EFFECT OF EXCITATION RELAXATION ON ELECTRON ENERGY DISTRIBUTIONS. Shaw, David Tai-ko (State Univ. of New York, Buffalo). J. Appl. Phys.; 42: 490-2(Jan 1971).

The depression of the electron energy distribution function in a cesium thermionic discharge was studied in the inelastic region (E > threshold energy for inelastic collisions). The possible departure from the Maxwellian distribution due to excitation relaxation near the emitter of a thermionic converter is considered. It is shown that, at low electron densities, the deviation from the Saha–Boltzmann distribution is significant and the distribution is not Maxwellian. However, the assumption of a Maxwellian distribution is justified, since its relaxation length is very small for typical thermionic plasma conditions. (D.L.C.)

9268 PLAZMENNO TERMOEMISSIONNOE PREOBRAZOVANIE ENERGII. (Plasma Thermionic Energy Conversion). Stakhanov, I. P.; Stepanov, A. S.; Pashchenko, V. P.; Gus'kov, Yu. K. Moscow; Atomizdat (1968). 392p.

Classification of different working regimes of the thermionic converter and the transport theory for 3-component plasma (electrons, ions, and atoms) are presented. Volt–ampere characteristics, density distributions, temperatures, and the electric field between electrodes under different conditions are studied. The methodology of the experimental investigations is stated. Results of calculations are compared with experiment. The effect of different impurities on performance of the cesium thermionic converter was analyzed. (M.H.R.)

Fluid Physics

Refer also to abstract 9263.

9269 (AD-706106) HYPERLIPTIC MAGNETOHYDRODYNAMIC STEADY FLOW PAST A POINT SOURCE. Friedlander, Stanley (New York Univ., N. Y. Courant Inst. of Mathematical Sciences). Mar 1970. 97p. (MF-61; AFOSR-70-527-TR). NTIS.

The disturbance field generated by a point source is obtained for steady, three-dimensional, isentropic, magnetohydrodynamic flow. The flow is governed by the Lindquist equations linearized about constant velocity, matter density, and magnetic field. The flow is assumed to be hyperliptic, i.e., the negative of the free stream velocity lies within the fast wave front of the time-dependent characteristic surface but outside the two cusped slow wave fronts of this surface. There are both real and complex characteristics. (auth) (USGRDR)

9270 HYDROMAGNETIC FREE CONVECTION FOR HIGH AND LOW PRANDTL NUMBERS. Nanda, R. S.; Mohanty, H.K. (Indian Inst. of Tech., Kharagpur). J. Phys. Soc. Jap.; 29: 1608-18(Dec 1970).

Free-convection boundary-layer flow of an electrically conducting fluid past a vertical flat plate in the presence of a magnetic field, perpendicular to the force of gravity, is analyzed. Thermal and viscous boundary layers are separately treated with different polynomials, representing the velocity and temperature profiles in different regions of the boundary layers. The flow, the rate of heat transfer, and the skin friction are discussed for high and low Prandtl numbers. (auth)

9271 TWO-DIMENSIONAL DISTRIBUTION OF CURRENT ALONG MAGNETOHYDRODYNAMIC CHANNELS. Argyropoulos, G. S.; Casteel, M. A.; Demetriades, S. T. (STD Research Corp., Pasadena, Calif.). Energy Convers.; 10: 189-92(Nov 1970).

The distributions of current density, electric field, and plasma properties over the entire length of multi-electrode MHD channels were determined in a realistic two-dimensional solution. It is shown that geometrical effects are often overshadowed by the influence of finite reaction rates, electron energy convection, thermal diffusion, and gasdynamic (thermal and velocity) boundary layers. This theory can analyze and predict experimental results accurately and reliably. (auth) (UK)

9272 CALCULATIONS OF MAGNETOHYDRODYNAMIC GAS-IONIZING SHOCK WAVES. Popov, Yu. P. Zh. Vychisl. Mat. i Mat. Fiz.; 10: 1238-46(Sep-Oct 1970). (In Russian).

The structure of magnetohydrodynamic gas-ionizing shock waves was quantitatively analyzed as a function of various parameters. Characteristic features of the shock transition, particularly the slight dependence of the effective width on conductivity of the media, were determined. A series of peculiarities was found in the calculations of gas-ionizing shock waves in the unsteady state during solution of the total system of MHD equations, including an unusual method for obtaining an accurate "mean time" solution. The influence of pseudo viscosity on the solution is analyzed. (tr-auth)

9273 ELEKTROMAGNITYNE METODY IZMERENIYA PARAMETROV MGD-PROTSESSOV. (Electromagnetic Methods of Measuring the Parameters of MHD Processes). Kisis, A. Yu. (ed.). Riga; Izdatel'stvo Zinatne (1968). 108p.

The following topics are covered: skin-effect of a traveling magnetic field and its use for MHD measurements, differential measurement methods for measuring the flow velocity of electroconducting media, measurement of the flow velocity and calibration of flowmeters by absence of the effect of the traveling magnetic field on liquid metals, measurement of the flow velocity of electroconducting media by the force of the reaction acting on the inductor of the traveling magnetic field, a contactless gage for measuring the flow velocity of a liquid metal using a pulsed magnetic field, effects of inductor geometry and temperatures of the transporting media on the contactless velocity meter for liquid metals, pulse methods for measurement of the flow velocity of liquid metals, an apparatus for the measurement of flow velocity by the pulse method, a conduction pump as a flowmeter, and a contactless measurement of the level of a liquid metal. (M.H.R.)

9274 EFFECT OF A MAGNETIC FIELD ON THERMAL INSTABILITY IN A LAYER OF MAXWELL FLUID. Takashima, M. (Osaka City Univ.). Phys. Lett.; 33A: 371-2(30 Nov 1970).

The stability of a layer of Maxwell fluid heated from below and subject to a magnetic field is considered. Elasticity is found to destabilize the fluid, and the magnetic field is found to be stabilizing. (auth)

9275 PRIKLADNAYA MAGNITNAYA GIDRODINAMIKA. (Applied Magnetohydrodynamics). Novikov, I. I. Moscow; Atomizdat (1969). 360p.

Questions of applied magnetohydrodynamics and magnetogasdynamics are studied in connection with technical applications (particularly, for the analysis and calculations of magnetohydrodynamic generators and electromagnetic pumps). Resistance to movement and heat transfer are investigated in the flow of electroconducting fluids in a magnetic field. The most important kinds of MHD flows are examined, and their calculation methods are given. The properties of MHD flows are systematized and examined. (M.H.R.)

9276 FLOW OF FLUIDS WITH TEMPERATURE-DEPENDENT TRANSFER COEFFICIENTS IN A FLAT CHANNEL. Filippov, S. S. Heat Transfer-Sov. Res.; 2: No. 5, 1-5(Sep 1970).

The effect of temperature dependence of viscosity and electrical conductivity coefficients on the laminar flow of an incompressible fluid between parallel, nonconducting walls in crossed electric and magnetic fields (the latter applied perpendicular to the walls) is studied. A pressure gradient exists along the flow. Nonisothermal analogies of Hartman, Poiseuille, and Couette flows are described by a nondecomposable system of nonlinear equations for velocity and temperature as particular cases, depending on the selection of the problem's parameters and boundary conditions for the velocity. However, unlike the case of constant transfer coefficients, the behavior of the flow depends markedly also on the boundary conditions for the temperature; thus, an asymmetric temperature distribution produces an asymmetry in the velocity distribution. Cases are considered of decreasing as well as of increasing transfer coefficients with increasing temperature, depending on the different behavior of this relationship for liquid metals, electrolytes, and ionized gases. A number of qualitative physical regularities, obtained by numerical solution of the problem on an electronic computer and illustrated by graphs, are discussed. (auth)

9277 DISTRIBUTION OF THE CONCENTRATION OF A BINARY MIXTURE IN A FILM MOVING ALONG THE WALLS OF A ROUND PIPE IN THE PRESENCE OF AN EXTERNAL INHOMOGENEOUS MAGNETIC FIELD. Voronina, S. M.; Atroshchenko, L. S. Heat Transfer - Sov. Res.; 2: No. 5, 6-13(Sep 1970).

An analytic expression is obtained for the distribution of components of a binary mixture in the liquid film in the form of rapidly converging infinite series. The magnetic part is isolated and the extent is determined of the effect of the magnetic field on the redistribution of components and on the length of the initial segment. The known distribution is obtained in the absence of a magnetic field. It is shown that the magnetic field appreciably intensifies the component redistribution process and reduces the length of the initial segment, which makes it possible to improve the design-parameter variables of film-type separating devices by using an external inhomogeneous magnetic field. (auth)

9278 PRESSURE SHOCKS IN DISSIPATIVE MAGNETO-GASDYNAMICS. Rao, M. P. Ranga; Chaturani, P. (Indian Inst. of Tech., Bombay). Indian J. Pure Appl. Math.; 1: 258-64 (Apr 1970).

The propagation of pressure shocks through a finitely electrically conducting, viscous, and heat-conducting gas in the presence of a uniform magnetic field is studied theoretically. The novel features of the problem are the anisotropic nature of the wave propagation and the existence of a simple relation between the vorticity jumps and the current density. (auth)

9279 HYDROMAGNETIC STABILITY OF STATICALLY UNSTABLE HETEROGENEOUS SHEAR FLOW. Agrawal, S. C.; Agrawal, G. S. (Indian Inst. of Tech., Kanpur). Indian J. Pure Appl. Math.; 1: 235-42(Apr 1970).

The stability of nondissipative heterogeneous shear flow in the presence of a uniform magnetic field applied in the streaming direction is investigated theoretically. The density increases vertically upwards. It is shown that the presence of a magnetic field inhibits the onset of instability, and the bounds for the complex wave velocity of an arbitrary unstable mode are also discussed. If the magnetic force number is small, then the entire wave-number range is discussed, and it is shown that short-wavelength perturbations are damped in its presence while the instability for long wavelengths is not affected. (auth)

9280 HYDROMAGNETIC FLOW NEAR AN ACCELERATED FLAT PLATE. Dube, Shishir Kumar (Lucknow Univ., India). Indian J. Pure Appl. Math.; 1: 170-7(Apr 1970).

Unsteady flow of a viscous incompressible and electrically conducting fluid past an infinite flat plate in the presence of a uniform transverse magnetic field is studied for the two cases when the plate is (i) a perfect conductor, and (ii) an insulator.

XUM

The plate is assumed to start at time t = 0 with velocity U(t) in its plane. Using the Laplace transform technique, general formulas for the velocity, induced magnetic field, and current density are obtained as a function of U when the magnetic Prandtl number is unity. The case of a uniformly accelerated plate is studied in detail. (auth)

9281 INTERACTIONS OF FLOWING ARGON PLASMA IN A CHANNEL WITH A TRANSVERSE MAGNETIC FIELD. Petrova, G. P.; Chekalin, E. K. pp 101-5 of Svoistva Gazov pri Vysokikh Temperaturakh. Predvoditelev, A. S. (ed.). Moscow; Izdatel'stvo Nauka (1967). (In Russian).

An attempt was made to determine the magnetohydrodynamic properties of a steady argon plasma flowing in a channel with cooled walls. (R.V.J.)

9282 BEHAVIOR OF FREE-BURNING ELECTRIC ARCS IN TRANSVERSE MAGNETIC FIELDS AND GAS FLOWS. Bartels, K.; Uhlenbusch, J. (RWTH, Aachen). Atomkernenergie; 16: 263-9(1970). (In German).

Methods for magnetohydrodynamic treatment of a free-burning arc in transverse magnetic fields and gas flows are surveyed. The solid-body model, mechanical similarity behavior, the arc as a source of volume, and mechanisms of retrograde motion are discussed. Experimental investigations of the magnetohydrodynamic response of the arc column to external oscillating magnetic fields are reported. (auth)

Geophysics (Upper Atmosphere)

9283 (AD-709888) IONOSPHERIC ELECTRON DENSITY PROFILE MODEL. Damon, Thomas D.; Hartranft, Franklin,R. (Weather Wing (4th), Ent AFB, Colo.). Jul 1970. 39p. (WW-TM-70-3). NTIS.

The ionospheric electron-density profile model presented consists of the sum of three Chapman layers (E, F1, F2). Electron densities in the topside ionosphere are controlled by complex motions rather than a production-loss balance and cannot be successfully described strictly by a Chapman layer. After some experimentation, a best fit was obtained by simply using the Chapman equation for the topside ionosphere, but computing the electron densities by using a variable scale height throughout the region. The program described was used routinely for eight months to predict profiles for radar refraction. Improvements in accuracy will be required as the model is evaluated for different purposes. (auth) (USGRDR)

9284 (JPRS-52023) AURORAL STUDIES AT CONJUGATE POINTS. Isaev, S. I. Translated from pp 3-18 of Kompleksnye Issledovaniya Polyarnoy Ionosfery. Leningrad; Izd-vo Nauka (1970). 16p. NTIS.

A review is presented of various phenomena that have been observed or detected at auroral conjugate points. Roderer classified conjugate phenomena by classes and types. The information is confined to areas of a finite section bounded by lines of force. Conjugacy by visual observation and on photographic data is discussed. Simultaneous photoelectric investigations were made from Nov. 1961 through Apr. 1962 by the USSR Academy of Sciences and the French National Space Research Center. During investigations of the conjugacy of the auroral hydrogen emission, it is noted that not only form of the zone, its position, size, and dynamics were conjugate, but also the difference in the intensity of hydrogen emission on the daytime and nighttime sides of the Earth was always situated approximately 5° closer to the equator than visual auroral forms. Total conjugacy of aurorae is not probable and continued investigations are necessary. 33 references. (J.C.W.)

9285 (MPI-PAE/EXTRATERR-49/70) MEASUREMENTS OF ELECTRIC FIELDS IN EQUATORIAL AND MEDIUM LATITUDES DURING TWILIGHT USING BARIUM ION CLOUDS. Rieger, E. (Max-Planck-Institut fuer Physik und Astronphysik, Munich (West Germany)). Sep 1970. 19p. Dep. NTIS (U. S. Sales Only).

Measurements of the ionospheric electric field at low and medium magnetic latitudes, using barium ion clouds, are summarized. The measured field strengths range from 0.3 to about 4.0 V/km. The field vectors are pointing preferentially southward during evening twilight and northward during morning twilight on the northern hemisphere at midlatitudes. At the equator, the vertical component exceeds the horizontal by a factor of about 3. Here the drifts are west and upward in the evening and east and downward in the morning. The implications of the observations on the Sq current are discussed, and evidence for the dynamo action of the atmosphere is derived in some cases, preferentially evening experiments. At the geomagnetic equator the ionospheric current appears to be driven by the electric polarization field. (auth)

9286 (TT-67-51394/1) ATMOSPHERIC ELECTRICITY. VOLUME I. FUNDAMENTALS, CONDUCTIVITY, IONS. Israel, H. Translation of Probl. Kosm. Phys.; 29: (1957). 326p. (IPST-Cat.-1995). NTIS.

Authorized and revised translation from the second German edition.

Topics covered in this treatise include a brief historical survey, nonself-sustaining discharges, self-sustaining discharges, ionizing agencies, atmospheric electric phenomena, conductivity, ions, nuclei, ion balance of the atmosphere, measuring techniques, and reference tables. (W.D.M.)

9287 MID- TO HIGH-LATITUDE IONOSPHERIC ELECTRON CONTENT. Lyon, G. F. (Univ. of Western Ontario, London). J. Atmos. Terrest. Phys.; 32: 1737-45(Nov 1970).

Steep content gradients associated with the main trough are observed in high-latitude beacon satellite observations. Data from two stations in line on the sub-satellite track are examined for evidence of solar control of the ionosphere equatorward of the trough. While such control is sometimes exercised, there are many occasions when it is either absent or masked by other effects. No clear pattern of behavior could be established. (auth) (UK)

9288 ON THE INFLUENCE OF ENERGETIC ELECTRON PRECIPITATION ON THE WATER CLUSTER ION POPULATION IN THE UPPER D REGION. Brown, R. R. (Univ. of California, Berkeley). J. Atmos. Terrest. Phys.; 32: 1747-53(Nov 1970).

Calculations were carried out to show the influence of energetic electron precipitation on the water-cluster ion composition in the 80- to 100-km region. The results obtained indicate that the relative abundance of cluster ions is shifted; disturbed conditions favor the emergence of intermediate ions at the expense of water cluster ions further along the cluster chain. The extent of this shift is shown for various water mixing ratios. (auth) (UK)

9289 COMPARISONS BETWEEN CALCULATED IONOSPHERIC ABSORPTION AND RIOMETER MEASUREMENTS. Heisler, R.; Hower, G. L. (Washington State Univ., Pullman). J. Atmos. Terrest. Phys.; 32: 1755-64(Nov 1970).

Calculations of the absorption that a given riometer system would expect to measure are made for both solar maximum and solar minimum conditions. These calculations utilize ray-tracing procedures and are based on available electron density and collision frequency or temperature profiles. For middle latitudes during the solar minimum, nearly all cosmic-noise absorption occurs in the D and E layers and is the result of electron-neutral collisions. During the solar maximum, about half of the total absorption occurs in the F layer. Approximately half of the apparent F-layer absorption is a result of the window effect, while the remaining half arises through electron-ion collisions. A comparison between calculated and measured absorption leads to the conclusion that high nighttime-absorption levels observed at many stations are the result of errors in setting the level of the quiet-day curve. It is also argued that daytime-absorption levels are significantly affected by the presence of solar noise during the solar maximum period. (auth) (UK)

9290 ON THE OCCURRENCE OF SPREAD F AND THE GEOMAGNETIC ACTIVITY OVER TAIPEI, TAIWAN. Huang, Yinn-nien; Yeh, Chung-yauw (Ministry of Communications, Chung-li, Taiwan). J. Atmos. Terrest. Phys.; 32: 1765-72(Nov 1970).

The ionospheric data obtained at Taipei during the period of July 1957 to June 1968 is used to investigate the solar cycle and seasonal and diurnal changes of the effects of the geomagnetic activity on the occurrence of spread-F activity. The cross-correlation analysis is also used to determine the correlation coefficients with time shifts up to 10 days. The results show that the spread-F activity is negatively correlated with the geomagnetic activity throughout the years under investigations except for the year 1961; there are two types of spread-F activity: one is the equinoctial-type that usually occurs during high solar activity and has its seasonal-activity peaks in equinoctial months and diurnal peak in 2200 LST; the other is the summer-type that usually occurs during low solar activity and has its seasonal activity peak in summer, and diurnal peak in 0200 LST. It is suggested that the equinoctial-type is closely associated with the appearance of the post-sunset peak of f_0F2 and is formed by the field aligned ionization irregularities caused by the fountain effect; and the summer type is formed by the ionization irregularities, which are always existing in the topside ionosphere. (auth) (UK)

9291 EQUATORIAL F2-LAYER ANOMALY AND THE q-TYPE SPORADIC-E LAYER OF THE IONOSPHERE. Kotadia, K. M.; Patel, J. C. (Bujarat Univ., Ahmedabad, India). J. Atmos. Terrest. Phys.; 32: 1773-80(Nov 1970).

A study is made of the midday (0900–1500 hr) critical frequencies of the F2 layer and the q-type sporadic-E layer for the IGY, IGC and IGCE years 1957–1960 to examine the association of the F2 layer anomalies with the equatorial electrojet. It is concluded from normal, abnormal, and lunar tidal variations of f_0F2, f_0E_{sq}, and the H component of the Earth's magnetic field that the equatorial F2-layer anomalies are largely due to the vertical drift of electrons caused by the E–W electric field associated with the current in the electrojet or the dynamo E region and the Earth's magnetic field. (auth) (UK)

9292 ATTENUATION OF ELF AND VLF RADIO WAVES PROPAGATING BELOW INHOMOGENEOUS ISOTROPIC IONOSPHERES. Barr, R. (King's Coll., London). J. Atmos. Terrest. Phys.; 32: 1781-91(Nov 1970).

Computations were made of the attenuation suffered by elf and vlf radio waves propagating under ionospheres having realistic variations of electron density and collisional frequency with height. In all cases, attenuation values were observed that are much greater than values obtained previously for propagation under accepted ionosphere models, especially in the region 1 to 4 kHz. These high values of attenuation are also much greater than the presently accepted experimental attenuation values in this region. Modal interference was also shown to play an important role in the propagation in this heavily attenuated region. (auth) (UK)

9293 GRAVITY WAVES GENERATED DURING MAGNETIC SUBSTORMS. Testud, J. (Centre National d'Etudes des Telecommunications, Issy-les-Moulineaux, France). J. Atmos. Terrest. Phys.; 32: 1793-1805(Nov 1970).

During magnetically disturbed days, wind and temperature data obtained in the F-region from incoherent scatter, show strong oscillations of the ion temperature and velocity with period of some 2 hr. These oscillations can be interpreted as due to atmospheric gravity waves traveling southwards. The data are compared to auroral magnetograms. Temperature and velocity oscillations appear to follow magnetic events such as substorms, with a time delay of about one hour. Theoretical computations show that the intense heat deposited in the auroral E region during a magnetic substorm, can generate atmospheric waves which propagate towards middle latitudes. The characteristics of the computed waves are in close agreement with the observed ones. Finally, the calorific energy deposited at middle latitudes by dissipation of such waves is evaluated. The resulting thermospheric temperature increase is comparable to that predicted by Jacchia's model. (auth) (UK)

9294 SOME GEOGRAPHIC AND GEOPHYSICAL ASPECTS OF ELECTRON CONTENT MEASUREMENTS FROM SATELLITE RADIO BEACON TRANSMISSIONS. Tyagi, Tuhi Ram; Mitra, A. P. (National Physical Lab., New Delhi). J. Atmos. Terrest. Phys.; 32: 1807-18(Nov 1970).

Geographic distribution of the ionospheric electron content was studied from the Faraday rotation of satellite radio transmissions recorded at several stations in the Indian zone. The effect of large-scale ionospheric irregularities on the Faraday rotation rate and rotation angle was demonstrated. The integrated electron production rate was obtained as a function of solar activity from the rate of change of electron content around sunrise for the period October (1964) to September (1968) (the rising half of the present solar cycle) and compared with other estimates, both theoretical and experimental. There are days of unusually high electron content apparently unrelated to any observed geophysical event; these days also show high 30-MHz cosmic radio noise absorption and the two are linearly related. (auth) (UK)

9295 TRAVELING DISTURBANCES IN THE IONOSPHERIC F REGION AND THE SPORADIC-E REGION. Sharadze, Z. S. (Tomsk State Univ., USSR). Izv. Vyssh. Ucheb. Zaved., Radiofiz.; 13: 1001-11(1970). (In Russian).

Results are given from investigations of traveling disturbances (TD) over Tbilisi for the period 1964 to 1967. The relation of TD with E_s region is analyzed. TD may be associated with internal gravity waves propagated in the ionosphere. (auth)

9296 D-REGION SUNRISE AURORAL ROCKET FLIGHT. Armstrong, R. J.; Folkestad, K.; Troeim, J. (Norwegian Defence Research Establishment, Kjeller). J. Atmos. Terrest. Phys.; 32: 1505-17(Sep 1970).

The flight of a rocket (F16) from Andöya, Northern Norway, into a sunrise aurora in winter is described and certain aspects of the experimental payload discussed. The results obtained with ultraviolet and visible sensors, an ion analyzer, and from Faraday rotation experiment indicate that a sharp transition occurred in ionospheric properties at about 73 km probably connected with the appearance of solar radiation of about 3180 Å at that altitude. There is also clear evidence that the total ozone concentration above 40 km was less than that observed on earlier midlatitude rocket flights. (auth) (UK)

9297 CHANGES IN D-REGION CHEMISTRY CONSISTENT WITH RADIO OBSERVATIONS. Doherty, R. H. (ESSA Research Lab., Boulder, Colo.). J. Atmos. Terrest. Phys.; 32: 1519-33 (Sep 1970).

Radio propagation may be related to D-region chemistry through the control of electron concentrations by atomic oxygen and ozone. A meteorological variable, water vapor, can appreciably affect the atomic oxygen and ozone concentrations in the height range where H_2O is dissociated by solar radiation or particle influx. Furthermore, the chemical reactions between the H_2O dissociation products and the O and O_3, produce heating that could influence the atmospheric temperatures. Winter variability and summer stability of both the radio propagation and the upper atmospheric temperatures, at high latitudes, could be related to the change of the water vapor height distribution. Seasonal changes in the radio observations at high latitudes are shown to be consistent with the proposed theory at frequencies from vlf to hf. Low frequency observations during a solar eclipse and following a nuclear detonation are interpreted on the basis of photochemical changes in the $[O]/[O_3]$ ratio. In the summer a large negative temperature gradient exists between 50 and 80 km, but winter measurements show higher temperatures and a smaller or no negative temperature gradient. It is suggested that water vapor concentrations above 50 km, which are less in the summer than in the winter, may explain these observations. Lower H_2O concentrations in the summer, caused by increased solar radiation capable of dissociating H_2O, would tend to reduce variations in temperature and electron densities, which are produced by changes in the H_2O dissociation rates and subsequent reactions with other constituents. In fall and winter the temperatures in the 50 to 80 km height range may rise as a result of increased water vapor, because there is less solar dissociation in the lower (<60 km) regions, allowing eddy and molecular diffusion to increase H_2O higher in the atmosphere. Particle influx may become relatively more important in dissociating water vapor in the winter. (auth) (UK)

9298 ELECTRON PRECIPITATION ASSOCIATED WITH SUDDEN COMMENCEMENT OF A GEOMAGNETIC STORM. Ullaland, S. L. (Univ. of Bergen, Norway); Wilhelm, K.; Kangas, J.; Riedler, W. J. Atmos. Terrest. Phys.; 32: 1545-53(Sep 1970).

Balloon observations of x-rays produced by precipitated electrons were made in the morning sector of the auroral zone at the time of the geomagnetic storm sudden commencement (SSC) of July 27, 1966. The impulsive precipitation event lasted 4 min, both the rise and fall times being nearly 1 min. On a shorter time scale, a pronounced variation with a period of 1.8 to 1.9 sec existed, which occurred together with hm emissions of the same period range. Besides the rapid fluctuations in the precipitation, a 50-sec period was also present. The energy spectrum of the observed x-ray flux was rather steep, characterized by an e-folding energy of E_0 = 18 to 22 keV. The SSC apparently triggered a polar magnetic substorm in the midnight sector of the auroral zone. (auth) (UK)

9299 THEORY FOR QUASI-PERIODIC OSCILLATIONS OBSERVED IN THE IONOSPHERE. Jones, W. L. (National Center for Atmospheric Research, Boulder, Colo.). J. Atmos. Terrest. Phys.; 32: 1555-66(Sep 1970).

Particular characteristics of the normal modes of oscillation of the atmosphere are brought forth to explain quasi-periodic motions observed in the ionosphere. These include disturbances of periods of 1 min associated with low-level nuclear explosions, 2 to 5 min associated with thunderstorms, and 10 to 15 min found under quiet ionospheric conditions. (auth) (UK)

9300 OBSERVATIONS OF ELECTRON DENSITY DURING A SOLAR FLARE. Rowe, J. N. (Pennsylvania State Univ., University Park); Ferraro, A. J.; Lee, H. S.; Kreplin, R. W.; Mitra, A. P. J. Atmos. Terrest. Phys.; 32: 1609-14(Sep 1970).

Electron density profiles were obtained from high power wave interaction measurements at The Pennsylvania State University during a solar flare which occurred on October 21, 1968. The results indicate increases in electron density at all heights in the D-region, but especially above 70 km. The electron production rates were calculated from the NRL measured 0 to 3 and 0 to 8 Å flux, and compared with the changes in electron density. It is concluded that the non-x-ray production rate at 80 km is less than 10 cm^{-3} sec^{-1}. (auth) (UK)

XUM

9301 INVESTIGATION OF THE OPERATION OF A DC ELECTRIC FIELD DETECTOR. Fahleson, U. V.; Kelley, M. C.; Mozer, F. S. (Univ. of California, Berkeley). Planet. Space Sci.; 18: 1551-61(Nov 1970).

Double Langmuir-probe detector systems were flown successfully on three rockets in the past two years to measure quasi-static and ac electric fields in the auroral-zone ionosphere. Diagnostic tests and redundancy features associated with these experiments are investigated to show that the instruments performed as expected theoretically and that dc electric fields with typical magnitudes of 20 to 40 mV/m have been measured with 10 to 20% accuracy. Uncertainties of the measurement that are considered include sheath potential and sheath resistance effects, photoemission, energetic particle currents, wake effects, asymmetries from the presence of the booms and the rocket body, contact potentials, and the subtraction of $\bar{v} \times \bar{B}$ from the rocket data to obtain electric fields in an Earth-fixed frame of reference. (auth) (UK)

9302 TRANSPORT PROPERTIES OF THE IONOSPHERIC ELECTRON GAS. Schunk, Robert W.; Walker, James C. G. (Yale Univ., New Haven). Planet. Space Sci.; 18: 1535-50 (Nov 1970).

The transport coefficients of the ionospheric electron gas—thermal conductivity, electrical conductivity, current flow conductivity due to thermal gradients, and heat flow conductivity due to electric fields—were evaluated. Shkarofsky's formulation was used, making it possible to allow rigorously for the velocity dependence of electron–electron, electron–ion, and electron–neutral collision frequencies. The transport coefficients at all altitudes from the weakly ionized limit at 100 km to the fully ionized limit at 600 km were calculated. The accuracy of an expression for the thermal conductivity in the ionosphere derived by Banks was confirmed but an error in the expression for the electrical conductivity was used in some ionospheric studies. Possible thermoelectric effects on ionospheric electron temperatures were explored and it is concluded that temperatures are significantly affected by field-aligned currents of about 10^{-5} amp m^{-2}, such as appear to flow in the auroral oval. (auth) (UK)

9303 PARALLEL AND PERPENDICULAR ELECTRIC FIELDS IN AN AURORA. Mozer, F. S.; Fahleson, U. V. (Univ. of California, Berkeley). Planet. Space Sci.; 18: 1563-71(Nov 1970).

Previously reported results of a rocket-borne electric field experiment flown near local midnight from Andenes, Norway were transformed to an Earth-fixed coordinate system and compared with plasma temperature and density measurements, energetic particle fluxes, and perpendicular electric field variations, to strengthen the earlier conclusion that ~10 mV/m electric fields existed parallel to the magnetic field line during the flight. Perpendicular electric field measurements made as the rocket crossed six auroral-arc boundaries indicated that the mean electric field strength did not vary across the boundary of an arc but that the boundary was often characterized by charge oscillations having periods of a few seconds. (auth) (UK)

9304 SEMI-ANNUAL VARIATION IN THE UPPER ATMOSPHERE DURING 1967 AND 1968. Cook, G. E. (Royal Aircraft Establishment, Farnborough, Eng.). Planet. Space Sci.; 18: 1573-84(Nov 1970).

The orbits of five satellites were analysed to reveal the semi-annual variation in air density at heights between 300 and 505 km during the period of high solar activity in 1967 and 1968, and the results combined with data from other satellites. The semi-annual effect shows considerable variation from cycle to cycle, both in magnitude and in the form of the height dependence. The dates of the maxima and minima given by the individual satellites each year are in very good agreement with each other and are close to the mean values obtained by Jacchia, Slowey and Campbell for the years 1958–1966; this suggests the effect is more regular in its timing than has previously been assumed. The main difficulty in interpreting the results is the lack of data at heights below 250 km. At times the observed magnitudes are compatible with a variation solely in exospheric temperature due to temperature changes in the thermosphere, whereas at other times a variation in conditions at the lower boundary near the turbopause (about 110 km) is required. (auth) (UK)

9305 ATMOSPHERIC GAMMA RAYS AT BALLOON ALTITUDES. Cortellessa, Paolo; di Benedetto, Paolo; Paizis, Constantinos (CNR, Milan). Planet. Space Sci.; 18: 1607-10(Nov 1970).

The omnidirectional intensity of atmospheric γ rays at balloon altitudes was measured at three energy thresholds. A value of 3.3×10^{-1} cm^{-2} sec^{-1} was found for energies greater than 20 MeV. A flattening of the integral spectrum was observed at lower energies. (auth) (UK)

9306 DISCONTINUITIES IN AN ANISOTROPIC PLASMA AND THEIR IDENTIFICATION IN THE SOLAR WIND. Hudson, P. D. (Imperial Coll. of Science and Tech., London). Planet. Space Sci.; 18: 1611-22(Nov 1970).

The types of discontinuity which can occur in a magnetohydrodynamic fluid with anisotropic pressure are discussed. Rules are given for the identification of the type of discontinuity together with equations to determine their orientation and velocity. In general, rotational discontinuities do not conserve density and field strength, and some of these in the solar wind may have been misidentified as shocks or tangential discontinuities. (auth) (UK)

9307 METEOR IONISATION IN THE E LAYER. Lebedinets, V. N.; Shushkova, V. B. (Academy of Science, Moscow). Planet. Space Sci.; 18: 1659-63(Nov 1970).

Active meteor ionisation, which is due to the collision of fast meteor atoms and molecules with atmospheric molecules while a meteoroid is moving in the atmosphere, is discussed. The contribution to ionization from (1) evaporation, which gives the main contribution to the ablation process in the case of meteroids and (2) sputtering, which is largely responsible for the ablation of micrometeorites is considered. Graphs showing the contribution to ionisation by meteors and micrometeorites are given, discussed and explained. (UK)

9308 COMPARISONS OF SIMULTANEOUS SATELLITE AND GROUND-BASED MEASUREMENTS OF IONOSPHERIC PARAMETERS. Taylor, G. N.; Wrenn, G. L. (Royal Radar Establishment, Malvern, Eng.). Planet. Space Sci.; 18: 1663-6 (Nov 1970).

Measurements of electron temperature, positive ion temperature, and plasma concentration made simultaneously by the Langmuir plate and spherical ion probe experiments on the Explorer 31 satellite, and by an incoherent scatter radar at Malvern, England, are compared. No significant systematic discrepancies are found. (auth) (UK)

9309 IONOSPHERIC OBSERVATIONS DURING THE ANNULAR SOLAR ECLIPSE OF MAY 20, 1966. I. INTENSITY AND ATMOSPHERIC ABSORPTION OF HYDROGEN LYMAN-α RADIATION. Hall, J. E. (Radio and Space Research Station, Ditton Park, Eng.). J. Atmos. Terrest. Phys.; 32: 1849-54 (Dec 1970).

The intensity of hydrogen Lyman-α was measured before and during the solar eclipse of May 20, 1966. The intensity of the full Sun was 3.6 erg cm^{-2} s^{-1} and of the 56% eclipsed Sun, 2.1 erg cm^{-2} s^{-1}. An estimate was made of the production of ionization in the D region by Lyman-α acting on nitric oxide. The molecular oxygen density from 70 to 85 km was deduced from the absorption of Lyman-α in the atmosphere, and the height variation of electron collision frequency was calculated from the air pressure. (auth) (UK)

9310 IONOSPHERIC OBSERVATIONS DURING THE ANNULAR SOLAR ECLIPSE ON MAY 20, 1966. II. POSITIVE ION PROBE OBSERVATIONS. Willmore, A. P. (University Coll., London). J. Atmos. Terrest. Phys.; 32: 1855-8(Dec 1970).

Results obtained from a cylindrical ion probe on each Arcas rocket fired in the solar eclipse campaign of May 20, 1966 in Greece were described and analysed by Bowling et al. (1967). However, results obtained from a subsequent study of the operation of these probes are used in a rediscussion of the observations, and in particular, it is found that the original conclusion that solar x-rays are responsible, even under quiet conditions, for an important fraction of the ionization near 75 km, is no longer justified. (auth) (UK)

9311 IONOSPHERIC OBSERVATIONS DURING THE ANNULAR SOLAR ECLIPSE OF MAY 20, 1966. III. FOUR D-REGION ELECTRON DENSITY PROFILES MEASURED BY ROCKET TECHNIQUES. Jespersen, M.; Pedersen, B. Moeller (Danish Space Research Inst., Lyngby). J. Atmos. Terrest. Phys.; 32: 1859-63 (Dec 1970).

Measurements of Faraday rotation and of differential absorption on frequencies 2.2, 3.9, and 7.8 MHz were used to determine the height distribution of collision frequency and electron concentration during the annular solar eclipse of May 20, 1966 and on a comparison day. (auth) (UK)

9312 IONOSPHERIC OBSERVATIONS DURING THE ANNULAR SOLAR ECLIPSE OF MAY 20, 1966. IV. D-REGION ELECTRON DENSITIES DERIVED FROM MEASUREMENTS OF PARTIAL REFLECTIONS. Haug, A. (Norwegian Defence Research Es-

tablishment, Kjeller); Thrane, E. V.; Tsagakis, E.; Anastassiades, M. J. Atmos. Terrest. Phys.; 32: 1865-71(Dec 1970).

The partial reflection technique was used to measure the time variations of D-region electron densities at 74 and 80 km throughout the solar eclipse of May 20, 1966. The average diurnal variation of the electron density was also derived from measurements over a period of about two weeks prior to the eclipse. The results are presented and compared with A_1-absorption measurements. (auth) (UK)

9313 IONOSPHERIC OBSERVATIONS DURING THE ANNULAR SOLAR ECLIPSE OF MAY 20, 1966. V. INTERPRETATION OF OBSERVED RESULTS. Landmark, B. (European Space Research Organization, Neuilly-sur-Seine, France); Haug, A.; Thrane, E. V.; (and others). J. Atmos. Terrest. Phys.; 32: 1873-83(Dec 1970).

The interpretation of results from ionospheric observations during the annular solar eclipse of 20 May 1966 is discussed. Observations were made of Lyman-α intensities, positive ion density, and electron density. From the observational results it is possible to estimate how the effective loss rate $\alpha_{eff} = q/N^2$ varies through the eclipse. It is concluded that the observed results can be explained in terms of a model of recombination in which two types of positive ions having markedly different recombination rates are present. Near 80 km this model predicts, and the results show, that electron density, N, is proportional to production, q, rather than $q^{\frac{1}{2}}$ as usually assumed. (auth) (UK)

9314 YIELD OF O(^{1}D) BY DISSOCIATIVE RECOMBINATION OF O_2^+ FROM NIGHT AIRGLOW OBSERVATIONS. Forbes, Jeffrey M. (Univ. of Illincis, Urbana). J. Atmos. Terrest. Phys.; 32: 1901-8(Dec 1970).

Ground-based photometer observations of the O I(6300 Å) night airglow compared with theoretical calculations of the integrated 6300-Å vertical volume emission rate indicate a yield of 0.15 ± 0.07 O(^{1}D) atoms per recombination of O_2^+ at 1000 K, including the $^1S \rightarrow {}^1D$ cascade effect. Implications of this result on the possible contribution of the dissociative recombination of NO^+ to the O I (6300 Å) night airglow are also discussed. (auth) (UK)

9315 EFFECT OF ELECTRIC FIELDS ON THE F-REGION BEHAVIOUR AS COMPARED WITH NEUTRAL WIND EFFECTS. Stubbe, P. (Max-Planck Institut fuer Aeronomie, Lindau, Ger.); Chandra, S. J. Atmos. Terrest. Phys.; 32: 1909-19(Dec 1970).

Numerical solutions of the coupled-ion and electron-continuity equations, ion and neutral dynamical equations, and ion and electron heat conduction equations are used to determine the relative importance of neutral winds and electric fields in the diurnal behaviour of the F-layer. The main results, derived for the mid-latitude ionosphere at equinox and medium solar activity, are given. (1) The W–E electric field giving about the same effect in F layer as a N–S wind based on Jacchia's model has a maximum of 7 V/km at 0200 hr and a minimum of –5 V/km at 1800 hr; (2) At night, the total vertical electron–ion velocity above 300 km is about zero; (3) Above 300 km, therefore, the electron–ion velocity along the magnetic lines of force is proportional to the W–E electric field strength E_y. Vasseur's measurements indicate that E_y is smaller than 2 V/km at night. (4) Ion temperature measurements with the incoherent backscatter technique give a much larger temperature amplitude than assumed in Jacchia's model. If Jacchia's model is modified correspondingly, an unrealistically large rise is obtained of the F-layer height at night. The electric W–E field that would suitably reduce the height rise is much larger than permitted by Vasseur's results. The solution to this problem seems to lie in introducing variable lower boundary conditions in the atmospheric model. (auth) (UK)

9316 TEMPERATURE AND COMPOSITION OF THE IONOSPHERE: DIURNAL VARIATIONS AND WAVES. Wand, R. H. (Univ. of Sydney); Perkins, F. W. J. Atmos. Terrest. Phys.; 32: 1921-43(Dec 1970).

The ion temperature, electron temperature, and the relative concentration of atomic ions (O^+) to molecular ions (NO^+ and O_2^+) are derived from Thomson scatter measurements in the height range 115 to 430 km above Arecibo, Puerto Rico. A double-pulse measurement technique was employed, permitting autocorrelation functions of the ion component of the Thomson scatter signal to be obtained with an altitude resolution of 15 km. In general, only two of the three unknowns could be determined directly from each measured autocorrelation function and two alternative methods of supplying the other parameter were used, viz. ion temperature models and ion composition models. The use of an ion composition model was appropriate when wave-like variations in ion temperature were found to be present in addition to the expected diurnal ion temperature variation due to solar heating. On occasions when the temperature waves were absent, temperature models were used to derive the diurnal ion composition variation. The average ion composition was substantially in agreement with rocket measurements. Daytime electron and ion temperatures were equal at 130 km while at greater heights the electrons were hotter than the ions. Above approximately 200 km, the shape of the electron temperature profile was strongly influenced by the electron density. (auth) (UK)

9317 POLAR MAXIMUM OF ELECTRON CONCENTRATION AT 1000-km ALTITUDE. Brace, L. H. (Goddard Space Flight Center, Greenbelt, Md.); Mayr, H. G.; Mahajan, K. K. J. Atmos. Terrest. Phys.; 32: 1945-57(Dec 1970).

Satellite probe measurements from a circular, polar orbit at 1000 km revealed a broad enhancement of ionization within the polar cap. The latitude of the maximum concentration closely followed the seasonal movement of the solar terminator across the polar cap. The peak is bounded on its nightside by a solar zenith angle of about 110° and on its dayside by a broad mid-latitude trough near 60° geomagnetic latitude. Thus one boundary of the peak, and the location of the maximum, is strongly influenced by solar zenith angle while the other boundary is geomagnetically fixed. Although the ionization and heating observed in the peak clearly arises from solar radiation, the most intriguing question is why a peak should be formed at all since this cannot be produced by zenith angle variations alone. The answer appears to lie in the mechanisms which produce the mid-latitude trough on the dayside. To explain the trough the effects of neutral atmospheric winds flowing poleward on the dayside of the Earth in response to solar heating are invoked. The observations are shown to agree quantitatively with solutions of the energy and particle equations of the plasma when a neutral wind field derived from a Jacchia model atmosphere is introduced and suitable allowance is made for an upward proton flux at high latitudes. It is concluded that the polar peak discussed here and the one observed by Nishida and interpreted as a neutral point phenomenon may actually be the same feature. Nishida's study employed only data acquired near equinox, thus he could not resolve the seasonal movement described here. (auth) (UK)

9318 BEHAVIOUR OF THE ARCTIC F REGION IN WINTER. Challinor, R. A. (Radio and Space Research Station, Ditton Park, Eng.). J. Atmos. Terrest. Phys.; 32: 1959-65(Dec 1970).

The behaviour of the Arctic F region was examined in order to investigate further the tentative conclusion (DUNCAN, 1962) that a certain degree of "Universal Time control" is observed there during winter. Secondary maxima in the F2-layer critical frequency, which are not associated with local noon, do indeed appear at a number of Arctic stations during winter. These appear at various Universal Times, and so do not demonstrate the existence of any Universal Time control. It is shown that they could be produced by vertical ionospheric drifts caused by horizontal neutral-air winds in the F region. (auth) (UK)

9319 LOW IONIZATION PROBLEM IN IONOSPHERIC TRUE-HEIGHT ANALYSES. Saha, A. K. (Univ. of Queensland, Brisbane). J. Atmos. Terrest. Phys.; 32: 1967-73(Dec 1970).

In the light of information available from various sources about ionization below the nighttime F-layer, an attempt is made to estimate possible errors involved when true-height reduction of nighttime ionograms are used at about 1 MHz at the low-frequency end assuming a flat base of the F layer below the f_{min}. It is shown that the errors are usually not as high as is often believed. A simple approximate procedure to allow for the low-lying ionization, applicable in certain cases, is suggested. (auth) (UK)

9320 ASSOCIATION BETWEEN X RAYS AND AURORAL RADAR ECHOES IN THE SOUTHERN AURORAL ZONE. Keys, J. G. (PEL Auroral Station, Omakau, N. Z.). J. Atmos. Terrest. Phys.; 32: 1975-81(Dec 1970).

Balloon-borne x ray detectors were flown under the beam of a vhf auroral radar that looks south from Slope Point, New Zealand, in order to compare radar echoes and bremsstrahlung x rays. The evidence suggests that particle precipitation is not directly responsible for either diffuse or discrete auroral radar echoes, but at times can show an association with the diffuse type. (auth) (UK)

9321 ION-REFLECTION OF DOWNWARD-PROPAGATING WHISTLERS AT LOW LATITUDES. Egeland, A.; Leer, E.; Holtet, J. A. (Norwegian Inst. of Cosmic Physics, Oslo). J. Atmos. Terrest. Phys.; 32: 1983-7(Dec 1970).

The real-time ac (10 to 1500 Hz) electric field measurements, received on May 2, 1967 when the Satellite OV1-10 (altitude about 700 km) moved from 0 to 20°N geomagnetic latitude, are presented. Several long fractional hop whistlers, strongly influenced by ions, were observed. For downward-propagating whistlers, a

XUM

frequency band is reflected. The width and the location of this band are latitude-dependent. Whistler pairs separated in time by 0.15 sec and with a 15% difference in dispersion were observed. These pairs are probably generated by the same lightning stroke and propagate along different ray paths. Whistlers propagating on higher L shells seem to be less connected to the magnetic-field lines than those on lower L shells. Resonance damping may be important for a limited-frequency band. (auth) (UK)

9322 DIURNAL DEVELOPMENT OF THE SEASONAL ANOMALY PHENOMENON IN THE MIDDLE-LATITUDE TOPSIDE F2 REGION. Fatkullin, M. N. (Academy of Sciences, Moscow). J. Atmos. Terrest. Phys.; 32: 1989-94(Dec 1970).

Data obtained by means of the ionospheric topside sounder satellite Alouette-1 were used to determine the mean seasonal (summer 1963 and winter 1963–1964) daily variations of electron density in the middle-latitude topside ionosphere. It is shown that the altitudinal extension of the seasonal anomaly in the topside electron density changes with local time. Maximum of the extension is observed at 1400 to 1500 hr (up to h ≃ 500 km). (auth) (UK)

9323 ON SOME NONDISSIPATIVE PHENOMENA AFFECTING A_1 ABSORPTION MEASUREMENTS. Ganguly, S.; Rao, Manoranjan (Bose Inst., Calcutta). J. Atmos. Terrest. Phys.; 32: 1995-8(Dec 1970).

The irregular variations in the strength of ionospherically reflected waves caused, for example, by focusing and by ionospheric irregularities are studied with reference to their diurnal distribution. (auth) (UK)

9324 RIOMETER OBSERVATIONS OF RADIO-WAVE ABSORPTION IN THE ANTARCTIC IONOSPHERE. Cowley, F. C.; Ecklund, W. L.; Reid, G. C.; Sauer, H. H. (Space Disturbances Lab., Boulder, Colo.). Antarctic J. U. S.; 5: 173-4(Sep-Oct 1970).

Riometers were operated at frequencies of 30 and 50 MHz at Byrd, South Pole, and Vostok during the austral winter of 1969, which was close to the peak of the solar activity cycle. The most outstanding PCA event occurred Apr. 12 to 16. The event apparently originated in a flare just beyond the east limb of the Sun that was invisible from the Earth, but was observed by a Pioneer spacecraft in solar orbit well to the east of the Earth. The event is being compared with other known east-limb proton events. (J.C.W.)

9325 VLF STUDIES OF THE MAGNETOSPHERE. Helliwell, R. A. (Stanford Univ., Calif.). Antarctic J. U. S.; 5: 170-1(Sep-Oct 1970).

A successful measurement of the net interchange of ionization between the F region and the protonosphere above was accomplished in 1969, verifying the role of the protonosphere in supplying ionization to the nighttime ionosphere. During a magnetic storm or series of intense polar substorms, ionization content is slow compared to similar recovery in the ionosphere. An attempt was made to develop a technique of worldwide plasmapause monitoring in Aug. 1969, at Byrd Station and Kerguelen Island. The walking-trace mode of whistler propagation between hemispheres was discovered on OGO-4 telemetry records from Byrd Station data. (J.C.W.)

9326 COOPERATIVE MICROPULSATION RESEARCH AT HIGH LATITUDES. Hessler, V. P.; Heacock, R. R. (Univ. of Alaska, College). Antarctic J. U. S.; 5: 169-70(Sep-Oct 1970).

Cooperative research is reported by the authors with Soviet scientists at Vostok, Antarctica; Danish scientists at Qanaq, Greenland; Finnish scientists at Sodankylä and Nurmijaavi observatories; senior scientists in Moscow, Helsinki, and Copenhagen; and Boeing Scientific Research Laboratories. The natural electromagnetic activity is sensed in the magnetic mode with induction magnetometers and in the electric mode with the telluric-current technique. Using 180 in/hr tapes, the polarization and direction of arrival of narrow-band electromagnetic waves down to periods of the order of 1 sec are studied. The new tapes make it possible to time the arrival of an event to the order of 0.1 sec, an accuracy essential to the study of the propagation of micropulsation activity. The authors and their Danish and Finnish collaborators now have the facility to study micropulsation propagation completely across the northern polar cap. The Vostok telluric-current recording experiment has shown that the special problem of installing satisfactory electrodes in the high-resistivity snow and ice of the antarctic ice cap can be solved. (J.C.W.)

9327 INVESTIGATIONS OF ENERGETIC PARTICLES AND RADIATION IN THE POLAR CAP WITH BALLOON-BORNE INSTRUMENTS. Pomerantz, Martin A.; Baird, George A. (Bartol Research Foundation, Swarthmore, Pa.). Antarctic J. U. S.; 5: 168-9(Sep-Oct 1970).

All charged particles that reach McMurdo have access through the magnetospheric tail. The propagation toward the Earth of the lower-energy cosmic rays can just penetrate the residual atmosphere above the ceiling altitude of balloons. Balloon flights have been very successful and new techniques have been developed. A new ballasting device, coupled with a much improved pressure sensor with roughly a tenfold increase in resolution, made it possible to obtain outstanding data for studying both the diurnal variation and longer-term transient and steady-state intensity fluctuations, and for relating these to the simultaneous observations with the ground-based detectors at McMurdo. It had been assumed that at synchronous altitude, the solar proton flux measured at ATS-1 is representative of the flux in interplanetary space and over the polar caps. This theory is upset by these observations, which reveal that this event was highly anisotropic. In this event, the first solar cosmic-ray influx observed with balloon-borne instruments in either polar cap occurred during a remarkable Forbush decrease that, at McMurdo, set in rather slowly at about 2300 on Jan. 28, 1970. (J.C.W.)

9328 EXPONENTIAL MODEL OF THE IONOSPHERIC D REGION. Nestorov, G. (Inst. of Geophysics, Sofia). Compt. Rend. Acad. Bulg. Sci.; 23: 939-42(1970).

A model based on absorption measurements with a reflection from E or E_s layers is proposed for the calm D region. Several N(h) distributions for describing the D region during daytime are shown. (M.O.W.)

9329 ELECTRON DENSITY VARIATIONS IN THE IONOSPHERE. Velinov, P. (Inst. of Geophysics, Sofia). Compt. Rend. Acad. Bulg. Sci.; 23: 943-6(1970).

General equations are deduced for variations of electron density on different types of ionospheric layers. The variation equations derived are for the α, β, and $\alpha\beta$ layers. (M.O.W.)

9330 POSSIBLE EVALUATION OF SOLAR HARD X RADIATION BY THE ABSORPTION IN D REGION. Nestorov, G. (Inst. of Geophysics, Sofia). Compt. Rend. Acad. Bulg. Sci.; 23: 771-4(1970).

Calculations are given for the integral flux radiation with $\lambda \leq 8$ Å and $\lambda \leq 3$ Å in the lower ionosphere. (M.O.W.)

9331 OZONE SCREENING HEIGHTS DEDUCED FROM SUNRISE EFFECTS AT VERY LOW FREQUENCIES. Schaal, R. E.; Ananthakrishnan, S. (Mackenzie Univ., Sao Paulo, Brazil). J. Atmos. Terres. Phys.; 32: 1831-4(Nov 1970).

During the August–September period of any year, the entire NAA–São Paulo path is illuminated almost simultaneously at sunrise, resulting in a sharp drop in the phase of the received signal. Using sunrise phase transitions and an assumed nighttime reflection height of 90 km, an ozone-screening height of 58 km was deduced. A calculation of the wavelength of the photodetaching radiation, using this value of the screening height, yielded a value of $\lambda = 3015$ Å. (auth) (UK)

9332 CORRELATION OF THE OCCURRENCE OF SIMULTANEOUS SUDDEN MAGNETOSPHERIC COMPRESSIONS AND GEOMAGNETIC BAY ONSETS WITH SELECTED GEOPHYSICAL INDICES. Schieldge, J. P.; Siscoe, G. L. (Univ. of California, Los Angeles). J. Atmos. Terrest. Phys.; 32: 1819-30(Nov 1970).

The results of a study of the conditions that affect the occurrence of simultaneous magnetospheric compressions, as indicated by geomagnetic sudden commencements and sudden impulses, and negative geomagnetic bays are presented. Data from the IGY period were used. Of 155 SC and positive SI events with amplitudes greater than 10 γ found during the period of study, 29 (18.7 per cent) produced simultaneous negative geomagnetic bays with depressions greater than 200 γ. (Of 98 negative SI events, 10 (10.2 per cent) produced simultaneous bays. The following correlation study used only positive compression events.) The probability of a simultaneous event was found to be independent of the k_p index and the value of $D_{(st)}$. However, the probability is larger for greater compression amplitudes; it is larger during PCA events; and it is larger when the low latitude H-component of the geomagnetic field in the pre-midnight sector is depressed relative to earlier local time values. These results are discussed in relation to bay production mechanisms that involve the state of the ionosphere, the ring current, and the tail current. It is concluded that only the last possibility is consistent with all the observed correlations. (auth) (UK)

9333 IONOSPHERIC ELECTRON CONCENTRATION ENHANCEMENT DURING A SOLAR FLARE. Taylor, G. N.; Watkins, C. D. (Royal Radar Establishment, Malvern, Eng.). Nature (London); 228: 653-4(14 Nov 1970).

Sudden increases of euv and x-ray fluxes during solar flares are known to produce abrupt increases of electron concentration (N_e) in the sunlit part of the ionosphere. Because of their short duration, and the accompanying blackout in hf propagation, however, such enhancements have been difficult to investigate, especially in the E region. Some results from the application of the new technique of incoherent-scatter radar to this problem are presented. The observations were made at Malvern during a solar flare on Feb. 20, 1970, using pulsed vertically pointing radar equipment at 400.5 MHz, with a transmitted pulse length of 33 μs (5 km radar length). Scattered signal power was measured in 90 consecutive range-sampling intervals, each 3 km wide, spanning the altitude range from 50 km upwards. The measurements were converted from scattered power to profiles of N_e against height. At all heights up to 150 km the measurements showed a rapid increase of N_e at the start of the disturbance; the magnitude and duration of the enhancement varied with height. At 90 km there was a large enhancement of N_e, lasting for at least 3 hr; whereas, at greater heights there were only marginally significant enhancements, probably not lasting longer than about an hour. The variation with height of the maximum enhancements is shown graphically. Enhancements approaching an order of magnitude appeared to be indicated at the bottom of the E region. It is considered significant that both the agreement between the time histories of the ionospheric and x-ray events, and the height variation of the N_e enhancement, indicate x rays as the main cause of the terrestrial flare effects. It is also interesting that the decimetric radio flux appeared a better indicator of the magnitude and duration of the ionospheric effects than were the Hα flare data. (UK)

9334 INVESTIGATION OF THE AURORAL ELECTROJET. Heinrich, H.; Reimer, D.; Siemann, H. (Univ., Brunswick). Z. Geophys.; 36: 399-420(Sep 1970).

The program PEJ 1 was planned in 1967 to investigate the Auroral Electrojet (AEJ). Three rockets of the Black Brant III type with magnetometers for measuring the field components, an impedance probe and a retarded-potential analyzer on board were launched in late 1968 from ESRANGE in Kiruna, Sweden. A position-finding system, based on magnetometer measurements was used to calculate the position of the ionospheric current system and to control the countdown. The gross structure of the AEJ was resolved by comparing the available data from ground-based magnetometers with the height profiles of the total intensity. Above an altitude of 130 km a sudden change in the phase shift of the transverse magnetic field was measured and can be interpreted as being due to a magnetospheric current system that is closed in the ionosphere. From the height profiles of the electron density, the conductivities were computed. The electric fields as derived from the combined results of these data and from the magnetometer measurements are comparable to results obtained by barium-cloud experiments. (auth)

9335 ELECTRIC FIELDS DERIVED FROM PLASMA MEASUREMENTS IN THE POLAR ELECTROJET. Kist, R.; Spenner, K. (Arbeitsgruppe fuer Physikalische Weltraumforschung, Freiburg i. B.). Z. Geophys.; 36: 421-49(Sep 1970). (In German).

With a variable-frequency impedance probe, electron density profiles were measured on board three Black Brant rockets, fired at ESRANGE/Kiruna. The profile obtained during ascent for rocket 1 can be represented quite well by a CHAPMAN–ELIAS function, with an "effective scale height" of 15 km, and height of maximum 115 km. At the two other occasions, considerable deviations from this particular profile were found. They could be due to a more complex ionization function as is particularly indicated in case of rocket 3 by the magnetometer measurements after which the rocket moved towards a second current-density peak. In fact, as the rockets were intended to be fired into an Auroral Electrojet (AEJ) the position of which was determined from ground observations, the probability is very high that the ionization profile as function of latitude was rather variable. Conductivity profiles were computed, using the measured electron densities and collision-frequency profiles, which had to be chosen carefully. After height integration of the calculated conductivities, they were brought together with height-integrated current densities determined by magnetometer measurements, so that an electric field could be computed. It was assumed that this field, in the height range concerned, is independent of height. Electric fields determined in this way agree well with results obtained independently from the retarding-potential analyzer for the height of the AEJ. In an AEJ the electric field is considerably increased. For rocket 3, which did not hit directly an AEJ but went into a region between two current density peaks, the NS component was only 5 mV/m. Thus, at ionospheric heights, electron density in situ profile observations, together with data on collision frequencies and magnetic field observations, allow the electric field to be deduced reasonably well. (auth (TSS)

9336 REVIEW OF THE SCIENTIFIC RESEARCH PROGRAM IN THE SPACE SCIENCE DEPARTMENT OF ESTEC. Trendelenburg, E. A.; Fitton, B.; Page, D. E.; Pedersen, A. (Gauthier-Villars, Paris). ELDO/ESRO Sci. Tech. Rev.; 2: No. 1, 1-74 (1970).

The Space Science Department of the European Space Research and Technology Centre (ESTEC) was originally created in 1965 under the title of the European Space Research Laboratory (ESLAB). Research is primarily on satellite and sounding-rocket projects and aims to complement work conducted in national space laboratories, with which the Department maintains close liaison and with which it sometimes undertakes joint projects. The Department comprises three Divisions, namely Cosmic Rays, Ionospheric Physics and Surface Physics. Results achieved to 1969 are discussed here. (auth)

9337 INTERPRETATION OF COSMIC RADIO-NOISE ABSORPTION MEASUREMENTS. Heisler, Rodney. Pullman, Wash.; Washington State Univ. (1970). 91p. University Microfilms Order No. 70-16, 810.

Thesis.

A procedure is presented for calculating the cosmic radio-noise absorption that one would expect to measure with a given riometer system. These calculations are made from electron-density and collision-frequency profiles and include the effects of deviative ray paths, different antenna beamwidths in space quadrature, variation of the refractive index with altitude, and ionospheric windowing. The results are compared with riometer measurements taken during solar minimum and maximum periods at Pullman, Washington, in order to establish a better understanding of riometer measurements. For middle latitudes it is found that nearly all of the cosmic-noise absorption occurs in the D and E layers during solar-minimum years. During solar-maximum years more than half of the cosmic-noise absorption occurs in the F layer. Approximately half of this F-layer absorption is a spurious absorption due to ionospheric windowing. The other half is the result of electron–ion collisions. The unexpectedly high nighttime absorption measured at most riometer stations is explained. The nighttime absorption measured at Pullman, Washington, in 1959 is determined to be in error due to an error in the level of the quiet-day curve. Since there is no known method of accurately setting the level of a quiet-day curve, it is concluded that this is the source of the high nighttime absorption measured at most stations. It is demonstrated that an error in the level of a quiet-day curve will introduce an anomaly in the monthly median curves. The effect of solar radio noise emission during solar maximum years upon riometer absorption measurements is investigated. It is determined that the solar radio emission at 27.6 MHz is appreciable, in comparison to the cosmic-noise background. Consequently, the daytime cosmic-noise absorption calculated from the riometer records is significantly less than is actually occurring in the ionosphere. It is suggested that a solution to this problem is to decrease the beamwidth of the receiving antenna to about 20° × 20°. During solar-minimum years the solar radio noise emission is reduced, and this problem does not exist. (Diss. Abstr. Int., B)

9338 PROPAGATION OF GEOMAGNETIC Pc1 PULSATIONS IN THE F REGION OF THE IONOSPHERE. Kato, Yoshio (Tokai Univ., Tokyo); Tamura, Kazushi. Sci. Rep. Tohoku Univ., Fifth Ser.; 19: 107-16(Mar 1970).

Propagation of hydromagnetic waves through the ionospheric F region is investigated for an explanation of geomagnetic Pc1 pulsations. The ray-tracing method is employed, and profiles of the refractive indices of hydromagnetic waves of the extraordinary mode versus height are obtained for a given model of the ionosphere. Results of the numerical calculation confirm that the ionospheric F region behaves as a waveguide for the waves. It is also found that attenuation of hydromagnetic waves passing through this waveguide is not so strong in the nighttime condition. This may explain the fact that geomagnetic Pc1 pulsations are more frequently observed during nighttime than during daytime at middle and low latitudes. (auth)

9339 CONTRIBUTION OF CORPUSCULAR RADIATION IN IONIZING THE D LAYER OF THE IONOSPHERE. Tulinov, V. F.; Yakovlev, S. G. Cosmic Res. (USSR) (Engl. Transl.); 7: 110-13 (Jan-Feb 1969).

Translated from Kosm. Issled.; 7: 122-6(Jan-Feb 1969).

The contribution of corpuscular streams in ionizing the D region is discussed on the basis of direct intensity measurements at heights up to 90 to 95 km. It is shown that the corpuscular radiation might be responsible for maintaining the high level of ionization of the D region at night. (tr-auth)

9340 SOURCES OF E-REGION HEATING. Breus, T. K. Cosmic Res. (USSR) (Engl. Transl.); 7: 114-19(Jan-Feb 1969).

XUM

Translated from Kosm. Issled.; 7: 127-33(Jan-Feb 1969).

The specific intensity of the thermal sources heating the E region is computed on the basis of results of rocket measurements of electron temperature during a solar eclipse. The intensity of possible thermal sources is estimated and compared with the computed intensity, using experimental data on the electron temperature. (tr-auth)

9341 CORPUSCULAR FLOW AND HEATING OF THE ELECTRON GAS AT E-LAYER ALTITUDES. Lazarev, V. I.; Breus, T. K. Cosmic Res. (USSR) (Engl. Transl.); 7: 120-2(Jan-Feb 1969).

Translated from Kosm. Issled.; 7: 134-6(Jan-Feb 1969).

The degree of heating of the electron gas by the absorption of electrons of small energies in the upper atmosphere is estimated. The results are compared with the value of the heat of the electron gas from additional sources required for maintenance of the high values of electron temperature in the E layer; these were measured by rocket experiments at the time of solar eclipse. (tr-auth)

9342 CURRENTS OF QUASI-CAPTURED PARTICLES AND THEIR INTERACTION WITH THE GEOMAGNETIC FIELD (SYMMETRIC APPROXIMATION). Pletnev, V. D.; Troshichev, O. A. Cosmic Res. (USSR) (Engl. Transl.); 6: 593-603(Sep-Oct 1968).

Translated from Kosm. Issled.; 6: 707-19(Sep-Oct 1968).

A model ring current of quasi-captured particles at high latitudes in the magnetosphere is discussed. Various special cases of particle distribution in the current are discussed for an anisotropy of the form $f_0 = K_\alpha p \sin^{\alpha+1}\theta_0 \cos^\beta \theta_0$. The latitude distribution of the current density and the effect of the current on the geomagnetic field are estimated. It is shown that the main phase of magnetic storms can be explained by the interaction between the current of quasi-captured particles and the field of the magnetosphere. (tr-auth)

9343 MEASUREMENTS OF THE PARAMETERS OF IONOSPHERE BY INCOHERENT RADIOWAVE SCATTERING. Misyura, V. A.; Tkachev, G. N.; Erokhin, Yu. G.; (and others). Cosmic Res. (USSR) (Engl. Transl.); 6: 610-13(Sep-Oct 1968).

Translated from Kosm. Issled.; 6: 726-9(Sep-Oct 1968).

Using the incoherent scattering (IS) method, taking into account collisions of ν for three values of the parameter $D = q^2d^2$ that satisfies the condition $D_3 \ll D_2 < D_1 < 1$, profiles are obtained of 1967–1968 measurements carried out in the middle latitudes of the Soviet Union. These profiles show the electron concentration N for the condition $\Delta z_3 > \Delta z_2 \gg \Delta z_1$, where q is the wave number of the directly scattered field, d is the Debye radius of an electron, Δz is the extent of the scattering volume with respect to height, that could be regulated using well-known methods. A corresponding IS theory is developed for a collision multicomponent temperature-nonequilibrium plasma in the absence of a magnetic field. The initial data were obtained and processed by different methods for D_1 and $D_{2,3}$. The measurement errors were estimated using various methods, including a comparison of the profiles of N obtained in the same region during the same time of day using various radiophysical methods (IS, vertical sounding, the Faraday effect, and the Doppler difference effect of coherent signals of AES and of a vertical space probe, etc.) (tr-auth)

9344 MEASUREMENT OF THE DISPERSED L_α RADIATION IN THE EARTH'S ATMOSPHERE AT ALTITUDES OF 1000 TO 3500 km. Sheffer, E. K. Cosmic Res. (USSR) (Engl. Transl.); 6: 619-21(Sep-Oct 1968).

Translated from Kosm. Issled.; 6: 735-7(Sep-Oct 1968).

Results are presented of measurements of the dispersed Lyman-α radiation of the Sun in the Earth's upper atmosphere at altitudes of 1000 to 3500 km taken during the flight of the "Vertical Cosmic Probe" in October, 1967. An empirical distribution model for neutral hydrogen was constructed for these altitudes. (tr-auth)

9345 MEASUREMENT OF THE ENERGY OF SOFT ELECTRONS IN THE UPPER ATMOSPHERE ON DECEMBER 21, 1966. Kazachevskaya, T. V. Cosmic Res. (USSR) (Engl. Transl.); 6: 679-81(Sep-Oct 1968).

Translated from Kosm. Issled.; 6: 795-7(Sep-Oct 1968).

A meteorological rocket was used in December, 1966, to determine the flux of ionizing radiation in the upper atmosphere at altitudes of 120 to 178 km. The "Fosfor" device was used to determine the energy of electrons with $E \gtrsim 2$ keV. The radiation detector was a $CaSO_4$(Mn) phosphor. After exposure to short-wave radiation ($\lambda \leq 1300$ Å, or to β and γ radiation, this phosphor reemits the stored energy in the visible range ($\lambda_{eff} = 5000$ Å) when it is heated. The radiation flux intercepted by the phosphor during the exposure time is characterized by the light sum Σ, defined as the total number of photons emitted by the phosphor during the heating process. The phosphor can be used to carry out absolute measurements in the short-wave part of the spectrum ($\lambda \leq 1300$ Å). The $CaSO_4$(Mn) phosphor can also be used to determine the energy of soft electrons in the upper atmosphere. Nosenko et al. have shown that the quantum yield of the phosphor for electrons with energies between 0.5 and 10 keV is similar to the quantum yield for x rays. Laboratory measurements of the sensitivity of the $CaSO_4$(Mn) phosphor to 0.3 to 5-keV electrons resulted in the same values as those reported for the quantum yield of the phosphor for 10-keV electrons, $\approx 3 \cdot 10^9$ per 1 erg of energy, while for x rays it is 10^9 to 2×10^9 in the same units. Measurements were carried out for the total flux of ionizing radiation and the radiation emitted in individual spectral ranges with the aid of 3 μ-thick terylene filters and 5 μ-thick aluminum filters. To determine the total flux of ionizing radiation (short-wave radiation, and the flux of electrons with energies in excess 1 to 2 keV) plates without filters were used. An additional experiment using an LiF filter was performed to determine the flux of solar Lyman-α radiation. The measurements showed that, for energies $E \gtrsim 2$ to 3 keV, the electron flux is $W = 0.15$ to 0.2 erg/cm$^2 \cdot$ sec $\cdot$ ster, and for electrons with $E \geq 17$ keV, the result is $W = 6 \times 10^{-3}$ to 7×10^{-3} erg/cm$^2 \cdot$ sec $\cdot$ ster. Finally, for electrons with $E \geq 30$ keV, $W < 2 \times 10^{-3}$ erg/cm$^2 \cdot$ sec $\cdot$ ster. The electron flux is thus seen to fall rapidly with increasing electron energy. (J.C.W.)

9346 DETECTION OF PERTURBATIONS OF THE GEOMAGNETIC FIELD IN THE MAGNETOSPHERE BASED ON DYNAMIC SPECTRA OF ATMOSPHERIC WHISTLERS. Likhter, Ya. I.; Molchanov, O. A. Cosmic Res. (USSR) (Engl. Transl.); 7: 83-92(Jan-Feb 1969).

Translated from Kosm. Issled.; 7: 92-102(Jan-Feb 1969).

The effect of the real configuration of the magnetic field in the magnetosphere during a period of moderate magnetic disturbance on the dynamic spectra of atmospheric whistlers is calculated. Dynamic spectra are demonstrated to be capable not only of establishing the existence of geomagnetic disturbances in the magnetosphere, but also of estimating the characteristics of the disturbance: shifts in the dipole line of force ΔL and field variations δH at the equator. The δH and δL values found for the recovery phase of the February 8, 1967 storm, viz. $\delta H \approx -130$ γ and $\Delta L \approx 0.15$ for the region $L \sim 3$, are in excellent agreement with these calculations. It was also found that the bend in the electron concentration profile for the magnetosphere took shape during a magnetic storm, and was situated at $L' \approx 3.5$, characterized by a depth ~ 0.25 R_E and a threefold-to-fivefold drop in concentration. (tr-auth)

9347 CURRENTS OF QUASI-TRAPPED PARTICLES WITH DISCONTINUITIES ON THE DAYTIME AND NIGHTTIME SIDES OF THE EARTH. Pletnev, V. D.; Troshichev, O. A. Cosmic Res. (USSR) (Engl. Transl.); 7: 93-7(Jan-Feb 1969).

Translated from Kosm. Issled.; 7: 103-8(Jan-Feb 1969).

The effect of the presence of a source (or discontinuity) in the drift current of a collisionless plasma is investigated. An estimate of possible effects related to discontinuities in currents of quasi-trapped particles on the daytime and nighttime sides of the Earth is made in application to the geomagnetic field. (tr-auth)

9348 SIMULATION OF FLOW OF INTERPLANETARY PLASMA PAST THE MAGNETOSPHERE OF THE EARTH OR PLANETS. Baranov, V. B. Cosmic Res. (USSR) (Engl. Transl.); 7: 98-104(Jan-Feb 1969).

Translated from Kosm. Issled.; 7: 109-16(Jan-Feb 1969).

The study of many of the physical processes related to flow of interplanetary plasma past the Earth or other planets can be aided substantially by setting up experiments simulating these processes under laboratory conditions. The model simulating these processes will properly match the physical phenomenon occurring in outer space only when a complete system of dimensionless ratios has been selected correctly so that the ratios obtained in the laboratory and those found in outer space will correspond to physically similar phenomena. A theoretical analysis of the problem was incomplete, rather general in nature, and often based on formulas whose range of applications was too limited (e.g., the use of the generalized Ohm's law, relationships for a collisionless shock wave, etc.). The present article constitutes an attempt at a consistent theoretical analysis of the possibilities inherent in exact and approximate simulation of flow of interplanetary plasma past the Earth and planets, based on the use of kinetic equations for particle distribution functions, Maxwell's equations for the electromagnetic field, and boundary conditions. Initial conditions are not presented since a quasi-stationary problem is treated here. (tr-auth)

9349 SPATIAL DISTRIBUTION OF SINGLY CHARGED PARTICLES AND HELIUM NUCLEI ABOVE THE ATMOSPHERE IN THE EQUATORIAL REGION. Basilova, R. N.; Grigorov,

N. L.; Savenko, I. A. Cosmic Res. (USSR) (Engl. Transl.); 7: 802-5(Nov-Dec 1969).

Translated from Kosm. Issled.; 7: 895-9(Nov-Dec 1969).

The distribution by zenith and azimuth of the intensity (density) of energetic particles with charges $Z \geq 1$ and $Z \geq 2$ is given. The distribution of particles with $Z \geq 1$ is nearly isotropic. The intensity distributions of particles with charge $Z \geq 2$ have a clear east–west asymmetry over all ranges of zenith. The measurements were made by the artificial satellite "Proton-2" at a height of 450 km. (tr-auth)

9350 MODEL EXPERIMENT ON DIFFUSION OF ELECTRONS IN THE MAGNETOSPHERE. Bocharov, V. N.; Volosov, V. I. Cosmic Res. (USSR) (Engl. Transl.); 7: 822-8(Nov-Dec 1969).

Translated from Kosm. Issled.; 7: 918-24(Nov-Dec 1969).

Results of a model experiment in the study of diffusion of charged particles in the Earth's magnetosphere are given. The diffusion was simulated in a trap having magnetic mirrors in the presence of axially nonsymmetrical magnetic field pulses (ΔH). The parameters of the experimental equipment were: magnetic field ~0.5 kG; pulsed magnetic field $\Delta H \approx 10$ G; pulse length ~2 μsec; trap dimensions, length ~30 cm and diameter 10 cm; and electron energy 30 keV. The observed experimental diffusion was in satisfactory agreement with the theoretical estimates given. (tr-auth)

9351 COMPUTATION OF SPECTRAL DISTRIBUTION OF ABSORBED ENERGY OF X RADIATION IN THE EARTH'S ATMOSPHERE. Kozlov, S. I.; Kudimov, A. V. Cosmic Res. (USSR) (Engl. Transl.); 7: 128-34(Jan-Feb 1969).

Translated from Kosm. Issled.; 7: 143-9(Jan-Feb 1969).

A method is described for computing the spectral distribution of the absorbed energy of x radiation in the Earth's atmosphere assuming existence of an isotropic point source, with some temperature T, whose initial radiation spectrum corresponds to the law of black-body radiation. The determined distribution is used in finding the spectrum of forming high-energy photoelectrons. It is shown that, at altitudes greater than 150 km, the maximum of photoelectron distribution, in contrast to the distribution of absorbed energy, falls at approximately 20 Å and is not dependent on T. (tr-auth)

9352 VARIATIONS IN THE MEAN LEVEL OF RADIO EMISSION AT THE FREQUENCIES 1.1 AND 2.3 MHz ACCORDING TO MEASUREMENTS MADE BY THE ARTIFICIAL EARTH SATELLITE ELEKTRON-4. Benediktov, E. A.; Getmantsev, G. G.; Mityakov, N. A.; Rapoport, V. O.; Tarasov, A. F. Cosmic Res. (USSR) (Engl. Transl.); 7: 141-2(Jan-Feb 1969).

Translated from Kosm. Issled.; 7: 156-7(Jan-Feb 1969).

From July to Dec., 1964, measurements were made of the intensities of the cosmic radio emission at the satellite Elektron-4. The bursts were identified with a sporadic radio emission that could arise in the upper parts of the ionosphere of the Earth when there is an increase in the fluxes of relatively fast electrons in the radiation belts. Processing of the results of the measurements has shown that the minimum level of the radio emission received also varied in time. In finding the intensities of the radio emission the low sections of the satellite orbit were excluded, because the ionospheric plasma could have influenced the results of the measurements. In principle, the level of the cosmic radio emission at sufficiently low frequencies can change as a result of a change in the absorption of the radio emission in the interplanetary plasma. Another possibility can be associated with screening of locally bright regions of the sky by the supercorona of the Sun. The variations of the level of the radio emission can also be due to shot noise caused in the antenna by fluxes of the effective temperature of the shot noise at a frequency of $f \approx 1$ MHz is $T_{eff} \approx 10^7$ K. (J.C.W.)

9353 RELATION OF STABLE PULSATIONS OF THE GEOMAGNETIC FIELD WITH PARAMETERS OF THE MAGNETOSPHERE. Kopytenko, Yu. A.; Raspopov, O. M.; Fang Wang Ch'ih. Cosmic Res. (USSR) (Engl. Transl.); 7: 238-42(Mar-Apr 1969).

Translated from Kosm. Issled.; 7: 266-72(Mar-Apr 1969).

The relation of the period of stable geomagnetic pulsations Pc2, 3, 4 with the intensity of D_{St} variations of the geomagnetic field and with the location of the density discontinuity of the plasma in the magnetosphere (the plasmapause) is analyzed. It is shown that the period of Pc2, 3 pulsations correlate with the variation of the location of the plasmapause, and the period of the Pc4 pulsation is connected with the magnitude of the D_{St} variation. Empirical relationships are derived which connect with the period of the Pc2, 3 pulsations with the position of the plasmapause. The results obtained are analyzed based on a possible model, proposed previously, of the excitation of stable pulsations of the geomagnetic field. The characteristics of the diurnal variations of the Pc3, 4 pulsation periods are explained. (tr-auth)

9354 RESULTS OF MEASUREMENTS OF FAST-CHARGED PARTICLES ON THE SATELLITE COSMOS-137. Vernov, S. N.; Gorchakov, E. V.; Getselev, I. V.; Ignat'ev, P. P.; Ternovskaya, M. V. Cosmic Res. (USSR) (Engl. Transl.); 7: 243-7(Mar-Apr 1969).

Translated from Kosm. Issled.; 7: 273-8(Mar-Apr 1969).

Results are discussed of data obtained on the satellite Cosmos-137 with a global Cherenkov counter that was designed for the detection of fast charged particles. In the inner region of the inner radiation belt the measured fluxes of particles (electrons with $E > 7$ MeV and protons with $E \geq 600$ MeV) differed slightly from the fluxes recorded in 1961 by Explorer 11. The difference in fluxes before and after the conduction of the high-altitude thermonuclear tests is apparently due to energetic electrons of artificial origin left in the inner radiation belt at the end of 1966. The orbit of Cosmos-137 provided information about the radiation belts in a much wider region of space than the flight of Explorer 11. It was found that in the region $L > 3.3$ the flux of trapped electrons with $E > 7$ MeV is small in comparison with the cosmic-ray flux. An outer belt of hard electrons, however, was found in the region $L \sim 2.8$. Also presented is the integral cosmic-ray spectrum for the beginning of 1967, calculated from the latitude–intensity relationships recorded in the flight outside the region of the radiation belts. (tr-auth)

9355 COMPARISON OF IONOSPHERIC FEATURES OF PLANETS IN THE TERRESTRIAL GROUP: MARS, VENUS, AND EARTH. Gringauz, K. I.; Breus, T. K. Cosmic Res. (USSR) (Engl. Transl.); 7: 782-97(Nov-Dec 1969).

Translated from Kosm. Issled.; 7: 871-90(Nov-Dec 1969).

The comparable features of the ionospheres of Mars, Venus, and Earth are summarized, along with the methods of investigating planetary ionospheres, the results of the experiments on board the Mariner-4, Venus-4, and Mariner-5 spacecraft, and the ionospheric models for these planets. The model ionospheres are compared with the terrestrial ionosphere. (tr-auth)

9356 DISTRIBUTION OF SOLAR-WIND DISTURBANCES CAUSED BY CHROMOSPHERIC FLARES. Korobeinikov, V. P.; Nikolaev, Yu. M. Cosmic Res. (USSR) (Engl. Transl.); 7: 798-801(Nov-Dec 1969).

Translated from Kosm. Issled.; 7: 891-4(Nov-Dec 1969).

Propagation of a shock wave induced by a chromospheric flare is studied in the approximation of a model of a strong explosion, taking into account the quasi-radial motion of the quiet solar wind. Estimates of flare energy and the degree of shock-wave attenuation are made. Theoretical results are compared with physical measurements made in space. (tr-auth)

Low-Temperature Physics and Cryogenic Equipment

Refer also to abstract 10018.

Superfluidity

9357 GAUGE FIELDS IN THE MANY-BODY PROBLEM AND SUPERFLUIDITY. Lee, H. J.; De Celles, P. C.; Marshalek, E. R. (Univ. of Notre Dame, Ind.). Contract AT(11-1)-427. Lett. Nuovo Cim.; 4: 1033-6(28 Nov 1970).

The idea is proposed that the Yang–Mills gauge field theory may be directly applicable to low-energy many-body problems. Adopting this point of view as a working hypothesis, some theoretical consequences for He II superfluidity are derived. In this approach, a gauge field is introduced, which arises from the constraint that the total number of particles in the system is conserved. (M.H.R.)

9358 LOW-TEMPERATURE MOBILITY OF TRAPPED IONS IN ROTATING He II. Fetter, Alexander L.; Iguchi, Ienari (Stanford Univ., Calif.). Phys. Rev., A; 2: 2067-74(Nov 1970).

A classical vortex with a movable impurity in its core is used to study the interaction of vortex waves with a trapped ion in rotating He II. The reflection probability is evaluated in the long- and short-wavelength limits. An approximate interpolation formula allows a calculation of the low-temperature mobility of an ion along the vortex axis. (auth)

9359 SUPERFLUID VORTEX MOTION. Campbell, L. J. (Los Alamos Scientific Lab., N. Mex.). J. Low Temp. Phys.; 3: 175-82(Aug 1970).

The two-dimensional path functions are derived for (1) a superfluid vortex subject to unbounded potential flows (of normal and superfluid) and an external force; and (2) a vortex "ring" parallel to a plane boundary. The sign of the phase changes due to vortex flow, and the temperature dependence of vortex damping due to the normal fluid, are discussed. (auth)

9360 THIRD SOUND IN SUPERFLUID HELIUM. Bengtson, Kurt Lennart. Riverside, Calif.; Univ. of California (1970). 71p. University Microfilms Order No. 70-22,856.

Thesis.

A set of coupled nonlinear differential equations obtained by Cummings, Herold, and Sarfatt for the superfluid order parameter and "depletion potential" (the CHS equations) is used to interpret recent experiments determining the velocity of third sound in unsaturated films of He II. The experiments indicate that the third sound velocity falls abruptly to zero at a temperature dependent "onset thickness." The CHS equations are solved by numerical integration for film geometries and the parameters occurring in the equations are chosen to give the observed decrease in the superfluid density for thicknesses greater than the onset thickness. It is shown that there is insufficient information relating the boundary conditions for the depletion potential to the external parameters to establish whether or not the solutions to the CHS equations behave discontinuously or decrease rapidly to zero at some critical film thickness. However, an interpretation is proposed to explain the discontinuous behavior of the third sound velocity which occurs without the appearance of a latent heat for the transition which can be interpreted as a first-order phase transition. (Diss. Abstr. Int., B)

9361 CHARGE MOBILITIES IN SUPERFLUID HELIUM UNDER PRESSURE. Brody, Burton Alan. Ann Arbor, Mich.; Univ. of Michigan (1970). 131p. University Microfilms Order No. 70-21,626.

Thesis.

Measurements of the mobilities of positive and negative charge carriers and the ratio of these at each point, at elevated pressures in He II are presented. The data proceed along ten isotherms at 1.315 to 1.83 K from the vapor pressure to the melting curve, and along cross-hatching isobars at intermediate pressures through the lambda line as well. This mapping extends through the regimes of roton scattering kinetic theory and viscous dynamics, accommodating to various analyses of mobility theories and charge carrier models, and of the roton parameters under pressure. All analyses are not pursued in depth, but almost five hundred mobility data are tabulated and plotted, for each carrier separately and as ratios, against pressure and inverse temperature, to reveal previously unobserved structure. The technique is a measurement of the drift time for charge carriers of either sign, generated by a 0.46-mCi americium alpha source and received by a fast electrometer as a current pulse of less than 10^{-11} A with a signal-to-noise ratio of less than unity. The time-of-flight varies from a fraction of a second to several seconds for a distance of five and a half centimeters under a uniform field of 100 V/cm. Signal-to-noise is improved by signal averaging with a multichannel pulse height analyzer/time averaging computer, whose analog output is measured by hand. (Diss. Abstr. Int., B)

9362 DETECTION OF SINGLE QUANTIZED VORTEX LINES IN ROTATING LIQUID HELIUM. Packard, Richard Erwin. Ann Arbor, Mich.; Univ. of Michigan (1969). 80p. University Microfilms Order No. 70-21,749.

Thesis.

The appearance of individual quantized vortex lines was detected in liquid He II in narrow (~1 mm) diameter, rotating, cylindrical vessels slowly accelerated from rest. The angular velocities where the lines appear are qualitatively consistent with theory based upon minimization of the free energy. However, it is found that the detailed behavior of the He II is quite history-dependent and cannot be uniquely determined from existing theory. The detection technique involves trapping electrons on the vortex lines for a fixed length of time. A subsequent measurement of the amount of charge trapped provides an indication of the number of vortex lines present. To determine the small amount of charge trapped on a single line, the trapped electrons were injected through the meniscus and detected in the vapor with a proportional counter. Vortex lines that persist after stopping rotation were observed. The apparent destruction of vortices by mechanically disturbing the rotating container was also disturbed. (Diss. Abstr. Int., B)

Superconductivity

Refer also to abstracts 9591 and 9921.

9363 (NYO-2150-64) INTERPHASE BOUNDARY WAVES IN THE INTERMEDIATE STATE OF LEAD. Kushnir, A. J.; McLean, W. L. (Rutgers-The State Univ., New Brunswick, N. J. Dept. of Physics); Kasdan, A.; Maxfield, B. W. (Cornell Univ., Ithaca, N. Y.). Oct 1970. 36p. Dep. NTIS.

The propagation of waves similar to helicon waves was studied in the superconducting intermediate state of lead in polycrystalline samples and in single crystals of varying quality. The theories of Nozières and Vinen and of Andreev were found to agree well with the results from the highest quality specimen. The behavior of the other specimens, although resembling in some respects that predicted recently by Maki for unpure systems, is probably due to pinning effects. The results in lead are compared with those obtained in earlier work on indium and tin. (auth)

9364 NEW APPROACH TO THE JOSEPHSON EFFECT. Leplae, L.; Mancini, F.; Umezawa, H. (Univ. of Wisconsin, Milwaukee). Lett. Nuovo Cim.; 4: 963-8(21 Nov 1970).

Recent results obtained in the study of the structure of vortex lines in Type-II superconductors show that the boson method presents certain advantages with respect to other approaches and may give some new insights in the theory of superconductivity. The boson method is applied here to the study of the Josephson effect, and it is shown how this effect can be derived from general principles and how all the observable quantities can be computed without using any phenomenological assumption such as $J = J \sin \varphi$. The principal results of the Josephson effect are derived by solving the Laplace equation without making any use of the Josephson equation. The results of these computations differ from others, although they behave qualitatively in a similar way. The derivation of the net current crossing the barrier shows that, only in a simple case, does this current obey the theoretical diffraction pattern predicted through the use of the Josephson assumption; more generally, the results predict a periodic behavior not necessarily of the form $\sin(X)/X$. (M.H.R.)

9365 INFLUENCE OF MAGNETIC FIELD ON THE ABSORPTION OF ULTRASOUND BY SUPERCONDUCTING TIN IN THE INTERMEDIATE STATE. Bezuglyi, P. A.; Denisenko, V. P.; Fil, V. D.; Gorodinskii, V. F. (Physical-Technical Inst. of Low Temperature, Kiev). JETP Lett. (USSR) (Engl. Transl.); 12: 169-71(5 Sep 1970).

Translated from Zh. Eksp. Teor. Fiz., Pis'ma Red.; 12: 249-51 (5 Sep 1970).

It has been shown that when the conditions for the existence of geometric-resonance oscillations in the normal state are observed, a nonmonotonic dependence of ultrasound absorption on the magnetic field should likewise be observed in the intermediate state. The general expression for the oscillating part of the absorption is given and its ramifications discussed. It is pointed out that the picture of sound absorption in the intermediate state depends significantly on the dislocation structure of the sample, and reproducible results can be obtained only for well-annealed samples. (M.H.R.)

9366 FLUX-FLOW NOISE SPECTRUM IN TYPE II SUPERCONDUCTORS. Shen, S. W. (Univ. of Minnesota, Minneapolis). Appl. Phys. Lett.; 17: 415-16(15 Nov 1970).

Experimental verification is given of Burgess' theory of the flux-flow noise spectrum in type-II superconductors. The measurements made on vanadium foil biased in the linear V-I region show quantitative agreement with the modified theory. (auth)

9367 THEORETICAL STUDY OF THE PROPERTIES OF THE EXCITONIC INSULATOR. Henson, Wallace Ray. Tucson Ariz.; Univ. of Arizona (1970). 71p. University Microfilms Order No. 70-15,423.

Thesis.

The superconductive properties of the excitonic insulator are investigated by considering a simple two-band model. A superconductive response to an electromagnetic perturbation is demonstrated by establishing the existence of the Meissner effect. The interband scattering of electrons plays a crucial role in the calculation. By showing that persistent current states exist, the superconductivity notion is supported. These states are characterized as being the states of lowest free energy, subject to the constraints of charge neutrality and finite current flow due to exciton pairs. The self-consistency of the resulting quasiparticle distributions is proven by solving the energy gap equation for all temperatures below the critical temperature. Critical currents are then found which denote the currents at which the excitonic insulator undergoes a first-order phase transition and returns to the normal phase. (Diss. Abstr. Int., B)

9368 HYPERSOUND ATTENUATION IN SUPERCONDUCTORS BY QUASI-PARTICLE CREATION. Garfunkel, M. P.; Lue, J. W.; Pike, G. E. (Univ. of Pittsburgh). Phys. Rev. Lett.; 25: 1649-52(14 Dec 1970).

The attenuation of 10-GHz longitudinal sound waves in superconducting molybdenum (T_c = 0.914 K) and cadmium (T_c = 0.500 K) shows the high-frequency behavior predicted by the BCS theory. In particular, the onset of the rapid drop in attenuation with decreasing temperature that is characteristic of superconductors is shifted downward to the temperature T_v (0.905 K in molybdenum and 0.490 K in cadmium) at which the superconducting energy gap equals the phonon energy. The analysis of the measurements indicates a large anisotropy in the energy gaps of both metals. (auth)

9369 APPARENT UNIVERSAL BEHAVIOR OF FLUCTUATION-INDUCED DIAMAGNETISM IN SUPERCONDUCTORS. Gollub, J. P.; Beasley, M. R.; Tinkham, M. (Harvard Univ., Cambridge, Mass.). Phys. Rev. Lett.; 25: 1646-9(14 Dec 1970).

The dependence on temperature and magnetic field of the diamagnetism due to fluctuations above T_c, while showing marked deviations from the behavior expected on the basis of the Ginzburg–Landau theory, appears to follow a universal behavior if one introduces a new characteristic field H_s, which may be expressed in terms of other known material-dependent parameters. (auth)

9370 THERMAL CONDUCTION IN IRREVERSIBLE, TYPE-II SUPERCONDUCTORS. Ward, D.; Dew-Hughes, D. (Univ. of Lancaster, Eng.). J. Phys., C (London); 3: 2245-65(Nov 1970).

Previous experimental and theoretical work on thermal conduction in dirty type-II superconductors is discussed, with particular reference to possible effects of irreversibility on the theoretical models. Thermal conductivity and magnetization measurements have been made on a series of superconducting lead alloys. Mixed-state conductivity results cannot be explained in terms of existing models particularly for decreasing magnetic fields. It is shown that magnetic induction may be used as a parameter in describing the mixed-state conductivity for both increasing and decreasing fields even when specimens exhibit strong irreversibility. A model based on this observation is proposed. The theoretical results obtained are in good agreement with experiment for a wide range of alloy compositions, including those where there is a conductivity minimum, and for differing degrees of irreversibility. (auth) (UK)

9371 EFFECT OF APPLIED STRAIN ON THE ELECTRICAL RESISTANCE AND SUPERCONDUCTING TRANSITION TEMPERATURE OF THIN LEAD FILMS. Hutcheson, Edward Thomas. Clemson, S. C.; Clemson Univ. (1969). 79p. University Microfilms Order No. 70-17,447.

Thesis.

The normal-state resistance and superconducting transition temperature of thin lead films were measured as a function of film thickness and applied strain over a broad thickness range. Thin lead films varying in thickness from <100 to ≃ 1000A were vapor deposited at 77K under high vacuum conditions onto mica substrates which had previously been coated with a thin layer of silicon monoxide. Tensile and compressive strain was applied to the films by substrate bending methods and the corresponding changes in electrical resistance and T_c were observed. All strain-effect measurements were performed on the films before and after annealing to room temperature. Tensile strain increased the film resistance and compressive strain decreased the film resistance in qualitative agreement with previous experimental results on bulk lead. The strain resistance coefficient, γ, varied with unstrained lead film resistance in a manner which is characteristic of results obtained for most other conducting thin films. Films that had been annealed to room temperature exhibited larger values of γ than did unannealed films. A calculated value of the variation in film resistance as a function of strain induced volume changes for the thickest annealed film is in reasonable agreement with results obtained by hydrostatic pressure measurements on bulk lead. The superconducting transition temperature of both annealed and unannealed lead thin films showed a monotonic decrease with increasing residual film resistance. Applied compressive strain decreased T_c, in qualitative agreement with the results of hydrostatic pressure measurements on bulk lead, and applied tensile strain increased T_c. The sensitivity of T_c to applied strain generally decreased with increasing residual film resistance. A calculated value of the variation in transition temperature as a function of strain-induced volume changes for an annealed film, which showed the maximum sensitivity to strain, was in reasonable agreement with results obtained by hydrostatic pressure measurements on bulk lead. (Diss. Abstr. Int., B)

9372 PRESSURE-ENHANCED SUPERCONDUCTIVITY IN V_3X COMPOUNDS. Smith, T. F. (Univ. of California, San Diego, La Jolla). Phys. Rev. Lett.; 25: 1483-6(23 Nov 1970).

The superconducting transition temperature of the compounds V_3Si, V_3Ga, and V_3Ge is found to increase linearly with the application of hydrostatic pressure. This behavior is compared with predictions based upon measurements of the elastic moduli. (auth)

9373 MEASUREMENT OF THE FERMI VELOCITY IN SINGLE-CRYSTAL FILMS OF LEAD BY ELECTRON TUNNELING. Lykken, G. I.; Geiger, A. L.; Mitchell, E. N. (Univ. of North Carolina, Chapel Hill). Phys. Rev. Lett.; 25: 1578-80 (30 Nov 1970).

The Tomasch effect in quasi-particle tunneling from thick, superconducting, single-crystal Pb films was used to measure Fermi velocities in three high-symmetry directions. Multiple gaps were observed in all of these directions which agree with those reported earlier in bulk single-crystal studies, indicating that these films behave in a fashion similar to bulk Pb. (auth)

9374 EFFECT OF LOCALIZED SPIN FLUCTUATIONS ON THE SUPERCONDUCTING CRITICAL TEMPERATURE OF DILUTE ALLOYS. Zuckermann, M. J. (McGill Univ., Montreal Imperial Coll., London). J. Phys., C (London); 3: 2130-9(Oct 1970).

The effects of localized spin fluctuations (LSF) on the properties of dilute superconducting alloys are investigated in both the weak magnetic and strong magnetic limits. In the weak magnetic limit, the inverse lifetime Γ_s of the LSF is long compared with kT_c where T_c is the superconducting critical temperature of the alloy. The renormalized random phase approximation is applied to obtain an expression in this limit. The theory accounts for the decrease in T_c with impurity concentration in AlMn. In the strong magnetic limit $\Gamma_s \ll kT_c$, the result of Abrikosov and Gorkov for the pair-breaking effect of localized impurity spins on superconductivity is recovered. (auth) (UK)

9375 EXPANDED VORTEX' STATES IN SUPERCONDUCTING FILMS AND SURFACE SHEATH IN INCLINED FIELDS. Tilley, D. R.; Ward, R. (Univ. of Essex, Colchester, Eng.). J. Phys., C (London); 3: 2119-29(Oct 1970).

Because of the large demagnetizing factor, a thin superconducting film in an inclined field has vortices running normal to the plane of the film. The effect of the parallel component of the field is to enlarge the core radius of the vortex. Similar physical arguments are applied to the surface sheath in an inclined field, and an expression for the angular dependence of the critical field is derived that is in good agreement with the experimental results of Burger et al. In the experimental part, tunnelling measurements on N/S junctions were made, showing good agreement with the theory for expanded vortices in both thin films and the surface sheath. (auth) (UK)

9376 INFLUENCE OF THE PHYSICAL LATTICE IMPERFECTIONS ON A TYPE II SUPERCONDUCTOR. Van Der Klein, C. A. M. (Kamerlingh Onnes Laboratorium, Leiden); Elen, J. D.; Wolf, R.; De Klerk, D. Physica; 49: 98-124(12 Oct 1970).

Magnetic properties and resistive transitions were investigated on five samples of niobium which, after plastic deformation, were heat treated at different temperatures up to 1600°C. Electron micrographs show the decreasing dislocation density with increasing temperature of the heat treatment. The magnetization curves show increasing reversibility with increasing temperature. The susceptibility curves of samples heat treated up to 1200°C can be interpreted by means of a model based on surface effects only. Susceptibility curves of samples heat treated at higher temperatures, however, show that here bulk effects also play an essential role. Here the $\chi''(\chi')$ plots are asymmetric. Also, the resistive transitions can be interpreted by different models. (auth)

9377 MODEL FOR THE CURRENT ON A SUPERCONDUCTING TRANSMISSION LINE. Shadowitz, A. (Fairleigh Dickinson Univ., Teaneck, N. J.). Physica; 49: 141-52(12 Oct 1970).

A model is proposed for the flow of current on the superconducting wires connecting a battery and resistor. A longitudinal E component, present near the leading edge of a transient wave just outside the conductors, but not present in the steady-state field, provides an impulse to the electrons, causing them to move thereafter with constant velocity. Since some electrons receive an impulse before other electrons, the negative surface-charge density is changed by the leading edge of a wave. When an impulse is opposite to the wave direction the surface becomes positive; when both are in the same direction the surface becomes negative. Equations are derived for surface-charge density, electron drift velocity, and the force between the two wires. It is found that the drift velocities on the two wires are slightly different and that the force between wires can be attractive, zero, or repulsive. (auth)

9378 INVESTIGATION OF SUPERCONDUCTING PROXIMITY EFFECTS WITH ACOUSTIC SURFACE WAVES. Kraetzig, E. (Philips Forschungslaboratorium, Hamburg). Phys. Lett.; 33A: 343-4(30 Nov 1970).

The leakage of Cooper pairs from a superconductor into a nor-

XUM

mal metal is studied by measuring the attenuation of acoustic surface waves. (auth)

9379 PINNING OF FLUX LINES IN SUPERCONDUCTING NIOBIUM DUE TO POINT DEFECTS. Ullmaier, H.; Papastaikoudis, K.; Takacs, S.; Schilling, W. (Kernforschungsanlage, Juelich, Ger.). Phys. Status Solidi; 41: 671-9(1 Oct 1970).

Measurements of pinning forces due to statistically distributed vacancies and interstitials (Frenkel pairs) in niobium are reported. The defects were produced by low-temperature 3-MeV electron irradiation. The results indicate that fluctuations in the defect density and not the interaction between a single point defect and a flux line are responsible for the observed pinning effects. (auth)

9380 LEAD-ALLOYING EFFECTS ON THE SUPERCONDUCTING CRITICAL FIELD CURVE OF INDIUM. Carriker, R. C.; Reynolds, C. A. (Univ. of Connecticut, Storrs). Phys. Rev., B; 2: 3991-4001(15 Nov 1970).

The effects of lead alloying on several features of the superconducting critical-field curve of indium were studied. Both the anisotropy and linear effects were observed in T_c for the 0 to 4 at. % lead alloys. The coefficient of the linear effect K^{Pb} was measured directly and found to be 0.144°K/$\mu\Omega$ cm. Using the theory of Markowitz and Kadanoff, the value of the mean-squared anisotropy $\langle a^2 \rangle$ of the superconducting energy gap in indium is found to be 0.0072 ± 0.0007, and in indium doped with lead the mean collision time for transport is found to be at least three times larger than that for the smoothing out of the gap anisotropy. The superconducting transition temperature T_c is found to increase linearly with doping in the 3 to 4 at. % lead concentration range. This confirms earlier work and raises a question as to why there is no unusual behavior in T_c near 3.5 at. % lead, since several other properties of the system including residual resistivity, thermoelectric power, lattice spacings, and electronic specific heat all exhibit anomalous behavior near both 3.5 and 7.0 at. % lead, whereas T_c only exhibits unusual behavior near 7.0 at. % lead. Critical-field-curve measurements in 0 to 0.8 at. % lead samples are found to qualitatively confirm the predictions of Clem for effects of alloying on the critical-field curve of an anisotropic superconductor. Using the analysis of Clem, $\langle a^2 \rangle = 0.007$ is found from data on $dH_c/dT|_{T_c}$. The similarity conditions on $H_0(x)/T_c(x)$ and $h(x,t)$, where x is impurity content, are found to be violated for indium doped with lead. A linear effect in $H_0(x)$ which is stronger than the linear effect in $T_c(x)$ is also observed. (auth)

9381 CONFERENCE ON SUPERCONDUCTING MATERIALS, AUSSOIS, FRANCE, MARCH 10–12, 1969. Rev. Phys. Appl.; 4: 543-91(Dec 1969). (In French). (CONF-690343).

Various industrial laboratory, public, semi-public, and university representatives interested in the study, fabrication, and use of superconductors attended this conference, which was devoted mostly to various aspects of materials for superconductors. The program included both talks and round-table discussions. Separate abstracts were prepared for the eleven items published here. (L.M.T.)

For abstracts of individual papers see: 9382–9387, 9394–9397, and 9921.

9382 ELECTRONIC PROPERTIES AND SUPERCONDUCTIVITY. Barisic, S. (Faculte des Sciences, Orsay, France). Rev. Phys. Appl.; 4: 545-8(Dec 1969). (In French).

From Conference on Superconducting Materials, Aussois, France. See CONF-690343.

Some recent achievements in thermodynamics of superconductors, viewed from the microscopic theory, are briefly discussed. Emphasis is put on the systems with high transition temperatures. 16 references. (tr-auth)

9383 SOME MAGNETIC EFFECTS IN SUPERCONDUCTORS. Pincus, P. (Faculte des Sciences, Orsay, France). Rev. Phys. Appl.; 4: 549-52(Dec 1969). (In French).

From Conference on Superconducting Materials, Aussois, France. See CONF-690343.

The effects of magnetic forces that are not time-reversal invariant on the transition temperature and critical fields of superconductors are discussed. For example, paramagnetic impurities, external fields, superimposed magnetic films, etc., are considered. 11 references. (tr-auth)

9384 JOSEPHSON EFFECTS. Libchaber, A. (Ecole Normale Superieure, Paris). Rev. Phys. Appl.; 4: 553-5(Dec 1969). (in French).

From Conference on Superconducting Materials, Aussois, France. See CONF-690343.

Tunnel effects are mentioned briefly, after which a simplified theory of the Josephson effect is derived. References are cited that deal with specific applications of the Josephson effect. 16 references. (L.M.T.)

9385 SUPERCONDUCTING THIN FILMS. Combet, H. A.; Guyon, E.; Maldy, J. Rev. Phys. Appl.; 4: 569-73(Dec 1969). (In French).

From Conference on Superconducting Materials, Aussois, France. See CONF-690343.

The following topics are briefly discussed: problems of purity and structure of films; techniques of measurement of various properties; superconducting memories; tunnel effect and Josephson effect; and proximity effects between superconducting and non-superconducting films. Preparation of superconducting thin films is presented in one table, displaying the technique, materials, and observations. Another table displays the parameters influencing the normal or superconducting state and the structural state of layers. A third table presents techniques used in preparation of thin insulating barriers (10 to 50 Å). 50 references. (L.M.T.)

9386 SUPERCONDUCTING MATERIALS. Bethoux, O.; Dosdat, J. Rev. Phys. Appl.; 4: 575-7(Dec 1969). (In French).

From Conference on Superconducting Materials, Aussois, France. See CONF-690343.

Development of superconducting alloys and compounds is briefly discussed, and a table summarizes the information as follows: laboratory or firm; materials studied; problems studied; and methods utilized in their study. (L.M.T.)

9387 VORTEX TRAPPING. Rocher, Y. A.; Nemoz, A. Rev. Phys. Appl.; 4: 579-80(Dec 1969). (In French).

From Conference on Superconducting Materials, Aussois, France. See CONF-690343.

A brief resumé of the activities of various firms or laboratories in the subject area, as was presented by the researchers in a round-table discussion is included. In the course of the discussion, interest centered on the mechanisms of vortex trapping; a few of the more pertinent comments are included here. (L.M.T.)

9388 ONSET OF SURFACE SUPERCONDUCTIVITY. Schmidt, Hartwig (Technische Hochschule, Munich); Mikeska, Hans-Juergen. J. Low Temp. Phys.; 3: 123-35(Aug 1970).

The onset of superconductivity due to fluctuations of the order parameter is investigated in the presence of a surface. The onset of the Meissner effect is calculated in close analogy to the Landau diamagnetism of a free-electron gas, both phenomena being due to surface currents. In the framework of the static Ginzburg–Landau theory the current density induced by a magnetic field parallel to the surface is calculated as a function of the distance from the surface. It is shown that for magnetic fields above the surface-nucleation field H_{c3}, the integrated current density is the same for the two boundary conditions of vanishing-order parameter and vanishing-order-parameter derivative at the surface, and leads to the bulk expression for the fluctuation magnetization. Using the time-dependent Ginzburg–Landau theory, the dynamical conductivity in the surface sheath is calculated. Apart from numerical factors of order unity, the surface-sheath conductivity is found to diverge on approaching T_{c3} in the same manner as the conductivity of a thin film diverges on approaching the bulk transition temperature, and is isotropic in contrast to the bulk case in the presence of a magnetic field. (auth)

9389 SUPERCONDUCTIVITY AND NORMAL-STATE PROPERTIES OF Th–U ALLOYS. Maple, M. B.; Huber, J. G.; Coles, B. R.; Lawson, A. C. (Univ. of California, San Diego, La Jolla). J. Low Temp. Phys.; 3: 137-45(Aug 1970).

Anomalies in the normal-state electric resistivity, thermoelectric power, and magnetic susceptibility were observed in dilute alloys of uranium dissolved in thorium. These anomalies appear to be due to localized spin fluctuations with a characteristic temperature $T_0 \sim 100$ K, which are associated with 5f virtual bound states on the U atoms. The depression of the superconducting transition temperature of Th by U impurities is large and deviates markedly from the form given by the Abrikosov–Gor'kov theory. (auth)

9390 SUPERCONDUCTING TUNNELING IN SINGLE CRYSTAL AND POLYCRYSTALLINE THIN FILMS OF TIN. Fowler, John David Jr. Chapel Hill, N. C.; Univ. of North Carolina (1970). 82p. University Microfilms Order No. 70-21,196.

Thesis.

Measurement of anisotropy of the superconducting energy gap in thin films and in bulk materials is discussed in relation to the effect of scattering on the electron mean free path. Theories of subharmonic structure and multiparticle tunneling are also discussed. A procedure is listed for growing single-crystal thin films of tin on sodium chloride substrates by evaporation of the

melt in ultrahigh vacuum. Electron tunneling data for (001) single crystal and [100] textured polycrystalline films of tin are presented. The measured difference in anisotropy of the energy gap between these orientations is found to be 3%, in contrast to the 30% difference reported in the literature. It is believed that the observed reduction in anisotropy is due to the limitations imposed on the electron mean free path by surface scattering in the films. (Diss. Abstr. Int., B)

9391 INTERACTION OF A MAGNETIC IMPURITY WITH ELECTRONS IN METALS AND IN SUPERCONDUCTORS. Ting, Chin-sen. San Diego, Calif.; Univ. of California (1970). 135p. University Microfilms Order No. 70-23,044.

Thesis.

The interaction of a magnetic impurity with electrons in metals and in superconductors is treated on the basis of the s–d exchange model. First, the free energy of a dilute magnetic alloy is obtained on the basis of Suhl's theory from which the temperature dependent entropy and specific heat of the system are calculated at all temperature ranges. The finite temperature result on the entropy shift constitutes an advance beyond the existing literatures in which only T = 0 is available. Next, the magnetic susceptibility and the magnetization of the impurity spin in metals are calculated within the Abrikosov and Suhl approach and in a manner that respects conservation laws. The spin flip vertex function which appears in the susceptibility and the magnetization diagrams is approximated by Suhl's spin flip scattering amplitude. The result for the zero field magnetic susceptibility has the desirable property that it agrees with the perturbation theory calculation at high temperature and at T = 0 and for S = $\frac{1}{2}$, the localized impurity spin is completely compensated by conduction electrons. In the last part of the work, the thermodynamic effect of a magnetic impurity in superconductors is treated also within the s–d model. The free energy shift due to the presence of the impurity is calculated by using Maki's approach. Combining this with the phenomenological Ginsburg and Landau theory, the shift of transition temperature and specific heat jump at transition point can easily be obtained. Because of the mathematical complexities the calculation is restricted to $T_c > T_k$ only, where T_c is the superconducting transition temperature and T_k is the Kondo temperature. The essential feature of the result is that the presence of the magnetic impurity is simply to decrease the jump of the specific heat at the transition temperature T_c. (Diss. Abstr. Int., B)

9392 THERMAL CONDUCTIVITY OF PURE TYPE II SUPERCONDUCTORS. Schmidbauer, E. (Technische Hochschule, Munich); Wenzl, H.; Umlauf, E. Z. Phys.; 240: 30-41 (1970). (In German).

The thermal conductivity was measured on two niobium samples of different purity (ratio of mean free path to coherence length 220 and 10, respectively), in the mixed state, with heat current parallel ($k_\parallel$) and normal ($k_\perp$) to the magnetic field. The experimental results are compared with theories; the range of validity is discussed. Maki's relation $(k - k_n) \sim (H_{c2} - H)^{1/2}$ could be verified only for the purer sample in the field range $(H_{c2} - H) \simeq$ 140 Oe. The relations $k_\parallel/k_\perp > 1$ for $T \lesssim T_c$ and $k_\parallel/k_\perp < 1$ for $T \ll T_c$ were found to be valid for the whole range of fields in the mixed state. (auth)

Equipment and Devices

Refer also to abstracts 8580 and 9903.

9393 MAGNETIC FIELD CALCULATIONS FOR THICK SOLENOIDS. Merrill, John R. (Dartmouth Coll., Hanover, N. H.). Rev. Sci. Instrum.; 41: 1849-50(Dec 1970).

A simple computer program is described that calculates the magnetic field B inside the bore of any system of coaxial uniform current density solenoid of rectangular cross section using Garrett's method [J. Appl. Phys. 22, 1091 (1951)]. Two versions of the program exist, the first in the Dartmouth form of the language BASIC, the second in the language FORTRAN IV. Both versions are ideally suited to modern digital computers, including time-shared computers. Copies or listings of the programs are available upon request. The programs are based on those used to design a miniature superconducting magnet for dip experiments. (auth)

9394 APPLICATIONS OF SUPERCONDUCTORS IN ELECTRICITY TECHNOLOGY. Chabrerie, J. P. Rev. Phys. Appl.; 4: 565-8(Dec 1969). (In French).

From Conference on Superconducting Materials, Aussois, France. See CONF-690343.

After a quick survey of the various applications of superconductors in such fields as energy transport, energy storage, and energy conversion, only applications of superconductivity to rotating machinery are considered. The feasibility of heteropolar engines is examined, and two kinds of superconducting homopolar engines being built at the present time (I.R.D. and L.C.I.E. engines) are described. Developments and current directions of research in this field are summarized. 12 references. (tr-auth)

9395 COILS AND ENERGY STORAGE. Sauzade, M.; Sole, J. Rev. Phys. Appl.; 4: 581-2(Dec 1969). (In French).

From Conference on Superconducting Materials, Aussois, France. See Conf-690343.

A round-table discussion was devoted to the different problems posed by the storage and liberation of magnetically accumulated energy in a superconducting coil. Activities of various firms and laboratories in this field are discussed briefly under the following headings: energy storage, stabilization of superconducting materials, and coils for bubble chambers. (L.M.T.)

9396 HYPERFREQUENCIES. Combe, Rene. Rev. Phys. Appl.; 4: 583-8(Dec 1969). (In French).

From Conference on Superconducting Materials, Aussois, France. See CONF-690343.

Methods of calculation and theoretical problems concerning the surface impedance of metal superconductors, superconducting waveguides and wave propagation, high-frequency resistance of metals, and influence of a magnetic field on high-frequency absorption are briefly presented. Applications discussed include deposition of thin superconductors, high-frequency oscillators using a superconducting cavity, "monotron"-type oscillators, and guides and cavities for particle accelerators. 31 references. (L.M.T.)

9397 CRYOGENIC DEVICES FOR APPLICATIONS OF SUPERCONDUCTIVITY. Lacaze, A. Rev. Phys. Appl.; 4: 589-91(Dec 1969). (In French).

From Conference on Superconducting Materials, Aussois, France. See CONF-690343.

The round-table discussions of 40 participants considered the technical questions posed by utilization of very low temperatures in the area of superconductivity and the French efforts in this area. General points investigated were: production, transfer, and storage of liquid helium; thermal insulation and heat transfer; and measurement and regulation of temperature in the region 1 to 15°K. (L.M.T.)

Plasma and Thermonuclear Physics

Confinement and Heating

Refer also to abstracts 9420 and 9487.

9398 (ORO-3895-15) HELIOS PROGRAM. Progress Report. Robertson, Harry S. (Miami Univ., Coral Gables, Fla. Dept. of Physics). 15 Sep 1970. 56p. Dep. NTIS.

Helios is an experimental facility in which electrons and lithium ions are heated by electromagnetic broad-band noise covering a spectral range around the electron and ion cyclotron frequencies. Sections are given concerning the following: (1) description of Helios, (2) optical diagnostics, (3) kinetic theory, statistical mechanics, and continuum thermodynamics of plasmas, (4) cesium plasma; basic data, and (5) wave studies and instability analysis of cesium magnetoplasmas. (M.O.W.)

9399 PLASMA CONTAINMENT IN A COMBINED MIRROR-MULTIPOLE MAGNETIC FIELD. Yatsu, K. (Tokyo Univ.); Morimoto, S.; Uchida, T. Phys. Lett.; 33A: 361-2(30 Nov 1970).

Plasma containment in a combined mirror–multipole magnetic field is studied experimentally. The plasma containment time increases with the increase of the octopole field, and the plasma density is constant on equipotential surfaces of the octopole field. (auth)

9400 CLASSICAL DIFFUSION OF A PLASMA IN TOROIDAL SYSTEMS. Pogutse, O. P. (Inst. of Atomic Energy, Moscow). Nucl. Fusion; 10: 399-403(Dec 1970).

The effects of plasma rotation on classical diffusion in toroidal systems are studied. Within the framework of the hydrodynamic description of a plasma it is shown that, if the pressure gradient is not too great ($\rho/a < B_\theta/B_z$, where ρ is the ion Larmor radius, $a^{-1} = d\ln p/dr$, B_θ is the azimuthal field, and B_z the longitudinal field), then there is only one direction in which the plasma column can rotate with a velocity of the order of the drift velocity and at the same time become negatively charged—the diffusion coefficients differing only by a numerical factor of the order of unity from those previously known. It is also shown that there occurs in the plasma a transverse electric field that is much stronger

XUM

than the Pfirsh–Schluter field, the direction of which depends on the path length of the particles. (auth)

9401 ION HEATING IN THE DENSE PLASMA FOCUS. Toepfer, A. J.; Smith, D. R.; Beckner, E. H. (Sandia Labs., Albuquerque, N. Mex.). Phys. Fluids; 14: 52-61(Jan 1971).

The collapse phase of a dense plasma focus gun operating in deuterium was studied, using streak photography and time-resolved x-ray and neutron measuring techniques. The streak photographs, showing the radial motion of the luminous front at various axial positions, indicate a collapsing luminous front at the time of the current collapse followed by an expanding front and a recompression. The luminosity then disappears for a period of several hundred nanoseconds, during which time the neutrons are emitted. Estimates of shock heating and magnetic compressional heating were made from the streak pictures, and a calculation of plasma heating due to viscous forces arising from axial motion of the plasma was carried out. The effects of shock heating, magnetic compressional heating, and viscous heating are shown to be sufficient to produce an ion temperature of several kilovolts. (auth)

9402 PLASMA MOTION IN A TIME-CHANGING TOROIDAL OCTUPOLE MAGNETIC FIELD. Lencioni, Donald E. (Univ. of Wisconsin, Madison). Phys. Fluids; 14: 160-4(Jan 1971).

A gun-injected hydrogen plasma was contained in a toroidal octupole magnetic field. The plasma motion due to the changing magnetic field was studied and compared to a model based on the flux invariance of the motion. For early injection (while the field was rising) there was a strong motion toward the multipole rods while for late injection the motion was toward the wall. Magnetohydrodynamic theory shows that the plasma becomes unstable near the separatrix due to this motion. Although fluctuations were observed in this region, the plasma was found to be distributed stably. (auth)

9403 STATISTICAL DESCRIPTION OF CYCLOTRON HEATING IN A NONUNIFORM MAGNETIC FIELD. Nekrasov, A. K. (Inst. of Atomic Energy, Moscow). Nucl. Fusion; 10: 387-90(Dec 1970).

Criteria of stochasticity (conditions of randomization of Larmor-rotation phases) are obtained for cyclotron heating in a nonuniform magnetic field. It is shown that randomization of phases is possible with the sufficiently large electric field of the wave. Criteria of stochasticity are given in the form suitable for the fields of the type of the magnetic trap. For the case of fulfilment of these conditions, an equation is given that describes the variation in the distribution function and has the form of a Fokker–Planck equation. (auth)

9404 CYCLOTRON HEATING OF A PLASMA IN A NONUNIFORM MAGNETIC FIELD. Timofeev, A. V.; Nekrasov, A. K. (Inst. of Atomic Energy, Moscow). Nucl. Fusion; 10: 377-81(Dec 1970).

A circularly polarized electromagnetic wave propagating along a nonuniform magnetic field was studied. A general wave equation describing the propagation of the wave is obtained, and by means of this equation the physical processes that occur when the wave frequency coincides with the cyclotron frequency and which lead to absorption of the oscillations are analyzed. Corrections to the absorption coefficient to allow for the Doppler effect, particle acceleration, and the nonlinear character of the variation in an unperturbed magnetic field are found. It is shown that, in calculating the coefficient of absorption, use of the adiabatic wave equation leads to the same result as direct consideration of the resonance interaction. (auth)

9405 ONE-DIMENSIONAL LASER HEATING OF A STATIONARY PLASMA. Steinhauer, Loren C.; Ahlstrom, Harlow G. (Univ. of Washington, Seattle). Phys. Fluids; 14: 81-93(Jan 1971).

The problem of laser energy addition to a nonuniform one-dimensional plasma is considered. The object is to study plasmas that may achieve temperatures and densities of interest for application to controlled thermonuclear reactions. The advent of the nanosecond and picosecond lasers makes it possible to consider the heating of stationary, nonthermally conducting plasmas with a nonuniform density distribution in which only the electrons are heated. The solutions show that for a wide range of relevant parameters these assumptions are valid. The temperatures that can be produced are of interest in controlled thermonuclear reactions. Depending on the steepness of the density gradient, either wavelike or simultaneous heating is produced. Also, the temperature distribution is very much nonuniform and can significantly affect the subsequent dynamics of the plasma. (auth)

9406 EFFECT OF CO-ORDINATE SPACE PHENOMENA ON END LOSSES FROM, AND DISTRIBUTIONS INSIDE, MAGNETIC MIRROR SYSTEMS. Englert, Gerald W. (Colorado State Univ., Fort Collins). Nucl. Fusion; 10: 361-8(Dec 1970).

Refinement to existing methods of determining distributions of charged particles inside, and end losses from, magnetic mirror systems is made possible by a random-walk procedure. Co-ordinate space, as well as velocity space, can now be considered in detail in the analysis. It is shown that the usual loss-cone criterion far overestimates end-loss rates unless the mean free path is much greater than the distance between the mirrors. The extent of population of the loss cone is evaluated for a range of mean free paths and mirror ratios. (auth)

Diagnostics

Refer also to abstracts 9171, 9172, 9485, and 9510.

9407 (CEA-N-1391) SPECTROSCOPIC MEASUREMENT OF THE ELECTRON TEMPERATURE OF A PLASMA IN THE VACUUM UV. Bernard, A.; Genta, P.; Jolas, A. (Commissariat a l'Energie Atomique, Limeil-Brevannes (France). Centre d'Etudes). [nd]. 37p. (In French). Dep. NTIS (U.S. Sales Only).

The electronic temperature of a deuterium plasma was measured using vacuum spectroscopy. The Z pinch studied was of a noncylindrical revolution type. The method consisted of measuring the rates of the intensities of two lines of an additional gas as a function of time. Two adjacent oxygen lines corresponding to the O V and O VI ionization states were chosen; these wavelengths are particularly suitable for monochromator measurements. The characteristic plasma time was such that a quasi-equilibrium (corona type) was established. The theoretical value of the ratio between the intensities was calculated as a function of the electron temperature for electron densities of 10^{17} cm^{-3} and 3.10^{17} cm^{-3}. During a 1-μsec interval, the plasma temperature is almost constant at 16 eV. The experimental difficulties encountered are underlined. (France)

9408 (COO-1789-1) CYCLOTRON WAVE PLASMA STUDIES. Final Report. Scharer, J. E.; Beyer, J. B.; Horng, Chingshie (Wisconsin Univ., Madison). 1 Dec 1970. Contract AT (11-1)-1789. 12p. Dep. NTIS.

The diagnostic measurement of plasma density and collisional frequency in the presence of a magnetic field is studied. The gridded electrodes and 10-GHz microwave transmitting and receiving antennas were re-designed and the correlation of the theoretical model with the measurements was made. As an alternative, a 35-GHz Fabry–Perot cavity resonator system was constructed. The plasma was a cold collisional plasma in the presence of a magnetic field with an assumed relaxation collisional model. An electromagnetic wave was propagated along a uniform static magnetic field with a propagation phase constant β_p and an attenuation constant α_p. (auth)

9409 (CTO-733) SPECTRUM OF SCATTERED LASER RADIATION AND THE MEASUREMENT OF ELECTRON DENSITY IN A PULSED PLASMA. Besshaposhnikov, A. A.; Voloshin, A. E.; Kuchuberiya, I. Kh.; Sidorov, V. P.; Simonova, N. V. Translated by J. B. Sykes for Culham Lab., Abingdon, Eng., from Zh. Prikl. Spektrosk.; 6: 172-5(1967). 6p. Dep. NTIS (U. S. Sales Only).

An abstract of this paper, prepared from the original language, appeared as NSA 21: 25117. (M.O.W.)

9410 (CTO-736) POSSIBILITY OF MEASURING DIRECTED FLUXES IN A PLASMA CONTAINED IN A TOROIDAL MAGNETIC TRAP. Berezhetskii, M. S.; Grebenshchikov, S. E.; Kossyi, I. A.; Shpigel, I. S. (Akademiya Nauk SSSR, Moscow. Institut Fiziki). Translated by J. B. Sykes for Culham Lab., Abingdon, Eng., from report NP-18372. 15p. Dep. NTIS (U. S. Sales Only).

An abstract of this paper, prepared from the original language, appeared as NSA 24: 45223. (M.O.W.)

9411 (ECRC/N-288) NEW TECHNIQUE FOR MEASURING THE TEMPERATURE OF L.T.E. PLASMAS. Johnston, P. D. (Electricity Council Research Centre, Capenhurst (England)). Jul 1970. 13p. Dep. NTIS (U.S. Sales Only).

A method of defining the temperature at a given point in a discharge by means of a maximum in a ratio of measureable quantities and relating other ratios to this maximum is described. Measurements of the continuum velocity across the discharge and the intensity of a hydrogen line are all that is required. Both the line intensity and the continuum intensity can be converted, in the case of an inhomogeneous circularly symmetric discharge, from observed integrated profiles to radial profiles by an Abel inversion technique. The advantages of this method are: no knowledge of either the transition probability or the spectral band width

is required; enough continuum intensity can be accepted by the detector to provide a good signal-to-noise ratio; and no calibration whatsoever is involved. (UK)

9412 (LA-tr-70-25) INVESTIGATION OF FINE STRUCTURE OF A PLASMA FOCUS USING THE METHOD OF A MULTI-PERFORATED PINHOLE CAMERA. Agafonov, V. I.; Moiseeva, M. P.; Filippova, T. I.; Filippova, N. V. (Gosudarstvennyi Komitet po Ispol'zovaniyu Atomnoi Energii SSSR, Moscow. Institut Atomnoi Energii). Translated by Helen Dahlby (Los Alamos Scientific Lab., N. Mex.), from report IAE-2015. 9p. Dep. NTIS.

A method using x-ray pinhole cameras for investigating the final stage of cumulation of a shell with a noncylindrical constriction of the z pinch is discussed. The use of a set of apertures from 4 to 44 μ and photographing from two mutually perpendicular directions permitted refining the diameter of the plasma focus, finding the complex fine structure, and comparing the experimental values of the plasma focus dimensions with the calculated ones. From the experimental results obtained, an estimate of the charged-particle density in the plasma focus, $n \geq 1.5 \times 10^{20}$ cm^{-3}, was made. (auth)

9413 (SC-T-71-3001) MEASUREMENT OF THE ION TEMPERATURE IN A HYDROGEN ARC BY MEANS OF THE THERMAL DOPPLER EFFECT. Ludwig, D.; Raeder, J. Translated by D. P. Aeschliman (Sandia Labs., Albuquerque, N. Mex.), from Z. Naturforsch.; 25a: 473-81(1970). 26p. Dep. NTIS.

The determination of ion temperatures from the half-width of Doppler-broadened spectral lines (using side-on observation) was found to be possible, within reasonable error bounds, in plasma columns whose rotational velocity is sufficiently small that the Doppler broadening from that effect is negligible compared to the thermal Doppler effect. If the rotational velocity is large, the radial velocity distribution must be known in order that the macroscopic and thermal Doppler effects can be clearly separated. The result of the Abel inversion for the axis region with side-on observation depends ultimately on the shape of the radial emission coefficient of the spectral line used for the measurement. The error in the inversion will be small if this emission coefficient has its maximum on the arc axis. (auth)

9414 INVESTIGATION OF A THREE-COMPONENT PLASMA STREAMING INTO A DIPOLE MAGNETIC FIELD. Miller, Donald David. College Station, Tex.; Texas A and M Univ. (1970). 118p. University Microfilms Order No. 70-16,746.

Thesis.

Thomson-scattered laser light was used to determine time-resolved electron temperature and density as a hydrogen plasma, with helium and argon ions in 25 and 10% concentrations, drifted into a dipole magnetic field. Doppler broadening of the H_α line yielded data on the hydrogen ion temperature. The plasma was not trapped and was monitored while drifting through the dipole cusp. A two-phase plasmoid model is proposed in order to explain the behavior of the observed densities and temperatures. A given plasmoid is followed from its initiation until it passes the observation point while undergoing a collisionless transfer of directed ion energy to cyclotron energy due to the magnetic field gradient and then thermalizing through Coulomb collisions. Calculations using this model approximate the observed behavior and the trends pertinent to the effect of the heavy ions added as impurities. (Diss. Abstr. Int., B)

9415 EFFECT OF APERTURE ON PLASMA PARAMETERS DETERMINED DURING DIAGNOSTICS BY THE SCATTERING METHOD. Pyatnitskii, L. N.; Khaustovich, G. P.; Korobkin, V. V. High Temp. (USSR) (Engl. Transl.); 7: 325-7(Mar-Apr 1969).

Translated from Teplofiz. Vys. Temp.; 7: 359-61(Mar-Apr 1969).

The equations for calculating electron density and temperature from the spectral density of scattered light I_ω are discussed for the cases $\Omega < \Omega_{cr}$ and $\Omega > \Omega_{cr}$, where Ω_{cr} is the maximum solid angle at which the equation can be used. A similarity between $\Delta\omega$ (frequency shift) and the dimensionless frequency is derived, which holds true only for given constants θ_0 and Ω. The effect of the aperture on the scattering spectrum is illustrated for $\alpha_\theta = a/\sin(\theta/2) = 3.0$ for $\theta_0 = 90°$ and $\Omega = 0.35$. (D.L.C.)

9416 SPECTROSCOPIC METHODS OF DETERMINING THE CONCENTRATION OF CHARGED PARTICLES UNDER THE CONDITIONS OF A PULSE PLASMA GENERATOR. Bakanovich, G. I.; Grechikhin, L. I. (Inst. of Physics, Moscow). High Temp. (USSR) (Engl. Transl.); 7: 303-6(Mar-Apr 1969).

Translated from Teplofiz. Vys. Temp.; 7: 338-41(Mar-Apr 1969).

The concentration of charged particles in the jet of a pulse plasma generator was measured from the broadening of the H_δ hydrogen line, from the disappearance of the boundaries of the hydrogen series, from the broadening of the 4530.8-Å copper line, and from the ratio of the intensity of the forbidden transition to the permitted transition. Different methods yield sharply differing results. Limits of applicability of the various methods and their errors are evaluated. It is shown that, under conditions of high concentrations of charged particles in a plasma, the broadening of the auto-ionization lines is mainly due to the influence of the quadratic Stark effect. (auth)

9417 AFTERGLOW STUDIES IN HELIUM. Cronin, J. C.; Sexton, M. C. (University Coll., Cork, Eng.). Proc. Roy Irish Acad., Sect A; 70: 13-(1970).

A 9-GHz free-space microwave interferometer is used to measure the electron density decay in a pulsed helium discharge in the range 10^{11} to 10^{10} cm^{-3} over the pressure range 0.07 to 5.70 torr. The various decay mechanisms present are discussed in detail and values for recombination coefficients and mobilities are extracted. The possible existence of second-order diffusion at low pressures is also discussed. The values of recombination rates obtained indicate that a two-body recombination process is responsible for the volume removal of the electrons. (auth) (UK)

9418 ELECTRON TEMPERATURE AND DENSITY DISTRIBUTION OF AN ARGON PLASMA IN INDUCTIVE HYDRODYNAMIC SHOCK WAVE TUBES AND THEIR TIME DEPENDENCE. Liebich, V.; Persianzew, L.; Sacharow, A.; Rothhardt, L. (Institutsteil VI Magnetoplasmadynamik, Jena, Ger.). Monatsber. Deut. Akad. Wiss. Berlin; 12: 173-9(1970). (In German).

The electron temperature and plasma density distributions along the axis in the inductive hydrodynamic shock tube were analyzed by spectroscopic methods, and their time dependence was measured. It was found that the plasma has a steep front that moves, under the experimental conditions, with a velocity of 3×10^5 cm/sec in the axis direction. Charge-carrier density and electron temperature are $\approx 10^{16}$ cm^{-3} and ≈ 2 eV; both depend only slightly on the position and the time. (tr-auth)

9419 MEASUREMENTS ON THE ELECTRON ENERGY DISTRIBUTION FUNCTION IN A LOW-PRESSURE CESIUM DISCHARGE. Postma, A. J. (EURATOM-FOM, Jutphaas, Netherlands). Physica; 49: 77-91(12 Oct 1970).

Electron-energy distribution functions were determined from the second derivatives of Langmuir-probe characteristics in the positive column of a discharge in cesium vapor. To explain second-derivative curves at energies below 0.5 eV, it was assumed that reflection of electrons on the probe surface is important in this region. The reflection coefficient was determined as a function of the energy from a comparison of second-derivative curves measured at large discharge currents with the Maxwellian distribution functions that can be expected in this case. The second derivative was compared with distribution functions corrected for this reflection coefficient under circumstances where one cannot expect a Maxwellian distribution function. Good agreement was obtained at high energy; at low energy correctness of the theoretical distribution functions is in doubt. A conclusion from the work is that, in the case of reflection of electrons on the probe surface, the plasma potential, in general, is not related to the energy at which the second derivative of the probe current is zero or where it has a minimum or a maximum value. (auth)

9420 GENERAL SCHEME OF STUDYING TRAPPED PARTICLES IN FUSION DEVICES. Liu, Chuan Sheng; Wong, Alfred Y. (Univ. of California, Los Angeles). Phys. Rev. Lett.; 25: 1702-6(21 Dec 1970).

A general scheme of detecting magnetically trapped particles in fusion devices through the observation of echo phenomena is proposed. The conditions for temporal echoes due to the trapped particles are derived, and a physical explanation of trapped-particle echoes is given. (auth)

9421 DETERMINATION OF THE ELECTRON DENSITY IN AN IONIZED CESIUM VAPOR FROM MEASUREMENTS OF THE STARK BROADENING OF THE 5D-nF ($n \geq 10$) LINES. Sayer, Bernard (CEA, Saclay, France); Sassi, Mohamed; Jeannet, Jean-Claude. Compt. Rend., Ser. B; 271: 839-42(19 Oct 1970). (In French).

The experimental profiles of the 5D-nF ($n \geq 10$) lines were compared with calculated Stark profiles. Excellent agreement was obtained in the electron density range 0.8 to 3×10^{13} cm^{-3}. (tr-auth) (France)

9422 DETERMINATION OF THE ELECTRON DENSITY OF A XENON PLASMA, PRODUCED IN A SHOCK TUBE, BY LASER INTERFEROMETRY AND SPECTROSCOPY. Richou, Jacques; Molitor, Alain (Observatoire de Paris, Meudon, France). Compt. Rend., Ser. B; 271: 753-6(12 Oct 1970). (In French).

Spectroscopy and laser interferometry were used to study a xenon plasma produced in a shock tube. The relaxation time for the ionization process was deduced from measurements of the electron

XUM

density as a function of time. A discrepancy of 15% occurred between results derived from the two methods. (tr-auth) (France)

9423 MEASUREMENT OF THE ABSOLUTE INTENSITIES OF THE SPECTRAL LINES AND THE BACKGROUND CONTINUUM OF AN ARGON PLASMA PRODUCED IN A SHOCK TUBE. Larcher, Ghislain; Thenard, Claude; Maillot, Patrice; Valentin, Pierre (Rouen Univ., Mont-Saint-Aignan, France). Compt. Rend., Ser. B; 271: 765-8(12 Oct 1970). (In French).

A method of calibrating the sensitivities of fast-response spectrometers is described. The luminance of a plasma produced by a shock wave could thus be measured. The structure of an argon plasma in the equilibrium region was studied. (auth) (France)

9424 MICROWAVE DIAGNOSTICS OF STRONG-CURRENT DISCHARGES WITH SKIN EFFECT. II. DETERMINATION OF PLASMA PARAMETERS IN A NITROGEN ARC DISCHARGE AT ATMOSPHERIC PRESSURE. Koernicke, H.; Suess, W.; Prinzler, H. (Zentralinstitut fuer Elektronenphysik, Berlin). Beitr. Plasmaphys.; 10: 139-59(1970). (In German).

Microwave diagnostics of an inhomogeneous, dense, cylindrical plasma column may be used to determine the complex impedance and a mean noise temperature in the range of strong skin effect. This case is realized if the specific dc impedance E/I falls below a critical value, e.g., 20 Ω/cm for $\omega = 10^{10}$. It is shown that, for any radial conductivity profile, the complex impedance is a function of E/I only. A formula is derived for calculating the noise temperature of the column as a weighted mean value due to the local plasma temperature and conductivity. In the case of strong skin effect this mean value equals the electron temperature of plasma regions near the boundary of the conducting diameter. These results, together with spectroscopic diagnostics, are used to determine some plasma parameters of an arc discharge in a streaming nitrogen atmosphere at 760 torr. The temperature profile was obtained from the intensity of the 3371-Å molecular band, and then the conductivity profile was calculated using an energy balance equation. The results show that, even in the 10-Å case, the arc plasma is not in thermal equilibrium, the difference $T_e - T_g$ being about 1500°K. This large difference is due to the flow of neutral gas streaming downward the discharge chamber. The length of the discharge (1 to 3 cm) is not sufficient for the neutral atoms to reach their equilibrium temperature. (auth)

9425 MICROWAVE DIAGNOSTICS OF INSTABILITIES IN COLUMN PLASMAS. ELECTRON DENSITY AND TEMPERATURE AND LIGHT EMISSION IN SELF-EXCITED MOVING STRIATIONS IN HYDROGEN DISCHARGES. Schockenhoff, F.; Stirand, O.; Prinzler, H. (Zentralinstitut fuer Elektronenphysik, Berlin. Tschechoslowakischen Akademic der Wisconschaften, Prague). Beitr. Plasmaphys.; 10: 123-37(1970). (In German).

Microwave methods are used to obtain the periodic variations in time and space of some plasma parameters. The electron density is obtained, using a time display of the reflection coefficient due to a plasma-perturbed cavity, and the electron temperature is obtained from the noise signal of a DICKE radiometer gated periodically. Assuming simple one-dimensional sinusoidal variations of temperature and density, the fundamental convolution integrals relating the appropriate cavity parameters to the plasma properties are solved and formulas are obtained to calculate the real fluctuating quantities. Also, in the case where the length of the cavity field region equals the dimension of the variations, the correct phase relation between electron temperature and density is obtained. The method is used for diagnostics of self-excited moving striations in hydrogen. The striations (frequency 24 kHz, striation lengths ~1 cm) move from cathode to anode and the sequence of the different maxima for an observer at rest is electron density, temperature, and light emission. The phase shift between density and temperature is about 90°, the appropriate density variation 10 : 1, and the temperature variation >2 : 1. (auth)

9426 SPECTRAL MEASUREMENTS OF PLASMA TEMPERATURE IN THE ROD PLASMA INJECTION (RPI). Suckewer, Szymon (Inst. of Nuclear Research, Swierk, Poland). Nukleonika; 15: 1-19(1970).

Results of ion and electron temperature measurements for the focusing injector "RPI" are given for different initial conditions. The ion temperature measurements were performed with plasma being observed lengthwise and perpendicularly to the gun axis to eliminate the influence of the correlated axial motion of plasma. It was found that T_i increases with rise in ion charge and decreases with increase of initial gas pressure in the discharge tube. The ion temperature drop is also observed when applying an external magnetic field $H_z = 5$ kG. The highest value of $T_i = 1.5 \times 10^6$ °K is found for the air initial pressure $p = 10^{-4}$ torr, whereas maximum electron temperatures do not exceed $T_e = 5 \times 10^4$ °K. The ion and the electron temperatures are determined as functions of the distance from the gun axis. The considerable differences observed between the electron and the ion temperatures are also discussed. (auth)

9427 MEASUREMENT OF MAGNETIC FIELD IN A LABORATORY PLASMA BY THOMSON SCATTERING OF LASER LIGHT. Evans, D. E.; Carolan, P. G. (Culham Lab., Abingdon, Eng.). Phys. Rev. Lett.; 25: 1605-8(7 Dec 1970).

A 2.7-Å band of the spectrum of ruby-laser light scattered by a plasma (20 eV, 10^{15} electrons/cm^3) in the presence of a magnetic field of about 15 kG was isolated and passed through a 0.1-Å resolution interferometer. Magnetic modulation of the spectrum was detected. There is reasonable agreement between the field strength calculated from the modulation and that measured by Faraday rotation. (auth)

9428 MICROWAVE DIAGNOSTICS OF STRONG-CURRENT DISCHARGES WITH SKIN EFFECT. I. FIELD DISTRIBUTION, SURFACE IMPEDANCE, AND RADIATION TRANSPORT. Prinzler, H. Beitr. Plasmaphys.; 9: 359-70(1969). (In German).

Using the methods of microwave diagnostics in the case of a dense cylindrical plasma column, a complex surface impedance and a mean noise temperature due to the real part of this impedance may be obtained, instead of electron density, collision-frequency and noise (electron-) temperature in the usual low-density case. These quantities, including the skin effect, are calculated for the axial-symmetric plasma mode of an inhomogeneous plasma column. The mean noise temperature is obtained, using a new method based on relations between the corresponding wave equation and the four pole equations. The result is a differential equation similar to the equation of radiation transfer, but without the well-known restrictions of this tool (approximation of ray optics, low damping of the wave). (auth)

9429 STUDIES OF THE LARGE-SHEATH CONCEPT FOR THE CONTINUUM PROBE THEORY. Chen, Sin-li; Chang, Jen-shih; Matsumura, S. (Musashi Inst. of Tech., Tokyo). J. Appl. Phys.; 42: 499-501(Jan 1971).

The continuum probe theory using the concept of "collision-dominated sheath" for low-density ($N_e = 10^6$ to 10^{10} cm^{-3}) plasmas has been studied by Kiel, and some simple forms representing ion current characteristics of both spherical and cylindrical probes were also presented by him for the use of electron density determinations. Experimental comparisons with his theory are made, and it is shown that the sheath concept is valid only for the case of high-density plasmas for which $\xi_e > 1$, where $\xi_e = r_p/h_e$, r_p is the probe radius and h_e is the electron Debye length, respectively. Experiments were performed in dc glow discharge argon plasmas produced in a cylindrical tube with an inside diameter of 60 mm. Spherical probes ($r_p = 0.39$ and 0.75 mm) made of platinum were used. (M.O.W.)

9430 IONIZATION GAUGE FOR MEASURED MOLECULAR FLUX DENSITIES IN OGRA-II. Zubarev, V. F. (Inst. of Atomic Energy, Moscow). Instrum. Exp. Tech. (USSR) (Engl. Transl.); No. 1, 191-3(Jan-Feb 1970).

Translated from Prib. Tekh. Eksp.; No. 1, 168-70(Jan-Feb 1970).

An ionization gage for measuring the density of a molecular flux of gas passing through the region of plasma buildup in the Ogra-II apparatus is described. The gage has a linear characteristic in the range 10^{-10} to 10^{-5} torr and a sensitivity of 10^5 torr^{-1}. (auth)

Kinetics (General)

Refer also to abstract 10221.

9431 (SC-T-70-4050) ESTABLISHMENT OF A GENERAL RULE FOR A HOLLOW-CATHODE ARC DISCHARGE. Delcroix, J. L.; Minoo, H.; Trindade, A. R. Translated by Anna Vakar (Sandia Labs., Albuquerque, N. Mex.), from J. Phys. (Paris), 29: 605-10(Jul 1968). 17p. Dep. NTIS.

An abstract of this paper, prepared from the original language, appeared as NSA 22: 52784. (M.O.W.)

9432 (SC-T-70-4051) NEW OPERATION MODE FOR A HOLLOW-CATHODE ARC DISCHARGE. Delcroix, Jean-Loup; Minoo, Habibollah; Trindade, Armando Rocha. Translated by Anna Vakar (Sandia Labs., Albuquerque, N. Mex.), from Compt. Rend., Ser. B; 266: 762-4(Mar 1968). 5p. Dep. NTIS.

A hollow-cathode arc operation without cathode gas flow is described. The method is developed, starting from the operation mode known as "hollow-cathode with gas flow." (auth)

9433 (SC-T-70-4053) STUDY OF HOLLOW-CATHODE DISCHARGES DEPENDENT ON GAS FLOW IN ARC OPERATION. Delcroix, J. L.; Minoo, H.; Trindade, A. R. Translated by Anna Vakar (Sandia Labs., Albuquerque, N. Mex.), from Rev. Roum. Phys.; 13: 401-22(1968). 35p. Dep. NTIS.

An abstract of this paper, prepared from the original language, appeared as NSA 22: 44176. (M.O.W.)

9434 EXPERIMENTAL INVESTIGATION OF DISTRIBUTION OF PARAMETERS IN ONE-PHASE AND TWO-PHASE SUBSONIC PLASMA JETS. Surov, N. S. (Inst. of Aviation Tech., Moscow). High Temp. (USSR) (Engl. Transl.); 7: 276-82(Mar-Apr 1969).

Translated from Teplofiz. Vys. Temp.; 7: 304-12(Mar-Apr 1969).

The distribution of velocity and temperature in single-phase and two-phase plasma jets (two-phase factor up to ~4.4) was investigated experimentally. It was found that the temperature and velocity of a gas may be lowered appreciably by introducing the condensed phase into a plasma stream. It was established that a marked reduction of the jet parameters downstream occurs. It is shown that the distribution of parameters in transverse sections of the main part of the jet is described satisfactorily by the appropriate Schlichting curves. Values were found for the Reynolds number characteristic of change of flow regime in an argon plasma stream at the nozzle exit. (auth)

9435 NONEQUILIBRIUM LOW-TEMPERATURE PLASMA. III. ELECTRON CONCENTRATION IN NONEQUILIBRIUM PLASMA. Biberman, L. M.; Vorob'ev, V. S.; Yakubov, I. T. (High Temperature Inst., Moscow). High Temp. (USSR) (Engl. Transl.); 7: 183-91(Mar-Apr 1969).

Translated from Teplofiz. Vys. Temp.; 7: 193-202(Mar-Apr 1969).

Stationary nonequilibrium plasma was examined. The unbalance was caused by the emission of radiation, the diffusion of charged particles toward the plasma boundaries, collisions involving the participation of atoms and ions, and the external field. The electron concentration was determined. The criterion governing applicability of the Saha equation was derived. A comparison was made with experimental data available in the literature. (auth)

9436 PISTON PROBLEMS WITH IONIZING SHOCK WAVES. Bausch, H. Monatsber. Deut. Akad. Wiss. Berlin; 12: 135-45 (1970). (In German).

In the tube, in the presence of a transverse electromagnetic field, it is assumed that the piston moves with constant velocity into a gas at rest. Further, the cross section of the tube is assumed sufficiently large so that the effect of the boundary walls can be neglected. The shock wave propagated in front of the piston should be a weak ionizing wave. The current behind the shock wave and the induced magnetic field are calculated with the help of a series development in powers of R_m. The velocity distribution obtained is used for a more accurate determination of the induced magnetic field. The induction equations are solved with the help of Laplace transformations. (tr-auth)

9437 FORMATION AND STRUCTURE OF ELECTROSTATIC COLLISIONLESS SHOCKS. Forslund, D. W.; Shonk, C. R. (Los Alamos Scientific Lab., N. Mex.). Phys. Rev. Lett.; 25: 1699-1702(21 Dec 1970).

A one-dimensional, two-species numerical-simulation code was used to study the formation and structure of collisionless electrostatic shocks formed by two colliding plasmas and by a plasma striking a perfectly reflecting piston. Collisionless shocks were formed in hydrogen up to a maximum piston velocity of $M \equiv v_D/c_s \sim 3.5$. Shocks with velocities up to $M \sim 4$ were produced that have a predominantly laminar structure accompanied by strong collisionless dissipation. (auth)

9438 CONTINUOUSLY OPERATING PLASMA PROPULSION. Peters, Theo (Deutsche Forschungs- und Versuchsanstalt fuer Luft- und Raumfahrt, Stuttgart). pp 369-78 of l'Evoluzione della Propulsione Spaziale Negli Anni '70. Roma; XVII Rassengna Internazionale Elettronica Nucleare e Teleradiocinematografica (1970).

From 10th International Technical-Scientific Meeting on Space. Rome, Italy. See CONF-700318.

Continuously working plasma thrusters are discussed under the following headings: (1) principles of stationary electromagnetic acceleration, (2) plasma thruster with self-magnetic acceleration, and (3) Hall-current acceleration. Theoretically, both self-magnetic and Hall-current acceleration appear promising, and experiments have shown the feasibility of arc discharges operating under conditions necessary to maintain stable conditions. However, the complexity of the acceleration mechanism and the thermodynamic nonequilibrium state of the plasma dictate that much more experimentation is necessary. (L.M.T.)

9439 HIGH-TEMPERATURE ENERGY SYSTEMS WITH PLASMA REACTORS AND INDUCTIVE MAGNETOPLASMADYNAMIC CONVERTERS. Peschka, Walter (Deutsche Forschungs- und Versuchsanstalt fuer Luft- und Raumfahrt e.V., Stuttgart). pp 379-88 of l'Evoluzione della Propulsione Spaziale Negli Anni '70. Roma; XVII Rassengna Internazionale Elettronica Nucleare e Teleradiocinematografica (1970).

From 10th International Technical-Scientific Meeting on Space, Rome, Italy. See CONF-700318.

The present status of research on nuclear propulsion and magnetoplasmadynamic power generation (using fission- or fusion-type reactors and electrodeless inductive converters) is very briefly summarized. (L.M.T.)

9440 RADIATIVE TRANSFER IN AN LTE ATMOSPHERE: AN INTEGRAL KERNEL FORMULATION OF THE COMPTON SCATTER SOURCE TERM. Babuel-Peyrissac, J. P.; Rouvillois, G. (CEA, Bruyeres-le-Chatel, France). J. Quant. Spectrosc. Radiative Transfer.; 10: 1277-90(Dec 1970).

The spectrum of the radiation scattered by an LTE atmosphere irradiated by a given spectrum is computed. The expression given for the integral kernel of Compton scatter takes into account both the Doppler shift and the Compton frequency shift. Collective (plasma) phenomena are neglected, and the binary encounter approximation is used throughout. The result is accurate to terms of 2nd order in v/c (v being the electron velocity, c the light velocity). A comparison is made with previous results. (auth) (UK)

9441 GVOSDOVER EFFECT IN A LOW-PRESSURE ARC CONSTRAINED BY ITS OWN MAGNETIC FIELD. Hoyaux, M. F. (Univ. of Pittsburgh). Appl. Sci. Res. (The Hague); 22: 321-37 (Jul 1970).

Calculations are continued for a preceding paper (Theoretical investigation of the first-order magnetic self-striction in a low-pressure arc with remote walls) and a method for adding the Gvosdover effect (reduction in electron mobility by ion–electron scattering) to the corrections introduced in that paper is described. The case of mercury vapor is, again, treated as an example. The model predicts the slightly rising volt–ampere characteristics pertaining to related cylindrical arcs and also shows some discontinuities and instabilities not found in the cylindrical case. (auth)

9442 INITIATION OF ARCS BY ION BOMBARDMENT. Lloyd, O.; Gozna, C. F.; Jervis-Hunter, G. (Central Electricity Generating Board, Marchwood, Eng.). J. Phys., D (London); 3: 1670-7(Nov 1970).

The arcing behavior of a number of refractory metals and graphite was examined by negatively biasing specimen electrodes in the presence of a pulsed rf discharge in order to select anode materials for gas-filled valves which would reduce their tendency to arc-back under severe commutation conditions. The voltage at which about 5% of the pulses resulted in an arc, at an argon ion current density of 1.2 kA m^{-2}, was used as a figure of merit. Of the materials examined, tungsten was the best with a figure of merit of 15 kV and graphite the worst with 6 kV. A good correlation was obtained between the results and the published values for the vacuum arc voltages. (auth) (UK)

9443 ANOMALOUS PLASMA RESISTIVITY AT LOW ELECTRIC FIELDS. Coppi, B. (Massachusetts Inst. of Tech., Cambridge. Princeton Univ., N. J.); Mazzucato, E. Phys. Fluids; 14: 134-49(Jan 1971).

Experiments have shown the appearance of "nonclassical" resistivity, higher than that predicted by the known transport theory based on electron–ion collisions, in magnetically confined plasmas where the electron gyrofrequency is larger than the Langmuir frequency and the electric field is well below the runaway threshold. A theoretical interpretation of the anomalous resistivity onset is proposed observing that (at long but finite mean free paths) nonresonant modes, associated with the effects of electron–electron collisions, are excited when the electron flow velocity along the magnetic field is roughly larger than the ion sound-wave velocity. The magnitude of anomalous resistivity is then discussed in relation to the nonlinear effects of resulting fluctuations and of related modes with wavelengths shorter than the mean free path. A comparison between several experiments on plasma confined in different stellarator and tokamak configurations is given. The differences in physical regimes that lead to various mechanisms for the appearance of "nonclassical" resistivity and the relationship with anomalous diffusion are pointed out. (auth)

9444 SVOISTVA GAZOV PRI VYSOKIKH TEMPERATURAKH. FIZICHESKAYA GAZODINAMIKA, TEPMODINAMIKA I FIZIKA GORENIYA. (Properties of Gases at High Temperatures. Physics of Gasdynamics, Thermodynamics, and Combustion Physics).

XUM

Predvoditelev, A. S. (ed.). Moscow; Izdatel'stvo Nauka (1967). 184p.

Twenty-nine articles are included on theoretical and experimental studies of gas flow at high temperatures, thermodynamic functions, and physicochemical processes in heterogeneous systems of gas–solid bodies. Experimental results are presented on the processes of ionization and dissociation of gases and on properties of ionized gases in magnetic fields. Separate abstracts were prepared for three of the articles. (R.V.J.)

For abstracts of individual sections see: 9281, 9445, and 9446.

9445 STUDIES OF THE STRUCTURE OF IONIZED GAS FLOW IN ELECTROMAGNETIC SHOCK TUBES. Bashilov, V. A.; Shevelev, V. P. pp 89-94 of Svoistva Gazov pri Vysokikh Temperaturakh. Predvoditelev, A. S. (ed.). Moscow; Izdatel'stvo Nauka (1967). (In Russian).

Studies of discharge processes in a conical discharge chamber revealed the formation of a rotating pinch effect that equalized the plasma flow from the cone without any converging shock wave. The structure of the plasma flow at various initial discharge conditions was analyzed, and plasma flow interactions with solids were investigated. (R.V.J.)

9446 DETERMINATION OF ELECTRON CONCENTRATION BEHIND THE SHOCK-WAVE FRONT AND IN GAS-DISCHARGE PLASMA IN A MAGNETOHYDRODYNAMIC SHOCK TUBE. Bashilov, V. A. pp 95-7 of Svoistva Gazov pri Vysokikh Temperaturakh. Predvoditelev, A. S. (ed.). Moscow; Izdatel'stvo Nauka (1967). (In Russian).

Electron density measured along the $H\beta$ line half-width, with the assumption of Stark broadening of the hydrogen line, showed the existence of a transition area from the discharge plasma to the pure gas. Moreover, the concentration of plasma increased evenly in the direction of discharge plasma, which may be explained by electron diffusion from the discharge plasma into the pure gas region. (R.V.J.)

Kinetics (Experimental)

9447 INSTABILITIES DUE TO INTERACTION BETWEEN A SLOW ELECTRON BEAM AND A PLASMA. Amagishi, Yoshimitsu (Fukushima Tech. Coll., Japan). J. Phys. Soc. Jap.; 29: 1592-7 (Dec 1970).

A mercury plasma is perturbed experimentally by a slow electron beam whose velocity is of the order of a thermal velocity of medium electrons. A special, but simple, gun is used to drive the slow electron beam into the plasma region. The beam is therefore considered to be of drifted Maxwellian distribution. Instabilities are classified into two types; one of them is a wave of beam–electron coupling, and the other is a wave of beam–ion coupling. Unstable regions are shown as a function of the frequency and the electron beam velocity, and explained on the basis of the theory of drift instability in a three-component plasma system. (auth)

9448 ENHANCED RADIATION FROM A THETA-PINCH PLASMA. Chin-Fatt, C.; Griem, Hans R. (Univ. of Maryland, College Park). Phys. Rev. Lett.; 25: 1644-6(14 Dec 1970).

Radiation exceeding thermal bremsstrahlung by more than three orders of magnitude was observed from a theta-pinch plasma. The spectrum consists of two broad and partially overlapping bands centered approximately at the electron plasma frequency and its first harmonic. (auth)

9449 EFFECT OF IRRADIATION ON THE CURRENT PULSES IN A LOW-FREQUENCY ELECTRODELESS ARGON DISCHARGE. Kher, V. G.; Hirde, J. P.; Kshirsagar, S. R. (Inst. of Science, Nagpur, India). J. Phys., B (London); 3: 1539-43(Nov 1970).

The effect of irradiation from an incandescent light source on the average current of a discharge in argon (the Joshi effect) was studied for pressures of 0.7 to 10 torr using a cylindrical glass vessel (length 1.2 cm, diameter 5.3 cm) and applying an ac voltage (of frequency 20 to 500 Hz) to external electrodes. The first current pulse group in each half cycle was found to consist of a steady wide low pulse that appears at a constant phase angle and a flickering narrow high pulse erratic in phase angle. Irradiation with a 200-W lamp placed 30 cm from the vessel reduces the amplitude of the second pulse considerably. By increasing the applied voltage beyond threshold the relative change in average current $\Delta I/I$ was found to increase continuously whereas other workers have always observed a decrease in $\Delta I/I$ with rising V. It is suggested that argon metastables from the discharge diffuse to the glass walls thus increasing the density of the low-work-function electron layer. The flickering part of the first pulse is thought to be caused by the fast photoelectric secondary mechanism and hence its peak increases with the applied voltage. Irradiation partly destroys the electron layer so that the peak of the flickering pulse is considerably reduced. (auth) (UK)

9450 EXPERIMENTAL STUDY OF THE SCATTERING OF AN ION BEAM IN HOT-ELECTRON PLASMA. Kirichenko, G. S.; Khmaruk, V. G. At. Energ. (USSR); 29: 136-8(Aug 1970). (In Russian).

The ion–acoustic instability that arises upon passage of an ion beam through the plasma may serve as an effective mechanism of the collision-free relaxation of the beam and the heating of the plasma. In connection with this, experiments were carried out to achieve a two-beam ion instability in the plasma at temperatures higher than those obtained with gas discharges for the purpose of studying the effective scattering of the beam. Argon plasma was used, the temperature of which could be increased from ~10 to 50 to 60 eV by electron-beam heating in a homogeneous magnetic field. The heating was continued by changing the parameters and the pressure of the natural gas. A monoenergetic potassium ion beam was introduced in the plasma; its energy could be adjusted within the limits of 200 and 1600 eV, the current from 0 to 2 mA at a maximum beam concentration of 5×10^8 cm^{-3} and a plasma concentration of (1 to 2) $\times 10^9$ cm^{-3}; the external magnetic field was varied from 600 to 1700 Oe. The experiments indicated that passage of the ion beam through the plasma is accompanied by the excitation of low-frequency oscillations, observed by means of a probe. The frequency spectrum exhibited narrow-band maxima. The amplitude of the noise decreased with decrease of the electron temperature and the ion beam current. The instability was related to a strong deformation of the ion beam energy function. The experiments indicated that an effective relaxation may be achieved by a fast ion beam in a turbulent plasma. (TTT)

9451 INCREASE OF ELECTRIC CONDUCTIVITY OF AN ARGON PLASMA IN SUPERSONIC FLOW SUBJECTED TO AN ELECTRIC DISCHARGE. Inglesakis, Georges; Bournot, Philippe; Forrestier, Bernard (Institut de Mecanique des Fluides, Marseille). Compt. Rend., Ser. B; 271: 769-72(12 Oct 1970). (In French).

It was shown that, although the initial ionization rate and pressure are rather high, a high-intensity electric current applied to a plasma can appreciably increase its conductivity. (auth) (France)

9452 EXPERIMENTAL STUDY OF THE MAGNETIC PISTON-SHOCK WAVE PROBLEM IN A COLLISIONLESS PLASMA. DeSilva, A. W. (Univ. of Maryland, College Park); Dove, W. F.; Spalding, I. J.; Goldenbaum, G. C. Phys. Fluids; 14: 42-51(Jan 1971).

The time-dependent problem of piston and shock-wave formation in a low-density (collision-free) magnetized plasma was experimentally studied in a high-voltage theta pinch. The applied field strongly interacts with the plasma: either exciting instabilities that cause a fast resistive penetration and very low force density, or exerting a sufficiently large force density to produce high Mach number (5 to 20) shock waves. The data on piston formation are discussed in terms of a magnetic-field-dependent resistivity such as might be expected from an ion plasma drift-wave instability. The piston ejects ions possibly by the interaction of ions with ion plasma waves. The shock wave is seen to evolve from an initially one-dimensional disturbance. (auth)

9453 WAVE NATURE OF MOVING STRIATIONS IN A LONGITUDINAL MAGNETIC FIELD. Sato, Masumi (Yamagata Univ., Yonezawa, Japan). Beitr. Plasmaphys.; 9: 371-81(1969).

The wave nature of stationary moving striations in helium and neon discharges in a uniform longitudinal magnetic field is studied. With increase of the magnetic field, the frequency of natural striations decreases while the wavelength increases, and they damp out at high field regions. Artificial excitations in these gases show that the wavelength is proportional to the excitation frequency for a given magnetic field, and the slope of linear lines increases with the field. The wave nature of the striations is explained, following the dispersion relation derived from the consideration of ionization waves and including effects of the magnetic field on the ionization. (auth)

9454 STUDY OF LOCAL THERMODYNAMIC EQUILIBRIUM IN THE ARGON PLASMA JETS. Bourasseau, D.; Cabannes, F.; Chapelle, J. (Faculte des Sciences, Orleans-la-Source, France). Astron. Astrophys.; 9: 339-49(Dec 1970). (In French).

Experimental measurements in an argon plasma jet were made to test the LTE at electron density $1.02 \times 10^{17} > N_e > 4.4 \times 10^{14}$ cm^{-3}. N_e is fixed by pressure smaller than 1 atm down to 5 torr. Relative intensities of two lines, arising from upper levels, give the Boltzmann temperature T_B. Absolute intensity of the line 4158 Å gives the excitation temperature T_{exc}. Measurements of N_e give the ionization temperature T_S on using the Saha equa-

tion. In this electron density range, the experimental values of T_B, T_{exc}, and T_S are in good agreement and the laws of LTE can be used. A discussion for validity of LTE in an argon plasma is given. The comparison of experimental data with critical electron densities calculated shows that the absorption of resonance lines must be taken into account. The assumption that absorption of the resonance lines is 100%, is necessary to obtain a good agreement. (auth)

Kinetics (Theoretical)

Refer also to abstract 9503.

9455 (AD-705265) STUDY OF HYDROMAGNETIC WAVE-PARTICLE BEAM INTERACTIONS. Final Report, December 1, 1964-November 30, 1969. Boley, Forrest I. (Dartmouth Coll., Hanover, N. H. Dept. of Physics). 28 Feb 1970. Contract AF-49(638)-1481. 10p. (AFOSR-70-444-TR). NTIS.

The behavior of organized groups of particles in a plasma was studied to determine the effects of the scattering and diffusion of these particles on the plasma. In one experiment the particle group was an electron beam injected into a neutral gas, thereby producing ionization and turbulent effects. Energy and spectral analysis of the beam particles and plasma turbulence are presented. In another experiment the particle group consisted of the plasma electrons gyrating at the upper hybrid frequency. The scattering of radiation from a column of such a magnetoplasma was studied. Amplitude and spectral measurements were correlated with an improved theoretical model. (auth) (USGRDR)

9456 (JUL-663-PP) ON THE TREATMENT OF AN ELLIPTIC BOUNDARY VALUE PROBLEM IN PLASMA PHYSICS WITH THE AID OF FORMAC. Belitz, H. J. (Kernforschungsanlage, Juelich (West Germany). Institut fuer Plasmaphysik). May 1970. 35p. (CONF-700631-1). Dep. NTIS (U. S. Sales Only).

From 2nd Meeting of the Seas Symbolic Mathematical Computation Project, Darmstadt, Germany.

The elliptic differential equation $\{(\partial^2/\partial z^2) - [(\Lambda/r)(\partial/\partial r)] + (\partial^2/\partial r^2)\}\Psi(x,z) = f_0(x,z) + f_1(x,z;\Psi)$, where $x = r - R_0$, and f_1 is a polynom in Ψ up to Ψ^4 is treated with the boundary condition $\Psi = 0$ on a surface Σ, defined by $\Sigma: x^2 + z^2 - \rho^2 = 0$. Assuming $\Psi = (x^2 + z^2 - \rho^2)\sum_{i=0}^{i_{max}}\sum_{j=0}^{j_{max}} C_{ij}x^i z^j)$, the coefficients C_{ij} are calculated up to $i_{max} + j_{max} = 10$. The method is applicable to higher orders in x and z; a general recurrent formula for the coefficients has not yet been found. The convergence problem is still open and will be treated in a later paper. Two numerical examples of a parameter study are given. (auth)

9457 (UCRL-72604) NOISE SUPPRESSION TECHNIQUES IN MACROPARTICLE MODELS OF COLLISIONLESS PLASMAS. Byers, J. A. California Univ., Livermore. Lawrence Radiation Lab.). 2 Nov 1970. 20p. (CONF-701113-1). Dep. NTIS.

From 4th Conference on Numerical Simulation of Plasmas, Washington, D. C.

Noise-reduction techniques are examined as applied to macroparticle computer models of collisionless plasmas. The quiet-start technique, particle weighting, and the usefulness of forcing the system to a linear one are discussed. (auth)

9458 (UCRL-72613) FORMULATION OF SELF-CONSISTENT 2- AND 2½-DIMENSIONAL ELECTROMAGNETIC AND RELATIVISTIC SIMULATIONS. Sinz, Kurt H. (California Univ., Livermore. Lawrence Radiation Lab.). 15 Oct 1970. 16p. (CONF-701113-3). Dep. NTIS.

From 4th Conference on Numerical Simulation of Plasmas, Washington, D. C.

A formulation for self-consistent 2- and 2½-dimensional electromagnetic and relativistic particle simulations is presented. The particles are infinitely long charged rods that move under the influence of their self-consistent fields. The numerical algorithms that numerically solve the appropriate Maxwell's equations and the Lorentz-force law in a first- order central difference scheme are given. The principal results are also applicable to simulations in one or three dimensions. (auth)

9459 (UCRL-72635) NONPHYSICAL MODIFICATIONS TO OSCILLATIONS, FLUCTUATIONS, AND COLLISIONS DUE TO SPACE-TIME DIFFERENCING. Langdon, A. Bruce (California Univ., Livermore. Lawrence Radiation Lab.). 2 Nov 1970. (CONF-701113-2) Dep. NTIS.

From 4th Conference on Numerical Simulation of Plasmas, Washington, D. C.

Oscillations, fluctuations, and collisions are examined in the idealized case of uniform and infinite or periodic plasma. Even in this simple situation there are several instances in which the models fail (mildly to grossly) to reproduce plasma behavior. This paper outlines the theory and discusses such nonphysical behavior caused by the finite-difference methods. The plasma interacts coherently with the periodicity of the spatial grid on which the electromagnetic fields are defined and with the periodicity of the finite-difference time integration. Various parametric instabilities are sometimes induced, which may be either weak or strong and may be difficult to distinguish from real instabilities. There is also high-frequency noise associated with the rate at which particles cross the spatial grid cells. If the time step is large enough that the frequency of this noise exceeds the time-sampling frequency, then this noise degrades normal fluctuations and collisions and can become excessive. The theory has helped others examine experimentally the nature of such nonphysical effects. Some suggestions are made as to how researchers using these models might respond to these results. (auth)

9460 FINITE-DIFFERENCE METHOD FOR THE SOLUTION OF FREE-BOUNDARY PROBLEMS. Bloch, Eugene. New York; New York Univ. (1969). 119p. University Microfilms Order No. 70-16,038.

Thesis.

A systematic iterative procedure is described that yields finite-difference solutions to steady free-boundary problems of plasma physics and fluid dynamics. By application of the method of steepest descent to minimize certain energy functionals connected with conformal mapping and free-boundary problems, a system of artificially time-dependent equations is produced that converges to a steady state as the time parameter goes to infinity. The solution is obtained in a parametric form in which the physical plane is the conformal image of a fixed rectangle. The use of a fixed rectangle as the parameter domain enables one to treat effectively the difficulties engendered by the singular behavior of the stream function at the point of separation between the fixed and free boundaries. As a result the scheme can be made convergent to second order in the mesh width h. The method was applied successfully to the vena contracta and Riabouchinsky models of classical hydrodynamics for both plane and axially symmetric geometries. An accuracy of four significant figures in the calculation of quantities of physical interest can be obtained without difficulty. A plane equilibrium model of plasma physics is also computed. The scheme can be applied to a variety of problems with two independent variables. (Diss. Abstr. Int., B)

9461 SHOCK WAVES IN A COLLISION-FREE MAGNETOPLASMA. Evers, William Henry Jr. Ithaca, N. Y.; Cornell Univ. (1970). 196p. University Microfilms Order No. 70-14,380.

Thesis.

Planar magnetoplasmadynamic disturbances, propagating exactly perpendicular to the magnetic field in a warm, collision-free plasma, are studied by solving numerically the equations of motion appropriate to the one-dimensional magnetic piston problem. The present analysis considers plasmas with initial ion temperatures such that $\beta_i^0 = 0.05$ to 0.50 and presents the results in terms of ion fluid properties. (TSS) (Diss. Abstr. Int., B)

9462 IONIZATION NONEQUILIBRIUM STATE OF COLD PULSE-DISCHARGE PLASMA. Snopko, V. N.; Razuvaeva, L. A. Zh. Prikl. Spektrosk.; 12: 203-7(Feb 1970). (In Russian).

The ionization equilibria of the plasma were investigated during expansion and adiabatic cooling. Plots are shown for log changes in ratios of intensities and of electron density along the axis of the plasma escaping at different pressure differentials. (M.O.W.)

9463 HIGH-FREQUENCY CONDUCTIVITY OF NONEQUILIBRIUM PLASMAS. Aono, Osamu (Tokyo Univ.). J. Phys. Soc. Jap.; 29: 1577-9(Dec 1970).

A new concept of a dressed ion (as not being a point particle) is proposed. The electrons are regarded as a dielectric medium. The dressed ion polarizes the medium, causing a frictional force between them, which governs the electric current. Concise expression is obtained, which is valid for any stable and uniform plasma in the absence of external magnetic field, and to which complicated expressions based on former theories reduce after careful rearrangement. (auth)

9464 ELECTRON ENERGY DISTRIBUTION FUNCTIONS AND TRANSPORT COEFFICIENTS IN HELIUM AND NEON. Hughes, M. H. (University Coll. of Swansea, Eng.). J. Phys., B (London); 3: 1544-51(Nov 1970).

The transport of electrons through gases in the régime of elastic and inelastic collisions is discussed and it is shown how the equation for the energy distribution derived by Smit (1936) follows more simply from consideration of the velocity diagram. The present analysis was applied to helium, neon and helium-neon mixtures where numerical integration techniques were employed to calculate electron energy distribution functions and transport coefficients in the range $3 \leq E/p_0 \leq 40$ V cm^{-1} torr^{-1}. The present results

XUM

are compared with previous theoretical calculations and experimental measurements of electron transport coefficients and it is shown that approximations involved in some previous calculations can lead to significant errors. In the pure gases helium and neon there is good agreement between the present theory and experiment; in helium–neon mixtures, however, the values of the Townsend primary ionization coefficient α/p_0, calculated on the assumption that only ionization by direct electron impact occurs, differ greatly from the values of α/p_0 measured experimentally. It is suggested that this may be due to an additional process of ionization in helium–neon mixtures although this is not a Penning mixture. (auth) (UK)

9465 SELF-EXCITED STEADY LAYERS IN ARGON LOW-PRESSURE COLUMNS IN HOMOGENEOUS, AXIAL MAGNETIC FIELDS. Popow, G.; Rothhardt, L. (Institutsteil VI Magnetoplasmadynamik, Jena, Ger.). Monatsber. Deut. Akad. Wiss. Berlin; 12: 168-71(1970). (In German).

The characteristics of the moving layer in an argon low-pressure column in a homogeneous axial magnetic field were calculated. It was found that, in strong magnetic fields, deviations from the Novák rule, $E_z \times \lambda$ = const., occur that are rigidly correlated with collective phenomena. These show clearly in the variation of the radial profile of the charge-carrier density. (tr-auth)

9466 NONLINEAR THEORY OF BEAM–PLASMA INTERACTIONS. III. PREPARATION OF NUMERICAL SOLUTIONS. Leven, Ronald (Univ., Greifswald, Ger.). Beitr. Plasma-phys.; 9: 293-305(1969). (In German).

In order to prepare the system of ordinary differential equations for the nonlinear behavior of a beam–plasma system, the dispersion relations are analyzed. In particular it is shown that, in the case of a three-component plasma, the complex wave number $k = k_r + i\gamma$ can be found without difficulties as a function of frequency ω and the plasma parameters, if the electron densities n_b and n_p are treated as the two dependent quantities. The expressions on the right hand sides of the differential equations are transformed in such a way that all complex integrals can be found as functions of one basic integral, tabulated in the literature, not only for negative values of γ (amplification) but also for positive values of γ (evanescence). In this way it will be possible to describe the behavior of the wave amplitude, not only for short distances from the input, where amplification of the wave takes place, but also for larger distances, where nonlinear Landau damping may occur. (auth)

9467 SCATTERING PROBABILITY FOR FAST TEST PARTICLES IN A PLASMA. Husseiny, A. A.; Forsen, H. K. (Univ. of Wisconsin, Madison). Phys. Rev., A; 2: 2019-24(Nov 1970).

An effective total cross section is calculated for elastic scattering of a monoenergetic beam of test particles in a plasma of arbitrary velocity distribution. Closed-form solutions are obtained for the special case of Maxwellian field particles taking into account small-angle scattering. The results are compared with those obtained using the Debye cutoff technique, and it is shown that such an arbitrary cutoff can lead to erroneous results in the effective cross section and can lead to different conclusions with regard to the relative importance of plasma ions and electrons in test-particle scattering. (auth)

9468 NUMERICAL SOLUTION OF THE DIFFUSION EQUATION. Burger, Jacques (Rennes Univ., France). Compt. Rend., Ser. B; 271: 761-4(12 Oct 1970). (In French).

The diffusion equation is solved numerically, and the profile of the electron density of a plasma determined, taking into account volume recombination. A comparison was made with experimental results. (auth) (France)

9469 NONLINEAR THEORY OF BEAM–PLASMA INTERACTIONS. IV. NUMERICAL RESULTS OF ELECTRON OSCILLATIONS. Leven, Ronald (Univ., Greifswald, Ger.). Beitr. Plasmaphys.; 10: 27-50(1970). (In German).

The spatial variations of the electric field E and the electron distribution function f_s for the case of beam–plasma amplification are computed on the basis of a nonlinear approximation developed earlier. The essential results are: with increasing distance x from the point where the beam enters the plasma, the amplitude A_1 of the first harmonic increases, reaches a maximum value at some point x_m, and then decreases monotonically without reaching a further maximum; in the region around x_m one finds a large increase of the higher harmonics, i.e., increasing nonlinearity, and also an increasing phase velocity, which soon approaches the beam velocity. The nonoscillating part of the distribution function of the beam electrons deforms, but not so much as the quasi-linear theory predicts, so that amplitude settling must be interpreted as a nonlinear but not as a quasi-linear effect. The results show a good agreement with some typical experiments on beam–plasma interactions. (auth)

9470 GENERAL SOLUTION OF THE ELECTRON DISTRIBUTION FUNCTION FOR WEAKLY IONIZED PLASMAS IN ARBITRARILY TIME-DEPENDENT ELECTROMAGNETIC FIELDS. Koch, Eckhard (Arbeitsstelle fuer Statistische Physik, Leipzig). Beitr. Plasmaphys.; 9: 306-23(1969). (In German).

The behavior of a weakly ionized plasma in external, arbitrarily time-dependent, electromagnetic fields is treated within the framework of kinetic theory. The Boltzmann kinetic equation is solved using the Lorentz ansatz, taking into account elastic collisions between electrons and neutral particles and assuming that the collision frequency is independent of the electron velocity. The drift velocity of electrons enters into the isotropic part f_0 and into the direction-dependent part f_1 of the electron distribution function. A method is given for calculation of the drift velocity, which is calculated explicitly for the important but difficult case of a sinusoidal electric field in the presence of a magnetic switching field, f_0 and f_1 are calculated; f_0 is investigated generally. f_0 consists of an expansion in generalized Laguerre polynomials. The influence of the electromagnetic fields on the distribution function and its time variation is discussed, and the relaxation behavior is shown. The following two special cases are calculated explicitly: a linear rising electric field and a sinusoidal electric field, both in the presence of a constant magnetic field. (auth)

9471 INFLUENCE OF A DIAPHRAGM ON THE ELECTRON DISTRIBUTION FUNCTION IN A GAS-DISCHARGE PLASMA. I. ELECTRON DISTRIBUTION FUNCTION FOLLOWING A POTENTIAL DIFFERENCE (THEORY). Wiesemann, K. (Univ., Marburg, Ger.). Ann. Phys. (Leipzig); 23: 104-12(Jun 1969). (In German).

The distribution function was calculated for plasma electrons accelerated by a potential difference. The calculation assumed that an isotropic distribution of electrons prevailed prior to acceleration. Interaction between electrons and other particles was neglected. If the accelerated layer was restricted by an aperture, electrons behind the aperture showed an energy-dependent decrease in density. (tr-auth)

9472 INFLUENCE OF INHOMOGENEITY OF PLASMA ON THE RELAXATION OF AN ULTRARELATIVISTIC ELECTRON BEAM. Breizman, B. N.; Ryutov, D. D. (Inst. of Nuclear Physics, Novosibirsk, USSR). JETP Lett. (USSR) (Engl. Transl.); 11: 421-4(20 Jun 1970).

Translated from Zh. Eksp. Teor. Fiz., Pis'ma Red.; 11: 606-9(20 Jun 1970).

The problem is considered for a beam with concentration n_b and particle energy $E \gg mc^2$. This beam is injected into a plasma whose concentration $n \gg n_b$ is a function with a characteristic scale L. The relaxation process due to Cherenkov interaction of the beam particles with the waves built up by the beam is considered. Different cases for plasma inhomogeneities are treated. (M.O.W.)

9473 CONVERGENCY PROBLEM IN THE CALCULATION OF THE ELECTRON VELOCITY DISTRIBUTION FUNCTION IN A LORENTZ PLASMA WITH HOMOGENOUS STATIONARY ELECTRIC FIELD. Wilhelm, J.; Winkler, R. (Institut fuer Gasentladungsphysik, Greifswald, Ger.). Ann. Phys. (Leipzig); 23: 28-48(Jun 1969). (In Germany).

Studies were based on the Boltzmann equation for electron velocity distributions (EV). Using the assumption of short mean free path, equations were obtained for the EV development in a Lorentz plasma. With spherical functions, the effect of an electric field on the EV development was studied under stationary homogeneous conditions for various electron velocities. It was found that the convergency of the EV development breaks down within the region of small electron velocities; the region depended on both strength of the electric field and width of the transport channel. Results were confirmed quantitatively between EV computation and experimental findings on a neon plasma. (tr-auth)

9474 ELECTRON VELOCITY DISTRIBUTION FUNCTION IN A HOMOGENOUS STATIONARY LORENTZ PLASMA IN NEON WITH CORRECT DESCRIPTION OF INELASTIC COLLISIONS. Winkler, R.; Wilhelm, J. (Zentralinstitut fuer Elektronenphysik, Greifswald, Ger.). Ann. Phys. (Leipzig); 24: 163-71(Mar 1970). (In German).

The velocity distribution was computed for a homogenous stationary weakly ionized Lorentz plasma in neon, using the assumption of a homogenous stationary electric field. The term for inelastic collisions in Boltzmann's equation was correctly calculated and compared with the usually applied approximation procedure

that assumes a delta-function pattern of influx at zero velocity. Effect of the approximation calculation was quantitatively studied on velocity distribution functions of interesting electron balance parameters such as velocity, diffusion coefficient, mean kinetic energy, and collision frequency for directly exciting and ionizing collisions. (tr-auth)

9475 CORRELATIONS OF TURBULENT PULSATIONS IN PLASMA. Makhankov, V. G.; Tsytovich, V. N. (Joint Inst. of Nuclear Research, Dubna, USSR). Nucl. Fusion; 10: 405-12 (Dec 1970).

Equations are derived for the correlation functions of a weakly turbulent plasma (both for decay and non-decay spectra). It is shown that the shape of the correlation curves close to the resonance frequencies is that of a Lorentz curve and the equation describing their structure is obtained by summation of the perturbation theory series. Estimates are given of the width of the correlation function of Langmuir pulsations. (auth)

9476 EFFECT OF OBLIQUE INCIDENCE ON OPTICAL ABSORPTION OF LASER LIGHT BY A PLASMA. Shearer, J. W. (Univ. of California, Livermore). Phys. Fluids; 14: 183-5(Jan 1971).

The reflection coefficient of laser light is an increasing function of the angle of incidence relative to the density gradient at a diffuse plasma boundary, because refraction bends the light away from denser regions where the absorption coefficient is high. (auth)

9477 PARTICLE ORBITS IN TWO WAVES OF ARBITRARY AMPLITUDE. Kaw, P. K.; Kruer, W. L. (Princeton Univ., N. J.). Contract AT(30-1)-1238. Phys. Fluids; 14: 190-2(Jan 1971).

The effect of a second wave, of arbitrary amplitude and phase, on the one-dimensional motion of a particle trapped in a large-amplitude electrostatic wave was analytically investigated. (auth)

9478 FAR-WAKE STRUCTURE IN RAREFIED PLASMA FLOWS PAST CHARGED BODIES. Sanmartin, Juan R.; Lam, S. H. (Princeton Univ., N. J.). Phys. Fluids; 14: 62-71(Jan 1971).

The asymptotic structure of the far wake behind a charged body in a rarefied plasma flow is investigated under the assumption of small ion-to-electron temperature ratio and of flow speed hypersonic with respect to the ions but not with respect to the electrons. It is found that waves are excited even if the flow is subacoustic (flow velocity less than the ion–acoustic speed). For both superacoustic and subacoustic velocities a steep wave front develops separating the weakly perturbed, quasi-neutral plasma ahead, from the region behind where ion waves appear. Near the axis a trailing front develops; the region between this and the axis is quasi-neutral for superacoustic speeds. The decay laws in all of these regions, the self-similar structure of the fronts and the general character of the waves are determined. The damping of the waves and special flow detail for bodies large and small compared with the Debye length are discussed. A nonlinear analysis of the leading wave front in superacoustic flow is carried out. A hyperacoustic equivalence principle is presented. (auth)

9479 SNOWPLOWING IN A PLASMA RAIL GUN. Collier, D. W.; Zinke, O. H. (Univ. of Arkansas, Fayetteville). Phys. Fluids; 14: 72-80(Jan 1971).

Agreement between data from a plasma rail gun as analyzed by a time-of-flight technique and predicted by snowplow theory indicates that there is no necessity for any theory of drag force in the gun and seems to indicate that one theory for drag force, which also accounts for the conduction of electrical current into a moving plasma, should be re-examined. (auth)

9480 EFFECT OF ELECTRON–ELECTRON COLLISIONS ON THE ELECTRICAL CONDUCTIVITY OF PLASMAS WITH TRAPPED PARTICLES. Salat, A. (Institut fuer Plasmaphysik, Garching, Ger.). Nucl. Fusion; 10: 369-76(Dec 1970).

Plasmas with electrons trapped in magnetic mirrors have a lower electrical conductivity than plasmas in homogeneous fields. It is shown that like-particle collisions reduce this difference by about 20%. Electron–electron encounters are simulated by the BGK model, whose validity for this case is discussed. (auth)

9481 SCATTERING OF RADIATION WITHIN A SPECTRAL LINE EMITTED BY TURBULENT PLASMA. Kaplan, S. A.; Tsytovich, V. N. (Scientific-Research Radiophysics Inst., Gorky, USSR. Inst. of Physics, Moscow). Astrophysics (Engl. Transl.); 5: 8-12(Spring 1969).

Translated from Astrofizika; 5: 21-30(1969).

The formation of satellites and the broadening of spectral lines during radiative transfer through turbulent plasma are discussed. A radiation pumping mechanism is proposed within the spectral lines, which can, in principle, give rise to a master effect under natural conditions. (auth)

Production

Refer also to abstract 9423.

9482 CURRENT DISTRIBUTION IN AN E × H DISCHARGE WITH SECTIONALIZED ELECTRODES FOR NONEQUILIBRIUM CONDUCTIVITY OF THE PLASMA. Glushkov, I. S.; Karpukhin, V. T.; Nedospasov, A. V. (Inst. of Atomic Energy, Moscow). High Temp. (USSR) (Engl. Transl.); 7: 208-15(Mar-Apr 1969).

Translated from Teplofiz. Vys. Temp.; 7: 223-32(Mar-Apr 1969).

Results are presented of an investigation of distribution of the current and principal parameters of a nonequilibrium plasma, as well as the Hall voltages, in an E × H discharge in the presence of sectionalized electrodes, using a pulsed discharge in an argon–cesium mixture. Starting from a certain value of the magnetic field, the current distribution at the surface of the electrodes ceases to depend on H, while as regards timing, it is in no way associated with the moment at which magnetic strata appear. For a fairly strong magnetic field, a discharge arises in the form of independent current "pinches"; these affect the saturation of the current density. (auth)

9483 PRODUCTION OF QUIESCENT PLASMAS WITH $T_i > T_e$. Honzawa, T.; Aihara, S.; Kawai, Y. (Nagoya Univ., Japan). Phys. Lett.; 33A: 395-6(30 Nov 1970).

The new type of plasma source described produces quiescent plasmas with ion temperature higher than electron temperature, and the plasmas are somewhat controllable in a magnetic field. (auth)

9484 ENERGETIC IONS PRODUCED BY SUBNANOSECOND LASER PULSES. Caruso, A.; De Angelis, A.; Gatti, G.; Gratton, R.; Martellucci, S. (EURATOM–CNEN, Frascati, Italy). Phys. Lett.; 33A: 336-7(30 Nov 1970).

The interaction of subnanosecond laser pulses with Ni targets leads to the production of an energetic pulsed plasma beam, whose main parameters were measured. (auth)

9485 TEMPORAL AND SPATIAL CHANGES IN THE ELECTRON DENSITY IN A XENON PLASMA PRODUCED BY A RUBY LASER BEAM. Hugenschmidt, Manfred (Institut Franco-Allemand de Recherches, Saint-Louis, France). Compt. Rend., Ser. B; 271: 757-60(12 Oct 1970). (In French).

In an interval of between 9 nanoseconds and a few microseconds after the creation of a xenon plasma by a laser beam, it was possible to obtain profiles of the electron density using differential interferometry. (auth) (France)

9486 INVESTIGATION ON PRECURSOR IONIZATION IN AN ELECTROMAGNETICALLY DRIVEN SHOCK TUBE. Geile, H. J. (Technische Hochschule, Aachen). Atomkernenergie; 16: 187-90(1970). (In German).

Pre-ionization phenomena observed during the discharge of a electromagnetically driven shock tube in the form of a conical theta pinch are discussed. It could be shown that this ionization is built up by short vacuum-uv flashes that occur during the compression phases of the pinch discharge. Because of the short periods of the swinging discharge, the electron density of the precursor ionization grows in several steps. The electron density shows a strong dependence from the pressure in all investigated gases. A relation between the neutral gas density and several parameters of the observed gases was found. By this relation the energy could be estimated which the shock wave and the plasma lose by ionizing rays. (auth)

Stability

Refer also to abstracts 9450 and 9524.

9487 (LRP–42/70) STUDY OF SHORT WAVELENGTH INSTABILITIES IN THE CONFINEMENT OF A COLLISION DOMINATED PLASMA BY A ROTATING MAGNETIC FIELD. Troyon, F. (Centre de Recherches en Physique des Plasmas, Lausanne (Switzerland)). Oct 1970. 14p. Dep. NTIS (U.S. Sales Only).

A collision-dominated plasma confined by a rotating magnetic field is stable if $f \cong 0.02\nu_i$ where f is the frequency of rotation and ν_i the ion collision frequency. Short-wavelength perturbations are the most difficult to stabilize. Growth rates of parametric instabilities are shown to be so large as to make impossible any attempt to use a frequency much lower than the above limit. A simple interpretation of a wide region of instability,

XUM

which cannot be ascribed to any parametric instability, is given in terms of an equivalent negative resistance. (auth)

9488 (LRP-45/70) THEORY OF THE DYNAMIC STABILIZATION OF THE RAYLEIGH-TAYLOR INSTABILITY. Troyon, F.; Gruber, R. (Centre de Recherches en Physique des Plasmas, Lausanne (Switzerland)). Oct 1970. 15p. Dep. NTIS (U.S. Sales Only).

Recent experiments by G. H. Wolf have demonstrated the possibility of dynamically stabilizing the Rayleigh-Taylor instability of the interface between two heavy fluids. This problem is considered here. It is shown quite generally that both viscosity and interfacial tension are necessary to stabilize the short-wavelength perturbations. As an example the experimental results on the liquid/air interface are reproduced. Dynamic stabilization of plasma confinement can be conceived by analogy with the fluid case. The differences between a plasma and a fluid are examined to show the limitations of the analogy. (auth)

9489 EXPERIMENTAL INVESTIGATIONS ON A TOROIDAL SCREW PINCH. Wilhelm, Rolf; Zwicker, Hartmut (Institut fuer Plasmaphysik, Garching, Ger.). Z. Phys.; 240: 295-305(1970).

High-β deuterium plasmas in a temperature range of 0.1 to 1 keV were produced in the fast toroidal screw pinch experiment ISAR IV ($B_{max} \approx 33$ kG, $I_{z\,max} \approx 100$ to 150 kA, coil diameter 12 cm, aspect ratio 5). The experimentally determined growth rates of the appearing instabilities, especially the m = 1 mode, are compared with two simple models and a more exact numerical calculation. This comparison and direct measurements of the magnetic field distribution show that the constant-pitch model of Bobeldijk is a suitable first approximation for the normal screw pinch. Using a delay of the z and θ-bank as a first simple method of field programming, this constant pitch profile could be varied in different directions. The results are discussed in more detail and confirm the theoretical picture of stability behavior of the high-β screw pinch. (auth)

9490 TRAPPED-PARTICLE EFFECT ON DRIFT-WAVE INSTABILITY IN TOROIDAL SYSTEMS. Liu, Chuan Sheng; Bhadra, Dilip K. (Gulf General Atomic, San Diego, Calif.). Contract AT(04-3)-167. Phys. Rev. Lett.; 25: 1706-9(21 Dec 1970).

Effects of the radial drift of the trapped particles on the drift-wave instability in toroidal systems are analyzed. These effects appear as $O(\sqrt{\epsilon})$ corrections to the dispersion relation, ϵ being the toroidicity. Instabilities due to the drift orbit are found in the following limits: (a) $a_e \gg \omega/k_{||} \gg a_i$, $\epsilon^{\frac{1}{2}}a_e, a_i$, (b) $\epsilon^{\frac{1}{2}}a_e, a_i \gg \omega/k_{||} > \epsilon^{\frac{1}{2}}a_i$, where a_e and a_i are the thermal speeds of the electrons and ions, respectively. (auth)

9491 EQUILIBRIUM AND STABILITY OF PLASMA IN CLOSED MAGNETIC TRAPS WITHOUT ROTATIONAL TRANSFORMATION. Shafranov, V. D.; Yurchenko, E. I. At. Energ. (USSR); 29: 106-11(Aug 1970). (In Russian).

Magnetic traps consisting of a crimped torus may be used for confining plasma because they have a large $\beta = 8\pi P/B^2$ value; therefore, calculations were made to estimate the highest possible β value with respect to the equilibrium and the stability of the confined plasma. It is not possible to determine through which closed magnetic line the plasma's constant pressure surface passes, on the basis of only a single magnetic line of force for traps without rotational transformation. Calculation of the P = const. system of magnetic surfaces is outlined. In view of the difficulties encountered with applied external fields under realistic boundary conditions, the problem was simplified, estimating the effect of the plasma pressure on the basis of a configuration in vacuum, with P = 0, with the same magnetic axis. The equations derived were used to calculate the equilibrium plasmas, the crimped torus, stability conditions, and the stabilizing torus. The results satisfy the stable equilibrium of a plasma with a $\beta \approx 1$ to 2% within a wide range of the third harmonic in the presence of a magnetic vacuum depression. In systems without rotational transformation, there is a stable equilibrium gap at $\beta \sim 1\%$. The possible existence of the required strongly flattened magnetic surfaces may be determined by computations. (TTT)

9492 KINK INSTABILITY OF A TOROIDAL PLASMA COLUMN. Schuurman, W.; Bobeldijk, C. (EURATOM-FOM, Jutphaas, Netherlands). Phys. Lett.; 33A: 381-2(30 Nov 1970).

It is shown that the toroidal effect on the growth rate for the kink instability of a plasma column vanishes in first order of the inverse aspect ratio of the torus. (auth)

9493 ELECTROMAGNETIC INSTABILITY OF COUNTERSTREAMING PLASMAS IN A MAGNETIC FIELD. Tzoar, N.; Yang, T. P. (Univ. of New York, N. Y.). Phys. Rev., A; 2: 2000-4(Nov 1970).

Using the Vlasov equation, σ_{zz} of the conductivity tensor is calculated for counterstreaming plasmas in a magnetic field. Using the dispersion relations for ordinary waves, the electromagnetic instability is considered. The spectrum of the instability and its growth rate are calculated. (auth)

9494 INFLUENCE OF COLLISIONS ON THE INSTABILITY OF COLD AND WARM ELECTRON BEAMS IN A PLASMA. Boehmer, H.; Chang, J.; Raether, M. (Univ. of Illinois, Urbana). Phys. Fluids; 14: 150-9(Jan 1971).

The effect of Coulomb collisions on the growth of the instability of monoenergetic beams and beams of finite initial velocity spread in a plasma was investigated experimentally. The results are compared with existing theories and with computations based on a beam with Lorentzian distribution function. It is shown that the instability is suppressed by collisions if the beam has a sufficiently large velocity spread in agreement with the prediction of Ascoli and Singhaus and that their stability criterion is valid over a larger parameter range than had previously been assumed. Evidence is presented for a self-quenching of the instability of an initially monoenergetic beam due to the combined effect of collisions and the smearing out of the beam distribution function by the unstable waves. (auth)

9495 AMPLITUDE LIMITATION OF A COLLISIONAL DRIFT-WAVE INSTABILITY. Hinton, F. L.; Horton, C. W. Jr. (Univ. of Texas, Austin). Phys. Fluids; 14: 116-23(Jan 1971).

A nonlinear analysis of collisional drift waves is presented in which a systematic expansion is made in powers of the wave amplitude. The two-fluid equations are used, including the effects of resistivity, viscosity, and thermal transport. The result, for the wave amplitude as a function of magnetic field in the linearly unstable region close to marginal stability, agrees reasonably well with experiment. (auth)

9496 VELOCITY SHEAR AND LOW-FREQUENCY PLASMA INSTABILITIES. Perkins, F. W.; Jassby, D. L. (Princeton Univ., N. J.). Phys. Fluids; 14: 102-15(Jan 1971).

The effects of transverse velocity shear on the low-frequency stability of a plasma are examined theoretically for a low-β resistive plasma in a uniform magnetic field. Cylindrical geometry is used, and the velocity shear is introduced by a nonuniform E × B rotation. Both numerical and analytic methods are used. The principal analytic result is a dispersion relation for instabilities caused by a thin-velocity shear layer. This dispersion relation describes the Q-machine edge oscillation, which is identified either as a Kelvin-Helmholtz instability or as a velocity-shear analog of the resistive drift wave, depending on the parallel wavelength. The numerical results show that properties of instabilities observed in several experiments agree reasonably well with theory. The effect of velocity shear on the drift instability is to make it into either a local or nonlocal type of normal mode. (auth)

9497 APPLICATION OF FINITE-LARMOR-RADIUS EQUATIONS FOR COLLISIONLESS PLASMAS TO A θ PINCH. Bowers, E.; Haines, M. G. (Imperial Coll. of Science and Tech., London). Phys. Fluids; 14: 165-73(Jan 1971).

Using finite-Larmor-radius equations developed in an earlier paper, the stability of an arbitrary β rotating θ pinch with straight lines of force in equilibrium is worked out in detail. The resulting differential equation, together with boundary conditions and the specification of radial density profiles, yields an eigenvalue problem that is solved with the aid of a computer. The results obtained show that an m = 1 rotational instability can occur in a θ pinch and that finite-Larmor-radius stabilization of this mode is present. It is also found that the rotating plasma should be stable to perturbations with an axial wavelength $\gtrsim 1$ m. This provides an explanation of why long θ pinches tend to go unstable uniformly along their length. Finite-Larmor-radius stabilization is critically dependent on the radial density profile, the steeper gradient favoring stability. Results are also presented showing how a large parallel temperature and shear in the axial flow can modify the rotational instability. (auth)

9498 STABILITY OF A HIGH-β, HELICALLY SYMMETRIC PINCH. Freidberg, J. P.; Marder, B. M. (Los Alamos Scientific Lab., N. Mex.). Phys. Fluids; 14: 174-8(Jan 1971).

Previous results obtained with a sharp boundary model on the stability of a high-β theta pinch with l = 1 windings are generalized to include diffuse profiles. The encouraging sharp boundary result is found to be valid for a large class of diffuse profiles: to lowest order, the system is weakly stable to the m = 1 mode. (auth)

9499 INFLUENCE OF HIGH-FREQUENCY ELECTRIC FIELDS ON EQUILIBRIUM AND STABILITY OF TOROIDAL PLASMAS. Dobrowolny, M.; Pogutse, O. P. (International Centre for Theoretical Physics, Trieste, Italy). Phys. Rev. Lett.; 25: 1608-11(7 Dec 1970).

The effect of a high-frequency toroidal electric field on equilibrium and stability of a toroidal plasma is considered. It is shown that, for some values of the electric field, one can change the particle orbits considerably with important consequences to diffusion and stability. (auth)

9500 ELECTROSTATIC INSTABILITIES IN MULTICOMPONENT PLASMAS. Schulz, Michael; Koons, H. C. (Aerospace Corp., El Segundo, Calif.). Phys. Fluids; 14: 188-90(Jan 1971).

A commonly employed heuristic method for evaluating phase velocities and growth rates of ion and electron plasma oscillations is generalized here to multicomponent plasmas. The new formulation exhibits the correct Galilean transformation properties. (auth)

9501 SOME POSSIBLE METHODS OF STABILIZING A CORRUGATED THETA PINCH WITH RESPECT TO LONG-WAVE PERTURBATIONS WITH m = 1. Nikulin, M. G. (Radiotechnical Inst., Moscow). Nucl. Fusion; 10: 395-8(Dec 1970).

The problem of stabilizing a corrugated theta pinch having high β with respect to long-wave perturbations with m = 1 is considered. The suggestion of Ribe and Riesenfeld that the variable axial high-frequency current, excited in the plasma column in addition to the azimuthal current, should be used for this purpose is discussed. It is shown that the stabilizing effect may result, in this case, only from the interaction of the axial current with the conducting wall surrounding the pinch. Consideration is also given to the possibility of suppressing the m = 1 mode with a quadrupole magnetic field. The stabilizing effect is, under these conditions, due to the interaction of the quadrupole field with the axial high-frequency current and to the presence of a magnetic well formed by the quadrupole field. (auth)

9502 COLLISIONAL EFFECTS ON THE RAYLEIGH–TAYLOR INSTABILITY IN A COMPOSITE MEDIUM. Bhatia, P. K. (Monash Univ., Clayton, Australia). Nucl. Fusion; 10: 383-5(Dec 1970).

The dynamic stability of a semi-infinite composite medium was studied to include the effects of collisions with neutral atoms. The case of one-dimensional density gradient in the fluid medium was studied. It is found that the collisions have a stabilizing influence in the case of the transverse mode of propagation. For the longitudinal mode, however, the stability criterion is found to remain unchanged by the inclusion of collisions. (auth)

Thermonuclear Processes

9503 (COO–1726-70) TECHNICAL PROGRESS REPORT [ON PLASMA PHYSICS]. (Wisconsin Univ., Madison). [1970]. Contract AT(11-1)-1726. 24p. Dep. NTIS.

Research areas described in this report are the following: (1) octupole studies, (2) theory, (3) plasma transport toward hoops, (4) superconducting studies, (5) microwave diagnostics, (6) engineering feasibility studies, (7) filling studies, and (8) abstracts, talks, and publications. (M.O.W.)

9504 (FOA–4-4438) THEORETICAL PARTICLE EMISSION SPECTRA IN FUSION REACTIONS. Gustafsson, H. I. (Forsvarets Forskningsanstalt, Stockholm (Sweden)). Sep 1970. 100p. Dep. NTIS (U. S. Sales Only).

Pure and superimposed three-dimensional, isotropic, and time-independent Maxwellian and monoenergetic test distributions are considered in order to investigate the relation between the rate of emission of reaction-product particles in a fusion plasma and the velocity distributions of the plasma ions. These simplifying tentative distributions are applied in evaluations of differential rates of binary, isotropic reactions. The rate formulas are reduced to numerically convenient one-dimensional integrals. The extensive analytical calculations for obtaining these are presented separately in three appendices. (auth) (Sweden)

9505 (KFK–896) MEASUREMENT OF HIGH SURGE CURRENT. Will, F. (Kernforschungszentrum, Karlsruhe (West Germany). Labor fuer Elektronik und Messtechnik). Aug 1970. 20p. (In German). Dep. NTIS (U. S. Sales Only).

The measurement of high surge current is feasible with small energy losses by application of an ohmic resistance, provided that the inductive fraction is negligible. Coaxial or bifilar types for ac-current measurements generate high mechanical forces. This disadvantage can be avoided by a suitable arrangement of the measurement conductors. Current measurement with a Rogowski coil followed by an integrator has the advantage of electrical isolation between the measurement circuit and the main circuit. It is easy to calculate Rogowski coils and their fabrication does not involve major problems. Current measurement by magnetic induction performed close to the surge-current conductor with a Hall generator shows good agreement with the two other methods, but the results were not investigated in further detail. (auth)

9506 (ORNL-TM–3207) PROSPECTS OF A MULTI-MeV H_2^+ INJECTION-ACCUMULATION EXPERIMENT. McNally, J. Rand Jr. (Oak Ridge National Lab., Tenn.). Nov 1970. Contract W-7495-eng-26. 21p. (CONF-701114–1). Dep. NTIS.

From Meeting on Division of Plasma Physics, Washington, D. C.

Crocker, Blow, and Watson discuss fusion reactors at ~200 kG, ion temperatures ~1 MeV, and lithium and deuterium as primordial fuel. The possibility of fusion start-up at MeV temperatures and more modest fields was discussed earlier. The prospects of a 2-mA, 4-MeV H_2^+ injection–accumulation experiment at 10^{-8} torr H_2 in a 40/20 kG mirror field with 5.5-mm ECH (electron cyclotron heating) are presented. Neglecting instabilities one should obtain an $n\tau \sim 5 \times 10^{14}$ sec cm^{-3} before nuclear elastic scattering losses limit the exponential buildup. Such an experiment would test the basic principle of plasma exponentiation, which has yet to be demonstrated in injection–accumulation experiments. (auth)

9507 (ORNL-TM–3233(Rev.)) NUCLEAR FUSION RESONANCE REACTIONS OF POSSIBLE CTR INTEREST. McNally, J. Rand Jr. (Oak Ridge National Lab., Tenn.). Jan 1971. Contract W-7405-eng-26. 6p. Dep. NTIS.

Some speculations are presented on possible nuclear fusion resonance reactions that may be of importance in the development of "clean" controlled thermonuclear reactors of either toroidal or mirror type. (auth)

9508 IMPROVEMENT OF l = 2 STELLARATOR AND TORSATRON. Mohri, Akihiro (Nagoya Univ., Japan); Azumi, Masafumi. J. Phys. Soc. Jap.; 29: 1580-92(Dec 1970).

Magnetic field systems with l = 2 helical windings of fairly short pitch have large rotational transform and high shear. This high shear promises the formation of an average magnetic well, when a vertical field is externally applied. A hybrid field having mainly l = 2 and l = 3 helical fields can be produced by deforming l = 2 helical windings. This field has a deep well, and its current system is very simple. Numerical calculations using Biot–Savart's law show that these improvements are realized in practice. (auth)

9509 VERY SIMPLE COIL GIVING A STELLARATOR-TYPE MAGNETIC CONFIGURATION. Gourdon, Christian; Hubert, Pierre; Marty, Denis (EURATOM–CEA, Fontenay-aux-Roses, France). Compt. Rend., Ser. B; 271: 843-5(19 Oct 1970). (In French).

Helical conductors, wound on a former, and following a certain pitch modulation law can yield good quality magnetic configurations. Analytical studies led to numerical calculations confirming this. Such a simplification might greatly facilitate the eventual development of a thermonuclear reactor. (tr-auth) (France)

9510 DEVELOPMENT OF A CLEAN SHOCK TUBE FOR MAKING SPECTROSCOPIC MEASUREMENTS ON A PLASMA. Larcher, Ghislain; Thenard, Claude; Maillot, Patrice (Rouen Univ., Mont-Saint-Aignan, France). Compt. Rend., Ser. B.; 271: 677-80(5 Oct 1970). (In French).

A special clean shock tube is described. This tube can retain a gas in a high state of purity. Absolute measurements of the line intensities and the background continuum of an argon plasma can be made. (auth) (France)

9511 STELLARATOR AS A NONLINEAR PLASMA-CURRENT TRANSFORMER. Furth, H. P. (Princeton Univ., N. J.). Contract AT(30-1)-1238. Phys. Fluids; 14: 194-6(Jan 1971).

Oscillation of the helical winding current of a stellarator induces toroidal plasma currents proportional to the square of the winding current. (auth)

Wave Phenomena

Refer also to abstracts 9459 and 9475.

9512 (NP–18554) HELICON RESONANCES IN LOW-PRESSURE PLASMAS. Sager, Otto (Eidgenoessische Technische Hochschule, Zurich (Switzerland)). 1970. 117p. (In German). Dep. NTIS (U. S. Sales Only).

A phenomenon in low-pressure discharges similar to what is known in solid-state plasmas as helicon resonances is investigated. Theoretical considerations based on a two-dimensional plasma sheet are extended by taking into account the influence of the electron temperature and the nonuniform density distribution. Experimental results obtained in rectangular and circular confinements of a high-frequency discharge with applied external static crossed

XUM

magnetic fields agree with the improved theory. Measurements on surface-ionized Cs plasmas show that the resonance behavior is not significantly influenced by the plasma generation. The general behavior of the electrodeless ring discharge can be described by calculating the power per unit area transferred to the plasma by the right- and left-handed circularly polarized waves. The necessary coil current and voltage for maintaining the discharge are determined by establishing the power balance. The numerical results compare favorably with measurements, especially in the case of applied constant current and constant voltage of the hf generator. It can be shown that the discharge is sustained in a state of helicon resonances over a wide range of the external static magnetic field. (auth)

9513 WAVE–WAVE COUPLING IN ION WAVE PROPAGATION. Ohnuma, Toshiro; Hatta, Yoshisuke (Tohoku Univ., Sendai). J. Phys. Soc. Jap.; 29: 1597-1608(Dec 1970).

Wave–wave coupling among ion waves was investigated experimentally and theoretically. When two ion waves of different frequencies of f_1 and f_2 are excited by one grid, the signals of the harmonic ($2f_1$) and $f_1 - f_2$ are detected by another grid. They are found to grow spatially in some regions, contrary to those of f_1 and f_2 that decrease monotonously in the region. The growing regions of the harmonic and $f_1 - f_2$ are in accord with those obtained from the theory of the wave–wave coupling among ion waves. The propagation of small-amplitude waves under large-amplitude waves and the propagation of large-amplitude ion waves were also investigated. (auth)

9514 NONLINEAR INTERACTION OF WAVES IN A BOUNDED MAGNETOACTIVE PLASMA. Kondratenko, A. N.; Shaptala, V. G. Izv. Vyssh. Ucheb. Zaved., Radiofiz.; 13: 1012-18(1970). (In Russian).

The decay instability of waves in a plasma cylindrical waveguide in a constant magnetic field is considered. General expressions and nonlinear boundary conditions were derived for the fields on the assumption of three-plasmon interaction. The interactions of hf surface waves with ion–acoustic surface or volume waves are investigated in detail at different radii of the waveguide. (auth)

9515 WAVE OSCILLATIONS IN WEAKLY TURBULENT PLASMA. Suramlishvili, G. I. Soobshch. Akad. Nauk Gruz. SSR; 60: 57-60(Oct 1970). (In Russian).

The question of wave oscillations in weakly turbulent plasma is discussed. It is shown that the presence of an overthermal background of pulsations in unstable plasma decreases the upper value of the phase velocities of the oscillating waves by a value proportional to the intensity of plasma oscillations. (auth)

9516 STUDY OF LONGITUDINAL WAVES IN A RELATIVISTIC PLASMA. Gupta, R. M. (Univ. of Rajasthan, Jaipur, India). Phys. Lett.; 33A: 341-2(30 Nov 1970).

The dispersion relation for the longitudinal waves in relativistic plasma, as obtained earlier, is analyzed further under different situations. Here it is observed that, even in the relativistic case, the longitudinal wave propagating parallel to the static magnetic field is free from magnetic effects but does show the effects in the transverse field. (auth)

9517 ANALOG DEVICE FOR COMPUTING THE PLASMA DISPERSION FUNCTION. Stainov, G. (Inst. of Physics, Sofia). Compt. Rend. Acad. Bulg. Sci.; 23: 931-4(1970).

An analog device for modeling harmonic functions and, in particular, for computing the plasma dispersion function is described. The functions are modeled in a round electrolytic bath. The modeling of the dispersion function is done by applying voltages proportional to the values of the distribution function on the cylindrical probes situated along a straight line simulating the real axis. (M.O.W.)

9518 EXCITATION OF LONGITUDINAL OSCILLATIONS OF A MAGNETIZED PLASMA BY A TRANSVERSE ELECTROMAGNETIC WAVE. Kotsarenko, N. Ya.; Yukhimuk, A. K. (Kiev State Univ.). Ukr. Fiz. Zh.; 15: 1349-52(Aug 1970). (In Russian).

The excitation of longitudinal oscillations in a magnetized plasma by transverse electromagnetic wave is studied. The propagation of a strong electromagnetic wave in plasma causes the drift of electrons with respect to ions. This drift may be a reason for low-frequency plasma instabilities. (auth)

9519 ECHO THEORY IN PLASMA: SPATIAL ECHO. Sitenko, A. G.; Nguyen Van Trong; Pavlenko, V. M. (Inst. of Theoretical Physics, Kiev). Ukr. Fiz. Zh.; 15: 1372-80(Aug 1970). (In Russian).

Spatial echo effects in plasma that arise as a result of interaction of external perturbations applied in various places are considered. Spatial echo vibrations associated with the transformation of waves in plasma, spatial echo vibrations conditioned by the distribution function perturbations, and spatial echo vibrations in nonequilibrium plasma are studied theoretically. (auth)

9520 MICROWAVE SCATTERING BY LOW-FREQUENCY OSCILLATIONS IN THETA-PINCH PLASMA. Adamov, I. Yu.; Dushin, L. A.; Berezhnyi, V. L.; Kononenko, V. I. (Physical-Technical Inst., Kharkov). Ukr. Fiz. Zh.; 15: 1353-8(Aug 1970). (In Russian).

Microwave scattering by low-frequency oscillations was studied in a theta-pinch plasma. The experimental value of the scattering coefficient was $\sigma_e \approx 2.5 \times 10^{-9}$ cm^{-1} to 5×10^{-7} cm^{-1}. It is shown that microwave scattering takes place on longitudinal plasma oscillations with frequencies $\omega \sim \sqrt{\omega_{He}\omega_{Hi}}$. (auth)

9521 GENERATION OF A HARMONIC OF AN ELECTROMAGNETIC WAVE AT THE UPPER HYBRID FREQUENCY IN AN INHOMOGENEOUS PLASMA. Cano, Renato; Fidone, Ignazio; Granata, Giovanni (CEN, Fontenay-aux-Roses, France). Compt. Rend., Ser. B.; 271: No. 14, 673-6(5 Oct 1970). (In French).

The generation of the first harmonic of an electromagnetic wave in a plasma was observed. It was propagated in a direction perpendicular to the confining magnetic field ($\omega_p < \omega_c$). An interpretation, based upon the resonance properties of the incident wave at the upper hybrid frequency in an inhomogeneous plasma, is proposed. (auth) (France)

9522 Q DEVICE. Andersen, H. K. (Danmarks Ingenioer-Akademi, Copenhagen). Fys. Tidsskr.; 68: No. 1, 7-38(1970). (In Danish).

The design of the Risoe Q device is described in some detail. The derivation of the dispersion relation for ion–acoustic waves from the fluid equations is surveyed. Experiments on propagation of ion–acoustic waves in fully ionized and in partly ionized Q-machine plasmas are reported. The results of the equations are compared with theoretical predictions. (Denmark)

9523 HARMONIC GENERATION IN COLD NONUNIFORM PLASMA IN A MAGNETIC FIELD. Blum, F. A. (Massachusetts Inst. of Tech., Lexington). Phys. Fluids; 14: 196-8(Jan 1971).

Theoretical discussion of harmonic generation in cold bounded nonuniform magnetoplasmas predicts weak even-order harmonic generation (compared to odd-order) and strong resonances near cyclotron and maximum upper hybrid resonances for small collision frequencies. (auth)

9524 ONE-DIMENSIONAL QUASI-LINEAR CALCULATION WITH ALLOWANCE FOR SPONTANEOUS EMISSION. Gratzl, H. (Institut fuer Plasmaphysik, Garching, Ger.). Nucl. Fusion; 10: 391-4(Dec 1970).

The one-dimensional quasi-linear instability of electron plasma waves considered by Drummond and Pines is calculated, with allowance for spontaneous emission. If the initial electron plasma wave spectrum is assumed to be in equilibrium with the thermal electrons, the spontaneous emissive power is inversely proportional to the number N of electrons in the Debye volume. For $N \lesssim 10^3$, it is found that the spontaneous emission drives the instability to overcome the quasi-linear asymptotic state, which is recovered for larger N if the initial values used by Drummond and Pines are applied. Relations between the one-dimensional problem and the physical problems entailed by more dimensions are discussed. (auth)

9525 ION ACOUSTIC WAVES IN FINITE-GEOMETRY PLASMAS. Shoucri, M. M. (International Centre for Theoretical Physics, Trieste, Italy). Nucl. Fusion; 10: 431-3(Dec 1970).

The dispersion relation for the ion acoustic waves in a finite-geometry plasma is derived. The finite-geometry solution will also allow the ion acoustic surface waves to be studied. The excitation of these waves by a small density beam will be considered, and it will be shown that the instability resulting from the interaction of the beam with the ion acoustic waves is convective. (M.O.W.)

9526 NONLINEAR PLASMA WAVES. Klozenberg, J. P. (Imperial Coll. of Science and Tech., London). Phys. Fluids; 14: 94-101(Jan 1971).

A numerical solution of the equations for unstable electrostatic plasma waves propagating in a uniform infinite plasma with a weak beam is performed. Space-dependent variables are Fourier transformed, and the computations are done first with only one and then with two harmonics included. In both cases the first harmonic electric field reaches a maximum amplitude and thereafter oscillates periodically, the period being different in the two cases. Thus, the time evolution of the field depends strongly on the pres-

ence of the second harmonic. The second harmonic electric field itself has negligible amplitude compared with the fundamental but the corresponding perturbed distribution functions are comparable in the vicinity of the wave resonance. In the frame of the background plasma the frequency of the first harmonic electric field is close to the plasma frequency ω_p but the nonlinearly generated second harmonic frequency is $2\omega_p$. Because of this it is found that the wave–wave interaction terms are important and resonant processes occur. The neglect of such terms in quasi-linear theory is questioned. (auth)

9527 KINETIC THEORY OF WAVE PROPAGATION. I. ONE-COMPONENT SYSTEMS. Bramlette, T. Taz (Bell Aerospace Co., Buffalo, N. Y.); Huang, A. Ben. Phys. Fluids; 14: 25-33(Jan 1971).

The problem of wave propagation in one-component systems is treated using the discrete-ordinate method. Forced and free oscillations in a monatomic gas and longitudinal electrostatic oscillations in a one-component plasma are considered. The governing equation is the linearized ellipsoidal model of the Boltzmann equation. When the ratio of collision frequency to a characteristic frequency of the wave is greater than one, the present technique yields results that are in excellent agreement with other theories and experimental data. For values of this ratio less than one, the present theory is very similar to the polynomial expansion theories. (auth)

9528 INTERACTION AMONG THREE EXTRAORDINARY WAVES IN A HOT ELECTRON PLASMA. Das, K. P. (Jalpaiguri Government Engineering Coll., India). Phys. Fluids; 14: 124-8(Jan 1971).

The Krylov–Bogolyubov–Mitropolsky method is applied to the study of the interaction among three extraordinary waves propagating perpendicularly to a uniform magnetic field in a hot electron plasma. The frequency and wavenumber of the three waves satisfy the conditions $\omega_1 + \omega_2 = \omega_3$ and $\kappa_1 + \kappa_2 = \kappa_3$. When the external magnetic field is small, the first and the third waves show a transverse character and the second wave shows a longitudinal character; in the case of a zero magnetic field, they reduce, respectively, to transverse and longitudinal waves. In the absence of a magnetic field the analysis shows a mechanism, through which the energy of a longitudinal wave may be converted into the energy of a transverse wave. (auth)

9529 LARGE-AMPLITUDE DISTURBANCES IN A POSITIVE COLUMN. Andrews, J. G. (Central Electricity Generating Board, Marchwood, Eng.). Phys. Fluids; 14: 129-33(Jan 1971).

A theory is given for treating large-amplitude disturbances to ion flow in a low-pressure positive column, using a characteristics method of solution. (auth)

9530 MICROWAVE PROPAGATION IN THE PRESENCE OF A FINITE-AMPLITUDE HELICAL INSTABILITY. Ventrice, Carl A. (Tennessee Technological Univ., Cookeville). Phys. Fluids; 14: 192-4(Jan 1971).

Phase-shift measurements are made in the presence of a finite-amplitude instability, using a 30-GHz microwave interferometer. A large discrepancy exists between the measured phase shifts and those calculated from the time-averaged particle density profiles. (auth)

9531 REFLECTION OF PSEUDOWAVES. Estabrook, K.; Alexeff, I.; Jones, W. D.; Lonngren, K. E. (Oak Ridge National Lab., Tenn.). Phys. Fluids; 14: 185-7(Jan 1971).

Ion bursts (pseudowaves) in a low-temperature discharge plasma are reflected from the potential barrier of a gridded energy analyzer. The energy of the reflected ions increases monotonically with the increasing potential. (auth)

9532 LONGITUDINAL OSCILLATIONS IN BOUNDED MAGNETOPLASMAS. Stenzel, R. L.; Gould, R. W. (California Inst. of Tech., Pasadena). Contract AT(04-3)-767. Phys. Fluids; 14: 187-8(Jan 1971).

Fine structure in absorption due to Buchsbaum–Hasegawa modes is observed over a wider range of magnetic fields than previously reported (ω_c/ω = 0.5 to 0.985). The basic theory is satisfactory only near the cyclotron harmonic. (auth)

9533 KINETIC THEORY OF WAVE PROPAGATION. II. BINARY GAS MIXTURES. Bramlette, T. Taz (Bell Aerospace Co., Buffalo, N. Y.); Huang, A. Ben. Phys. Fluids; 14: 34-41 (Jan 1971).

Solutions to the problems of forced- and free-wave propagation in binary gas mixtures are presented that were obtained using the discrete-ordinate method. The governing equations for the mixtures are the model equations proposed by Hamel. The solution is in excellent agreement with existing experimental data. (auth)

9534 HIGHER-ORDER TEMPORAL AND SPATIAL PLASMA WAVE ECHOES. Sauer, K.; Bachmann, P.; Wallis, G. (Zentralinstitut fuer Elektronenphysik, Berlin). Beitr. Plasmaphys.; 10:: 199-206(1970).

The collisionless Boltzmann equation is solved in two ways by the method of characteristics. The solution is used for an exact treatment of higher-order temporal and spatial plasma wave echoes in the absence of steady magnetic fields. The second-order spatial echo is treated separately and analyzed numerically. (auth)

9535 STATISTICAL ANALYSIS OF OSCILLATIONS EXCITED IN A PLASMA–BEAM SYSTEM. Gashevskii, V. A.; Kovtun, R. I.; Kharchenko, I. F. Radiotekh. Elektron.; 15: 1647-50(Aug 1970). (In Russian).

The numerical treatment of rapid scanning of plasma signals was used in studies of the statistical nature of random oscillations excited in a plasma–beam system. Data obtained revealed that the random oscillations represent a quasi-stationary multiplicative process with normal distributions. (tr-auth)

Shielding

Refer also to abstracts 8960, 9601, 9619, 9944, 9948, 9950, 10192, and 10296.

9536 (CEA-CONF–1669) COMPARATIVE PERFORMANCES OF MONTE CARLO AND DISCRETE ORDINATE ONE DIMENSIONAL TRANSPORT CODES IN AN IRON BULK SHIELD CALCULATION. Devillers, Christian (Commissariat a l'Energie Atomique, Fontenay-aux-Roses (France). Centre d'Etudes Nucleaires). 1970. 17p. (CONF-701020–1). Dep. NTIS (U. S. Sales Only).

From Monte Carlo Seminar Workshop, Oak Ridge, Tenn.

A comparative study was made on the propagation of neutrons through a large thickness of iron for two one-dimensional transport codes, NIOBE and ANISN and the one-dimensional POKER code. The comparison between the results obtained from the NIOBE and POKER codes indicated the influence of different data treatments using the same library (UNC). NIOBE uses a pseudo-multigroup calculation and POKER a linear interpolation. The comparison of the results obtained using the POKER and the ANISN codes contrasts the use of the ENDF/B library in place of the UNC library. The comparison between the measured and the calculated responses demonstrates the possible inadequacy of the cross sections used. The experimental results were obtained from the iron column of the Harmonie reactor using sulfur-, rhodium-, and manganese-activated detectors. (France)

9537 (N–70-34007) RADIATION FLUX MAPPING OF OPE SPACECRAFT MODELS, PHASE 1. (Hittman Associates, Inc., Columbia, Md.). Mar 1970. Contract NAS5-11225. 26p. (NASA-CR–109876; HIT–439). NTIS.

Spacecraft equipped with radioisotope thermoelectric generators (RTG) presents a unique problem with respect to any of the on-board radiation sensors. Photon and neutron emission from the radioisotopic fuel can seriously perturb the measurement of the extremely low particle flux fields in the vicinity of the spacecraft. Even when sufficient shadow shielding of primary RTG radiation is present between the RTG and the radiation sensor, scattered radiation can be a problem. The RTG and sensor booms, and the spacecraft itself, constitute potential scatter zones for the RTG radiation. Analytical techniques are developed and applied in evaluating the primary and scattered RTG radiations with respect to selected OPE spacecraft models. (auth) (STAR)

9538 (ORNL-TM-3251) ACTIVITIES OF THE ANS-6 SUBCOMMITTEE ON RADIATION SHIELDING STANDARDS. Claiborne, H. Clyde; Dudziak, Donald J.; Schaeffer, Norman M. (Oak Ridge National Lab., Tenn.). Dec 1970. Contract W-7405-eng-26. 17p. Dep. NTIS.

A special report is given on the activities of the ANS-6 Subcommittee on Radiation Shielding Standards that was prepared for presentation at the special session entitled "Current Status of Nuclear Standards Development" at the 1970 winter meeting of the American Nuclear Society at Washington, D. C. A brief discussion of the history, organization, and philosophy of the ANS-6 Subcommittee and a report on the accomplishments and current activities of the existing working groups are presented, which include: shielding cross section standards, benchmark problems, shield performance evaluation, shield materials, and shielding nomenclature. (auth)

9539 DISK SOURCE ENERGY AND ANGULAR DISTRIBUTIONS. Rubin, Richard Mark. Manhattan, Kan.; Kansas State Univ. (1970). 144p. University Microfilms Order No. 70-16,646.

XUM

Thesis.

Angular flux densities and exposure angular distributions for points along the axis of plane disk isotropic ^{60}Co sources in an infinite air medium were calculated, using the moments method solution to the gamma-ray transport equation. The method is based on the expansion of the gamma-ray flux density at a distance z above an infinite plane isotropic source as a Legendre polynomial expansion. The coefficients of the Legendre expansion were reconstructed, using standard biorthogonal polynomial expansion techniques. Using extrapolation techniques similar to those recommended by Spencer for extrapolation of the Legendre coefficients, the exposure angular distribution was reconstructed with 61 Legendre coefficients. Standard geometric transformations allowed evaluation of exposure angular distributions for isotropic point, ring, and disk sources as well as infinite plane isotropic sources. Selected energy-angular flux densities were computed for comparison with experimental data. (Diss. Abstr. Int., B)

9540 AKTIVNAYA ZASHCHITA KOSMICHESKIKH KORABLEI. (Effective Protection of Space Ships). Trukhanov, K. A.; Ryabova, T. Ya.; Morozov, D. Kh. Moscow; Atomizdat (1970). 232p.

The problems of effective protection of space vehicles, based on deflection of charged-particle fluxes (protons and electrons) by magnetic and electric fields are presented. The radiation environment, principles of electrostatic shielding, and calculations of electrostatic shielding against high-energy electrons are discussed, as well as the weight factors in the electrostatic shielding. Physical principles and fundamental characteristics of electromagnetic shielding are treated in two separate chapters, and another chapter is devoted to determination of the forbidden zone in electromagnetic shielding. (R.V.J.)

Solid-State Physics

Refer also to abstracts 9970, 9971, 10017, and 10018.

Radiation Effects

Refer also to abstracts 8485, 8964, and 9379.

9541 (CEA-CONF-1680) ELECTRON IRRADIATION OF Fe AND Ni. Bourret, A. (Commissariat a l'Energie Atomique, Grenoble (France). Centre d'Etudes Nucleaires). 1970. 2p. (In French). (CONF-700809-4). Dep. NTIS (U. S. Sales Only).

From 7th International Congress on Electron Microscopy, Grenoble, France.

Nickel and iron foils were exposed to 1.5-MeV electrons in an electron microscope. In both cases dislocation loops were observed. These loops were formed by the agglomeration of interstitials produced by collisions between the electrons and the atoms of the crystal. The number of loops produced remained constant with respect to the dose; the nucleation of loops occurred in a homogeneous way and the process could be analyzed with kinetic chemistry. Comparison with theory indicated that, in nickel, the nucleation occurred about the impurities, while in iron, the interstitial pairs dissociated, accounting for the high doses necessary before the defects were observed. The use of additional results obtained with a Van de Graaff generator indicated that the nucleation process was no more homogeneous at 3 MeV than it was at 1 MeV. At 3 MeV there was a sensible variation between the number of loops produced and the dose, which was much greater than would be expected from the number of defects produced. Thus, it was shown that electron irradiation can directly produce nucleation centers when the average number of atoms displaced by primary collisions exceeds 1.3. (tr-auth) (France)

9542 (CEA-CONF-1681) OBSERVATION AT VERY LOW TEMPERATURES OF THE ANNEALING PROCESS IN SPECIMENS WITH RADIATION DEFECTS. Bourret, A. (Commissariat a l'Energie Atomique, Grenoble (France). Centre d'Etudes Nucleaires). 1970. 2p. (In French). (CONF-700809-3). Dep. NTIS (U. S. Sales Only).

From 7th International Congress on Electron Microscopy, Grenoble, France.

A platinum microscope cooled to 10°K was used to study the annealing of specimens in which defects had been created by neutron irradiation. The specimens were in the form of thin foils and had received a dose of 4.10^{18} nvt at an energy in excess of 1 MeV. The absence of visible defects in Fe at 77°K indicated that the depleted zones were not directly visible and that at that temperature no mobile species had yet diffused. The visible observation of faults at 77°K in Ni, Al, and Mg indicated that they had been produced by agglomeration of the interstitials during the neutron irradiation. The loops rearrange themselves until a vacancy-type fault becomes mobile. This fault then destroys the loops in the case of Al and Mg (because the vacancies are then highly dispersed: strong stage III) or as in the case of Ni begins to partially annihilate them (because of the very inhomogeneous way in which the vacancies are already grouped: weak stage III). (France)

9543 CHANNELING OF ELECTRONS AND POSITRONS IN SILICON AND ANTHRACENE MONOCRYSTALS. Ok, H. H. Armagan (Univ., Goettingen, Ger.). Z. Phys.; 240: 314-22(1970). (In German).

Channeling of 148-keV electrons and 247-keV positrons in monocrystals of silicon and anthracene is found in transmission experiments. In anthracene the measurements are carried out at T = 130°K. The number of transmitted electrons incident along the [110] axis of silicon and the [001] axis of anthracene is remarkably reduced. The number of transmitted positrons incident along these axes shows pronounced peaks. The theoretical critical angles for channeling are compared with the observed values. (auth)

9544 ELECTRON SPIN RESONANCE INVESTIGATION OF A Li CENTER IN MgO. Rius, Gerard; Cox, Ronald; Picard, Robert; Santier, Christian (CEA, Grenoble, France). Compt. Rend., Ser. B; 271: 824-7(19 Oct 1970). (In French).

A paramagnetic center consisting of a hole trapped by an oxygen ion, situated near a substitutional impurity, was created in Li-doped MgO by gamma irradiation at 77°K. (France)

9545 ESR IN IRRADIATED SILICON CARBIDE. Balona, L. A. de S.; Loubser, J. H. N. (Univ. of the Witwatersrand, Johannesburg). J. Phys., C (London); 3: 2344-51(Nov 1970).

Thirty samples of n- and p-type 6H and n-type 3C silicon carbide single crystals were irradiated at room temperature with either 0.8- or 1.0-MeV electrons or reactor neutrons. Seven different radiation-induced ESR spectra were found. Some of these have been described before, but further investigations of production rates and annealing behavior have necessitated changes in the previously proposed models. The ESR parameters of these centers are given. Three of the spectra are tentatively ascribed to (1) the uncharged carbon vacancy, (2) the negatively charged carbon divacancy, and (3) the uncharged silicon vacancy trapped at a boron site. Tentative models for three other centers are discussed. (auth) (UK)

9546 STRUCTURE OF SOME TRAPPED HOLE CENTERS IN CaF_2. II. Hall, T. P. P.; Leggeat, A.; Twidell, J. W. (Univ. of Essex, Colchester, Eng.). J. Phys., C (London); 3: 2352-8(Nov 1970).

Electron spin resonance studies were made of trapped hole centers in CaF_2 that have a F_2^- molecular ion structure with nearly axial symmetry along ⟨110⟩ directions, and unequal hyperfine interaction with the two ^{19}F nuclei involved in each center. The centers are formed in samples containing trivalent Y and Lu substitutional impurity ions by x irradiation at low temperatures and subsequent warming, or by irradiation at room temperature. A model is proposed in which the hole is trapped at a pair of nearest-neighbor interstitial F^- ions which themselves form an aggregate defect complex with the trivalent cation impurities. (auth) (UK)

9547 EFFECTS OF FAST NEUTRON IRRADIATION ON INTERNAL FRICTION AND YOUNG'S MODULUS OF SODIUM CHLORIDE SINGLE CRYSTALS. French, I. E.; Pollard, H. F. (Univ. of New South Wales, Kensington, Australia). J. Phys., C (London); 3: 1866-76(Sep 1970).

Sodium chloride single crystals were irradiated with fast neutrons at incident dose rates of between 5×10^7 and 3.4×10^8 neutrons per second whilst their internal friction and elastic modulus were being continuously measured. The effects of neutron dose rate, temperature (near room temperature), and interruptions in the irradiation were studied. The results are found to agree with the dislocation pinning theory of Granato and Lücke (1956) so that analysis in terms of this theory is justified. It is found that the rate at which dislocations are pinned is directly proportional to neutron dose rate. The dislocation damping coefficient B is found to vary when the irradiation is interrupted. An approximate activation energy of 0.7 ± 0.1 eV is found for the process that causes the variation in damping coefficient. A model is proposed to explain the results. (auth) (UK)

9548 THERMOLUMINESCENCE SPECTRUM OF γ-IRRADIATED NATURAL CALCIUM FLUORIDE. Sunta, C. M. (Bhabha Atomic Research Centre, Bombay). J. Phys., C (London); 3: 1978-83(Sep 1970).

The thermoluminescence glow curve of natural calcium fluoride crystals shows three distinct glow peaks between room temperature and 350°C. Emission spectrum is investigated separately for each of the glow peaks in the range 200 to 1000 nm. The spectral

similarity of emission associated with these glow peaks leads to the conclusion that they are associated with the release of either holes or electrons from different trapping sites and that the released carriers recombine with the same type of emitting centers It is concluded that the glow peaks are due to the release of holes which on recombination with electrons trapped at rare-earth impurity ions give rise to their characteristic spectra. (auth) (UK)

9549 IMPURITY EFFECTS ON ANNEALING OF RADIATION DEFECTS IN p-TYPE SILICON. Fang, P. H. (Electronics Research Center, Cambridge, Mass.); Tarko, H.; Drevinsky, P. J.; Iles, P. Appl. Phys. Lett.; 17: 426-7(15 Nov 1970).

A study of p-type silicon shows that (1) the annealing temperature of electron-irradiation damage increases as the acceptor concentration increases and (2) the isochronal annealing behavior of damage in samples with gallium and aluminum impurities is different from that in boron-containing samples, which show a higher annealing temperature. (auth)

9550 LOCALIZED MODES AND DIVACANCY ABSORPTION IN OXYGEN-ION-IMPLANTED Si. Stein, H. J.; Beezhold, Wendland (Sandia Labs., Albuquerque, N. Mex.). Appl. Phys. Lett.; 17: 442-4(15 Nov 1970).

Optical absorption bands characteristic of localized vibrational modes for both interstitial and substitutional oxygen were observed in crystalline Si implanted with 220-keV oxygen ions at 330°K. In addition, the fluence dependences for the vibrational modes and also for an electronic transition of the divacancy (1.8-μ band) were measured. Implanted oxygen ions are found to enhance divacancy formation. This effect was not observed for Sb implantation. The sum of the observed interstitial and substitutional oxygen centers is approximately equal to the number of implanted oxygen ions. An ion fluence 300 times larger than that to detect divacancies was required to detect the vibrational modes of oxygen as expected from the relative production rates and absorption coefficients. At these high fluences, the strengths of the vibrational bands increase in magnitude with fluence, while the divacancy band decreases. At even higher fluences amorphous layer formation, as indicated by a milky coloration of the surface, caused a decrease in the spacing interference fringes and in the magnitude of the oxygen vibrational bands. (auth)

9551 SPECIFIC VOLUME RESISTANCE OF STEATITE CERAMICS IN HIGH-INTENSITY γ FIELDS. Kostyukov, N. S.; Mazitov, B. S.; Muminov, M. I.; Shmid, O. I. (Inst. of Nuclear Physics, Tashkent). Dokl. Akad. Nauk Uzb. SSR; No. 2, 26-8 (1970). (In Russian).

The specific volume resistance of SNB, SNTs, SK-1, and SPK-2 specimens was studied as a function of irradiation dose and time. Disc-shaped specimens 50 mm in diameter and 1 to 2 mm in thickness were studied under 500-V intensities and γ doses varying from 270 to 4.8×10 r/sec. The results showed for SNB and SNTs specimens a minimum resistance at 2×10 r/sec and at 4.8×10^3 r/sec an increase in resistance reaching the point beyond the measuring instrument capacity. For SK-1 and SPK-2, the volume resistance never reached the minimum point. It was observed that irradiated steatites acquired nonlinear properties similar to that of certain ceramic semiconductor materials. It was assumed that the dependence of conductivity current on the doses or applied voltage is regulated by the same process. (R.V.J.)

9552 RADIATION ENHANCEMENT OF CAPRONE COLORATION AND POSSIBILITIES OF APPLICATION OF HIGH-CURRENT ACCELERATORS FOR THIS PURPOSE. Kaipov, D. K.; Tuktarov, N. S.; Zakharova, R. P. Izv. Akad. Nauk Kaz. SSR, Ser. Fiz.-Mat.; No. 6, 48-53(Nov-Dec 1969). (In Russian).

Results of enhancement of the coloration of caprone under the action of fast electrons are presented. Irradiation doses and stability characteristics are adduced, and the possibilities of using high-current accelerators for the enhancement of the coloration are considered. (tr-auth)

9553 ROLE OF MOBILE HOLES, ANION VACANCIES, AND EXCITONS IN THE RADIOINDUCED COLOURATION OF KCl CRYSTALS. Muradov, S.; Elango, M. (Inst. of Nuclear Physics, Tashkent). Izv. Akad. Nauk Est. SSR, Fiz. Mat.; 19: 320-7(1970).

The radiative production of F centers in KCl, KCl(Ag), KCl(Pb), and KCl(H) and B centers in KCl(Ag) as well as the radiative destruction of B centers in KCl (Ca, Ag) and reproduction of U centers by the optical bleaching of F centers in preliminarily irradiated KCl(H) were studied at temperatures between 80 and 400°K. The processes associated with the migration of holes (the 2nd stage of F-center production), anion vacancies (B-center production, optical F → U conversion) and excitons (the 1st stage of F-center production, radiative B-center destruction) were clarified. The temperatures for delocalization of holes (205°K), anion vacancies (235°K), and excitons (250°K) in KCl crystals were determined. (auth)

9554 PLASMA RADIATION FROM ELECTRON-BOMBARDED Be FILMS. Braundmeier, A. J. Jr.; Arakawa, E. T. (Oak Ridge National Lab., Tenn.). Opt. Commun.; 2: 257-8(Nov 1970).

A plasma energy of (18.1 ± 0.4) eV was determined for Be. Thin evaporated films of Be were bombarded by normally incident 80-keV electrons, with the emitted radiation being observed at 30° from the incident electron beam. Peaks in the emission spectrum were identified as due to plasma radiation or transition radiation. (auth)

9555 RELATIVE ENERGY LOSSES OF CHANNELED D^+ IONS IN GOLD. Hines, R. L. (Northwestern Univ., Evanston, Ill.). Phys. Lett.; 33A: 348-9(30 Nov 1970).

Measurements of the relative energy losses of 20 to 28 keV D^+ ions channeled in ⟨001⟩, ⟨112⟩, and ⟨011⟩ directions in gold crystal foils show that the ⟨001⟩ direction gives the largest energy loss and the ⟨011⟩ direction gives the smallest energy loss. (auth)

9556 MECHANISM OF ION SCATTERING BY CRYSTALS. Mashkova, E. S.; Molchanov, V. A.; Skripka, Yu. G. (Moscow State Univ.). Phys. Lett.; 33A: 373-4(30 Nov 1970).

On the basis of new experimental data for the (110) and (100) faces of copper, a simple qualitative mechanism of ion scattering by crystals is proposed. (auth)

9557 X-RAY DIFFRACTION OF ION-BOMBARDED DIAMONDS. Guseva, M. I.; Ershova, L. M.; Kiseleva, K. V.; Krasnopevtsev, V. V.; Milyutin, Yu. V. (Inst. of Physics, Moscow). Sov. Phys.-Cryst. (Engl. Transl.); 15: 441-4(Nov-Dec 1970).

Translated from Kristallografiya; 15: 523-7(May-Jun 1970).

With the aid of the Lang method, it is established that when diamond is bombarded with lithium ions with energy 40 keV and total dose $\sim 10^{16}$ cm^{-2}, a thin surface region is formed with a markedly disturbed crystal lattice. It consists of two layers with different degrees of disturbance and a total thickness of about 0.6 μ. This "sandwich" creates elastic stresses in the adjoining crystal lattice, and these stretch up to 180 μ into the specimen. (auth)

9558 LITHIUM-DEFECT INTERACTIONS IN ELECTRON-IRRADIATED n-TYPE SILICON. Goldstein, Bernard (Radio Corp. of America Labs., Princeton, N. J. Faculte des Sciences, Paris). Phys. Rev., B; 2: 4110-17(15 Nov 1970).

Single-crystal silicon specimens, both with and without oxygen, were diffused with lithium to concentrations $\sim 10^{17}$/cm^3, irradiated with 1–1.5-MeV electrons, and the ensuing defects studied by EPR and electrical measurements. The presence of oxygen strongly affects the properties of these defects. In O-containing material, the room-temperature carrier-removal rate is 0.25 cm^{-1}, and the carrier concentration continues to decrease after the cessation of the irradiation; in O-free material, the carrier-removal rate is 0.39 cm^{-1}, but here the carrier concentration can either increase or decrease after cessation of the irradiation. EPR measurements indicated the presence of two new defects that involve Li, one in O-containing material and one in O-free material. Their introduction rates are much smaller than the carrier-removal rates. The defect in O-containing Si exhibits a strong hyperfine interaction with the ^{7}Li nucleus, while that in O-free Si exhibits no hyperfine structure. Their g values are 2.0046 and 2.0090, respectively, and are isotropic. The defects are observed in their electron-filled state, and indicate a net electron spin of ½. The defect spectra disappear (with time) at room temperature, and this, together with the carrier-concentration changes, can be explained by the formation of other Li-involved defects which lie deeper in the energy band gap and are not visible by EPR. Electron irradiation at 40°K followed by annealing at higher temperatures shows that both EPR defects described above begin to form at about 200°K and begin to decrease at about 275°K, just as does the 250°K reverse annealing observed generally for n-type Si. Based on these data, and the work of others, it is suggested that both defects form as a result of the motion of Si interstitials, which produce a (Li–O interstitial) complex in O-containing Si, and a (Li interstitial) complex in O-free Si. (auth)

9559 ANION-VACANCY PROCESSES OCCURRING AFTER ROOM-TEMPERATURE F-LIGHT BLEACHING OR IRRADIATION OF NaCl. Jaque, F.; Agullo-Lopez, F. (Junta de Energia Nuclear, Madrid). Phys. Rev., B; 2: 4225-33(15 Nov 1970).

The thermally activated processes occurring in the dark after room-temperature F-light bleaching of x- or γ-irradiated NaCl were investigated. It was found that, near room temperature, the concentration of free-anion vacancies decays exponentially with

XUM

time. The kinetics of the process was studied by putting the crystal in the dark for a variable time after bleaching, and then subjecting it to a short illumination or irradiation pulse that detects the disappearance of the vacancies. It was observed that the decay in vacancy concentration is closely associated with a decrease in the F′-band intensity and with increases in the F- and M-band intensities. The experimental information led to the conclusion that vacancies become trapped at F′ centers according to a first-order reaction, giving rise to F and M centers through the mechanisms F′ + anion vacancy → 2F, and F′ + anion vacancy → M, respectively. The activation energy for the trapping process was found to be $E = 0.48 \pm 0.06$ eV. These phenomena also occur after an x or γ irradiation, and are shown to provide a coherent picture of the previously reported anomalous coloring behavior appearing at the start of a new irradiation period. (auth)

9560 P–N JUNCTION FORMATION IN ION-IMPLANTED ZnTe. Marine, J. (CENG, Grenoble, France); Rodot, H. Appl. Phys. Lett.; 17: 352-4(15 Oct 1970).

Chlorine ion implantation in ZnTe gives a highly resistive n-type layer. The technological process used for the doping is described, and the different tests that showed that type conversion of ZnTe was accomplished are discussed. (auth)

9561 ION IMPLANTATION OF SODIUM, LITHIUM, AND NEON IN CADMIUM SULFIDE. Tell, B. (Bell Telephone Labs., Holmdel, N. J.); Gibson, W. M.; Rogers, J. W. Appl. Phys. Lett.; 17: 315-18(15 Oct 1970).

Sodium, Li, and Ne were implanted into CdS in order both to study the luminescence and to attempt to achieve type conversion. Acceptor luminescence, due to the alkali impurities, was produced with significant intensity, but type conversion was not observed. The luminescence efficiency and the induced emission intensity as a function of annealing temperature have been obtained. (auth)

9562 ION-IMPLANTATION INDUCED OPTICAL ABSORPTION EDGE SHIFTS IN GaP. Davey, J. E.; Pankey, T.; Malmberg, P. R.; Lucke, W. H. (Naval Research Lab., Washington, D. C.). Appl. Phys. Lett.; 17: 323-5(15 Oct 1970).

The effects of implantation of argon on the optical properties of GaP films and bulk were investigated for doses of 10^{13} to $10^{15}/cm^2$ and energies between 1.5 and 3 MeV. Implantation of ordered films and bulk GaP results in a marked change in the optical absorption edge from about 2.3 eV to less than 1.0 eV, similar to behavior observed for amorphous films and for those subject to neutron irradiation. A maximum value of 3.22 was observed for the index of refraction of implanted films, as compared with 3.06 for bulk or highly ordered films. Bulk optical behavior can be recovered for implanted GaP with annealing at temperatures below 600°C. (auth)

9563 EFFECTS OF ELECTRON IRRADIATION ON CONDUCTIVITY IN CdS. Yoshida, Toshio; Kitagawa, Michiharu; Fujino, Takahiro (Radiation Center of Osaka Prefecture, Osaka). Appl. Phys. Lett.; 17: 337-8(15 Oct 1970).

Variations in radiation-induced conductivity of two different types of CdS single crystals near liquid-nitrogen temperature during 5-MeV electron irradiation were investigated. The conductivity of a high-conductivity crystal is decreased, and that of a low-conductivity crystal is increased with irradiation. Both conductivities come nearer to each other and seem to approach a limiting value as irradiation is continued. Two possible interpretations for the experimental result are presented. (auth)

9564 COMPARISON OF LATTICE-PARAMETER AND RESISTIVITY CHANGE IN ELECTRON-IRRADIATED ALUMINUM. Wagner, H.; Dworschak, F.; Schilling, W. (Kernforschungsanlage, Juelich, Ger.). Phys. Rev., B; 2: 3856-63(15 Nov 1970).

Lattice-parameter and residual-resistivity measurements were performed on high-purity aluminum samples irradiated simultaneously with 3-MeV electrons at 4.5°K. For the lattice-parameter measurements, a rotating single-crystal backreflection x-ray technique with monochromatic radiation (Cu $K\alpha_1$) was used with a resolution of $\Delta a/a \approx 6.5 \times 10^{-6}$. In four runs, the ratio $\eta = (\Delta a/a)/\Delta\rho$ was determined as a function of defect concentration and of thermal recovery. During defect production, the ratio η amounts to $(1.61 \pm 0.10) \times 10^3\ (\Omega\ cm)^{-1}$ and remains unaffected by the radiation annealing processes up to defect densities of about 2×10^{-3}. Furthermore, the ratio η stays constant throughout the recovery stages I, II, and III. This behavior suggests that the rearrangement in the local distribution of the interstitials and vacancies accompanying the radiation annealing and thermal recovery processes — especially the interstitial clustering processes — does not appreciably affect the lattice-parameter expansion and the electrical resistivity per unit of Frenkel-defect concentration. (auth)

9565 X-RAY MEASUREMENTS OF NEUTRON-IRRADIATED LiF. Hayashida, Hideto (Maritime Safety Academy, Hiroshima). Kaijo Hoan Daigakko Kenkyu Hokoku, Dai-2-Bu; 21-5(Mar 1970). (In Japanese).

The thermal recovery of a neutron-irradiated LiF single crystal was investigated by an x-ray-diffraction method. Measurements of changes in the lattice parameter and x-ray-reflection half-breadth during the successive thermal anneals were made. Assuming that the fractional lattice parameter change $(\Delta a/a)_x$ is proportional to defect concentration, it was shown that the annealing process is of second order and the activation energy is 2.4 eV. A particle size of about 500 Å for the irradiated crystal was obtained. (auth) (Japan)

9566 RADIATION INDUCED DEFECTS IN DIELECTRIC–SEMICONDUCTOR STRUCTURES. Mordkovich, V. N.; Zhukova, G. A.; Temper, E. M. Fiz. Tekh. Poluprov.; 4: 1583-5(Aug 1970). (In Russian).

An attempt is made to show that radiation-induced positive charges in dielectrics are not the only processes influencing the change in the structure of dielectric–semiconductor (d–s) structures as was stated by E. Snow et al., Proc. IEEE, 55: 1168(1967). Experiments with various specimens revealed that, depending on the method of production of silicon dioxides, irradiation with low-energy ($E \leq 50$ keV) protons produced both a positive and a negative charge in Si–SiO_2 structures. It was also shown that neutron irradiation may produce a negative charge in a dielectric, with the negative charge first increasing with the increase of neutron flux, followed subsequently by increase of positive charge. Thus, it is suggested that studies of radiation-induced effects in d–s systems should consider the complex processes that produce the defects in dielectrics. (R.V.J.)

9567 STUDIES OF RECOMBINATION CENTERS IN GAMMA-IRRADIATED p-TYPE SILICON. Nakashima, Kenshiro (Nagoya Inst. of Tech., Japan); Inuishi, Yoshio. J. Phys. Soc. Jap.; 29: 1500-12(Dec 1970).

Recombination centers produced by ^{60}Co γ-ray irradiation at room temperature were investigated by measuring the temperature dependence and the annealing behavior of the minority-carrier lifetime. Both isochronal and isothermal annealing of the lifetime at a fixed measured temperature were observed to investigate the characteristic of the individual recombination center. The measurements at 150°K show that A center at $E_C - 0.17$ eV is the most effective recombination center about the region of this temperature in all p-type specimens. The first-order annealing process, with an activation energy of 1.27 eV, was found in agreement with the values reported earlier. The capture cross sections for electrons and holes were estimated to be 1.2×10^{-15} cm² and 1.8×10^{-14} cm², respectively. The introduction rate of inverse lifetime measured at 150°K seems to show that A center is introduced at nearly the same rate in both floating-zone and pulled crystals. At and above room temperature the recombination center at $\sim E_V + 0.3$ eV was found to control the lifetime. The annealing activation energy of this center was found to be dependent on the kind of impurities and estimated to be 1.27 and 0.98 eV in boron- or gallium-doped floating-zone specimens, respectively. The reaction order of recovery process of this center was less than one. This center seems to be a complex defect containing a dopant impurity. (auth)

9568 VOLUME GRADIENT OF γ-EMF IN p-Si. Dubovoi, V. K.; Konozenko, I. D.; Semenyuk, A. K. (Inst. of Physics, Kiev). Fiz. Tekh. Poluprov.; 4: 1575-6(Aug 1970). (In Russian).

The volume-gradient γ-emf, studied as a function of ^{60}Co γ-radiation dose and temperature for p-type silicon at 20 to 60°C, decreased with increased temperature and had a logarithmic character with doses from 1700 to 100 r/sec. (R.V.J.)

9569 ENHANCED DIFFUSION OF HIGH-TEMPERATURE ION-IMPLANTED ANTIMONY INTO SILICON. Gamo, Kenji; Masuda, Kohzoh; Namba, Susumu (Osaka Univ.). Appl. Phys. Lett.; 17: 391-3(1 Nov 1970).

Concentration profiles of 20-keV high-temperature ion-implanted antimony into a silicon single crystal were measured by means of radioactivation analysis and the enhanced diffusion was observed. The concentration profiles were found to be independent of temperature over the range between 500 and 800°C and to be dependent on the dose rate of ion implantation. The diffusion coefficient of antimony is estimated to be about 1.1×10^{-15}/cm² sec for the dose rate of about 1.2×10^{12} ions/cm² sec and about 6.6×10^{-15} cm²/sec for that of about 7.2×10^{12} ions/cm² sec. The measured concentration profiles are in good agreement with the calculated concentration profile. These results are explained on the basis of a vacancy mechanism. (auth)

9570 OPTICAL ABSORPTION AND ELECTRICAL CONDUCTION IN KBr CRYSTALS CONTAINING DIFFUSED MAGNE-

SIUM. Sootha, G. D.; Kumar, N. (National Physical Lab., New Delhi). J. Phys., (London); 3: 1963-6(Nov 1970).

The conductivity of KBr crystals containing diffused magnesium is smaller in the free vacancy conduction region II (where the conductivity is due to the cation vacancies present in the crystal as a result of the presence of divalent cation impurities, and all the vacancies are in the free state) than in a pure crystal. These crystals show an optical absorption band peaking at 228 nm. It is suggested that the decrease in the conductivity and the 228 nm band are associated with the reduction of background divalent cations like Pb^{2+} to mono- or zero-valent form and formation of U centres, respectively. (auth) (UK)

9571 KOHLER'S RULE FOR THE LONGITUDINAL MAGNETORESISTANCE OF NEUTRON-IRRADIATED COPPER AT 4.6 K. Boening, K.; Fenzl, H. J.; Welter, J.-M.; Wenzl, H. (Technische Hochschule, Munich). Phys. Kondens. Mater.; 12: 72-80(1970). (In German).

The longitudinal magnetoresistance of pure single- and polycrystalline copper was measured after structural defects were introduced at low temperature with fast neutrons and subsequent step-annealing. There are deviations from Kohler's rule if the scattering anisotropies of the defects change. The result of the measurement is that, during irradiation and recovery state I, almost the same scattering configuration is present, which rearranges to another configuration that dominates after stage III. (auth)

9572 DIRECT OBSERVATION OF THE EFFECTS OF IRRADIATION WITH GAMMA RAYS AND FAST NEUTRONS ON SILICON. Gerward, L. (Chalmers Tekniska Hogskola, Goteborg). Phys. Scr.; 1: 147-9(1970).

X-ray topography was used to study the production of lattice defects by 1.25-MeV gamma photons and by fast neutrons in silicon single crystals. It was found that no changes occur in the dislocation configuration, and no defects are created with strain fields larger than 1 μ in size. Though electrical measurements indicate the existence of overlapping disordered regions in crystals irradiated with doses exceeding 10^{19} fast neutrons per cm^2, it is shown that the defects are sufficiently dilute to maintain a well-defined lattice with regard to x-ray diffraction properties. (auth) (Sweden)

9573 PRIMARY-RECOIL ATOM SPECTRA FROM ENDF/B DATA. Jenkins, J. D. (Oak Ridge National Lab., Tenn.). Nucl. Sci. Eng.; 41: 155-63(Aug 1970).

Information from the Evaluated Nuclear Data File (ENDF/B) was used to construct energy-exchange kernels describing the energy transfer probabilities between neutrons and material lattice atoms. The kernels correctly incorporate all the available information on elastic scattering and inelastic scattering contained in ENDF/B. Their use removes much of the uncertainty in the calculation of primary-recoil spectra. Primary-recoil atom spectra for Ni, Nb, and Fe in different reactor spectra were generated. The influence of inelastic scattering on the recoil spectra is discussed. Results obtained with the ENDF/B data are compared with previously published information. (auth)

Physical Properties

Refer also to abstracts 8882, 8908, 8934, 8936, 9391, 9608, and 9964.

9574 ANNEALING EFFECTS AND OPTICAL ABSORPTION OF THERMOLUMINESCENT LITHIUM FLUORIDE. Jackson, J. H.; Harris, A. M. (Central Electricity Generating Board, Berkeley, Eng.). J. Phys., C (London); 3: 1967-77(Sep 1970).

The changes in the optical absorption of thermoluminescent dosimetry-grade lithium fluoride observed as functions of various pre-irradiation and post-irradiation heat treatments were related to the thermoluminescent properties of the material. Correlations were made of the 3.23-eV absorption band to the glow peaks at 115°C and 160°C, and the 3.99-eV absorption band to the peaks at 195°C and 210°C. Determinations of the trap depths and frequency factors yield figures in reasonable agreement with those previously obtained from thermoluminescent data. A model for the trap distribution and movement is presented that is consistent with the observations and with the variation of thermoluminescent sensitivity reported previously. (auth) (UK)

9575 FERMI SURFACE IN NIOBIUM. Scott, G. B.; Springford, M. (Univ. of Sussex, Eng.). Proc. Roy. Soc. (London), Ser. A; 320: 115-30(24 Nov 1970).

The low-frequency field modulation technique was employed to study the de Haas–van Alphen effect in single crystals of niobium in fields up to 10 tesla. The frequency determination of the oscillations was performed by computer-based Fourier analysis and gave five sets of frequencies, which were studied in {100} and {110} planes. Effective masses and Dingle temperatures of some orbits were measured in the symmetry directions ⟨100⟩, ⟨110⟩, and ⟨111⟩. Interpretation of the results was based on the results of a recent augmented plane-wave band structure calculation of Mattheiss (1970). Three of the observed frequency branches can be explained in terms of, and are in good agreement with, the Fermi surface predicted by this calculation. The remaining frequencies can be accounted for, if a slight distortion of the proposed model is made. Comparison of the measured effective masses with those calculated from the band structure gives a value of 2.14 ± 0.17 for the mass enhancement factor due to many-body effects. Using the theory of McMillan (1968), the superconducting isotope shift coefficient is evaluated to be 0.24. (auth) (UK)

9576 MAGNETIC COUPLING AND PHASE BOUNDARIES FOR SOME C15 AND C22 PSEUDOBINARY ALLOYS CONTAINING LANTHANIDES. Leon, Burke. Pittsburgh; Univ. of Pittsburgh (1969). 168p. University Microfilms Order No. 70-14,833.

Thesis.

Magnetic and structural properties were determined for a series of "pseudobinary" alloys of the C15 and C22 structures: $LnNi_xAl_{2-x}$ and $Pr_xLn_{1-x}T_2$ where Ln = Ce, Pr, Nd, Gd, Tb, Dy, Ho, Er, Y, and Lu for the first case, and Ln = Dy and Ho, and T = Ni and Co for the second case. Samples were prepared by induction melting and their crystal structures examined by powder x-ray diffraction. Magnetic susceptibilities were determined by the Faraday method. Susceptibilities were measured as a function of temperature over the range 4.2 to 300°K, and as a function of selected field strength values between 2 and 20 kOe. The phase diagrams were determined for all cases. For the $LnNi_xAl_{2-x}$ system, the phase diagram from x = 0 to x = 2 consisted of two terminal regions of C15 structure separated from a central region of C22 structure by two-phase regions. The outstanding feature of these phase diagrams was the appearance of a second phase at an electron concentration of 1.16 electrons per atom for all the heavy lanthanides, in agreement with predictions based on a theory of Fermi surface Brillouin zone interactions. For $Pr_xLn_{1-x}T_2$, a single-phase region of C15 structure was observed from x = 0 to x = 1. Magnetic measurements were made on one sample in each of the one-phase regions of $LnNi_xAl_{2-x}$. All samples except Ln = Ce, Lu, Y, and Pr were ferromagnetic at low temperatures. In all cases the effective paramagnetic moment at 18 kOe was that of the free ion, while the saturation moment, Weiss constant, and Curie temperature for these ternaries differed from the corresponding binary compounds in a somewhat systematic manner. Detailed magnetic investigation of the aluminum-rich single-phase region for Ln = Tb and Er produced a variation of magnetic properties which could be interpreted using the RKKY interaction. For the $Pr_xLn_{1-x}T_2$ systems, the magnetic measurements made on samples from x = 0 to x = 1 gave an indication of Pr magnetic moment with Ln concentration. For T = Ni, the Pr was paramagnetic until a "threshold" concentration of Ln was substituted for Pr. The moment then rose to its maximum of 3.2 Bohr magnetons as x increased to x = 1. For T = Co, a rise from a Pr moment of 1.2 to 3.2 Bohr magnetons was observed as x increased to x = 1. All ternary samples of the $Pr_xLn_{1-x}T_2$ exhibited ferrimagnetic coupling. (Diss. Abstr. Int., B)

9577 ELECTRICAL PROPERTIES AND DEFECT STRUCTURE OF ThO_2. Bransky, I. (Ohio State Univ., Columbus); Tallan, N. M. J. Amer. Ceram. Soc.; 53: 625-9(Nov 1970).

The electrical conductivity and thermoelectric power of high-purity polycrystalline ThO_2 in thermodynamic equilibrium with the gas phase were measured as a function of temperature from 1000 to 1600°C and as a function of oxygen partial pressure from 1 to 10^{-22} atm. An n-type electronic contribution to the conductivity was observed above 1400°C at low oxygen pressures. An analytic solution is presented for the oxygen pressure dependence of the total conductivity in the mixed ionic–electron hole conduction region observed at higher oxygen pressures. The activation energies for p-type and ionic conduction are 1.0 and 0.9 eV, respectively. The combined conductivity and thermal emf data give a lower limit of ≈6 cm^2/V-s for the electron hole mobility. (auth)

9578 MEASUREMENT OF THE MAGNETIC SUSCEPTIBILITY OF BERYLLIUM. Bowring, C. S.; Wynn, V. T. (Exeter Univ., Eng.). Phys. Lett.; 33A: 401-2(30 Nov 1970).

Measurements of the total magnetic susceptibility and the electron spin susceptibility were made for beryllium. The results are still at variance with recent theoretical work. (auth)

9579 TEMPERATURE DEPENDENCE OF SPONTANEOUS MAGNETIZATION IN HOLMIUM DURING HEATING-COOLING CYCLE. Mandzhavidze, A. G.; Gogava, V. V.; Kolesnikova, L. M.; Megeryan, R. G. (Inst. of Physics, Tbilisi, USSR). Soobshch. Akad. Nauk Gruz. SSR.; 60: 65-8(Oct 1970). (In Russian)

XUM

Temperature dependence of spontaneous magnetization in polycrystalline Ho was investigated by small-angle monochromatic neutron scattering in the heating-cooling cycle near absolute zero. Thermal hysteresis of magnetization was found. This suggests that magnetic transformation in Ho has the character of a phase transition of first order. (auth)

9580 ELECTRICAL PROPERTIES OF V_8O_{15} SINGLE CRYSTAL. Okinaka, H. (Kyoto Univ.); Kosuge, K.; Kachi, S.; Nagasawa, K.; Bando, Y.; Takada, T. Phys. Lett.; 33A: 370-1(30 Nov 1970).

Electrical resistivity and thermoelectric power measurements on V_8O_{15} single crystals clarified that V_8O_{15} shows the metal-to-semiconductor phase transition at 70°K. (auth)

9581 ELECTRICAL PROPERTIES OF V_2O_5. Haemers, Johan. Ghent; State Univ. of Ghent (1969). (In Dutch).

Thesis.

A purified V_2O_5 is obtained by transforming distilled $VOCl_3$ into NH_4VO_3 as an intermediate step. Thermal decomposition of the latter in oxygen atmosphere, yields a better starting material for the zone refining. Applying zone refining to the purified material yields large single crystals (15 cm × 1cm × 1cm). The impurity content is about 100 ppM, Pt being the most important one. On those single crystals electrical measurements were performed. The temperature dependence of the conductivity showed three different ranges. Between room temperature and ±140°K, an activation energy of 0.52 ± 0.04 eV could be derived. On the same samples, Hall measurements were performed. No Hall voltages could be detected for mobilities as low as 10^{-3} cm^2/V-sec. Most recent theories by Cohen and Mott, in which the problem of the transition from a perfect to an amorphous semiconductor is treated, gave good qualitative agreement with the experimental results. On the basis of experimental results obtained on undoped and doped single crystals, a model for the band structure and the conduction mechanism in V_2O_5 is proposed. (TSS) (Diss. Abstr. Int., B)

9582 ANALYSIS OF THE ELECTRON-PARAMAGNETIC-RESONANCE LINESHAPE OF Tb^{4+} IN POLYCRYSTALLINE TbO_2. Azzoni, C. B.; Del Nero, G. L.; Lanzi, G.; Cola, M. (Univ., Pavia, Italy). Lett. Nuovo Cim.; 4: 959-62(21 Nov 1970).

The Tb^{4+} ion in face-centered cubic TbO_2 was studied by EPR techniques. A single line was obtained at g = 2.0147 ± 0.0002, with Lorentzian shape and linewidth ΔH = (3.06 ± 0.08) kG. The signal parameters were independent of temperature for temperatures between −196 and +200°C. The experimental results were simulated theoretically; a g value of 2.0023 was predicted. (R.W.R.)

9583 CHARACTERISTIC ENERGY LOSS STUDIES OF V_2O_5 AND VANADIUM. Fiermans, L.; Vennik, J. (Rijksuniversiteit, Ghent). Phys. Status Solidi; 41: 621-9(1 Oct 1970).

The characteristic energy losses of V_2O_5 are interpreted, using collective oscillations of groups of electrons forming the O2p valence band. These observations provide valuable information concerning the energy band model of this material. The losses observed on vanadium are interpreted as due to free electron bulk and surface plasmons and combinations of both. Characteristic ionization losses confirm the ODS peaks observed in the vanadium valence band and indicate high transition probabilities for the top and bottom of this band. (auth)

9584 THERMAL RADIATION AND ELECTRONIC DENSITY OF STATES OF W−Ta ALLOYS. Thomas, L. K. (Technische Univ., Berlin). Phys. Status Solidi; 41: 681-9(1 Oct 1970).

The normal spectral emissivity of W, Ta−50 W, and Ta is calculated in the wavelength range 0.35 to 2.3 μm for the temperature 2400 °K using literature values of the electronic density of states for W. At 0.57 μm, calculations are made for the temperatures 2800 and 2000 °K. The calculations follow the theory of radiative energy transfer in gases and the theory of Einstein's transition probabilities. The matrix element of the electron−phonon interaction is used for the comparison of the theoretical and experimental results. The calculated temperature coefficient of the emissivity has the correct sign. (auth)

9585 ISOTOPE SPLITTING OF THE F-CENTER IN-GAP MODE IN KI AND KBr. Baeuerle, D. (Cornell Univ., Ithaca, N. Y.); Huebner, R. Phys. Rev., B; 2: 4252-62(15 Nov 1970).

High-resolution measurements at the F-center in-gap mode in KI and KBr revealed a threefold structure in the absorption spectrum with lines at 82.62 ± 0.02, 81.98 ± 0.02, 81.19 ± 0.05 cm^{-1} and at 99.60 ± 0.03, 99.07 ± 0.04, 98.50 ± 0.05 cm^{-1}, respectively. This structure is interpreted as due to the presence of two stable isotopes, ^{39}K and ^{41}K, in the crystal. In a three-dimensional-model calculation, which uses as parameters changes in the force constants between the defect and the first nearest neighbors (A01) and changes in the force constant between the first and fourth nearest neighbors (A14), it is found that the in-gap mode frequencies are extremely sensitive to the value of the latter. The position and splitting in the absorption lines can be explained in the calculation by using A01 = −0.50, A14 = −0.060 for KI and A01 = −0.50, A14 = +0.002 for KBr. Stress experiments on the strongest lines in KI are in agreement with the model. Extending the calculation to Cl^- and Br^- centers in KI, it is shown that the measured isotope splitting for ^{35}Cl, ^{37}Cl, and ^{79}Br, ^{81}Br centers can be explained by taking into account not only changes in A01 but also changes in A14. (auth)

9586 MULTIPLE KINK EFFECT IN GRAPHITE. Yugo, Shigemi; Hayashi, Haruhisa; Yazawa, Kazuhiko (Univ. of Electro-Communications, Tokyo). Appl. Phys. Lett.; 17: 339-40(15 Oct 1970).

It is found that (1) the current−voltage relation of graphite has three kink points under the influence of a transverse magnetic field, and (2) the kink effect is observed even at such a high temperature as 300°K. These kinks are attributed to the interaction between conduction electrons and various modes of phonons that are unique in the lamellar structure material. (auth)

9587 INCREASE OF CURIE TEMPERATURE IN EuO FILMS BY Fe DOPING. Ahn, K. Y. (IBM Thomas J. Watson Research Center, Yorktown Heights, N. Y.). Appl. Phys. Lett.; 17: 347-9 (15 Oct 1970).

A large increase of ferromagnetic Curie temperature from 69.5 to ~180°K was discovered in EuO films by Fe doping. In films containing Fe up to 8% by weight, the structure is essentially the same as bulk EuO, the magnetic moment (at 4.2°K) is reduced slightly to 190 emu/g, the longitudinal Faraday rotation shows a similar wavelength dependence as that of pure EuO with a maximum positive rotation of 2.4×10^5 deg/cm at 6500 Å at an incidence angle of 65°, square hysteresis loops extend to ~160°K, and the optical absorption characteristics are modified by Fe doping with a peak absorption coefficient of 2.4×10^5/cm (at 300°K) at 5800 Å. (auth)

9588 NEW FIRST-ORDER PHASE TRANSITION IN HIGH-PURITY YTTERBIUM METAL. Bucher, E.; Schmidt, P. H.; Jayaraman, A.; (and others). (Bell Telephone Labs., Murray Hill, N. J.). Phys. Rev., B; 2: 3911-17(15 Nov 1970).

A first-order magnetic phase transition was observed in high-purity Yb metal. It is characterized by a paramagnetic-to-diamagnetic transition with a large degree of hysteresis between 100 and 360°K, and appears to be associated with an fcc−hcp martensitic transformation. The occurrence of this transition is characteristic of high-purity metal and has not been previously reported. Several other properties such as the specific heat at 0 and 106 kOe, the volume and resistance changes of the low-temperature resistivity, x-ray data, and the pressure and strain dependence of the transition are discussed. The diamagnetic phase is not superconducting above 0.015°K. The fcc phase was obtained from the hcp phase by applying strain at room temperature and was also investigated. It shows a strongly temperature-dependent paramagnetic susceptibility down to 1.4°K, but no magnetic ordering could be detected down to 1.0°K. (auth)

9589 LATTICE-DYNAMICAL THEORY OF THE DIFFUSION PROCESS. I. ISOTOPE EFFECT IN CUBIC METALS. Achar, B. N. Narahari (Argonne National Lab., Ill.). Phys. Rev., B; 2: 3848-55(15 Nov 1970).

A lattice-dynamical theory of diffusion based on the fluctuations in a certain reaction coordinate first used by Flynn is presented. The theory of vibrations of isotopic impurities in a crystal is applied to evaluate the parameter ΔK that describes the isotope effect in diffusion. Numerical results for Cu, Ag, Au, Al, Ni, Co, Pb, Na, and α-Fe are presented. The effect of both relaxation near the vacancy and temperature on ΔK are also studied. (auth)

9590 METODY ISSLEDOVANIYA TERMOELEKTRICHESKIKH SVOISTV POLUPROVODNIKOV. (Methods of Investigation of Thermoelectric Properties of Semiconductors). Glazov, V. M.; Okhotin, A. S.; Borovikova, R. P.; Pushkarskii, A. S. Moscow, Atomizdat (1969). 176p.

The physical essence of thermoelectric phenomena and properties of semiconductors are first described briefly. Then the theoretical bases of methods of measurement of thermal emf, electric conductivity, thermal conductivity, and the Hall effect are discussed. For each method, equipment for measurement is described, and a comparative analysis of the different methodology is presented. Finally, the methods of measurement of thermoelectric properties of liquid semiconductors are clarified in detail. 251 references. (tr-auth)

9591 INCIPIENT ANTIFERROMAGNETISM IN SCANDIUM. Capellmann, Herbert (Univ. of Pennsylvania, Philadelphia). J. Low Temp. Phys.; 3: 189-96(Aug 1970).

The influence of the magnetic properties of the elements on the left-hand side of the transition series on their superconducting transition temperature T_c is discussed. In particular, in the case of a scandium, there is experimental evidence for the existence of strong antiferromagnetic spin fluctuations. They lead to a repulsive electron–electron interaction. This possibly explains why Sc has not been found to be superconducting. (auth)

9592 METALLIC CHARACTER OF A METAL HYDRIDE, V_2H. Westlake, D. G.; Ockers, S. T. (Argonne National Lab., Ill.). Phys. Rev. Lett.; 25: 1618-19(7 Dec 1970).

Both the residual and ideal electrical resistivities of V_2H approximate those of vanadium metal down to 4.2°K. The addition of hydrogen to the metal lowers the superconducting transition temperature. This is discussed from the standpoints of both lower crystal symmetry and higher electron-to-atom ratios. (auth)

Moessbauer Effects and NMR

Refer also to abstract 8575.

9593 RESONANCE SPECTROSCOPY OF γ-RADIATION ON Au(I) AND Au(III) COMPOUNDS. Bartunik, H. D. (Technische Hochschule, Munich); Potzel, W.; Moessbauer, R. L.; Kaindl, G. Z. Phys.; 240: 1-16(1970).

Isomer shift and electric quadrupole splitting of the 77-keV γ rays of ^{197}Au were investigated for a large number of Au(I) and Au(III) compounds at 4.2 °K by nuclear γ-resonance spectroscopy. A close correlation between the observed isomer shifts and the spectrochemical series of the ligands was observed. For each oxidation state, isomer shift and electric quadrupole splitting show approximately a linear relationship. On the basis of LCAO–MO theory, the experimental results are interpreted by covalency effects in the molecular orbitals, synergic coupling of σ- and π-bonds, and the empirically known donor and acceptor properties of the ligands. (auth)

9594 MOESSBAUER EFFECT STUDY OF HYPERFINE INTERACTIONS IN ^{145}Nd. Kaindl, G. (Univ. of California, Berkeley). Z. Phys.; 240: 100-22(1970).

The magnetic hyperfine splitting of the 72.5-keV γ rays of ^{145}Nd was investigated in intermetallic compounds of Nd and in the paramagnetic salts $Nd_xY_{1-x}Cl_3 \cdot 6H_2O$ (with x = 0.02 and x = 0.05) at 4.2°K. With the magnetic hyperfine tensor A of $Nd_{0.01}Y_{0.99}Cl_3 \cdot 6H_2O$ known from EPR spectroscopy, the analysis of the unresolved magnetic hyperfine spectra yields $I_e = 5/2$ for the spin of the 72.5-keV state, in contradiction of a previous result. The multipolarity of the 72.5-keV γ transition was found to be essentially M1 with $\delta^2 = 0.010 \pm 0.014$, and the magnetic moment of the 72.5-keV state was determined as $\mu(5/2) = -0.319 \pm 0.004$ nm. For various divalent and trivalent Nd compounds as well as for metallic Nd, the isomer shift IS of the 72.5-keV γ line was measured. A value for the change of the mean square nuclear charge radius during the 72.5-keV γ transition of $\Delta\langle r^2\rangle = +(1.9 \pm 0.9) \cdot 10^{-3}$ fm² was deduced, using electron density differences from free-ion Hartree–Fock calculations. (auth)

9595 PREPARATION OF MOESSBAUER SOURCE. Lipka, Jozef; Sitek, Jozef (Slovak Technical Univ., Bratislava). Jad. Energ.; 16: 378-9(1970). (In Czech).

The Moessbauer source ^{57}Co in Cu was prepared. The Doppler-shift curve was measured to find the effective width $\Gamma_{exp} = 0.700 \pm 0.023$ mm/sec and peak absorption $D = 0.238 \pm 0.021$. The recoil-free fraction, $f = 0.685 \pm 0.012$, was obtained by the area method. Such sources give a single-line spectrum. (auth)

9596 RESONANT BRAGG SCATTERING OF GAMMA RAYS BY NUCLEI IN HIGH ORDERS OF REFLECTION, AND PRODUCTION OF DIRECTED BEAMS OF PURE MOESSBAUER RADIATION. Voitovetskii, V. K.; Korsunskii, I. L.; Pazhin, Yu. F.; Silakov, R. S. JETP Lett. (USSR) (Engl. Transl.); 12: 212-15 (20 Sep 1970).

Translated from Zh. Eksp. Teor. Fiz., Pis'ma Red.; 12: 314-18(20 Sep 1970).

The use of high reflection orders suppresses scattering by electrons and makes it possible to observe only nuclear scattering. Bragg scattering of γ rays was observed in a Moessbauer setup with a $^{119m}SnO_2$ source and a ^{119}Sn single crystal. A diffraction peak was found in the tenth order of reflection when the velocity was at resonance. The Moessbauer spectra at 100 and 210°K agreed with calculations for the 1-μ and the mosaic (5 and 16 μ) crystals, but not for the perfect 420-μ crystal. The sharp asymmetry of the spectra, which is opposite to that at low reflection orders, is noted. (D.L.C.)

Theory

Refer also to abstract 9606.

9597 SELF-CONSISTENT BAND CALCULATIONS FOR VANADIUM AND CHROMIUM. Yasui, Masaru; Hayashi, Eisuke; Shimizu, Masao (Nagoya Univ., Japan). J. Phys. Soc. Jap.; 29: 1446-55(Dec 1970).

Self-consistent band calculations are carried out for vanadium and chromium. The modified tight-binding method and the orthogonalized-plane-wave method are used for the wave functions of d- and s-electrons, respectively. The crystal potential and wave function are determined self-consistently by an iteration method. The calculations are carried out in the two cases where the coefficient of the Slater exchange potential is 1 and 0.725. The band structures, Fermi surfaces, and density of states curves are obtained for both metals and compared with previously reported results. (auth)

9598 MODEL POTENTIAL CALCULATION OF THE RAMAN TENSOR FOR Be, Mg, AND Zn. Swanson, L. R.; Maradudin, A. A. (Univ. of California, Irvine). Phys. Rev., B; 2: 3891-4(15 Nov 1970).

A model potential calculation of the first derivative of the electronic polarizability with respect to an atomic displacement for Be, Mg, and Zn is presented. The magnitudes of these derivatives, which govern the intensity of the first-order Raman effect in the corresponding crystals at the argon-ion laser wavelength of 4880 Å, are 39.7 Å² for Be, 11.2 Å² for Mg, and 18.9 Å² for Zn. The dependence of the real and imaginary parts of the polarizability derivative on the frequency of the incident light is also calculated for these crystals. (auth)

Theoretical Physics

Refer also to abstracts 9054, 9055, 9839, 9840, and 9869.

9599 (JINR–P2-5314) NONRELATIVISTIC TRANSFORMATIONS APPLIED TO THE DIRAC EQUATION. Strel'tsov, V. N. (Joint Inst. for Nuclear Research, Dubna (USSR). Lab. of High Energy). 1970. 5p. (In Russian). Dep. NTIS (U. S. Sales Only).

Nonrelativistic transformations are applied to the Dirac equation. It is shown, for example, that in this case the wave functions obey the transformation formulae of the type $\psi' = s\psi$, where $s = (1 + \beta^2/8) + i\gamma_1\gamma_4 (1 + 3\beta^2/8)$, and $\beta = v/c$. (auth)

9600 (JINR–P4-5040) PROBLEM OF TWO CENTRES IN QUANTUM MECHANICS. V. ALGORITHM. Ponomarev, L. I.; Puzynina, T. P. (Joint Inst. for Nuclear Research, Dubna (USSR)). 1970. 42p. (In Russian). Dep. NTIS (U. S. Sales Only).

Algorithms for calculation of eigenvalues $P_i(R)$ and $\lambda_i(R)$ of the two center problem of quantum mechanics, its wave functions $\phi_i(\xi, \eta, R)$, and some matrix elements on these wave functions are described. Matrix elements were calculated for the $Z_1 = 1$; $Z_2 = 1$; 2 charge system and internuclear spacing R = 0.1(0.1)5(0.2)11 (0.5)20. (auth)

9601 (LA–4539) ANDYMG3: THE BASIC PROGRAM OF A SERIES OF MONTE CARLO PROGRAMS FOR TIME-DEPENDENT TRANSPORT OF PARTICLES AND PHOTONS. Harris, D. R. (Los Alamos Scientific Lab., N. Mex.). Oct 1970. Contract W-7405-eng-36. 21p. Dep. NTIS.

ANDYMG3 is the basic program of a series of Monte Carlo programs designed to solve applied problems in time-dependent particle and photon transport for general geometries. Particle or photon type and energy are identified by multi-energy-group number. Cross sections are read in S_N format with scattering pattern components up to P_3. Particle splitting and termination routines permit negative weights. Particle and photon emission can be delayed. A library of reaction cross sections is provided so that practically useful results are computed after execution of the Monte Carlo. The ANDYMG3 program, in FORTRAN-IV for the CDC-6600 and UNIVAC-1108 computers, requires 0.5 to 2 msec per collision (CDC-6600) and a field length less than 60_8K for most problems. (auth)

9602 (LA–4554) TRANSPORT THEORY: DISCRETE ORDINATES QUADRATURE OVER THE UNIT SPHERE. Carlson, Bengt G. (Los Alamos Scientific Lab., N. Mex.). Sep 1970. 16p. Dep. NTIS.

Symmetric quadrature sets, defined over the surface of the unit

XUM

sphere, are developed for use with the discrete ordinates method in transport theory to improve the quality of numerical solutions, especially in the case of geometries with two or more dimensions. The sets are constructed so that the quadrature points are invariant with respect to certain reflections and rotations of the unit sphere. (auth)

9603 PROBLEM IN THE QUANTUM THEORY OF MEASUREMENT. Burba, David Alexander. Nashville; Vanderbilt Univ. (1970). 51p. University Microfilms Order No. 70-16,416.

Thesis.

The probability that a particle with a given initial wave function will be in a given volume V at least one time between two distinct fixed times, t_0 and t_α, is discussed. One approach to solving this particle-probability problem is to assume that the volume V is occupied by a 100%-efficient counter (which is designed to detect the presence of a single particle should the particle pass through the volume of the counter and which is assumed to be capable of recording the time at which a count occurs) and to determine the counting probability of that counter. Four main approaches to solving the counting-probability problem are discussed. One of these approaches involves assuming that the counter accomplishes the necessary "collapse" of the particle's wave function by acting as a black or absorbing sphere. There are two black-sphere methods discussed: 1) the use of a negative imaginary potential to obliterate the particle's wave function in the volume of the counter, and 2) direct obliteration of some of the outgoing components of the particle's wave function without trying to write a Hamiltonian to produce the effect of absorption. The second main approach to solving the counting-probability problem is to consider Hamiltonian methods which explicitly involve interaction of the particle with a counter system which has its own degrees of freedom. The third approach toward a solution of the counting-probability problem is an attempt to represent the case of a continuous observation (in which the interaction of counter and particle goes on simultaneously with a continuous collapse of the state vector) by breaking the relevant time interval up into (n+1) equally-spaced instants separated by intervals of duration Δ, with $n\Delta = t_\alpha - t_0$, and assuming that the counter is turned on instantaneously at each of these instants. One would then hope to let $n \to \infty$, $\Delta \to 0$ in such a way that $n\Delta \equiv t_\alpha - t_0$ to achieve the desired description of a continuous observation. Various attempts at carrying out this program and their results are discussed. No complete results are obtained. The fourth approach to solving the counting-probability problem consists of breaking the relevant time interval up into many different sets of increments of unequal duration and averaging all the resulting state vectors. (TSS) (Diss. Abstr. Int., B)

9604 DISTRIBUTION OF EIGENFREQUENCIES FOR THE WAVE EQUATION IN A FINITE DOMAIN. I. THREE-DIMENSIONAL PROBLEM WITH SMOOTH BOUNDARY SURFACE. Balian, R.; Bloch, C. (Centre d'Etudes Nucleaires, Saclay, France). Ann. Phys. (New York); 60: 401-47(Oct 1970).

The distribution of eigenvalues of the equation $\Delta\phi + E\phi = 0$ is calculated for a volume V of arbitrary shape, and for the general boundary condition $\partial\phi/\partial n = \kappa\phi$ on the surface S, assumed to be smooth. A time-independent Green function method is used, involving a multiple reflection expansion. (M.O.W.)

9605 LOW-TEMPERATURE PROPERTIES OF A DENSE CHARGED BOSE GAS. Fetter, Alexander L. (Stanford Univ., Calif.). Contract F44620-68-C-0075. Ann. Phys. (New York); 60: 464-83(Oct 1970).

The zero-temperature excitation spectrum E_k of a dense charged Bose gas with mass M and charge e is combined with Landau's quasi-particle model to derive the thermodynamic functions at low temperature. The finite long-wavelength limit $\hbar^{-1}E_0 = \Omega_0$ (the plasma frequency) implies that the normal-fluid density $\rho_n(T)$ and the specific heat both vanish like $\exp(-\hbar\Omega_0/k_B T)$ as $T \to 0$. A microscopic calculation with the Bogolyubov approximation gives the low-temperature correction to the depletion $n'(T) - n'(0) = \frac{3}{2}M^{-1}\rho_n(T)$. The transverse current j(q) induced by a transverse vector potential A(q) is evaluated in the same Bogolyubov approximation. For the two cases examined (long wavelengths at $T \geq 0$ and short wavelengths at $T = 0$), j(q) reduces to the London form $-[\rho - \rho_n(T)](e^2/M^2c)A(q)$. Nonlocal contributions to the zero-temperature integral kernel $K(x - x')$ are of order n'/n and hence small in the high-density limit. (auth)

9606 MANY-BODY THEORY FOR NEARLY FREE ELECTRONS AND ITS APPLICATION TO ANNIHILATION OF POSITRONS IN A PERIODIC FIELD. Fujiwara, Kunio (Tokyo Univ.). J. Phys. Soc. Jap.; 29: 1479-90(Dec 1970).

A many-body theory for nearly free electrons is constructed by introducing "Bloch-pair operators," α_k and β_k, which are related to free-particle operators through the transformation

$$\begin{pmatrix}\alpha_k \\ \beta_k\end{pmatrix} = \begin{pmatrix}1/\sqrt{2} & \theta_h/\sqrt{2} \\ -\theta_h/\sqrt{2} & 1/\sqrt{2}\end{pmatrix}\begin{pmatrix}\alpha_k^- \\ \alpha_{k+h}\end{pmatrix}$$

where h is 2π times a reciprocal lattice vector, and θ_h is the sign of the relevant Fourier component, v_h, of the periodic field. This theory is then applied to the annihilation of positrons in the periodic field. The interaction between a positron and a Bloch electron is, for the first time, taken into account by a few simple diagrams. The result shows that a fairly sharp break of the angular-correlation curve occurs at the hexagonal-zone-face position in copper just as expected from the previous experiments. (auth)

9607 DERIVATION OF A SCHROEDINGER TYPE EQUATION WITH DAMPING FOR THE DYNAMICAL SYSTEM WEAKLY COUPLED TO A THERMAL BATH. Walasek, K.; Zubarev, D. N.; Kuzemskii, A. L. (Joint Inst. for Nuclear Research, Dubna, USSR). Teor. Mat. Fiz.; 5: 281-92(Nov 1970). (In Russian).

A Schroedinger type of equation with damping is derived for a dynamical system weakly coupled to a thermal bath on the basis of the method of the nonequilibrium statistical operator. The system of coupled Schroedinger- and kinetic-type nonlinear equations is obtained for the case of Bose statistics. (auth)

9608 KINETICS OF HOT ELECTRONS IN QUANTIZED MAGNETIC FIELDS. I. EFFECTIVE PARAMETER APPROXIMATION. Kalashnikov, V. P. (Inst. of Physics of Metals, Moscow). Teor. Mat. Fiz.; 5: 293-304(Nov 1970). (In Russian).

Using the many-electron nonequilibrium statistical operator, the equations of momentum and energy balance are constructed that determine the kinetics of the spatially homogeneous distributions of current carriers of conducting crystals in strong crossed electrical and magnetic fields. The case of high concentrations of the conductive electrons is considered, when the nonequilibrium state of the electrons can be characterized by mean values of the total energy, total momentum, and particle number. (auth)

9609 CONCERNING THE CONE OF RADIATION IN THE SOLUTION OF THE KINETIC TRANSPORT EQUATION. Kostritsa, A. A.; Neimotin, E. I. Izv. Akad. Nauk Kaz. SSR, Ser. Fiz.-Mat.; No. 2, 58-62(Mar-Apr 1968). (In Russian).

It is shown that in radiation diffusion in media the cone of radiation affiliated with the velocity of the medium (or source) emerges with a velocity less than the velocity of the particles emitted by the source. Discussion is based on the premise that scattering is isotropic in the center-of-mass system. (tr-auth)

9610 REDUCTION OF THE POTENTIAL OF THE SCHROEDINGER EQUATION ACCORDING TO SCATTERING DATA BY THE METHOD OF M. G. KREIN. Poplavskii, I. V. (Odessa Construction-Engineering Inst.). Izv. Vyssh. Ucheb. Zaved., Fiz.; No. 9, 13-18(1968). (In Russian).

The reduction of the potential of the Schroedinger equation (for the case of scattering) is considered, according to the data from the scattering technique of M. G. Krein. The mathematical problem is reduced to the solution of inhomogeneous algebraic equations of relatively precise functions. The equations for the problems of different special cases utilize Bargmann potentials determined previously by other methods. (tr-auth)

9611 SOLUTION OF THE EQUATION OF RADIATION TRANSFER. Senina, A. V.; Paskar, S. V. (Siberian Physical-Technical Inst., Tomsk, USSR). Izv. Vyssh. Ucheb. Zaved., Fiz.; No. 9, 57-61(1968). (In Russian).

Questions relating to the integro-differential equation of radiation transport of Boltzmann type are considered. The final form of the source function, calculated by the method of Ritz, is influenced both by the geometry of the medium and the nature of the broadening of the spectral lines, as well as precision of the intermediate operations after selection of test functions and determination of integral matrix elements and the intrinsic value of the variational method. (tr-auth)

9612 INSOLUBILITY OF THE QUANTUM MEASUREMENT PROBLEM. Fine, Arthur (Cornell Univ., Ithaca, N. Y.). Phys. Rev., D; 2: 2783-7(15 Dec 1970).

The problem of whether a measurement interaction can leave the joint object-apparatus system in a mixture of states, in each state of which the apparatus's observable displays a definite value, is set within the most general quantum-theoretic framework for treating measurements. It is shown that the question posed by this problem admits only a negative answer. Some schemes for approximating the true object-apparatus state by means of such mixtures are examined. It is argued that such schemes constitute fundamental changes in the interpretation of quantum theory. (auth)

9613 EVANESCENT WAVES AND THE ELECTROMAGNETIC FIELD OF A MOVING CHARGED PARTICLE. Asby, R.; Wolf, E. (Univ. of Rochester, N. Y.). J. Opt. Soc. Amer.; 61: 52-9(Jan 1971).

An angular-spectrum representation is obtained of the electromagnetic field in a homogeneous medium, arising from any prescribed motion of a charged particle in a plane. The field on either side of the plane of motion is expressed as a superposition of monochromatic waves in general, homogeneous as well as evanescent ones. The homogeneous waves are propagated away from the plane of motion of the particle, the evanescent ones decay exponentially with increasing distance from this plane. For each plane wave, the appropriate dispersion relation is satisfied and hence the representation is a true mode expansion in each of the two half-spaces. The results are illustrated by considering the field of a uniformly moving charged particle. In free space, the Coulomb field of the particle, as would be observed in a fixed laboratory system, is shown to arise from the superposition of evanescent waves to which the moving particle gives rise. The main formulas relating to the Čerenkov field both above and below threshold are also obtained, as an illustration of this technique. (auth)

9614 PROPERTIES OF IRRADIATED ENSEMBLES. Bragard, Leopole (Institut de Mathematique, Liege). Bull. Soc. Roy. Sci. Liege; 39: 264-8(1970). (In French).

It is shown that the irradiated sets of a linear topological space enjoy some properties very close to those of convex bodies. If a set A is neither a point nor a half-line of a linear topological space of dimension 1, then $\nu(\bar{A}) = \nu(A) = \nu(\bar{\bar{A}})$, where $\nu(A)$ is the irradiation kernel of A. Finally, the irradiated sets are characterized in terms of convex kernels. Similar results are obtained for algebraically irradiated sets in a linear space. (auth)

9615 COMPTON EFFECT AND POWER ABSORPTION BY SPACE CHARGE. Bokov, O. G.; Yudovich, M. V. (Saratov Polytechnic Inst., USSR). Izv. Vyssh. Ucheb. Zaved., Fiz.; No. 9, 95-9(1970). (In Russian).

Compton scattering of light on space charge is studied. The space charge energy absorption and electron gas heating are estimated. The possibility of measuring the intensity of powerful coherent light beams is discussed. (tr-auth)

9616 HIGH-ORDER SCATTERING IN DIFFUSE REFLECTION FROM A SEMI-INFINITE ATMOSPHERE. van de Hulst, H. C. (Sterrewacht, Leiden). Astron. Astrophys.; 9: 374-9 (Dec 1970).

An asymptotic formula representing the terms with a relative error 0 (n^{-2}) is found for the radiation intensity diffusely reflected from a semi-infinite atmosphere after n successive scatterings. The method, valid for an arbitrary phase function, is to transform a power series in k, the diffusion exponent, into one in $t = (1 - a)^{\frac{1}{2}}$ and then into one in a, the albedo for single scattering. Four examples, including isotropic and highly anisotropic scattering, show the method to be accurate and convenient. If exact values for the orders n = 1 to 6 are known, values for all higher orders can be estimated to within a percent by this method. (auth)

9617 APPROXIMATE EQUATIONS AND SOLUTIONS OF INTERNAL PROBLEM FOR A BEAM IN A STRONG MAGNETIC FIELD. Danilov, V. N. Radiotekh. Elektron.; 15: 1761-3(Aug 1970). (In Russian).

The approximate equations and solutions obtained for electron beams can be used in calculations for magnetotron guns and guns with crossed fields for forming beams of specified shapes, under inhomogeneous conditions on the surfaces of curvilinear cathodes. (R.V.J.)

9618 APPROXIMATE SOLUTION OF THE INTERNAL PROBLEM OF THE THEORY OF FORMATION OF ELECTRON BEAMS. Ovcharov, V. T.; Penzyakov, V. V. Radiotekh. Elektron.; 15: 1651-8(Aug 1970). (In Russian).

An approximate solution is obtained for the problem of formation of laminar axisymmetric powerful electron beams, with prescribed trajectories described by two functions, each having a single coordinate. (tr-auth)

9619 EXPLICIT SOLUTIONS OF HALF SPACE PROBLEMS IN THE TWO-GROUP TRANSPORT THEORY. Thielheim, K. O.; Bloecker, W. (Univ., Kiel). Atomkernenergie; 16: 281-4(1970).

The restricted two-group transport theory in which there is, per definition, a one-way coupling between the two groups of energy, is applied to half-space problems. The half-range completeness theorem of eigenfunctions is presented. The explicit solution of Milne's problem is given, together with expressions for extrapolated boundaries. For application in more general half-space problems, Green's function is presented. (auth)

PHYSICS (HIGH ENERGY)

Particle Interactions and Properties (Experimental)

Refer also to abstracts 9685 and 9694.

Electromagnetic

Refer also to abstract 9727.

9620 (LUNP–7007) PHOTOPRODUCTION OF CHARGED PIONS FROM NUCLEI. Blomqvist, I.; Nydahl, G.; Forkman, B. (Lund Univ. (Sweden). Dept. of Physics. Lund Inst. of Tech. (Sweden). Dept. of Nuclear Physics). Apr 1970. 31p. Dep. NTIS (U. S. Sales Only).

The yields of the reaction $^{41}K(\gamma,\pi^+)^{41}Ar$, $^{65}Cu(\gamma,\pi^+)^{65}Ni$, $^{88}Sr(\gamma,\pi^+)^{88}Rb$ and $^{138}Ba(\gamma,\pi^+)^{138}Cs$ were measured by activation analysis. Data on the reactions $^{11}B(\gamma,\pi^-)^{11}C$, $^{27}Al(\gamma,\pi^+)^{27}Mg$ and $^{51}V(\gamma,\pi^+)^{51}Ti$ obtained earlier were also analysed. The experimental cross sections are compared with predictions from simple model calculations. (auth) (Sweden)

9621 (NP–18581) PRELIMINARY RESULTS ON BHABHA SCATTERING, MUON PAIR ANNIHILATION AND HADRON PRODUCTION BY e^+, e^- COLLIDING BEAMS IN THE GeV REGION. Note No. 281. Conversi, M. (Rome Univ. (Italy). Istituto di Fisica. Istituto Nazionale di Fisica Nucleare, Rome (Italy)). 15 Sep 1970. 54p. Dep. NTIS (U. S. Sales Only).

Preliminary results are reported of an experiment carried out at the Frascati storage ring, Adone, to investigate wide angle Bhabha scattering (WABS: $53° < \theta < 127°$), annihilation into muon pairs and hadron production by e^+, e^- colliding beams of total energy ranging from 1.4 to 2.4 GeV. These reactions were studied at the same time and with the same apparatus, consisting of a number of optical spark chambers and plastic scintillators, with an electronics suitable for time-of-flight and pulse-height measurements. A monitoring system based on small angle Bhabha scattering ($3.5 < \theta < 6.1°$) was also used during the runs, to obtain an absolute determination of the luminosity of Adone. The results refer to a preliminary analysis of data collected in the period from January to June 1970, corresponding to an integrated luminosity of about $75(10)^{33}$ cm^{-2}. They can be summarized as follows: The analysis of the WABS events is based on more than 3000 recorded events. Both, the absolute values and energy dependence of the cross section integrated over the solid angle of the apparatus, agree well with the predictions of quantum electrodynamics. The analysis of the process $e^+e^- \rightarrow \mu^+\mu^-$ is based for the time being on about 140 recorded events. The cross-section integrated over the apparatus is found to be 2.7 ± 4 nb (1 nb = 10^{-33} cm^2), to be compared with 3.35 nbarn, which is the theoretical value computed at the average four momentum squared of 3.3 $(GeV)^2$. The analysis of the process $e^+e^- \rightarrow \pi^+\pi^-$ (or $\rightarrow K^+K^-$) is based only on 14 recorded events. The integrated cross-section is estimated and found to be, with ~50% uncertainty, nearly half the value computed for point-like pions from quantum electrodynamics. Finally, more than 100 multi-body events were observed of which there were 66 with three or more visible tracks. For the latter events no background was observed running the machine with one beam alone. Arguments are given in favor of the hadronic nature of these multi-body events which appear then to occur with a cross section of the same order of magnitude as that for e^+e^- annihilation into muon pairs. (auth)

9622 REDETERMINATION OF THE MAGNETIC MOMENT OF THE PROTON IN NUCLEAR MAGNETONS. Fystrom, Dell O. (Univ. of Colo., Boulder). Phys. Rev. Lett.; 25: 1469-72(23 Nov 1970).

A redetermination of the magnetic moment of the proton in nuclear magnetons was performed using an omegatron. Special care was taken to make the phase of the rf electric field uniform inside the omegatron, and an almost rectangular line shape consistent with simple theory was obtained. Measurements were made both before and after gold plating the omegatron to check on the effects of nonuniform surface potentials. The value obtained uncorrected for diamagnetism was 2.792 783 ± 0.000 016 (±6 ppM). (auth)

9623 PHOTOPRODUCTION OF POSITIVE PIONS ON PROTONS IN THE REGION OF RESONANCE $P_{33}(1236)$. Aleksandrov, Yu. M. (Lebedev Inst. of Physics, Moscow); Grushin, V. F.; Leikin, E. M.; Rotvain, A. Ya. Yadern. Fiz.; 12: 770-81(Oct 1970). (In Russian)

Absolute differential cross sections of the process $\gamma p \rightarrow n\pi^+$ in the photon energy region 260 to 350 MeV and pion emission region in c.m.s. 49 to 173° are measured. The phenomenological analysis is made which enables one to compare and to treat the data obtained in combination with polarized and nonpolarized radiation. The S- and P-wave multipole amplitudes for process $\gamma p \rightarrow n\pi^+$ are estimated. The dependence of $ReM_{1-}^{3/2}$ on the energy shows the appearance of resonance $P_{11}(1470)$ in the channel $\gamma p \rightarrow n\pi^+$ and confirms that it is a member of the unitary octet. (auth)

9624 SMALL MOMENTUM TRANSFER π^+ PRODUCTION WITH LINEARLY POLARIZED PHOTONS. Burfeindt, H.; Buschhorn, G.; Geweniger, C.; (and others) (DESY, Hamburg). Phys. Lett.; 33B: 509-10(7 Dec 1970).

Previous measurements of the cross section asymmetry for single π^+ production on protons with linearly polarized photons of 3.4 GeV are extended to momentum transfers within the forward peak, i.e., $-t = 0.0026$, 0.006 and 0.01 $(GeV/c)^2$. The results are in good agreement with pion exchange models. (auth)

9625 π^0 ELECTROPRODUCTION AT $\Delta(1236)$ AND A FOUR-MOMENTUM TRANSFER OF 15 fm^{-2}. Albrecht, W. (Deutsche Elektronen Synchrotron, Hamburg); Brasse, F. W.; Dorner, H.; (and others). Nucl. Phys.; B25: 1-8(1971).

The electroproduction of the $\Delta(1236)$ was investigated through the π^0 channel at a four-momentum transfer of 15 fm^{-2}. Angles and momenta of the secondary electron and of the proton were measured in coincidence to obtain the differential cross section for the reaction $ep \rightarrow ep\pi^0$. The angular distribution for s- and p-waves of the outgoing pion and nucleon in their c.m. system was fitted to the cross sections. The resultant coefficients of the angular distributions are given as functions of the mass W of the pion nucleon system for 15 fm^{-2}. In a small range of W around the resonance, the contributions of the resonant multipoles M_{1+}, E_{1+} and S_{1+} to the cross section are also given. Further results with respect to non-resonant multipoles, as well as for momentum transfers of 25 and 40 fm^{-2}, will be published later. (auth)

Weak

9626 (COO–1545-87) MEASUREMENT OF THE UP-DOWN ASYMMETRIES IN THE BETA DECAY OF POLARIZED LAMBDAS. Lindquist, J.; Sumner, R. L.; Watson, J. M.; Winston, R.; Wolfe, D. M. (Chicago Univ., Ill.); Phillips, P. R.; Swallow, E. C. (Washington Univ., St. Louis, Mo.); Reibel, K.; Schwartz, D. M.; Stevens, A. J. (Ohio State Univ., Columbus); Romanowski, T. A. (Argonne National Lab., Ill.). [1970]. 16p. (CONF-700806–54). Dep. NTIS.

From 15th International Conference on High Energy Physics, Kiev, USSR.

The experiment on the beta decay of the lambda hyperon was performed in order to study the form of the weak interaction in this decay by measuring the up-down asymmetries of neutrinos, electrons, and protons with respect to the lambda spin. Spark chambers and counters were used for this study. (J.F.P.)

9627 (NP–18558) ON THE EXPERIMENTAL POSSIBILITY OF REVEALING THE REACTOR $l^+ + l^- \rightarrow \nu + \bar{\nu} + \gamma$. Tikhonin, F. F. (Gosudarstvennyi Komitet po Ispol'zovaniyu Atomnoi Energii SSSR, Serpukhov. Institut Fiziki Vysokikh Energii). 1969. 11p. (In Russian). Dep. NTIS (U. S. Sales Only).

Consideration of possible ways for detecting γ-quanta, generated in the reaction $l^+ + l^- \rightarrow \nu + \bar{\nu} + \gamma$ is presented. Two possibilities, suitable for registration of this process were chosen from many others (such as angular, energy distribution, polarization, etc.). These are: measuring photon-circular polarization and observation of showers, generated by γ-quanta of large energies, when showers from charged particles and other protons are absent. (auth)

9628 (UCLA–1052) A STUDY OF THE DECAY MODE $K_L^0 \rightarrow \pi^+\pi^-\pi^0$. Buchanan, C. D. (California Univ., Los Angeles); Chien, C. -Y. (Johns Hopkins Univ., Baltimore, Md.); Dally, E.; (and others) (Stanford Linear Accelerator Center, Calif.). [1970]. 12p. (JHU–7018(Rev.)). Dep. NTIS.

The decay process $K_L^0 \rightarrow \pi^+\pi^-\pi^0$ was studied in the 3^0 K_L^0 beam at the Stanford Linear Accelerator Center using a wire chamber magnetic spectrometer. The three pion decay was separated from leptonic decays using kinematics and muon identification. The average detection efficiency is 58.5% with a variation of less than 10% over the Dalitz plot. For a matrix element expressed as $|M|^2 = 1 + 2\,a_0(M_K/M_\pi^{+2})(2T_0 - T_{max}) + \beta_0(M_K/M_\pi^{+2})(2T_0 - T_{max})^2$

it is found that $a_0 = -0.257 \pm 0.005$. The squared term is consistent with zero. (auth)

9629 (UCLA-1054) A MEASUREMENT OF THE FORM FACTORS FOR THE DECAY $K_L^0 \rightarrow \pi\mu\nu$. Chien, C. Y. (Johns Hopkins Univ., Baltimore, Md.); Dally, E. (Stanford Linear Accelerator Center, Calif.); Buchanan, C. D.; (and others) (California Univ., Los Angeles). [1970]. 12p. (JHU-7016 (Rev.)). Dep. NTIS.

The decay process $K_L^0 \rightarrow \pi\mu\nu$ was studied in a wire chamber experiment using the three-degree K_L^0 beam at SLAC. A sample of 26,500 $K\mu_3$ events were identified to obtain information on the form factors f_i associated with the V-A hypothesis for this decay. Expressing the energy dependence of the form factors as $f_i = f_i(0)(1 + \lambda_i q^2/m_\pi^2)$, where $q^2 = (p_K - p_\pi)^2$, the experiment yields the value $\lambda_+ = 0.08 \pm 0.01$ and reveals a strong coupling between λ_- and $\xi(0) = f_-(0)/f_+(0)$. (auth)

9630 EXPERIMENTAL STUDY OF THE DECAY $K_L^0 \rightarrow \pi^+\pi^-\pi^0$. Albrow, M. G. (Manchester Univ., Eng.) Aston, D.; Barber, D. P.; (and others). Phys. Lett.; 33B: 516-20(7 Dec 1970).

In a study of 70,000 K_L^0 decays a sample of 29,000 $K_L^0 \rightarrow \pi^+\pi^-\pi^0$ decays has been isolated. In the parametrisation of the π^0 spectrum $|M\ T_0|^2\alpha| + (cQ/M_\pi)\ (3T_0 - Q)/Q$ (where Q = Q value of the decay and T_0 = C.M. kinetic energy) c is found to be -5.14 ± 0.09. A linear form for the dependence of M on T_0 does not fit the data. It was found that the dependence of $|M|^2$ on $X = \sqrt{3}\ (T_+ - T_-)/Q$ was weak, where $T_i = \pi^i$ cm kinetic energy. (auth)

9631 MAGNITUDE OF THE $K_1^0 - K_2^0$ MASS DIFFERENCE AND Λp INTERACTIONS AT HIGH ENERGIES. Bassano, Daniel Anthony. Syracuse, N. Y.; Syracuse Univ. (1969). 66p. University Microfilms Order No. 70-15, 204.

Thesis.

The data obtained for this experiment were part of an extensive study of K^-p interactions at 4.6 and 5.0 GeV/c conducted by groups from Syracuse University and Brookhaven National Laboratory. As of 1967, approximately 300,000 pictures had been taken in a series of exposures of the 80-inch liquid hydrogen bubble chamber to a separated K^- beam at the Brookhaven A.G.S., half of which were used for this work. The $\bar{K}^0$ beam was obtained from K^-p interactions in the hydrogen bubble chamber. The time dependence of $\bar{K}^0$ interactions coming from a pure $\bar{K}^0$ beam at t = 0 was analyzed to determine the $K_S - K_L$ mass difference, Δm. The result $\Delta m = (0.54 \pm^{0.19}_{0.20})\ \tau_s\ \hbar^{-1}$ MeV is in good agreement with less accurate measurements using a similar technique as well as with more accurate measurements using different techniques. Secondly a Λ beam produced from K^-p interactions was studied and cross sections were determined in the Λ momentum range of ~1 to 5 GeV/c. The elastic and total cross sections averaged over the full energy range are found to be ~10 mb and ~35 mb, respectively. These values are in good agreement with predictions of various versions of the quark model. Also observed were final state resonance production and these are discussed in terms of meson exchange models. (Diss. Abstr. Int., B)

9632 NARROW MUON BUNDLES BELOW GROUND. Shibata, Hiroyuki; Kaneko, Tatsunosuke; Kishimoto, Syunsuke (Okayama Univ., Japan). J. Phys. Soc. Jap.; 29: 1427-35(Dec 1970).

The observation of muon bundles caused by cosmic rays was carried out for 17,000 hours by means of spark chamber at 30 m.w.e. below ground. The muon bundles in a narrow region of 20 ~ 30 cm in diameter were observed over the expectation from the fluctuation of spatial distribution of muons by the Monte Carlo method. Their frequency was about $2 \times 10^{-4}\ m^{-2}\ h^{-1}$. The frequency of these muon bundles cannot be explained as known interaction processes without extreme assumptions. (auth)

9633 π^+-MESIC DECAY OF THE $^4_\Lambda$He HYPERFRAGMENT. Gerber, J. P. (CERN, Strasbourg); Bechdolff, A.; Baumann, G. Nucl. Phys.; B24: 576-8(1970). (In French).

A mesic hyperfragment $^4_\Lambda\text{He} \rightarrow n + {}^3\text{H} + \pi^+$ was identified. The ratio π^+/π^- from this type of events is found to be equal to ≈4%. (auth)

Strong (Baryon-Induced)

9634 (COO-1764-115) MOMENTUM SPECTRA IN HIGH-ENERGY HADRON-DEUTERON INTERACTIONS. Coleman, E. (Minnesota Univ., Minneapolis. School of Physics). [1970]. 10p. Dep. NTIS.

Momentum spectra were measured for the scattering of protons by deuterons at 2.784 GeV/c and for the scattering of negative pions by deuterons at 5.53 GeV/c. The measurements test multiple scattering theories. The roles of double scattering processes, interference phenomena, nucleon-nucleon correlations, and production processes were examined. (J.F.P.)

9635 (INP-722) HADRON INTERACTION AT ULTRA HIGH ENERGIES. Miesowicz, M. (Institute of Nuclear Physics, Krakow (Poland)). 1970. 50p. (CONF-700708-3). Dep. NTIS (U. S. Sales Only).

From 6th Interamerican Seminar on Cosmic Rays, La Paz, Bolivia.

Recent data concerning the interaction of nucleons in the energy interval 100 GeV to 100 TeV and of pions at energies 45 GeV to 200 GeV are presented. With reference to the proposed definition of a fireball, a review of evidence for fireball production in the mentioned energy interval is given. The common general features of interaction of pions at Serpukhov energies and of cosmic ray pions at ~200 GeV are given. Coherent production of 3π and 5π -bodies by pions up to primary energy ~200 GeV is discussed. (auth)

9636 (TID-25610) COHERENT $\bar{p}d$ INTERACTIONS AND RELATED DISSOCIATION REACTIONS AT 7.0 GeV/c. Antich, P.; Callahan, A.; Carson, R.; (and others) (Johns Hopkins Univ., Baltimore, Md.). [1970] 45p. (JHU-7009(Rev.)). Dep. NTIS.

In a 3.5 event/μb exposure of the BNL 80″ bubble chamber the following reactions were observed: $\bar{p}d \rightarrow \bar{p}d\pi^+\pi^-$ (1), $\bar{p}d \rightarrow \bar{p}pn\pi^+\pi^-$ (2), and $\bar{p}d \rightarrow \bar{p}d\pi^+\pi^-\pi^0$ (3). The incident $\bar{p}$ momentum was 7.0 GeV/c. Cross sections are given for the reactions, as well as for other reactions involving production of $\bar{\Lambda}$. Detailed descriptions of the coherent final states (1) and (3) are given. It is observed that reactions (1 to 3) are dominated by production of $\bar{\Delta}^{--}$ (1236). A Deck model, both in Reggeized and non-Reggeized form, is applied to the reaction: $\bar{p}d \rightarrow \bar{\Delta}^{--}\pi^+d$ and satisfactory fits to the distributions of all kinematic variables were obtained. In particular, the π^+d mass spectrum, which shows a prominent peak—the "d*"—at a mass $M(\pi d) \sim 2170$ MeV, is well reproduced by the predictions of the model without introducing a resonant interpretation for this effect. Modified versions of this model are applied to the reactions: $\bar{p}d \rightarrow \bar{\Delta}^{--}\pi^+pn$ and $\bar{p}d \rightarrow \bar{\Delta}^{--}\pi^0\pi^+d$ which occur as sub-samples of the final states (2) and (3) respectively. Here also, prominent peaks are observed in the π^+pn mass spectrum (in the former reaction) and in the π^+d and π^0d mass spectrum (in the latter reaction). Again, the predictions of the model agree well with the observed distributions of all the kinematic variables. (auth)

9637 STUDY OF HYPER-FRAGMENTS PRODUCED IN HIGH ENERGY INTERACTIONS OF PIONS AND PROTONS WITH EMULSIONS. Ganguli, S. N. Bombay; Bombay Univ. (1969).

Thesis.

The thesis deals with the analysis of short range hyperfragments produced in nuclear emulsions by high energy protons and pions. The analysis yielded results on mass distribution of short range hyperfragments and non-mesic to mesic ratios in decay of HFs. The role of fission process in production of hyperfragments is discussed. The rare decay modes of hyperfragments observed are presented. (Indian Sci. Abstr.)

9638 CHARGED-PARTICLE MULTIPLICITIES OF PROTON-PROTON INTERACTIONS BETWEEN 90 AND 800 GeV. Jones, L. W. (Univ. of Michigan, Ann Arbor); Bussian, A. E.; DeMeester, G. D.; (and others). Phys. Rev. Lett.; 25: 1679-83(14 Dec 1970).

A cosmic-ray experiment at Echo Lake, Colorado, employing a 2000-liter liquid-hydrogen target together with spark chambers and an ionization calorimeter was performed to study the interaction of protons with protons above 70 GeV. The quantitative results on the distribution of secondary charged-particle multiplicity and the energy dependence of the average charged multiplicity are reported. (auth)

9639 ANTIDEUTERON ABSORPTION CROSS SECTIONS ON NUCLEI Li, C, Al, Cu, AND Pb AT 25 GeV/c. Binon, F.; Gorin, Yu. P.; Denisov, S. P.; (and others). (Inst. of High Energy Physics, Serpukhov, USSR). Yadern. Fiz.; 12: 806-9(Oct 1970). (In Russian).

Antideuteron absorption cross sections on nuclei Li, C, Al, Cu, and Pb at the incident momentum of 25 GeV/c are measured. The cross sections are described by the dependence of $A^{0.67 \pm 0.05}$. (auth)

9640 TOTAL CROSS SECTION MEASUREMENTS. Giacomelli, G. (CERN, Geneva). Progr. Nucl. Phys.; 12: 77-225(1970).

The subject is dealt with under the following headings: Experimental methods; the transmission method for charged particles (principle of a transmission measurement, the beam, the counters, the electronics, the targets, experimental procedure and corrections), bubble chamber measurements for charged particles, measurements of total cross sections of neutral particles (neutrons, absorption coefficients for photons), other methods. The computation of the pure isospin cross sections—the deuteron problem; the pure isospin cross sections, the shadow effect, the Fermi motion is given. Analysis of the experimental errors, analysis of the

XUM

total cross section data; the pion-nuclear system, the K^--nucleon, the K^+-nucleon system, the nucleon-nucleon system, the ΛN and ΣN systems, the antinucleon-nucleon system, comparison of the high-energy behavior, dispersion relations, absorption cross sections of nuclei, and interpolated values of total cross sections and a listing of all measured total cross sections are given. (UK)

9641 DETAILED INVESTIGATION OF AN 80-TeV NUCLEAR INTERACTION. Nozaki, Tadao (Tokyo Univ.). J. Phys. Soc. Jap.; 29: 1403-27(Dec 1970).

An 80-TeV nuclear interaction of type (15 + 15 + 49) p detected in a large emulsion stack was analyzed in detail. The target diagram of charged secondary particles and γ-rays in the extreme forward cone together with their energy estimates was found to be consistent with the production of an aleph baryon and its subsequent decay into (p + φ) in the extreme forward cone. The masses of the wide angle secondary charged particles were identified and the results were found to be consistent with the production of an aleph baryon decaying into (p + φ) in the extreme backward cone of the center of mass system. (auth)

9642 EMISSION OF LIGHT PARTICLES IN THE INTERACTIONS PRODUCED BY 26-GeV PROTONS IN NUCLEAR EMULSIONS. Tsai-Chu (Faculte des Sciences, Paris). Compt. Rend., Ser. B; 271: 802-5(12 Oct 1970). (In French).

The study of secondary branches in 26-GeV proton jets revealed an excess of light particles in relation to the Dalitz pairs. The light particles might be heavier than an electron and have similar properties to pions; the particles might be named mini- or L-mesons. (France)

9643 SEARCH FOR DOUBLY CHARGED MESONS IN $\bar{p}p$ ANNIHILATIONS INTO PIONS NEAR 1.9 GeV/c. Lys, J.; Chapman, J. W. (Univ. of Michigan, Ann Arbor). Phys. Rev., D; 2: 2525-8(1 Dec 1970).

A search was made for evidence of doubly charged mesons in 45,000 events of the type $\bar{p}p \rightarrow \pi^+\pi^+\pi^-\pi^- + n\pi^0$, $n \geq 0$, at incident antiproton momenta 1.6 to 2.2 GeV/c. No evidence for such mesons is found, and upper limits are given for production cross sections. (auth)

9644 MEASUREMENT OF ANTIPROTON–PROTON FORWARD CHARGE-EXCHANGE SCATTERING. Atwood, W. (California Inst. of Tech., Pasadena); Barish, B.; Nicholson, H. W.; (and others). Contract AT(11-1)-68. Phys. Rev., D; 2: 2519-25(1 Dec 1970).

There is a well-known forward peak in the np forward charge-exchange cross section, for momentum transfers $|t| \lesssim m_\pi^2$. An experiment to look for analogous behavior in the reaction $\bar{p}p \rightarrow \bar{n}n$. The data cover the kinematical region $0 \leq |t| \leq 1.5 m_\pi^2$ at an incident antiproton momentum of 1.80 GeV/c. A forward peak is observed, which is estimated (from results of other experiments) to be considerably smaller than that for np charge exchange. This result can be understood in terms of interference between one-pion exchange and exchange of a particle with even G parity. (auth)

9645 FRACTION OF STOPPED ANTIPROTONS WHICH ANNIHILATE ON FREE HYDROGEN IN PROPANE. Pawlewicz, W. T. (Carnegie–Mellon Univ., Pittsburgh); Murphy, C. T.; Fetkovich, J. G.; (and others). Phys. Rev., D; 2: 2538-44(1 Dec 1970).

Antiprotons were stopped in a liquid-propane bubble chamber. In a sample of film containing 75,000 annihilations at rest, 21 examples of the reactions $\bar{p}p \rightarrow \pi^+\pi^-$ or $\bar{p}p \rightarrow K^+K^-$ were identified. This number, together with the previously measured branching ratios of these channels in liquid hydrogen, leads to a determination that (11 ± 3)% of the antiprotons annihilate on free protons. The remaining 89% annihilate on bound nucleons in carbon. This fraction is markedly higher than the fraction of π^- at rest which charge exchange on free protons in similar hydrocarbons. An explanation of the large difference is suggested. (auth)

9646 EXPERIMENTAL STUDY OF THE POLARIZATION OF ANTIPROTONS FROM LOW-ENERGY $\bar{p}$–p ELASTIC SCATTERING. Ceschia, Mario (Univ., Trieste, Italy). Phys. Rev., D; 2: 2555-63(1 Dec 1970).

The polarization of elastically scattered antiprotons in hydrogen, averaged with respect to the energy over the range 49.4 to 181.0 MeV, is evaluated as a function of the cm scattering angle between 16° and 100°. The result is based on an analysis of approximately 50,000 pictures taken in the 81-cm Saclay hydrogen bubble chamber, which was exposed to a separated beam from the CERN proton synchrotron. The events used for measuring the polarization were double elastic scatterings of antiprotons. The resulting polarization appears to be rather strong, and does not agree with the predictions given by the current theoretical models. (auth)

9647 RHO–OMEGA INTERFERENCE IN $\bar{p}p \rightarrow 4\pi$ AT 1.6 TO 2.2 GeV/c. Chapman, J. W.; Davidson, J.; Green, R.; (and others) (Univ. of Michigan, Ann Arbor). Nucl. Phys.; B24: 445-52(1970).

The $\pi^+\pi^-$ mass spectrum from over 3000 events of the reaction $pp \rightarrow \pi^+\pi^+\pi^-\pi^-$ at 1.63 to 2.20 GeV/c shows evidence for ρ-ω interference. If ρ-background interference is taken into account the evidence is weak in the total data, but is strong when a particular cut is made on the momentum transfer, from the proton or antiproton to the $\pi^+\pi^-$. A fit to the data with this cut gives a lower limit on the branching ratio $\omega \rightarrow \pi^+\pi^-$ to $\omega \rightarrow \pi^+\pi^-\pi^0$ of 1.9 (95% confidence level). (auth)

9648 DIRECT MEASUREMENT OF n–p AND n–d TOTAL CROSS SECTIONS FROM 700 TO 2900 MeV/c. Mischke, R. E. (Princeton Univ., N. J.); Devlin, T. J.; Johnson, W.; (and others). Contract AT(30-1)-4159. Phys. Rev. Lett.; 25: 1724-7(21 Dec 1970).

Neutron-proton and neutron-deuteron total cross sections were measured directly at the Princeton-Pennsylvania Accelerator using time of flight to determine the incident neutron momentum. The results cover the region from 700 to 2900 MeV/c with a typical accuracy of 0.8% for each of 26 momentum bins. The data are not consistent with the most precise previous measurements in the same momentum range. (auth)

9649 ANTIPROTON–NEUTRON ELASTIC CROSS SECTION AT 3.5 GeV/c. Weaver, Kelly Edward. Athens, Ohio; Ohio Univ. (1970). 123p. University Microfilms Order No. 70-20,104. Thesis.

The experiment was done in the deuterium-filled 30-inch MURA bubble chamber at the Argonne National Laboratories, using the 7° beam from the Zero Gradient Synchrotron. A total of 74,000 pictures taken in this chamber were scanned for events with a two-prong topology. From this scan 4041 events were selected which met the following criteria: The lab scattering angle was greater than 5° and the spectator proton had a projected stopping range which was less than 2 cm. but large enough to be measureable. These criteria were introduced to aid in the elimination of antiproton-proton interactions. These selected events were measured and then processed through geometric reconstruction and kinematic fitting computer programs; 1107 were found to have fits to the elastic antiproton-neutron hypothesis. After ionization and equal-mass scattering checks 373 events were finally selected as being true antiproton-neutron scatters in the range of t, the square of the four momentum transfer greater than 0.15 $(GeV/c)^2$. In addition these events were restricted to a fiducial volume in the chamber shown to be free of geometrical biases which would have placed in question the selection criteria or the value of t for any event. The sample was then corrected in accordance with scattering plane azimuthal symmetry, spectator proton directional isotropy, the Hulthen momentum distribution of the spectator proton, scan efficiency and fitting and reconstruction program failures. The final corrected sample was extrapolated to t = 0, a differential cross section was constructed and the total elastic cross section computed. (TSS) (Diss. Abstr. Int., B)

Strong (Meson-Induced)

9650 (COO–1195-202) ON THE COHERENCE OF ISOSCALAR AND ISOVECTOR EXCHANGE AMPLITUDE IN $\pi^\pm p \rightarrow A_2^\pm p$. Brockway, D. V.; Ascoli, G.; Eisenstein, L.; Ioffredo, M. L.; Kruse, U. E. (Illinois Univ., Urbana). Oct 1970. 11p. (CONF-701108–1). Dep. NTIS.

From Meeting of the Division of Particles and Fields of the American Physical Society, Austin, Tex.

A study of $\pi^\pm p \rightarrow \pi^+\pi^-\pi^\pm p$ at incident momenta from 5 to 8.5 GeV/c and a comparison with published data on $\pi^+ n \rightarrow A_2^0 p$ indicate that charged A_2 production involves both isoscalar and isovector exchange amplitudes of comparable magnitude. There appears, however, to be very little, if any, interference between these amplitudes thus leaving unexplained the difference between A_2^+ and A_2^- mass spectra recently reported. (auth)

9651 (COO-1764-111) OBSERVATION OF THE DECAY $\eta' \rightarrow \gamma\gamma$. Harvey, E. H.; Marquit, E.; Peterson, E.; Rhoades, T. G.; Romer, H.; Ruddick, K.; Satovich, G.; Smith, J. R.; Tooley, J. G. (Minnesota Univ., Minneapolis. School of Physics); Randolph, J. Kemp (Michigan Univ., Ann Arbor. Dept. of Physics). [1968]. 9p. Dep. NTIS.

The reaction $\pi^- p \rightarrow n\gamma\gamma$ was studied at an incident pion momentum of 3.65 GeV/c. The gamma rays were detected in steel plate optical spark chambers and neutrons in an array of scintillation counters and thin plate spark chambers. A preliminary value of 3.1 ± 1.2 per cent for the branching ratio $\eta' \rightarrow \gamma\gamma$ was determined. (auth)

9652 (COO-1764-112) MEASUREMENTS OF π^-p ELASTIC SCATTERING FROM 1.71 TO 5.53 GeV/c. Fellinger, M.; Gutman, E.; Lamb, R. C.; Peterson, F. C.; Schroeder, L. S. (Ames Lab., Iowa); Chase, R. C.; Coleman, E.; Rhoades, T. G. (Minnesota Univ., Minneapolis. School of Physics). [1969]. 23p. Dep. NTIS.

The π^-p elastic scattering differential cross section was obtained at eighteen incident momenta from 1.71 to 5.53 GeV/c. The measurements were taken over a limited range of squared four-momentum transfer, t, near the forward direction. The statistical accuracy and resolution of these data are comparable to, or better than, existing data. The parameter b in the expression $d\sigma/dt = Ae^{bt}$ has been determined at each of our incident momenta, and a large (~25%) enhancement in b as a function of momentum is observed at a center of mass energy of ~2290 MeV. The relation of this bump in b with the well established bump in the total π^-p cross section at ~2200 MeV is discussed. (auth)

9653 (COO-1764-113) π^-p CHARGE EXCHANGE AT BACKWARD ANGLES. Chase, R. C.; Coleman, E.; Courant, H. W. J.; Marquit, E.; Petraske, E. W.; Romer, H. F.; Ruddick, K. (Minnesota Univ., Minneapolis. School of Physics). [1970]. 50p. Dep. NTIS.

Results of a measurement of the π^-p charge-exchange process at backward angles are presented. Differential cross sections were measured in the angular region $-0.5 < \cos\theta < -1.0$ at incident momenta of 2, 3, 4, 5, 6 GeV/c. The 6 GeV/c data were combined with existing measurements of the differential cross sections for backward π^+p and π^-p elastic scattering to yield values for the isotopic spin $\frac{1}{2}$ and $\frac{3}{2}$ u-channel and s-channel amplitudes for backward pion nucleon scattering and for the magnitude of the phases between them. It is found that the u-channel amplitudes can be explained by pure Regge pole (Δ_δ,N_α) exchange only near the extreme backward direction, but that a Reggeized absorption model agrees at least qualitatively with the data. The phase difference between the $I = \frac{1}{2}$ and $\frac{3}{2}$ s-channel amplitudes is approximately 90° over the region $-0.8 < u < 0$ $(GeV/c)^2$. (auth)

9654 (COO-1764-114) REACTION $\pi^-p \rightarrow n\pi^+\pi^-$ AT HIGH MOMENTUM TRANSFER. Romer, H. F.; Chase, R. C.; Coleman, E.; Courant, H. W. J.; Marquit, E.; Petraske, E. W.; Ruddick, K. (Minnesota Univ., Minneapolis). [1970]. Contract AT(11-1)-1764. 9p. Dep. NTIS.

The production of $\pi^+\pi^-$ pairs in the backward hemisphere of the reaction $\pi^-p \rightarrow n\pi^+\pi^-$ was studied at incident pion momenta of 2, 3, 4, 5, and 6 GeV/c. The process is dominated by ρ^0 and f^0 production. Differential cross sections and density matrix elements are presented. (auth)

9655 (ITEF-767) STUDY OF THE $\pi^-\pi^-$ INTERACTION IN THE REACTION $\pi^-p \rightarrow N^{*++}(1236)\pi^-\pi^-$ WITH MOMENTUM 4.47 GeV/c. Beketov, G. V.; Zombkovskii, S. M.; Kaidalov, A. B.; Konovalov, B. S.; Kruchinin, S. P.; Selektor, Ya. M.; Shulyachenko, V. N. (Gosudarstvennyi Komitet po Ispol'zovaniyu Atomnoi Energii SSSR, Moscow. Institut Teoreticheskoi i Eksperimental'noi Fiziki). 1970. 28p. (In Russian). Dep. NTIS (U. S. Sales Only).

The reaction $\pi^-p \rightarrow N^{*++}$ (1236) $\pi^-\pi^-$ at incident momentum of 4.47 GeV/c was studied using the 50-cm hydrogen bubble chamber. This reaction was analyzed in terms of the π-pole exchange Regge model and three versions of the OPE model. The $\pi^-\pi^-$-scattering cross sections were obtained for mass ranges of the $\pi^-\pi^-$-system from 0.28 GeV to 1.4 GeV. The angular distributions of $\pi^-\pi^-$- and π^+p-virtual scattering are presented. The angular distributions seem to show the considerable dependence from the background reaction $\pi^-p \rightarrow \pi^-p\rho^0$. (auth)

9656 (ITEF-775) STUDY OF THE REACTION $\pi^-p \rightarrow \rho^0\pi^-p$ WITH MOMENTUM 4.45 GeV/c. Beketov, G. V.; Zombkovskii, S. M.; Kaidalov, A. B.; Konovalov, B. S.; Kruchinin, S. P.; Selektor, Ya. M.; Shulyachenko, V. N. (Gosudarstvennyi Komitet po Ispol'zovaniyu Atomnoi Energii SSSR, Moscow. Institut Teoreticheskoi i Eksperimental'noi Fiziki). 1970. 16p. (In Russian). Dep. NTIS (U. S. Sales Only).

The reaction $\pi^-p \rightarrow \rho^0\pi^-p$ was studied in the liquid-hydrogen bubble chamber at 4.45 GeV/c. The obtained data are in good agreement with the Regge π-pole exchange model. (auth)

9657 (ORO-3948-2) PION INTERACTIONS AT MEDIUM ENERGIES. Progress Report. Allred, John C.; Goodman, Clark (Houston Univ., Tex.). 1 Jan 1971. Contract AT(40-1)-3948. 25p. Dep. NTIS.

The summary of research given includes the small-angle scattering of protons and π^+ and π^-, data analysis programs, incident pion flux measurements, and the development of scintillation counters. A list of presented papers is included. (J.F.P.)

9658 (TID-25611) STUDY OF THE REACTION $K^-n \rightarrow K^-\pi^-p$ AT 12.6 GeV/c. Antich, P.; Callahan, A.; Carson, R.; (and others) (Johns Hopkins Univ., Baltimore, Md.). [1970] 27p. (JHU-7013(Rev.)). Dep. NTIS.

From a 2.5 event/μb K^-d exposure of the BNL 80" bubble chamber 351 events were obtained which successfully fit the reaction $K^-d \rightarrow K^-\pi^-pp_s$. The $(p\pi^-)$ mass spectrum exhibits a strong enhancement, centered at 1400 MeV and 400 MeV wide, which cannot be clearly resolved into individual resonances. The reaction is analyzed with a diffraction dissociation model and the relevant cross sections are given. From a study of the low $K^-\pi^-$ mass region we find that the $K\pi$ elastic scattering cross section in the isospin $\frac{3}{2}$ state is of the order of 2 mb. (auth)

9659 (UCRL-19789) STUDY OF THE Σ (1915) RESONANCE IN THE REACTION $K^-p \rightarrow \Lambda\pi^0$. Ely, R. P. Jr.; Birge, R. W.; Hoven, J.; Kalmus, G. E.; Kane, D.; Van Horn, A. (California Univ., Berkeley. Lawrence Radiation Lab.). Aug 1970. Contract W-7405-eng-48. 16p. (CONF-700806-53). Dep. NTIS.

From 15th International Conference on High Energy Physics, Kiev, USSR.

The interactions $K^- + p \rightarrow \Lambda + \pi^0$ were studied at the energies 1.865 to 2.001 GeV in a hydrogen bubble chamber. The purpose of the study was to check the mass, width, coupling, and relative phase of the Σ (1915) resonance. Also alternative spin-parity assignments were sought but not found. The mass was found to be 1911^{+15}_{-5} MeV, the width was 74 ± 10 MeV, t = 0.085 ± 0.01, and the phase was $179°^{+20}_{-10}$. (J.F.P.)

9660 PRODUCTION OF He NUCLEI IN INTERACTIONS OF PIONS WITH ENERGY OF 60 GeV WITH HEAVY NUCLEI OF EMULSION. Borisenko, A. I.; Goryachikh, A. A.; Kazanskaya, A. P.; (and others). (Kazakh State Univ., Alma-Ata, USSR). Yadern. Fiz.; 12: 810-14(Oct 1970). (In Russian).

An analysis is given of the He nuclei with momenta more than 800 MeV/c, emitted from interactions of the 60-GeV pions with heavy nuclei of emulsion. The results are compared with data obtained investigating the fast He nuclei produced in proton- and pion-induced nuclear spallations in the energy range 2 to 20 GeV. Dependence of the cross section and the He angular and energy distributions on the energy and the nature of the projectile is studied. It is shown that the yield of the two-charge particles increases with the number of the grey-black tracks following the law: $W \sim \exp(0.06 N_h)$. It is noted that the results indicate a relation between the internuclear cascade processes and the emission of fast He nuclei. The conclusion is drawn that the emission of the fast He nuclei can not be explained by the existing theoretical models. (auth)

9661 DIRECT PRODUCTION OF ELECTRON-POSITRON PAIRS BY 2.94-GeV/c NEGATIVE PIONS. Vaisenberg, A. O.; Kel'ner, S. R.; Minervina, Z. V.; Novikov, L. S.; Shishov, N. N. (Inst. of Theoretical and Experimental Physics, Moscow). Yadern. Fiz.; 12: 782-7(Oct 1970). (In Russian).

Direct production of electron-positron pairs by 2.94 GeV/c negative pions was studied. It is shown that the number of pairs observed and their spectrum are in qualitative agreement with the theory. (auth)

9662 DETERMINATION OF RESONANCE PRODUCTION CROSS SECTION IN π^+p INTERACTIONS AT 2.34 GeV/c. Angelov, N.; Gramenitskii, I. M.; Kanazirskii, Kh.; (and others). (Joint Inst. for Nuclear Research, Dubna, USSR). Yadern. Fiz.; 12: 788-99(Oct 1970). (In Russian).

A method to determine parameters of resonances in 4- and 5-particle reactions is described. Production cross sections of the N^{*++}_{1238}, N^{*-}_{1238}, ρ^0, ω^0, and η^0 resonances in π^+p interactions at 2.34 GeV/c are determined. (auth)

9663 STUDY OF REACTION $\pi^-p \rightarrow \rho^0\pi^-p$ AT 4.45 GeV/c. Beketov, G. V.; Zombkovskii, S. M.; Kaidalov, A. B.; (and others). (Inst. of Theoretical and Experimental Physics, Moscow). Yadern. Fiz.; 12: 800-5(Oct 1970). (In Russian).

The reaction $\pi^-p \rightarrow \rho^0\pi^-p$ at 4.45 GeV/c was studied using a 50-cm liquid hydrogen bubble chamber. The data obtained are in good agreement with the model of the Regge π pole exchange. (auth)

9664 STUDY OF THE REACTION $\pi^+d \rightarrow (p)p\pi^+\pi^-\pi^0$ AT INCIDENT PION MOMENTA BETWEEN 1.1 AND 2.4 GeV/c. Danburg, Jerome Samuel. Berkeley, Calif.; Univ. of California (1969). 172p. University Microfilms Order No. 70-13,033. Thesis.

The reaction $\pi^+d \rightarrow (p)p\pi^+\pi^-\pi^0$ was studied in a 264,000-picture bubble chamber experiment with pion beam momentum between 1.1 and 2.4 GeV/c. The most significant features of the final state are production of η and ω mesons in the reactions $\pi^+n \rightarrow \eta p$ and

XUM

$\pi^+n \rightarrow \omega p$. The η production characteristics are well described by a Reggeized A_2-exchange model using Veneziano-type residue functions. The ω production and decay characteristics are presented, and it is found that a ρ-exchange model with absorptive corrections is inadequate to describe the data. (Diss. Abstr. Int., B)

9665 BACKWARD ρ^+ PRODUCTION IN π^+p REACTIONS AT 5.2 GeV/c. Carlson, P. J.; Fleury, P.; Lundby, A.; Mukhin, S.; Myrheim, J. (CERN, Geneva). Phys. Lett.; 33B: 502-4(7 Dec 1970).

Using wire spark chambers the backward production of ρ^+ mesons was observed in the reaction $\pi^+p \rightarrow p$ (missing mass) at 5.2 GeV/c. In the four-momentum interval $-0.80 < u < -0.006$ $(GeV/c)^2$ the angular distribution shows a backward peak. In contrast to backward π^+p elastic scattering, there is no dip in the angular distribution at $u \approx -0.15$ $(GeV/c)^2$. The ρ^+ decay is found to be compatible with isotropy. (auth)

9666 BUBBLE CHAMBER MEASUREMENT OF $\eta'(960) \rightarrow \gamma\gamma$ AND $\eta'(960) \rightarrow \pi^0\pi^0\eta$ $(\eta \rightarrow 3\pi^0)$ DECAY RATES. Bensinger, J.; Erwin, A. R.; Thompson, M. A.; Walker, W. D. (Univ. of Wisconsin, Madison). Contract AT(11-1)-881. Phys. Lett.; 33B: 505-8(7 Dec 1970). (COO-881-291).

The reaction $\pi^+d \rightarrow p(p) + k\gamma$, k = 2, 3, 4, 5 and 6 was studied at a beam momentum of 2.15 GeV/c. From the k = 2 sample a branching ratio $BR_1 = \Gamma(\eta' \rightarrow \gamma\gamma)/\Gamma(\eta' \rightarrow \text{all}) = 0.126 \pm 0.075$ was found. Using the k = 6 data, $BR_2 = \Gamma(\eta' \rightarrow \pi^0\pi^0\eta; \eta \rightarrow 3\pi^0)/\Gamma(\eta' \rightarrow \text{all}) = 0.11 \pm 0.06$ was found. (auth)

9667 $\bar{K}N$ ELASTIC AMPLITUDES BETWEEN 1 AND 1.3 GeV/c. Bricman, C.; Ferro-Luzzi, M.; Lagnaux, J. P. (CERN, Geneva). Phys. Lett.; 33B: 511-15(7 Dec 1970).

Recent measurements of the polarization and differential cross section of $K^-p \rightarrow K^-p$ were used to determine the $\bar{K}N$ partial wave amplitudes in the momentum region between 0.98 and 1.34 GeV/c. This analysis also uses earlier data on the same reaction, on $K^-p \rightarrow \bar{K}^0n$ and on the total $\bar{K}N$ cross section. The resulting amplitudes, obtained by an energy dependent method, are generally continuous with those at lower momenta and favor the existence of an isospin-0 S-wave resonance with mass near 1870 MeV. (auth)

9668 S-WAVE PION-PION SCATTERING LENGTH FROM REACTION $\pi^- + p \rightarrow \pi^0 + \pi^0 + n$ AT 378 MeV. Maung, T. (Univ. of California, San Diego, La Jolla); Masek, G. E.; Miller, E.; (and others). Phys. Lett.; 33B: 521-4(7 Dec 1970).

The differential energy distributions of neutrons from the reaction $\pi^- + p \rightarrow \pi^0 + \pi^0 + n$ were measured at four different neutron lab angles. Fitting the distributions with the Chew-Mandelstam solution for $\pi-\pi$ phase shift, we obtain a value $a_{SO} = (0.28 \pm 0.21)\ \mu^{-1}$ for the S-wave $\pi-\pi$ scattering length. (auth)

9669 $\pi^+\pi^-$ ELASTIC CROSS SECTION FROM CHEW-LOW EXTRAPOLATIONS OF $\pi^-p \rightarrow \pi^+\pi^-n$ REACTION AT 2.77 GeV/c. Baton, J. P.; Laurens, G.; Reignier, J. (CEN, Saclay, France). Phys. Lett.; 33B: 525-7(7 Dec 1970).

The elastic cross section for $\pi^+\pi^-$ scattering is determined up to 1.2 GeV by applying the Chew-Low extrapolation method on a high statistics experiment. Different types of extrapolation procedure are used and their results compared. (auth)

9670 $\pi\pi$ PHASE SHIFTS FROM CHEW-LOW EXTRAPOLATIONS OF $\pi^-p \rightarrow \pi\pi N$ AT 2.77 GeV/c. Baton, J. P.; Laurens, G.; Reignier, J. (CEN, Saclay, France). Phys. Lett.; 33B: 528-32 (7 Dec 1970).

A phase shift analysis is made from the $\pi^-\pi^0$ and $\pi^+\pi^-$ elastic scattering data obtained through Chew-Low extrapolation with high statistics of the $\pi^-p \rightarrow \pi^-\pi^0p$ and $\pi^-p \rightarrow \pi^+\pi^-n$ reactions at 2.77 GeV/c. The well known up-down ambiguity for the I = 0 S-wave is solved in the low energy region where the down solution is the only one compatible with the data. The ambiguity remains at higher energies and it appears furthermore that there the inelasticity starts to play an important role. (auth)

9671 EVIDENCE FOR AN $n\pi^-\pi^-$ ENHANCEMENT AT A MASS OF 1.627 GeV/c^2 IN $K^-d \rightarrow p_s\ \pi^+\pi^-\pi^-n\ \bar{K}^0$ AT 4.91 GeV/c. Price, R. R.; Berg, R. E.; Salant, E. O. (Vanderbilt Univ., Nashville). Phys. Lett.; 33B: 533-5(7 Dec 1970).

Evidence is presented for an enhancement in the $n\pi^-\pi^-$ invariant mass distribution at (1.627 ± 0.012) GeV/c^2 with its full width at half maximum less than 0.030 GeV/c^2 at the 90 percent confidence level. Charge independence implies its isospin is $\frac{1}{2}$. (auth)

9672 A_2 MESON PRODUCTION IN K^-d REACTIONS. Garfinkel, A. F. (Purdue Univ., Lafayette, Ind.); Ammann, A. C.; Carmony, D. D.; Yen, W. L. Phys. Lett.; 33B: 536-40(7 Dec 1970).

New data on the reactions $K^-n \rightarrow \Lambda^0 A_2^-$ and $K^-n \rightarrow \Sigma^0 A_2^-$ are presented which are compatible with $J^{PC} = 2^{2+}$ for the A_2^-. Previously published data on the reaction $K^-n \rightarrow AA_2^-$ favored $J^{PC} = 1^{-+}$ and would thus be incompatible with the simple quark model. (auth)

9673 KAON-NUCLEON TOTAL CROSS SECTIONS FROM 0.36 TO 0.72 GeV/c. Bowen, T.; Caldwell, P. K.; Dikmen, F. Ned; (and others) (Univ. of Arizona, Tucson). Phys. Rev., D; 2: 2599-2608(1 Dec 1970).

The K^+ and K^- total cross sections were measured on both hydrogen and deuterium at a series of momenta between 360 MeV/c and 720 MeV/c by the transmission method. The data were corrected for Coulomb and decay effects, and the isospin states were extracted. The K^+N, I = 1 cross section was found to be free from resonances, although the presence of a small dip at about 700 MeV/c was confirmed. No convincing evidence was found for structure in the K^+N, I = 0 cross section, which was observed to be steeply rising with increasing momentum throughout this range. The prominence of the $\Lambda'(1520)$ was verified in the K^-N, I = 0 system in which no additional structure was seen. In the K^-N, I = 1 system no new structure was clearly established, though there appears to be a small enhancement with a mass about 1600 MeV. (auth)

9674 π^-p CHARGE EXCHANGE AT BACKWARD ANGLES. Chase, R. C.; Coleman, E.; Courant, H. W. J.; (and others) (Univ. of Minnesota, Minneapolis). Contract AT(11-1)-1764. Phys. Rev., D; 2: 2588-99(1 Dec 1970).

Results of a measurement of the π^-p charge-exchange process at backward angles are presented. Differential cross sections were measured in the angular region $-0.5 < \cos\theta^* < -1.0$ at incident momenta of 2, 3, 4, 5, and 6 GeV/c. An additional background subtraction to a version of the data published previously has a significant effect at 6 GeV/c and brings the data into agreement with more recent measurements. The 6-GeV/c data were combined with existing measurements of the differential cross sections for backward π^+p and π^-p elastic scattering to yield values for the isotopic-spin-$\frac{1}{2}$ and -$\frac{3}{2}$ u-channel and s-channel amplitudes for backward pion-nucleon scattering and for the magnitude of the phases between them. It is found that the u-channel amplitudes can be explained by pure Regge-pole $(\Delta_\delta, N_\alpha)$ exchange only near the extreme backward direction, but that a Reggeized absorption model agrees at least qualitatively with the data. The phase difference between the I = $\frac{1}{2}$ and $\frac{3}{2}$ s-channel amplitudes is approximately 90° over the region $-0.8 < u < 0$ $(GeV/c)^2$. (auth)

9675 PRODUCTION AND DECAY OF η AND ω MESONS IN THE REACTION $\pi^+d \rightarrow (p)p\pi^+\pi^-\pi^0$ BETWEEN 1.1 AND 2.4 GeV/c. Danburg, Jerome S.; Abolins, Maris A.; Dahl, Orin I.; (and others) (Univ. of California, Berkeley). Phys. Rev., D; 2: 2564-88(1 Dec 1970).

The reaction $\pi^+d \rightarrow (p)p\pi^+\pi^-\pi^0$ was studied in a bubble-chamber experiment with pion beam momentum between 1.1 and 2.4 GeV/c; the exposure size was 14 events/μb. The most significant features of the final state are production and decay of η and ω mesons in the reactions $\pi^+n \rightarrow \eta p$ and $\pi^+n \rightarrow \omega p$. The η-production characteristics are well described by a Reggeized A_2-exchange model using Veneziano-type residue functions. The ω production and decay characteristics are presented, and it is found that a ρ-exchange model with absorptive corrections is inadequate to describe these data. (auth)

9676 STUDY OF THE REACTIONS $\pi^-p \rightarrow p\pi^-MM^0$ AND $\pi^-p \rightarrow p\pi^+\pi^-\pi^-MM^0$ AT 8 GeV/c. Dzierba, A. R.; Shephard, W. D.; Biswas, N. N.; (and others) (Univ. of Notre Dame, Ind.). Phys. Rev., D; 2: 2544-54(1 Dec 1970).

Results are presented from a hydrogen-bubble-chamber study of the final states $p\pi^-MM^0$ and $p\pi^+\pi^-\pi^-MM^0$, where MM^0 represents a neutral boson state of mass $\geq 2m(\pi^0)$. The proton was identified by ionization for all events in the sample. Production of η^0, ω^0, and f^0 mesons with decays into all neutral particles is observed in the $p\pi^-MM^0$ final state. Peaks are observed in the $\eta^0\pi^-$ spectrum at 1080 and 1310 MeV. The higher-mass peak has mass 1306 ± 8 MeV and width 41^{+21}_{-11} MeV and is identified as the A_2. The branching ratio for $A_2 \rightarrow \eta^0\pi^-/A_2 \rightarrow (\rho\pi)^-$ was measured as (18 ± 7)%. There is no evidence for a 980-MeV $\eta^0\pi^-$ enhancement. Data on the $p\pi^+\pi^-\pi^-MM^0$ final state show evidence for η^0 and ω^0 production. (auth)

9677 STUDY OF $\Delta^{++}(1236)$ + BOSON PRODUCTION IN π^+p INTERACTIONS AT 18.5 GeV/c. Biswas, N. N.; Cason, N. M.; Farber, M. S.; (and others) (Univ. of Notre Dame, Ind.). Phys. Rev., D; 2: 2529-37(1 Dec 1970).

The production of the ρ^0, f^0, g^0, η^0, and ω^0 bosons in the pseudo-two-body final state with the $\Delta^{++}(1236)$ baryon is studied. The cross sections and their t dependence are discussed. The s dependence of $\Delta^{++}\rho^0$ and $\Delta^{++}\omega^0$ final states is fitted with the expres-

sion $\sigma = k\,(p/p_0)^{-n}$ and yields values of n in the range 1.5–2.5. Using SU(3) invariance, the phase angle between ρ^0 and ω^0 production is determined as a function of incident momentum. The t dependence for $\rho^0\Delta^{++}$ production shows that the Regge model of the conspiring pion is not correct. Correlations between the Δ^{++} and ρ^0 decays are observed and are consistent with quark-model predictions. (auth)

9678 DENSITY MATRIX ELEMENTS AND DONOHUE-HOEGAASEN PARAMETERS OF RESONANCES PRODUCED IN π^+p AND γp REACTIONS. Aderholz, M. (Technische Hochschule, Aachen); Beaupre, J. V.; Deutschmann, M.; (and others). Nucl. Phys.; B24: 509-26(1970).

Density matrix elements are presented for several quasi two-body processes produced in π^+p interactions at 8 GeV/c. The decay of vector mesons and of $\Delta^{++}(1236)$ isobar is then studied in terms of the Donohue–Høgaasen (DH) spin population parameters α, β and γ and the rotation angle Θ. The data used are from π^+p scattering at 4 and at 8 GeV/c and from γp interactions in the photon energy region below 5.8 GeV. It is found that the DH parameters have the tendency to be less dependent on momentum transfer than the density matrix elements in the Jackson or in the helicity systems. The stronger variation of the matrix elements in the latter two systems is shown to be a kinematic consequence of the rotation of the frames. This effect is particularly well seen in the reaction $\gamma p \rightarrow \Delta^{++}\pi^-$ where the rotation angle strongly depends on the photon energy. The suggestion of Donohue and Høgaasen, that the DH reference system is a more natural frame than the others is well confirmed by our experimental results. (auth)

9679 STUDY OF $K\pi\pi$ STATES PRODUCED IN 10 GeV/c K^+p INTERACTIONS. Barnham, K. W. J. (Univ. of Birmingham, Eng.); Colley, D. C.; Dodd, W. P.; (and others). Nucl. Phys.; B25: 49-74(1971).

An analysis of the $K\pi\pi$ system produced in 10 GeV/c K^+p interactions is presented. It is shown that the low-mass enhancement between 1.2 and 1.4 GeV/c^2 in the $K\pi\pi$ mass spectrum is predominantly 1^+ throughout, the relative amplitudes for the decay of this system into $K^*(890)\,\pi$ and $K\rho$ are given, and new evidence is offered for the presence of two 1^+ resonances in this mass region. (auth)

9680 ELASTIC SCATTERING OF POSITIVE PIONS ON POLARIZED PROTONS BETWEEN 0.82 AND 2.74 GeV/c. Albrow, M. G.; Andersson, Almehed, S.; Bosnjakovic, B.; (and others) (CERN; Geneva). Nucl. Phys.; B25: 9-48(1971).

Polarization and differential cross-section data for elastic scattering of positive pions on protons between 0.82 and 2.74 GeV/c are presented. A dip in the polarization, at constant $u \approx -0.65$ GeV^2 is observed. The data are compared with published phase-shift analyses. (auth)

9681 ELASTICITY OF THE $\Sigma(2030)$. Campbell, J. R. (Univ. of Glasgow); Morton, W. T.; Negus, P. J.; Goyal, D. P.; Miller, D. B. Nucl. Phys.; B25: 75-84(1971).

The elastic scattering reaction $K^-n \rightarrow K^-n$, was studied using a deuterium filled bubble chamber in the range of c.m. energies from 1860 to 2150 MeV. A partial-wave analysis gives an estimate of 0.17 ± 0.04 for the elasticity of the $\Sigma(2030)$. (auth)

9682 STUDY OF CROSS SECTIONS AND SPIN-DENSITY MATRIX ELEMENTS IN 5 GeV/c π^+p FOUR-PRONGED INTERACTIONS. Pols, C. L. (Univ. of Nijmegen, Netherlands); Schotanus, D. J.; Toet, D. Z.; (and others). Nucl. Phys.; B25: 109-40(1971).

Results are presented on differential and total cross sections for seven quasi two-body reactions ($\pi^+p \rightarrow pA_2^+$, pB^+, $\Delta^{++}\eta^0$, $\Delta^{++}\rho^0$, $\Delta^{++}\omega^0$, $\Delta^{++}f^0$ and $\Delta^{++}A_2^0$) obtained from a sample of approximately 25,000 four-pronged interactions at 5 GeV/c incident momentum. In the forward direction the $d\sigma/dt'$ distributions of reactions with final state $\Delta^{++}\eta^0$, $\Delta^{++}\omega^0$ and $\Delta^{++}A_2^0$ show a dip or flat region. Reaction $\Delta^{++}\rho^0$ and $\Delta^{++}f^0$ require a "double slope" fit. The spin-density matrix elements of reaction $\Delta^{++}\rho^0$ and $\Delta^{++}\omega^0$ present evidence for non-sense wrong signature zero's in the π- and ρ-trajectory contributions respectively. For the reaction $\Delta^{++}\omega^0$ both $d\sigma/dt'$ and the ω ρ^{00} spin-density decay element show a remarkable dip around $t' \approx 0.1-0.15$ GeV^2. Several other features in the "forward" differential cross sections of the reactions observed are discussed and compared with models. Significant backward peaks are seen in reactions pB^+, $\Delta^{++}\eta^0$, $\Delta^{++}\rho^0$ and $\Delta^{++}\omega^0$. For two of the most prominent two-body reactions ($\Delta^{++}\rho^0$ and $\Delta^{++}\omega^0$) background studies were made by applying subtractions and studying t' dependences over the complete Goldhaber plot. (auth)

9683 EVIDENCE FOR THE EXISTENCE OF A NEW MESON IN THE 955-MeV MASS REGION. Aguilar-Benitez, M. (Brookhaven National Lab., Upton, N. Y.); Bassano, D.; Eisner, R. L.; (and others). Phys. Rev. Lett.; 25: 1635-8(7 Dec 1970).

Evidence is reported for the existence of a new meson, which is called the M(953), with mass 953 ± 2 MeV and width <10 MeV, produced in the final state $K^-p \rightarrow pK^-M^0$ at incident momenta 3.9 and 4.6 GeV/c. These results are based primarily on a signal of 68 ± 12 events in the decay mode $M \rightarrow \pi^+\pi^-\gamma$ where the $\pi\pi$ system does not show a ρ^0 signal, in sharp distinction to the $\rho^0\gamma$ decay mode of the $\eta'(958)$. (auth)

9684 HIGH-ENERGY HADRON–PROTON ELASTIC SCATTERING. Carlson, Per J. Stockholm; Univ. of Stockholm (1969). Thesis.

Within the field of elementary particle physics, three experiments are described and the implications of their results are given. The experiments were performed at the CERN Proton Synchrotron, and utilized the spark chamber technique. The elastic scattering of pions, kaons and antiprotons on protons was studied with the emphasis on the large and backward angles. The scattering of pions on protons was studied for incident momenta of 2.85, 3.30, 3.55, 5.2 and 6.9 GeV/c, that of positive kaons on protons at 3.55, 5.2 and 6.9 GeV/c, that of negative kaons on protons at 3.55 and 6.9 GeV/c and that of antiprotons on protons at 3.55 GeV/c. (TSS) (Diss. Abstr. Int., B)

Particle Interactions and Properties (Theoretical)

General

Refer also to abstract 9870.

9685 (COO–1764-86) THEORETICAL AND HIGH ENERGY PHYSICS PROGRAMS. Progress Report, September 1, 1969–August 31, 1970. (Minnesota Univ., Minneapolis. School of Physics). Contract AT(11-1)-1764. 55p. Dep. NTIS.

Research in high-energy physics and nuclear physics is summarized. The nuclear research is all theoretical, and the particle research is both theoretical and experimental. A list of publications is included. (J.F.P.)

9686 (COO–1764-100) THEOREM ON INTUITIVE TESTS OF PARITY CONSERVATION VIA SPIN POLARIZATION PROCESSES. Saenger, Robert M. (Minnesota Univ., Minneapolis. School of Physics). [1969]. Contract AT(11-1)-1764. 15p. Dep. NTIS.

Working in the helicity formalism it is shown that if parity is violated in a nontrivial way by the amplitudes for a two-body scattering reaction, then at least one of the parity violating polarization correlation measurements, $M_{\overline{\gamma}\delta;\alpha\beta}(\theta)$, all of which would vanish in the case of parity conserving amplitudes, is nonvanishing. More precisely, it is proven that $\Sigma|M_{\overline{\gamma}\delta;\alpha\beta}|^2 = 2|F_+|^2|F_-|^2$ where F_+ and F_- are the parts of the scattering helicity matrix which are even and odd under reflection and $\{M_{\overline{\gamma}\delta;\alpha\beta}\}$ is the set of all parity violating correlations taken from an orthonormal basis for the initial and final density matrices. This type of result is more general than the specific case considered and applies, for example, to decay processes as well. (auth)

9687 (ITF–70-58-P) DEFINITION OF QUASI-AVERAGES. Bogolubov, N. N. Jr. (Akademiya Nauk Ukrainskoi SSR, Kiev. Institut Teoreticheskoi Fiziki). 1970. 20p. (In Russian). Dep. NTIS (U. S. Sales Only).

Some difficulties connected with definition of quasi-averages for the model systems with a negative four-fermion interaction are considered. A new method of introducing the auxiliary system and definition of quasi-averages is developed. At the same time the problem of limiting expressions for the free energy (when $V \rightarrow \infty$) is solved. (auth)

9688 (JINR–P2-5336) ON THE BOUND STATES OF THE RELATIVISTIC THREE-PARTICLE SYSTEM. Atanasov, A. (Joint Inst. for Nuclear Research, Dubna (USSR). Lab. of Theoretical Physics). 1970. 14p. (In Russian). Dep. NTIS (U. S. Sales Only).

In the quasipotential approach the problem of determination of the bound state masses in the three-particle system with the quasi-pair interaction is reduced to the analysis of the eigenvalues of the Hermitian operator. Under some assumptions concerning two-particle interaction an estimate is obtained for the upper limit of the bound state number and for the algorithm of the approximate calculation of the bound state masses. (auth)

9689 (LNF–70/22) HAMILTONIAN THAT IMPLIES THE EXCLUSION PRINCIPLE. Note No. 478. Sacerdoti, G. (Comi-

XUM

tato Nazionale per l'Energia Nucleare, Frascati (Italy). Laboratori Nazionali di Frascati). 25 May 1970. 10p. (In Italian). Dep. CFSTI (U. S. Sales Only).

The explicit function H'_0 of a hamiltonian which has by mean of self-functions of the type $\varphi_k(x_1x_2x_n)^0 = \Sigma P(a_1a_2a_n)u_{a1}(x_1)....u_{a_n}(x_n)$ (with $a_1 < a_2... < a_n$ and $u_i(x)$ functions of a complete orthonormal set) is derived with the same eigenvalues E_k of those of a normal hamiltonian H of a system of interacting many bodies having as self-functions those obtained from $\varphi(x_1x_2...x_n)$ antisymmetrically. The condition $a_1 < a_2... < a_n$ is equivalent to the Pauli exclusion principle. The hamiltonian H'_0 derived is expressible as $H'_0 = \lambda \underline{\lim}_{\lambda} \lambda_{min}H'_0(\lambda)$ where λ is a numerical parameter. The exclusion principle can be a limiting case in which $\lambda \to 0$. For the bosons on the contrary the valid hamiltonian can be that of the photon. Valid statistical and intermediate particles for quasi fermions are possible which in high energy states can behave as quasi bosons. The theoretical consequences of this formulation of the many-body problem was not studied either in the interpretation of experimental results or in the suggestions of mathematical methods to resolve possible problems caused by this formulation. (tr-auth)

9690 (NYO-2171-331) BOOTSTRAPS IN LOCAL FIELD THEORY. Whippman, M. L. (Pennsylvania Univ., Philadelphia. Dept. of Physics). 10 Dec 1970. 22p. Dep. NTIS.

The problem of formulating a bootstrap in terms of vanishing renormalization constants is discussed. It is pointed out that the equations Z = 0 need not determine masses and coupling constants, but might be identities or else possess no solution. It is argued that this always occurs in theories in which particles are treated as made up of arbitrarily many other particles and this is illustrated in a soluble model. Finally, various consequences of this idea are mentioned. (auth)

9691 (RLO-1388-592) LOOP DIAGRAMS IN DUAL RESONANCE THEORIES WITH NONLINEAR TRAJECTORIES. Baker, M. (Washington Univ., Seattle. Dept. of Physics); Coon, D. D. (Minnesota Univ., Minneapolis. School of Physics and Astronomy). Sep 1970. 32p. Dep. NTIS.

Rules are presented for calculating loop diagrams in a dual resonance theory with nonlinear trajectories. Explicit expressions for the self-energy graph, the vacuum bubble graph and the vertex graph are given. In the limit of linear trajectories the integrands of these graphs diverge. This is in contrast to the behavior of the tree graphs which approach the Veneziano tree graphs in the same linear limit. It is also shown that when the trajectories are nonlinear the self-energy graph including the $\int d^4k$ is finite. It should be emphasized that these rules have been developed without consideration of the factorization properties of the nonlinear n point Born term. In this sense they are analogous to the original Veneziano loop diagram rules of Kikkawa, Sakita and Virasoro, which were subsequently modified by the requirements of factorization. However, although the rules may likewise be modified, they present a simplified context for developing techniques which are of general value for the study of the nonlinear theory. (auth)

9692 STUDY OF A POINT PROCESS CHARACTERIZED BY ITS MULTICOINCIDENCES. Macchi, Odile (Paris Univ., Orsay, France). Compt. Rend., Ser. A; 171: 660-3(5 Oct 1970). (In French).

A point process model, characterized by its multicoincidences, is presented. The integral equation of Fredholm was used to study the function characteristic of the number of points in an interval. A necessary condition for the validity of this model is stated and its physical interpretation given. (France)

9693 DUALITY OF THE NONPLANAR TETRAHEDRON GRAPH. Minami, Masatsugu; Miyata, Hideo (Kyoto Univ.). Progr. Theor. Phys. (Kyoto); 44: 783-95(Sep 1970).

The notion of duality of linear graphs is extended in connection with the reciprocity between analytic properties of the position-space functions and those of the momentum-space ones. A proposition concerning the analyticity associated with the torus graphs is proved. (auth)

9694 INTERMEDIATE ENERGY NUCLEAR PHYSICS. Lock, W. O.; Measday, D. F. London; Methuen and Company, Ltd. (1970). 320p. 85s.

The subject is dealt with under the following headings; properties of the elementary particles, some mathematical tools, fundamental concepts, pion interactions with nucleons, interactions of gamma rays and electrons with nucleons, nucleon-nucleon elastic scattering, nucleon-nucleon inelastic reactions, interactions of leptons and photons with nuclei, interactions of nucleons with nuclei, interactions of pions with nuclei. (UK)

9695 OFF-SHELL FUNCTIONS OF THE DUAL RESONANCE. Shirafuji, Takeshi (Saitama Univ., Japan). Progr. Theor. Phys. (Kyoto); 44: 823-5(Sep 1970).

An attempt is made to generalize the propagator of the scalar meson in the proper-time formalism to the particle with two proper-times (τ, ξ), following the Feynman path integral approach. Using an off-function, a simple interaction with scalar particles is introduced and the N-point Veneziano amplitude is obtained. (L.B.S.)

9696 LAGRANGIAN FORMULATION OF DUAL RESONANCE MODEL. Biyajima, Minoru; Miyamoto, Yoneji (Tokyo Univ. of Education). Progr. Theor. Phys. (Kyoto); 44: 825-7(Sep 1970).

The invariance properties of the Lagrangian formulation of the dual resonance model are discussed, and the conservation of currents, which corresponds to the Ward-like identities, is derived. (L.B.S.)

9697 QUASI-POTENTIAL EQUATIONS FOR SPIN PARTICLES OF UNEQUAL MASS. Bogolyubov, P. N. (Joint Inst. for Nuclear Research, Dubna, USSR). Teor. Mat. Fiz.; 5: 244-52(Nov 1970). (In Russian).

Possible forms of the quasipotential equations for spin-½ particles of unequal mass are considered. It is shown that by means of the Markov-Yukava type conditions the quasipotential equations of the Logunov-Tavkhelidze type can be received for the case of spin particles of unequal mass. (auth)

9698 FINITE-DIMENSIONAL SPECTRUM-GENERATING ALGEBRAS. Dothan, Yossef (Inst. for Advanced Study, Princeton, N. J.). Phys. Rev., D; 2: 2944-54(15 Dec 1970).

It is suggested that the generators of a spectrum-generating algebra are all constants of the motion, some of them having an explicit time dependence. Also suggested is a specific form of the Hamiltonian action on the spectrum-generating algebra for systems with a finite number of degrees of freedom. Well-known examples of spectrum-generating algebras are shown to fit into this framework. The stability of the suggested structure against small perturbation is discussed. The question of the generalization of the suggested structure to systems with an infinite number of degrees of freedom is briefly commented upon. (auth)

9699 PARTICLES, SOURCES, AND FIELDS. Schwinger, Julian. Addison-Wesley Series in Physics. Reading, Mass.; Addison-Wesley Publishing Company, Inc. (1970). 431p. $14.95.

A detailed presentation is given of the ideas and methods of source theory—a new theory for high-energy particle theory that emphasizes its unity with electrodynamics, gravitational theory, and many-particle cooperative phenomena. (L.B.S.)

9700 WAVE EQUATIONS IN DE-SITTER SPACE. Vidal, A. (Centro Brasileiro de Pesquisas Fisicas, Rio de Janeiro). An. Acad. Brasil, Cienc.; 42: 163-5(Jun 1970).

Equations are formulated in tensor and spin-tensor forms for the case of free particles of spins 1, 2, and 3/2 respectively. This is done using a treatment similar to that previously used. The wave equations are constructed with the help of the ten Dirac symmetric operators and the original spinors. (J.F.P.)

Electromagnetic

Refer also to abstracts 9780 and 9867.

9701 (ITF-70-73) ASYMPTOTIC PROPERTIES OF THE ELECTRON-PROTON SCATTERING AMPLITUDE AND THE SUM RULES FOR THE SCHWINGER TERM. Miranskii, V. A.; Zinov'ev, G. M. (Akademiya Nauk Ukrainskoi SSR, Kiev. Institut Teoreticheskoi Fiziki). 1970. 6p. Dep. NTIS (U.S. Sales Only).

A connection is established between the asymptotic behavior of the electron-proton scattering amplitude, the Jost-Lehmann-Dyson (JLD) spectral function of the commutator of currents, and the sum rules for the Schwinger term. It is shown that the restrictions on the JLD spectral function are less rigorous than those resulting in the property of the "scale invariance" of the scattering amplitude. (auth)

9702 (JINR-E2-5333) ANOMALOUS MAGNETIC MOMENT OF NUCLEONS. Goloskokov, S. V. (Joint Inst. for Nuclear Research, Dubna (USSR). Lab. of Theoretical Physics). 1970. 15p. Dep. NTIS (U. S. Sales Only).

Self-consistent solution is received for the anomalous magnetic moment of the nucleon μ' on the basis of the sidewise dispersion relations for μ' and the dispersion relations for the πN scattering amplitudes. (auth)

9703 (JINR-P2-5042) TRANSITION RADIATION ON RESONANCE γ-QUANTA. Perelstein, E. A.; Podgoreisky, M. I. (Joint Inst. for Nuclear Research, Dubna (USSR)). 1970. 11p. (In Russian). Dep. NTIS (U. S. Sales Only).

The effect of the absorption nuclear lines on the transition radiation of resonance γ quanta by relativistic electrons passing through a plate of a finite thickness is considered. It is shown that the radiation intensity inside the absorption line can considerably exceed the intensity outside the line. (auth)

9704 (NP-18540) HIGH-ENERGY SCATTERING OF CHARGED PARTICLES AND BETHE FORMULA. Kaffiev, Yu. N. (Akademiya Nauk SSSR, Novosibirsk. Institut Matematiki). 1970. 16p. Dep. NTIS (U. S. Sales Only).

Coulomb corrections to the nuclear amplitude are considered. It is shown that in general the Bethe formula doesn't hold, and its breaking is due to the presence in the amplitude potentials with different radio or rescatterings. Regge behavior of the amplitude at high energies is assumed and the radiation phase shift and its asymptote are found. In conclusion the experimental situation is discussed. (auth)

9705 (SLAC-123) THEMI: MONTE CARLO GENERATION OF ELECTROMAGNETIC EVENTS. Blanchard, Dennis C.; Swanson, William P. (Stanford Linear Accelerator Center, Calif.). Oct 1970. Contract AT(04-3)-515. 13p. Dep. NTIS.

A set of FORTRAN subroutines THEMI was written which gives the total cross sections for hydrogen and random events whose kinematics are distributed according to theoretical models which have been confirmed by numerous experiments. The spectrum of an incident bremsstrahlung beam determined by measuring electron pairs from photoproduction on hydrogen using a streamer chamber is discussed as an illustration of the set of routines. (J.F.P.)

9706 (SLAC-PUB-843) THEORIES OF HIGHLY INELASTIC ELECTRON SCATTERING. Smith, C. H. Llewellyn (Stanford Linear Accelerator Center, Calif.). Nov 1970. 22p. (CONF-701108-3). Dep. NTIS.

From Meeting of the Division of Particles and Fields of the American Physical Society, Austin, Tex.

The review of highly inelastic electron scattering covers the Parton model, survival of resonance contributions at large $|q^2|$ Regge behavior, finite-energy sum rules and fixed poles, recent e^- N research, and related processes. (J.F.P.)

9707 PHOTOPRODUCTION OF W-MESON PAIRS ON ELECTRONS. Kompaniets, V. G. (Inst. of High Energy Physics, Serpukhov, USSR). Yadern. Fiz.; 12: 826-33(Oct 1970). (In Russian).

An analytical expression, in form of a double integral on invariant variables, is obtained for the cross section of W-meson pair photoproduction on electrons with the meson anomalous magnetic moment equal to 0, ±1. The threshold and asymptotical behaviors of the cross section are analyzed. (auth)

9708 INTEGRAL EQUATIONS OF CASCADE KINEMATICS. Grishin, V. G.; Kopylova, D. K.; Kopylov, G. I.; Lyubimov, V. B.; Yuldashev, B. S. (Joint Inst. for Nuclear Research, Dubna, USSR). Yadern. Fiz.; 12: 757-69(Oct 1970). (In Russian).

The case is considered when in cascade decays the effective masses of two groups of particles from different branches of a cascade are measured. Two-dimensional distributions of these quantities are characterized by the internal structure: their level lines are determined by the kinematics of a cascade (by conservation laws) but not by the spectrum of the effective mass of the whole particle system. A similar structure is also possible in two-dimensional energy distributions. A concept on kinematical potential as a function of one variable determining two-dimensional distributions is introduced. The integral equations are derived that allow one to determine the m_{eff} spectrum of the whole particle system without detecting all the final products. For instance, the spectrum $m(\pi^+\pi^-\pi^0)$ is reconstructed from the measurements of $m(\pi^+\pi^-\gamma)$ and $m(\pi^+\pi^-)$ with the help of the equations. (auth)

9709 PARADOX OF RADIATION FROM A UNIFORMLY ACCELERATED POINT ELECTRON AND A CONSISTENT PHYSICAL FRAMEWORK FOR ITS RESOLUTION. Leiter, Darryl (Univ. of Windsor, Ont.). Int. J. Theor. Phys.; 3: 387-93(Oct 1970).

The problem of an electron in an external, uniform electric field is studied. The problem is analyzed within the framework of a new theory of Maxwell electrodynamics in which the problems and paradoxes of infinite self-energies are omitted by considering only the interactions between charged particles as the basic building blocks of the theory. For this case of uniform acceleration, the manifest consistency and physical transparency of this new electrodynamic formalism allows a simple and physically clear interpretation to be ascribed to the "acceleration energy", and the role it plays in acting as the source of the energy which is radiated from the accelerated charge. The relation of the acceleration energy to the internal energy of the electron is clarified in terms of the "total coupled radiation field" of the system. At the same time the new formulation of electrodynamics is shown to represent a completely consistent theory of a classical electron in an external field, which in many aspects is a superior alternative to either Maxwell-Lorentz theory or Wheeler-Feynman theory. (auth) (UK)

9710 LOW-ENERGY THEOREMS FOR COMPTON SCATTERING OFF ARBITRARY-SPIN TARGETS. Saito, Satoru. Madison, Wis.; Univ. of Wisconsin (1969). 121p. University Microfilms Order No. 70-3688.

Thesis.

Low-energy theorems for Compton scattering on targets with arbitrary spin are studied. The scattering amplitude is dominated at threshold by the Born term, which is calculated explicitly. Other contributions at threshold are uniquely determined by requiring that the total amplitude be the gauge invariant. In this way, each intrinsic electromagnetic moment of the target is obtained in terms of the threshold value of the amplitude. To linear order in ω (photon frequency) this information completely determines the amplitude and gives a generalization to the arbitrary-spin case of the low-energy theorem of Low, Gell-Mann and Goldberger. It is also found that two structure-dependent parameters (electric and magnetic polarizabilities of the target) are necessary to describe the spin nonflip amplitude to order ω^2. It is necessary to introduce two additional parameters to completely determine the total amplitude to this order in ω. (Diss. Abstr. Int., B)

9711 INFINITELY DEGENERATE PARTICLES AND MECHANISM OF MASS SPLITTING: BOSON CASE. Miyazaki, Tadashi (Tokyo Univ.). Progr. Theor. Phys. (Kyoto); 44: 796-800(Sep 1970).

Presenting the model Lagrangian which expresses the particles degenerate infinitely around a mass, the mass split was performed based on the mechanism of the tadpole-type interaction. (auth)

9712 PHOTOPRODUCTION OF ETA MESONS IN THE VENEZIANO MODEL. Hori, Setsuko; Hosoda, Masataka (Osaka Univ.). Progr. Theor. Phys. (Kyoto); 44: 746-57(Sep 1970).

The Veneziano Model is applied to photoproduction of eta mesons off nucleons. The model is written with inclusion of the trajectories ρ, ω, φ, B, N_α and N_γ, the last two of which are assumed to be parity-doublet and not exchange-degenerate. From the requirement of duality H' meson with $J^{PG} = 1^{+-}$ and I = 0 is introduced within the framework of the nonet scheme. The four amplitudes of Veneziano type are constructed on which a number of requirements are imposed: (1) gauge invariance, (2) crossing symmetry, (3) asymptotic behavior for both fixed t and fixed u as $s \to \infty$, (4) signatures of trajectories and (5) correct pole structure. Secondly the general features predicted by the model are studied and a new fit to the experimental data is obtained. Particular attention is paid to angular distributions of the differential cross section at forward angles ($0 \lesssim -t \lesssim 1.6$) for the 4 GeV and 6 GeV laboratory energies of photons. The dependence of $d\sigma/dt$ on the energy of the incident photons is also discussed. (auth)

9713 HIGH-ENERGY PHOTOPRODUCTION OF VECTOR MESONS IN A QUARK MODEL. Chand, Ramesh (Matscience, Madras). Progr. Theor. Phys. (Kyoto); 44: 758-64(Sep 1970).

Within the framework of SU(3) quark model, the production of vector mesons in high energy photonuclear reactions is investigated in the t-channel. Defining the physical baryon octet as 8 (physical) = 8' cos θ + 8 sin θ, where 8 and 8' arise from $3 \otimes \bar{3}$ and $3 \otimes 6$ respectively, a number of predictions are made using $\theta = 20°$. Also, independent of θ, a number of sum rules are derived. (auth)

9714 SELF-ENERGY OF LEPTONS. Fukuda, Reijiro (Tokyo Univ.). Progr. Theor. Phys. (Kyoto); 44: 827-8(Sep 1970).

The self-energy of leptons due to gravitational, weak and electromagnetic interaction is considered and the condition for elimination of divergences is studied. (L.B.S.)

9715 COULOMB EFFECTS IN HIGH ENERGY ^{4}He-^{4}He ELASTIC SCATTERING. Czyz, W. (American Univ., Washington, D. C.); Maximon, L. C. Ann. Phys. (New York); 60: 484-6(Oct 1970).

The results of previous work for high-energy ^{4}He-^{4}He elastic scattering are extended to include the Coulomb corrections. These corrections are found important around the diffractive minima. (auth)

XUM

9716 CHENG–WU PICTURE APPLIED TO $\gamma p \to \rho^0 p$ AND φp. Nelson, Charles A. (City Univ. New York). Phys. Rev., D; 2: 2669-76(1 Dec 1970).

The Cheng-Wu physical picture, with some additional assumptions, is applied to ρ^0 (φ) photoproduction and comparison is made with available experimental data. The comparison is not favorable for the assumption that the intermediate particles are two pions (kaons). On the other hand, the asymptotic prediction for $\gamma p \to \rho^0 p$ is consistent with extrapolation of present data under an alternative assumption that the intermediate particles are a quark-antiquark pair. In addition, under the latter assumption there is a justification for the additivity hypothesis of the quark picture of high-energy scattering. (auth)

9717 PION PHOTOPRODUCTION IN THE VENEZIANO MODEL. Ahmad, Masud; Fayyazuddin (Univ. of Islamabad, Rawalpindi, Pakistan). Phys. Rev., D; 2: 2718-24(1 Dec 1970).

The Veneziano representation is constructed for pion photoproduction amplitudes. Keeping the π,π_c,A_1 and the ρ trajectories, zero-free parameter fits for the sum and the difference of the differential cross sections for unpolarized photons $d\sigma/dt$ ($\gamma p \to \pi^+ n$) $\pm$ $d\sigma/dt$ ($\gamma n \to \pi^- p$) and the asymmetry function $\Sigma(\pi^+ + \pi^-)$ are obtained. The agreement with experiment is fairly good. (auth)

9718 SPECTRAL-FUNCTION SUM RULES FOR $\rho-\omega$ AND $\rho-\phi$ TRANSITIONS. Sanda, A. I.; Suzuki, Mahiko (Columbia Univ., New York). Phys. Rev., D; 2: 2676-81(1 Dec 1970).

Assuming the field algebra of Lee, Weinberg, and Zumino, it is pointed out that two spectral-function sum rules remain valid when the electromagnetic interaction is turned on. From these sum rules formulas are derived for calculating the electromagnetic $\rho-\omega$ and $\rho-\phi$ transitions. A tentative numerical estimate gives a value for the $\rho-\omega$ transition close to quark-model predictions, but an opposite sign for the $\rho^+-\rho^0$ mass splitting (−7.5 MeV). The branching ratio $\Gamma(\omega \to 2\pi)/\Gamma(\omega \to 3\pi)$ is estimated to be ~1%, and the phase of the $\omega \to 2\pi$ amplitude relative to the $\rho \to 2\pi$ amplitude is between 80° and 130°. (auth)

9719 MODEL OF $\epsilon \to 2\gamma$ AND $\delta \to 2\gamma$ DECAYS. Sarker, A. Q. (Univ. of Oregon, Eugene). Phys. Rev., D; 2: 2732-3 (1 Dec 1970).

A model of DeCelles and Goehl for $\epsilon \to 2\gamma$ decay is generalized so as to give the correct SU(3)-symmetric result for both $\epsilon \to 2\gamma$ and $\delta \to 2\gamma$. The question of symmetry breaking is also discussed. (auth)

9720 CONSTRAINT ON THE UNIVERSAL FUNCTION IN ELECTROPRODUCTION. Choudhury, S. Rai; Rajaraman, R. (Univ. of Delhi). Phys. Rev., D; 2: 2728-9(1 Dec 1970).

It is shown that analyticity and asymptotic behavior impose a severe constraint on the scale-invariant function widely suggested for the behavior of $\nu W_2(q^2\nu)$ as $q^2 \to \infty$. If the asymptotic behavior of the off-mass-shell Compton scattering amplitude is dominated by the usual (nonfixed) Regge trajectories, then our constraint is violated by the experimental candidates for the νW_2 curve. On the other hand, the introduction of a fixed pole corresponding to the one used by Damashek and Gilman alters the constraint, which is then consistant with the 18° data. (auth)

9721 IMPROVEMENT OF THE KROLL–RUDERMAN THEOREM. De Baenst, P. (University Coll., Dublin). Nucl. Phys.; B24: 633-52(1970).

The Fubini–Furlan–Rossetti theorem is rederived in a simple way by using the PCAC hypothesis extended in a minimal way so as to take into account the electromagnetic interactions up to the first order in e. This low-energy theorem, as well as crossing symmetry, is used to improve the Kroll–Ruderman results concerning the slopes of the differential cross sections for π-photoproduction at threshold. Specifically, it is proved that in an expansion in $\mu \equiv m_\pi/M$ (M is the nucleon mass) the slopes can be exactly predicted up to and including terms of order μ^1, μ^1, μ^3 and μ^4 for $\gamma p \to n\pi^+$, $\gamma n \to p\pi^-$, $\gamma p \to p\pi^0$ and $\gamma n \to n\pi^0$ respectively if the simplest extrapolation from $q^2 = 0$ to $q^2 = m_\pi^2$ is valid. It is believed that the fair agreement obtained with the available experimental data (particularly for the photoproduction of π^0 on protons) provides added support for the extended PCAC hypothesis. (auth)

9722 THRESHOLD THEOREM FOR THE RADIUS OF THE F_2 NUCLEON FORM FACTOR. Royer, Jeffrey Paul (Stanford Univ., Calif.). Phys. Rev., D; 2: 3040-53(15 Dec 1970).

A method is developed for expanding the absorptive part of the sidewise dispersion relation for the nucleon F_{2N} radius. It is assumed that a threshold expansion is valid and the exact first-order terms in this expansion can be obtained in the limit of the pion mass going to zero. It is proved that the first-order terms in this expansion come solely from the π-N intermediate state. Thus, the expansion provides justification for the retention of only the π-N intermediate state in a first attempt at describing the radius, as in Drell and Silverman. Furthermore, the expansion provides a handhold for attempting to estimate the corrections to the first-order term coming from the 2π-N and higher intermediate states. It must be emphasized that we are not providing justification for the assumption of threshold dominance. An attempt is made to follow that assumption to its logical conclusion. That is, if the threshold dominance idea is good, then a threshold expansion provides a logical way to calculate low-energy parameters. Such an expansion is provided for the F_{2v} radius. (auth)

9723 LORENTZ INVARIANT FORMULATION OF VECTOR-MESON DOMINANCE IN PHOTOPRODUCTION. Berlad, G.; Eilam, G. (Technion–Israel Inst. of Tech., Haifa). Nucl. Phys.; B25: 321-31(1971).

The vector-meson dominance (VMD) for photoproduction is reformulated in a frame-independent way, by assuming weak dependence of the Poincaré (ls)-reduced T matrix elements for the reaction "vector meson + target → hadrons" on the mass of the external vector meson. It then follows that the T matrix elements for this reaction smoothly approach at high energy the corresponding matrix elements for the reaction "photon + target → hadrons", provided the vector meson is transversely polarized in the s-channel c.m. frame. Some advantages of the new VMD formulation are pointed out, and some illustrative examples are explicitly studied. (auth)

9724 SOME REMARKS ON THE INTERCONNECTION BETWEEN THE KROLL–RUDERMAN THEOREM AND THE RELIABILITY OF THE BORN APPROXIMATION FOR THE NON-SPIN-FLIP p-WAVE PHOTOPRODUCTION MULTIPOLES AT LOW ENERGIES. Verzegnassi, C. (Daresbury Nuclear Physics Lab., Eng.). Nucl. Phys.; B25: 308-16(1971).

A generalization of the Kroll–Ruderman theorem is given for the non-spin-flip p-wave photoproduction multipoles near threshold. The reliability of the Born approximation for low-energy photoproduction p-waves is consequently discussed. (auth)

9725 OFF-SHELL SINGLE-CURRENT AMPLITUDE IN THE VENEZIANO APPROACH. Humpert, B. (Cavendish Lab., Cambridge, Eng.). Nucl. Phys.; B25: 291-307(1971).

A simplified model for an off-shell single-current amplitude in the Veneziano approach is proposed which satisfies current conservation and has an explicit dependence on the current mass. It exhibits the correct J-plane structure with moving Regge poles as well as fixed poles and gives the expected low-energy behavior. Using this model the vector meson dominance assumption is investigated and it is found that the continuation in the current mass does not affect considerably the matrix elements. Charged-pion photoproduction near the forward direction with this model is studied. (auth)

9726 NON-MINIMAL CURRENTS IN CHIRAL LAGRANGIANS WITH AN APPLICATION TO PION PHOTOPRODUCTION. Pantin, C. F. A. (Cambridge Univ., Eng.). Nucl. Phys.; B25: 245-59 (1971).

Nonminimal currents are constructed to describe nucleon anomalous magnetic moments and related effects in the chiral Lagrangian formalism without upsetting current algebra and PCAC. The construction is applied to give a more realistic description of pion photoproduction at low energies. (auth)

9727 FIT TO HIGH-ENERGY PION PHOTOPRODUCTION. Kellett, B. H. (Univ. of Manchester, Eng.). Nucl. Phys.; B25: 205-17(1971).

A simultaneous fit to all the available data on high-energy pion photoproduction is performed. The model assumes dominance of the electric Born term in charged-pion photoproduction and dominance of ω-exchange in the neutral case. Good fits are obtained with the inclusion of phenomenological cuts as well as evasive ρ, ω and A_2 Regge poles. (auth)

9728 MULTIPOLE ANALYSIS FOR THE REACTIONS $\gamma p \to K^+\Lambda$ AND $\gamma p \to K^+\Sigma^0$. Schorsch, W.; Tietge, J.; Weilnboeck, W. (Max-Planck-Institut fuer Physik und Astrophysik, Muenchen, Ger.). Nucl. Phys.; B25: 179-96(1971).

A multipole analysis of the reactions $\gamma p \to K^+\Lambda$ and $\gamma p \to K^+\Sigma^0$ was performed for cm energies from threshold up to 2.0 GeV. The multipole amplitudes were parametrized by a generalized Breit–Wigner formula together with and without smooth background contributions. No exchange terms were explicitly included in the analysis. Fits to the experimental data with various combinations of at most three resonating waves were attempted by means of a χ^2 minimization procedure. In the case of $K^+\Lambda$

photoproduction the fits obtained favor solutions with S_{11}, P_{11} and D_{13} wave contributions, whereas for the $K^+\Sigma^0$ photoproduction $S_{\#}$, P_1 and F_5 or F_7 wave contributions are needed. (auth)

9729 DIBARIC PARTICLE IN A CONSTANT ELECTRIC FIELD. Polovina, N. N.; Yaroshenko, A. P. (Dnepropetrovsk State Univ., USSR). Ukr. Fiz. Zh.; 15: 1338-41(Aug 1970). (In Russian).

The mass state particle behavior was considered in a constant electric field. The complete separation of variables in the corresponding wave equation was carried out by means of projection operators. The exact solution of the problem is obtained. (auth)

9730 ELECTROMAGNETIC ANNIHILATION OF LEPTON–ANTILEPTON PAIR IN HYPERON PAIRS WITH CONSIDERATION OF POLARIZATION AND FORM FACTORS. Kasumov, Yu. M. (Moscow State Univ.). Izv. Vyssh. Ucheb. Zaved., Fiz.; No. 9, 75-81(1968). (In Russian).

The process of lepton–antilepton pair annihilation into pairs of $\bar{\Lambda}^0\Sigma^0$ or $\Lambda^0\bar{\Sigma}^0$ hyperons is studied. Expressions for the differential cross sections, the strange particle form factor calculations, and also arbitrary polarizations of the initial and final particles are obtained in the cms system. (tr-auth)

9731 INITIAL STAGE OF AVALANCHE DEVELOPMENT. Gedalin, E. V.; Krasnov, Yu. K. (Inst. of Physics, Tbilisi, USSR). Soobshch. Akad. Nauk Gruz. SSR; 60: 61-4(Oct 1970). (In Russian).

The diagram technique is used to study the initial stage of development of avalanches for nuclear particles of two kinds: pions and nucleons. The assumptions are made that the coefficient of inelasticity is constant and that there is power dependence of secondary particle multiplicity on the energy of the incident particle in the event of nuclear interaction. It is shown that even for sufficiently thin targets (~0.1 of the nuclear path) the contribution of secondary interactions is quite essential and leads to an increase of about 20% of the average multiplicity for the initial energy of 10^2 to 10^3 GeV. (auth)

Weak

Refer also to abstract 9839.

9732 (BNL-50260) REMARKS ON THE $|\Delta I| = 1/2$ RULE IN NONLEPTONIC WEAK DECAYS AND THE USE OF THE PHENOMENOLOGICAL LAGRANGIAN. Lee, T. D. (Columbia Univ., New York). May 1970. 62p. Dep. NTIS.

It is shown that the validity of the usual "soft-pion" limit and the existence of a $|\Delta\vec{I}| = 1/2$ rule for nonleptonic weak interactions are two independent assumptions. The alleged derivation of the $|\Delta\vec{I}| = 1/2$ rule for nonleptonic K decays by using the "soft-pion" limit is, therefore, incorrect. As examples, several different phenomenological Lagrangian models for nonleptonic K decays are examined which illustrate the logical independence of these two assumptions. A speculative possibility, based on a previous idea, concerning the origin of the $|\Delta\vec{I}| = 1/2$ rule is analyzed. (auth)

9733 (ITF–70-52) DEFINITION OF QUASI-AVERAGES. Bogolyubov, N. N. Jr. (Akademiya Nauk Ukrainskoi SSR, Kiev. Institut Teoreticheskoi Fiziki). 1970. 20p. Dep. NTIS (U.S. Sales Only).

Some difficulties are considered connected with definition of quasi-averages for the model systems with a negative four-fermion interaction. A new method of introducing the auxiliary system and definition of quasi-averages is developed. At the same time the problem of limiting expressions for the free energy (when $V \to \infty$) is solved. (auth)

9734 (ITF–70-53) OBTAINING THE LIMITING RELATIONS FOR CORRELATION AVERAGES. Bogolyubov, N. N. Jr. (Akademiya Nauk Ukrainskoi SSR, Kiev. Institut Teoreticheskoi Fiziki). 1970. 16p. Dep. NTIS (U.S. Sales Only).

The theorems necessary for obtaining many-time correlation averages are formulated under some rather general auxiliary conditions. The technique proposed is valid for a wide class of model systems with four-fermion interaction. (auth)

9735 (NYO–1932(2)-186) HISTORY OF WEAK INTERACTIONS. Lee, T. D. (Columbia Univ., New York). Jul 1970. Contract AT(30-1)-1932. 16p. Dep. NTIS.

This review of weak interactions covers the early history from the idea of the neutrino and the phenomenological Lagrangian of the beta decay interaction to the theory of the intermediate boson and the electron spectrum in muon decay. The transition period is discussed and covers the decays of strange particles to the discovery of the electronic and the muonic neutrinos. Finally the present status of weak interactions is described listing the general properties of these interactions and important unresolved problems. (J.F.P.)

9736 DETERMINATION OF PION SCATTERING LENGTHS FROM RATIO OF TOTAL PROBABILITIES OF THE $K \to 3\pi$ DECAYS. Dakhno, L. G. (Inst. of High Energy Physics, Serpukhov, USSR). Yadern. Fiz.; 12: 840-6(Oct 1970). (In Russian).

The effect is considered of the nonlinear character of the pion spectra on the ratio of the total probabilities of the decay $\gamma^{2+-}/4\gamma^{00+} - 3\gamma^{+0}/2\gamma^{000}$. These ratios are calculated up to terms $\sim E^2$ (E is the total energy released in the decay), their values being determined by the pion interaction, as well as by the spectrum slope in the middle of the Dalitz plot. Comparison with the experimental data enable one to find possible values of the pion scattering lengths. (auth)

9737 LIMITS ON ELECTRIC CHARGE, MAGNETIC MOMENT, AND MONOPOLE MOMENT OF THE NEUTRINO. Ereshchenko, S. K. (Moscow Physical-Technical Inst.). Yadern. Fiz.; 12: 834-9(Oct 1970). (In Russian).

Electromagnetic production of neutrino–antineutrino pairs in the sun interior is considered. Upper limits for the electric charge, magnetic moment and monopole moment of the massless neutrino, obtained originally in previous work, are made more precise. Dependence of the upper limit for the neutrino electric charge on the neutrino mass is obtained in the interval $0 \leq m_\nu \leq 10$ keV. (auth)

9738 $K_2^0 \to 2\pi 2\gamma$ BY CURRENT ALGEBRA. Heiko, Lance (Centro de Investigacion y Estudios Avanzados del I.P.N., Mexico City); Kannenberg, Lloyd C.; Kannenberg, Susan L. Progr. Theor. Phys. (Kyoto); 44: 809-11(Sep 1970).

A current-algebra analysis was made of $K_2^0 \to 2\pi 2\gamma$ decay in the soft-pion limit. The branching ratio $K_2^0 \to 2\pi 2\gamma / K_2^0 \to$ all modes was found to be 1.1×10^{-6}, a value within present experimental detectability. (L.B.S.)

9739 CLUSTER MODEL AND NONLEPTONIC HYPERON DECAYS. Noda, Hujio (Kyushu Univ., Fukuoka); Toyoda, Fumihiko. Progr. Theor. Phys. (Kyoto); 44: 811-13(Sep 1970).

The nonleptonic hyperon decays are treated on the basis of the cluster structure of the baryon. The main properties of the S-wave and P-wave decays are obtained. The model is also applied to the Ω^- nonleptonic decay. (L.B.S.)

9740 WEAK INTERACTION AS AN S MATRIX. Maheshwari, Amar; Miyazawa, Hironari (Tokyo Univ.). Progr. Theor. Phys. (Kyoto); 44: 772-6(Sep 1970).

Transition amplitudes for weak processes are constructed so that they satisfy unitarity relation and analyticity, and coincide with the phenomenological weak interaction Hamiltonian in the low energy limit. As an example of higher order process, K_L–K_S mass difference is calculated. (auth)

9741 CAUSALITY FUNCTION IN A FOUR-FERMION MODEL WITH AN INDEFINITE METRIC. Demidova, N. S.; Naumov, A. I. Vestn. Mosk. Univ., Ser. III. Fiz. Astron.; No. 2, 215-17(Mar-Apr 1970). (In Russian).

After determining the parameters of causality function and including the internal characteristics of isospin and hypercharge the four-fermion model with an indefinite metric was used for calculating the mass and coupling constants of the hadron similar to the calculations of spinor theory. (R.V.J.)

9742 g_A AND g_V FROM MIRROR NUCLEI. Leonardi, R. (Univ., Bologna). Phys. Rev. Lett.; 25: 1731-4(21 Dec 1970).

The superallowed β transitions of mirror nuclei were analyzed, and the Gamow–Teller matrix elements were calculated in order to determine g_A and g_V. Agreement with the more recent measurements is obtained. (auth)

9743 CHIRAL SYMMETRY BREAKING AND THE K_{l4} AXIAL-VECTOR FORM FACTORS. Lane, Kenneth D. (Johns Hopkins Univ., Baltimore). Phys. Rev., D; 2: 2703-10(1 Dec 1970).

The axial-vector form factors of K_{l4} decay are calculated in the framework of current algebra and approximate chiral symmetry. They are obtained with the neglect of terms involving second and higher orders in both the symmetry breaking and the momenta of the π and K mesons. The Gell-Mann–Oakes–Renner model is used to evaluate matrix elements of the usual σ commutators between pseudoscalar-meson states. The calculated form factors are then compared with the existing experimental data on these decays. First-order symmetry-breaking corrections to the s-wave $K\pi$ scattering lengths are also determined in this procedure, and the results are presented. (auth)

XUM

9744 POSSIBLE DUALITY CONSTRAINTS ON P-WAVE NONLEPTONIC DECAYS. Inami, Takeo (Tokyo Univ.); Kawarabayashi, Ken; Kitakado, Shinsaku. Phys. Rev., D; 2: 2711-13 (1 Dec 1970).

Assuming minimal exchange-degeneracy patterns for mesons and baryons consistent with duality and the absence of exotic resonances, an argument is given for possible constraints on P-wave nonleptonic baryon decays. The $\Delta I = \frac{1}{2}$ rule and $P(\Sigma^-) = 0$ then follow in the SU(3) limit. (auth)

9745 AXIAL-VECTOR-MESON DOMINANCE AND A NEW ESTIMATE FOR THE DECAY $K^+ \to \pi^+\gamma\gamma$. Intemann, Gerald W. (State Univ. of New York, Binghamton). Phys. Rev., D; 2: 2630-4(1 Dec 1970).

The radiative decay mode $K^+ \to \pi^+\gamma\gamma$ is studied within the framework of an axial-vector dominance model (AVDM) with the exchange of the $A_1^+(1070)$, $B^+(1235)$, and $K_A^+(1320)$ dominating the decay. A new estimate is obtained for the branching ratio $R = \Gamma(K^+ \to \pi^+\gamma\gamma)/\Gamma(K^+ \to \text{all}) = 1.5 \times 10^{-6} - 2.1 \times 10^{-6}$ depending on the d-wave-to-s-wave ratio in axial-vector-meson decays. For a modest amount of d wave, the AVDM result is comparable to the value for R based on the π^0-pole model and is also in good agreement with experiment. The π^+ energy spectrum is also calculated using AVDM and compared with the spectrum found in the π^0-pole model. The significance of these results for the testing of a proposed mechanism for $K^+ \to \pi^+\pi^0$ is also discussed. (auth)

9746 V−A ELASTIC SCATTERING OF ELECTRONS BY FISSION ANTINEUTRINOS. Avignone III, F. T. (Univ. of South Carolina, Columbia). Contract AT(38-1)-474. Phys. Rev., D; 2: 2609-12(1 Dec 1970).

The energy spectrum of electron antineutrinos from ^{235}U fission products in secular equilibrium has been recalculated. Assuming the validity of V−A theory, cross sections for the elastic scattering reaction $\bar{\nu}_e + e^- \to \bar{\nu}_e + e^-$, integrated over recoil electron energy for this antineutrino spectrum, are given for several values of minimum electron energy from 1 to 5.5 MeV. Theoretical error bars, which reflect the uncertainties in the input data, are given for the antineutrino spectrum and the cross sections. (auth)

9747 COLLINEAR DISPERSION RELATIONS AND THE K_{e4} DECAY RATE. Nasrallah, N. F. (Lebanese Univ., Beirut); Schilcher, K. Phys. Rev., D; 2: 2698-2702(1 Dec 1970).

The K_{e4} decay form factors using a method introduced by Fubini and Furlan are studied. The amplitudes which are extrapolated from the soft-pion limits to the physical point differ slightly from the previously used ones. The choice is motivated by the collinear parametrization. These amplitudes are simply related to the K_{e4} form factors and to the K-π scattering amplitudes, which appear on equal footing. The calculated decay rate $\Gamma = (2.3 \pm 0.3) \times 10^3$ sec^{-1} lies within the experimental error. (auth)

9748 POSSIBILITY OF EXPERIMENTAL DETERMINATION OF THE NATURE OF THE NEUTRAL PARTICLES IN MUON DECAY. Kalbfleisch, George R. (Brookhaven National Lab., Upton, N. Y.). Nucl. Phys.; B25: 197-204(1971).

The nature of the neutral particles from muon decay can be checked through their interactions in the bubble chamber in neutrino exposures of the near future. In particular it can be determined whether the lepton conservation law is additive or multiplicative. (auth)

Strong (General)

Refer also to abstracts 9253 and 9886.

9749 (JINR−E2-5341) REPRESENTATION FOR THE RELATIVISTIC SCATTERING AMPLITUDE AT HIGH ENERGIES. Garsevanishvili, V. R.; Kadyshevskii, V. G.; Mir-Kasimov, R. M.; Skachkov, N. B. (Joint Inst. for Nuclear Research, Dubna (USSR). Lab. of Theoretical Physics). 1970. 36p. Dep. NTIS (U. S. Sales Only).

In the framework of the quasipotential approach high-energy representation for the relativistic scattering amplitude is obtained. A basic point is an application of the Fourier analysis in terms of the nonabelian group of translations embedded as a subgroup in the Lorentz group. The representation obtained corresponds to the eikonal one in quantum mechanics. (auth)

9750 PROBLEM ON THE ROLE OF ρ AND σ MESONS IN STRONG INTERACTIONS. Lend'el, V. I.; Marina, D. M. (Uzhgorod State Univ., USSR). Yadern. Fiz.; 12: 860-4(Oct 1970). (In Russian).

The universal formulas for the contributions of ρ and σ mesons in different strong interaction processes are obtained. It is shown that within a certain accuracy a selfconsistent description of the strong interaction processes of nonstrange particles can be obtained with the help of these formulas. (auth)

9751 STRAIGHT-LINE PATHS APPROXIMATION FOR STUDYING HIGH-ENERGY ELASTIC AND INELASTIC HADRON COLLISIONS IN QUANTUM FIELD THEORY. Barbashov, B. M.; Kuleshov, S. P.; Matveev, V. A.; (and others) (Joint Inst. for Nuclear Research, Dubna, USSR). Phys. Lett.; 33B: 484-8(7 Dec 1970).

The problem of the asymptotic behavior of high-energy elastic and inelastic amplitudes is studied by means of the functional methods of quantum field theory. The straight-line paths approximation (SLPA), making it possible to effectively calculate the functional integrals which arise, is formulated. (auth)

9752 PARTIALLY LATENT INTERACTION IN ELEMENTARY PARTICLE FORMATION. Suh, Kiu S. (Grumman Aerospace Research Center, Bethpage, N. Y.). Int. J. Theor. Phys.; 3: 359-66(Oct 1970).

In order to surmount difficulties currently encountered by strong interaction theory, modifications appear to be needed. A possible modification is conjectured by introducing the concept of quasidynamical strong interaction at very short distances. The feasibility of tightly binding quasidynamical $\bar{K}-N$ interaction to deliver hyperons is considered. The quasidynamical interaction, if proved correct, may provide an essential interaction mechanism for the formation of strongly interacting particle states. (auth) (UK)

9753 HADRON BOOTSTRAP: TRIUMPH OR FRUSTRATION? Chew, Geoffrey F. (Univ. of California, Berkeley). Phys. Today; 23: No. 10, 23-8(Oct 1970).

The fundamentalist and hadron bootstrap points of view are discussed. A proof of the superiority of one theory over the other is considered impossible at the present time. Even the discovery of quarks would not resolve the problem, since quarks may also be constructed of more fundamental particles. The characteristics and possibilities of both theories are pointed out. (J.F.P.)

9754 CLASSIFICATION OF LOCAL CURRENT ALGEBRAS. Joseph, A. (Tel-Aviv Univ., Israel). Commun. Math. Phys.; 19: 106-18(1970).

A simple, yet rigorous derivation of all possible forms of a local Lie algebra L g subject to a certain finiteness condition is presented. This result is used to describe all possible continuous finite dimensional representations of L g. (auth)

9755 EIKONAL REGGE FITS TO SMALL-ANGLE ELASTIC SCATTERING DATA. Hamer, C. J.; Ravndal, F. (California Inst. of Tech., Pasadena). Contract AT(11-1)-68. Phys. Rev., D; 2: 2687-92(1 Dec 1970).

A fit is made to the elastic scattering data at $|t| \lesssim 0.1$ GeV^2 for the reactions $\pi^\pm p$, $K^\pm p$, pp, and $\bar{p}p$, employing the eikonal Regge model of Frautschi and Margolis. It is shown that the model is capable of explaining all aspects of the existing data, with the exception of the $\pi^- p$ total cross section, where our fit does not flatten out as much as the high-energy results from Serpukhov. Extrapolating to still higher energies, it is predicted that the pp total inelastic cross section should increase by 15% from 10 GeV to 10^3 GeV, a result of interest in connection with recent cosmic-ray observations by Grigorov et al. (auth)

9756 PRODUCTION CROSS SECTIONS IN THE MULTIPERIPHERAL MODEL. Ball, James S.; Marchesini, G. (Univ. of California, Berkeley). Phys. Rev., D; 2: 2665-8(1 Dec 1970).

The total cross section for the multiperipheral model is obtained by solving a Bethe-Salpeter equation. It is shown that the N-particle production cross sections are given directly in terms of the eigenvalues and eigenfunctions of this Bethe-Salpeter equation, and hence are directly related to the Regge-pole parameters. In simple models of Regge poles based on the multiperipheral model the production cross sections are completely determined. Results are given for several simple cases including the Chew and Snider model of the Pomeranchon. (auth)

9757 STUDY OF A MULTIPERIPHERAL BOOTSTRAP. Halliday, I. G.; Saunders, L. M. (Imperial Coll. of Science and Tech., London). Phys. Rev., D; 2: 2969-75(15 Dec 1970).

A simple example of the multiperipheral Regge bootstrap is discussed in detail, both numerically and qualitatively. The model, which contains one trajectory and one kind of particle, uses both elastic and inelastic unitarity to calculate the trajectory α, the two-particle−Reggeon coupling G, and the two-Reggeon−particle coupling g. Many properties of the equations are discussed qualitatively. The trajectory α and coupling G have been computed numerically for a variety of g but we are unable to close the bootstrap by computing a self-consistent g. The numerical results ob-

XUM

tained strongly suggest considerable structure, both in angular dependence and momentum transfers, in the coupling g. (auth)

9758 STUDIES OF MULTIPERIPHERAL INTEGRAL EQUATIONS. Ting, Peter D. (Univ. of California, Berkeley). Phys. Rev., D; 2: 2982-3004(15 Dec 1970).

The Chew–Goldberger–Low type of multiperipheral integral equation is derived in terms of invariant variables, without assuming subenergies to be large compared with momentum transfers and particle masses. Both forward direction and nonforward direction are worked out in detail, and the multiperipheral model with Toller-angle-dependent vertex functions is discussed. It is furthermore demonstrated that all the qualitative physical properties of the model proposed by Amati, Bertocchi, Fubini, Stanghellini, and Tonin in 1962 remain true in this generalized multiperipheral model. (auth)

9759 HADRODYNAMICS AND QUARK STRUCTURE. Ellis, Stephen (California Inst. of Tech., Pasadena); Frampton, Paul H.; Freund, Peter G. O.; Gordon, David. Nucl. Phys.; B24: 465-89 (1970).

It is proved that conformal invariance of dual dynamics unambiguously fixes the possible quark configurations of all (exotic and non-exotic) hadrons. All these configurations follow a simple star-of-David rule. Rules for computing amplitudes for arbitrary hadronic processes involving external and/or intermediate exotic hadrons are given. The existence of quark diagrams such that one diagram has poles in all three channels of a four-point function is pointed out. The total quark number of a hadron is identified with a Casimir operator of a new "D-spin" group. (auth)

9760 QUARK FOCUSING AT HADRONIC VERTICES. Frampton, Paul H.; Freund, Peter G. O. (Univ. of Chicago). Nucl. Phys.; B24: 453-64(1970).

A basis for dual theory of processes that involve external and/or intermediate exotic hadrons is found in the form of a quark-focusing principle. This principle, derived from the conformal invariance of the theory, requires that at a hadronic vertex all active quarks be focused to a point of their world sheet and act together (as a point-like particle) in the transfer of momentum. It is found that all hadronic couplings (including the coupling of any three exotic hadrons) can be expressed in terms of a single (say the $\rho\pi\pi$) coupling constant. Applications to $B\bar{B}$ scattering are made. (auth)

9761 OCTET BEHAVIOUR OF SINGLE-PARTICLE MATRIX ELEMENTS $\langle B'|Hw|B\rangle$ AND $\langle M'|Hw|M\rangle$ USING A WEAK CURRENT–CURRENT QUARK HAMILTONIAN. Koerner, Juergen G. (Univ., Heidelberg). Nucl. Phys.; B25: 282-90(1971).

The SU(3) transformation behavior of single-particle matrix elements $\langle B'|H_W(0)|B\rangle$ and $\langle M'|H_W(0)|M\rangle$ is investigated under the assumption that the transitions are induced by a weak current–current type quark Hamiltonian. The baryons B and mesons M are taken to be members of the 56 and 35 multiplets, respectively. For Fermi quarks the baryon matrix elements vanish identically and the meson matrix elements transform as octets. For para quarks and in the three-triplet model the baryon elements have a strong 27 component. A slightly modified Hamiltonian is introduced which induces octet transitions for both mesons and baryons. (auth)

9762 LINEAR CURRENT-FIELD ALGEBRAS, BROKEN SCALE INVARIANCE, AND NUCLEON INTERACTIONS. Genz, H. (Univ. of Karlsruhe, Ger.). Nucl. Phys.; B25: 269-81(1971).

For a particular nucleon source term two possible values are calculated for the effective πN coupling constant from assumed equal-time commutators and observed ρ-meson coupling constants. Neglecting renormalization, one of these is in surprisingly good agreement with experiment. It disagrees however with ρ-meson universality. In the Kastrup–Mack scheme of broken scale invariance a self-contained derivation is then given of an expression for the ϵN coupling constant in terms of the length dimension of the pion field (defined by PCAC). The relation obtained this way is compared to experiment and to other models. (auth)

Strong (Baryon No. = 0)

Refer also to abstracts 9668–9670, 9743, and 9813.

9763 (COO-1428-239) THE ANALYTIC STRUCTURE OF THE OFF-MASS-SHELL S-WAVE $\pi^+\pi^-$ SCATTERING AMPLITUDE. Gutay, L. J.; Scharenguivel, J. H. (Purdue Univ., Lafayette, Ind.). Meiere, F. T. (Indiana–Purdue Univ., Indianapolis). [1970]. Contract AT(11-1)-1428. 8p. Dep. NTIS.

Using rather general assumptions, it is shown that the on-mass-shell P-wave determines the off-mass-shell dependence of the S-wave $\pi^+\pi^-$ amplitude. This is used to determine $(2a_0 + a_2)/a_1$ experimentally. (auth)

9764 (DESY–70/58) EMPIRICAL TEST OF TENSOR MESON DOMINANCE. Renner, B. (Deutsches Elektronen-Synchrotron, Hamburg (West Germany)). Nov 1970. 7p. Dep. NTIS (U. S. Sales Only).

The assumption of meson pole dominance for matrix elements of the energy momentum tensor is tested using empirical results on tensor meson decay widths and nucleon coupling constants. Its most significant consequence is the decoupling of the f-exchange contribution from the A amplitude in pion-nucleon scattering. (auth)

9765 (NP–18578) A STUDY OF THE $K\bar{K}\pi$ FINAL STATES FOR $N\bar{N}$ ANNIHILATION AT REST IN THE VENEZIANO LANGUAGE. Note No. 277. Benfatto, G.; Cassandro, M.; Lusignoli, M.; Nicolo, F. (Rome Univ. (Italy). Istituto di Fisica. Istituto Nazionale di Fisica Nucleare, Rome (Italy)). 8 Jul 1970. 32p. Dep. NTIS (U. S. Sales Only).

The $N\bar{N} \to K\bar{K}\pi$ processes are studied in terms of four-point Veneziano functions "à la Lovelace." A duality breaking correction term is added to describe the φ bump. The theoretical mass spectra and angular distributions are in good qualitative agreement with the experimental data. Being the daughter resonances a specific feature of any Veneziano model their contributions to the various bumps were evaluated and found quite important. (auth)

9766 LEPTONIC DECAYS OF VECTOR MESONS WITH THE ACCOUNT OF RADIATIVE CORRECTIONS. RADIATIVE LEPTONIC DECAYS OF VECTOR MESONS. Kerimov, B. K.; Tsvetkov, V. P. (Moscow State Univ.). Yadern. Fiz.; 12: 821-5(Oct 1970). (In Russian).

A radiative correction of the first order in α to the probability of the vector meson decay ($V = \rho^0, \omega, \varphi$) into an electron–positron (or muon) pair is calculated. The leptonic decay of the vector meson with the emission of a hard photon is also considered. The expressions for the energy spectra of photons and leptons of the decay are obtained as well as the constant $\gamma_V^2/4\pi$ of the vector dominance model taking into account the radiative corrections. (auth)

9767 DETERMINATION OF $\pi\pi$ SCATTERING PHASE SHIFTS IN REACTION $\gamma p \to \pi\pi p$ AT HIGH ENERGY. Velikson, B. A. (Ioffe Inst. of Physics and Tech., Leningrad). Yadern. Fiz.; 12: 847-55(Oct 1970). (In Russian).

Explicit expressions for the angular distributions of reaction $\gamma p \to \pi\pi p$ at high energies are obtained when the main contribution to the amplitude appears to be from the vacuum Regge pole exchange. These expressions explicitly contain the $\pi\pi$ scattering phase shifts. The interference of the one-photon and one-reggeon exchange is also taken into account. The formulas obtained may be used for the experimental determination of the $\pi\pi$ phase shifts. (auth)

9768 SHARP STATES IN THE SPECTRUM OF LOW-LYING MESONS. Rosner, J. L. (Univ. of Minnesota, Minneapolis). Contract AT(11-1)-1764. Phys. Lett.; 33B: 493-8(7 Dec 1970).

The existence of a family of narrow, low-lying mesons of ordinary I, Y is suggested. These would coexist with the wider states usually assigned to $q\bar{q}$: L = 1 in a quark model, and in particular would give rise to the A_2 splitting. The assignment of these states to a $qq\bar{q}\bar{q}$ multiplet leads to their narrowness. Such states were predicted by applying duality to baryon-antibaryon scattering. Their partners of "exotic" I and Y would lie higher in mass (at least one below 1.9 GeV, probably), and need not be so narrow. (auth)

9769 LINEAR RISING TRAJECTORIES THEORY OF NUCLEON–ANTINUCLEON ANNIHILATION. Rubinstein, H. R. (Chalmers Univ., Goteborg. Weizmann Inst. of Science, Rehovot, Israel). Phys. Lett.; 33B: 477-80(7 Dec 1970).

Using linear rising trajectories from threshold on, the multiplicity structure and its energy dependence are explained for all annihilation channels. Many striking features are predicted and whenever data are available they are very well verified. It turns out, not surprisingly, that the π trajectory dominates the problem. (auth)

9770 NOVEL INTERPRETATION OF THE HOLE STRUCTURE IN $\bar{p}n \to \pi^-\pi^-\pi^+$. Odorico, R. (CERN, Geneva). Phys. Lett.; 33B: 489-92(7 Dec 1970).

A natural interpretation of the hole structure exhibited by the recent data for $\bar{p}n \to \pi^-\pi^-\pi^+$ in flight, and not explained by the Veneziano model, is proposed. A dual formula with properties

XUM

analogous to those of Veneziano, Virasoro and Mandelstam, but with a different dynamical content, is presented. (auth)

9771 DUAL RESONANCE MODEL AND EXTENDED PARTICLE MODEL WITH ARBITRARY NUMBER OF QUARK–ANTIQUARK PAIRS. Fujimura, Kimio (Waseda Univ., Tokyo); Kobayashi, Tsunehiro. Progr. Theor. Phys. (Kyoto); 44: 821-3 (Sep 1970).

It is shown that the dual resonance model can be represented in the previously proposed extended particle model with an arbitrary number of quark-antiquark pairs which are described by harmonic oscillator variables. The meson–meson scattering is discussed for simplicity, where spin-unitary spin indices of quarks are neglected. (L.B.S.)

9772 ANALYTICAL PROPERTIES OF THE EXACTLY SOLVABLE NONRELATIVISTIC TWO-CHANNEL SCATTERING PROBLEM. Kharakhan, M. L. (Moscow State Univ.). Teor. Mat. Fiz.; 5: 262-75(Nov 1970). (In Russian).

An exactly solvable nonrelativistic example is investigated of the two-channel scattering problem for the system of two neutral spinless bosons. The explicit form of the S-matrix is obtained as the quotient of matrices of the Jost type. The assumption made that the identities $S_{12} = S_{21} = 0$, $S_{22} = 1$ hold in the region between the thresholds is checked, and it is found that the identities mentioned can be violated. The connection was observed between the identities and the T-invariance condition. The peculiar features of the scattering and reaction cross section are investigated for the case when the pole is present on the nonphysical sheet near the upper threshold in the region between the thresholds. (auth)

9773 MAGNITUDE OF HIGH-ENERGY MESON–MESON TOTAL CROSS SECTIONS. Abarbanel, H. D. I.; Chew, G. F.; Goldberger, M. L.; Saunders, L. M. (Princeton Univ., N. J.). Phys. Rev. Lett.; 25: 1735-7(21 Dec 1970).

The total cross section for meson–meson scattering at high energy is calculated using a simple, but plausible, SU(n)-symmetric multiperipheral model. The resulting σ_T is of the order $16\pi^3/NM_V^2$, where M_V is the central mass of the dominant low-energy resonance multiplet in elastic meson–meson scattering and N is the dimensionality of the multiplet of the incident mesons. The nongeometric character of this result is discussed. (auth)

9774 DECAY OF RESONANCE STATES AND DETERMINATION OF THEIR QUANTUM NUMBERS. Dubovikov, M. S.; Suimonov, Yu. A. (Moscow Physical-Technical Inst.). Usp. Fiz. Nauk; 101: 655-96(Aug 1970). (In Russian).

In a review on the basis of the unitarity approach the general method of determination of the spins and parities of resonances was stated, based on the law of conservation of momentum and parity in resonance production and decay reactions. This method is that of polarizing moments. The sequence of specific decays was examined. As an illustration of the method, results of experimental works are cited. (tr-auth)

9775 HARD-PION CURRENT ALGEBRA, UNITARIZATION, AND I = 0 s-WAVE $\pi\pi$ SCATTERING. Rockmore, Ronald (Rutgers–The State Univ., New Brunswick, N. J.). Phys. Rev., D; 2: 2628-30(1 Dec 1970).

Using current algebra and a method of pole and cut dominance, a two-parameter effective-range formula for the scalar $\pi\pi$ form factor is obtained. The fit to the I = 0 s-wave $\pi\pi$ phase shift derived from this result favors the "up-down" solution and supports the existence of a broad ϵ resonance. (auth)

9776 EIKONAL REGGE MODEL FOR ELASTIC SCATTERING PROCESSES. Frautschi, S. C.; Hamer, C. J.; Ravndal, F. (California Inst. of Tech., Pasadena). Contract AT(11-1)-68. Phys. Rev., D; 2: 2681-6(1 Dec 1970).

The Frautschi-Margolis version of the Regge eikonal model is extended to include secondary Regge trajectories. Physical properties of the model are discussed. In particular, the "shrinkage" of $d\sigma/dt$ observed at present energies (rapid shrinkage for pp and K^+p, little or no shrinkage for π^+p and K^-p, antishrinkage for $\bar{p}p$) is related to the energy dependence of σ_{tot} (pp and K^+p nearly flat, π^+p and K^-p falling slowly, $\bar{p}p$ falling rapidly). (auth)

9777 SCALAR FORM FACTORS JUST BEYOND THE TREE APPROXIMATION. Rockmore, Ronald (Rutgers–The State Univ., New Brunswick, N. J.). Phys. Rev., D; 2: 2693-8(1 Dec 1970).

Using the algebra of currents and current divergences derived from the chiral SU(3) symmetry-breaking model of Gell-Mann, Oakes, and Renner and a method of pole and cut dominance, two-parameter effective-range formulas are derived for scalar (I = J = ½)Kπ and (I = J = 0)$\pi\pi$ form factors. The fit to the I = ½ s-wave Kπ phase-shift data of Antich et al. favors their "lower" solution with m_k = 1150 MeV and supports the existence of a broad k resonance. It is shown that the introduction of the similarly broad ϵ resonance which emerges from these considerations into the weak-interaction scheme $K_L^0 \to \epsilon \to \pi\pi$ makes agreement with the experimental value of the K_L^0-K_S^0 mass difference difficult, if the K_L^0 mass shift is not small. (auth)

9778 CALCULATION OF THE MASS SHIFTS OF THE K_S MESON. Coulter, Philip W. (Univ. of California, Irvine). Phys. Rev., D; 2: 2725-7(1 Dec 1970).

The mass shifts of the K_S meson are calculated in a multichannel ND^{-1} formalism by considering coupling of the K_S meson to both the I = 0 and I = 2 (J = 0) $\pi\pi$ states. A pole approximation is used for the weak coupling of the K_S meson to the $\pi\pi$ channel. The results for the coupling of K_S to the I = J = 0 $\pi\pi$ partial wave give a value of $\Delta m_s^{(0)}/(\frac{1}{2}\gamma_s^{(0)})$ of the order of −1, in agreement with previous calculations. The ratio $\Delta m_s^{(2)}/(\frac{1}{2}\gamma_s^{(2)})$ is sensitive to the high-energy behavior of the I = 2, J = 0 phase shift and may be larger than previously expected. (auth)

9779 ESTIMATES OF THE MASS OF THE NINTH PSEUDOSCALAR MESON. Rodenberg, R.; Zerwas, P. (Technische Hochschule, Aachen). Phys. Rev., D; 2: 2730-1(1 Dec 1970).

Using Gell-Mann's ansatz for the SU(3) × SU(3) symmetry-breaking part in the strong Hamiltonian density, a sum rule for the spin-zero spectral functions of the pseudoscalar axial-vector current octet is derived. Saturating the sum rule with the lowest-lying states, the mass of the ninth pseudoscalar meson can be estimated as m ≈ 1 GeV. (auth)

9780 COMMENT ON A MESON DECAY FROM A CHIRAL LAGRANGIAN MODEL. Gounaris, G. J. (Brookhaven National Lab., Upton, N. Y.). Phys. Rev., D; 2: 2734-7(1 Dec 1970).

The decay rates of $\omega \to 3\pi$, $\eta \to \pi^+\pi^-\gamma$, $X^0 \to \pi^+\pi^-\gamma$, $\eta \to \pi^0\gamma\gamma$, and $X^0 \to \pi^0\gamma\gamma$ are calculated using a chiral Lagrangian model suggested previously. The effects of the contact interaction and the σ-pole terms in these decay modes are studied in detail. (auth)

9781 CHIRAL SU(2) × SU(2) DYNAMICS FOR A_1, ρ, AND π MESONS. Ogievetsky, V. I.; Zupnik, B. M. (Joint Inst. for Nuclear Research, Dubna, USSR). Nucl. Phys.; B24: 612-22(1970).

It is remarked that the conventional effective Lagrangian with ρ and A_1 mesons contains trilinear and quadrilinear derivative couplings. Thus one should add independently all terms with three and four field derivatives; the theory should then contain a number of arbitrary parameters. A new Lagrangian for the A_1 $\rho\pi$ system containing no more than two field derivatives in each term is suggested. This model is determined by only four parameters g_ρ, g_A, m_ρ, M_A and gives the smoothest momentum dependence for the contact vertices. The reasonable value $\delta = -1$ is derived for the anomalous magnetic moment of A_1 if the KSFR relation holds and also the model is applied to $\pi\pi$ scattering and A_1 decay. (auth)

9782 SUMMING SOFT PSEUDOSCALAR PIONS. Fried, H. M. (Brown Univ., Providence). Phys. Rev., D; 2: 3035-40 (15 Dec 1970).

Momentum-transfer-dependent damping of the nucleon form factors due to the virtual exchange of soft nonchiral pseudoscalar-pion pairs is estimated. When chirality is enforced, by embedding the calculation in the nonlinear σ model, these soft effects are shown to cancel to all orders in the strong coupling. By themselves, the contributions described here do not easily fit the experimental data. (auth)

9783 SUMMING SOFT PIONS. Brown, Lowell S. (Univ. of Washington, Seattle); Weinberg, Steven. Contracts AT(45-1)-1388; AT(30-1)-2098. Phys. Rev., D; 2: 3083-5(15 Dec 1970).

A simple derivation of Weinberg's result on the chiral-symmetric coupling of soft pions to a high-energy process is presented. His formula for soft-virtual-pion corrections is shown to be not invariant under canonical transformation of the pion field. Thus this formula is model dependent and not a consequence of chiral symmetry. A reply is given by Weinberg, who suggests that the error made in the use of the tree approximation does not affect the physical significance of the results. (L.B.S.)

9784 RESTRICTIONS ON PION–PION SCATTERING FROM CROSSING SYMMETRY AND UNITARITY. Dilley, James (Ohio Univ., Athens). Nucl. Phys.; B25: 227-44(1971).

Using only analyticity, crossing symmetry, and unitarity, two distinct types of pion–pion scattering amplitudes are found. One class includes a wide range of non-physical solutions of the "s-wave dominant" type: these can be rejected only through assumptions other than crossing symmetry and unitarity. The second class, also found by other authors, contains the physical amplitudes. The solutions, plus some further experimental information, agree well with the scattering lengths suggested by Morgan and Shaw, $a_0 = 0.16 \pm 0.04$, $a_2 = -0.05 \pm 0.01$. (auth)

XUM

Strong (Baryon No. = 1)

Refer also to abstracts 9667, 9878, and 9894.

9785 (DESY-70/55) NEW VACUUM TRAJECTORY FOR PION-NUCLEON SCATTERING. Sundermeyer, Kurt (Deutsches Elektronen-Synchrotron, Hamburg (West Germany)). Oct 1970. 24p. Dep. NTIS (U. S. Sales Only).

It is shown that the asymptotic behavior of the isospin-zero part $A^{(+)}$ of the invariant amplitude A in πN-scattering is determined by a vacuum trajectory with $\alpha(0) = -0.47 \pm 0.17$. With duality arguments and continuous-moment sum rules the assumption is confirmed that s-channel helicity is conserved in πN-scattering. Because of the smallness of the trajectory, the influence of strong contributions of $\Delta(1236)$ and possible complications by wrong-signature nonsense points the slope cannot be satisfactorily determined. (auth)

9786 POSSIBILITY OF OBSERVING ρ'' DAUGHTER RESONANCE IN $\pi \to 2\pi$ REACTION IN NUCLEAR FIELD. Iroshnikov, G. S.; Nikitin, Yu. P. (Moscow Engineering-Physics Inst.). Yadern. Fiz.; 12: 856-9(Oct 1970). (In Russian).

Possible experimental observation of the ρ'' daughter resonance is discussed. It is shown that the Veneziano model predicts a small contribution from this resonance to the amplitudes of the processes studied previously. A reaction where the ρ'' meson may be detected is proposed. (auth)

9787 ANGULAR DISTRIBUTIONS OF SECONDARY PARTICLES IN THE THERMODYNAMIC MODEL. Ranft, J. (Karl-Marx Univ., Leipzig). Phys. Lett.; 33B: 481-3(7 Dec 1970).

Angular distributions obtained from the thermodynamic model of multi-particle production are compared with cosmic ray results at 175 GeV/c and with angular distributions obtained according to parametrizations with Feynman like scaling behavior. (auth)

9788 USE OF SIMPLE-HARMONIC FORCES IN THE NON-RELATIVISTIC QUARK MODEL. Faiman, David. Urbana, Ill.; Univ. of Illinois (1969). 102p. University Microfilms Order No. 70-13,301.

Attention is drawn to a possible band structure displayed by the known N* resonances. The observed spectrum is similar to that predicted by a paraquark harmonic-oscillator shell model. Exact three-body Schroedinger wave functions are used to compute the Nπ partial decay widths, assuming the pion emission takes place via a one-quark de-excitation. The agreement with experiment is sufficiently good to warrant an investigation of the Nπ decay widths of all resonances predicted to have masses up to about 2 GeV, and such an investigation is performed. The model is then used to estimate the radiative widths of the observed N* resonances. In the "second resonance region" of pion photoproduction, both the $S_{11}(1550)$ and $D_{13}(1525)$ resonances (and possibly the $D_{11}(1470)$, depending on what should be taken as its Nπ width) are expected to be important, while in the "third resonance region" $F_{15}(1690)$, $S_{11}(1710)$ and $D_{13}(1690)$ are expected to have comparable contributions. The mixing angle between the two S_{11} resonances is determined to be about 35°. In inelastic electron scattering $ep \to eN^*$, the $S_{11}(1550)$ and $D_{13}(1525)$ resonances are expected to dominate over the $P_{11}(1470)$. The neutral $P_{11}(1470)$ radiative width is found to be smaller than the charged width, in contrast to an SU(3) $\underline{10}$ assignment for this resonance. The model is extended to include the strangeness-zero meson resonances, and the root mean square pion radius is found to be larger than that of the nucleon. The principal failures of the model are its inability to predict the correct shape for the nucleon electromagnetic form factors, and both the proton magnetic moment and the pion-nucleon coupling constant are predicted to be 40% larger than the experimental findings. (Diss. Abstr. Int., B)

9789 SUM RULES FOR THE RATIO OF THE $\pi^{\pm}$p-SCATTERING AMPLITUDES. Baluni, V. Z.; Vernov, Yu. S. (Inst. of Physics, Moscow). Teor. Mat. Fiz.; 5: 235-43(Nov 1970). (In Russian).

Using the principles of analyticity, unitarity and crossing symmetry the exact integral relation between $|f + (E)/f - (E)|$ and the difference of phases of $f + (E)$ and $f - (E)$, and also the analogous relation between $|f + (E)/f - (E)|$ and the sum of the phases of these amplitudes (here $f \pm (E)$ are $\pi^{\pm}$p-forward scattering amplitudes) are derived. The restrictions on $\int_1^{\infty} \ln|f + (E')|/|f - (E')|\, (dE')/(\sqrt{E'^2 - 1})$ are found. (auth)

9790 FERMION REGGE TRAJECTORY. Iwasaki, Yoichi (Kyoto Univ.). Progr. Theor. Phys. (Kyoto); 44: 777-82(Sep 1970).

It is shown that there is no relation between the MacDowell symmetry and the existence of parity doublets, and that there are examples, satisfying the MacDowell symmetry in which the Regge parameter is not regular at the point W = 0. The asymptotic behavior in the ladder model was also calculated and an explicit form of the Regge trajectory was obtained. (auth)

9791 STUDY OF π^--MESIC ATOMS BY MEANS OF SCATTERING LENGTHS. Lambert, E. (Univ., Neuchatel, Switzerland). Helv. Phys. Acta; 43: 713-31(1 Oct 1970). (In French).

From measurements on pionic atoms the π-nucleus experimental scattering lengths are determined. These s and p scattering lengths are then connected to those of the π-N elementary process through a multiple scattering theory. The binding of the nucleons is neglected, and the nuclear structure is introduced in a simple way by means of the independent particle model. The absorption is treated phenomenologically by taking complex values for the π-N scattering parameters. A set of these parameters is then adjusted to the experimental results. (auth)

9792 MESON-BARYON CONSISTENCY CONDITIONS FROM DUALITY. Capps, Richard H. (Purdue Univ., Lafayette, Ind.). Phys. Rev., D; 2: 2640-5(1 Dec 1970).

A duality requirement and a simple proportionality hypothesis involving the residues of baryonic Regge trajectories are used to derive a self-consistency condition for the scattering of pseudoscalar mesons from spin-$\frac{1}{2}$ baryons. Essentially, the condition states that the differences between the residues of even- and odd-signature baryon trajectories are the components of an eigenvector of the $s \leftrightarrows u$ channel crossing matrix. Several different forms of the consistency condition are discussed, one of which involves residues of trajectories in the physical region, at the energies of the lowest resonances on the trajectories. Experimental values of partial widths of resonances are used to check this latter form for πN, $\pi\Lambda$, and $\pi\Sigma$ scattering. The agreement with experiment is good. (auth)

9793 πN CHARGE-EXCHANGE POLARIZATION IN THE VENEZIANO MODEL. Maharana, J.; Ramachandran, R. (Indian Inst. of Tech., Kanpur). Phys. Rev., D; 2: 2713-17(1 Dec 1970).

Pion-nucleon charge-exchange polarization is calculated in various Veneziano representations for πN scattering. The results are in qualitative agreement with the experimental data for some sets of parameters. It is not possible, however, to resolve the non-uniqueness of the Veneziano representation from this information alone. (auth)

9794 PHENOMENOLOGICAL LAGRANGIAN MODEL OF CHIRAL SU(3) × SU(3) FOR MESONS AND BARYONS WITH SYMMETRY BREAKING. Lam, Yuk-Ming P.; Lee, Yee Yen (Univ. of Chicago). Phys. Rev., D; 2: 2976-82(15 Dec 1970).

Using the techniques of nonlinear realization of SU(3) × SU(3), a Lagrangian is written for the pseudoscalar nonet and $\frac{1}{2}^+$-baryon octet with a symmetry-breaking term transforming like a vector in a $(3,3^*) \oplus (3^*,3)$ representation of SU(3) × SU(3). This Lagrangian yields a mass formula (different from the Gell-Mann-Okubo mass formula) for the pseudoscalar octet, and, if η-η' mixing is neglected, then this formula fits the experimental masses to an accuracy of about 1 MeV. From this Lagrangian, explicit expressions for the axial-vector currents in terms of particle fields are obtained. The tree-diagram prescription then yields a modified Goldberger-Treiman relation consistent with experimental measurements. (auth)

9795 BOX DIAGRAM FOR THE INTERACTION OF PSEUDOSCALAR BOSONS WITH SPIN-$\frac{1}{2}$ FERMIONS. Brunet, Robert C. (Univ., Montreal). Phys. Rev., D; 2: 3064-73(15 Dec 1970).

Explicit expressions are found for the invariant-amplitude contributions of the box diagrams in the interaction of pseudoscalar bosons with spin-$\frac{1}{2}$ fermions. The spin complications are reduced using unitarity such that the A and B amplitudes can be expressed as single-variable integrals over closed-form analytic functions. The problem is solved for the elastic-process amplitudes and is useful in calculations including fourth-order terms. Previous calculations used mainly numerical methods; we rely on exact partial-fraction expansions to obtain amplitudes from a few key analytic functions. The amplitudes are calculated independently for both the s and t channels and are tested by three different consistency checks. Various useful dispersion-integral forms are given, with emphasis on those suitable for partial-wave expansions. The closed forms obtained also yield "natural" subtraction points for the s-variable integrals. In writing the crossed box amplitude for convenient partial-wave expansion, a relation free from any formal dependence on a subtraction is found. This is due to an improved convergence of the absorptive parts in the new functional dependence which arises. The partial-wave contributions are also given explicitly. (auth)

9796 LOCAL DUALITY IN THE INVARIANT AMPLITUDES FOR πN SCATTERING. Shiga, Kunio (Kyushu Univ., Fukuoka); Kinoshita, Kisei; Toyoda, Fumihiko. Nucl. Phys.; B24: 490-508 (1970).

XUM

Local duality for πN scattering in the low- and intermediate-energy regions is investigated from comparisons of the invariant amplitudes constructed from phase-shift data with the interpolated Regge ones. The following results are obtained: (i) Local duality is satisfied with the order $A'^{(+)}$, $B^{(-)}$, $A'^{(-)}$ and $B^{(+)}$. In particular, local duality for the $A'^{(+)}$ amplitude is valid even for the c.m. energy down to 1.5 GeV and finite t-region. (ii) The crossing-even amplitudes having excellent local duality are made up constructively by the prominent resonances which lie on the leading trajectories and have the regularity of the Kycia–Riley rule. (iii) The Freund–Harari conjecture is examined for isospin nonflip amplitudes $A'^{(+)}$ and $B^{(+)}$. The conjecture works well for the imaginary part but not for the real part. Moreover, the modified interference model proposed by Coulter, Ma and Shaw is also examined for the $B^{(-)}$ amplitude: The real part of the background term fills up the dip near $t = -0.6$, in contradiction with the observations. (auth)

9797 TEST OF DOUBLE-REGGE BEHAVIOR OF GENERALIZED VENEZIANO MODEL. Jerome, J. A.; Simmons, W. A. (Univ. of Hawaii, Honolulu). Contract AT(04-3)-511. Nucl. Phys.; B24: 623-32(1970).

A model based upon the generalized Veneziano model is constructed in order to compare the behavior of the B_5 function with that of a conventional double-Regge model and with experimental data. The model is patterned after the recent work of Petersson and Törnqvist and of Chan et al., and is constructed to describe the reaction $K^+p \to K^+p\omega$ at 9.0 GeV/c. This reaction has been described accurately by a double-Regge model in which the omega is treated as a stable particle and in which the pomeron is ignored. The B_5 model, also constructed for a stable omega and without a pomeron contribution, reproduces, with only a single adjustable parameter, the general features of the data; sharply peaked momentum transfer distribution and smooth mass plots with no prominent resonances. There is a statistically significant disagreement with the height of the pp momentum transfer peak. The assumptions underlying the model are discussed. A modified version is applied to data which have been subjected to a phase-space cut. The model is compared with available data at 4.6 GeV/c. (auth)

9798 PHOTOPRODUCTION OF THE ISOBAR Δ (1238). Dogyust, I. V.; Naisteter, S. I. (Uzhgorod State Univ., USSR). Ukr. Fiz. Zh.; 15: 1381-3(Aug 1970). (In Russian).

Angular distribution asymmetry of π meson emissions during photoproduction of Δ(1238) isobar at 0.7 to 1 GeV photon energies was calculated and results obtained were compared with experimental data. (R.V.J.)

9799 BUILDING MESON–BARYON SCATTERING AMPLITUDES FROM DUALITY. Auvil, P. R.; Halzen, F.; Michael, C.; (CERN, Geneva). Nucl. Phys.; B25: 317-20(1971).

Duality constraints are extended to include the interrelation of the structure of the s-channel spectrum with that of u- and t-channels. Predictions for t-channel meson couplings are presented within an SU(3) framework. (auth)

9800 REGGE CUTS AND ASYMPTOTIC SUM RULES FOR πN FORWARD SCATTERING. Martin, A. D.; Wit, R. (CERN, Geneva). Nucl. Phys.; B25: 85-92(1971).

A dispersion representation for the inverse of the forward scattering amplitude is derived, which leads to a useful sum-rule constraint on the high-energy data. The sum rule is applied to an analysis of pion–nucleon forward scattering data. (auth)

9801 DIRECT-CHANNEL REGGE POLES AS A MEANS OF TREATING THE UNPHYSICAL REGION IN FINITE-ENERGY SUM RULES. Bowcock, J. E.; Ng, P. H. (Univ. of Birmingham, Eng.). Nucl. Phys.; B25: 93-108(1971).

In using FESR at fixed momentum transfer an analytic continuation of the amplitude into the unphysical region near to threshold is necessary. It is shown how direct channel Regge poles may be used to facilitate this and a detailed application to the πN amplitudes is given. (auth)

9802 MESON-EXCHANGES IN THE ISOSPIN ZERO t-CHANNEL OF PION–NUCLEON SCATTERING. Engels, J. (Univ. of Karlsruhe, Ger.). Nucl. Phys.; B25: 141-58(1971).

The πN backward dispersion relations for even isospin ($I_t = 0$) are investigated with phase shifts and the baryon Regge-exchange model as input. The $\pi\pi N\bar{N}$ cut contributions to the dispersion relations are then used to estimate in an $\epsilon(700)$ and $f^0(1260)$ exchange model the meson–nucleon coupling constants. (auth)

Strong (Baryon No. ≥ 2)

9803 (ITEF-759) MANY-BARYON RESONANCES. Kondratyuk, L. A.; Shapiro, I. S. (Gosudarstvennyi Komitet po Ispol'zovaniyu Atomnoi Energii SSSR, Moscow. Institut Teoreticheskoi i Eksperimental'noi Fiziki). 1970. 32p. (In Russian). Dep. NTIS (U. S. Sales Only).

The quasinuclear model of many baryon resonance, which results from Δ-N potential interaction, is formulated. The interaction Δ-N, decay modes and production mechanisms of two- and three-baryon resonances, involving Δ-isobar, are investigated. The experimental data on two-baryon resonances with isospin $T = 1$ are analyzed. (auth)

9804 (JINR-P2-5231) CROSS SECTION OF $\bar{K}d \to KY_1Y_2$. Lapidus, L. I.; Tarasov, A. V.; Tseren, Ch. (Joint Inst. for Nuclear Research, Dubna (USSR). Lab. of Nuclear Problems). 1970. 9p. (In Russian). Dep. NTIS (U. S. Sales Only).

The interactions of $\bar{K}$ mesons with nuclei which generate hyperon and meson pairs, are currently widely investigated; therefore, their cross section is of great general interest. The study indicated that the cross section of the $\bar{K}d \to KY_1Y_2$ is related in a simple manner to the cross section of single collisions of elementary particles with nucleons. The problem was examined on the basis of the pion chain in the $\bar{K}d \to KY_1Y_2$ ($\bar{K}d \to \pi Y_1N_2 \to KY_1Y_2$) reaction. The derived expression leads directly to a formula obtained in a previous paper on the interaction of $\bar{K}$ mesons with nuclei. (TTT)

9805 CONNECTION BETWEEN INELASTIC PROTON–PROTON REACTIONS AND DEEP INELASTIC ELECTRON SCATTERING. Berman, S. M. (Imperial Coll. of Science and Tech., London. Stanford Univ., Calif.); Jacob, M. Phys. Rev. Lett.; 25: 1683-6(14 Dec 1970).

Following the idea that the electromagnetic and nuclear distributions behave similarly for large momentum transfers the possibility of relating the deep inelastic electron scattering to large-momentum-transfer and high-energy inelastic proton–proton reactions is examined. (auth)

9806 BREAKDOWN OF POMERANCHUK'S CONJECTURE AND THE COMPOSITE STRUCTURE OF HADRONS. Takada, Yoshio (Tokyo Inst. of Tech.). Progr. Theor. Phys. (Kyoto); 44: 765-71(Sep 1970).

Quark model is applied to high energy asymptotic limit scattering processes. It is shown that the Pomeranchuk's conjecture may break down for hadron–hadron scattering even if it holds good for quark–quark scattering. (auth)

9807 TWO-PION EXCHANGE CONTRIBUTION TO NUCLEON–NUCLEON SCATTERING ON THE BASIS OF PION–PION DYNAMICS. Furuichi, Susumu (Rikkyo Univ., Tokyo); Kanada, Hiroyuki; Watanabe, Keiji. Progr. Theor. Phys. (Kyoto); 44: 711-28(Sep 1970).

Calculation of nucleon–nucleon scattering is presented as a completion of our works on the systematic studies of low energy strong interactions. The essential part of the present work is a quantitative evaluation of the two-pion-exchange contribution to nucleon–nucleon scattering, starting from the pion–pion scattering phase shifts in the $I = L = 0$ and $I = L = 1$ states. In this calculation, the parameters for the two-pion contribution with $I = L = 1$ state are predetermined from the iso-vector part of the nucleon electromagnetic form factors. For the $I = L = 0$ state, both cases of the up-down and the down-up solutions for S-wave pion–pion scattering are examined. The $I = 0$ S-wave pion–pion phase shift $\delta^{0(0)}$ in the former case shows a very broad enhancement below 1 GeV region, whereas $\delta^{0(0)}$ in the latter case contains a sharp resonance in the neighborhood of the ρ-meson mass. For the higher angular momentum two-pion states $L \geq 2$, pion–pion correlations are neglected. In addition to these two-pion contributions and the one-pion contribution, inclusion of the ω- and the η-meson contributions leads to the results which agree well with the experimentally determined nucleon–nucleon scattering amplitudes, when the up-down solution is taken for $\delta^{0(0)}$. However, the down-up solution for $\delta^{0(0)}$ makes the $I = L = 0$ part of the two-pion contribution too large and reasonable fit with the experiment on nucleon–nucleon scattering cannot be obtained for the latter case. From the present analysis it is concluded that the up-down solution for S-wave pion–pion scattering is superior to the down-up solution. This gives another indication to the importance of the non-resonant part of two-pion contribution as well as that given by the analysis of the nucleon electromagnetic form factors. It is also shown that in the present treatment the η-meson contribution becomes rather large. (auth)

9808 SURFACE EXCITATION MODEL OF HADRON RESONANCES. Aihara, Yoshinao; Bando, Masako; Monden, Yoshimi; Wakaizumi, Seiichi (Kyoto Univ.). Progr. Theor. Phys. (Kyoto); 44: 729-45(Sep 1970).

The surface excitation model widely known in nuclear physics is applied to the hadron reactions. The resonance production processes with the exchange of no quantum number except angular

momentum, i.e. with Pomeron exchange are analyzed and it is shown that the model nicely explains the empirical selection rule proposed by Morrison and other characteristic features of these processes. For this kind of Pomeron, we name the "Pomeron of the second kind." (auth)

9809 DERIVATION OF THE WU–YANG CONJECTURE IN THE BOOTSTRAP MODEL. Hwa, Rudolph C. (State Univ. of New York, Stony Brook. California Inst. of Tech., Pasadena). Phys. Rev. Lett.; 25: 1728-31(21 Dec 1970).

On the basis that the Pomeranchukon is a branch point with vanishing strength at the tip, the small-t dependence of the Pomeranchukon is related to the properties of the secondary trajectory P′. Then the exchange degeneracy between P′ and ρ is used to deduce the (form factor)^4 behavior as conjectured by Wu and Yang. Multiple-scattering correction at large t then modifies the t dependence in accordance with the Chou–Yang description. High-energy behavior is discussed. (auth)

9810 MESON FACTORIES AND THE TWO-NUCLEON PROBLEM. Moravcsik, Michael J. (Univ. of Oregon, Eugene). Phys. Today; 23: No. 10, 40-6; 46(Oct 1970).

The interest in the two nucleon problem is considered with regard to the development of ultra-high energy accelerators. Nuclear structure, the charge-independence hypothesis, relevance to particle physics, and resonance formation are discussed. (J.F.P.)

9811 THEORETICAL ESTIMATES OF QUARK PRODUCTION CROSS SECTIONS AT ULTRAHIGH ENERGIES. Tuan, S. F. (Univ. of Hawaii, Honolulu). Phys. Rev., D; 2: 2646-55(1 Dec 1970).

Various theoretical models for the production of quarks at ultrahigh energy are discussed. In particular, a well-defined temperature model (suggested by Yang sometime back) is used to illustrate the type of production cross section expected in this picture for a given quark mass and c.m. energy. (auth)

9812 DETERMINATION OF THE $\pi\Lambda\Sigma$ AND $\pi\Sigma\Sigma$ COUPLING CONSTANTS UTILIZING ADLER'S CONSISTENCY CONDITION. Chan, C. H.; Smalley, L. L. (Univ. of Alabama, Huntsville). Phys. Rev., D; 2: 2635-9(1 Dec 1970).

An independent method to determine the $\pi\Sigma\Lambda$ and $\pi\Sigma\Sigma$ coupling constants is presented. It is accomplished by writing a once-subtracted dispersion relation for $\pi\Lambda$ and $\pi\Sigma$ scattering amplitudes slightly off the incident-pion mass shell and evaluating the subtraction constant at the point where Adler's consistency condition is valid. The results obtained are $g_{\pi\Sigma\Lambda}{}^2/4\pi = 20.9 \pm 6.7$ and $g_{\pi\Sigma\Sigma}{}^2/4\pi = 11.4 \pm 5.5$, in good agreement with the earlier calculation of Chan and Meiere using a completely different method. (auth)

9813 REGGE-POLE MODEL FOR pp AND $\bar{p}p$ ELASTIC SCATTERING AT HIGH ENERGIES. Austin, Donald M.; Greiman, William H.; Rarita, William (Univ. of California, Berkeley). Phys. Rev., D; 2: 2613-27(1 Dec 1970).

High-energy data for pp and $\bar{p}p$ elastic scattering are confronted with the simple Regge-pole model in an attempt to discover which features of these data, if any, are beyond the power of this model. The simplest representation, with only three poles (P, P′, and ω), gives a reasonable fit to all the data except the "dip" structure in the $\bar{p}p$ differential cross sections (DCS). Several types of parametrizations were tested, including various ghost-eliminating mechanisms, and all produced comparable fits. To account for the $\bar{p}p$ DCS structure, and simultaneously circumvent the factorization difficulties caused by the universal zero in the ω amplitude, a fourth pole (the ω') was introduced. The four-pole parametrizations (several were tested) provide adequate fits to all the data, including the $\bar{p}p$ DCS structure, and in addition come much closer to satisfying the sum-rule constraints imposed, through factorization, by the πN and KN analyses. For completeness, another vacuum-type pole (the P″) is introduced and five-pole fits parametrized as in cut models are compared with pure pole models. The results are somewhat ambiguous, showing that the high-energy differential and total cross sections, polarization, ratio of real to imaginary part, and Serpukhov slope data all together are still not sufficient for determining the differences between many possible parametrizations. (auth)

9814 CHARACTERISTICS OF THE PROTON–PROTON INTERACTION DEDUCED FROM THE DATA BELOW 30 MeV. Sher, Michael S. (Michigan State Univ., East Lansing); Signell, Peter; Heller, Leon. Contract AT(11-1)-2061. Ann. Phys. (N. Y.); 58: 1-46(May 1970).

A two-parameter description for each of the low-energy ^{3}P phase shifts is justified and used to perform the first comprehensive analysis of all of the proton–proton scattering data below 30 MeV. Particular attention is paid to magnetic moment, vacuum polarization, and finite electromagnetic structure effects. Effective-range parameters for the ^{1}S and ^{3}P states are determined as well as possible, but distressing irregularities are noted in all of the data between 1 and 10 MeV. Nevertheless, some parameters are determined with precision, such as the singlet scattering length with a value of $a_{pp}^{E} = -7.822 \pm 0.004$ F. It is found that the central, tensor, and spin-orbit P-wave parameters reflect the uncertainties in the low energy data much more accurately than do the phase shifts themselves, and values of the parameters derived from experiment are given. The vacuum polarization interaction is shown to be present with a strength about equal to its theoretical value, but again with some irregularities. Finite electromagnetic structure effects deduced from the Hofstadter–Wilson dipole formula are found to be quite different from those found in previous calculations. The neutron–neutron scattering length, corrected for finite structure effects, is predicted to be $a_{nn} = -17.06$ F. (auth)

9815 Σ-SUPPRESSION IN $^5_\Lambda$He. Law, J.; Nguyen, T. D. (Univ. of Guelph, Ont.). Nucl. Phys.; B24: 579-90(1970).

An approximate way of estimating Σ-suppression in $^5_\Lambda$He by using the scattering data is considered. It is found that the binding in $^5_\Lambda$He can be reduced by 2 to 3 MeV by coupling to the Σ-channel. (auth)

9816 O(2,1) ANALYSIS OF SINGLE-PARTICLE SPECTRA AT HIGH ENERGY. Mueller, A. H. (Brookhaven National Lab., Upton, N. Y.). Phys. Rev., D; 2: 2963-8(15 Dec 1970).

Processes of the type proton + proton → pion + anything at high energy are discussed. The differential cross section for such reactions is expressed in terms of a three-particle → three-particle amplitude. This amplitude is then expanded into O(2,1) representations. If the Pomeranchuk trajectory is the dominant O(2,1) singularity at high energy, the existence of pionization and limiting fragmentation is obtained. Furthermore, the pionization products are essentially independent of the target and projectile, while the fragments of the target are independent of the projectile. Modifications in the presence of strong Regge cuts at J = 1 are discussed. (auth)

9817 DISPERSION METHODS AND THE TWO-NUCLEON INTERACTION IN CHARGED SCALAR THEORY. Scarfone, Leonard M. (Univ. of Vermont, Burlington. Univ. of Miami, Coral Gables). Phys. Rev., D; 2: 3054-63(15 Dec 1970).

The charged scalar static model is studied from the viewpoint of dispersion theory with the aim of including two-meson effects in the binding energy between two nucleons at zero separation. The method of analysis is that due to Blankenbecler and Cook, who advocate the use of vertex functions for investigating bound-state properties. In this case a deuteron vertex is examined in terms of Bronzan's one-nucleon two-meson solution which possesses two- and three-particle unitarity and a crossing-symmetric scattering amplitude. On the one hand, matrix elements containing the deuteron state at one end and two- or three-particle states at the other are contracted with respect to mesons. In this approach a summation over intermediate states involving two nucleons and zero, one, or more mesons is neglected. On the other hand, this summation may be avoided by contracting nucleons, but it appears that this approach leads to an intractable system of coupled integral equations. For this reason, only the simplest matrix element is treated this way, and even then some two- and three-particle contributions are ignored. Under these conditions, it is found that a factorization property of the one-nucleon two-meson connected scattering matrix leads to inhomogeneous Omnès equations having solutions which transform the two-meson dispersion expansion of the deuteron vertex into a condition for the determination of the binding energy. (auth)

9818 SYMMETRIES IMPOSED ON TWO-PARTICLE SYSTEMS. III. ENERGY DEPENDENCE OF PARTIAL-WAVE AMPLITUDES. Klink, William H.; Smith II, Granville J. (Univ. of Iowa, Iowa City). Phys. Rev., D; 2: 2912-26(15 Dec 1970).

From the assumption that the S operator transforms as an irreducible tensor operator under an aproximate symmetry group, called a two-particle symmetry group, it is shown that partial-wave scattering amplitudes can be calculated. Two models, based on different two-particle symmetry groups, are presented. Investigation of the first model makes it clear that an energy-dependent amplitude can be calculated, but the amplitude cannot be identified as a unique partial-wave amplitude. This problem suggests the investigation of the second model, which is then used to calculate S-wave proton–proton elastic scattering phase shifts. Further research along these lines is suggested. (auth)

9819 (3,3) RESONANCE AND NUCLEON POLE FOR NN → NNπ AT LOW AND MODERATE ENERGY. Drechsel, D.; Weber, H. J. (Univ. of Virginia, Charlottesville). Nucl. Phys.; B25: 159-72(1971).

The nucleon pole as generated by soft-pion techniques and the

XUM

(3,3) resonance pole of the isobar model are included in a relativistic treatment of $pp \rightarrow pp\pi^0$ for low and moderate incident proton energies. The total and various differential cross section is calculated and found in agreement with experiment. Except for several well-known coupling constants this description is parameter-free. (auth)

Particle Invariance Principles and Symmetries

General

Refer also to abstract 9839.

9820 RECURRENCE RELATION FOR KOSTANT'S FORMULA. Gruber, B. (St. Louis Univ.); Weber, H. J. Proc. Roy. Irish Acad., Sect. A; 70: 27-(1970).

For the series of groups SU(l + 1) an explicit and closed formula for the multiplicity of weights was obtained which expresses this multiplicity in terms of Kostant's formula for the subgroup SU(l) of the group SU(l + 1) rather than in terms of the familiar formula of Kostant for the group SU(l + 1) itself. (auth) (UK)

9821 CLEBSCH–GORDAN FORMULAS OF THE SU(1,1) GROUP. Ui, Haruo (Tohoku Univ., Sendai). Progr. Theor. Phys. (Kyoto); 44: 689-702(Sep 1970).

The Clebsch–Gordan formulas for d-function are studied for both nonunitary finite dimensional representation and unitary infinite dimensional representation of the SU(1,1) group. It is shown that, in addition to the usual Clebsch–Gordan formulas for the above-mentioned two representations, there exists an additional type of Clebsch–Gordan formula connecting the nonunitary and unitary d-functions. The new kind of Clebsch–Gordan coefficient of the SU(1,1) obtained previously arises naturally in this formula. The three Clebsch–Gordan formulas are proved to be interrelated with each other by analytic continuation. It is further pointed out that all the recurrence formulas of the unitary d-functions —obtainable from the known recurrence relations of Jacobi polynomials —belong actually to this new type of Clebsch–Gordan formula. Explicit algebraic formulas of d-functions are derived by employing an elementary algebraic method analogous to the standard treatment of angular momentum. (auth)

9822 BOSON BOGOLYUBOV TRANSFORMATION AND THE SU(1,1) GROUP. Ui, Haruo (Tohoku Univ., Sendai). Progr. Theor. Phys. (Kyoto); 44: 703-10(Sep 1970).

The homogeneous canonical transformation of boson operators is studied from the standpoint of the SU(1,1) quasi-spin formalism. It is shown that this transformation can be regarded as a rotation in the SU(1,1) quasi-spin space. This situation is just analogous to the SU(2) quasi-spin formalism of many-fermion problem, in which fermion Bogolyubov transformation can be regarded as a rotation in the SU(2) quasi-spin space. The transformation law of state vectors under this boson Bogolyubov transformation is then written down explicitly in terms of the SU(1,1) d-functions obtained in the preceding paper. For clarity, the simplest nontrivial example of one-dimensional harmonic oscillator or, equivalently, a system consisting of one kind of bosons is treated. Generalization to many-boson problem and its possible applications to Bose fluid and nuclear structure are briefly discussed. (auth)

9823 UNITARY REPRESENTATIONS OF THE CONFORMAL GROUP. Leznov, A. N.; Fedoseev, I. A. (Inst. of High Energy Physics, Moscow). Teor. Mat. Fiz.; 5: 181-9(Nov 1970). (In Russian).

An explicit expression of the invariant Hermitian form is found for all representations of the conformal group where such a form exists. Unitary representations are selected by the condition of the positive definiteness of the form. (auth)

9824 REPRESENTATIONS OF GELL-MANN–DASHEN ALGEBRA. Klimyk, A. U. (Inst. of Theoretical Physics, Kiev). Teor. Mat. Fiz.; 5: 167-80(Nov 1970). (In Russian).

The representations of Gell-Mann–Dashen algebra with the structure constants of the arbitrary Lie algebra, in a direct integral of Hilbert spaces are considered. In the case of the structure constants of semisimple Lie algebra a direct integral of spaces can be reduced to the orthogonal sum of the spaces. The case with the structure constants of the group 0(3) is considered in detail. (auth)

9825 KUO TRANSFORMATION IN LINEAR AND NONLINEAR CHIRAL-SYMMETRY THEORIES. Okubo, Susumu (Univ. of Rochester, N. Y.). Phys. Rev., D; 2: 3005-15(15 Dec 1970).

Model Hamiltonians with $(3,3^*) \oplus (3^*,3)$-violating interaction in the theory of Gell-Mann, Oakes, and Renner are investigated for both cases of linear and nonlinear realizations of the SW(3) theory in connection with the Kuo transformation. For the linear case, all mass formulas remain unchanged under the transformation, but not for the nonlinear case. Also, scattering amplitudes are found not to be invariant in general under the Kuo transformation for the nonlinear case. Physical interpretations of these puzzling facts are discussed in detail. (auth)

Applications (Electromagnetic and Weak)

9826 (NYO–2171-329) ON THE POSSIBILITY THAT PULSES OF A LONG RANGE FIELD ARE THE SOURCE OF CP NONINVARIANCE. Atkins, K. R.; Lande, K. (Pennsylvania Univ., Philadelphia. Dept. of Physics). 4 Dec 1970. 6p. Dep. NTIS.

The possibility that pulses of a long range field are the source of CP noninvariance in K_L^0 decays is explored. An experimental test involving correlation in the decay of two $K_L^0 \rightarrow \pi^+\pi^-$ is proposed. (auth)

9827 CP VIOLATION AND MODELS WITH SUPPLEMENTARY PARTICLES. Nikolaev, N. N.; Ryndin, R. M. (Joint Inst. for Nuclear Research, Dubna, USSR). Yadern. Fiz.; 12: 865-70 (Oct 1970). (In Russian).

A test of the CP violation in the $K_L \rightarrow 2\pi$ and $K_L \rightarrow \pi l\nu$ decays is discussed. A pure phenomenological scheme with supplementary particles is considered that is able, though with quite artificial assumptions, to explain the K_L–K_S interference in the two-pion decays and the charge asymmetry in the $K_L \rightarrow \pi l\nu$ decays, retaining the CP conservation. Possible experimental tests of such a scheme are discussed. (auth)

9828 CP VIOLATION IN THE NEUTRAL K SYSTEM (A BRIEF REVIEW OF THE THEORY). Yun, Suk Koo (Syracuse Univ., N. Y.). Int. J. Theor. Phys.; 3: 367-85(Oct 1970).

The theoretical aspect of CP-violation is reviewed. The K_S and K_L states, the unitarity relation, parametrization and analysis, the electric dipole moment of the neutron, η asymmetry and C noninvariance in $\eta_{3\pi}$ are all discussed. Then five theoretical models concerning neutral $K \rightarrow 2\pi$ are dealt with. (auth) (UK)

9829 EXPERIMENTAL TEST OF TIME-REVERSAL INVARIANCE IN $\Sigma^0 \rightarrow \Lambda^0 + e^+ + e^-$. Baggett, Millicent Joan. College Park, Md.; Univ. of Maryland (1969). 148p. University Microfilms Order No. 70-16,019.

Thesis.

There were 1100 events of the type $\Sigma^0 \rightarrow \Lambda^0 e^+ e^-$ analyzed for which the Σ^0 was produced by the interaction of a stopping K^- or Σ^- with a proton in the 30'' hydrogen bubble chamber at the Brookhaven National Laboratory AGS. If time reversal invariance is violated in the electromagnetic interactions of the strongly interacting particles, the Λ^0 could be polarized along the normal to the Σ^0 decay plane, defined by $\vec{N} = \hat{p}_A \times (\hat{k}_+ + \hat{k}_-)$, where $\hat{p}_A$, $\hat{k}_+$, $\hat{k}_-$ are unit vectors along the directions of the lambda, the positron, and the electron in the Σ^0 rest frame. As a measurement of this polarization, the average value of the cosine of the angle between $\vec{N}$ and the direction of the lambda-decay proton in the lambda rest frame was computed. For the unweighted average -0.032 ± 0.017, and for the weighted average (using the magnitude of $\vec{N}$ as weight) -0.030 ± 0.027 are found. Combining the results with the 907 events from the previous Maryland-Heidelberg-Columbia collaboration gives an unweighted average of -0.0092 ± 0.013 and a weighted average of $+0.010 \pm 0.020$. This result is consistent with the absence of any T violation. (Diss. Abstr. Int., B)

9830 ASYMPTOTIC SU(3) SYMMETRY: BROKEN SU(3) AND RELATIONS BETWEEN BARYON MASS DIFFERENCES AND NON-LEPTONIC HYPERON DECAY AMPLITUDES. Danskin, J. H. (Univ. of Edinburgh). Nucl. Phys.; B25: 260-8 (1971).

The technique of asymptotic SU(3) symmetry is extended to the non-vanishing equal-time commutators between vector charges and the time-derivatives of other vector charges. Relations are obtained between the mass splittings in the $\frac{1}{2}^+$ baryon octet and the s-wave amplitudes for non-leptonic hyperon decays. Numerical results agree reasonably well with experimental data. (auth)

Applications (Strong)

Refer also to abstract 9818.

9831 NONEXISTENCE OF AMBIGUITIES IN SU(3) ⊗ SU(3) BREAKING. Mahanthappa, K. T. (Univ., Rome); Maiana, L. Phys. Lett.; 33B: 499-501(7 Dec 1970).

It is shown that a careful treatment of symmetry breaking of

SU(3) ⊗ SU(3) does not lead to any ambiguity in the determination of the $(3,\bar{3}) \oplus (\bar{3},3)$ breaking lagrangian, contrary to the result of Kuo. (auth)

9832 THREE-DIMENSIONAL CANONICAL ALGEBRA AND SO(4,2) DYNAMICAL GROUP. Kobayashi, Kozo (Saitama Univ., Japan). Progr. Theor. Phys. (Kyoto); 44: 817-19(Sep 1970).

The relation between the three-dimensional canonical algebra and the SO(4,2) dynamical symmetry is discussed for the hydrogen atom and baryons. (L.B.S.)

9833 SCHWINGER TERMS AND PSEUDOSCALAR MESONS. Barnes, K. J.; Dondi, P. H. (Queen Mary Coll., London). Nucl. Phys.; B25: 218-16(1971).

Effective meson operators are exhibited for a class of chiral SU(2) current models, and the general ($\frac{1}{2}$N, $\frac{1}{2}$N) symmetry breaking Hamiltonian is constructed from Schwinger terms. A closed form is thus found for the corresponding non-linear pion Lagrangian in general coordinates. (auth)

Field Theories

General

Refer also to abstract 9709.

9834 (RLO-1388-584) CLASSICAL SCHWINGER TERMS. Boulware, David G. (Washington Univ., Seattle. Dept. of Physics); Deser, S. (Brandeis Univ., Waltham, Mass. Dept. of Physics). [1970]. Contract AT(45-1)-1388B. 11p. Dep. NTIS.

Schwinger terms must be present in equal-time ground-state Poisson brackets among currents unless the latter are stationary in that state. (auth)

9835 ADVANCED AND RETARDED SOLUTIONS IN FIELD THEORY. Schwebel, Solomon L. (Boston Coll., Chestnut Hill, Mass.). Int. J. Theor. Phys.; 3: 347-53(Oct 1970).

The appearance of retarded and advanced solutions to the wave equation and the ad hoc choice of one of them in preference to the other led to the claim that electromagnetic theory is incomplete. It is contended that some other condition outside that theory must be invoked in order to make a meaningful physical choice. However, both a physical and mathematical analysis show, that, in fact, both retarded and advanced solutions are necessary and that the rejection of the advanced type of solution is not valid; that its rejection is based on an ambiguous mathematical technique and a faulty physical interpretation. A unique form for the Green's function is obtained which is related to all other types of Green's functions by the appropriate adjunction of solutions to the homogeneous equation. (auth) (UK)

9836 ANOMALOUS PROPERTIES OF VECTOR CURRENTS IN EXACTLY SOLVABLE FIELD THEORY MODELS. Tyutin, I. V. (Lebedev Inst. of Physics, Moscow). Teor. Mat. Fiz.; 5: 253-61(Nov 1970). (In Russian).

Anomalous properties of vector and axial currents are studied in two exactly solvable field theory models in two-dimensional space-time: the interaction of the massless fermion with the external vector and axial fields; the current-current interaction of the two different massless fermions. The method proposed earlier is used for the rigorous determination of the models. Both models are constructed nonambiguously. Heisenberg operators of fields and currents are found. It is shown that the axial current in the first model is not conserving. In the second model the first fermion vector current does not commute with the second fermion field operator at equal times, although the field operators satisfy the canonical anticommutation relations. (auth)

Quantum Field Theory

Refer also to abstracts 9357 and 9690.

9837 (ITF-70-57) EQUAL-TIME COMMUTATOR, SUM RULES AND WARD IDENTITIES IN AXIOMATIC QUANTUM FIELD THEORY. Miranskii, V. A. (Akademiya Nauk Ukrainskoi SSR, Kiev. Institut Teoreticheskoi Fiziki). 1970. 17p. Dep. NTIS (U.S. Sales Only).

The equal-time commutator of currents in the axiomatic quantum field theory is considered. Using some V. A. Vladimirov's theorems the number and the structure of Schwinger terms depending on the asymptotical behavior the Fourier transforms of the retarded functions at infinity are established. As a consequence sufficient conditions for the validity of Gell-Mann-Fubini sum rules are obtained. The validity of normal Ward identities in axiomatic field theory is discussed. (auth)

9838 (NYO-3829-60) CHARGE OPERATORS IN GENERAL QUANTUM FIELD THEORY: THE RIGGED HILBERT SPACE APPROACH. Antoine, J. P. (Pittsburgh Univ., Pa. Dept. of Physics. Louvain Univ. (Belgium). Inst. for Theoretical Physics). Sep 1970. 19p. (CONF-700710-1) Dep. NTIS.

From Conference on Special Topics in Quantum Field Theory, St. Louis, Mo.

The mathematical definition of a charge operator given by the formal integral of a density is studied. It is assumed only that the current density is a local Wightman field, i.e. an operator-valued tempered distribution satisfying the axiom of locality and the strong spectral condition. The current is not assumed a priori to be conserved. (J.F.P.)

9839 (NYO-3829-64) HIGH-ENERGY PHYSICS AT THE UNIVERSITY OF PITTSBURGH. Progress Report, December 1, 1969-December 1, 1970. (Pittsburgh Univ., Pa. Dept. of Physics). Nov 1970. Contract AT(30-1)-3829. 22p. Dep. NTIS.

Summaries are given of the research which includes weak interactions, quantum field theory, group theory, quantum mechanics, and mathematical physics. A list of publications is given. (J.F.P.)

9840 FORMULATIONS OF CLASSICAL AND QUANTUM DYNAMICAL THEORY. Rosen, Gerald. A Series of Monographs and Textbooks. Mathematics in Science and Engineering, Volume 60. New York; Academic Press Inc. (1969). 163p. $9.50.

Classical mechanics is formulated according to Lagrange, Hamilton, and Poisson; quantum mechanics according to Feynman, Schroedinger, and Dirac. The calculus of functional differentiation and integration and the theory of Lie groups and algebras are included. Recent quantum field theory applications of the functional differential operator formulations are also included. (C.E.S.)

9841 RELATIVISTIC QUANTUM MECHANICS OF FERMIONS. Marx, Egon (Drexel Univ., Philadelphia). Int. J. Theor. Phys.; 3: 401-12(Oct 1970).

A modification of the Dirac equation is presented that allows a relativistic quantum mechanics to be formulated for spin-$\frac{1}{2}$ fermions in an external electromagnetic field, with a probabilistic interpretation similar to that in nonrelativistic quantum mechanics and based on an indefinite charge density. It is found that stationary states cannot be interpreted in this manner, and they are replaced by quasistationary states. Also included is a general discussion of the difficulties and possible generalizations of this approach. (auth) (UK)

9842 INTERACTION OF MOLECULAR MULTIPOLES WITH THE ELECTROMAGNETIC FIELD IN THE CANONICAL FORMULATION OF NONCOVARIANT QUANTUM ELECTRODYNAMICS. Atkins, P. W.; Woolley, R. G. (Oxford Univ.). Proc. Roy. Soc. (London), Ser. A; 319: 549-63(10 Nov 1970).

The procedure devised by Dirac for the canonical quantization of systems described by degenerate lagrangians is used to construct the hamiltonian for molecules interacting with the electromagnetic field. The hamiltonian obtained is expressed in terms of the gauge invariant field strengths and the electric and magnetic multipole moments of the molecules. The Coulomb gauge is introduced but other gauge conditions could be used. Finally, a physical interpretation of the unitary transformation that may be used to generate the multipole hamiltonian is given. (auth) (UK)

9843 CAUCHY PROBLEM FOR THE RELATIVISTIC BOLTZMANN EQUATION. Bancel, Daniel (Univ., Paris). Compt. Rend., Ser. A; 271: 694-6(5 Oct 1970). (In French).

The Cauchy problem was studied for the nonlinear Boltzmann equation, in the framework of the special relativity theory.

9844 CRITERION OF ALGEBRAIC CLOSENESS OF THE COMMUTANT OF QUANTUM FIELD. Vasil'ev, A. N. (Leningrad State Univ.). Teor. Mat. Fiz.; 5: 161-6(Nov 1970). (In Russian).

The necessary and sufficient condition of the algebraic closeness (i.e. the closeness with respect to all algebraic operations) of the commutant of a given quantum field is formulated. If the field satisfies the usual requirements of Wightman approach, then the suggestion that the field commutant is a *-algebra implies that this *-algebra is abelian. (auth)

9845 QUANTUM ELECTRODYNAMICS IN EXTERNAL FIELDS. I. Batalin, I. A.; Fradkin, E. S. (Lebedev Inst. of Physics, Moscow). Teor. Mat. Fiz.; 5: 190-218(Nov 1970). (In Russian).

By means of the functional method the solutions are obtained of the Klein-Gordon and Dirac equations in the external field of a special form. The field represents the superposition of an arbitrary stationary homogeneous electromagnetic field and the field of an electromagnetic plane wave with arbitrary spectrum and polarization. The four-momentum of the plane wave is an eigenvector of the stress-tensor of the stationary field. (auth)

XUM

9846 MODIFIED PHOTON PROPAGATOR IN THE ρ-DOMINANCE MODEL. Buchl, R. A.; Nigam, B. P. (Arizona State Univ., Tempe). Progr. Theor. Phys. (Kyoto); 44: 815-17(Sep 1970).

In the ρ-dominance model, a local Lagrangian field theory can be constructed for the ρ meson. A modified photon propagator is obtained in the chain approximation by insertions of ρ^0 propagators and photon mass terms. (L.B.S.)

9847 VACUUM EXPECTATION VALUES OF SOME EXPONENTIAL OPERATORS. Blomer, R. J. (American Univ., Beirut, Lebanon). Progr. Theor. Phys. (Kyoto); 44: 590-8(Sep 1970).

The vacuum expectation values (VEV) of operators $\exp(A + B)^n$, $n > 2$, where $[A,B]$ is a c-number are given as formal (divergent) power series. A generalization of the Borel summation is used to construct from those divergent power series the VEVs in integral representation which fulfill the requirements of generalized Padé approximation. A correspondence with the S-matrix elements in the Peres model is shown. (auth)

9848 FUNCTIONAL RELATIONS FOR RENORMALIZATIONS IN QUANTUM ELECTRODYNAMICS. Truten, V. I.; Fomin, P. I. (Inst. of Physics, Tashkent). Teor. Mat. Fiz.; 5: 219-34(Nov 1970). (In Russian).

Functional relations of the type of Gell-Mann–Low asymptotical functional relations for Green functions are deduced for the electron mass renormalization $\delta m = mF(\Lambda/m,\alpha)$ and the photon and electron wave function renormalization constants $Z_3(\Lambda/m,\alpha)$, $Z_2(\Lambda/m,\alpha)$ considered as functions of cut-off parameter Λ and renormalized mass m and coupling constant α. On the basis of relations obtained the following problems are investigated: existence of "superconducting type" solution for the electron self-energy; character of the divergences in quantum electrodynamics; self-consistency of the theory. For calculation of the functions of interest the approximation scheme is developed which is based on the functional relations obtained and the perturbation theory. (auth)

9849 $\lambda(\phi^4)_2$ QUANTUM FIELD THEORY WITHOUT CUTOFFS. III. THE PHYSICAL VACUUM. Glimm, James; Jaffe, Arthur (New York Univ., N. Y. Harvard Univ., Cambridge, Mass.). Acta Math. (Uppsala); 125: 203-67(1970).

A quantum field theory model is constructed. The model describes a spin-zero boson field with a nonlinear ϕ^4 selfinteraction in two-dimensional space time. The physical representation and renormalization, one-particle operators, quantized operators in Fock space, vacuum expectation values of local number operators, norm compactness of the approximate vacuums, and finite vacuum self-energy per unit volume are discussed. (J.F.P.)

9850 FERMION STATES OF A BOSON FIELD. Streater, R. F.; Wilde, I. F. (Univ. of Lund, Sweden). Nucl. Phys.; B24: 561-75(1970).

Certain non-Fock representations of the canonical commutation relations are constructed for the zero-mass scalar field in two-dimensional space-time. These are obtained from the free-field representation by applying localized automorphisms, are strongly locally Fock, and have a positive energy-momentum spectrum. The model is suggested by an early paper of Skyrme, and provides a concrete example of the algebraic theory of observables and charges. It satisfies some, but not all, of the postulates of Doplicher, Haag and Roberts. The Bose–Fermi alternative does not hold: instead, a continuum of representations is found which interpolates between the Bose and Fermi sectors. The local field algebra can then be constructed, which provides a unitary multiplier representation of a gauge group of the second kind. (auth)

9851 STUDIES IN THE YANG–MILLS FIELD. Wu, Alfred C. T. (CERN, Geneva, Univ. of Michigan, Ann Arbor). Phys. Rev., D; 2: 3081-2(15 Dec 1970).

By explicit calculation, the cancellation between longitudinal and scalar components is verified in the lowest-order scattering of massless Yang–Mills fields. The problem of stability of the subsidiary condition under a local gauge transformation is briefly discussed. The question is raised as to whether the (infinitesimal) non-Abelian gauge function should be quantized. A possible connection between the fictitious ghost of Feynman and DeWitt and the fictitious gauge quanta is mentioned. (auth)

9852 SCHWINGER TERMS IN FERMION ELECTRODYNAMICS. Chanowitz, Michael S. (Cornell Univ., Ithaca, N. Y.). Phys. Rev., D; 2: 3016-23(15 Dec 1970).

The c-number Schwinger term and a possible operator Schwinger term in fermion electrodynamics, to the lowest nontrivial orders in perturbation theory. The results of our direct method of calculation agree with results previously obtained from the Bjorken–Johnson–Low high-energy limit. In particular, no evidence is found for the existence of an operator Schwinger term. The structure of the results helps to understand the calculations by the split-point method of Schwinger, according to which there seems to be an operator Schwinger term. In the examples considered, an analogy between the direct perturbation-theory calculations, which are performed in momentum space, and the split-point calculations, which are performed in coordinate space is discovered. Interchanging the equal-time limit with the phase-space integration is analogous to interchanging the equal-time limit with the split-point limit. Pursuing the analogy, it is concluded that the split-point definition of the current probably is consistent with perturbation theory, and that the apparent discrepancies are due to the improper interchange of the equal-time limit with the split-point limit in previous calculations by the split-point method. (auth)

9853 GENERALIZED WAVE EQUATIONS. II. Tripathy, Kishor C. (Univ. of Delhi. Inst. of Theoretical Physics, Goteborg). Phys. Rev., D; 2: 2955-62(15 Dec 1970).

A type of field equation is investigated which describes particles with spin $J = 0, \frac{1}{2}, 1, \frac{3}{2}, 2, \ldots$, and $I = 0, \frac{1}{2}, 1, \frac{3}{2}, 2$. The fields transform under the combined representation of SL(2,C) (Majorana) $\otimes$ D(Dirac) $\otimes$ $O(3)_I$. Explicit expressions for the mass spectra and the "wave functions" were obtained. Finally, the conservation laws and the quantization scheme are discussed. (auth)

9854 INTERACTION OF A GAUGE-INDEPENDENT SPIN-ONE FIELD. Palmer, Roger; Takahashi, Sushi (Univ. of Alberta, Edmonton). Phys. Rev., D; 2: 3086-9(15 Dec 1970).

In a recent paper a massive spin-1 field was considered that was gauge invariant, at least in the free-field case. It was pointed out that when an interaction was in order to maintain the gauge invariance certain conditions had to be imposed on the source functions. The object of this paper is to construct the interaction Hamiltonian and to consider the consequences of these conditions. (auth)

9855 METHODS FOR THE BETHE–SALPETER EQUATION. I. SPECIAL FUNCTIONS AND EXPANSIONS IN SPHERICAL HARMONICS. Kershaw, David (Univ. of California, Berkeley); Snodgrass, Herschel; Zemach, Charles. Phys. Rev., D; 2: 2806-19 (15 Dec 1970).

Elements of the structure of the Bethe–Salpeter equation are studied. Properties of useful special functions are obtained and free-particle solutions to the truncated expansion of the equation in four-dimensional spherical harmonics are derived in terms of known special functions. The validity of the truncation approximation is examined in terms of a convenient representation of the Green's function. In particular, it is shown that the method of truncating the differential Bethe–Salpeter equation cannot succeed for scattering. The development of alternative procedures is deferred. As a by-product, a simple computational technique for the approximation of integrals by Gaussian quadrature is derived. (auth)

9856 METHODS FOR THE BETHE–SALPETER EQUATION. II. BRACKETS AND THE N/D METHOD. Kershaw, David (Univ. of California, Berkeley); Zemach, Charles. Phys. Rev., D; 2: 2819-40(15 Dec 1970).

A systematic study of the Bethe–Salpeter relativistic two-body equation is continued. The equation is treated in Wick-rotated coordinate space. A bilinear combination of functions, called a bracket, is defined. Its relation to scattering amplitudes and their residues at poles, and to questions of structure of the equation and numerical accuracy of solutions, is developed. N and D matrices similar to the Jost function of potential theory are defined in terms of complete sets of solutions to the equation characterized by appropriate boundary conditions. Scattering and bound-state properties are defined in terms of them, by formulas analogous to the N/D methods of S-matrix theory, and properties of symmetry, unitarity, and behavior at poles are derived. Various methods for computing wave functions and bound-state and scattering data are presented. A generalization of the variable-phase method of potential theory, which substitutes for the Bethe–Salpeter equation a coupled set of ordinary linear first-order differential equations, is given. (auth)

9857 S MATRIX FOR YANG–MILLS AND GRAVITATIONAL FIELDS. Fradkin, E. S.; Tyutin, I. V. (Lebedev Inst. of Physics, Moscow). Phys. Rev., D; 2: 2841-57(15 Dec 1970).

A method is suggested (and applied to the Yang–Mills and gravitational fields) for the construction of the generating functional (S matrix) for fields possessing an invariance group. The unitarity and gauge independence of the S matrix on the mass shell are seen explicitly. (auth)

9858 EQUIVALENT FORMULATIONS OF MASSIVE VECTOR FIELD THEORIES. Salam, Abdus; Strathdee, J. (International Centre for Theoretical Physics, Miramare, Italy). Phys. Rev., D; 2: 2869-76(15 Dec 1970).

Generalizations of the Stückelberg decomposition of a vector field are developed by means of the Feynman functional-integral technique. The modified perturbation series which result are of interest because they can be used to express the nonrenormalizable parts of the interaction of a system of charged massive vector particles in a form to which recently developed nonpolynomial techniques of computation can be applied. (auth)

9859 RENORMALIZATION, DIAGRAMS, AND GAUGE INVARIANCE. Bialynicki-Birula, I. (Univ. of Pittsburgh. Univ., Warsaw). Contract AT(30-1)-3829. Phys. Rev., D; 2: 2877-86 (15 Dec 1970).

A compact formula for the renormalized transition probability in quantum electrodynamics is derived and its interpretation in terms of the diagrams is given. This formula is used next to prove the equivalence of the Coulomb gauge and the Feynman gauge. It is shown that, contrary to widespread belief, the problem of the gauge invariance becomes a very delicate one when the radiative corrections are included. The common practice of dropping k_μ and k_ν terms in the photon propagator $D_{\mu\nu}(k)$ is justified, but the justification requires a nontrivial analysis of the gauge transformations of the propagators involved. (auth)

9860 FIELD-THEORY REALIZATION OF THE DROPLET MODEL. Chang, Shau-jin (Univ. of Illinois, Urbana. Stanford Univ., Calif.). Phys. Rev., D; 2: 2886-98(15 Dec 1970).

It is demonstrated with two field-theoretic models that the operator droplet model proposed by Chou and Yang can be understood as due to the contribution from a class of leading Feynman diagrams at $s = \infty$. In the first model, a theory is considered which consists of both a strong and an electromagnetic interaction. The purpose of introducing two types of interactions is to supply a natural division between the production of particles and the interaction between the jets. In this model, the sum of pure photon-exchange diagrams leads automatically to an expression identical to that of the operator droplet model. Limitations and generalizations of the model are investigated. The second model is derived from pure quantum electrodynamics. It is found that an operator-droplet-model formulation can reproduce leading amplitudes in quantum electrodynamics, including those which give rise to $(\ln s)^N$ behavior. This confirms and generalizes an earlier result of Lee. It is demonstrated explicitly how the N-bubble diagrams should be treated in this calculation. By including diagrams related to one another by covariance, a reference-frame-independent result always emerges. These frame-independent results coincide with earlier calculations based on the usual Feynman rules. (auth)

9861 CONSEQUENCES OF RENORMALIZABILITY. I. Rae, Anil C. (Indian Inst. of Tech., Kanpur). Phys. Rev., D; 2: 2899-2908(15 Dec 1970).

The photon propagator in quantum electrodynamics is studied in the high-energy limit. The approach is to regulate the Feynman integrals which give contributions to the photon self-energy and then to use the fact that when an appropriate set of renormalization subtractions is made, the resulting functions must be independent of the regulating mass. In addition, one makes the plausible assumption that the regulated functions are not singular in the limit where the electron mass approaches zero. To any finite order, one finds functional equations which must be satisfied by the various functions involved. These functional equations are used in two ways. The first is to find the possible form of the functions in each order of perturbation theory and relationships between the functions of different orders. It is found that in nth order (in the fine-structure constant α) the functions are specified by n constants (if $n > 1$); however, using the relationships between orders, $n - 2$ of these constants can be expressed in terms of the ones found in lower order. The second use of the functional equation involves the complete function. It is shown that the general function of two arguments is completely determined by two functions of a single argument. It will be recognized that the aim and methods of this work parallel those of studies of the "renormalization group." The principal differences are a more explicit and careful discussion of the details of renormalization and a more complete study of the implications for the perturbation expansion. (auth)

9862 ENERGY–MOMENTUM TENSORS AND SCALE INVARIANCE IN THE THIRRING MODEL. Georgi, Howard (Yale Univ., New Haven). Phys. Rev., D; 2: 2908-11(15 Dec 1970).

It is shown that in the Thirring model the Sugawara form of the energy-momentum tensor, $T_{S\mu\nu}$, is a more natural choice than the usual form in terms of canonical fields, $T_{C\mu\nu}$, in the sense that $\int x_\mu T_S^{\mu 0}(x)dx^1$ is the generator of scale transformations which leave the solution of the model invariant. (auth)

9863 PROBLEMS OF STABILITY FOR QUANTUM FIELDS IN EXTERNAL TIME-DEPENDENT POTENTIALS. Schroer, Bert (Univ. of Pittsburgh); Seiler, Rudolf; Swieca, Jorge Andre. Contract AT(30-1)-3829. Phys. Rev., D; 2: 2927-37(15 Dec 1970).

The algebraic aspect of the time evolution for various types of fields interacting with external potentials is discussed. This is a pure c-number problem for the classical wave equations. In the case of interaction, the equation for $s \geq 3/2$ exhibits the well-known consistency troubles and the breakdown of causality studied by Velo and Zwanziger. Other equations, for example, a modified form of the Joos–Weinberg equations, are shown to lead to different troubles. As for the question of a unitary operator implementing the time-evolution automorphism in the Fock space of the in-fields, a peculiar property is encountered: The scalar coupling of $s = 0$ fields (superrenormalizable) leads to the existence of a time-evolution operator, whereas electromagnetic-type couplings (renormalizable) possess at most an S matrix and no evolution operator in the interaction region. This Haag's phenomenon holds for arbitrary smooth and short-range external fields. (auth)

9864 INDEFINITE METRIC AND STATIONARY EXTERNAL INTERACTIONS OF QUANTIZED FIELDS. Schroer, Bert (Univ. of Pittsburgh); Swieca, Jorge Andre. Contract AT(30-1)-3829. Phys. Rev., D; 2: 2938-44(15 Dec 1970).

The necessary modifications of the state space for quantum fields interacting with strong stationary external fields are discussed. In addition to the introduction of an indefinite metric, the possibility of having a positive-definite metric without a vacuum state is discussed. (auth)

9865 LOGARITHMIC BEHAVIOR IN SHORT-DISTANCE FIELD PRODUCTS. de Mottoni, P. (CNR, Rome); Genz, H. Nucl. Phys.; B25: 173-8(1971).

The square of a local spin-zero field, in the short-distance limit, is shown to be as singular as its vacuum expectation value. The proof does not require scale invariance; the Wightman functions $\langle\phi(y_1) \ldots \phi(y_{k'})A(\lambda x_1)A(\lambda x_2)\phi(y_{k'+1}) \ldots \phi(y_k)\rangle_0$ are only assumed to behave like products of powers of λ and $|\ln\lambda|$ in the limit $\lambda \to 0$. The same result holds for any even power of a local spin-zero field. (auth)

9866 LEVER PROBLEM IN SPECIAL RELATIVITY. Strnad, J. (Univ. of Ljubljana, Yugoslavia. Jozef Stefan Nuclear Inst., Ljubljana, Yugoslavia). Fizika (Zagreb); 2: 169-76(Oct 1970).

Previously an attempt was made to avoid the statement in the special theory of relativity that the torque on a mechanical system in a moving inertial frame differs from zero though the corresponding torque in the proper frame is zero. It was claimed that the consideration of the nonsimultaneity of the acting forces, which act simultaneously in the proper frame only, leads to the conclusion that the torque is zero in the moving frame also. A simple example is given to show that the consideration of the nonsimultaneity of forces does not invalidate the traditional statement. The above statement can be avoided with a new invariant definition of the torque, according to Butler. It can be shown, however, that this definition can be of use in static problems only. If the forces are switched on and off net change of angular momentum in the moving frame is not equal to zero though it should be, since the corresponding change in the proper frame is equal to zero. (auth)

9867 FINITE FIELD ENERGIES OF POINT CHARGES IN A POLARIZED VACUUM. Bagge, Erich (Institut fuer Reine und Angewandte Kernphysik, Kiel). Atomkernenergie; 16: 165-76 (1970). (In German).

It will be shown that a Lorentz-invariant electrodynamics may be formulated in such a way that the field energy of a point charge will be finite. For that purpose it is necessary to introduce the polarization of the vacuum in the theory in a fundamental way and to have a linear correlation between the four vectors of the field instead of between the six vectors. With the help of a polarization function given, it can be demonstrated that the field energy of a point charge e is equal to the rest energy of the particle mass. The same polarization function allows one to calculate the anomalous magnetic moments of an electron and proton and gives practically correctly the observed values of the momenta. The theory leads also to a new expression for the interaction term of an electron in the radiation field. This term automatically must give a finite value for self-energy of the electron, deduced by quantumelectrodynamics. (auth)

9868 MODEL FIELD THEORY IN FIVE DIMENSIONS. Oliveira, Colber G.; Vidal, A. (Centro Brasileiro de Pesquisas Fisicas, Rio de Janeiro). An. Acad. Brasil. Cienc.; 42: 167-8(Jun 1970).

A theory for interacting spin-2, -1 and -0 fields is constructed by 4 + 1 decomposition of a symmetric tensor in five-dimensional

XUM

flat space. The field equations are a natural consequence of the existing symmetry principles. (auth)

9869 LECTURES ON NON-LINEAR ELECTRODYNAMICS, COPENHAGEN, 1968. Plebanski, Jerzy. Copenhagen; Nordisk Institut for Teoretisk Atomfysik (1970). 153p. (NP-18512).

A compact exposition of nonlinear electrodynamics is given stressing the algebraic aspects, and an exhaustive study of characteristic surfaces is presented. A survey is given of some general conclusions that follow from the equations of motion as derived by variational techniques. (J.F.P.)

Gravitation and General Relativity

Refer also to abstracts 9052 and 9154.

9870 (JINR-P2-5289) ON THE FRIEDMAN THEORY. (ON THE ROLE OF GRAVITATION IN THE ELEMENTARY PARTICLE THEORY). Markov, M. A. (Joint Inst. for Nuclear Research, Dubna (USSR). Lab. of Theoretical Physics). 1970. 31p. (In Russian). (CONF-700806-29). Dep. CFSTI (U. S. Sales Only).

From 15th International Conference on High Energy Physics, Kiev, USSR.

The work is based on the hypothesis that systems with external microscopic parameters (Friedman) are produced in time automatically independently of the initial and randomly large macroscopic values of these parameters. Friedman uses as a phenomenological model extensive elementary particles, avoiding the known difficulties of nonlocal theory. A detailed analysis indicates that during systematic descriptions of the elementary particles in the general theory of relativity the Friedman character of the system under consideration develops automatically. (tr-auth)

9871 CONSERVED QUANTITIES IN GRAVITATIONAL RADIATION THEORY. Glass, Edward Nathan. Syracuse, N. Y.; Syracuse Univ. (1969). 120p. University Microfilms Order No. 70-15,211.

Thesis.

In 1965 E. T. Newman and R. Penrose announced the existence of 10 absolutely conserved quantities in the theory of gravitational radiation. Since such quantities as energy momentum and angular momentum are not absolutely conserved by radiative processes it was felt that an understanding of these interesting quantities was essential. The main aim is to achieve insight into these quantities and extend the initial work. Since all constants of the motion generate invariant transformations of the field variables, this is the initial direction of study. J. N. Goldberg investigated the N-P constants for the Maxwell field in Minkowski space. By using Green's theorem he was able to demonstrate that the N-P constants generate transformations that for the tensor wave equation map solutions into solutions. D. C. Robinson extended this work by making use of generalized Hertz potentials for zero mass fields. Using a conformal technique developed by R. Penrose which allowed him to calculate "at infinity," Robinson extended the results to curved space and to mappings of solutions of the field equations themselves. The present research examines these results in the full physical space. Since the generalized Hertz potentials (super-potentials) for gravitation exist only at infinity, the metric is used directly. Using a new generalization of Green's theorem for nonlinear equations, the N-P constants are found by examining the shear of outgoing null geodesics (the bicharacteristics of the surfaces along which radiation from zero mass fields propagates). Since Robinson used a Lorentz gauge, his calculation is not conformally invariant (although the final 2-surface integral expressing the constants is). This investigation improves on Robinson's results by adopting a null gauge (Bondi gauge) which is conformally invariant so the whole calculation can be taken over intact to the unphysical conformal space. The invariant transformations generated by the gravitational N-P constants are found to be incoming quadrupole pulses with support limited to future null infinity. The supertranslation invariance of the constants is shown directly since the calculation is performed on an arbitrary outgoing null surface (this is a distinct advance, since the only prior proof had to make use of the unphysical conformal space). The nonexistence of higher order constants is discussed and related to the wave tail structure of the higher order incoming perturbations. (Diss. Abstr. Int., B)

9872 QUANTIZATION OF GENERAL RELATIVITY. Brill, D. R.; Gowdy, R. H. (Yale Univ., New Haven). Contract AT(30-1)-3935. Rep. Progr. Phys.; 33: 413-88(May 1970).

Several theories of quantum general relativity have been formulated. Each of these theories has elements of arbitrariness and ambiguity as well as technical difficulty which make it less than satisfactory. However, the construction of these theories has revealed much about the structure of general relativity as a dynamical system and has spurred the development of new approaches to quantum theory. Canonical, sum-over-histories and source theory approaches to the quantization of the gravitational field in the absence of matter are reviewed in terms of a unified notation. Discussions of quantum theory and general relativity are provided to make the review self-contained. The quantization of open space-time geometries (graviton scattering) is treated in sufficient detail to reveal the basic mathematical structure of the formalism. The quantization of closed universes (quantum cosmology) is discussed with particular attention to the superspace concept and the construction of finite-dimensional model quantum theories. Superspace, the domain manifold of the quantum state functional in general relativity, is also discussed separately. (auth) (UK)

9873 CYLINDRICAL WAVE SOLUTIONS OF FIELD EQUATIONS OF GENERAL RELATIVITY CONTAINING ELECTROMAGNETIC FIELDS. Lal, K. B.; Prasad, H. (Univ. of Gorakhpur, India). Tensor; 20: 45-52(1969).

Einstein's gravitational field equations of general relativity containing the electromagnetic energy tensor along with Maxwell's electromagnetic field equations were solved in a cylindrically symmetric space-time. When the electromagnetic field tensor F_{ij} is taken as functions of (r-t), the cylindrically symmetric space-time is reduced to a plane symmetric space-time in the sense of Taub. But by using the concept of physical components of tensors, it has been shown that even if the electromagnetic field tensor F_{ij} is taken as any functions of (r,t), to within some restrictions, exact cylindrical wave solutions of these field equations exist. (auth)

9874 MOTION OF PARTICLES WITH SPIN IN GENERAL RELATIVITY. Souriau, Jean-Marie (CNRS, Marseille, France). Compt. Rend., Ser. A; 271: 751-3(12 Oct 1970). (In French).

It is shown that particles with spin do not describe geodesics; but the gravitational acceleration is very weak and can only be described for the case of very intense gravitational waves. Elementary particles have a mass and a spin independent of their motion; in this case the motion is derived from a symplectic principle. (France)

9875 DYNAMICS OF EXTENDED BODIES IN GENERAL RELATIVITY. II. MOMENTS OF THE CHARGE-CURRENT VECTOR. Dixon, W. G. (Cambridge Univ., Eng.). Proc. Roy. Soc. (London), Ser. A; 319: 509-47(10 Nov 1970).

The problem is considered of defining multipole moments for a tensor field given on a curved spacetime, with the aim of applying this to the energy-momentum tensor and charge-current vector of an extended body. Consequently, it is assumed that the support of the tensor field is bounded in spacelike directions. A definition is proposed for "a set of multipole moments" of such a tensor field relative to an arbitrary bitensor propagator. This definition is not fully determinate, but any such set of moments completely determines the original tensor field. By imposing additional conditions on the moments in two different ways, two uniquely determined sets of moments are obtained for a vector field J^{α}. The first set, the complete moments, always exists and agrees with moments defined less explicitly by Mathisson. If $\nabla_{\alpha} J^{\alpha} = 0$, as is the case for the charge-current vector, these moments are interrelated by an infinite set of corresponding restrictions. The second set, the reduced moments, exists if and only if $\nabla_{\alpha} J^{\alpha} = 0$. These avoid such an infinite set of interrelations, there being instead only one such restriction, the constancy of the total charge of the body. (auth) (UK)

9876 STATIC EQUILIBRIUM STATES OF SPHERICALLY SYMMETRIC MASSES WITH ARBITRARY BARYON NUMBER IN THE TETRAD THEORY OF TREDER. Kreisel, E. (Institut fuer Relativistiche und Extragalaktische Forschung, Potsdam, Ger.). Ann. Phys. (Leipzig); 23: 180-91(Jul 1969). (In German).

Equilibrium conditions were studied for static spherically symmetrical distributions of material by means of Treder's tetrad theory. Solution for vacuum conditions necessitated two constants. One of these constants corresponded to Schwarzschild's mass, the other one deviated significantly from it at high central densities. Conversely to Einstein's theory, the baryon number grows unlimited with increasing central density. (tr-auth)

9877 OSCILLATORY APPROACH TO A SINGULAR POINT IN THE RELATIVISTIC COSMOLOGY. Belinskii, V. A.; Khalatnikov, I. M.; Lifshitz, E. M. Advan. Phys.; 19: 525-73(Jul 1970).

A new type of singularity in the cosmological solutions of the Einstein equations, which are of a complex oscillatory nature, is described. The singularities are discussed mainly in the case of homogeneous models although there are indications that the singularity in the general solution of the gravitational equations is of the same type. This conclusion is supported by the concept that the oscillatory approach to a singular point is caused by the type of perturbation that makes the generalized Kasner solution, and

the analytic construction of the solution corresponding to small oscillations confirms the generality of the regime. These ideas are discussed. (UK)

9878 PROTON AND NEUTRON MASSES AND A CONJECTURE FOR THE GRAVITATIONAL CONSTANT. Good, I. J. (Virginia Polytechnic Inst., Blacksburg. Virginia State Univ., Blacksburg). Phys. Lett.; 33A: 383-4(30 Nov 1970).

Some formulas are suggested connecting the velocity of light, Planck's constant, the fine-structure constant, the gravitational constant, and the masses of the electron, proton and neutron. They are accurate enough to suggest that Eddington's fundamental theory is likely to be partly right. (auth)

9879 FERMIONS IN GENERAL RELATIVITY. Lawrence, John K. (Univ., Vienna). Ann. Phys. (N. Y.); 58: 47-55(May 1970).

A discussion is given of the interaction of fermions with linearized gravitational fields in general relativity by means of the covariant Dirac equation. A formulation of the Dirac equation is used in which the "spin–spin" interaction terms do not appear. The trajectories of the fermions in a gravitational field are found by means of a WKB type limit. The resulting equations of motion are comparable to those of previous work and lack certain ambiguities of the equations for classical spinning bodies. Although massless particles must follow null geodesics, massive particles exhibit nongeodetic motion. Any effect on the result of an Eötvös–Dicke type experiment would be of at least second order in the gravitational field strengths, but anomalous deflections are found for high-energy fermions passing near a massive body. (auth)

9880 GRAVITATIONAL–SCALAR FIELD COUPLING. Deser, S. (Brandeis Univ., Waltham, Mass. NORDITA, Copenhagen); Higbie, J. Ann. Phys. (N. Y.); 58: 56-75(May 1970).

Spherically symmetric initial solutions of coupled gravitational–massless scalar fields, generated by a physical particle source of both, are obtained. These solutions exhibit unusual behavior in terms of the source parameters (bare mass m_0, Einstein constant κ, scalar coupling constant f, and source size ϵ): There are no solutions for some ranges of these parameters, while two (nonsingular) branches exist elsewhere. In each of the limits $f \to 0$, $\kappa \to 0$ or $\epsilon \to \infty$ there is a normal and an anomalous branch, the latter involving essential singularities in f, κ, ϵ^{-1} through factors $\sim f^2\epsilon^{-1}$ exp $[\epsilon^2 f^{-2}\kappa^{-1}]$ in the mass and the fields. There is a minimum finite particle extension for all solutions. The analogous system: particle source of the scalar–tensor gravitational field is also treated in the scalar–tensor theory of gravitation where the results are qualitative as in general relativity. (auth)

9881 ACTION FUNCTIONAL OF GENERAL RELATIVITY AS A PATH LENGTH. I. CLOSED EMPTY UNIVERSES. Gowdy, Robert H. (Yale Univ., New Haven). Contract AT(30-1)-3935. Phys. Rev., D; 2: 2774-83(15 Dec 1970).

For the case of closed empty universes it is established (up to a uniqueness conjecture) that the action functional of general relativity is a Riemannian path length in superspace, an infinite-dimensional manifold whose points represent three-dimensional geometries. Each procedure for representing spacetimes by trajectories in superspace yields a corresponding superspace metric. These metrics are just the "geodesic sheaf" metrics found by DeWitt. A general expression for all of these metrics is obtained in terms of arbitrary coordinates on superspace. The expression requires an explicit and unique solution to the spacelike constraints ($G^{0i} = 0$, $i = 1, 2, 3$) of general relativity. Supertrajectories are separated into "timelike" ones which are permitted because they have real actions and "spacelike" ones which are forbidden because their actions are imaginary. By varying the path-length action, it is found that solutions of Einstein's source-free field equations correspond to a class of timelike geodesics in superspace. This class of geodesics is subject to conserved constraints which are homogeneous and quadratic in time derivatives. The truncated superspace which contains the empty "mixmaster" universes studied by Misner is discussed as an application of the supergeometric approach. The approach is particularly useful for analyzing the maximum expansion stage of the universe. Universes at this stage of their evolution encounter a real singularity of superspace. Time-symmetric universes end their supertrajectories on this singularity, while all other universes penetrate it in a well-defined way. The singularity, together with the causal structure of superspace, limits the anisotropy of empty mixmaster universes which are a finite number of e-foldings from the stage of maximum expansion. (auth)

9882 GRAVITATIONAL FIELD OF SHELLS AND DISKS IN GENERAL RELATIVITY. Morgan, Lesley (Univ. of Nebraska, Lincoln); Morgan, Thomas. Phys. Rev., D; 2: 2756-61(15 Dec 1970).

The problem of obtaining the gravitational field of static, axially symmetric, thin shells is elucidated. In particular, a clear distinction between global and local frames is made. An algorithm is given for obtaining the fields of disks. There are two significant gravitational potentials λ and ϕ. The potential λ is straightforwardly determined from the radial stresses by solving a two-dimensional potential problem. This potential is analytic everywhere except on the disk and, together with its stream function $\bar{z}$, can be used to generate a conformal transformation which brings the equation for ϕ into the form of Laplace's equation. This potential can then be found by solving a Neumann boundary-value problem. However, the surface in the new coordinate system is not a disk since $\bar{z}$ is discontinuous across the disk. This is due to the fact that the Cauchy–Riemann equations imply that if the normal derivative of $\bar{p}$ is discontinuous, then the tangential derivative of z will be discontinuous. (auth)

9883 EXPANSION OF EINSTEIN'S THEORY OF GRAVITATION AROUND A NEWTONIAN-TYPE THEORY IN FLAT AND CURVED THREE-DIMENSIONAL SPACE. Gonzalez-Martin, Gustavo R. Boston; Boston Univ. (1970). 272p. University Microfilms Order No. 70-22,389.

Thesis.

The coordinate invariant concept of a limit applied to spacetimes, given by Geroch for the case of metric spaces, is extended to affine spaces with singular metric. Newton's theory is shown to be a limit solution of Einstein's equation, in the limit of instantaneity. The necessary postulates that distinguish this limit from others are given. The metric is split covariantly by using singular tensors of rank three, and one. The limit affine connection is shown to be the same connection given by the four-dimensional formulation of Newton's theory. Furthermore, using this Newtonian connection, the Einstein field equations reduce in this limit to Poisson's equations. This is in contrast to what happens when the usual slow motion and weak field limit, which leads to an affine connection which is flat in the limit and consequently to a theory without gravitation is taken. (TSS) (Diss. Abstr. Int., B)

Scattering Theory

Refer also to abstract 9749.

9884 (COO-1764-90) DUAL RESONANCE THEORY WITH NONLINEAR TRAJECTORIES. Baker, M. (Washington Univ., Seattle. Dept. of Physics); Coon, D. D. (Minnesota Univ., Minneapolis. School of Physics and Astronomy). [1970]. Contracts AT(45-1)-1388; AT(11-1)-1764. 51p. Dep. NTIS.

A dual resonance model with nonlinear trajectories which includes the Veneziano model as a limiting case is discussed. Rules are given for constructing the N-point function in such a model, and an explicit expression for the N-point planar tree graph is derived. A conjectured rule for loop diagrams is also presented. Representations of four-point function satellite terms which admit straightforward generalization to the N-point function are derived. (auth)

9885 (COO-1764-98) RULES FOR CONSTRUCTING GENERALIZATIONS OF THE VENEZIANO N-POINT FUNCTION. Baker, M. (Washington Univ., Seattle. Dept. of Physics); Coon, D. D. (Minnesota Univ., Minneapolis. School of Physics and Astronomy). [1969]. Contracts AT(45-1)-1388; AT(11-1)-1764. 11p. Dep. NTIS.

Rules are presented for constructing N-point functions in dual resonance models with nonlinear trajectories. The planar tree graph five-point function is discussed and an explicit expression for the N-point function is given. (auth)

9886 (DESY–70/57) ON THE CONSEQUENCES OF THE ASSUMPTION THAT THE S-MATRIX COMMUTES WITH THE AXIAL CHARGE. Fabricius, K. (Deutsches Elektronen-Synchrotron, Hamburg (West Germany)). Nov 1970. 21p. Dep. NTIS (U. S. Sales Only).

The aim is to derive the consequences of the assumption that the axial charge commutes with the S-matrix. Therefore some properties of the axial charge are studied first in perturbation theory and subsequently in a general manner. As a result of the above assumption the self-consistency condition of Adler and in addition the universality of the two-pion isovector coupling are found. (auth)

9887 (ITF-70-43) DUAL RESONANCE MODELS. I. (REVIEW). Jenkovszky, L. L.; Kukhtin, V. V.; Shelest, V. P. (Akademiya Nauk Ukrainskoi SSR, Kiev. Institut Theoreticheskoi Fiziki). 1970. 51p. (In Russian). Dep. NTIS.

The origin, properties, some applications and possible generalizations of dual resonance models are reviewed. (auth)

XUM

9888 (ITF–70-78) A GENERALIZED VENEZIANO MODEL. Miranskii, V. A.; Shelest, V. P.; Zinov'ev, G. M. (Akademiya Nauk Ukrainskoi SSR, Kiev. Institut Teoreticheskoi Fiziki). 1970. 8p. Dep. NTIS (U.S. Sales Only).

It is shown that from the generalized Veneziano model one can construct the amplitude with a finite number of daughter Regge trajectories which corresponds to the generalized interference model. (auth)

9889 (JINR–P4-5366) ON THE USE OF K-HARMONICS IN THE SCATTERING PROBLEMS. Lkhagva, O. (Joint Inst. for Nuclear Research, Dubna (USSR). Lab. of Theoretical Physics). 1970. 15p. (In Russian). Dep. NTIS (U. S. Sales Only).

It is suggested to use the method of hyperspherical functions for obtaining the lower bounds on the scattering parameters, as well as for the generalization of the time delay theory for the case of the reactions with the fragment number $N \geq 3$. (auth)

9890 EXACTLY SOLUBLE THREE-BODY MODEL OF RESONANCE SCATTERING. Beregi, P. (Central Research Inst. for Physics, Budapest); Lovas, I.; Revai, J. Ann. Phys. (N. Y.); 61: 57-77(Nov 1970).

A simple model is constructed consisting of two particles and a potential having two bound states. The model is solved exactly, applying Faddeev's method, and approximately, using the basic assumptions of the microscopic nuclear reaction theories. In the elastic scattering channel a compound-type resonance is produced and the properties of this resonance are studied in order to make comparison between exact and approximate solutions. (auth)

9891 ALTERNATIVE TREATMENT OF THE THREE-BODY PROBLEM. Hannover, H. (Ruhr Univ., Bochum, Ger.). Z. Phys.; 240: 272-80(1970).

For solving the three-body problem with local potentials a model Hamiltonian H_0 containing an interaction between one particle and the center-of-mass of the other two interacting particles is introduced. The total Hamiltonian H is obtained by $H = H_0 + W$ where W is a "residual interaction" in close analogy to the nuclear shell model. At a certain stage of the calculations H_0 has to be replaced by a new model Hamiltonian $\tilde{H}_0$ containing plane waves. The resolvent (and thereby the T-matrix) of the three-body problem is calculated by operator techniques. It is possible to draw some conclusions conerning three-body properties from these general expressions. Therefore this attempt may be considered as a supplementary treatment, in addition to the Faddeev-equations, of the three-body problem: it exhibits the discrete spectrum, the simple and the twofold continuum of H arising from the corresponding states of H_0, and provides some approximation methods. (auth)

9892 PADE AND FREDHOLM APPROXIMANTS IN SCATTERING THEORY. Moiseiwitsch, B. L. (Queen's Univ., Belfast). J. Phys., B (London); 3: 1417-25(Nov 1970).

It is shown that Padé approximants can be obtained directly from the Fredholm expansion for scattering phase shifts. The accuracies of various Padé and Fredholm approximants taken up to the third order in the strength of the interaction potential are assessed by evaluating the S-wave phase shifts for the elastic scattering of particles by square-well and exponential potentials. The second-order Padé and Fredholm approximants are found to be quite accurate and both superior to the second Born approximation, while taken to third order they generally yield very accurate values for the phase shifts. (auth) (UK)

9893 GRIBOV–POMERANCHUK POLE IN THE REGGE-POLE RESIDUES. Chiu, Charles B.; Matsuda, Satoshi (California Inst. of Tech., Pasadena). Contract AT(11-1)-68. Phys. Rev., D; 2: 2655-64(1 Dec 1970).

A mechanism is considered for generating a nonsense wrong-signature fixed pole in the scattering amplitude based on a certain class of Feynman diagrams. It is shown that the presence of a fixed pole in the Regge-pole residue is expected when an effect of the third double-spectral function is included in an appropriate way, and its phenomenological implications are discussed in connection with dip-bump structures in differential cross sections. In particular, a certain channel-independent feature of a fixed-pole effect is pointed out and a comparison with the data is made. (auth)

9894 BEHAVIOR OF RESONANCES FOR SOME SIMPLE POTENTIALS. Lyberg, Mats Douglas (Univ. of Lund, Sweden). Nucl. Phys.; B24: 527-36(1970).

Different resonance approximations are compared to the exact expressions for some simple potentials in potential scattering. Specially it is investigated how accurately the pole position can be determined from the peak position and the width of the resonance. A parameter is also introduced which in a natural way can be regarded as describing the contribution from the nonresonant background. This parameter is also used in a simple fit of the ρ-meson. (auth)

9895 WEIGHT FUNCTIONS AND SUBTRACTIONS IN DISPERSION THEORY. Ciulli, S.; Fischer, J. (NORDITA, Copenhagen). Nucl. Phys.; B24: 537-60(1970).

The extrapolation of the scattering amplitude through "Carleman" weighted dispersion relations to a general interior point of the analyticity domain is considered, assuming that the experimental data are available on some limited part of the boundary. Besides some suitable chosen weight function (similar to those used in Carleman kernels) the method uses essentially a Poisson kernel instead the Cauchy one of the conventional dispersion relations. A rigorous proof is given that this is the best extrapolation procedure of the dispersion-relation type (linear with respect to the input data), in the sense that any other weighted dispersion relation leads to greater error-bounds in the result. (auth)

9896 SPIN, PARITY, SIGNATURE AND DUALITY, AND FACTORIZATION CONSTRAINTS ON THE MESON SPECTRUM. Canning, Gerald P. (Tel-Aviv Univ., Israel). Nucl. Phys.; B24: 591-611(1970).

Using the technique of "normality-conserving" helicity amplitudes, the constraints placed on the meson spectrum by construction of dual amplitudes for inelastic reactions of the type (spin) $1 \times 0 \to 1 \times 0$ are examined. In the absence of parity doublets, it is found that mixed-signature abnormal-parity trajectories spaced one unit from signatured normal-parity trajectories are predicted for the meson spectrum. (auth)

9897 RELATIVISTIC EIKONAL EXPANSION. Blankenbecler, R. (Stanford Univ., Calif.); Sugar, R. L. Phys. Rev., D; 2: 3024-30(15 Dec 1970).

A systematic study is made of the relativistic analog of the eikonal expansion. Approximate amplitudes are obtained for the scattering of a high-energy projectile off a single particle and off a compound system. For the two-body problem our results are valid for all momentum transfers, while for the three-body amplitude the relativistic analog of the Glauber formula is obtained. (auth)

9898 UNITARITY AND FIXED POLES OF WEAK AMPLITUDES IN A PERTURBATION-THEORY MODEL. Baker, H. C.; Lu, Eugene Y. C.; Wood, L. E. (Washington Univ., St. Louis). Phys. Rev., D; 2: 3031-4(15 Dec 1970).

It is shown that weak unitarity equations in general require the existence of fixed simple poles in weak amplitudes at right-signature nonsense–nonsense points and are consistent with the presence of higher-order fixed poles with constant or polynominal residues. These fixed poles are exhibited in a perturbation-theory model. (auth)

9899 INVESTIGATION OF SOME DUAL AMPLITUDES WITH CUTS. Abo-Shaeer, Muhsin A. R. (International Centre for Theoretical Physics, Miramar, Italy). Phys. Rev., D; 2: 3073-8(15 Dec 1970).

Two simple ways of adding an infinite number of direct-channel two-particle thresholds to the Veneziano picture are studied, which usually contains only resonances in the direct channel. The high-energy behavior, positivity, and l-plane structure of the resulting amplitudes are investigated, which turn out to have Regge cuts in addition to Regge poles in the crossed channel. (auth)

9900 UNITARIZATION OF THE VENEZIANO AMPLITUDE: A SIMPLE POTENTIAL-THEORY MODEL. Yaes, Robert J. (Univ. of Texas, Austin). Phys. Rev., D; 2: 2803-5(15 Dec 1970).

In order to see what we would expect to happen to the poles in the Veneziano amplitude if we were able to unitarize it, a potential-theory model with an energy-dependent potential with poles on the real axis is considered. It is shown how in the T matrix the poles are removed from the real axis since their residues vanish. In the unitarized single-pole approximation, it is explicitly seen how corresponding poles appear on the second sheet. (auth)

9901 FORMULATION OF DUAL THEORY IN TERMS OF FUNCTIONAL INTEGRATIONS. Hsue, C. S.; Sakita, B.; Virasoro, M. A. (Univ. of Wisconsin, Madison). Contract AT(11-1)-881. Phys. Rev., D; 2: 2857-68(15 Dec 1970).

A formulation of dual-symmetric theory is given in terms of functional integrations. Known formulas of the theory, such as the N-particle Veneziano amplitude and both planar and nonplanar one-loop amplitudes, are explicitly given in terms of the new formulation. The new formulation is also shown to be equivalent to the other formulations such as the harmonic-oscillator formulation. (auth)

Particle Accelerators

Refer also to abstracts 8482, 8490, 8553, 8711, 9617, 9618, 9692, 9966, 9971, and 9978.

9902 (AECL-3669) FITTING OF AN ORDERED SET OF MODE FREQUENCIES. Schriber, S. O. (Atomic Energy of Canada Ltd., Chalk River (Ontario). Chalk River Nuclear Labs.). Oct 1970. 37p. Dep. NTIS (U. S. Sales Only). AECL $1.00.

A computer program called DISPER has been developed for weighted, non-linear, least-squares fitting of an ordered set of mode frequencies from coupled rf cavities to frequency-phase relationships developed from equivalent circuit analysis using coupled R, L, C loops. Fits can be done for either singly- or doubly-periodic systems with different combinations of first- and second-neighbour coupling. The report describes the equivalent circuit equations, the logic of the program and illustrates the use of the latter with a few examples. (auth)

9903 (BNL-15368) RIBBON EFFECT IN A SUPERCONDUCTING SEPTUM MAGNET. Parzen, G.; Jellett, K. (Brookhaven National Lab., Upton, N. Y.). 18 Nov 1970. 4p. Dep. NTIS.

The septum of a superconducting septum magnet is wound out of a thin superconducting ribbon. Only a small fraction of the ribbon and of the septum carries current. The effect of the number of ribbon layers on the leakage field is studied for particular application to the septum magnet for the AGS slow extraction system. (auth)

9904 (CERN-70-24) EFFECTS OF MAGNETIC FIELD PERTURBATIONS OF A SYNCHROTRON ON THE CLOSED ORBIT AND BETATRON OSCILLATIONS, AS WELL AS THEIR COMPENSATION. Guignard, G. (European Organization for Nuclear Research, Geneva (Switzerland)). 14 Sep 1970. 141p. (In French). Dep. NTIS (U. S. Sales Only).

The aim of this work is to analyze the effects of various field perturbations of a synchrotron on the beam and to determine the elements necessary for their compensation. Dipolar magnetic perturbations are treated, and an analytic estimation of the effect of the corrections is developed as well as three correction methods and a numerical simulation of proton dynamics. The instabilities due to multipolar perturbations and their compensation are studied analytically. Finally, these obtained results are applied to a new injector for the CERN proton synchrotron. (tr-auth)

9905 (CERN-70-28) AN INSTRUMENT FOR MEASURING THE RATE OF CHANGE OF THE RF FREQUENCY IN PARTICLE ACCELERATORS. Blandamura, F.; Giannini, R.; Susini, A.; Zanaschi, C. (European Organization for Nuclear Research, Geneva (Switzerland)). 29 Sep 1970. 22p. Dep. NTIS (U. S. Sales Only).

An electronic device is described which measures the time derivative of a time-dependent frequency function. There are systematic and random errors; the latter can be decreased significantly if f(t) is periodic as in the case of particle accelerators. The device has been constructed to monitor the accelerating frequency program of the CERN Synchro-cyclotron (SC) and it allows a relative accuracy better than 2.5 $^{0}/_{00}$. Circuits are given. (auth)

9906 (IFVE-SKU-69-95) TOPOGRAPHY OF THE MAGNETIC FIELD AT THE 70-GeV ACCELERATOR. Komarov, V. V.; Korol'kov, I. Ya.; Lednev, A. A.; Marshanskii, V. S. (Gosudarstvennyi Komitet po Ispol'zovaniyu Atomnoi Energii SSSR, Serpukhov. Institut Fiziki Vysokikh Energii). 1969. 23p. (In Russian). Dep. NTIS (U. S. Sales Only).

The data on measuring the magnetic field topography in the gap of the open and closed units of the electromagnet of the IHEP accelerator and in the region of fringing fields during injection are given. The measurement methods and the apparatus used for this purpose are briefly described. (auth)

9907 (KFK-tr-335) DETERMINATION OF THE CRITICAL CURRENT IN A SECTION WITH RADIAL SLOTS IN THE IRIS DISK. Zykov, A. I.; Grizhko, V. M.; Grishaev, I. A.; Fursov, G. L.; Kramskoi, G. D. (Akademiya Nauk Ukrainskoi SSR, Kharkov. Fiziko-Tekhnicheskii Institut). Translated by Rosemarie Corssen (Kernforschungszentrum, Karlsruhe, Ger.), from report KHFTI-69-25. 6p. (In German). Dep. CFSTI (U. S. Sales Only).

A beam of accelerated electrons penetrating an iris-loaded waveguide produces non-rotational symmetrical waves of the higher modes. These waves cause a transverse amplification of the beam electrons leading to its destruction under certain conditions. The value of the current in the beam at which destruction occurs is called the critical current. The critical current was calculated for a section of the Kharkov 2-GeV accelerator with radial slots in the iris disk. The results showed that with the help of a single section with radial slots in the iris disk the accelerated current can be increased at least tenfold, and it was established that at $W_0 = 40$ MeV the critical current of the single section was not less than 1.5 amp. It is emphasized that this current value in the single section can not be accelerated to $W_0 = 40$ MeV, but is only a stability measurement. (J.S.R.)

9908 (KFK-tr-337) ELECTRON-ION BUNCH DIAGNOSTICS BY BREMSSTRAHLUNG. Iovnovich, M. L.; Sarantsev, V. P.; Fiks, M. M. (Joint Inst. for Nuclear Research, Dubna (USSR)).

Translated by Rosemarie Corssen (Kernforschungszentrum, Karlsruhe, Ger.), from report JINR-P9-4850. 8p. (In German). Dep. CFSTI (U. S. Sales Only).

The method of accelerating heavy atoms to high energies, based on the possibility of producing electron-ion bunches which are accelerated as a whole through an external magnetic field, produces a bremsstrahlung of the electrons during the capture process. The use of this bremsstrahlung for the diagnosis of the electron-ion bunch was investigated, both theoretically and experimentally. The theoretical study showed that the number of γ quanta recorded during the capture process depends on the spectral sensitivity of the detector and the detection probability. In the experimental use of a Ge(Li) detector in the acceleration of Xe, the results showed that the capture process of Xe in bunches can be studied with the electron number $N_e \gtrsim 3 \times 10^{12}$. (J.S.R.)

9909 (LNF-70/17) STUDY OF SOME PROBLEMS OF CAVITY RESONATORS BY MEANS OF FINITE DIFFERENCES. Note No. 473. Florean, R.; Tazzioli, F.; Verri, G. (Comitato Nazionale per l'Energia Nucleare, Frascati (Italy). Laboratori Nazionali di Frascati). 11 May 1970. 13p. (In Italian). Dep. CFSTI (U. S. Sales Only).

The problem of the determination of the electromagnetic field behavior of resonators consists in the resolution of the Helmholtz equations with partial derivatives with determined conditions at the cavity interior. These equations were solved in the present study by the expression of the equation by means of finite differences. The solution of the problem is then reduced directly to that of a system of algebraic equations. This method was used to determine the resonance frequency, the merit factor, and the shunt impedance of some resonators. The comparison with the theoretical values from former reports made it possible to determine an order of magnitude of the error. The numerical method, applied by others to the fundamental mode, was extended to higher modes with devices regarding the convergence criterion. The method does not give high precision on the absolute values of the resonance frequency. It does, however, give an approximation of the field configuration and is useful in studying small variations on the form of a given model by varying a certain parameter as for example the resonance frequency of one mode with respect to that of another. (tr-auth)

9910 (LUSY-7007) COMPUTER PROGRAMME FOR CALCULATION OF SOLID ANGLES AND ANGULAR ACCEPTANCES. Kivikas, Toeivelemb (Lund Univ. (Sweden). Dept. of Physics). Sep 1970. 75p. Dep. NTIS (U. S. Sales Only).

SOLAN, a FORTRAN program, for the calculation of solid angles and angular acceptances relevant to commonly-encountered target-detector geometries is described. Some illustrations of typical calculations are given as a listing appendix of the program. (auth) (Sweden)

9911 (LYCEN-6949) METHOD OF CALCULATION OF TRAJECTORIES OF IONS BEFORE INJECTION INTO THE PROPOSED HEAVY-ION LINEAR ACCELERATOR. Bajard, M.; Ero, I.; Hadinger, G.; Tauth, T. (Lyon Univ. (France). Institut de Physique Nucleaire). 17 Oct 1969. 13p. (In French). Dep. NTIS (U. S. Sales Only).

A mathematical method of calculation using the matrix of trajectories in the focusing elements of deflection and transport is studied. Such a method is quite useful for calculations using computers. The matrix of ion motion, calculation of the admittance of focusing system, and programing are discussed. (J.F.P.)

9912 (LYCEN-6953) DETERMINATION OF CERTAIN PARAMETERS OF "REFLEX"-TYPE ION SOURCES. Bajard, M.; Fiks, M.; Hadinger, G.; Tauth, T. (Lyon Univ. (France). Institut de Physique Nucleaire). 25 Nov 1969. 15p. (In French). Dep. NTIS (U. S. Sales Only).

Certain quantitative relations among the most important parameters of the discharge in reflex-type ion sources are studied theoretically in order to determine the optimum performance. An isolated plasma is considered which does not touch the walls of the discharge chamber in which surface phenomena can be neglected. (J.F.P.)

9913 (NP-18594) SEXTUPOLE LENSES WITH "DIRECT" NONLINEARITY IN A SLOW EJECTION SYSTEM. Gal'chuk,

XUM

A. V.; Sivkov, Yu. P. (Scientific Research Inst. of Electro-Physical Apparatus, Leningrad (USSR)). 1970. 10p. (In Russian). Dep. NTIS (U. S. Sales Only).

Application of sextupole lenses with considerable drop-off of the field on the aperture edge in the slow ejection system has been considered. Calculations have shown that application of these lenses allows to decrease the swing amplitude and to improve slightly the emittance of the external beam as well as to reduce the total length of lenses on the ring. (auth)

9914 (NP-tr-1926) BEAM REGULATION IN A 100-MeV PROTON LINEAR ACCELERATOR. Batalin, V. A.; Ilievskii, S. A.; Kapchinskii, I. M.; Ni'egorodzev, V. V.; Plotnikov, V. K.; Poninenkova, L. M.; Tepliakov, V. A.; Tichin, V. G. (Gosudarstvennyi Komitet po Ispol'zovaniyu Atomnoi Energii SSSR, Serpukhov. Institut Fiziki Vysokikh Energii). Translated by H. Polge (CEA, Saclay, France), from report IFVE-69-9. 17p. (In French). Dep. CFSTI (U.S. Sales Only).

The discussion of beam regulation in a 100-MeV accelerator covers a description of the accelerator components, method of beam regulation, the gradual adjustment of the acceleration region in the various parts of the accelerator, and the physical starting of the accelerator. The alignment of the pre-injector accelerator tube, betatron oscillations, the maximal dimensions and divergence angles of the beam in the median planes, and the variation of the current as a function of the field gauge are considered. (J.F.P.)

9915 (SLAC-Trans-124) DISCONTINUOUS PHASE OSCILLATIONS IN PARTICLE ACCELERATORS. Bathow, G.; Freytag, E. (Deutsches Elektronen-Synchrotron, Hamburg (West Germany)). Translated for Stanford Linear Accelerator Center, Calif., from report DESY-69/29. 41p. Dep. NTIS.

Phase oscillations in particle accelerators are comprehensively treated for the case of discontinuous acceleration. A phase-oscillation parameter Z is introduced into the difference equation for the phase and energy deviations. The quantity Z covers the influence of the characteristic accelerator parameters on the phase motion; it also describes the phase-amplitude damping. The results given show that, for accelerators having a constant Z of the order of unity, resonances will occur which critically influence the phase stability. Analytic approximations are given for a qualitative survey of the numerical results. Microtrons, mesotrons, synchrotrons, cyclotrons, storage rings, and linacs are considered. (auth)

9916 (UCRL-19313) THIN LENS OPTICS WITH SPACE CHARGE. Garren, A. A. (California Univ., Berkeley. Lawrence Radiation Lab.). Aug 1969. Contract W-7405-eng-48. 57p. (CONF-690811-17). Dep. NTIS.

From 7th International Conference on High Energy Accelerators, Moscow, USSR.

The beam-envelope theory of Kapchinskij and Vladimirskij is applied to the case of a drifting relativistic beam of circular cross section focused by thin lenses. Numerical integration of the envelope equation in dimensionless form produces a single family of envelope curves that represent all possible beam envelopes for any particular choice of momentum, emittance, and intensity. From these curves the minimum possible beam radius for any particular lens spacing may be determined, as well as the corresponding lens strength. (auth)

9917 (UCRL-20125) STATUS OF THE ERA RESEARCH AT BERKELEY. Keefe, Denis (California Univ., Berkeley. Lawrence Radiation Lab.). Oct 1970. Contract W-7405-eng-48. 12p. (CONF-700929-3). Dep. NTIS.

From Proton Linear Accelerator Conference, Batavia, Ill.

The Compressor III experiment at the Astron facility is reviewed, and the Berkeley 2-MeV electron linear induction accelerator and the Compressor IV apparatus are described. Also, conceptual studies of an electron-ring accelerator for acceleration of protons to high energies at high intensities are outlined. (W.H.K.)

9918 PROTON ACCELERATOR WITH ENERGY SMOOTHLY CHANGING FROM 10 TO 100 keV FOR INVESTIGATING CRYSTAL STRUCTURE BY THE SHADOW EFFECT METHOD. Polandov, A. G. (Moscow State Univ.). Izv. Akad. Nauk Arm. SSR, Ser. Fiz.; 5: 129-35(1970). (In Russian).

A proton electrostatic accelerator to investigate crystalline structure by the shadow effect method is described. The specific feature of the accelerator is a separating magnet placed immediately under the ion source. The accelerator beam current is 90 to 120 muA. The proton energy changes from 10 to 100 keV. (auth)

9919 ELECTRON POSITRON COLLISIONS IN THE ORSAY STORAGE RING. Marin, Pierre (Ecole Normale Superieure, Orsay, France). Sci. Progr. Decouverte; No. 3425, 5-15(Sep 1970). (In French).

The principles of existing storage rings and of those being developed are discussed. The plan of the Orsay storage ring (A.C.O.) used for electron-positron collisions is given. The injection equipment and the guidance and focussing systems are shown; and the principal characteristics and physics experiments which can be performed are discussed. (France)

9920 MODIFICATION OF THE SAXONBURG SYNCHROCYCLOTRON. Dupont, F. M. (Thomson-CSF, Orsay, France). Rev. Tech. Thomson-CSF; 3: 441-57(Sep 1970). (In French).

The modification project consists in converting the Saxonburg synchrocyclotron into a heavy ion isochronous cyclotron. A system comprising a heavy ion source and a linear accelerator for preaccelerating the ions before their peripheral electrons are peeled off inside the modified synchrocyclotron allows the heavy ions to be accelerated up to 125 MeV/a.m.u. This machine consequently represents a unique tool with which chemists and especially biologists can conduct their experiments. Many technical problems arise in the project because of the need to retain a beam intensity sufficient for experimental purposes, through the various sections of the machine (ion source, linear accelerator, injection system, cyclotron). (France)

9921 SUPERCONDUCTING LINEAR ACCELERATOR AND PROBLEMS ASSOCIATED WITH ITS CONSTRUCTION. Septier, A. (CNRS, Orsay, France). Rev. Phys. Appl.; 4: 559-64(Dec 1969). (In French).

From Conference on Superconducting Materials, Aussois, France. See CONF-690343.

After a brief survey of hf losses in a linear accelerator, it is shown that the use of a superconducting waveguide allows a continuous working of the machine, but the residual surface resistance R_0 is to be reduced to maximum by improving the preparation technique of the superconducting material. Other problems examined include waveguide technology, frequency stability, focusing, and phasing of cavities. 28 references. (tr-auth)

9922 OPTICS OF THE ION SOURCE EXTRACTION SPACE. Majumdar, N. K. (Saha Inst. of Nuclear Physics, Calcutta). Nucl. Instrum. Methods; 88: 205-11(1970).

A reasonable potential distribution has been assumed in the extraction space of an ion source and the extracted ion beam has been calculated. The formulation is geometry-dependent and geometrical parameters could be adjusted in actual design consideration for best results in a typical ion source. The focussing property of the extraction space has also been investigated. It is seen that, depending on the potential parameters, the focussing could be a function of time, or independent of time. (auth)

9923 EXPERIMENTAL METHOD TO DETERMINE AVERAGE CROSS-SECTIONS. Shotter, A. C.; Takacs, J.; Fisher, P. S. (Nuclear Physics Lab., Oxford). Nucl. Instrum. Methods; 88: 233-7(1970).

A method is described for directly measuring energy averaged cross sections using a Van de Graaff accelerator. The effective averaging range can be fixed between 5 keV to 400 keV. The deterioration of the energy resolution of the reaction particle spectrum, which normally occurs if the incident beam has a large energy spread, is avoided by the use of electronic techniques. (auth)

9924 LINE SHAPE CALCULATION FOR NUCLEAR SCATTERING FROM GASEOUS TARGETS. Kemper, K. W.; Haynes, D. S.; Fletcher, N. R. (Florida State Univ., Tallahassee). Nucl. Instrum. Methods; 88: 289-93(1970).

A line shape calculation combining geometric and straggling effects for the energy spectrum of nuclear scattering from a gas target is described. The calculated full widths at half maximum are in agreement with values extracted from scattering data to within about 1%. The nearly Gaussian calculated line shape is shown to accurately describe a measured spectral line shape over an energy range of $\pm 2\sigma$ of a fitted Gaussian. The effect of large angle double scattering originating outside the geometric target volume, which is the principal contribution near three standard deviations from the centroid, has not been included. (auth)

9925 PROFILES OF UNIFORMLY ACCELERATED ION BEAMS. Morrone, T. (Adelphi Univ., Garden City, N. Y.). Nucl. Instrum. Methods; 88: 323(1970).

An approximation of Moak's integral is derived which may replace Moak's tables over a useful range of parameters. (Moak's tables are used for the calculation of the profile of uniformly accelerated ion beams which are significantly affected by space charge forces.) (auth)

9926 MONOCHROMATIZATION SYSTEM FOR THE EXTERNAL BEAMS OF THE 2.4-m ISOCHRONOUS CYCLOTRON. Basargin, Yu. G.; Bogdanova, V. I.; Venikov, N. I.; (and others). At. Energ. (USSR); 29: 112-16(Aug 1970). (In Russian).

The energy scatter of a cyclotron beam may be greatly reduced without any loss of intensity by taking advantage of methods used for linear accelerators, such as the high-frequency compensation by longitudinal separation of particles on the basis of their pulses. This approach was used to determine the parameters of the compensation system designed to monochromatize the beam of the 100 MeV U-240 cyclotron. The energy stabilization and control system was developed without rebuilding the cyclotron. The trajectory changes of particles caused by the aberration of the longitudinal motion could also partially be compensated. Thus, the energy scatter may be reduced from 2×10^{-3} to 2×10^{-4}, if the phase width of the clusters in the cyclotron is about 5. (TTT)

9927 SYSTEM FOR FORMING BEAMS AND BEAM PARAMETERS IN THE OUTPUT CHANNELS OF THE 360-MeV ELECTRON LINEAR ACCELERATOR. Grishaev, I. A.; Dem'yanenko, G. K.; Makhnenko, L. A.; Rubtsov, K. S.; Ryabka, P. M. At. Energ. (USSR); 29: 138-40(Aug 1970). (In Russian).

The particle dynamics of a linac is affected by the perturbations caused by the external magnetostatic field and by the high-frequency field resulting from the asymmetry of the transformers. Steps were taken to overcome the shortcoming: the external field was greatly reduced by shielding, and the influence of the longitudinal field of the temperatures was compensated for by introducing a doublet of quadrupole lenses. The special accelerating and beam extraction system is described. The beam analyzer consisted of a deflecting magnet with a Faraday cylinder and a monochromator; its resolution is determined by the gap width of the monochromator. The two intermediate output canals of the accelerator were used for injecting electrons and for carrying out radiation physics experiments. When the specified scatterers are used at the output, the system yields a beam of up to 10 cm, with a particle density unevenness at the edges of up to 30%. (TTT)

9928 DEMOUNTABLE MAGNETIC LENS. Wolfe, W. A.; Harvey, A. Canadian Patent 855,320. 3 Nov 1970.

A multipole magnetic lens assembly, using either permanent or electromagnets for the focusing of a particle beam is adapted to be placed about or removed from a particle beam tube without interfering with the beam tube. The lens assembly is divided into separable sections with each section displaceable laterally with respect to the beam tube. (Canada)

9929 10-MeV LINEAR ELECTRON ACCELERATOR DESIGNATED AS U-13. Val'dner, O. A.; Milovanov, O. S.; Ostanin, V. A.; (and others). At. Energ. (USSR); 29: 140-1(Aug 1970). (In Russian).

During 1968-69 two U-13 type, 10-MeV linear accelerators were designed and built at the Moscow Engineering Physics Institute. They are currently used as ionizing radiation sources and for carrying out resolution chemistry studies. The energy and flux of accelerated electrons may be adjusted within a wide range. The high-frequency supply consists of 2 mutually synchronized magnetrons; the injector is a 2-electrode Pierce gun with a T-shaped, flat, tantalum cathode operating at an injected electron energy of 50 keV. At a power input of 1.2 MW the two accelerators reach a maximum energy of 9.6 MeV. Increasing the power to 1.4 to 1.5 MW results in an increase of the output energy of the accelerating electron up to 10.0 to 10.2 MeV at a current of 80 to 100 μA; this indicates a good agreement between the calculated and experimental values. Equipment is being installed to stabilize the output current with a precision of ~1% while maintaining the stabilized monochromatized energy within 1.2 to 2%. (TTT)

9930 AUTOMATIC VAN DE GRAAFF VOLTAGE CONDITIONER. Holm, L.; McLarnon, B.; Elliott, J. B.; Neilson, G. C. (Univ. of Alberta, Edmonton). Nucl. Instrum. Methods; 88: 177-9(1970).

The automatic voltage conditioner described will condition a 5.5 MeV Van de Graaff accelerator up to a required energy without direct supervision. It has built-in features to safeguard against excessive sparks, vacuum and Van de Graaff belt failures. (auth)

9931 HIGH-VOLTAGE PULSE SOURCE FOR THE DEFLECTOR PLATES IN AN ION CLUSTER INPUT SYSTEM TO THE SYNCHROTRON CHAMBER. Barabash, L. Z.; Grachev, A. S.; Kyrzhanovskii, O. I.; Lebedev, P. I. (Inst. of Theoretical and Experimental Physics, Moscow). Instrum. Exp. Tech. (USSR) (Engl. Transl.); No. 1, 130-2(Jan-Feb 1970).

Translated from Prib. Tekh. Eksp.; No. 1, 119-21(Jan-Feb 1970).

The circuit for supplying a high-voltage pulse to the deflecting plates in an ion cluster input system to the chamber of a synchrotron is described. The circuit differs from the one described previously in that it uses as a high-voltage source the standard rectifier V-100-20, whose primary circuit is switched by a controllable diode. The circuit forms pulses of the amplitude ±50 kV with a break time of less than 0.1 μsec. (auth)

9932 HIGH-VOLTAGE PULSE GENERATOR. Barabash, L. Z.; Kryzhanovskii, O. I.; Lebedev, P. I. (Inst. of Theoretical and Experimental Physics, Moscow). Instrum. Exp. Tech. (USSR) (Engl. Transl.); No. 1, 133-4(Jan-Feb 1970).

Translated from Prib. Tekh. Eksp.; No. 1, 121-3(Jan-Feb 1970).

A generator of high-voltage pulses for feeding the inflector of an input system injecting an ion beam into the chamber of the ITEP proton synchrotron is described. The generator forms symmetrical different polarity pulses the amplitude of which is adjusted from ±5 to ±25 kV; the time of establishing the voltage on the inflector is 150 μsec, and the interruption time is <0.1 μsec. (auth)

9933 QUASISTOCHASTIC INSTABILITY OF THE VIBRATIONS OF PARTICLES IN ANNULAR ACCELERATORS AND STORAGE RINGS. Zenkevich, P. R. (Inst. of Theoretical and Experimental Physics, Moscow). Instrum. Exp. Tech. (USSR) (Engl. Transl.); No. 1, 18-23(Jan-Feb 1970).

Translated from Prib. Tekh. Eksp.; No. 1, 25-9(Jan-Feb 1970).

The quasistochastic vibrations (oscillations) of particles arising as a result of external noise factors on passing through a single resonance are studied. (auth)

9934 INSTABILITY OF THE MOTION OF PARTICLES IN A SYNCHROTRON FOR HIGH FREQUENCIES OF THE ACCELERATING FIELD. Kheifets, S. A.; Orlow, Yu. F. (Erevan Physical Inst.). Instrum. Exp. Tech. (USSR) (Engl. Transl.); No. 1, 24-7(Jan-Feb 1970).

Translated from Prib. Tekh. Eksp.; No. 1, 29-31(Jan-Feb 1970).

For a sufficiently high multiplicity of the frequency of the accelerating field, either the longitudinal or the radial motion of the particles in a synchrotron is unstable. This instability takes place both for synchrotrons with discrete acceleration and for waveguide synchrotrons. (auth)

9935 MEASURING THE CONSTANCY OF THE MAXIMUM ENERGY IN THE BREMSSTRAHLUNG SPECTRUM OF A SYNCHROTRON. Ratner, B. S. (Inst. of Physics, Moscow). Instrum. Exp. Tech. (USSR) (Engl. Transl.); No. 1, 28-30(Jan-Feb 1970).

Translated from Prib. Tekh. Eksp.; No. 1, 32-4(Jan-Feb 1970).

A method of measuring the constancy of the maximum energy in the bremsstrahlung spectrum of a synchrotron is described. An accuracy of ±2 keV may be achieved in a period of 1 h. The energy of the synchrotron measured over a month remains constant within a mean-square error of 1.7 keV. (auth)

9936 STUDY OF RAPID FLUCTUATIONS OF INTENSITY IN THE GAMMA RADIATION OF A BETATRON. Ishkhanov, B. S.; Kapitonov, I. M.; Piskarev, I. M.; Ekivin, V. V. (Moscow State Univ.). Instrum. Exp. Tech. (USSR) (Engl. Transl.); No. 1, 31-2 (Jan-Feb 1970).

Translated from Prib. Tekh. Eksp.; No. 1, 34-5(Jan-Feb 1970).

A method is proposed for measuring the instability in the intensity of the 35-MeV betatron of the Scientific-Research Institute of Nuclear Physics in Moscow State University by reference to the recording of the neutrons arising as a result of photonuclear reactions. The neutrons were recorded with a detector of 45% efficiency. The relative fluctuations in intensity were characterized by $\delta = (4 \pm 0.4)\%$. (auth)

9937 HIGH-FREQUENCY OPERATING CONDITIONS IN LINEAR INDUCTION ACCELERATORS. Grishin, V. K. (Moscow State Univ.). Instrum. Exp. Tech. (USSR) (Engl. Transl.); No. 1, 33-5(Jan-Feb 1970).

Translated from Prib. Tekh. Eksp.; No. 1, 35-6(Jan-Feb 1970).

The operating conditions for linear induction accelerators (LIA) are considered. It is shown that, under conditions of high-frequency supply of the accelerating ring inductors, the LIA efficiency increases, reaching the efficiency of wave guide accelerators. The accelerated current intensity, however, is much higher in LIA's than in waveguide accelerators. (auth)

9938 INCREASING THE POWER OF A LINEAR ELECTRON ACCELERATOR. Flerov, N. N.; Lipatov, V. P.; Konyashev, E. I. (Inst. of Atomic Energy, Moscow). Instrum. Exp. Tech. (USSR) (Engl. Transl.); No. 1, 36-7(Jan-Feb 1970).

XUM

Translated from Prib. Tekh. Eksp.; No. 1, 37-8(Jan-Feb 1970).

To increase the power of the linear electron accelerator of the Institute of Atomic Energy, the hf klystron power source was put into forced operation through an increase of the pulse repetition frequency to 244 sec^{-1}. Klystrons can be used in this manner because they are extremely reliable, have quite high reserve capacity, and are used with high-voltage pulses of short duration ~1.2 μsec. The klystron modulator and several units of the accelerator were modified for the new operating conditions. The reliability of the accelerator was improved as a result of these modifications. The power of the source of electrons, gammas, and neutrons was doubled. (auth)

9939 HIGH-FREQUENCY SEPARATOR OF PARTICLES OPERATING ON AN EH_{12} WAVE. Aver'yanov, V. N.; Glazkov, A. A.; Sobenin, N. P. (Moscow Engineering-Physics Inst.). Instrum. Exp. Tech. (USSR) (Engl. Transl.); No. 1, 38-41(Jan-Feb 1970).

Translated from Prib. Tekh. Eksp.; No. 1, 38-41(Jan-Feb 1970).

High-frequency characteristics of a circular iris waveguide operating on EH_{13} and EH_{11} waves at $\theta = \pi/2$ and $\beta_d = 1$ are measured experimentally. It is shown that in using an EH_{12} wave in a high-frequency separator of ultra-relativistic particles the acceptance is ~10% higher than with the use of an EH_{11} wave. (auth)

PHYSICS (NUCLEAR)

Neutron Interactions with Matter

Refer also to abstracts 8537, 8574, 8579, 9573, and 9995.

9940 (BARC-499) 14-MeV NEUTRON GENERATOR FOR CALIBRATION OF FAST NEUTRON DETECTORS. Misra, S. C.; Gupta, U. C. (Bhabha Atomic Research Centre, Bombay (India)). 1970. 21p. Dep. NTIS (U. S. Sales Only).

A 14 MeV neutron generator developed for the calibration of fast neutron detectors is described. The constructional details and the performance of the generator are given. Some of the factors that affect the measurement of the neutron flux from the generator are discussed. (auth)

9941 (CEA-N-1361) DETAILS CONCERNING THE USE OF THE ELF PROGRAM. Gervaise, Francois (Commissariat a l'Energie Atomique, Fontenay-aux-Roses (France). Centre d'Etudes Nucleaires). Oct 1970. 35p. (In French). Dep. NTIS (U. S. Sales Only).

Several improvements to the ELF program are described. They refer to the following points: the establishment of an ELF library tape, the reduction of the volume of the ELF-NEUTRON program and its use with the MAJONG system, and the study of the variance of the results using the W test. (France)

9942 (CTC-42) THE POPOP4 LIBRARY OF NEUTRON-INDUCED SECONDARY GAMMA-RAY YIELD AND CROSS SECTION DATA. POPOP 4 Memo No. 1. Ford III, W. E. (Union Carbide Corp., Oak Ridge, Tenn. Computing Technology Center). 10 Sep 1970. Contract W-7405-eng-26. 88p. Dep. NTIS.

The data set titles and literature sources of the data in the initial distribution of the POPOP4 library are listed. This library is a compendium of secondary γ-ray data for the various neutron-induced reactions and is available on magnetic tape from the Radiation Shielding Information Center. The data are in a format for use with the POPOP4 system of codes in the preparation of multigroup cross sections for coupled neutron-γ transport calculations. Input and output from sample cases using data from the library with the POPOP4 system of codes are shown. (8 references) (auth)

9943 (GA-10223) INTEGRAL NEUTRON THERMALIZATION. Quarterly Progress Report, April 1, 1970-June 30, 1970. Slaggie, E. L.; Houston, D. H. (Gulf General Atomic, Inc., San Diego, Calif.). 10 Jul 1970. Contract AT(04-3)-167. 18p. Dep. CFSTI.

Research progress in integral neutron thermalization studies at Gulf General Atomic in the period April 1, 1970 through June 30, 1970 is summarized. (J.W.R.)

9944 (ORNL-TM-3156) CALCULATED NEUTRON FLUX DISTRIBUTION RESULTING FROM A FISSION SOURCE LOCATED AT THE CENTER OF A 10-METER-DIAMETER SPHERE OF SODIUM. Thompson, C. L. (Oak Ridge National Lab., Tenn.). 27 Oct 1970. 26p. Dep. NTIS.

A Monte Carlo calculation using the 06R code was made to determine the neutron flux distribution resulting from a point isotropic fission source located at the center of a 10-meter-diameter sphere of sodium. The purpose was to obtain data that will be helpful in evaluating the accuracy of calculations involving neutron transport in sodium. (auth)

9945 (RPI-328-190) LINEAR ACCELERATOR PROJECT. Progress Report, April 1, 1970-June 30, 1970. (Rensselaer Polytechnic Inst., Troy, N. Y.). Contract AT(30-1)-328. 104p. Dep. CFSTI.

Progress is summarized for neutron cross section measurements in reactor fuel and structural materials and experimental and theoretical fast reactor physics studies. (H.D.R.)

9946 (TID-25165(Suppl.2)) CINDA 69: AN INDEX TO THE LITERATURE ON MICROSCOPIC NEUTRON DATA. (Division of Technical Information Extension (AEC), Oak Ridge, Tenn. Gosudarstvennyi Komitet po Ispol'zovaniyu Atomnoi Energii SSSR, Obninsk. Fiziko-Energeticheskii Institut. ENEA Neutron Data Compilation Centre, Gif-sur-Yvette (France). International Atomic Energy Agency, Vienna (Austria). Nuclear Data Unit). 15 Aug 1970. 372p. DTIE Free.

New information added to the CINDA library since the publication of CINDA 69 is presented. (G.M.C.)

9947 (TRG-Report-1990) SNAP: A TWO-DIMENSIONAL NEUTRON DIFFUSION CODE. McCallien, C. W. J. (United Kingdom Atomic Energy Authority, Risley (England). Reactor Group). 1970. 76p. Dep. NTIS (U. S. Sales Only). UK 10s.

SNAP is a FORTRAN IV program that solves the finite-difference form of the group diffusion equations in one or two dimensions. The four co-ordinate systems (x,y), (r,z), (r, θ) and one-dimensional spherical are allowed. Mesh points are positioned at the centers of cells of constant composition. In the (x,y) case the cells may be rectangles, or equal equilateral triangles, or equal regular hexagons. In (r,z) the cells are rectangular. In (r,θ) each cell is bounded by two radii and two concentric arcs. Numerous symmetry options are available. Extrapolation lengths can be specified at internal and external boundaries. Up to sixty energy groups are allowed. Options include adjoint problems, fixed source problems and the determination of the critical buckling or critical cell sizes. (auth)

9948 BYULLETEN' INFORMATSIONNOGO TSENTRA PO YADERNYM DANNYM (VYPUSK CHETVERTYI). (Bulletin of the Russian Nuclear Data Center (Fourth Issue)). Leipunskii, A. I. (ed.). Moscow; Atomizdat (1967). 540p. (NP-18104).

Forty reports are contained in three chapters. The first chapter includes the data on nuclear physics constants. The following subjects are considered: slow-neutron reactions with Dy isotopes; penetrability of potential barriers by protons from (n,p) reactions; cross sections for the production of γ quanta with over 2-MeV energy during 14-MeV neutron reactions with Li, Be, B, C, N, O, F, and Al; elastic and inelastic neutron scattering; thermal cross sections and resonance integrals for the capture and fission of ^{241}Am, ^{242}Am, and ^{243}Am; cross section ratios for fission of ^{233}U, ^{235}U, and ^{239}Pu by fast neutrons; and the quasi-stationary states of fissioning nuclei. Reactor constants and parameters are discussed in the second chapter. The third chapter covers the characteristics and parameters of shielding, calculations of shielding, angular coefficients for fast neutrons in anhydrous media, and determination of the minimum total cross section of fast neutrons in iron. Corrections for penetration of potential barriers from reactions and magnitude of Q(n,d) and (n,p) reactions are included in the brief supplement. (R.V.J.)

9949 NEUTRON POLARIZATION IN THE SCATTERING ON THICK LAYERS OF MATTER. Gnedin, Yu. N.; Dolginov, A. Z.; Silant'ev, N. A.; Shibanov, Yu. A. (Ioffe Inst. of Physics and Tech., Leningrad). Yadern. Fiz.; 12: 815-20(Oct 1970). (In Russian).

Polarization and angular distribution of neutrons scattered in a thick layer of matter is determined. Numerical calculations are performed for the targets consisting of the nucleus of carbon, oxygen and helium. It is shown that the scattered beam gets a considerable polarization. This allows one to obtain neutron beams with the polarization of some dozens percents without a large loss of the initial intensity. (auth)

9950 SECONDARY GAMMA-RAY PRODUCTION AND TRANSPORT IN LIQUID NITROGEN. Reynolds, G. M.; Sperling, S. M.; Selph, W. E. (Gulf General Atomic Inc., San Diego, Calif.). Nucl. Sci. Eng.; 42: 324-34(Dec 1970).

High-resolution measurements have been made of the gamma-ray spectrum produced in liquid nitrogen by a 14-MeV neutron source. The spectra of gamma rays from neutron inelastic scattering were measured to a distance of six feet by pulsing the source. Comparison of the inelastic photon flux with discrete ordinates calculations using ENDF/B neutron cross sections and recent gamma-ray production cross sections shows good agreement for the strong well-resolved lines. The results of unfolding the continuum part of the spectrum reveal a flux of high energy lines that is a sizable fraction of the total flux of resolved lines. These normally unresolved gamma rays account for part of the gap in the nitrogen nonelastic cross section. (auth)

9951 APPLICATION OF CHANDRASEKHAR'S METHOD TO DEEP PENETRATION PROBLEMS. Clancy, B. E. (Australian Atomic Energy Commission Research Establishment, Lucas Heights). J. Nucl. Energy; 24: 261-8(Sep 1970).

A method is developed for solving the one dimensional multigroup transport equation in a homogeneous semi infinite medium with anisotropic scattering. A variational treatment is then used to enable the method to be applied to finite slabs where only the emergent angular fluxes are of interest. The method which is not limited by any restriction on the number of spatial mesh intervals used is shown to be competitive in computing time with conventional discrete ordinate techniques. (auth) (UK)

9952 BOUNDARY-VALUE PROBLEMS OF LINEAR TRANSPORT THEORY: GREEN'S FUNCTION APPROACH. Kanal,

XUM

Madhoo (Univ. of Michigan, Ann Arbor). J. Math. Phys. (N. Y.); 11: 3042-52(Oct 1970).

Case's technique utilizing Green's functions for dealing with boundary-value problems of the neutron linear-transport theory is exploited. It is shown that the Fourier coefficients of the Green's functioh over the Case spectrum are precisely the normal modes. In particular, if it is assumed that the scattering kernel is rotationally invariant and approximate it by a degenerate kernel consisting of spherical harmonics, the set of modes is deficient for problems lacking azimuthal symmetry. It is also shown that the expansion of the scattering kernel, in terms of spherical harmonics (or any set of orthogonal functions for that matter), permits the linear factorization of the Fourier coefficients of the Green's function in terms of the lowest element, with the proportionality functions consisting of complete orthogonal polynomials. As a consequence of this attribute of Fourier coefficients, the eigenfunctions (continuum and discrete) also factorize, which then permits decoupling of the appropriate singular integral equations. To illustrate the idea, the half-space and slab problems are solved. However, the basic procedure is kept sufficiently general so that the extension to problems involving other geometrics remains straightforward. (auth)

9953 LINEAR INTEGRAL EQUATIONS FOR A CERTAIN CLASS OF H-FUNCTIONS APPLICABLE TO THE THEORY OF NEUTRON TRANSPORT AND RADIATIVE TRANSFER. Burniston, E. E. (North Carolina State Univ., Raleigh); Siewert, C. E. J. Math. Phys. (N. Y.); 11: 3091-5(Oct 1970).

A matrix version of the classical Riemann–Hilbert problem defined on an open contour is discussed. The problem is reduced to a quasiregular integral equation for cases where the sufficient Hölder continuity condition is satisfied and the component indices are nonnegative. As an illustration of this procedure, linear integral equations (rather than the usual nonlinear forms), for Chandrasekhar's functions $H_1(\mu)$ and $H_r(\mu)$ are established in a form amenable to solution by numerical iteration. (auth)

9954 VERY INTENSE NEUTRON SOURCE. Brugger, R. M. (Idaho Nuclear Corp., Idaho Falls); Russell, G. J.; Johnson, B. W.; DeVault, G. P. Nucl. Technol.; 10: 188-203(Feb 1971).

The conceptual design of a neutron source is described. This device, called Very Intense Neutron Source (VINS) would produce bursts of neutrons to be used for fast and thermal neutron beam experiments by time-of-flight methods. The source would have an effective source flux for beam experiments several orders of magnitude above those fluxes now available at the best neutron sources. In the concept the neutrons produced by an electron linear accelerator would be multiplied by fast reactor modules. These modules would be arranged to provide maximum multiplication while limiting the shock and heat and limiting multiplication of those neutrons from the delayed neutron precursors. The experimental arrangement and uses of VINS are stressed. (auth)

9955 PRODUCTION AND CHARACTERISTICS OF A 14-MeV NEUTRON BEAM. Loude, J. F.; Perroud, J. P. (Univ., Lausanne, Switzerland). Nucl. Instrum. Methods; 88: 261-5 (1970). (In French).

Detection of the α particle associated with the neutrons emitted in the reaction d(150 keV) + $^3H \rightarrow n + \alpha$ was used to determine a 14 MeV neutron beam. The use of a slowly rotating target and of closed-loop regulation of the neutron intensity permitted uninterrupted and stable operation for more than 100 h at 3×10^8 n/s over 4π. The spatial extension and energy spread of the neutron beam have been calculated by a Monte Carlo method, the results of which are in excellent agreement with the experiment. (auth)

9956 EXPERIMENTAL METHOD FOR MEASUREMENT OF THE EVOLUTION AND POPULATION OF FAST NEUTRONS IN NON-MULTIPLYING ASSEMBLIES. Deconninck, G. (Univ., Louvain, Belg. Univ., Namur, Belg.); Monseu, Pn. Nucl. Instrum. Methods; 88: 309-15(1970). (In French).

A method is described which allows the measurement of neutron time and energy spectra. Neutron bursts are produced by the pulsed beam of a 4 MeV Van de Graaff using the T(p,n) and V(p,n) reactions. The time and energy behaviour of these neutrons in non multiplying assemblies is followed by means of a stilbene detector placed at the surface of the assemblies, the energy spectrum being obtained by unscrambling the proton recoil spectra. The response function to monoenergetic neutrons has been recorded experimentally between 0.7 and 1.6 MeV; these spectra are considered as basis vectors, the components of a neutron spectrum into this basis are easily obtained with the help of a PDP 9 computer. Different geometries have been experimentally realized in graphite and in lead, the bombarding energy has been fixed to 1.66 MeV. The T(p,n) reaction is utilised for producing a plane wave of neutrons incident on cubic assemblies, the V(p,n) reaction is utilised as an isotropic neutron source located at the centre of spherical assemblies. These simple experimental conditions will make further calculations easier. Experimentally it can be seen that the neutron modes decay monotonically with time, however, in the case of lead the inelastic scattering of neutrons is clearly dominating the low energy groups. (auth)

9957 DETERMINATION OF THE DIFFERENTIAL NEUTRON SOURCE STRENGTH FROM THE T(d,n)^{4}He REACTION. Haussen, W.; Schweitzer, T.; Seeliger, D.; Seidel, K. (Technische Univ., Dresden). Nucl. Instrum. Methods; 88: 251-6 (1970). (In German).

The accuracy of determination of the differential source strength of 14 MeV neutrons from the T(d,n)^{4}He reaction by α-particle counting is analysed at a concrete arrangement. This monitor is completed by two neutron monitors including a BF_3-counter and a scintillation detector The behavior of this system during measurements of inelastic scattering is studied. (auth)

9958 TOTAL COHERENT CROSS SECTIONS FOR THE SCATTERING OF NEUTRONS FROM CRYSTALS. Binder, K. (Technische Hochschule, Munich). Phys. Status Solidi; 41: 767-79(1 Oct 1970).

A calculation of the cross sections for polycrystalline bismuth and aluminum is presented. Various methods are applied to calculate the incoherent part and the interference part of the cross section. A description of the scattering is obtained which is valid for the whole range of neutron energies. Previous treatments are critically discussed. (auth)

9959 AVERAGE ANGLE OF SCATTERING IN ENERGY-DEPENDENT PROBLEMS. McGirt, Frank; Becker, Martin (Rensselaer Polytechnic Inst., Troy, N. Y.). Contract AT (30-1)-328. Nucl. Sci. Eng.; 42: 104-6(Oct 1970).

The average of the cosine of the scattering angle in the laboratory system, $\bar{\mu}$, is used in approximations that account for anisotropic scattering. These approximations include correcting the diffusion coefficient in diffusion theory and replacing the detailed anisotropic scattering treatment by a transport approxi-nation in higher-order transport theory methods. However, in the energy-dependent case, several different procedures have been used to define effective average $\bar{\mu}$. An attempt is made here to test the sensitivity of $\bar{\mu}$, as a function of energy, to the averaging procedure used. Substantial differences were obtained from different common definitions of $\bar{\mu}$. These differences were observed to have significant consequences for the calculation of time-dependent spectra. Significant consequences might also be expected in high-leakage situations, as in thin lattices The preferred definition is indicated. (M.H.R.)

9960 INVESTIGATION OF CRITICALITY FOR ENERGY-DEPENDENT TRANSPORT IN SLAB GEOMETRY Nelson, Paul Jr. Albuquerque, N. Mex.; Univ. of New Mexico (1969). 173p. University Microfilms Order No. 70-10,126.

Thesis.

An abstract model of neutron transport in slab geometry is considered. The abstraction is intended to encompass both the classical neutron transport problem and some discrete approximations to this problem. The classical problem has the mathematical form $\varphi = \gamma K\varphi + q$. Here φ is the angular flux of neutrons, K is the (linear) integral transport operator, γ is an eigenparameter, and q is the known source contribution to the flux. Physically, γ is the maximum expected number of neutrons resulting from a collision. The operator K is defined so that $K\varphi(z,\underline{v})$ is the contribution to the angular flux at the point z and velocity $\underline{v}$ from neutron collisions at all points and velocities. The abstraction consists in replacing the velocity vector $\underline{v}$ by a state vector ranging over a measure space which satisfies certain natural requirements. Under some basic hypotheses on the slab material it is shown that K is a continuous linear operator in the space $L^1(\tau)$ where τ is a naturally occurring measure. If γ is a positive real number and q a nonnegative element of $L^1(\tau)$, then the pair (γ,q) is defined to be subcritical if the Neumann series $\Sigma\, \gamma^n K^n q$ converges, and γ is defined to be uniformly subcritical if (γ,q) is subcritical for every $q \geq 0$ in $L^1(\tau)$. It is shown that there exists a number $\gamma_1 \geq 1$ such that γ is uniformly subcritical if, and only if, $\gamma < \gamma_1$. Physical considerations suggests that γ_1 should actually satisfy the inequality $\gamma_1 > 1$ and, under slightly stronger hypothesis, it is shown that this is the case. An example is given to show that $\gamma_1 = 1$ is possible under the fundamental hypotheses. This somewhat pathological possibility is associated with the singular directions parallel to the slab faces. In order to study the concept of subcriticality it seems necessary to assume that K is an eventually compact operator in the space $L^1(\tau)$. Sufficient conditions for K to have this property are given in terms of properties of the slab material. The fundamental result on subcriticality is the following. Assume K is eventually compact, and let $\Gamma = \{\gamma_1, \gamma_2, \ldots\}$ be the

(finite or countably infinite) collection of positive eigenvalues of K which are associated with positive eigenfunctions, with Γ indexed so that $\gamma_i < \gamma_{i+1}$. Then to each γ_i there is associated a τ-measurable B_i, with B_i contained properly in B_{i+1}, and such that the collection $\{B_i\}$ has the following property: If $q \geq 0$, $q \in L^1(\tau)$, and j is the smallest index such that q is not almost everywhere (modulo τ) zero on B_j, then (γ,q) is subcritical if, and only if, $0 \leq \gamma < \gamma_j$. If q is almost everywhere zero on every B_i, then (γ,q) is subcritical for every $\gamma > 0$. The proof of the above fundamental result on subcriticality uses the adjoint operator K^* and, in particular, uses those functions which are annihilated by some iterate of $\gamma I - K^*$. This rather naturally causes inquiry into the physical meaning of these functions. Although a general physical interpretation is not found, it is shown that the function describing the importance of a collision for a barely critical slab is an eigenfunction of K^*. This result is similar to, but not identical with, some early results from neutron transport theory, in which the neutron importance function for a barely critical reactor was shown to be an eigenfunction of the differential transport equation. (Diss. Abstr. Int., B)

9961 TRANSVERSE PROPAGATION OF NEUTRON WAVES. Klinc, Tomaz Ladislav. Ithaca, N. Y.; Cornell Univ. (1970). 74p. University Microfilms Order No. 70-12,631.

Thesis.

Cercignani's method of singular eigenfunctions is developed to study transverse propagation of one-speed neutron waves in a medium with isotropic scattering. A close relationship between this and the Case method is displayed. Cercignani's method can be applied to transport problems characterized by two-dimensional eigenvalue spectra. The half-space problem with the wave propagating along the surface is solved exactly. The complex extrapolated endpoint is determined from the asymptotic part of the solution. An expansion for the extrapolated endpoint is given in terms of two characteristic parameters. No closed-form solution is found for the slab problem. This problem, like the critical problem, is reduced to an integral equation which can be solved by iteration. The asymptotic distribution is determined in the zeroth-order approximation; this yields a complex transverse buckling. The effect of transverse propagation on the measurement of the diffusion coefficient on large assemblies is found to be negligible. (Diss. Abstr. Int., B)

9962 STUDY OF SOME ASPECTS OF THE NEUTRON THERMALIZATION PROBLEM. Kuehn III, Nicholas Henry. Raleigh, N. C.; North Carolina State Univ. (1968). 192p. University Microfilms Order No. 68-14,665.

Thesis.

Three aspects of the neutron thermalization problem are studied: the angular moments of the scattering kernel, the infinite-medium Green's function for a proton gas, and a modified spherical-harmonics solution of the Boltzmann transport equation. A method is presented for calculating the scattering moments $K_n(v',v)$ as single integrals over the relative velocity v_r for a general cross section $\sigma_s(v_r)$. This method employs reduced variables, which display basic symmetries and cancelation patterns. The explicit calculation of $K_2(v',v)$, not previously reported in the literature, is presented in detail to demonstrate the technique. The collision-density Green's function for a proton gas is developed in terms of solutions of a second-order differential equation, which is derived from the integral transport equation. Series solutions for the equation are investigated and their range of application is discussed. A technique is developed for solving the one-dimensional, energy-dependent transport equation in which the angular dependence is expanded in Legendre polynomials, the energy dependence is expressed as a dominant distribution multiplied by a sum of Chebychev polynomials, and the spatial dependence is exponential. The treatment of sources and the formulation of boundary conditions is discussed; the computational methods needed for this analysis are then presented. Finally, the eigenvalues and eigenvectors, needed for the general solution of the transport equation, are calculated on a digital computer for a proton gas for four different energy ranges. (Diss. Abstr. Int., B)

9963 COHERENT DOUBLE SCATTERING OF NEUTRONS. Men'shikov, A. Z.; Bogdanov, S. G. (Inst. of the Physics of Metals, Moscow). Sov. Phys.-Cryst. (Engl. Transl.); 15: 383-6(Nov-Dec 1970).

Translated from Kristallografiya; 15: 452-6(May-Jun 1970).

The theory of coherent double scattering of neutrons is discussed for neutron passage through a plate. General expressions are obtained for the intensities of nuclear-nuclear, nuclear-magnetic, magnetic-nuclear, and magnetic-magnetic scattering, taking account of the crystallographic anisotropy. (auth)

9964 NEUTRON SCATTERING FROM PHONONS IN SOLID HELIUM. Werthamer, N. R. (Bell Telephone Labs., Murray Hill, N. J.). Phys. Rev., A; 2: 2050-60(Nov 1970).

The usual interpretation of the inelastic-coherent-neutron-scattering cross section from phonons in crystal lattices preserves the existence of a one-phonon peak, varying rapidly with neutron energy loss, on top of a smooth multiphonon background, with negligible interference between the two. It is pointed out that previous theoretical analyses arriving at these conclusions are not necessarily applicable to solid helium, since the dimensionless product of neutron momentum transfer and mean atom zero-point displacement is not, in this case, a small parameter. A new expression for the differential cross section is derived, based on a functional variation technique, which allows the dimensionless product to take on an arbitrary value. In the first order of approximation, the one-phonon peak is broadened and shifted from the equilibrium self-consistent phonon spectrum. Estimates are made of the extent to which interference terms distort the observed neutron cross sections in solid helium. The mathematical techniques are also applicable to the model of Feynman et al. for the polaron mobility. (auth)

Nuclear Properties and Reactions, A≤5

Refer also to abstracts 9949, 9955, 9957, and 9974.

9965 (AD-710384) ELECTROMAGNETIC STRUCTURE OF THE ^{3}He NUCLEUS. McCarthy, J. S.; Sick, I.; Whitney, R. R.; Yearian, M. R. (Stanford Univ., Calif. High-Energy Physics Lab.). Jul 1970. Contract Nonr-225(67). 15p. (HEPL-635). NTIS.

The electromagnetic structure of ^{3}He was investigated by means of high energy electron scattering. A separation of the charge and magnetic form factors was accomplished. The charge form factor data extend to q squared = 20 fm sup (-2) and exhibit a diffraction minimum at q squared = 11.6 fm sup (-2); the magnetic scattering is measured to q squared = 12.5 fm sup (-2). The results are discussed in terms of models for the charge and magnetic distributions of the nucleus. (auth) (USGRDR)

9966 (COO-1265-94) ANNUAL REPORT, 1970. (Minnesota Univ., Minneapolis. John H. Williams Lab. of Nuclear Physics). Contract AT(11-1)-1265. 184p. Dep. NTIS.

ALUMINUM-27—deuteron reactions (d, He-3) at 20 MeV, angular distributions for, (E)
—deuteron elastic and inelastic scattering at 20 MeV, angular distributions for, (E)
ASTATINE-212—alpha decay of ground-state and isomeric, half-lives for, (E)
CADMIUM-114—proton elastic scattering at 18.6 MeV, angular distribution for, (E)
CALCIUM-40—deuteron reactions (d,p) at 19 MeV, angular distributions for, (E)
CALCIUM-42—alpha reactions (α,d) at 26.5 MeV, deuteron spectra and angular distributions for, (E)
CALCIUM-44—helium-3 reactions (He-3,t) at 29 MeV, angular distributions for, (E)
HELIUM-4—helium-3 elastic scattering at 20 to 51 MeV, exchange effects in, (E)
—helium-3 elastic scattering at 30 MeV, resonating group calculation for, (T)
MAGNESIUM-26—energy levels from aluminum-27 (d, He-3) reactions, spectroscopic factors for, (E)
—helium-3 elastic and inelastic scattering at 17.7 MeV, angular distributions for, (E)
NICKEL-58—alpha elastic scattering at 26.5 MeV, angular distribution for, (E)
PALLADIUM-106—energy levels from palladium-108 (p,t) reactions, (E)
PALLADIUM-108—proton reactions (p,t) at 19 MeV, angular distributions for, (E)
POLONIUM-210—energy levels from bismuth-209 (He-3,d) reactions, (E)
POLONIUM-211—alpha decay of ground-state and isomeric, half-lives for, (E)
SAMARIUM-148—energy levels from samarium-150 (p,t) reactions, (E)
SAMARIUM-150—proton reactions (p,t) at 19 MeV, triton spectra from, (E)
SAMARIUM-152—energy levels from samarium-154 (p,t) reactions, (E)
SAMARIUM-154—proton reactions (p,t) at 19 MeV, triton spectra from, (E)
SCANDIUM-44—energy levels from scandium-45 (α,d) reactions, spectroscopic factors for, (E)
SCANDIUM-45—energy levels from titanium-46 (d, He-3) reactions, spectroscopic factors for, (E)

XUM

SCANDIUM-47—energy levels from titanium-48 (d, He-3) reactions, spectroscopic factors for, (E)
SILVER-107—energy levels from silver-109 (p,t) reactions, (E)
SILVER-109—proton reactions (p,t) at 19 MeV angular distributions for, (E)
TITANIUM—deuteron reactions (d,α) at 19 MeV, angular distributions for, (E)
TITANIUM-49—helium-3 reactions (He-3,d) at 22 MeV, deuteron spectra and angular distributions for, (E)
TITANIUM-50—deuteron reactions (d,p) at 18 MeV, angular distributions for, (E)
VAN DE GRAAFF ACCELERATORS—operation of University of Minnesota tandem
—experimental facilities at University of Minnesota tandem, development of
VANADIUM-50—energy levels from titanium-49 (He-3,d) reactions, (E)
YTTERBIUM-176—proton elastic and inelastic scattering at 19 MeV, angular distributions for, (E)
ZINC-68—proton elastic scattering at 18.6 MeV, angular distribution for, (E)
ZIRCONIUM-90—proton elastic scattering at 18.6 MeV, angular distribution for, (E) (J.W.R.)

9967 (JINR-P2-5335) INTERACTION CROSS SECTIONS OF FAST PARTICLES WITH TRITIUM AND ^{3}He NUCLEI. Barashenkov, V. S.; Eliseev, S. M.; Ostapenko, A. A. (Joint Inst. for Nuclear Research, Dubna (USSR). Lab. of Theoretical Physics). 1970. 9p. (In Russian). Dep. NTIS (U. S. Sales Only).

In the framework of the Glauber theory, energy dependence is calculated for the cross sections of interaction of pions and nucleons with T and ^{3}He nuclei. (auth)

9968 (NP-18488) ABSOLUTE MEASUREMENTS IN FAST NEUTRON REACTIONS: THE n + D → nnp REACTION AT 14 MeV. Kossentini, Abdelmajid (Grenoble Univ. (France). Faculte des Sciences). 8 May 1970. 70p. (In French). Dep. NTIS (U. S. Sales Only).

The problem of the absolute measurement of the cross sections for fast neutron reactions with energies between 1 and 15 MeV was studied: the application envisaged was the study of a three-nucleon system by the reaction n + D → nnp at 14.5 MeV at different points on the Dalitz plot. The spectra of the neutrons and the absolute value of their energy E_0 for the T (d,n)^{4}He reaction used, were measured by time-of-flight techniques; the precision with which the energy (~14.5 MeV) was measured was better than 1 percent and the overall resolution $\Delta t \sim 1$ ns corresponded to an energy dispersion of $\Delta E \sim 260$ keV. Using three series of measurements the efficiency of the neutron detector was determined with equally good precision (2–5 percent): the relative measurement by the usual method of (n–H) scattering from approximately 2 to 15 MeV, the absolute measurement at 14.5 MeV using the T(d,n)^{4}He reaction, and the absolute measurement at 2.5 MeV using the D(d,n)^{3}He reaction. A value of the differential cross section $d^4\sigma/d\Omega_1\Omega_2$ for the reaction D(n,nnp) with (30°,30°) and (30°,80°) geometries corresponding to the singularities nn or np was determined. An approximate calculation was made using the experimental results and then a Monte Carlo simulation method was used. This value was not directly comparable to the theoretical value. In contrast, the value of the differential cross section $d^5\sigma/d\omega_1\, d\omega_2\, dE_1$ in mb/sr^2 MeV (which is dependent upon the transition amplitude chosen) may be compared to the theoretical value. The reason why the values for the differential cross section $d^5\sigma/d\omega_1\, d\omega_2\, dE_1 \sim 6.7$ mb/sr^2 MeV for (30°,30°) geometry and ~3.4 mb/sr^2 MeV for (30°,80°) geometry differ by a factor of 2 can be explained in terms of the spin factor. (France)

9969 LOW-MOMENTUM K^-–^{4}He SCATTERING AT 115 TO 160 MeV/c. McComas, John Glenn. Chicago; Illinois Inst. of Tech. (1970). 207p. University Microfilms Order No. 70-13,561.

Thesis.

The differential cross section for K^-–^{4}He elastic scattering based on 254 events with K^- laboratory momenta in the interval 115 to 160 MeV/c is reported for an experiment in the Argonne–Carnegie Tech 10-inch helium bubble chamber with superconducting magnet. The elastic data and measurements of the total absorption cross section were fitted with a Coulomb-modified partial-wave series comprised of s- and p-wave terms with complex phase shifts, yielding two solutions with comparable confidence levels. The scattering lengths are calculated in the presence of the Coulomb field. These parameters are used for predicting the result of a K-mesic X-ray experiment in helium. It is found that ≥99% of those K^- that reach the 2p state are captured from that state. The results are not consistent with an absolute K_α X-ray yield exceeding 1%. For data in the 115 to 160 MeV/c interval, d-wave terms in the partial-wave series do not improve the confidence level of the fitted solutions. This apparent absence of d-wave scattering implies a low 3d capture rate, $\Gamma = 3^{+3}_{-3} \times 10^9$ sec^{-1}. This value is two orders of magnitude smaller than the rate required if 3d capture competes with 3d → 2p radiation; thus there is disagreement with the value of Γ required by a very recent K-mesic X-ray experiment. The s- and p-wave results are in good agreement with those from another K^-–^{4}He scattering experiment. The experimental scattering lengths are compared with values computed with a simplified model based on $\bar{K}$–N scattering lengths under the assumption that (complex) $\bar{K}$–N potentials can be summed and smeared to approximate the K^-–^{4}He potential. In addition the s-wave scattering lengths are calculated assuming that the K^-–^{4}He interaction may be described by a purely imaginary potential, and scattering lengths are found in reasonable agreement with our solution. (Diss. Abstr. Int., B)

Nuclear Properties and Reactions, 6 ≤ A ≤ 19

Refer also to abstracts 8513, 9948, 9949, 10002, 10004, 10006, 10010, 10014, 10055, and 10076.

9970 (AECL-3668) PHYSICS DIVISION PROGRESS REPORT, APRIL 1-JUNE 30, 1970. (Atomic Energy of Canada Ltd., Chalk River (Ontario). Chalk River Nuclear Labs.). 123p. (PR-P-86). Dep. NTIS (U. S. Sales Only). AECL $2.50.

Research by the physics division of Chalk River Nuclear Laboratories in the period April 1 to June 30, 1970 is reported. Nuclear and solid-state physics research was conducted by the nuclear physics branch, the general physics branch, the neutron physics branch, the theoretical physics branch, and the mathematics and computation branch. (J.W.R.)

9971 (ANL-7698) PHYSICS DIVISION SUMMARY REPORT, OCTOBER-DECEMBER 1969. (Argonne National Lab., Ill.). Contract W-31-109-eng-38. 44p. Dep. CFSTI.

Research highlights at the Physics Division of Argonne National Laboratory during the period October through December, 1969 are summarized. (J.W.R.)

9972 (ANU-P-496) SYSTEMATIC SEARCH FOR THE LOWEST T = 2 STATE OF ^{12}C USING DEUTERON AND ^{3}He-INDUCED REACTIONS. Black, J. L.; Caelli, W. J.; Watson, R. B. (Australian National Univ., Canberra. Dept. of Nuclear Physics). 1970. 8p. Dep. CFSTI (U. S. Sales Only).

The reactions ^{10}B(d,p), ^{10}B(d,α), and ^{10}B(d,2γ) were used to search for the lowest T = 2 state of ^{12}C. No resonance was observed, and upper limits have been set on partial widths. A possible candidate for the state was observed in ^{9}Be(^{3}He,2γ) at $E_x = 27.585 \pm 0.005$ MeV. (auth) (Australia)

9973 (ITF-70-42) KNOCKOUT OF NUCLEONS FROM LIGHT NUCLEI UNDER THE INELASTIC SCATTERING OF HIGH-ENERGY ELECTRONS. Pasichnyi, A. A. (Akademiya Nauk Ukrainskoi SSR, Kiev. Institut Teoreticheskoi Fiziki). 1970. 25p. (In Russian). Dep. NTIS (U. S. Sales Only).

An investigation is made of the shell structure of light nuclei under the inelastic scattering of high-energy electrons accompanied by knockout of a nucleon from the nucleus. The distortion of the nucleon motion in the final state under the interaction of the nucleon and the residual nucleus is taken into account. The nucleon momenta distributions in different shells of the nuclei ^{12}C, ^{16}O, ^{40}Ca are investigated. The influence of the interaction of the nucleon and nucleus in the final state on the electron distribution over the angles and energies in coincidence experiments is shown. The allowance for the distortion effect results in improving the agreement of theory and experiment when studying the knockout of protons from the different shells of ^{12}C in coincidence experiments, as well as in experiments on the investigation of the continuous spectrum of the nonelastically scattered high-energy electrons. (auth)

9974 (JINR-P2-5286) PROCESSES OF THE TYPE OF DOUBLE CHARGE EXCHANGE AT LIGHT NUCLEI. Tarasov, A. V.; Tseren, Ch. (Joint Inst. for Nuclear Research, Dubna (USSR). Lab. of Nuclear Problems). 1970. 14p. (In Russian). Dep. NTIS (U. S. Sales Only).

The processes of double charge exchange of mesons at light nuclei are considered. It is shown that the cross sections of such processes contain, besides the cross sections of elementary acts occurring on nucleons, an important characteristic of the nucleon distribution in the nucleus (an average value of inverse square of the distance between nucleons) which, apparently, is sensitive to the nucleon pair correlations. (auth)

9975 (JINR-P15-5143) INVESTIGATION OF THE REACTION $^{7}Li(d,n)^{8}Be$. Osetinskii, G. M.; Sikora, B.; Tyke, Ya.; Fryshchin, B. (Joint Inst. for Nuclear Research, Dubna (USSR). Lab. of Neutron Physics). 1970. 17p. (In Russian). Dep. CFSTI (U. S. Sales Only).

The differential cross sections and angular distributions of the neutrons from the reactions $^{7}Li(d,n_0)^{8}Be$ and $^{7}Li(d,n_1)^{8}Be^{*}$ were measured in the deuteron energy range of 1.1 to 4 MeV. The total cross sections were obtained for the reaction $^{7}Li(d,n_0)^{8}Be$ at six energy values. It is established that the reaction proceeds through the compound nucleus mechanism; the neutron spectra indicate the existence of the 4.5 ± 0.15 MeV level in the ^{8}Be nucleus and the absence of other ^{8}Be nucleus levels in the range of the excitation energies up to 9 MeV. 15 references. (auth)

9976 (JINR-P15-5148) INVESTIGATION OF THE $^{9}Be(t,n)^{11}B$ REACTION AT 1.10 MeV. Maluszynska, K.; Niedzwiedziuk, K.; Przytula, M.; Salatskii, V. I. (Joint Inst. for Nuclear Research, Dubna (USSR). Lab. of Neutron Physics). 1970. 8p. (In Russian). Dep. CFSTI (U. S. Sales Only).

The angular distributions of neutrons from the $^{9}Be(t,n)^{11}B$ reaction at 1.10 MeV were measured for four groups of neutrons corresponding to the ground, first, second, and sixth levels of ^{11}B. The expansion coefficients of the angular distributions over the Legendre polynomials are given. It is observed that in the investigated reaction at 1.10 MeV a notable contribution from the compound nucleus mechanism is not excluded. (4 references) (auth)

9977 (LUNP-7009) PHOTOMESON EFFECTS IN (γ,n) AND (γ,p)-REACTIONS IN LIGHT NUCLEI. Friberg, B.; Anderson, G.; Forkman, B. (Lund Univ. (Sweden). Dept. of Physics. Lund Inst. of Tech. (Sweden). Dept. of Nuclear Physics). Sep 1970. 34p. Dep. NTIS (U. S. Sales Only).

Yield curves have been determined for (γ,n)-reactions in ^{14}N, ^{16}O, ^{19}F and ^{31}P and for the reaction $^{30}Si(\gamma,p)^{29}Al$ at maximum bremsstrahlung energies between 100 and 800 MeV. Above 200 MeV there is a difference between the determined yield and that predicted from the contributions from the giant resonance and, at higher energies, the quasi-deuteron absorption process. From the difference, which is assumed to represent the (γ,n) or (γ,p)-reaction via meson production, the number of nucleons that can contribute to the reaction is calculated. The results are in good agree ment with simple shell-model considerations. (auth) (Sweden)

9978 (ORO-3398-26) RESEARCH AND OPERATION OF THE TEXAS A AND M VARIABLE ENERGY CYCLOTRON. Progress Report, June 1, 1969-June 1, 1970. (Texas Agricultural and Mechanical Univ., College Station. [Cyclotron Inst.]). Contract AT(40-1)-3398. 162p. Dep. CFSTI.

ALUMINUM-27—deuteron reactions (d, Li-6) at 50 MeV, lithium-6 spectra and angular distributions for, (E)
CALCIUM-40—deuteron reactions (d, Li-6) at 50 MeV, lithium-6 spectra and angular distributions for, (E)
CARBON-12—alpha inelastic scattering at 35 MeV, α-γ angular correlations for, (E)
—helium-3 inelastic scattering at 44 MeV, particle-γ angular correlations for, (E)
COPPER—alpha reactions at 30 to 80 MeV, k-shell ionization cross sections for, (E)
—alpha reactions with, x-ray fluorescence yields from, (E)
CYCLOTRONS—experimental facilities at Texas A & M variable-energy, development of
—operation of Texas A & M variable-energy, in period June 1, 1969 to June 1, 1970
GADOLINIUM-152—energy-level scheme from terbium-152 m decay, (E)
IRON—alpha reactions at 30 to 80 MeV, k-shell ionization cross sections for, (E)
LEAD—alpha reactions with, x-ray fluorescence yields from, (E)
MAGNESIUM-26—deuteron reactions (d, Li-6) at 50 MeV, lithium-6 spectra and angular distributions for, (E)
MOLYBDENUM-92—helium-3 reactions (He-3,d) at 35 MeV, angular distributions for, (E)
NEODYMIUM-142—proton reactions (p,d) with, angular distributions for, (E)
NICKEL—alpha reactions at 30 to 80 MeV, k-shell ionization cross sections for, (E)
NIOBIUM—alpha reactions at 30 to 80 MeV, k-shell ionization cross sections for, (E)
OXYGEN-16—deuteron reactions (d, Li-6) at 50 MeV, lithium-6 spectra and angular distributions for, (E)
PALLADIUM—alpha reactions at 30 to 80 MeV, k-shell ionization cross sections for, (E)
POLONIUM-210—decay of, in-beam measurement of internal conversion electrons from, (E)
POTASSIUM-39—deuteron reactions (d, Li-6) at 50 MeV, lithium-6 spectra and angular distributions for, (E)
PRASEODYMIUM-141—proton reactions (p,d) with, angular distributions for, (E)
RHODIUM—alpha reactions at 30 to 80 MeV, k-shell ionization cross sections for, (E)
SAMARIUM-144—proton elastic scattering at 30 MeV, optical model analysis of, (E)
—proton reactions (p,t) with, angular distributions and Q-value for, (E)
—proton reactions (p,d) with, angular distributions for, (E)
SAMARIUM-150—alpha reactions (α,xnγ) at 25 and 30 MeV, γ spectra from, (E)
SAMARIUM-152—alpha reactions (α,xnγ) at 40 and 45 MeV, γ spectra from, (E)
SILVER—alpha reactions at 30 to 80 MeV, k-shell ionization cross sections for, (E)
—alpha reactions at 85 MeV, spectra of light fragments from, (E)
SODIUM-20—alpha decay of, α spectra from β-delayed, (E)
STRONTIUM-88—deuteron reactions (d, He-3) at 35 MeV, angular distributions for, (E)
—deuteron elastic scattering at 30 to 40 MeV, angular distributions for, (E)
—helium-3 elastic scattering at 33.4 MeV, angular distribution for, (E)
SULFUR-32—helium-3 reactions (He-3,d) at 35 MeV, angular distributions for, (E)
TERBIUM-152—beta and electron-capture decay of isomeric, γ energies from, (E)
THALLIUM-197—electron-capture decay of, in-beam measurement of internal conversion electrons from, (E)
TIN—alpha reactions at 30 to 80 MeV, k-shell ionization cross sections for, (E)
YTTRIUM-89—deuteron reactions (d, He-3) at 30 to 40 MeV, angular distributions for, (E)
—deuteron elastic scattering at 30 to 40 MeV, angular distributions for, (E)
ZIRCONIUM—alpha reactions at 30 to 80 MeV, k-shell ionization cross sections for, (E) (J.W.R.)

9979 PROTON CAPTURE GAMMA DECAY TO EXCITED STATES OF ^{16}O. Barnett, A. R.; Tanner, N. W. (Nuclear Physics Lab., Oxford). Nucl. Phys.; A152: 257-62(1970).

The excitation function of the yield from the $^{15}N(p,\gamma_1+\gamma_2)^{16}O$ reaction was measured from 4.1-12.8 MeV (E_x = 16-24 MeV in ^{16}O) together with that of the ground state capture reaction $^{15}N(p,\gamma_0)^{16}O$. The target thickness was kept at ≈50 keV; energy increments of ≦50 keV were made below 9 MeV, and of 100 keV above. The two reactions γ_0 and $\gamma_1+\gamma_2$ show no correlation at all, which suggests that the γ_1 radiation to the 6.06 MeV 0^+ state of ^{16}O is very weak. The possibility that the strong $\gamma_1+\gamma_2$ doublet at 19.91 and 20.40 MeV is related to the T = 0, T = 1, $J^{\pi}=1^-$ doublet near 13 MeV by weak coupling (to the 3^- state of ^{16}O) is examined, and some predictions of the model are compared with the experimental results. (auth)

9980 STUDY OF ^{18}O THROUGH $^{14}C+\alpha$ REACTIONS. Morgan, G. L. (North Carolina State Univ., Raleigh. Triangle Universities Nuclear Lab., Durham, N. C.); Tilley, D. R.; Mitchell, G. E.; Hilko, R. A.; Roberson, N. R. Nucl. Phys.; A148: 480-91 (1970).

The reaction $^{14}C(\alpha,\alpha)^{14}C$ has been studied over the bombarding energy range 3.5 to 16.5 MeV. Yield curves at eight angles were measured over the entire energy range; angular distributions were measured on resonances in the energy region below 8 MeV. Measurement was made of the relative yield from the reaction $^{14}C(\alpha,n)^{17}O$ from 4.9 to 8.5 MeV. Seventeen new levels have been observed and spin and parity assignments made for a majority of these. Evidence for the existence of rotational bands in ^{18}O is discussed. (auth)

9981 A STUDY OF THE $^{16}O(^3He,n)$ AND $^{12}C(^3He,n)$ STRIPPING REACTIONS AND A COMPARISON OF ANALOGOUS $(^3He,n)$, $(^3He,p)$, AND (t,p) TRANSITIONS. Adelberger, E. G.; McDonald, A. B. (California Inst. of Tech., Pasadena). Nucl. Phys.; A145: 497-533(1970).

The $^{16}O(^3He,n)$ and $^{12}C(^3He,n)$ reactions were studied at incident energies between 9 and 13.5 MeV using a time-of-flight neutron spectrometer. Neutron angular distributions were obtained at several different bombarding energies from both reactions, and fitted with DWBA calculations. The intensities and shapes of the angular distributions of analogue (t,p), $(^3He,p)$ and $(^3He,n)$ transitions are compared with DWBA predictions. With a few exceptions, the theory is able to reproduce the shapes of the angular distributions fairly well and gives relative strengths to ±25%. Excited states

XUM

of ^{18}Ne were observed at 1.89, 3.38, 3.56, 3.61, 4.51, 4.57, and 5.14 MeV. Spins and parities of 2^+, 4^+, (0^+) and 2^+ were found for the first four excited states. (auth)

9982 MICROSCOPIC DESCRIPTION OF THE ABSORPTION OF BOUND PIONS. Chung, Kyu Nung (Univ., Erlangen, Ger.); Huber, Max Georg; Danos, Michael. Z. Phys.; 240: 195-216(1970).

The absorption rates of bound 1s and 2p pions in some light nuclei have been investigated on the basis of a shell model picture modified by short range nucleon–nucleon correlations. It turns out that the total absorption rate, the missing energy spectra and the single neutron energy spectra depend sensitively on the details of the correlation functions. The results of the present analysis indicate that one can obtain informations on the short range correlations from pion absorption experiments. (auth)

9983 ELASTIC SCATTERING OF 1-GeV PROTONS ON ^{12}C. Guardiola, R. (International Centre for Theoretical Physics, Trieste, Italy). Lett. Nuovo Cim.; 4: 1005-9(28 Nov 1970).

The differential cross section for the elastic scattering of 1-GeV protons on ^{12}C is calculated using the most general ^{12}C wave function with mixing of the $1p_{\frac{3}{2}}$ and $1p_{\frac{1}{2}}$ shells, in an attempt to remove the discrepancy between a previous calculation and experiment. It is concluded that the configuration-mixing mechanism cannot explain the disagreement. (L.B.S.)

9984 NEUTRON POLARIZATIONS IN THE ^{6}Li(d,n) AND ^{7}Li(d,n) REACTIONS FOR DEUTERON ENERGIES FROM 2.5 TO 3.7 MeV. Thomason, R. S.; Spalek, G.; Walter, R. L. (Duke Univ., Durham, N. C. Triangle Universities Nuclear Lab., Durham, N. C.). Nucl. Phys.; A155: 659-72(1970).

Angular distributions of the neutron polarizations for the n_0 and n_1 groups from the ^{6}Li(d,n) and ^{7}Li(d,n) reactions were measured for deuteron energies from 2.5 to 3.7 MeV. Helium was used as a polarization analyzer and a spin precession solenoid was used to simulate interchange of the "side" detectors. The polarization distributions for the four groups studied have shapes that are very constant with energy over the energy range studied. The maximum absolute value of the measured polarizations is greater than about 0.40 for all except the ^{7}Li(d,n_1) reaction. Distorted wave Born approximation calculations in which capture of the proton in the 1p shell with $j = \frac{3}{2}$ was assumed, were made for the ^{6}Li(d,n_1) and ^{7}Li(d,n_0) reactions at 3.7 MeV. Using optical-model parameters that were obtained from published values, reasonable agreement with cross-section data was obtained and the predicted polarizations resembled the measured data somewhat. (auth)

9985 ^{18}O(^{3}He,d)^{19}F REACTION AT $E_{^3He}$ = 16 MeV. Schmidt, C.; Duhm, H. H. (Max-Planck-Institut fuer Kernphysik, Heidelberg). Nucl. Phys.; A155: 644-58(1970).

^{18}O(^{3}He,d)^{19}F angular distributions were obtained at 16 MeV bombarding energy using a magnetic spectrograph. Levels were observed up to about 10.5 MeV excitation energy. Standard DWBA analysis yields l-assignments and spectroscopic factors for about 30 states. For the strong transitions good agreement is found with a previous experiment at 11 MeV. For some weaker transitions, however, the present data yield smaller spectroscopic factors and some discrepancies with previous l-assignments which may partly be attributed to the difficulties in the analysis resulting from the lack of structure of the angular distributions (momentum mismatch) at higher excitation energies. The attempt of extrapolating the DWBA calculations to the unbound $\frac{1}{2}^+$, $T = \frac{3}{2}$ state at 8.795 MeV yields a much too small spectroscopic factor which again may partly be due to the momentum mismatch conditions for negative Q-values in the (^{3}He,d) reaction. (auth)

9986 MANY-NUCLEON TRANSFER REACTIONS BETWEEN HEAVY IONS. Roynette, J. C. (Institut de Physique Nucleaire, Orsay, France). Nucl. Phys.; A155: 548-60(1970). (In French).

Population of n-particles–n-hole states is studied in three, four and five nucleon stripping reactions by heavy ions, leading to the ^{16}O residual nucleus. High-energy excitation levels of ^{16}O are obtained up to 26 MeV. All of these reactions are very selective, especially alpha transfer reactions. Several 2p–2h and 4p–4h states are populated by three and five nucleons transfer reactions. Angular distributions measured at forward angles ($\geq$1.5° lab) exhibit a typically diffractional pattern suggesting that a direct interaction mechanism is predominant. (auth)

9987 THEORETICAL ANALYSIS OF $(\alpha,2\alpha)$ REACTIONS USING TRIANGULAR GRAPHS. Mithra, B.; Laverriere, R. (Univ., Lyon). Nucl. Phys.; A155: 535–47(1970).

This study concerns $(\alpha,2\alpha)$ reactions in the scheme of the dispersion theory. Triangular graphs are considered, taking into account a final state interaction. Numerical calculations are made for 56 MeV incident energy, with ^{6}Li, ^{9}Be, ^{12}C and ^{16}O as targets and in the case of a coplanar and symmetrical geometry. A good agreement is obtained especially for carbon and oxygen. (auth)

9988 ONE-NEUTRON TRANSFER REACTIONS WITH BERYLLIUM, CARBON, AND OXYGEN NUCLEI. Barker, P. H.; Huber, A.; Knoth, H.; (and others) (Laboratorium fuer Kernphysik, Zurich). Nucl. Phys.; A155: 401-16(1970).

The differential cross sections of the reactions ^{9}Be(^{12}C, ^{13}C)^{8}Be, ^{9}Be(^{16}O, ^{17}O)^{8}Be and ^{13}C(^{16}O, ^{17}O)^{12}C were measured at energies near the Coulomb barrier. DWBA calculations were used to extract the spectroscopic factors of the neutron states involved. (auth)

9989 EXCITATION FUNCTIONS FOR ^{3}He INDUCED REACTIONS WITH ^{12}C. Singh, J. (Univ. of Birmingham, Eng.). Nucl. Phys.; A155: 443-52(1970).

The excitation function for ^{12}C(^{3}He,n)^{14}O$_{g.s.}$, ^{12}C(^{3}He,d)^{13}N$_{g.s.}$ and ^{12}C(^{3}He,p)^{14}N (g.s., 2.31 MeV and 3.945 MeV) reactions was measured up to an incident ^{3}He energy of 30.6 MeV. Very little evidence of resonance structures was observed. (auth)

9990 RESONANCES IN THE INTERACTION OF ^{3}He PARTICLES WITH ^{12}C AND ^{10}B. Singh, J. (Univ. of Birmingham, Eng.). Nucl. Phys.; A155: 453-64(1970).

The excitation functions for the ^{12}C(^{3}He, ^{3}He')^{12}C* (15.11 MeV), ^{12}C(^{3}He,t)^{12}N$_{g.s.}$ and ^{10}B(^{3}He,n)^{12}N$_{g.s.}$ reactions were measured up to 30.6 MeV ^{3}He energy. The excitation functions show broad resonance structures which indicate the possibility of a compound nucleus mechanism at higher excitation energies. In the ^{12}C(^{3}He, ^{3}He')^{12}C* (15.1 MeV) reaction, a strong peak is seen at an incident ^{3}He energy of 21.5 MeV. (auth)

9991 VALIDITY OF THE AUSTERN–BLAIR METHOD FOR INELASTIC SCATTERING OF DEUTERONS AND ALPHA PARTICLES. Hermans, W. C. (Inst. for Nuclear Physics Research, Amsterdam); Tjin A Djie, H. R. E.; Tolsma, L. D.; Verhaar, B. J. Nucl. Phys.; A141: 431-48(1970).

The Austern-Blair method (AB) for inelastic scattering with collective excitation has been compared with DWBA for the excitation of the first 2^+ level of a number of doubly even nuclei by medium-energy deuterons and alpha particles. The derivatives of the phase shifts were obtained from optical-model calculations or from parametrized phase-shift distributions. For alpha particles with energies above 20 MeV the angular distributions of AB and DWBA are very similar. For deuterons (with $11.9 \leq E \leq 52$ MeV) and for alpha particles with energy below 20 MeV the AB results show strong discrepancies with respect to the corresponding DWBA angular distributions, which are due to large contributions from the radial integrals for the lower partial waves, for which the AB assumptions are not valid. This is probably related to an increased transmission, observed in the phase-shift distributions. An optical-model parameter for predicting the success of the AB method in fitting angular distributions is introduced. (auth)

9992 REALISTIC ONE-BOSON-EXCHANGE POTENTIALS AND THEIR APPLICABILITY IN THE SHELL MODEL OF ^{16}O. Ganas, P. S. (Univ. of Florida, Gainesville). Phys. Rev., C; 2: 93-102(Jul 1970).

Realistic, generalized, and regularized, velocity-dependent one-boson-exchange potential models of the nucleon–nucleon interaction are applied to calculate the low-lying energy levels of the nucleus ^{16}O in the harmonic-oscillator shell model. In these calculations, the short-range correlations are excluded which, if they were included, would suppress the repulsive core. Also, core-polarization effects are excluded which take account of the excitations of the ^{16}O core. It is found that the shell-model matrix elements are too repulsive, and the energy levels lie too high. Good agreement with experiment is obtained after weakening the ω-meson interaction to compensate for the neglect of the effects. This also provides a simple way of incorporating the effect of the nuclear medium upon the nuclear interaction. (auth)

9993 INVESTIGATION OF (^{3}He,^{3}He) AND (^{3}He,t) REACTIONS ON ^{10}B, ^{11}B, AND ^{13}C. Nuesslin, F.; Braun-Munzinger, P. (Max-Planck-Institut fuer Kernphysik, Heidelberg). Z. Phys.; 240: 217-32(1970).

^{3}He elastic scattering and (^{3}He,t) reactions on ^{10}B, ^{11}B, and ^{13}C were studied. Excitation functions for the reactions ^{10}B(^{3}He,t)^{10}C and ^{11}B(^{3}He,t)^{11}C were measured at incident energies between 11 and 17 MeV. All angular distributions were taken at 14 MeV ^{3}He energy. From an optical-model analysis of the ^{3}He elastic-scattering data the parameters of the optical potentials are determined. Best fits are obtained using surface-peaked potentials. The (^{3}He,t) reactions are interpreted in terms of a microscopic model, which, in general, gives a good account of the data. Corrections due to nonlocality effects are included in the calculations. A satisfactory agreement of the predicted and

the measured cross sections requires an effective nucleon–nucleon interaction of the Yukawa form (α^{-1} = 1.2 fm). With a Serber exchange mixture the isospin-dependent and the spin–isospin-dependent strength parameters of the potential are deduced to be V_τ = 21.4 ± 2.3 MeV and $V_{\sigma\tau}$ = 19.5 ± 2.7 MeV, respectively. (auth)

9994 13- TO 27-MeV ^{3}He ELASTIC SCATTERING FROM SEVERAL LIGHT NUCLEI. Buffa, Anthony John Jr. Urbana, Ill.; Univ. of Illinois (1969). 227p. University Microfilms Order No. 70-13,258.

Thesis.

^{9}Be, ^{10}B, ^{11}B, ^{12}C, ^{24}Mg, ^{25}Mg, ^{26}Mg, and ^{27}Al targets were bombarded with a ^{3}He beam. Elastic scattering angular distributions were obtained in the approximate beam-energy range of 13 to 27 MeV insteps of about 2 MeV and in the angular range 8° to 150° (lab). The data were analyzed in terms of a local optical potential and a sharp-edge diffraction model; and the results, compared to other experiments. Each isotope is discussed, and possible explanations for some of the experimental discrepancies with these models are given. (Diss. Abstr. Int., B)

9995 FAST NEUTRON STUDY. Arai, E.; Ito, S.; Toda, I.; Yamauchi, T.; Yamamuro, N. (Tokyo Inst. of Tech.). Bull. Tokyo Inst. Technol. (Engl. Ed.); No. 96, 113-22(Mar 1970).

The transient behavior of monoenergetic fast neutrons in nonmultiplying systems was investigated both experimentally and theoretically. The transient phenomena can be represented by a telegrapher's equation. Decay measurement was performed at the neutron energy of 3 MeV. The dimensions of lead assemblies were 20 × 40 × 60 (cm) and 30 × 40 × 60 (cm). Neutrons were pulsed. The employed detector was a plastic scintillator combined with a 56 AVP photomultiplier. The result of time response behavior after pulse injection was compared with calculation. It was evident that the experimental decay curves were different from the single exponential mode derived from the diffusion theory. This fact suggested that a predominant spatial mode had never existed during the measurement. The angular distribution of the elastic scattering cross section of ^{12}C and ^{9}Be was measured by means of the time-of-flight method at the incident neutron energy of 14.6 MeV. Optical-model calculation was applied to the result for ^{12}C. The measured cross section of ^{9}Be was also compared with the previous study. The result for ^{12}C was in good agreement with the calculation. Particularly, the agreement with Nodvik's calculation indicated that the Coulomb term contribution to this reaction was negligible. The result for ^{9}Be was also in agreement with the other results. (Japan)

Nuclear Properties and Reactions, 20 ≤ A ≤ 89

Refer also to abstracts 9660, 9966, 9970, 9973, 9977, 9978, 9991, 9994, 10032, 10040, 10051, 10053, 10055, and 10073.

9996 (ANU-P–466) ANGULAR CORRELATION STUDIES OF THE ^{42}Ca(α,pγ)^{45}Sc REACTION. Zuk, W. M.; Symons, G. D.; Baugh, D. J. (Australian National Univ., Canberra. Dept. of Nuclear Physics). 1970. 32p. Dep. CFSTI (U. S. Sales Only).

The spins and decay modes of levels of ^{45}Sc up to an excitation energy of 1663 keV were investigated via particle–gamma angular correlation measurements of the reaction ^{42}Ca(α,pγ)^{45}Sc. From data obtained here and in previous experiments spin and parity assignments were deduced for levels at 376.2 ($3/2^-$), 542.8 ($5/2^+$), 720.7 ($5/2^-$), 974.9 ($7/2^+$), 1067.1 ($3/2^-$, $1/2^-$), 1237.3 ($11/2^-$), 1302.3 ($3/2^+$), 1409.5 ($5/2^-$, $7/2^-$), 1432.9 ($9/2^+$, $5/2^+$), 1556 ($1/2^-$, $3/2^-$) and 1662.8 ($9/2^-$) keV. Discrepancies in the decay schemes for the 1067.1-, 1302.3-, 1432.9- and 1556-keV levels were resolved. (auth) (Australia)

9997 (JINR-E4-5350) GENERALIZED DWBA MODEL APPLIED TO THE ^{24}Mg(d,p)^{25}Mg REACTION AT E_d = 13.5 MeV. Schulz, H.; Wiebicke, H. J.; Fuelle, R.; Netzband, D.; Schlott, K. (Joint Inst. for Nuclear Research, Dubna (USSR). Lab. of Theoretical Physics). 1970. 28p. Dep. NTIS (U. S. Sales Only).

By the code POLLUX angular distributions for the reaction ^{24}Mg(d,p)^{25}Mg were calculated and compared with the experimental data covering the $5/2^+$ [202], $1/2^+$ [211], $1/2^+$ [200], and $1/2^-$ [330] rotational bands. The code considers indirect transitions arising via intermediate rotational excitations of the target and final nuclei. The optical and deformation parameters for both the entrance and exit channels were taken from the elastic and inelastic scattering data. The wave function of the transferred neutron was obtained in a deformed Saxon–Woods potential. The experimental data are sufficiently well described, as is shown by the comparison between calculation and measurement, with respect to the shape as well as the absolute cross section. In particular, remarkable agreement is obtained for the stripping-forbidden transition to the $7/2$ $5/2^+$ [202] state. (auth)

9998 (NP–18439) MEASUREMENT OF THE ORIENTATION OF THE RESIDUAL NUCLEUS AND SEVERAL DIFFERENTIAL INTERACTION CROSS SECTIONS IN THE REACTION ^{56}Fe(d,p)^{57}Fe. Bueche, G. (Kernforschungszentrum, Karlsruhe (West Germany). Institut fuer Experimentelle Kernphysik). Jun 1970. 87p. (In German). Dep. CFSTI (U. S. Sales Only).

Thesis. Submitted to Univ. Technische Hochschule, Karlsruhe, Germany.

The spin dependence of the nuclear energy orients the angular momentum of the particles in the final states of a reaction. After (d,p) stripping reactions, the rest nucleus polarization was investigated in comparison with the rare nucleon polarization. The Moessbauer effect opened for some nuclei the possibility that, from the hyperfine structure splitting of its states, information could be obtained on the orientation of the nucleus after reaction. For residual nuclei of the reaction ^{56}Fe(d,p)^{57}Fe (14 keV), from the intensity distribution of the hyperfine structure transition ($3/2$, $\pm 3/2$) → ($1/2$, $\pm 1/2$) in coincidence with protons, the orientation in the ($3/2$, $\pm 3/2$) states are measured. The possible disturbances to the orientation of the residual nucleus is discussed. The differential cross section at a deuteron energy of 5.5 MeV was measured for excitation energies below 3 MeV. (tr-auth)

9999 (ORNL–4552) NEUTRON ELASTIC- AND INELASTIC-SCATTERING CROSS SECTIONS FOR YTTRIUM IN THE ENERGY RANGE 4.19 TO 8.56 MeV. Perey, F. G.; Kinney, W. E. (Oak Ridge National Lab., Tenn.). Dec 1970. Contract W-7405-eng-26. 52p. Dep. NTIS.

Numerical values are presented for neutron elastic- and inelastic-scattering cross sections for Yttrium for incident neutron energies from 4.19 to 8.56 MeV. The data are in good agreement with the results of others. (auth)

10000 (PH–2) MEASUREMENT OF THE REACTION ^{35}Cl (n,γ)^{36}Cl USING A THREE-CRYSTAL PAIR AND ANTI-COMPTON SPECTROMETER. Jafar, J. D.; Abdulla, A. A.; Al-Quraishi, N. H.; Alwash, M. S.; Kajfosz, J.; Khalil, M. A.; Al-Kaissy, M. H.; Kosina, Z. (Atomic Energy Commission, Baghdad (Iraq). Nuclear Research Inst.). Sep 1970. 21p. Dep. NTIS (U. S. Sales Only).

The Cl(n,γ) reaction was investigated, and the energies and intensities of 190 resolved γ rays are reported. A three-crystal NaI–Ge pair and anti-Compton spectrometer was used. A computer program useful in the automatic analysis of γ-ray spectra is briefly described. A boot-strap technique generated a self-consistent energy calibration, and the binding energy of ^{36}Cl was determined to be 8580.7 ± 1 keV. (auth)

10001 COLLECTIVE LEVELS IN ^{72,74,76,78}Se. Lieder, Rainer M.; Draper, James E. (Univ. of California, Davis). Phys. Rev., C; 2: 531-43(Aug 1970).

The even selenium isotopes ^{72}Se, ^{74}Se, ^{76}Se, and ^{78}Se have been investigated by means of the Ge(α,2nγ)Se and Ge(α,4nγ)Se reactions. The γ radiation from these nuclei was studied during the irradiation using techniques of in-beam spectroscopy. The energies of the γ rays, their relative intensities, their angular distributions, and their time distributions relative to the 2-nsec beam bunch have been measured. Quasirotational ground-state bands were observed up to 10+ for ^{76}Se, up to 8+ for ^{74}Se and ^{78}Se, and up to 6+ for ^{72}Se. The level energies are compared to a semiempirical formula. (auth)

10002 STUDY OF THE EXCITED STATES OF ^{22}Ne FROM THE REACTION ^{18}O(α,γ)^{22}N BETWEEN 16 AND 5.0 MeV. Chouraqui, G.; Muller, Th.; Port, M.; Thirion, J. M. (Univ., Strasbourg). J. Phys. (Paris); 31: 249-54(Apr 1970). (In French).

The excitation curve for the 350-keV radiation from the ^{18}O (α,nγ)^{21}Ne reaction was measured. Six new resonances were observed corresponding to the following ^{22}Ne levels: E_x = 11.199 MeV(E_α = 1.873 MeV; Γ_t = 7 keV), 11.271 (1.961; 7), 11.431 (2.156; 47), 11.519 (2.263; 6), 11.577 (2.335; 16), 11.745 (2.540; 41). The gamma decay spectra were observed for all levels and the angular distributions measured for levels with strong enough gamma yield. Actually this only occurred for three previously observed resonances. For the Ex = 11.462 MeV (2.194; 9) level, the angular distribution analysis led to the $J^\pi = 1^-$ assignment. For the levels Ex = 11.682 MeV (2.463; 8) and Ex = 11.751 MeV (2.547; 8), the earlier J^π assignments of respectively 2^+ and 1^- were confirmed. The branching ratios (γ0/γ1) were determined for these three levels as well as the multipole mixing coefficients for the γ1 radiations. Upper limits of the γ0 + γ1 transition strengths ωγ are given for the other levels. (auth)

10003 ENERGY LEVELS OF ^{45}Ti EXCITED IN THE ^{45}Sc(p,n)^{45}Ti REACTION. Iyengar, K. V. K.; Wong, E.; Neilson, G. C. (Univ. of Alberta, Edmonton). Nucl. Phys.; A155: 582-96(1970).

XUM

The energy levels of ^{45}Ti excited in the reaction ^{45}Sc(p,n)^{45}Ti were investigated by neutron time-of-flight technique. Levels in ^{45}Ti at 1.521, 1.800, 1.880 and 2.020 MeV were observed for the first time through this reaction. Angular distributions of the neutron groups to the ground state, 0.040, 0.330, 0.744, 1.226, 1.353 and 1.468 MeV levels were measured at a mean proton energy of 5.330 MeV. The neutron distributions to the ground state, 0.040, 0.330 and 0.744 MeV levels of ^{45}Ti were compared with the predictions from Hauser–Feshbach statistical model and a spin of $\frac{5}{2}$ was assigned to the 0.744 MeV level. Gamma rays from the interaction of protons with scandium were observed using a Ge(Li) detector and γ-rays of 293, 414, 482, 707, 896, 1186, 1226, 1313, 1353, 1468 and 1484 keV were observed to arise from transitions between levels of ^{45}Ti. The angular distributions of the 293 and 414 keV γ-rays were measured at protón bombarding energies of 3.45 and 3.85 MeV respectively and were found to be isotropic. (auth)

10004 LOW-LYING LEVELS OF ^{20}F. Quin, P. A.; Bissinger, G. A.; Chagnon, P. R. (Univ. of Notre Dame, Ind.). Contract Nonr-1623(05). Nucl. Phys.; A155: 495-512(1970).

Directional-correlation measurements of γ-rays with protons in the reaction ^{18}O(^{3}He,pγ)^{20}F through several of the levels of ^{20}F up to 3 MeV in excitation were made in collinear reaction geometry. With this extension of earlier work there was combined an extensive review of all available experimental work bearing on each of the levels discussed. The spin and parity assignments ensuing are compatible with earlier publications; usually they are more restricted and in two cases unambiguous: 656 keV, $J^\pi = 3^+$, and 2044 keV, $J^\pi = 2^+$. Branching ratios for all of the levels in this range were measured and are reported, as are the multipole mixing ratios deduced for all of the γ-ray transitions studied. (auth)

10005 REACTION MECHANISM IN (p,pn) REACTIONS AT 17 MeV. Cohen, B. L.; Fink, C. L.; van der Weerd, J. C.; Petty, R. J. (Univ. of Pittsburgh). Phys. Rev., C; 1: 1237-59(Apr 1970).

(p,pn) reactions induced by 17-MeV protons on 12 different nuclei are studied by coincidence detection and energy measurements of the emitted neutron and proton. Probabilities of exciting various final states and of (p,p′γ) reactions (i.e., no neutron emission) are measured as a function of the energy of the emitted particles, and attempts are made to explain the results with a model assuming that these are (p,p′) reactions followed by neutron boil-off. There are many disagreements with the predictions of this model, and many inconsistencies between results from the different nuclei under this interpretation. It is shown that including contributions from (p,n) reactions followed by proton boil-off does little to improve the situation. The results might be explained if both particles are emitted in a direct reaction, although there is difficulty with the simplest such reaction, a single collision knockout, in that there is poor correlation between states excited in these reactions and in pickup reactions such as (p,d). (auth)

10006 ^{20}Ne(p,t)^{18}Ne REACTION AS A TEST OF THE ^{18}Ne AND ^{20}Ne WAVE FUNCTIONS. L'Ecuyer, J. (Oxford Univ.); Gill, R. D.; Ramavataram, K.; Chant, N. S.; Montague, D. G. Phys. Rev., C.; 2: 116-24(Jul 1970).

The differential cross sections for the reaction ^{20}Ne(p,t) leading to states of ^{18}Ne were measured at a proton energy of 50 MeV. The angular distributions were analyzed in the distorted-wave Born approximation (DWBA) and the transferred angular momentum was extracted. This led to the following energy-level sequence in ^{18}Ne: ground state, 0^+; 1.83 MeV, 2^+; 3.36 MeV, 4^+; 3.58 MeV, 0^+ and 2^+; 4.46 MeV, 1^-; 5.12 MeV, and 6.34 MeV. A comparison was made with the predictions of DWBA calculations for the relative cross section, using various wave functions for both initial and final nuclei. It is concluded that only the wave functions which include the $1p_{\frac{1}{2}}$ and $1d_{\frac{5}{2}}$ configurations give satisfactory agreement with the data. The calculation of the form factor is also discussed, and its effect on the cross section is found to be large. On the whole, better agreement is achieved when using the same binding energy instead of the same well depth for all configurations. (auth)

10007 NUCLEAR STRUCTURE EFFECTS IN THE γ DECAY OF ISOBARIC ANALOG STATES IN ^{24}Mg, ^{27}Al, AND ^{28}Si. Lawergren, B. (Columbia Univ., New York); Taylor, I. J.; Nessin, M. Phys. Rev., C; 1: 994-99(Mar 1970).

The ^{23}Na(d,n), the ^{26}Mg(d,n), and the ^{27}Al(d,n) reactions were used to populate isobaric analog states. Their γ decays were measured with a Ge(Li) detector (i) in coincidence with the neutron groups, (ii) in singles arrangements using a bare detector, and (iii) in a three-crystal configuration. The observed branching ratios are compared to the approximate selection rules operating in the rotational and the Hartree–Fock model. It is found that the 4.23-MeV state in ^{24}Mg has a wave function with admixtures of angular momentum projection K = 0 and K = 2. This fact supports the model proposed by Kelson et al. which gives an ellipsoidally symmetric deformation to ^{24}Mg. The observed transitions in ^{28}Si indicate that the analog of the ground-state doublet in ^{28}Al has an oblate deformation. (auth)

10008 ADDENDUM TO HARTREE–FOCK–BOGOLYUBOV CALCULATIONS IN THE 2s, 1d SHELL. Goss, David (Nebraska Wesleyan Univ., Lincoln). Phys. Rev., C; 2: 1168-70(Sep 1970).

The mass hexadecapole moments obtained from the Hartree–Fock–Bogolyubov variational calculation of Satpathy, et al. (Phys. Rev. 183, 887 (1969)) were compared with those of Swiniarski, et al. (Phys. Rev. Letters 23, 317(1969)). Values of the deformation parameter for second- and fourth-order axial deformation are given for ^{20}Ne, ^{24}Mg, ^{28}Si, and ^{32}S. (M.C.G.)

10009 BRANCHING RATIOS AND INTENSITIES OF SOME TRANSITIONS IN ^{35}Cl(n,γ)^{36}Cl REACTION. Honzatko, J.; Kajfosz, J.; Konecny, K. (Nucl. Research Inst., Rez, Czech.). Czech. J. Phys.; 20: 1059-61(1970).

A Ge(Li) detector was used to measure branching ratios and intensities of some transitions in the ^{35}Cl(n,γ) reaction. The placement of the transitions in the ^{36}Cl level scheme is discussed. The results are compared with previous data. (J.W.R.)

10010 INELASTIC ELECTRON SCATTERING AND SUPERMULTIPLETS IN THE PARTICLE–HOLE MODEL FOR ^{12}C, ^{16}O, ^{28}Si, ^{32}S, AND ^{40}Ca. Donnelly, T. W.; Walker, G. E. (Stanford Univ., Calif.). Contract F44620-68-C-0075. Ann. Phys. (N. Y.); 60: 209-72(Sep 1970).

Within the framework of the simple particle–hole model electron inelastic scattering form factors are obtained and the usefulness of Wigner supermultiplet theory as a predictive tool in studying weak and electromagnetic processes in light closed-shell nuclei is investigated. In the cases of ^{12}C and ^{16}O the Serber–Yukawa residual interaction yields wave functions and electron inelastic scattering form factors in essential agreement with recent experimental data, and prompts the study of heavier nuclei in the same manner. Therefore, by interpreting the particle–hole states as the doorway states for electroexcitation and grouping states neighboring in energy into complexes, form factors to be compared with averaged electron scattering data are obtained. Interesting structure is predicted over a wide range of momentum transfer, particularly at high momentum transfer where the excitation function contains a few well-separated strongly-excited complexes dominated by high spin states. These results suggest future experimental studies of electroexcitation which may serve as tests of the particle–hole model. (auth)

10011 ANALOG STATES OF ^{89}Sr AND THE PARTICLE-CORE MODEL IN THE N = 50 REGION. Cosman, E. R. (Los Alamos Scientific Lab., N. Mex.); Kalish, R.; Armstrong, D. D.; Britt, H. C. Contract AEC(30-1)-2098. Phys. Rev., C; 1: 945-57(Mar 1970).

Analog resonances in (p,p) and (p,p′) excitation functions on ^{88}Sr are studied, and previous data are extended to complete the range from E_p = 4.8 to 12 MeV and include residual channels up to E_x = 4.5 MeV in the target system. The various reaction mechanisms contributing to the observed structure are assayed. A comparison of the present data with similar experimental results in this mass region is made, and the empirical evidence for particle-core coupling in the spectra of several odd-A nuclei near N = 50 is stressed. The possible existence of composite particle-core structure involving the 0_1^+ and collective 2_1^+ and 3_1^- cores is discussed and a consequent means of populating two-phonon $2_1^+ \times 3_1^-$ state is suggested. Evidence for particle coupling to non-collective core excitations is also cited. (auth)

10012 EXCITATION OF NUCLEAR FRAGMENTS FOLLOWING K^- ABSORPTION BY NEON. Garrett, N. E. (Univ. of Tennessee, Knoxville. Oak Ridge National Lab., Tenn.); Bugg, W. M.; Condo, G. T.; (and others). Nucl. Phys.; B24: 653-6(1970).

A study of internally converted electron-positron pairs associated with K^- neon absorption at rest reveals that 0.67 ± 0.15 γ-rays are emitted per nuclear absorption, indicating a large probability for residual nuclear excitation following K^- absorption. (auth)

10013 SENSITIVITY OF THE (^{3}He,t) REACTION TO FINAL-STATE CONFIGURATIONS. Holden, J. E.; Fortune, H. T.; Balamuth, D. P.; Zurmuehle, R. W. (Univ. of Pennsylvania, Philadelphia). Phys. Rev. Lett.; 25: 1677-9(14 Dec 1970).

The reactions ^{27}Al(^{3}He,t)^{27}Si and ^{23}Na(^{3}He,t)^{23}Mg were studied at a bombarding energy of 18 MeV. Within each nucleus angular distributions leading to states of the same spin and parity are found to show a pronounced dependence on the configuration of the final state, contrary to previous suggestions. Such a dependence is consistent with the results of microscopic distorted-wave Born-approximation calculations. (auth)

10014 STUDY OF ATOMIC NUCLEUS BY ELECTRON SCATTERING. Torizuka, Yoshiharu; Kimura, Motoharu; Kojima, Yuzo; Oyamada, Masayuki; Nakahara, Kazuo (Tohoku Univ., Sendai). Kakuriken Kenkyu Hokoku; 2: No. 2, 1-31(Dec 1969). (In Japanese).

The study of atomic nuclei was made with electron scattering on ^{9}Be, ^{12}C, ^{16}O, ^{40}Ca, ^{58}Ni, ^{60}Ni, and ^{197}Au. The experimental result on ^{9}Be already reported was analyzed in accordance with the medium coupling model and the strong coupling model. The spectrum near the giant resonance of ^{12}C was examined and compared with the quantitative theory. $|F|^2$ of 25.5-MeV level was in agreement with giant resonance theory. The 19-MeV level of ^{16}O was found to be multiple, and separated into levels at 18.6 MeV and 19.1 MeV. Modes were assigned to each level. The measurement of ^{40}Ca was extended to higher q. The difficulty of the one-particle–one-hole model became more evident. The measurement of $|F|^2$ of ^{58}Ni and ^{60}Ni was extended to higher q. Elastic scattering from ^{197}Au was measured, and the change distribution in the ground state was determined from the data. (Japan)

Nuclear Properties and Reactions, A ≥ 90

Refer also to abstracts 8238, 8465, 8830, 8831, 9594, 9596, 9660, 9948, 9966, 9970, 9978, 9991, 10005, and 10008.

10015 (ANL-7699) PHYSICS DIVISION SUMMARY REPORT, JANUARY-MARCH 1970. (Argonne National Lab., Ill.). Contract W-31-109-eng-38. 47p. Dep. NTIS.

Research highlights at the Physics Division of Argonne National Laboratory in the period January through March 1970 are summarized. (J.W.R.)

10016 (ANU-P-503) SEARCH FOR THE 3446 keV LEVEL IN ^{29}P VIA THE ^{28}Si(p,γ) REACTION. Zuk, W. M.; Black, J. L.; Davidson, W. F. (Australian National Univ., Canberra. Dept. of Nuclear Physics). 1970. 9p. Dep. CFSTI (U. S. Sales Only).

A search for a resonance in the ^{28}Si(p,γ)^{29}P reaction, corresponding to excitation of the 3.446 MeV level in ^{29}P, was carried out utilizing a high-efficiency coincidence system. No resonance was observed and an upper limit of 0.7×10^{-3} eV was set on $(2J+1)\Gamma_p\Gamma_\gamma\Gamma$, which is 7 times lower than previous limits. (auth) (Australia)

10017 (BARC-501) ANNUAL REPORT OF THE NUCLEAR PHYSICS DIVISION, 1969-70. Iyengar, P. K.; Murthy, N. S. Satya (Bhabha Atomic Research Centre, Bombay (India)). 1970. 112p. Dep. CFSTI (U. S. Sales Only).

Research at the nuclear physics division of Bhabha Atomic Research Center in 1969 is summarized. The work includes nuclear physics, solid state physics, reactor neutron physics, seismology, and development of special nuclear instruments. (J.W.R.)

10018 (BMBW-FBK-70-10) ANNUAL REPORT, 1969. (Technische Hochschule, Munich (West Germany). Teilinstitut Maier-Leibnitz im Physikdepartment). Jul 1970. 187p. (In German). Dep. NTIS (U. S. Sales Only).

Some results from nuclear physics including measurements and calculations of (n, γ), (n, e$^-$) and (n, n′γ)-reactions and cross sections for slow and fast neutrons are reported. Experiments in solid state physics and low temperature irradiation at the FRM include Hall effect on Al, Mössbauer-effect on ferromagnetic platinum alloys and influence on electrical, magnetic and lattice properties of metals, and scattering experiments and calculations with slow neutrons on polycrystals. New apparative developments include a 1 Å-neutron guide tube, a monochromator with circular ringslits for lightsources of small luminosity density, Michelson-spectrometer for fourier-spectroscopy, measurement of half-lives up to 10 seconds by the aid of a small on line computer, improvement of an arrangement for measurements of Debye-Waller-factors as function of temperature, and an arrangement for activation analysis of frozen liquids by means of low temperature irradiation. (auth)

10019 (BNL-50242) STUDIES OF THE CAPTURE CROSS SECTION OF ^{237}Np AND ^{241}Am IN DIFFERENT REACTOR SPECTRA. Hellstrand, E.; Phelps, J.; Sastre, C. (Brookhaven National Lab., Upton, N. Y.). Jun 1970. 14p. Dep. NTIS.

Reactor oscillator technique was used for studying the capture cross section of ^{237}Np and ^{241}Am in two different reactor spectra. Because of unforeseen difficulties in ascertaining accurate weights of the samples, separate values of 2200-m/sec cross section σ_0 and the resonance integral RI could not be derived from the experiments. For the same reason no results could be obtained from measurements on ^{238}Pu and the ^{239}Pu substandard used for correcting the ^{238}Pu sample result for the ^{239}Pu contribution. Assuming $\sigma_0 = 169 \pm 5$ b, a value of RI = 640 ± 50 b was obtained for ^{237}Np. For ^{241}Am the measurements yielded the relation RI = 6.1 σ_0 − 2210 between the cross sections involved. The low-energy limit for RI is 0.55 eV. (auth)

10020 (BNL-tr-379) EMPIRICAL NEUTRON TRANSMISSION COEFFICIENTS FOR HEAVY NUCLEI IN THE ENERGY REGION 0.05-2 MeV. Vorotnikov, P. E. Translated by S. J. Amoretty (Brookhaven National Lab., Upton, N. Y.), from At. Energy, (USSR); 29: 48(1970). 6p Dep. NTIS.

Transmission coefficients $T_l(E_n)$ are determined directly from the experimental data for energies between 0.05 and 2 MeV from excited levels in ^{232}Th and ^{238}U. Contributions from direct processes and fission were ignored. The cross sections calculated from these T_l are compared with experiment. (R.W.R.)

10021 (CEA-N-1273) CRITICAL EXAMINATION OF ^{240}Pu NEUTRON CROSS SECTIONS. L'Heriteau, Jean-Pierre; Ribon, Pierre (Commissariat a l'Energie Atomique, Saclay (France). Centre d'Etudes Nucleaires). Mar 1970. 51p. (In French). (EANDC(E)-126-AL). Dep. CFSTI (U. S. Sales Only).

Neutron data concerning ^{240}Pu is presented; the most recent experimental results are taken into account and errors dependent upon energy are estimated. Problems arising from discrepancies between resonance parameters and $\bar{\nu}(E)$ are dealt with. Essentially data applicable to energies less than 1 MeV are considered. A set of suggested data is given. (auth) (France)

10022 (CEA-N-1338) MEASUREMENT AND ANALYSIS OF HOLMIUM TOTAL CROSS SECTION FOR NEUTRONS AT ENERGIES BETWEEN 0.005 AND 1.7 keV. Tellier, Henry (Commissariat a l'Energie Atomique, Saclay (France). Centre d'Etudes Nucleaires). Nov 1970. 20p. (In French). Dep. NTIS (U. S. Sales Only).

The total cross section of holmium was measured by the time-of-flight method, at liquid nitrogen temperature. Resonance parameters were obtained by a shape analysis of the transmission curve. The values of the strength function, the level-density parameter, and the neutron-width and level-spacing distributions were determined. (auth) (France)

10023 (CEA-N-1372) RADIOACTIVE CHARACTERISTICS NECESSARY FOR STUDYING FISSION PRODUCTS: BETA RADIATION AND CONVERSION ELECTRONS. Kostic, S.; Le Meur, R. (Commissariat a l'Energie Atomique, Saclay (France). Centre d'Etudes Nucleaires). 6 Aug 1970. 26p. (In French). Dep. NTIS (U. S. Sales Only).

In order to use them in semiconductor spectrometry, the energies of the electrons emitted by fission products were grouped in two tables. The first table refers to the electrons emitted in β disintegration and the second to the internal conversion electrons emitted. The name and period of the nuclide are indicated for each energy. The energies and their associated abundances are given. (auth) (France)

10024 (FEI-190) ANGULAR ANISOTROPY OF THE PHOTOFISSION OF ^{239}Pu. Soldatov, A. S.; Tsipenyuk, Yu. M.; Smirenkin, G. N. (Gosudarstvennyi Komitet po Ispol'zovaniyu Atomnoi Energii SSSR, Obninsk. Fiziko-Energeticheskii Institut). 1970. 15p. (In Russian). Dep. NTIS (U. S. Sales Only).

The energy dependence of the cross section and angular anisotropy of the photofission of ^{239}Pu was studied near the threshold. Also performed was combined analysis of experimental data on reactions of ^{239}Pu(γ,f) and ^{238}Pu(n,f). The quasi-stationary state of the ^{239}Pu nucleus, fissioning at the excitation energy of 5.6 MeV, was found to be 0.5 MeV below the height of the barrier. (tr-auth)

10025 (INDC(NDS)-19/N) ENERGY DEPENDENT $\bar{\nu}$-VALUES FOR ^{235}U, ^{239}Pu, ^{233}U, ^{240}Pu, ^{241}Pu, AND THE STATUS OF $\bar{\nu}$ FOR SPONTANEOUS FISSION ISOTOPES. Konshin, V. A.; Manero, F. (International Nuclear Data Committee). Jun 1970. 63p. Dep. CFSTI (U. S. Sales Only).

10026 (JINR-E3-5371) COHERENT SCATTERING AMPLITUDE OF TUNGSTEN-186 MEASURED BY SMALL ANGLE SCATTERING. Alexandrov, Yu. A.; Koester, L.; Samosvat, G. S. (Joint Inst. for Nuclear Research, Dubna (USSR). Lab. of Neutron Physics). 1970. 11p. Dep. NTIS (U. S. Sales Only).

The "Christiansen-Filter" technique was used. The scattering amplitude of tungsten was determined from the condition of identity of the refractive indices of a powder and a liquid when the small-angle scattering of neutrons passing through the filter is negligible. For the mixture of tungsten isotopes containing 90.7% of ^{186}W, the coherent scattering amplitude of neutrons with the

XUM

average wavelength of about 15 Å was found to be (−0.466 ± 0.006) F. (auth)

10027 (JINR-E6-5379) TWO-QUASIPARTICLE $(h_{9/2})^2$ ISOMERIC STATE IN ^{202}Po. Hagemann, U.; Neubert, W.; Schulze, W. (Joint Inst. for Nuclear Research, Dubna (USSR). Lab. of Nuclear Reactions). 1970. 11p. Dep. NTIS (U. S. Sales Only).

In ^{202}Po a two-quasi-particle state of the configuration $(h_{9/2})^2$ with half-life $T_{1/2}$ = 165 ± 20 ns and transition energies 443, 571, and 677 keV was found. In ^{204}Po the half-life of the $I^\pi = 8^+$ isomeric state was measured as $T_{1/2}$ = 140 ± 5 ns. (auth)

10028 (JINR-P4-5228) NON-ROTATIONAL STATE OF DEFORMED NUCLEI WITH AN ODD NUMBER OF NEUTRONS IN THE RANGE 165 ≤ A ≤ 175. Malov, L. A.; Solov'ev, V. G.; Fedolov, S. I. (Joint Inst. for Nuclear Research, Dubna (USSR). Lab. of Theoretical Physics). 1970. 14p. (In Russian). Dep. NTIS (U. S. Sales Only).

A superfluid nuclear model was used for calculating the ground and excited states of odd N nuclei in the range of 165 ≤ A ≤ 175. The single-particle energies and wave functions of the Saxon–Woods potential were used in the computations. Data obtained were in good agreement with experimental data. (tr-auth)

10029 (JINR-P6-5200) LIFETIME OF EXCITED STATES IN SPHERICAL NUCLEI ^{139}La, ^{135}La, AND ^{133}La. Babadzhanov, R.; Morozov, V. A.; Muminov, T. M.; Razov, V. I.; Khalikulov, A. B. (Joint Inst. for Nuclear Research, Dubna (USSR). Lab. of Nuclear Problems). 1970. 16p. (In Russian). Dep. CFSTI (U. S. Sales Only).

Determination of the probability of forbidden transitions is an effective method for the study of the structure of spherical nuclei; therefore, the lifetimes of the lower excited states were measured in the spherical nuclei ^{133}La, ^{135}La, and ^{139}La. The lifetimes of the 119.4-keV level of ^{135}La and the 97- and 130.7-keV levels of ^{133}La were determined by means of an e−γ coincidence instrument; the 165.8-keV level of the ^{139}La nucleus was measured by γ−γ coincidence. The decay of the radioactive cerium isotopes served as basis of the study. The results indicated that the above transitions are forbidden by the orbital quantum number. The quantum characteristics of the ground and lower excited levels of ^{139}La and ^{135}La nuclei were confirmed in the same experiments. The spin of the 130.7-keV level was found to be $J^\pi = {}^7/_2{}^+$. The transition may be considered as a one-particle one only in the first approximation. (TTT)

10030 (KFK-tr−329) IDENTIFICATION OF ELEMENTS 102 AND 104 WITH THE HELP OF THE COLLIMATION METHOD. Oganesyan, Yu. Ts.; Lobanov, Yu. V.; Tret'yakova, S. P.; Lazarev, Yu. A.; Kolesov, I. V.; Gavrilov, K. A.; Plotko, V. M.; Poluboyarinov, Yu. V. (Joint Inst. for Nuclear Research, Dubna (USSR)). Translated by Rosemarie Corssen (Kernforschungszentrum, Karlsruhe, Ger.), from report JINR−P7-4797. 23p. (In German). Dep. CFSTI (U. S. Sales Only).

The sharp contrast of the reactions and properties of the element 104 synthesized at Dubna and Berkeley was outlined. Possible errors in the identification of the isotope produced at Berkeley were discussed. The synthesis of elements 102 and 104 was repeated at Dubna using a collimation method for the identification of the elements. The results obtained agreed with the previous Dubna results. The collimation method of identification is described in detail and it was recommended that the measurement of the integral angular distribution of the nuclear reaction products permits a reliable identification of the atomic number of an element. This method is very easy in the synthesis of new elements in reactions with accelerated heavy ions. (J.S.R.)

10031 (ORNL-4627) CURRENT NUCLEAR LEVEL SCHEMES: A = 91 TO 117. (First Edition). "AN INVITATION TO PARTICIPATE." Bass, W. T.; Horen, D. J.; Ewbank, W. B. (Oak Ridge National Lab., Tenn.). Dec 1970. Contract W-7405-eng-26. 283p. Dep. NTIS.

Recent literature containing experimental nuclear structure data were scanned to extract level energies and spins and parities for nuclei in the mass region A = 91 to 117. A summary of "current" data for these nuclei is presented in the form of "ladder" diagrams and accompanying tables. These data mainly represent the conclusions of the authors cited and were not thoroughly evaluated. This report should provide the reader with useful and usable level information in a mass region for which more thorough compilations are mostly outdated. (auth)

10032 (ORNL-tr-2345) DECAY SCHEMES OF ^{59}Fe AND ^{192}Ir. Legrand, Jean; Morel, Jean; Clement, Christophe. Translated by Martha Gerrard and J. J. Pinajian (Oak Ridge National Lab., Tenn.), from Nucl. Phys.; A142: 63-71(1970). 13p. Dep. NTIS.

Gamma-ray transitions following the decay of ^{59}Fe to ^{59}Co and ^{192}Ir to ^{192}Pt and ^{192}Os were investigated with calibrated Ge(Li) detectors. Transitions of ^{59}Co at 381 and 1481 keV were confirmed. The absolute intensities for γ rays and β transitions are deduced, particularly, the electron capture intensity in ^{192}Ir: (4.7 ± 0.4)%. The K-capture probability is calculated: P_K = 0.811 ± 0.05. (tr-auth)

10033 DOUBLET IN THE NUCLEI ^{207}Pb AND ^{207}Tl. Hamamoto, Ikuko (NORDITA, Copenhagen). Nucl. Phys.; A148: 465-79(1970).

The following properties of the doublet (particle-vibration states) in ^{207}Pb and ^{207}Tl are investigated by solving the inhomogeneous differential equations obtained from the Schroedinger equation: the energy splitting, the one-particle structure, the decay scheme, and the strength of the octupole vibration. (auth)

10034 EXCITED STATES OF ^{156}Gd STUDIED BY THE CONVERSION ELECTRON SPECTRA OF 5.4 d ^{156}Tb. Fujioka, M. (Tokyo Inst. of Tech.). Nucl. Phys.; A153: 337-82(1970).

Excited states of ^{156}Gd were studied by the measurement of conversion electron spectra of 5.4 d ^{156}Tb, using a newly constructed iron-free $\pi\sqrt{2}$ spectrometer having a mean radius of 75 cm. Conversion lines associated with 90 transitions in ^{156}Gd were observed. The K-conversion coefficients were deduced for 33 transitions, using the previous gamma-ray data. A level scheme of ^{156}Gd comprising 22 excited states and 81 transitions was proposed with the use of energy sums. By an additional least-squares analysis the energies of the excited states were determined with errors of 0.02-0.07 keV. The L-subshell ratios were determined for the 88.97, 111.93, 115.61, 155.15, 199.19, 212.74, 262.54, 267.07, 296.49, 356.38, 381.10, 422.34, 534.29 and 1222.34 keV transitions and the multipolarities were deduced. The spins and parities were assigned, transition intensities estimated and log ft values deduced. The proposed level scheme contains the 4^+ and the 5^+ members of the β- and the γ-bands, respectively, the 1^-, 3^- and 2^- members of the octupole bands, the 2^+ member of another, recently proposed $K^\pi = 0^+$ band, and levels at ≈2 MeV feeding these states. The excited states of ^{156}Gd are discussed in comparison with theoretical predictions. (auth)

10035 PROPERTIES OF EXCITED STATES OF ^{151}Sm. Begzhanov, R. B.; Gaffarov, D. G.; Il'khamdzhanov, I.; Muminov, A. I.; Salikhaev, K. T. (Inst. of Nuclear Physics, Tashkent). Dokl. Akad. Nauk Uzb. SSR; No. 1, 18-20(1970). (In Russian).

Data were obtained for γ−γ angular correlations of seven cascades and the g-factor of the 167-keV state. Consequent quantum characteristics and multipole compositions of transitions in ^{151}Sm are tabulated. (R.V.J.)

10036 BETA DECAY OF ^{239}Pu FISSION PRODUCTS AT SHORT TIMES AFTER FISSION. Iyer, M. R.; Ganguly, A. K. (Bhabha Atomic Research Centre, Bombay). J. Nucl. Energy; 24: 171-9(Jul 1970).

The beta activity of ^{239}Pu fission products at short times after fission down to 1 msec was measured using a slow neutron chopper and a time analyser. The technique adopted for the experiment is described. The lower limit for the composite half-life of fission product beta decay was estimated as 0.2 sec. The maximum beta energy of the fission product betas at 0.96 sec of decay was found to be 5.7 MeV. (auth) (UK)

10037 NUCLEONIC COMPOSITION AND EXCITATION ENERGY OF FISSIONING NUCLEI IN IRRADIATION OF ^{209}Bi AND ^{197}Au TARGETS WITH 1-GeV PHOTONS. Komar, A. P.; Bochagov, B. A.; Kotov, A. A.; Semenchuk, G. G.; Solyakin, G. E. (Ioffe Physico-Technical Inst., Leningrad). Dokl. Akad, Nauk SSSR; 190: 1308-11(21 Feb 1970). (In Russian).

The nucleon composition A, Z and the excitation energy E_{exc} of nuclei undergoing fission by high-energy particles have been derived on the basis of processes preceding the fission. It was attempted to use data derived from the fission for this purpose, examining specifically the effect of the decrease of the kinetic energy of the fission fragments on the emission of neutrons and calculating the mass and energy distribution of the fragments for a given temperature of the nucleus. The authors' earlier data on light target nuclei ^{209}Bi and ^{197}Au and more recent data of H. W. Schmitt et al. with ^{208}Pb targets and more precise values for ^{197}Au targets calibrated with ^{252}Cf nuclei were used for the study; the Seaborg–Viola formula was used to calculate the mean kinetic energy of the fragments before the emission of neutrons. The number of the emitted neutrons was calculated on the basis of the decrease of the excitation caused by the emission of neutrons and γ quanta. The result revealed that identification of the basic fissioning ^{193}Ir nucleus in the irradiation of gold targets agrees with the experimental data. Contradictions arise, if it is assumed that either the original ^{197}Au target nucleus or the ^{192}Os nucleus undergo fission. Similar calculations for ^{209}Bi and ^{208}Pb indicate that ^{205}Pb and ^{205}Tl, respectively, undergo fission. (TTT)

10038 ACCURACY OF ANALYTICAL TREATMENTS FOR RESONANCE ABSORPTION IN DOPPLER RESONANCE REGIONS. Takano, Hideki; Nakagawa, Masayuki; Ishiguro, Yukio; Katsuragi, Satoru (Japan Atomic Energy Research Inst., Tokai). J. Nucl. Sci. Technol. (Tokyo); 7: 500-10(Oct 1970).

Resonance shielding factors based on the assumption of constant collision density were compared with those obtained by solving rigorously the slowing down equation. The results obtained by calculating numerically the flux for this assumption were thoroughly examined for several compositions and temperatures. This detailed investigation was based on consideration of the interaction effects between neighboring resonances in both the same and different nuclear species. The results obtained permitted determination of the limits of accuracy obtained with conventional analytical methods. The accuracy of two typical methods of approximation based on the above basic assumption was also investigated for important Doppler resonance regions in large fast reactor. The study covered the resonance regions below 21.5 keV for ^{238}U, and below 10 keV for ^{235}U and ^{239}Pu. It was found that the results obtained numerically from the assumption of constant collision density are fairly good at higher energies, but the errors become large with decreasing neutron energy and the increasing concentration of fuel. Furthermore the shielding factor and the temperature coefficient of ^{239}Pu are affected considerably by superposition of the resonances of ^{238}U, and the errors are thereby accentuated by a factor of more than two. And the errors resulting from the analytical methods were found larger than those incurred by the assumption of constant collision density. (auth)

10039 MEASUREMENT OF ENERGY SPECTRA AND AVERAGE NUMBER $\bar{\nu}$ OF PROMPT FISSION NEUTRONS. Kroshkin, N. I.; Zanyatnin, Yu. S. At. Energ. (USSR); 29: 95-8(Aug 1970). (In Russian).

Prompt neutron spectra of ^{244}Cm and ^{252}Cf spontaneous fission and ^{229}Th, ^{235}U, ^{238}Pu, ^{242m}Am and ^{245}Cm thermal fission were measured by the time-of-flight method. The pulse from fission fragments in gas scintillation chamber was used as start signal. Using spectra approximation by the expression $N(E) \sim \sqrt{E}e^{-E/T}$ the T parameter values were obtained to be (1.38 ± 0.03) MeV, (1.48 ± 0.03) MeV, (1.24 ± 0.04) MeV, (1.35 ± 0.04) MeV, (1.42 ± 0.03) MeV and (1.50 ± 0.05) MeV, respectively, for ^{244}Cm and ^{252}Cf spontaneous fission and for ^{229}Th, ^{238}Pu, ^{242m}Am and ^{245}Cm thermal fission. The values of fission neutron average number for above nuclei were found to be 2.77 ± 0.08, 3.77 ± 0.08, 2.05 ± 0.10, 2.92 ± 0.12, 3.28 ± 0.10 and 3.83 ± 0.16, respectively. The measurements were performed relative to ^{235}U, supposing T = 1.29 MeV and $\bar{\nu}$ = 2.426 for ^{235}U. (auth)

10040 ACTIVATION CROSS-SECTIONS, DETERMINED FROM EXPERIMENTAL STUDY OF SECOND-ORDER REACTIONS. Gijbels, R.; De Vos, M.; De Neve, R.; Hoste, J. (State Univ., Ghent) Radiochem. Radioanal. Lett.; 5: 145-57(6 Nov 1970).

Three second-order reactions were studied experimentally by irradiating highly purified osmium, germanium, and platinum during varying periods at various neutron fluxes. By determining the apparent iridium, arsenic, and gold concentrations, respectively, it was possible to determine the thermal and resonance activation cross sections for the reactions ^{190}Os(n,γ)^{191m}Os; ^{75}Ge(n,γ)^{76m}Ge; and ^{196}Pt(n,γ)^{197m}Pt, without absolute countings of the radionuclides ^{191m}Os, ^{76m}Ge, and ^{197m}Pt and without any detailed knowledge of their decay schemes. A satisfactory agreement with the latest literature data was observed. (auth)

10041 DOPPLER EFFECT OF 6.24 eV RESONANCE IN ^{121}Sb. Mateiciuc, V.; Aldea, L.; Constantinescu, M.; Dobrescu, S.; Stadnicov, T. (Inst. for Atomic Physics, Bucharest). J. Nucl. Energy; 24: 245-51(Sep 1970).

The measured influence of the Doppler effect on the 6.24 eV resonance in ^{121}Sb at room and liquid nitrogen temperature is presented. The experimental results are compared with Lamb's gas model. The 6.24 eV resonance parameters were calculated using the values on the center of the transmission in both cases. The following values were obtained: Γ = 81 ± 9 meV; Γ_γ = 79 ± 9 meV and $2g\Gamma_n$ = 2.0 ± 0.7 meV. (auth)

10042 SEMI-MICROSCOPIC DESCRIPTION OF EVEN TELLURIUM ISOTOPES. Lopac, V. (Institut Rudjer Boskovic, Zagreb. Institut de Physique Nucleaire, Orsay, France). Nucl. Phys.; A155: 513-25(1970).

The properties of even tellurium isotopes are calculated assuming two protons coupled to a quadrupole vibrator. The obtained energy levels, wave functions and electromagnetic transitions are compared with experimental data. The observed quadrupole moment of the first excited state is reproduced and its structure is analyzed in terms of the perturbation theory. (auth)

10043 NUCLEAR OCTUPOLE VIBRATIONS IN THE ISOTOPES OF Pb. Hamamoto, Ikuko (NORDITA, Copenhagen). Nucl. Phys.; A155: 362-84(1970).

By using the particle-vibration coupling model the frequency and the oscillator strength of the octupole vibrations in the nuclei of the lead isotopes are evaluated and compared with experiments. It is shown that in the heavy even-A isotopes (i.e., ^{210}Pb, ^{212}Pb etc.) the oscillator strength of the lowest 3$^-$ state (at 2.62 MeV) of ^{208}Pb is divided approximately into two low-lying states. The quadrupole moment of 3$^-$ state in ^{208}Pb is also calculated by using the present model and compared with the recent measurement. (auth)

10044 STUDY OF $^7/_2^-$ ISOBARIC ANALOGUE RESONANCE IN ODD ISOTOPES OF Sb. Arking, R. (Rutgers — The State Univ., New Brunswick, N. J.); Boyd, R. N.; Lombardi, J. C.; Robbins, A. B.; Gonsior, B. Nucl. Phys.; A155: 480-94(1970).

A study was made of the lowest-lying $^7/_2^-$ isobaric analog resonances in the odd isotopes of antimony by analysis of the elastic scattering of protons from even isotopes of tin. These resonances correspond to low-lying states in odd isotopes of tin. The states of interest are the 2.76 MeV state in ^{125}Sn, the 2.73 MeV state in ^{123}Sn and the 2.59 MeV and 2.69 MeV states in ^{121}Sn. Measurements of cross section and polarization were made for protons scattered from ^{124}Sn, ^{122}Sn and ^{120}Sn at bombarding energies from 9.85 MeV to 10.90 MeV. Theoretical fits to the data were made using resonance terms of the Breit–Wigner form in the collision matrix. The fits to the data established the spins and parities of the resonances. The resonance parameters from these fits were used to calculate spectroscopic factors for the states, using the approaches of Thompson, Adams and Robson, and of Mahaux and Weidenmüller. The optical-model parameters used to describe the non-resonant background scattering were obtained by fitting off-resonance angular distributions. An investigation has shown large sensitivities to various parameters of the optical potential. Cross-section measurements for the decay of the $^7/_2^-$ resonances to 2$^+$ and 3$^-$ excited states were made in order to obtain information about the admixtures to the analog states. (auth)

10045 PROPERTIES OF THE ^{209}Bi GROUND-STATE ANALOG IN ^{209}Po. Crawley, G. M. (Michigan State Univ., East Lansing); Benenson, W.; Miller, P. S.; Bayer, D. L.; St. Onge, R.; Krominga, A. Phys. Rev., C; 2: 1071-7(Sep 1970).

The analog of the ground state of ^{209}Bi was investigated by both the ^{209}Bi(p,n)^{209}Po and the ^{209}Bi(p,nγ)^{209}Bi reactions. The Coulomb energy difference ^{209}Po–^{209}Bi was determined as 18.92 ± 0.03 MeV, and the relative partial widths for proton decay into the $p_{\frac{1}{2}}$, $f_{\frac{5}{2}}$, and $p_{\frac{3}{2}}$ channels were determined. The total width of the analog state was found to be 380 ± 80 keV. (auth)

10046 INELASTIC ELECTRON SCATTERING BY ^{140}Ce UP TO 3.5 MeV. Pitthan, R. (Technische Hochschule, Darmstadt, Ger.). Z. Naturforsch.; 25a: 1358-9(Aug-Sep 1970). (In German).

From electron scattering experiments (scattering angle 141°, primary energies 60 and 50 MeV) ground state radiation widths were determined for the levels at 1.60 (2$^+$), 2.08 (4$^+$), 2.46 (3$^-$), 2.90, 3.12, and 3.32 MeV. Spins and parities of the last three levels, which were known as 1$^+$ or 2$^+$, could be classified as 2$^+$. (auth)

10047 EVIDENCE FOR NONSTATISTICAL EFFECTS IN THE REACTION ^{163}Dy(n,γ)^{164}Dy. Mughabghab, S. F.; Chrien, R. E.; Wasson, O. A. (Brookhaven National Lab., Upton, N. Y.). Phys. Rev. Lett.; 25: 1670-3(14 Dec 1970).

γ-ray intensities from 17 resonances with J = 3 to 22 final states in ^{164}Dy reveal that there are significant correlations between partial radiative widths and reduced neutron widths. The two-particle–one-hole doorway-state concept and channel-capture mechanisms may be invoked to explain these correlations. (auth)

10048 CONVERSION ELECTRON SPECTRUM IN THE DECAY OF ^{195}Au. Toburen, L. H.; Albridge, R. G. (Vanderbilt Univ., Nashville). Z. Phys.; 240: 185-94(1970).

Twenty-four internal conversion lines in the decay of ^{195}Au were studied at high resolution by means of an iron-free spectrometer. The electron intensities of this work and previously published photon intensities were used to calculate the percentage decay to each level in ^{195}Pt. Conversion coefficients and L-subshell ratios were used to assign the following multipolarities: 30.8 keV, pure M1; 98.8 keV, (99 ± 1)% M1; 129.8 keV, pure E2; and 210 keV, pure E2. Measured L-subshell ratios are not in good agreement with theoretical values. (auth)

10049 β–γ DECAY OF THE 5$^+$ LEVEL IN ^{116}In AND γ-BRANCHING RATIOS IN ^{116}Sn. Rabenstein, Dietrich (Technische Hochschule, Munich). Z. Phys.; 240: 244-55(1970). (In German).

The γ spectrum, emitted in the β–γ decay of the 5$^+$ state of ^{116}In, was measured with a Ge(Li) detector. Nineteen unknown transitions in ^{116}Sn were found, most of which could be fitted

XUM

uniquely into the established level scheme. A new β transition (log ft = 5.6) to the 3096-keV level was found. Branching ratios are given and a possible band structure in ^{116}Sn is discussed. (auth)

10050 THEORETICAL STUDY OF THE BETA-DECAY TRANSITIONS $0^- \rightarrow 2^+$ AND $0^- \rightarrow 0^+$ OF THE ^{166}Ho NUCLEUS. Bogdan, D. (Inst. for Atomic Physics, Bucharest); Carjan, N.; Fuia, H. Z. Phys.; 240: 233-43(1970).

The theoretical beta-decay observables are compared with the experimental values for the $0^- \rightarrow 2^+$ and $0^- \rightarrow 0^+$ transitions. By considering a ^{166}Ho ground-state configuration inferred from (d,p) reaction experiments and using all the matrix elements, satisfactory results are obtained for the $0^- \rightarrow 2^+$ transition. For the $0^- \rightarrow 0^+$ transition an important cancellation effect is found which determines the failure of the ξ approximation and results in an energy-dependent spectrum shape. (auth)

10051 ON THE STRUCTURE OF THE PAIRED STATES. Fomenko, V. N. (Leningrad State Univ.). J. Phys., A (London); 3: 520-3(Sep 1970).

The quasi-particle structure of the ground state of the pairing Hamiltonian is analysed for the Ni isotopes and ^{206}Pb. The particle-number projected Bardeen–Cooper–Schrieffer states are used for describing the states under consideration. The quasi-particle amplitudes are evaluated in the saddle-point approximation. The amplitudes with the number of quasi-particles a multiple of four are shown to be comparable with the quasi-particle vacuum amplitude. The value of the other quasi-particle amplitudes depends essentially on the system considered. In particular, the two-quasi-particle component can sometimes be comparable with the four-quasi-particle one (^{206}Pb). On the basis of the data obtained it is concluded that the random-phase-approximation ground-state wave function with small admixture of the quasi-particle components, the components with the odd number of quasi-particle pairs being neglected completely, is rather poor. (auth) (UK)

10052 CHARGED PARTICLE FISSION OF ^{238}U. Kandil, Abdel–Hakim Taha. Tallahassee; Florida State Univ. (1969). 103p. University Microfilms Order No. 70-11,131.

Thesis.

Peak-to-valley ratios for the proton and deuteron fission of ^{238}U were measured as a function of particle energy. The proton peak-to-valley ratios were in excellent agreement with the previous work of Choppin et al. The deuteron peak-to-valley ratios showed fluctuations at 10.75 MeV and 12 MeV, which are assigned tentatively to the onset of (d, d'n) and (d, 3n) reactions. A Ge(Li) spectrometer was used to measure the cross-sections of some 20 nuclides formed in the 11.2-MeV proton and 10.6-MeV deuteron fission of ^{238}U. From the estimated cross sections, mass yield curves for both the 11.2-MeV proton and 10.6-MeV deuteron fission of ^{238}U are constructed. The cross-sections of the shielded and quasi-shielded nuclides are used in testing the various prescriptions proposed for explaining the nuclear charge distribution of fission. The most satisfactory description of low-energy fission induced by charged particles is provided by the postulate of minimum potential energy although in some cases the equal-charge-displacement rule is equally good. (TSS) (Diss. Abstr. Int., B)

10053 STUDY OF ISOBARIC ANALOGUE STATE BY (γ,p) REACTION. Shoda, Katsufusa; Sugawara, Masumi; Saito, Teijiro; Miyase, Haruhisa; Oikawa, Shiro (Tohoku Univ., Sendai). Kakuriken Kenkyu Hokoku; 2: No. 2, 32-46(Dec 1969). (In Japanese).

Isobaric analogue state was studied by (e, e'p) reaction with ^{138}Ba, ^{209}Bi, ^{208}Pb, ^{88}Sr, ^{89}Y, and ^{90}Zr. A broad-range magnetic spectrometer was used to measure the energy distribution of emitted protons. By varying the energy of incident electrons, the yield curve was obtained. The result obtained with ^{138}Ba was compared with the previous measurement for ^{140}Ce, ^{142}Nd, and ^{144}Sm, and the similar resonance was found, which can be attributed to the same isobaric analogue state. The energy distribution from ^{209}Bi and ^{208}Pb showed a strong proton group around 11 MeV. The sudden increase in the proton yield of ^{209}Bi was found around Ee ≃ 18.7 MeV, which corresponds to the E1 IAS of the ground state ($2g_{9/2}$ neutron state) of ^{209}Pb. Most protons through this IAS leave the residual nucleus ^{208}Pb in several excited states. This seems to correspond to the proton group around 11 MeV. The yield curves for ^{88}Sr, ^{89}Y, and ^{90}Zr showed resonance at about 21 MeV. (Japan)

10054 LOW ENERGY FISSION OF ^{232}Th. Tofe, Andrew John. Tallahassee; Florida State Univ. (1969). 114p. University Microfilms Order No. 70-11,169.

Thesis.

A study of the mass and charge distributions of ^{232}Th with 11.3-MeV protons and 11.5-MeV deuterons was performed. Cumulative and independent yields were measured for rare-earth fission-product nuclides. Yields were also measured for iodine fission-product nuclides in the 11.5-MeV deuteron fission. Computerized analysis of Ge(Li) spectra was used to determine the nuclides from complex spectra of rare-earth and iodine fission products. The Minimum Potential Energy (MPE), Equal Charge Displacement (ECD), and Unchanged Charge Distribution (UCD) postulates were tested with an experimentally measured neutrons function. The MPE was found to best fit the 11.5-MeV deuteron data with a shell-corrected mass equation. For the proton data it was not possible to make a definitive choice between the MPE and ECD postulates. (Diss. Abstr. Int., B)

10055 COMPILATION OF COEFFICIENTS FOR ADJUSTMENT OF COMPLEX SCATTERING FACTORS FOR FAST ELECTRONS. II. THOMAS–FERMI–DIRAC CASE. Haase, Joachim (Univ., Ulm, Ger.). Z. Naturforsch.; 25a: 1219-35(Aug-Sep 1970). (In German).

Formulas and coefficients are presented for computing the magnitudes and phases of the complex scattering factors for nuclei with Z = 6 to 92; constant accelerating voltages of 40, 60, 80, 100, and 120 kV are considered, as well as a voltage-independent representation between 40 and 120 kV. (tr-auth)

10056 DELAYED NEUTRONS FROM ^{3}He AND ^{4}He INDUCED FISSION OF ^{238}U, ^{232}Th, AND ^{209}Bi AND FROM SPONTANEOUS FISSION OF ^{252}Cf. Chulick, Eugene Thomas. St. Louis; Washington Univ. (1969). 191p. University Microfilms Order No. 70-10,948.

Thesis.

Delayed neutrons were investigated from the ^{3}He- and ^{4}He-induced fission of ^{238}U and ^{232}Th, the ^{3}He-induced fission of ^{209}Bi, and the spontaneous fission of ^{252}Cf. Experiments were done at bombarding energies of 20 to 29 MeV for ^{4}He and 22 to 34 MeV for ^{3}He. Fission yields of ^{99}Mo were measured and used to monitor the beam intensities. Delayed-neutron decay curves from the ^{3}He and ^{4}He fission of ^{238}U and ^{232}Th were resolved into seven half-life groups of 55, 24, 16, 5, 2, 0.5, and 0.2 sec. The three longest-lived groups are attributed to ^{87}Br, ^{137}I, and ^{88}Br, respectively. Delayed-neutron precursor cross sections were found to peak at about 38 MeV excitation energy for ^{3}He fission. The number of delayed neutrons per fission generally decreases with increasing excitation energy but shows a slight increase at 38 MeV. The increase is attributed to the onset of new precursors or increases in the fission-chain yields. Chain yields for the mass 87, 88, and 137 chains were calculated from the delayed-neutron yields of ^{87}Br, ^{88}Br, and ^{137}I, the previously known neutron emission probabilities, and the previously known charge distribution curves. Data from the ^{3}He fission of ^{209}Bi were resolved into four half-life groups of 55, 16, 3.2, and 1.4 sec. These half-lives are similar to the half-lives of known bromine precursors. This similarity shows that the yield of heavy-mass precursors (^{137}I, etc.) is greatly reduced for symmetric fission of ^{209}Bi. Four delayed-neutron groups were found in the spontaneous fission of ^{252}Cf with half-lives of 0.5 ± 0.1, 2.0 ± 0.3, 6.1 ± 1.4, and 26.8 ± 1.1 sec and relative abundances of 0.17 ± 0.05, 0.30 ± 0.03, 0.22 ± 0.02, and 0.31 ± 0.01, respectively. The energy spectrum of delayed neutrons from spontaneous fission of ^{252}Cf was observed with a time-of-flight spectrometer. Timing conditions were set to emphasize the 2-sec group with some contribution from the 0.5-sec group. Neutron peaks were found in the energy interval from 100 to 400 keV. The neutron spectral data below 2 MeV gave a straight line when the fifth root of the number of neutrons was plotted versus neutron energy. The mean neutron energy obtained from this plot was 1.5 MeV. (Diss. Abstr. Int., B)

10057 DECAY SCHEMES OF ^{91}Mo AND ^{91m}Mo. de Barros, S. (Centro Brasileiro de Pesquisas Fisicas, Rio de Janeiro); Maurenzig, P. R.; Baptista, G.; Canto, L. F.; de Pinho, A. G.; Jeronymo, J. M. F. Z. Naturforsch.; 25a: 1250-4(Aug-Sep 1970).

Seven previously unreported gamma rays in the decay of ^{91g}Mo were observed. For ^{91m}Mo two new gamma rays were observed and the levels fed by its decay were identified with l = 1 levels found by (^{3}He, d) reaction. (auth)

Nuclear Theory

Refer also to abstracts 9600, 9637, 9685, 9694, 9703, 9742, 9791, 9810, 9890, 9949, 9978, 9994, 10008, 10052, and 10054.

10058 (ITF–70–38) QUASI-ELASTIC KNOCKOUT OF NUCLEONS FROM LIGHT NUCLEI BY HIGH ENERGY ELECTRONS. Tartakovskii, V. K.; Pasichmyi, A. A. (Akademiya Nauk Ukrainskoi SSR, Kiev. Institut Teoreticheskoi Fiziki). 1970. 17p. (In Russian). Dep. NTIS (U. S. Sales Only).

Inelastic high-energy electron scattering by light nuclei accompanied by knockout of nucleons is considered. The one-particle nucleon wave functions used in the bound state and in the state with positive energy were taken in the form of the exact solutions of Schrödinger's equation with the Woods–Saxon potential. The dependence of the disintegration process cross-section on the potential parameters is investigated. The calculated cross sections are compared with the experimental ones for ^{12}C. The possibility of taking into account the nucleon-wave deformation in the finite state is shown. (auth)

10059 (LYCEN–7039) ROLE OF POLAR AND TRIANGULAR DIAGRAMS IN THE INTERPRETATION OF $(\alpha,2\alpha)$ REACTIONS. Perrin, Martine (Lyon Univ. (France). Institut de Physique Nucleaire). Jun 1970. 63p. (In French). Dep. NTIS (U. S. Sales Only).

Thesis. Submitted to Univ. of Lyon, France.

The way in which the Shapiro model arises from formal scattering theory was recalled. The most simple graphs capable of explaining break-up reactions, in particular $(\alpha,2\alpha)$ were then described. This reaction was then envisaged as a three body problem. A development in the transition operator for the break-up reaction, whose first terms correspond to certain mechanisms described by graphs deduced from the Shapiro model, was established. Expressions for the amplitudes corresponding to virtual polar and triangular graphs, when all the particles are outside the mass shell were deduced. These expressions were applied to different real polar and triangular graphs capable of describing the $(\alpha,2\alpha)$ reactions. The theoretical results were compared with experimental results obtained using ^{6}Li, ^{12}C, and ^{16}O targets. (auth) (France)

10060 (NP–18538) HARTREE–BOGOLYUBOV THEORY AND APPLICATION TO THE NEUTRON–PROTON PAIRING PROBLEM. Jean, Maurice (Paris Univ., Orsay (France). Institut de Physique Nucleaire). [1969]. 107p. Dep. NTIS (U. S. Sales Only).

The general Hartree–Bogoliubov (HB) theory is derived, and its properties are discussed. The Hartree–Fock and BCS theories are considered as special cases of the HB theory. After application to T = 1 or T = 0 neutron–proton pairing, the theory is generalized in such a way that both T = 1 and T = 0 paring are included. It is shown that the HB theory can be used to treat on an equal footing both T = 1 and T = 0 pairing correlations among nucleons. (R.W.R.)

10061 (NYO–2171-330) GIANT MONOPOLE STATE: ISOSPIN MIXING IN NUCLEAR GROUND STATES. Noble, J. V. (Pennsylvania Univ., Philadelphia. Dept. of Physics). [1970]. 8p. Dep. NTIS.

The Coulomb-induced $\Delta T = 1$ admixture in nuclear ground states is evaluated by assuming that the mixing is entirely through the giant monopole state $|\Phi\rangle \propto (\Sigma_p r_p^2 - \Sigma_n r_n^2)|$ g.s.$\rangle$. (auth)

10062 (RLO-1388-131) FINITE NUCLEAR SIZE AND RADIATIVE CORRECTIONS IN THE CONSTRUCTION AND ASSESSMENT OF KURIE PLOTS FOR ALLOWED BETA-DECAY. Wilkinson, D. H. (Washington Univ., Seattle). [1970]. 13p. Dep. NTIS.

If only a small fraction of a β spectrum is available for Kurie plot analysis because of the existence of strong branches of lower energy, it may become important to take into account finite nuclear size and radiative effects in the construction and assessment of the Kurie plot. Failure to do this may result in errors of many percent in the extraction of the high energy β branch. These effects are analyzed, and numerical estimates are made of the possible errors. (auth)

10063 (RLO-1925-46) BOOTSTRAP THEORY OF VIBRATIONS IN NUCLEI. Nalcioglu, Orhan (Oregon Univ., Eugene). Sep 1970. 132p. Dep. NTIS.

Thesis.

The bootstrap theory of vibrations is formulated for nuclei. This is first done for the closed-shell region, and it is shown how the ground-state correlations for the odd-mass nuclei can and must be taken into account. The modification of single-particle spectroscopic factors and particle–hole splittings is explicitly demonstrated. The Random–Phase Approximation(RPA) is obtained in the weak-coupling limit. The theory is then applied to heavy spherical nuclei in the quasi-particle representation. The development of the quadrupole moment for the 2^+ state is demonstrated, and the quadrupole moment is calculated for ^{110}Pd. The effect of core anharmoniticity on the odd-mass spectrum is also pointed out. In the weak-coupling limit the QRPA is again obtained. The bootstrap theory is next developed for the pairing vibrations; in the strong-coupling limit, it gives rise to the BCS theory except for a better treatment of the number problem. The modified TDA is proposed as an alternative approach in the weak-coupling limit. Finally, the bootstrap theory is used to study the quadrupole–quadrupole force in the intermediate- and strong-coupling limits; and it is shown that the bootstrap theory gives the correct limiting cases. (R.W.R.)

10064 UNIQUE FIRST FORBIDDEN β-TRANSITIONS. Abecasis, S. M. (Laboratorio de Radiaciones, Buenos Aires); Krmpotic, F. Nucl. Phys.; A151: 641-55(1970).

Theoretical expressions which include higher-order terms in the multipole expansion of the weak Hamiltonian and terms induced by strong interaction together with the variation of the lepton wave functions over the nuclei are presented for different β-decay observables. A detailed investigation of the experiments concerning ^{142}Pr and ^{166}Ho has been performed. Shape factor measurements for ^{42}K, ^{86}Rb, ^{90}Y, and ^{90}Sr are also re-analyzed. No useful information about pseudoscalar and pseudotensor interactions can be extracted from the available experimental data. Precise experiments determining shape factors, together with longitudinal polarization and/or $\beta\gamma$ directional correlation, combined with better knowledge of the nuclear structure are required in order to draw definite conclusions. (auth)

10065 APPLICATION OF THE DIFFERENTIAL EQUATION METHOD TO THE STUDY OF A NONRELATIVISTIC FEYNMAN AMPLITUDE. Giffon, Maurice; Joseph, Jacques; Meyer, Jacques (Univ., Lyon). Compt. Rend., Ser.B; 271: 809-12(19 Oct 1970). (In French).

The method of differential equations is used to study the mathematical properties of the Feynman function associated with the fourth order diagram occurring in numerous nuclear reactions. (auth)

10066 ENERGY GAP IN NUCLEAR MATTER AND VELOCITY-DEPENDENT NUCLEON–NUCLEON INTERACTION. Bhattacharya, Purabi (Indian Inst. of Tech., Kharagpur). Indian J. Pure Appl. Phys.; 8: 302-3(Jun 1970).

The energy gap in nuclear matter was calculated using velocity-dependent, nucleon–nucleon interaction. The results agree well with the values calculated with hard core potential by earlier workers, thus showing that velocity-dependent potential can replace the hard core potential in the low energy region of nuclear matter. (auth)

10067 SOME STUDIES OF REALISTIC FORM FACTORS FOR (d,p) AND (p,d) REACTIONS IN THE LEAD REGION. Edwards, V. R. W. (Nuclear Physics Lab., Oxford). Nucl. Phys.; A138: 671-84(1969).

A formalism is developed for the calculation of the form factors of one-nucleon transfer reactions using a perturbation treatment which is correct to all orders and techniques originally employed in photonuclear reaction theory to sum the contributions of bound and continuum terms. A simplified version of this formalism is used to analyze the reactions $^{206}Pb(d,p)^{207}Pb$, $^{209}Bi(d,p)^{210}Bi$ and $^{210}Pb(p,d)^{209}Pb$ and the results are employed to determine the sensitivity of the ground state wave function predictions for the target nuclei to the form factor prescription. It is shown that significant corrections are required in certain cases. (auth)

10068 APPLICATIONS OF t-MATRIX PERTURBATION THEORY. Lu, A. H. (Rensselaer Polytechnic Inst., Troy, N. Y.). Nucl. Phys.; A149: 86-94(1970).

The energy correction to the trinucleon (with a central spin-dependent potential) due to high partial waves in the two-body interaction is calculated by using Fuda's first-order t-matrix perturbation theory. It is found that waves beyond the $^1S_0$ and $^3S_1 + {}^3D_1$ contribute less than 0.01 MeV. (auth)

10069 DIPOLE GIGANTIC RESONANCES OF NONMAGIC NUCLEI. Bazhenov, A. A.; Gamalya, I. A.; Cherdantsev, P. A. (Tomsk Polytechnic Inst., USSR). Izv. Vyssh. Ucheb. Zaved., Fiz.; No. 1, 7-13(1970). (In Russian).

A method for calculating dipole gigantic resonances of nonmagic nuclei using deformed single-particle orbits for constructing the wave functions of nuclei is presented. The potential of residual interaction, taking into account calculation of dipole states, also includes the relation of quantum numbers K, which represent the integrals of motion. (tr-auth)

10070 GROUND STATE PROPERTIES OF ALPHA MATTER. Mueller, G. P. (Naval Research Lab., Washington, D. C.); Clark, J. W. Nucl. Phys.; A155: 561-81(1970).

The ground state of a uniform, extended system of alpha particles at zero temperature is studied by a variational method. The alpha particles are treated as elementary bosons and are assumed to interact through two-body potentials fitting the alpha-alpha elastic scattering data. A cluster development is used to evaluate the expectation value of the energy for a trial ground state wave

XUM

function of Jastrow form. The conventional Bose cluster expansion is modified to cope with the rather strong angular-momentum dependence of the best phenomenological alpha–alpha potentials. Numerical calculations of the two- and three-body cluster contributions to the energy have been performed over a wide range of densities and variational parameters. Some estimates of the four-body terms have also been made. The convergence of the cluster expansions, for the optimally determined variational parameters, appears quite satisfactory. The resulting equations of state for zero-temperature alpha matter are of interest in relation to the theory of low-density nuclear matter and, more specifically, the problems of nucleon clustering in the nuclear surface. (auth)

10071 SHORT-RANGE CORRELATIONS IN A WOODS–SAXON SHELL MODEL. Zabolitsky, J. G.; Gari, M.; Kuemmel, H. (Ruhr-Univ., Bochum, Ger.). Nucl. Phys.; A155: 526-34(1970).

A method for separating the Woods–Saxon potential and wave functions into relative and c.m. coordinates is developed. The Bethe–Goldstone equation is solved in the case of ^{16}O. The results are compared with the oscillator model case. For some pairs the wave functions turn out to be quite different, the healing effect being smaller for higher excited nucleons. (auth)

10072 EFFECTIVE OPERATORS IN THE NUCLEAR SHELL MODEL. II. PHENOMENOLOGY OF E2 OPERATORS. Harvey, M.; Khanna, F. C. (Chalk River Nuclear Labs., Ont.). Nucl. Phys.; A155: 337-61(1970).

The coupling operator discussed in paper I is defined in terms of a buffer space and parameterized to fit the observed E2 effective charge in the oxygen region. Variations in the exchange character of the coupling operator resulting from changes in the assumed effective charges are studied. The effect on the E3 effective charge and the magnitude of the two-body E2 operator are discussed. (auth)

10073 FINE-STRUCTURE ANALYSIS OF ISOBARIC ANALOG RESONANCES. Di Toro, M. (Univ., Catania, Italy). Nucl. Phys.; A155: 385-400(1970).

A method to extract the characteristic parameters of an isobaric analog resonance (IAR) from the analysis of the fine-structure experiments is discussed. An application is performed for the IAR $3/2^-$ and $1/2^+$ in $^{40}Ar + p$, $3/2^-$ and $3/2^+$ in $^{22}Ne + p$ and $3/2^-$ in $^{48}Ca + p$ observed by proton elastic scattering. The results are compared with a theoretical investigation allowing a study of the effects of the anti-analog state on the proton escape width. Spectroscopic factors of the parent states are evaluated. (auth)

10074 CALCULATION OF OSCILLATOR MATRIX ELEMENTS DIRECTLY FROM THE NUCLEON–NUCLEON PHASE SHIFTS. Galonska, J. E. (Univ., Muenster, Ger.); Faessler, Amand; Appel, Kurt. Nucl. Phys.; A155: 465-79(1970).

A method is derived and applied for the calculation of the oscillator matrix elements directly from the nucleon–nucleon phase shifts. It is an extension of the Distorted Wave Born Approximation (DWBA) method of Elliott: The Elliott method is restricted to the use of a cut-off oscillator potential as a first-order approximation to the realistic nucleon–nucleon interaction. Since the input into this method consists only of the nucleon–nucleon phase shifts (on-energy-shell data) and this unrealistic auxiliary potential one expects and gets poor results for the off-shell elements. Here the short-comings of the Elliott method are avoided by a procedure which allows that more realistic auxiliary potentials can be used. The connection between the radial wave functions of the respective auxiliary potentials and the oscillator wave functions is established by an integral equation. The DWBA corrected oscillator matrix elements for the Eikemeier–Hackenbroich and the Orsay potential as auxiliary potentials are tabulated for the oscillator lengths b = 1.4 (0.2) 2.4 fm. (auth)

10075 REARRANGEMENT OF GOLDSTONE LINKED-CLUSTER EXPANSION FOR FERMI GAS. Arponen, J. (NORDITA, Copenhagen). Nucl. Phys.; A155: 597-624(1970).

The Goldstone expansion for a momentum-conserving Fermi gas is rearranged in terms of certain partial summations chosen on the basis of the factorization properties of the "generalized time-order" graphs. The linked-cluster sum is replaced by a reduced set of diagrams in which all the hole energies are shifted from ϵ_k^0 to $\epsilon_k = \epsilon_k^0 + \delta_k$. The "generalized Hartree–Fock" self-energies δ_k are represented by similar partial sums. Formulas are derived to express the average values of static (instantaneous) one- and two-body operators in terms of reduced graphs. The counting problem is treated properly, since no overcounting of diagrams appears at any stage of the development or in any approximations based on the method. The scheme makes it to a certain extent possible to trace the analytic properties of the ground state energy as a function of the interaction coupling constant g, and to analytically continue the Goldstone sum beyond the range of convergence of the power-series expansion in g. Applications of the method are considered, especially to nuclear matter problems, and the Brueckner approximation is treated in detail. (auth)

10076 RPA GROUND STATE CORRELATIONS FROM PERTURBATION THEORY. Ellis, P. J. (Rutgers — The State Univ., New Brunswick, N. J.). Nucl. Phys.; A155: 625-43(1970).

A correlated ground state wave function is derived for a non-degenerate system by explicitly summing up the perturbation theory diagrams of the RPA to all orders. Exact expressions are also given for the correlation energy, wave function normalization and single-particle occupation probabilities. The major difference from previous results obtained with the quasi-boson approximation lies in the treatment of the lowest order diagrams. These are overcounted by a factor of two by the quasi-boson approximation if antisymmetrized matrix elements are used. As an example the case of ^{16}O is discussed. (auth)

10077 DERIVATION OF THE RELATION BETWEEN THE TRANSMISSION COEFFICIENT AND THE RATIO OF THE AVERAGE WIDTH TO THE AVERAGE SPACING. Ullah, Nazakat (Univ. of Toronto). Phys. Rev., C; 2: 1174-5(Sep 1970).

The expansion developed previously for the derivation of the relation between the transmission coefficient and the ratio of the average width to the average spacing is reexamined. By rewriting the series in a more convenient form, not only is the objection raised against the expansion removed, but also an estimate of the smallness of the terms that are usually thrown out can be easily made. (auth)

10078 FIVE-DIMENSIONAL QUASISPIN TOWARD A COMPLETE CLASSIFICATION OF THE ISOSPIN CHARACTERISTICS OF SHELL-MODEL STATES IN THE SENIORITY SCHEME. Hemenger, R. P.; Hecht, K. T. (Univ. of Michigan, Ann Arbor). Nucl. Phys.; A145: 468-96(1970).

A solution is proposed for the inner multiplicity problem associated with the five-dimensional quasispin description of shell-model states. A classification scheme, in terms of an orthonormal basis, leads to tractable results with definite symmetry properties under particle-hole conjugation. Explicit constructions are given for the R(5) irreducible representations $(\omega_1\ 1)$, $(\omega_1\ 3/2)$, $(t+1,\ t)$ for which the inner multiplicities are never greater than two. For states of seniority v = 2, reduced isospin t = 1, of a configuration j^n general expressions are given for the matrix elements of an arbitrary two-body interaction, to determine their n, T dependence, and to isolate those features of the actual interaction among nucleons which are most effective in splitting the isospin degeneracy of such states. (auth)

10079 INTERACTION OF TWO NUCLEONS IN A NUCLEUS. Kirson, M. W.; Zamick, L. (Weizmann Inst. of Science, Rehovot, Israel). Ann. Phys. (N. Y.); 60: 188-208(Sep 1970).

With a two-nucleon G matrix as given, the effective interaction between two nucleons in a nucleus is calculated in a variety of approximations, all of which involve selected sums of diagrams in perturbation theory. It is shown that many important effects can be classified as either vertex modifications or propagator modifications. Whereas an RPA calculation of the modified propagator leads to very large core-polarization corrections, one finds that this large effect is cancelled by a modification of the vertex, which is carried out to second order in perturbation theory. The results for the effective interaction are compared with those of effective charge where apparently the vertex modification is not so important. A multipole (spin, isospin) analysis of the transferred particle–hole pair shows that with a modified vertex the $J'' = 2$, $T'' = 0$ contribution gets cut down considerably, and other components such as $J'' = 5$ sometimes become large. This means that core polarization no longer provides a justification for the quadrupole–quadrupole force. (auth)

10080 THEORY OF NUCLEAR MATTER. Bethe, Hans A. (Atomic Research Inst., Seoul). New Phys. (S. Korea); 9: 114-18(Dec 1969).

An elementary discussion of nuclear matter is presented. By using the local density approximation the results are applied in a qualitative way to various nuclei and compared with the experimental data. (R.W.R.)

10081 ESTIMATION OF THE ENERGY WIDTH OF A QUASI-STATIONARY LEVEL. Arsen'ev, A. A. (Moscow State Univ.). Teor. Mat. Fiz.; 5: No. 1, 94-7(Oct 1970). (In Russian).

The energy width of a quasistationary level is estimated in terms of the parameters of the potential. (auth)

10082 DIRECT TRANSFER REACTIONS DERIVED FROM THE GREEN'S FUNCTIONS METHOD. Froebrich, Peter

(Technische Univ., Munich. Teilinstitut Theorie, Munich). Phys.; 240: 256-71(1970).

Direct transfer reactions are extracted from the general many-body theory of nuclear reactions. The case of single- and two-nucleon transfer reactions to the ground state is emphasized. For this the two- and the three-particle Green's functions are used. In deriving the T matrices of scattering theory, plausible assumptions about the energy dependence of the corresponding K matrices are made. Expressions for direct reactions, which look similar to DWBA, are obtained. The resulting T matrices contain microscopic many-body expressions for the effective interaction and the optical potentials instead of the phenomenological ones of DWBA. (auth)

10083 DYNAMIC COLLECTIVE MODEL OF THE GIANT RESONANCE. Rezwani, V. (Univ., Frankfurt am Main); Gneuss, G.; Arenhoevel, H. Phys. Rev. Lett.; 25: 1667-70(14 Dec 1970).

The dynamic model of the giant dipole resonance is extended to describe nuclei of quite different collective character, e.g., rotators, vibrators, and transition cases, on an equal footing. (auth)

10084 CLASSICAL ANALOG OF THE VARIABLE MOMENT OF INERTIA FORMULAS FOR ROTATIONAL STATES IN EVEN-EVEN NUCLEI. Thieberger, P. (Brookhaven National Lab., Upton, N. Y.). Phys. Rev. Lett.; 25: 1664-6(14 Dec 1970).

A simple mechanical model has been found which gives the same angular-velocity dependence of energy and angular momentum as postulated in the variable-moment-of-inertia description of rotational states. The possibility for one of the two coefficients of this description to adopt negative values follows naturally from this model. Also, the nonzero ground-state energies, which in some cases result from the variable-moment-of-inertia description, are easily understood. (auth)

10085 INDEPENDENT-PARTICLE-MODEL ENERGY LEVELS. Lodhi, M. A. K. (Texas Tech. Univ., Lubbock). J. Phys. A (London); 3: 533-5(Sep 1970).

This paper reports some results obtained in an attempt to determine a nucleon-nuclear potential of the Morse function type that contains velocity-dependent, spin-orbit splitting, energy-dependent, centrifugal interaction, etc., terms. The single-particle energy formula for all nuclei in the Morse-type potential well has been shown as convenient as in the harmonic type and as reliable as perhaps Hartree-Fock calculations. In particular, the neutron separation energies for ^{16}O and ^{40}Ca have been calculated and compared with the recently published results obtained from similar calculations and also with the other theoretical and experimental works. The results are found to be in very good agreement with the data and are consistent with the other calculations except with those published recently. (auth) (UK)

10086 ENERGIES SPREAD OF THE GAUSSIAN DISTRIBUTED BEAM IN NUCLEAR SCATTERING EXPERIMENTS. Mizia, I. (Academy of Mining and Metallurgy, Krakow); Zipper, W. Acta Phys. Pol.; B1: 275-9(Jul-Sep 1970).

An analysis of the energy spread of the products of a nuclear reaction in thin targets for a Gaussian-distributed beam of incident particles is presented. (auth)

10087 EVALUATION OF THE MOTT SCATTERING CROSS SECTION AND THE GOUDMIT-SAUNDERSON MULTIPLE SCATTERING DISTRIBUTION FOR ELECTRON TRANSPORT CALCULATIONS. Felder, R. M. (North Carolina State Univ., Raleigh). Nucl. Sci. Eng.; 42: 232-3(Nov 1970).

Electron transport calculations often require evaluation of cross sections for the scattering of relativistic electrons by point nuclei, and the use of these cross sections to calculate angular deflections of electrons that have traversed specified path lengths. The most accurate known single-scattering cross-section formula is that of Mott, and the best available multiple-scattering theory is that of Goudsmit and Saunderson. The convergence of both series is improved by applying the Yennie-Ravenhall-Wilson transformation in the evaluation of the Legendre expansion. The results of typical calculations are given. (R.W.R.)

XUM

REACTOR TECHNOLOGY

Commercial Power Reactors

Refer also to abstracts 8321 and 8326.

10088 (CONF-690967-1) NUCLEAR SYSTEM MANUFACTURE AND CONSTRUCTION PROGRESS. McNelly, M. J.; Koke, L. C. (General Electric Co., San Jose, Calif. Atomic Power Equipment Dept.). [nd]. 17p.

From Joint Power Conference, Charlotte, N. C.

The current status of the water reactor industry is reviewed, reference is made to the backlog of commitments, the facilities in place, and some of the critical phases lying immediately ahead. Specific data on cost trends, on quality and reliability as evidenced through operating experience, and on nuclear plant construction schedules are presented as an illustration of the basic strengths of the industry. (auth)

10089 (CONF-691020-3) PLANNING OF THE FIRST NUCLEAR POWER PROJECT IN TAIWAN. Chu, David S. L. (Taiwan Power Co., Taipei). [1969]. 9p. (SM-126/43). Dep. NTIS (U. S. Sales Only).

The Taiwan Power Company is planning to construct a 550 to 600 MW(e) nuclear power plant at a site north of Taipei. Operation is scheduled for 1975. The reactor will be light water cooled and moderated. The planning studies, both technical and economic, leading to the decision to construct the plant are described. (H.D.R.)

10090 (CONF-700335-1) HEAT DISCHARGES FROM NUCLEAR REACTORS. Amato, Charles G. (New Jersey State Dept. of Health, Trenton). [1969]. 10p. Dep. NTIS.

From Conference on the International and Interstate Regulation of Water Pollution, New York, N. Y.

The performance characteristics of coal fired and nuclear power plants in terms of heat energy releases to the environment are examined. Various approaches to waste heat management, including cooling ponds, cooling towers, and surface water discharge, are discussed. (H.D.R.)

10091 (NP-18595) MAXIMUM LIKELIHOOD IDENTIFICATION OF DYNAMICS OF THE AGESTA REACTOR AND COMPARISON WITH RESULTS OF SPECTRAL ANALYSIS. Gustavsson, I. (Lund Inst. of Tech. (Sweden). Div. of Automatic Control). Feb 1969. 33p. Dep. NTIS (U. S. Sales Only).

The reactivity to power transfer function was determined by identification of dynamic measurements of the Agesta power reactor. Two different methods were used. A parametric model of the process was developed by the maximum likelihood method. This model was compared with the results of spectral analysis of the same measurements. Differences in the results show that the maximum likelihood method may be preferable if the noise to signal ratio is high. An example with simulated data indicates that the differences between the results from the two methods may be considerable and that it may be difficult to get a reasonable parametric model from the results of the spectral analysis. 12 references. (auth) (Sweden)

10092 (NP-18600) TWELFTH ACTIVITY REPORT, PARIS, NOVEMBER 1970. (European Nuclear Energy Agency, Paris (France)). 117p. Dep. NTIS (U. S. Sales Only).

A review of activities for ENEA during 1970 is presented. Activities are discussed under the following main headings: joint undertakings and common services; nuclear power; scientific and technical cooperation; health and safety; and legal affairs. (D.C.C.)

10093 (NP-tr-1928) RELIABILITY STUDY MADE AT RHEINSBERG NUCLEAR POWER PLANT. Graupe, H. Translated from Kernenergie; 13: 279-83(1970). 8p.

In case of a total network failure, the safe cooling down of the reactor core is to be ensured by certain automatic switching functions in the Rheinsberg Nuclear Power Plant. The system components essentially consist of relays, rectifiers, cables and terminals. To ensure the continuous operational readiness of this protection system, the maintenance cycle required as well as the weak points of the system must be determined, so that it will be ready for operation between two maintenance operations with a high degree of probability. Based on a logic coupling between the input values (triggering criteria of the automatic circuitry) and the output values (switching functions of the automatic system) a reliability block diagram was set up. In the calculations, it was assumed that the life of the system components is distributed exponentially. As a result of the large number of system components, the reliability of the system had to be determined on a digital computer, using the Monte Carlo method. (auth)

10094 (ORNL-HUD-14) USE OF STEAM-ELECTRIC POWER PLANTS TO PROVIDE THERMAL ENERGY TO URBAN AREAS. Miller, A. J.; Payne, H. R.; Lackey, M. E.; Samuels, G.; Heath, M. T.; Hagen, E. W.; Savolainen, A. W. (Oak Ridge National Lab., Tenn.). Jan 1971. Contract W-7405-eng-26. 195p. Dep. NTIS.

With coordinated planning of energy centers and new cities, it would be feasible to provide thermal energy from steam-electric power plants to urban areas. With nuclear plants the siting with respect to nearby populations could be in accordance with present-day practice. An analysis was made of a 1980 reference city of 389,000 people with a climate similar to that of Philadelphia. Thermal energy extracted from the turbines of a generating plant that employed light-water reactors would be used for providing space heat, hot water, and air conditioning for the commercial buildings and the two-thirds of the city's inhabitants who lived in three-story apartment buildings. The apartment areas were considered to have an average population density of 21,500 people per square mile in one arrangement and 14,333 people per square mile in an alternate layout. Heat would also be supplied for manufacturing processes and desalting sewage plant effluent for reuse. The use of heat in the reference city would reduce the average heat rejected to the plant's cooling water to about 63% of that which would be rejected from a single-purpose plant, and this heat rejection would be reduced to 21% of that from a single-purpose plant during the period of maximum heat consumption in the summer. The cost of distributed hot water in the reference city was estimated to be 142.5¢/MBtu, which is competitive for most U. S. cities. (75 references) (auth)

10095 (WASH-1098) POTENTIAL NUCLEAR POWER GROWTH PATTERNS. (Division of Reactor Development and Technology (AEC), Washington, D. C.). Dec 1970. 266p. GPO $2.00.

An analytical program of an idealized model of the U. S. electrical power economy is described. The application of the model to evaluate the benefits of alternate courses of electric power system developments is discussed. The reactor types considered were: light water reactors, heavy water reactors, high temperature gas reactors, liquid metal fast breeder reactors, gas cooled fast breeder reactors, steam cooled fast breeder reactors, and molten salt breeder reactors. The period from 1970 to 2020 was projected with anticipated improvements in the technical and economic performance of fuels and overall fuel cycle. The design information was based on 1000 MW(e) reactor models. (D.C.C.)

10096 (ZJE-65) PRETIGHTENING OF LARGE PRESSURE VESSEL FLANGE JOINTS. Kuchta, J.; Sneberger, J. (Skoda Concern, Pilsen (Czechoslovakia). Nuclear Power Plants Div.). 1970. 34p. Dep. NTIS (U. S. Sales Only).

Calculations for the design of auxiliary devices and certain experiments for the pretightening of free flange joints with 5500 mm pitch diameter and 42 bolts with 200 mm thread diameter and 4000 mm length are described. The angles of rotation of the nuts for the method of simultaneous pretightening of several bolts under the condition of equal final forces in all bolts were established. The bolts were stressed by means of three hydraulic jacks and in other experiments by means of thermal preheating. Pretightening and releasing of the bolts in the actual flange joint was checked by the detailed strain gauge measurement of each bolt. This experiment was repeated several times with mild rubber and also with metal sealing between the flanges. Measured values are compared to theoretical solutions. (auth)

10097 DISQUIET OVER WEST GERMAN REACTORS. Marks, D. New Sci.; 48: 267-8(5 Nov 1970).

Difficulties encountered in the nuclear power programme suggest that Europe should co-operate rather than compete on the nuclear front. Since 1960 the Nuclear Research Centre in Karlsruhe has worked on fast breeder reactors both the sodium cooled version and the steam cooled version, the latter being dropped in 1969. Optimistic predictions for the KNK test reactor and the 300-MW prototype at Weisweiler were made, but numerous technical difficulties with the fuel elements have made the programme behind schedule. There is also uneasiness about the potential hazards of building nuclear power stations close to densely populated areas. Permission for the construction of the 300-MW prototype has since been withdrawn because of safety risks and alternative sites suggested which would mean a delay in the programme of at least two

years. Future developments are discussed and it is concluded that the system whereby government departments are advised by experts should be re-examined. (UK)

10098 PAKISTAN GOES NUCLEAR. Kidwai, A. New Sci.; 48: 266-7(5 Nov 1970).

Pakistan's 137-MW nuclear power plant near Karachi should be in commercial operation within a few months, and a nuclear plant of 200 MW power at Rooppur in E. Pakistan is to be commissioned by 1975. Pakistan also wishes to use nuclear power for desalination and a study is to be made aided by the U.K.A.E.A. for setting up a 600-MW plant near Karachi. Pakistan's main development problem is the harvesting of energy for its fast growing industrial sector as well as for its agricultural needs. The natural resources can no longer meet the country's increasing need for power, and without nuclear power a deficit of 16800 MW for West Pakistan and 12000 MW for East Pakistan is forecast by the year 2000. It is felt that the economics of atomic power, costing about one penny per kWh, should easily compete with the power generated from fossil fuels. India's extensive nuclear power programme, adopted in spite of her vast natural resources is discussed, and it is felt that in Pakistan is an even greater need for the development of nuclear power resources. (UK)

10099 SOME ASPECTS OF NUCLEAR DEVELOPMENTS IN THE USSR. Rojkov, V. J. Brit. Nucl. Energy Soc.; 9: 258-62 (Oct 1970).

Problems arising in the search for the optimum core arrangement for large fast reactors are discussed. Methods of improving performance by flux flattening or by modification of shape by changing the diameter to height ratio of the core are described. The main advantages of channel type stations compared with the pressure vessel type are presented and performance data are tabulated for graphite-moderated water cooled channel reactors. Economics aspects of the light water vessel type station at Novo-Voroneahskaja are referred to briefly. (UK)

10100 PROJECTION OF NUCLEAR FUEL COST TRENDS. Hoffmeister, A. J.; Houser, H. G.; Smith, E. E. (Westinghouse Electric Corp., Pittsburgh). Atompraxis; 16: 333-7(Sep-Oct 1970).

The light water reactor fuel cycle is analyzed by the discrete elements of which it is composed and future economic trends for each of these elements are projected. As the volume of light water fuel being processed increases and as engineering advancements and materials developments and improved utilization combine to provide higher recovery of available energy content, light water fuel cycle costs will decrease considerably. The effects of inflation, if it continues in the future, will strongly influence the fossil versus nuclear plant economic balance in favor of the nuclear plant. 6 references. (auth)

10101 STATE OF DEVELOPMENT OF ADVANCED REACTOR FUEL ELEMENTS. Eisner, J. H. Atompraxis; 16: 337-9(Sep-Oct 1970). (In German).

The advances in the development of fuel elements for thermal light water reactors of the second generation as well as for fast breeders as representatives of the third reactor generation are described. (auth)

10102 SURVEY OF THE U.S.A. Nucl. Eng. Int.; 15: 897-929(Nov 1970).

The survey comprises eleven articles. A review of the reactor development program covers light water reactors, liquid metal and also gas-cooled fast reactors, molten-salt breeders and high-temperature gas-cooled reactors. The nuclear fuel-cycle industry and the electricity supply industries are described. There are discussions of health and safety issues, regulatory procedures and principles involved in licensing and the role of accident analysis. The work of the Joint Committee on Atomic Energy is described. Brief descriptions are given of the activities of several major nuclear companies. A folding chart is presented showing the organization of the nuclear industry, including national bodies, main contractors and their nuclear interests. (UK)

10103 IMPORTANCE OF THE MARKET FOR COMPONENTS FOR NUCLEAR POWER STATIONS AND PROBLEMS OF ITS NATIONALIZATION. Kaibel, Enrique. Energ. Nucl. (Madrid); 13: 499-508(Nov-Dec 1969). (In Spanish).

The National Electric Plan for Spain calls for 8.5 million kilowatts of installed nuclear power by 1981 and an estimated installed power of the order of 70 million kilowatts by 2000. The potential market for fabricators of components of nuclear power stations is very important. The typical power reactors are reduced to their basic components, and the economic value of these components is estimated. Analysis of the required components shows the lack of adequate fabrication installations in Spain at the present time. The difficulties of establishing such facilities are outlined, and the positive aspects in their establishment are discussed. A schedule for the establishment of necessary facilities is proposed. (J.S.R.)

10104 SURVEY OF NUCLEAR POWER. Martinez, Francisco Pascual (Junta de Energia Nuclear, Madrid). Energ. Nucl. (Madrid); 13: 488-98(Nov-Dec 1969). (In Spanish).

The development of nuclear energy in Spain up to the year 2000 can be logically divided into two sections: the first extending to 1981 and the second to the turn of the century. The first section corresponds to the recently approved National Electrical Plan, which estimates the electrical needs of Spain for the next ten years and calls for about 21.8% of the installed power to be nuclear. The long-term plan extending to 2000 must take into consideration the types of nuclear power plants, the introduction of fast reactors, and the nuclear market. Each of these aspects is briefly considered. (J.S.R.)

10105 NUCLEAR POWER ENGINEERING: ANALYSIS OF TRENDS IN POLICY AND TECHNOLOGY. Olds, F. C. Power Eng.; 74: No. 11, 20(Nov 1970).

The development status of nuclear power plants in Germany is reviewed. Delays in reactor construction are analyzed. (D.C.C.)

10106 RELIABILITY OF THE EVAPORATING CHANNELS OF THE BELOYARSK POWER PLANT TYPE REACTORS. Konstantinov, L. V.; Postnikov, V. V.; Vetyukov, V. N.; Lunina, L. I. At. Energ. (USSR); 29: 208-9(Aug 1970). (In Russian).

The efficiency of the Beloyarsk type reactors depends to a large extent on the optimum ratio between the maximum permissible power level and the safe operation of each of the evaporating canals. The latter factor depends on the random defects in the basic engineering properties of the system, such as the strength of the canal, water consumption, and its outlet pressure and temperature. The boundary conditions were determined for operating the system at a given probability of the defects of the evaporating canals at the critical heat exchange level. It was assumed that the parameters were measured independently and the error distribution of the measurements followed the usual law. The known relationship between the critical power level of the canals, the water consumption, and its outlet pressure and temperature was used to set up a second-order critical equation on the basis of experimentally obtained data. The numerical value of the derived equations was determined by computer calculations. It was also shown that the thermoenergetic reliability of the canals, i.e., the probability that no runaway accident will occur within the specified time period, may be calculated from Poisson's distribution law. (TTT)

10107 EXPERIENCE WITH OPERATION OF THE IN-CORE DETECTORS OF THE GARIGLIANO NUCLEAR POWER PLANT. Foti, Guido. Ing. Nucl.; 10: No. 6, 19-24(Nov-Dec 1969). (In Italian).

The in-core detectors have undergone significant and continuous improvements with respect to those of the Dresden Center; these come from experience gained during many years of operation at different reactors, in which were used several hundred neutron flux detectors. The behavior of detectors during excursions, the substitutions made, and the safety criteria in the Garigliano Nuclear Power Plant are described. (tr-auth)

10108 RELIABILITY STUDY OF AN AUTOMATIC SYSTEM IN THE RHEINSBERG NUCLEAR POWER PLANT AND ESTIMATION OF ITS UPKEEPING CYCLE TAKING THE SUPPLY RELIABILITY OF MAINS SYSTEMS INTO ACCOUNT. Graupe, H. (VEB Kernkraftwerk, Rheinsberg, Ger.). Kernenergie; 13: 279-83(Sep 1970). (In German).

In the Rheinsberg nuclear power plant an automatic system maintains safe cooling of the reactor core by starting certain switching operations in the case when mains voltage totally fails. The components of this system chiefly are relays, rectifiers, cable joints, and terminal points. For warranting permanent readiness of this safety system for operation, both the necessary upkeeping cycle and poor points of the system had to be determined. On the basis of logic operations between input quantities (energizing criteria for the automatic system) and outputs (switching operations of the automatic system) a reliability block diagram has been established. For working out the calculations, the lifetime of the system elements was suggested to be distributed according to an exponential law. As the result of the large number of the system elements the reliability of the system was determined by means of a digital computer using the Monte Carlo technique. 3 references. (auth)

XUM

Operation and Economics

10109 (BNL-50238) COMBINED HYDROELECTRIC PUMPED STORAGE AND NUCLEAR POWER GENERATION. Susskind, Herbert; Raseman, Chad J. (Brookhaven National Lab., Upton, N. Y.). Apr 1970. 83p. Dep. NTIS.

The U.S. market potential of hydroelectric pumped storage power used in conjunction with nuclear base-load plants was investigated. Pumped storage power was analyzed in its relation to other types of peaking power, as well as to nuclear and fossil-fueled sources of pumping energy. The effects of pumped storage power on the generating system's operating characteristics were assessed. Pumped storage is an accepted method of producing peaking or even intermediate power, the extent of its use depending on the requirements of each individual utility and topographical conditions. Although the ideal combination of plants in the generating system is a mix of nuclear and pumped storage units, the actual mix depends on many factors which must be considered by each utility. At any given time, the pumping power will only be supplied by the most economical generating unit—either nuclear or fossil-fueled underground pumped storage plants appear to have great merit and should be investigated further. 29 references. (auth)

10110 (DOCKET-1155-86) LA CROSSE BOILING WATER REACTOR. Monthly Operating Report, September 1970. (Dairyland Power Cooperative, La Crosse, Wis.). 21 Dec 1970. Contract AT(11-1)-851. 37p. (DPC-851-16). Dep. NTIS.

10111 (DOCKET-1155-88) LA CROSSE BOILING WATER REACTOR. Monthly Operating Report, October 1970. (Dairyland Power Cooperative, La Crosse, Wis.). 13 Jan 1971. Contract AT(11-1)-851. 27p. (DPC-851-17). Dep. NTIS.

10112 (DOCKET-50016-88) ENRICO FERMI ATOMIC POWER PLANT, UNIT 1. [Operations] Report, August 1970. (Power Reactor Development Co., Detroit, Mich.). 30 Dec 1970. 15p. (PRDC-EF-84). Dep. NTIS.

10113 (DOCKET-50029-141) YANKEE NUCLEAR POWER STATION. Operation Report No. 119, November 1970. (Yankee Atomic Electric Co., Westboro, Mass.). 21 Dec 1970. 16p. Dep. NTIS.

10114 (DOCKET-50171-75) PEACH BOTTOM ATOMIC POWER STATION, UNIT 1. Monthly Operations Report No. 57, November 1970. (Philadelphia Electric Co., Pa.). 11 Jan 1971. 11p. Dep. NTIS.

10115 (DOCKET-50171-76) PEACH BOTTOM ATOMIC POWER STATION, UNIT 1. Moisture Detectors. (Philadelphia Electric Co., Pa.). 8 Jan 1971. 9p. Dep. NTIS.

10116 (DOCKET-50206-100) SAN ONOFRE NUCLEAR GENERATING STATION, UNIT 1. Operation Report, November 1970. (Southern California Edison Co., Los Angeles). Dec 1970. Contract AT(30-1)-3270. 7p. (NYO-3270-44). Dep. NTIS.

10117 (DOCKET-50206-102) SAN ONOFRE NUCLEAR GENERATING STATION, UNIT 1. Operation Report, December 1970. (Southern California Edison Co., Los Angeles). Jan 1971. Contract AT(30-1)-3270. 5p. (NYO-3270-45). Dep. NTIS.

10118 (DOCKET-50219-117) OYSTER CREEK NUCLEAR POWER PLANT, UNIT NO. 1. Surveillance Test Failure of Vacuum Breaker Block Valves. (Jersey Central Power and Light Co., Morristown, N. J.). 23 Dec 1970. 2p. Dep. NTIS.

10119 (DOCKET-50237-124) DRESDEN NUCLEAR POWER STATION, UNIT 2. Spent Radwaste Demineralizer. (Commonwealth Edison Co., Chicago, Ill.). 21 Dec 1970. 2p. Dep. NTIS.

10120 (DOCKET-50237-125) DRESDEN NUCLEAR POWER STATION, UNIT 2. Failure of Standby Diesel Generator to Start Following a Manual Initiation Signal. (Commonwealth Edison Co., Ill.). 2 Dec 1970. 2p. Dep. NTIS.

10121 (DOCKET-50245-49) MILLSTONE NUCLEAR POWER STATION, UNIT 1. Abnormal Occurrence Report No. 7 and No. 8. (Millstone Point Co., Wethersfield, Conn.). 2 Jan 1971. 2p. Dep. NTIS.

Safety analysis of the failure of the select control rod drive to function on December 23, 1970 is presented. A correction in the wiring configuration is described. The incident involving decrease of condenser vacuum is also discussed. Repair of a cracked seal weld is described. (D.C.C.)

10122 (DOCKET-50245-50) MILLSTONE NUCLEAR POWER STATION, UNIT 1. Abnormal Occurrence Report No. 10. (Millstone Point Co., Wethersfield, Conn.). 8 Jan 1971. 1p. Dep. NTIS.

The failure of a D.C. emergency lube oil pump during a simulated test of the gas turbine generator is reviewed. Corrective maintenance is described. (D.C.C.)

10123 (DOCKET-50261-49) H. B. ROBINSON UNIT NO. 2. Stuck Rod Control Cluster Assembly. (Carolina Power and Light Co., Raleigh, N. C.). 22 Dec 1970. 19p. Dep. NTIS.

10124 (DOCKET-50266-37) POINT BEACH NUCLEAR PLANT, UNIT 1. Abnormal Occurrence Report: Improper Valve Lineup for Radioactive Liquid Release. (Wisconsin Electric Power Co., Milwaukee). 19 Dec 1970. 2p. Dep. NTIS.

10125 (NP-18573) OECD HALDEN REACTOR PROJECT. Tenth Annual Report, 1969. (Organization for Economic Co-operation and Development, Paris (France)). 165p. Dep. NTIS (U. S. Sales Only).

HALDEN BOILING REACTOR—operations during 1969
—maintenance during 1969
—control system for, development of on-line digital computer
—fuel elements for, radiation testing of Zircaloy 2 clad uranium oxide (UO_2) pin type
—instrumentation for, development of test
NEUTRONS—effects on mechanical properties of uranium oxide (UO_2) and Zircaloy 2
REACTOR CONTROL SYSTEMS—development of on-line digital computer
REACTOR FUEL ELEMENTS—radiation testing of Zircaloy 2 clad uranium oxide (UO_2) pin type
URANIUM OXIDES UO_2—radiation effects on mechanical properties of, neutron
ZIRCALOY-2—radiation effects on mechanical properties of, neutron (D.C.C.)

10126 (TID-25608) GARIGLIANO NUCLEAR POWER STATION OPERATION REPORT FOR THE 2nd QUARTER, 1970. (Ente Nazionale per l'Energia Eletrica, Rome (Italy)). 30 Jun 1970. 19p. Dep. NTIS.

During April and May 1970 the Garigliano power plant operated at a power level of 150 MW(e) and a capacity factor of 94%. The plant was shut down for refueling and general maintenance on June 13. Plant operating statistics for the quarter are tabulated, and the reactor core performance, plant chemistry, health physics, and maintenance are discussed. (H.D.R.)

10127 (TID-25628) ARDENNES NUCLEAR POWER PLANT. Report of Activities for September 1970. (Societe d'Energie Nucleaire Franco-Belge des Ardennes, Chooz-lez-Givet (France)). 17p. Dep. NTIS.

Operations and maintenance requirements during September 1970 are described. Fuel inventory is itemized. (D.C.C.)

10128 (TID-25629) SENA NUCLEAR POWER PLANT. Monthly Report, August 1970. (Societe d'Energie Nucleaire Franco-Belge des Ardennes, Chooz-lez-Givet (France)). 15p. Dep. NTIS.

Operations and maintenance requirements during August 1970 are described. Fuel inventory is itemized. (D.C.C.)

10129 (WAPD-MRP-131) PRESSURIZED WATER REACTOR (PWR) PROJECT. Technical Progress Report, October 25, 1969-January 23, 1970. (Bettis Atomic Power Lab., Pittsburgh, Pa.). Contract AT(11-1)-Gen-14. 26p. Dep. NTIS.

Plant operations and testing on 3 loops continued satisfactorily. The investigation into the extent and cause of the "D" steam generator primary to secondary plant tube leak continued. Tubing removed from the "D" steam generator was metallographically inspected. A series of low pressure blowdown tests were continued to evaluate various cooling strategies. Seed 2 thermal power capabilities were evaluated for full power and swing load operation from 2500 to 6000 EFPH and indicate design power ratios greater than 1.05 for this period. An assessment was completed of the Seed 2 power capability for the interval 2500 to 6000 EFPH based on fuel element conditions which indicate no limitations on power will be required except perhaps for startup conditions. (auth)

10130 OPTIMIZAREA PARAMETRILOR CENTRALELOR NUCLEARE-ELECTRICE. (Optimization of Parameters for Nuclear Power Plants). Haiduc, Constantin. Bucuresti; Editura Academiei Republicii Socialiste Romania (1970). 323p.

Techniques for the optimization of the parameters of nuclear power stations and for the design of nuclear reactors, steam generators, and thermodynamic cycles are presented. Particular at-

tention is paid to the method for determining the optimum type of nuclear power station and to the examination of the efficiency of nuclear fuel cycles of thermal neutron reactors and fast breeder reactors. (auth)

10131 DISPOSAL OF THE LOW ACTIVITY SOLID WASTE AT A NUCLEAR POWER PLANT. Antonucci, L.; Della Rocca, C.; Turricchia, A. Ing. Nucl.; 10: No. 6, 25-32(Nov-Dec 1969). (In Italian).

The problem of the disposal of low activity solid wastes is considered in its general aspects. Among the various methods, that of burial in trenches is analyzed in greater detail. The aspects and the technico-economic advantages of this method are illustrated. The criteria, the analyses, and the procedures adopted for the application of this method at the Garigliano Nuclear Power Plant are discussed. (tr-auth)

Safety and Siting

Refer also to abstract 8667.

10132 (BNWL-SA-3564) NUCLEAR PLANTS AND THE ENVIRONMENTAL "CRISIS." Foster, R. F. (Battelle-Northwest, Richland, Wash. Pacific Northwest Lab.). 30 Sep 1970. Contract AT(45-1)-1830. 16p. (CONF-701021-1). Dep. NTIS.

From Thermal Power Generation Conference, Pullman, Wash.

The major kinds of pollutants from thermal power generation, both fossil fuel and nuclear plants, are examined. Fossil fuel plants are seen to be the second largest contributor to air pollution in the U. S. Nuclear plants add radioactivity in small amounts and heat in large amounts to the environment. The magnitude of these releases and some of the possible problems they may cause are discussed. (H.D.R.)

10133 (BNWL-SA-3581) THERMAL POLLUTION AND ITS TREATMENT. THE IMPLICATIONS OF UNRESTRICTED ENERGY USAGE WITH SUGGESTIONS FOR MODERATION OF THE IMPACT. Jaske, R. T. (Battelle-Northwest, Richland, Wash. Pacific Northwest Lab.). 7 Oct 1970. Contract AT-(45-1)-1830. 31p. Dep. NTIS.

The state of the art in energy technology, primarily electrical power technology, is briefly reviewed. The potential environmental impact of heat release from U.S. energy requirements by the year 2000 is discussed. Various schemes for energy production and utilization which would lessen this impact are examined. A basic concept of a series of canal-lake cooling systems to provide an extended heat sink away from present population centers is described. 14 references. (H.D.R.)

10134 (DOCKET-1153-17) HALLAM NUCLEAR POWER FACILITY. Semiannual Report of the Environmental Surveillance. (Nebraska Dept. of Health, Lincoln. Div. of Radiological Health). 29 Dec 1970. Contract AT(11-1)-2097. 3p. Dep. NTIS.

10135 (DOCKET-1155-87) LA CROSSE BOILING WATER REACTOR. Nuclear Instrumentation Automatic Gain Control System, Addendum No. 2. (Allis-Chalmers Mfg. Co., Bethesda, Md. Atomic Energy Div.). Jan 1971. 20p. (ACNP-70503.2). Dep. NTIS.

10136 (DOCKET-50010-75) DRESDEN NUCLEAR POWER STATION, UNIT 1. Minimizing Radioactive Off-Gas Release Rate. (Commonwealth Edison Co., Chicago, Ill.). 1 Dec 1970. 1p. Dep. NTIS.

10137 (DOCKET-50146-67) SAXTON REACTOR. License No. DPR-4; Technical Specifications Change No. 40. (Division of Reactor Licensing (AEC), Washington, D. C.). 24 Dec 1970. 2p. Dep. NTIS.

Authorization for Core 3 exposure to 4000 MWd before midlife fuel examination is presented. Revised control rod scram tests schedules are included. (D.C.C.)

10138 (DOCKET-50155-56) BIG ROCK POINT NUCLEAR PLANT. License No. DPR-6; Proposed Technical Specifications Change No. 23. (Consumers Power Co., Jackson, Mich.). 18 Dec 1970. 10p. Dep. NTIS.

Revised technical specifications concerning an instrumented type F fuel rod are presented. The instrumented type F fuel rod will provide means for monitoring cladding temperatures. (D.C.C.)

10139 (DOCKET-50155-57) BIG ROCK POINT NUCLEAR PLANT. License No. DPR-6; Proposed Technical Specifications Change No. 24. (Consumers Power Co., Jackson, Mich.). 21 Dec 1970. 32p. Dep. NTIS.

Technical specifications concerning the New Centermelt fuel bundles are presented. (D.C.C.)

10140 (DOCKET-50213-88) CONNECTICUT YANKEE ATOMIC POWER PLANT. License No. DPR-14; Technical Specifications Change No. 16. (Division of Reactor Licensing (AEC), Washington, D.C.). 24 Dec 1970. 15p. Dep. NTIS.

Revised technical specifications concerning administrative controls are presented. Monitoring and reporting requirements are listed. (D.C.C.)

10141 (DOCKET-50213-90) CONNECTICUT YANKEE ATOMIC POWER PLANT. Ultrasonic Inspection Main Coolant Pump Flywheels (Keyways). (Connecticut Yankee Atomic Power Co., Hartford). 6 Jan 1971. 4p. Dep. NTIS.

10142 (DOCKET-50213-91) CONNECTICUT YANKEE NUCLEAR POWER PLANT, UNIT NO. 1. Reference Plant Design Report. Includes Appendixes A and B. (Connecticut Yankee Atomic Power Co., Haddam. Stone and Webster Engineering Corp., Boston, Mass. Weston Geophysical Engineers, Inc., Mass.). Dec 1963. Contract AT(30-1)-3250. 337p. Dep. NTIS.

Information on Connecticut Yankee Power Reactor is presented under the following broad topics: site; containment; reactor design; nuclear steam supply systems; shielding; instrumentation and controls; secondary systems; tests and operation; administration and training; and accidents and potential hazards. (D.C.C.)

10143 (DOCKET-50219-118) OYSTER CREEK NUCLEAR POWER PLANT, UNIT NO. 1. Application for an Increase in Power Level. Preliminary Safety Analysis Report, Amendment 65. (Jersey Central Power and Light Co., Morristown, N. J.). 31 Dec 1970. 144p. Dep. NTIS.

Revised and additional information required for an operating power level of 1930 MW(t) is presented. Technical specification changes are described. (D.C.C.)

10144 (DOCKET-50219-119) OYSTER CREEK NUCLEAR POWER PLANT, UNIT NO. 1. Provisional Operating License DPR-16. Technical Specifications Change No. 2. (Division of Reactor Licensing (AEC), Washington, D. C.). 5 Jan 1971. 2p. Dep. NTIS.

Revised technical specifications concerning the control rod withdrawal prohibit function of the source range monitoring system are described. The revised specifications allow function control by either the intermediate range monitoring system or the source range monitoring system during reactor startup. (D.C.C.)

10145 (DOCKET-50237-123) DRESDEN NUCLEAR POWER STATION, UNIT 2. Proposal to Use Fuel Containing Gadolinia. (Commonwealth Edison Co., Chicago, Ill.). 28 Dec 1970. 2p. Dep. NTIS.

10146 (DOCKET-50249-52) DRESDEN NUCLEAR POWER STATION, UNIT 3. Detailed Statement on the Environmental Considerations. (Division of Reactor Licensing (AEC), Washington, D. C.). 31 Dec 1970. 184p. Dep. NTIS.

Information concerning chemical, radioactive, and thermal discharges from the reactor is presented. The effects of reactor operations on the environment are analyzed. (D.C.C.)

10147 (DOCKET-50250-37) TURKEY POINT PLANT, UNIT 3. Containment Dome Report. (Florida Power and Light Co.). 23 Dec 1970. 107p. Dep. NTIS.

10148 (DOCKET-50269-30) OCONEE NUCLEAR STATION, UNIT 1. Notice of Proposed Issuance of Facility Operating License. (Duke Power Co., Charlotte, N. C.). 31 Dec 1970. 14p. Dep. NTIS.

10149 (DOCKET-50269-31) OCONEE NUCLEAR STATION, UNITS 1, 2, AND 3. Preliminary Safety Analysis Report, Amendment 25. (Duke Power Co., Charlotte, N. C.). 30 Dec 1970. 109p. (DOCKET-50270-30; DOCKET-50287-27). Dep. NTIS.

Revised and additional information concerning reactor building instrumentation is presented. Results of dye-penetrant tests for cladding of straight piping and elbows of the cooling system are included. (D.C.C.)

10150 (DOCKET-50269-32) OCONEE NUCLEAR STATION, UNIT 1. Safety Evaluation. (Division of Reactor Licensing (AEC), Washington, D. C.). 29 Dec 1970. 114p. Dep. NTIS.

10151 (DOCKET-50285-39) FORT CALHOUN STATION, UNIT NO. 1. Preliminary Safety Analysis Report, Amendment 22 (Includes Final Safety Analysis Report, Suppl. No. 5). (Omaha Public Power District, Nebr.). 8 Jan 1971. 107p. Dep. NTIS.

Revised design parameters of the Fort Calhoun Power Reactor Unit 1 are presented. Included also are additional data on the reactor requested by the Division of Reactor Licensing. (D.C.C.)

XUM

10152 (DOCKET-50289-30) THREE MILE ISLAND NUCLEAR STATION, UNIT 1. Reactor Coolant Flow Tubes. (Metropolitan Edison Co., Reading, Pa.). 21 Dec 1970. 1p. Dep. NTIS.

10153 (DOCKET-50289-31) THREE MILE ISLAND NUCLEAR STATION, UNIT 1. Preliminary Safety Analysis Report, Amendment 16. (Metropolitan Edison Co., Reading, Pa. Jersey Central Power and Light Co., Morristown, N. J. Pennsylvania Electric Co., Johnstown) 12 Jan 1971. 28p. Dep. NTIS.

Financial data on the owners of the Three Mile Island Power Reactor Unit 1 are presented in support of the application for operating license. The 1969 Annual Report for the Pennsylvania Electric Company is included. (D.C.C.)

10154 (DOCKET-50317-21) CALVERT CLIFFS NUCLEAR POWER PLANT, UNITS 1 AND 2. Preliminary Safety Analysis Report, Amendment 11 (Includes Final Safety Analysis Report, Vol. 1). (Baltimore Gas and Electric Co., Md.). 4 Jan 1971. 369p. (DOCKET-50318-21). Dep. NTIS.

Information on Calvert Cliffs Power Reactor Units 1 and 2 is presented under the following broad topics: introduction and summary; proposed AEC general design criteria; quality assurance program; and site and environment. (D.C.C.)

10155 (DOCKET-50317-22) CALVERT CLIFFS NUCLEAR POWER PLANT, UNITS 1 AND 2. Preliminary Safety Analysis Report, Amendment 11 (Includes Final Safety Analysis Report, Vol. 2). (Baltimore Gas and Electric Co., Md.). 4 Jan 1971. 506p. (DOCKET-50318-22). Dep. NTIS.

Information on Calvert Cliffs Power Reactor Units 1 and 2 is presented under the following broad topics: reactor; reactor coolant system; structures; engineered safety features; instrumentation and control; and electrical systems. (D.C.C.)

10156 (DOCKET-50317-23) CALVERT CLIFFS NUCLEAR POWER PLANT, UNITS 1 AND 2. Preliminary Safety Analysis Report, Amendment 11 (Includes Final Safety Analysis Report, Vol. 3). (Baltimore Gas and Electric Co., Md.). 4 Jan 1971. 502p. (DOCKET-50318-23). Dep. NTIS.

Information on Calvert Cliffs Power Reactor Units 1 and 2 is presented under the following broad topics: auxiliary systems; steam and power conversion system; waste processing and radiation protection; conduct of operations; initial tests and operation; safety analysis; and technical specifications. (D.C.C.)

10157 (DOCKET-50320-20) THREE MILE ISLAND NUCLEAR STATION, UNIT 2. Preliminary Safety Analysis Report, Amendment 11, Suppl. 7. (Metropolitan Edison Co., Reading, Pa. Jersey Central Power and Light Co., Morristown, N. J. Pennsylvania Electric Co., Johnstown). 6 Jan 1971. 195p. Dep. NTIS.

Requested information concerning tendon anchorage for prestressed concrete containment structure is presented. (D.C.C.)

10158 (DOCKET-50382-1) WATERFORD STEAM ELECTRIC STATION, UNITS 3 AND 4. Application for Licenses. (Louisiana Power and Light Co., New Orleans). Jan 1971. 38p. (DOCKET-50383-1). Dep. NTIS.

Financial data on the owners of the Waterford Power Reactor Units 3 and 4 are presented in support of the application for construction permit and operating license. The 1969 Annual Report of the Louisiana Power and Light Company is included. (D.C.C.)

10159 (ORNL-NSIC-81) INDEXED BIBLIOGRAPHY OF THERMAL EFFECTS LITERATURE-1. Morgan, J. G.; Franzreb, J. K. (Oak Ridge National Lab., Tenn.). Dec 1970. Contract W-7405-eng-26. 163p. Dep. NTIS.

References concerning thermal effluents are cataloged under the following categories: General Safety Criteria; Siting of Nuclear Facilities; Transportation and Handling of Radioactive Materials; Aerospace Safety; Heat Transfer and Thermal Transients; Reactor Transients, Kinetics, and Stability; Fission Product Release, Transport, and Removal; Sources of Energy Release Under Accident Conditions; Nuclear Instrumentation, Control, and Safety Systems; Electrical Power Systems; Containment of Nuclear Facilities; Plant Safety Features-Reactor; Plant Safety Features-Nonreactor; Radionuclide Release and Movement in the Environment; Environmental Surveys, Monitoring, and Radiation Dose Measurements; Meteorological Considerations; Operational Safety and Experience; Safety Analysis and Design Reports; Radiation Dose to Man from Radioactivity Release to Environment; Effects of Thermal Modifications on Ecological Systems; and Effects of Radionuclides and Ionizing Radiation on Ecological Systems. (D.C.C.)

10160 (ORNL-tr-2402) GAS PRESSURE APPARATUS PRESTRESSED CONCRETE NUCLEAR REACTOR VESSELS. Translated for Oak Ridge National Lab., Tenn., from J. Offic. Repub. Fr.; No. 70-103, 3207-38(Jun 1970). 54p. Dep. NTIS.

Presented is a decree from the French Minister of Industrial and Scientific Development dealing with regulations for the design, construction, testing, and operation of prestressed concrete pressure vessels for reactors. Included is a circular which discusses the factors involved in the application of various technical provisions of the new regulations. (H.D.R.)

10161 PERMISSIBLE ACTIVITY RATES IN THE EXHAUST AIR DISCHARGED BY NUCLEAR REACTOR PLANTS. Stauber, E. (AEG-Telefunken, Frankfurt am Main). Atompraxis; 16: 303-5(Sep-Oct 1970). (In German).

In the general pollution of our environment, radioactive exposure caused by nuclear reactors plays only a minor part due to consistent preventive measures, both technical and administrative. Such measures must already be planned at an early stage. This situation should also be taken into account in the method used to estimate the permissible activity rates of the exhaust air discharged by nuclear reactor plants. It is likewise essential that the calculation of these values be performed on a uniform basis. A method is proposed to serve these purposes. (auth)

10162 EFFECT OF THE VARIOUS REGIMES OF OPERATION OF A NUCLEAR INSTALLATION ON THE VOLATILE RADIOACTIVE RELEASE. Schimmel, W. (Staatliche Zentrale fuer Strahlenschutz, Berlin). Kernenergie; 13: 274-9(Sep 1970). (In German).

The problem of radiation protection and nuclear safety of nuclear installations with respect to their effect on environment by release of radioactive matter which cannot absolutely be excluded is described. The various regimes of operation are characterized, arrangements for radiation protection are presented, a method of determining the probabilities of high-activity release is blocked out, and trends of development are given. 16 references. (auth)

Power Reactor Development

Refer also to abstracts 8829, 8849, and 8912.

10163 (ANL-7619) VIBRATION OF A BEAM WITH MOTION-CONSTRAINT STOPS. Chen, S. S.; Rosenberg, G. S.; Wambsganss, M. W. (Argonne National Lab., Ill.). Mar 1970. Contract W-31-109-eng-38. 44p. Dep. NTIS.

As the result of clearances imposed by manufacturing practices and design considerations, reactor fuel pins are susceptible to impacting with their supporting grid members, and heat-exchanger tubes can be expected to contact flow-directing baffles, which also serve as their intermediate supports. This intermittent contact will affect the vibrational characteristics and response of the component. To gain insight into the dynamics of the phenomenon, a theoretical analysis of a sinusoidally force-excited beam with motion-limiting stops is performed and a method of solution is presented. The "gross" motion is obtained through reduction of the system to a bilinear vibrating model. Information obtained from this model is used in a classical modal analysis in which many modes are included to give the dynamic stresses and impact in explicit form. Numerical results are given, and the character of impact is also investigated. The method is applied to study the tube-baffle interaction induced by cross-flow in the EBR-II superheater. 12 references. (auth)

10164 (ANL-7758) REACTOR DEVELOPMENT PROGRAM PROGRESS REPORT, NOVEMBER 1970. (Argonne National Lab., Ill.). 23 Dec 1970. Contract W-31-109-eng-38. 129p. Dep. NTIS.

Highlights of project activities for November 1970 are summarized. Fuels, components, and physics development for the Liquid Metal Fast Breeder Reactor are described. The EBR-2 research and development programs, fuel fabrication, and operations are reviewed. General reactor fuels and materials development, physics studies, engineering development, fuel cycle chemistry, and LMFBR safety studies are reported. Operations and analyses of ZPR-3, ZPR-6, ZPR-9, and ZPPR are presented. (H.D.R.)

10165 CISE-R-233) SOURCES OF RADIATION AND ENERGY RELEASE IN A THERMAL REACTOR. Technical Report No. 37. Tonolini, F. (Centro Informazioni Studi Esperienze, Milan (Italy)). Jan 1967. Contract 008.65.1-NTRI. 38p. (In Italian). Dep. NTIS (U. S. Sales Only).

The sources of γ and β radiation in a thermal reactor were analyzed with the purpose of being able to evaluate the radiation emission after the shutdown of the reactor. 34 references. (tr-auth)

10166 (GA-10265) SPECIAL DEVELOPMENT PROBLEMS OF HIGH-TEMPERATURE GAS-COOLED REACTOR SYSTEMS. Goodjohn, A. J.; Trauger, D. B. (Gulf General Atomic, Inc., San Diego, Calif.). 21 Aug 1970. Contracts AT(04-3)-167; AT(04-3)-314; AT(04-3)-633; W-7405-eng-26. 42p. (CONF-700904-1). Dep. NTIS.

From Conference on Power Reactor Systems and Components, Williamsburg, Va.

The major development areas of the HTGR system are described. Topics discussed include: fuel development; prestressed concrete reactor vessel development; helium circulator development; steam generator development; steam generator materials development; and refueling equipment development. 11 references. (auth)

10167 (WAPD-TM-714) EFFECT OF CLADDING OVALITY AND DIAMETRAL CREEP ON FUEL ROD SUPPORT SYSTEMS (LWBR DEVELOPMENT PROGRAM). Harden III, W. H. (Bettis Atomic Power Lab., Pittsburgh, Pa.). Dec 1970. Contract AT-11-1-GEN-14. 13p. Dep. NTIS.

The results of a study to determine optimum grid dimple spacing in fuel rod support grids are presented. The spring movement due to rod ovality and diameter change is calculated as a function of rod orientation and dimple spacing. (auth)

10168 IMPROVEMENTS IN OR RELATING TO NUCLEAR REACTORS. Rennie, Compton Alexander; Lockett, George Edward; Hosegood, Samuel Britan (to United Kingdom Atomic Energy Authority). British Patent 1,212,696. 18 Nov 1970. Filed 11 Dec 1968.

The system described aims to provide, for gas-cooled reactors, a core configuration having a favorable fuel/moderator volume ratio and which will accommodate the usual control rod and fuel handling facilities. The core comprises a number of prismoidal columns of moderator material, containing nuclear fuel, arranged in parallel form, the arrangement being such that the fuel is replaceable by replacing at least some of the columns, or parts thereof. A series of longitudinal members are provided in channels extending parallel to and between at least some of the adjacent columns, at least alternate members being removable and when removed allowing replacement only of adjacent columns, while the other columns are retained in interlocking relationship by virtue of the remaining longitudinal members and the prismoidal shape of the columns. Longitudinal spreader rods and control rods may be located in alternate channels, at least some of the former being removable to allow replacement of adjacent columns or parts thereof. Various alternative geometrical arrangements are described. (UK)

10169 NUCLEAR PLANT. (to Sulzer Freres SA). French Patent 1,573,792. 27 May 1969. Priority date 19 Sep 1967, Switzerland. (In French).

The design is given of a nuclear plant that contains a reactor vessel and a chamber that contains conventional plant equipment, which is pressure tight and capable of supporting the pressure of the working fluid in case of an accident. The top of the chamber supports the reactor vessel. The top is proportioned in such a way that it produces an internal surface for maximum possible pressure suppression of the working fluid and supports a large portion of the weight of the reactor vessel. The cylindrical reactor vessel base rests on top of the chamber. The base of the reactor vessel and the top of the chamber are supported by a single base. (P.C.H.)

10170 FAST BREEDER REACTORS. (to Siemens Aktiengesellschaft). British Patent 1,211,526. 11 Nov 1970. Priority date 27 Apr 1968, Germany.

REACTORS, BREEDER—core for fast, with unclad fuel elements of uniform enrichment

REACTORS, FAST—core for breeder, with unclad fuel elements of uniform enrichment (H.D.R.)

10171 INSTRUMENTED SUBASSEMBLY SYSTEM IN EBR-II Smaardyk, A.; Divona, C. J.; Hutter, E. (Argonne National Lab., Ill.). Nucl. Technol.; 10: 139-59(Feb 1971).

The Instrumented Subassembly System supplies the means of measuring operating parameters of specimen fuels, instruments, and related components in the EBR-II core. The system consists of an instrumented subassembly, an extension tube with seals and connections for the instrument lead wires, a drive to make it compatible with fuel handling operations, and recording and data logging equipment. The instrumented subassembly is located in the fifth row of the core (replacing a control rod), is cooled by flowing sodium of 700°-900°F, and is exposed to a total flux of approximately 1.9×10^{15} n/cm^2 sec at 50 MW reactor power. A prototype subassembly, containing 23 instruments was successfully tested in the reactor for 140 days (3856 MWd). (auth)

10172 AEG SUPERHEATED STEAM REACTOR. Seyfferth, Ludwig (AEG-Kernenergieversuchsanlage, Grosswelzeim, Ger.). Ind. At.; 14: No. 7-8, 33-44(Jul-Aug 1970). (In French).

The target of a development program begun by AEG in 1961 was the testing of a system with nuclear superheating by the construction of a prototype plant. At the moment this prototype is being put into operation at Grosswelzheim. The special feature of the design developed by AEG is the tubular fuel elements, at the outer side of which, as with a boiling water reactor, saturated steam is produced, which is then superheated on the inner side. Further new features of the prototype reactor are special instruments for experimental purposes and a high degree of adaptability in regard to its use as a test device for light water reactors. Certain problems arose during the construction, particularly in the production of the fuel elements. The experience gained forms a reliable basis for the further development of this design. (auth) (France)

Kinetics and Dynamics

Refer also to abstracts 9945, 10217, 10258, 10303, and 10306.

10173 (ANL-7542) CATALOG OF ROD-DROP AND TRANSFER-FUNCTION DATA FROM EBR-II RUNS 25 THROUGH 30A. EBR-II Project. Engen, I. A.; Hyndman, R. W. (Argonne National Lab., Ill.). May 1970. Contract W-31-109-eng-38. 73p. Dep. NTIS.

Reactivity-perturbation experiments have been conducted in EBR-II during many reactor runs. The results of the experiments conducted during runs 25 through 30A are presented here to provide a large amount of data in a compact form suitable for reference. Experimental rod-drop and oscillator methods used are discussed. The application of the results to reactor evaluation is not included. (5 references) (auth)

10174 (LFEN-109-B) EXPERIMENTAL STUDY OF THE KINETICS AND DYNAMICS OF CRITICAL ASSEMBLIES FOR THERMAL NEUTRONS. Oliveira, Jaime M. Costa (Junta de Energia Nuclear, Sacavem (Portugal). Laboratorio de Fisica e Engenharia Nucleares). 1969. 171p. (In French). Dep. NTIS (U. S. Sales Only).

Thesis. Submitted to Univ. of Paris, Faculte des Sciences, Orsay, France.

The theory of the kinetic and dynamic characteristics of reactors is reviewed. The various experimental methods used for the study of the kinetic and dynamic behavior are outlined and classified as active or passive. The results obtained by the use of one active method, reactivity modulation, and two passive methods, Rossi α method and correlation method are described with emphasis on the conditions of application of each method and the precision obtainable. The experimental values are compared with theoretical values and a critical analysis is made of the three methods. It was established that spatial effects play a large role in the dynamics of reactors and that the point model is not always sufficient to interpret the results. The usefulness of the cross correlation method was experimentally proven. The importance of statistical methods for the experimental study of reactors, particularly power reactors, was emphasized. 42 references. (J.S.R.)

10175 PHYSICS STUDIES ON BWR VOID SIMULATED CORES. II. Kikuchi, Hiroshi (Hitachi Ltd., Kawasaki, Japan). J. Nucl. Sci. Technol. (Tokyo); 7: 545-52(Nov 1970).

The steam void effect on core reactivity and flux distribution was experimentally studied on cores loaded with fuel assemblies of various void fractions. The voids were simulated by hollow polyethylene tubes. The study proved that the reactivity calculation can be improved by considering the double heterogeneity that characterizes an assembly lattice simulating the BWR core, by means of the following treatments: consideration of the spatial variation of the thermal neutron spectrum around water gaps which gives good results for the analyses of local flux distributions; and adoption of the effective Dancoff factor, which evaluates the difference in the resonance neutron shielding effect between fuel rods lining the water gap and those others closed in by similar rods. 4 references. (auth)

10176 DOPPLER EFFECT AND NUCLEAR SAFETY OF A FAST REACTOR. Usynin, G. B.; Polyanin, L. N. At. Energ. (USSR); 29: 216-18(Aug 1970). (In Russian).

The negative Doppler effect in a fast reactor, related to the temperature dependence of the reactivity changes, is caused by various factors, such as the initiation of boiling of the sodium in the reactor core which under certain conditions could lead to the uncontrollable runaway condition of the reactor. Two cases of the Doppler effect were examined: the delay time of this effect with respect to the change of the neutron density, and the influence of the heterogeneity

XUM

of the fuel composition. The calculations indicated that there is no delay of the Doppler effect with respect to the sudden change of neutron density. The Doppler temperature coefficient of the reactivity of a fast breeder reactor consists at least of a positive ^{239}Pu component and a negative ^{238}U one; as a rule the absolute value of the second component is larger. The behavior of the reactor depends not only on the sign and amount of the reactivity but also on its delayed function with respect to the original perturbation; this is determined by the difference of Pu and U in the fuel. Under stationary conditions, the fact that the heterogeneity of the fuel has not been taken into account does not cause serious errors, although the energy release in Pu is about 50 times higher than in uranium. The calculation indicated that the critical radius of ^{239}Pu particles, assuming ideal contact between them and ^{238}U, is about 15μ. This is the minimal radius of heterogeneity. (TTT)

10177 EXPERIMENTAL NEUTRON FLUX-TO-PRESSURE FREQUENCY RESPONSE FOR THE MOLTEN-SALT REACTOR EXPERIMENT: DETERMINATION OF VOID FRACTION IN FUEL SALT. Robinson, J. C. (Univ. of Tenn., Knoxville); Fry, D. N. Nucl. Sci. Eng.; 42: 397-405(Dec 1970).

Small pressure perturbations were introduced into the primary fuel pump bowl of the Molten-Salt Reactor Experiment (MSRE) operating at its nominal power of 8 MW(th). The experimental neutron flux-to-pressure frequency response was then obtained from a cross-power and auto-power spectral density analysis of the resulting signals from a neutron sensitive ionization chamber and a pressure transducer. By comparing the frequency dependence of the experimental frequency response determined for the reactor operating at power with the frequency response determined from analysis of mathematical models, the selection of the more appropriate boundary condition set from a choice of two possible boundary condition sets was possible. Then, the analytical frequency response was fitted by the least-squares method to the experimental frequency response to obtain the void fraction in the molten salt fuel. A void fraction of 0.61 ± 0.04% was determined from the frequency response; this value compares favorably with a value of 0.6 ± 0.1% determined by other techniques. Conclusions from this work are that the analytical model leads to acceptable results for the neutron flux-to-pressure frequency response and that properly designed dynamic tests involving small reactivity perturbations (introduced by means other than rod motion) can be used to extract specific nuclear parameters for a nuclear system operation at power. (auth)

10178 ANALYTICAL DETERMINATION OF THE NEUTRON FLUX-TO-PRESSURE FREQUENCY RESPONSE: APPLICATION TO THE MOLTEN-SALT REACTOR EXPERIMENT. Robinson, J. C. (Univ. of Tenn., Knoxville). Nucl. Sci. Eng.; 42: 382-96 (Dec 1970).

The neutron flux-to-pressure frequency response for a molten-salt-fueled reactor with a small amount of gas entrained in the molten salt was determined analytically. The one-dimensional conservation equations describing the flow of the compressible molten-salt gas mixture and the one-group neutron diffusion equations were written in the linearized perturbed form, and Laplace transformation in time was performed. The coupled set of equations describing the conservation of mass for the molten salt, conservation of mass for the gas, and conservation of momentum for the salt-gas mixture (the hydraulic equations) was solved by employing matrix exponential techniques. The remaining equations were solved by more conventional schemes. The matrix exponential technique was selected to obtain a solution for the hydraulic equations over the techniques normally employed (nodal or modal) for stability studies in boiling water systems because the validity of the solution is independent of the frequency of interest, and the total number of simultaneous equations required to be solved for application of boundary conditions (closing the flow loop) is small. Results from the computed neutron flux-to-pressure frequency response for the molten-salt-fueled reactor under study show that the shape of the modulus of the frequency response for frequencies below 1 to 2 cycles/sec is independent of the void fraction (volume fraction occupied by the gas), and the magnitude of the modulus of the frequency response is proportional to the void fraction. Therefore, it is concluded that the amount of void in the system can be inferred by comparing the analytical frequency response with an experimental frequency response. (auth)

10179 EFFECT OF ERRORS IN THE DELAYED-NEUTRON DATA ON FAST REACTOR STATIC AND DYNAMIC CALCULATIONS. Saphier, D.; Yiftah, S. (Soreq Nuclear Research Center, Yavne, Israel). Nucl. Sci. Eng.; 42: 272-7(Dec 1970).

The effect of the errors in presently available delayed-neutron data on various calculations and measurements in reactor physics is analyzed. It is shown that these errors have very little influence on static calculations but may cause an error of 5 to 9% in reactivity calculations and measurements; this is a third of the discrepancy between presently observed measurements and calculations. Very large errors in predicting the dynamic behavior of large fast reactors resulted when uncertainties in the delayed-neutron spectra were considered. (auth)

10180 SPACE–TIME EFFECTS IN FAST REACTOR DYNAMICS. Jackson, James F.; Kastenberg, William E. (Univ. of California, Los Angeles). Nucl. Sci. Eng.; 42: 278-94(Dec 1970).

A numerical investigation of space-time effects in the dynamic behavior of fast breeder reactors is presented. The basic approach is to compare results from point kinetics and time-dependent diffusion theory. The accuracy of point kinetics is determined for different approximations to the shape function used in calculating the initiating reactivity and feedback coefficients. Several space-dependent feedback models are studied. The importance of considering spatial effects that arise from two sources is shown. The first type consists of those induced by local reactivity perturbations. Usually, these can be adequately accounted for through the proper selection of a shape function. For example, it is found that when calculating rapid, localized ramp insertions, a good choice is the flux shape at prompt critical. The second type consists of those induced by feedback with strong space dependence. Spatial effects of this type are shown to be difficult to cope with when applying point kinetics. (auth)

10181 FAST NEUTRON DOSIMETRY WITH TWO THRESHOLD DETECTORS IN CRITICALITY ACCIDENTS OF NUCLEAR REACTORS. Ro, Seung Gy (Reactor Centrum Nederland, Petten, Netherlands). J. Korean Nucl. Soc.; 2: 85-95(Jun 1970).

An attempt has been made to do interpretation of the fast neutron dose with two threshold detectors incorporated with the Harwell criticality locket. This method is based on the assumption that the spectral distribution of fission neutrons in criticality accidents may be governed by one spectral parameter. The surface-absorbed dose for a unit fission neutron fluence seems to be insensitive to spectral shifts of the fission neutron spectrum. The average cross-sections for the activation detectors, however, are considerably changed with the neutron spectral shape, which may lead to a large error in calculating the dose from the reaction rate if one uses a fixed value for the average cross sections regardless of the neutron spectral distribution. 46 references. (auth)

10182 EXPERIENCES WITH DYNAMIC TESTING METHODS AT THE MOLTEN-SALT REACTOR EXPERIMENT. Kerlin, T. W. (Oak Ridge National Lab., Tenn.); Ball, S. J.; Steffy, R. C.; Buckner, M. R. Nucl. Technol.; 10: 103-17(Feb 1971).

A series of reactivity-to-power frequency response measurements was made on the Molten-Salt Reactor Experiment. This was done for ^{233}U fuel and ^{235}U fuel, for a range of operating power levels, at several points in the system operating history, and for several different test procedures. A comparison of experimental results with prior theoretical predictions confirmed the validity of the theoretical predictions. The test program included measurements using the pseudorandom binary sequence, pseudorandom ternary sequence, n-sequence and the multi-frequency binary sequence. 13 references. (auth)

10183 THEORETICAL DYNAMICS ANALYSIS OF THE MOLTEN-SALT REACTOR EXPERIMENT. Kerlin, T. W.; Ball, S. J.; Steffy, R. C. (Oak Ridge National Lab., Tenn.). Nucl. Technol.; 10: 118-32(Feb 1971).

The dynamic characteristics of the MSRE were calculated for operation with ^{235}U fuel and ^{233}U fuel. The analysis included calculation of the transient response for reactivity perturbations, frequency response for reactivity perturbations, stability, and sensitivity to parameter variations. The calculations showed that the system dynamic behavior is satisfactory for both fuel loadings. 12 references. (auth)

10184 DEVELOPMENT OF AN AUTOMATED FUEL LOADING OPTIMIZATION SCHEME FOR PRESSURIZED WATER REACTORS. Naft, Barry N. Lafayette, Ind.; Purdue Univ. (1970). 263p. University Microfilms Order No. 70-18,698.

Thesis.

A direct search scheme is developed to optimize the fuel loading pattern of a power reactor. An optimal pattern is achieved when the peak-to-average radial power is at a minimum and all constraints on assembly and region-average burnups are met. The optimization scheme utilizes a simplified function to represent the two dimensional power profile. This function is the product of a slowly varying component, which is a one dimensional analytic solution to the diffusion equation, and a rapidly varying component, which uses the material buckling as a parameter to rep-

resent the material properties of the nearest neighbors of an assembly. The function itself is completely general. Through the use of a variational approach several undetermined coefficients are set for each specific case. The simplified function is operated on by a discrete direct optimization scheme which treats discrete nonlinear variables through a univariate search. Through this search, a graded table of possible moves is created which specifies a direction or pattern in which the optimization proceeds. In a test of the optimization procedure using the San Onofre reactor as a model, the initial core power was described by the simplified power function to within about one percent. In addition, the optimization scheme duplicated the initial core loading pattern as well as a replacement core loading pattern. (Diss. Abstr.)

Control Systems

Refer also to abstract 10125.

10185 (CEA-R-3988) STUDY OF TWO CONTROL SCHEMES WITH DYNAMIC CONSTRAINTS ON A MULTIVARIABLE NON-LINEAR SYSTEM. Tomei, Alain (Commissariat a l'Energie Atomique, Cadarache (France). Centre d'Etudes Nucleaires). May 1970. 89p. (In French). Dep. NTIS (U. S. Sales Only).

Thesis. Submitted to Univ. of Marseille, France.

A study was made on a hybrid computer of two control schemes, operating on a multivariable, nonlinear system with respect to dynamic constraints. The multivariable system chosen is a nuclear reactor with its heat exchangers. The dynamic constraints operate on the input and output temperature derivatives of the cooling fluid in the reactor. These control schemes are used to change the reactor power or the input temperature of the coolant with respect to dynamic constraints. After a theoretical study of the control schemes, a more complete study was carried out on a hybrid computer. 10 references. (auth) (France)

10186 (KFK-1179) INFLUENCE OF THE CORRECT DEAD TIME SIMULATION ON THE DYNAMIC BEHAVIOR OF THE MODEL FOR CONTROLLED Na 2 REACTORS. Koepp, C. (Kernforschungszentrum, Karlsruhe (West Germany). Institut fuer Reaktorentwicklung). Jul 1970. 63p. (In German). (EUR-3708). Dep. NTIS (U. S. Sales Only).

The influence of the correct deadtime simulation upon the automatic control behavior of the Na2-reactor model has been analyzed. A comparison between deadtime-simulation and the generally applied simulation of deadtime relations by 1st order time delays has been made. The result was that only those deadtime relations, which have a great influence upon the dynamic behavior of the model (such as the transport time of the coolant in the primary Na circuit tubes), produce a significantly worse automatic control behavior when they are simulated by deadtime blocks as compared to 1st order delay blocks. The analysis was carried out with the digital dynamic simulator DAS2 on an IBM 360/65 computer. (5 references) (auth)

10187 DYNAMIC BEHAVIOUR OF TWO-PHASE FLOW RODS FOR NUCLEAR REACTOR CONTROL. Luminari, M.; Masini, G.; Peterlongo, G.; Tacconi, F. A. (CISE, Milan). Energ. Nucl. (Milan); 17: 637-42(Nov 1970).

The operation principle of a two-phase flow rods system for the fast control of nuclear reactor power is briefly outlined. After discussing the steady-state characteristics of the circuit, experimental results obtained in transient conditions are presented. The density in the rod was measured with the quickclosing valve technique, while transfer functions between the control signal and some hydraulic parameters (flowrates, pressure drops) were obtained by a digital transfer function analyzer. The dynamic behavior of the system allows a fast control of the reactor neutron flux. 12 references. (auth)

10188 HYDRAULICALLY OPERATED CONTROL ROD DRIVE SYSTEM FOR PRESSURISED WATER AND BOILING WATER REACTORS. Meusel, Wilhelm; Schluter, Heinz (to Maschinenfabrik Augsburg-Nurnberg Aktiengesellschaft). British Patent 1,209,953. 28 Oct 1970. Filed 30 Jan 1968.

The system described comprises two hydraulically operated interconnected pistons of different diameters, movable in a stepped cylinder, with a valve means such that in the event of a fault in the hydraulic drive system the latter is shut off and allows hydraulic pressure from the reactor to act on the large diameter piston and insert the control rod for normal operation and also for scram operation. Various alternative designs are described. Operation may be in the vertical, horizontal, or any desired diagonal direction. (UK)

10189 DESIGN AND DEVELOPMENT OF A CAPILLARY VALVE FOR USE IN VENTING FISSION GASES FROM FAST BREEDER REACTOR CONTROL RODS. Heenan II, William Andrew. Detroit; Univ. of Detroit (1969). 123p. University Microfilms Order No. 70-12,600.

Thesis.

A "capillary valve" having no moving parts, suited for use in corrosive media, has been designed and developed. The valve permits the bleeding of a gas into a liquid region if a certain pressure difference is exceeded and also prevents the counterflow of liquid. The valve consists of a porous metallic disk or plug which has small-diameter interconnected pores which average between 0.1 and 5 microns and have the essential property of being wet by the liquid involved. This valve was developed as a solution to the problem of venting control rods and possibly fuel rods in liquid-sodium fast breeder reactors. Due to the buildup of fission gases in these rods, it is desirable to vent these gases and thereby increase length of service without permitting sodium to enter the rods and possibly cause deterioration. While this specific design was developed for the Fermi reactor, the fundamental problem is characteristic of all liquid-metal fast breeder reactors. (Diss. Abstr. Int.)

10190 UPRAVLENIE YADERNYMI ENERGETICHESKIMI USTANOVKAMI. VYPUSK 4. (Control of Nuclear Power Reactors. Issue 4). Filipchuk, E. V. Moscow; Atomizdat (1970). 144p.

A collection of articles on the dynamics of circulating fuel reactors and on the calculation of the spatial distribution of the neutron flux in reactors is presented. The design and operation of automatic control systems and the optimization of control systems are examined. Reliability aspects of reactor components are discussed. 86 references. (tr-auth)

10191 INSTRUMENTATION OF NUCLEAR REACTORS. Foster, Kenneth; Wolfenden, Bryan; Cartmell, John; Price, Michael Anthony (to United Kingdom Atomic Energy Authority). British Patent 1,211,561. 11 Nov 1970. Filed 18 Jan 1968.

A method for keeping electrical insulators within a gas-cooled, graphite-moderated reactor pressure vessel clean by sweeping gas over them is presented. The instrumentation described comprises an electrical connector having gas passages for sweeping gas over the surfaces of its insulation. A number of lead-through insulators are supported in a skeletal frame fabricated from suitable material, such as stainless steel strip, the open nature of the frame providing the passages. A set of contacts may be provided for cooperation with a second set of contacts on a complementary connector, both sets being mounted within a bore passing through a stack of dished separated insulating plates supporting one set of contacts so that a flow gas parallel to the bore will be scooped into the passages defined by insulating plates. The plates are separated so as to create a radial flow of gas sweeping the surface of the plates. Some of the lead-through insulators may incorporate resilient plungers. (UK)

Shielding

10192 (CEA-N-1354) STUDY OF THE VALIDITY OF THE SABINE CODE IN CALCULATIONS ON THE SHIELDING OF HEAVY AND LIGHT WATER REACTORS. Guezenec, Jean-Yves; Hot, Michel; Pepin, Pierre (Commissariat a l'Energie Atomique, Fontenay-aux-Roses (France). Centre d'Etudes Nucleaires). Oct 1970. 31p. (In French). Dep. NTIS (U. S. Sales Only).

A test of the SABINE program for the determination of neutron fluxes in iron-water lamellar shields is discussed. A preliminary study using the NIOBE code determined the boundary conditions which were to be introduced into the SABINE program. 7 references. (auth) (France)

10193 (CEA-N-1359) THREE-DIMENSIONAL MONTE-CARLO CALCULATION (TRIPOLI CODE) OF THE NEUTRON SPECTRA IN THE LOWER SHIELD OF PHENIX. Nimal, Jean-Claude; Vergnaud, Therese (Commissariat a l'Energie Atomique, Fontenay-aux-Roses (France). Centre d'Etudes Nucleaires). Oct 1970. 40p. (In French). Dep. NTIS (U. S. Sales Only).

Results of calculations made on the lower part of the PHENIX reactor using the TRIPOLI code are presented. These calculations represent the first step towards the lateral calculation intended to determine the secondary sodium activation. The case considered is practically two-dimensional and involves very strong attenuation of the neutron fluxes. For a similar case, calculations were made in spherical geometry using the NIOBE code. (auth) (France)

XUM

Cooling Systems

Refer also to abstract 8394.

10194 (CEA-R-3895) STATISTICAL INTERPRETATION OF UNCERTAINTY COEFFICIENTS IN THERMAL CALCULATIONS FOR NUCLEAR REACTORS. PARTICULAR PROBLEMS IN THE APPLICATION OF THE σ METHOD. APPLICATION TO REDISTRIBUTION OF THE FLOW. Fabrega, Serge (Commissariat a l'Energie Atomique, Grenoble (France). Centre d'Etudes Nucleaires). Oct 1970. 69p. (In French). Dep. NTIS (U. S. Sales Only).

Various statistical methods for taking into account the uncertainties involved in calculations on the thermal characteristics of nuclear reactors are described. The variance addition theorem (σ method) is currently used for calculating the probabilities of thermal accidents in reactors. It is shown that the use of this method can be extended if certain elementary variances are replaced (the variance in the local flux peak or the variance in the uranium charge between the channel entrance and the hot point) by different calculated values. It is found, for example, that it is necessary to divide the local heat flux peaks by a factor of the order of 2, in order to take into account: the limited amplitude of the flux peak, the random position of the flux peak, the non linearities, and the existence of threshold values. The same reduction is applicable to the velocity effect occurring in the local air gap in the hot channel. The 3σ method is applied to calculations on safety margins with respect to the redistribution of the flow. Numerical results are given in the case of high flux reactors. The gain in performance using statistical methods is demonstrated; losses due to incertainties are reduced by a factor of at least 2. (France)

10195 (DP-Report-500) KINETICS OF CARBON DEPOSITION REACTIONS IN HIGH TEMPERATURE GAS COOLED REACTORS. Project DRAGON. Everett, M. R. (Atomic Energy Establishment, Winfrith (England)). Jan 1967. 39p. (CONF-670341-1). Dep. NTIS.

From Conference on Gas-Metal Reactions in Environments Containing CO_2, London, England.

Corrosion of the graphite core of a He cooled high temperature reactor by inleakage of steam from heat exchangers will result in small equilibrium partial pressures of H_2O, H_2, CO and CO_2 impurities being maintained in the primary coolant by the competing influences of the graphite core and the primary circuit purification system. Under certain conditions, decomposition of CO on catalytically active Fe surfaces such as areas of steel heat exchanger tubing operating at temperatures of the order of 500°C can deposit C and regenerate oxidizing impurities such as H_2O or CO_2. The kinetics of these reactions were investigated and found to be controlled by the chemical balance and partial pressures of reducing and oxidizing impurities in the He coolant, the chemical composition of heat exchanger steels, their operating temperature and surface condition. It is shown that these metal/gas reactions do not constitute a major problem in HTGCRs. 10 references. (auth)

10196 (ORNL-TM-3229) FLUID DYNAMIC STUDIES OF THE MOLTEN-SALT REACTOR EXPERIMENT (MSRE) CORE. Kedl, R. J. (Oak Ridge National Lab., Tenn.). 19 Nov 1970. 36p. Dep. NTIS.

In the MSRE reactor vessel, fluid fuel is circulated at 1200 gpm down through an annular region and up through 1140 passages in the graphite core. The core design was based on preliminary tests in a one-fifth scale model, followed by detailed measurements with water solutions in a full-scale mockup of the reactor vessel and internals. Presented are the models, the testing, and the data from which velocity, pressure drop and flow patterns are deduced. Also described is how the measurements were extrapolated to molten salt at 1200°F in the actual reactor. The few observations possible in the reactor were consistent with the predicted behavior. (10 references) (auth)

10197 DESIGN CRITERIA AND STEEL CHARACTERISTICS FOR BWR AND PWR REACTOR PRESSURE VESSELS. Ermini, E.; Salmoni, G. Energ. Nucl. (Milan); 17: 654-64(Nov 1970). (In Italian).

The design criteria for BWR and PWR reactor pressure vessels and the problems of their in-site assembling are outlined. The steel types and characteristics required for their fabrication are reviewed in detail. 7 references. (auth)

10198 IMPROVEMENTS IN OR RELATING TO NUCLEAR REACTORS. Proudlove, Michael Joseph (to Nuclear Power Group Ltd.). British Patent 1,210,787. 28 Oct 1970. Filed 27 Feb 1969.

Reference is made to gas-cooled, graphite-moderated, prestressed concrete pressure vessel reactors, in which the heat exchangers are located in bores (or "pods") within the wall of the pressure vessel. In order to facilitate access to the heat-exchanger tube banks the tubes are housed in pods that open into the outer surface of the pressure vessel and the pods are sealed by closure members during reactor operation. Such closure members must be capable of withstanding the reactor gas pressure and may have a bayonet-type fitting or may be held down by bolts; both kinds of fitting present some complications, especially when high gas pressures are involved. In the system described the closure members are held in position by some of the stressing tendons used to prestress the pressure vessel and are in the form of a cylinder with one end closed and the other end having a flange resting on a seating at the outer end of the pod to form a seal. The stressing tendons pass through openings in the flange and have tensioning devices adapted to act against the flange to hold the closure member in position and the flange in sealing engagement with the seating. The tendons may lie on concentric rings. (UK)

10199 THERMAL SHIELD SYSTEM FOR A NUCLEAR REACTOR VESSEL. Costes, Didier; Desisle, Jean-Paul; Gallo, Sabino; Schaller, Karl (to Commissariat a l'Energie Atomique). British Patent 1,214,439. 2 Dec 1970. Priority date 4 Apr 1969, France.

REACTOR CONTAINMENT STRUCTURES—thermal insulation for liquid sodium cooled, description of liquid sodium
REACTORS, FAST—containment structure for liquid sodium cooled, description of liquid sodium thermal insulation for
REACTORS, LIQUID METAL-COOLED—containment structure for fast, description of liquid sodium thermal insulation for
SODIUM—use for thermal insulation of liquid
THERMAL INSULATION—design parameters for liquid sodium cooled fast reactor containment structures (D.C.C.)

10200 IMPROVEMENTS IN OR RELATING TO NUCLEAR REACTORS. Blacker, Peter Thomas; Holmes, John Arthur Godfrey; Pickering, Alan Roy; Stevens, George Frederick William (to United Kingdom Atomic Energy Authority). British Patent 1,214,314. 2 Dec 1970. Filed 13 Jul 1967.

PIPES—design parameters of spaced in-core, with multiple injection nozzles
REACTORS, BOILING—cooling system for, description of spaced in-core ducts with multiple injection nozzles (D.C.C.)

10201 IMPROVEMENT IN OR RELATING TO NUCLEAR REACTORS. Jaquiss, Michael Thornton; Domingey, Derek Alan (to United Kingdom Atomic Energy Authority). British Patent 1,211,011. 4 Nov 1970. Filed 27 Jun 1967.

Reference is made to the use of methane, in the presence of CO, as an inhibitor of the irradiation induced reaction between graphite and CO_2 in a gas-cooled, graphite-moderated reactor. The use of methane was found to enhance the inhibition achieved by CO alone and thus reduce the required content of CO in the coolant. This is advantageous since with CO alone as inhibitor there is a tendency for C deposition to occur in the coolant circuit outside the reactor. It was also observed that the rate at which methane is destroyed in the reactor coolant is reduced with increasing CO concentration. A saving may be effected by adjusting the CO and methane concentrations so as to give the required inhibition and a reduced methane destruction rate. The preferred methane concentration is 400 to 2500 ppM by volume, with a maintained CO concentration between 1 and 5% by volume. (UK)

10202 NUCLEAR REACTOR CORE STRUCTURE. (to English Electric Co.). French Patent 1,572,687. 19 May 1969. Priority date 21 Jun 1967, Great Britain. (In French).

The design is given of a core structure for a gas-cooled nuclear reactor with a passage for outflow of the gas coolant through a channel between graphite columns. The gas then passes the length of an annular space in the fuel canals in a contrary direction and finally passes through the fuel in the first direction. In other words the gas descends through the fuel. (P.C.H.)

10203 HEAT TRANSFER IN REACTOR COMPONENTS HAVING TEMPERATURE-DEPENDENT THERMAL CONDUCTIVITY. Sparrow, E. M.; Koopman, R. N. (Univ. of Minnesota, Minneapolis). Nucl. Sci. Eng.; 42: 406-14(Dec 1970).

A solution method for steady heat conduction in convectively cooled solids having temperature-dependent thermal conductivity is described and applied. The method provides solutions in algebraic form from which the temperature and its spatial derivatives can be evaluated at any point in the solid. To illustrate the application of the method, consideration is given to an internally heat-generating solid pierced by circular cooling pas-

XUM

sages. Results for the hot spot temperature are presented for a range of geometrical and thermal parameters. The results indicate a substantial influence of variable thermal conductivity when the temperature variation across the solid is large. (auth)

10204 HEAT EXCHANGE UNIT FOR A NUCLEAR REACTOR. Fonteray, P. J.; Thome, P.; Noel, R. (to CEA). French Patent 1,569,732. 28 Apr 1969. Filed 8 Mar 1968. (In French).

The heat exchange unit is of modular construction and built essentially in the form of a right prism where the two bases are open. A transverse network of parallel tubes connects the heat exchange circuit to the pumps for the primary cooling system. (J.G.B.)

10205 NUCLEAR COMPARISON OF COOLANTS IN HEAVY WATER PRESSURE TUBE REACTORS. Schludi, H. N. Atomkernenergie; 16: 225-9(1970).

Heavy water pressure tube reactors having reached the stage of power reactors or at least of power demonstration-reactors use heavy water, carbon dioxide, and boiling light water as coolant. These three coolant variants are briefly described and evaluated as far as their nuclear characteristics are concerned. The evaluation shows a superiority of the coolants with low neutron absorption, namely, D_2O and CO_2 for higher values of the ratio $N(D_2O)/N(U)$. (auth)

10206 WATER LEAK DETECTORS. Bancroft, A. R.; Dombra, A. H. Canadian Patent 850,004. 25 Aug 1970.

A high temperature stable indicator is formulated for detecting light or heavy water leaks from nuclear reactors or conduits associated with them. Stability up to 550°F has been achieved. The sensitive material comprises a carrier and a $SrCrO_4/Ag_2SO_4$ couple as the active indicator or a carrier and a $KyFe(CN)_6/Fe_2(SO_4)_3$ couple as the active indicator or a carrier and a $K_4Fe(CN)_6/CuSO_4$ couple as the active indicator. These materials are applied to the pipes by a variety of methods and though unaffected by high humidity, they show a distinct color change if touched by light or heavy water. (F.S.A.)

Fuels

Refer also to abstracts 8835, 8910, 8911, 8951, 10257, and 10328.

10207 (BNWL-SA-3286) DEVELOPMENT AND RESULTS OF AN ELECTRICALLY HEATED SEVEN-PIN BUNDLE ASSEMBLY FOR THERMAL HYDRAULIC TESTING IN LIQUID METALS. Collingham, R. E.; Hill, V. R.; Yatabe, J. M.; Thorne, W. L. (Battelle-Northwest, Richland, Wash. Pacific Northwest Lab.). 21 May 1970. Contract AT(45-1)-1830. 22p. (CONF-701110-2). Dep. NTIS.

From ASME Winter Annual Meeting, New York, N. Y.

The development, design, and results of an electrically heated seven-pin instrumented bundle assembly for LMFBR thermal hydraulic testing are presented. The test assembly was capable of operating in liquid metals at typical temperatures (800°F) and nominal heat fluxes (500,000 Btu/hr-ft^2) of LMFBR's and was typical of LMFBR geometry. Wire wraps were used as spacers. Heat transfer data were taken over a tenfold range of Peclet number (50 to 500), and the results are presented as local coolant enthalpy rises, local coolant temperatures, and local clad temperatures. Even though considerable forced diversion of the coolant by the wire wraps was evident, significant coolant and clad temperatures gradients did exist across pins of the outer row. A severe hot spot did not exist beneath a wire wrap. (auth)

10208 (GEAP-13562) TRANSIENT OVERPOWER IRRADIATION OF AXIALLY-RESTRAINED, ZERO-BURNUP, FAST REACTOR FUEL SPECIMENS. Thomas, G. R.; Field, J. H. (General Electric Co., Sunnyvale, Calif. Breeder Reactor Development Operation). Sep 1969. Contract AT(04-3)-189. 92p. Dep. NTIS.

The results of an experimental program for evaluating the transient overpower limits of Liquid Metal Fast Breeder Reactor (LMFBR) fuel specimens as a function of fuel column axial restraint, fuel density, and fuel form (pellet versus powder fuel) are presented. The test specimens contained zero-burnup $(Pu_{0.2}U_{0.8})O_2$ fuel. In size, they were one-quarter of an inch in diameter with a fuel column length of ≈14 inches. The specimens were clad by Type 316 stainless steel. The results indicate that the transient failure threshold for zero-burnup fuel is a strong function of the combination of fuel density and molten fuel volume. Following cladding failure, molten fuel can exhibit high mobility, and under the conditions of the experiment, the resultant interaction between molten fuel, cladding, and sodium coolant is not violent. 21 references. (auth)

10209 (JUL-654-RG) THE DEVELOPMENT AND EXPLANATION OF A PROTOTYPE FUEL ELEMENT FOR A HEAVY-WATER-MODERATED AND-COOLED THORIUM BREEDER REACTOR WITH VIBRATIONALLY COMPACTED FUEL PARTICLES. Fritz, Rolf (Kernforschungsanlage, Juelich (West Germany). Institut fuer Reaktorentwicklung). Apr 1970. 144p. (In German). Dep. NTIS (U. S. Sales Only).

The thorium heavy-water breeder reactor, as it was studied in the thermal breeder studies at Juelich, promises an economic use of the large natural thorium reserves in the thorium–uranium cycle. The fuel element developed in the course of these studies is a vibrationally compacted fuel which appears especially suitable for automatic and simple handling. In addition to an accurate analysis of the thermal and mechanical stresses to be expected, a series of special preliminary studies were made and evaluated. The calculation methods were confirmed or supplemented. The principles for the test element installation, the reactor proposed in the breeder study, and an evaluation of the studies on similar fuel materials are described. The physical installation of the reactor is briefly discussed. Special attention was placed on the investigation of the thermal and mechanical stresses which at individual points can not be described with the usual methods. The conceivable error deviations and the corresponding safety factors introduced were considered. The extrapolation possibilities of the research results are discussed and the irradiation method is reported. 53 references. (tr-auth)

10210 (ORNL-4434) LOW-PRESSURE DISTILLATION OF MOLTEN FLUORIDE MIXTURES: NONRADIOACTIVE TESTS FOR THE MSRE DISTILLATION EXPERIMENT. Hightower, J. R. Jr.; McNeese, L. E. (Oak Ridge National Lab., Tenn.). Jan 1971. Contract W-7405-eng-26. 52p. Dep. NTIS.

Equipment was designed and built to demonstrate the low-pressure distillation of a 48-liter batch of irradiated fuel salt from the Molten Salt Reactor Experiment. The equipment consisted of a 48-liter feed tank, a 12-liter, one-stage still reservoir, a condenser, and a 48-liter condensate receiver. The equipment was tested by processing six 48-liter batches of nonradioactive $LiF-BeF_2-ZrF_4-NdF_3$ (65-30-5-0.3 mole %) at a temperature of 1000°C. A distillation rate of 1.5 ft^3 of salt per day per square foot of vaporization surface was achieved in the nonradioactive tests. Evidences of concentration polarization and/or entrainment were noted in some runs but not in others. Automatic operation was easily maintained in each run, although certain deficiencies in the liquid-level measuring devices were noted. Condensation of volatile salt components in the vacuum lines and metal deposition in the feed line to the still pot are problems needing further attention. Since a postoperational inspection of the equipment showed essentially no dimensional changes, the equipment was judged to be satisfactory for use with radioactive material. The results of these nonradioactive tests indicate that the application of distillation to MSBR fuel salt processing is feasible. (10 references) (auth)

10211 (ORNL-4616) PREPARATION AND HANDLING OF SALT MIXTURES FOR THE MOLTEN SALT REACTOR EXPERIMENT. Shaffer, James H. (Oak Ridge National Lab., Tenn.). Jan 1971. Contract W-7405-eng-26. 41p. Dep. NTIS.

A molten mixture of LiF, BeF_2, ZrF_4, and UF_4 served as the circulating fuel for the Molten-Salt Reactor Experiment. Its secondary coolant for transferring heat to an air-cooled radiator was a molten mixture of LiF and BeF_2. A third mixture that was chemically identical to the coolant mixture was used in place of the fuel for premuclear operations and subsequently to flush the reactor core after a fuel drain. Approximately 26,000 lb of these fused fluoride mixtures were prepared from component fluoride salts and loaded into the reactor facility. Techniques for handling molten fluorides and their production process for attaining high chemical purity were developed and applied simultaneously with the development of the molten-salt nuclear reactor concept. The plans and operations which were a part of the fueling of the MSRE are described. (26 references) (auth)

10212 (TID-25590) REPORT OF MEETING ON METHODS AND MODELS USED TO DESIGN FUEL PINS AND PREDICT IN-PILE PERFORMANCE, APRIL 8-9, 1970, GERMANTOWN. Kelman, L. R.; Rough, F. A. 10 Nov 1970. 56p. Dep. NTIS.

Computer programs used to predict the performance of fuel elements are reviewed. Comparisons of calculational models with experimental programs are made to establish performance characteristics of fast breeder reactor fuel elements. (D.C.C.)

10213 (WCAP-3385-25) SAXTON PLUTONIUM PROJECT. Quarterly Progress Report for the Period Ending September 30, 1970. Smalley, W. R. (Westinghouse Electric Corp., Pittsburgh, Pa. Nuclear Fuel Div.). Oct 1970. Contract AT(30-1)-3385. 26p. Dep. NTIS.

XUM

The physics section of the final report on Core II fuel evaluation was revised to reflect corrected values of $^{239}Pu/^{238}U$ ratio. After the interim shutdown the Saxton reactor operated at power for approximately 22 days during the quarter. As of September 30, the cumulative energy generated in Core III was 2133 megawatt-days, with a total of 184 load follow cycles. The peak burnups in the loose lattice region were: (1) For peak power rod: 27,600 MWD/MTM; (2) For highest burnup rod: 37,100 MWD/MTM. One of the four rods was removed from the center 3 × 3 subassembly during the interim shutdown. The rod was transferred to the WPIF Hot Laboratory, where it was visually examined and gamma scanned. The examination revealed no evidence of swelling, hydride blisters, cracks, or other defects. (auth)

10214 OUTLOOK FOR NUCLEAR REACTORS AND FUEL. Stewart, H. B. (Gulf General Atomic, Inc., San Diego, Calif.). pp 56-60 of Mining Year Book 1970. Denver; Colorado Mining Association (1970).

From 73rd National Western Mining Conference and Exhibition, Denver, Colo. See CONF-700216.

The possible directions that nuclear power plant designs might take and the fuel cycles for these plants are reviewed. The factors that affect the introduction of new reactor types are illustrated, with emphasis on the effects of developments in the uranium mining industry. (H.D.R.)

10215 SOME CONSIDERATIONS ON CRITICAL HEAT FLUX IN ROD CLUSTERS IN ANNULAR DISPERSED VERTICAL UPWARD TWO-PHASE FLOW. Gaspari, G. P.; Hassid, A.; Vanoli, G. (CISE, Milan). Energ. Nucl. (Milan); 17: 643-53(Nov 1970).

Critical heat flux in rod clusters is being investigated at CISE in connection with the development of the CIRENE reactor (pressure tube, D_2O moderated, evaporating H_2O cooled). The studies are being carried out on 19 rod clusters (7 rod clusters have also been considered) to determine the influence of some geometrical parameters. The results so far obtained, in particular with reference to the influence of a number of parameters, such as rod diameter, rod spacing, length, number of rods, and radial power distribution are discussed. Experimental data are studied according to an approach based on a rod-centered subchannel division of the cross section. A brief analysis is also given of the limitations of the existing correlations. 36 references. (auth)

10216 ESTIMATING AVERAGE NUCLEAR FUEL COSTS. Bader, J. F.; Kitzke, K. J.; Nordman, D. A. (Westinghouse Electric Corp., Pittsburgh). Atompraxis; 16: 305-8(Sep–Oct 1970).

A form called the seven-page is useful when analyzing the effects on nuclear fuel cost of various changes in fuel design parameters, economic and time period assumptions and operating modes. The completed form yields accurate estimates of average fuel cost for each core loading and for each fuel region comprising the loading. The systematic form expedites estimates of average nuclear fuel costs for each fuel region of each core loading. (auth)

10217 MEASUREMENT OF RELATIVE CONVERSION RATIO IN PARTICULATE FUEL. Taylor, W. H.; Murphy, M. F.; Grattan, J.; Millington, R. A. (United Kingdom Atomic Energy Authority, Winfrith, Eng.). J. Brit. Nucl. Energy Soc.; 9: 244-58(Oct 1970).

Measurements of relative conversion ratio are made for particulate fuel as part of the study of Mk III gas cooled reactor lattices at AEE Winfrith. A liquid source coincidence technique has been developed in order to overcome the difficulty of detecting the low energy coincident gamma rays from thermal capture events in ^{238}U with the same efficiency as the resonance capture events, which are concentrated close to the surface of the kernel. More than one hundred separate determinations are made with total random errors of ±0.7%; comparisons with an independent chemistry method show agreement to within ±1%. (auth) (UK)

10218 IMPROVEMENTS IN NUCLEAR REACTORS. Sodergard, Bengt Martin (to Allmanna Svenska Elektriska Atiebolaget). British Patent 1,213,397. 25 Nov 1970. Priority date 25 Apr 1967, Sweden.

REACTOR CONTROL ELEMENTS—guide tubes for boiling water cooled, description of removable

REACTOR FUEL ELEMENTS—guide tubes for boiling water cooled, description of removable

REACTORS, BOILING—core for, description of parallel arranged removable guide tubes in

TUBES—design parameters of removable guide, for reactor refueling (D.C.C.)

10219 FUEL ELEMENT FOR A NUCLEAR REACTOR. Lofroth, E. (to Aktiebolaget Atomenergi). British Patent 1,210,127. 28 Oct 1970. Filed 29 Feb 1968.

Reference is made to fuel elements for mounting in a vertical position in a reactor. The fuel element described has a tubular metal casing containing a number of cylindrical fuel bodies all of which contain at least one gas-filled opening in an axial direction; the channels defined by these openings are divided into shorter sections separated by partitions. Fuel bodies containing channels offer some advantages over solid fuel bodies, such as a reduced tendency for cracking and a layer cooled surface. It has been found that the fuel material in a vertical fuel element tends to collect on the bottom of the channels, resulting in a local temperature increase. This danger can be eliminated or reduced by use of partitions; each partition will receive only a small quantity of fissile material and the temperature increase will be negligible. Each channel should be divided into at least 10 sections, and preferably into at least 20 sections. This type of fuel element is particularly suitable for use in superheated water cooled reactors. The partitions may be provided in each fuel body, or between each two adjacent fuel bodies, or if the fuel bodies are very short the partitions may be provided in or at each second or third fuel body. Various alternative arrangements of openings in the fuel bodies are described. (UK)

10220 FUEL AND/OR BREEDING ELEMENT FOR NUCLEAR REACTORS. (to Kernforschungsanlage Julich GmbH). British Patent 1,213,425. 25 Nov 1970. Priority date 12 Mar 1969, Germany.

REACTOR FUEL ELEMENTS—design parameters of water cooled zirconium alloy clad pyrolytic graphite coated particle type

REACTORS, WATER-COOLED—fuel elements for, description of zirconium alloy clad pyrolytic graphite coated particle type (D.C.C.)

10221 USE OF URANIUM HEXAFLUORIDE IN NUCLEAR POWER INSTALLATIONS. Dmitrievskii, V. A.; Voinov, E. M.; Tetel'baum, S. D. At. Energ. (USSR); 29: 251-5(Oct 1970). (In Russian).

A short survey of Soviet and foreign publications concerning the use of uranium hexafluoride in nuclear reactors, nuclear power installations and MHD-generators is presented. From these data a conclusion is made of advantages of using UF_6 in nuclear power installations. 17 references. (auth)

10222 COMMERCIAL PLUTONIUM RECYCLE. Roll, J. B. Power Eng.; 74: No. 11, 34-6(Nov 1970).

The development of plutonium fuel cycles for pressurized-water reactors is described. Cost factors and safety problems related to the plutonium fuels are reviewed. Plutonium availability predictions are presented. (D.C.C.)

10223 FUEL RODS WITH INTERNAL FINS. Ihle, P.; Rust, K. (Kernforschungszentrum, Karlsruhe, Ger.). Atomkernenergie; 16: 231-2(1970). (In German).

Fuel rods are equipped with internal fins or cams to increase the rod power and, hence, reduce the fissile material inventory. Such an internal fin geometry increases the thermal conductivity of the outer fuel zone considerably. Calculations have shown this measure to increase the rod power of oxide fuel rods by 25 to 50 percent relative to the power of fuel rods with a smooth inner surface. (auth)

10224 FUEL LATCH DESIGN. Lambert, J. E. Canadian Patent 854,399. 20 Oct 1970.

A latch is described for connecting, in serially disposed relation, fuel bundles for nuclear power reactors. The latch has a thin bowed profile and is more or less a continuous ring. As such, it has a low neutron capture ratio; readily interlocks and disconnects with adjacent latches; and, axially displaces some of the fuel elements in each bundle to present a more uniform or consistent radiation density across interconnecting latches. (F.S.A.)

10225 NUCLEAR REACTORS. Wheeler, David John (to English Electric Co. Ltd.). British Patent 1,211,954. 11 Nov 1970. Filed 13 Mar 1970.

In gas-cooled reactors vertical channels provided in the core structure for accommodation of control rods have previously been positioned not directly below the fueling standpipes but below a second set of standpipes interstitially located in the top cap between the fueling standpipes. The provision of this second set of standpipes adds considerably to the cost of the top cap. In the system described the core structure has vertically extending channels for the control rods and each of these channels is located directly below a fueling standpipe. The operating mechanisms for the control rods are housed in the standpipes and the additional standpipes provided for the control rod mechanisms are dispersed with, thus simplifying construction of the

top cap and reducing the cost of the biological shield. The control rod operating mechanisms in the respective standpipes are removed when it is required to refuel the reactor core. The standpipes are so disposed in relation to the regular arrangement of the blocks of the core structure that blocks at the top of the core structure are accessible for removal through the standpipes. Various geometrical arrangements of the blocks, control rod channels and standpipes are described. The blocks may be loaded or unloaded individually, and it is only necessary to provide a clearance between the top of the core structure and the top cap of depth slightly greater than the vertical height of a block. The height of the refueling mechanism may also be considerably reduced, compared with previous arrangements, if the blocks are handled individually. (UK)

10226 OPTIMIZATION OF THE CELL DIMENSIONAL PARAMETERS OF AN INCORE THERMIONIC FUEL ELEMENT. Wolf, E.; Haug, W. (Univ., Stuttgart). Atomkernenergie; 16: 213-18(1970). (In German).

Performance data of incore thermionic fuel elements with series-connected converters are determined by means of a theoretical model in a wide range of operational and geometrical parameters. In general the single cells are differently heated in the reactor core. The effect of this non-uniform heat generation on the total output data is investigated. A method for power enhancement by means of variation of converter lengths or interconnection lead geometries in the fuel elements is discussed. 11 references. (auth)

10227 GAS ANALYSIS OF NUCLEAR FUEL ELEMENTS. Takahashi, S. (Hydro-Electric Power Commission of Ontario, Toronto). Ont. Hydro Res. Quart.; 22: 24-5(3rd quarter 1970).

The presence of approximately 1.25×10^{-6} gram or more of H_2 per gram UO_2 in nuclear fuel elements could result in failure of the element tube. A procedure has been developed to extract and analyze the cover and pellet gases, as a quality control measure. Analyses to date indicate an average total content of about 0.05×10^{-6} gram H_2 per gram of fuel. (auth) (Canada)

Auxiliary and Emergency Systems

Refer also to abstract 10244.

10228 (ANL-7665) STUDY OF THE RESPONSE OF THE EBR-II PLANT PROTECTIVE SYSTEM TO HYPOTHETICAL MALFUNCTIONS IN THE REACTOR SYSTEM. EBR-II Project. Campise, A. V. (Argonne National Lab., Ill.). Jun 1970. Contract W-31-109-eng-38. 91p. Dep. NTIS.

The prompt response of the EBR-II plant protective system to hypothetical malfunctions of reactor components has been investigated by means of a comprehensive dynamic simulation and analysis. The hypothetical malfunctions investigated are those listed in the EBR-II Hazard Summary Report. The AIROS-IIA dynamic-simulation digital code was used to model the principal neutronic, thermal, and hydraulic characteristics of typical driver-fuel and experimental-oxide-fuel elements. Response times of the EBR-II protective system were taken from in situ measurements made at the reactor plant on circuits sensing neutron flux, coolant flow rates, and temperatures. The studies indicate that the present EBR-II plant protective system provides responsive and redundant protection for all hypothetical malfunctions of components listed in the Hazard Summary Report. 4 references. (auth)

10229 (WCAP-7544) PWR FLECHT (FULL LENGTH EMERGENCY COOLING HEAT TRANSFER) GROUP II TEST REPORT. Cadek, F. F.; Dominicis, D. P.; Leyse, R. H. (Westinghouse Electric Corp., Pittsburgh, Pa. Nuclear Energy Systems Div.). Sep 1970. Contract AT(10-1)-1230; Subcontract S-7045. 226p. Dep. NTIS.

For Idaho Nuclear Corp., Idaho Falls.

The objective of the PWR FLECHT (Full Length Emergency Cooling Heat Transfer) test program is to obtain experimental reflooding heat transfer data under simulated loss-of-coolant accident conditions. These data will be used in evaluating the heat transfer capabilities of pressurized water reactor emergency core cooling systems. The test program is divided into three Groups, according to the type heater rods used. The results of twenty-seven Group II tests are presented. The Group II test series extended the range of initial temperatures, flooding rates and flow blockages investigated in Group I and examined the effects of power decay rate, variable flooding rate and entrained water "fallback." The test results reported include transient heat transfer coefficients and clad temperatures at different radial and axial locations. Typical axial and radial pressure drop data, local coolant temperature data and measurements of carry-over water are also presented. The results of this test series provide further verification of the ability of bottom flooding emergency core cooling systems to terminate the temperature increase during a loss-of-coolant accident. In particular, it has been shown that the effects of a variable flooding rate can be predicted, using constant flooding rate data; that reactor "fallback" will significantly reduce second peak temperatures; and that complete blockage of as many as sixteen adjacent channels will not significantly impair bottom flooding emergency core cooling system effectiveness. (auth)

10230 IMPROVEMENTS IN OR RELATING TO GAS-COOLED NUCLEAR REACTORS. Neilson, Thomas Christopher (to United Kingdom Atomic Energy Authority). British Patent 1,212,458. 18 Nov 1970. Filed 8 Jul 1969.

Reference is made to refuelling standpipes in gas-cooled reactors. Alignment of these standpipes and fuel channels presents a problem because of temperature differentials, and charging guides must allow for this. Arrangements of standpipes and charging guides have been devised in which the standpipes are expanded at their lower ends to provide a relatively wide mouth that overlaps the upper end of the corresponding guide. Coolant gas is then discharged from the guide into the hot gas plenum through the annulus between the upper end of the guide and the mouth of the standpipe. It has been found, however, that discharge through such an annulus is liable to be unstable, and improvements have been sought. In the system described the standpipe is provided at its lower end with a circumferential fitting of wire mesh, or perforated metal sheet, for the passage of coolant. This fitting may be conical in form. (UK)

10231 NUCLEAR REACTOR CONTAINMENT SYSTEM. (to Westinghouse Electric Corp.). British Patent 1,212,299. 11 Nov 1970. Priority date 23 Sep 1968, United States.

REACTOR CONTAINMENT SYSTEMS—design with means for using primary coolant as emergency core coolant
REACTORS, PRESSURIZED WATER—emergency core cooling system for, use of lost primary coolant in (H,D,R.)

10232 ANALYTICAL MODEL FOR THE DERIVATION OF DESIGN PARAMETERS OF DRY CONTAINMENTS AND ANCILLARY ENGINEERED SAFEGUARDS OF WATER REACTORS. Aisch, Dietrich E. (Steinkohlen-Elektrizitaet Aktiengesellschaft, Essen). Atomkernenergie; 16: 219-24(1970).

A computer program for the analysis of the consequences of a loss-of-coolant accident in dry-well containments of water reactors is presented. The calculational model provides information on temperature and pressure transients in the containment vessel without assuming thermodynamic equilibrium between water and vapor. It further allows the prediction of temperature gradients throughout the containment structure and of the effectiveness of engineered safeguards, such as containment spray and emergency cooling. The program satisfactorily correlates the experimental data obtained in the tests simulating the design basis accident of the CVTR containment. The results of a sample calculation for the containment and ancillary engineered safeguards of a 2000 MW pressurized water reactor are discussed. (10 references) (auth)

Operation and Economics

10233 (BNWL-SA-3605) FACTORS AFFECTING THE OPTIMUM FUEL CYCLE. Deonigi, D. E.; Merrill, E. T. (Battelle-Northwest, Richland, Wash. Pacific Northwest Lab.). Oct 1970. Contract AT(45-1)-1830. 14p. (CONF-701022-1). Dep. NTIS.

From Regional Meeting of the AIChE, Richland, Wash.

Some of the fuel cycle codes which use different techniques for fuel cycle cost calculations are examined. A comparison of the codes shows that the figures used for working capital are responsible for the only variations in the calculated costs. It is shown that a theoretically optimum fuel cycle can be calculated simply by determining the fuel cycle cost resulting from fuel operating to a given exposure without regard to control requirements and system load factors. (H,D,R.)

10234 (DOCKET-50231-62) SOUTHWEST EXPERIMENTAL FAST OXIDE REACTOR. Malfunction of an Emergency Electrical System Circuit Breaker. (General Electric Co., Sunnyvale, Calif. Breeder Reactor Development Operation). 22 Dec 1970. 3p. Dep. NTIS.

10235 (DOCKET-50231-64) SOUTHWEST EXPERIMENTAL FAST OXIDE REACTOR. Quarterly Plant Operations Report No. 6, August 1-October 31, 1970. (General Electric Co., Sunnyvale, Calif. Breeder Reactor Development Operation). 4 Jan 1971 28p. Dep. NTIS.

XUM

Safety and Siting

10236 (AERE-R-6242) DESCRIPTION OF THE COMPUTER PROGRAMME ICON FOR THE CALCULATION OF FISSION PRODUCT INVENTORIES. Faircloth, R. L.; Hopper, M. J. (Atomic Energy Research Establishment, Harwell (England)). Nov 1970. 38p. Dep. NTIS (U. S. Sales Only). UK 5s. 6d.

A description is given of the Fortran IV computer code ICON, used to determine the complete fission product inventory for a reactor after a particular history of operating conditions taking into account the structure of the individual decay chains and also the effects of neutron capture. Each chain is fitted to a generalised decay scheme and a method for solving the simultaneous differential equations is described. (auth)

10237 (BAW-1344) 1000-MWe LMFBR ACCIDENT ANALYSIS AND SAFETY SYSTEM DESIGN STUDY. PHASE I. FAULT TREES AND MALFUNCTION CATALOG. (Babcock and Wilcox Co., Lynchburg, Va. Nuclear Power Generation Dept.). Dec 1969. Contracts 31-109-38-2339; 847-0501. 67p. Dep. NTIS.

For Argonne National Lab., Ill.

Component and system faults associated with the 1000 MW(e) LMFBR reference design are identified and cataloged. Fault trees are summarized in verbal descriptions that trace key failure paths in systems and subsystems. These fault trees are to be used as an aid in identifying necessary LMFBR protective systems and safety features. (H.D.R.)

10238 (BMI-1890) EVALUATION OF THE APPLICABILITY OF EXISTING DATA TO THE ANALYTICAL DESCRIPTION OF A NUCLEAR-REACTOR ACCIDENT. Quarterly Progress Report, July-September 1970. Carbiener, Wayne A.; Ritzman, Robert L. (Battelle Memorial Inst., Columbus, Ohio). Oct 1970. Contract W-7405-eng-92. 36p. Dep. NTIS.

Work related to the development of simplified models for estimating the effectiveness of emergency-core-cooling (ECC) systems is described. The simplified models are based on a balance between energy changes in the fuel and coolant regions during a specified time interval. PWR-FLECHT quench times at the axial mid-plane of the core were used as a basis of comparison. It was found that a simple heat balance could be used to reproduce the quench data and predict temperature turnaround times reasonably well; however, the relationship that was developed considerably overpredicted the temperature rise observed in the experiments. The two transient neutron kinetics codes, ADEP-1 and ADEP-2, were combined into a single code capable of accommodating either one- or two-dimensional analyses. Several additional features were added to ADEP to improve its versatility and efficiency. Rod-ejection accident calculations were extended to cases wherein the accidents were initiated at low power. Comparisons were made between one-dimensional and point-kinetics results for a 12-ft slab from initial conditions of 1 and 10 percent of full power. Analytical studies of iodine removal by containment sprays were continued with an examination of the effects of the volatilization of hypoiodous acid (HIO) from spray solutions. The development of a model including the effects of iodine removal by an ice condenser chamber within a general analysis of containment processes is described. Efforts related to the development of the emergency-core-cooling computer codes, ECCSA and MUCHA, were concentrated on the reflood portions of the loss-of-coolant accident. Both steady-flow and variable-flow PWR-FLECHT tests were used as comparative bases in order to test the ability of the model to predict the fuel-rod simulator response. Reformulation of the ECCSA fluid model in order to obtain significant decreases in computing time requirements is described. 24 references. (auth)

10239 (DOCKET-50231-61) SOUTHWEST EXPERIMENTAL FAST OXIDE REACTOR. Restrictions on the Use of Special Fuel Rods. (General Electric Co., Sunnyvale, Calif. Breeder Reactor Development Operation). 18 Dec 1970. 4p. Dep. NTIS.

10240 (DOCKET-50231-63) SOUTHWEST EXPERIMENTAL FAST OXIDE REACTOR. License No. DR-15; Technical Specifications Proposed Change No. 4, Rev. 2. (General Electric Co., Sunnyvale, Calif. Breeder Reactor Development Operation). 22 Dec 1970. 17p. Dep. NTIS.

Revised operating requirements of the gross cover gas monitor system for fuel failure detection are described. The revised requirements relate to operation with failed fuel. (D.C.C.)

10241 (GEAP-13608) THE FREADM-1 CODE: A FAST REACTOR EXCURSION AND ACCIDENT DYNAMICS MODEL. Freeman, D. D.; Leff, E. G.; Bender, D. J.; Meinhardt, W. G. (General Electric Co., Sunnyvale, Calif. Breeder Reactor Development Operation). Sep 1970. Contract AT(04-3)-189. 236p. Dep. NTIS.

FREADM-1 is a fast reactor multi-channel accident analysis program designed to efficiently simulate a reactor transient from initiation to the point of core disassembly. Models are included for nuclear kinetics (point model), core thermo-hydraulics, voiding, fuel redistribution, failure propagation, programmed reactivity insertion, and the dynamics of primary system coolant flow. A broad range of assumed accident initiating and propagating activities may be simulated using triggering logic included in the code. FREADM-1 is restricted to accidents which initiate and propagate uniformly within annular or cylindrical co-axial core regions. (auth)

10242 (IN-1444) COMPARISON OF PREDICTIONS FROM THE REACTOR PRIMARY SYSTEM DECOMPRESSION CODE (RELAP3) WITH DECOMPRESSION DATA FROM THE SEMI-SCALE BLOWDOWN AND EMERGENCY CORE COOLING (ECC) PROJECT. Slater, C. E. (Idaho Nuclear Corp., Idaho Falls). Dec 1970. Contract AT(10-1)-1230. 21p. Dep. NTIS.

RELAP3, a computer code developed for predicting the thermal-hydraulic response of pressurized-water nuclear reactor systems to a loss-of-coolant accident (LOCA), was partially evaluated by comparing RELAP3-predicted transient pressures and residual water with experimental data from the Semiscale Blowdown and Emergency Core Cooling (ECC) Project. The blowdown tests were conducted in a cylindrical vessel having a height of approximately 5.3 feet and an inside diameter of approximately 1.2 feet. Initial test pressures and temperatures were about 2350 psia and 540°F. RELAP3 predicted the pressure behavior as a function of time within a maximum deviation ±100 psi of the experimentally measured pressure data; agreement was generally much better. Agreement between analytical and experimental results depended on the value of discharge coefficient selected in the analysis. A discharge coefficient of 0.6 gave best agreement with experimental data for the 100% breaks (100% break of four-inch ID pipe) whereas a value of 0.8 gave the best agreement for the 2% breaks. The residual water in the semiscale vessel was predicted within a maximum deviation of ±20% of the measured residual water. (auth)

10243 (NP-18535) OBSERVATIONS OF THE DECLINE OF INTERFERENCE IN THE D_2O LOOP OF THE MULTIPURPOSE RESEARCH REACTOR. INVESTIGATION OF THE DYNAMIC BEHAVIOR MADE WITH AN ANALOG COMPUTATION MODEL OF A CARBIDE IRRADIATION UNIT IN THE EMERGENCY COOLING CASE. Figge, A. (Kernforschungszentrum, Karlsruhe (West Germany). Institut fuer Reaktorentwicklung). Jul 1970. 68p. (In German). Dep. NTIS(U. S. Sales Only).

Within the studies of incidents made for the preliminary safety report on the D_2O loop of the Multipurpose Research Reactor (MZFR) the dynamic behavior of a test rig for carbide fuel (UC/PuC) irradiations was examined with an analog computation model for the main incidents possible. The results shown as temperature curves are preliminary information based on estimated curves for coolant throughput and system pressure which have to be checked upon the termination of a planned out-of-pile test of the aggregate assembly. Previous results show that the loop designed to irradiate a representative 2 MW oxide fuel rig (maximum rod power 800 W/cm) can be operated without modifications also with a carbide fuel rig of the same power level (maximum rod power 1500 W/cm). (6 references) (auth)

10244 (ORNL-TM-3212) ORNL NUCLEAR SAFETY RESEARCH AND DEVELOPMENT PROGRAM BIMONTHLY REPORT, SEPTEMBER-OCTOBER 1970. Cottrell, Wm. B. (Oak Ridge National Lab., Tenn.). Jan 1971. Contract W-7405-eng-26. 142p. Dep. NTIS.

The accomplishments during the months of September and October in the research and development program under way at ORNL as part of the U. S. Atomic Energy Commission's Nuclear Safety Program are summarized. Much of this work is in general support of water-cooled power reactor technology, including LOFT and industry programs, and reflects current safety problems, such as measurements of prompt fuel element failure phenomena and the efficacy of containment-spray and filter systems for the removal of accident-released fission products and aerosols from gas streams. Several projects are also conducted in support of the high-temperature gas-cooled reactor (HTGR) and liquid-metal fast breeder reactor (LMFBR) programs. Other major projects include studies of primary piping, steel pressure-vessel technology, and seismic design consideration. Experimental work relative to pressure-vessel technology includes investigations of the attachment of nozzles to shells and the implementation of joint AEC-PVRC programs on heavy-section steel technology and nuclear piping, pumps, and valves. Several of the projects are directly related to the AEC's standards program, which entails development of engineering safeguards and the establishment of codes and standards for government-owned or -sponsored reactor

facilities. The recent activities of NSIC and the Nuclear Safety journal in behalf of the nuclear community are also discussed. Of particular interest in both of these activities is the recent emphasis on environmental effects. (auth)

10245 (ORO-3822-5) INTERACTION BETWEEN SOIL AND NUCLEAR REACTOR FOUNDATIONS DURING EARTHQUAKES. Isenberg, J. (Agbabian-Jacobsen Associates, Los Angeles, Calif.). 10 Jun 1970. Contract AT(40-1)-3822. 201p. Dep. NTIS.

For Toledo Univ., Ohio. Research Foundation.

A study of the dynamic response of a nuclear reactor structure and surrounding soil that is subjected to earthquake motion is presented. The case of a reactor structure whose foundation is embedded below ground surface is analyzed. The structure and soil are represented by an assembly of two-dimensional finite elements. In some examples, elastic properties are assumed for the soil, and in others, inelastic properties are assumed. The computer programs used to perform the analyses and the version of plasticity theory used to represent inelastic soil properties are described. The study indicates that the horizontal response of the structure foundation, as measured either by its response spectrum or peak acceleration, is less than the corresponding response at the surface of the free field. The structural response appears to be suppressed by a greater amount if its natural frequencies are about the same as the dominant frequencies of the earthquake input. Suppression is also greater if the stiffness of the soil is decreased. 23 references. (auth)

10246 STUDIES ON THE LOSS-OF-COOLANT ACCIDENT IN WATER-COOLED NUCLEAR POWER REACTORS. PART 3. Nishiwaki, Ichiro; Shimizu, Sadaaki; Inami, Kuniaki; Kasuga, Yasuhiro. Denki Shikensho Iho; 34: 540-71(1970). (In Japanese).

The blowdown test facility, which is being built at the Electrotechnical Laboratory, has been used to develop information on core-heatup phenomena associated with a loss-of-coolant accident in water-cooled nuclear power reactors. The research program consists of blowdown and core-heatup experiments during the loss-of-coolant accidents. The entire primary coolant system includes both BWR and PWR loops. Instrumentation is provided to measure the transient thermal behavior of the electrically heated reactor core. Parametric blowdown tests have been performed to evaluate the influence of the break size and the break location on the transient core-heatup phenomena during the blowdown. The major experimental results are stated as follows: (1) Top blowdown experiments show that the time required for uncovering the reactor core is shorter for large break as compared with that for small break, and that the clad temperature after uncovering is relatively high for larger break. (2) Bottom blowdown experiments indicate the reverse situation as compared with the top blowdown ones, namely, the time required for uncovering is rather shorter and the clad temperature is relatively high in the case of smaller break. These results are mainly attributed to the phase-separation phenomena in the reactor vessel, that is, the separated steam during the bottom blowdown is likely to be accumulated in the top portion of the core and this possibly makes the faster uncovering of the core as compared with that for the blowdown. Simulated double-ended blowdown experiments show that the transient thermal response of the reactor core for the double-ended blowdown is similar to that for the top blowdown. This result indicates that heat removal from the reactor core during the double-ended blowdown is mainly predominated by the behavior of the coolant discharged from the top break located close to the outlet nozzle of the reactor vessel. (auth)

10247 ENERGY ABSORBER STRUCTURE FOR A NUCLEAR POWER PLANT CONTAINMENT SYSTEM. Marko, Myroslaw (to North American Rockwell Corp.). British Patent 1,212,480. 18 Nov 1970. Priority date 12 Nov 1968, United States.

REACTOR CONTAINMENT SYSTEMS—blast energy absorption by, core vessel top shield assembly for

REACTORS, POWER—shield assembly for, blast energy absorber structure for top (H.D.R.)

10248 ANALYSIS OF NUCLEAR REACTOR EQUIPMENT RESPONSE TO EARTHQUAKE FORCES. Wang, George Shih-chang. Los Angeles; Univ. of California (1970). 196p. University Microfilms Order No. 70-19,912.

Thesis.

The results of forced vibration experiments on a large central nuclear power station are presented. A calculational procedure that reproduces the experimental results is described. Based upon the experimental data, a set of aseismic design criteria for the reactor components are also proposed and a comparison between the proposed criteria and a reference design is made. It is proposed that if the integrity of the reactor components can be guaranteed, the reactor containment structure could be considered unnecessary. The forced vibration experiment was conducted at the 450 MW(e) San Onofre Nuclear Generating Station Unit No. 1. Modal analysis was used to establish the calculation model. The displacements of reactor components are nonlinear with respect to the applied force, even in the low level force range used during the vibration tests. They would be nonlinear when earthquake-like motion impinges upon the reactor building foundation. The proposed design criteria for the steam generator, the primary coolant pump, the pressurizer and the vital connecting piping take this nonlinear response into account. The peak displacements computed using the proposed design criteria are in close agreement with the existing design and the effects due to earthquake-like input of ground motion records from Taft 1952 and El Central 1940 earthquakes. (Diss. Abstr.)

Power Conversion Systems

10249 COMBINED CARBON DIOXIDE TURBINES EQUIPMENT AND NUCLEAR REACTOR. (to Sulzer Freres SA). French Patent 1,570,301. 28 Apr 1969. Priority date 27 Jul 1967, Switzerland. (In French).

The design is given of a closed cycle CO_2 turbine combined with a nuclear reactor which consists of at least two shafts and two expansion stages between which the reheating stage is effected by the heat coming from the reactor. The available power is furnished by the stage of low pressure expansion in which one part of the motor fluid removed from the gaseous circuit is liquified by heat extraction, pressurized at least to an intermediate pressure, and is restored in the principal circuit. Means is provided for removing a portion of the coolant, liquefying it by heat removal, and returning it to the circuit at an intermediate pressure. (P.C.H.)

10250 CARBONIC GAS TURBINES EQUIPMENT COMBINED WITH A NUCLEAR REACTOR. (to Sulzer Freres SA). French Patent 1,570,300. 28 Apr 1969. Priority date 27 Jul 1967, Switzerland. (In French).

The design is given of a closed cycle CO_2 turbine with at least two shafts in connection with a nuclear reactor. The installation consists of at least two stages of gas expansion with an intermediate reheating stage. The useful power is produced during expansion at low pressure. (P.C.H.)

10251 STATIONARY BEHAVIOR OF GAS TURBINES IN NUCLEAR PLANTS. Dibelius, G. (Instituts fuer Dampf- und Gasturbinen, Aachen); Hlubek, W. Brennst.-Waerme-Kraft; 22: 503-8(Nov 1970). (In German).

Data concerning the part load behavior of nuclear gas turbine plants are presented for various arrangements of the components and for various control systems. Simple- and multiple-shaft arrangements as well as pressure level-, temperature-, by-pass- and blade-angle-control of the stationary vanes in the low pressure turbine are investigated. Economical aspects of the choice of the arrangement- and of the control system are discussed. The two-shaft arrangement with the generator on the high-pressure-shaft seems to be particularly promising. (auth)

Research and Test Reactors

Refer also to abstracts 10164 and 10207.

10252 (AAEC/M-9) REACTOR HIFAR: THE SAFETY ROD CIRCUITS. Hopkinson, J. B. (Australian Atomic Energy Commission Research Establishment, Lucas Heights). Aug 1969. 12p. Dep. NTIS (U. S. Sales Only).

The manual describes the safety rod circuits of the HIFAR reactor. Control circuits, maintenance facilities, position indicators and guard switches are described and a drawing of a complete rod circuit is enclosed. (Australia)

10253 (AAEC/M-32) REACTOR HIFAR: THE SAFETY ROD SYSTEM. Hopkinson, J. B. (Australian Atomic Energy Commission Research Establishment, Lucas Heights). Jul 1970. 16p. Dep. NTIS (U. S. Sales Only).

A description is given of the main components of the safety rod system in the HIFAR reactor. (Australia)

10254 (ANL-Trans-865) SAFETY REPORT FOR THE "SCARABEE" LOOP. (Commissariat a l'Energie Atomique, Cadarache (France). Centre d'Etudes Nucleaires). Translated for Argonne National Lab., Ill.), from French report DEP/GTSP/Ca-28/70. 149p. Dep. NTIS.

A sodium loop in the CABRI reactor facility is designed to

investigate the consequences of a single fuel pin meltdown in fast sodium-cooled reactors. The loop is described and its operating and safety characteristics are defined. (H.D.R.)

10255 (BNWL-916) TECHNICAL BASES FOR FFTF DRIVER FUEL INSTRUMENTATION. Regimbal, J. J. (comp.) (Battelle-Northwest, Richland, Wash. Pacific Northwest Lab.). Oct 1968. Contract AT(45-1)-1830. 136p. Dep. NTIS.

Technical bases for instrumentation requirements to protect the core of the Fast Flux Test Reactor are evaluated in detail for driver fuel. Power excursions, loss of flow, and fuel failure are characterized to establish sensitivity and response time requirements. Surveillance and reliability requirements are also considered. Preliminary safety criteria relative to core instrumentation are formulated and brief rationale presented. A comprehensive assessment of present instrument technology is presented and used as a basis for establishing instrument development goals. (49 references) (auth)

10256 (BNWL-1485) EFFECT OF CONTINUOUS SPRAY OPERATION ON THE REMOVAL OF AEROSOLS AND GASES IN THE CONTAINMENT SYSTEMS EXPERIMENT. Postma, A. K.; Coleman, L. F. (Battelle-Northwest, Richland, Wash. Pacific Northwest Lab.). Dec 1970. Contract AT(45-1)-1830. 147p. Dep. NTIS.

Results of two large scale experiments on fission product removal by sprays are reported in detail. For these two Containment Systems Experiment (CSE) tests, spraying was begun prior to injection of fission product simulants into the gas phase. Spraying with recirculated liquid was continued for 24 hours at an average temperature of 250°F. In one of the tests the spray additive was sodium hydroxide at pH 9.4 and in the other the hydroxide was augmented by 1 wt % sodium thiosulfate. These tests showed that aerosol particles and inorganic iodine are rapidly removed from the gas phase by spray, and that the degree of removal continued to increase over the 24 hour period of spray recirculation. The methyl iodide removal rate, which was slow for caustic spray, was increased an order of magnitude by the presence of thiosulfate. The experimental results are in agreement with previously published data obtained in the Containment Systems Experiment. 38 references. (auth)

10257 (EURFNR-764) SAFETY REPORT FOR FR-2 EXPERIMENTAL CAPSULE RIGS WITH SINGLE-WALLED NaK CAPSULES FOR IRRADIATION OF HIGH-POWER FUEL PINS. Haefner, H. (Kernforschungszentrum, Karlsruhe (West Germany). Institut fuer Reaktorentwicklung). Translation of report KFK-1143. 72p. Dep. NTIS.

Work Performed under United States-Euratom Fast Reactor Exchange Program.

Irradiation of mixed UC-PuC fuel pins of lengths up to 1 m will be performed in the FR2 reactor. At the initial stage, pins of 475 mm length (300 mm fuel length and 10 mm outer diameter of the cladding tube) will be introduced including pins with He and Ar bonding as well as with Na bonding. The central fuel temperature (2,000°C max.) will be measured in the case of fuel pins with gas bonding. Maximum pin power is intended to be 1,150 W/cm for a temperature of the cladding tube surface of 630°C; the burnup is limited to 50,000 MWd/te of fuel. For the purposes of this irradiation experiment, a capsule for a high pin power was developed using NaK as heat transfer medium which surrounds the fuel pin. The separation between NaK and the reactor cooling water is achieved by only one wall which consists of a capsule tube of Nb-1%Zr. An intermediate tube with good thermal conductivity is fitted into the NaK gap in order to achieve lower heat flux densities on the capsule surfaces and to avoid convection in the NaK. In addition to the description of the capsule rigs and their operational behavior, the actual safety considerations which play a particularly important part because of the possible risks of NaK/water reactions resulting from a leak in the capsule are included. (29 references) (auth)

10258 (EURFNR-848) PHYSICS INVESTIGATIONS OF STEAM-COOLED FAST REACTOR CORES WITH A PLUTONIUM-FUELED CENTRAL ZONE. SNEAK-ASSEMBLY 3 B. Fischer, E. A.; Helm, F.; Werle, H. (comps.) (Kernforschungszentrum, Karlsruhe (West Germany)). Sep 1970. 70p. (KFK-1266; EUR-3969). Dep. NTIS (U. S. Sales Only).

Work Performed under United States-Euratom Fast Reactor Exchange Program.

In SNEAK Assembly 3B the physics parameters of a steam-cooled fast reactor core were investigated, the steam being simulated by polyethylene foils. The core had a central zone fuelled with Pu and a surrounding U zone. It was also modified by introducing Ni and Mo for the simulation of Inconel and by introducing platelets containing a mockup of fission products. The experiments were compared to calculations, often using various nuclear data sets or calculational methods. (34 references) (auth)

10259 (GEAP-5550) FAST FLUX TEST FACILITY BACKUP DESIGN PROJECT FIRST QUARTERLY REPORT, MAY-AUGUST 1967. (General Electric Co., Sunnyvale, Calif. Advanced Products Operation). Oct 1967. Contract BDR-341. 46p. Dep. NTIS.

Development of backup design systems during May to August 1967 is described under the following main headings: plant performance; plant systems; reactor vessel and internals; refueling cell and fuel handling; driver fuel instrumentation; nuclear characteristics; shield design; thermal hydraulics analysis; and safeguards. (D.C.C.)

10260 (GEAP-5552) CONCEPTUAL DESIGN OF THE BACK-UP REACTOR SYSTEM FOR THE FAST FLUX TEST FACILITY. (General Electric Co., Sunnyvale, Calif. Advanced Products Operation). Aug 1967. Contract BDR-341. 166p. Dep. NTIS.

Design parameters for the FFTF backup systems are described. Design information is presented under the following headings: test facilities; cooling system; containment; reactor core; fuel loading and storage facilities; physics measurements; shielding; and engineered safeguards. (12 references) (D.C.C.)

10261 (GEAP-5614) FAST FLUX TEST FACILITY BACKUP DESIGN PROJECT SECOND QUARTERLY REPORT, SEPTEMBER-NOVEMBER 1967. (General Electric Co., Sunnyvale, Calif. Advanced Products Operation). Apr 1968. Contract BDR-341. 128p. Dep. NTIS.

Development of backup design systems during September to November 1967 is described under the following main headings: plant performance; plant systems; reactor vessel and internals; refueling cell and fuel handling; nuclear characteristics; shielding; thermal hydraulics analysis; and engineered safeguards. (13 references) (D.C.C.)

10262 (GEAP-5641) FAST FLUX TEST FACILITY BACKUP DESIGN PROJECT THIRD QUARTERLY REPORT, DECEMBER 1967-FEBRUARY 1968. (General Electric Co., Sunnyvale, Calif. Advanced Products Operation). Jul 1968. Contract BDR-341. 97p. Dep. NTIS.

Development of backup design systems during December 1967 to February 1968 is described under the following main headings: plant performance; reactor vessels and internals; refueling cell and fuel handling; nuclear characteristics; shielding; and thermal hydraulics analysis. (5 references) (D.C.C.)

10263 (GEAP-5650) FAST FLUX TEST FACILITY BACKUP DESIGN PROJECT FOURTH QUARTERLY REPORT, MARCH-MAY 1968. (General Electric Co., Sunnyvale, Calif. Advanced Products Operation). Jul 1968. Contract BDR-341. 130p. Dep. NTIS.

Development of backup design systems during March to May 1968 is described under the following main headings: plant performance; core structures; control rods; fuel elements; nuclear characteristics; shielding; and engineered safeguards. (5 references) (D.C.C.)

10264 (GEAP-5684) FAST FLUX TEST FACILITY BACKUP DESIGN PROJECT FIFTH QUARTERLY REPORT, JUNE-AUGUST 1968. (General Electric Co., Sunnyvale, Calif. Advanced Products Operation). Sep 1968. Contract BDR-341. 146p. Dep. NTIS.

Development of backup design systems during June to August 1968 is described under the following main headings: control system; core structures; physics; shielding; containment; and pressure vessel. (20 references) (D.C.C.)

10265 (GEAP-5715) FINAL FAST FLUX TEST FACILITY BACKUP DESIGN DEVELOPMENT REQUIREMENT REPORT. Pluta, P. R. (comp.) (General Electric Co., Sunnyvale, Calif. Advanced Products Operation). Dec 1968. Contract BDR-341. 14p. Dep. NTIS.

The backup design for the FFTF provides the capability for replacing the reference FFTF dispersed core design at any point in its evolution, with an open lattice vertical core and associated handling system, instrumentation, control rod, head configuration making use of the reference design vessel, hot cell, and cooling system. Backup design development requirements are listed. (auth)

10266 (GEAP-5721) FFTF BACKUP DESIGN INTERFACE DEFINITION DISCUSSION OF SYSTEM REQUIREMENTS. Kruger, G.; Kendall, W.; Mitome, D. (General Electric Co., Sunnyvale, Calif. Breeder Reactor Development Operation). Aug 1968. Contract BDR-341. 122p. Dep. NTIS.

System requirements for the FFTF backup design are discussed under the following headings: containment system; cooling system;

irradiation test facilities; cover gas system; radioactive gas waste system; and emergency power supply system. (D.C.C.)

10267 (IN-1442) ULTRASONIC LIQUID LEVEL DETECTOR USING SHEAR WAVE ATTENUATION IN A BAR. Arave, A. E. (Idaho Nuclear Corp., Idaho Falls). Nov 1970. Contract AT(10-1)-1230. 14p. Dep. NTIS.

An ultrasonic liquid level detector is being designed for the 200°F to 1000°F, 2500 psi water environment of the Loss of Fluid Test, LOFT, at the National Reactor Testing Station, NRTS. The detection technique is new in the ultrasonic liquid level detector field. Attenuation of an ultrasonic shear wave as it propagates in a steel bar is a function of the water covering the bar. The bar takes on different dimensions depending on the application. Magnetostrictive transducers are used to transmit and receive the 200 kHz shear waves. (auth)

10268 (LA-4399-TR) HIGH-FLUX STATIONARY RESEARCH REACTORS AND THEIR OUTLOOK. Feinberg, S. M. (Gosudarstvennyi Komitet po Ispol'zovaniyu Atomnoi Energii SSSR, Moscow. Institut Atomnoi Energii). Translated by Helen J. Dahlby (Los Alamos Scientific Lab., N. Mex.), from report IAE-1693. 10p. Dep. NTIS.

Successful operation of stationary research intermediate-neutron reactors with a thermal-neutron trap is described. The prospects of further enlargement of the neutron flux are discussed. A comparison is made with the design of a fast-neutron accelerator used as the source of an intensive field of thermal neutrons. (10 references) (auth)

10269 (NP-18498) SAFETY REPORT FOR THE CORE ARRANGEMENT WITH TWO FISSION ZONES. Supplement to the Authorization Authority Safety Report Submitted in 1966 for the Research and Measurement Reactor (FMRB). (Physikalisch-Technische Bundesanstalt, Brunswick (West Germany)). Aug 1968. 55p. (In German). Dep. NTIS (U. S. Sales Only).

The Braunschweig Research and Measurement Reactor possesses two physically separated fission zones, which are coupled by a heavy water tank of about 60 cm width. The special characteristics of this reactor are described. The physical and engineering data are compiled. The physics properties of the nuclear arrangement with two fission zones are discussed. The safety measures taken are outlined. The nuclear startup program is given. (J.S.R.)

10270 (ORNL-TM-3256) OAK RIDGE RESEARCH REACTOR QUARTERLY REPORT, JULY-SEPTEMBER OF 1970. Hurt III, S. S.; Tabor, W. H. (Oak Ridge National Lab., Tenn.). 4 Dec 1970. 52p. Dep. NTIS.

The ORR operated at an average power level of 29.9 MW 87.3% of the time during July, August, and September of 1970. Thirty-four fuel elements were declared spent during the quarter, bringing the number of spent fuel elements for the year to 93. The average burnup (loss of ^{235}U) for the quarter and for the year to date was 49%. The reactor was scheduled down on only seven occasions, two of which were end-of-cycle shutdowns. Unscheduled downtime (one shutdown) totaled 0.433 hours. The fission chamber preamplifier assembly (snake) for the No. 1 counting-rate channel was replaced, as was the ionization chamber for the No. 2 safety channel. The poolside facility (flat side of the reactor tank) was checked dimensionally on the inside and visually on the outside. There was no indication of dimensional changes of any consequence and no visible evidence of damage or excessive corrosion. Shim-rod-worth measurements were made in July when all shim-rod positions were filled with rods originally containing 167 g of ^{235}U. Thermal fluxes in the fuel positions were measured in September. (auth)

10271 (WHAN-FR-21) CONDUCTIVITY CELLS FOR FLOW INDUCED VIBRATION MEASUREMENTS. Sawtelle, G. R. (WADCO Corp., Richland, Wash.). Oct 1970. Contract AT-(45-1)-2170. 42p. Dep. NTIS.

The development of a conductivity cell instrumentation for measuring flow induced vibrations in long, slender fuel pins is described. The design, construction and evaluation of conductivity cells and associated signal conditioning equipment are discussed in detail, providing the background for the underlying theory, operating procedure and limitations of a particular instrument, the PNL Impedance Detector. 11 references. (auth)

10272 (WHAN-FR-35) COMPARISON OF NUCLEAR DESIGN MODELS FOR POWER AND FLUX DISTRIBUTIONS NEAR THE FTR CORE-REFLECTOR INTERFACE. O'Dell, L. D.; Rothrock, R. B. (WADCO Corp., Richland, Wash.). Nov 1970. Contract AT(45-1)-2170. 20p. Dep. NTIS.

Diffusion and transport (Sn) calculations in one and two dimensions are described. The model detail required to accurately calculate flux and power distributions near the Fast Test Reactor (FTR) core-reflector interface is analyzed. 8 references. (auth)

10273 UNIVERSITY OF MISSOURI RESEARCH REACTOR FACILITY. Emmons, A. H.; Cox, E. L.; Alger, D. M. (Univ. of Missouri, Columbia). Isotop. Radiat. Technol.; 8: 137-45 (1970-71).

The Research Reactor Facility at the University of Missouri in Columbia is described. This flux-trap reactor is designed to operate at 10 MW power but is currently operating at 5 MW. The reactor is cooled and moderated by light water and uses beryllium and graphite as reflectors. The laboratories and other facilities related to the reactor operation are also described. (auth)

10274 HYDRAULIC RABBIT FACILITY. Stechemesser, H.; Sachse, K. (Kernforschungsanlage, Juelich, Ger.). Kerntechnik; 12: 449-55(Oct 1970). (In German).

For the irradiation of large samples at temperatures below 20°C, a hydraulic rabbit system was constructed at the reactor DIDO in Jülich. The principle of operation and the design data are explained. Special points of safety considerations, instrumentation and design are pointed out. (auth)

10275 CROSS-SPECTRAL-DENSITY SINK FREQUENCY BEHAVIOR FOR COUPLED-CORE ARGONAUT REACTORS. Nagy, Mohamed El-Sayed; Danofsky, Richard A. (Iowa State Univ., Ames). Nucl. Sci. Eng.; 42: 419-21(Dec 1970).

The results of a parametric study, based on the mathematical model by Danofsky, of the sensitivity of the sink frequency to core spacing and the thermal absorption and fast removal cross sections of the internal reflector or coupling region are presented. The cross-spectral-density function and corresponding sink frequency are determined for symmetric observation points located at the midplane of the two fuel regions of the one-dimensional reactor model. All systems investigated are delayed critical and, in the two-energy group analysis used, absorption in the fast group and fast fission are assumed to be negligible. (auth)

10276 POOL NUCLEAR REACTOR. Giraud, J.; Lorin, C. (to CEA). French Patent 1,575,859. 16 Jun 1969. Filed 10 Jun 1968. (In French).

A pool-type reactor with an independent cooling system is described. The fuel elements are arranged in vertical tubes which carry the coolant upward to a collection vessel. The vessel contains a filter for trapping particles from failed fuel elements which may be carried away by the coolant. The trapped particles are then deposited in a vertical conduit under the filter. (P.C.H.)

10277 MEASUREMENT OF FAST NEUTRON SPECTRUM AND FLUX IN CENTRAL THIMBLE OF TRIGA MARK-II REACTOR. Kim, Dong Hoon; Kim, Hong Sik; Yang Jae Choon (Atomic Energy Research Inst., Seoul). J. Korean Nucl. Soc.; 2: 67-72(Jun 1970).

The measurements of the fast neutron flux and its spectrum have been carried out by the threshold detectors in the central thimble of TRIGA Mark-II reactor operating at 250 kW. The following reactions have been employed for these measurements: $^{58}Ni(n,p)^{58}Co$; $^{24}Mg(n,p)^{24}Na$; $^{27}Al(n,\alpha)^{24}Na$. From the activation data the fast neutron spectrum was calculated by CDC-3600 computer making use of two semi-empirical methods. It has been verified that the validity of assumption of a fission spectrum in the central thimble exists only above 1 to 2 MeV energy level. With this spectrum, a fast neutron flux in the range of 1×10^{12} n/cm^2-sec above the energy of 2.6 MeV was observed in the central thimble of TRIGA MARK-II reactor. 10 references. (auth)

10278 ADDITIONAL COMMENTS ON THE CROSS-SPECTRAL-DENSITY SINK FREQUENCY BEHAVIOR FOR COUPLED CORE ARGONAUT REACTORS. Danofsky, R. A. (Iowa State Univ., Ames). Nucl. Sci. Eng.; 42: 430(Dec 1970).

The sink frequency as measured in the FMRB reactor by Viehl and Seifritz has been compared with that calculated by Nagy and Danofsky using a one-dimensional model of an Argonaut-type reactor. It is reported that the observed sink frequency is higher than that predicted for a 60-cm-thick D_2O coupling region. It should be noted that the results represent a draftsman's fit to the calculated values. A calculated value for a 60-cm-thick D_2O model was not obtained in the original study and thus the value for the 60-cm coupling region is estimated. The predicted sink frequency is approximately 40 rad/sec. This is less than the observed 250 rad/sec. The difference between the observed and predicted sink frequency may be due in part to the one-dimensional nature of the model used and in part to the two-energy group approximation used with the associated choice of nuclear constants. Also, the model used in the study had external graphite reflectors and 15-cm fuel regions and it is not known if variations in these properties might alter the predicted sink frequency. (auth)

XUM

10279 CROSS-SPECTRAL-DENSITY SINK FREQUENCY BEHAVIOR IN COUPLED CORE REACTORS. Viehl, E. (Physikalisch-Technische Bundesanstalt, Brunswick, Ger.); Seifritz, W. Nucl. Sci. Eng.; 42: 430(Dec 1970).

The sensitivity of the sink frequency to core spacing and the thermal-absorption and fast-removal cross sections of the coupling medium of a two-slab coupled core reactor have been theoretically investigated. It was found that for a 60-cm-wide heavy water coupling region the sink frequency was predicted to occur at the very low angular frequency of 15 rad/sec. However, two-detector cross correlation measurements at the Forschungs- und Me β reaktor Braunschweig (FMRB) which are being carried out presently cannot confirm this result. The FMRB is a swimming pool type reactor with two weakly coupled cores which are moderated and reflected by light water. Each core contains a 4×7 loading of MTR fuel elements with 90% ^{235}U enriched uranium. The coupling region consists of a 60-cm-wide heavy water tank. The quality of the heavy water is better than 99.75%. The aluminum walls of the tank are 8-mm-thick and there is a 6-mm-thick light water layer between each core and the side of the heavy water tank. First evaluations of cross power spectral density measurements with the reactor at delayed critical and at a symmetrical power distribution lead to a sink frequency of about 250 rad/sec which is in poor agreement with the predicted theoretical value of Nagy and Danofsky. (auth)

10280 POOL-REACTOR. Giraud, J.; Lorin, C. (to CEA). French Patent 1,575,858. 16 Jun 1969. Filed 10 Jun 1968. (In French).

A pool-type reactor is described in which fuel elements are arranged vertically in a mass of water, which assures biological protection and relies on an independent cooling circuit. The fuel elements are extended vertically by tubes leading up to a collection vessel. (P.C.H.)

10281 MODEL FOR CALCULATION OF SELF-LIMITING POWER EXCURSIONS IN A REACTOR WITH NATURAL URANIUM FUEL ELEMENTS IN PRESSURE TUBES OF VARIABLE PITCH. Markovina, A.; Palinski, R. (EURATOM, Ispra, Italy). Ing. Nucl.; 10: No. 6, 7-17(Nov-Dec 1969). (In Italian).

A mathematical model for the calculation of the power excursions, generated by accidental insertions of reactivity, was illustrated for a research reactor with natural uranium, moderated with D_2O and cooled with organic liquid, and with fuel elements in pressure tubes of variable pitch. The intrinsic mechanisms of reactivity compensation, evaluated in part by directly measured parameters and in part by calculations, were emphasized. The Doppler effect and the effects connected with the thermal expansion of the materials are considered. The calculation results are discussed with reference to the self-limiting power of the reactor. (tr-auth)

10282 SHORT-INTERVAL SERIES PULSING-EXPERIMENTAL STUDIES AND NUMERICAL EXPERIMENTS. Kurstedt, H. A. Jr.; Miley, G. H. (Univ. of Illinois, Urbana). Nucl. Technol., 10: 168-78(Feb 1971).

The technique of short-interval series pulsing a thermal reactor has been studied experimentally using the University of Illinois TRIGA Reactor. Pulse repetition rates varying from 0.5 to 3.0 pulses/minute were involved. These rates represent an order of magnitude decrease in time interval between pulses compared to previous TRIGA pulsing experience. It was found that the equilibrium pulse amplitudes are strongly affected by the pulse rod reactivity, the rod drop time, and the time interval between pulses; and in the experiments, each of these parameters was maintained at a fixed value during any given series. A unique method of analysis involving the reactor kinetics equations solved in temperature has been developed to study series pulsing. This analysis shows that a further improvement by a factor of two to five for present reactor and fuel designs can be expected with certain techniques which do not require major modifications to reactor geometry or fuel. These include changing the pulse rod reactivity values between pulses, changing the time interval between pulses, increasing the rod drop reactivity, and series pulsing from elevated powers. 10 references. (auth)

10283 DETECTION AND LOCATION OF LEAKING TRIGA REACTOR FUEL ELEMENTS. Bouchey, G. D.; Gage, S. J. (Univ. of Texas, Austin). Nucl. Technol.; 10: 211-14(Feb 1971).

The radioactive fission gases and their daughter products which are observed as a result of a typical cladding break in a TRIGA reactor fuel element are discussed. Methods of detection of these fission products as airborne particulate activity are described. Finally, a device for selectively locating a failed fuel element by measuring the particulate activity in gas collected directly above the test element during reactor operation is described. (auth)

10284 RADIATION PROTECTION EXPERIENCE AT THE ONE-MEGAWATT POOL REACTOR THOR AND ITS AFFILIATED FACILITIES. Weng, P. S.; Lin, H. H. (National Tsing Hua Univ., Hsinchu, China). Hoken Butsuri; 5: 129-33(Sep 1970).

In an eight-year period of operating THOR and its affiliated facilities, since it went to critical on April 13, 1961, twenty incidents involving more or less serious radiation exposure or reactor hazards were recorded. Some of these incidents are described. The incidents described were chosen to give a representative picture of what could be expected in the operation of a reactor facility of similar design and similar purpose under similar operating conditions. The difficulties which exist or have existed in the radiation protection work were reviewed, and the possible solutions were suggested and practiced. (auth) (Japan)

10285 NEUTRON AMPLIFICATION AND APPLICATION TO A FLUX-TRAP REACTOR. Karousakis, Panayiotis. Lafayette, Ind.; Purdue Univ. (1970). 143p. University Microfilms Order No. 70-18,679.

Thesis.

The feasibility of a high flux research reactor is studied based on Borst's idea of the convergatron, a device which employs successive layers of moderator, fuel, and absorber regions in such a way as to enhance a forward movement and an amplification of neutrons. The problem is studied from various points of view with the main emphasis on generalized multienergy group point kinetics, derived from the Boltzmann transport equation and reduced to a diffusion theory formulation. An explicit treatment and definitions of the effective surface sources at the various interfaces is included. The approximation made is a two group approximation, a fast group, referred to as group one extending down to 0.683 ev, and a thermal group, referred to as group two extending from 0.683 ev to 0.025 ev. Two computer codes, the DTF IV transport code and the EQUIPOISE diffusion code, are extensively employed and the results are analyzed and used in obtaining coupling coefficients and kinetics parameters. These values are then used in the set of integrodifferential equations of the two group approach, and the coupled equations are solved. Use is made here of the MIMIC program. Preliminary results show that such a reactor system is indeed feasible up to second order effects and holds promise for future research in realizing very high neutron fluxes for irradiation and other purposes. The proposed reactor furthermore is superior to a reactor system of the same size and critical mass, but with the fissile material uniformly dispersed over the whole core, and compares favorably with other flux trap reactors such as the HFIR and the ATR reactors. (Diss. Abstr. Int., B)

Rocket and Space Reactors

10286 CONCEPTUAL DESIGN OF A 2-Mw_t (375 kw_e) NUCLEAR-ELECTRIC SPACE POWER SYSTEM. Pitts, John H.; Walter, Carl E. (Univ. of California, Livermore). J. Spacecraft Rockets; 7: 1282-6(Nov 1970).

The power system described includes a unique nuclear reactor-boiler unit operating at 1500°K that utilizes heatpipes in lieu of a conventionally pumped primary loop. An efficient heatpipe radiator rejects waste heat at 1035°K. Over-all system efficiency is 18.8% yielding a net electrical output of 375 kW(e). The system specific mass is 10 kg/kW(e) including a generous shadow shield for unmanned payloads. 15 references. (auth)

10287 DEEP SPACE SHUTTLES: CHEMICAL vs NUCLEAR; DIRECT FLIGHT vs NEAR-ORBIT RENDEZVOUS. Salkeld, Robert. J. Spacecraft Rockets; 7: 1369-71(Nov 1970).

Costs related to the operating modes and vehicle types used for space activities are compared. Nuclear and chemical propelled vehicles and their operation alternatives are analyzed. (D.C.C.)

10288 COLLECTION OF TECHNICAL PAPERS ON STRUCTURES AND MATERIALS. AIAA/ASME 10th Structures, Structural Dynamics, and Materials Conference, New Orleans, Louisiana, April 14–16, 1969. New York; American Society of Mechanical Engineers (1969). 476p. $22.00 (CONF-690415).

Information on structures and materials is presented with emphasis placed on aerospace applications. A separate abstract is included for 1 of the 47 papers presented. (D.C.C.)

For abstract of the individual paper see: 10289.

10289 LAUNCH AND MISSION INFLUENCES ON SPACE PROPULSION SYSTEM DESIGN. Garcia, D. S.; Fahrner, T.; Johnson, K. P. (McDonnell Douglas Astronautics Co., Huntington Beach, Calif.). pp 319-29 of Collection of Technical Papers on Structures

and Materials. New York; American Society of Mechanical Engineers (1969).

From 10th Structures, Structural Dynamics, and Material Conference, New Orleans, La. See CONF-690415.

Various aspects of launch and mission influences on structural design of upper stages for space applications have been evaluated. A nuclear stage of 250 K lb–LH_2 capacity with a NERVA 1 engine has been used for this purpose. Both load-bearing tank and thermos bottle configurations were compared employing various insulation systems for a range of mission requirements. The thermos bottle configuration was subjected to a detailed parametric evaluation emphasizing the interaction between launch and mission design conditions for different stage geometries. A top-down analytical technique is presented which translates mission requirements into allowable loading envelopes and launch vehicle interactions, providing a basis for launch vehicle design and integration with the space propulsion system. Also, the space mission performance sensitivity to stage structural requirements of the various launch and mission influences was evaluated. A computer program was developed to facilitate the analyses. The program consists of a series of interrelated subroutines which combine geometry, loads/inert weight evaluation, mission requirements, and system integration requirements to accomplish total system design. 8 references. (auth)

10290 MUTUAL NEUTRON INTERCHANGE THROUGH VACUUM BETWEEN BOUNDARY SURFACES OF REACTOR PARTS. Speidel, V.; Wolf, E. (Univ., Stuttgart). Atomkernenergie; 16: 196-200(1970).

A theoretical model for studying the mutual neutron interchange through vacuum between arbitrarily arranged parts of reactor medium is presented. For the special case of plane polar coordinates the model is formulated in the form of boundary conditions of the diffusion theory and compared to experimental data of SNAP Experimental Reactor. The method is suitable for reactor physics calculations of reactors having movable reflector parts for control purposes. (11 references) (auth)

Process Heat and Desalination Reactors

Refer also to abstract 10094.

10291 (TID–25630) THE IMPACT OF NUCLEAR ENERGY CENTERS ON THE ECONOMY OF PUERTO RICO. Holmes, John M. (Tennessee Univ., Knoxville. Dept. of Chemical and Metallurgical Engineering. Oak Ridge National Lab., Tenn.). Jul 1970. 239p. Dep. NTIS.

Thesis.

An economic model was developed for determining: an optimum combination of industrial activities for a nuclear energy center as a function of energy cost, and the economic impact of the center on its economic region. The model is derived from the coupling of two research techniques, separable programming and input-output analysis, in a mutually consistent manner. Separable programming was used to optimize the mix of energy-intensive industries proposed for an energy center; maximization of premium worth at a 10% minimum acceptable rate of return was adopted as the optimization criterion. The program used energy cost as a parameter in order to study the variations in industrial activity and total energy demand as a function of energy cost. Problems associated with the achievement of local optima in the separable program were corrected through development of a search routine based on inserting activity vectors into the basis of each prior solution and running the problem until an optimum which was believed to be reasonably close to the global optimum for this particular study was achieved. Results of the separable program served as the data for an input-output program which examined the effect of the center on its economic region in terms of increases in gross product, employment, and capital demands. A feedback of information from the input-output program permitted adjustment of the capital and employment constraints in the separable program so that consistent relationships were maintained between the project demands and the resources of the economy. Projection of the input-output data to show the effects of an energy center over both short- and long-term time periods was developed employing a dynamic procedure which took into account the changes in the final demands of the economy as a function of the growth of gross product. Puerto Rico was selected as a test region for this model. Results of the optimization are presented. 132 references. (auth)

10292 PROCESS AND EQUIPMENT FOR THE WORKING OF NUCLEAR ENERGY. (to Kernforschungsanlage, Julich GmbH). French Patent 1,572,233. 19 May 1969. Priority date 17 Feb 1967, Germany. (In French).

A procedure for utilizing energy produced by a nuclear reactor is described. A refrigerant circulating through pipes transfers the heat produced by the reactor to vessels containing substances destined to participate in a particular chemical reaction. In the production of hydrogen, water vapor is passed over a metal oxide in a CO atmosphere. The metal carbonate formed is dissociated with regeneration of the oxide and evolution of CO_2, some of which is passed over finely divided carbon, producing CO, which is returned to the reaction vessel. Products of the reaction are hydrogen gas and CO_2. (J.G.B.)

10293 COST ECONOMICS OF A FERTILIZER COMPLEX ON THE WEST PAKISTAN SEA COAST. Ahmad, Mohammad (Pakistan Atomic Energy Commission, Karachi). Nucleus (Karachi); 7: 4-20(Jan-Apr 1970).

The results of a theoretical exercise on the cost economics of a fertilizer complex using imported phosphate rock and excess naphtha from the refineries for an unspecified site on the West Pakistan sea-coast are reported. Ammonia and phosphorus are the primary products which are easily converted into secondary fertilizers. The gross profit for four types of product-mix varies from 17 to 30%. The water and power requirements of the complex are assumed to be met from a dual-purpose nuclear station. Whereas the electrical load in the complex varies from about 70 to 200 MW at 90% load factor depending on the product-mix, the process water requirement is not large. It is also found that the additional supply of 30% of the cooling water requirement in the complex from the desalination plant does not practically affect the manufacturing cost of the fertilizer; this industry can, therefore, bear higher rates for the cooling water. 6 references. (auth)

10294 METHOD FOR UTILIZING NUCLEAR ENERGY IN THE PRODUCTION OF HYDROGEN. Wolfgang, Hans; Wolff, Gerhard (to Kernforschungsanlage). U. S. Patent 3,535,082. 20 Oct 1970. Priority date 17 Feb 1967, Germany.

Nuclear energy is utilized in the production of H_2 by heating $CaCO_3$ or $MgCO_3$ so as to form the respective metal oxide and CO_2, using a portion of the thus obtained CO_2 for conversion thereof in contact with C to CO, heating the thus obtained metal oxide and CO in the presence of steam so as to form H_2 gas and metal carbonate, the latter being reused for producing metal oxide and CO_2 and the H_2 gas being recovered, and supplying the heat required for these reactions and for the production of the needed steam by indirect heat exchange with a heat exchange medium such as He which passes in a closed cycle between a high temperature nuclear reactor in which the heat exchange medium is heated and the above described reaction mixtures which are heated by the heat exchange medium under simultaneous cooling of the latter. (auth)

Marine and Portable Power Reactors

10295 (JPRS–51939) SAFE OPERATION OF ATOMIC SHIPS. Sarkisov, A. A. Translated from Morsk. Sb.; No. 10, 66-71(1970). 10p. NTIS.

Safety factors which are not concerned with ship reactor design and operation are reviewed. Various aspects of reactor location aboard the ship and measures needed to protect the reactor in the event of collision, grounding, fire, sinking, etc. are discussed. (H.D.R.)

10296 (NSJ-tr–157) GAMMA-RAY LEAKAGE THROUGH A JUNCTION BETWEEN LEAD AND CONCRETE WALLS. Miyasaka, Shun-ichi; Kanemori, Yoshihiko; Fukushima, Yutaka; Yamada, Takeshi. Translated from Nippon Genshiryoku Gakkaishi; 11: 144-9(Mar 1969). 14p. Dep. NTIS (U. S. Sales Only).

A study was performed as part of a series of mock-up tests undertaken in relation to the shielding design for the first Japanese nuclear propelled ship. The subject is reactor γ-ray leakage through a part of the shielding forming the junction between 15 cm thick lead and 75 cm thick concrete slabs, with the lead wall abutting at right angles against the side of the concrete shielding. The experimental results are expressed as functions of slit width, beam incident angle, and point of observation. The observed data are compared with calculations based on ray-analysis for penetration components, and on single scattering method for streaming components. (13 references) (auth)

10297 NUCLEAR POWER OPERATIONS, DEEP FREEZE 69–70. Alexander, Robert F. (Naval Nuclear Power Unit, Fort Belvoir, Va.). Antarctic J. U. S.; 5: 205-6(Sep-Oct 1970).

The operation of the Pm-3A nuclear power plant at McMurdo

XUM

Station during the 1969-70 season is reviewed. Electrical plant availability and output and water distillation plant output are tabulated. Maintenance and modifications to the plant are summarized. (H.D.R.)

10298 SMALL NUCLEAR REACTOR FOR UNDERSEA USE. Mills, Carroll B. (Los Alamos Scientific Lab., N. Mex.). Nucl. Technol.; 10: 133-8(Feb 1971).

Requirements for underseas nuclear reactor power systems for small vessels include: simplified, small reactor and plant control and instrumentation; long-term compatibility of fuel, structure and coolant; and extended fuel lifetime, safety, and low cost. Neutronic qualities that reflect these requirements are: lowest critical mass, for low cost and small size; low fuel concentration in the fuel elements, consistent with extended fuel lifetime, small fuel effects on fuel element materials properties, and small fission-product effects; negative temperature and core geometry coefficients of reactivity, in the interest of minimizing safety and control problems; and 100 g fuel burnup (100 MW days of energy). A reactor design that has these qualities uses a pressurized water moderated, beryllium (4 in.) reflected, solid fuel geometry with 0.070 g/ml ^{235}U in the core, and zirconium fuel elements, with a fuel mass including 0.1 kg for burnup of under 0.8 kg of ^{235}U. This reactor core is 8 in. long and 8 in. in diameter, and contains 85% by volume of water at an operating temperature around 500°F, for a power level of 300 kW(t). 13 references. (auth)

Reactor Theory

10299 INVESTIGATION OF FISSION-PRODUCT BEHAVIOR AND DECAY HEATING IN NUCLEAR REACTORS. England, Talmadge Ray. Madison, Wis.; Univ. of Wisconsin (1970). 335p. University Microfilms Order No. 70-12,727.

Thesis.

Fission product decay heating by release of delayed beta and gamma emission is extensively studied by first principle calculations. Fissile and fissionable fuels ^{235}U, ^{233}U, ^{239}Pu, ^{238}U and ^{232}Th are included. Variations in reactor dependent parameters (spectrum, flux and power level, and flux-time) are made. A comprehensive set of nuclide data is included; the list contains neutron cross sections, half-lives, direct yields from each fuel nuclide, decay branching fractions, beta and gamma energies per decay, and chain structure. A digital source program capable of an exact description of the individual and collective behavior of the fission product data, arbitrary fuel chains, or any other set of coupled nuclides in a realistic, time-dependent flux and spectrum is included. Extensive tabular and graphical results are presented that show the detailed behavior of beta and gamma radiation (in MeV/fission) both during fuel irradiation and over a ten year shutdown interval. Comprehensive comparisons with the ^{235}U heating data generally used in nuclear design for all fuels and with some experimental data are presented. Intercomparisons of results are included. (Diss. Abstr. Int., B)

Kinetics

Refer also to abstracts 9948, 10177–10179, 10272, 10275, 10278, and 10279.

10300 (AECL-3671(Add.1)) FORGAD: A ONE DIMENSIONAL FEW GROUP FINITE DIFFERENCE REACTOR CODE. Sills, H. E. (Atomic Energy of Canada Ltd., Chalk River (Ontario). Chalk River Nuclear Labs.). Dec 1970. 24p. Dep. NTIS (U. S. Sales Only). AECL $1.00.

The program, FORGOD, was modified to include more input options. The major modifications include the calculation of the adjoint flux, a criticality search on a region boundary and "supercell" calculations. The physics calculations remain unchanged from FORGOD and so no explanation is given. Only the modifications and input structure for FORGAD are described. (auth)

10301 (AEEW-R-701) THERMAL NEUTRON DIFFUSION DATA AND THE WIMS SCATTERING MODELS FOR LIGHT WATER. Butland, A. T. D.; Chudley, C. T. (Atomic Energy Establishment, Winfrith (England)). Aug 1970. 31p. Dep. NTIS (U. S. Sales Only). UK 6s. 6d.

Available integral data on the neutron diffusion coefficient and differential measurements of the total neutron cross-section of light water are examined and used to test the validity of the Effective Width and Nelkin Models for thermal neutron scattering in light water. (46 references) (auth) (UK)

10302 (BARC-502) DETERMINATION OF THE REACTOR POWER RESPONSE TO A SINUSOIDAL REACTIVITY INPUT BY USE OF IDEMPOTENT MATRICES. Trasi, M. S. (Bhabha Atomic Research Centre, Bombay (India)). 1970. 7p. Dep. NTIS (U. S. Sales Only).

The point-reactor kinetic equations, with one group of delayed neutrons and a sinusoidal reactivity input, are integrated by the method of small parameters. The properties of certain idempotent matrices are used to facilitate the integration, and the mean gradient and the amplitude of the oscillations of the logarithm of the power are obtained. (auth)

10303 (CEA-CONF-1684) HYBRID SOLUTION OF THE SPACE-TIME PROBLEMS IN POWER REACTORS. Caillet, Claude (Commissariat a l'Energie Atomique, Saclay (France). Centre d'Etudes Nucleaires). 21 Oct 1970. 43p. (In French). (CONF-701019-2). Dep. NTIS (U. S. Sales Only).

From CREST Meeting on Reactivity Effects in Large Power Reactors, Ispra, Italy.

The ways in which analog or hybrid computers are used to solve the partial differential equations encountered in the running problems associated with large power reactors are reviewed. Two problems recently studied at the Analog and Hybrid Computing Center of the Electronic Reactor Service Group at Saclay are described. A series solution method was used to solve a thermal neutron gas-graphite reactor (Bugey reactor) problem, while a series-parallel method was used with a fast neutron reactor problem. (auth) (France)

10304 (EUR-4539) CONDOR 3: A TWO-DIMENSIONAL REACTOR LIFETIME PROGRAM WITH LOCAL AND SPECTRUM DEPENDENT DEPLETION. Salina, E. (Applicazioni e Ricerche Scientifiche, Milan (Italy)). 1970. 82p. Dep. NTIS (U.S. Sales Only). EUR Fr.F 13.80.

CONDOR 3, as the preceding nuclear codes of the CONDOR series is a few-group bidimensional lifetime program written in Fortran IV for the IBM 360/65. It couples the method of the spatial modal expansion with the 5 point finite difference method. By means of the spatial modal expansion the program determines the eigenvalue of the reactor, which can be in turn the K_{eff} (multiplication factor), the (H) (dilution factor of a diluted poison), the Σ_p or the boundary of a prefixed control region. By means of the finite difference method, the program improves the calculation of the K_{eff} and the group flux spatial distribution. 18 references. (auth)

10305 (IAE-1955) EFFECT OF DELAYED NEUTRONS ON THE DYNAMIC REACTIVITY OF A REACTOR ORIGINATING DURING OSCILLATIONS OF THE DENSITY OF THE FUEL. Blinkin, V. L.; Novikov, V. M. (Akademiya Nauk SSSR, Moscow. Institut Atomnoi Energii). 1970. 23p. (In Russian). Dep. NTIS (U. S. Sales Only).

Delayed neutrons influence upon the alteration of the reactivity in reactor due to the fuel density oscillations is investigated. It is shown that the calculations taking into account the delayed neutrons do not lead to the change of the sign of the resulted reactivity. However, the dynamic reactivity dependence upon the delayed neutrons parameters essentially differs from that for the constant supercriticality. The dynamic reactivity of the system with delayed neutrons may be even more than that calculated for the system without delayed neutrons. 3 references. (auth)

10306 (NP-18547) DIGITAL SIMULATION OF SPATIAL XENON OSCILLATIONS. Olsson, Gustaf (Lund Inst. of Tech. (Sweden). Div. of Automatic Control). Jul 1969. 117p. Dep. NTIS (U. S. Sales Only).

A nonlinear model of xenon spatial oscillations in one dimension based on one group diffusion theory and finite differences is presented. The process has been simulated on a digital computer. The domain of linearity of the model is discussed. The influence of different core parameters on reactor stability and on amplitude of the oscillations is presented. The results are compared to other models. Influence of nonlinear terms, such as temperature feedback and control rod, indicates that periodic solutions can appear. This has been predicted earlier with a simple two point model. The rod movement has a very big influence on amplitude and character of the oscillations. It can be explained from a very simple model of the core. The simulations have indicated suitable approximations to get a space independent nonlinear model of the process. Physical interpretation and drawbacks of this model are discussed. (auth) (Sweden)

10307 (ORNL-TM-3136) NEW CALCULATIONAL METHOD FOR SPACE-ENERGY-ANGULAR DEPENDENT REACTOR KINETICS. Dodds, Harold Lebron Jr. (Oak Ridge National Lab., Tenn.). Jan 1971. Contract W-7405-eng-26. 91p. Dep. NTIS.

Thesis. Submitted to Tennessee Univ., Knoxville.

In order to aid the interpretation of kinetic experiments in nuclear reactors, a new calculational method for solving the zero-power reactor kinetic equations in the frequency domain was developed. The algorithm that was developed is valid for either multigroup diffusion theory or discrete ordinate transport theory in one-dimensional slab geometry. The numerical technique that is used employs a combined transfer-scattering (or response) matrix concept which includes spatially distributed extraneous sources. The technique is explicitly designed to control truncation and round-off error problems. Results calculated using the new technique were compared with experimental results for a D_2O moderated, natural-uranium fueled, subcritical assembly. Good agreement with experiment was achieved. A comparison with results calculated independently using a more conventional calculational technique was also performed. Excellent agreement was achieved in this comparison. Finally, in order to demonstrate its usefulness, the method was utilized in a theoretical investigation into the validity of using the point model to describe the subcritical kinetics of a symmetrically reflected, fast reactor. The results of this theoretical study indicated that, in general, the point model was not valid for interpreting experimental results obtained with a detector located in the reflector and was only approximately valid for a detector located in the center of the core. (45 references) (auth)

10308 CALCULATION OF BURNT FUEL ACTIVITY BY OPTIMIZATION METHOD. El-Mekkawi, L. S. (Atomic Energy Establishment, Cairo). Atompraxis; 16: 340-2(Sep–Oct 1970).

The method of optimization gives a quick comparison of the activity of isotopes of burnt fuel and shows how to select the higher activity isotopes for given fuel irradiation and cooling times. It gives simplified calculations of the activity of the hazardous fission products, as well as the burnt fuel activity. 6 references. (auth)

10309 REACTIVITY MEASUREMENTS BY PULSE METHODS. Stumbur, E. A. At. Energ. (USSR); 29: 212-15(Aug 1970). (In Russian).

The amount of introduced reactivity k_{eff} is a useable value for reactor calculations. Following up the theoretical studies of k_{eff} by L. N. Usachev, its highest eigenvalue, for which the solution of $\psi(r,v)$ is non-negative, was considered. The $\psi(r,v)$ may be practically achieved only for critical reactors, that is when $k_{eff} = 1$; in every other case the spatial and energy distribution of the neutrons will be different. Taking advantage of Laplace transform with a parameter s for the nonstationary equation, two values of s were found to be of special importance: $s = \alpha_0$ indicating the decrement of the asymptotic dampening of the prompt neutron flux measured by pulse experiments, and $s = \alpha_T$ indicating the inverse value of the reactor period T. The pulse method makes it possible to measure considerable subcritical states but applicability of the α method is greatly limited. More recently the integral pulse methods have been widely used; they are based on the application of the whole time behavior of the neutron flux excited by the pulse of an external source. The various pulse methods yield correct results only if the measurements are made within the reactor core; the assumptions made should not be generalized. The combined integral method is laborious but the results do not depend on the kinetic limitations, location of the pulse source, or on the effect of higher harmonics. (TTT)

10310 EXTENDED EQUIVALENCE RELATION. Kelber, Charles N. (Argonne National Lab., Ill.). Nucl. Sci. Eng.; 42: 257-9(Dec 1970).

The equivalence relation for the calculation of resonance capture employs a modified rod radius to account for inaccuracies in the Wigner rational approximation of the probability of escape from the rod. An extension of the work is presented to derive a correction to the mean chord length which depends on the peak resonance cross section, the potential scattering, and the rod radius. Such a formula represents a useful compromise between use of the less accurate but computationally convenient equivalence relation and accurate but computationally complex methods. (auth)

10311 PHASE SPACE ANALYSIS OF REACTOR KINETICS. Vreekse, Simon A.; Sandquist, Gary M. (Univ. of Utah, Salt Lake City). Nucl. Sci. Eng.; 42: 295-305(Dec 1970).

A method for studying systems of differential equations employing an interactive computer system with a display screen is presented and applied to three nonlinear problems in reactor kinetics. Interactively it is possible to construct phase space solutions of second- and third-order systems of equations. It is also possible to project from the three-dimensional space and to consider the solutions of the equations as explicit functions of the independent variable. The method is demonstrated on three different nonlinear problems of interest to nuclear reactor kinetics. A second-order problem with temperature-dependent reactivity is considered. Two third-order problems with reactivity a function of two effective temperatures and ^{135}Xe concentration, respectively, are also considered. The method of analysis makes it possible to efficiently study the effect of various parameter values on the solutions of the equations. Limit cycle behavior is investigated and the effect of the parameters of the model on the limit cycles is studied with greater effectiveness than can be achieved by an analytical study. (auth)

10312 STUDIES OF NUMERICAL METHODS FOR SOLVING ONE-POINT REACTOR KINETIC EQUATIONS. Koyama, Shigeo; Wakamatsu, Seiji. Denki Shikensho Iho; 34: 600-14(1970). (In Japanese).

A comparative examination is given into several numerical methods for solving one-point reactor kinetic equations, well-known as one of the most difficult problems to solve rapidly, stably, and precisely through numerical methods. Taylor series expansion of the kinetic equations is employed to clarify the convergency of several numerical methods. It is concluded that the numerical instability occurs mainly due to the truncation error which is inherently based on each method. Numerical examples suggest the length of the time interval "h" to be selected to perform stable and reasonably precise calculation as follows: $h \leq T_{min}$ in the 4th order Runge–Kutta method and the Runge–Kutta–Gill method; $h \leq 2T_{min}$ in the Runge–Kutta–Merson method and the 5th order Runge–Kutta method; where T_{min} is the minimum time constant of a set of kinetic equations. (auth)

10313 CALCULATION OF FLUX DISTRIBUTIONS IN REACTOR SUB-REGIONS WITH GENERALIZED MULTIPLE COLLISION PROBABILITIES. Mayer, L. (Kernforschungszentrum, Karlsruhe, Ger.). J. Nucl. Energy; 24: 337-58(Nov 1970).

The theory of multiple collision probabilities for one-dimensional problems was extended for handling thick zones and strongly anisotropic fluxes. This entailed the treatment of space dependent scattering sources and anisotropic fluxes at the boundaries of sub-zones. For plane geometry anisotropic scattering sources were included. A multigroup collision probability code STOWA based on the extended theory was written. It may be used in connection with diffusion calculations or independently and may perform cell calculations or determine flux distributions in special layers of a reactor, e.g., in the blanket or the shielding. Results are given and compared with other transport codes and measurements. Different approximations to angular scattering on hydrogen are evaluated with the code. (auth) (UK)

10314 MONTE CARLO INVESTIGATION OF TIME-DEPENDENT THERMAL NEUTRON BEHAVIOR IN SMALL, NONCRYSTALLINE MODERATORS. Conn, Robert (EURATOM-CCR, Ispra, Italy). J. Nucl. Energy; 24: 359-66(Nov 1970).

The time-dependent behavior of a burst of neutrons in small, noncrystalline moderators (H_2O and D_2O) is investigated using a simplified scattering kernel, the time-dependent Monte Carlo method, and the variance reducing technique of Expected Leakage Probability. Both the neutron density and the average energy, as functions of time, are presented with primary emphasis placed on systems having decay rates greater than the minimum collision frequency. A discussion is included of the connection between the results and certain predictions made based upon an approximate treatment of the spatial dependence. It is suggested that valuable information on the time-dependent behavior of a pulse in such small systems can be extracted from a measurement of either the average energy or average velocity as a function of time. Measurements of the neutron density alone can mask the actual behavior of the pulse. (auth) (UK)

10315 BEHAVIOR OF A NEUTRON PULSE IN THE VICINITY OF AN INELASTIC THRESHOLD. Beynon, T. D.; Coleman, M.; Mondal, M. A. W. (Univ. of Birmingham, Eng.). J. Nucl. Energy; 24: 367-83(Nov 1970).

A multigroup energy formalism is used to investigate the effect of inelastic scattering on neutron pulses in both infinite and finite moderators. Having established the accuracy of this technique in the case of purely elastic scattering by comparison with transport theory calculations, it is shown that the presence of inelastic scattering can produce anomalous behavior in the neutron slowing down times. In particular, over certain energies, the slowing down time can decrease with decreasing energy. Accompanying this is a marked spatial dependence of the slowing down time. (auth) (UK)

10316 APPROACH TO THE STABILITY CRITERION FOR A NUCLEAR REACTOR. Imasaki, Masahide; Sueoka, Yoshitaka (Kyushu Inst. of Tech., Kitakyushu City, Japan). Nucl. Sci. Eng.; 42: 415-28(Dec 1970).

The question of stability is very important in control-system

XUM

theory and practice. Therefore, many research workers have studied the stability of the space-time nuclear reactor kinetics by expansion functions or trial functions. Among these expansion functions, the natural mode has an excellent property of finality. The eigenvalues of the natural modes are closely related to the stability of the modes. Wiberg has shown the method to evaluate the eigenvalues and eigenfunctions of the natural mode. However, the complexity of the characteristic equation requires a very laborious calculation for its solution. In practical applications the exact location of the eigenvalue in the complex plane is not required and a determination of the half-plane in which they lie suffices. An alternate method that determines the stability without actually solving for the eigenvalues of the characteristic equation is proposed. (auth)

10317 NUCLEAR REACTOR THEORY. Bell, George I.; Glasstone, Samuel. New York; Van Nostrand Reinhold Company (1970). 635p. $24.50. (TID-25606).

The treatment of nuclear reactor theory based on neutron transport theory is presented under the following topics: neutron transport equation; one-speed transport theory; numerical methods for one-speed problems, simple P_N approximations; solution of transport equation by multigroup methods; discrete ordinates and discrete S_N methods; adjoint equation, perturbation theory, and variational methods; neutron thermalization; resonance absorption; reactor dynamics; and space-dependent reactor dynamics and related topics. (D.C.C.)

10318 DEVELOPMENT OF DESIGN PROCEDURES TO DETERMINE REACTOR PHYSICS CHARACTERISTICS OF HIGHLY ENRICHED HEAVY WATER MODERATED REACTORS. Kim, Yong Su. Washington, D. C.; Catholic Univ. of America (1970). 280p. University Microfilms Order No. 70-17,418.

Thesis.

Analytical procedures were formulated to determine the reactor physics characteristics of high-enriched heavy water moderated reactors. The method selected is similar to that which is used for the light water moderated reactors; namely, (1) generation of few group neutron cross sections, (2) calculation of reactivity and neutron flux distribution using a two dimensional neutron diffusion equation, and (3) synthesis of one and two dimensional results to obtain the three dimensional characteristics of a reactor. The method of analysis was applied to the National Bureau of Standards Reactor for a detailed analysis of its initial zero power core. The method gave a calculated initial criticality which is much closer to the measured value than the original design estimate. (Diss. Abstr. Int., B)

10319 EFFECT OF RANDOM FUEL ELEMENT DISPLACEMENT UPON NEUTRON REACTION RATES. Barrett, P. R. (Univ. of New South Wales, Sydney). Atomkernenergie; 16: 191-5(1970).

The effect of random displacements of fuel elements (induced by, for example, fuel element bowing owing to neutron irradiation) upon neutron fluxes and reaction rates in a lattice cell is examined for the case of an array of a large number of lattice cells in each of which the probability distribution for the fuel element displacement is the same. This is illustrated in the example of a single thermal neutron energy group with a slowing down source that is spatially uniform in the moderator and zero in the fuel, using the collision probability approach to transport theory in the flat flux approximation. It is shown that relatively small magnitude random displacements of the fuel elements can lead to significant variance to mean ratios in the neutron flux levels. (auth)

Dynamics

Refer also to abstracts 10091 and 10180.

Experimental Applications

10320 (AE-405) SPECTRAL PARAMETERS IN WATER-MODERATED LATTICES. A Survey of Experimental Data with the Aid of Two-Group Formulae. Sokolowski, E. K. (Aktiebolaget Atomenergi, Studsvik (Sweden)). Oct 1970. 23p. Dep. NTIS (U. S. Sales Only).

A set of analytical two-group formuls for the Westcott spectral indices $r\sqrt{T_n}$ and T_n is used as basis for comparison of a large number of experimental data on heavy- and light-water moderated lattices. The consistency of the data is generally found to be within the experimental errors. A comparison with multigroup transport calculations indicates that the latter over-estimate the epithermal spectrum component, which could in part explain the empirical need for reducing the ^{238}U resonance cross section in such calculations. 18 references. (auth) (Sweden)

10321 DETERMINATION OF THE RESERVE REACTIVITY BY THE DOUBLE OVER-COMPENSATION METHOD. Dideikin, T. S.; Shishin, B. P. At. Energ. (USSR); 29: 215-16(Aug 1970). (In Russian).

The supercritical character of a given reactor may be determined on the basis of reserve reactivity, as measured by the differential reactivity. A method was developed for carrying out such measurements in a subcritical reactor. The positive reactivity may be compensated by changing one of the parameters of the breeding medium while keeping the other parameters unchanged. Similarly, an originally supercritical system may be turned into a critical one by changing the other parameters. A simultaneous change of these two parameters renders the reactor subcritical. The relation between the sub and supercritical system may be expressed by an expansion of a Taylor series. An expression was derived to find the supercriticality of the system expressed as the reserve reactivity, on the basis of a subcritical reactivity measurement. The negative reactivity may be measured by the pulsed method, by noise analysis, or by any convenient technique. In order to verify the calculations, the reserve reactivity was experimentally measured on the basis of the differential reactivity by changing the water level in the reactor and by determining the supercriticality, using the pulse method which involved a double over-compensation technique by introducing supplementary absorber in the form of boric acid solution and reducing the height of the core in a uranium-water critical assembly with a $H : ^{235}U$ ratio of about 80. The experimental data agreed with the calculated values. (TTT)

10322 CALCULATION OF NEUTRON DETECTOR RESPONSE IN A SUBCRITICAL REACTOR. Waltz, W. R.; Walter, J. F. (Westinghouse Electric Corp., West Mifflin, Pa.). Nucl. Technol.; 10: 160-8(Feb 1971).

Comparisons of calculation and experiment were performed to test the adequacy of few group subcritical diffusion theory in predicting neutron detector response induced from material changes in a subcritical water moderated reactor. Comparisons show that diffusion theory may be used successfully; however, certain limitations of the model must be recognized and avoided. The breakdown of the calculational model in certain cases can be related ultimately to the inability of few-group diffusion theory to predict the absolute magnitude of detector flux for large distances through a water (or metal-water) shield. This inability can result in inaccuracies in predicted count rate response when applied to a specific source-core-detector arrangement with the characteristic that a given material change results in gross changes in the axial flux distribution. These effects can be overcome by the suitable locationing of the neutron source and detector relative to the subcritical assembly. (auth)

Reactor Components, Fuels, and Accessories

Refer also to abstracts 8371, 8392, 8401, 8413, 8454, 8828, 8836, 8848, 8857, 8896, 8899, 8909, 8915, 8919, 8921, 8925, 8941, 8952, 8953, and 10164.

10323 (EURFNR-774) DETERMINATION OF OPERATIONAL THERMAL CONDUCTIVITY OF CERAMIC NUCLEAR FUEL AND HEAT TRANSFER COEFFICIENT OF FUEL/CAN GAP BY BALANCED OSCILLATOR METHOD. Daenner, W. (Kernforschungszentrum, Karlsruhe (West Germany). Institut fuer Reaktorentwicklung). Translation of report KFK-1125. 191p. Dep. NTIS.

Work Performed under United States-Euratom Fast Reactor Exchange Program.

The Balanced Oscillator Method is described in respect to in-pile application for measuring the thermal conductivity of ceramic fuels and the gap conductance. It is based upon a comparison of the experimentally and analytically determined transfer function between sinusoidal oscillations in coolant flow and specimen power at constant coolant temperatures. The analytical solution of the transfer function is deduced from the instationary differential equation for heat conduction, taking into consideration radial variation of heat source, heat capacity of the canning and time dependence of heat transfer coefficient. The result of out-pile experiments using coal as specimens proves the feasibility of such experiments and the completeness of the assumptions set up for the analytical solution. (66 references) (auth)

10324 (EURFNR-755) RESULTS OF ERROR ANALYSIS FOR IN-PILE THERMAL CONDUCTIVITY MEASUREMENT USING THE BALANCED OSCILLATOR TECHNIQUES. Daenner, W. (Kernforschungszentrum, Karlsruhe (West Germany). In-

stitut fuer Reaktorentwicklung). Translation of report KFK-1140. 45p. Dep. NTIS.

Work Performed under United States-Euratom Fast Reactor Exchange Program.

With respect to the in-pile application of the balanced oscillator method for measuring the fuel thermal conductivity and the gap conductance, a detailed error analysis has been performed. Observing the postulated optimal test conditions the thermal conductivity could be obtained with a precision of about 15 to 20%, the gap conductance with about 20 to 40% during the entire burnup of the specimen. Necessary improvements of the test loop instrumentation and essential experiments are advised. Some experimental problems of running the measurements in the FR2 are discussed. 8 references. (auth)

10325 (ORNL-TM-3246) AN INVESTIGATION OF THE TIME-DEPENDENT BEHAVIOR OF PRESTRESSED CONCRETE PRESSURE VESSELS. Whitman, G. D.; Callahan, J. P.; Corum, J. M. (Oak Ridge National Lab., Tenn.). 10 Dec 1970. Contract W-7405-eng-26. 25p. (CONF-701007-2). Dep. NTIS.

From Meeting on Concretes Used in Nuclear Reactors, Berlin, Germany.

The effects of the thermal conditions imposed on a prestressed concrete pressure vessel (PCRV) present a major uncertainty in predicting long-term vessel behavior. In current vessel designs insulating and cooling are provided to limit concrete temperatures to 200°F (93°C) or less; however, the time-dependent behavior of the structures may be significantly affected by this relatively low temperature. A thermal cylinder model has been designed for the purpose of providing a structure which simulates a portion of the barrel of a cylindrical vessel. Provision is made for applying internal pressure and a temperature profile simulating the thermal conditions in an operating PCRV. All surfaces are sealed to prevent moisture loss and the model will be instrumented to measure stress, strain, moisture level and temperature at selected locations. Time-dependent predictions of the behavior of this structure using finite element methods of analysis in conjunction with concrete material properties obtained in complementary portions of an overall PCRV research and development program will provide a unique verification of the adequacy of such techniques. It is also planned to subject the specimen to off-design conditions at the end of the experimental life by producing hot spots and thus obtain information on the capability of the structure to endure prolonged accidental over-temperature loads. 6 references. (auth)

10326 (RT/FI-(70)7) MICROWAVE TECHNIQUE FOR MEASUREMENT OF HIGH TEMPERATURE AND NEUTRON FLUX IN NUCLEAR REACTORS. Rosatelli, C. (Comitato Nazionale Energia Nucleare, Rome (Italy)). 22 Jan 1970. 32p. (In Italian). Dep. NTIS (U.S. Sales Only).

A brief survey of the microwave technique application to the temperature and neutron flux measurements within nuclear reactors is given. Some results of a preliminary study carried out at the CNEN Computing Centre are illustrated. Further developments in the field of the instrumentation for nuclear reactors are suggested. 19 references. (auth)

10327 SITUATION DE L'APPROVISIONNEMENT EN COMBUSTIBLES NUCLEAIRES. (Situation Concerning the Supplying of Nuclear Fuels). Commission des Communautes Europeennes, Serie Energie, No. 3. Bruxelles; Office des Publications Officielles des Communautes Europeennes (1970). 39p. FF 16,70; FB 150,-; DM 10,90; Lire 1870; Fl. 11,-.

The actual situation on supplying nuclear fuels in the Community and future developments are discussed. Data on the situation are tabulated. The nuclear fuels discussed include: natural uranium; enriched uranium; plutonium; and thorium. Policies of supplying and the market for nuclear fuels in the principal western countries (U.S., Canada, Japan, South Africa, and United Kingdom) are also considered. (P.C.H.)

10328 MINING YEAR BOOK 1970. Transactions of the 73rd National Western Mining Conference and Exhibition, Denver, February 14, 1970. Denver; Colorado Mining Association (1970). 143p. $5.00. (CONF-700216).

The mining, milling, processing, prospecting, and marketing activities in the western United States during 1969 are reviewed. Three of the speeches concern uranium mining and utilization as nuclear reactor fuel. A separate abstract was prepared for each of these 3 speeches. (H.D.R.)

For abstracts of individual papers see: 8373, 8374, and 10214.

10329 LOADING MACHINE FOR FUEL ELEMENTS AND CONTROL RODS IN A NUCLEAR REACTOR. (to Siemens AG). French Patent 1,570,724. 5 May 1969. Filed 3 Apr 1968. (In French).

The main feature of the loading machine described for fuel elements and control rods in a water cooled reactor is double prehension which is mobile in the vertical sense and which can be operated separately. The interior contains a guiding mast, and the exterior contains a centering scuttle that can slide in a telescopic manner in the mast. (P.C.H.)

10330 IMPROVEMENTS IN THE PLUGGING OF DEFECTIVE TUBES IN TUBE BUNDLES. Boniface, Cyril Edward (to Foster Wheeler John Brown Boilers Ltd.). British Patent 1,210,212. 28 Oct 1970. Filed 28 Nov 1966.

Reference is made to the plugging of defective tubes in heat exchangers, condensers or other apparatus having a closely spaced bundle of tubes. A problem encountered in conventional techniques is that a plug may become loose and lead to a leakage and mixing of fluids, one of which may be radioactive. The method described comprises the insertion of a tightly fitting plug into each end of the defective tube, so as to block it off. The plug is circumferentially welded to the wall of the tube. The method has particular application to the plugging of small bore tubes. Various designs of plug are described. (UK)

10331 IMPROVED SYSTEM FOR THE LOADING AND UNLOADING OF FUEL ELEMENTS IN A NUCLEAR REACTOR. Angelo, S. (to SNAM Progetti SpA). French Patent 2,000,788. 24 Jan 1969. Priority date 26 Jan 1968, Italy. (In French).

The arrangement for the loading and unloading of fuel elements in a nuclear reactor consists of a combination of unique movable shaft connected to the means for controlling the control rod's motion and an apparatus for admission in place and removing of some integral fuel elements through the movable shaft. (P.C.H.)

10332 SPACING GRID FOR A NUCLEAR REACTOR FUEL ELEMENT. Demaison, Paul; Menissier, Pierre; Sionnet, Jean (to Societe Industrielle de Combustible Nucleaire SA). French Patent 1,571,496. 12 May 1969. Filed 6 May 1968. (In French).

Description is given of a spacing grid for nuclear reactor fuel elements that includes a rod cluster of fissile or fertile material placed in a case and supported by two rigid grids containing at the top a frame surrounded by several superposed helical tangential springs in the rods. The successive layers are directed alternately in two perpendicular directions and the spirals of the layers in the same direction are displaced in a half step. (P.C.H.)

10333 FUEL CARTRIDGE MADE OF TWO SEPARATE PARTS TO BE INTRODUCED FROM THE SEAT OF A REACTOR. Goran, Karl; Froman, Ernst; Johnsson, Erik Boerge (to Aktiebolaget Atomenergi). French Patent 1,566,809. 31 Mar 1969. Priority date 3 Apr 1967, Sweden. (In French).

Description is given of a fuel cartridge for a nuclear reactor capable of being engaged from the base of the reactor in a fuel channel comprising a part containing the fuel and a support part. The upper extremity of the support-part secures the part containing the fuel while the base of the support-part is itself supported by a stopping element closing the orifice in the bottom of the fuel channel. The part containing the fuel and the support is composed of two parts which are assembled separately. (P.C.H.)

10334 POROUS METAL HYDRIDE BODIES. (to Martin Marietta Corp.). British Patent 1,211,886. 11 Nov 1970. Priority date 15 Nov 1966, United States.

HYDRIDES—production process for porous metal
REACTOR MODERATORS—production process for porous metal hydride particles with capacity for controlled absorption and release of hydrogen (H.D.R.)

10335 THERMALLY INSULATING JACKET FOR A NUCLEAR REACTOR. Lepert, Claude; Sauvage, Michel (to Commissariat a l'Energie Atomique). French Patent 1,589,148. 23 Mar 1970. Filed 13 Sep 1968. (In French).

A thermally insulating jacket designed to avoid undesirable temperature increases in the fuel core assembly is described. This jacket must dissipate from the circuits the heat produced by the fission reaction, in the case of damage or even sudden breakdown in these circuits. The jacket consists of an assembly of laminated metallic layers whose apparent conductivity increases rapidly with temperature. It may be placed against the outside wall of the reactor tank or against the inside wall of the biological protection cavity encircling the tank; it is placed against only part of the tank wall. (auth) (France)

XUM

GENERAL

10336 (ACRH-1000-214) EFFECTS OF HYPERTROPHY AND HYPOXIA ON THE TURNOVER OF MYOCARDIAL COMPONENTS. Rabinowitz, Murray; Zak, Radovan; Aschenbrenner, Vaclav; Albin, R. (Chicago Univ., Ill. Argonne Cancer Research Hospital, Chicago, Ill.). [1970]. 28p. (CONF-700936-1). Dep. NTIS.
From Symposium on Cardiac Hypertrophy, Bratislava, Czechoslovakia.

10337 (AECOP-621) PROGRAM USER'S MANUAL CAPITAL BUDGETING PROBLEM. Halcomb, B. D. (Atomic Energy Commission Combined Operations Planning, Oak Ridge, Tenn.). 28 Aug 1970. Contract W-7405-eng-26. 30p. Dep. NTIS.

10338 (ANL-Trans-866) PINOCYTOSIS AND LOCOMOTION OF AMOEBAS. III. THE FUNCTION OF THE GOLGI APPARATUS OF AMOEBA PROTEUS AND CHAOS CHAOS. Stockem, W. Translated for Argonne National Lab., Ill., from Histochemie; 18: 217-40(1969). 29p. Dep. NTIS.

10339 (ANL-Trans-868) ION AND ELECTRON MOTION IN SOLID SILVER SULFIDE, SILVER SELENIDE, AND SILVER TELLURIDE. Valverde, Nilo. Translated for Argonne National Lab., Ill., from Z. Phys. Chem. (Frankfurt); 70: 128-38(1970). 11p. Dep. NTIS.

10340 (ANL/ES-1) EFFECTS OF THERMAL DISCHARGES ON THE MASS/ENERGY BALANCE OF LAKE MICHIGAN. Asbury, J. G. (Argonne National Lab., Ill.). Jul 1970. Contract W-31-109-eng-38. 24p. Dep. NTIS.

10341 (BDX-613-166) TRANSFER MOLDING CLOSE TOLERANCE PARTS. Hishaw, R. J. (Bendix Corp., Kansas City, Mo.). Nov 1970. Contract AT(29-1)-613. 18p. Dep. NTIS.

10342 (BDX-613-252) FILLED FOAM MANUFACTURING AND TESTING TECHNIQUES. Fender, J. R. (Bendix Corp., Kansas City, Mo.). Oct 1970. Contract AT(29-1)-613. 6p. Dep. NTIS.

10343 (BNL-15437) INTERNAL LOGIC MANUAL FOR THE PROGRAMMED COMMUNICATIONS CONTROLLED (PCC). Felberbaum, Joan (Brookhaven National Lab., Upton, N. Y.). [nd]. 115p. Dep. NTIS.

10344 (BNL-tr-386) ELECTRICAL RESISTANCE AND TRANSPARENCY OF FILMS OF Mg-Sb, Mg-Bi, AND Mg-Sn ALLOYS. Kurov, G. A. Translated by S. J. Amoretty (Brookhaven National Lab., Upton, N. Y.), from Dokl. Akad. Nauk SSSR; 94: 207-8(1954). 7p. Dep. NTIS.

10345 (BNL-tr-387) INVESTIGATION OF FILMS OF VARIABLE COMPOSITION OF THE Mg-Sb SYSTEM. Mochan, I. V. Translated by S. J. Amoretty (Brookhaven National Lab., Upton, N. Y.), from Dokl. Akad. Nauk SSSR; 98: 579-84(1954). 9p. Dep. NTIS.

10346 (BNL-tr-389) INVESTIGATION OF THE HEISENBERG MODEL OF THE IMPURE FERROMAGNETS. [PART] I. Provetski, E. (Joint Inst. for Nuclear Research, Dubna (USSR). Lab. of Theoretical Physics). Translated by S. J. Amoretty (Brookhaven National Lab., Upton, N. Y.), from Russian report. 17p. Dep. NTIS.

10347 (CALT-822-20) KONDO TEMPERATURE AND UNITARITY LIMIT IN NON-DILUTE MAGNETIC AMORPHOUS ALLOYS. Liang, V. K. C.; Tsuei, C. C. (California Inst. of Tech., Pasadena. W. M. Keck Lab. of Engineering Materials). Jan 1971. Contract AT(04-3)-822. 11p. Dep. NTIS.

10348 (CALT-822-21) RADIAL DISTRIBUTION FUNCTION OF AN AMORPHOUS Mn-P-C ALLOY. Sinha, Ashok K.; Duwez, Pol (California Inst. of Tech., Pasadena. W. M. Keck Lab. of Engineering Materials). Jan 1971. Contract AT(04-3)-822. 14p. Dep. NTIS.

10349 (CONF-700545-1) DYNAMIC MICROPLASTICITY OF B.C.C. METALS AND SOLID SOLUTIONS. Arsenault, R. J.; Crowe, C. R. (Maryland Univ., College Park. Engineering Materials Group); Carnahan, R. D. (Universal Oil Products Co., Des Plaines, Ill. Materials Science Lab.). May 1970. Contract AT(40-1)-3612. 47p. Dep. NTIS.
From 3rd International Symposium on Pure Materials in Science and Technology, Dresden, East Germany.

10350 (LA-4555) CONVERT: AN IBM-TO-CDC PROGRAM CONVERSION CODE. Hopkins, George C. (Los Alamos Scientific Lab., N. Mex.). Oct 1970. Contract W-7405-eng-36. 9p. Dep. NTIS.

10351 (LA-4556) STATISTICAL ASPECTS OF DECONVOLUTION. Hunt, B. R. (Los Alamos Scientific Lab., N. Mex.). Oct 1970. Contract W-7405-eng-36. 37p. Dep. NTIS.

10352 (LA-tr-70-26) ON THE QUESTION OF HIGH-PRESSURE SCALE. Vereshchagin, L. F.; Semerchan, A. A.; Kuzin, N. I.; Sadkov, Yu. A. Translated by Alois D. Cernicek (Los Alamos Scientific Lab., N. Mex.), from Dokl. Akad. Nauk SSSR; 191: 557-60(1970). 9p. Dep. NTIS.

10353 (ORNL-4605) SPECTRAN: A COMPUTER SYSTEM TO ANALYZE HIGH RESOLUTION SPECTRUM. VOLUME I. USER'S MANUAL. Joseph, A. F. (Oak Ridge National Lab., Tenn.). Jan 1971. Contract W-7405-eng-26. 20p. Dep. NTIS.

10354 (ORNL-4632) OAK RIDGE NATIONAL LABORATORY-NATIONAL SCIENCE FOUNDATION INTERDISCIPLINARY RESEARCH RELEVANT TO PROBLEMS OF OUR SOCIETY. PROGRESS REPORT OF SUMMER STUDY, 1970. (Oak Ridge National Lab., Tenn.). Dec 1970. Contract W-7405-eng-26. 128p. Dep. NTIS.

10355 (ORNL-4642) TOBACCO SMOKE ANALYSIS PROGRAM. Progress Report, January 1, 1970-September 1, 1970. Guerin, M. R.; Shults, W. D. (Oak Ridge National Lab., Tenn.). Jan 1971. Contract W-7405-eng-26. 207p. Dep. NTIS.

10356 (ORNL-TM-3175) FOREST MANAGEMENT PLAN, AEC OAK RIDGE RESERVATION: 1970-1975. Strock, W. G., Jr. (Oak Ridge National Lab., Tenn.). Dec 1970. Contract W-7405-eng-26. 28p. Dep. NTIS.

10357 (ORNL-tr-2314) STRUCTURAL STABILITY OF AUSTENITIC Cr-Ni STAINLESS STEELS TO DEFORMATION AND EXTREMELY LOW TEMPERATURE. Rousseau, D.; Blanc, G.; Tricot, R.; Gueussier, A. Translated by R. Gregg Mansfield (Oak Ridge National Lab., Tenn.), from Mem. Sci. Rev. Met.; 67: 315-34(1970). 44p. Dep. NTIS.

10358 (ORNL-tr-2392) ELEMENTARY MECHANISMS OF HETEROGENEOUS GAS-SOLID KINETICS. EFFECT OF THE PRESSURE OF THE GAS ON THESE KINETICS. Besson, Jean; Azzopardi, Max; Caillet, Marcel; Sarrazin, Pierre; Soustelle, Michel. Translated by R. Gregg Mansfield (Oak Ridge National Lab., Tenn.), from J. Chim. Phys.; 61: 1018-22(1964). 10p. Dep. NTIS.

10359 (ORNL-tr-2411) RECENT DEVELOPMENTS AT KUWAIT IN THE CONTROL OF SCALE AT ELEVATED TEMPERATURE. Khalaf, K. A.; Watson, B. M. Translated by R. Gregg Mansfield (Oak Ridge National Lab., Tenn.), from pp 147-51 of 3rd International Symposium on Fresh Water from Sea, Vol. 4, Dubrovnik, Yugoslavia, September 13-17, 1970. 4p. (CONF-700926-3). Dep. NTIS.

10360 (ORNL-tr-2412) CORROSION TESTS ON VARIOUS MATERIALS IN SEAWATER UP TO 150°C. Boisde, G.; Coriou, H.; Grall, L.; Mahieu, C.; Mahut, R.; Pelras, M. (Commissariat a l'Energie Atomique, Fontenay-aux-Roses (France). Centre d'Etudes Nucleaires). Translated by R. Gregg Mansfield (Oak Ridge National Lab., Tenn.), from pp 570-90 of 3rd International Symposium on Fresh Water from the Sea, Vol. 1, Dubrovnik, Yugoslavia, September 13-17, 1970. 13p. (CONF-700926-2). Dep. NTIS.

10361 (ORNL-tr-2413) ALUMINUM ALLOYS IN SEAWATER DESALINATION INSTALLATIONS. Vargel, C.; Pelletier, M. Translated by R. Gregg Mansfield (Oak Ridge National Lab., Tenn.), from pp 501-15 of 3rd International Symposium on Fresh Water from the Sea, Vol. 1, Dubrovnik, Yugoslavia, September 13-17, 1970. 16p. (CONF-700926-4). Dep. NTIS.

10362 (ORNL-tr-2418) NEUROTROPIC CARCINOGENIC EFFECT OF PHENYL-DIMETHYL TRIAZENE ON RATS. Druckrey, H.; Ivankovic, S.; Preussmann, R. Translated by R. Gregg Mansfield (Oak Ridge National Lab., Tenn.), from Naturwissenschaften; 54: 171(1967). 3p. Dep. NTIS.

10363 (ORO-1637-21) THE ORIGIN AND FATE OF THIOCYANATE ION IN METABOLISM. Summary Progress Report,

XUM

May 1954–October 1970. Wood, John L. (Tennessee Univ., Memphis. Dept. of Biochemistry) Contract AT(40-1)-1637. 15p. Dep. NTIS.

10364 (ORO-3628-11) MECHANISMS OF INNATE IMMUNITY. IV. BIOLOGICAL PROPERTIES OF POLYMORPHONUCLEAR LEUKOCYTE CYTOPLASMIC GRANULES AND THEIR COMPONENTS. Progress Report, December 1, 1969–November 30, 1970. Spitznagel, John K. (North Carolina Univ., Chapel Hill). Contract AT(40-1)-3628. 11p. Dep. NTIS.

10365 (ORO-3895-9) ENTROPY OSCILLATION AND THE H THEOREM FOR FINITE SEGMENTS OF INFINITE COUPLED-HARMONIC-OSCILLATOR CHAINS. Robertson, Harry S.; Huerta, Manuel A. (Miami Univ., Coral Gables, Fla. Dept. of Physics). Nov 1969. 15p. (MIAPH-TP–69-23). Dep. NTIS.

10366 (RLO-2225-T-19-9) MACROMOLECULE SYNTHESIS AND WALL EXTENSIBILITY IN RELATION TO THE MECHANISM OF AUXIN-INDUCED CELL ELONGATION. Cleland, Robert; Thompson, William F.; Haughton, Peter M.; Rayle, David L. (Washington Univ., Seattle. Dept. of Botany). [1970]. 20p. Dep. NTIS.

10367 (RLO-2227-T-5-1) PROPERTIES OF ENZYMES FROM THERMOMORPHS AND HALOPHILES. Progress Report (Three Year), April 1, 1968–December 15, 1970. Becker, R. R. (Oregon State Univ., Corvallis. Dept. of Biochemistry and Biophysics). Contract AT(45-1)-2059. 14p. Dep. NTIS.

10368 (RLO-2227-T-5-2) PROPERTIES OF ENZYMES FROM THERMOMORPHS AND HALOPHILES. Progress Report, December 1969–December 1970. Becker, R. R. (Oregon State Univ., Corvallis. Dept. of Biochemistry and Biophysics). Contract AT(45-1)-2059. 11p. Dep. NTIS.

10369 (RLO-2227-T-5-4) THE EFFECT OF UNIVALENT CATIONS ON THE CIRCULAR DICHROISM OF PYRUVATE KINASE. Wildes, R. A.; Evans, H. J.; Becker, R. R. (Oregon State Univ., Corvallis. Dept. of Biochemistry and Biophysics). [1970]. 12p. Dep. NTIS.

10370 (SC-CR-69-3266) DEVELOPMENT AND ANALYSIS OF TECHNIQUES FOR CALIBRATION OF KERR CELL PULSE-VOLTAGE MEASURING SYSTEMS. [PART] III. Cassidy, Esther C.; Cones, H. N. (National Bureau of Standards, Washington, D. C.). Aug 1969. 97p. Dep. NTIS.
For Sandia Labs., Albuquerque, N. Mex.

10371 (SC-CR-70-6092) ANALYSIS OF DSB/FM TELEMETRY SYSTEM ERRORS. Uglow, Kenneth M. Dec 1970. Contract 72-8647. 112p. Dep. NTIS.
For Sandia Labs., Albuquerque, N. Mex.

10372 (SC-CR-70-6152) INTERIM REPORT: RESPONSE OF A MULTICONDUCTOR CABLE TO EXCITATION AT AN OPEN BREAK IN THE SHIELD. (Frankel (Sidney) and Associates, Menlo Park, Calif.). Nov 1970. Contract DO-AF(29-601)-64-4457. 35p. Dep. NTIS.
For Sandia Labs., Albuquerque, N. Mex.

10373 (SC-DR-70-698) PULSED SOLID-STATE SOURCES FOR MICROWAVE APPLICATION. Wilson, W. E. (Sandia Labs., Albuquerque, N. Mex.). Oct 1970. 52p. Dep. NTIS.

10374 (SC-M-70-684) AN INTRODUCTION TO AM FREQUENCY DIVISION MULTIPLEX TELEMETRY SYSTEMS. Johnson, C. S. (Sandia Labs., Albuquerque, N. Mex.). Dec 1970. 102p. Dep. NTIS.

10375 (SC-RR-70-544) REALIZATION OF NEAR-TIME-OPTIMAL FEEDBACK CONTROLLERS. Veneruso, Anthony F. (Sandia Labs., Albuquerque, N. Mex.). Nov 1970. 173p. Dep. NTIS.

10376 (SC-RR-70-775) PRECISELY CONTROLLED, LOW RANGE HUMIDITY SYSTEM. Garst, Daniel M.; Lindell, Kermit F. (Sandia Labs., Albuquerque, N. Mex.). Nov 1970. 20p. Dep. NTIS.

10377 (SC-T-70-4048) EFFECT OF COMPONENT TOLERANCES ON THE TRANSFER CHARACTERISTICS IN THE FREQUENCY RANGE. Mildenberger, Otto. Translated for Sandia Labs., Albuquerque, N. Mex.), from NTZ-Nachrtech. Z.; 23: 85-92(1970). 26p. Dep. NTIS.

10378 (SC-T-70-4052) FLUORESCENCE OF TETRACYANOPLATINATES. Khvostikov, J. A. Translated for Sandia Labs., Albuquerque, N. Mex., from Phys. Z. Sowjetunion; 9: 210-36(1936). 32p. Dep. NTIS.

10379 (SC-T-71-3000) INVESTIGATION OF THE SPECTRA OF STOCHASTIC OPERATORS ARISING IN LATTICE MODELS OF A GAS. Minlos, R. A.; Sinay, Ya. G. Translated by Fredric D. Killebrew (Sandia Labs., Albuquerque, N. Mex.), from Teor. Mat. Fiz.; 2: No. 2, 230-43(1970). 24p. Dep. NTIS.

10380 (SCL-DR-70-108) SPECTRE: A FINITE DIFFERENCE COMPUTER PROGRAM FOR CALCULATING THE DYNAMIC RESPONSE OF A CYLINDRICAL SHELL. Birnbaum, M. R.; Cupps, F. J.; Emery, A. F. (Sandia Labs., Livermore, Calif.). Dec 1970. Contract AT(29-1)-789. 186p. Dep. NTIS.

10381 (SCL-DR-70-130) MODEL 50-600-75 MANGANIN PULSE POWER SUPPLY. Williams, E. O. (Sandia Labs., Livermore, Calif.). Dec 1970. 32p. Dep. NTIS.

10382 (STAN-CS-70-158(App.5)) PARALLEL PROCESSING WITH THE PERFECT SHUFFLE. Stone, Harold S. (Stanford Univ., Calif. Dept. of Computer Science). Mar 1970. Contract AT(04-3)-326. 36p. Dep. NTIS.

10383 (STAN-CS-70-165(App.2)) SCHEDULING OF N TASKS WITH M OPERATIONS ON TWO PROCESSORS. Bauer, Henry; Stone, Harold (Stanford Univ., Calif. Dept. of Computer Science). Jul 1970. Contract AT(04-3)-326. 34p. Dep. NTIS.

10384 (TID-25609) ONE SWEEP NUMERICAL METHOD FOR VECTOR-MATRIX DIFFERENCE EQUATIONS WITH TWO-POINT BOUNDARY CONDITIONS. Technical Report No. 70-16. Angel, E.; Kalaba, R. (University of Southern California, Los Angeles. Dept. of Electrical Engineering). Apr 1970. Contract AT(11-1)-113. 16p. Dep. NTIS.

10385 (TID-25612) FUNCTIONAL EQUATIONS IN THE THEORY OF DYNAMIC PROGRAMMING. XVIII. MINIMUM CONVOLUTIONS AND GREEN'S FUNCTIONS. Bellman, Richard (University of Southern California, Los Angeles). Jan 1970. Contract AT(21-1)-113. 4p. Dep. NTIS.

10386 (TID-25613) ON A GENERALIZATION OF CONTINUED FRACTIONS AND THE ESTIMATION OF SOME INTEGRALS. Technical Report No. 69-26. Bellmann, Richard (University of Southern California, Los Angeles). Nov 1969. Contract AT(11-1)-113. 5p. Dep. NTIS.

10387 (TID-25614) TRUNCATION AND PRESERVATION OF MOMENT PROPERTIES FOR FOKKER–PLANCK MOMENT EQUATIONS. Technical Report No. 69-25. Wilcox, Ralph M.; Bellman, Richard (University of Southern California, Los Angeles). Nov 1969. Contract AT(11-1)-113. 14p. Dep. NTIS.

10388 (TID-25615) FUNCTIONAL EQUATIONS IN THE THEORY OF DYNAMIC PROGRAMMING. XVII. POLICIES DEPENDENT ON CRITICAL STATE VARIABLES. Technical Report No. 69-29. Bellman, Richard (University of Southern California, Los Angeles). Dec 1969. Contract AT(11-1)-113. 5p. Dep. NTIS.

10389 (TID-25616) DIFFERENTIAL QUADRATURE AND LONG-TERM INTEGRATION. Technical Report No. 70-9. Bellman, Richard (University of Southern California, Los Angeles); Casti, John (RAND Corp., Santa Monica, Calif.). Jan 1970. Contract AT(11-1)-113. 5p. Dep. NTIS.

10390 (TID-25617) USE OF SPLINES WITH UNKNOWN END POINTS IN THE IDENTIFICATION OF SYSTEMS. Technical Report No. 70-6. Bellman, Richard (University of Southern California, Los Angeles. Dept. of Electrical Engineering); Roth, Robert S. (Avco Corp., Wilmington, Mass. Avco Systems Div.). Jan 1970. Contract AT(11-1)-113. 11p. Dep. NTIS.

10391 (TID-25618) THE RESPONSE OF THE SAVANNAH RIVER GUYED STACK UNDER WIND AND EARTHQUAKE ACTION. Davenport, A. G.; Vickery, B. J. (University of Western Ontario, London). Jun 1968. 144p. (BLWT-5-68). Dep. NTIS.
For Du Pont de Nemours (E. I.) and Co., Aiken, S. C., Savannah River Lab.

10392 (TID-25619) ANNUAL PROGRESS REPORT [ON HYPOTHALAMUS CONTROL OF ANTERIOR PITUITARY GLAND FUNCTION], MARCH 1, 1970–FEBRUARY 28, 1971. (Pennsylvania State Univ., University Park). Contract AT(30-1)-3827. 26p. Dep. NTIS.

10393 (TID-25620) ON ADDITION CHAINS. Technical Report No. 70-8. Kato, Hatsuhiko (University of Southern California, Los Angeles. Dept. of Electrical Engineering). Jan 1970. Contract AT(11-1)-113. 67p. Dep. NTIS.

10394 (TID-25622) MICRO-COMPUTER MODEL FOR THE DEFINITION AND EXECUTION OF COMPLEX INFORMATION

XUM

PROCESSING SYSTEMS. Lesser, V. R. (Stanford Univ., Calif. Dept. of Computer Science). May 1969. 50p. Dep. NTIS.

10395 (TID-25623) A VARIABLE CONTROL STRUCTURE MICRO-COMPUTER ARCHITECTURE OR EMULATION VIA AN INSTANTIATION LANGUAGE. Lesser, Victor R. (Stanford Univ., Calif. Dept. of Computer Science). Jul 1970. Contract AT(04-3)-326. 65p. Dep. NTIS.

10396 (TID-25624) APPROXIMATION TECHNIQUES IN DISCRETE DYNAMIC PROGRAMMING. PART I. FOUNDATIONS. Technical Report No. 69-21. Lew, Art (University of Southern California, Los Angeles. Dept. of Electrical Engineering). Oct 1969. Contract AT(11-1)-113. 28p. Dep. NTIS.

10397 (TID-25625) APPROXIMATION TECHNIQUES IN DISCRETE DYNAMIC PROGRAMMING. PART II. REDUCTION OF DIMENSIONALITY. Technical Report No. 69-24. Lew, Art (University of Southern California, Los Angeles. Dept. of Electrical Engineering). Nov 1969. Contract AT(11-1)-113. 21p. Dep. NTIS.

10398 (TID-25627) BOUNDS FOR APPROXIMATE SOLUTIONS TO THE OPERATOR DIFFERENTIAL EQUATION $Y(t) = M(t)Y(t)$; APPLICATIONS TO MAGNUS EXPANSION AND TO $u + [1 + f(t)]u = 0$. Technical Report No. 70-15. Wilcox, Ralph (University of Southern California, Los Angeles. Dept of Electrical Engineering). Mar 1970. Contract AT(11-1)-113. 32p. Dep. NTIS.

10399 (UCB-34-P-186-X-1) THE RECOVERY AND ANALYSIS OF MUTANTS CONTROLLING DEVELOPMENT IN DROSOPHILA MELANOGASTER. Progress Report [for] Period Ending August 31, 1970. (California Univ., Berkeley. Dept. of Genetics). Contract AT(04-3)-34. 8p. Dep. NTIS.

10400 (UCLA-12-788) STUDIES ON RNA AND HISTONE RELATIONSHIPS DURING THE SYNCHRONIZED TETRAHYMENA LIFE CYCLE. Lee, Young C.; Byfield, John E. (California Univ., Los Angeles. Lab. of Nuclear Medicine and Radiation Biology). [1970]. Contract AT-04-1-GEN-12. 28p. Dep. CFSTI.

10401 (UCLA-12-801) USE OF CIRCULAR DICHROISM TO STUDY THE INTERACTIONS OF CARBOXYPEPTIDASE A (ANSON) AND $A_{\alpha+\beta}$ WITH SUBSTRATES AND INHIBITORS. Fretto, Larry; Strickland, E. Hardin (California Univ., Los Angeles. Lab. of Nuclear Medicine and Radiation Biology). [1970]. Contract AT(04-1)-Gen-12. 36p. Dep. NTIS.

10402 (UCLA-12-802) EFFECT OF TEMPERATURE UPON THE CONFORMATIONS OF CARBOXYPEPTIDASE A (ANSON), A_{γ}^{Leu}, A_{γ}^{Val}, AND $A_{\alpha+\beta}$. Fretto, Larry; Strickland, E. Hardin (California Univ., Los Angeles. Lab. of Nuclear Medicine and Radiation Biology). [1970]. Contract AT(04-1)-Gen-12. 41p. Dep. NTIS.

10403 (UCRL-19615) TRANSFER PROCESSES IN ECM. Landolt, D.; Muller, R. H.; Tobias, C. W. (California Univ., Berkeley. Lawrence Radiation Lab.). Oct 1970. Contract W-7405-eng-48. 28p. (CONF-701016-2). Dep. NTIS.
From Symposium on Fundamental Aspects of Electrochemical Machining, Atlantic City, N. J.

10404 (UCRL-19618) PERIODIC PHENOMENA IN COPPER DISSOLUTION AT CONSTANT CURRENT. Cooper, J.; Muller, R. H.; Tobias, C. W. (California Univ., Berkeley. Lawrence Radiation Lab.). Oct 1970. Contract W-7405-eng-48. 17p. (CONF-701016-1). Dep. NTIS.
From Symposium on Fundamental Aspects of Electrochemical Machining, Atlantic City, N. J.

10405 (UCRL-20139) ELECTRON DIFFRACTION TECHNIQUE FOR THE DETERMINATION OF CRYSTALLINE STRUCTURE OF β GLYCINE. Quon, Wai-Kit (California Univ., Berkeley. Lawrence Radiation Lab.). Oct 1970. Contract W-7405-eng-48. 147p. Dep. NTIS.
Thesis.

10406 (UCRL-20358) NONLINEAR OPTICAL EFFECTS. Shen, Y. R. (California Univ., Berkeley. Lawrence Radiation Lab.). Oct 1970. Contract W-7405-eng-48. 30p. (CONF-701026-1). Dep. NTIS.
From Conference of the Physics of Opto-Electronic Materials, General Motors Research Symposium, Warren, Mich.

10407 (UCRL-72390) EXPERIMENTAL RESULTS ON PHASE-LOCKED LOOPS WITH ADDED NONLINEARITIES. Cleland, L. L. (California Univ., Livermore. Lawrence Radiation Lab.). 4 May 1970. 5p. (CONF-701024-1). Dep. NTIS.
From UMR-Mervin J. Kelly Communications Conference, St. Louis, Mo.

10408 (UCRL-72648) CYCLE-ALLOCATION DISCIPLINES FOR MULTIACCESS MEMORY SYSTEMS. Hill, J. Carver (California Univ., Livermore. Lawrence Radiation Lab.). 20 Nov 1970. 5p. (CONF-710101-1). Dep. NTIS.
From International Conference on Systems, Networks, and Computers, Oaxtepec, Mexico.

10409 (UCRL-72770) SHOCK WAVES. II. TRANSPORT AND OTHER PROPERTIES. Keeler, R. N. (California Univ., Livermore. Lawrence Radiation Lab.). 5 Nov 1970. 12p. Dep. NTIS.

10410 (UCRL-Trans-1414) ELECTRON DIFFRACTION PATTERNS OF Pb-Bi ALLOYS AT VERY LOW TEMPERATURES. Baier, Peter. Translated for Univ. of California Lawrence Radiation Lab., Berkeley, from Z. Phys.; 213: 89-100(1968). 22p. Dep. NTIS.

10411 (UCRL-Trans-1424) EFFECT OF TRAINING NERVOUS PROCESSES ON THE WEIGHT OF THE BRAIN AND THE CHOLINESTERASE ACTIVITY. Obraztsova, G. A.; Pigareva, Z. D.; Fedorov, V. K. Translated by Marie Kassatkin (Univ. of California Lawrence Radiation Lab., Berkeley), from Dokl. Akad. Nauk SSSR; 186: 1349-51(1969). 7p. Dep. NTIS.

10412 (UCRL-Trans-1427) SPECTRA OF THE PHOTOCONDUCTIVITY OF GREEN LEAVES AND CHLOROPLASTS AT A FREQUENCY OF 10^{10} CYCLES PER SECOND. Blyumenfel'd, L. A.; Kafalieva, D. I.; Livshits, V. A.; Solov'ev, I. S.; Chetverikov, A. G. Translated by Marie Kassatkin (Univ. of California, Lawrence Radiation Lab., Livermore), from Dokl. Akad. Nauk SSSR; 193: 700-2(1970). 6p. Dep. NTIS.

10413 (UCRL-Trans-1428) ISOELECTRIC SEPARATION IN PROTEIN CHEMISTRY REVIEW. Reis, H. E.; Wetter, O. Translated for Univ., of California, Lawrence Radiation Lab., Berkeley, from Klin. Wochensch.; 48: 643-50(1970). 10p. Dep. NTIS.

10414 (UCRL-Trans-1429) ELECTROPHORESIS IN A CARRIER-FREE BUFFER STREAM. I. CONTINUOUS SEPARATIONS IN AMPHOLYTE GRADIENTS. Seiler, Nikolaus; Thobe, Josef; Werner, Gottfried. Translated for Univ. of California, Lawrence Radiation Lab., Berkeley, from Z. Physiol. Chem.; 351: 865-8(1970). 5p. Dep. NTIS.

10415 (UCRL-Trans-1431) CHARACTERISTICS AND USES OF HEXAGONAL FERRITES. Winkler, G. Translated for Univ. of California, Lawrence Radiation Lab., Berkeley, from Z. Angew. Phys.; 21: 282-6(1966). 7p. Dep. NTIS.

10416 (UCRL-Trans-10504) VOLCANIC CYCLES AND METALLOGENY OF NOVAYA ZEMLYA. Mutafi, N. N. Translated by A. Mincer for Univ. of California, Lawrence Radiation Lab., Livermore, from Probl. Sov. Geol.; 17: No. 3, 210-25(1937). 40p. Dep. NTIS.

10417 (USCEE-344) NOTE ON THE ASYMPTOTIC BEHAVIOR OF SOLUTION OF NONLINEAR DIFFERENTIAL EQUATIONS. Bellman, Richard (University of Southern California, Los Angeles). Apr 1969. (Contract AT(11-1)-113. 4p. Dep. NTIS.

10418 (USCEE-350) REDUCTION OF DIMENSIONALITY BY APPROXIMATION TECHNIQUES: DIFFUSION PROCESSES. I. Lew, Art (University of Southern California, Los Angeles. Dept. of Electrical Engineering). Apr 1969. Contract AT-(11-1)-113. 18p. Dep. NTIS.

10419 (USCEE-377) REDUCTION OF DIMENSIONALITY IN DYNAMIC PROGRAMMING VIA THE METHOD OF DIAGONAL DECOMPOSITION. Collins, David C. (University of Southern California, Los Angeles. Dept. of Electrical Engineering). Aug 1969. Contract AT(11-1)-113. 15p. Dep. NTIS.

10420 L'EVOLUZIONE DELLA PROPULSIONE SPAZIALE NEGLI ANNI '70. X CONVEGNO INTERNAZIONALE TECNICO-SCIENTIFICO SULLO SPAZIO, ROMA, 9-11 MARZO 1970. (Evolution of Space Vehicle Propulsion in the 1970's. 10th International Technical-Scientific Meeting on Space, Rome, March 9-11, 1970). Roma; XVII Rassegna Internazionale Elettronica Nucleare e Teleradiocinematografica (1970). 528p. (In several languages). (CONF-700318).
This proceeding contains thirty-nine papers, nine abstracts, and one title (only). Separate abstracts were prepared for two papers pertaining to plasma propulsion. (L.M.T.)

For abstracts of individual papers see: 9438 and 9439.

CORPORATE AUTHOR INDEX

In the Corporate Author Index, technical report literature is indexed by the organization or institution responsible for issuing the report. Entries are given for all report literature and for published literature for which a corporate author approach is especially desirable, e.g., symposium and conference proceedings.

Each entry under a corporate author gives the publication title and the *NSA* volume and abstract numbers. Report numbers, where applicable, are given in parentheses at the end of the entry.

A

AGBABIAN-JACOBSEN ASSOCIATES, LOS ANGELES, CALIF.
Interaction between soil and nuclear reactor foundations during earthquakes, 25:10245 (ORO-3822-5)
AIR FORCE MATERIALS LAB., WRIGHT-PATTERSON AFB, OHIO.
Thermodynamics of vanadium alloys. I, 25:8862 (AD-709957)
AKADEMIYA NAUK SSSR, MOSCOW. INSTITUT ATOMNOI ENERGII.
Effect of delayed neutrons on the dynamic reactivity of a reactor originating during oscillations of the density of the fuel, 25:10305 (IAE-1955)
AKADEMIYA NAUK SSSR, MOSCOW. INSTITUT FIZIKI.
Possibility of measuring directed fluxes in a plasma contained in a toroidal magnetic trap, 25:9410 (CTO-736)
AKADEMIYA NAUK SSSR, NOVOSIBIRSK. INSTITUT MATEMATIKI.
High-energy scattering of charged particles and bethe formula, 25:9704 (NP-18540)
AKADEMIYA NAUK UKRAINSKOI SSR, KHARKOV. FIZIKO-TEKHNICHESKII INSTITUT.
Determination of the critical current in a section with radial slots in the iris disk, 25:9907 (KFK-tr-335)
AKADEMIYA NAUK UKRAINSKOI SSR, KIEV. INSTITUT TEORETICHESKOI FIZIKI.
Asymptotic properties of electron--proton scattering amplitude and sum rules for Schwinger term, 25:9701 (ITF-70-73)
Definition of quasi-averages, 25:9733 (ITF-70-52)
Definition of quasi-averages, 25:9687 (ITF-70-58-P)
Dual resonances models. I, 25:9887 (ITF-70-43)
Equal-time computator, sum rules and ward identities in axiomatic quantum field theory, 25:9837 (ITF-70-57)
Generalized Veneziano model, 25:9888 (ITF-70-78)
Knockout of nucleons from light nuclei under the inelastic scattering of high-energy electrons, 25:9973 (ITF-70-42)
Obtaining the limiting relations for correlation averages, 25:9734 (ITF-70-53)
Quasi-elastic knockout of nucleons from light nuclei by high energy electrons, 25:10058 (ITF-70-38)
AKTIEBOLAGET ATOMENERGI, STUDSVIK (SWEDEN).
Correlation for burnout predictions in vertical rod bundles, 25:8408 (CONF-660675-1)
Spectral parameters in water-moderated lattices, 25:10320 (AE-405)
ALBERT EINSTEIN MEDICAL CENTER, PHILADELPHIA, PA.
Prog. rpt. on effects of ionizing radiation on germinal epithelium of human testes, 1970, 25:8789 (NYO-4034-2)
ALLIS-CHALMERS MFG. CO., BETHESDA, MD. ATOMIC ENERGY DIV.
La Crosse Boiling Water Reactor. Nuclear instrumentation automatic gain control system, Addendum No. 2, 25:10135 (DOCKET-1155-87)
AMES LAB., IOWA.
Measurements of π^-p elastic scattering from 1.71 to 5.53 GeV/c, 25:9652 (COO-1764-112)
ANDERSON (M. D.) HOSPITAL AND TUMOR INST., HOUSTON, TEX.
Prog. rpt. on radiation and biophysical studies on viruses and cells, 10/16/69--10/15/70, 25:8605 (ORO-2832-85)
APPLICAZIONI E RICERCHE SCIENTIFICHE, MILAN (ITALY).
CONDOR 3: two-dimensional reactor lifetime program with local and spectrum dependent depletion, 25:10304 (EUR-4539)
APPLIED NUCLEAR CO., LA JOLLA, CALIF.
Chemistry of the Gasbuggy chimney, 25:8384 (PNE-G-68)
ARGONNE CANCER RESEARCH HOSPITAL, CHICAGO, ILL.
Effects of hypertrophy and hypoxia on the turnover of myocardial components, 25:10336 (ACRH-1000-214)
ARGONNE NATIONAL LAB., ILL.
1000-MWe LMFBR accident analysis and safety system design study: fault trees and malfunction catalog, 25:10237 (BAW-1344)
Catalog of rod-drop and transfer-function data from EBR-II runs 25 through 30A. EBR-II Project, 25:10173 (ANL-7542)
Cesium-137 in various Chicago foods (collection month, July 1970), 25:8659 (HASL-237, pp III.14-17)
Effects of thermal discharges on mass/energy balance of Lake Michigan, 25:10340 (ANL-ES-1)
Engineering development of fluid-bed fluoride volatility processes. Part 16. A safety manual for the engineering-scale alpha facility, 25:8446 (ANL-7672)
Guidelines for sodium fire prevention, detection, and control: report of the Ad Hoc Committee on sodium fires, 25:8827 (ANL-7691)
Measurement of the up-down asymmetries in the beta decay of polarized lambdas, 25:9626 (COO-1545-87)
Physics Division summary report, 1--3/1970, 25:10015 (ANL-7699)
Prog. rpt. on physics, 10--12/69, 25:9971 (ANL-7698)
Prog. rpt. on reactor development, 11/70, 25:10164 (ANL-7758)
Study of the response of the EBR-II plant protective system to hypothetical malfunctions in the reactor system. EBR-II Project, 25:10228 (ANL-7665)
Vibration of a beam with motion-constraint stops, 25:10163 (ANL-7619)
ARMY ENGINEER WATERWAYS EXPERIMENT STATION, VICKSBURG, MISS.
Grouting and materials control, Operation Flint Lock, 25:8962 (POR-4013)
ATLANTIC RICHFIELD HANFORD CO., RICHLAND, WASH.
Pyrochemical process for the reduction of plutonium dioxide to metal, 25:8236 (ARH-SA-72)
ATOMIC BOMB CASUALTY COMMISSION, HIROSHIMA (JAPAN).
Bibliography of published papers of the Atomic Bomb Casualty Commission, 25:8741 (ABCC-TR-G-69)
ATOMIC BOMB CASUALTY COMMISSION, NAGASAKI (JAPAN).
Bibliography of published papers of the Atomic Bomb Casualty Commission, 25:8741 (ABCC-TR-G-69)
ATOMIC ENERGY COMMISSION, BAGHDAD (IRAQ). NUCLEAR RESEARCH INST.
Determination of uranium content in geological samples by neutron activation, 25:8219 (PH-3)
Measurement of reaction $^{35}Cl(n,\gamma)^{36}Cl$ using a three-crystal pair and anti-Compton spectrometer, 25:10000 (PH-2)
Versatile and modular data acquisition system useful in nuclear experiments, 25:8483 (PH-1)
ATOMIC ENERGY COMMISSION COMBINED OPERATIONS PLANNING, OAK RIDGE, TENN.
Program user's manual capital budgeting problem, 25:10337 (AECOP-621)
ATOMIC ENERGY ESTABLISHMENT, WINFRITH (ENGLAND).
Correlation between effective diffusion coefficient and porous structure in nuclear graphite, 25:8924 (DP-Report-437)
Kinetics of carbon deposition reactions in high temperature gas cooled reactors, 25:10195 (DP-Report-500)
Thermal neutron diffusion data and WIMS scattering models for light water, 25:10301 (AEEW-R-701)
ATOMIC ENERGY OF CANADA LTD., CHALK RIVER (ONTARIO). CHALK RIVER NUCLEAR LABS.
Choice of bath materials for the inert gas fusion method for the determination of oxygen in metals, 25:8194 (AECL-3743)
Fitting of an ordered set of mode frequencies, 25:9902 (AECL-3669)
FORGAD: one dimensional few group finite difference reactor code, 25:10300 (AECL-3671(Add.1))
Prog. rpt. on biology and health physics, 4--6/70, 25:8666 (AECL-3728)
Prog. rpt. on physics, 4--6/70, 25:9970 (AECL-3668)
Use of ^{41}Ar to study dispersion of effluent from stacks, 25:8363 (AECL-3731)
ATOMIC ENERGY RESEARCH ESTABLISHMENT, HARWELL (ENGLAND).
Chemical determination of N in nitrides of B, Ti, Zr, Cr, Mo, Nb, Ta, and V, 25:8195 (AERE-R-6491)

Description of computer program ICON for calculation of fission product inventories, 25:10236 (AERE-R-6242)
First British radioactive isotope powered thermoelectric generators, 25:8421 (AERE-M-1594)
High temperature furnace for compatibility studies, 25:8389 (AERE-M-1990)
Homogenizing structures and mechanical properties of welding Zircaloy 2 tubes, 25:8844 (AERE-M-1561)
Metallographic examination of sodium, 25:8845 (AERE-R-5483)
Photon activation analysis using electron linear accelerator at Harwell, 25:8216 (AERE-R-5363)
Preliminary corrosion tests on some steam treated zirconium alloys, 25:8833 (AERE-M-1854)
Processing in limited geometry. XVI, 25:8445 (AERE-R-5104)
Radioactive fallout in air and rain, 25:8364 (AERE-R-6556)
Simultaneous reaction, diffusion and bulk flow in tubular specimens of graphite. V, 25:8906 (AERE-R-4857)
Sodium purification and general handling facility, 25:8390 (AERE-R-5502)

AUSTRALIAN ATOMIC ENERGY COMMISSION RESEARCH ESTABLISHMENT, LUCAS HEIGHTS.
Heavy water production, 25:8315 (AAEC/TM-562)
On-line computer system for a mass spectrometer, 25:8571 (AAEC/TM-568)
Reactor HIFAR: safety rod circuits, 25:10252 (AAEC/M-9)
Reactor HIFAR: safety rod system, 25:10253 (AAEC/M-32)

AUSTRALIAN NATIONAL UNIV., CANBERRA. DEPT. OF NUCLEAR PHYSICS.
Angular correlation studies of the $^{42}Ca(\alpha,p\gamma)^{45}Sc$ reaction, 25:9996 (ANU-P-466)
Search for the 3446 keV level in ^{29}P via the $^{28}Si(p,\gamma)$ reaction, 25:10016 (ANU-P-503)
Systematic search for the lowest T = 2 state of ^{12}C using deuteron and ^{3}He induced reactions, 25:9972 (ANU-P-496)

AVCO CORP., WILMINGTON, MASS. AVCO SYSTEMS DIV.
Use of splines with unknown end points in the identification of systems, 25:10390 (TID-25617)

B

BABCOCK AND WILCOX CO., LYNCHBURG, VA. NUCLEAR POWER GENERATION DEPT.
1000-MWe LMFBR accident analysis and safety system design study: fault trees and malfunction catalog, 25:10237 (BAW-1344)

BALTIMORE GAS AND ELECTRIC CO., MD.
Calvert Cliffs Nuclear Power Plant, Units 1 and 2. Preliminary safety analysis report, Amendment 11 (includes final safety analysis report, Vol. 3), 25:10156 (DOCKET-50317-23)
Calvert Cliffs Nuclear Power Plant, Units 1 and 2. Preliminary safety analysis report, Amendment 11 (includes final safety analysis report, Vol. 1), 25:10154 (DOCKET-50317-21)
Calvert Cliffs Nuclear Power Plant, Units 1 and 2. Preliminary safety analysis report, Amendment 11 (includes final safety analysis report, Vol. 2), 25:10155 (DOCKET-50317-22)

BATTELLE MEMORIAL INST., COLUMBUS, OHIO.
Development of mechanical-property design data for reactor materials, 25:8864 (BMI-1891, Sect.A)
Prog. rpt. on applicability of existing data to analytical description of reactor accident, 7--9/70, 25:10238 (BMI-1890)
Prog. rpt. on LMFBR cladding, structural and component materials, 7--9/70, 25:8863 (BMI-1891)
Stesses in out-of-round pipe due to internal pressure, 25:8871 (ORNL-TM-3244)
Studies of the effects of irradiation on cladding and structural alloys, 25:8895 (BMI-1891, Sect.B)

BATTELLE-NORTHWEST, RICHLAND, WASH. PACIFIC NORTHWEST LAB.
Absolute cross sections, differential in energy and angle, for ejection of electrons from xenon by fast protons, 25:9191 (BNWL-SA-3631)
Anuglar and energy distributions of electrons from hydrogen ion breakup, 25:9190 (BNWL-SA-3498)
Counter for the direct measurement of ^{55}Fe in blood and other liquid samples, 25:8466 (BNWL-SA-3624)
Development and results of an electrically heated seven-pin bundle assembly for thermal hydraulic testing in liquid metals, 25:10207 (BNWL-SA-3286)
Effect of continuous spray operation on the removal of aerosols and gases in the containment systems experiment, 25:10256 (BNWL-1485)
Electron distributions from hydrogen for 0.6, 1.0 and 1.5 MeV hydrogen ions, 25:9189 (BNWL-SA-3482)
Evaluation of hydroxylamine nitrate monitoring systems, 25:8199 (BNWL-CC-2502)
Eventual whole body exposure rate from ^{85}Kr released to the atmosphere, 25:8667 (BNWL-SA-3233)
Factors affecting the optimum fuel cycle, 25:10233 (BNWL-SA-3605)
Integrated LMFBR aqueous fuel reprocessing concepts, 25:8316 (BNWL-CC-1939)
Materials for nuclear reactors, 25:8828 (BNWL-SA-3426)
Mathematical simulation of groundwater transport of radionuclides at Hanford, 25:8345 (BNWL-SA-3494)
Nuclear plants and the environmental ''crisis'', 25:10132 (BNWL-SA-3564)
Reasons for differences in calculated estimates of the cloud dose, 25:8668 (BNWL-SA-3424)
Solid state x-ray-alpha coincidence counter, 25:8465 (BNWL-SA-1514)
Studies of inhaled radon daughters, uranium ore dust, diesel exhaust, and cigarette smoke in dogs and hamsters, 25:8623 (BNWL-SA-3419)
Technical bases for FFTF driver fuel instrumentation, 25:10255 (BNWL-916)
Thermal pollution and its treatment, 25:10133 (BNWL-SA-3581)
Total quality control concept for material balance measurements, 25:8448 (BNWL-SA-3336)

BENDIX CORP., KANSAS CITY, MO.
Filled foam manufacturing and testing techniques, 25:10342 (BDX-613-252)
Transfer molding close tolerance parts, 25:10341 (BDX-613-166)

BETTIS ATOMIC POWER LAB., PITTSBURGH, PA.
Effect of cladding ovality and diametral creep on fuel rod support systems (LWBR development program), 25:10167 (WAPD-TM-714)
Prog. rpt. on PWR project, 10/25/69--1/23/70, 25:10129 (WAPD-MRP-131)

BHABHA ATOMIC RESEARCH CENTRE, BOMBAY (INDIA).
Determination of the reactor power response to a sinusoidal reactivity input by use of idempotent matrices, 25:10302 (BARC-502)
In-line analytical methods for fuel reprocessing streams. I, 25:8197 (BARC-510)
Neutron generator for calibration of fast neutron detectors, 25:9940 (BARC-499)
Prog. rpt. on nuclear physics, annual, 1969--70, 25:10017 (BARC-501)
Sintering of UO_2: relation between electrical conductivity and microstructure of sintered UO_2, 25:8908 (BARC-507)
Spectrographic determination of Ru in silicious materials used in radioactive waste disposal, 25:8196 (BARC-504)

BONN UNIV. (WEST GERMANY). INSTITUT FUER STRAHLEN UND KERNPHYSIK.
Multiwire spark and/or proportional chambers for the Bonn split-pole magnetic spectrograph, 25:8478 (JUL-CONF-4, pp 141-7)

BRANDEIS UNIV., WALTHAM, MASS. DEPT. OF PHYSICS.
Classical Schwinger terms, 25:9834 (RLO-1388-584)

BROOKHAVEN NATIONAL LAB., UPTON, N. Y.
Capture cross section of ^{237}Np and ^{241}Am in different reactor spectra, 25:10019 (BNL-50242)
Combined hydroelectric pumped storage and nuclear power generation, 25:10109 (BNL-50238)
Determination of Ag, Cd, In, Sn, and Sb in Na solubility studies, 25:8198 (BNL-50271)
Internal logic manual for programmed communications controlled (PCC), 25:10343 (BNL-15437)
Remarks on the ΔI absolute value = $^1/_2$ rule in non-leptonic weak decays and use of phenomenological Lagrangian, 25:9732 (BNL-50260)
Ribbon effect in a superconducting septum magnet, 25:9903 (BNL-15368)
Two-phase pressure drop for potassium with and without net vaporization, 25:8405 (BNL-13957)

BUREAU OF RADIOLOGICAL HEALTH, WINCHESTER, MASS. NORTHEASTERN RADIOLOGICAL HEALTH LAB.
Calibration and initial field testing of ^{85}Kr detectors for environmental monitoring, 25:8467 (BRH/NERHL-70-4)

C

CALIFORNIA INST. OF TECH., PASADENA. W. M. KECK LAB. OF ENGINEERING MATERIALS.
Kondo temperature and unitarity limit in non-dilute magnetic amorphous alloys, 25:10347 (CALT-822-20)
Radial distribution function of an amorphous Mn--P--C alloy, 25:10348 (CALT-822-21)

CALIFORNIA UNIV., BERKELEY.
Prog. rpt. on effects of radiation on brain activity and development, 1961--1970, 25:8758 (UCB-34-P-82-10)

CALIFORNIA UNIV., BERKELEY. DEPT. OF GENETICS.
Prog. rpt. on recovery and analysis of mutants controlling development in D. melanogaster, 8/31/70, 25:10399 (UCB-34-P-186-X-1)

CALIFORNIA UNIV., BERKELEY. LAWRENCE RADIATION LAB.
Computer based laboratory-wide data acquisition, analysis, and retrieval system, 25:8193 (UCRL-20132)
Electron diffraction technique for the determination of crystalline structure of beta glycine, 25:10405 (UCRL-20139)
Finding events in a sea of bubbles, 25:8548 (UCRL-20126)
Neutron flux distribution resulting from fission source located at center of sphere of sodium, 25:9944 (ORNL-TM-3156)
Nonlinear optical effects, 25:10406 (UCRL-20358)
Periodic phenomena in copper dissolution at constant current, 25:10404 (UCRL-19618)
Status of the ERA research at Berkeley, 25:9917 (UCRL-20125)
Study of Σ (1915) resonance in reaction $K^-p \to \Lambda \pi^0$,

XUM

25:9659 (UCRL-19789)
Thin lens optics with space charge, 25:9916 (UCRL-19313)
Transfer processes in ECM, 25:10403 (UCRL-19615)
CALIFORNIA UNIV., LIVERMORE. LAWRENCE RADIATION LAB.
Anharmonic lattice dynamical properties of solid neon, argon, krypton, and xenon, 25:8262 (UCRL-50903)
Computer code for the analysis of digitized seismic signals, 25:8382 (UCRL-50939)
Cycle-allocation disciplines for multiaccess memory systems, 25:10408 (UCRL-72648)
Digital data acquisition system for displacement measurement, 25:8397 (UCRL-72509)
Experimental results on phase-locked loops with added nonlinearities, 25:10407 (UCRL-72390)
Formulation of self-consistent 2- and 2 $^{1}/_{2}$-dimensional electromagnetic and relativistic simulations, 25:9458 (UCRL-72613)
Noise suppression techniques in macroparticle models of collisionless plasmas, 25:9457 (UCRL-72604)
Nonphysical modifications to oscillations, fluctuations, and collisions due to space--time differencing, 25:9459 (UCRL-72635)
Preamplifier noise effects on spectrometer energy resolution, 25:8532 (UCRL-72481)
Shock waves. II, 25:10409 (UCRL-72770)
Transient flow in a gas reservoir stimulated by a nuclear explosion: Project Gasbuggy, 25:8387 (UCRL-71868)
Water waves produced by cratering explosions in shallow water, 25:8386 (UCRL-50940)
CALIFORNIA UNIV., LOS ANGELES.
Measurement of form factors for decay K/sub L/^{0} + $\pi\mu\nu$, 25:9629 (UCLA-1054)
Study of decay mode K/sub L/^{0} + $\pi^{+}\pi^{-}\pi^{0}$, 25:9628 (UCLA-1052)
CALIFORNIA UNIV., LOS ANGELES. LAB. OF NUCLEAR MEDICINE AND RADIATION BIOLOGY.
Effect of temperature upon conformations of carboxypeptidase A, A/sub γ//sup Leu/, A/sub γ//sup Val/, and A/sub $\alpha+\beta$/, 25:10402 (UCLA-12-802)
Effects of coronary arterial injection of radioalbumin macroaggregates on coronary hemodynamics and myocardial function, 25:8713 (UCLA-12-798)
Studies on RNA and histone relationships during the synchronized Tetrahymena life cycle, 25:10400 (UCLA-12-788)
Use of circular dichroism to study interactions of carbosypeptidase A (Anson) and A/sub $\alpha+\beta$/ with substrates and inhibitors, 25:10401 (UCLA-12-801)
CAMBRIDGE ELECTRON ACCELERATOR, MASS.
Simple threshold and delay circuit for multi-wire proportional chambers, 25:8468 (CEAL-1054)
CAROLINA POWER AND LIGHT CO., RALEIGH, N.C.
H. B. Robinson Unit No. 2. Stuck rod control cluster assembly, 25:10123 (DOCKET-50261-49)
CEKMECE NUCLEAR RESEARCH CENTER, ISTANBUL (TURKEY).
Uptake of ^{203}Hg by Tapes decussatus L, 25:8625 (NP-18429)
CENTRAL ELECTRICITY GENERATING BOARD, BERKELEY (ENGLAND). BERKELEY NUCLEAR LABS.
Method of superposition of temperature distributions in forced convection heat transfer experiments, 25:8409 (RD/B/N-1755)
CENTRE DE RECHERCHES EN PHYSIQUE DES PLASMAS, LAUSANNE (SWITZERLAND).
Short wavelength instabilities in confinement of collision dominated plasma by rotating magnetic field, 25:9487 (LRP-42/70)
Theory of dynamic stabilization of Rayleigh--Taylor instability, 25:9488 (LRP-45/70)
CENTRE D'ETUDE DE L'ENERGIE NUCLEAIRE, BRUSSELS (BELGIUM).
Fabrication of Ge(Li) detectors, 25:8463 (BLG-447)
CENTRO INFORMAZIONI STUDI ESPERIENZE, MILAN (ITALY).
Sources of radiation and energy release in a thermal reactor, 25:10165 (CISE-R-233)
CHICAGO UNIV., ILL.
Effects of hypertrophy and hypoxia on the turnover of myocardial components, 25:10336 (ACRH-1000-214)
Measurement of the up-down asymmetries in the beta decay of polarized lambdas, 25:9626 (COO-1545-87)
CINCINNATI UNIV., OHIO.
Thermodynamics of vanadium alloys. I, 25:8862 (AD-709957)
COLOGNE UNIV. (WEST GERMANY). INSTITUT FUER KERNPHYSIK.
Position-sensitive proportional counter for measurement of β spectra, 25:8472 (JUL-CONF-4, pp 22-9)
COLORADO STATE UNIV., FORT COLLINS. DEPT. OF RADIOLOGY AND RADIATION BIOLOGY.
Polonium-210 in soils and plants, 25:8593 (COO-1733-11)
COLORADO UNIV., BOULDER. DEPT. OF CHEMISTRY.
Fractionation and analysis of gamma irradiated lysozyme, 25:8604 (COO-690-41)
COLUMBIA UNIV., NEW YORK.
History of weak interactions, 25:9735 (NYO-1932(2)-186)
Remarks on the Δ I absolute value = $^{1}/_{2}$ rule in non-leptonic weak decays and use of phenomenological Lagrangian, 25:9732 (BNL-50260)
COLUMBIA UNIV., NEW YORK. DEPT. OF CHEMISTRY.
Effect of chemical exchange between D_2 and HBr on thermal diffusion separation of D and H in a trennschaukel, 25:8422 (CU-755-7, Sect.5)
Exchange equilibria between methylacetylene-d and water by mass spectrometry, 25:8241 (CU-755-7, Sect.3)
Hold-up of amines and amine carbamates on column packings, 25:8320 (CU-755-7, Sect.6)
Preparation of ^{13}C by chemical exchange between amine carbamates and carbon dioxide, 25:8318 (CU-755-7, Sect.2)
Prog. rpt. on separation of isotopes, annual, 9/70, 25:8317 (CU-755-7)
Separation of isotopic isomers of NO by low-temperature gas chromatography, 25:8319 (CU-755-7, Sect.4)
COLUMBIA UNIV., NEW YORK. RADIOLOGICAL RESEARCH LAB.
Biophysics, 25:8756 (NYO-2740-7, pp 164-217)
Prog. rpt., 7/70, 25:8676 (NYO-2740-7)
Radiobiology, 25:8757 (NYO-2740-7, pp 218-56)
Radiological physics: I. Dosimetry, 25:8677 (NYO-2740-7, pp 5-51)
Radiological physics: II. Measurements of microscopic distribution of radiation energy, 25:8563 (NYO-2740-7, pp 52-110)
Radiological physics: III. Ancillary problems, 25:8482 (NYO-2740-7, pp 112-53)
COLUMBIA UNIV., PALISADES, N. Y. LAMONT-DOHERTY GEOLOGICAL OBSERVATORY.
Closed basin lakes as a tool in geochemistry. II, 25:8348 (CU-2493-11, App.2)
Closed basin lakes as a tool in geochemistry. III, 25:8349 (CU-2493-11, App.3)
Geochemical studies on Cranberry and Sterling Lakes, 25:8350 (CU-2493-11, App.4)
Mixing and gas exchange rates in Experimental Lakes Area, Western Ontario, 25:8352 (CU-2493-11, App.6)
Prog. rpt. on geochemical studies on continental waters, annual, 10/70, 25:8346 (CU-2493-11)
Project Ross, 25:8351 (CU-2493-11, App.5)
Tritium in Crater Lake, Oregon, 25:8347 (CU-2493-11, App.1)
COMITATO NAZIONALE PER L'ENERGIA NUCLEARE, FRASCATI (ITALY). LABORATORI NAZIONALI DI FRASCATI.
Hamiltonian that implies the exclusion principle, 25:9689 (LNF-70/22)
Study of some problems of cavity resonators by means of finite differences, 25:9909 (LNF-70/17)
COMITATO NAZIONALE PER L'ENERGIA NUCLEARE, ROME (ITALY).
Microwave technique for measurement of high temperature and neutron flux in nuclear reactors, 25:10326 (RT/FI-(70)7)
COMMISSARIAT A L'ENERGIE ATOMIQUE, CADARACHE (FRANCE). CENTRE D'ETUDES NUCLEAIRES.
Safety report for the ''Scarabee'' loop, 25:10254 (ANL-Trans-865)
Two control schemes with dynamic constraints on a multivariable nonlinear system, 25:10185 (CEA-R-3988)
COMMISSARIAT A L'ENERGIE ATOMIQUE, FONTENAY-AUX-ROSES (FRANCE). CENTRE D'ETUDES NUCLEAIRES.
Characteristics of ordinary concrete relative to radioprotection calculation, 25:8960 (CEA-N-1355)
Clearance of radioisotopes from lungs of rats, 25:8591 (CEA-CONF-1677)
Comparative performances of Monte Carlo and discrete ordinate one dimensional transport codes in an iron bulk shield calculation, 25:9536 (CEA-CONF-1669)
Corrosion tests on various materials in seawater up to 150°C, 25:10360 (ORNL-tr-2412)
Details concerning the use of ELF program, 25:9941 (CEA-N-1361)
Diffusion coefficients of Ni--U system, 25:8865 (CEA-R-4066)
Experimental research on the treatment of contamination by transplutonium elements, 25:8590 (CEA-CONF-1658)
Oxidation of uranium carbides in gaseous environments, 25:8907 (CEA-Bib-183)
Three-dimensional Monte-Carlo calculation (TRIPOLI code) of neutron spectra in lower shield of Phenix, 25:10193 (CEA-N-1359)
Validity of SABINE code in calculations on shielding of heavy and light water reactors, 25:10192 (CEA-N-1354)
COMMISSARIAT A L'ENERGIE ATOMIQUE, GRENOBLE (FRANCE). CENTRE D'ETUDES NUCLEAIRES.
Electron irradiation of Fe and Ni, 25:9541 (CEA-CONF-1680)
Heat exchange for two-phase flow in horizontal and vertical tubes, 25:8406 (CEA-CONF-1649)
Observation at very low temperatures of the annealing process in specimens with radiation defects, 25:9542 (CEA-CONF-1681)
Statistical interpretation of uncertainty coefficients in thermal calculations for nuclear reactors, 25:10194 (CEA-R-3895)
COMMISSARIAT A L'ENERGIE ATOMIQUE, LA HAGUE (FRANCE).
Accidental release of ^{131}I at UP 2 plant on October 2nd and 3rd 1968, 25:8657 (CEA-R-4008)
COMMISSARIAT A L'ENERGIE ATOMIQUE, LIMEIL-BREVANNES (FRANCE). CENTRE D'ETUDES.
Spectroscopic measurement of the electron temperature of a plasma in the vacuum uv, 25:9407 (CEA-N-1391)
COMMISSARIAT A L'ENERGIE ATOMIQUE, SACLAY (FRANCE). CENTRE D'ETUDES NUCLEAIRES.
Critical examination of ^{240}Pu neutron cross sections, 25:10021 (CEA-N-1273)
Hybrid solution of the space--time problems in power reactors, 25:10303 (CEA-CONF-1684)
Information Bulletin on Isotopic Generators, 25:8425

(NP-18563)
Measurement and analysis of holmium total cross section for neutrons at energies between 0.005 and 1.7 keV, 25:10022 (CEA-N-1338)
Radioactive characteristics necessary for studying fission products: beta radiation and conversion electrons, 25:10023 (CEA-N-1372)

COMMONWEALTH EDISON CO., CHICAGO, ILL.
Dresden Nuclear Power Station, Unit 1. Minimizing radioactive off-gas release rate, 25:10136 (DOCKET-50010-75)
Dresden Nuclear Power Station, Unit 2. Failure of standby diesel generator to start following a manual initiation signal, 25:10120 (DOCKET-50237-125)
Dresden Nuclear Power Station, Unit 2. Proposal to use fuel containing gadolinia, 25:10145 (DOCKET-50237-123)
Dresden Nuclear Power Station, Unit 2. Spent radwaste demineralizer, 25:10119 (DOCKET-50237-124)

CONNECTICUT YANKEE ATOMIC POWER CO., HADDAM.
Connecticut Yankee Nuclear Power Plant, Unit No. 1. Reference plant design report. Includes Appendixes A and B, 25:10142 (DOCKET-50213-91)

CONNECTICUT YANKEE ATOMIC POWER CO., HARTFORD.
Connecticut Yankee Atomic Power Plant. Ultrasonic inspection main coolant pump flywheels (keyways), 25:10141 (DOCKET-50213-90)

CONSUMERS POWER CO., JACKSON, MICH.
Big Rock Point Nuclear Plant. License No. DPR-6; proposed technical specifications Change No. 24, 25:10139 (DOCKET-50155-57)
Big Rock Point Nuclear Plant. License No. DPR-6; proposed technical specifications Change No. 23, 25:10138 (DOCKET-50155-56)

CORNELL UNIV., ITHACA, N. Y.
Interphase boundary waves in the intermediate state of lead, 25:9363 (NYO-2150-64)

D

DAIRYLAND POWER COOPERATIVE, LA CROSSE, WIS.
La Crosse Boiling Water Reactor. Monthly operating report, September 1970, 25:10110 (DOCKET-1155-86)
La Crosse Boiling Water Reactor. Monthly operating report, October 1970, 25:10111 (DOCKET-1155-88)

DANISH ATOMIC ENERGY COMMISSION, RISOE. RESEARCH ESTABLISHMENT.
Properties of He: density, specific heats, viscosity, and thermal conductivity at pressures from 1 to 100 bar and from room temperature to about 1800 K, 25:8261 (RISO-224)

DARTMOUTH COLL., HANOVER, N.H. DEPT. OF PHYSICS.
Hydromagnetic wave--particle beam interactions, 25:9455 (AD-705265)

DEUTSCHES ELEKTRONEN-SYNCHROTRON, HAMBURG (WEST GERMANY).
Consequences of assumption that S-matrix commutes with axial charge, 25:9886 (DESY-70/57)
Discontinuous phase oscillations in particle accelerators, 25:9915 (SLAC-Trans-124)
Empirical test of tensor meson dominance, 25:9764 (DESY-70/58)
New vacuum trajectory for pion--nucleon scattering, 25:9785 (DESY-70/55)
Storing tracks in streamer chambers, 25:8543 (DESY-70/60)

DIVISION OF REACTOR DEVELOPMENT AND TECHNOLOGY (AEC), WASHINGTON, D. C.
Potential nuclear power growth patterns, 25:10095 (WASH-1098)

DIVISION OF REACTOR LICENSING (AEC), WASHINGTON, D. C.
Connecticut Yankee Atomic Power Plant. License No. DPR-14; technical specifications Change No. 16, 25:10140 (DOCKET-50213-88)
Dresden Nuclear Power Station, Unit 3. Detailed statement on the environmental considerations, 25:10146 (DOCKET-50249-52)
Oconee Nuclear Station, Unit 1. Safety evaluation, 25:10150 (DOCKET-50269-32)
Oyster Creek Nuclear Power Plant, Unit No. 1. Provisional Operating License DPR-16. Technical specifications Change No. 2, 25:10144 (DOCKET-50219-119)
Saxton Reactor. License No. DPR-4; technical specifications Change No. 40, 25:10137 (DOCKET-50146-67)

DIVISION OF TECHNICAL INFORMATION EXTENSION (AEC), OAK RIDGE, TENN.
CINDA 69: index to literature on microscopic neutron data, 25:9946 (TID-25165(Suppl.2))
Engineering materials list, 25:8396 (TID-4100(Suppl.61))

DOW CHEMICAL CO., GOLDEN, COLO. ROCKY FLATS DIV.
Explosive nature of uranium-base niobium alloys after immersion in nitric acid, 25:8840 (RFP-1575)

DU PONT DE NEMOURS (E.I.) AND CO., AIKEN, S. C. SAVANNAH RIVER LAB.
Deuteration in slow neutron radiography of biological media, 25:8709 (DP-1229)
Response of Savannah River guyed stack under wind and earthquake action, 25:10391 (TID-25618)

DUKE POWER CO., CHARLOTTE, N.C.
Oconee Nuclear Station, Unit 1. Notice of proposed issuance of facility operating license, 25:10148 (DOCKET-50269-30)
Oconee Nuclear Station, Units 1, 2, and 3. Preliminary safety analysis report, Amendment 25, 25:10149 (DOCKET-50269-31)

E

EIDGENOESSISCHE TECHNISCHE HOCHSCHULE, ZURICH (SWITZERLAND).
Helicon resonances in low-pressure plasmas, 25:9512 (NP-18554)

EL PASO NATURAL GAS CO., FARMINGTON, N.MEX.
Petrographic analysis, Gasbuggy No. 1 and Gasbuggy No. 3, 25:8385 (PNE-G-69)

ELECTRICITY COUNCIL RESEARCH CENTRE, CAPENHURST (ENGLAND).
New technique for measuring temperature of LTE plasmas, 25:9411 (ECRC/N-288)

ENEA NEUTRON DATA COMPILATION CENTRE, GIF-SUR-YVETTE (FRANCE).
CINDA 69: index to literature on microscopic neutron data, 25:9946 (TID-25165(Suppl.2))

ENGINEERING PHYSICS CO., ROCKVILLE, MD.
Hydro shock experiment, 25:8383 (AD-706767)

ENTE NAZIONALE PER L'ENERGIA ELETTRICA, ROME (ITALY).
Garigliano Nuclear Power Station operations report, 6/70, 25:10126 (TID-25608)

EUROPEAN ATOMIC ENERGY COMMUNITY.
CONDOR 3: two-dimensional reactor lifetime program with local and spectrum dependent depletion, 25:10304 (EUR-4539)
Crushing behaviour of pyrocarbon coated fuel particles, 25:8925 (EUR-4501)
Design and construction of a programmer for an electron beam welding machine, 25:8391 (EUR-4537)

EUROPEAN ATOMIC ENERGY COMMUNITY, ISPRA (ITALY). JOINT NUCLEAR RESEARCH CENTER.
Design and construction of a programmer for an electron beam welding machine, 25:8391 (EUR-4537)
Protection service, site survey and meteorology section quarterly report, 25:8370 (HASL-237, pp III.18-23)

EUROPEAN ATOMIC ENERGY COMMUNITY, PETTEN (NETHERLANDS). JOINT NUCLEAR RESEARCH CENTER.
Crushing behaviour of pyrocarbon coated fuel particles, 25:6925 (EUR-4501)

EUROPEAN COMMUNITIES, LUXEMBOURG. COMMISSION.
Radioactive contamination of foodstuffs in countries of the Community in 1968, 25:8624 (EUR-4509)

EUROPEAN NUCLEAR ENERGY AGENCY, PARIS (FRANCE).
Information Bulletin on Isotopic Generators, 25:8425 (NP-18563)
Prog. rpt. on activities, annual, 11/70, 25:10092 (NP-18600)

EUROPEAN ORGANIZATION FOR NUCLEAR RESEARCH, GENEVA (SWITZERLAND).
Approach to a rem dosimeter using ionization chambers, 25:8562 (CERN/DI/HP-29)
Effects of magnetic field perturbations of synchrotron on closed orbit and betatron oscillations, 25:9904 (CERN-70-24)
Instrument for measuring rate of change of RF frequency in particle accelerators, 25:9905 (CERN-70-28)

F

FLORIDA POWER AND LIGHT CO.
Turkey Point Plant, Unit 3. Containment dome report, 25:10147 (DOCKET-50250-37)

FORSVARETS FORSKNINGSANSTALT, STOCKHOLM (SWEDEN).
Theoretical particle emission spectra in fusion reactions, 25:9504 (FOA-4-4438)

FRANKEL (SIDNEY) AND ASSOCIATES, MENLO PARK, CALIF.
Response of multiconductor cable to excitation at open break in shield, 25:10372 (SC-CR-70-6152)

G

GENERAL ELECTRIC CO., PLEASANTON, CALIF. NUCLEONICS LAB.
Prog. rpt. on thermodynamic data program involving plutonia and uranias at high temperatures, 5--7/70, 25:8926 (GEAP-12133)

GENERAL ELECTRIC CO., SAN JOSE, CALIF. ATOMIC POWER EQUIPMENT DEPT.
Nuclear system manufacture and construction progress, 25:10088 (CONF-690967-1)
Status of pipe rupture study at General Electric Company. III, 25:8866 (GEAP-10205)

GENERAL ELECTRIC CO., SAN JOSE, CALIF. REACTOR FUELS AND REPROCESSING DEPT.
Prog. rpt. on Zircaloy--clad UO_2 fuel rod evaluation program, 5--7/70, 25:8951 (GEAP-10217)

GENERAL ELECTRIC CO., SUNNYVALE, CALIF. ADVANCED PRODUCTS OPERATION.
Conceptual design of backup reactor system for Fast Flux Test Facility, 25:10260 (GEAP-5552)
Final Fast Flux Test Facility backup design development requirement report, 25:10265 (GEAP-5715)
Prog. rpt. on Fast Flux Test Facility Backup Design

Project, 12/67--2/68, 25:10262 (GEAP-5641)
Prog. rpt. on Fast Flux Test Facility Backup Design Project, 9-11/67, 25:10261 (GEAP-5614)
Prog. rpt. on Fast Flux Test Facility Backup Design Project, 6--8/68, 25:10264 (GEAP-5684)
Prog. rpt. on Fast Flux Test Facility Backup Design Project, 3--5/68, 25:10263 (GEAP-5650)
Prog. rpt. on Fast Flux Test Facility Backup Design Project, 5--8/67, 25:10259 (GEAP-5550)

GENERAL ELECTRIC CO., SUNNYVALE, CALIF. BREEDER REACTOR DEVELOPMENT OPERATION.
FFTF backup design interface definition discussion of system requirements, 25:10266 (GEAP-5721)
Southwest Experimental Fast Oxide Reactor. License No. DR-15; technical specifications Proposed Change No. 4, Rev. 2, 25:10240 (DOCKET-50231-63)
Southwest Experimental Fast Oxide Reactor. Malfunction of an emergency electrical system circuit breaker, 25:10234 (DOCKET-50231-62)
Southwest Experimental Fast Oxide Reactor. Quarterly plant operations report No. 6, August 1--October 31, 1970, 25:10235 (DOCKET-50231-64)
Southwest Experimental Fast Oxide Reactor. Restrictions on the use of special fuel rods, 25:10239 (DOCKET-50231-61)
The FREADM-1 code: a fast reactor excursion and accident dynamics model, 25:10241 (GEAP-13608)
Transient overpower irradiation of axially-restrained, zero-burnup, fast reactor fuel specimens, 25:10208 (GEAP-13562)

GEOLOGICAL SURVEY, DENVER, COLO.
Bibliography of published reports by U. S. Geological Survey personnel on the geology and hydrology of the Nevada Test Site, 1957--1969, 25:8355 (USGS-474-88)
Lithologic log of Pahute Mesa exploratory drill hole No. 1, Nevada Test Site, 25:8357 (USGS-474-96)
U20e post shot fractures, Jorum event, 25:8356 (USGS-474-92)

GEORGIA INST. OF TECH., ATLANTA.
Formation of metastable hydrogen atoms by charge transfer, 25:9193 (ORO-2591-52)

GEORGIA INST. OF TECH., ATLANTA. SCHOOL OF PHYSICS.
Prog. rpt. on formation of excited hydrogen atoms by charge transfer and dissociation, 12/69--11/70, 25:9192 (ORO-2591-51)

GESELLSCHAFT FUER KERNFORSCHUNG m.b.H., KARLSRUHE (WEST GERMANY).
Plutonium-documentation, Vol. 4, No. 10, 1970, 25:8830
Plutonium-documentation, Vol. 4, No. 7-9, 1970, 25:8831

GOODYEAR ATOMIC CORP., PIKETON, OHIO.
Prog. rpt. on health and safety, 1969, 25:8692 (GAT-627)

GOSUDARSTVENNYI KOMITET PO ISPOL'ZOVANIYU ATOMNOI ENERGII SSSR, MOSCOW. INSTITUT ATOMNOI ENERGII.
Fine structure of plasma focus using method of multiperforated pinhole camera, 25:9412 (LA-tr-70-25)
High-flux stationary research reactors and their outlook, 25:10268 (LA-4399-TR)

GOSUDARSTVENNYI KOMITET PO ISPOL'ZOVANIYU ATOMNOI ENERGII SSSR, MOSCOW. INSTITUT TEORETICHESKOI I EKSPERIMENTAL'NOI FIZIKI.
Interaction $\pi^-\pi^-$ in the reaction $\pi^-p \to N^{***}(1236)\pi^-\pi^-$ with impulse 4.47 GeV/c, 25:9655 (ITEF-767)
Many-baryon resonances, 25:9803 (ITEF-759)
Reaction $\pi^-p \to rho^0\pi^-p$ with impulse 4.45 GeV/c, 25:9656 (ITEF-775)

GOSUDARSTVENNYI KOMITET PO ISPOL'ZOVANIYU ATOMNOI ENERGII SSSR, OBNINSK. FIZIKO-ENERGETICHESKII INSTITUT.
Angular anisotropy of photofission of ^{239}Pu, 25:10024 (FEI-190)
CINDA 69: index to literature on microscopic neutron data, 25:9946 (TID-25165(Suppl.2))

GOSUDARSTVENNYI KOMITET PO ISPOL'ZOVANIYU ATOMNOI ENERGII SSSR, SERPUKHOV. INSTITUT FIZIKI VYSOKIKH ENERGII.
Beam regulation in a 100-MeV linear accelerator, 25:9914 (NP-tr-1926)
Experimental possibility of revealing the reaction $1^+ + 1^- \to \nu + \text{anti } \nu + \gamma$, 25:9627 (NP-18558)
Topography of magnetic field at 70-GeV accelerator, 25:9906 (IFVE-SKU-69-95)

GRENOBLE UNIV. (FRANCE). FACULTE DES SCIENCES.
Absolute measurements in fast neutron reactions: the n + D → nnp reaction at 14 MeV, 25:9968 (NP-18488)

GRONINGEN RIJKSUNIVERSITEIT (NETHERLANDS).
Isotope encephalography: diagnosis of intracranial focal lesions, 25:8710 (NP-18560)

GULF GENERAL ATOMIC, INC., SAN DIEGO, CALIF.
Cloud chemistry of fallout formation, 25:8362 (AD-707427)
Nonlinear quasi-static analysis of two-dimensional concrete structures. I and II, 25:8392 (GA-9994)
Prog. rpt. on integral neutron thermalization, 4--6/70, 25:9943 (GA-10223)
Special development problems of high-temperature gas-cooled reactor systems, 25:10166 (GA-10265)

H

HAHN-MEITNER-INSTITUT FUER KERNFORSCHUNG, BERLIN (WEST GERMANY).
Contamination of the river water by the fallout after extreme reactor accidents, 25:8660 (HMI-B-87)
Estimation of the surface water's contamination by the near fallout by nuclear explosions, 25:8354 (HMI-B-86)
Modular program system for experimental programing for the PDP-9, 25:8572 (HMI-B-96)

HARVARD UNIV., BOSTON, MASS.
Case study in technological innovation: food irradiation, 25:8813 (NP-18236)

HITTMAN ASSOCIATES, INC., COLUMBIA, MD.
Radiation flux mapping of OPE spacecraft models, 25:9537 (N-70-34007)

HOUSTON UNIV., TEX.
Prog. rpt. on pion interactions at medium energies, 25:9657 (ORO-3948-2)

I

IDAHO NUCLEAR CORP., IDAHO FALLS.
Comparison of predictions from the reactor primary system decompression code (RELAP3) with decompression data from the semiscale blowdown and emergency core cooling (ECC) project, 25:10242 (IN-1444)
Development of a fluidized-bed burner for processing Rover fuel, 25:8322 (IN-1423)
Particle size control by jet grinding in a fluidized-bed denitrator, 25:8323 (IN-1439)
Prog. rpt. on silver zeolite: iodine adsorption studies, semiannual, 7/1--12/31/69, 25:8321 (IN-1363)
PWR FLECHT (Full Length Emergency Cooling Heat Transfer) Group II test report, 25:10229 (WCAP-7544)
Release of radioiodine from open pools, 25:8450 (IN-1449)
Ultrasonic liquid level detector using shear wave attenuation in a bar, 25:10267 (IN-1442)

ILLINOIS STATE WATER SURVEY, URBANA.
Prog. rpt. on study of rainout of radioactivity in Illinois, 11/70, 25:8365 (COO-1199-19)

ILLINOIS UNIV., URBANA.
Coherence of isoscalar and isovector exchange amplitudes in $\pi^+p \to A_2^+p$, 25:9650 (COO-1195-202)

ILLINOIS UNIV., URBANA. DEPT. of VETERINARY PHYSIOLOGY AND PHARMACOLOGY.
Prog. rpt. on animal metabolic studies of Sr and Ca, 8/16/69--8/15/70, 25:8592 (COO-1339-43)

INDIANA-PURDUE UNIV., INDIANAPOLIS.
Analytic structure of off-mass-shell S-wave π, 25:9763 (COO-1428-239)

INSTITUTE OF NUCLEAR PHYSICS, KRAKOW (POLAND).
Hadron interaction at ultra high energies, 25:9635 (INP-722)

INTERNATIONAL ATOMIC ENERGY AGENCY, VIENNA (AUSTRIA).
Directory of high-energy radiotherapy centers, 1970, 25:8728 (STI/PUB-251)
Manual on mutation breeding, 25:8635 (STI/DOC-10/119)
Panel on nuclear techniques for studying pesticide residue problems, Vienna, Austria, 12/68, 25:8583 (STI/PUB-252)
Training manual on food irradiation technology and techniques, 25:8814 (STI/DOC-10/114)

INTERNATIONAL ATOMIC ENERGY AGENCY, VIENNA (AUSTRIA). NUCLEAR DATA UNIT.
CINDA 69: index to literature on microscopic neutron data, 25:9946 (TID-25165(Suppl.2))

INTERNATIONAL COMMISSION ON RADIATION UNITS AND MEASUREMENTS, WASHINGTON, D.C.
Linear energy transfer, 25:8671 (ICRU-16)
Radiation dosimetry: x rays generated at potentials of 5 to 150 kV, 25:8672 (ICRU-17)

INTERNATIONAL NUCLEAR DATA COMMITTEE.
Energy dependent anti ν-values for ^{235}U, ^{239}Pu, ^{233}U, ^{240}Pu, ^{241}Pu, and the status of anti ν for spontaneous fission isotopes, 25:10025 (INDC(NDS)-19/N)

IOWA UNIV., IOWA CITY. DEPT. OF MECHANICAL ENGINEERING.
Fatigue behavior of molybdenum, 25:8861 (AD-709580)

ISTITUTO NAZIONALE DI FISICA NUCLEARE, ROME (ITALY).
K anti K ν final states for N anti N annihilation at rest in Venezziano language, 25:9765 (NP-18578)
Muon pair annihilation and Hadron production by e^+, e^- colliding beams in GeV region, 25:9621 (NP-18581)

J

JAPAN ATOMIC ENERGY RESEARCH INST., TOKAI. TOKAI RESEARCH ESTABLISHMENT.
Nuclear accidents in nuclear installations, 25:8661 (JAERI-4052)

JAPAN ATOMIC ENERGY RESEARCH INST., TOKYO.
Health physics and safety at Oarai Research Establishment, 4/69--3/70, 25:8673 (JAERI-Memo-4098)
Prog. rpt. on activities in Division of Health Physics and Safety, annual, 4/69--3/70, 25:8693 (JAERI-5025)
Study on the radiation-induced chain crosslinking and crosslinking polymerization, 25:8276 (JAERI-Memo-4147)

JERSEY CENTRAL POWER AND LIGHT CO., MORRISTOWN, N. J.
Oyster Creek Nuclear Power Plant, Unit No. 1. Application for an increase in power level. Preliminary safety analysis report, Amendment 65, 25:10143 (DOCKET-50219-118)
Oyster Creek Nuclear Power Plant, Unit No. 1. Surveillance test failure of vacuum breaker block

valves, 25:10118 (DOCKET-50219-117)
Three Mile Island Nuclear Station, Unit 1. Preliminary safety analysis report, Amendment 16, 25:10153 (DOCKET-50289-31)
Three Mile Island Nuclear Station, Unit 2. Preliminary safety analysis report, Amendment 11, Suppl. 7, 25:10157 (DOCKET-50320-20)
JOHNS HOPKINS UNIV., BALTIMORE, MD.
Coherent anti pd interactions and related dissociation reactions at 7.0 GeV/c, 25:9636 (TID-25610)
Measurement of form factors for decay K/sub L/^{0} + $\pi\mu\nu$, 25:9629 (UCLA-1054)
Study of decay mode K/sub L/^{0} + $\pi^+\pi^-\pi^0$, 25:9628 (UCLA-1052)
Study of reaction K$^-$n + K$^-\pi^-$p at 12.6 GeV/c, 25:9658 (TID-25611)
JOINT INST. FOR NUCLEAR RESEARCH, DUBNA (USSR).
Electron--ion bunch diagnostics by bremsstrahlung, 25:9908 (KFK-tr-337)
Identification of elements 102 and 104 with the help of the collimation method, 25:10030 (KFK-tr-329)
Magnetic spark chamber spectrometer for K/sub L/^{0}--K/sub S/^{0} regeneration investigations at high energies, 25:8544 (JINR-P1-5361)
Problem of two centers in quantum mechanics. V, 25:9600 (JINR-P4-5040)
Transition radiation on resonance γ-quanta, 25:9703 (JINR-P2-5042)
JOINT INST. FOR NUCLEAR RESEARCH, DUBNA (USSR). LAB. OF HIGH ENERGY.
Nonrelativistic transformations applied to Dirac equation, 25:9599 (JINR-P2-5314)
Pulse shaper with the zero time of regeneration for the apparatus blocking at the large loading, 25:8545 (JINR-P13-5377)
JOINT INST. FOR NUCLEAR RESEARCH, DUBNA (USSR). LAB. OF NEUTRON PHYSICS.
Coherent scattering amplitude of ^{186}W measured by small angle scattering, 25:10026 (JINR-E3-5371)
Investigation of ^{9}Be(t,n)^{11}B reaction at 1.10 MeV, 25:9976 (JINR-P15-5148)
Reaction ^{7}Li(d,n)^{8}Be, 25:9975 (JINR-P15-5143)
JOINT INST. FOR NUCLEAR RESEARCH, DUBNA (USSR). LAB. OF NUCLEAR PROBLEMS.
Cross section of anti Kd + KY_1Y_2, 25:9804 (JINR-P2-5231)
Lifetime of excited states in spherical nuclei ^{139}La, ^{138}La, and ^{133}La, 25:10029 (JINR-P6-5200)
Processes of the type of double charge exchange at light nuclei, 25:9974 (JINR-P2-5286)
JOINT INST. FOR NUCLEAR RESEARCH, DUBNA (USSR). LAB. OF NUCLEAR REACTIONS.
Two-quasiparticle (h/sub 9/2/)^2 isomeric state in ^{202}Po, 25:10027 (JINR-E6-5379)
JOINT INST. FOR NUCLEAR RESEARCH, DUBNA (USSR). LAB. OF THEORETICAL PHYSICS.
Anomalous magnetic moment of nucleons, 25:9702 (JINR-E2-5333)
Bound states of relativistic three-particle system, 25:9688 (JINR-P2-5336)
Friedman theory, 25:9870 (JINR-P2-5289)
Generalized DWBA model applied to ^{24}Mg(dp)^{25}Mg reaction at E/sub d/ = 13.5 MeV, 25:9997 (JINR-E4-5350)
Interaction cross sections of fast particles with tritium and ^{3}He nuclei, 25:9967 (JINR-P2-5335)
Investigation of Heisenberg model of impure ferromagnets. I, 25:10346 (BNL-tr-389)
Non-rotational state of deformed nuclei with an odd number of neutrons in range 165 less than or equal to A less than or equal to 175, 25:10028 (JINR-P4-5228)
Representation for relativistic scattering amplitude at high energies, 25:9749 (JINR-E2-5341)
Use of K-harmonics in scattering problems, 25:9889 (JINR-P4-5366)
JUNTA DE ENERGIA NUCLEAR, SACAVEM (PORTUGAL). LABORATORIO DE FISICA E ENGENHARIA NUCLEARES.
Experimental study of the kinetics and dynamics of critical assemblies for thermal neutrons, 25:10174 (LFEN-109-B)
Study of determination of fluorine in uranium concentrates: outline of the volumetric method, 25:8201 (LFEN-N1.-36-a)

K

KERNFORSCHUNGSANLAGE, JUELICH (WEST GERMANY).
Conference on position-sensitive detectors in nuclear physics, Juelich, Ger., 7/69, 25:8469 (JUL-CONF-4)
KERNFORSCHUNGSANLAGE, JUELICH (WEST GERMANY). INSTITUT FUER CHEMISCHE TECHNOLOGIE.
Reprocessing of thorium-containing nuclear fuels, 25:8324 (ORNL-tr-2405)
KERNFORSCHUNGSANLAGE, JUELICH (WEST GERMANY). INSTITUT FUER FESTKOERPER- UND NEUTRONENPHYSIK.
Position-sensitive counters, 25:8470 (JUL-CONF-4, pp 1-10)
KERNFORSCHUNGSANLAGE, JUELICH (WEST GERMANY). INSTITUT FUER KERNPHYSIK.
Analog-division stage for use with position-sensitive detectors, 25:8471 (JUL-CONF-4, pp 11-21)
KERNFORSCHUNGSANLAGE, JUELICH (WEST GERMANY). INSTITUT FUER PLASMAPHYSIK.
Elliptic boundary value problem in plasma physics, 25:9456 (JUL-663-PP)
KERNFORSCHUNGSANLAGE, JUELICH (WEST GERMANY). INSTITUT FUER REAKTORENTWICKLUNG.
Development and explanation of prototype fuel element for heavy-water-moderated and-cooled thorium breeder reactor, 25:10209 (JUL-654-RG)
KERNFORSCHUNGSANLAGE, JUELICH (WEST GERMANY). ZENTRALLABOR FUER ELEKTRONIK.
Position resolving detector bank for neutron scattering experiments, 25:8473 (JUL-CONF-4, pp 30-47)
KERNFORSCHUNGSZENTRUM, KARLSRUHE (WEST GERMANY).
Physics investigations of steam-cooled fast reactor cores with a Pu-fueled central zone, 25:10258 (EURFNR-848)
KERNFORSCHUNGSZENTRUM, KARLSRUHE (WEST GERMANY). INSTITUT FUER ANGEWANDTE REAKTORPHYSIK.
Measurement of neutron spectra in energy range from 1 eV to 10 keV with help of sandwich techniques, 25:8481 (KFK-1233)
KERNFORSCHUNGSZENTRUM, KARLSRUHE (WEST GERMANY). INSTITUT FUER EXPERIMENTELLE KERNPHYSIK.
Measurement of the orientation of the residual nucleus and several differential interaction cross sections in the reaction ^{58}Fe(d,p)^{59}Fe, 25:9998 (NP-18439)
Wire spark chambers at the Inst. for Experimental Nuclear Physics, Karlsruhe, 25:8480 (JUL-CONF-4, pp 165-71)
KERNFORSCHUNGSZENTRUM, KARLSRUHE (WEST GERMANY). INSTITUT FUER MATERIAL UND FESTKOERPERFORSCHUNG.
Dispersion fuel for high-flux reactors (UAl_3--Al), 25:8846 (KFK-1252)
Preparation of uranium mononitride pellets of differing densities by cold pressing and sintering, 25:8913 (ORNL-tr-2365)
Relations between stereometric microstructure and properties of cermets and porous materials, 25:8944 (KFK-1236)
KERNFORSCHUNGSZENTRUM, KARLSRUHE (WEST GERMANY). INSTITUT FUER RADIOCHEMIE.
Complex formation of tetravalent actinides with pyridine- and α-aminopolycarboxylic acids, 25:8237 (KFK-1210)
System UO_2--UO_3--$LaO_{1.5}$, 25:8943 (KFK-1235)
KERNFORSCHUNGSZENTRUM, KARLSRUHE (WEST GERMANY). INSTITUT FUER REAKTORENTWICKLUNG.
Determination of operational thermal conductivity of ceramic nuclear fuel and heat transfer coefficient of fuel/can gap by balanced oscillator method, 25:10323 (EURFNR-774)
Influence of correct dead time simulation on the dynamic behavior of model for controlled Na 2 reactors, 25:10186 (KFK-1179)
Observations of decline of interference in D_2O loop of multipurpose research reactor, 25:10243 (NP-18535).
Results of error analysis for in-pile thermal conductivity measurment using the balanced oscillator techniques, 25:10324 (EURFNR-775)
Safety report for FR-2 experimental capsule rigs with single-walled NaK capsules for irradiation of high-power fuel pins, 25:10257 (EURFNR-764)
KERNFORSCHUNGSZENTRUM, KARLSRUHE (WEST GERMANY). LABOR FUER ELEKTRONIK UND MESSTECHNIK.
CAMAC: system of computer-controlled electronics, 25:8573 (KFK-1241)
Measurement of high surge current, 25:9505 (KFK-896)

L

LEIDEN RIJKSUNIVERSITEIT (NETHERLANDS).
Genetic investigation of radiation-sensitive mutant of Escherichia coli, 25:8633 (NP-18483)
LOS ALAMOS SCIENTIFIC LAB., N. MEX.
ANDYMG3: basic program for time-dependent transport of particles and photons, 25:9601 (LA-4539)
Controlled-potential coulometric and potentiometric titrations of uranium and plutonium in ceramic-type materials, 25:8200 (LA-4537)
CONVERT: IBM-to-CDC program conversion code, 25:10350 (LA-4555)
Statistical aspects of deconvolution, 25:10351 (LA-4556)
TEPLO: heat conduction code for studying thermal explosions in laminar composites, 25:8961 (LA-4511)
Transport theory: discrete ordinates quadrature over the unit sphere, 25:9602 (LA-4554)
Vela V and VI solar x-ray atlas. II, 25:9097 (LA-4454(Vol.2))
LOUISIANA POWER AND LIGHT CO., NEW ORLEANS.
Waterford Steam Electric Station, Units 3 and 4. Application for licenses, 25:10158 (DOCKET-50382-1)
LOUVAIN UNIV. (BELGIUM). INST. FOR THEORETICAL PHYSICS.
Charge operators in general quantum field theory, 25:9838 (NYO-3829-60)
LOYOLA UNIV., MAYWOOD, ILL. STRITCH SCHOOL OF MEDICINE.
Argonne radium studies, 25:8669 (COO-2088-1)
LUND INST. OF TECH. (SWEDEN). DEPT. OF NUCLEAR PHYSICS.
Photomeson effects in (γ, n) and (γ,p)-reaction in light nuclei, 25:9977 (LUNP-7009)
Photoproduction of charged pions from nuclei, 25:9620 (LUNP-7007)
LUND INST. OF TECH. (SWEDEN). DIV. OF AUTOMATIC CONTROL.
Digital simulation of spatial xenon oscillations, 25:10306 (NP-18547)

XUM

Maximum likelihood identification of dynamics of the agesta reactor and comparison with results of spectral analysis, 25:10091 (NP-18595)

LUND UNIV. (SWEDEN). DEPT. OF PHYSICS.
Computer programme for calculation of solid angles and angular acceptances, 25:9910 (LUSY-7007)
Photomeson effects in (γ, n) and (γ,p)-reaction in light nuclei, 25:9977 (LUNP-7009)
Photoproduction of charged pions from nuclei, 25:9620 (LUNP-7007)

LYON UNIV. (FRANCE).
Polar and triangular diagrams in interpretation of (α,2α) reactions, 25:10059 (LYCEN-7039)

LYON UNIV. (FRANCE). INSTITUT DE PHYSIQUE NUCLEAIRE.
Fabrication and utilization of lithium-drifted silicon detectors, 25:8546 (LYCEN-6847)
Method of calculation of trajectories of ions before injection into the proposed heavy-ion linear accelerator, 25:9911 (LYCEN-6949)
Parameters of ''Reflex''-type ion sources, 25:9912 (LYCEN-6953)
Polar and triangular diagrams in interpretation of (α,2α) reactions, 25:10059 (LYCEN-7039)
Transient effects of radiation on diodes and bipolar transistors, 25:8581 (LYCEN-6933)

M

MARBURG UNIV. (WEST GERMANY). PHYSIKALISCHES INSTITUT.
Use of position-fixing semiconductor counters in magnetic spectrographs, 25:8474 (JUL-CONF-4, pp 48-58)

MARYLAND UNIV., COLLEGE PARK. ENGINEERING MATERIALS GROUP.
Dynamic microplasticity of B.C.C. metals and solid solutions, 25:10349 (CONF-700545-1)

MASSACHUSETTS GENERAL HOSPITAL, BOSTON.
Prog. rpt. on positron scanning with computer interface, 1--10/70, 25:8711 (NYO-3937-2)

MAX-PLANCK-INSTITUT FUER KERNPHYSIK, HEIDELBERG (WEST GERMANY).
Construction of a multiwire proportional chamber, 25:8479 (JUL-CONF-4, pp 148-64)

MAX-PLANCK-INSTITUT FUER PHYSIK UND ASTROPHYSIK, MUNICH (WEST GERMANY).
Extensive air showers, 25:9253 (MPI-PAE/EXTRATERR-47)
Gamma ray and neutron emissions from the sun, 25:9098 (MPI-PAE/EXTRATERR-48)
Measurements of electric fields in equatorial and medium latitudes during twilight using barium ion clouds, 25:9285 (MPI-PAE/EXTRATERR-49/70)

MECHANICAL TECHNOLOGY INC., LATHAM, N. Y.
Prog. rpt. on liquid metal bearings technology, 11/69--4/70, 25:8394 (NYO-3930-7)

MEDICAL COLL. OF GEORGIA, AUGUSTA. DEPT. OF PHYSIOLOGY.
Prog. rpt. on mechanism of radiation effects on transport and bioelectric properties of rat intestine, 9/70, 25:8607 (ORO-3882-3)

METROPOLITAN EDISON CO., READING, PA.
Three Mile Island Nuclear Station, Unit 1. Preliminary safety analysis report, Amendment 16, 25:10153 (DOCKET-50289-31)
Three Mile Island Nuclear Station, Unit 1. Reactor coolant flow tubes, 25:10152 (DOCKET-50289-30)
Three Mile Island Nuclear Station, Unit 2. Preliminary safety analysis report, Amendment 11, Suppl. 7, 25:10157 (DOCKET-50320-20)

MIAMI UNIV., CORAL GABLES, FLA. DEPT. OF PHYSICS.
Entropy oscillation and the h theorem for finite segments of infinite coupled-harmonic-oscillator chains, 25:10365 (ORO-3895-9)
Prog. rpt. on HELIOS Program, 9/15/70, 25:9398 (ORO-3895-15)

MIAMI UNIV., FLA. ROSENSTIEL SCHOOL OF MARINE AND ATMOSPHERIC SCIENCES.
Inoculated pack studies on low-dose irradiated marine products: shrimp, 25:8804 (TID-25556)

MICHIGAN UNIV., ANN ARBOR. DEPT. OF CHEMISTRY.
Prog. rpt. on low temperature chemical thermodynamics, annual, 11/69--11/70, 25:8260 (COO-1149-180)

MICHIGAN UNIV., ANN ARBOR. DEPT. OF PHYSICS.
Observation of the decay eta' → γ γ, 25:9651 (COO-1764-111)

MILLSTONE POINT CO., WETHERSFIELD, CONN.
Millstone Nuclear Power Station, Unit 1. Abnormal occurrence report No. 7 and No. 8, 25:10121 (DOCKET-50245-49)
Millstone Nuclear Power Station, Unit 1. Abnormal occurrence report No. 10, 25:10122 (DOCKET-50245-50)

MINNESOTA UNIV., MINNEAPOLIS.
Reaction $\pi^- p \to n\pi^+\pi^-$ at high momentum transfer, 25:9654 (COO-1764-114)

MINNESOTA UNIV., MINNEAPOLIS. JOHN H. WILLIAMS LAB. OF NUCLEAR PHYSICS.
Prog. rpt. on nuclear physics, annual, 1970, 25:9966 (COO-1265-94)

MINNESOTA UNIV., MINNEAPOLIS. SCHOOL OF PHYSICS.
Measurements of $\pi^- p$ elastic scattering from 1.71 to 5.53 GeV/c, 25:9652 (COO-1764-112)
Momentum spectra in high-energy Hadron-deuteron interactions, 25:9634 (COO-1764-115)
Observation of the decay eta' → γ γ, 25:9651 (COO-1764-111)
Prog. rpt. on theoretical and high energy physics programs, 9/69--8/70, 25:9685 (COO-1764-86)
$\pi^- p$ charge exchange at backward angles, 25:9653 (COO-1764-113)
Theorem on intuitive tests of parity conservation via spin polarization processes, 25:9686 (COO-1764-100)

MINNESOTA UNIV., MINNEAPOLIS. SCHOOL OF PHYSICS AND ASTRONOMY.
Dual resonance theory with nonlinear trajectories, 25:9884 (COO-1764-90)
Loop diagrams in dual resonance theories with nonlinear trajectories, 25:9691 (RLO-1388-592)
Rules for constructing generalizations of Veneziano N-point function, 25:9885 (COO-1764-98)

MOUND LAB., MIAMISBURG, OHIO.
Disproportionation of tetravalent and pentavalent plutonium ions in the presence of hexavalent plutonium, 25:8239 (MLM-1744)
Investigations into the determination of mercury in copper, 25:8217 (MLM-1772)
Peak Stripping Program for the Nuclear Data 50/50 Analyzer System, 25:8531 (MLM-1773)
Stable gaseous isotope separation and purification: July--September 1970, 25:8424 (MLM-1768)
Thermal diffusion column coefficients for the separation of N_2^{14}--$N^{14}N^{15}$ and O_2^{16}--$O^{16}O^{18}$, 25:8423 (MLM-1439(Rev.))

MUNICH UNIV. (WEST GERMANY).
Applications of spark chambers and multiwire proportional counters in magnetic spectrographs, 25:8476 (JUL-CONF-4, pp 71-120)

N

NATIONAL ACADEMY OF SCIENCES--NATIONAL RESEARCH COUNCIL, WASHINGTON, D.C. COMMITTEE ON RADIOACTIVE WASTE MANAGEMENT.
Disposal of solid radioactive wastes in bedded salt deposits, 25:8455 (TID-25576)

NATIONAL BUREAU OF STANDARDS, WASHINGTON, D. C.
Development and analysis of techniques for calibration of Kerr cell pulse-voltage measuring systems. III, 25:10370 (SC-CR-69-3266)

NATIONAL LEAD CO. OF OHIO, CINCINNATI.
Elevated-temperature tensile tests of cast uranium-base dilute quinary alloys, 25:8867 (NLCO-1060)

NATIONAL RADIATION LAB., CHRISTCHURCH (NEW ZEALAND).
Annual report for the year 1969, 25:8675 (NP-18529)

NRBRASKA DEPT. OF HEALTH, LINCOLN. DIV. of RADIOLOGICAL HEALTH.
Hallam Nuclear Power Facility. Semiannual report of the environmental surveillance, 25:10134 (DOCKET-1153-17)

NEW JERSEY STATE DEPT. OF HEALTH, TRENTON.
Heat discharges from nuclear reactors, 25:10090 (CONF-700335-1)

NEW YORK OPERATIONS OFFICE (AEC), N. Y. HEALTH AND SAFETY LAB.
Accumulated fallout ^{90}Sr in the Rocky Flats area, 25:8353 (HASL-237, pp I.11-26)
HASL fallout program data, 25:8658 (HASL-237, pp II.1-16)
Prog. rpt. on fallout program, 10/70, 25:8670 (HASL-237(App.))
Prog. rpt. on fallout program, 6--9/70, 25:8367 (HASL-237)
Strontium-90 deposition in the Atlantic Ocean. III, 25:8368 (HASL-237, pp I.27-37)

NEW YORK UNIV., N. Y.
Comparisons of observed concentrations of nuclides in the stratosphere with predictions by the Streak model, 25:8369 (HASL-237, pp I.38-62)

NEW YORK UNIV., N. Y. COURANT INST. OF MATHEMATICAL SCIENCES.
Hyperliptic magnetohydrodynamic steady flow past a point source, 25:9269 (AD-706106)

NORDISK INSTITUT FOR TEORETISK ATOMFYSIK, COPENHAGEN (DENMARK).
Lectures on non-linear electrodynamics, Copenhagen, 1968, 25:9869

NORTH CAROLINA UNIV., CHAPEL HILL.
Prog. rpt. on mechanisms of innate immunity, IV, 12/69--11/70, 25:10364 (ORO-3628-11)

NUCLEAR FUEL SERVICES, INC., WEST VALLEY, N.Y.
West Valley Reprocessing Plant. Quarterly report, July 1--September 30, 1970, Revision, 25:8366 (DOCKET-50201-56)

O

OAK RIDGE NATIONAL LAB., TENN.
Activities of ANS-6 subcommittee on radiation shielding standards, 25:9538 (ORNL-TM-3251)
Advanced materials for steam generators, 25:8838 (ORNL-4600, pp 282-6)
Behavior of refractory materials under irradiation, 25:8957 (ORNL-4600, pp 250-1)
Cladding materials for space isotopic heat sources, 25:8850 (ORNL-4600, pp 181-5)
Corrosion studies of advanced refractory metals, 25:8837

(ORNL-4600, pp 216-22)
Current nuclear level schemes: A = 91 to 117, 25:10031 (ORNL-4627)
Design and safety considerations of shipping solidified high-level radioactive wastes, 25:8451 (ORNL-TM-2971)
Development of advanced LMFBR fuels, 25:8910 (ORNL-4600, pp 41-56)
Development of fast-reactor neutron-absorber materials, 25:8912 (ORNL-4600, pp 167-74)
Development of fast-reactor oxide fuels, 25:8909 (ORNL-4600, pp 3-40)
Development of fuel element fabrication, 25:8956 (ORNL-4600, pp 235-48)
Development of uranium mononitride fuels, 25:8953 (ORNL-4600, pp 177-80)
Effect of fast neutron irradiation on the creep-rupture properties of type 304 stainless steel at 600°C, 25:8897 (ORNL-TM-3169)
Effect of power cycling on LMFBR fuel-cladding behavior, 25:8835 (ORNL-4600, pp 57-64)
Effects of chronic irradiation and temperature on populations of aquatic snail Physa heterostropha, 25:8750 (ORNL-4612)
Eigenvalues, radial expectation values, and potentials for free atoms from Z = 2 to 126 as calculated from relativistic Hartree--Fock--Slater atomic wave functions, 25:9168 (ORNL-4614)
Examination of nickel heat pipes containing potassium, 25:8395 (ORNL-TM-3077)
Fabrication development for LMFBR stainless steel tubing, 25:8847 (ORNL-4600, pp 126-30)
Fast-neutron irradiation effects on electrical insulators, 25:8954 (ORNL-4600, pp 210-15)
Fission-gas release and physical properties of fuel materials during irradiation, 25:8955 (ORNL-4600, pp 225-34)
Fluid dynamic studies of the Molten-Salt Reactor Experiment (MSRE) core, 25:10196 (ORNL-TM-3229)
Forest management plan, AEC Oak Ridge reservation: 1970--1975, 25:10356 (ORNL-TM-3175)
Glove box vacuum system for radioisotopic targets, 25:8453 (ORNL-TM-3209)
Heavy section steel technology program. Technical report No. 11. Notch preparation in compact tension specimens, 25:8872 (WCAP-7579)
Impact of nuclear energy centers on economy of Puerto Rico, 25:10291 (TID-25630)
Improvement of Hastelloy N and related compositions, 25:8870 (ORNL-4600, pp 271-81)
Indexed bibliography of thermal effects literature--1, 25:10159 (ORNL-NSIC-81)
Joining research on nuclear materials, 25:8854 (ORNL-4600, pp 252-65)
LMFBR fuel element design and model development, 25:8911 (ORNL-4600, pp 65-80)
Low-pressure distillation of molten fluoride mixtures: nonradioactive tests for the MSRE distillation experiment, 25:10210 (ORNL-4434)
Mechanical properties of alloys in reactor environments and development of LMFBR cladding and structural materials, 25:8952 (ORNL-4600, pp 81-125)
Neutron elastic- and inelastic-scattering cross sections for yttrium in the energy range 4.19 to 8.56 MeV, 25:9999 (ORNL-4552)
New calculational method for space--energy--angular dependent reactor kinetics, 25:10307 (ORNL-TM-3136)
Nondestructive testing techniques for LMFBR, 25:8439 (ORNL-4600, pp 153-6)
Nondestructive testing, 25:8440 (ORNL-4600, pp 266-70)
Nonlinear quasi-static analysis of two-dimensional concrete structures. I and II, 25:8392 (GA-9994)
Nuclear fusion resonance reactions of possible CTR interest, 25:9507 (ORNL-TM-3233(Rev.))
Physical and mechanical metallurgy of refractory alloys, 25:8851 (ORNL-4600, pp 186-97)
Preparation and handling of salt mixtures for the Molten Salt Reactor Experiment, 25:10211 (ORNL-4616)
Prog. rpt. on fuels and materials development, 6/30/70, 25:8829 (ORNL-4600)
Prog. rpt. on nuclear safety, 9--10/70, 25:10244 (ORNL-TM-3212)
Prog. rpt. on Oak Ridge Research Reactor, 7--9/70, 25:10270 (ORNL-TM-3256)
Prog. rpt. on ORNL isotopic power fuels, 9/30/70, 25:8427 (ORNL-4639)
Prog. rpt. on ORNL--NSF interdisciplinary research relevant to problems of our society, summer/1970, 25:10354 (ORNL-4632)
Prog. rpt. on tobacco smoke analysis program, 1/70--9/70, 25:10355 (ORNL-4642)
Progress in Zircaloy cladding failure modes research, 25:8839 (ORNL-TM-3188)
Properties of ferritic steel welds, 25:8869 (ORNL-4600, pp 147-52)
Prospects of a multi-MeV H_2^+ injection-accumulation experiment, 25:9506 (ORNL-TM-3207)
Selected abstracts of world literature on production and industrial uses of radioisotopes (from NSA July--September 1970), 25:8428 (ORNL-IIC-30(Pt.3))
Shielded metal-arc welding for LMFBR components, 25:8849 (ORNL-4600, pp 142-6)
Sodium corrosion studies, 25:8836 (ORNL-4600, pp 157-66)
Some techniques for estimating the results of the emission of radioactive effluent from ORNL stacks, 25:8452 (ORNL-TM-3187)
SPECTRAN: computer system to analyze high resolution spectrum. I, 25:10353 (ORNL-4605)
Stesses in out-of-round pipe due to internal pressure, 25:8871 (ORNL-TM-3244)
Technetium-99m in medicine: a supplementary bibliography, 25:8712 (ORNL-TM-2091(Suppl.1))
Technical assistance in procurement of fuel elements, 25:8853 (ORNL-4600, pp 249)
Thorium ceramics data manual. II, 25:8927 (ORNL-4503(Vol.2))
Time-dependent behavior of prestressed concrete pressure vessels, 25:10325 (ORNL-TM-3246)
Tungsten metallurgy, 25:8852 (ORNL-4600, pp 198-209)
Tunneling: an annotated bibliography with permuted-title and key-word index, 25:8444 (ORNL-HUD-17)
Use of steam-electric power plants to provide thermal energy to urban areas, 25:10094 (ORNL-HUD-14)
Welding development for LMFBR vessels and components, 25:8848 (ORNL-4600, pp 131-41)

OHIO STATE UNIV., COLUMBUS.
Measurement of the up-down asymmetries in the beta decay of polarized lambdas, 25:9626 (COO-1545-87)

OHIO STATE UNIV. RESEARCH FOUNDATION, COLUMBUS.
Prog. rpt. on stress corrosion cracking in Fe--Ni--Cr alloys, 12/69--3/70, 25:8834 (COO-2069-6)

OMAHA PUBLIC POWER DISTRICT, NEBR.
Fort Calhoun Station, Unit No. 1. Preliminary safety analysis report, Amendment 22 (includes final safety analysis report, Suppl. No. 5), 25:10151 (DOCKET-50285-39)

OREGON STATE UNIV., CORVALLIS. DEPT. OF BIOCHEMISTRY AND BIOPHYSICS.
Effect of univelent cations on circular dichroism of pyruvate kinase, 25:10369 (RLO-2227-T-5-4)
Prog. rpt. on properties of enzymes from thermomorphs and halophiles, 3 yrs, 4/1/68--12/15/70, 25:10367 (RLO-2227-T-5-1)
Prog. rpt. on properties of enzymes from thermomorphs and halophiles, annual, 12/69--12/70, 25:10368 (RLO-2227-T-5-2)

OREGON UNIV., EUGENE.
Bootstrap theory of vibrations in nuclei, 25:10063 (RLO-1925-46)

ORGANIZATION FOR ECONOMIC CO-OPERATION AND DEVELOPMENT, PARIS (FRANCE).
Prog. rpt. on Halden Reactor project, annual, 1969, 25:10125 (NP-18573)

P

PAKISTAN INST. OF NUCLEAR SCIENCE AND TECHNOLOGY, NILORE.
Description of hot facilities at Pakistan Inst. of Nuclear Science and Tech., Pakistan, 25:8449 (CONF-691008-18)

PARIS UNIV., ORSAY (FRANCE). FACULTE DES SCIENCES.
Diffusion coefficients of Ni--U system, 25:8865 (CEA-R-4066)
Experimental study of the kinetics and dynamics of critical assemblies for thermal neutrons, 25:10174 (LFEN-109-B)

PARIS UNIV., ORSAY (FRANCE). INSTITUT DE PHYSIQUE NUCLEAIRE.
Hartree--Bogolyubov theory and application to neutron--proton pairing problem, 25:10060 (NP-18538)

PAVIA UNIV. (ITALY).
Work of Euratom Study Group on radiation and human cytogenetics of Univ. of Pavia, 4/63--3/68, 25:8632 (EUR-4526)

PENNSYLVANIA ELECTRIC CO., JOHNSTOWN.
Three Mile Island Nuclear Station, Unit 1. Preliminary safety analysis report, Amendment 16, 25:10153 (DOCKET-50289-31)
Three Mile Island Nuclear Station, Unit 2. Preliminary safety analysis report, Amendment 11, Suppl. 7, 25:10157 (DOCKET-50320-20)

PENNSYLVANIA STATE UNIV., UNIVERSITY PARK.
Prog. rpt. on hypothalamus control of anterior pituitary gland function, 3/70--2/71, 25:10392 (TID-25619)

PENNSYLVANIA UNIV., PHILADELPHIA. DEPT. OF PHYSICS.
Bootstraps in local field theory, 25:9690 (NYO-2171-331)
Giant monopole state: isospin mixing in nuclear ground states, 25:10061 (NYO-2171-330)
Possibility that pulses of long range field are source of CP non-invariance, 25:9826 (NYO-2171-329)

PHILADELPHIA ELECTRIC CO., PA.
Peach Bottom Atomic Power Station, Unit 1. Moisture detectors, 25:10115 (DOCKET-50171-76)
Peach Bottom Atomic Power Station, Unit 1. Monthly operations report No. 57, November 1970, 25:10114 (DOCKET-50171-75)

PHYSIKALISCH-TECHNISCHE BUNDESANSTALT, BRUNSWICK (WEST GERMANY).
Safety report for the core arrangement with two fission zones, 25:10269 (NP-18498)

PITTSBURGH UNIV., PA. DEPT. OF PHYSICS.
Charge operators in general quantum field theory, 25:9838 (NYO-3829-60)

XUM

Prog. rpt. on high-energy physics, 12/69--12/70, 25:9839 (NYO-3829-64)
POWER REACTOR DEVELOPMENT CO., DETROIT, MICH.
Enrico Fermi Atomic Power Plant, Unit 1. Operations report, August 1970, 25:10112 (DOCKET-50016-88)
PRINCETON UNIV., N.J. DEPT. OF PHYSICS.
Performance of large-volume two-phototube neutron detector, 25:8547 (PURC-4159-13)
PUERTO RICO NUCLEAR CENTER, MAYAGUEZ.
Prog. rpt., annual, 1969, 25:8574 (PRNC-140)
PURDUE UNIV., LAFAYETTE, IND.
Analytic structure of off-mass-shell S-wave π, 25:9763 (COO-1428-239)

R

RAND CORP., SANTA MONICA, CALIF.
Differential quadrature and long-term integration, 25:10389 (TID-25616)
REACTOR CENTRUM NEDERLAND, PETTEN.
Accurate and precise titrimetric analysis of uranium in nuclear fuels, 25:8202 (RCN-126)
Determination of oxygen-to-uranium ratio in hyperstoichiometric uranium dioxide, 25:8203 (RCN-127)
Determination of oxygen-to-uranium ratio in hypostoichiometric uranium dioxide, 25:8204 (RCN-128)
RENSSELAER POLYTECHNIC INST., TROY, N. Y.
Linear accelerator project. Progress report, April 1, 1970--June 30, 1970, 25:9945 (RPI-328-190)
Prog. rpt. on pulse radiolysis of gases, annual, 11/70, 25:8285 (RPI-3821-5)
REYNOLDS ELECTRICAL AND ENGINEERING CO., INC., MERCURY, NEV. RADIOLOGICAL SCIENCES DEPT.
Model 102 air sampler, 25:8393 (NVO-410-6)
ROCHESTER UNIV., N. Y. DEPT. OF PHYSICS AND ASTRONOMY.
Some remarks concerning the precision of 1 to 2 meter bubble chambers, 25:8549 (UR-875-324)
ROME UNIV. (ITALY). ISTITUTO DI FISICA.
K anti K π final states for N anti N annihilation at rest in Veneziano language, 25:9765 (NP-18578)
Muon pair annihilation and Hadron production by e^+, e^- colliding beams in GeV region, 25:9621 (NP-18581)
RUTGERS--THE STATE UNIV., NEW BRUNSWICK, N. J. DEPT. OF PHYSICS.
Interphase boundary waves in the intermediate state of lead, 25:9363 (NYO-2150-64)

S

SANDIA CORP., ALBUQUERQUE, N. MEX.
Development and analysis of techniques for calibration of Kerr cell pulse-voltage measuring systems. III, 25:10370 (SC-CR-69-3266)
SANDIA LABS., ALBUQUERQUE, N. MEX.
Acceptable imperfections in impulsive loads for simulation tests on circular cylindrical shells, 25:8441 (SC-RR-70-600)
AM frequency division multiplex telemetry systems, 25:10374 (SC-M-70-684)
Analysis of DSB/FM telemetry system errors, 25:10371 (SC-CR-70-6092)
Atomic subshell photoionization cross sections for Z less than or equal to Z less than or equal to 54, 25:9194 (SC-RR-70-721)
Differential ionization cross section in Born approximation, 25:9195 (SC-RR-70-773)
Precisely controlled• low range humidity system, 25:10376 (SC-RR-70-775)
Prog. rpt. on planetary quarantine, 6/30/70, 25:8803 (TID-25468)
Pulsed solid-state sources for microwave application, 25:10373 (SC-DR-70-698)
Range--energy relations for He ions and protons in N_2, O_2, and air (0.2 to 2.0 MeV), 25:9162 (SC-RR-70-788)
Realization of near-time-optimal feedback controllers, 25:10375 (SC-RR-70-544)
Response of multiconductor cable to excitation at open break in shield, 25:10372 (SC-CR-70-6152)
SANDIA LABS., LIVERMORE, CALIF.
Model 50-600-75 Manganin Pulse Power Supply, 25:10381 (SCL-DR-70-130)
SPECTRE: finite difference program for calculating dynamic response of cylindrical shell, 25:10380 (SCL-DR-70-108)
SCIENTIFIC RESEARCH ATOMIC REACTOR INST., MELEKESS (USSR).
Analysis of variation of deformation processes of construction materials after reactor irradiation. I, 25:8898 (SRARI-P-85)
Mechanism of gas release from ceramic nuclear fuels, 25:8958 (SRARI-P-73)
SCIENTIFIC RESEARCH INST. OF ELECTRO-PHYSICAL APPARATUS, LENINGRAD (USSR).
Sextupole lenses with direct nonlinearity in slow ejection system, 25:9913 (NP-18594)
SIEMENS A.G., ERLANGEN (WEST GERMANY).
Small rod-shaped silicon-detectors for medical and biological applications, 25:8464 (BMBW-FBK-70-15)
SKODA CONCERN, PILSEN (CZECHOSLOVAKIA). NUCLEAR POWER PLANTS DIV.
Neutron irradiation induced changes in mechanical properties of pressure vessel steel for A-1 nuclear power plant, 25:8900 (ZJE-90)
Neutron irradiation induced changes in mechanical properties of base material and welding joints of A-1 pressure vessel steel, 25:8901 (ZJE-91)
Pretightening of large pressure vessel flange joints, 25:10096 (ZJE-65)
Radiation stability of steels for pressure vessels of Czechoslovak nuclear reactors, 25:8899 (ZJE-89)
SOCIETE D'ENERGIE NUCLEAIRE FRANCO-BELGE DES ARDENNES, CHOOZ-LEZ-GIVET (FRANCE).
Ardennes Nuclear Power Plant operations report, 9/70, 25:10127 (TID-25628)
SENA Nuclear Power Plant operations report, 8/70, 25:10128 (TID-25629)
SOUTHERN CALIFORNIA EDISON CO., LOS ANGELES.
San Onofre Nuclear Generating Station, Unit 1. Operation report, November 1970, 25:10116 (DOCKET-50206-100)
San Onofre Nuclear Generating Station, Unit 1. Operation report, December 1970, 25:10117 (DOCKET-50206-102)
STAATLICHE ZENTRALE FUER STRAHLENSCHUTZ, BERLIN (EAST GERMANY).
Classification of the new nuclear fuel elements for water-moderated reactors with regard to the regulations for the transport of radioactive materials, 25:8454 (SZS-14/70 (pp 11-21))
Influence of short-term activity releases into the atmosphere on the annual radiation burden in the environment of nuclear power plants, 25:8371 (SZS-14/70 (pp 1-10))
Methods of application of gamma emitters in contact therapy with regard to radiation protection, 25:8688 (SZS-6/70)
Methods of application of gamma emitters in contact therapy with regard to radiation protection, 25:8729 (SZS-6/70, pp 1-8)
Methods of application of gamma emitters, especially radio-gold-seeds in contact therapy with special regard to radiation protection, 25:8689 (SZS-6/70, pp 19-27)
Need for measuring radiation burden of the bladder and rectum, 25:8679 (SZS-6/70, pp 9-18)
Quantitative alpha-autoradiography: a documentation, 25:8584 (SZS-15/70)
Situation and trend of contact therapy in treatment of gynecologic carcinomas, 25:8730 (SZS-6/70, pp 28-35)
STANFORD LINEAR ACCELERATOR CENTER, CALIF.
Measurement of form factors for decay K/sub L^0 • $\pi\mu\nu$, 25:9629 (UCLA-1054)
Study of decay mode K/sub L^0 • $\pi^+\pi^-\pi^0$, 25:9628 (UCLA-1052)
THEMI: Monte Carlo generation of electromagnetic events, 25:9705 (SLAC-123)
Theories of highly inelastic electron scattering, 25:9706 (SLAC-PUB-843)
STANFORD UNIV., CALIF. DEPT. OF BIOLOGICAL SCIENCES.
Repair replication: its role in genetic stability, 25:8636 (SU-326-P-7-X-22)
STANFORD UNIV., CALIF. DEPT. OF COMPUTER SCIENCE.
Micro-computer model for the definition and execution of complex information processing systems, 25:10394 (TID-25622)
Parallel processing with the perfect shuffle, 25:10382 (STAN-CS-70-158(App.5))
Scheduling of N tasks with M operations on two processors, 25:10383 (STAN-CS-70-165(App.2))
Variable control structure micro-computer architecture, 25:10395 (TID-25623)
STANFORD UNIV., CALIF. DEPT. OF MINERAL ENGINEERING.
Prog. rpt. on nitride formation in liquid uranium alloys and their applications to reprocessing of spent nuclear fuel, 6/69--3/70, 25:8325 (SU-326-P-28-X-2)
STANFORD UNIV., CALIF. HIGH-ENERGY PHYSICS LAB.
Electromagnetic structure of ^{3}He nucleus, 25:9965 (AD-710384)
STONE AND WEBSTER ENGINEERING CORP., BOSTON, MASS.
Connecticut Yankee Nuclear Power Plant, Unit No. 1. Reference plant design report. Includes Appendixes A and B, 25:10142 (DOCKET-50213-91)
STUTTGART UNIV. (WEST GERMANY). INSTITUT FUER GASENTLADUNGSTECHNIK UND PHOTOELEKTRONIK.
Multiwire proportional detectors, particularly for the detection of low-energy particles, 25:8477 (JUL-CONF-4, pp 121-40)

T

TAIWAN POWER CO., TAIPEI.
Planning of the first nuclear power project in Taiwan, 25:10089 (CONF-691020-3)
TECHNISCHE HOCHSCHULE, KARLSRUHE (WEST GERMANY).
Measurement of neutron spectra in energy range from 1 eV to 10 keV with help of sandwich techniques, 25:8481 (KFK-1233)
Measurement of the orientation of the residual nucleus and several differential interaction cross sections in the reaction ^{54}Fe(d,p)^{57}Fe, 25:9998 (NP-18439)

TECHNISCHE HOCHSCHULE, MUNICH (WEST GERMANY). TEILINSTITUT MAIER-LEIBNITZ IM PHYSIKDEPARTMENT.
Prog. rpt. on physics, annual, 1969, 25:10018 (BMBW-FBK-70-10)
TECHNISCHE HOGESCHOOL, DELFT (NETHERLANDS).
Activation analysis of oxygen with the aid of tritium, 25:8218 (NP-18592)
TECHNISCHE HOGESCHOOL, EINDHOVEN (NETHERLANDS).
Position-sensitive detectors for the simultaneous determination of several parameters of a particle, 25:8475 (JUL-CONF-4, pp 59-70)
TENNESSEE UNIV., KNOXVILLE.
New calculational method for space--energy--angular dependent reactor kinetics, 25:10307 (ORNL-TM-3136)
TENNESSEE UNIV., KNOXVILLE. DEPT. OF CHEMICAL AND METALLURGICAL ENGINEERING.
Impact of nuclear energy centers on economy of Puerto Rico, 25:10291 (TID-25630)
TENNESSEE UNIV., MEMPHIS. DEPT. OF BIOCHEMISTRY.
Prog. rpt. on origin and fate of thiocyanate ion in metabolism, 5/54--10/70, 25:10363 (ORO-1637-21)
TEXAS AGRICULTURAL AND MECHANICAL UNIV., COLLEGE STATION. CYCLOTRON INST.
Prog. rpt. on research and operation of Texas A and M variable energy cyclotron, annual, 6/69--6/70, 25:9978 (ORO-3398-26)
TEXAS AGRICULTURAL AND MECHANICAL UNIV., COLLEGE STATION. DEPT. OF CHEMISTRY.
Prog. rpt. on high energy radioactive atoms resulting from nuclear transformations in systems of silicon-containing compounds, 2/70--1/71, 25:8310 (ORO-3898-2)
TEXAS UNIV., DALLAS.
Prog. rpt. on photorepair of UV damage to DNA, 1/2/71, 25:8606 (ORO-3630-10)
TEXAS UNIV., HOUSTON. GRADUATE SCHOOL OF BIOMEDICAL SCIENCES.
Prog. rpt. on effect of radiation-sensitive mutations and radiation on recombination in partially diploid derivatives of Escherichia coli, 9/70, 25:8634 (ORO-4024-1)
TOLEDO UNIV., OHIO. RESEARCH FOUNDATION.
Interaction between soil and nuclear reactor foundations during earthquakes, 25:10245 (ORO-3822-5)

U

UNION CARBIDE CORP., OAK RIDGE, TENN. COMPUTING TECHNOLOGY CENTER.
Neutron-induced secondary gamma-ray yield and cross section data, 25:9942 (CTC-42)
UNION CARBIDE CORP., OAK RIDGE, TENN. Y-12 PLANT.
Automatic sample changer for the beryllium analyzer, 25:8220 (Y-1744)
Compensating tool-path data in numerical control machine tapes, 25:8398 (Y-1750)
UNITED KINGDOM ATOMIC ENERGY AUTHORITY, ABINGDON (ENGLAND). CULHAM LAB.
VORTEX: 2-dimensional hydrodynamics simulation code, 25:8407 (CLM-R-106)
UNITED KINGDOM ATOMIC ENERGY AUTHORITY, RISLEY (ENGLAND). REACTOR GROUP.
SNAP: two dimensional neutron diffusion code, 25:9947 (TRG-Report-1990)
UNITED NUCLEAR CORP., ELMSFORD, N. Y. RESEARCH AND ENGINEERING CENTER.
Prog. rpt. on enriched uranium active assay program, 4--6/70, 25:8447 (BHO-65-1)
UNITED STATES-EURATOM FAST REACTOR EXCHANGE PROGRAM.
Determination of operational thermal conductivity of ceramic nuclear fuel and heat transfer coefficient of fuel/can gap by balanced oscillator method, 25:10323 (EURFNR-774)
Physics investigations of steam-cooled fast reactor cores with a Pu-fueled central zone, 25:10258 (EURFNR-848)
Results of error analysis for in-pile thermal conductivity measurment using the balanced oscillator techniques, 25:10324 (EURFNR-775)
Safety report for FR-2 experimental capsule rigs with single-walled NaK capsules for irradiation of high-power fuel pins, 25:10257 (EURFNR-764)
UNIVERSAL OIL PRODUCTS CO., DES PLAINES, ILL. MATERIALS SCIENCE LAB.
Dynamic microplasticity of B.C.C. metals and solid solutions, 25:10349 (CONF-700545-1)
UNIVERSITY OF SOUTHERN CALIFORNIA, LOS ANGELES.
Differential quadrature and long-term integration, 25:10389 (TID-25616)
Functional equations in theory of dynamic programming. XVIII, 25:10385 (TID-25612)
Functional equations in theory of dynamic programming. XVII, 25:10388 (TID-25615)
Generalization of continued fractions and estimation of some integrals, 25:10386 (TID-25613)
Note on the asymptotic behavior of solution of nonlinear differential equations, 25:10417 (USCEE-344)
Truncation and preservation of moment properties for Fokker--Planck moment equations, 25:10387 (TID-25614)
UNIVERSITY OF SOUTHERN CALIFORNIA, LOS ANGELES. DEPT. OF ELECTRICAL ENGINEERING.
Addition chains, 25:10393 (TID-25620)
Approximation techniques in discrete dynamic programming. I, 25:10396 (TID-25624)
Approximation techniques in discrete dynamic programming. II, 25:10397 (TID-25625)
Bounds for approximate solutions to operator differential equation $Y(t) = M(t)Y(t)$, 25:10398 (TID-25627)
One sweep numerical method for vector-matrix difference equations with two-point boundary conditions. technical report no. 70-16, 25:10384 (TID-25609)
Reduction of dimensionality by approximation techniques: diffusion processes. I, 25:10418 (USCEE-350)
Reduction of dimensionality in dynamic programming via the method of diagonal decomposition, 25:10419 (USCEE-377)
Use of splines with unknown end points in the identification of systems, 25:10390 (TID-25617)
UNIVERSITY OF WESTERN ONTARIO, LONDON.
Response of Savannah River guyed stack under wind and earthquake action, 25:10391 (TID-25618)

W

WADCO CORP., RICHLAND, WASH.
Comparison of nuclear design models for power and flux distributions near the FTR core-reflector interface, 25:10272 (WHAN-FR-35)
Conductivity cells for flow induced vibration measurements, 25:10271 (WHAN-FR-21)
WASHINGTON UNIV., ST. LOUIS, MO.
Measurement of the up-down asymmetries in the beta decay of polarized lambdas, 25:9626 (COO-1545-87)
WASHINGTON UNIV., SEATTLE.
Finite nuclear size and radiative corrections in the construction and assessment of Kurie plots for allowed beta-decay, 25:10062 (RLO-1388-131)
WASHINGTON UNIV., SEATTLE. DEPT. OF BOTANY.
Macromolecule synthesis and wall extensibility in relation to the mechanism of auxin-induced cell elongation, 25:10366 (RLO-2225-T-19-9)
WASHINGTON UNIV., SEATTLE. DEPT. OF PHYSICS.
Classical Schwinger terms, 25:9834 (RLO-1388-584)
Dual resonance theory with nonlinear trajectories, 25:9884 (COO-1764-90)
Loop diagrams in dual resonance theories with nonlinear trajectories, 25:9691 (RLO-1388-592)
Rules for constructing generalizations of Veneziano N-point function, 25:9885 (COO-1764-98)
WEATHER WING (4TH), ENT AFB, COLO.
Ionospheric electron density profile model, 25:9283 (AD-709888)
WESTINGHOUSE ELECTRIC CORP., PITTSBURGH, PA. NUCLEAR ENERGY SYSTEMS DIV.
Heavy section steel technology program. Technical report No. 11. Notch preparation in compact tension specimens, 25:8872 (WCAP-7579)
PWR FLECHT (Full Length Emergency Cooling Heat Transfer) Group II test report, 25:10229 (WCAP-7544)
WESTINGHOUSE ELECTRIC CORP., PITTSBURGH, PA. NUCLEAR FUEL DIV.
Prog. rpt. on Saxton Plutonium Project, 9/70, 25:10213 (WCAP-3385-25)
WESTON GEOPHYSICAL ENGINEERS, INC., MASS.
Connecticut Yankee Nuclear Power Plant, Unit No. 1. Reference plant design report. Includes Appendixes A and B, 25:10142 (DOCKET-50213-91)
WISCONSIN ELECTRIC POWER CO., MILWAUKEE.
Point Beach Nuclear Plant, Unit 1. Abnormal occurrence report: improper valve lineup for radioactive liquid release, 25:10124 (DOCKET-50266-37)
WISCONSIN UNIV., MADISON.
Cyclotron wave plasma studies, 25:9408 (COO-1789-1)
Prog. rpt. on plasma physics, 1970, 25:9503 (COO-1726-70)

Y

YANKEE ATOMIC ELECTRIC CO., WESTBORO, MASS.
Yankee Nuclear Power Station. Operation report No. 119, November 1970, 25:10113 (DOCKET-50029-141)

Z

ZENTRALINSTITUT FUER KERNPHYSIK, ROSSENDORF BEI DRESDEN (EAST GERMANY).
Technology of isotope production. I, 25:8429 (ORNL-tr-2400)

XUM

PERSONAL AUTHOR INDEX

Authors' names are indexed in the form appearing in the abstracted publication. Each entry under an author's name gives the publication title and the *NSA* volume and abstract numbers. Report numbers, where applicable, are given in parentheses at the end of the entry.

Because of problems involved in the mechanical preparation of this index, all accent marks are omitted. The following changes in spelling have been introduced to reduce some of the confusion which might result from omitting the accents:

Germanic	ä appears as	ae
Germanic	ö	oe
Germanic	ü	ue
Scandinavian	ϕ	oe

A

ABARBANEL, H. D. I., Magnitude of high-energy meson--meson total cross sections, 25:9773
ABBOSOV, O., Determination of Be by (γ,n) reaction in linac, 25:8225
ABDULLA, A. A., Determination of uranium content in geological samples by neutron activation, 25:8219 (PH-3)
Measurement of reaction $^{35}Cl(n,\gamma)^{36}Cl$ using a three-crystal pair and anti-Compton spectrometer, 25:10000 (PH-2)
ABE, Ryuji, Effect of γ irradiation on dielectric constants of KH_2PO_4, 25:8275
ABECASIS, S. M., Unique first forbidden β-transitions, 25:10064
ABEND, K., Position resolving detector bank for neutron scattering experiments, 25:8473 (JUL-CONF-4, pp 30-47)
ABOLINS, Maris A., Production and decay of eta and ω mesons in reaction $\pi^+d \rightarrow (p)p\pi^+\pi^-\pi^0$ between 1.1 and 2.4 GeV/c, 25:9675
ABO-SHAEER, Muhsin A. R., Dual amplitudes with cuts, 25:9899
ABRAMS, I. A., Determination of Be by (γ,n) reaction in linac, 25:8225
ABT, Helmut A., Rotational velocities in short-period A-type binaries, 25:9003
Rotational velocities in the Orion Nebula cluster, 25:8981
ACHAR, B. N. Narahari, Lattice-dynamical theory of diffusion process. I, 25:9589
ACKERMANN, G., Extreme red stars in Cygnus, 25:8991
ADAMEK, A., Complementary to 14-MeV neutron generator, 25:8579
ADAMOV, I. Yu., Microwave scattering by low-frequency oscillations in theta-pinch plasma, 25:9520
ADELBERGER, E. G., Stripping reactions $^{16}O(^3He,n)$ and $^{12}C(^3He,n)$, 25:9981
ADERHOLZ, M., Density matrix elements and parameters of resonances produced in π^+p and γp reactions, 25:9678
AGAFONOV, V. I., Fine structure of plasma focus using method of multiperforated pinhole camera, 25:9412 (LA-tr-70-25)
AGARWAL, G. S., Master-equation approach to spontaneous emission, 25:9244
AGNIHOTRI, P. K., Sintering of UO_2: relation between electrical conductivity and microstructure of sintered UO_2, 25:8908 (BARC-507)
AGRAWAL, G. S., Hydromagnetic stability of statically unstable heterogeneous shear flow, 25:9279
AGRAWAL, S. C., Hydromagnetic stability of statically unstable heterogeneous shear flow, 25:9279
AGUILAR-BENITEZ, M., New meson in 955-MeV mass region, 25:9683
AGULLO-LOPEZ, F., Anion-vacancy processes after F-light bleaching or irradiation of NaCl, 25:9559
AHLSTROM, Harlow G., One-dimensional laser heating of a stationary plasma, 25:9405
AHMAD, Masud, Pion photoproduction in Veneziano model, 25:9717
AHMAD, Mohammad, Cost economics of fertilizer complex, 25:10293
AHMAD, S. Y., Axial distribution of bulk temperature and void fraction in a heated channel with inlet subcooling, 25:8417
AHMED, M. R., Determination of uranium content in geological samples by neutron activation, 25:8219 (PH-3)
AHN, K. Y., Increase of Curie temperature in EuO films by Fe doping, 25:9587
AHNSTROEM, G., Killing and mutagenic action in E. coli associated with Auger effect during ^{125}I decay, 25:8654
AHRENS, L. H., Composition of stony meteorites. VIII, 25:8967
Composition of stony meteorites. VII, 25:8966
Composition of stony meteorites. VI, 25:8965
AIHARA, S., Production of quiescent plasmas with T/sub i/ > T/sub e/, 25:9483
AIHARA, Yoshinao, Surface excitation model of hadron resonances, 25:9808
AISCH, Dietrich E., Analytical model for the derivation of design parameters of dry containments and ancillary engineered safeguards of water reactors, 25:10232
AITKEN, E. A., Prog. rpt. on thermodynamic data program involving plutonia and urania at high temperatures, 5--7/70, 25:8926 (GEAP-12133)
AIZENMAN, Morris L., Early evolution of Population II stars. II, 25:9041
AKERMAN, M., Gammagraphy in the diagnosis of cerebral abscess, 25:8714
ALBIN, R., Effects of hypertrophy and hypoxia on the turnover of myocardial components, 25:10336 (ACRH-1000-214)
ALBRECHT, L., Classification of the new nuclear fuel elements for water-moderated reactors with regard to the regulations for the transport of radioactive materials, 25:8454 (SZS-14/70 (pp 11-21))
ALBRECHT, W., π^0 electroproduction at Δ(1236), 25:9625
ALBRIDGE, R. G., Conversion electron spectrum in decay of ^{195}Au, 25:10048
ALBROW, M. G., Elastic scattering of positive pions on polarized protons between 0.82 and 2.74 GeV/c, 25:9680
Experimental study of decay $K/sub\ L/^0 \rightarrow \pi^+\pi^-\pi^0$, 25:9630
ALDEA, L., Doppler effect of 6.24 eV resonance in ^{121}Sb, 25:10041
ALDERSON, T., Photosensitizing effect of 8-methoxypsoralen on inactivation and mutation of Aspergillus conidia, 25:8702
ALEKSANDROV, E. B., Certain misunderstanding concerning counting photon coincidences, 25:8518
ALEKSANDROV, Yu. M., Photoproduction of positive pions on protons in region of resonance $P_{33}(1236)$, 25:9623
ALEXANDER, Robert F., Nuclear power operations, Deep Freeze 69--70, 25:10297
ALEXANDROV, Yu. A., Coherent scattering amplitude of ^{184}W measured by small angle scattering, 25:10026 (JINR-E3-5371)
ALEXEFF, I., Reflection of pseudowaves, 25:9531
ALEY, Maxwell, Some financing approaches for small uranium operators, 25:8374
ALGER, D. M., University of Missouri Research Reactor Facility, 25:10273
AL-KAISSY, M. H., Measurement of reaction $^{35}Cl(n,\gamma)^{36}Cl$ using a three-crystal pair and anti-Compton spectrometer, 25:10000 (PH-2)
AL-KAYSI, B., Versatile and modular data acquisition system useful in nuclear experiments, 25:8483 (PH-1)
ALLER, L. H., Continuous spectrum of neutral helium from gaseous nebulae, 25:9046
ALLRED, John C., Prog. rpt. on pion interactions at medium energies, 25:9657 (ORO-3948-2)
ALPER, T., Inactivation of the scrapie agent by near monochromatic ultraviolet light, 25:8805
ALPER, Tikvah, Decrease in anoxic sensitivity, and resultant increase in O enhancement ratio, with decrease in energy of fast electrons, 25:8811
AL-QURAISHI, N. H., Measurement of reaction $^{35}Cl(n,\gamma)^{36}Cl$ using a three-crystal pair and anti-Compton spectrometer, 25:10000 (PH-2)
Versatile and modular data acquisition system useful in nuclear experiments, 25:8483 (PH-1)
AL-SHAHIRY, G. Y., Determination of uranium content in

geological samples by neutron activation, 25:8219 (PH-3)
ALSIS, M., French nuclear-powered pacemaker program, 25:8430
ALWASH, M. S., Measurement of reaction $^{35}Cl(n,\gamma)^{36}Cl$ using a three-crystal pair and anti-Compton spectrometer, 25:10000 (PH-2)
AMAGISHI, Yoshimitsu, Instabilities due to interaction between a slow electron beam and a plasma, 25:9447
AMANO, M., Effect of uv-irradiated vesicular stomatitis virus on nucleic acid synthesis in chick embryo cells, 25:8806
AMATO, Charles G., Heat discharges from nuclear reactors, 25:10090 (CONF-700335-1)
AMBRUS, Julian L., Strain and substrain differences in the recovery of thymus function after whole-body x-irradiation of mice, 25:8776
AMEY, E. A., Effect of erythropoietin in combination with radioprotective agents on erythropoietic recovery and survival in irradiated mice, 25:8775
AMMANN, A. C., A_2 meson production in K-d reactions, 25:9672
AMOS, A. T., Perturbed generalized eigenvalue equation for the helium atom, 25:9185
ANANDAN, N. S., Sintering of UO_2: relation between electrical conductivity and microstructure of sintered UO_{2+x}, 25:8908 (BARC-507)
ANANTHAKRISHNAN, S., Ozone screening heights deduced from sunrise effects at very low frequencies, 25:9331
ANASTASSIADES, M., Ionospheric observations during annular solar eclipse of May 20, 1966. IV, 25:9312
ANDERSEN, H. K., Q device, 25:9522
ANDERSON, A., Studies of the cellular radiosensitivity of transplants of murine ependymomas irradiated in vivo, 25:8759
ANDERSON, Alfred B., Studies in the single-center method, 25:9251
ANDERSON, C. A., TEPLO: heat conduction code for studying thermal explosions in laminar composites, 25:8961 (LA-4511)
ANDERSSON, G., Photomeson effects in (γ, n) and (γ,p)-reaction in light nuclei, 25:9977 (LUNP-7009)
ANDERSSON/ALMEHED, S., Elastic scattering of positive pions on polarized protons between 0.82 and 2.74 GeV/c, 25:9680
ANDREEV, E. A., Fast current preamplifier for operation in an electronic neutron collimation system, 25:8519
ANDREEVA, L. S., Sensitivity of spherical neutron detectors in energy range from thermal to 10 MeV, 25:8522
ANDREWS, J. G., Large-amplitude disturbances in a positive column, 25:9529
ANGEL, E., One sweep numerical method for vector-matrix difference equations with two-point boundary conditions. technical report no. 70-16, 25:10384 (TID-25609)
ANGELO, S., Improved of system for the loading and unloading of fuel elements in a nuclear reactor, 25:10331
ANGELOV, N., Determination of resonance production cross section in π^+p interactions at 2.34 GeV/c, 25:9662
ANOSOVA, Zh. P., Investigation of the dynamics of triple systems by the Monte Carlo method. III, 25:9007
ANTICH, P., Coherent anti pd interactions and related dissociation reactions at 7.0 GeV/c, 25:9636 (TID-25610)
Study of reaction $K^-n \rightarrow K^-\pi^-p$ at 12.6 GeV/c, 25:9658 (TID-25611)
ANTOINE, J. P., Charge operators in general quantum field theory, 25:9838 (NYO-3829-60)
ANTONUCCI, L., Disposal of the low activity solid waste, 25:10131
AONO, Osamu, High-frequency conductivity of nonequilibrium plasmas, 25:9463
AOYAMA, Hideyuki, Auxiliary equipment for a nuclear power generation turbine, 25:8399
APPEL, Kurt, Calculation of oscillator matrix elements, 25:10074
APPENZELLER, I., Mass loss rates for vibrationally unstable very massive main-sequence stars, 25:9023
APTE, V. P., Voltammetric study of molybdenum reduction, 25:8211
ARAI, E., Fast neutron study, 25:9995
ARAKAWA, E. T., Plasma radiation from electron-bombarded Be films, 25:9554
ARAKELYAN, M. A., Curve of growth for an expanding atmosphere, 25:9012
ARAVE, A. E., Ultrasonic liquid level detector using shear wave attenuation in a bar, 25:10267 (IN-1442)
ARENHOEVEL, H., Dynamic collective model of the giant resonance, 25:10083
ARGYROPOULOS, G. S., Two-dimensional distribution of current along magnetohydrodynamic channels, 25:9271
ARKING, R., $^7/_2^-$ isobaric analogue resonances in odd isotopes of Sb, 25:10044
ARMAN, I. P., Recovery phenomena in yeast. II, 25:8797
ARMANTROUT, G. A., Preamplifier noise effects on spectrometer energy resolution, 25:8532 (UCRL-72481)
ARMSTRONG, D. D., Analog states of ^{89}Sr, 25:10011
ARMSTRONG, R. J., D-region sunrise auroral rocket flight, 25:9296
ARNETT, W. David, Supernova light curves and presupernova models, 25:9038
ARNOLD, G. W., Lattice expansion and strain in ion-bombarded GaAs and Si, 25:8964
ARP, Halton, Faint outer regions of elliptical galaxies, 25:9139
ARPONEN, J., Rearrangement of Goldstone linked-cluster expansion for Fermi gas, 25:10075
ARSENAULT, R. J., Dynamic microplasticity of B.C.C. metals and solid solutions, 25:10349 (CONF-700545-1)
ARSEN'EV, A. A., Estimation of the energy width of a quasistationary level, 25:10081
ASBRINK, L., Photoelectron spectrum of H_2, 25:9199
ASBURY, J. G., Effects of thermal discharges on mass/energy balance of Lake Michigan, 25:10340 (ANL-ES-1)
ASBY, R., Evanescent waves and the electromagnetic field of a moving charged particle, 25:9613
ASCHENBRENNER, Vaclav, Effects of hypertrophy and hypoxia on the turnover of myocardial components, 25:10336 (ACRH-1000-214)
ASCOLI, G., Coherence of isoscalar and isovector exchange amplitudes in $\pi^+p \rightarrow A_2^+p$, 25:9650 (COO-1195-202)
ASHBY, George Elliott, Preparing microspheres, 25:8916
ASHLEY, R. W., Choice of bath materials for the inert gas fusion method for the determination of oxygen in metals, 25:8194 (AECL-3743)
ASKONAS, B. A., Selection of a single antibody-forming cell clone and its propagation in syngeneic mice, 25:8769
ASLAM, K. M., Bacteria-aided water leaching of uranium ores, 25:8337
ASLAM, M., Bacteria-aided water leaching of uranium ores, 25:8337
ASQUIEDGE, M., High temperature ceramic conductors and insulators, 25:8936
ASTON, D., Experimental study of decay K/sub L/$^0 \rightarrow \pi^+\pi^-\pi^0$, 25:9630
ATANASOV, A., Bound states of relativistic three-particle system, 25:9688 (JINR-P2-5336)
ATKINS, H. L., Oxygen enhancement ratio for protracted irradiation with ^{252}Cf, 25:8704
ATKINS, K. R., Possibility that pulses of long range field are source of CP non-invariance, 25:9826 (NYO-2171-329)
ATKINS, P. W., Interaction of molecular multipoles with the electromagnetic field in the canonical formulation of noncovariant quantum electrodynamics, 25:9842
ATLAN, Henri, Stimulating effects of ionizing radiation, thermal energy, and other environmental factors, 25:8742
ATROSHCHENKO, L. S., Distribution of concentration of film moving along walls of pipe in presence of magnetic field, 25:9277
ATWOOD, W., Antiproton--proton forward charge-exchange scattering, 25:9644
AUBERT, Jacques, Experimental study of liquid-vapor equilibrium of a UF_6--WF_6 hexafluoride binary mixture under a pressure of 2,600 torr, 25:8265
Experimental study of the UF_6--MoF_6 binary mixture under a pressure of 2,600 torr, 25:8264
AUERBACH, C., Determination of Ag, Cd, In, Sn, and Sb in Na solubility studies, 25:8198 (BNL-50271)
AUERBACH, H., Diurnal variation in labeling index of mouse epidermis, 25:8589
AUSTIN, Donald M., Regge-pole model for pp and anti pp elastic scattering at high energies, 25:9813
AUVIL, P. R., Building meson--baryon scattering amplitudes from duality, 25:9799
AVAKYAN, R. M., Models of static configurations, 25:9008
AVER'YANOV, V. N., High-frequency separator of particles, 25:9939
AVIGNONE III, F. T., V--A elastic scattering of electrons by fission antineutrinos, 25:9746
AXEL, Leon, Mass accretion and pulsational stability, 25:9040
AYYANGAR, K. M. M. S., Relative biological effectiveness of the $^{10}B(n,\alpha)^7Li$ reaction in HeLa cells, 25:8745
AZALBERT, Jean-Paul, Noble-gas closed MHD loop fired with fossil fuels, 25:9264
AZUMI, Masafumi, Improvement of l = 2 Stellarator and Torsatron, 25:9508
AZZONI, C. B., Analysis of electron-paramagnetic-resonance lineshape of Tb^{4+} in polycrystalline TbO_2, 25:9582
AZZOPARDI, Max, Elementary mechanisms of heterogeneous gas-solid kinetics, 25:10358 (ORNL-tr-2392)

B

BABADZHANOV, R., Lifetime of excited states in spherical nuclei ^{139}La, ^{138}La, and ^{133}La, 25:10029 (JINR-P6-5200)
BABIKOV, Yu. M., Thermophysical properties of organic coolants, 25:8412
BABUEL-PEYRISSAC, J. P., Radiative transfer in an LTE atmosphere, 25:9440
BACHMANN, P., Higher-order temporal and spatial plasma wave echoes, 25:9534
BACHNER, D., Multiwire spark and/or proportional chambers for the Bonn split-pole magnetic spectrograph, 25:8478 (JUL-CONF-4, pp 141-7)
BACKER, D. C., Correlated subpulse structure in PSR 1237 + 25, 25:9064
BADER, J. F., Estimating average nuclear fuel costs,

XUM

25:10216
BAEUERLE, D., Isotope splitting of F-center in-gap mode in KI and KBr, 25:9585
BAGGE, Erich, Finite field energies of point charges in a polarized vacuum, 25:9867
BAGGETT, Millicent Joan, Experimental test of time-reversal invariance in $\Sigma^0 + \Lambda^0 + e^+ + e^-$, 25:9829
BAHCALL, John N., Inferences from spectrophotometry of quasi-stellar sources, 25:9074
Quark fusion in quasi-stellar objects, 25:9075
BAIER, Peter, Electron diffraction patterns of Pb--Bi alloys at very low temperatures, 25:10410 (UCRL-Trans-1414)
BAIRD, George A., Energetic particles and radiation in polar cap, 25:9327
BAJARD, M., Method of calculatibn of trajectories of ions before injection into the proposed heavy-ion linear accelerator, 25:9911 (LYCEN-6949)
Parameters of ''Reflex''-type ion sources, 25:9912 (LYCEN-6953)
BAKANOVICH, G. I., Determining concentration of charged particles of pulsed plasma generator, 25:9416
BAKER, C. A., Photon activation analysis using electron linear accelerator at Harwell, 25:8216 (AERE-R-5363)
BAKER, H. C., Unitarity and fixed poles of weak amplitudes in a perturbation-theory model, 25:9898
BAKER, M., Dual resonance theory with nonlinear trajectories, 25:9884 (COO-1764-90)
Loop diagrams in dual resonance theories with nonlinear trajectories, 25:9691 (RLO-1388-592)
Rules for constructing generalizations of Veneziano N-point function, 25:9885 (COO-1764-98)
BAKER, P. S., Selected abstracts of world literature on production and industrial uses of radioisotopes (from NSA July--September 1970), 25:8428 (ORNL-IIC-30(Pt.3))
BALAMUTH, D. P., Sensitivity of (^{3}He,t) reaction to final-state configurations, 25:10013
BALASHOV, V. D., Analysis of variation of deformation processes of construction materials after reactor irradiation. I, 25:8898 (SRARI-P-85)
BALASHOV, V. V., Resonance photoionization of helium and helium-like ions, 25:9239
BALIAN, R., Distribution of eigenfrequencies for the wave equation in a finite domain. I. Three-dimensional problem with smooth boundary surface, 25:9604
BALL, J. A., Search for extraterrestrial $H_2{}^{18}O$ emission, 25:9076
BALL, James S., Production cross sections in the multiperipheral model, 25:9756
BALL, John A., Detection of methyl alcohol in Sagittarius, 25:9060
Search for excited state of OH in W3, 25:9093
BALL, S. J., Experiences with dynamic testing methods at Molten-Salt Reactor Experiment, 25:10182
Theoretical dynamics analysis of Molten-Salt Reactor Experiment, 25:10183
BALOGH, L., Radioactivity of honey, 25:8665
BALONA, L. A. de S., ESR in irradiated silicon carbide, 25:9545
BALUNI, V. Z., Sum rules for the ratio of the π^+--p scattering amplitudes, 25:9789
BANCEL, Daniel, Cauchy problem for the relativistic Boltzmann equation, 25:9843
BANCROFT, A. R., Water leak detectors, 25:10206
BANDO, Masako, Surface excitation model of hadron resonances, 25:9808
BANDO, Shoji, Choice of activable tracer for spraying agricultural insecticides by helicopter, 25:8426 (NSJ-tr-155)
BANDO, Y., Electrical properties of V_6O_{13} single crystal, 25:9580
BANERJEE, S. N., Radiation-induced division and mitotic delay studies in green algs (Oedogonium cardiacum), 25:8644
BANKSTON, C. A., Quasi-developed turbulent pipe flow with heat transfer, 25:8420
BAPTIST, J. E., Glucose-induced resistance to gamma-rays in E. coli, 25:8812
BAPTISTA, G., Decay schemes of ^{91}Mo and /sup 91m/Mo, 25:10057
BAQUEY, Ch., Radiolysis of 1 M aqueous ethanol solutions of potassium nitrate, 25:8301
BARABAS, B., Radioactivity of honey, 25:8665
BARABASH, L. Z., High-voltage pulse generator, 25:9932
High-voltage pulse source for the deflector plates in an ion cluster input system to the synchrotron chamber, 25:9931
BARAN, Vaclav, Possibility of luminescence of U/sub aq/$^{++}$ ion, 25:8267
BARANOV, V. B., Simulation of flow of interplanetary plasma, 25:9348
BARASHENKOV, V. S., Interaction cross sections of fast particles with tritium and ^{3}He nuclei, 25:9967 (JINR-P2-5335)
BARBASHOV, B. M., High-energy elastic and inelastic hadron collisions, 25:9751
BARBER, D. P., Experimental study of decay K/sub L/^{0} + $\pi^+\pi^-\pi^0$, 25:9630
BARISH, B., Antiproton--proton forward charge-exchange scattering, 25:9644
BARISIC, S., Electronic properties and superconductivity, 25:9382
BARKAT, Z., Evolution of growing stellar cores and presupernova models, 25:9006
BARKER, P. H., One-neutron transfer reactions with Be, C, and O nuclei, 25:9988
BARNES, Charles D., Effect of brain stem irradiation on descending systems to the spinal cord, 25:8771
BARNES, K. J., Schwinger terms and pseudoscalar mesons, 25:9833
BARNETT, A. R., Proton capture gamma decay to excited states of ^{14}O, 25:9979
BARNHAM, K. W. J., Kπ states produced in 10 GeV/c K$^+$p interactions, 25:9679
BARONENKO, V. A., Effect of ultraviolet irradiation on blood serum, 25:8782
BARR, R., Attenuation of radio waves propagating below inhomogeneous isotropic ionospheres, 25:9292
BARRETT, P. R., Effect of random fuel element displacement upon neutron reaction rates, 25:10319
BARRY, P. J., Use of ^{41}Ar to study dispersion of effluent from stacks, 25:8363 (AECL-3731)
BARSOVA, L. I., Formation and kinetics of accumulation of NO_2 radicals in γ-irradiated $BaSO_4$, 25:8286
BARTELS, K., Behavior of free-burning electric arcs in transverse magnetic fields and gas flows, 25:9282
BARTUNIK, H. D., Resonance spectroscopy of γ-radiation on Au(I) and Au(III) compounds, 25:9593
BARUFFA, A., Creation of an installation for enrichment of U in the European Community, 25:8435
BASARGIN, Yu. G., Monochromatization system for the external beams of the 2.4-m isochronous cyclotron, 25:9926
BASHILOV, V. A., Electron concentration behind shock-wave front, 25:9446
Structure of ionized gas flow in electromagnetic shock tubes, 25:9445
BASILADZE, S. G., Magnetic spark chamber spectrometer for K/sub L/^{0}--K/sub S/^{0} regeneration investigations at high energies, 25:8544 (JINR-P1-5361)
BASILOVA, R. N., Spatial distribution of singly charged particles and helium nuclei above the atmosphere in the equatorial region, 25:9349
BASS, W. T., Current nuclear level schemes: A = 91 to 117, 25:10031 (ORNL-4627)
BASSANO, D., New meson in 955-MeV mass region, 25:9683
BASSANO, Daniel Anthony, Magnitude of the K/sub L^0/--K/sub S^0/ mass difference and Ap interactions at high energies, 25:9631
BASTON, V. F., Release of radioiodine from open pools, 25:8450 (IN-1449)
BATALIN, I. A., Quantum electrodynamics in external fields. I, 25:9845
BATALIN, V. A., Beam regulation in a 100-MeV linear accelerator, 25:9914 (NP-tr-1926)
BATALLER, Simone, Radiation sealed x-ray diffraction camera, 25:8577
BATCHELOR, R. A., Observations of pulsar spectra, 25:9059
BATHOW, G., Discontinuous phase oscillations in particle accelerators, 25:9915 (SLAC-Trans-124)
BATON, J. P., Pi$^+\pi^-$ elastic cross section, 25:9669
Piν phase shifts, 25:9670
BAUCHINGER, M., Time wise behaviour of irradiation induced chromosome aberrations in humans, 25:8788 (LIB/Trans-296)
BAUDEL, L., Hα/[N II] ratio in Orion Nebula, 25:9028
BAUER, Henry, Scheduling of N tasks with M operations on two processors, 25:10383 (STAN-CS-70-165(App.2))
BAUGH, D. J., Angular correlation studies of the ^{42}Ca(α,pγ)^{45}Sc reaction, 25:9996 (ANU-P-466)
BAUM, J. W., Relative biological effectiveness of heavy ions in producing mutations, tumors, and growth inhibition in the crucifer plant, arabidopsis, 25:8800
BAUM, S. J., Hematopoietic recovery in irradiated dogs, 25:8774
BAUMANN, G., Pi$^+$-mesic decay of /sub Λ/^{4}He hyperfragment, 25:9633
BAUMANN, M., Stark-mixing signals in n = 3 term of singly ionized He, 25:9181
BAUSCH, H., Piston problems with ionizing shock waves, 25:9436
BAUTZ, L. P., Classification of the forms of clusters of galaxies, 25:9125
BAXENDALE, J. H., Pulse radiolysis study of transitory species Au II, 25:8306
BAYER, D. L., Bismuth-209 ground-state analog in ^{209}Po, 25:10045
BAZHENOV, A. A., Dipole gigantic resonances of nonmagic nuclei, 25:10069
BEASLEY, M. R., Apparent universal behavior of fluctuation-induced diamagnetism in superconductors, 25:9369
BEAUPRE, J. V., Density matrix elements and parameters of resonances produced in π$^+$p and γp reactions, 25:9678
BECHDOLFF, A., Pi$^+$-mesic decay of /sub Λ/^{4}He hyperfragment, 25:9633
BECK, R. J., Measurement of the broadening of silicon lines by electrons and hydrogen atoms, 25:9187
BECKER, H., Construction of a multiwire proportional chamber, 25:8479 (JUL-CONF-4, pp 148-64)
BECKER, Kurt M., Correlation for burnout predictions in vertical rod bundles, 25:8408 (CONF-660675-1)
BECKER, Martin, Average angle of scattering in energy-dependent problems, 25:9959

BECKER, R. R., Effect of univalent cations on circular dichroism of pyruvate kinase, 25:10369 (RLO-2227-T-5-4)
Prog. rpt. on properties of enzymes from thermomorphs and halophiles, 3 yrs, 4/1/68--12/15/70, 25:10367 (RLO-2227-T-5-1)
Prog. rpt. on properties of enzymes from thermomorphs and halophiles, annual, 12/69--12/70, 25:10368 (RLO-2227-T-5-2)
BECKER, W., Galactic halo in the direction to the northern galactic pole, 25:9144
BECKNER, E. H., Ion heating in the dense plasma focus, 25:9401
BEEZHOLD, Wendland, Localized modes and divacancy absorption in oxygen-ion-implanted Si, 25:9550
BEGGS, David Phillip, Ion--molecule reactions in gaseous hydrocarbon--silane mixtures, 25:8294
BEGZHANOV, R. B., Properties of excited states of ^{151}Sm, 25:10035
BEKETOV, G. V., Interaction $\pi^-\pi^-$ in the reaction $\pi^-p \to N^{*++}(1236)\pi^-\pi^-$ with impulse 4.47 GeV/c, 25:9655 (ITEF-767)
Reaction $\pi^-p \to rho^0\pi^-p$ with impulse 4.45 GeV/c, 25:9656 (ITEF-775)
Study of reaction $\pi^-p \to rho^0\pi^-p$ at 4.45 GeV/c, 25:9663
BEKIER, A., Diagnostic use of ^{89}Sr in the preoperative evaluation of non-union, 25:8720
BEKRENEV, V. S., Wire spark chamber system with magnetostrictive information retrieval, 25:8552
BELINSKII, V. A., Oscillatory approach to a singular point in the relativistic cosmology, 25:9877
BELITSKAYA, R. A., Biomedical problems of space flight, 25:8755 (JPRS-51660)
BELITZ, H. J., Elliptic boundary value problem in plasma physics, 25:9456 (JUL-663-PP)
BELL, George I., Nuclear reactor theory, 25:10317
BELL, K. L., Comments on the photoionization of helium, 25:9205
BELL, Kenneth G., Uraninite-bearing contact metamorphic deposits, Heaths Peak, Carbon County, Wyoming, 25:8379
BELLI DONINI, M. L., Gamma irradiation of table grape variety hoanes, 25:8817
BELLMAN, Richard, Differential quadrature and long-term integration, 25:10389 (TID-25616)
Functional equations in theory of dynamic programming. XVII, 25:10388 (TID-25615)
Functional equations in theory of dynamic programming. XVIII, 25:10385 (TID-25612)
Generalization of continued fractions and estimation of some integrals, 25:10386 (TID-25613)
Note on the asymptotic behavior of solution of nonlinear differential equations, 25:10417 (USCEE-344)
Truncation and preservation of moment properties for Fokker--Planck moment equations, 25:10387 (TID-25614)
Use of splines with unknown end points in the identification of systems, 25:10390 (TID-25617)
BELOTSVETOV, A. E., Communication system between a scintillation hodoscope and Minsk-22 computer, 25:8560
BELOV, D. G., Effect of electron bombardment on luminescence of ZnS--Cu phosphor, 25:8485
BEL'SKAYA, E. A., An experimental study of the thermal conductivity of high-porosity graphitic carbon, 25:8942
BELYAEVSKII, L. V., Communication system between a scintillation hodoscope and Minsk-22 computer, 25:8560
BENAVENTE, Carmen Marin, Photogeology uses in exploration of uraniferous deposits, 25:8375
BENCINI, M., Factors influencing haematopoietic spleen colony formation in whole-body irradiated mice. I, 25:8765
BENDER, D. J., The FREADM-1 code: a fast reactor excursion and accident dynamics model, 25:10241 (GEAP-13608)
BENEDETTO, A., Computer dosimetry of the radioiridium castings, 25:8684
BENEDIKTOV, E. A., Variations in mean level of radio emission at 1.1 and 2.3 MHz, 25:9352
BENENSON, W., Bismuth-209 ground-state analog in ^{209}Po, 25:10045
BENESOVSKY, F., Plasma spraying of tungsten, 25:8855
BENFATTO, G., K anti K π final states for N anti N annihilation at rest in Veneziano language, 25:9765 (NP-18578)
BENGTSON, Kurt Lennart, Third sound in superfluid helium, 25:9360
BENSINGER, J., Bubble chamber measurement of eta'(960) $\to \gamma\gamma$ and eta'(960) $\to \pi^0\pi^0$eta (eta $\to 3\pi^0$) decay rates, 25:9666
BENTON, C. U., Technique for obtaining neutron radiographs in the resonance region, 25:8442
BENZEL, Martin, Assembly for closing an aperture, 25:8403
BEREGI, P., Exactly soluble three-body model of resonance scattering, 25:9890
BERENDT, Richard F., Effect of Na fluorescein and plating medium on recovery of irradiated E. coli, 25:8807
BEREZHETSKII, M. S., Possibility of measuring directed fluxes in a plasma contained in a toroidal magnetic trap, 25:9410 (CTO-736)
BEREZHNYI, V. L., Microwave scattering by low-frequency oscillations in theta-pinch plasma, 25:9520
BERG, Chr, Linear ratemeter with noise suppression, 25:8503
BERG, R. E., $n\pi^-\pi^-$ enhancement at 1.627 GeV/c^2 in K-d $\to$ p/sub s/$\pi^+\pi^-\pi^-$n anti K^0 GeV/c, 25:9671
BERGER, R., French nuclear-powered pacemaker program, 25:8430
BERGSTRESSER, Karl S., Controlled-potential coulometric and potentiometric titrations of uranium and plutonium in ceramic-type materials, 25:8200 (LA-4537)
BERLAD, G., Vector-meson dominance in photoproduction, 25:9723
BERMAN, S. M., Connection between inelastic proton--proton reactions and deep inelastic electron scattering, 25:9805
BERNAOLA, O. A., Fast drying shippable protective cover for radioactive decontamination, 25:8663
BERNARD, A., Spectroscopic measurement of the electron temperature of a plasma in the vacuum uv, 25:9407 (CEA-N-1391)
BERRY, H. G., Observations of He II n = 3 to 5, 3204-A transition, 25:9182
BERTOLA, Francesco, Faint outer regions of elliptical galaxies, 25:9139
BERTON, Yves, Decontaminating radioactive effluents, 25:8344
BESKORSKII, A. I., Miniature end window counter for soft beta-radiation, 25:8521
Portable internally loaded counter for measuring low levels of gas activity, 25:8520
BESPALOVA, T. V., Magnetic spark chamber spectrometer for K/sub L/^{0}--K/sub S/^{0} regeneration investigations at high energies, 25:8544 (JINR-P1-5361)
BESSHAPOSHNIKOV, A. A., Spectrum of scattered laser radiation and the measurement of electron density in a pulsed plasma, 25:9409 (CTO-733)
BESSIS, Marcel, Partial cell irradiation by uv and visible light, 25:8744
BESSON, Jean, Elementary mechanisms of heterogeneous gas-solid kinetics, 25:10358 (ORNL-tr-2392)
BETHE, Hans A., Theory of nuclear matter, 25:10080
BETHOUX, O., Superconducting materials, 25:9386
BETTY, Robert Warren, Radiation-initiated homogeneous grafting of styrene to benzylcelluiose, 25:8271
BEYER, H. D., Correlation between effective diffusion coefficient and porous structure in nuclear graphite, 25:8924 (DP-Report-437)
BEYER, J. B., Cyclotron wave plasma studies, 25:9408 (COO-1789-1)
BEYNON, T. D., Behaviour of a neutron pulse in the vicinity of an inelastic threshold, 25:10315
BEZUGLYI, P. A., Absorption of ultrasound by superconducting Sn, 25:9365
BHADRA, Dilip K., Trapped-particle effect on drift-wave instability in toroidal systems, 25:9490
BHARGAVA, V. K., In-line analytical methods for fuel reprocessing streams. I, 25:8197 (BARC-510)
BHATIA, P. K., Collisional effects on Rayleigh--Taylor instability in composite medium, 25:9502
BHATTACHARYA, Purabi, Energy gap in nuclear matter and velocity-dependent nucleon--nucleon interaction, 25:10066
BIALYNICKI-BIRULA, I., Renormalization, diagrams, and gauge invariance, 25:9859
BIBERMAN, L. M., Nonequilibrium low-temperature plasma. III, 25:9435
BIBLARZ, Oscar, Analysis of optimum charged-particle size of EGD generators, 25:9262
BIGELEISEN, Jacob, Isotope separation practice, 25:8328
Theoretical analysis of chemical isotope fractionation by orthogonal polynomial methods, 25:8335
BIJAOUI, A., Short-period variable stars. III, 25:9035
BINDER, K., Total coherent cross sections for the scattering of neutrons from crystals, 25:9958
BINFORD, F. T., Some techniques for estimating the results of the emission of radioactive effluent from ORNL stacks, 25:8452 (ORNL-TM-3187)
BINON, F., Antideuteron absorption cross sections on nuclei Li, C, Al, Cu, and Pb at 25 GeV/c, 25:9639
BIRGE, R. W., Study of Σ (1915) resonance in reaction K-p $\to$ $\Lambda \pi^0$, 25:9659 (UCRL-19789)
BIRNBAUM, M. R., SPECTRE: finite difference program for calculating dynamic response of cylindrical shell, 25:10380 (SCL-DR-70-108)
BIRULEV, V. K., Magnetic spark chamber spectrometer for K/sub L/^{0}--K/sub S/^{0} regeneration investigations at high energies, 25:8544 (JINR-P1-5361)
BISSINGER, G. A., Low-lying levels of ^{20}F, 25:10004
BISWAS, N. N., Reactions $\pi^-p \to p\pi^-MM^0$ and $\pi^-p \to p\pi^+\pi^-\pi^-MM^0$ at 8 GeV/c, 25:9676
Study of $\Delta^{++}(1236)$ + boson production in π^+p interactions at 18.5 GeV/c, 25:9677
BIYAJIMA, Minoru, Lagrangian formulation of dual resonance model, 25:9696
BJOERLYKKE, K., Autoradiography of neutron-activated rock slabs, 25:8234
BLACK, J. L., Search for the 3446 keV level in ^{29}P via the ^{28}Si(p,γ) reaction, 25:10016 (ANU-P-503)
Systematic search for the lowest T = 2 state of ^{12}C using deuteron and ^{3}He induced reactions, 25:9972 (ANU-P-496)
BLACKER, Peter Thomas, Improvements in reactors, 25:10200
BLAKE, E. R., Toxicity and radiosensitizing activity of triacetoneamine-N-oxyl, 25:8701
BLANC, Claude, Process for separating isotopic compounds by

XUM

absorption, 25:8343
BLANC, G., Structural stability of austenitic Cr--Ni stainless steels to deformation and extremeley low temperature, 25:10357 (ORNL-tr-2314)
BLANCHARD, Dennis C., THEMI: Monte Carlo generation of electromagnetic events, 25:9705 (SLAC-123)
BLANDAMURA, F., Instrument for measuring rate of change of RF frequency in particle accelerators, 25:9905 (CERN-70-28)
BLANKENBECLER, R., Relativistic eikonal expansion, 25:9897
BLICHERT-TOFT, M., Normal plasma cortisol values determined by a double isotope derivative technique, 25:8585
BLINKIN, V. L., Effect of delayed neutrons on the dynamic reactivity of a reactor originating during oscillations of the density of the fuel, 25:10305 (IAE-1955)
BLOCH, C., Distribution of eigenfrequencies for the wave equation in a finite domain. I. Three-dimensional problem with smooth boundary surface, 25:9604
BLOCH, Eugene, Finite-difference method for the solution of free-boundary problems, 25:9460
BLOCH, Peter, Gamma-ray spectrometric method using a lithium-drifted silicon detector to determine the antimony deposits in the lung in vivo, 25:8726
BLOCK, L. P., Conjugate photoelectron impact ionization, 25:9127
BLOCKER, N. K., Vela V and VI solar x-ray atlas. II, 25:9097 (LA-4454(Vol.2))
BLOECKER, W., Explicit solutions of half space problems in the two-group transport theory, 25:9619
BLOK, J., Internal source scintillation spectrometer, 25:8514
BLOMEKE, J. O., Design and safety considerations of shipping solidified high-level radioactive wastes, 25:8451 (ORNL-TM-2971)
BLOMER, R. J., Vacuum expectation values of some exponential operators, 25:9847
BLOMQVIST, I., Photoproduction of charged pions from nuclei, 25:9620 (LUNP-7007)
BLOOM, E. E., Effect of fast neutron irradiation on the creep-rupture properties of type 304 stainless steel at 600°C, 25:8897 (ORNL-TM-3169)
BLOOM, S. G., Ecological models applied to radionuclide transfer in tropical ecosystems, 25:8626
BLUM, F. A., Harmonic generation in cold nonuniform plasma, 25:9523
BLUM, P. W., Lyman-α scattering during the solar radiation period, 25:9108
BLUMENBERG, F. E., Multiwire spark and/or proportional chambers for the Bonn split-pole magnetic spectrograph, 25:8478 (JUL-CONF-4, pp 141-7)
BLYUMENFEL'D, L. A., Spectra of photoconductivity of green leaves and chloroplasts at a frequency of 10^{10} cycles per second, 25:10412 (UCRL-Trans-1427)
BOBELDIJK, C., Kink instability of a toroidal plasma column, 25:9492
BOCHAGOV, B. A., Composition and excitation energy of fissioning nuclei in irradiation of ^{209}Bi and ^{197}Au 1 GeV photons, 25:10037
BOCHAROV, V. N., Model experiment on diffusion of electrons in the magnetosphere, 25:9350
BODENSTEDT, E., Investigation of photon--photon angular correlations in atomic mercury, 25:9206
BOEHM, F., Atomic 2s/sub $^1/_2$/--1s/sub $^1/_2$/ transition, 25:9183
BOEHMER, H., Instability of electron beams in plasma, 25:9494
BOEHM-VITENSE, E., Convection in A and F stars and metallicism, 25:8989
UBVr colors of main-sequence stars, 25:8988
BOENING, K., Longitudinal magnetoresistance of neutron-irradiated copper, 25:9571
BOERGER, D., Determination of oxygen-to-uranium ratio in hypostoichiometric uranium dioxide, 25:8204 (RCN-128)
BOGATYREV, V. K., Use of ^{3}He counters in antineutrino experiments, 25:8550
BOGDAN, D., Beta-decay transitions $0^- \to 2^+$ and $0^- \to 0^+$ of the ^{166}Ho nucleus, 25:10050
BOGDANOV, S. G., Coherent double scattering of neutrons, 25:9963
BOGDANOVA, N., Changes in DNA template after x-ray irradiation in vitro, 25:8610
BOGDANOVA, V. I., Monochromatization system for the external beams of the 2.4-m isochronous cyclotron, 25:9926
BOGOLUBOV, N. N. Jr., Definition of quasi-averages, 25:9687 (ITF-70-58-P)
BOGOLYUBOV, N. N. Jr., Definition of quasi-averages, 25:9733 (ITF-70-52)
Obtaining the limiting relations for correlation averages, 25:9734 (ITF-70-53)
BOGOLYUBOV, P. N., Quasi-potential equations for spin particles of unequal mass, 25:9697
BOISDE, G., Corrosion tests on various materials in seawater up to 150°C, 25:10360 (ORNL-tr-2412)
BOKOV, O. G., Compton effect and power absorption by space charge, 25:9615
BOLEY, Forrest I., Hydromagnetic wave--particle beam interactions, 25:9455 (AD-705265)
BOLGAR, A. S., Evaporation rates of carbides of Ti, Zr, Hf, Nb, and Ta at high temperatures, 25:8929
BONIFACE, Cyril Edward, Plugging of defective tubes, 25:10330
BOOKHART, T. W., Compensating tool-path data in numerical control machine tapes, 25:8398 (Y-1750)
BOOZ, J., Energy dependence of the mean energy per ion pair at low electron energies, 25:9161 (LA-tr-70-24)
BORDUIN, L. C., Development of a fluidized-bed burner for processing Rover fuel, 25:8322 (IN-1423)
BORISENKO, A. I., Production of He nuclei at interactions of pions with energy of 60 GeV with heavy nuclei of emulsion, 25:9660
BORISOV, I. Ye., Portable internally loaded counter for measuring low levels of gas activity, 25:8520
BORMANN, M., Fast neutron flux measurements with stilbene-scintillator, 25:8509
BOROB'EV, Yu. A., Properties of ^{6}LiI(Eu) crystals at low temperatures, 25:8529
BOROVIKOVA, R. P., Methods of investigation of thermoelectric properties of semiconductors, 25:9590
BORRELLO, G., Factors influencing haematopoietic spleen colony formation in whole-body irradiated mice. I, 25:8765
BOSNJAKOVIC, B., Elastic scattering of positive pions on polarized protons between 0.82 and 2.74 GeV/c, 25:9680
BOTSULA, R. A., Twin star systems with atmospheres of zeta Aurigae eclipsing type, 25:8983
BOTTINO, P. J., Effects of simulated radioactive fallout buildup and decay on survival and yield of lettuce, maize, radish, squash, and tomato, 25:8796
BOUCHER, J. D., French nuclear-powered pacemaker program, 25:8430
BOUCHEY, G. D., Detection and location of leaking TRIGA reactor fuel elements, 25:10283
BOUDRY, Jean Claude, Processes for simultaneously purifying and concentrating plutonium solutions, 25:8338
BOUESC, Jacky, Potential distribution between electrodes of Faraday MHD tube, 25:9263
BOULESTEIX, J., Kinematic study of ionized hydrogen in NGC 4490-85, 25:8994
Mass distribution and a stellar population model in the spiral galaxy M 33, 25:9149
BOULWARE, David G., Classical Schwinger terms, 25:9834 (RLO-1388-584)
BOURASSEAU, D., Study of local thermodynamic equilibrium in the argon plasma jets, 25:9454
BOURNOT, Philippe, Potential distribution between electrodes of Faraday MHD tube, 25:9263
BOURNOT, Phillippe, Electric conductivity of Ar plasma in supersonic flow subjected to electric discharge, 25:9451
BOURRET, A., Electron irradiation of Fe and Ni, 25:9541 (CEA-CONF-1680)
Observation at very low temperatures of the annealing process in specimens with radiation defects, 25:9542 (CEA-CONF-1681)
BOUVIER, P., Disruption of star clusters through passing interstellar clouds investigated by numerical experiments, 25:9050
BOWCOCK, J. E., Direct-channel Regge poles as a means of treating the unphysical region in finite-energy sum rules, 25:9801
BOWEN, T., Kaon--nucleon total cross sections from 0.36 to 0.72 GeV/c, 25:9673
BOWERS, E., Finite-Larmor-radius equations for theta pinch, 25:9497
BOWRING, C. S., Measurement of the magnetic susceptibility of beryllium, 25:9578
BOYD, R. N., $^7/_2^-$ isobaric analogue resonances in odd isotopes of Sb, 25:10044
BOYER, R., Numerical experiments on photospheric line profiles, 25:9119
BOZZINI, A., Relative frequency of chlorophyll to morphological and sterility mutations induced in durum wheat, 25:8641
BRACE, L. H., Polar maximum of electron concentration at 1000-km altitude, 25:9317
BRAGARD, Leopold, Properties of irradiated ensembles, 25:9614
BRAMLETTE, T. Tex, Kinetic theory of wave propagation. I, 25:9527
Kinetic theory of wave propagation. II, 25:9533
BRANCH, David Reed, Solar magnesium isotopic abundance ratios, 25:9101
BRANSKY, I., Electrical properties and defect structure of ThO_{2-x}, 25:9577
BRAR, S. S., Cesium-137 in various Chicago foods (collection month, July 1970), 25:8659 (HASL-237, pp III.14-17)
BRASSE, F. W., π^0 electroproduction at Δ(1236), 25:9625
BRAUNDMEIER, A. J. Jr., Plasma radiation from electron-bombarded Be films, 25:9554
BRAUN-MUNZINGER, P., Investigation of (^{3}He,^{3}He) and (^{3}He,t) reactions on ^{10}B, ^{11}B, and ^{13}C, 25:9993
BREIZMAN, B. N., Influence of inhomogeneity of plasma on the relaxation of an ultrarelativistic electron beam, 25:9472
BREUS, T. K., Comparison of ionospheric features of planets in terrestrial group, 25:9355
Corpuscular flow and heating of the electron gas at E-layer altitudes, 25:9341
Sources of E-region heating, 25:9340
BRICMAN, C., anti KN elastic amplitudes between 1 and 1.3 GeV/c, 25:9667

BRILL, D. R., Quantization of general relativity, 25:9872
BRINKMAN, A., Internal source scintillation spectrometer, 25:8514
BRINKMAN, A. C., Satellite-borne instrument for the measurement of soft solar x rays, 25:8499
BRISAC, Michel, Improvements in protective closures, 25:8458
BRITT, H. C., Analog states of ^{89}Sr, 25:10011
BROCKWAY, D. V., Coherence of isoscalar and isovector exchange amplitudes in π^+-p + A_2^+-p, 25:9650 (COO-1195-202)
BRODERICK, John, Distribution functions of star clusters, 25:8971
BRODY, Burton Alan, Charge mobilities in superfluid helium under pressure, 25:9361
BROECKER, W. S., Geochemical studies on Cranberry and Sterling Lakes, 25:8350 (CU-2493-11, App.4)
Project Ross, 25:8351 (CU-2493-11, App.5)
BROECKER, Wallace S., Mixing and gas exchange rates in Experimental Lakes Area, Western Ontario, 25:8352 (CU-2493-11, App.6)
Prog. rpt. on geochemical studies on continental waters, annual, 10/70, 25:8346 (CU-2493-11)
BROIDA, H. P., Optical spectra observed during ion--molecule collisions, 25:9213
BROOKEMAN, Valerie A., Digital computer data acquisition, display, and analysis system for the gamma camera, 25:8725
BROOKS, C. B., Tunneling: an annotated bibliography with permuted-title and key-word index, 25:8444 (ORNL-HUD-17)
BROOKS, W. L., Radioactive fallout in air and rain, 25:8364 (AERE-R-6556)
BROSSET, C., Conference on science of ceramics, Ronneby Brunn, Sweden, 4/69. V, 25:8933
BROSZKIEWICZ, R. K., Errors in ferrous sulphate dosimetry, 25:8564
BROWN, Daniel G., Clinical and gross pathological findings in swine relative to late effects of mixed gamma-neutron and x-irradiation, 25:8773
BROWN, L. M., Characterization of alkoxy-derived yttria-stabilized hafnia, 25:8949
Study of neutron damage in Be-doped Cu, 25:8902
BROWN, Lowell S., Summing soft pions, 25:9783
BROWN, M., Deuteration in slow neutron radiography of biological media, 25:8709 (DP-1229)
BROWN, R., Spark source mass spectrometric survey analysis of air pollution particulates, 25:8208
BROWN, R. R., Energetic electron precipitation on water cluster ion population in D region, 25:9288
BRUBIDGE, G. R., Heavy elements in peculiar A stars, 25:8984
BRUECKNER, K. A., Convergence of the density gradient expansion for atoms, 25:9245
BRUES, A. M., Diurnal variation in labeling index of mouse epidermis, 25:8589
BRUGGER, R. M., Very intense neutron source, 25:9954
BRUMOVSKY, M., Neutron irradiation induced changes in mechanical properties of pressure vessel steel for A-1 nuclear power plant, 25:8900 (ZJE-90)
Neutron irradiation induced changes in mechanical properties of base material and welding joints of A-1 pressure vessel steel, 25:8901 (ZJE-91)
Radiation stability of steels for pressure vessels of Czechoslovak nuclear reactors, 25:8899 (ZJE-89)
BRUNDLE, C. R., Ionization and dissociation energies of HF and DF and their bearing on D_0^0 (F_2), 25:8251
BRUNET, Robert C., Box diagram for interaction of pseudoscalar bosons with spin-$^1/_2$ fermions, 25:9795
BRUNFELT, A. O., Autoradiography of neutron-activated rock slabs, 25:8234
BRUNINX, E., Measurement of fast neutron flux densities above 0.5 MeV by a simple moderation method, 25:8495
BRUNO, Fred P., Digital computer data acquisition, display, and analysis system for the gamma camera, 25:8725
BRUNSKILL, Gregg, Mixing and gas exchange rates in Experimental Lakes Area, Western Ontario, 25:8352 (CU-2493-11, App.6)
BRUSENTSEVA, S. A., Salt effects during pulse radiolysis of neutral water and alkali solutions, 25:8291
BRYAN, C. A., Mathematical simulation of groundwater transport of radionuclides at Hanford, 25:8345 (BNWL-SA-3494)
BRYANT, P. E., Effect of hypoxia on recovery from sublethal damage in Chlamydomonas, 25:8795
BRYANT, Pamela M., Derivation of working limits for continuous release rates of ^{129}I to atmosphere, 25:8681
BUCHANAN, C. D., Measurement of form factors for decay K/sub L/^{0} + $\pi\mu\nu$, 25:9629 (UCLA-1054)
Study of decay mode K/sub L/^{0} + $\pi^+\pi^-\pi^0$, 25:9628 (UCLA-1052)
BUCHANAN, James W., Radiation chemistry of phosphine--ammonia mixtures in gas phase, 25:8299
Use of phosphine as a free radical scavenger in the radiolysis of methyl iodide vapor, 25:8303
BUCHER, E., New first-order phase transition in high-purity ytterbium metal, 25:9588
BUCHL, R. A., Modified photon propagator in rho-dominance model, 25:9846
BUCKNER, M. R., Experiences with dynamic testing methods at Molten-Salt Reactor Experiment, 25:10182
BUECHE, G., Measurement of the orientation of the residual nucleus and several differential interaction cross sections in the reaction $^{56}Fe(d,p)^{57}Fe$, 25:9998 (NP-18439)
BUFFA, Anthony John Jr., Helium-3 elastic scattering (13- to 27-MeV) from several light nuclei, 25:9994
BUGG, W. M., Excitation of nuclear fragments following K-absorption by neon, 25:10012
BUHL, David, Molecules in the interstellar medium. II, 25:9071
BULDAKOV, L. A., Problems of plutonium toxicology, 25:8594 (LF-tr-41)
BULHAK, Z., Errors in ferrous sulphate dosimetry, 25:8564
BULIEN, D., Metabolic and hemodynamic disturbances in the liver subdued to extracorporeal perfusion, 25:8783
BURBA, David Alexander, Quantum theory of measurement, 25:9603
BURBIDGE, E. M., 3C 390.3: an N system with two emission redshifts, 25:9147
BURBIDGE, G. R., 3C 390.3: an N system with two emission redshifts, 25:9147
BURBIDGE, Geoffrey, Nature of galactic nuclei, 25:9130
BURESCH, F. E., Effect of cyclic fast neutron irradiation damage on modulus of rupture of BeO, 25:8959
BURFEINDT, H., Small momentum transfer π^+ production with linearly polarized photons, 25:9624
BURGER, Jacques, Numerical solution of the diffusion equation, 25:9468
BURKE, P. C., Electron scattering by atomic hydrogen using a pseudo-state expansion. III, 25:9208
BURNASHOVA, V. V., Investigation of Nb--Fe--Al and Nb--Co--Al systems, 25:8890
BURNETT, W. L., Grouting and materials control, Operation Flint Lock, 25:8962 (POR-4013)
BURNISTON, E. E., Linear integral equations for a certain class of H-functions applicable to the theory of neutron transport and radiative transfer, 25:9953
BUSCHHORN, G., Small momentum transfer π^+ production with linearly polarized photons, 25:9624
BUSCHOW, K. H. J., Crystal structure of Th_2Co_7, 25:8893
Erbium--copper system, 25:8887
BUSH, S. H., Materials for nuclear reactors, 25:8828 (BNWL-SA-3426)
BUSSIAN, A. E., Charged-particle multiplicities of proton--proton interactions between 90 and 800 GeV, 25:9638
BUSSON, N., High temperature ceramic conductors and insulators, 25:8936
BUSUOLI, G., Mixed radiation dosimetry with LiF (TLD-100), 25:8567
BUTIU, Doina, Radioactivity of honey, 25:8665
BUTLAND, A. T. D., Thermal neutron diffusion data and WIMS scattering models for light water, 25:10301 (AEEW-R-701)
BUUS, O., Normal plasma cortisol values determined by a double isotope derivative technique, 25:8585
BYAKOV, V. M., Notes on the properties of intermediate particles during radiolysis of aqueous oxygen solutions, 25:8293
BYERS, J. A., Noise suppression techniques in macroparticle models of collisionless plasmas, 25:9457 (UCRL-72604)
BYFIELD, John E., Studies on RNA and histone relationships during the synchronized Tetrahymena life cycle, 25:10400 (UCLA-12-788)
BYRNE, J., Energy dependence of proportional counter pulse-height resolution, 25:8505

C

CABANNES, F., Study of local thermodynamic equilibrium in the argon plasma jets, 25:9454
CABASSA, N., Lung scintiphotography with /sup 113m/In $Fe(OH)_3$ aggregates, 25:8721
CABELLA, A., Two years of operation of Eurochemic, 25:8327
CACHEUX, J. A., Ionizing radiation detector, 25:8498
CADEK, F. F., PWR FLECHT (Full Length Emergency Cooling Heat Transfer) Group II test report, 25:10229 (WCAP-7544)
CAELLI, W. J., Systematic search for the lowest T = 2 state of ^{12}C using deuteron and ^3He induced reactions, 25:9972 (ANU-P-496)
CAILLET, Claude, Hybrid solution of the space--time problems in power reactors, 25:10303 (CEA-CONF-1684)
CAILLET, Marcel, Elementary mechanisms of heterogeneous gas-solid kinetics, 25:10358 (ORNL-tr-2392)
CAIRNS, J. A., New end-window variable geometry x-ray proportional counter, 25:8510
CALDWELL, James, X- and Y-functions of Chandrasekhar, 25:9045
CALDWELL, P. K., Kaon--nucleon total cross sections from 0.36 to 0.72 GeV/c, 25:9673
CALLAHAN, A., Coherent anti pd interactions and related dissociation reactions at 7.0 GeV/c, 25:9636 (TID-25610)
Study of reaction K-n + K-π-p at 12.6 GeV/c, 25:9658 (TID-25611)
CALLAHAN, J. P., Time-dependent behavior of prestressed concrete pressure vessels, 25:10325 (ORNL-TM-3246)
CALLAN, C. G. Jr., Quark fusion in quasi-stellar objects, 25:9075
CAMBRAY, R. S., Radioactive fallout in air and rain,

XUM

25:8364 (AERE-R-6556)
CAMERON, A. G. W., Processes of nucleosynthesis, 25:8987
CAMPANI, E., Lamb shift in muonic helium ions, 25:9188
CAMPBELL, J. R., Elasticity of the I(2030), 25:9681
CAMPBELL, L. J., Superfluid vortex motion, 25:9359
CAMPBELL, William J., Use of selective ion exchange paper in x-ray spectrography and neutron activation. Application to the determination of gold, 25:8221
CAMPISE, A. V., Study of the response of the EBR-II plant protective system to hypothetical malfunctions in the reactor system. EBR-II Project, 25:10228 (ANL-7665)
CANIGGIA, A., Factors influencing haematopoietic spleen colony formation in whole-body irradiated mice. I, 25:8765
CANNING, Gerald P., Duality and factorization constraints on meson spectrum, 25:9896
CANO, Renato, Generation of harmonic EM wave at upper hybrid frequency in inhomogeneous plasma, 25:9521
CANT, J. Stanley, Assessment and treatment of endocrine exophthalmos, 25:8733
CANTO, L. F., Decay schemes of ^{91}Mo and /sup 91m/Mo, 25:10057
CAO, S., Two years of operation of Eurochemic, 25:8327
CAPELLMANN, Herbert, Incipient antiferromagnetism in scandium, 25:9591
CAPET, Henri, Device for the packing of radioactive material, 25:8456
CAPPS, Richard H., Meson--baryon consistency conditions from duality, 25:9792
CARBIENER, Wayne A., Prog. rpt. on applicability of existing data to analytical description of reactor accident, 7--9/70, 25:10238 (BMI-1890)
CARJAN, N., Beta-decay transitions $0^- \rightarrow 2^+$ and $0^- \rightarrow 0^+$ of the ^{166}Ho nucleus, 25:10050
CARLES, Maurice, Experimental study of liquid-vapor equilibrium of a UF_6--WF_6 hexafluoride binary mixture under a pressure of 2,600 torr, 25:8265
Experimental study of the UF_6--MoF_6 binary mixture under a pressure of 2,600 torr, 25:8264
CARLETON, N. P., Results of a search for optical pulsars, 25:9090
CARLEY-MACAULY, K. W., Processing in limited geometry. XVI, 25:8445 (AERE-R-5104)
CARLS, E. L., Engineering development of fluid-bed fluoride volatility processes. Part 16. A safety manual for the engineering-scale alpha facility, 25:8446 (ANL-7672)
CARLSON, Bengt G., Transport theory: discrete ordinates quadrature over the unit sphere, 25:9602 (LA-4554)
CARLSON, P. J., Backward rho$^+$ production in π^+p reactions at 5.2 GeV/c, 25:9665
CARLSON, Per J., High-energy hadron--proton elastic scattering, 25:9684
CARLSON, T. A., Eigenvalues, radial expectation values, and potentials for free atoms from Z = 2 to 126 as calculated from relativistic Hartree--Fock--Slater atomic wave functions, 25:9168 (ORNL-4614)
CARMONY, D. D., A_2 meson production in K$^-$d reactions, 25:9672
CARNAHAN, R. D., Dynamic microplasticity of B.C.C. metals and solid solutions, 25:10349 (CONF-700545-1)
CAROLAN, P. G., Measurement of magnetic field in a laboratory plasma by Thomson scattering of laser light, 25:9427
CAROUBALOS, C., Space radioastronomy of solar bursts at all frequencies, 25:9124
CARPENTER, C. P., Asymptotic electron capture in hydrogen, 25:9211
CARRIKER, R. C., Lead-alloying effects on the superconducting critical field curve of indium, 25:9380
CARROLL, John M., Radioactive scleral shell in the treatment of conjunctival tumors, 25:8731
CARRUTHERS, George R., Encapsulation of helical channel multipliers for space flight applications, 25:8489
CARSON, R., Coherent anti pd interactions and related dissociation reactions at 7.0 GeV/c, 25:9636 (TID-25610)
Study of reaction K$^-$n $\rightarrow$ K$^-\pi^-$p at 12.6 GeV/c, 25:9658 (TID-25611)
CARTER, Gary M., Alkali--alkali differential spin-exchange scattering. I, 25:9223
CARTMELL, John, Instrumentation of nuclear reactors, 25:10191
CARUSO, A., Energetic ions produced by subnanosecond laser pulses, 25:9484
CASALINA, Samuel L., Irradiating mushrooms and their growing soil, 25:8821
CASON, N. M., Study of Δ^{++}(1236) + boson production in π^+p interactions at 18.5 GeV/c, 25:9677
CASSABOIS, Georges, Accidental release of ^{131}I at UP 2 plant on October 2nd and 3rd 1968, 25:8657 (CEA-R-4008)
CASSANDRO, M., K anti K π final states for N anti N annihilation at rest in Veneziano language, 25:9765 (NP-18578)
CASSEN, Benedict, Liquid scintillation counting of /sup 113m/In conversion electrons in the presence of ^{3}H and ^{14}C, 25:8213
CASSIDY, Esther C., Development and analysis of techniques for calibration of Kerr cell pulse-voltage measuring systems. III, 25:10370 (SC-CR-69-3266)
CASTEEL, M. A., Two-dimensional distribution of current along magnetohydrodynamic channels, 25:9271
CASTI, John, Differential quadrature and long-term integration, 25:10389 (TID-25616)
CAUDRON, R., Study of tantalum--hydrogen system, 25:8885 (ANL-Trans-867)
CAUSSORGUES, C., Exchange excitation of 2s state of hydrogen in close collisions with protons, 25:9201
CAVALLINI, A., Mixed radiation dosimetry with LiF (TLD-100), 25:8567
CAVALLO, Giacomo Giulio Francesco, Pi^0 decay and the diffuse γ-background radiation, 25:9254
CAYLOR, J. D., Automatic sample changer for the beryllium analyzer, 25:8220 (Y-1744)
CEARLOCK, D. B., Mathematical simulation of groundwater transport of radionuclides at Hanford, 25:8345 (BNWL-SA-3494)
CECH, O., Diagnostic use of ^{85}Sr in the preoperative evaluation of non-union, 25:8720
CELINSKI, Z., Optimum number of load circuits in Hall-type MHD generator, 25:9265
CERMAK, J. O., Departure from nucleate boiling in rod bundles during pressure blowdown, 25:8418
CESARI, L., Factors influencing haematopoietic spleen colony formation in whole-body irradiated mice. I, 25:8765
CESCHIA, Mario, Polarization of antiprotons from low-energy anti p--p elastic scattering, 25:9646
CHABRERIE, J. P., Applications of superconductors in electricity technology, 25:9394
CHADWICK, K. H., Interpretation of the optical density-dose relationship in irradiated clear polymethyl methacrylate, 25:8273
CHAGNON, P. R., Low-lying levels of ^{20}F, 25:10004
CHALLINOR, R. A., Behavior of Arctic F region in winter, 25:9318
CHAMBERLAIN, G. E., Absolute measurement of differential cross sections for electron scattering in helium, 25:9222
CHAMBERS, W. H., Vela V and VI solar x-ray atlas. II, 25:9097 (LA-4454(Vol.2))
CHAMBON, Marcel, Processes for simultaneously purifying and concentrating plutonium solutions, 25:8338
CHAMPLIN, Jerry B. Francis, Transport of radioisotopes by fine particulate matter in aquifers, 25:8361
CHAN, C. H., Determination of $\pi\Lambda\Sigma$ and $\pi\Sigma\Sigma$ coupling constants utilizing Adler's consistency condition, 25:9812
CHAND, Ramesh, High-energy photoproduction of vector mesons in a quark model, 25:9713
CHANDRA, S., Effect of electric fields on F-region behavior, 25:9315
CHANDRASEKHARAN, E. S., In-line analytical methods for fuel reprocessing streams. I, 25:8197 (BARC-510)
CHANG, C. K., Na--Cs differential spin-exchange scattering, 25:9212
CHANG, J., Instability of electron beams in plasma, 25:9494
CHANG, Jen-shih, Large-sheath concept for continuum probe theory, 25:9429
CHANG, Shau-jin, Field-theory realization of the droplet model, 25:9860
CHANOWITZ, Michael S., Schwinger terms in fermion electrodynamics, 25:9852
CHANT, N. S., ^{20}Ne(p,t)^{18}Ne reaction as a test of the ^{18}Ne and ^{20}Ne wave functions, 25:10006
CHAPELLE, J., Study of local thermodynamic equilibrium in the argon plasma jets, 25:9454
CHAPMAN, J. W., Doubly charged mesons in anti pp annihilations into pions near 1.9 GeV/c, 25:9643
Rho--omega interference in anti pp $\rightarrow 4\pi$ at 1.6 to 2.2 GeV/c, 25:9647
CHAPPEL, C. I., Effect of gamma radiation on vitamin content of enriched flour, 25:8816
CHAPPELL, C. R., Efficiency measurements for channel electron multipliers, 25:8490
CHASE, R. C., Measurements of π^-p elastic scattering from 1.71 to 5.53 GeV/c, 25:9652 (COO-1764-112)
Pi$^-$p charge exchange at backward angles, 25:9674
π^-p charge exchange at backward angles, 25:9653 (COO-1764-113)
Reaction π^-p $\rightarrow n\pi^+\pi^-$ at high momentum transfer, 25:9654 (COO-1764-114)
CHASE, R. L., Digital rf pulse burst generator, 25:8575
CHATURANI, P., Pressure shocks in dissipative magnetogasdynamics, 25:9278
CHAU, W. Y., Gravitational radiation and the oblique rotator model, 25:9063
CHAUVET, Pierre, Decontaminating radioactive effluents, 25:8344
CHAVYCHALOVA, T. P., Optimum neutron irradiation conditions for radioisotope production, 25:8308
CHECHETINA, N. A., Miniature end window counter for soft beta-radiation, 25:8521
CHEKALIN, E. K., Interactions of flowing argon plasma in a channel with a transverse magnetic field, 25:9281
CHEKHOVSKII, V. Ya., Integrated hemispherical emissivity of zirconium carbide, 25:8931
CHEN, John C., Two-phase pressure drop for potassium with and without net vaporization, 25:8405 (BNL-13957)
CHEN, Joseph C. Y., Coupled equations for scattering and

rearrangement collisions, 25:9220
CHEN, K. W., Calibration of large neutron counter, 25:8512
CHEN, S. S., Vibration of a beam with motion-constraint stops, 25:10163 (ANL-7619)
CHEN, Sin-li, Large-sheath concept for continuum probe theory, 25:9429
CHERDANTSEV, P. A., Dipole gigantic resonances of nonmagic nuclei, 25:10069
CHERNOV, E. N., Sensitivity of spherical neutron detectors in energy range from thermal to 10 MeV, 25:8522
CHERVONSKAYA, N. V., Mitotic cycle in normal and irradiated cells of the human diploid strain WI-38, 25:8743
CHETVERIKOV, A. G., Spectra of photoconductivity of green leaves and chloroplasts at a frequency of 10^{10} cycles per second, 25:10412 (UCRL-Trans-1427)
CHEW, G. F., Magnitude of high-energy meson--meson total cross sections, 25:9773
CHEW, Geoffrey F., Hadron bootstrap: triumph or frustration, 25:9753
CHIEN, C. Y., Measurement of form factors for decay K/sub L/^{0} + $\pi\mu\nu$, 25:9629 (UCLA-1054)
CHIEN, C.-Y., Study of decay mode K/sub L/^{0} + $\pi^+\pi^-\pi^0$, 25:9628 (UCLA-1052)
CHIHARA, Tsutomu, Conformation therapy technique on 6 MeV linear accelerator in treatment of the carcinoma of cervix uteri, 25:8740
CHIN-FATT, C., Enhanced radiation from a theta-pinch plasma, 25:9448
CHIU, Charles B., Gribov--Pomeranchuk pole in Regge-pole residues, 25:9893
CHOUDHURY, S. Rai, Constraint on the universal function in electroproduction, 25:9720
CHOURAQUI, G., Excited states of ^{22}Ne, 25:10002
CHRIEN, R. E., Nonstatistical effects in reaction ^{163}Dy(n,γ)^{164}Dy, 25:10047
CHRISTEN, H., New aspects in the field of gamma irradiation plants, 25:8432
CHRISTIANSEN, J. P., VORTEX: 2-dimensional hydrodynamics simulation code, 25:8407 (CLM-R-106)
CHRISTODOULOU, Demetrios, Reversible and irreversible transformations in black-hole physics, 25:9153
CHU, David S. L., Planning of the first nuclear power project in Taiwan, 25:10089 (CONF-691020-3)
CHU, Frank Y., Alkali--alkali differential spin-exchange scattering. I, 25:9223
Alkali-alkali differential spin-exchange scattering. II, 25:9224
CHUBARYAN, E. V., Slow rotation of relativistic polytropic models, 25:9078
CHUDLEY, C. T., Thermal neutron diffusion data and WIMS scattering models for light water, 25:10301 (AEEW-R-701)
CHULICK, Eugene Thomas, Delayed neutrons from ^{3}He and ^{4}He induced fission of ^{238}U, ^{232}Th, and ^{209}Bi and from spontaneous fission of ^{252}Cf, 25:10056
CHUNG, Kwong T., Coupled equations for scattering and rearrangement collisions, 25:9220
CHUNG, Kyu Nung, Microscopic description of the absorption of bound pions, 25:9982
CHUPP, E. L., Gamma ray and neutron emissions from the sun, 25:9098 (MPI-PAE/EXTRATERR-48)
CHURCH, K., Meiosis in the grasshopper after x-rays, 25:8754
CHURCHWELL, E., Shapes of recombination lines at lambda3 cm in M 42, M 17, and IC 1795, 25:9060
CHURG, Antonie, Magnetic resonance spectrum of vibrationally excited OH and a prediction of the radio-astronomy spectrum, 25:8975
CHUSHKIN, Yu. V., Mechanism of gas release from ceramic nuclear fuels, 25:8958 (SRARI-P-73)
CISNEROS-PARRA, J. U., Apsidal motion in close binaries with and without mass exchange, 25:9033
CISSEL, D. W., Guidelines for sodium fire prevention, detection, and control: report of the Ad Hoc Committee on sodium fires, 25:8827 (ANL-7691)
CITTADINI, G., Factors influencing haematopoietic spleen colony formation in whole-body irradiated mice. II, 25:8767
CIULLI, S., Weight functions and subtractions in dispersion theory, 25:9895
CIZERON, G., Low--temperature tensile device for tests on mono- and polycrystalline microsamples, 25:8881
CLAIBORNE, H. Clyde, Activities of ANS-6 subcommittee on radiation shielding standards, 25:9538 (ORNL-TM-3251)
CLANCY, B. E., Chandrasekhar's method to deep penetration problems, 25:9951
CLARK, J. W., Ground state properties of alpha matter, 25:10070
CLARK, Willie E., Engineering materials list, 25:8396 (TID-4100(Suppl.61))
CLARKE, M. C., Inactivation of the scrapie agent by near monochromatic ultraviolet light, 25:8805
CLELAND, L. L., Experimental results on phase-locked loops with added nonlinearities, 25:10407 (UCRL-72390)
CLELAND, Robert, Macromolecule synthesis and wall extensibility in relation to the mechanism of auxin-induced cell elongation, 25:10366 (RLO-2225-T-19-9)
CLEMENT, Christophe, Decay schemes of ^{59}Fe and ^{192}Ir, 25:10032 (ORNL-tr-2345)
CLEMENTE, Gianfelice, Techniques for measuring gamma radioactivity in the human body, 25:8687
COCHRAN, J. A., Calibration and initial field testing of ^{85}Kr detectors for environmental monitoring, 25:8467 (BRH/NERHL-70-4)
COHEN, B. L., Reaction mechanism in (p,pn) reactions, 25:10005
COLA, M., Analysis of electron-paramagnetic-resonance lineshape of Tb^{4+} in polycrystalline TbO_2, 25:9582
COLE, David LeRoy, Kinetic investigation of metal ion hydrolysis and indicator reactions using a square wave dissociation field effect apparatus, 25:8240
COLEMAN, E., Measurements of π^-p elastic scattering from 1.71 to 5.53 GeV/c, 25:9652 (COO-1764-112)
Momentum spectra in high-energy Hadron-deuteron interactions, 25:9634 (COO-1764-115)
π^-p charge exchange at backward angles, 25:9674
π^-p charge exchange at backward angles, 25:9653 (COO-1764-113)
Reaction $\pi^-p \to n\pi^+\pi^-$ at high momentum transfer, 25:9654 (COO-1764-114)
COLEMAN, L. F., Effect of continuous spray operation on the removal of aerosols and gases in the containment systems experiment, 25:10256 (BNWL-1485)
Guidelines for sodium fire prevention, detection, and control: report of the Ad Hoc Committee on sodium fires, 25:8827 (ANL-7691)
COLEMAN, M., Behaviour of a neutron pulse in the vicinity of an inelastic threshold, 25:10315
COLES, B. R., Superconductivity and normal-state properties of Th--U alloys, 25:9389
COLGATE, Stirling A., Neutron-star formation, thermonuclear supernovae, and heavy-element reimplosion, 25:8998
COLLET, J., Lunar occultation satellite for high-resolution studies of cosmic x-ray sources, 25:9065
COLLEY, D. C., $K\pi\pi$ states produced in 10 GeV/c K^+p interactions, 25:9679
COLLIER, D. W., Snowplowing in a plasma rail gun, 25:9479
COLLINGHAM, R. E., Development and results of an electrically heated seven-pin bundle assembly for thermal hydraulic testing in liquid metals, 25:10207 (BNWL-SA-3286)
COLLINS, David C., Reduction of dimensionality in dynamic programming via the method of diagonal decomposition, 25:10419 (USCEE-377)
COMBET, H. A., Superconducting thin films, 25:9385
CONDO, G. T., Excitation of nuclear fragments following K-absorption by neon, 25:10012
CONES, H. N., Development and analysis of techniques for calibration of Kerr cell pulse-voltage measuring systems. III, 25:10370 (SC-CR-69-3266)
CONGDON, C. C., Secondary disease mortality in rat-mouse radiation chimeras, 25:8619
CONKLING, John Alexander, Alpha- and beta-deuterium isotope effects on the solvolysis of norbornyl brosylates, 25:8254
CONN, Robert, Monte Carlo investigation of time-dependent thermal neutron behavior in small, noncrystalline moderators, 25:10314
CONSTANTINESCU, M., Doppler effect of 6.24 eV resonance in ^{121}Sb, 25:10041
CONTI, P. S., Coarse analysis of the helium-weak B star iota Ori B, 25:8995
CONTI, Peter S., Presence of metallic line stars in young clusters, 25:9051
CONTOPOULOS, G., Preference of trailing spiral waves, 25:9138
CONVERSI, M., Muon pair annihilation and Hadron production by e^+, e^- colliding beams in GeV region, 25:9621 (NP-18581)
COOK, G. E., Semi-annual variation in the upper atmosphere during 1967 and 1968, 25:9304
COOK, J. D., Counter for the direct measurement of ^{55}Fe in blood and other liquid samples, 25:8466 (BNWL-SA-3624)
COOLEY, J. L., Effects of chronic irradiation and temperature on populations of aquatic snail Physa heterostropha, 25:8750 (ORNL-4612)
COON, D. D., Dual resonance theory with nonlinear trajectories, 25:9884 (COO-1764-90)
Loop diagrams in dual resonance theories with nonlinear trajectories, 25:9691 (RLO-1388-592)
Rules for constructing generalizations of Veneziano N-point function, 25:9885 (COO-1764-98)
COOPER, Edwin L., Bone marrow restoration of transplantation immunity in the leopard frog Rana pipiens, 25:8620
COOPER, J., Periodic phenomena in copper dissolution at constant current, 25:10404 (UCRL-19618)
COPE, Beth H., Some techniques for estimating the results of the emission of radioactive effluent from ORNL stacks, 25:8452 (ORNL-TM-3187)
COPPI, B., Anomalous plasma resistivity at low electric fields, 25:9443
COPPINGER, E. A., Formation of intimate oxide--carbon mixtures of fuel materials as an intermediate for carbide and nitride fuels, 25:8923
CORDES, O. L., Release of radioiodine from open pools, 25:8450 (IN-1449)
CORIOU, H., Corrosion tests on various materials in seawater up to 150°C, 25:10360 (ORNL-tr-2412)
CORTELLESSA, Paolo, Atmospheric gamma rays at balloon altitudes, 25:9305
CORTISSONE, C., Control of contaminated air in a reactor fuel element fabrication plant, 25:8695

CORUM, J. M., Time-dependent behavior of prestressed concrete pressure vessels, 25:10325 (ORNL-TM-3246)
COSMAN, E. R., Analog states of ^{89}Sr, 25:10011
COSTA, A., Radiation attenuation around medical Curietron-type radioactive probe, 25:8683
COSTA, P., Study of tantalum--hydrogen system, 25:8885 (ANL-Trans-867)
COSTES, Didier, Thermal shield for a reactor vessel, . 25:10199
COTTRELL, Wm. B., Prog. rpt. on nuclear safety, 9--10/70, 25:10244 (ORNL-TM-3212)
COUCHAT, Philippe, Neutron method of soil moisture measurement, 25:8570
COULTER, Philip W., Mass shifts of the K/sub s/ meson, 25:9778
COURANT, H. W. J., Pi-p charge exchange at backward angles, 25:9674
  π^-p charge exchange at backward angles, 25:9653 (COO-1764-113)
  Reaction π^-p → n$\pi^+\pi^-$ at high momentum transfer, 25:9654 (COO-1764-114)
COURVOISIER, Pierre, Isotopic exchange between hydrogen and liquid ammonia catalyzed by alkali amides, 25:8244
COWLEY, F. C., Riometer observations of radio-wave absorption in the antarctic ionosphere, 25:9324
COX, Donald Peyton, Calculations of cooling rates and spectral emission of gaseous nebulae, 25:8974
COX, E. L., University of Missouri Research Reactor Facility, 25:10273
COX, Ronald, ESR investigation of Li center in MgO, 25:9544
CRAWLEY, G. M., Bismuth-209 ground-state analog in ^{209}Po, 25:10045
CREAN, P. A., Calibration of large neutron counter, 25:8512
CRESP, Jean, Action of x-rays on the morphogenesis of buds in Salmacina incrustans, 25:8753
CREZE, M., Estimation of the parameters of galactic rotation and solar motion with respect to population I Cepheids, 25:9151
  Influence of the accuracy of stellar distances on the estimations of kinematical parameters from radial velocities, 25:9150
CRINQUETTE, J., Radiotherapeutic cardiomyopathy, 25:8708
CRISTY, G. A., Tunneling: an annotated bibliography with permuted-title and key-word index, 25:8444 (ORNL-HUD-17)
CRONIN, J. C., Afterglow studies in helium, 25:9417
CROOKS, G. B., Experimental evidence for the mechanism of charge transfer into continuum states, 25:9241
CROSS, Marian, Nitrous oxide as a sensitizer of bacterial spores to x-rays, 25:8810
CROWE, C. R., Dynamic microplasticity of B.C.C. metals and solid solutions, 25:10349 (CONF-700545-1)
CUNNINGHAM, M. E., X-ray production in ion--atom collisions, 25:9164
CUPERMAN, S., Electron temperature in the two-component solar wind, 25:9114
CUPPS, F. J., SPECTRE: finite difference program for calculating dynamic response of cylindrical shell, 25:10380 (SCL-DR-70-108)
CURTIS, C. E., Thorium ceramics data manual. II, 25:8927 (ORNL-4503(Vol.2))
CUSHING, Vincent J., Hydro shock experiment, 25:8383 (AD-706767)
CZIRR, J. B., Scintillator solvents for pulse shape discrimination, 25:8504
CZYZ, W., Coulomb effects in high energy ^{4}He--^{4}He elastic scattering, 25:9715

D

DABOSI, F., High-temperature embrittlement of binary Mg--Zr alloy by hydrogenation, 25:8874
DADYKIN, V. L., Liquid scintillators for large scintillator detectors, 25:8527
DAENNER, W., Determination of operational thermal conductivity of ceramic nuclear fuel and heat transfer coefficient of fuel/can gap by balanced oscillator method, 25:10323 (EURFNR-774)
  Results of error analysis for in-pile thermal conductivity measurment using the balanced oscillator techniques, 25:10324 (EURFNR-775)
DAHL, Orin I., Production and decay of eta and ω mesons in reaction π^+d → (p)p$\pi^+\pi^-\pi^0$ between 1.1 and 2.4 GeV/c, 25:9675
DAKHNO, L. G., Pion scattering lengths from total probabilities of K → 3π decays, 25:9736
DAKIN, J. T., Calibration of large neutron counter, 25:8512
  Performance of large-volume two-phototube neutron detector, 25:8547 (PURC-4159-13)
DALLY, E., Measurement of form factors for decay K/sub L/^{0} → πμν, 25:9629 (UCLA-1054)
  Study of decay mode K/sub L/^{0} → $\pi^+\pi^-\pi^0$, 25:9628 (UCLA-1052)
DALTON, D. R., Electron spin resonance studies on neutral aromatic hydrocarbon radicals, 25:8252
DAMASCELLI, B., Concentrations of tritiated desacetyl-lanatoside C after injections in cardiopathic subjects, 25:8724
D'AMATO, F., Embryo--endosperm relations in irradiated water soaked seeds of durum wheat, 25:8655
DAMBURG, N. A., Application of cadmium filter in activation analysis with reactor neutrons, 25:8226
DAMON, Thomas D., Ionospheric electron density profile model, 25:9283 (AD-709888)
DANBURG, Jerome S., Production and decay of eta and ω mesons in reaction π^+d → (p)p$\pi^+\pi^-\pi^0$ between 1.1 and 2.4 GeV/c, 25:9675
DANBURG, Jerome Samuel, Reaction π^+d → (p)p$\pi^+\pi^-\pi^0$ at incident pion momenta between 1.1 and 2.4 GeV/c, 25:9664
DANIEL, E. E., Effects of altered external calcium concentrations on fluxes of ^{45}Ca in rat myometrium, 25:8601
DANIELS, Raymond D., Correlation of hydrogen evolution with surface blistering in proton-irradiated aluminum, 25:8905
DANILOV, V. N., Solutions of internal problem for a beam in a strong magnetic field, 25:9617
DANKS, A. C., Observations of the [S II] doublet 6717 A, 6731 A in Orion, 25:9020
DANOFSKY, R. A., Additional comments on the cross-spectral-density sink frequency behavior for coupled core Argonaut reactors, 25:10278
DANOFSKY, Richard A., Cross-spectral-density sink frequency behavior for coupled-core Argonaut reactors, 25:10275
DANOS, Michael, Microscopic description of the absorption of bound pions, 25:9982
DANSKIN, J. M., Asymptotic SU(3) symmetry, 25:9830
DANTEL, M., Short period variable stars. II, 25:9025
  Short-period variable stars. III, 25:9035
DAPKVIASHVILI, A. G., Mass-spectrometric investigation of low-temperature radiolysis of organic sulfides, 25:8290
DAS, K. P., Interaction among three extraordinary waves in a hot electron plasma, 25:9528
DAS, T. P., Indirect spin--spin coupling constant in HD molecule, 25:9180
DASHEN, Roger, Quark fusion in quasi-stellar objects, 25:9075
DATSCHEW, B., Some changes in the gingival connective tissue in acute radiation sickness, 25:8786
DAVENPORT, A. G., Response of Savannah River guyed stack under wind and earthquake action, 25:10391 (TID-25618)
DAVEY, J. E., Ion-implantation induced optical absorption edge shifts in GaP, 25:9562
DAVID, B., Behavior of some ion-exchangers, made in Romania, in the conditions of uranium hydrometallurgy, 25:8963
DAVIDSON, J., Rho--omega interference in anti pp → 4π at 1.6 to 2.2 GeV/c, 25:9647
DAVIDSON, W. F., Search for the 3446 keV level in ^{29}P via the ^{28}Si(p,γ) reaction, 25:10016 (ANU-P-503)
DAVIES, J. M., Homogenizing structures and mechanical properties of welding Zircaloy 2 tubes, 25:8844 (AERE-M-1561)
DAVIS, Michael A., Relative biological effectiveness of the ^{10}B(n,α)^{7}Li reaction in HeLa cells, 25:8745
DAVYDOV, E. F., Mechanism of gas release from ceramic nuclear fuels, 25:8958 (SRARI-P-73)
DE ANGELIS, A., Energetic ions produced by subnanosecond laser pulses, 25:9484
DE BAENST, P., Improvement on Kroll--Ruderman theorem, 25:9721
DEBARBAT, S., Polarization of continuum at the solar limb, 25:9109
DE BARROS, S., Decay schemes of ^{91}Mo and /sup 91m/Mo, 25:10057
DE CELLES, P. C., Gauge fields in the many-body problem and superfluidity, 25:9357
DECONNINCK, G., Fast neutrons in non-multiplying assemblies, 25:9956
DEGENHARDT, K. H., Modular program system for experimental programing for the PDP-9, 25:8572 (HMI-B-96)
DE GOEIJ, Jeroen Joannes Maria, Activation analysis of oxygen with the aid of tritium, 25:8218 (NP-18592)
DEHARVENG, J. M., Observations of faint extragalactic H II regions, 25:9143
DEIGHTON, M., Solubility of $M_{23}C_6$ in Type 316 stainless steel, 25:8875
DEKALB, Edward L., Quaternary oxide systems as hosts for x-ray excited optical fluorescence detection of rare earths in nuclear materials as the part per giga (part per 10^9) level, 25:8207
DE KERSGIETER, A., Hα-emission objects in two selected regions of southern Milky Way, 25:9032
DE KLERK, D., Influence of physical lattice imperfections on a type II superconductor, 25:9376
DELAND, R. J., Comparisons of observed concentrations of nuclides in the stratosphere with predictions by the Streak model, 25:8369 (HASL-237, pp I.38-62)
DELCLOS, Luis, Afterloading vaginal irradiators, 25:8736
DELCROIX, J. L., Establishment of a general rule for a hollow-cathode arc discharge, 25:9431 (SC-T-70-4050)
  Hollow-cathode discharges dependent on gas flow in arc operation, 25:9433 (SC-T-70-4053)
DELCROIX, Jean-Loup, New operation mode for a hollow-cathode arc discharge, 25:9432 (SC-T-70-4051)
DELISLE, Jean-Paul, Electromagnetic flow measurement device, 25:8400

DELLA ROCCA, C., Disposal of the low activity solid waste, 25:10131
DELMAS, Robert, Isotopic exchange between hydrogen and liquid ammonia catalyzed by alkali amides, 25:8244
DEL NERO, G. L., Analysis of electron-paramagnetic-resonance lineshape of Tb^{++} in polycrystalline TbO_2, 25:9582
DEL VECCHIO, E., Enzyme activities in rabbits after pan-irradiation, 25:8779
DEMAISON, Paul, Spacing grid for a nuclear reactor fuel element, 25:10332
DEMARQUE, Pierre, Early evolution of Population II stars. II, 25:9041
DEMEESTER, G. D., Charged-particle multiplicities of proton--proton interactions between 90 and 800 GeV, 25:9638
DEMETRIADES, S. T., Two-dimensional distribution of current along magnetohydrodynamic channels, 25:9271
DEMIDOVA, N. S., Causality function in a four-fermion model with an indefinite metric, 25:9741
DE MOTTONI, P., Logarithmic behavior in short-distance field products, 25:9865
DEM'YANENKO, G. K., Forming beams and beam parameters in output channels of 360-MeV electron linear accelerator, 25:9927
DE NEVE, R., Activation cross-sections, determined from second-order reactions, 25:10040
DENISENKO, V. P., Absorption of ultrasound by superconducting Sn, 25:9365
DENISOV, S. P., Antideuteron absorption cross sections on nuclei Li, C, Al, Cu, and Pb at 25 GeV/c, 25:9639
DENOYELLE, J., Hα-emission objects in two selected regions of southern Milky Way, 25:9032
DIONIGI, D. E., Factors affecting the optimum fuel cycle, 25:10233 (BNWL-SA-3605)
DE PINHO, A. G., Decay schemes of ^{91}Mo and /sup 91m/Mo, 25:10057
DER, R. C., X-ray production in ion--atom collisions, 25:9164
DEREVSHCHIKOV, A. A., Communication system between a scintillation hodoscope and Minsk-22 computer, 25:8560
DESBOROUGH, C. L., New end-window variable geometry x-ray proportional counter, 25:8510
DESER, S., Classical Schwinger terms, 25:9834 (RLO-1388-584)
  Gravitational--scalar field coupling, 25:9880
DESILVA, A. W., Magnetic piston-shock wave in collisionless plasma, 25:9452
DESISLE, Jean-Paul, Thermal shield for a reactor vessel, 25:10199
DESPOTAKIS, J. A., Computer based laboratory-wide data acquisition, analysis, and retrieval system, 25:8193 (UCRL-20132)
DETILLEUX, E., Two years of operation of Eurochemic, 25:8327
DE TOURNEMINE, R., Concerning an ordered solid solution of beryllium in U_3Si_2, 25:8947
  Ordered solid solution of Be in U_3Si_2, 25:8888
DEUTSCHMANN, M., Density matrix elements and parameters of resonances produced in π^+p and γp reactions, 25:9678
DEVAN, J. H., Examination of nickel heat pipes containing potassium, 25:8395 (ORNL-TM-3077)
DEVAULT, G. P., Very intense neutron source, 25:9954
DEVILLERS, Christian, Comparative performances of Monte Carlo and discrete ordinate one dimensional transport codes in an iron bulk shield calculation, 25:9536 (CEA-CONF-1669)
DEVLIN, T. J., Direct measurement of n--p and n--d total cross sections from 700 to 2900 MeV/c, 25:9648
DE VOS, M., Activation cross-sections, determined from second-order reactions, 25:10040
DEWEY, D. L., Action of atomic hydrogen, hydrated electrons, and ionizing radiation on bacteriophage T_7 in aqueous solution, 25:8808
DEW-HUGHES, D., Thermal conduction in irreversible, Type-II superconductors, 25:9370
DHANESHWAR, R. G., Voltammetric study of molybdenum reduction, 25:8211
DHARKAR, S. D., Radiation preservation of Chapaties, 25:8819
DIBELIUS, G., Stationary behavior of gas turbines in nuclear plants, 25:10251
DI BENEDETTO, Paolo, Atmospheric gamma rays at balloon altitudes, 25:9305
DICKENS, R. J., Photometry of RR Lyrae variables in globular cluster NGC 6171, 25:8970
DICKINSON, Deanne, Empirical model for safe pipe intersections containing fissile solution, 25:8459
DICKINSON, H. O., Total elastic scattering and spin-change cross sections for collisions between alkali atoms, 25:9202
DIDEIKIN, T. S., Determination of the reserve reactivity by the double over-compensation method, 25:10321
DIEFALLAH, El-Hussieny M., Chemical consequences of Auger effect: iodine yield from iodoamino acids as function of x-ray dose and energy, 25:8304
DIEHL, Hans Guenther, System UO_2--UO_3--$LaO_{1.5}$, 25:8943 (KFK-1235)
DIEHN, Bodo, Chemical consequences of Auger effect: iodine yield from iodoamino acids as function of x-ray dose and energy, 25:8304
DIERKS, R. D., Evaluation of hydroxylamine nitrate monitoring systems, 25:8199 (BNWL-CC-2502)
DIETZE, R., Methods of application of gamma emitters in contact therapy with regard to radiation protection, 25:8688 (SZS-6/70)
  Methods of application of gamma emitters, especially radio-gold-seeds in contact therapy with special regard to radiation protection, 25:8689 (SZS-6/70, pp 19-27)
DIKMEN, F. Nad, Kaon--nucleon total cross sections from 0.36 to 0.72 GeV/c, 25:9673
DILLEY, James, Restrictions on pion--pion scattering from crossing symmetry and unitarity, 25:9784
DILLON, R. S., Design and safety considerations of shipping solidified high-level radioactive wastes, 25:8451 (ORNL-TM-2971)
DILWORTH-OCCHIALINI, C., Lunar occultation satellite for high-resolution studies of cosmic x-ray sources, 25:9065
DIMICH, A. B., Computer-analyzed counting and scanning, 25:8716
DIRKS, Johan F., Generalized variational bounds on positron--hydrogen reaction matrix. I, 25:9216
DISNEY, Richard K., Implantable circulatory support system, 25:8436
DI TORO, M., Fine-structure analysis of isobaric analog resonances, 25:10073
DIVONA, C. J., Instrumented subassembly system in EBR-II, 25:10171
DIXON, W. G., Dynamics of extended bodies in general relativity. II, 25:9875
DJIRKOLOVA, T., Changes in DNA template after x-ray irradiation in vitro, 25:8610
DMITRIEV, V. F., O(2,1) algebra and H atom, 25:9179
DMITRIEVSKII, V. A., Use of uranium hexafluoride in nuclear power installations, 25:10221
DOAZAN, V., Envelope of the Be star HD 218393, 25:9017
  Study of Be stars: width of emission lines, 25:9034
DOBRESCU, S., Doppler effect of 6.24 eV resonance in ^{121}Sb, 25:10041
DOBROWOLNY, M., Influence of high-frequency electric fields on equilibrium and stability of toroidal plasmas, 25:9499
DOBRZANSKI, Z., Clinical value of liver function appraisal by means of ^{131}I-rose bengal. III, 25:8722
DODD, W. P., $K\pi\nu$ states produced in 10 GeV/c K^+p interactions, 25:9679
DODDS, Harold Lebron Jr., New calculational method for space--energy--angular dependent reactor kinetics, 25:10307 (ORNL-TM-3136)
DODSON, Ronald Franklin, Ultrastructural study of control and acute, whole body gamma-irradiated medulla oblongata tissue, 25:8787
DOGYUST, I. V., Photoproduction of the isobar A (1238), 25:9798
DOHERTY, R. H., Changes in D-region chemistry consistent with radio observations, 25:9297
DOI, Hideo, Effect of flow pattern in gaseous diffusion process, 25:8438
DOLGINOV, A. Z., Neutron polarization at the scattering on thick layers of matter, 25:9949
DOLYA, G. P., Electronic apparatus for rapidly identifying charged particles, 25:8530
DOMBRA, A. H., Water leak detectors, 25:10206
DOMINEY, Derek Alan, Improvement in nuclear reactors, 25:10201
DOMINICIS, D. P., PWR FLECHT (Full Length Emergency Cooling Heat Transfer) Group II test report, 25:10229 (WCAP-7544)
DONDES, S., Photochemical separation of the carbon isotopes, 25:8331
  Prog. rpt. on pulse radiolysis of gases, annual, 11/70, 25:8285 (RPI-3821-5)
DONDI, P. H., Schwinger terms and pseudoscalar mesons, 25:9833
DONNELLY, T. W., Inelastic electron scattering and supermultiplets in the particle--hole model for ^{12}C, ^{16}O, ^{28}Si, ^{32}S, and ^{40}Ca, 25:10010
DORNER, H., π^0 electroproduction at Δ(1236), 25:9625
DORSEY, Emerson L., Effect of Na fluorescein and plating medium on recovery of irradiated E. coli, 25:8807
DOSDAT, J., Superconducting materials, 25:9386
DOTHAN, Yossef, Finite-dimensional spectrum-generating algebras, 25:9698
DOVE, W. F., Magnetic piston-shock wave in collisionless plasma, 25:9452
DOVZHENKO, A. S., Potential danger of embrittlement for structures of steel 22K type, 25:8903
DOWNS, G. S., Interstellar scintillations of pulsar signals at 2388 MHz, 25:9091
DRAGO, A., Crushing behaviour of pyrocarbon coated fuel particles, 25:8925 (EUR-4501)
DRAGUN, G. S., Cosmic-ray mu-meson intensity meter, 25:8556
DRAPER, James E., Collective levels in ^{72} ^{74} ^{76} ^{78}Se, 25:10001
DRECHSEL, D., (3,3) resonance and nucleon pole for NN → NNπ, 25:9819
DREVINSKY, P. J., Impurity effects on annealing of radiation defects in p-type silicon, 25:9549
DREW, R. M., Oxygen enhancement ratio for protracted irradiation with ^{252}Cf, 25:8704
DRUCKREY, H., Neurotropic carcinogenic effect of phenyl--

XUM

dimethyl triazene on rats, 25:10362 (ORNL-tr-2418)
DRURY, J. S., Chemical fractionation of boron isotopes, 25:8329
DRUZHININ, V. P., Emittance of Re in range from 1200 to 2600° K, 25:8878
D'SILVA, Arthur P., Quaternary oxide systems as hosts for x-ray excited optical fluorescence detection of rare earths in nuclear materials as the part per giga (part per 10^9) level, 25:8207
DUBE, Shishir Kumar, Hydromagnetic flow near an accelerated flat plate, 25:9280
DUBENSKY, R. G., Fatigue behavior of molybdenum, 25:8861 (AD-709580)
DUBIS, Krystyna, Morpho-functional study of hypothalamic neurosecretion. VI, 25:8764
DUBOUT-CRILLON, R., Kinematic study of ionized hydrogen in NGC 4490-85, 25:8994
DUBOVIKOV, M. S., Decomposition of resonance states and determination of their quantum numbers, 25:9774
DUBOVOI, V. K., Volume gradient of γ-emf in p-Si, 25:9568
DUCASTELLE, F., Study of tantalum--hydrogen system, 25:8885 (ANL-Trans-867)
DUDZIAK, Donald J., Activities of ANS-6 subcommittee on radiation shielding standards, 25:9538 (ORNL-TM-3251)
DUFF, R. E., Chemistry of the Gasbuggy chimney, 25:8384 (PNE-G-68)
DUFFEY, D., Construction materials for neutron capture-gamma-ray measurement assembly using ^{252}Cf, 25:8537
DUGGAL, Shakti P., Cosmic-ray intensity variations in Antarctica, 25:9259
DUHM, H. H., Reaction $^{18}O(^3He,d)^{19}F$, 25:9985
DUMONT, S., Polarization of continuum at the solar limb, 25:9109
DUNBAR, Robert C., Method for studying ion--molecule collision and charge-transfer rates, 25:9233
DUNN, Jerry L., Fluorescence efficiencies of nitrogen excited by 1- to 5-MeV positive ions, 25:9234
DUNN, P. D., First British radioactive isotope powered thermoelectric generators, 25:8421 (AERE-M-1594)
DUPONT, F. M., Modification of the Saxonburg synchrocyclotron, 25:9920
DUPUY, David L., New observations of blue Haro galaxies, 25:9128
DURNEY, B., Differential rotation, meridional velocities, and temperature of rotating convective spherical shell, 25:9111
DUSHIN, L. A., Microwave scattering by low-frequency oscillations in theta-pinch plasma, 25:9520
DUTCHAK, Ya. I., Correlation between structure and electric conductivity of In--Sn, In--Zn, and In--Pb alloys in liquid state, 25:8882
DUTHIE, J. G., Accurate timing of light flashes from the pulsar in the Crab Nebula, 25:9089
DUTREIX, Andree, Radiation attenuation around medical Curietron-type radioactive probe, 25:8683
DUTTA, C. M., Indirect spin--spin coupling constant in HD molecule, 25:9180
DUTTA, N. C., Indirect spin--spin coupling constant in HD molecule, 25:9180
DUVALL, R. E., Elevated-temperature tensile tests of cast uranium-base dilute quinary alloys, 25:8867 (NLCO-1060)
DUWEZ, Pol, Radial distribution function of an amorphous Mn--P--C alloy, 25:10348 (CALT-822-21)
DWORSCHAK, F., Comparison of lattice-parameter and resistivity change in electron-irradiated aluminum, 25:9564
DWYER, A. J., Computer-analyzed counting and scanning, 25:8716
DYAL, P., Moon: global electromagnetic sounding using the solar wind, 25:9159
DYMOV, B. K., Integrated hemispherical emissivity of zirconium carbide, 25:8931
DZHAVRISHVILI, A. K., Characteristics and capabilities of a discharge--condensation chamber, 25:8551
DZIEDZIC-GOCLAWSKA, Anna, ESR study of bone tissue sterilized by gamma radiation, 25:8825
DZIERBA, A. R., Reactions $\pi^-p \to p\pi^-MM^0$ and $\pi^-p \to p\pi^+\pi^-\pi^-MM^0$ at 8 GeV/c, 25:9676

E

EASON, Charles F., AEC workmen compensation standards, 25:8697
EASTERDAY, R. J., Compensating tool-path data in numerical control machine tapes, 25:8398 (Y-1750)
EBERHARDT, J. E., High-resolution nuclear radiation detectors from epitaxial n-GaAs, 25:8491
EBERT, H. G., Energy dependence of the mean energy per ion pair at low electron energies, 25:9161 (LA-tr-70-24)
ECKARDT, V., Storing tracks in streamer chambers, 25:8543 (DESY-70/60)
ECKLUND, W. L., Riometer observations of radio-wave absorption in the antarctic ionosphere, 25:9324
EDER, O. J., Dynamical behavior of a chopper-rotating crystal system in a neutron time-of-flight experiment, 25:8533
EDMOND, John M., Radium in Indian--Antarctic Ocean south of Australia, 25:8380
EDWARDS, J. L., Prog. rpt. on formation of excited hydrogen atoms by charge transfer and dissociation, 12/69--11/70, 25:9192 (ORO-2591-51)
EDWARDS, V. R. W., Form factors for (d,p) and (p,d) reactions in the lead region, 25:10067
EGELAND, A., Ion-reflection of downward-propagating whistlers at low latitudes, 25:9321
EGGEN, O. J., Narrow- and broad-band photometry of red stars. V, 25:9002
EHRENBERG, L., Killing and mutagenic action in E. coli associated with Auger effect during ^{125}I decay, 25:8654
Mutagenic effect of ^{90}Sr in barley, 25:8648
EIBOFNER, A., Stark-mixing signals in n = 3 term of singly ionized He, 25:9181
EICHHORN, H., Influence of short-term activity releases into the atmosphere on the annual radiation burden in the environment of nuclear power plants, 25:8371 (SZS-14/70 (pp 1-10))
EICHNER, H., Position-sensitive proportional counter for measurement of β spectra, 25:8472 (JUL-CONF-4, pp 22-9)
EILAM, G., Vector-meson dominance in photoproduction, 25:9723
EINASTO, Ya. I., Andromeda galaxy M 31. I, 25:9141
EISENSTEIN, L., Coherence of isoscalar and isovector exchange amplitudes in $\pi^+p \to A_2^+p$, 25:9650 (COO-1195-202)
EISNER, J. H., State of development of advanced reactor fuel elements, 25:10101
EISNER, R. L., New meson in 955-MeV mass region, 25:9683
EKIVIN, V. V., Rapid fluctuations of intensity in the gamma radiation of a betatron, 25:9936
ELAKOV, L. S., Portable internally loaded counter for measuring low levels of gas activity, 25:8520
ELANGO, M., Role of mobile holes, anion vacancies, and excitons radioinduced coloration of KCl crystals, 25:9553
ELEN, J. D., Influence of physical lattice imperfections on a type II superconductor, 25:9376
ELISEEV, S. M., Interaction cross sections of fast particles with tritium and ^3He nuclei, 25:9967 (JINR-P2-5335)
ELKE, M., Biphasic scan in cirrhotic liver disturbances based on various physiological principals, 25:8715
EL-LAKANY, Mohamed Hosny Hassan, Studies on the effects of ionizing radiation on some western coniferous species, 25:8799
ELLIOTT, J. B., Automatic Van de Graaff voltage conditioner, 25:9930
ELLIS, P. J., RPA ground state correlations, 25:10076
ELLIS, Stephen, Hadrodynamics and quark structure, 25:9759
EL-MEKKAWI, L. S., Calculation of burnt fuel activity by optimization method, 25:10308
ELSTON, M. J. H., Method of superposition of temperature distributions in forced convection heat transfer experiments, 25:8409 (RD/B/N-1755)
ELY, R. P. Jr., Study of Σ (1915) resonance in reaction $K^-p \to A\pi^0$, 25:9659 (UCRL-19789)
EMERSON, Steve, Mixing and gas exchange rates in Experimental Lakes Area, Western Ontario, 25:8352 (CU-2493-11, App.6)
EMERY, A. F., SPECTRE: finite difference program for calculating dynamic response of cylindrical shell, 25:10380 (SCL-DR-70-108)
EMMERICH, W.-D., Timing with surface barrier detectors, 25:8517
EMMONS, A. H., University of Missouri Research Reactor Facility, 25:10273
ENGELS, J., Meson-exchanges in the isospin zero t-channel of pion-nucleon scattering, 25:9802
ENGEN, I. A., Catalog of rod-drop and transfer-function data from EBR-II runs 25 through 30A. EBR-II Project, 25:10173 (ANL-7542)
ENGLAND, Talmadge Ray, Fission-product behavior and decay heating in nuclear reactors, 25:10299
ENGLERT, Gerald W., Effect of coordinate space phenomena on end losses from, and distributions inside, magnetic mirror systems, 25:9406
ENSTROM, James E., Convergence of series expansion solution to Thomas--Fermi--Dirac equation, 25:9250
EPPLE, E., Multiwire proportional detectors, particularly for the detection of low-energy particles, 25:8477 (JUL-CONF-4, pp 121-40)
EPSTEIN, R. B., Bone marrow chimeras in man and animals, 25:8617
ERESHCHENKO, S. K., Limits on electric charge, magnetic moment, and monopole moment of the neutrino, 25:9737
ERIKSSON, G., Mutagenic effect of ^{90}Sr in barley, 25:8648
ERMAN, Peter, Differences in single, plural, and multiple scattering of electrons and positrons through intermediate angles, 25:9225
ERMINI, E., Design criteria and steel characteristics for reactor pressure vessels, 25:10197
ERO, I., Method of calculation of trajectories of ions before injection into the proposed heavy-ion linear accelerator, 25:9911 (LYCEN-6949)
EROKHIN, Yu. G., Measurements of the parameters of ionosphere by incoherent radiowave scattering, 25:9343
ERSHOV, B. G., Formation and kinetics of accumulation of NO_2 radicals in γ-irradiated $BaSO_4$, 25:8286
Kinetics of thermal and photostimulated extinctions of trapped electrons in γ-irradiated vitreous alkaline

ice, 25:8287
ERSHOVA, L. M., X-ray diffraction of ion-bombarded diamonds, 25:9557
ERWIN, A. R., Bubble chamber measurement of eta'(960) + γγ and eta'(960) + π⁰π⁰eta (eta + 3π⁰) decay rates, 25:9666
ESPAGNO, Lucien, Process for separating isotopic compounds by absorption, 25:8343
ESTABROOK, K., Reflection of pseudowaves, 25:9531
ETO, Terukazu, Drops of oxides on tungsten oxide needles and nuclei of dendritic crystals, 25:8859
EU, Byung Chan, Classical theory of scattering: three-body problems, 25:9231
EVANS, A. G., Construction materials for neutron capture-gamma-ray measurement assembly using ^{252}Cf, 25:8537
EVANS, D. E., Measurement of magnetic field in a laboratory plasma by Thomson scattering of laser light, 25:9427
EVANS, H. J., Effect of univalent cations on circular dichroism of pyruvate kinase, 25:10369 (RLO-2227-T-5-4)
EVANS, J. P., High temperature furnace for compatibility studies, 25:8389 (AERE-M-1990)
EVANS, S. K., Prog. rpt. on thermodynamic data program involving plutonia and urania at high temperatures, 5--7/70, 25:8926 (GEAP-12133)
EVERETT, M. R., Kinetics of carbon deposition reactions in high temperature gas cooled reactors, 25:10195 (DP-Report-500)
EVERS, William Henry Jr., Shock waves in a collision-free magnetoplasma, 25:9461
EVETTS, M. A., Sodium purification and general handling facility, 25:8390 (AERE-R-5502)
EVSYUKOV, E. P., Biomedical problems of space flight, 25:8755 (JPRS-51660)
EWALD, H., Mass spectrometer with energy dispersion, 25:8578
EWBANK, W. B., Current nuclear level schemes: A = 91 to 117, 25:10031 (ORNL-4627)
EWERT, Michael A., Effects of ionizing radiation on populations of Manitoba toads, Bufo hemiophrys, 25:8628
EWING, M. S., Observations of pulsar spectra, 25:9059

F

FABREGA, Serge, Statistical interpretation of uncertainty coefficients in thermal calculations for nuclear reactors, 25:10194 (CEA-R-3895)
FABRICIUS, K., Consequences of assumption that S-matrix commutes with axial charge, 25:9886 (DESY-70/57)
FAESSLER, Amand, Calculation of oscillator matrix elements, 25:10074
FAGER, D. N., Solid cadmium embrittlement: titanium alloys, 25:8879
FAHLESON, U. V., Operation of dc electric field detector, 25:9301
Parallel and perpendicular electric fields in an aurora, 25:9303
FAHR, H. J., Lyman-α scattering during the solar radiation period, 25:9108
FAHRNER, T., Launch and mission influences on space propulsion system design, 25:10289
FAIMAN, David, Use of simple-harmonic forces in the non-relativistic quark model, 25:9788
FAIRCHILD, R. G., Oxygen enhancement ratio for protracted irradiation with ^{252}Cf, 25:8704
FAIRCLOTH, R. L., Description of computer program ICON for calculation of fission product inventories, 25:10236 (AERE-R-6242)
FAIRHALL, A. W., Radiocarbon in the southern oceans, 25:8361
FAIRWEATHER, I. L., Polarization sensitivity of rectangular Li drifted silicon detector, 25:8508
FALTHAMMAR, C.-G., Conjugate photoelectron impact ionization, 25:9127
FANG, P. H., Analysis of dose-rate dependence of radiation injury, 25:8748
Impurity effects on annealing of radiation defects in p-type silicon, 25:9549
FANG WANG CH'IH, Relation of stable pulsations of the geomagnetic field with parameters of the magnetosphere, 25:9353
FARBER, M. S., Study of $\Delta^{++}(1236)$ + boson production in π⁺p interactions at 18.5 GeV/c, 25:9677
FARMAN, R. F., Departure from nucleate boiling in rod bundles during pressure blowdown, 25:8418
FAROOQUI, W. A., Inhibition of the germination in gamma irradiated onions, 25:8815
FASSEL, Velmer A., Quaternary oxide systems as hosts for x-ray excited optical fluorescence detection of rare earths in nuclear materials as the part per giga (part per 10^9) level, 25:8207
FASSO, A., Mixed radiation dosimetry with LiF (TLD-100), 25:8567
FATKULLIN, M. N., Seasonal anomaly phenomenon in middle-latitude topside F2 region, 25:9322
FAUGERAS, Pierre, Processes for simultaneously purifying and concentrating plutonium solutions, 25:8338
FAYYAZUDDIN, Pion photoproduction in Veneziano model, 25:9717
FEDOLOV, S. I., Non-rotational state of deformed nuclei with an odd number of neutrons in range 165 less than or equal to A less than or equal to 175, 25:10028 (JINR-P4-5228)
FEDORENKO, N. V., Electron binding energy in negative ion He^-, 25:9169
FEDOROV, V. K., Effect of training nervous processes on the weight of the brain and the cholinesterase activity, 25:10411 (UCRL-Trans-1424)
FEDOSEEV, I. A., Unitary representations of the conformal group, 25:9823
FEHLAU, P. E., Vela V and VI solar x-ray atlas. II, 25:9097 (LA-4454(Vol.2))
FEINBERG, S. M., High-flux stationary research reactors and their outlook, 25:10268 (LA-4399-TR)
FEINER, M., Accumulated fallout ^{90}Sr in the Rocky Flats area, 25:8353 (HASL-237, pp I.11-26)
FEIX, G., Correlation of the impulsive component of mm-bursts and the gradual rise of soft x-ray emission, 25:9121
FELBERBAUM, Joan, Internal logic manual for programmed communications controlled (PCC), 25:10343 (BNL-15437)
FELDER, R. M., Mott scattering cross section and the Goudsmit--Saunderson multiple scattering distribution for electron transport calculations, 25:10087
FELLINGER, M., Measurements of π⁻p elastic scattering from 1.71 to 5.53 GeV/c, 25:9652 (COO-1764-112)
FELT, R. E., Pyrochemical process for the reduction of plutonium dioxide to metal, 25:8236 (ARH-SA-72)
FENDER, J. R., Filled foam manufacturing and testing techniques, 25:10342 (BDX-613-252)
FENZL, H. J., Longitudinal magnetoresistance of neutron-irradiated copper, 25:9571
FERRARO, A. J., Observations of electron density during a solar flare, 25:9300
FERRO-LUZZI, M., anti KN elastic amplitudes between 1 and 1.3 GeV/c, 25:9667
FESENKO, V. V., Evaporation rates of carbides of Ti, Zr, Hf, Nb, and Ta at high temperatures, 25:8929
FETKOVICH, J. G., Fraction of stopped antiprotons which annihilate on free hydrogen in propane, 25:9645
FETTER, Alexander L., Low-temperature mobility of trapped ions in rotating He II, 25:9358
Low-temperature properties of a dense charged Bose gas, 25:9605
FETTWEIS, P., Fabrication of Ge(Li) detectors, 25:8463 (BLG-447)
FIALA, Werner, Simple total-reflecting low-energy neutron spectrometer, 25:8536
FIDONE, Ignazio, Generation of harmonic EM wave at upper hybrid frequency in inhomogeneous plasma, 25:9521
FIEGE, A., Observations of decline of interference in D_2O loop of multipurpose research reactor, 25:10243 (NP-18535)
FIELD, J. H., Transient overpower irradiation of axially-restrained, zero-burnup, fast reactor fuel specimens, 25:10208 (GEAP-13562)
FIELD, S. B., Measurement of LET spectra, 25:8492
FIERMANS, L., Characteristic energy loss studies of V_2O_5 and V, 25:9583
FIKS, M., Parameters of ''Reflex''-type ion sources, 25:9912 (LYCEN-6953)
FIKS, M. M., Electron--ion bunch diagnostics by bremsstrahlung, 25:9908 (KFK-tr-337)
FIL, V. D., Absorption of ultrasound by superconducting Sn, 25:9365
FILEVICH, A., Fast drying shippable protective cover for radioactive decontamination, 25:8663
FILIPCHUK, E. V., Control of nuclear power reactors. IV, 25:10190
FILIPPOV, S. S., Flow of fluids with temperature-dependent transfer coefficients in a flat channel, 25:9276
FILIPPOVA, N. V., Fine structure of plasma focus using method of multiperforated pinhole camera, 25:9412 (LA-tr-70-25)
FILIPPOVA, T. I., Fine structure of plasma focus using method of multiperforated pinhole camera, 25:9412 (LA-tr-70-25)
FILYUSHKIN, I. V., Sensitivity of spherical neutron detectors in energy range from thermal to 10 MeV, 25:8522
FINE, Arthur, Insolubility of the quantum measurement problem, 25:9612
FINK, C. L., Reaction mechanism in (p,pn) reactions, 25:10005
FINK, R. L., Computer based laboratory-wide data acquisition, analysis, and retrieval system, 25:8193 (UCRL-20132)
FINKEL, Asher J., Argonne radium studies, 25:8669 (COO-2088-1)
FIRSOV, E. I., Semiconductor gamma spectrometer, 25:8541
FISCHER, E. A., Physics investigations of steam-cooled fast reactor cores with a Pu-fueled central zone, 25:10258 (EURFNR-848)
FISCHER, J., Weight functions and subtractions in dispersion theory, 25:9895
FISCHER, R. P., Similarities, differences, and some genetic problems of the Wyoming and Colorado Plateau types of uranium deposits in sandstone, 25:8377
FISHER, E. M. R., Radioactive fallout in air and rain, 25:8364 (AERE-R-6556)
FISHER, H. L., Relationship of ^{210}Pb and short lived ^{222}Rn

XUM

daughter products, 25:8680
FISHER, P. S., Average cross-sections, 25:9923
FITTON, B., Scientific research in space science at ESTEC, 25:9336
FITZGERALD, Gordon M., Practical radiation protection and their factors, 25:8690
FITZWILSON, R. L., Formation of metastable hydrogen atoms by charge transfer, 25:9193 (ORO-2591-52)
Prog. rpt. on formation of excited hydrogen atoms by charge transfer and dissociation, 12/69--11/70, 25:9192 (ORO-2591-51)
FLACK, Herbert Paul, Preparing microspheres, 25:8916
FLEISCHER, R. L., Particle-track identification: application of a new technique to Apollo helmets, 25:9255
FLEISCHHAUER, Gerhard, Production of spherical oxidic or carbidic particles from heavy metal salt solutions, 25:8922
FLEROV, N. N., Increasing the power of a linear electron accelerator, 25:9938
FLETCHER, Gilbert H., Afterloading vaginal irradiators, 25:8736
FLETCHER, N. R., Line shape calculation for nuclear scattering from gaseous targets, 25:9924
FLEURY, P., Backward rho⁺ production in π⁺p reactions at 5.2 GeV/c, 25:9665
FLOREAN, R., Study of some problems of cavity resonators by means of finite differences, 25:9909 (LNF-70/17)
FLORIS, C., Embryo--endosperm relations in irradiated water soaked seeds of durum wheat, 25:8655
FLOYD, Brenda, Effects of simulated radioactive fallout buildup and decay on survival and yield of lettuce, maize, radish, squash, and tomato, 25:8796
FOERSTER, Walter, Gas determination in metals. I, 25:8205
FOLKESTAD, K., D-region sunrise auroral rocket flight, 25:9296
FOMENKO, V. N., Structure of paired states, 25:10051
FOMIN, P. I., Functional relationships for renormalizations in quantum electrodynamics, 25:9848
FOMINA, N. V., Radiation-thermal isomerization of alkyl bromides, 25:8279
FONTERAY, P. J., Heat exchange unit for a nuclear reactor, 25:10204
FORAGE, A. J., Decrease in anoxic sensitivity, and resultant increase in O enhancement ratio, with decrease in energy of fast electrons, 25:8811
FORBES, Jeffrey M., Yield of O(¹D) by dissociative recombination of O_2^+ from night airglow observations, 25:9314
FORD, J. C., Prog. rpt. on formation of excited hydrogen atoms by charge transfer and dissociation, 12/69--11/70, 25:9192 (ORO-2591-51)
FORD III, W. E., Neutron-induced secondary gamma-ray yield and cross section data, 25:9942 (CTC-42)
FORESTI, A., Concentrations of tritiated desacetyl-- lanatoside C after injections in cardiopathic subjects, 25:8724
FORKMAN, B., Photomeson effects in (γ, n) and (γ,p)- reaction in light nuclei, 25:9977 (LUNP-7009)
Photoproduction of charged pions from nuclei, 25:9620 (LUNP-7007)
FORMAN, L., Technique for obtaining neutron radiographs in the resonance region, 25:8442
FORMENTINI, A., Concentrations of tritiated desacetyl-- lanatoside C after injections in cardiopathic subjects, 25:8724
FORRESTIER, Bernard, Electric conductivity of Ar plasma in supersonic flow subjected to electric discharge, 25:9451
FORSEN, H. K., Scattering probability for fast test particles in a plasma, 25:9467
FORSLUND, D. W., Formation and structure of electrostatic collisionless shocks, 25:9437
FORTUNE, H. T., Sensitivity of (³He,t) reaction to final-state configurations, 25:10013
FOSTER, Kenneth, Instrumentation of nuclear reactors, 25:10191
FOSTER, R. F., Nuclear plants and the environmental ''crisis'', 25:10132 (BNWL-SA-3564)
FOTI, Guido, Operation of in-core detectors of Garigliano nuclear power plant, 25:10107
FOWLER, John David Jr., Superconducting tunneling in single crystal and polycrystalline thin films of tin, 25:9390
FOWLER, William A., How now, no cosmological helium, 25:9156
FOZZARD, J. A. F., Teratogenic activity of x irradiation, 25:8703
FRADKIN, E. S., Quantum electrodynamics in external fields. I, 25:9845
S matrix for Yang--Mills and gravitational fields, 25:9857
FRADKIN, G. M., Optimum neutron irradiation conditions for radioisotope production, 25:8308
FRAMPTON, Paul H., Hadrodynamics and quark structure, 25:9759
Quark focusing at hadronic vertices, 25:9760
FRANCHI, R., Lung scintiphotography with /sup 113m/In Fe(OH)₃ aggregates, 25:8721
FRANTSEVICH, V. M., Current generator for studying superconductivity by an impulse method, 25:8580
FRANZREB, J. K., Indexed bibliography of thermal effects literature--1, 25:10159 (ORNL-NSIC-81)
FRAUEN, L. L., Fatigue behavior of molybdenum, 25:8861 (AD-709580)
FRAUTSCHI, S. C., Eikonal Regge model for elastic scattering processes, 25:9776
FREEMAN, D. D., The FREADM-1 code: a fast reactor excursion and accident dynamics model, 25:10241 (GEAP-13608)
FREIDBERG, J. P., Stability of high-β, helically symmetric pinch, 25:9498
FRENCH, I. E., Effects of fast neutron irradiation on internal friction and Young's modulus of NaCl single crystals, 25:9547
FRENKEL, Eugene P., Bacteria as specific binding agents for an isotopic assay of serum folate, 25:8809
FRETTO, Larry, Effect of temperature upon conformations of carboxypeptidase A, A/sub γ//sup Leu/, A/sub γ//sup Val/, and A/sub α+β/, 25:10402 (UCLA-12-802)
Use of circular dichroism to study interactions of carboxypeptidase A (Anson) and A/sub α+β/ with substrates and inhibitors, 25:10401 (UCLA-12-801)
FREUND, Peter G. O., Hadrodynamics and quark structure, 25:9759
Quark focusing at hadronic vertices, 25:9760
FREVERT, Erich, Method for determining the content of cement in concrete, 25:8232
FREVERT, L., Modular program system for experimental programing for the PDP-9, 25:8572 (HMI-B-96)
FREYTAG, E., Discontinuous phase oscillations in particle accelerators, 25:9915 (SLAC-Trans-124)
FRIBERG, B., Photomeson effects in (γ, n) and (γ,p)- reaction in light nuclei, 25:9977 (LUNP-7009)
FRIDMAN, Sh. D., Method for separating γ radiation dose rate of artificial and natural radioactive isotopes in ground, 25:8360
FRIED, H. M., Summing soft pseudoscalar pions, 25:9782
FRIEDLANDER, Stanley, Hyperliptic magnetohydrodynamic steady flow past a point source, 25:9269 (AD-706106)
FRIEFELD, R. D., Observations of pulsar spectra, 25:9059
FRIEMERT, R., Quantitative alpha-autoradiography: a documentation, 25:8584 (SZS-15/70)
FRIES, J. F., Low--temperature tensile device for tests on mono- and polycrystalline microsamples, 25:8881
FRIESEN, B. S., Glucose-induced resistance to gamma-rays in E. coli, 25:8812
FRISCH, H., Coupling between radiative transfer and thermal conduction in the chromosphere, 25:9116
FRITZ, Rolf, Development and explanation of prototype fuel element for heavy-water-moderated and-cooled thorium breeder reactor, 25:10209 (JUL-654-RG)
FRITZE, K., Development of a star with 0.6 sun mass, 25:8978
FROEBRICH, Peter, Direct transfer reactions derived from Green's functions method, 25:10082
FROEMAN, Nanny, Energy levels of double-well potentials. II, 25:9248
FROMAN, Ernst, Fuel cartridge made of two separate parts to be introduced from the seat of a reactor, 25:10333
FRY, D. N., Experimental neutron flux-to-pressure frequency response for the Molten-Salt Reactor Experiment: determination of void fraction in fuel salt, 25:10177
FRYSHCHIN, B., Reaction $^7Li(d,n)^8Be$, 25:9975 (JINR-P15-5143)
FUCIK, Vladimir, Induction of segment extension and chromatid structural changes in Vicia faba chromosomes, 25:8639
FUELLE, R., Generalized DWBA model applied to $^{24}Mg(dp)^{25}Mg$ reaction at E/sub d/ = 13.5 MeV, 25:9997 (JINR-E4-5350)
FUIA, H., Beta-decay transitions 0⁻ → 2⁺ and 0⁻ → 0⁺ of the ^{166}Ho nucleus, 25:10050
FUJIMURA, Kimio, Dual resonance model and extended particle model with arbitrary number of quark--antiquark pairs, 25:9771
FUJINO, Takahiro, Effects of electron irradiation on conductivity in CdS, 25:9563
FUJIOKA, M., Excited states of ^{156}Gd, 25:10034
FUJIWARA, Kishio, Drops of oxides on tungsten oxide needles and nuclei of dendritic crystals, 25:8859
FUJIWARA, Kunio, Many-body theory for nearly free electrons and application to annihilation of positrons, 25:9606
FUKADA, Eiichi, Effect of gamma irradiation on the very dilute solution of collagen in the atmosphere of air and nitrogen, 25:8307
FUKATSU, T., Sintering and structure of TiC--Ni--Mo compacts, 25:8928 (UCRL-Trans-10505)
FUKAYA, Kiyoshi, Development of a device for measuring circumferential mechanical properties of cladding tubes, 25:8883
FUKUDA, Reijiro, Self-energy of leptons, 25:9714
FUKUSHIMA, Yutaka, Gamma-ray leakage through a junction between lead and concrete walls, 25:10296 (NSJ-tr-157)
FULLER, E. L. Jr., Gravimetric adsorption studies of thorium oxide. V. Water adsorption between 25 and 500°, 25:8266
FULLER, J. C., Vela V and VI solar x-ray atlas. II, 25:9097 (LA-4454(Vol.2))
FULS, G. M., Effect of bubble stabilization on pool boiling heat transfer, 25:8419
FURSOV, G. L., Determination of the critical current in a section with radial slots in the iris disk, 25:9907

(KFK-tr-335)
FURTH, H. P., Stellarator as a nonlinear plasma-current transformer, 25:9511
FURUICHI, Susumu, Two-pion exchange contribution to nucleon--nucleon scattering, 25:9807
FURUKAWA, George T., Heat capacity and thermodynamic properties of α-beryllium nitride, Be_3N_2, from 20 to 315 K, 25:8939
FYSTROM, Dell O., Magnetic moment of the proton, 25:9622

G

GAFFAROV, D. G., Properties of excited states of ^{151}Sm, 25:10035
GAGE, S. J., Detection and location of leaking TRIGA reactor fuel elements, 25:10283
GAHM, Goesta F., Mass loss from T Tauri stars, 25:9029
GAILLARD, Remi, Transient effects of radiation on diodes and bipolar transistors, 25:8581 (LYCEN-6933)
GAL'CHUK, A. V., Sextupole lenses with direct nonlinearity in slow ejection system, 25:9913 (NP-18594)
GALIMULLIN, V. N., Calculation of plane electron beam in intersected fields by Monte Carlo method, 25:9165
GALLO, Sabino, Thermal shield for a reactor vessel, 25:10199
GALONSKA, J. E., Calculation of oscillator matrix elements, 25:10074
GAMALYA, I. A., Dipole gigantic resonances of nonmagic nuclei, 25:10069
GAMBEL, D., Technique for afterloading implants using radioactive Ir wire, 25:8737
GAMO, Kenji, Enhanced diffusion of high-temperature ion-implanted antimony into silicon, 25:9569
GANAS, P. S., Realistic one-boson-exchange potentials and their applicability in the shell model of ^{18}O, 25:9992
GANDON, Remi, Accidental release of ^{131}I at UP 2 plant on October 2nd and 3rd 1968, 25:8657 (CEA-R-4008)
GANGULI, S. N., Study of hyper-fragments produced in high energy in tractions of pions and protons with emulsions, 25:9637
GANGULY, A. K., Beta decay of ^{239}Pu fission products, 25:10036
GANGULY, S., Nondissipative phenomena affecting A_1 absorption measurements, 25:9323
GANTOIS, M., Mechanisms of plastic deformation in a nickel--chromium--niobium alloy precipitation hardened at 700°C, 25:8884
GARBINCIUS, P. H., Range--energy relation in hydrogen, 25:9166
GARCIA, D. S., Launch and mission influences on space propulsion system design, 25:10289
GARCIA, W. J. Jr., Water waves produced by cratering explosions in shallow water, 25:8386 (UCRL-50940)
GARDINER, D. A., Secondary disease mortality in rat-mouse radiation chimeras, 25:8619
GARDNER, Angela, Physical and dosimetric aspects of the radiotherapy of malignant lymphomas. II. The inverted-Y technique, 25:8734
Physical and dosimetric aspects of the radiotherapy of malignant lymphomas. I. The mantle technique, 25:8735
GARFINKEL, A. F., A_2 meson production in K-d reactions, 25:9672
GARFUNKEL, M. P., Hypersound attenuation in superconductors by quasi-particle creation, 25:9368
GARI, M., Short-range correlations in a Woods--Saxon shell model, 25:10071
GARREN, A. A., Thin lens optics with space charge, 25:9916 (UCRL-19313)
GARRETT, D. A., Technique for obtaining neutron radiographs in the resonance region, 25:8442
GARRETT, N. E., Excitation of nuclear fragments following K- absorption by neon, 25:10012
GARSEVANISHVILI, V. R., Representation for relativistic scattering amplitude at high energies, 25:9749 (JINR-E2-5341)
GARST, Daniel M., Precisely controlled low range humidity system, 25:10376 (SC-RR-70-775)
GARZ, T., Experimental oscillator strengths for Ni I lines, 25:9117
GARZOLI, Silvia L., Distribution of atomic hydrogen in Carina, 25:9146
GASHEVSKII, V. A., Statistical analysis of oscillations excited in a plasma--beam system, 25:9535
GASPARI, G. P., Some considerations on critical heat flux in rod clusters in annular dispersed vertical upward two-phase flow, 25:10215
GATTI, G., Energetic ions produced by subnanosecond laser pulses, 25:9484
GATZKE, J., Population inversion in He transitions, 25:9170
GAUTHIER, R., Polarization sensitivity of rectangular Li drifted silicon detector, 25:8508
GAVRILOV, K. A., Identification of elements 102 and 104 with the help of the collimation method, 25:10030 (KFK-tr-329)
GAYET, R., Average Gaunt factor for free--free emission, 25:9081
GEDALIN, E. V., Initial stage of avalanche development, 25:9731
GEGUSCH, M., Applications of vacuum technology in nuclear installations, 25:8461
GEIGER, A. L., Fermi velocity in single-crystal films of Pb, 25:9373
GEIGER, G. E., Effect of bubble stabilization on pool boiling heat transfer, 25:8419
GEIGER, J., Electron energy loss spectra of graphite single crystals and evaporated carbon films in the range 0.02 to 0.4 ev, 25:9167
GEILE, H. J., Investigation on precursor ionization in an electromagnetically driven shock tube, 25:9486
GENNARI, C., Factors influencing haematopoietic spleen colony formation in whole-body irradiated mice. I, 25:8765
GENTA, P., Spectroscopic measurement of the electron temperature of a plasma in the vacuum uv, 25:9407 (CEA-N-1391)
GENZ, H., Linear current-field algebras, broken scale invariance, and nucleon interactions, 25:9762
Logarithmic behavior in short-distance field products, 25:9865
GEOGHEGAN, G. R. H., Uranium enrichment in the UK, 25:8431
GEORGELIN, Y. M., Galactic rotation from H II regions, 25:9145
GEORGELIN, Y. P., Galactic rotation from H II regions, 25:9145
GEORGI, Howard, Energy--momentum tensors and scale invariance in Thirring model, 25:9862
GERARD, E., Observations of Jupiter at 11.13 cm, 25:9160
GERASIMOV, V. V., Effect of treatment of steel with Trylon B on its hydrogen absorption, 25:8842
GERBER, J. P., Pi^+-mesic decay of /sub Λ/^{5}He hyperfragment, 25:9633
GERNER, C. P., Internal source scintillation spectrometer, 25:8514
GERRARD, Martha, Selected abstracts of world literature on production and industrial uses of radioisotopes (from NSA July--September 1970), 25:8428 (ORNL-IIC-30(Pt.3))
GERVAISE, Francois, Details concerning the use of ELF program, 25:9941 (CEA-N-1361)
GERWARD, L., Effects of irradiation with gamma rays and fast neutrons on Si, 25:9572
GETMANTSEV, G. G., Variations in mean level of radio emission at 1.1 and 2.3 MHz, 25:9352
GETSELEV, I. V., Measurements of fast-charged particles on Cosmos-137, 25:9354
GEWENIGER, C., Small momentum transfer π^+ production with linearly polarized photons, 25:9624
GHATE, Madhav R., Preparation of ^{13}C by chemical exchange between amine carbamates and carbon dioxide, 25:8318 (CU-755-7, Sect.2)
GIACOMELLI, G., Total cross section measurements, 25:9640
GIANNINI, R., Instrument for measuring rate of change of RF frequency in particle accelerators, 25:9905 (CERN-70-28)
GIARD, P., Radiotherapeutic cardiomyopathy, 25:8708
GIARD, W. R., Particle-track identification: application of a new technique to Apollo helmets, 25:9255
GIBADULIN, R. A., Mitotic cycle in normal and irradiated cells of the human diploid strain WI-38, 25:8743
GIBSON, J. A., Simultaneous reaction, diffusion and bulk flow in tubular specimens of graphite. V, 25:8906 (AERE-R-4857)
GIBSON, J. R., Glove box vacuum system for radioisotopic targets, 25:8453 (ORNL-TM-3209)
GIBSON, W. M., Ion implantation of sodium, lithium, and neon in cadmium sulfide, 25:9561
GIDALEVICH, E. Ya., Nature of interplanetary gas, 25:9115
GIFFON, Maurice, Application of the differential equation method to the study of a nonrelativistic feynman amplitude, 25:10065
GIJBELS, R., Activation cross-sections, determined from second-order reactions, 25:10040
GILL, R. D., $^{20}Ne(p,t)^{18}Ne$ reaction as a test of the ^{18}Ne and ^{20}Ne wave functions, 25:10006
GILLESPIE, P. J., Ratemeter controlled rectilinear scanning, 25:8494
GILLETTE, Edward L., Age sensitivity of epithelial cells of mouse small intestine, 25:8785
GILLETTE, R. K., Investigations into the determination of mercury in copper, 25:8217 (MLM-1772)
GILLS, Thomas E., Determination of trace elements in glass by activation analysis using hydrated antimony pentoxide for sodium removal, 25:8223
GINZBURG, V. L., Coherent mechanisms of emission and their application to pulsars. I, 25:9070
GIRAUD, J., Pool nuclear reactor, 25:10276
Pool-reactor, 25:10280
GIULIANELLI, James Louis, Reactions of S atoms produced by $^{35}Cl(n,p)^{35}S$ in KCl, 25:8312
GIVORD, Francoise, Crystalline structures of the intermetallic compound (Gd/sub 2/3/2Fe/sub 1/3/)Fe_3, 25:8891
GLAETZLE, R., Plasma spraying of tungsten, 25:8855
GLASEL, J. A., Digital rf pulse burst generator, 25:8575
GLASER, F. H., Methods of application of gamma emitters in contact therapy with regard to radiation protection, 25:8688 (SZS-6/70)
Need for measuring radiation burden of the bladder and rectum, 25:8679 (SZS-6/70, pp 9-18)
GLASOW, P., Small rod-shaped silicon-detectors for medical and biological applications, 25:8464 (BMBW-FBK-70-15)

XUM

GLASS, Edward Natham, Conserved quantities in gravitational radiation theory, 25:9871
GLASSTONE, Samuel, Nuclear reactor theory, 25:10317
GLAZKOV, A. A., High-frequency separator of particles, 25:9939
GLAZOV, V. M., Methods of investigation of thermoelectric properties of semiconductors, 25:9590
GLENCROSS, W. M., Six-minute periodicity during x-ray flares, 25:9104
GLIMM, James, Lambda(phi⁴)$_2$ quantum field theory without cutoffs. III, 25:9849
GLUSHKOV, I. S., Current distribution in an E x H discharge with sectionalized electrodes for nonequilibrium conductivity of the plasma, 25:9482
GLUSHKOVA, V. B., Kinetics and mechanism of solid state reactions in the systems of refractory oxides, 25:8935
GNEDIN, Yu. N., Neutron polarization at the scattering on thick layers of matter, 25:9949
GNEUSS, G., Dynamic collective model of the giant resonance, 25:10083
GOEDBLOED, W., Internal source scintillation spectrometer, 25:8514
GOERNER, W., Multichannel counting of short-lived nuclides, 25:8515
GOGAVA, V. V., Temperature dependence of spontaneous magnetization in holmium during heating--cooling cycle, 25:9579
GOIKHBERG, E. Ya., Portable internally loaded counter for measuring low levels of gas activity, 25:8520
GOLDBERGER, M. L., Magnitude of high-energy meson--meson total cross sections, 25:9773
GOLDEN, Lawrence B., Semi-empirical cross sections and rates for excitation and ionization of hydrogen by electron impact, 25:9184
GOLDENBAUM, G. C., Magnetic piston-shock wave in collisionless plasma, 25:9452
GOLDSTEIN, Bernard, Lithium-defect interactions in electron-irradiated n-type silicon, 25:9558
GOLLUB, J. P., Apparent universal behavior of fluctuation-induced diamagnetism in superconductors, 25:9369
GOLOSKOKOV, S. V., Anomalous magnetic moment of nucleons, 25:9702 (JINR-E2-5333)
GOLUTVINA, I. G., Effect of natural lighting on plastic scintillators, 25:8528
GONSALVES, Neil Ignatius, Mechanism of wound healing in irradiated mouse skin, 25:8772
GONSIOR, B., $^7/_2^-$ isobaric analogue resonances in odd isotopes of Sb, 25:10044
GONZALEZ-MARTIN, Gustavo R., Expansion of Einstein's theory of gravitation in flat and curved three-dimensional space, 25:9883
GOOD, I. J., Proton and neutron masses and a conjecture for the gravitational constant, 25:9878
GOODJOHN, A. J., Special development problems of high-temperature gas-cooled reactor systems, 25:10166 (GA-10265)
GOODMAN, Clark, Prog. rpt. on pion interactions at medium energies, 25:9657 (ORO-3948-2)
GORAN, Karl, Fuel cartridge made of two separate parts to be introduced from the seat of a reactor, 25:10333
GORCHAKOV, E. V., Measurements of fast-charged particles on Cosmos-137, 25:9354
GORDEEV, V. A., Wire spark chamber system with magnetostrictive information retrieval, 25:8552
GORDON, David, Hadrodynamics and quark structure, 25:9759
GORDON, M. A., Shapes of recombination lines at lambda3 cm in M 42, M 17, and IC 1795, 25:9080
GORE, M. S., Dehydro-irradiation process for tropical shrimps, 25:8820
GORIN, Yu. P., Antideuteron absorption cross sections on nuclei Li, C, Al, Cu, and Pb at 25 GeV/c, 25:9639
GORNITZ, Vivien, Uranium mineralization and alteration, Orphan Mine, Grand Canyon, Arizona, 25:8376
GORODINSKII, V. F., Absorption of ultrasound by superconducting Sn, 25:9365
GORYACHIKH, A. A., Production of He nuclei at interactions of pions with energy of 60 GeV with heavy nuclei of emulsion, 25:9660
GORYAEV, V. M., Influence of ionizing radiation on the structure and properties of modified kapron fibers, 25:8270
GOSS, David, Addendum to Hartree--Fock--Bogolyubov calculations in the 2s, 1d shell, 25:10008
GOTO, H., Effects of acridine orange on the biological action of gamma-ray, 25:8707
GOTTLIEB, C. A., Search for extraterrestrial $H_2{}^{18}O$ emission, 25:9076
GOTTLIEB, Carl A., Detection of methyl alcohol in Sagittarius, 25:9060
Search for excited state of OH in W3, 25:9093
GOULD, R. W., Longitudinal oscillations in bounded magnetoplasmas, 25:9532
GOULD, Robert F., Conference on isotope effects in chemical processes, Miami Beach, Fla., 4/67, 25:8243
GOUNARIS, G. J., Meson decay from a chiral Lagrangian model, 25:9780
GOURDON, Christian, Coil giving stellarator-type magnetic configuration, 25:9509
GOVERSE, S. C., Internal source scintillation spectrometer, 25:8514
GOWDY, R. H., Quantization of general relativity, 25:9872
GOWDY, Robert H., Action functional of general relativity as a path length. I, 25:9881
GOYAL, D. P., Elasticity of the I(2030), 25:9681
GOZNA, C. F., Initiation of arcs by ion bombardment, 25:9442
GRABAN, Wieslaw, Use of ^{133}Xe for studies on effects of insulin and glucose on blood flow in resting muscle. II, 25:8586
GRACHEV, A. S., High-voltage pulse source for the deflector plates in an ion cluster input system to the synchrotron chamber, 25:9931
GRAEBER, H., Heat transfer in smooth tubes, between parallel plates, in annuli, and tube bundles, 25:8416
GRAEFEN, W., Mass spectrometer with energy dispersion, 25:8578
GRALL, L., Corrosion tests on various materials in seawater up to 150°C, 25:10360 (ORNL-tr-2412)
GRAMENITSKII, I. M., Determination of resonance production cross section in π^+p interactions at 2.34 GeV/c, 25:9662
GRAMMAGE, R. B., Gravimetric adsorption studies of thorium oxide. V. Water adsorption between 25 and 500°, 25:8266
GRANATA, Giovanni, Generation of harmonic EM wave at upper hybrid frequency in inhomogeneous plasma, 25:9521
GRANKINA, Z. A., Infrared spectra and molecular properties of tetrahydroborates of metals of the M(BH$_4$)$_n$ type, 25:8263
GRATTAN, J., Measurement of relative conversion ratio in particulate fuel, 25:10217
GRATTON, R., Energetic ions produced by subnanosecond laser pulses, 25:9484
GRATZL, H., One-dimensional quasi-linear calculation with allowance for spontaneous emission, 25:9524
GRAUPE, H., Reliability study made at Rheinsberg Nuclear Power Plant, 25:10093 (NP-tr-1928)
Reliability study of automatic system in Rheinsberg nuclear power plant, 25:10108
GREBENSHCHIKOV, S. E., Possibility of measuring directed fluxes in a plasma contained in a toroidal magnetic trap, 25:9410 (CTO-736)
GRECHIKHIN, L. I., Determining concentration of charged particles of pulsed plasma generator, 25:9416
GREEN, Louis C., Pulsars today. II, 25:9072
GREEN, R., Rho--omega interference in anti pp → 4π at 1.6 to 2.2 GeV/c, 25:9647
GREEN, T. S., Parallel plate electrostatic spectrograph, 25:8576
GREEN, Thomas E., Use of selective ion exchange paper in x-ray spectrography and neutron activation. Application to the determination of gold, 25:8221
GREENBERG, E. J., Computer-analyzed counting and scanning, 25:8716
GREENE, Arthur E., Brightening of uv spectrum of carbon star HD 59643, 25:9001
GREGORY, W. D., Production of thin metallic single crystals, 25:8858
GREIG, J. R., Measurement of the stark broadening of the resonance lines of neutral argon and neon, 25:9171
GREIMAN, William H., Regge-pole model for pp and anti pp elastic scattering at high energies, 25:9813
GREIN, F., Configuration interaction combined with a correlation factor for two-electron atoms, 25:9242
GREVESSE, N., Identification of SiH⁺ in the solar photospheric spectrum, 25:9120
GREWE, H., Growing of structure-components in WC--TaC--Co hardmetal-alloys, 25:8877
GRIEM, Hans R., Enhanced radiation from a theta-pinch plasma, 25:9448
Measurement of the stark broadening of the resonance lines of neutral argon and neon, 25:9171
GRIGOR'EV, Yu. G., Biomedical problems of space flight, 25:8755 (JPRS-51660)
GRIGOROV, N. L., Spatial distribution of singly charged particles and helium nuclei above the atmosphere in the equatorial region, 25:9349
GRIGOR'YAN, D. G., Proteins of the brain and blood serum of animals subjected to the effect of microwaves, 25:8784
GRINBERG, E. M., Track autoradiography for the study of the microdistribution of certain elements in metals, 25:8235
GRINGAUZ, K. I., Comparison of ionospheric features of planets in terrestrial group, 25:9355
GRISHAEV, I. A., Determination of the critical current in a section with radial slots in the iris disk, 25:9907 (KFK-tr-335)
Forming beams and beam parameters in output channels of 360-MeV electron linear accelerator, 25:9927
GRISHANOVA, S. I., Resonance photoionization of helium and helium-like ions, 25:9239
GRISHIN, V. G., Integral equations of cascade kinematics, 25:9708
GRISHIN, V. K., High-frequency operating conditions in linear induction accelerators, 25:9937
GRIZHKO, V. M., Determination of the critical current in a section with radial slots in the iris disk, 25:9907 (KFK-tr-335)
GROSSE, W., Small rod-shaped silicon-detectors for medical and biological applications, 25:8464 (BMBW-FBK-70-15)
GROSSER, J., Reactive scattering of hydrogen and deuterium atoms from halogen molecules, 25:8256
GROSSMANN, H., Methods of application of gamma emitters in

contact therapy with regard to radiation protection, 25:8688 (SZS-6/70)
Situation and trend of contact therapy in treatment of gynecologic carcinomas, 25:8730 (SZS-6/70, pp 28-35)
GROVE, E. L., Conference of the seventh national meeting of the Society for Applied Spectroscopy (Nineteenth Annual Mid-America Spectroscopy Symposium), Chicago, 5/68, 25:8538
GRUBE, D. D., Diurnal variation in labeling index of mouse epidermis, 25:8589
GRUBER, B., Recurrence relation for Kostant's formula, 25:9820
GRUBER, R., Theory of dynamic stabilization of Rayleigh--Taylor instability, 25:9488 (LRP-45/70)
GRUSHIN, V. F., Photoproduction of positive pions on protons in region of resonance $P_{33}(1236)$, 25:9623
GUARDIOLA, R., Elastic scattering of 1-GeV protons on ^{12}C, 25:9983
GUERIN, M. R., Prog. rpt. on tobacco smoke analysis program, 1/70--9/70, 25:10355 (ORNL-4642)
GUEUSSIER, A., Structural stability of austenitic Cr--Ni stainless steels to deformation and extremeley low temperature, 25:10357 (ORNL-tr-2314)
GUEZENEC, Jean-Yves, Validity of SABINE code in calculations on shielding of heavy and light water reactors, 25:10192 (CEA-N-1354)
GUIDINI, Joseph, Charge transfer during collisions between H^+ and Kr, Xe, NH_3, C_2H_2, C_6H_6, 25:9229
GUIGNARD, G., Effects of magnetic field perturbations of synchrotron on closed orbit and betatron oscillations, 25:9904 (CERN-70-24)
GUILLOU, M., High temperature ceramic conductors and insulators, 25:8936
GUPTA, R. M., Study of longitudinal waves in a relativistic plasma, 25:9516
GUPTA, U. C., Neutron generator for calibration of fast neutron detectors, 25:9940 (BARC-499)
GURCHUMELIYA, A. D., Local exchange potential in the theory of electron scattering on atoms, 25:9237
GUSEVA, M. I., X-ray diffraction of ion-bombarded diamonds, 25:9557
GUS'KOV, Yu. K., .asma thermionic energy conversion, 25:9268
GUSTAFSSON, H. I., Theoretical particle emission spectra in fusion reactions, 25:9504 (FOA-4-4436)
GUSTAVSSON, I., Maximum likelihood identification of dynamics of the agesta reactor and comparison with results of spectral analysis, 25:10091 (NP-18595)
GUTAY, L. J., Analytic structure of off-mass-shell S-wave π, 25:9763 (COO-1428-239)
GUTMAN, E., Measurements of π^-p elastic scattering from 1.71 to 5.53 GeV/c, 25:9652 (COO-1764-112)
GUYON, E., Superconducting thin films, 25:9385
GUYOT, M., Gravitational instability of a two-component fluid: matter and radiation, 25:9157

H

HAAS, F. X., Peak Stripping Program for the Nuclear Data 50/50 Analyzer System, 25:8531 (MLM-1773)
HAAS, R. E., Radiosensitivity of mice exposed to various temperatures and low-dose rate radiation, 25:8768
HAASE, Joachim, Coefficients for adjustment of complex scattering factors for fast electrons. II, 25:10055
HABER, Alan H., RBE of fast neutrons in growth inhibition: evidence for a component requiring cell division, 25:8801
HABERLAND, H., Reactive scattering of hydrogen and deuterium atoms from halogen molecules, 25:8256
HACKSTEIN, Karl-Gerhard, Production of spherical oxidic or carbidic particles from heavy metal salt solutions, 25:8922
HADINGER, G., Method of calculation of trajectories of ions before injection into the proposed heavy-ion linear accelerator, 25:9911 (LYCEN-6949)
Parameters of ''Reflex''-type ion sources, 25:9912 (LYCEN-6953)
HADLEY, J. H. Jr., Positron annihilation in irradiated acetyl methionine, 25:8269
HAEFNER, H., Safety report for FR-2 experimental capsule rigs with single-walled NaK capsules for irradiation of high-power fuel pins, 25:10257 (EURFNR-764)
HAEMERS, Johan, Electrical properties of V_2O_3, 25:9581
HAGEMANN, U., Two-quasiparticle (h/sub 9/2/)^2 isomeric state in ^{202}Po, 25:10027 (JINR-E6-5379)
HAGEN, E. W., Use of steam-electric power plants to provide thermal energy to urban areas, 25:10094 (ORNL-HUD-14)
HAGENAS, Lars, Uv-irradiation induced changes in the uptake of acridine orange in living mouse fibroblasts in vitro, 25:8770
HAGIWARA, Miyuki, Study on the radiation-induced chain crosslinking and crosslinking polymerization, 25:8276 (JAERI-Memo-4147)
HAHN, Yukap, Generalized variational bounds on positron--hydrogen reaction matrix. I, 25:9216
HAIDUC, Constantin, Optimization of parameters for nuclear power plants, 25:10130
HAIG, D. A., Inactivation of the scrapie agent by near monochromatic ultraviolet light, 25:8805
HAIGH, Mary V., Radiation responses of fern spores during their first cell-cycle, 25:8614
HAINES, M. G., Finite-Larmor-radius equations for theta pinch, 25:9497
HALKETT, James A. E., Allograft survival in nonsusceptible C57BL/6J mice hosts. Temporal relationship between whole-body x irradiation and the immune response, 25:8622
HALL, Donald F., Digital data acquisition system for displacement measurement, 25:8397 (UCRL-72509)
HALL, J. E., Ionospheric observations during annular solar eclipse of May 20, 1966. I, 25:9309
HALL, T. P. P., Structure of some trapped hold centers in CaF_2. II, 25:9546
HALLIDAY, I. G., Multiperipheral bootstrap, 25:9757
HALZEN, F., Building meson--baryon scattering amplitudes from duality, 25:9799
HAMAMOTO, Ikuko, Doublet in ^{207}Pb and ^{207}Tl, 25:10033
Nuclear octupole vibrations in the isotopes of Pb, 25:10043
HAMER, C. J., Eikonal Regge fits to small-angle elastic scattering data, 25:9755
Eikonal Regge model for elastic scattering processes, 25:9776
HAMRICK, T. P., Some techniques for estimating the results of the emission of radioactive effluent from ORNL stacks, 25:8452 (ORNL-TM-3187)
HANAWALT, Philip C., Repair replication: its role in genetic stability, 25:8636 (SU-326-P-7-X-22)
HANGAY, Gyoergy, Radio-sterilization of a hydrocortisone acetate- and chloramphenicol-containing ophthalmic ointment. I, 25:8826
HANNOVER, H., Alternative treatment of the three-body problem, 25:9891
HANRAHAN, Robert J., Radiation chemistry of phosphine--ammonia mixtures in gas phase, 25:8299
Use of phosphine as a free radical scavenger in the radiolysis of methyl iodide vapor, 25:8303
HANSEN, Wayne R., Polonium-210 in soils and plants, 25:8593 (COO-1733-11)
HARDEN III, W. H., Effect of cladding ovality and diametral creep on fuel rod support systems (LWBR development program), 25:10167 (WAPD-TM-714)
HARDY, E., Accumulated fallout ^{90}Sr in the Rocky Flats area, 25:8353 (HASL-237, pp I.11-26)
HARDY, Edward P. Jr., Prog. rpt. on fallout program, 6--9/70, 25:8367 (HASL-237)
HARM, Helga, Analysis of photoenzymatic repair of uv lesions in DNA by single light flashes. VI, 25:8651
Analysis of photoenzymatic repair of uv lesions in DNA by single light flashes. VII, 25:8650
HARM, Walter, Analysis of photoenzymatic repair of uv lesions in DNA by single light flashes. V, 25:8652
Analysis of photoenzymatic repair of uv lesions in DNA by single light flashes. VIII, 25:8649
HARNIE, R., Pilot plant for preparation of uranium hexafluoride by dry treatment of nuclear compounds, 25:8342
HARRAH, L. A., Stored-charge effects on electron dose-depth profiles in insulators, 25:8566
HARRINGTON, Robert S., Encounter phenomena in triple stars, 25:8979
HARRIS, A. M., Annealing effects and optical absorption of thermoluminescent LiF, 25:9574
HARRIS, D. E., Minimum observable diameter of radio sources, 25:9084
HARRIS, D. R., ANDYMG3: basic program for time-dependent transport of particles and photons, 25:9601 (LA-4539)
HARRIS, T. J., Pulse shape discrimination in proportional counters, 25:8516
HARSHMAN, E. N., Uraninite-bearing contact metamorphic deposits, Heaths Peak, Carbon County, Wyoming, 25:8379
HART, H. R. Jr., Particle-track identification: application of a new technique to Apollo helmets, 25:9255
HARTECK, P., Photochemical separation of the carbon isotopes, 25:8331
Prog. rpt. on pulse radiolysis of gases, annual, 11/70, 25:8285 (RPI-3821-5)
HARTEN, A., Electron temperature in the two-component solar wind, 25:9114
HARTMANN, V., Gamma-radiolysis of 2-deoxy-D-ribose in aqueous solution, 25:8305
HARTRANFT, Franklin R., Ionospheric electron density profile model, 25:9283 (AD-709888)
HARTWICK, F. D. A., Rate of star formation in M31, 25:9134
HARVEY, A., Demountable magnetic lens, 25:9928
HARVEY, E. H., Observation of the decay eta' → γ γ, 25:9651 (COO-1764-111)
HARVEY, M., Effective operators in the nuclear shell model. II, 25:10072
HARVEY, R. S., Temperature effects on the sorption of radionuclides by freshwater algae, 25:8598
HASAN, S., Computer-analyzed counting and scanning, 25:8716
HASEGAWA, Koichi, New varieties of malting barley produced by radiation breeding, 25:8656
HASEK, M., Host and graft factors in the homing of haematopoietic cells, 25:8616
HASHIMOTO, Hatsujiro, Drops of oxides on tungsten oxide needles and nuclei of dendritic crystals, 25:8859
HASSID, A., Some considerations on critical heat flux in rod clusters in annular dispersed vertical upward two-

phase flow, 25:10215
HASTERLIK, Robert J., Argonne radium studies, 25:8669 (COO-2088-1)
HATTA, Yoshisuke, Wave--wave coupling in ion wave propagation, 25:9513
HAUBACH, W. J., Isotope and ortho-para separations of the molecular hydrogens by adsorption at low temperatures, 25:8332
HAUG, A., Ionospheric observations during annular solar eclipse of May 20, 1966. IV, 25:9312
Ionospheric observations during annular solar eclipse of May 20, 1966. V, 25:9313
HAUG, U., Luminosity determination of OB stars by Hβ indices, 25:9049
HAUG, W., Optimization of the cell dimensional parameters of an incore thermionic fuel element, 25:10226
HAUGHTON, Peter M., Macromolecule synthesis and wall extensibility in relation to the mechanism of auxin-induced cell elongation, 25:10366 (RLO-2225-T-19-9)
HAUSER, M. G., Calibration of large neutron counter, 25:8512
Performance of large-volume two-phototube neutron detector, 25:8547 (PURC-4159-13)
Response of a mineral-oil based liquid scintillator to heavily ionizing particles, 25:8511
HAUSSEN, W., Differential neutron source strength from T(d,n)^{5}He, 25:9957
HAVLEN, Robert James, Observational aspects of cepheid evolution, 25:8977
HAWTIN, P., Simultaneous reaction, diffusion and bulk flow in tubular specimens of graphite. V, 25:8906 (AERE-R-4857)
HAYAKAWA, Shigeru, Formation, microstructure, and properties of barium zirconium sulfide ceramics, 25:8920
HAYASHI, Chushiro, Effects of electron capture on the temperature in dense stars, 25:8973
HAYASHI, Eisuke, Self-consistent band calculations for vanadium and chromium, 25:9597
HAYASHI, Haruhisa, Multiple kink effect in graphite, 25:9586
HAYASHIDA, Hideto, X-ray measurements of neutron-irradiated LiF, 25:9565
HAYE, C., Action of ionizing radiations on the eye, 25:8609
HAYNES, D. S., Line shape calculation for nuclear scattering from gaseous targets, 25:9924
HAYNIE, Gordon, Study of trace metals in fingernails and hair using neutron activation analysis, 25:8229
HAYWOOD, Fred F., RBE of fast neutrons in growth inhibition: evidence for a component requiring cell division, 25:8801
HEACOCK, R. R., Cooperative micropulsation research at high latitudes, 25:9326
HEALY, C., Chemical determination of N in nitrides of B, Ti, Zr, Cr, Mo, Nb, Ta, and V, 25:8195 (AERE-R-6491)
HEASLEY, James N. Jr., Apsidal-motion test for late-type stars, 25:9005
HEATH, M. T., Use of steam-electric power plants to provide thermal energy to urban areas, 25:10094 (ORNL-HUD-14)
HECHT, K. T., Five-dimensional quasispin, 25:10078
HECKER, R., Effect of cyclic fast neutron irradiation damage on modulus of rupture of BeO, 25:8959
HEENAN II, William Andrew, Design and development of a capillary valve for use in venting fission gases from fast breeder reactor control rods, 25:10189
HEERINGA, R., Old open cluster NGC 7142, 25:9022
HEIKO, Lance, $K_2^0 + 2\pi 2\gamma$ by current algebra, 25:9738
HEIL, Timothy G., Four new bound, low-lying states of cyanogen, 25:9110
HEINISCH, H. L. Jr., Polarizability of H$^-$, 25:9174
HEINRICH, H., Investigation of the auroral electrojet, 25:9334
HEINZINGER, K., Electromigration in metals, salts, and aqueous solutions, 25:8247
HEISE, H., Experimental oscillator strengths for Ni I lines, 25:9117
HEISLER, R., Comparisons between calculated ionospheric absorption and riometer measurements, 25:9289
HEISLER, Rodney, Intrepretation of cosmic radio-noise adsorption meesurements, 25:9337
HELLER, Leon, Characteristics of proton--proton interaction from data below 30 MeV, 25:9814
HELLIWELL, R. A., VLF studies of magnetosphere, 25:9325
HELLSTRAND, E., Capture cross section of ^{237}Np and ^{241}Am in different reactor spectra, 25:10019 (BNL-50242)
HELM, F., Physics investigations of steam-cooled fast reactor cores with a Pu-fueled central zone, 25:10258 (EURFNR-848)
HEMENGER, R. P., Five-dimensional quasispin, 25:10078
HENDRICKSON, M. M., Eventual whole body exposure rate from ^{85}Kr released to the atmosphere, 25:8667 (BNWL-SA-3233)
Reasons for differences in calculated estimates of the cloud dose, 25:8668 (BNWL-SA-3424)
HENSON, Wallace Ray, Properties of the excitonic insulator, 25:9367
HERBST, L. J., Electronics for nuclear particle analysis, 25:8488
HERMANS, M. E. A., Sol--Gel processes for ceramic nuclear fuels, 25:8915
HERMANS, W. C., Austern--Blair method for scattering of deuterons and alpha particles, 25:9991
HERZBERGER, P., Design and construction of a programmer for an electron beam welding machine, 25:8391 (EUR-4537)
HESSLER, V. P., Cooperative micropulsation research at high latitudes, 25:9326
HEWITT, H. B., Toxicity and radiosensitizing activity of triacetoneamine-N-oxyl, 25:8701
HEYDENREICH, A., Radiation-induced eye lesions, 25:8793
HEYS, H., Monitors and detectors for radiological protection, 25:8487
HIGASHI, Kunio, Effect of flow pattern in gaseous diffusion process, 25:8438
HIGASHIDE, Fukuji, ESR study of radiation-induced graft-polymerization of methyl methacrylate on flaky glass, 25:8277 (NSJ-tr-160)
HIGBIE, J., Gravitational--scalar field coupling, 25:9880
HIGHTOWER, J. R. Jr., Low-pressure distillation of molten fluoride mixtures: nonradioactive tests for the MSRE distillation experiment, 25:10210 (ORNL-4434)
HILKO, R. A., Reactions ^{14}C + α, 25:9980
HILL, J. Carver, Cycle-allocation disciplines for multiaccess memory systems, 25:10408 (UCRL-72648)
HILL, V. R., Development and results of an electrically heated seven-pin bundle assembly for thermal hydraulic testing in liquid metals, 25:10207 (BNWL-SA-3286)
HILLIER, R. R., Low-energy gamma rays from NP 0532, 25:9062
HILTNER, W. A., Optical monitoring of Sco X-1 for 1967-1969, 25:9086
HINES, R. L., Relative energy losses of channeled D$^+$ ions in Au, 25:9555
HINTON, F. L., Amplitude limitation of a collisional drift-wave instability, 25:9495
HIPPE, E., Normal plasma cortisol values determined by a double isotope derivative technique, 25:8585
HIRAI, Shin, New varieties of malting barley produced by radiation breeding, 25:8656
HIRAKI, Makoto, New varieties of malting barley produced by radiation breeding, 25:8656
HIRDE, J. P., Effect of irradiation on the current pulses in a low-frequency electrodeless argon discharge, 25:9449
HIRONO, Y., Relative biological effectiveness of heavy ions in producing mutations, tumors, and growth inhibition in the crucifer plant, arabidopsis, 25:8800
HIROTA, Kozo, Application of microwave spectroscopy to the self-exchange of deuterium in propylene-3-d_1 catalyzed by group VIII metals, 25:8258
HISHAW, R. J., Transfer molding close tolerance parts, 25:10341 (BDX-613-166)
HLUBEK, W., Stationary behavior of gas turbines in nuclear plants, 25:10251
HOBBS, R. W., Observations of seven compact sources in H II regions, 25:9077
HOCH, M., Thermodynamics of vanadium alloys. I, 25:8862 (AD-709957)
HOEHNEL, G., Multichannel counting of short-lived nuclides, 25:8515
HOFF, G. C., Grouting and materials control, Operation Flint Lock, 25:8962 (POR-4013)
HOFFMEISTER, A. J., Projection of nuclear fuel cost trends, 25:10100
HOFMANN, A., Timing with surface barrier detectors, 25:8517
HOGG, G. W., Particle size control by jet grinding in a fluidized-bed denitrator, 25:8323 (IN-1439)
HOKKYO, Noboru, Equivalence principle and geodesic De Broglie waves, 25:9152
HOLCOMB, B. D., Program user's manual capital budgeting problem, 25:10337 (AECOP-621)
HOLDEN, J. E., Sensitivity of (^{3}He,t) reaction to final-state configurations, 25:10013
HOLLAND, Redus F., Fluorescence efficiencies of nitrogen excited by 1- to 5-MeV positive ions, 25:9234
HOLLENBACH, David, Surface recombination of hydrogen molecules, 25:9087
HOLLENBACH, David J., Molecular H in H I regions, 25:9088
HOLLOWAY, D. F., New end-window variable geometry x-ray proportional counter, 25:8510
HOLM, L., Automatic Van de Graaff voltage conditioner, 25:9930
HOLMBERG, Adolph, Radioactive scleral shells in the treatment of conjunctival tumors, 25:8731
HOLMES, H. F., Gravimetric adsorption studies of thorium oxide. V. Water adsorption between 25 and 500°, 25:8266
HOLMES, John Arthur Godfrey, Improvements in reactors, 25:10200
HOLMES, John M., Impact of nuclear energy centers on economy of Puerto Rico, 25:10291 (TID-25630)
HOLTET, J. A., Ion-reflection of downward-propagating whistlers at low latitudes, 25:9321
HONSA, I., Bromopyrogallol red as colorimetric reagent. IV, 25:8212
HONZATKO, J., Branching ratios and intensities of some transitions in ^{35}Cl(n,γ)^{36}Cl reaction, 25:10009
HONZAWA, T., Production of quiescent plasmas with T/sub i/ > T/sub e/, 25:9483
HOOVER, Scott, Role of contamination in the kinetics of oxidation nucleation of tungsten and molybdenum, 25:8841

HOPKINS, George C., CONVERT: IBM-to-CDC program conversion code, 25:10350 (LA-4555)
HOPKINS, L. L. Jr., Determination of vanadium by neutron activation analysis at nanogram levels to formulate a low-vanadium diet, 25:8228
HOPKINSON, Eric C., Method and apparatus for neutron lifetime well logging using dual discrimination within one of two intervals, 25:8359
HOPKINSON, J. B., Reactor HIFAR: safety rod circuits, 25:10252 (AAEC/M-9)
Reactor HIFAR: safety rod system, 25:10253 (AAEC/M-32)
HOPPER, M. J., Description of computer program ICON for calculation of fission product inventories, 25:10236 (AERE-R-6242)
HORAK, Thomas B., Determination of elements of close binary system, 25:8980
HOREN, D. J., Current nuclear level schemes: A = 91 to 117, 25:10031 (ORNL-4627)
HORI, Setsuko, Photoproduction of eta mesons in Veneziano Model, 25:9712
HORIKAWA, Masakatsu, Radiation and carcinogenesis, 25:8611
HORNG, Ching-shie, Cyclotron wave plasma studies, 25:9408 (COO-1789-1)
HOROWITZ, P., Results of a search for optical pulsars, 25:9090
HORROCKS, Donald L., Nuclear applications of liquid scintillation systems, 25:8539
HORSLEY, R. J., Radiation-induced division and mitotic delay studies in green alga (Oedogonium cardiacum), 25:8644
HORTON, C. W. Jr., Amplitude limitation of a collisional drift-wave instability, 25:9495
HOSEGOOD, Samuel Britan, Improvements in nuclear reactors, 25:10168
HOSHI, Reiun, Effect of electron capture on the temperature in dense stars, 25:8973
HOSODA, Masataka, Photoproduction of eta mesons in Veneziano Model, 25:9712
HOSOI, Fumio, Study on the radiation-induced chain crosslinking and crosslinking polymerization, 25:8276 (JAERI-Memo-4147)
HOSTE, J., Activation cross-sections, determined from second-order reactions, 25:10040
HOT, Michel, Validity of SABINE code in calculations on shielding of heavy and light water reactors, 25:10192 (CEA-N-1354)
HOUSER, H. G., Projection of nuclear fuel cost trends, 25:10100
HOUSTON, D. H., Prog. rpt. on integral neutron thermalization, 4--6/70, 25:9943 (GA-10223)
HOVEN, J., Study of I (1915) resonance in reaction K⁻p → Λ π⁰, 25:9659 (UCRL-19789)
HOWARD, Alma, Radiation responses of fern spores during their first cell-cycle, 25:8614
HOWARD, Barry C., Computer code for the analysis of digitized seismic signals, 25:8382 (UCRL-50939)
HOWARD, Edwin B., Studies of inhaled radon daughters, uranium ore dust, diesel exhaust, and cigarette smoke in dogs and hamsters, 25:8623 (BNWL-SA-3419)
HOWARD III, William E., Search for strong radio spectral lines in the range 12.4 to 15.1 and 15.3 to 17.3 GHz, 25:9058
HOWER, G. L., Comparisons between calculated ionospheric absorption and riometer measurements, 25:9289
HOY, R. D., Effects of an annular solar eclipse on phase of VLF transmissions, 25:9105
HOYAUX, M. F., Gvosdover effect in a low-pressure arc constrained by its own magnetic field, 25:9441
HSIEH, K. C., Galactic ³He above 10 MeV per nucleon and the solar contributions of hydrogen and helium, 25:9257
Relative abundances and energy spectra of ³He and ⁴He from solar flares, 25:9103
HSU, F. H., Positron annihilation in irradiated acetyl methionine, 25:8269
HSUE, C. S., Formulation of dual theory in terms of functional integrations, 25:9901
HUA, C. T., Morphological and kinematical study of two planetary nebulae, 25:9048
HUANG, A. Ben, Kinetic theory of wave propagation. II, 25:9533
Kinetic theory of wave propagation. I, 25:9527
HUANG, Yinn-nien, Occurrence of spread F and geomagnetic activity over Taipei, Taiwan, 25:9290
HUBBARD, Lincoln B., Gamma-ray dose distributions in externally irradiated cylinders, 25:8686
HUBE, Douglas Peter, Distribution and kinematics of the late B-type stars, 25:8976
HUBER, A., One-neutron transfer reactions with Be, C, and O nuclei, 25:9988
HUBER, J. G., Superconductivity and normal-state properties of Th--U alloys, 25:9389
HUBER, Max Georg, Microscopic description of the absorption of bound pions, 25:9982
HUBER, W., Crushing behaviour of pyrocarbon coated fuel particles, 25:8925 (EUR-4501)
HUBERT, Pierre, Coil giving stellarator-type magnetic configuration, 25:9509
HUDSON, Katherine I., Rotational velocities in short-period A-type binaries, 25:9003
HUDSON, P. D., Discontinuities in plasma and identification in solar wind, 25:9306
HUEBNER, R., Isotope splitting of F-center in-gap mode in KI and KBr, 25:9585
HUERTA, Manuel A., Entropy oscillation and the h theorem for finite segments of infinite coupled-harmonic-oscillator chains, 25:10365 (ORO-3895-9)
HUGENSCHMIDT, Manfred, Temporal and spatial changes in electron density in xenon plasma, 25:9485
HUGHES, M. H., Electron energy distribution functions and transport coefficients in helium and neon, 25:9464
HUGHES, V. A., Optical depth and excitation temperature of galactic H in direction of W49, 25:9069
HUGO, P., Correlation between effective diffusion coefficient and porous structure in nuclear graphite, 25:8924 (DP-Report-437)
HUH, Yeon, Radiolysis reactions of colloidal silver and silver bromide, 25:8302
HUMPERT, B., Off-shell single-current amplitude in the Veneziano approach, 25:9725
HUNDHAUSEN, A. J., Composition and dynamics of the solar wind plasma, 25:9107
HUNT, B. R., Statistical aspects of deconvolution, 25:10351 (LA-4556)
HURT III, S. S., Prog. rpt. on Oak Ridge Research Reactor, 7--9/70, 25:10270 (ORNL-TM-3256)
HUSAIN, D., Low-energy positron--helium scattering, 25:9196
HUSSAIN, S., Killing and mutagenic action in E. coli associated with Auger effect during ¹²⁵I decay, 25:8654
HUSSEINY, A. A., Scattering probability for fast test particles in a plasma, 25:9467
HUTCHESON, Edward Thomas, Effect of strain on resistance and superconducting transition temperature of thin Pb films, 25:9371
HUTTER, E., Instrumented subassembly system in EBR-II, 25:10171
HUYNH, Chanh Trung, Process for separating isotopic compounds by absorption, 25:8343
HVATUM, Hein, Search for strong radio spectral lines in the range 12.4 to 15.1 and 15.3 to 17.3 GHz, 25:9058
HWA, Rudolph C., Derivation of the Wu--Yang conjecture in the bootstrap model, 25:9809
HYCHE, C. M., Neutron activation analysis of inorganic constituents of airborne particulates, 25:8231
HYMAN, L. G., Range--energy relation in hydrogen, 25:9166
HYNDMAN, R. W., Catalog of rod-drop and transfer-function data from EBR-II runs 25 through 30A. EBR-II Project, 25:10173 (ANL-7542)

I

IBEN, I. Jr., On the evolutionary status of stars above the horizontal branch in globular clusters, 25:8992
IGNAT'EV, P. P., Measurements of fast-charged particles on Cosmos-137, 25:9354
IGUCHI, Ienari, Low-temperature mobility of trapped ions in rotating He II, 25:9358
IHLE, P., Fuel rods with internal fins, 25:10223
ILARI, O., Control of contaminated air in a reactor fuel element fabrication plant, 25:8695
ILES, P., Impurity effects on annealing of radiation defects in p-type silicon, 25:9549
ILIEVSKII, S. A., Beam regulation in a 100-MeV linear accelerator, 25:9914 (NP-tr-1926)
IL'IN, R. N., Electron binding energy in negative ion He⁻, 25:9169
IL'KHAMDZHANOV, I., Properties of excited states of ¹⁸¹Sm, 25:10035
IMASAKI, Masahide, Approac to the stability criterion for a nuclear reactor, 25:10316
IMHOF, J. P., Satellite-borne instrument for the measurement of soft solar x rays, 25:8499
INAMI, Kuniaki, Loss-of-coolant accident in water-cooled nuclear power reactors. III, 25:10246
INAMI, Takeo, Possible duality constraints on P-wave nonleptonic decays, 25:9744
INGERSOLL, Andrew P., Temperature variation and the solar oblateness, 25:9113
INGLESAKIS, Georges, Electric conductivity of Ar plasma in supersonic flow subjected to electric discharge, 25:9451
Potential distribution between electrodes of Faraday MHD tube, 25:9263
INOUE, Mamoru, Development of a device for measuring circumferential mechanical properties of cladding tubes, 25:8883
INTEMANN, Gerald W., Axial-vector-meson dominance and a new estimate for decay K⁺ → π⁺γγ, 25:9745
INTRILIGATOR, D. S., Preliminary power spectra of the interplanetary plasma, 25:9102
INUISHI, Yoshio, Studies of recombination centers in gamma-irradiated p-type silicon, 25:9567
IOFFREDO, M. L., Coherence of isoscalar and isovector exchange amplitudes in π⁺⁻p → A₂⁺⁻p, 25:9650 (COO-1195-202)
IOVNOVICH, M. L., Electron--ion bunch diagnostics by bremsstrahlung, 25:9908 (KFK-tr-337)
IPOHORSKI, M., Study of neutron damage in Be-doped Cu, 25:8902
IRFAN, M., Relative photopeak efficiencies and photofractions of a 2'' x 2'' CsI(TL) crystal, 25:8502

XUM

IROSHNIKOV, G. S., Possibility to observe rho'' daughter resonance in π + 2π reaction in nuclear field, 25:9786
ISAEV, S. I., Auroral studies at conjugate points, 25:9284 (JPRS-52023)
ISENBERG, J., Interaction between soil and nuclear reactor foundations during earthquakes, 25:10245 (ORO-3822-5)
ISHIDA, Takanobu, Theoretical analysis of chemical isotope fractionation by orthogonal polynomial methods, 25:8335
ISHIGURO, Yukio, Accuracy of analytical treatments for resonance absorption in Doppler resonance regions, 25:10038
ISHKHANOV, B. S., Rapid fluctuations of intensity in the gamma radiation of a betatron, 25:9936
ISKRZHITSKAYA, A. I., Effect of ultraviolet irradiation on blood serum, 25:8782
ISRAEL, H., Atmospheric electricity. I, 25:9286 (TT-67-51394/1)
ISSERSTEDT, J., P Cygni and stellar ring 274, 25:9036
ITO, S., Fast neutron study, 25:9995
ITZKOWITZ, M. S., Computer based laboratory-wide data acquisition, analysis, and retrieval system, 25:8193 (UCRL-20132)
IVANCHENKO, V. G., Phase diagram of the chromium--terbium system, 25:8889
IVANKOVIC, S., Neurotropic carcinogenic effect of phenyl--dimethyl triazene on rats, 25:10362 (ORNL-tr-2418)
IVANOV, L. I., Track autoradiography for the study of the microdistribution of certain elements in metals, 25:8235
IVANOV, V. B., Improvement of characteristics of a double-diode restorer of base level, 25:8540
IWASAKI, Yoichi, Fermion Regge trajectory, 25:9790
IYENGAR, K. V. K., Energy levels of ^{48}Ti, 25:10003
IYENGAR, P. K., Prog. rpt. on nuclear physics, annual, 1969--70, 25:10017 (BARC-501)
IYER, M. R., Beta decay of ^{239}Pu fission products, 25:10036
IYER, P. S., Glucose-induced resistance to gamma-rays in E. coli, 25:8812
IYER, R. H., In-line analytical methods for fuel reprocessing streams. I, 25:8197 (BARC-510)

J

JACKSON, J. H., Annealing effects and optical absorption of thermoluminescent LiF, 25:9574
JACKSON, James F., Space--time effects in fast reactor dynamics, 25:10180
JACKSON, Ross J., Explosive nature of uranium-base niobium alloys after immersion in nitric acid, 25:8840 (RFP-1575)
JACKSON, W. R., Low-energy gamma rays from NP 0532, 25:9062
JACOB, M., Connection between inelastic proton--proton reactions and deep inelastic electron scattering, 25:9805
JACOBI, W., Contamination of the river water by the fallout after extreme reactor accidents, 25:8660 (HMI-B-87)
Estimation of the surface water's contamination by the near fallout by nuclear explosions, 25:8354 (HMI-B-86)
JACOBSON, Jerry H., Toxic effect of thermal neutrons on the rabbit electroretinogram, 25:8761
JACQUEMIN, J., Contraction of β and delta phases of Pu under the effect of self-irradiation at 4.2°K, 25:8904
JACQUIN, M., High temperature ceramic conductors and insulators, 25:8936
JAENTSCH, O., Small rod-shaped silicon-detectors for medical and biological applications, 25:8464 (BMBW-FBK-70-15)
JAFAR, J. D., Measurement of reaction ^{35}Cl(n,γ)^{36}Cl using a three-crystal pair and anti-Compton spectrometer, 25:10000 (PH-2)
JAFFE, Arthur, Lambda(phi^4)$_2$ quantum field theory without cutoffs. III, 25:9849
JANDACEK, R. J., Conformation of radioprotectant compounds. The crystal structures of 2-mercaptoethylamine hydrochloride and 3-mercaptopropylamine hydrochloride, 25:8268
JANIN, G., Disruption of star clusters through passing interstellar clouds investigated by numerical experiments, 25:9050
JANKOWSKI, K., Application of truncated multipolar expansion pair functions in atomic structure calculations, 25:9249
JANSEN, D. H., Examination of nickel heat pipes containing potassium, 25:8395 (ORNL-TM-3077)
JAQUE, F., Anion-vacancy processes after F-light bleaching or irradiation of NaCl, 25:9559
JAQUISS, Michael Thornton, Improvement in nuclear reactors, 25:10201
JASKE, R. T., Thermal pollution and its treatment, 25:10133 (BNWL-SA-3581)
JASSBY, D. L., Velocity shear and low-frequency plasma instabilities, 25:9496
JASWAL, S. S., Polarizability of H-, 25:9174
JAYARAMAN, A., New first-order phase transition in high-purity ytterbium metal, 25:9588
JEAN, Maurice, Hartree--Bogolyubov theory and application to neutron--proton pairing problem, 25:10060 (NP-18538)
JEANNET, Jean-Claude, Electron density in ionized Cs vapor, 25:9421
JEEVANADAM, M., Preparation of 99.5 percent ^{15}N by chemical exchange between oxides of nitrogen in a solvent carrier system, 25:8334
JELINEK, George E., Anharmonic lattice dynamical properties of solid neon, argon, krypton, and xenon, 25:8262 (UCRL-50903)
JELLETT, K., Ribbon effect in a superconducting septum magnet, 25:9903 (BNL-15368)
JENKINS, Evan C., Lithologic log of Pahute Mesa exploratory drill hole No. 1, Nevada Test Site, 25:8357 (USGS-474-96)
JENKINS, J. D., Primary-recoil atom spectra from ENDF/B data, 25:9573
JENKOVSZKY, L. L., Dual resonances models. I, 25:9887 (ITF-70-43)
JENSEN, C. A., He and H$^-$ 1^1S and 2^3S states computed from Feynman path integrals in imaginary time, 25:9177
JENSEN, H. Kaalund, Normal plasma cortisol values determined by a double isotope derivative technique, 25:8585
JEROME, J. A., Test of double-Regge behavior of generalized Veneziano model, 25:9797
JERONYMO, J. M. F., Decay schemes of ^{91}Mo and /sup 91m/Mo, 25:10057
JERVIS-HUNTER, G., Initiation of arcs by ion bombardment, 25:9442
JESPERSEN, M., Ionospheric observations during annular solar eclipse of May 20, 1966. III, 25:9311
JOHNS, Wilbur L., Explosive nature of uranium-base niobium alloys after immersion in nitric acid, 25:8840 (RFP-1575)
JOHNSON, B. M., Formation of intimate oxide--carbon mixtures of fuel materials as an intermediate for carbide and nitride fuels, 25:8923
JOHNSON, B. R., Classical and semiclassical limits in collision theory, 25:9228
JOHNSON, B. W., Very intense neutron source, 25:9954
JOHNSON, C. S., AM frequency division multiplex telemetry systems, 25:10374 (SC-M-70-684)
JOHNSON, Donald F., Clinical and gross pathological findings in swine relative to late effects of mixed gamma-neutron and x-irradiation, 25:8773
JOHNSON, Hugh M., Observation and classification of the Nebula YM 29, 25:9047
JOHNSON, K. P., Launch and mission influences on space propulsion system design, 25:10289
JOHNSON, L. L., Semiclassical treatment of collision-induced dissociation, 25:9197
JOHNSON, R. E., Oscillations in cross section of Ar$^+$--Ar charge transfer, 25:9236
JOHNSON, W., Direct measurement of n--p and n--d total cross sections from 700 to 2900 MeV/c, 25:9648
JOHNSSON, Erik Boerge, Fuel cartridge made of two separate parts to be introduced from the seat of a reactor, 25:10333
JOHNSTON, F. J., Radiolysis reactions of colloidal silver and silver bromide, 25:8302
JOHNSTON, K. J., Observations of seven compact sources in H II regions, 25:9077
JOHNSTON, P. D., New technique for measuring temperature of LTE plasmas, 25:9411 (ECRC/N-288)
JOLAS, A., Spectroscopic measurement of the electron temperature of a plasma in the vacuum uv, 25:9407 (CEA-N-1391)
JONATHAN, N., Photoelectron spectra of ground-state atomic H, N, and O, 25:9200
JONES, B. F., Membership of intermediate-age open cluster NGC 2420, 25:9031
JONES, Frank C., Fluctuation of cosmic-ray anisotropy and the dimensionality of propagation, 25:9258
JONES, L. W., Charged-particle multiplicities of proton--proton interactions between 90 and 800 GeV, 25:9638
JONES, Troyce D., Dose and LET distributions in small-animal sized cylinders for a fission neutron spectrum, 25:8685
JONES, W. D., Reflection of pseudowaves, 25:9531
JONES, W. L., Theory for quasi-periodic oscillations observed in the ionosphere, 25:9299
JOSEPH, A., Classification of local current algebras, 25:9754
JOSEPH, A. F., SPECTRAN: computer system to analyze high resolution spectrum. I, 25:10353 (ORNL-4605)
JOSEPH, Jacques, Application of the differential equation method to the study of a nonrelativistic feynman amplitude, 25:10065
JOSLIN, C. A. F., Use of high activity ^{60}Co sources for intracavitary and surface mould therapy, 25:8738
JULIAN, Carl L., Acceptable imperfections in impulsive loads for simulation tests on circular cylindrical shells, 25:8441 (SC-RR-70-600)

K

KABAKCHI, A. M., Determination of radiation yield of nitrite ions during irradiation of sodium nitrate solutions with small doses, 25:8297
KABAKCHI, S. A., Confirmation of the presence of monomolecular reactions during the radiolysis of aqueous

oxygen solutions, 25:8295
KACHI, S., Electrical properties of V_6O_{13} single crystal, 25:9580
KADYSHEVSKII, V. G., Representation for relativistic scattering amplitude at high energies, 25:9749 (JINR-E2-5341)
KAFALIEVA, D. I., Spectra of photoconductivity of green leaves and chloroplasts at a frequency of 10^{10} cycles per second, 25:10412 (UCRL-Trans-1427)
KAFFIEV, Yu. N., High-energy scattering of charged particles and bethe formula, 25:9704 (NP-18540)
KAGIYA, Tsutomu, Study on the radiation-induced chain crosslinking and crosslinking polymerization, 25:8276 (JAERI-Memo-4147)
KAIBEL, Enrique, Market for components for nuclear power stations and problems of its nationalization, 25:10103
KAIDALOV, A. B., Interaction $\pi^-\pi^-$ in the reaction $\pi^-p \to N^{*++}(1236)\pi^-\pi^-$ with impulse 4.47 GeV/c, 25:9655 (ITEF-767)
Reaction $\pi^-p \to rho^0\pi^-p$ with impulse 4.45 GeV/c, 25:9656 (ITEF-775)
Study of reaction $\pi^-p \to rho^0\pi^-p$ at 4.45 GeV/c, 25:9663
KAINDL, G., Moessbauer effect study of hyperfine interactions in ^{145}Nd, 25:9594
Resonance spectroscopy of γ-radiation on Au(I) and Au(III) compounds, 25:9593
KAIPOV, D. K., Radiation amplification of caprolactam coloration and possibilities of application to high-current accelerators, 25:9552
KAJFOSZ, J., Branching ratios and intensities of some transitions in $^{35}Cl(n,\gamma)^{36}Cl$ reaction, 25:10009
Measurement of reaction $^{35}Cl(n,\gamma)^{36}Cl$ using a three-crystal pair and anti-Compton spectrometer, 25:10000 (PH-2)
KAKEHI, Masae, Conformation therapy technique on 6 MeV linear accelerator in treatment of the carcinoma of cervix uteri, 25:8740
KALABA, R., One sweep numerical method for vector-matrix difference equations with two-point boundary conditions. technical report no. 70-16, 25:10384 (TID-25609)
KALASHNIKOV, V. P., Kinetics of hot electrons in quantized magnetic fields. I, 25:9608
KALBFLEISCH, George R., Experimental determination of neutral particles in muon decay, 25:9748
KALBITZER, S., Manufacturing of radiation detectors, 25:8484
KALER, J. B., Continuous spectrum of neutral helium from gaseous nebulae, 25:9046
KALISH, R., Analog states of ^{89}Sr, 25:10011
KALISH, Sheldon, Two-phase pressure drop for potassium with and without net vaporization, 25:8405 (BNL-13957)
KALMUS, G. E., Study of Σ (1915) resonance in reaction $K^-p \to \Lambda\pi^0$, 25:9659 (UCRL-19789)
KALYAZIN, E. P., Notes on the properties of intermediate particles during radiolysis of aqueous oxygen solutions, 25:8293
KALYNA, J., High speed pulse shape discriminator, 25:8507
Pulse shape discrimination, 25:8506
KAMAT, M. J., Spectrographic determination of Ru in silicious materials used in radioactive waste disposal, 25:8196 (BARC-504)
KAMINSKI, K. J., Thermal diffusion column coefficients for the separation of N_2^{14}--$N^{14}N^{15}$ and O_2^{16}--$O^{16}O^{18}$, 25:8423 (MLM-1439(Rev.))
KANADA, Hiroyuki, Two-pion exchange contribution to nucleon--nucleon scattering, 25:9807
KANAL, Madhoo, Boundary-value problems of linear transport theory, 25:9952
KANAZAWA, Yoshiko, ESR study of radiation-induced graft-polymerization of methyl methacrylate on flaky glass, 25:8277 (NSJ-tr-160)
KANAZIRSKII, Kh., Determination of resonance production cross section in π^+p interactions at 2.34 GeV/c, 25:9662
KANDIL, Abdel-Hakim Taha, Charged particle fission of ^{238}U, 25:10052
KANE, D., Study of Σ (1915) resonance in reaction $K^-p \to \Lambda\pi^0$, 25:9659 (UCRL-19789)
KANEKO, Shobu, van der Waals constants for two He atoms and three He atoms by coupled H--F approximation, 25:9176
KANEKO, Tatsunosuke, Narrow muon bundles below ground, 25:9632
KANEMORI, Yoshihiko, Gamma-ray leakage through a junction between lead and concrete walls, 25:10296 (NSJ-tr-157)
KANGAS, J., Electron precipitation associated with sudden commencement of a geomagnetic storm, 25:9298
KANNENBERG, Lloyd C., $K_2^0 \to 2\pi 2\gamma$ by current algebra, 25:9738
KANNENBERG, Susan L., $K_2^0 \to 2\pi 2\gamma$ by current algebra, 25:9738
KAPCHINSKII, I. M., Beam regulation in a 100-MeV linear accelerator, 25:9914 (NP-tr-1926)
KAPITOLA, J., Accumulation of /sup 99m/Tc in rat thyroid, 25:8599
KAPITONOV, I. M., Rapid fluctuations of intensity in the gamma radiation of a betatron, 25:9936
KAPLAN, R. W., Influence of host-cell reactivation and uv dose on formation of pure and mixed clones of c mutants in phage kappa, 25:8653
KAPLAN, S. A., Scattering of radiation within a spectral line emitted by turbulent plasma, 25:9481
KARAMYSHEV, M. I., Ternary systems Gd--(Y, Tb, Dy, Ho, Er, Sc)--Al in region to 25 at. percent rare-earth metals, 25:8886
KARANDASHOV, E. A., Effect of trinitrophenylation of myosin on isotopic exchange of oxygen in ATP--$H_2{}^{18}O$, 25:8248
KARO, Arnold M., Anharmonic lattice dynamical properties of solid neon, argon, krypton, and xenon, 25:8262 (UCRL-50903)
KAROUSAKIS, Panayiotis, Neutron amplification and application to a flux-trap reactor, 25:10285
KARPUKHIN, V. T., Current distribution in an E x H discharge with sectionalized electrodes for nonequilibrium conductivity of the plasma, 25:9482
KARZMARK, C. J., Physical and dosimetric aspects of the radiotherapy of malignant lymphomas. II. The inverted-Y technique, 25:8734
Physical and dosimetric aspects of the radiotherapy of malignant lymphomas. I. The mantle technique, 25:8735
KASDAN, A., Interphase boundary waves in the intermediate state of lead, 25:9363 (NYO-2150-64)
KASPAREK, L., Functional changes in the vestibulocochlear analyzer due to irradiation, 25:8792
KASSEM, Abdel-Hamid A., Use of ionizing radiation for the hydrolysis of pectins and the effect on the properties of the extracted pectins, 25:8823
KASTENBAUM, M. A., Secondary disease mortality in rat-mouse radiation chimeras, 25:8619
KASTENBERG, William E., Space--time effects in fast reactor dynamics, 25:10180
KASUGA, Yasuhiro, Loss-of-coolant accident in water-cooled nuclear power reactors. III, 25:10246
KASUMOV, Yu. M., Electromagnetic annihilation of lepton--antilepton pair in hyperon pairs with consideration of polarization and form factors, 25:9730
KATO, Hatsuhiko, Addition chains, 25:10393 (TID-25620)
KATO, Yoshio, Propagation of Pc1 pulsations in F region, 25:9338
KATORSKI, A., Isotope and ortho-para separations of the molecular hydrogens by adsorption at low temperatures, 25:8332
KATSURAGI, Satoru, Accuracy of analytical treatments for resonance absorption in Doppler resonance regions, 25:10038
KATTERWE, H., Electron energy loss spectra of graphite single crystals and evaporated carbon films in the range 0.02 to 0.4 ev, 25:9167
KATZ, B., Far infrared spectra of HCl and DCl in a N matrix, 25:8250
KATZ, Herbert Marvin, Preparing microspheres, 25:8916
KAUL, B. L., Effect of 1-methyl-3-nitro-1-nitrosoguanidine on x-ray-induced chromosomal lesions, 25:8705
KAVANAGH, T. M., X-ray production in ion--atom collisions, 25:9164
KAW, P. K., Particle orbits in two waves of arbitrary amplitude, 25:9477
KAWAI, Y., Production of quiescent plasmas with T/sub i/ > T/sub e/, 25:9483
KAWAKAMI, Yutaka, Choice of activable tracer for spraying agricultural insecticides by helicopter, 25:8426 (NSJ-tr-155)
KAWARABAYASHI, Ken, Possible duality constraints on P-wave nonleptonic decays, 25:9744
KAWASAKI, Satoru, Development of a device for measuring circumferential mechanical properties of cladding tubes, 25:8883
KAZACHEVSKAYA, T. V., Measurement of the energy of soft electrons in the upper atmosphere on December 21, 1966, 25:9345
KAZANSKAYA, A. P., Production of He nuclei at interactions of pions with energy of 60 GeV with heavy nuclei of emulsion, 25:9660
KEDL, R. J., Fluid dynamic studies of the Molten-Salt Reactor Experiment (MSRE) core, 25:10196 (ORNL-TM-3229)
KEEFE, Denis, Status of the ERA research at Berkeley, 25:9917 (UCRL-20125)
KEELER, R. N., Shock waves. II, 25:10409 (UCRL-72770)
KEHOE, R. B., Uranium enrichment in the UK, 25:8431
KEIRIM-MARKUS, I. B., Sensitivity of spherical neutron detectors in energy range from thermal to 10 MeV, 25:8522
KELBER, Charles N., Extended equivalence relation, 25:10310
KELLER, Donald L., Prog. rpt. on LMFBR cladding, structural and component materials, 7--9/70, 25:8863 (BMI-1891)
KELLETT, B. H., Fit to high-energy pion photoproduction, 25:9727
KELLEY, M. C., Operation of dc electric field detector, 25:9301
KELMAN, L. R., Report of meeting on methods and models used to design fuel pins and predict in-pile performance, April 8--9, 1970, Germantown, 25:10212 (TID-25590)
KEL'NER, S. R., Direct production of electron--positron pairs by 2.94-GeV/c negative pions, 25:9661
KEMPER, K. W., Line shape calculation for nuclear scattering from gaseous targets, 25:9924
KENDALL, W., FFTF backup design interface definition discussion of system requirements, 25:10266 (GEAP-5721)
KENNEDY, David James, Polarization of the decametric

XUM

radiation from Jupiter, 25:9158
KERIMOV, B. K., Leptonic decays of vector mesons, 25:9766
KERLIN, T. W., Experiences with dynamic testing methods at Molten-Salt Reactor Experiment, 25:10182
Theoretical dynamics analysis of Molten-Salt Reactor Experiment, 25:10183
KERR, Paul F., Uranium mineralization and alteration, Orphan Mine, Grand Canyon, Arizona, 25:8376
KERSHAW, David, Methods for the Bethe--Salpeter equation. I, 25:9855
Methods for the Bethe--Salpeter equation. II, 25:9856
KESSEL, Quentin C., Multiple ionization of iodine in 1.5- to 12.0-MeV I/sup n+/--Xe collisions, 25:9219
KEYES, W. I., Ratemeter controlled rectilinear scanning, 25:8494
KEYS, J. G., Association between x rays and auroral radar echoes in the southern auroral zone, 25:9320
KHACHIKYAN, E. E., Spectral observations of Markaryan galaxies with uv continuum. II, 25:9140
KHALAF, K. A., Recent developments at kuwait in the control of scale at elevated temperature, 25:10359 (ORNL-tr-2411)
KHALATNIKOV, I. M., Oscillatory approach to a singular point in the relativistic cosmology, 25:9877
KHALIKULOV, A. B., Lifetime of excited states in spherical nuclei ^{139}La, ^{135}La, and ^{133}La, 25:10029 (JINR-P6-5200)
KHALIL, M. A., Measurement of reaction ^{35}Cl(n,γ)^{36}Cl using a three-crystal pair and anti-Compton spectrometer, 25:10000 (PH-2)
KHALIZEV, A. E., Genetic mutations in cell cultures of mammals, 25:8638
KHALKIN, V. A., Determination of the boiling point of astatobenzene, 25:8259 (ANL-Trans-869)
Reaction with benzene of ^{129}I and ^{211}At formed from the noble gases during K-capture, 25:8284 (ANL-Trans-870)
KHANNA, F. C., Effective operators in the nuclear shell model. II, 25:10072
KHARAKHAN, M. L., Analytical properties of the exactly solvable nonrelativistic two-channel scattering problem, 25:9772
KHARCHENKO, I. F., Statistical analysis of oscillations excited in a plasma--beam system, 25:9535
KHAUSTOVICH, G. P., Effect of aperture on plasma parameters, 25:9415
KHAZEN, I. M., Biomedical problems of space flight, 25:8755 (JPRS-51660)
KHEIFETS, S. A., Instability of the motion of particles in a synchrotron for high frequencies of the accelerating field, 25:9934
KHER, V. G., Effect of irradiation on the current pulses in a low-frequency electrodeless argon discharge, 25:9449
KHIDESHELI, G. I., Mass-spectrometric investigation of low-temperature radiolysis of organic sulfides, 25:8290
KHITROVA, V. I., Phase transition in thin films of tantalum oxides, 25:8950
KHMARUK, V. G., Scattering of ion beam in hot-electron plasma, 25:9450
KHOKHLOVA, L. K., High-temperature combustion products for thermoelectric plants with MHD generator, 25:9261
KHORVAT, P., Pulse shaper with the zero time of regeneration for the apparatus blocking at the large loading, 25:8545 (JINR-P13-5377)
KHOZHAINOV, A. I., Magnetohydrodynamics in marine engineering, 25:9266
KHRENOV, A. N., Pulse shaper with the zero time of regeneration for the apparatus blocking at the large loading, 25:8545 (JINR-P13-5377)
KHVOSTIKOV, J. A., Fluorescence of tetracyanoplatinates, 25:10378 (SC-T-70-4052)
KIDWAI, A., Pakistan goes nuclear, 25:10098
KIEFFER, L. J., Angular distribution of O$^-$ from dissociative electron attachment to O_2, 25:9221
KIENBERGER, C. A., Automatic sample changer for the beryllium analyzer, 25:8220 (Y-1744)
KIGHT, Harry K., Model 102 air sampler, 25:8393 (NVO-410-6)
KIKUCHI, Hiroshi, Physics studies on BWR void simulated cores. II, 25:10175
KILIAN, D. C., Development of a fluidized-bed burner for processing Rover fuel, 25:8322 (IN-1423)
KILIN, S. F., Radioluminescence of organic substances. VIII, 25:8274
KILIN, V. S., Integrated hemispherical emissivity of zirconium carbide, 25:8931
KILLANDER, Dick, Uv-irradiation induced changes in the uptake of acridine orange in living mouse fibroblasts in vitro, 25:8770
KIM, Dong Hoon, Fast neutron spectrum and flux in central thimble of TRIGA Mark-II reactor, 25:10277
KIM, H. C., Effects of interstitial impurities on the yielding behaviour of niobium single crystals, 25:8880
KIM, Hong Sik, Fast neutron spectrum and flux in central thimble of TRIGA Mark-II reactor, 25:10277
KIM, Yong Su., Design procedures to determine characteristics of highly enriched heavy water moderated reactors, 25:10318
KIMURA, Motoharu, Study of atomic nucleus by electron scattering, 25:10014
KINGSTON, A. E., Comments on the photoionization of helium, 25:9205
KINNEY, W. E., Neutron elastic- and inelastic-scattering cross sections for yttrium in the energy range 4.19 to 8.56 MeV, 25:9999 (ORNL-4552)
KINOSHITA, Kisei, Local duality in invariant amplitudes for πN scattering, 25:9796
KINZLER, R. V., Engineering development of fluid-bed fluoride volatility processes. Part 16. A safety manual for the engineering-scale alpha facility, 25:8446 (ANL-7672)
KIPPENHAHN, R., Thermal behavior of rotating and magnetic stars, 25:9027
KIPPER, T. A., Spectrophotometry of F stars. IV, 25:9014
KIRICHENKO, G. S., Scattering of ion beam in hot-electron plasma, 25:9450
KIRSON, M. W., Interaction of two nucleons in a nucleus, 25:10079
KISELEVA, K. V., X-ray diffraction of ion-bombarded diamonds, 25:9557
KISHIMOTO, Syunsuke, Narrow muon bundles below ground, 25:9632
KISHKURNO, V. V., Momentum vector in a magnetic track spectrometer, 25:8561
KISIS, A. Yu., Electromagnetic methods of measuring the parameters of MHD processes, 25:9273
KIST, R., Electric fields derived from plasma measurements in the polar electrojet, 25:9335
KITAGAWA, Michiharu, Effects of electron irradiation on conductivity in CdS, 25:9563
KITAGAWA, Toshio, Conformation therapy technique on 6 MeV linear accelerator in treatment of the carcinoma of cervix uteri, 25:8740
KITAKADO, Shinsaku, Possible duality constraints on P-wave nonleptonic decays, 25:9744
KITZKE, K. J., Estimating average nuclear fuel costs, 25:10216
KIVIKAS, Toivolemb, Computer programme for calculation of solid angles and angular acceptances, 25:9910 (LUSY-7007)
KLEIN, M. P., Computer based laboratory-wide data acquisition, analysis, and retrieval system, 25:8193 (UCRL-20132)
KLEIN, S. S., Position-sensitive detectors for the simultaneous determination of several parameters of a particle, 25:8475 (JUL-CONF-4, pp 59-70)
KLEMM, A., Electromigration in metals, salts, and aqueous solutions, 25:8247
KLEPPNER, Daniel, Alkali--alkali differential spin-exchange scattering. I, 25:9223
KLIMYK, A. U., Representations of Gell-Mann--Dashen algebra, 25:9824
KLINC, Tomaz Ladislav, Transverse propagation of neutron waves, 25:9961
KLINK, William H., Symmetries imposed on two-particle systems. III, 25:9818
KLOZENBERG, J. P., Nonlinear plasma waves, 25:9526
KLYUSHNIKOV, O. I., Current generator for studying superconductivity by an impulse method, 25:8580
KNOLL, Peter, Technology of isotope production. I, 25:8429 (ORNL-tr-2400)
KNOPP, E., Conference on science of ceramics, Ronneby Brunn, Sweden, 4/69. V, 25:8933
KNOTH, H., One-neutron transfer reactions with Be, C, and O nuclei, 25:9988
KNUTSON, L. D., Charge-exchange collisions between metastable hydrogen atoms and iodine molecules, 25:9218
KOBAYASHI, Kozo, Three-dimensional canonical algebra and SO(4,2) dynamical group, 25:9832
KOBAYASHI, Tsunehiro, Dual resonance model and extended particle model with arbitrary number of quark--antiquark pairs, 25:9771
KOBZENKO, G. F., Phase diagram of the chromium--terbium system, 25:8889
KOCH, Eckhard, General solution of the electron distribution function for weakly ionized plasmas in arbitrarily time-dependent electromagnetic fields, 25:9470
KOCHESHKOV, K. A., Radiation-thermal isomerization of alkyl bromides, 25:8279
KODIRI, S., Determination of Be by (γ,n) reaction in linac, 25:8225
KOEHLER, E. K., Kinetics and mechanism of solid state reactions in the systems of refractory oxides, 25:8935
KOEPP, C., Influence of correct dead time simulation on the dynamic behavior of model for controlled Na 2 reactors, 25:10186 (KFK-1179)
KOERNER, Juergen G., Octet behavior of single-particle matrix elements (B' absolute value Hw B) and (M' absolute value Hw M), 25:9761
KOERNICKE, H., Microwave diagnostics of strong-current discharges with skin effect. II, 25:9424
KOESTER, L., Coherent scattering amplitude of ^{186}W measured by small angle scattering, 25:10026 (JINR-E3-5371)
KOGAN, R. M., Method for separating γ radiation dose rate of artificial and natural radioactive isotopes in ground, 25:8360
KOHNO, Kaku, Effect of gamma irradiation on the very dilute solution of collagen in the atmosphere of air and nitrogen, 25:8307
KOJIMA, Yuzo, Study of atomic nucleus by electron scattering, 25:10014
KOKE, L. C., Nuclear system manufacture and construction

progress, 25:10088 (CONF-690967-1)
KOLESNIKOVA, L. M., Temperature dependence of spontaneous magnetization in holmium during heating--cooling cycle, 25:9579
KOLESOV, I. V., Identification of elements 102 and 104 with the help of the collimation method, 25:10030 (KFK-tr-329)
KOLOMOITSEV, F. I., Effect of electron bombardment on luminescence of ZnS--Cu phosphor, 25:8485
KOMAR, A. P., Composition and excitation energy of fissioning nuclei in irradiation of ^{209}Bi and ^{197}Au 1 GeV photons, 25:10037
KOMAROV, V. V., Topography of magnetic field at 70-GeV accelerator, 25:9906 (IFVE-SKU-69-95)
KOMENDER, Andrzej, ESR study of bone tissue sterilized by gamma radiation, 25:8825
KOMITOWSKI, D., Accumulation of ^{85}Sr, 25:8597
KOMPANIETS, V. G., Photoproduction of W-meson pairs on electrons, 25:9707
KONDRASHOV, A. P., Effect of electron bombardment on luminescence of ZnS--Cu phosphor, 25:8485
KONDRATENKO, A. N., Nonlinear interaction of waves in a bounded magnetoactive plasma, 25:9514
KONDRATYUK, L. A., Many-baryon resonances, 25:9803 (ITEF-759)
KONECNY, K., Branching ratios and intensities of some transitions in ^{35}Cl(n,γ)^{36}Cl reaction, 25:10009
KONONENKO, V. I., Microwave scattering by low-frequency oscillations in theta-pinch plasma, 25:9520
KONOVALOV, B. S., Interaction $\pi^-\pi^-$ in the reaction π^-p + N^{*++}(1236)$\pi^-\pi^-$ with impulse 4.47 GeV/c, 25:9655 (ITEF-767)
Reaction π^-p + rho$^0\pi^-$p with impulse 4.45 GeV/c, 25:9656 (ITEF-775)
KONOZENKO, I. D., Volume gradient of γ-emf in p-Si, 25:9568
KONSHIN, V. A., Energy dependent anti ν-values for ^{235}U, ^{239}Pu, ^{233}U, ^{240}Pu, ^{241}Pu, and the status of anti ν for spontaneous fission isotopes, 25:10025 (INDC(NDS)-19/N)
KONSTANTINOV, L. V., Reliability of the evaporating channels of Beloyarsk power plant type reactors, 25:10106
KONTSEVOI, V. G., Ternary systems Gd--(Y, Tb, Dy, Ho, Er, Sc)--Al in region to 25 at. percent rare-earth metals, 25:8886
KONYASHEV, E. I., Increasing the power of a linear electron accelerator, 25:9938
KOONS, H. C., Electrostatic instabilities in multicomponent plasmas, 25:9500
KOOPMAN, David W., Single-electron capture by C^{++} in helium, neon, and argon below 40 keV, 25:9215
KOOPMAN, R. N., Heat transfer in reactor components having temperature-dependent thermal conductivity, 25:10203
KOPYLOV, G. I., Integral equations of cascade kinematics, 25:9708
KOPYLOVA, D. K., Integral equations of cascade kinematics, 25:9708
KOPYTENKO, Yu. A., Relation of stable pulsations of the geomagnetic field with parameters of the magnetosphere, 25:9353
KOROBEINIKOV, V. P., Distribution of solar-wind disturbances caused by chromospheric flares, 25:9356
KOROBKIN, V. V., Effect of aperture on plasma parameters, 25:9415
KOROLENKO, Frances Jane, Rex mutant in the house mouse, 25:8645
KOROL'KOV, I. Ya., Topography of magnetic field at 70-GeV accelerator, 25:9906 (IFVE-SKU-69-95)
KOROVYAKOVSKII, Yu. P., Gas motion in close binary systems, 25:9011
KORSUNSKII, I. L., Resonant Bragg scattering of gamma rays by nuclei, 25:9596
KOSINA, Z., Measurement of reaction ^{35}Cl(n,γ)^{36}Cl using a three-crystal pair and anti-Compton spectrometer, 25:10000 (PH-2)
KOSMOLINSKII, F. P., Biomedical problems of space flight, 25:8755 (JPRS-51660)
KOSSENTINI, Abdelmajid, Absolute measurements in fast neutron reactions: the n + D + nnp reaction at 14 MeV, 25:9968 (NP-18488)
KOSSYI, I. A., Possibility of measuring directed fluxes in a plasma contained in a toroidal magnetic trap, 25:9410 (CTO-736)
KOSTIC, S., Radioactive characteristics necessary for studying fission products: beta radiation and conversion electrons, 25:10023 (CEA-N-1372)
KOSTRITSA, A. A., Concerning the cone of radiation in the equation of the kinetic transport equation, 25:9609
KOSTYUKOV, N. S., Specific volume resistance of steatite ceramics in high-intensity γ fields, 25:9551
KOSUGE, K., Electrical properties of V_6O_{13} single crystal, 25:9580
KOTADIA, K. M., Equatorial F2-layer anomaly and q-type sporadic-E layer, 25:9291
KOTOV, A. A., Composition and excitation energy of fissioning nuclei in irradiation of ^{209}Bi and ^{197}Au 1 GeV photons, 25:10037
KOTSARENKO, N. Ya., Excitation of longitudinal oscillations of a magnetized plasma by a transverse electromagnetic wave, 25:9518
KOULKES-PUJO, Anne-Marie, Pulse radiolysis study of transitory species Au II, 25:8306
KOVTUN, R. I., Statistical analysis of oscillations excited in a plasma--beam system, 25:9535
KOYAMA, Shigeo, Numerical methods for solving one-point reactor kinetic equations, 25:10312
KOZLOV, S. I., Distribution of absorbed energy of x radiation in Earth's atmosphere, 25:9351
KRAETZIG, E., Investigation of superconducting proximity effects with acoustic surface waves, 25:9378
KRAMER, Gordon, Semiconductor dosimeter having low temperature diffused junction, 25:8565
KRAMER, Henry Herman, Saline solution containing radioactive gas, 25:8309
KRAMSKOI, G. D., Determination of the critical current in a section with radial slots in the iris disk, 25:9907 (KFK-tr-335)
KRASNOPEVTSEV, V. V., X-ray diffraction of ion-bombarded diamonds, 25:9557
KRASNOV, Yu. K., Initial stage of avalanche development, 25:9731
KRASSNOYAROV, N. V., Certain properties of fuel behavior of can structural material in fast reactor conditions, 25:8896 (BNWL-tr-57)
KRAUS, W., Quantitative alpha-autoradiography: a documentation, 25:8584 (SZS-15/70)
KREISEL, E., Static equilibrium states of spherically symmetric masses with arbitrary baryon number in the tetrad theory of Treder, 25:9876
KREISLER, M. N., Performance of large-volume two-phototube neutron detector, 25:8547 (PURC-4159-13)
KREJCI, I., Effects of altered external calcium concentrations on fluxes of ^{45}Ca in rat myometrium, 25:8601
KREPLIN, R. W., Observations of electron density during a solar flare, 25:9300
KREY, P., Accumulated fallout ^{90}Sr in the Rocky Flats area, 25:8353 (HASL-237, pp I.11-26)
KRISHTAL, M. A., Track autoradiography for the study of the microdistribution of certain elements in metals, 25:8235
KRISTIAN, Jerome, Limits for optical counterparts of fifteen radio pulsars, 25:9061
KRMPOTIC, F., Unique first forbidden β-transitions, 25:10064
KROHN, David L., Toxic effect of thermal neutrons on the rabbit electroretinogram, 25:8761
KROMMINGA, A., Bismuth-209 ground-state analog in ^{209}Po, 25:10045
KROSHKIN, N. I., Measurement of energy spectra and average number anti ν of prompt fission neutrons, 25:10039
KRTIL, J., Isolation of ^{95}Zr--^{95}Nb from solution of fission products, 25:8214
KRUCHININ, S. P., Interaction $\pi^-\pi^-$ in the reaction π^-p + N^{*++}(1236)$\pi^-\pi^-$ with impulse 4.47 GeV/c, 25:9655 (ITEF-767)
Reaction π^-p + rho$^0\pi^-$p with impulse 4.45 GeV/c, 25:9656 (ITEF-775)
KRUER, W. L., Particle orbits in two waves of arbitrary amplitude, 25:9477
KRUGER, G., FFTF backup design interface definition discussion of system requirements, 25:10266 (GEAP-5721)
KRUGER, Paul, Technology of nuclear explosions for peaceful uses, 25:8388
KRUGLOV, S. P., Wire spark chamber system with magnetostrictive information retrieval, 25:8552
KRUGLOVA, I. M., Resonance photoionization of helium and helium-like ions, 25:9239
KRUKOVSKII, V. K., Covering graphite with niobium from a vapor--gas mixture, 25:8917
KRUSE, U. E., Coherence of isoscalar and isovector exchange amplitudes in π^+p + A_2^+p, 25:9650 (COO-1195-202)
KRYSHKIN, V. I., Shower spark chambers for detecting particles moving at small angles with respect to the beam being stopped, 25:8553
KRYZHANOVSKII, O. I., High-voltage pulse generator, 25:9932
KSHIRSAGAR, S. R., Effect of irradiation on the current pulses in a low-frequency electrodeless argon discharge, 25:9449
KUCHTA, J., Pretightening of large pressure vessel flange joints, 25:10096 (ZJE-65)
KUCHUBERIYA, I. Kh., Spectrum of scattered laser radiation and the measurement of electron density in a pulsed plasma, 25:9409 (CTO-733)
KUDIMOV, A. V., Distribution of absorbed energy of x radiation in Earth's atmosphere, 25:9351
KUEHL, R., Fast neutron flux measurements with stilbene-scintillator, 25:8509
KUEHN III, Nicholas Henry, Study of some aspects of the neutron thermalization problem, 25:9962
KUEMMEL, H., Short-range correlations in a Woods--Saxon shell model, 25:10071
KUHL, David E., Computer processing of images in nuclear medicine, 25:8727
KUHLMANN, W., Analog-division stage for use with position-sensitive detectors, 25:8471 (JUL-CONF-4, pp 11-21)
KUKHTIN, V. V., Dual resonances models. I, 25:9887 (ITF-70-43)
KULEBAKINA, L. G., Radioecological studies of the Mediterranean Sea, 25:8630

XUM

KULESHOV, S. P., High-energy elastic and inelastic hadron collisions, 25:9751
KULEVA, N. V., Effect of trinitrophenylation of myosin on isotopic exchange of oxygen in ATP--$H_2{}^{18}O$, 25:8248
KULLEN, B. J., Engineering development of fluid-bed fluoride volatility processes. Part 16. A safety manual for the engineering-scale alpha facility, 25:8446 (ANL-7672)
KUMAO, Akihiro, Drops of oxides on tungsten oxide needles and nuclei of dendritic crystals, 25:8859
KUMAR, N., Optical absorption and electrical conduction in KBr crystals containing diffused Mg, 25:9570
KUMTA, U. S., Dehydro-irradiation process for tropical shrimps, 25:8820
KUNDU, M. R., Polarization of Tycho's supernova remnant at 2.8 cm, 25:9073
KUNZ, W. E., Vela V and VI solar x-ray atlas. II, 25:9097 (LA-4454(Vol.2))
KUPTSOV, V. M., Altitude distribution of ^{238}U, ^{232}Th, and ^{239}Pu in atmospheric fallout, 25:8372
KUROKI, Toshio, Chemical carcinogenesis in vitro, 25:8746
KUROV, G. A., Electrical resistance and transparency of films of Mg--Sb, Mg--Bi, and Mg--Sn alloys, 25:10344 (BNL-tr-386)
KURSTEDT, H. A. Jr., Short-interval series pulsing-experimental studies and numerical experiments, 25:10282
KURZ, Rudolf, Crack formation nitrided components of X6CrMo4, 25:8940
KUSHNIR, A. J., Interphase boundary waves in the intermediate state of lead, 25:9363 (NYO-2150-64)
KUYATT, C. E., Absolute measurement of differential cross sections for electron scattering in helium, 25:9222
KUZEMSKII, A. L., Derivation of a schroedinger type equation with damping for the dynamical system weakly coupled to a thermal bath, 25:9607
KUZIN, N. I., Question of high-pressure scale, 25:10352 (LA-tr-70-26)
KUZIN, V. I., Determination of the boiling point of astatobenzene, 25:8259 (ANL-Trans-869)
Reaction with benzene of ^{125}I and ^{211}At formed from the noble gases during K-capture, 25:8284 (ANL-Trans-870)
KUZ'MA, Yu. B., New ternary compounds with structure of $YCrB_4$ type, 25:8948
KUZNETSOVA, L. V., Mitotic cycle in normal and irradiated cells of the human diploid strain WI-38, 25:8743
KUZNETSOVA, O. B., Recovery phenomena in yeast. II, 25:8797
KYLES, J., Energy dependence of proportional counter pulse-height resolution, 25:8505
KYRZHANOVSKII, O. I., High-voltage pulse source for the deflector plates in an ion cluster input system to the synchrotron chamber, 25:9931

L

LAANER, G. S., Processing in limited geometry. XVI, 25:8445 (AERE-R-5104)
LACAZE, A., Cryogenic devices for applications of superconductivity, 25:9397
LACKEY, M. E., Use of steam-electric power plants to provide thermal energy to urban areas, 25:10094 (ORNL-HUD-14)
LACOMBE, P., Anion and cation diffusion in some transition metal oxides, 25:8934
LACROIX, Andre, Electromagnetic flow measurement device, 25:8400
LAFUMA, J., Experimental research on the treatment of contamination by transplutonium elements, 25:8590 (CEA-CONF-1658)
LAGNAUX, J. P., anti KN elastic amplitudes between 1 and 1.3 GeV/c, 25:9667
LAGRANGE, Philippe, Microdetermination of molybdenum by anodic stripping at constant current using the hanging mercury drop electrode, 25:8206
LAKHTIN, Yu. M., Metallurgy and the hot working of metals, 25:8894
LAL, K. B., Cylindrical wave solutions of field equations of general relativity containing electromagnetic fields, 25:9873
LALLEMENT, R., Contraction of β and delta phases of Pu under the effect of self-irradiation at 4.2°K, 25:8904
LAM, S. H., Far-wake structure in rarefied plasma flows past charged bodies, 25:9478
LAM, Yuk-Ming P., Phenomenological Lagrangian model of chiral SU(3) x SU(3) for mesons and baryons with symmetry breaking, 25:9794
LAMB, Eugene, Prog. rpt. on ORNL isotopic power fuels, 9/30/70, 25:8427 (ORNL-4639)
LAMB, R. C., Measurements of π^-p elastic scattering from 1.71 to 5.53 GeV/c, 25:9652 (COO-1764-112)
LAMBERT, E., Study of π^--mesic atoms by means of scattering lengths, 25:9791
LAMBERT, J. E., Fuel latch design, 25:10224
LAMBERT, J. P. F., Determination of vanadium by neutron activation analysis at nanogram levels to formulate a low-vanadium diet, 25:8228
Neutron activation analysis program of the food and drug administration, 25:8227
LAMERTON, L. F., Adaptation of hemopoietic systems to environmental conditions, 25:8608
LANCE, Joseph R., Implantable circulatory support system, 25:8436
LANDE, K., Possibility that pulses of long range field are source of CP non-invariance, 25:9826 (NYO-2171-329)
LANDMARK, B., Ionospheric observations during annular solar eclipse of May 20, 1966. V, 25:9313
LANDOLT, D., Transfer processes in ECM, 25:10403 (UCRL-19615)
LANE, Kenneth D., Chiral symmetry breaking and K/sub 14/ axial-vector form factors, 25:9743
LANGDON, A. Bruce, Nonphysical modifications to oscillations, fluctuations, and collisions due to space--time differencing, 25:9459 (UCRL-72635)
LANGE, C. S., Estimation of survival curve parameters for the cells of organized tissues in vivo from split dose data, 25:8777
LANGIE, St., Gammagraphy in the diagnosis of cerebral abscess, 25:8714
LANGLEY, Robert A., Range--energy relations for He ions and protons in N_2, O_2, and air (0.2 to 2.0 MeV), 25:9162 (SC-RR-70-788)
LANZI, G., Analysis of electron-paramagnetic-resonance lineshape of Tb^{4+} in polycrystalline TbO_2, 25:9582
LAPIDUS, L. I., Cross section of anti Kd + KY_1Y_2, 25:9804 (JINR-P2-5231)
LARCHER, Ghislain, Development of a clean shock tube for making spectroscopic measurements on a plasma, 25:9510
Intensities of spectral lines and background continuum of Ar plasma produced in a shock tube, 25:9423
LATARJET, R., Inactivation of the scrapie agent by near monochromatic ultraviolet light, 25:8805
LATOUR, Jean, Envelope models for A type-stars, 25:9019
LAUGHLIN, C., Perturbed generalized eigenvalue equation for the helium atom, 25:9185
LAUGHLIN, J. S., Computer-analyzed counting and scanning, 25:8716
LAURENS, G., $Pi^+\pi^-$ elastic cross section, 25:9669
Piπ phase shifts, 25:9670
LAVERRIERE, R., Theoretical analysis of (α,2α) reactions, 25:9987
LAW, J., SIGMA-suppression in /sub Λ/^{5}He, 25:9815
LAW, Stephen L., Use of selective ion exchange paper in x-ray spectrography and neutron activation. Application to the determination of gold, 25:8221
LAWANDE, S. V., He and H^- 1^1S and 2^3S states computed from Feynman path integrals in imaginary time, 25:9177
LAWERGREN, B., Isobaric analog states in ^{24}Mg, ^{27}Al, and ^{28}Si, 25:10007
LAWRENCE, John K., Fermions in general relativity, 25:9879
LAWSON, A. C., Superconductivity and normal-state properties of Th--U alloys, 25:9389
LAZAREV, V. I., Corpuscular flow and heating of the electron gas at E-layer altitudes, 25:9341
LAZAREV, Yu. A., Identification of elements 102 and 104 with the help of the collimation method, 25:10030 (KFK-tr-329)
LEBEDEV, I. G., Certain properties of fuel behavior of can structural material in fast reactor conditions, 25:8896 (BNWL-tr-57)
LEBEDEV, K. A., Morphological aspects of the effect of ionizing radiation on antibody formation, 25:8762
LEBEDEV, P. I., High-voltage pulse generator, 25:9932
High-voltage pulse source for the deflector plates in an ion cluster input system to the synchrotron chamber, 25:9931
LEBEDINETS, V. N., Meteor ionization in E layer, 25:9307
LE CONTEL, J. M., Short period variable stars. II, 25:9025
Short-period variable stars. III, 25:9035
L'ECUYER, J., $^{20}Ne(p,t)^{18}Ne$ reaction as a test of the ^{18}Ne and ^{20}Ne wave functions, 25:10006
LE DIEU DE VILLE, Alain, Characteristics of ordinary concrete relative to radioprotection calculation, 25:8960 (CEA-N-1355)
LEDNEV, A. A., Topography of magnetic field at 70-GeV accelerator, 25:9906 (IFVE-SKU-69-95)
LE DOUCEN, Roger, Charge transfer during collisions between H^+ and Kr, Xe, NH_3, C_2H_2, C_6H_6, 25:9229
LEE, D. A., Enrichment of lithium isotopes by extraction chromatography, 25:8330
LEE, H. J., Gauge fields in the many-body problem and superfluidity, 25:9357
LEE, H. S., Observations of electron density during a solar flare, 25:9300
LEE, Keenan, Remote sensing in exploration for mineral deposits, 25:8378
LEE, P., Continuous spectrum of neutral helium from gaseous nebulae, 25:9046
LEE, T. D., History of weak interactions, 25:9735 (NYO-1932(2)-186)
Remarks on the Δ I absolute value = $^1/_2$ rule in non-leptonic weak decays and use of phenomenological Lagrangian, 25:9732 (BNL-50260)
LEE, Yee Yen, Phenomenological Lagrangian model of chiral SU(3) x SU(3) for mesons and baryons with symmetry breaking, 25:9794
LEE, Young C., Studies on RNA and histone relationships during the synchronized Tetrahymena life cycle, 25:10400 (UCLA-12-788)
LEER, E., Ion-reflection of downward-propagating whistlers at low latitudes, 25:9321

LEFF, E. G., The FREADM-1 code: a fast reactor excursion and accident dynamics model, 25:10241 (GEAP-13608)
LEGGEAT, A., Structure of some trapped hold centers in CaF_2. II, 25:9546
LEGRAND, Jean, Decay schemes of ^{59}Fe and ^{192}Ir, 25:10032 (ORNL-tr-2345)
LEIKIN, E. M., Photoproduction of positive pions on protons in region of resonance $P_{33}(1236)$, 25:9623
LEIPUNSKII, A. I., Bulletin of the Russian Nuclear Data Center, 25:9948
LEITER, Darryl, Paradox of radiation from a uniformly accelerated point electron and a consistent physical framework for its resolution, 25:9709
LEMAIRE, R., Crystalline structures of the intermetallic compound (Gd/sub 2/3/2Fe/sub 1/3/)Fe_3, 25:8891
LEMBO, G., Control of contaminated air in a reactor fuel element fabrication plant, 25:8695
LE MEUR, R., Radioactive characteristics necessary for studying fission products: beta radiation and conversion electrons, 25:10023 (CEA-N-1372)
LENCIONI, Donald E., Plasma motion in a time-changing toroidal octupole magnetic field, 25:9402
LEND'EL, V. I., Problem on role of rho and sigma mesons in strong interactions, 25:9750
LENGEMANN, F. W., Determination of contained-milk volume of the mammary gland of the goat by ^{141}Ce and ^{14}C-PEG-4000, 25:8587
LENORMAND, Jean-Michel, Charge transfer during collisions between H^+ and Kr, Xe, NH_3, C_2H_2, C_6H_6, 25:9229
LEON, Burke, Magnetic coupling and phase boundaries for pseudobinary alloys containing lanthanides, 25:9576
LEONARDI, R., g/sub A/ and g/sub V/ from mirror nuclei, 25:9742
LEONOV, V. V., Emission of novas prior to light maximum, 25:9010
LEPERT, Claude, Thermally insulating jacket for a nuclear reactor, 25:10335
LEPLAE, L., New approach to the Josephson effect, 25:9364
LESSER, V. R., Micro-computer model for the definition and execution of complex information processing systems, 25:10394 (TID-25622)
LESSER, Victor R., Variable control structure micro-computer architecture, 25:10395 (TID-25623)
LEVAN, H., Radiosensitivity of mice exposed to various temperatures and low-dose rate radiation, 25:8768
LEVEN, Ronald, Nonlinear theory of beam--plasma interactions. III, 25:9466
Nonlinear theory of beam--plasma interactions. IV, 25:9469
LEVIN, A. A., Ecological models applied to radionuclide transfer in tropical ecosystems, 25:8626
LEVINE, R. D., Classical and semiclassical limits in collision theory, 25:9228
LEVINS, D. M., Heavy water production, 25:8315 (AAEC/TM-562)
LEVITZ, N. M., Engineering development of fluid-bed fluoride volatility processes. Part 16. A safety manual for the engineering-scale alpha facility, 25:8446 (ANL-7672)
LEVY, Donald H., Magnetic resonance spectrum of vibrationally excited OH and a prediction of the radio-astronomy spectrum, 25:8975
LEVY II, H., Born wave cross section calculations for excitation of $He(1^1S)$ to $He(N^1L)$, 25:9204
LEW, Art, Approximation techniques in discrete dynamic programming. I, 25:10396 (TID-25624)
Approximation techniques in discrete dynamic programming. II, 25:10397 (TID-25625)
Reduction of dimensionality by approximation techniques: diffusion processes. I, 25:10418 (USCEE-350)
LEYSE, R. H., PWR FLECHT (Full Length Emergency Cooling Heat Transfer) Group II test report, 25:10229 (WCAP-7544)
LEZNOV, A. N., Unitary representations of the conformal group, 25:9823
L'HERITEAU, Jean-Pierre, Critical examination of ^{240}Pu neutron cross sections, 25:10021 (CEA-N-1273)
LHEUREUX, Colette, Processes for simultaneously purifying and concentrating plutonium solutions, 25:8338
LIANG, V. K. C., Kondo temperature and unitarity limit in non-dilute magnetic amorphous alloys, 25:10347 (CALT-822-20)
LIBCHABER, A., Josephson effects, 25:9384
LIEBICH, V., Electron temperature and density distribution of an argon plasma in inductive hydrodynamic shock wave tubes and their time dependence, 25:9418
LIEBMAN, A., Electron spin resonance studies on neutral aromatic hydrocarbon radicals, 25:8252
LIEDER, Rainer M., Collective levels in ^{72} ^{74} ^{76} ^{78}Se, 25:10001
LIFSHITZ, E. M., Oscillatory approach to a singular point in the relativistic cosmology, 25:9877
LIKHTER, Ya. I., Detection of perturbations of geomagnetic field in the magnetosphere, 25:9346
LILLEY, A. E., Detection of methyl alcohol in Sagittarius, 25:9060
LIMBER, D. Nelson, Asymmetries in envelopes of Wolf--Rayet components of close binaries, 25:9004
LIN, H. H., Radiation protection experience at the one-megawatt pool reactor THOR and its affiliated facilities, 25:10284
LINDELL, Kermit F., Precisely controlled+ low range humidity system, 25:10376 (SC-RR-70-775)
LINDGREN, D., Mutagenic effect of ^{90}Sr in barley, 25:8648
LINDQUIST, J., Measurement of the up-down asymmetries in the beta decay of polarized lambdas, 25:9626 (COO-1545-87)
LINGERAK, W. A., Accurate and precise titrimetric analysis of uranium in nuclear fuels, 25:8202 (RCN-126)
Determination of oxygen-to-uranium ratio in hyperstoichiometric uranium dioxide, 25:8203 (RCN-127)
Determination of oxygen-to-uranium ratio in hypostoichiometric uranium dioxide, 25:8204 (RCN-128)
LIONS, Noel, Electromagnetic flow measurement device, 25:8400
LIPANINA, A. A., Effect of treatment of steel with Trylon B on its hydrogen absorption, 25:8842
LIPATOV, V. P., Increasing the power of a linear electron accelerator, 25:9938
LIPKA, Jozef, Preparation of Moessbauer source, 25:9595
LIPPMANN, Bernard A., Unique definition of the quasi-stationary state for resonant processes, 25:9209
LISSY, Margit, Crack formation nitrided components of X6CrMo4, 25:8940
LITTLE, John B., Relative biological effectiveness of the $^{10}B(n,\alpha)^7Li$ reaction in HeLa cells, 25:8745
LIU, Chalcie, Optical spectra observed during ion--molecule collisions, 25:9213
LIU, Chuan Sheng, General scheme of studying trapped particles in fusion devices, 25:9420
Trapped-particle effect on drift-wave instability in toroidal systems, 25:9490
LIUTI, G., Photochemical separation of the carbon isotopes, 25:8331
LIVSHITS, V. A., Spectra of photoconductivity of green leaves and chloroplasts at a frequency of 10^{10} cycles per second, 25:10412 (UCRL-Trans-1427)
LKHAGVA, O., Use of K-harmonics in scattering problems, 25:9889 (JINR-P4-5366)
LLORET, Polen, Gamma ray camera, 25:8497
LLOYD, O., Initiation of arcs by ion bombardment, 25:9442
LOBANOV, E. M., Activation methods for determining content of Ta and Cs in rocks, 25:8230
LOBANOV, Yu. V., Identification of elements 102 and 104 with the help of the collimation method, 25:10030 (KFK-tr-329)
LOCHER, J. Th., Biphasic scan in cirrhotic liver disturbances based on various physiological principals, 25:8715
LOCK, W. O., Intermediate energy nuclear physics, 25:9694
LOCKETT, George Edward, Improvements in nuclear reactors,. 25:10168
LODDING, A., Thermotransport in monatomic and ionic liquids, 25:8336
LODHI, M. A. K., Independent-particle-model energy levels, 25:10085
LOFROTH, E., Fuel element for a nuclear reactor, 25:10219
LOGAN, B. A., Polarization sensitivity of rectangular Li drifted silicon detector, 25:8508
LOMBARD, L., Formation and nature of twin crystals in U_3Si, 25:8946
LOMBARDI, J. C., $^7/_2^-$ isobaric analogue resonances in odd isotopes of Sb, 25:10044
LONGHURST, T. H., Choice of bath materials for the inert gas fusion method for the determination of oxygen in metals, 25:8194 (AECL-3743)
LONNGREN, K. E., Reflection of pseudowaves, 25:9531
LOONEN, J. P., Coarse analysis of the helium-weak B star iota Ori B, 25:8995
LOPAC, V., Semi-microscopic description of even tellurium isotopes, 25:10042
LOPRIENO, N., Effect of caffeine on mutation and recombination, 25:8637
LORIN, C., Pool nuclear reactor, 25:10276
Pool-reactor, 25:10280
LOUBSER, J. H. N., ESR in irradiated silicon carbide, 25:9545
LOUDE, J. F., Production and characteristics of a 14-MeV neutron beam, 25:9955
LOUISE, R., Morphological and kinematical study of two planetary nebulae, 25:9048
LOVAS, I., Exactly soluble three-body model of resonance scattering, 25:9890
LOVELACE, R. V., Minimum observable diameter of radio sources, 25:9084
LU, A. H., t-matrix perturbation theory, 25:10068
LU, C. C., Eigenvalues, radial expectation values, and potentials for free atoms from Z = 2 to 126 as calculated from relativistic Hartree--Fock--Slater atomic wave functions, 25:9168 (ORNL-4614)
LU, Eugene Y. C., Unitarity and fixed poles of weak amplitudes in a perturbation-theory model, 25:9898
LUCKE, W. H., Ion-implantation induced optical absorption edge shifts in GaP, 25:9562
LUCY, L. B., Formation of resonance lines in extended and expanding atmospheres, 25:9044
LUDWIG, D., Measurement of ion temperature in hydrogen arc by means of thermal Doppler effect, 25:9413 (SC-T-71-3001)
LUE, J. W., Hypersound attenuation in superconductors by quasi-particle creation, 25:9368
LUE, Phillip K., Southern hemisphere radio sources. I, 25:9067

Southern hemisphere radio sources. II, 25:9066
LUMINARI, M., Dynamic behaviour of two-phase flow rods for nuclear reactor control, 25:10187
LUNDAHL, L., Search for OH 18-cm emission in the Cepheus IV association, 25:9015
LUNDBY, A., Backward rho⁺ production in π⁺p reactions at 5.2 GeV/c, 25:9665
LUNINA, L. I., Reliability of the evaporating channels of Beloyarsk power plant type reactors, 25:10106
LUPSAN, V., Radioactivity of honey, 25:8665
LUSIGNOLI, M., K anti K π final states for N anti N annihilation at rest in Veneziano language, 25:9765 (NP-18578)
LUTZ, Barry L., Emission spectrum of CN*, 25:9186
LUTZ, Marc, Partial cell irradiation by uv and visible light, 25:8744
LYALIN, E. O., Properties of ⁶LiI(Eu) crystals at low temperatures, 25:8529
LYBERG, Mats Douglas, Behavior of resonances for some simple potentials, 25:9894
LYKKEN, G. I., Fermi velocity in single-crystal films of Pb, 25:9373
LYMAN, J. T., Relative biological effectiveness of heavy ions in producing mutations, tumors, and growth inhibition in the crucifer plant, arabidopsis, 25:8800
LYNGA, G., Distribution of OB stars in Southern Milky Way, 25:9026
LYON, G. F., Mid- to high-latitude ionospheric electron content, 25:9287
LYON, R. J. P., Remote sensing in exploration for mineral deposits, 25:8378
LYS, J., Doubly charged mesons in anti pp annihilations into pions near 1.9 GeV/c, 25:9643
LYUBCHANSKII, E. R., Problems of plutonium toxicology, 25:8594 (LF-tr-41)
LYUBIMOV, V. B., Integral equations of cascade kinematics, 25:9708

M

MACBETH, R. V., Forced convection burnout in water, 25:8410
MACCHI, Odile, Study of a point process characterized by its multicoincidences, 25:9692
MACHTA, Lester, Radioiodine levels in US public health service pasteurized milk network from 1963--1968 and their relationship to possible sources, 25:8629
MACKOWSKI, J. M., Fabrication and utilization of lithium-drifted silicon detectors, 25:8546 (LYCEN-6847)
MACQUEEN, K. F., Effect of gamma radiation on vitamin content of enriched flour, 25:8816
MAECK, William J., Prog. rpt. on silver zeolite: iodine adsorption studies, semiannual, 7/1--12/31/69, 25:8321 (IN-1363)
MAGER, T. R., Heavy section steel technology program. Technical report No. 11. Notch preparation in compact tension specimens, 25:8872 (WCAP-7579)
MAHAJAN, K. K., Polar maximum of electron concentration at 1000-km altitude, 25:9317
MAHANTHAPPA, K. T., Nonexistence of ambiguities in SU(3) x SU(3) breaking, 25:9831
MAHARANA, J., PiN charge-exchange polarization in Veneziano model, 25:9793
MAHESHWARI, Amar, Weak interaction as an S matrix, 25:9740
MAHIEU, C., Corrosion tests on various materials in seawater up to 150°C, 25:10360 (ORNL-tr-2412)
MAHLER, Delmar J., Study of trace metals in fingernails and hair using neutron activation analysis, 25:8229
MAHUT, R., Corrosion tests on various materials in seawater up to 150°C, 25:10360 (ORNL-tr-2412)
MAIANA, L., Nonexistence of ambiguities in SU(3) x SU(3) breaking, 25:9831
MAILLOT, Jean-Paul, Nuclear probe using a single cable, 25:8493
MAILLOT, Patrice, Development of a clean shock tube for making spectroscopic measurements on a plasma, 25:9510
Intensities of spectral lines and background continuum of Ar plasma produced in a shock tube, 25:9423
MAIRE, J., Boron carbide agglomerate, 25:8919
MAISIN, J. R., Ultrastructure of the lung of mice exposed to a supra-lethal dose of ionizing radiation on the thorax, 25:8778
MAJUMDAR, N. K., Optics of the ion source extraction space, 25:9922
MAKAR'IN, V. K., 70 kOe pulse magnet, 25:8555
MAKAROV, I. E., Kinetics of thermal and photostimulated extinctions of trapped electrons in γ-irradiated vitreous alkaline ice, 25:8287
MAKHANKOV, V. G., Correlations of turbulent pulsations in plasma, 25:9475
MAKHNENKO, L. A., Forming beams and beam parameters in output channels of 360-MeV electron linear accelerator, 25:9927
MAKSIMENKO, B. P., Recording of 10 to 100 keV electrons with surface-barrier silicon counters, 25:8524
MALAVIYA, V., Resonance charge transfer between protons and excited hydrogen atoms. III, 25:9203
MALDUEV, V. L., Miniature end window counter for soft beta-radiation, 25:8521
MALDY, J., Superconducting thin films, 25:9385
MALIK, F. B., Eigenvalues, radial expectation values, and potentials for free atoms from Z = 2 to 126 as calculated from relativistic Hartree--Fock--Slater atomic wave functions, 25:9168 (ORNL-4614)
MALMBERG, P. R., Ion-implantation induced optical absorption edge shifts in GaP, 25:9562
MALOV, L. A., Non-rotational state of deformed nuclei with an odd number of neutrons in range 165 less than or equal to A less than or equal to 175, 25:10028 (JINR-P4-5228)
MALUSZYNSKA, K., Investigation of ⁹Be(t,n)¹¹B reaction at 1.10 MeV, 25:9976 (JINR-P15-5148)
MANCINI, F., New approach to the Josephson effect, 25:9364
MANCINI, G., Factors influencing haematopoietic spleen colony formation in whole-body irradiated mice. II, 25:8767
MANDZHAVIDZE, A. G., Temperature dependence of spontaneous magnetization in holmium during heating--cooling cycle, 25:9579
MANDZHAVIDZE, Z. Sh., Characteristics and capabilities of a discharge--condensation chamber, 25:8551
MANERO, F., Energy dependent anti ν-values for ²³⁵U, ²³⁹Pu, ²³³U, ²⁴⁰Pu, ²⁴¹Pu, and the status of anti ν for spontaneous fission isotopes, 25:10025 (INDC(NDS)-19/N)
MANYUKOV, B. A., Distribution of random displacement of track points due to Coulomb multiple scattering, 25:8559
MAPLE, M. B., Superconductivity and normal-state properties of Th--U alloys, 25:9389
MARABINI, A., Lung scintiphotography with /sup 113m/In Fe(OH)$_3$ aggregates, 25:8721
MARADUDIN, A. A., Model potential calculation of Raman tensor for Be, Mg, and Zn, 25:9598
MARCHENKOV, V. V., Pulse generator for stabilizing a spectrometer circuit, 25:8542
MARCHESINI, G., Production cross sections in the multiperipheral model, 25:9756
MARCIANI, Dante Juan, Fractionation and analysis of gamma irradiated lysozyme, 25:8604 (COO-690-41)
MARCUS, R. A., Extension of the WKB method to inelastic or reactive collisions, 25:9198
MARDER, B. M., Stability of high-β, helically symmetric pinch, 25:9498
MARGULOVA, T. Kh., Effect of treatment of steel with Trylon B on its hydrogen absorption, 25:8842
MARIN, Pierre, Electron positron collisions in the Orsay storage ring, 25:9919
MARINA, D. M., Problem on role of rho and sigma mesons in strong interactions, 25:9750
MARINE, J., P--N junction formation in ion-implanted ZnTe, 25:9560
MARIN GORRIZ, D. Francisco, Various radiobiological considerations on therapeutic castration of women, 25:8732
MARKIV, V. Ye., Investigation of Nb--Fe--Al and Nb--Co--Al systems, 25:8890
MARKO, Myroslaw, Energy absorber for a nuclear plant, 25:10247
MARKOV, M. A., Friedman theory, 25:9870 (JINR-P2-5289)
MARKOVINA, A., Calculation of self-limiting power excursions, 25:10281
MARKS, D., Disquiet over West German reactors, 25:10097
MARLOW, William F., Determination of trace elements in glass by activation analysis using hydrated antimony pentoxide for sodium removal, 25:8223
MARQUIT, E., Observation of the decay eta' → γ γ, 25:9651 (COO-1764-111)
π⁻p charge exchange at backward angles, 25:9653 (COO-1764-113)
Reaction π⁻p → nπ⁺π⁻ at high momentum transfer, 25:9654 (COO-1764-114)
MARSHALEK, E. R., Gauge fields in the many-body problem and superfluidity, 25:9357
MARSHANSKII, V. S., Topography of magnetic field at 70-GeV accelerator, 25:9906 (IFVE-SKU-69-95)
MARTELLUCCI, S., Energetic ions produced by subnanosecond laser pulses, 25:9484
MARTIN, A. D., Regge cuts and asymptotic sum rules for πN forward scattering, 25:9800
MARTIN, Jean, Winches used for the handling of nuclear materials, 25:8460
MARTIN, Siegfried, Conference on position-sensitive detectors in nuclear physics, Juelich, Ger., 7/69, 25:8469 (JUL-CONF-4)
MARTIN, William C., Energies of 1snl(1 greater than or equal to 3) configurations in ⁴He I as calculated from polarization theory, 25:9173
MARTINEZ, Francisco Pascual, Survey of nuclear power, 25:10104
MARTY, Denis, Coil giving stellarator-type magnetic configuration, 25:9509
MARX, Egon, Relativistic quantum mechanics of fermions, 25:9841
MASEK, G. E., S-wave pion--pion scattering length, 25:9668
MASHKOVA, E. S., Mechanism of ion scattering by crystals, 25:9556
MASINI, G., Dynamic behaviour of two-phase flow rods for nuclear reactor control, 25:10187
MASLEY, A. J., Solar cosmic-ray observations during 1969, 25:9260
MASNOU-SEEUWS, F., Fine-structure transitions in sodium--

XUM

rare-gas collisions, 25:9207
MASUDA, Kohzoh, Enhanced diffusion of high-temperature ion-implanted antimony into silicon, 25:9569
MASUDA, Kouji, Effects of temperature on dose-response curve of HeLa S3 cells irradiated with x rays, 25:8747
MATCHERET, Georges, Oxidation of uranium carbides in gaseous environments, 25:8907 (CEA-Bib-183)
MATEICIUC, V., Doppler effect of 6.24 eV resonance in ^{121}Sb, 25:10041
MATHIESON, E., Pulse shape discrimination in proportional counters, 25:8516
MATHIEU, G., Geochemical studies on Cranberry and Sterling Lakes, 25:8350 (CU-2493-11, App.4)
MATHUR, B. P., Effect of chemical exchange between D_2 and HBr on thermal diffusion separation of D and H in a trennschaukel, 25:8422 (CU-755-7, Sect.5)
MATKIN, D. I., Fabrication and properties of high strength oxides and oxide composites, 25:8937
MATSUDA, Satoshi, Gribov--Pomeranchuk pole in Regge-pole residues, 25:9893
MATSUI, H., Effects of acridine orange on the biological action of gamma-ray, 25:8707
MATSUMURA, S., Large-sheath concept for continuum probe theory, 25:9429
MATTERN, Ina Elisabeth, Genetic investigation of radiation-sensitive mutant of Escherichia coli, 25:8633 (NP-18483)
MATTILA, K., Surface brightness observations of dark nebulae, 25:9131
MATVEEV, V. A., High-energy elastic and inelastic hadron collisions, 25:9751
MATVEEVA, E. N., Degradation of the luminescence of plastic polystrene scintillators, 25:8582
Effect of natural lighting on plastic scintillators, 25:8528
Mechanical quenching of the light of liquid scintillators, 25:8526
MAUNG, T., S-wave pion--pion scattering length, 25:9668
MAURENZIG, P. R., Decay schemes of ^{91}Mo and /sup 91m/Mo, 25:10057
MAXFIELD, B. W., Interphase boundary waves in the intermediate state of lead, 25:9363 (NYO-2150-64)
MAXIMON, L. C., Coulomb effects in high energy ^{4}He--^{4}He elastic scattering, 25:9715
MAYER, K., Computer-analyzed counting and scanning, 25:8716
MAYER, L., Calculation of flux distributions in reactor sub-regions with generalized multiple collision probabilities, 25:10313
MAYER-COERICKE, Claus, Conference on position-sensitive detectors in nuclear physics, Juelich, Ger., 7/69, 25:8469 (JUL-CONF-4)
MAYR, H. G., Polar maximum of electron concentration at 1000-km altitude, 25:9317
MAZDIYASNI, K. S., Characterization of alkoxy-derived yttria-stabilized hafnia, 25:8949
MAZITOV, B. S., Specific volume resistance of steatite ceramics in high-intensity γ fields, 25:9551
MAZZUCATO, E., Anomalous plasma resistivity at low electric fields, 25:9443
MCCALL, Mary S., Bacteria as specific binding agents for an isotopic assay of serum folate, 25:8809
MCCALLIEN, C. W. J., SNAP: two dimensional neutron diffusion code, 25:9947 (TRG-Report-1990)
MCCARROLL, R., Exchange excitation of 2s state of hydrogen in close collisions with protons, 25:9201
MCCARTHY, J. S., Electromagnetic structure of ^{3}He nucleus, 25:9965 (AD-710384)
MCCOMAS, John Glenn, Low-momentum K$^+$--^{4}He scattering at 115 to 160 MeV/c, 25:9969
MCDONALD, A. B., Stripping reactions $^{16}O(^{3}He,n)$ and $^{12}C(^{3}He,n)$, 25:9981
MCDONOUGH, J. W., Solar cosmic-ray observations during 1969, 25:9260
MCELIGOT, D. M., Quasi-developed turbulent pipe flow with heat transfer, 25:8420
MCGIRT, Frank, Average angle of scattering in energy-dependent problems, 25:9959
MCGUIRE, E. J., Atomic subshell photoionization cross sections for Z less than or equal to Z less than or equal to 54, 25:9194 (SC-RR-70-721)
Differential ionization cross section in Born approximation, 25:9195 (SC-RR-70-773)
MCKENNEY, Joel R., Prog. rpt. on mechanism of radiation effects on transport and bioelectric properties of rat intestine, 9/70, 25:8607 (ORO-3882-3)
MCKINLEY, T. W. Jr., Recovery from radiation injury with and without bone marrow transplantation: effects of splenectomy, 25:8706
MCLARNON, B., Automatic Van de Graaff voltage conditioner, 25:9930
MCLEAN, W. L., Interphase boundary waves in the intermediate state of lead, 25:9363 (NYO-2150-64)
MCNALLY, J. Rand Jr., Nuclear fusion resonance reactions of possible CTR interest, 25:9507 (ORNL-TM-3233(Rev.))
Prospects of a multi-MeV H_2^+ injection-accumulation experiment, 25:9506 (ORNL-TM-3207)
MCNEESE, L. E., Low-pressure distillation of molten fluoride mixtures: nonradioactive tests for the MSRE distillation experiment, 25:10210 (ORNL-4434)
MCNELLY, M. J., Nuclear system manufacture and construction progress, 25:10088 (CONF-690967-1)
MEASDAY, D. F., Intermediate energy nuclear physics, 25:9694
MEEKS, M. L., Search for excited state of OH in W3, 25:9093
MEGERTH, F. H., Prog. rpt. on Zircaloy--clad UO_2 fuel rod evaluation program, 5--7/70, 25:8951 (GEAP-10217)
MEGERYAN, R. G., Temperature dependence of spontaneous magnetization in holmium during heating--cooling cycle, 25:9579
MEHROTRA, K. N., Radiolysis reactions of colloidal silver and silver bromide, 25:8302
MEIERE, F. T., Analytic structure of off-mass-shell S-wave w, 25:9763 (COO-1428-239)
MEINHARDT, W. G., The FREADM-1 code: a fast reactor excursion and accident dynamics model, 25:10241 (GEAP-13608)
MEISTER, W., Some problems with evaporation in the UHV, 25:8462
MEJSTRIK, V., Uptake of ^{32}P by different kinds of ectotrophic mycorrhiza of Pinus, 25:8603
MELANDRI, C., Control of contaminated air in a reactor fuel element fabrication plant, 25:8695
MELETTI, P., Embryo--endosperm relations in irradiated water soaked seeds of durum wheat, 25:8655
MENGEL, John G., Early evolution of Population II stars. II, 25:9041
MENISSIER, Pierre, Spacing grid for a nuclear reactor fuel element, 25:10332
MEN'SHIKOV, A. Z., Coherent double scattering of neutrons, 25:9963
MERRILL, E. T., Factors affecting the optimum fuel cycle, 25:10233 (BNWL-SA-3605)
MERRILL, John R., Magnetic field calculations for thick solenoids, 25:9393
MERTEN, D., Determination of mercury and bromine in flour, 25:8588
METZ, Charles F., Controlled-potential coulometric and potentiometric titrations of uranium and plutonium in ceramic-type materials, 25:8200 (LA-4537)
MEULEMAN, J., Ionizing radiation detector, 25:8498
MEUSEL, Wilhelm, Control rod drive for reactors, 25:10188
MEYER, J., Measurement of the broadening of silicon lines by electrons and hydrogen atoms, 25:9187
MEYER, Jacques, Application of the differential equation method to the study of a nonrelativistic feynman amplitude, 25:10065
MEYN, R., Glucose-induced resistance to gamma-rays in E. coli, 25:8812
MICHAEL, C., Building meson--baryon scattering amplitudes from duality, 25:9799
MICHAELIS, Arnd, Induction of segment extension and chromatid structural changes in Vicia faba chromosomes, 25:8639
MIELCZAREK, S. R., Absolute measurement of differential cross sections for electron scattering in helium, 25:9222
MIESOWICZ, M., Hadron interaction at ultra high energies, 25:9635 (INP-722)
MIKESKA, Hans-Juergen, Onset of surface superconductivity, 25:9388
MIKHEEV, S. P., Efficiency of a spark chamber at the lower limit of ionization, 25:8557
MIKHEEV, V. P., Measuring devices for processing photographs of bubble chambers (review), 25:8554
MIKOLAJKOW, A., Technetium-99m scanning of the stomach, 25:8723
MILDENBERGER, Otto, Effect of component tolerances on the transfer characteristics in the frequency range, 25:10377 (SC-T-70-4048)
MILEY, G. H., Short-interval series pulsing-experimental studies and numerical experiments, 25:10282
MILKEY, R. W., Vela V and VI solar x-ray atlas. II, 25:9097 (LA-4454(Vol.2))
MILLER, A. J., Use of steam-electric power plants to provide thermal energy to urban areas, 25:10094 (ORNL-HUD-14)
MILLER, Charles E., Argonne radium studies, 25:8669 (COO-2088-1)
MILLER, D. B., Elasticity of the Ξ(2030), 25:9681
MILLER, David, Radioactive scleral shells in the treatment of conjunctival tumors, 25:8731
MILLER, Donald David, Three-component plasma streaming into dipole magnetic field, 25:9414
MILLER, E., S-wave pion--pion scattering length, 25:9668
MILLER, Edwin, Hydro shock experiment, 25:8383 (AD-706767)
MILLER, P. S., Bismuth-209 ground-state analog in ^{209}Po, 25:10045
MILLER, W. H., Classical S-matrix, 25:9227
MILLET, J., High temperature ceramic conductors and insulators, 25:8936
MILLET, P., Behavior of cans and centering devices, 25:8857
High-temperature embrittlement of binary Mg--Zr alloy by hydrogenation, 25:8874
MILLINGTON, R. A., Measurement of relative conversion ratio in particulate fuel, 25:10217
MILLS, Carroll B., Small nuclear reactor for undersea use, 25:10298
MILOVANOV, O. S., 10-MeV linear electron accelerator designated as U-13, 25:9929
MILYUTIN, Yu. V., X-ray diffraction of ion-bombarded

XUM

diamonds, 25:9557
MINAMI, Kentaro, Nuclear accidents in nuclear installations, 25:8661 (JAERI-4052)
MINAMI, Masatsugu, Duality of the nonplanar tetrahedron graph, 25:9693
MINERVINA, Z. V., Direct production of electron--positron pairs by 2.94-GeV/c negative pions, 25:9661
MINLOS, R. A., Investigation of the spectra of stochastic operators arising in lattice models of a gas, 25:10379 (SC-T-71-3000)
MINOO, H., Establishment of a general rule for a hollow-cathode arc discharge, 25:9431 (SC-T-70-4050)
Hollow-cathode discharges dependent on gas flow in arc operation, 25:9433 (SC-T-70-4053)
MINOO, Habibollah, New operation mode for a hollow-cathode arc discharge, 25:9432 (SC-T-70-4051)
MIRANSKII, V. A., Asymptotic properties of electron--proton scattering amplitude and sum rules for Schwinger term, 25:9701 (ITF-70-73)
Equal-time computator, sum rules and ward identities in axiomatic quantum field theory, 25:9837 (ITF-70-57)
Generalized Veneziano model, 25:9888 (ITF-70-78)
MIR-KASIMOV, R. M., Representation for relativistic scattering amplitude at high energies, 25:9749 (JINR-E2-5341)
MISCHKE, R. E., Direct measurement of n--p and n--d total cross sections from 700 to 2900 MeV/c, 25:9648
Performance of large-volume two-phototube neutron detector, 25:8547 (PURC-4159-13)
Response of a mineral-oil based liquid scintillator to heavily ionizing particles, 25:8511
MISHKIN, Fred S., Radionuclide angiogram and scan findings in a case of herpes simplex encephalitis, 25:8718
MISRA, S. C., Neutron generator for calibration of fast neutron detectors, 25:9940 (BARC-499)
MISYURA, V. A., Measurements of the parameters of ionosphere by incoherent radiowave scattering, 25:9343
MITCHELL, B., Criticality detection system, 25:8486
MITCHELL, E. N., Fermi velocity in single-crystal films of Pb, 25:9373
MITCHELL, G. E., Reactions $^{14}C + \alpha$, 25:9980
MITCHELL, T. J., Secondary disease mortality in rat-mouse radiation chimeras, 25:8619
MITHRA, B., Theoretical analysis of $(\alpha,2\alpha)$ reactions, 25:9987
MITOME, D., FFTF backup design interface definition discussion of system requirements, 25:10266 (GEAP-5721)
MITRA, A. P., Aspects of electron content measurements from satellite radio beacon transmissions, 25:9294
Observations of electron density during a solar flare, 25:9300
MITSUI, H., Effect of uv-irradiated vesicular stomatitis virus on nucleic acid synthesis in chick embryo cells, 25:8806
MITSUI, Hiroshi, Study on the radiation-induced chain crosslinking and crosslinking polymerization, 25:8276 (JAERI-Memo-4147)
MITTLEMAN, Marvin H., Intermediate-energy electron--atom scattering. I, 25:9214
MITYAKOV, N. A., Variations in mean level of radio emission at 1.1 and 2.3 MHz, 25:9352
MIYAMOTO, Yoneji, Lagrangian formulation of dual resonance model, 25:9696
MIYASAKA, Shun-ichi, Gamma-ray leakage through a junction between lead and concrete walls, 25:10296 (NSJ-tr-157)
MIYASE, Haruhisa, Study of isobaric analogue state by (γ,p) reaction, 25:10053
MIYATA, Hideo, Duality of the nonplanar tetrahedron graph, 25:9693
MIYAZAKI, Tadashi, Infinitely degenerate particles and mechanism of mass splitting, 25:9711
MIYAZAWA, Hironari, Weak interaction as an S matrix, 25:9740
MIZIA, I., Energies spread of Gaussian distributed beam in nuclear scattering experiments, 25:10086
MNATSAKANYAN, M. A., Models of static configurations, 25:9008
MOCHAN, I. V., Investigation of films of variable composition of Mg--Sb system, 25:10345 (BNL-tr-387)
MOEBIUS, W., Methods of application of gamma emitters in contact therapy with regard to radiation protection, 25:8688 (SZS-6/70)
Methods of application of gamma emitters in contact therapy with regard to radiation protection, 25:8729 (SZS-6/70, pp 1-8)
MOESSBAUER, R. L., Resonance spectroscopy of γ-radiation on Au(I) and Au(III) compounds, 25:9593
MOHANTY, H. K., Hydromagnetic free convection for high and low Prandtl numbers, 25:9270
MOHR, H. E., Determination of vanadium by neutron activation analysis at nanogram levels to formulate a low-vanadium diet, 25:8228
MOHRI, Akihiro, Improvement of l = 2 Stellarator and Torsatron, 25:9508
MOISEEVA, M. P., Fine structure of plasma focus using method of multiperforated pinhole camera, 25:9412 (LA-tr-70-25)
MOISEIWITSCH, B. L., Pade and Fredholm approximants in scattering theory, 25:9892
MOLCHANOV, O. A., Detection of perturbations of geomagnetic field in the magnetosphere, 25:9346
MOLCHANOV, V. A., Mechanism of ion scattering by crystals, 25:9556
MOLHO, S., Concerning an ordered solid solution of beryllium in U_3Si_2, 25:8947
Ordered solid solution of Be in U_3Si_2, 25:8888
MOLITOR, Alain, Electron density of xenon plasma by laser interferometry and spectroscopy, 25:9422
MOLNAR, Michael R., The r-process in a hydrodynamical model of the helium flash, 25:9037
MONDAL, M. A. W., Behaviour of a neutron pulse in the vicinity of an inelastic threshold, 25:10315
MONDEN, Yoshimi, Surface excitation model of hadron resonances, 25:9808
MONNET, G., Kinematic study of ionized hydrogen in NGC 4490-85, 25:8994
Mass distribution and a stellar population model in the spiral galaxy M 33, 25:9149
MONSE, E. U., Analysis of isotope-effect calculations illustrated with exchange equilibria among oxynitrogen compounds, 25:8245
MONSEU, Ph., Fast neutrons in non-multiplying assemblies, 25:9956
MONTAGUE, D. G., $^{20}Ne(p,t)^{18}Ne$ reaction as a test of the ^{18}Ne and ^{20}Ne wave functions, 25:10006
MOOK, D. E., Optical monitoring of Sco X-1 for 1967-1969, 25:9086
MOORE, Bailey, Afterloading vaginal irradiators, 25:8736
MOORTHY, V. K., Sintering of UO_2: relation between electrical conductivity and microstructure of sintered UO_2, 25:8908 (BARC-507)
MOO-YOUNG, G. A., Measurement of the stark broadening of the resonance lines of neutral argon and neon, 25:9171
MORAVCSIK, Michael J., Meson factories and the two-nucleon problem, 25:9810
MORAVEC, A., Isolation of ^{95}Zr--^{95}Nb from solution of fission products, 25:8214
MORAVEK, Frantisek, Pulmonary ascariasis in an irradiated organism. II, 25:8781
MORDKOVICH, V. N., Radiation induced defects in dielectric--semiconductor structures, 25:9566
MOREL, Jean, Decay schemes of ^{59}Fe and ^{192}Ir, 25:10032 (ORNL-tr-2345)
MORENO, Giuliana, Partial cell irradiation by uv and visible light, 25:8744
MORGAN, G. L., Reactions $^{14}C + \alpha$, 25:9980
MORGAN, J. G., Indexed bibliography of thermal effects literature--1, 25:10159 (ORNL-NSIC-81)
MORGAN, Lesley, Gravitational field of shells and disks in general relativity, 25:9882
MORGAN, Thomas, Gravitational field of shells and disks in general relativity, 25:9882
MORGAN, W. W., Classification of the forms of clusters of galaxies, 25:9125
MORI, Tomoyuki, Conformation therapy technique on 6 MeV linear accelerator in treatment of the carcinoma of cervix uteri, 25:8740
MORIMOTO, S., Plasma containment in a combined mirror--multipole magnetic field, 25:9399
MORIN, M., Experimental research on the treatment of contamination by transplutonium elements, 25:8590 (CEA-CONF-1658)
MORIYA, Makoto, Effects of halides on anodic polarization of zirconium in ammonium nitrate solution, 25:8832 (AEC-tr-7204)
MOROZOV, D. Kh., Effective protection of space ships, 25:9540
MOROZOV, V. A., Lifetime of excited states in spherical nuclei ^{139}La, ^{138}La, and ^{133}La, 25:10029 (JINR-P6-5200)
MOROZUMI, Takaaki, Effects of halides on anodic polarization of zirconium in ammonium nitrate solution, 25:8832 (AEC-tr-7204)
MORRIS, A., Photoelectron spectra of ground-state atomic H, N, and O, 25:9200
MORRONE, T., Profiles of uniformly accelerated ion beams, 25:9925
MORTON, W. T., Elasticity of the $\Sigma(2030)$, 25:9681
MOSKALEV, Yu. I., Problems of plutonium toxicology, 25:8594 (LF-tr-41)
Recommendations concerning the maximum permissible tritium oxide concentrations in the atmosphere of industrial premises, 25:8678 (ORNL-tr-2403)
MOTT, B. W., Metallographic examination of sodium, 25:8845 (AERE-R-5483)
Sodium purification and general handling facility, 25:8390 (AERE-R-5502)
MOULTON, R. J., Processing in limited geometry. XVI, 25:8445 (AERE-R-5104)
MOZER, F. S., Operation of dc electric field detector, 25:9301
Parallel and perpendicular electric fields in an aurora, 25:9303
MUBARAK, Mohammad A., Description of hot facilities at Pakistan Inst. of Nuclear Science and Tech., Pakistan, 25:8449 (CONF-691008-18)
MUEL, B., Inactivation of the scrapie agent by near monochromatic ultraviolet light, 25:8805
MUELLER, A. H., O(2,1) analysis of single-particle spectra at high energy, 25:9816
MUELLER, G. P., Ground state properties of alpha matter, 25:10070

MUELLER, Horst, Chemical effects of nuclear transformations in solids. II, 25:8314
Chemical effects of nuclear transformations in solids. I, 25:8313
MUELLER, Manfred, Measurement of neutron spectra in energy range from 1 eV to 10 keV with help of sandwich techniques, 25:8481 (KFK-1233)
MUELLER, W. H., Cesium-137-decontamination with colloidally soluble Prussian blue in rats, 25:8662 (UCRL-Trans-10488)
MUGHABGHAB, S. F., Nonstatistical effects in reaction $^{163}Dy(n,\gamma)^{164}Dy$, 25:10047
MUHAMMAD, Amir, Inhibition of the germination in gamma irradiated onions, 25:8815
MUHLBERGER, Friedrich, Method for determining the content of cement in concrete, 25:8232
MUKAI, Yoshihiro, Biological effects of 15 MeV electron beams of betatron to lymphoid tissues of mice, 25:8780
MUKHIN, S., Backward rho$^+$ production in π^+p reactions at 5.2 GeV/c, 25:9665
MUKHIN, S. V., Pulse shaper with the zero time of regeneration for the apparatus blocking at the large loading, 25:8545 (JINR-P13-5377)
MULLER, R. H., Periodic phenomena in copper dissolution at constant current, 25:10404 (UCRL-19618)
Transfer processes in ECM, 25:10403 (UCRL-19615)
MULLER, Th., Excited states of ^{22}Ne, 25:10002
MUMINOV, A. I., Properties of excited states of ^{151}Sm, 25:10035
MUMINOV, M. I., Specific volume resistance of steatite ceramics in high-intensity γ fields, 25:9551
MUMINOV, T. M., Lifetime of excited states in spherical nuclei ^{139}La, ^{135}La, and ^{133}La, 25:10029 (JINR-P6-5200)
MUMTAZ, Ali, Inhibition of the germination in gamma irradiated onions, 25:8815
MUNCASTER, George W., Rotational velocities in the Orion Nebula cluster, 25:8981
MURABAYASHI, Masayuki, Thermal conductivity of ceramic solid solutions, 25:8932
MURADOV, S., Role of mobile holes, anion vacancies, and excitons radioinduced coloration of KCl crystals, 25:9553
MURAI, Tadayuki, Effect of electron capture on the temperature in dense stars, 25:8973
MURATA, Mikio, Nuclear accidents in nuclear installations, 25:8661 (JAERI-4052)
MURATBEKOV, M. B., Role of charged particles and excited molecules during radiation oxidation of n-heptane by molecular oxygen, 25:8281
MURDIN, Paul, Accurate timing of light flashes from the pulsar in the Crab Nebula, 25:9089
MURPHY, C. T., Fraction of stopped antiprotons which annihilate on free hydrogen in propane, 25:9645
MURPHY, M. F., Measurement of relative conversion ratio in particulate fuel, 25:10217
MURPHY, W. A., Engineering development of fluid-bed fluoride volatility processes. Part 16. A safety manual for the engineering-scale alpha facility, 25:8446 (ANL-7672)
MURRAY, A., Low-energy gamma rays from NP 0532, 25:9062
MURTHY, N. S. Satya, Prog. rpt. on nuclear physics, annual, 1969--70, 25:10017 (BARC-501)
MURTHY, P. Sreerama, Spectrographic determination of Ru in silicious materials used in radioactive waste disposal, 25:8196 (BARC-504)
MUSHER, J. I., Hartree--Fock problem, 25:9247
MUTAFI, N. N., Volcanic cycles and metallogeny of Novaya Zemlya, 25:10416 (UCRL-Trans-10504)
MYAKISHEV, K. G., Infrared spectra and molecular properties of tetrahydroborates of metals of the $M(BH_4)_n$ type, 25:8263
MYERS, W. P. L., Computer-analyzed counting and scanning, 25:8716
MYHRMAN, Ulla, Energy levels of double-well potentials. II, 25:9248
MYRHEIM, J., Backward rho$^+$ production in π^+p reactions at 5.2 GeV/c, 25:9665

N

NADA, Hideyuki, Approximate solution and measurement of the steady temperature distribution in a finite region with many circular holes, 25:8413
NAFT, Barry N., Development of an automated fuel loading optimization scheme for pressurized water reactors, 25:10184
NAGAHARA, Sadao, Pathology of radiation fibrosis of the lung, 25:8791
NAGASAKI, Ryukichi, Development of a device for measuring circumferential mechanical properties of cladding tubes, 25:8883
NAGASAWA, K., Electrical properties of V_6O_{13} single crystal, 25:9580
NAGASE, Kaneomi, Formation, microstructure, and properties of barium zirconium sulfide ceramics, 25:8920
NAGIRNER, D. I., Nonstationary radiation fields in infinite media, 25:9009
NAGY, Mohamed El-Sayed, Cross-spectral-density sink frequency behavior for coupled-core Argonaut reactors, 25:10275
NAISTETER, S. I., Photoproduction of the isobar Δ (1238), 25:9798
NAJAC, Harold W., Toxic effect of thermal neutrons on the rabbit electroretinogram, 25:8761
NAKAGAWA, Masayuki, Accuracy of analytical treatments for resonance absorption in Doppler resonance regions, 25:10038
NAKAHARA, Kazuo, Study of atomic nucleus by electron scattering, 25:10014
NAKAMOTO, Shunsuke, Multiple scattering of protons and nitrogen ions on copper, 25:9163
NAKASHIMA, Kenshiro, Studies of recombination centers in gamma-irradiated p-type silicon, 25:9567
NAKAZAWA, Kiyoshi, Effect of electron capture on the temperature in dense stars, 25:8973
NALCIOGLU, Orhan, Bootstrap theory of vibrations in nuclei, 25:10063 (RLO-1925-46)
NAMBA, Susumu, Enhanced diffusion of high-temperature ion-implanted antimony into silicon, 25:9569
NANDA, R. S., Hydromagnetic free convection for high and low Prandtl numbers, 25:9270
NANOBASHVILI, H. M., Mass-spectrometric investigation of low-temperature radiolysis of organic sulfides, 25:8290
NASRALLAH, N. F., Collinear dispersion relations and K/sub e4/ decay rate, 25:9747
NATARAJAN, A. T., Killing and mutagenic action in E. coli associated with Auger effect during ^{125}I decay, 25:8654
NAUMOV, A. I., Causality function in a four-fermion model with an indefinite metric, 25:9741
NAZARE, S., Dispersion fuel for high-flux reactors (UAl_3--Al), 25:8846 (KFK-1252)
Relations between stereometric microstructure and properties of cermets and porous materials, 25:8944 (KFK-1236)
NAZAROV, I. M., Method for separating γ radiation dose rate of artificial and natural radioactive isotopes in ground, 25:8360
NAZHAT, N. B., Nature of bleached color centers in irradiated alkaline ice, 25:8272
NEDOSPASOV, A. V., Current distribution in an E x H discharge with sectionalized electrodes for nonequilibrium conductivity of the plasma, 25:9482
NEFEDOV, V. D., Determination of the boiling point of astatobenzene, 25:8259 (ANL-Trans-869)
Reaction with benzene of ^{125}I and ^{211}At formed from the noble gases during K-capture, 25:8284 (ANL-Trans-870)
NEFF, Everett L. Jr., Effect of Na fluorescein and plating medium on recovery of irradiated E. coli, 25:8807
NEGREI, S. A., Semiconductor gamma spectrometer, 25:8541
NEGUS, P. J., Elasticity of the $\Sigma(2030)$, 25:9681
NEILSON, G. C., Automatic Van de Graaff voltage conditioner, 25:9930
Energy levels of ^{45}Ti, 25:10003
NEILSON, Thomas Christopher, Improvements in nuclear reactors, 25:10230
NEIMOTIN, E. I., Concerning the cone of radiation in the equation of the kinetic transport equation, 25:9609
NEIRINCKX, Rudi Dominique, Neutron activation analysis of trace impurities in titanium and titanium dioxide, 25:8233
NEKHAI, A. P., Pulse generator for stabilizing a spectrometer circuit, 25:8542
NEKRASOV, A. K., Cyclotron heating in nonuniform magnetic field, 25:9403
Cyclotron heating of a plasma in a nonuniform magnetic field, 25:9404
NELSON, Charles A., Cheng--Wu picture applied to $\gamma p \to \rho^0 p$ and $\pi h p$, 25:9716
NELSON, D. L., Effects of chronic irradiation and temperature on populations of aquatic snail Physa heterostropha, 25:8750 (ORNL-4612)
NELSON, D. M., Cesium-137 in various Chicago foods (collection month, July 1970), 25:8659 (HASL-237, pp III.14-17)
NELSON, Gilbert B., Controlled-potential coulometric and potentiometric titrations of uranium and plutonium in ceramic-type materials, 25:8200 (LA-4537)
NELSON, Paul Jr., Investigation of criticality for energy-dependent transport in slab geometry, 25:9960
NEMOZ, A., Vortex trapping, 25:9387
NEMOZ, Alain, Radiation sealed x-ray diffraction camera, 25:8577
NENOT, J. C., Clearance of radioisotopes from lungs of rats, 25:8591 (CEA-CONF-1677)
Experimental research on the treatment of contamination by transplutonium elements, 25:8590 (CEA-CONF-1658)
NESSIN, M., Isobaric analog states in ^{24}Mg, ^{27}Al, and ^{28}Si, 25:10007
NESTOR, C. W. Jr., Eigenvalues, radial expectation values, and potentials for free atoms from Z = 2 to 126 as calculated from relativistic Hartree--Fock--Slater atomic wave functions, 25:9168 (ORNL-4614)
NESTOROV, G., Evaluation of solar hard x radiation by absorption in D region, 25:9330
Exponential model of ionospheric D region, 25:9328
NETZBAND, D., Generalized DWBA model applied to $^{24}Mg(dp)^{25}Mg$ reaction at E/sub d/ = 13.5 MeV, 25:9597 (JINR-E4-5350)
NEUBERT, W., Two-quasiparticle (h/sub 9/2/)^2 isomeric state

XUM

in ^{202}Po, 25:10027 (JINR-E6-5379)
NEWTON, Mary C. Barsa, Toxic effect of thermal neutrons on the rabbit electroretinogram, 25:8761
NG, P. H., Direct-channel Regge poles as a means of treating the unphysical region in finite-energy sum rules, 25:9801
NGUYEN, T. D., SIGMA-suppression in /sub A/^{3}He, 25:9815
NGUYEN-H-DOAN, Study of spectrograms of CH Cygni, 25:8990
NGUYEN VAN TRONG, Echo theory in plasma, 25:9519
NICHOLSON, H. W., Antiproton--proton forward charge-exchange scattering, 25:9644
NICOLO, F., K anti K w final states for N anti N annihilation at rest in Veneziano language, 25:9765 (NP-18578)
NIEDZWIEDZIUK, K., Investigation of $^{9}Be(t,n)^{11}B$ reaction at 1.10 MeV, 25:9976 (JINR-P15-5148)
NI'EGORODZEV, V. V., Beam regulation in a 100-MeV linear accelerator, 25:9914 (NP-tr-1926)
NIELUBOWICZ, J., Metabolic and hemodynamic disturbances in the liver subdued to extracorporeal perfusion, 25:8783
NIFATOV, A. P., Problems of plutonium toxicology, 25:8594 (LF-tr-41)
NIGAM, B. P., Modified photon propagator in rho-dominance model, 25:9846
NIKAIDO, Osamu, Radiation and carcinogenesis, 25:8611
NIKI, H., Kinetic isotope effects in the quenching of $O_2(b^1I/sub\ g/^+)$ by some deuterated compounds, 25:8249
NIKITIN, K. A., Covering graphite with niobium from a vapor--gas mixture, 25:8917
NIKITIN, Yu. P., Possibility to observe rho'' daughter resonance in w + 2w reaction in nuclear field, 25:9786
NIKOLAEV, N. N., CP violation and models with supplementary particles, 25:9827
NIKOLAEV, Yu. M., Distribution of solar-wind disturbances caused by chromospheric flares, 25:9356
NIKOLAEVA, V. A., Emissivity of carbides of Ta and Hf over range 1300 to 3000° K, 25:8930
NIKULIN, M. G., Methods of stabilizing corrugated theta pinch, 25:9501
NIMAL, Jean-Claude, Three-dimensional Monte-Carlo calculation (TRIPOLI code) of neutron spectra in lower shield of Phenix, 25:10193 (CEA-N-1359)
NININGER, Robert D., World uranium picture, 25:8373
NISHIHARA, Tomio, Effect of gamma irradiation on the very dilute solution of collagen in the atmosphere of air and nitrogen, 25:8307
NISHIWAKI, Ichiro, Loss-of-coolant accident in water-cooled nuclear power reactors. III, 25:10246
NISHIWAKI, Y., Effects of acridine orange on the biological action of gamma-ray, 25:8707
NISSL, Adolf, Crack formation nitrided components of X6CrMo4, 25:8940
NITTA, Tsuneharu, Formation, microstructure, and properties of barium zirconium sulfide ceramics, 25:8920
NOBLE, J. V., Giant monopole state: isospin mixing in nuclear ground states, 25:10061 (NYO-2171-330)
NODA, Hujio, Cluster model and nonleptonic hyperon decays, 25:9739
NOEL, R., Heat exchange unit for a nuclear reactor, 25:10204
NOERDLINGER, Peter D., Test for expansion of clusters of galaxies, 25:9133
NORDMAN, D. A., Estimating average nuclear fuel costs, 25:10216
NORDSIECK, Kenneth H., Dust--radiation instability in ionized nebulae, 25:8999
NORMAN, A., Unscheduled DNA synthesis at low x-ray doses, 25:8647
NORMAN, John H., Cloud chemistry of fallout formation, 25:8362 (AD-707427)
NORSEEV, Yu. V., Determination of the boiling point of astatobenzene, 25:8259 (ANL-Trans-869)
Reaction with benzene of ^{125}I and ^{211}At formed from the noble gases during K-capture, 25:8284 (ANL-Trans-870)
NOUZA, K., Host and graft factors in the homing of haematopoietic cells, 25:8616
NOVAK, L., Body temperature as an indicator of the radioprotective effect of sodium fluoroacetate in mice, 25:8700
NOVIKOV, A. M., Use of the /sup 125m/Te isotope as a source of x-ray radiation, 25:8434
NOVIKOV, I. I., Applied magnetohydrodynamics, 25:9275
NOVIKOV, L. S., Direct production of electron--positron pairs by 2.94-GeV/c negative pions, 25:9661
NOVIKOV, V. M., Effect of delayed neutrons on the dynamic reactivity of a reactor originating during oscillations of the density of the fuel, 25:10305 (IAE-1955)
NOWAK, Jurgen, Production of spherical oxidic or carbidic particles from heavy metal salt solutions, 25:8922
NOZAKI, Tadao, Detailed investigation of an 80-TeV nuclear interaction, 25:9641
NUESSLIN, F., Investigation of (^{3}He,^{3}He) and (^{3}He,t) reactions on ^{10}B, ^{11}B, and ^{13}C, 25:9993
NURMATOV, D., Activation methods for determining content of Ta and Cs in rocks, 25:8230
NYDAHL, G., Photoproduction of charged pions from nuclei, 25:9620 (LUNP-7007)
NYQUIST, Laurence Elwood, Cosmic-ray record in the metallic phase of chondrites, 25:8968

O

OBLINGER, C. J., Thermodynamics of vanadium alloys. I, 25:8862 (AD-709957)
OBRAZTSOVA, G. A., Effect of training nervous processes on the weight of the brain and the cholinesterase activity, 25:10411 (UCRL-Trans-1424)
OCCHIONERO, Franco, Newtonian electrodynamics from general-relativistic arguments, 25:9052
OCKERS, S. T., Metallic character of metal hydride, V_2H, 25:9592
O'DELL, L. D., Comparison of nuclear design models for power and flux distributions near the FTR core-reflector interface, 25:10272 (WHAN-FR-35)
ODORICO, R., Novel interpretation of hole structure in anti pn + w-w-w+, 25:9770
OFFORI, Evans Dunstan, Effects of gamma radiation on Stomoxys calcitrans, 25:8822
OGANESYAN, R. Kh., Spectrophotometric study of some stars of Of type, 25:8986
OGANESYAN, Yu. Ts., Identification of elements 102 and 104 with the help of the collimation method, 25:10030 (KFK-tr-329)
OGIEVETSKY, V. I., Chiral SU(2) x SU(2) dynamics for A_1, rho, and w mesons, 25:9781
OHANNESIAN, O. A., Versatile and modular data acquisition system useful in nuclear experiments, 25:8483 (PH-1)
OHASHI, Hiroshi, Effects of halides on anodic polarization of zirconium in ammonium nitrate solution, 25:8832 (AEC-tr-7204)
OHNUMA, Toshiro, Wave--wave coupling in ion wave propagation, 25:9513
OIKAWA, Shiro, Study of isobaric analogue state by (γ,p) reaction, 25:10053
OK, H. H. Armagan, Channeling of electrons and positrons in silicon and anthracene monocrystals, 25:9543
OKE, J. B., Inferences from spectrophotometry of quasi-stellar sources, 25:9074
Maffei 1: a new massive member of the Local Group, 25:9148
OKEL, J. G. R., Potential for the interaction of atoms and heavy polar molecules in thermal scattering, 25:9232
OKHOTIN, A. S., Methods of investigation of thermoelectric properties of semiconductors, 25:9590
OKINAKA, H., Electrical properties of V_6O_{13} single crystal, 25:9580
OKUBO, Susumu, Kuo transformation in linear and nonlinear chiral-symmetry theories, 25:9825
OKUDA, Atsuyuki, Radiation-induced binding of phenylalanine and OH substituted derivatives, 25:8280
OKUYAMA, Fumio, Observations of needle crystals of tungsten oxide, 25:8843
OLDENDORF, William H., Liquid scintillation counting of /sup 113m/In conversion electrons in the presence of ^{3}H and ^{14}C, 25:8213
OLDS, F. C., Nuclear power engineering: analysis of trends in policy and technology, 25:10105
OLIVEIRA, Colber G., Model field theory in five dimensions, 25:9868
OLIVEIRA, Jaime M. Costa, Experimental study of the kinetics and dynamics of critical assemblies for thermal neutrons, 25:10174 (LFEN-109-B)
OLIVO, O. M., Degeneration of cells in mitosis induced by x radiation (20,000 to 100,000 R), 25:8751
Mitosis in in vitro cultured fibroblasts following x irradiation, 25:8752
OLSON, Karin E., Effect of brain stem irradiation on descending systems to the spinal cord, 25:8771
OLSSON, Gustaf, Digital simulation of spatial xenon oscillations, 25:10306 (NP-18547)
OLSZEWSKI, W., Metabolic and hemodynamic disturbances in the liver subdued to extracorporeal perfusion, 25:8783
OLTEANU, V., Recovery phenomena in yeast. II, 25:8797
O'MALLEY, Thomas F., Unique definition of the quasi-stationary state for resonant processes, 25:9209
OMEL'YANENKO, A. A., Efficient separation of neutrons and gamma rays with a stilbene crystal, 25:8525
ONDRACEK, G., Dispersion fuel for high-flux reactors (UAl_3--Al), 25:8846 (KFK-1252)
Relations between stereometric microstructure and properties of cermets and porous materials, 25:8944 (KFK-1236)
ONDRISH, L., Pulse shaper with the zero time of regeneration for the apparatus blocking at the large loading, 25:8545 (JINR-P13-5377)
ONISHI, Takeshi, Nuclear accidents in nuclear installations, 25:8661 (JAERI-4052)
OPARIN, V. A., Electron binding energy in negative ion He^-, 25:9169
OREKHOV, V. D., Determination of radiation yield of nitrite ions during irradiation of sodium nitrate solutions with small doses, 25:8297
ORLOW, Yu. F., Instability of the motion of particles in a synchrotron for high frequencies of the accelerating field, 25:9934
OSADA, Tadanori, New varieties of malting barley produced by radiation breeding, 25:8656
OSANO, Katsuharu, Design and project of radioactive

treatment and disposal system in large capacity BWR nuclear power station, 25:8340
OSBORN, W., Measures of double stars on parallax plates, 25:9053
OSETINSKII, G. M., Reaction $^{7}Li(d,n)^{8}Be$, 25:9975 (JINR-P15-5143)
OSMOLSKI, Thaddeus Vincent, Factors influencing the expression of anophthalmia in the mouse, 25:8646
OSOSKOV, G. A., Maximum-probability method to determine the kinematic parameters of tracks, 25:8558
OSTANIN, V. A., 10-MeV linear electron accelerator designated as U-13, 25:9929
OSTAPENKO, A. A., Interaction cross sections of fast particles with tritium and ^{3}He nuclei, 25:9967 (JINR-P2-5335)
OSTENSON, Alan T., Radiocarbon in the southern oceans, 25:8381
OSTER, Ludwig, Free--free emission and absorption coefficients in the radio frequency range at very low temperatures, 25:9082
OSTROWSKI, Kazimierz, ESR study of bone tissue sterilized by gamma radiation, 25:8825
OTTAWAY, J. M., Determination of ruthenium by atomic absorption spectrophotometry, 25:8209
OVCHAROV, V. T., Approximate solution of the internal problem of the theory of formation of electron beams, 25:9618
OYAMADA, Masayuki, Study of atomic nucleus by electron scattering, 25:10014

P

PACAULT, R., Lunar occultation satellite for high-resolution studies of cosmic x-ray sources, 25:9065
PACINI, F., Secular decrease of the optical and x-ray luminosity of pulsars, 25:9092
PACKARD, Richard Erwin, Detection of single quantized vortex lines in rotating liquid helium, 25:9362
PACKER, A. D., Teratogenic activity of x irradiation, 25:8703
PAGE, D. E., Scientific research in space science at ESTEC, 25:9336
PAGE, Vera, Physical and dosimetric aspects of the radiotherapy of malignant lymphomas. I. The mantle technique, 25:8735
Physical and dosimetric aspects of the radiotherapy of malignant lymphomas. II. The inverted-Y technique, 25:8734
PAIZIS, Constantinos, Atmospheric gamma rays at balloon altitudes, 25:9305
PALINSKI, R., Calculation of self-limiting power excursions, 25:10281
PALKO, A. A., Chemical fractionation of boron isotopes, 25:8329
PALKO, Aloysius A., Method for fractionation of carbon isotopes, 25:8339
PALMER, H. E., Counter for the direct measurement of ^{55}Fe in blood and other liquid samples, 25:8466 (BNWL-SA-3624)
PALMER, Roger, Interaction of a gauge-independent spin-one field, 25:9854
PANCHVIDZE, M. V., Mass-spectrometric investigation of low-temperature radiolysis of organic sulfides, 25:8290
PANCNER, F. O., Guidelines for sodium fire prevention, detection, and control: report of the Ad Hoc Committee on sodium fires, 25:8827 (ANL-7691)
PANFILOVA, Z. I., Action of chemical mutagenes and uv on Escherichia coli B, 25:8642
PANKEY, T., Ion-implantation induced optical absorption edge shifts in GaP, 25:9562
PANSOLLI, P., Gamma irradiation of table grape variety hoanes, 25:8817
PANTELEEVA, N. S., Effect of trinitrophenylation of myosin on isotopic exchange of oxygen in ATP--$H_2{}^{18}O$, 25:8248
PANTIN, C. F. A., Non-minimal currents in chiral Lagrangians with an application to pion photoproduction, 25:9726
PAPALIOLIOS, C., Results of a search for optical pulsars, 25:9090
PAPASTAIKOUDIS, K., Pinning of flux lines in superconducting niobium due to point defects, 25:9379
PAPOYAN, V. V., Slow rotation of relativistic polytropic models, 25:9078
PARKER, A., Chemical determination of N in nitrides of B, Ti, Zr, Cr, Mo, Nb, Ta, and V, 25:8195 (AERE-R-6491)
PARKER, E. N., Generation of magnetic fields in astrophysical bodies. II, 25:9136
Generation of magnetic fields in astrophysical bodies. III, 25:9135
Origin of magnetic fields, 25:9129
PARKS, P. B., Deuteration in slow neutron radiography of biological media, 25:8709 (DP-1229)
PARLEE, Norman A. D., Prog. rpt. on nitride formation in liquid uranium alloys and their applications to reprocessing of spent nuclear fuel, 6/69--3/70, 25:8325 (SU-326-P-28-X-2)
PARZEN, G., Ribbon effect in a superconducting septum magnet, 25:9903 (BNL-15368)
PASCHMANN, G., Efficiency measurements for channel electron multipliers, 25:8490
PASHCHENKO, V. P., Plasma thermionic energy conversion, 25:9268
PASICHNYI, A. A., Knockout of nucleons from light nuclei under the inelastic scattering of high-energy electrons, 25:9973 (ITF-70-42)
Quasi-elastic knockout of nucleons from light nuclei by high energy electrons, 25:10058 (ITF-70-38)
PASKAR, S. V., Solution of the equation of radiation transfer, 25:9611
PATEL, J. C., Equatorial F2-layer anomaly and q-type sporadic-E layer, 25:9291
PATEMAN, J. A., Ultraviolet-light sensitive mutants of Aspergillus nidulans, 25:8640
PATRIARCA, P., Prog. rpt. on fuels and materials development, 6/30/70, 25:8829 (ORNL-4600)
PATRYN, A., Accumulation of ^{85}Sr, 25:8597
PAUL, M. Th., Complex formation of tetravalent actinides with pyridine- and α-aminopolycarboxylic acids, 25:8237 (KFK-1210)
PAVLENKO, V. N., Echo theory in plasma, 25:9519
PAVLOVSKAYA, T. F., Properties of $^{6}LiI(Eu)$ crystals at low temperatures, 25:8529
PAWLEWICZ, W. T., Fraction of stopped antiprotons which annihilate on free hydrogen in propane, 25:9645
PAWLOWICZ, Richard, Petrographic analysis, Gasbuggy No. 1 and Gasbuggy No. 3, 25:8385 (PNE-G-69)
PAYNE, H. R., Use of steam-electric power plants to provide thermal energy to urban areas, 25:10094 (ORNL-HUD-14)
PAZHIN, Yu. F., Resonant Bragg scattering of gamma rays by nuclei, 25:9596
PECKER, J.-C., Polarization of continuum at the solar limb, 25:9109
PEDERSEN, A., Scientific research in space science at ESTEC, 25:9336
PEDERSEN, B. Moeller, Ionospheric observations during annular solar eclipse of May 20, 1966. III, 25:9311
PEERY, Benjamin F. Jr., Technetium stars, 25:9057
PEGOUD, J., High-temperature embrittlement of binary Mg--Zr alloy by hydrogenation, 25:8874
PEIRSON, D. H., Radioactive fallout in air and rain, 25:8364 (AERE-R-6556)
PELEKIS, L. L., Application of cadmium filter in activation analysis with reactor neutrons, 25:8226
Determination of Be by (γ,n) reaction in linac, 25:8225
PELETSKII, V. E., Emittance of Re in range from 1200 to 2800° K, 25:8878
PELISSIER, J., Formation and nature of twin crystals in U_3Si, 25:8946
PELLET, A., Observations of faint extragalactic H II regions, 25:9143
PELLETIER, M., Aluminum alloys in seawater desalination installations, 25:10361 (ORNL-tr-2413)
PELRAS, M., Corrosion tests on various materials in seawater up to 150°C, 25:10360 (ORNL-tr-2412)
PENCE, Dallas T., Prog. rpt. on silver zeolite: iodine adsorption studies, semiannual, 7/1--12/31/69, 25:8321 (IN-1363)
PENG, T.-H., Mixing and gas exchange rates in Experimental Lakes Area, Western Ontario, 25:8352 (CU-2493-11, App.6)
PENNER, H., Histological identification of irradiated potatoes, 25:8802
PENZYAKOV, V. V., Approximate solution of the internal problem of the theory of formation of electron beams, 25:9618
PEPIN, Pierre, Characteristics of ordinary concrete relative to radioprotection calculation, 25:8960 (CEA-N-1355)
Validity of SABINE code in calculations on shielding of heavy and light water reactors, 25:10192 (CEA-N-1354)
PERELSTEIN, E. A., Transition radiation on resonance γ-quanta, 25:9703 (JINR-P2-5042)
PEREY, F. G., Neutron elastic- and inelastic-scattering cross sections for yttrium in the energy range 4.19 to 8.56 MeV, 25:9999 (ORNL-4552)
PEREZ, J. D., Convergence of the density gradient expansion for atoms, 25:9245
PERKINS, Alfred J., Conference of the seventh national meeting of the Society for Applied Spectroscopy (Nineteenth Annual Mid-America Spectroscopy Symposium), Chicago, 5/68, 25:8538
PERKINS, F. W., Velocity shear and low-frequency plasma instabilities, 25:9496
PERKINS, Francis, Mass accretion and pulsational stability, 25:9040
PERKINS, J. F., Hartree--Fock calculations of autoionization states, 25:9252
PERONA, J. J., Design and safety considerations of shipping solidified high-level radioactive wastes, 25:8451 (ORNL-TM-2971)
PERPER, Timothy Pelle, Physiological and genetic studies of x-ray resistance in budding yeast cells, 25:8798
PERRIN, Martine, Polar and triangular diagrams in interpretation of $(\alpha,2\alpha)$ reactions, 25:10059 (LYCEN-7039)
PERROUD, J. P., Production and characteristics of a 14-MeV neutron beam, 25:9955
PERRY, F. C., Thermoelastic dosimetry of relativistic electron beams, 25:8569
PERSIANZEW, I., Electron temperature and density distribution of an argon plasma in inductive hydrodynamic shock wave tubes and their time

XUM

dependence, 25:9418
PERVYSHEV, E. V., Miniature end window counter for soft beta-radiation, 25:8521
PESCHKA, Walter, High-temperature energy systems with plasma reactors and inductive magnetoplasmadynamic converters, 25:9439
PETERLONGO, G., Dynamic behaviour of two-phase flow rods for nuclear reactor control, 25:10187
PETERS, Theo, Continuously operating plasma propulsion, 25:9438
PETERSEN, Helge, Properties of He: density, specific heats, viscosity, and thermal conductivity at pressures from 1 to 100 bar and from room temperature to about 1800 K, 25:8261 (RISO-224)
PETERSON, Deane M., Investigation of six D-type spectra, 25:9042
PETERSON, E., Observation of the decay eta' → γ γ, 25:9651 (COO-1764-111)
PETERSON, F. C., Measurements of π⁻p elastic scattering from 1.71 to 5.53 GeV/c, 25:9652 (COO-1764-112)
PETERSON, Sigfred, Thorium ceramics data manual. II, 25:8927 (ORNL-4503(Vol.2))
PETON, A., Envelope of the Be star HD 218393, 25:9017
PETRAKIEV, Asparuch, Excitation temperature functions of some spectrum lines of He, Ne, Ar, Kr, and Xe, 25:9172
PETRASKE, E. W., π⁻p charge exchange at backward angles, 25:9653 (COO-1764-113)
Reaction π⁻p → nπ⁺π⁻ at high momentum transfer, 25:9654 (COO-1764-114)
PETRINI, D., Electron excitation rate of the green coronal line 5303 A, 25:9123
PETRINOVIC, M., Digital rf pulse burst generator, 25:8575
PETROV, V. A., Emissivity of carbides of Ta and Hf over range 1300 to 3000° K, 25:8930
Integrated hemispherical emissivity of zirconium carbide, 25:8931
PETROVA, G. P., Interactions of flowing argon plasma in a channel with a transverse magnetic field, 25:9281
PETROVA, O. N., Genetic mutations in cell cultures of mammals, 25:8638
PETTY, R. J., Reaction mechanism in (p,pn) reactions, 25:10005
PHELPS, J., Capture cross section of ^{237}Np and ^{241}Am in different reactor spectra, 25:10019 (BNL-50242)
PHILIPP, G., Timing with surface barrier detectors, 25:8517
PHILLIPS, P. R., Measurement of the up-down asymmetries in the beta decay of polarized lambdas, 25:9626 (COO-1545-87)
PIARCENTINI, R. D., Exchange excitation of 2s state of hydrogen in close collisions with protons, 25:9201
PICARD, Robert, ESR investigation of Li center in MgO, 25:9544
PICKERING, Alan Roy, Improvements in reactors, 25:10200
PIGAREVA, Z. D., Effect of training nervous processes on the weight of the brain and the cholinesterase activity, 25:10411 (UCRL-Trans-1424)
PIKAEV, A. K., Kinetics of thermal and photostimulated extinctions of trapped electrons in γ-irradiated vitreous alkaline ice, 25:8287
PIKE, G. E., Hypersound attenuation in superconductors by quasi-particle creation, 25:9368
PILLAY, K. K. S., Neutron activation analysis of inorganic constituents of airborne particulates, 25:8231
PINCUS, P., Some magnetic effects in superconductors, 25:9383
PINSKER, Z. G., Phase transition in thin films of tantalum oxides, 25:8950
PISKAREV, I. M., Rapid fluctuations of intensity in the gamma radiation of a betatron, 25:9936
PITTHAN, R., Inelastic electron scattering by ^{140}Ce up to 3.5 MeV, 25:10046
PITTS, John H., Conceptual design of a 2-Mw/sub t/ (375 kw/sub e/) nuclear-electric space power system, 25:10286
PLAVNIK, G. M., Influence of ionizing radiation on the structure and properties of modified kapron fibers, 25:8270
PLEBANSKI, Jerzy, Lectures on non-linear electrodynamics, Copenhagen, 1968, 25:9869
PLETNEV, V. D., Currents of quasi-captured particles and interaction with geomagnetic field, 25:9342
Currents of quasi-trapped particles, 25:9347
PLOTKO, V. M., Identification of elements 102 and 104 with the help of the collimation method, 25:10030 (KFK-tr-329)
PLOTNIKOV, V. K., Beam regulation in a 100-MeV linear accelerator, 25:9914 (NP-tr-1926)
PLUTA, P. R., Final Fast Flux Test Facility backup design development requirement report, 25:10265 (GEAP-5715)
PODGOREISKY, M. I., Transition radiation on resonance γ-quanta, 25:9703 (JINR-P2-5042)
PODZOROVA, E. A., Determination of radiation yield of nitrite ions during irradiation of sodium nitrate solutions with small doses, 25:8297
POE, Norman D., Effects of coronary arterial injection of radioalbumin macroaggregates on coronary hemodynamics and myocardial function, 25:8713 (UCLA-12-798)
POGUTSE, O. P., Classical diffusion of a plasma in toroidal systems, 25:9400
Influence of high-frequency electric fields on equilibrium and stability of toroidal plasmas, 25:9499
POHLIT, Helmut Martin, Hot-atom chemistry of low-energy carbon ions in benzene, 25:8311
POLANDOV, A. G., Proton accelerator with investigating crystal structure by shadow effect method, 25:9918
POLANSKI, J., Metabolic and hemodynamic disturbances in the liver subdued to extracorporeal perfusion, 25:8783
POLIKARPOV, G. G., Radioecological studies of the Mediterranean Sea, 25:8630
POLITIS, C., Fabrication of ceramic materials by melting in an overpressure electric arc furnace, 25:8914
POLLARD, H. F., Effects of fast neutron irradiation on internal friction and Young's modulus of NaCl single crystals, 25:9547
POLOVINA, N. N., Dibaric particle in a constant electric field, 25:9729
POLS, C. L., Cross sections and spin-density matrix elements in 5 GeV/c π⁺ p four-pronged interactions, 25:9682
POLUBOYARINOV, Yu. V., Identification of elements 102 and 104 with the help of the collimation method, 25:10030 (KFK-tr-329)
POLYANIN, L. N., Doppler effect and nuclear safety of a fast reactor, 25:10176
POMERANTZ, Martin A., Cosmic-ray intensity variations in Antarctica, 25:9259
Energetic particles and radiation in polar cap, 25:9327
POMYTKIN, A. P., Spatial distribution of radical during γ irradiation of methanol at 77°K, 25:8288
PONINENKOVA, L. M., Beam regulation in a 100-MeV linear accelerator, 25:9914 (NP-tr-1926)
PONOMAREV, L. I., Problem of two centers in quantum mechanics. V, 25:9600 (JINR-P4-5040)
POPLAVSKII, I. V., Reduction of potential of the Schroedinger equation, 25:9610
POPOV, Yu. P., Calculations of magnetohydrodynamic gas-ionizing shock waves, 25:9272
POPOVA, G. Yu., Formation and kinetics of accumulation of NO_2 radicals in γ-irradiated $BaSO_4$, 25:8286
POPOW, G., Self-excited steady layers in Ar low-pressure columns in homogeneous, axial magnetic fields, 25:9465
POPP, M., Investigation of photon--photon angular correlations in atomic mercury, 25:9206
PORT, M., Excited states of ^{22}Ne, 25:10002
POSPIESZCZYK, A., Kinetic temperature of cold H I galactic components, 25:9132
POSTMA, A. J., Electron energy distribution function in low-pressure Cs discharge, 25:9419
POSTMA, A. K., Effect of continuous spray operation on the removal of aerosols and gases in the containment systems experiment, 25:10256 (BNWL-1485)
POSTNIKOV, V. V., Reliability of the evaporating channels of Beloyarsk power plant type reactors, 25:10106
POTZEL, W., Resonance spectroscopy of γ-radiation on Au(I) and Au(III) compounds, 25:9593
POWERS, E. L., Nitrous oxide as a sensitizer of bacterial spores to x-rays, 25:8810
POZDEEV, V. V., Radiation-thermal isomerization of alkyl bromides, 25:8279
PRADERIE, F., Short-period variable stars. III, 25:9035
PRASAD, G. Eswara, Sintering of UO_2: relation between electrical conductivity and microstructure of sintered UO_2, 25:8908 (BARC-507)
PRASAD, H., Cylindrical wave solutions of field equations of general relativity containing electromagnetic fields, 25:9873
PRASAD, R. D. G., Relative photopeak efficiencies and photofractions of a 2'' x 2'' CsI(TL) crystal, 25:8502
PRATCHETT, A. G., Photon activation analysis using electron linear accelerator at Harwell, 25:8216 (AERE-R-5363)
PRATT, P. L., Effects of interstitial impurities on the yielding behaviour of niobium single crystals, 25:8880
PREDVODITELEV, A. S., Properties of gases at high temperatures, 25:9444
PREUSSMANN, R., Neurotropic carcinogenic effect of phenyl--dimethyl triazene on rats, 25:10362 (ORNL-tr-2418)
PRICE, Michael Anthony, Instrumentation of nuclear reactors, 25:10191
PRICE, R. M., Observations of pulsar spectra, 25:9059
PRICE, R. R., nπ⁻π⁻ enhancement at 1.627 GeV/c² in K⁻d → p/sub s/s⁺s⁻s⁻n anti K⁰ GeV/c, 25:9671
PRINZLER, H., Microwave diagnostics of instabilities in column plasmas, 25:9425
Microwave diagnostics of strong-current discharges with skin effect. II, 25:9424
Microwave diagnostics of strong-current discharges with skin effect. I, 25:9428
PRITCHARD, David E., Alkali--alkali differential spin-exchange scattering. I, 25:9223
Alkali-alkali differential spin-exchange scattering. II, 25:9224
PROCA, G. A., Parallel plate electrostatic spectrograph, 25:8576
PROCHOROV, V. I., Certain properties of fuel behavior of can structural material in fast reactor conditions, 25:8896 (BNWL-tr-57)
PRODI, V., Control of contaminated air in a reactor fuel element fabrication plant, 25:8695
PROKOPENKO, L. G., Biosynthesis stimulation of antibodies in irradiated organism, 25:8621
PRONKIN, N. S., Counting characteristics of semiconductor detectors, 25:8523

PROUDLOVE, Michael Joseph, Improvements in nuclear reactors. 25:10198
PROVETSKI, E., Investigation of Heisenberg model of impure ferromagnets. I, 25:10346 (BNL-tr-389)
PRZYTULA, M., Investigation of $^{9}Be(t,n)^{11}B$ reaction at 1.10 MeV, 25:9976 (JINR-P15-5148)
PUEHLHOFER, F., Use of position-fixing semiconductor counters in magnetic spectrographs, 25:8474 (JUL-CONF-4, pp 48-58)
PUJARA, C. M., Radiation-induced division and mitotic delay studies in green alga (Oedogonium cardiacum), 25:8644
PUSHKARSKII, A. S., Methods of investigation of thermoelectric properties of semiconductors, 25:9590
PUZYNINA, T. P., Problem of two centers in quantum mechanics. V, 25:9600 (JINR-P4-5040)
PYATNITSKII, L. N., Effect of aperture on plasma parameters, 25:9415

Q

QUIN, P. A., Low-lying levels of ^{20}F, 25:10004
QUON, Wai-Kit, Electron diffraction technique for the determination of crystalline structure of beta glycine, 25:10405 (UCRL-20139)

R

RABENSTEIN, Dietrich, Beta--γ decay of 5^+ level in ^{116}In and γ-branching ratios in ^{116}Sn, 25:10049
RABINOWITZ, Murray, Effects of hypertrophy and hypoxia on the turnover of myocardial components, 25:10336 (ACRH-1000-214)
RADEKA, V., Digital rf pulse burst generator, 25:8575
RADFORD, H. E., Detection of methyl alcohol in Sagittarius, 25:9060
Search for excited state of OH in W3, 25:9093
Search for extraterrestrial $H_2{}^{18}O$ emission, 25:9076
RADHAKRISHNA, P., Isotope and ortho-para separations of the molecular hydrogens by adsorption at low temperatures, 25:8332
RADVAN, Rostislav, Pulmonary ascariasis in an irradiated organism. II, 25:8781
RADZIEVSKII, G. B., Tritium targets for beta-irradiation experiments, 25:8437
RAE, Anil C., Consequences of renormalizability. I, 25:9861
RAEDER, J., Measurement of ion temperature in hydrogen arc by means of thermal Doppler effect, 25:9413 (SC-T-71-3001)
RAETHER, M., Instability of electron beams in plasma, 25:9494
RAGNI, G., Computer dosimetry of the radioiridium castings, 25:8684
RAHIM, M., Open cluster NGC 2236, 25:9024
RAHMAN, M., Low-energy positron--helium scattering, 25:9196
RAINES, G. E., Ecological models applied to radionuclide transfer in tropical ecosystems, 25:8626
RAITSIMRING, A. M., Spatial distribution of radical during γ irradiation of methanol at 77°K, 25:8288
RAJARAMAN, R., Constraint on the universal function in electroproduction, 25:9720
RAMACHANDRAN, R., PiN charge-exchange polarization in Veneziano model, 25:9793
RAMANISH, M. V., In-line analytical methods for fuel reprocessing streams. I, 25:8197 (BARC-510)
RAMAVATARAM, K., $^{20}Ne(p,t)^{18}Ne$ reaction as a test of the ^{18}Ne and ^{20}Ne wave functions, 25:10006
RANDALL, P. L., Elevated-temperature tensile tests of cast uranium-base dilute quinary alloys, 25:8867 (NLCO-1060)
RANDOLPH, J. Kemp, Observation of the decay eta' → γ γ, 25:9651 (COO-1764-111)
RANFT, J., Angular distributions of secondary particles in the thermodynamic model, 25:9787
RAO, G. U. V., Contrast perception in imaging systems, 25:8496
RAO, M. P. Ranga, Pressure shocks in dissipative magnetogasdynamics, 25:9278
RAO, Manoranjan, Nondissipative phenomena affecting A_1 absorption measurements, 25:9323
RAO, S. V. K., Sintering of UO_2: relation between electrical conductivity and microstructure of sintered UO_2, 25:8908 (BARC-507)
RAO, V. K., In-line analytical methods for fuel reprocessing streams. I, 25:8197 (BARC-510)
RAPOPORT, V. O., Variations in mean level of radio emission at 1.1 and 2.3 MHz, 25:9352
RARITA, William, Regge-pole model for pp and anti pp elastic scattering at high energies, 25:9813
RASEMAN, Chad J., Combined hydroelectric pumped storage and nuclear power generation, 25:10109 (BNL-50238)
RASHID, Y. R., Nonlinear quasi-static analysis of two-dimensional concrete structures. I and II, 25:8392 (GA-9994)
RASMUSSEN, Erik Gerhard, Strontium- and manganese concentrations in mandibular rat incisors following intraperitoneal injections, 25:8222
RASPOPOV, O. M., Relation of stable pulsations of the geomagnetic field with parameters of the magnetosphere, 25:9353
RASSKAZOV, D. S., Thermophysical properties of organic coolants, 25:8412
RATNER, B. S., Constancy of the maximum energy in the bremsstrahlung spectrum of a synchrotron, 25:9935
RAUDASKOSKI, Marjatta, New secondary B/sub β/ mutation in Schizophyllum, 25:8643
RAUZEN, F. V., Sorption of Sr and Ca cations on KU-2 type cation exchange resin, 25:8341
RAVNDAL, F., Eikonal Regge fits to small-angle elastic scattering data, 25:9755
Eikonal Regge model for elastic scattering processes, 25:9776
RAVOIRE, Jean, Isotopic exchange between hydrogen and liquid ammonia catalyzed by alkali amides, 25:8244
RAVVE, Abraham, Process for preparing polymerized aminoplast surface coatings using ionizing radiation, 25:8278
RAYLE, David L., Macromolecule synthesis and wall extensibility in relation to the mechanism of auxin-induced cell elongation, 25:10366 (RLO-2225-T-19-9)
RAZOV, V. I., Lifetime of excited states in spherical nuclei ^{139}La, ^{135}La, and ^{133}La, 25:10029 (JINR-P6-5200)
RAZUVAEVA, L. A., Ionization nonequilibrium state of cold pulse-discharge plasma, 25:9462
REDDY, A. R., Relative biological effectiveness of the $^{10}B(n,\alpha)^{7}Li$ reaction in HeLa cells, 25:8745
REDFERN, R. M., Low-energy gamma rays from NP 0532, 25:9062
REGIMBAL, J. J., Technical bases for FFTF driver fuel instrumentation, 25:10255 (BNWL-916)
REIBEL, K., Measurement of the up-down asymmetries in the beta decay of polarized lambdas, 25:9626 (COO-1545-87)
REICHARD, S. M., Deuteration in slow neutron radiography of biological media, 25:8709 (DP-1229)
REICHLEY, P. E., Interstellar scintillations of pulsar signals at 2388 MHz, 25:9091
REID, G. C., Riometer observations of radio-wave absorption in the antarctic ionosphere, 25:9324
REIFSNYDER, David N., Multiple echinococcus granulosus cysts of liver, 25:8719
REIGNIER, J., $Pi^+\pi^-$ elastic cross section, 25:9669
Piπ phase shifts, 25:9670
REILLY, Martin L., Heat capacity and thermodynamic properties of α-beryllium nitride, Be_3N_2, from 20 to 315 K, 25:8939
REIMER, D., Investigation of the auroral electrojet, 25:9334
REIS, H. E., Isoelectric separation in protein chemistry, 25:10413 (UCRL-Trans-1428)
RENNER, B., Empirical test of tensor meson dominance, 25:9764 (DESY-70/58)
RENNIE, Compton Alexander, Improvements in nuclear reactors, 25:10168
RESHETOV, N. N., Improvement of characteristics of a double-diode restorer of base level, 25:8540
REVAI, J., Exactly soluble three-body model of resonance scattering, 25:9890
REYES, E., Radiosensitivity of mice exposed to various temperatures and low-dose rate radiation, 25:8768
REYNES, Jean, Experimental study of liquid-vapor equillibrium of a UF_6--WF_6 hexafluoride binary mixture under a pressure of 2,600 torr, 25:8265
Experimental study of the UF_6--MoF_6 binary mixture under a pressure of 2,600 torr, 25:8264
REYNOLDS, C. A., Lead-alloying effects on the superconducting critical field curve of indium, 25:9380
REYNOLDS, G. M., Secondary gamma-ray production and transport in liquid nitrogen, 25:9950
REZANOV, I. I., Uranium level in foodstuffs, 25:8631
REZWANI, V., Dynamic collective model of the giant resonance, 25:10083
RHOADES, T. G., Measurements of π^-p elastic scattering from 1.71 to 5.53 GeV/c, 25:9652 (COO-1764-112)
Observation of the decay eta' → γ γ, 25:9651 (COO-1764-111)
RIBON, Pierre, Critical examination of ^{240}Pu neutron cross sections, 25:10021 (CEA-N-1273)
RICE, J. B., Oblique rotator model for the magnetic and spectrum variable HD 173650, 25:9021
RICHARDSON, Gerald L., Integrated LMFBR aqueous fuel reprocessing concepts, 25:8316 (BNWL-CC-1939)
RICHMOND, R. G., Dosimetry of proton radiation fields in space with nuclear emulsions, 25:8682
RICHOU, Jacques, Electron density of xenon plasma by laser interferometry and spectroscopy, 25:9422
RICHTER, J., Experimental oscillator strengths for Ni I lines, 25:9117
RICQUE, R., Heat exchange for two-phase flow in horizontal and vertical tubes, 25:8406 (CEA-CONF-1649)
RIEDLER, W., Electron precipitation associated with sudden commencement of a geomagnetic storm, 25:9298
RIEGER, E., Measurements of electric fields in equatorial and medium latitudes during twilight using barium ion clouds, 25:9285 (MPI-PAE/EXTRATERR-49/70)
RIEGER, Rigomar, Induction of segment extension and chromatid structural changes in Vicia faba chromosomes, 25:8639
RIEKSTINYA, D. V., Rapid neutron activation method for

XUM

aluminum determination in al coordination compounds, 25:8224
RIGLER, Rudolf, Uv-irradiation induced changes in the uptake of acridine orange in living mouse fibroblasts in vitro, 25:8770
RIKHVITSKII, S. V., Pulse shaper with the zero time of regeneration for the apparatus blocking at the large loading, 25:8545 (JINR-P13-5377)
RILEY, B., High temperature oxygen equilibrium in the plutonium--oxygen system, 25:8945
RIMONDI, O., Mixed radiation dosimetry with LiF (TLD-100), 25:8567
RISIK, N. S., Radioecological studies of the Mediterranean Sea, 25:8630
RITTENHOUSE, P. L., Progress in Zircaloy cladding failure modes research, 25:8839 (ORNL-TM-3188)
RITTER, F. W., Computer-analyzed counting and scanning, 25:8716
RITZMAN, Robert L., Prog. rpt. on applicability of existing data to analytical description of reactor accident, 7--9/70, 25:10238 (BMI-1890)
RIUS, Gerard, ESR investigation of Li center in MgO, 25:9544
RIVA, D., Concentrations of tritiated desacetyl--lanatoside C after injections in cardiopathic subjects, 25:8724
RIVEROS, Jose Manuel, Isotopic effect and temperature dependence of ESR spectrum of methyl radical, 25:8257
RIX, H., Interpretation of the east--west asymmetry of the initial appearance of sunspots, 25:9118
RIXEN, W., Effect of cyclic fast neutron irradiation damage on modulus of rupture of BeO, 25:8959
RO, Seung Gy, Fast neutron dosimetry with two threshold detectors in criticality accidents of nuclear reactors, 25:10181
ROBBINS, A. B., $^{7}/_{2}^{-}$ isobaric analogue resonances in odd isotopes of Sb, 25:10044
ROBERSON, N. R., Reactions $^{14}C + \alpha$, 25:9980
ROBERTS, Phillip Howard Jr., Velocity fields in magnetically disturbed regions of the Hα chromosphere, 25:9106
ROBERTS, R. E., Semiclassical treatment of collision-induced dissociation, 25:9197
ROBERTSON, Harry S., Entropy oscillation and the h theorem for finite segments of infinite coupled-harmonic-oscillator chains, 25:10365 (ORO-3895-9)
Prog. rpt. on HELIOS Program, 9/15/70, 25:9398 (ORO-3895-15)
ROBERTSON, James S., Toxic effect of thermal neutrons on the rabbit electroretinogram, 25:8761
ROBINSON, J. C., Analytical determination of the neutron flux-to-pressure frequency response: application to the Molten-Salt Reactor Experiment, 25:10178
Experimental neutron flux-to-pressure frequency response for the Molten-Salt Reactor Experiment: determination of void fraction in fuel salt, 25:10177
ROBINSON, T. W. E., Potentiation of primary virus infection by radiomimetic drugs, 25:8699
ROCHER, Y. A., Vortex trapping, 25:9387
ROCKMORE, Ronald, Hard-pion current algebra, unitarization, and I = 0 s-wave ππ scattering, 25:9775
Scalar form factors just beyond the tree approximation, 25:9777
RODABAUGH, E. C., Stesses in out-of-round pipe due to internal pressure, 25:8871 (ORNL-TM-3244)
RODDIER, F., Interpretation of the east--west asymmetry of the initial appearance of sunspots, 25:9118
RODENBERG, R., Mass of the ninth pseudoscalar meson, 25:9779
RODGERS, Jean-Marie, Glucose-induced resistance to gamma-rays in E. coli, 25:8812
RODIER, J., Water and the nuclear industry, 25:8326
RODKINA, T. E., Nature of interplanetary gas, 25:9115
RODOT, H., P--N junction formation in ion-implanted ZnTe, 25:9560
RODRIGUEZ DE QUESADA, Angel, Some complications in high energy therapy, 25:8739
RODRIGUEZ DE QUESADA, Blas, Some complications in high energy therapy, 25:8739
ROEH, A. P., Development of a fluidized-bed burner for processing Rover fuel, 25:8322 (IN-1423)
ROGACHEV, A. P., High-temperature combustion products for thermoelectric plants with MHD generator, 25:9261
ROGERS, J. W., Ion implantation of sodium, lithium, and neon in cadmium sulfide, 25:9561
ROINISHVILI, V. N., Characteristics and capabilities of a discharge--condensation chamber, 25:8551
ROITMAN, James Nathaniel, Studies in carbanion chemistry, 25:8253
ROJKOV, V., Some aspects of nuclear developments in USSR, 25:10099
ROLINSKI, Ednund J., Thermodynamics of vanadium alloys. I, 25:8862 (AD-709957)
ROLL, J. B., Commercial plutonium recycle, 25:10222
ROMANOV, E. P., Current generator for studying superconductivity by an impulse method, 25:8580
ROMANOV, P. V., Calculation of plane electron beam in intersected fields by Monte Carlo method, 25:9165
ROMANOWSKI, T. A., Measurement of the up-down asymmetries in the beta decay of polarized lambdas, 25:9626 (COO-1545-87)
ROMER, H., Observation of the decay eta' → γ γ, 25:9651 (COO-1764-111)
ROMER, H. F., $\pi^- p$ charge exchange at backward angles, 25:9653 (COO-1764-113)
Reaction $\pi^- p \rightarrow n\pi^+\pi^-$ at high momentum transfer, 25:9654 (COO-1764-114)
RON, A., Far infrared spectra of HCl and DCl in a N matrix, 25:8250
ROOD, R. T., On the evolutionary status of stars above the horizontal branch in globular clusters, 25:8992
ROSATELLI, C., Microwave technique for measurement of high temperature and neutron flux in nuclear reactors, 25:10326 (RT/FI-(70)7)
ROSEN, Gerald, Formulations of classical and quantum dynamical theory, 25:9840
ROSENBERG, G. S., Vibration of a beam with motion-constraint stops, 25:10163 (ANL-7619)
ROSHAL, A. S., Calculation of plane electron beam in intersected fields by Monte Carlo method, 25:9165
ROSNER, J. L., Sharp states in the spectrum of low-lying mesons, 25:9768
ROSS, K. J., Photoelectron spectra of ground-state atomic H, N, and O, 25:9200
ROSSI, A., Enzyme activities in rabbits after pan-irradiation, 25:8779
ROTH, Robert S., Use of splines with unknown end points in the identification of systems, 25:10390 (TID-25617)
ROTHHARDT, L., Electron temperature and density distribution of an argon plasma in inductive hydrodynamic shock wave tubes and their time dependence, 25:9418
Self-excited steady layers in Ar low-pressure columns in homogeneous, axial magnetic fields, 25:9465
ROTHROCK, R. B., Comparison of nuclear design models for power and flux distributions near the FTR core-reflector interface, 25:10272 (WHAN-FR-35)
ROTHSCHILD, E., Computer-analyzed counting and scanning, 25:8716
ROTHSTEIN, Stuart M., Pade-type variational wave function for H_2^+, 25:9175
ROTVAIN, A. Ya., Photoproduction of positive pions on protons in region of resonance $P_{33}(1236)$, 25:9623
ROUGH, F. A., Report of meeting on methods and models used to design fuel pins and predict in-pile performance, April 8--9, 1970, Germantown, 25:10212 (TID-25590)
ROUMY, R., Heat exchange for two-phase flow in horizontal and vertical tubes, 25:8406 (CEA-CONF-1649)
ROUSSEAU, D., Structural stability of austenitic Cr--Ni stainless steels to deformation and extremeley low temperature, 25:10357 (ORNL-tr-2314)
ROUTLEDGE, D., Optical depth and excitation temperature of galactic H in direction of W49, 25:9069
ROUTSON, R. C., Mathematical simulation of groundwater transport of radionuclides at Hanford, 25:8345 (BNWL-SA-3494)
ROUVILLOIS, G., Radiative transfer in an LTE atmosphere, 25:9440
ROUX, J. C., Radiolysis of 1 M aqueous ethanol solutions of potassium nitrate, 25:8301
ROWE, J. N., Observations of electron density during a solar flare, 25:9300
ROWSTON, W. B., Determination of ruthenium by atomic absorption spectrophotometry, 25:8209
ROYER, A., Mechanisms of plastic deformation in a nickel--chromium--niobium alloy precipitation hardened at 700°C, 25:8884
ROYER, Jeffrey Paul, Threshold theorem for the radius of nucleon form factor, 25:9722
ROYNETTE, J. C., Many-nucleon transfer reactions between heavy ions, 25:9986
ROZHANSKAYA, L. I., Radioecological studies of the Mediterranean Sea, 25:8630
ROZMAN, I. M., Radioluminescence of organic substances. VIII, 25:8274
ROZOV, B. S., Measuring devices for processing photographs of bubble chambers (review), 25:8554
RUBBIA, Carlo, Simple threshold and delay circuit for multi-wire proportional chambers, 25:8468 (CEAL-1054)
RUBIN, R. H., Radio observations of planetary nebulae and possible planetary nebulae, 25:8996
RUBIN, Richard Mark, Disk source energy and angular distributions, 25:9539
RUBIN, Robert H., Observation and classification of the Nebula YM 29, 25:9047
RUBINSTEIN, H. R., Linear rising trajectories theory of nucleon--antinucleon annihilation, 25:9769
RUBTSOV, K. S., Forming beams and beam parameters in output channels of 360-MeV electron linear accelerator, 25:9927
RUCKER, D. J., Prog. rpt. on fuels and materials development, 6/30/70, 25:8829 (ORNL-4600)
RUDD, M. E., Experimental evidence for the mechanism of charge transfer into continuum states, 25:9241
RUDDICK, K., Observation of the decay eta' → γ γ, 25:9651 (COO-1764-111)
$\pi^- p$ charge exchange at backward angles, 25:9653 (COO-1764-113)
Reaction $\pi^- p \rightarrow n\pi^+\pi^-$ at high momentum transfer, 25:9654 (COO-1764-114)
RUDGE, M. R. H., Total elastic scattering and spin-change cross sections for collisions between alkali atoms, 25:9202
RUEHLE, M., Production and properties of dispersion

hardened Cu. II, 25:8873
RUMER, Yu. B., O(2,1) algebra and H atom, 25:9179
RUPERT, Claud S., Analysis of photoenzymatic repair of uv lesions in DNA by single light flashes. VII, 25:8650
Analysis of photoenzymatic repair of uv lesions in DNA by single light flashes. VI, 25:8651
RUSSELL, G. J., Very intense neutron source, 25:9954
RUSSEV, G. K., Changes in DNA template after x-ray irradiation in vitro, 25:8610
RUST, K., Fuel rods with internal fins, 25:10223
RUTHERFORD, W. M., Thermal diffusion column coefficients for the separation of N_2^{14}--$N^{14}N^{15}$ and O_2^{16}--$O^{16}O^{18}$, 25:8423 (MLM-1439(Rev.))
RYABKA, P. M., Forming beams and beam parameters in output channels of 360-MeV electron linear accelerator, 25:9927
RYABOV, V. R., Investigation of Nb--Fe--Al and Nb--Co--Al systems, 25:8890
Ternary systems Gd--(Y, Tb, Dy, Ho, Er, Sc)--Al in region to 25 at. percent rare-earth metals, 25:8886
RYABOVA, T. Ya., Effective protection of space ships, 25:9540
RYAN, R. D., High-resolution nuclear radiation detectors from epitaxial n-GaAs, 25:8491
RYAZHSKAYA, O. G., Liquid scintillators for large scintillator detectors, 25:8527
RYBAKOVA, N. A., Shower spark chambers for detecting particles moving at small angles with respect to the beam being stopped, 25:8553
RYNDIN, R. M., CP violation and models with supplementary particles, 25:9827
RYTER, Charles, Location of x-ray sources and the galactic background, 25:9079
RYUTOV, D. D., Influence of inhomogeneity of plasma on the relaxation of an ultrarelativistic electron beam, 25:9472

S

SABAEV, E. F., Natural circulation stability of heat transfer agent in one-loop system, 25:8414
SACERDOTI, G., Hamiltonian that implies the exclusion principle, 25:9689 (LNF-70/22)
SACHAROW, A., Electron temperature and density distribution of an argon plasma in inductive hydrodynamic shock wave tubes and their time dependence, 25:9418
SACHS, Francis L., Engineering materials list, 25:8396 (TID-4100(Suppl.61))
SACHSE, K., Hydraulic rabbit facility, 25:10274
SACKMANN, I.-J., Rapid uniform rotation along main sequence. II, 25:9030
SADKOV, Yu. A., Question of high-pressure scale, 25:10352 (LA-tr-70-26)
SAENGER, Robert M., Theorem on intuitive tests of parity conservation via spin polarization processes, 25:9686 (COO-1764-100)
SAGER, Otto, Helicon resonances in low-pressure plasmas, 25:9512 (NP-18554)
SAHA, A. K., Low ionization problem in ionospheric true-height analyses, 25:9319
SAHLIN, H. L., He and H^- 1^1S and 2^3S states computed from Feynman path integrals in imaginary time, 25:9177
SAHOTA, H. S., Measurement of K-shell photoelectric cross sections in U, 25:9235
SAITO, Ryozo, Two phase flow in the bleed piping of a nuclear turbine, 25:8411
SAITO, Satoru, Low energy theorems for Compton scattering off arbitrary spin targets, 25:9710
SAITO, Teijiro, Study of isobaric analogue state by (γ,p) reaction, 25:10053
SAITO, Toru, Effect of flow pattern in gaseous diffusion process, 25:8438
SAKABE, Kiyozo, Fatigue strength of nuclear pressure vessel material ASTM A 302 B steel and its welded joints, 25:8868 (NSJ-tr-159)
SAKAKI, Takashi, Direct determination of molybdenum in high alloy steel by the spectrophotometric method, 25:8210
SAKISAKA, Masakatsu, Multiple scattering of protons and nitrogen ions on copper, 25:9163
SAKITA, B., Formulation of dual theory in terms of functional integrations, 25:9901
SAKKA, Masatoshi, Dependency of inhibition of imago formation in Sarcophaga pupae upon dose-rate, 25:8749 (NSJ-tr-156)
SALAM, Abdus, Equivalent formulations of massive vector field theories, 25:9858
SALANT, E. O., $n\pi^-\pi^-$ enhancement at 1.627 GeV/c^2 in K-d → p/sub s/$\pi^+\pi^-\pi^-$n anti K^0 GeV/c, 25:9671
SALAT, A., Effect of collisions on electrical conductivity of plasmas, 25:9480
SALATSKII, V. I., Investigation of $^9Be(t,n)^{11}B$ reaction at 1.10 MeV, 25:9976 (JINR-P15-5148)
SALE, R. G., Low-energy gamma rays from NP 0532, 25:9062
SALIKHAEV, K. T., Properties of excited states of ^{151}Sm, 25:10035
SALIN, A., Exchange excitation of 2s state of hydrogen in close collisions with protons, 25:9201
SALINA, E., CONDOR 3: two-dimensional reactor lifetime program with local and spectrum dependent depletion, 25:10304 (EUR-4539)
SALKELD, Robert, Deep space shuttles: chemical vs nuclear; direct flight vs near-orbit rendezvous, 25:10287
SALMONI, G., Design criteria and steel characteristics for reactor pressure vessels, 25:10197
SALPETER, E. E., Surface recombination of hydrogen molecules, 25:9087
SALPETER, Edwin E., Molecular H in H I regions, 25:9088
SAMOSVAT, G. S., Coherent scattering amplitude of ^{186}W measured by small angle scattering, 25:10026 (JINR-E3-5371)
SAMPIERE, Vincent, Afterloading vaginal irradiators, 25:8736
SAMPSON, Douglas H., Semi-empirical cross sections and rates for excitation and ionization of hydrogen by electron impact, 25:9184
SAMUELS, G., Use of steam-electric power plants to provide thermal energy to urban areas, 25:10094 (ORNL-HUD-14)
SANDA, A. I., Spectral-function sum rules for rho--ω and rho--phi transitions, 25:9718
SANDQUIST, Gary M., Phase space analysis of reactor kinetics, 25:10311
SANMARTIN, Juan R., Far-wake structure in rarefied plasma flows past charged bodies, 25:9478
SANNER, Tore, Effect of charged groups on the indirect action in frozen aqueous solutions, 25:8298
Intermolecular transfer of radiation energy at 77°K. An ESR study of irradiated mixtures of macromolecules and oxidized penicillamine, 25:8613
SANTIER, Christian, ESR investigation of Li center in MgO, 25:9544
SAPHIER, D., Effect of errors in the delayed-neutron data on fast reactor static and dynamic calculations, 25:10179
SARAEVA, V. V., Role of charged particles and excited molecules during radiation oxidation of n-heptane by molecular oxygen, 25:8281
SARANTSEV, V. P., Electron--ion bunch diagnostics by bremsstrahlung, 25:9908 (KFK-tr-337)
SAREYAN, J. P., Short period variable stars. II, 25:9025
Short-period variable stars. III, 25:9035
SARGENT, W. L. W., Heavy elements in peculiar A stars, 25:8984
Maffei 1: a new massive member of the Local Group, 25:9148
SARGENT, Wallace L. W., Isolated extragalactic H II regions, 25:9126
SARKER, A. Q., Model of epsilon → 2γ and delta → 2γ decays, 25:9719
SARKISOV, A. A., Safe operation of atomic ships, 25:10295 (JPRS-51939)
SARRAZIN, Pierre, Elementary mechanisms of heterogeneous gas-solid kinetics, 25:10358 (ORNL-tr-2392)
SASLAW, William C., Differences in stellar content of the nuclei of galaxies with measured rotation curves, 25:9137
SASSI, Mohamed, Electron density in ionized Cs vapor, 25:9421
SASTRE, C., Capture cross section of ^{237}Np and ^{241}Am in different reactor spectra, 25:10019 (BNL-50242)
SATO, Masumi, Wave nature of moving striations in a longitudinal magnetic field, 25:9453
SATO, Nobuyuki, Nuclear accidents in nuclear installations, 25:8661 (JAERI-4052)
SATOVICH, G., Observation of the decay eta' → γ γ, 25:9651 (COO-1764-111)
SATTAR, A., Inhibition of the germination in gamma irradiated onions, 25:8815
SATTERBLOM, P. R., Solar cosmic-ray observations during 1969, 25:9260
SAUER, H. H., Riometer observations of radio-wave absorption in the antarctic ionosphere, 25:9324
SAUER, K., Higher-order temporal and spatial plasma wave echoes, 25:9534
SAUNDERS, L. M., Magnitude of high-energy meson--meson total cross sections, 25:9773
Multiperipheral bootstrap, 25:9757
SAUVAGE, Michel, Thermally insulating jacket for a nuclear reactor, 25:10335
SAUVAL, A. J., Identification of SiH^+ in the solar photospheric spectrum, 25:9120
SAUZADE, M., Coils and energy storage, 25:9395
SAVAGAON, K. A., Radiation preservation of Chapaties, 25:8819
SAVENKO, I. A., Spatial distribution of singly charged particles and helium nuclei above the atmosphere in the equatorial region, 25:9349
SAVOLAINEN, A. W., Use of steam-electric power plants to provide thermal energy to urban areas, 25:10094 (ORNL-HUD-14)
SAWANT, P. L., Dehydro-irradiation process for tropical shrimps, 25:8820
SAWTELLE, G. R., Conductivity cells for flow induced vibration measurements, 25:10271 (WHAN-FR-21)
SAYER, Bernard, Electron density in ionized Cs vapor, 25:9421
SBORSHCHIKOV, V. G., Efficiency of a spark chamber at the lower limit of ionization, 25:8557
SCARASCIA-MUGNOZZA, G. T., Relative frequency of chlorophyll to morphological and sterility mutations induced in durum wheat, 25:8641
SCARFONE, Leonard M., Dispersion methods and the two-nucleon interaction in charged scalar theory, 25:9817

XUM

SCARICABAROZZI, Ricardo, Noble-gas closed MHD loop fired with fossil fuels, 25:9264
SCHAAL, R. E., Ozone screening heights deduced from sunrise effects at very low frequencies, 25:9331
SCHAEFER, D. William, Bone marrow restoration of transplantation immunity in the leopard frog Rana pipiens, 25:8620
SCHAEFER, G., Investigation of photon--photon angular correlations in atomic mercury, 25:9206
SCHAEFER, H. J., Dosimetry of proton radiation fields in space with nuclear emulsions, 25:8682
SCHAEFER, K., Fast neutron flux measurements with stilbene-scintillator, 25:8509
SCHAEFER III, Henry F., Four new bound, low-lying states of cyanogen, 25:9110
SCHAEFFER, Norman M., Activities of ANS-6 subcommittee on radiation shielding standards, 25:9538 (ORNL-TM-3251)
SCHALIT, L. M., Chemistry of the Gasbuggy chimney, 25:8384 (PNE-G-68)
SCHALLER, Karl, Thermal shield for a reactor vessel, 25:10199
SCHAMBERGER, R. D., Prog. rpt. on enriched uranium active assay program, 4--6/70, 25:8447 (BHD-65-1)
SCHARENGUIVEL, J. M., Analytic structure of off-mass-shell S-wave π, 25:9763 (COO-1428-239)
SCHARER, J. E., Cyclotron wave plasma studies, 25:9408 (COO-1789-1)
SCHEIDHAUER, Jean, Accidental release of ^{131}I at UP 2 plant on October 2nd and 3rd 1968, 25:8657 (CEA-R-4008)
SCHELBERG, A. D., Technique for obtaining neutron radiographs in the resonance region, 25:8442
SCHENK, L. U., Hold-up of amines and amine carbamates on column packings, 25:8320 (CU-755-7, Sect.6)
SCHERBAKOVA, L. G., Kinetics and mechanism of solid state reactions in the systems of refractory oxides, 25:8935
SCHIELDGE, J. P., Simultaneous sudden magnetospheric compressions and geomagnetic bay onsets, 25:9332
SCHILCHER, K., Collinear dispersion relations and K/sub e4/ decay rate, 25:9747
SCHILLING, W., Comparison of lattice-parameter and resistivity change in electron-irradiated aluminum, 25:9564
Pinning of flux lines in superconducting niobium due to point defects, 25:9379
SCHIMMEL, W., Applications of vacuum technology in nuclear installations, 25:8461
Effect of the various regimes of operation of a nuclear installation on the volatile radioactive release, 25:10162
SCHLOTT, K., Generalized DWBA model applied to $^{24}Mg(dp)^{25}Mg$ reaction at E/sub d/ = 13.5 MeV, 25:9997 (JINR-E4-5350)
SCHLUDI, H. N., Nuclear comparison of coolants in heavy water pressure tube reactors, 25:10205
SCHLUTER, Heinz, Control rod drive for reactors, 25:10188
SCHMID, E., Time wise behaviour of irradiation induced chromosome aberrations in humans, 25:8788 (LIB/Trans-296)
SCHMIDBAUER, E., Thermal conductivity of pure type II superconductors, 25:9392
SCHMIDT, C., Reaction $^{18}O(^3He,d)^{19}F$, 25:9985
SCHMIDT, Hartwig, Onset of surface superconductivity, 25:9388
SCHMIDT, P. H., New first-order phase transition in high-purity ytterbium metal, 25:9588
SCHMIDT-KALER, Th., Kinetic temperature of cold H I galactic components, 25:9132
SCHMIDT-PARZEFALL, W., Wire spark chambers at the Inst. for Experimental Nuclear Physics, Karlsruhe, 25:8480 (JUL-CONF-4, pp 165-71)
SCHMITT, John L., Stars with strong cyanogen absorption, 25:9043
SCHNEIDER, Barry, Inelastic scattering of high-energy electrons from atoms: the helium atom, 25:9217
SCHOCKENHOFF, F., Microwave diagnostics of instabilities in column plasmas, 25:9425
SCHOLZ, M., Investigation of six O-type spectra, 25:9042
SCHOOLMAN, Stephen Allan, Magnetic and spectral characteristics of small H-alpha solar plages, 25:9099
SCHORSCH, W., Multipole analysis for the reactions γp → K⁺Λ and γp → K⁺Σ⁰, 25:9728
SCHOTANUS, D. J., Cross sections and spin-density matrix elements in 5 GeV/c π⁺ p four-pronged interactions, 25:9682
SCHRIBER, S. O., Fitting of an ordered set of mode frequencies, 25:9902 (AECL-3669)
SCHROEDER, B., Electron energy loss spectra of graphite single crystals and evaporated carbon films in the range 0.02 to 0.4 ev, 25:9167
SCHROEDER, L. S., Measurements of π⁻p elastic scattering from 1.71 to 5.53 GeV/c, 25:9652 (COO-1764-112)
SCHROER, Bert, Indefinite metric and stationary external interactions of quantized fields, 25:9864
Problems of stability for quantum fields in external time-dependent potentials, 25:9863
SCHUELLEROVA, M., Accumulation of /sup 99m/Tc in rat thyroid, 25:8599
SCHULTE-FROHLINDE, D., Gamma-radiolysis of 2-deoxy-D-ribose in aqueous solution, 25:8305
SCHULZ, G. J., Vibrational excitation by electron impact in O_2, 25:9210
SCHULZ, H., Generalized DWBA model applied to $^{24}Mg(dp)^{25}Mg$ reaction at E/sub d/ = 13.5 MeV, 25:9997 (JINR-E4-5350)
SCHULZ, Michael, Electrostatic instabilities in multicomponent plasmas, 25:9500
SCHULZ, Milford D., Radioactive scleral shells in the treatment of conjunctival tumors, 25:8731
SCHULZ, Wallace W., Integrated LMFBR aqueous fuel reprocessing concepts, 25:8316 (BNWL-CC-1939)
SCHULZE, W., Two-quasiparticle (h/sub 9/2/)² isomeric state in ^{202}Po, 25:10027 (JINR-E6-5379)
SCHUNK, Robert W., Transport properties of the ionospheric electron gas, 25:9302
SCHUPBACH, M., Effect of caffeine on mutation and recombination, 25:8637
SCHUSKE, C. L., Empirical model for safe pipe intersections containing fissile solution, 25:8459
SCHUURMAN, W., Kink instability of a toroidal plasma column, 25:9492
SCHWARTZ, D. M., Measurement of the up-down asymmetries in the beta decay of polarized lambdas, 25:9626 (COO-1545-87)
SCHWEBEL, Solomon L., Advanced and retarded solutions in field theory, 25:9835
SCHWEDE, Harold F., Nuclear resonance well logging method and apparatus, 25:8358
SCHWEITZER, T., Differential neutron source strength from $T(d,n)^4He$, 25:9957
SCHWING, Jean-Paul, Microdetermination of molybdenum by anodic stripping at constant current using the hanging mercury drop electrode, 25:8206
SCHWINGER, Julian, Particles, sources, and fields, 25:9699
SCOBEL, W., Apparatus for the investigation of neutron induced α-activities in the order of seconds, 25:8513
SCOTT, Arthur F., Study of trace metals in fingernails and hair using neutron activation analysis, 25:8229
SCOTT, B. R., Photosensitizing effect of 8-methoxypsoralen on inactivation and mutation of Aspergillus conidia, 25:8702
SCOTT, G. B., Fermi surface in niobium, 25:9575
SEALANDER, John A., Short-term effects of acute sublethal gamma radiation on populations of the old-field mouse, 25:8760
SEARLE, Leonard, Isolated extragalactic H II regions, 25:9126
SEDRAKYAN, D. M., Slow rotation of relativistic polytropic models, 25:9078
SEEBECK, U., Fast neutron flux measurements with stilbene-scintillator, 25:8509
SEELIGER, D., Differential neutron source strength from $T(d,n)^4He$, 25:9957
SEGMUELLER, G., Diagnostic use of ^{85}Sr in the preoperative evaluation of non-union, 25:8720
SEIDEL, K., Differential neutron source strength from $T(d,n)^4He$, 25:9957
SEIFRITZ, W., Cross-spectral-density sink frequency behavior in coupled core reactors, 25:10279
SEILER, Nikolaus, Electrophoresis in a carrier-free buffer stream. I, 25:10414 (UCRL-Trans-1429)
SEILER, Rudolf, Problems of stability for quantum fields in external time-dependent potentials, 25:9863
SELEKTOR, Ya. M., Interaction π⁻π⁻ in the reaction π⁻p → N*⁺⁺(1236)π⁻π⁻ with impulse 4.47 GeV/c, 25:9655 (ITEF-767)
Reaction π⁻p → rho⁰π⁻p with impulse 4.45 GeV/c, 25:9656 (ITEF-775)
SELPH, W. E., Secondary gamma-ray production and transport in liquid nitrogen, 25:9950
SELZ, Allen, Implantable circulatory support system, 25:8436
SEMEL, M., Zeeman effects in solar spectral lines, 25:9122
SEMENCHUK, G. G., Composition and excitation energy of fissioning nuclei in irradiation of ^{209}Bi and ^{197}Au 1 GeV photons, 25:10037
SEMENYUK, A. K., Volume gradient of γ-emf in p-Si, 25:9568
SEMENYUSHKIN, I. N., Pulse shaper with the zero time of regeneration for the apparatus blocking at the large loading, 25:8545 (JINR-P13-5377)
SEMERCHAN, A. A., Question of high-pressure scale, 25:10352 (LA-tr-70-26)
SEMONIN, Richard G., Prog. rpt. on study of rainout of radioactivity in Illinois, 11/70, 25:8365 (COO-1199-19)
SENASHENKO, V. S., Resonance photoionization of helium and helium-like ions, 25:9239
SENFTLE, F. E., Construction materials for neutron capture-gamma-ray measurement assembly using ^{252}Cf, 25:8537
SENINA, A. V., Solution of the equation of radiation transfer, 25:9611
SENOO, Muneaki, Choice of activable tracer for spraying agricultural insecticides by helicopter, 25:8426 (NSJ-tr-155)
SEPTIER, A., Superconducting linear accelerator and problems associated with its construction, 25:9921
SERENKOV, I. T., Electron binding energy in negative ion He^-, 25:9169
SESSA, G., Enzyme activities in rabbits after pan-irradiation, 25:8779
SEVERA, F., Complementary to 14-MeV neutron generator, 25:8579
SEXTON, M. C., Afterglow studies in helium, 25:9417
SEYFFERTH, Ludwig, AEG superheated steam reactor, 25:10172

SHADOWITZ, A., Model for the current on a superconducting transmission line, 25:9377
SHAFFER, James H., Preparation and handling of salt mixtures for the Molten Salt Reactor Experiment, 25:10211 (ORNL-4616)
SHAFRANOV, M. D., Degradation of the luminescence of plastic polystrene scintillators, 25:8582
SHAFRANOV, V. D., Equilibrium and stability of plasma in closed magnetic traps without rotational transformation, 25:9491
SHAIKH, F., Energy dependence of proportional counter pulse-height resolution, 25:8505
SHAIKH, Mohammad U., Description of hot facilities at Pakistan Inst. of Nuclear Science and Tech., Pakistan, 25:8449 (CONF-691008-18)
SHALEK, Robert J., Prog. rpt. on radiation and biophysical studies on viruses and cells, 10/16/69--10/15/70, 25:8605 (ORO-2832-85)
SHANSHIASHVILI, M. I., Products of anthracene transformation under (n,γ) irradiation, 25:8289
SHAPIRO, I. S., Many-baryon resonances, 25:9803 (ITEF-759)
SHAPIRO, N. I., Genetic mutations in cell cultures of mammals, 25:8638
SHAPTALA, V. G., Nonlinear interaction of waves in a bounded magnetoactive plasma, 25:9514
SHARADZE, Z. S., Traveling disturbances in F region and sporadic-E region, 25:9295
SHARILOV, F. Kh., Dosimetric evaluation of radiation effects in rats by air containing thoron, 25:8763
SHARP, R. D., Efficiency measurements for channel electron multipliers, 25:8490
SHAW, David Tai-ko, Effect of excitation relaxation on electron energy distributions, 25:9267
SHAWHAN, S. D., Conjugate photoelectron impact ionization, 25:9127
SHCHETKOVSKII, A. I., Wire spark chamber system with magnetostrictive information retrieval, 25:8552
SHEARER, J. W., Absorption of laser light by plasma, 25:9476
SHEFFER, E. K., Measurement of the dispersed L/sub α/ radiation in the Earth's atmosphere at altitudes of 1000 to 3500 km, 25:9344
SHEINDLIN, A. E., Emissivity of carbides of Ta and Hf over range 1300 to 3000° K, 25:8930
SHELEST, V. P., Dual resonances models. I, 25:9887 (ITF-70-43)
Generalized Veneziano model, 25:9888 (ITF-70-78)
SHELLEY, E. G., Efficiency measurements for channel electron multipliers, 25:8490
SHEN, C. S., Pulsars and very high-energy cosmic-ray electrons, 25:9256
SHEN, S. W., Flux-flow noise spectrum in Type II superconductors, 25:9366
SHEN, Y. R., Nonlinear optical effects, 25:10406 (UCRL-20358)
SHEPHARD, W. D., Reactions π⁻p → pπ⁻MM⁰ and π⁻p → pπ⁺π⁻π⁻MM⁰ at 8 GeV/c, 25:9676
SHER, Lawrence D., Microwaves in the kitchen, 25:8790
SHER, Michael S., Characteristics of proton--proton interaction from data below 30 MeV, 25:9814
SHERER, A., Boron carbide agglomerate, 25:8919
SHERWOOD, A. E., Transient flow in a gas reservoir stimulated by a nuclear explosion: Project Gasbuggy, 25:8387 (UCRL-71868)
SHEVCHENKO, V. A., Fast current preamplifier for operation in an electronic neutron collimation system, 25:8519
SHEVELEV, V. P., Structure of ionized gas flow in electromagnetic shock tubes, 25:9445
SHIBANOV, Yu. A., Neutron polarization at the scattering on thick layers of matter, 25:9949
SHIBATA, Hiroyuki, Narrow muon bundles below ground, 25:9632
SHIGA, Kunio, Local duality in invariant amplitudes for πN scattering, 25:9796
SHIMIZU, Masao, Self-consistent band calculations for vanadium and chromium, 25:9597
SHIMIZU, Sadaaki, Loss-of-coolant accident in water-cooled nuclear power reactors. III, 25:10246
SHIMOZATO, Atou, Design and project of radioactive treatment and disposal system in large capacity BWR nuclear power station, 25:8340
SHIN, H. K., Dependence of vibrational transition probabilities on the orientation angle in the three-dimensional BC + A collision, 25:9226
SHIRAFUJI, Takeshi, Off-shell functions of the dual resonance, 25:9695
SHISHIN, B. P., Determination of the reserve reactivity by the double over-compensation method, 25:10321
SHISHOV, N. N., Direct production of electron--positron pairs by 2.94-GeV/c negative pions, 25:9661
SHLEIEN, B., Calibration and initial field testing of ^{85}Kr detectors for environmental monitoring, 25:8467 (BRH/NERHL-70-4)
SHLYAPNIKOV, P. V., Distribution of random displacement of track points due to Coulomb multiple scattering, 25:8559
Maximum-probability method to determine the kinematic parameters of tracks, 25:8558
SHMID, O. I., Specific volume resistance of steatite ceramics in high-intensity γ fields, 25:9551
SHODA, Katsufusa, Study of isobaric analogue state by (γ,p) reaction, 25:10053
SHONK, C. R., Formation and structure of electrostatic collisionless shocks, 25:9437
SHOTTER, A. C., Average cross-sections, 25:9923
SHOUCRI, M. M., Ion acoustic waves in finite-geometry plasmas, 25:9525
SHPENIK, O. B., Transfer of excitation energy in ion--atom interaction, 25:9238
SHPIGEL, I. S., Possibility of measuring directed fluxes in a plasma contained in a toroidal magnetic trap, 25:9410 (CTO-736)
SHPIRKAUSKAITE, N. K., Altitude distribution of ^{238}U, ^{232}Th, and ^{239}Pu in atmospheric fallout, 25:8372
SHTUKKENBERG, Yu. M., Recommendations concerning the maximum permissible tritium oxide concentrations in the atmosphere of industrial premises, 25:8678 (ORNL-tr-2403)
SHUBIN, V. N., Confirmation of the presence of mono-molecular reactions during the radiolysis of aqueous oxygen solutions, 25:8295
SHULTS, W. D., Prog. rpt. on tobacco smoke analysis program, 1/70--9/70, 25:10355 (ORNL-4642)
SHULYACHENKO, V. N., Interaction π⁻π⁻ in the reaction π⁻p → N*⁺⁺(1236)π⁻π⁻ with impulse 4.47 GeV/c, 25:9655 (ITEF-767)
Reaction π⁻p → rho⁰π⁻p with impulse 4.45 GeV/c, 25:9656 (ITEF-775)
SHUMATE, Donald J., Closed system generation and containerization of radioisotopes, 25:8433
SHUMYATSKII, B. Ya., High-temperature combustion products for thermoelectric plants with MHD generator, 25:9261
SHUSHKOVA, V. B., Meteor ionization in E layer, 25:9307
SICK, I., Electromagnetic structure of ^{3}He nucleus, 25:9965 (AD-710384)
SIDOROV, V. P., Spectrum of scattered laser radiation and the measurement of electron density in a pulsed plasma 25:9409 (CTO-733)
SIEBMANNS, W., Preparation of uranium mononitride pellets of differing densities by cold pressing and sintering, 25:8913 (ORNL-tr-2365)
SIEMANN, H., Investigation of the auroral electrojet, 25:9334
SIEWERT, C. E., Linear integral equations for a certain class of H-functions applicable to the theory of neutron transport and radiative transfer, 25:9953
SIGNELL, Peter, Characteristics of proton--proton interaction from data below 30 MeV, 25:9814
SIKORA, B., Reaction ^{7}Li(d,n)^{8}Be, 25:9975 (JINR-P15-5143)
SIKULOVA, J., Body temperature as an indicator of the radioprotective effect of sodium fluoroacetate in mice, 25:8700
SILAKOV, R. S., Resonant Bragg scattering of gamma rays by nuclei, 25:9596
SILANT'EV, N. A., Neutron polarization at the scattering on thick layers of matter, 25:9949
SILLS, H. E., FORGAD: one dimensional few group finite difference reactor code, 25:10300 (AECL-3671(Add.1))
SILVA, A. Jr., Study of determination of fluorine in uranium concentrates: outline of the volumetric method, 25:8201 (LFEN-NI.-36-a)
SILVER, D. M., Basis sets of gaussian and Slater-type atomic orbitals, 25:9243
SILVER, G. L., Disproportionation of tetravalent and pentavalent plutonium ions in the presence of hexavalent plutonium, 25:8239 (MLM-1744)
SILVESTRE, G., Formation and nature of twin crystals in U_3Si, 25:8946
SIMMONS, J. A., Calibration of clear Perspex for radiation dosimetry, 25:8568
SIMMONS, W. A., Test of double-Regge behavior of generalized Veneziano model, 25:9797
SIMONOV, Yu. A., Decomposition of resonance states and determination of their quantum numbers, 25:9774
SIMONOVA, N. V., Spectrum of scattered laser radiation and the measurement of electron density in a pulsed plasma, 25:9409 (CTO-733)
SIMONSON III, S. Christian, Problems in galactic spiral structure, 25:9142
SIMPSON, H. James, Tritium in Crater Lake, Oregon, 25:8347 (CU-2493-11, App.1)
SIMPSON, Harry James Jr., Closed basin lakes as a tool in geochemistry. II, 25:8348 (CU-2493-11, App.2)
Closed basin lakes as a tool in geochemistry. III, 25:8349 (CU-2493-11, App.3)
SIMPSON, J. A., Galactic ^{3}He above 10 MeV per nucleon and the solar contributions of hydrogen and helium, 25:9257
Relative abundances and energy spectra of ^{3}He and ^{4}He from solar flares, 25:9103
SIMPSON, R. E., Determination of venadium by neutron activation analysis at nanogram levels to formulate a low-vanadium diet, 25:8228
Neutron activation analysis program of the food and drug administration, 25:8227
SINAY, Ya. G., Investigation of the spectra of stochastic operators arising in lattice models of a gas, 25:10379 (SC-T-71-3000)
SINGER, Ralph M., Experimental demonstration of inert gas effects upon the incipient pool boiling of sodium, 25:8415
SINGH, J., Excitation functions for ^{3}He induced reactions with ^{12}C, 25:9989

XUM

Resonances in tHe interaction of ^{3}He particles with ^{12}C and ^{10}B, 25:9990

SINHA, Ashok K., Radial distribution function of an amorphous Mn--P--C alloy, 25:10348 (CALT-822-21)

SINIFF, Donald B., Effects of ionizing radiation on populations of Manitoba toads, Bufo hemiophrys, 25:8628

SINISTRERO, G., Computer dosimetry of the radioiridium castings, 25:8684

SINZ, Kurt H., Formulation of self-consistent 2- and 2 $^{1}/_{2}$-dimensional electromagnetic and relativistic simulations, 25:9458 (UCRL-72613)

SIONNET, Jean, Spacing grid for a nuclear reactor fuel element, 25:10332

SISCOE, G. L., Simultaneous sudden magnetospheric compressions and geomagnetic bay onsets, 25:9332

SISSON, Warden B., Liquid scintillation counting of /sup 113m/In conversion electrons in the presence of ^{3}H and ^{14}C, 25:8213

SISTEMICH, K., Position-sensitive counters, 25:8470 (JUL-CONF-4, pp 1-10)

SITEK, Jozef, Preparation of Moessbauer source, 25:9595

SITENKO, A. G., Echo theory in plasma, 25:9519

SIT'KO, S. P., Fast current preamplifier for operation in an electronic neutron collimation system, 25:8519

SIVKOV, Yu. P., Sextupole lenses with direct nonlinearity in slow ejection system, 25:9913 (NP-18594)

SKACHKOV, N. B., Representation for relativistic scattering amplitude at high energies, 25:9749 (JINR-E2-5341)

SKRIPKA, Yu. G., Mechanism of ion scattering by crystals, 25:9556

SLAGGIE, E. L., Prog. rpt. on integral neutron thermalization, 4--6/70, 25:9943 (GA-10223)

SLATER, C. E., Comparison of predictions from the reactor primary system decompression code (RELAP3) with decompression data from the semiscale blowdown and emergency core cooling (ECC) project, 25:10242 (IN-1444)

SLATEVA, M., Some changes in the gingival connective tissue in acute radiation sickness, 25:8786

SLATTERY, P., Some remarks concerning the precision of 1 to 2 meter bubble chambers, 25:8549 (UR-875-324)

SLINEY, David H., Evaluating health hazards from military lasers, 25:8694

SLONINA, J.-P., Boron carbide agglomerate, 25:8919

SMAARDYK, A., Instrumented subassembly system in EBR-II, 25:10171

SMALLEY, L. L., Determination of $\pi\Lambda\Sigma$ and $\pi\Sigma\Sigma$ coupling constants utilizing Adler's consistency condition, 25:9812

SMALLEY, W. R., Prog. rpt. on Saxton Plutonium Project, 9/70, 25:10213 (WCAP-3385-25)

SMIRENKIN, G. N., Angular anisotropy of photofission of ^{239}Pu, 25:10024 (FEI-190)

SMIRNOV, V. N., Use of the /sup 125m/Te isotope as a source of x-ray radiation, 25:8434

SMITH, C. H. Llewellyn, Theories of highly inelastic electron scattering, 25:9706 (SLAC-PUB-843)

SMITH, C. W., Use of high activity ^{60}Co sources for intracavitary and surface mould therapy, 25:8738

SMITH, D. G., Calibration and initial field testing of ^{85}Kr detectors for environmental monitoring, 25:8467 (BRH/NERHL-70-4)

SMITH, D. J., Photoelectron spectra of ground-state atomic H, N, and O, 25:9200

SMITH, D. R., Ion heating in the dense plasma focus, 25:9401

SMITH, E. E., Projection of nuclear fuel cost trends, 25:10100

SMITH, F. A., Guidelines for sodium fire prevention, detection, and control: report of the Ad Hoc Committee on sodium fires, 25:8827 (ANL-7691)

SMITH, H. H., Relative biological effectiveness of heavy ions in producing mutations, tumors, and growth inhibition in the crucifer plant, arabidopsis, 25:8800

SMITH, J. R., Observation of the decay eta' $\rightarrow \gamma\gamma$, 25:9651 (COO-1764-111)

SMITH, Jessie Gregory, Exchange equilibria between methylacetylene-d and water by mass spectrometry, 25:8241 (CU-755-7, Sect.3)

Separation of isotopic isomers of NO by low-temperature gas chromatography, 25:8319 (CU-755-7, Sect.4)

SMITH, L. F., Efficiency measurements for channel electron multipliers, 25:8490

SMITH, L. H., Recovery from radiation injury with and without bone marrow transplantation: effects of splenectomy, 25:8706

SMITH, Richard J., Engineering materials list, 25:8396 (TID-4100(Suppl.61))

SMITH, S. B., Quasi-developed turbulent pipe flow with heat transfer, 25:8420

SMITH, T. F., Pressure-enhanced superconductivity in V_3X compounds, 25:9372

SMITH II, Granville J., Symmetries imposed on two-particle systems. III, 25:9818

SNEBERGER, J., Pretightening of large pressure vessel flange joints, 25:10096 (ZJE-65)

SNIPES, M. B., Determination of contained-milk volume of the mammary gland of the goat by ^{141}Ce and ^{14}C-PEG-4000, 25:8587

SNODGRASS, Herschel, Methods for the Bethe--Salpeter equation. I, 25:9855

SNOPKO, V. N., Ionization nonequilibrium state of cold pulse-discharge plasma, 25:9462

SNYCKERS, F., Stereochemistry of sigma-complex intermediate in sterically hindered electrophilic aromatic substitutions, 25:8242

SNYDER, R. P., U20e post shot fractures, Jorum event, 25:8356 (USGS-474-92)

SOBENIN, N. P., High-frequency separator of particles, 25:9939

SODERGARD, Bengt Martin, Improvements in nuclear reactors, 25:10218

SOKOLOV, I. B., Influence of radiation dose and method of specimen preparation on the kinetics of radical accumulation in aniline, 25:8296

SOKOLOWSKI, E. K., Spectral parameters in water-moderated lattices, 25:10320 (AE-405)

SOKOL'SKII, A. G., High-temperature combustion products for thermoelectric plants with MHD generator, 25:9261

SOLDATOV, A. S., Angular anisotropy of photofission of ^{239}Pu, 25:10024 (FEI-190)

SOLE, J., Coils and energy storage, 25:9395

SOLOV'EV, E. S., Electron binding energy in negative ion He^{-}, 25:9169

SOLOV'EV, I. S., Spectra of photoconductivity of green leaves and chloroplasts at a frequency of 10^{10} cycles per second, 25:10412 (UCRL-Trans-1427)

SOLOV'EV, V. G., Non-rotational state of deformed nuclei with an odd number of neutrons in range 165 less than or equal to A less than or equal to 175, 25:10028 (JINR-P4-5228)

SOLYAKIN, G. E., Composition and excitation energy of fissioning nuclei in irradiation of ^{209}Bi and ^{197}Au 1 GeV photons, 25:10037

SONETT, C. P., Moon: global electromagnetic sounding using the solar wind, 25:9159

SOOTHA, G. D., Optical absorption and electrical conduction in KBr crystals containing diffused Mg, 25:9570

SOSHNIKOV, V. N., Simplest model of vibrational excitation of diatomic molecules by slow electrons, 25:9240

SOTIROVSKI, Pascal, Identification of MgO lines in spectrum of large sunspot, 25:9100

SOURIAU, Jean-Marie, Motion of particles with spin in general relativity, 25:9874

SOUSTELLE, Michel, Elementary mechanisms of heterogeneous gas-solid kinetics, 25:10358 (ORNL-tr-2392)

SPALDING, I. J., Magnetic piston-shock wave in collisionless plasma, 25:9452

SPALEK, G., Neutron polarizations in the $^{6}Li(d,n)$ and $^{7}Li(d,n)$ reactions, 25:9984

SPARROW, A. H., Effects of simulated radioactive fallout buildup and decay on survival and yield of lettuce, maize, radish, squash, and tomato, 25:8796

SPARROW, E. M., Heat transfer in reactor components having temperature-dependent thermal conductivity, 25:10203

SPECHT, J. H., Applications of spark chambers and multiwire proportional counters in magnetic spectrographs, 25:8476 (JUL-CONF-4, pp 71-120)

SPEIDEL, V., Mutual neutron interchange through vacuum between boundary surfaces of reactor parts, 25:10290

SPENCE, D., Vibrational excitation by electron impact in O_2, 25:9210

SPENNER, K., Electric fields derived from plasma measurements in the polar electrojet, 25:9335

SPERLING, S. M., Secondary gamma-ray production and transport in liquid nitrogen, 25:9950

SPIEGEL, E. A., Instabilities of differential rotation, 25:8985

SPIEGEL, Edward A., Temperature variation and the solar oblateness, 25:9113

SPIEGLER, P., Unscheduled DNA synthesis at low x-ray doses, 25:8647

SPINDEL, W., Analysis of isotope-effect calculations illustrated with exchange equilibria among oxynitrogen compounds, 25:8245

Theoretical analysis of chemical isotope fractionation by orthogonal polynomial methods, 25:8335

SPINRAD, Hyron, Maffei 1: a new massive member of the Local Group, 25:9148

Scanner abundance studies. III, 25:9000

SPITSYN, Vikt. I., Formation and kinetics of accumulation of NO_2 radicals in γ-irradiated $BaSO_4$, 25:8286

SPITZNAGEL, John K., Prog. rpt. on mechanisms of innate immunity, IV, 12/69--11/70, 25:10364 (ORO-3628-11)

SPITZYN, V. I., Influence of ionizing radiation on the structure and properties of modified kapron fibers, 25:8270

SPLICHAL, W. F. Jr., Self-auditing multichannel neutron monitor, 25:8501

SPRINGFORD, M., Fermi surface in niobium, 25:9575

SPURNY, F., Radioluminescence of organic substances. VIII, 25:8274

SPURR, W. F., Solid cadmium embrittlement: titanium alloys, 25:8879

SREBRO, Z., Morpho-functional study of hypothalamic neurosecretion. VI, 25:8764

SREENIVASAN, A., Dehydro-irradiation process for tropical shrimps, 25:8820

Radiation preservation of Chapaties, 25:8819

SRINIVASAN, N., In-line analytical methods for fuel reprocessing streams. I, 25:8197 (BARC-510)

ST. ONGE, R., Bismuth-209 ground-state analog in ^{209}Po,

25:10045
STACHOWICZ, Waclaw, ESR study of bone tissue sterilized by gamma radiation, 25:8825
STADNICOV, T., Doppler effect of 6.24 eV resonance in ^{121}Sb, 25:10041
STAEHLE, R. W., Prog. rpt. on stress corrosion cracking in Fe--Ni--Cr alloys, 12/69--3/70, 25:8834 (COO-2069-6)
STAELIN, D. H., Observations of pulsar spectra, 25:9059
STAHLBERG, Rudi, Gas determination in metals. I, 25:8205
STAINOV, G., Analog device for computing the plasma dispersion function, 25:9517
STAKHANOV, I. P., Plasma thermionic energy conversion, 25:9268
STANBURY, John B., Use of radioisotopes in human experimentation, 25:8717
STARCHIK, L. P., Determination of Be by (γ,n) reaction in linac, 25:8225
STAUBER, E., Permissible activity rates in the exhaust air discharged by nuclear reactor plants, 25:10161
STECHEMESSER, H., Hydraulic rabbit facility, 25:10274
STEER, C., Homogenizing structures and mechanical properties of welding Zircaloy 2 tubes, 25:8844 (AERE-M-1561)
STEFANI, S., Radiosensitivity of mice exposed to various temperatures and low-dose rate radiation, 25:8768
STEFFY, R. C., Experiences with dynamic testing methods at Molten-Salt Reactor Experiment, 25:10182
Theoretical dynamics analysis of Molten-Salt Reactor Experiment, 25:10183
STEIN, Gabriel, Action of atomic hydrogen, hydrated electrons, and ionizing radiation on bacteriophage T_7 in aqueous solution, 25:8808
STEIN, H. J., Localized modes and divacancy absorption in oxygen-ion-implanted Si, 25:9550
STEIN, W. A., Infrared emission from Be stars, 25:9018
STEINBERG, J.-L., Space radioastronomy of solar bursts at all frequencies, 25:9124
STEINHAUER, Loren C., One-dimensional laser heating of a stationary plasma, 25:9405
STELTER, Lothar, Chemical consequences of Auger effect: iodine yield from iodoamino acids as function of x-ray dose and energy, 25:8304
STEMPLE, Ruth M., Technetium-99m in medicine: a supplementary bibliography, 25:8712 (ORNL-TM-2091(Suppl.1))
STENZEL, R. L., Longitudinal oscillations in bounded magnetoplasmas, 25:9532
STEPANOV, A. S., Plasma thermionic energy conversion, 25:9268
STEPHENS, R. I., Fatigue behavior of molybdenum, 25:8861 (AD-709580)
STERLIGOV, A. G., Shower spark chambers for detecting particles moving at small angles with respect to the beam being stopped, 25:8553
STERN, Marvin J., Analysis of isotope-effect calculations illustrated with exchange equilibria among oxynitrogen compounds, 25:8245
STEVENS, A. J., Measurement of the up-down asymmetries in the beta decay of polarized lambdas, 25:9626 (COO-1545-87)
STEVENS, G. F., Forced convection burnout in water, 25:8410
STEVENS, George Frederick William, Improvements in reactors, 25:10200
STEWART, H. B., Outlook for nuclear reactors and fuel, 25:10214
STEWART, P., Power spectrum of electromagnetic radiation scattered by a relativistic beam, 25:9085
STIEGLER, J. O., Effect of fast neutron irradiation on the creep-rupture properties of type 304 stainless steel at 600°C, 25:8897 (ORNL-TM-3169)
STIRAND, D., Microwave diagnostics of instabilities in column plasmas, 25:9425
STOCKEM, W., Pinocytosis and locomotion of amoebas. III, 25:10338 (ANL-Trans-866)
STOLETOVA, I. M., Degradation of the luminescence of plastic polystrene scintillators, 25:8582
STOLTERFOHT, N., Contamination of the river water by the fallout after extreme reactor accidents, 25:8660 (HMI-B-87)
Estimation of the surface water's contamination by the near fallout by nuclear explosions, 25:8354 (HMI-B-86)
STONE, Harold, Scheduling of N tasks with M operations on two processors, 25:10383 (STAN-CS-70-165(App.2))
STONE, Harold S., Parallel processing with the perfect shuffle, 25:10382 (STAN-CS-70-158(App.5))
STORB, R., Bone marrow chimeras in man and animals, 25:8617
STOTT, A. N. B., Radiation-protective clothing, 25:8691
STOWE, R. L., Grouting and materials control, Operation Flint Lock, 25:8962 (POR-4013)
STOYE, Hilde, Influence of host-cell reactivation and uv dose on formation of pure and mixed clones of c mutants in phage kappa, 25:8653
STRATHDEE, J., Equivalent formulations of massive vector field theories, 25:9858
STRATTON, K., Studies of the cellular radiosensitivity of transplants of murine ependymomas irradiated in vivo, 25:8759
STREATER, R. F., Fermion states of a boson field, 25:9850
STREL'TSOV, V. N., Nonrelativistic transformations applied to Dirac equation, 25:9599 (JINR-P2-5314)
STRENGE, D. L., Reasons for differences in calculated estimates of the cloud dose, 25:8668 (BNWL-SA-3424)
STRICKLAND, E. Hardin, Effect of temperature upon conformations of carboxypeptidase A, A/sub γ//sup Leu/, A/sub γ//sup Val/, and A/sub $\alpha+\beta$/, 25:10402 (UCLA-12-802)
Use of circular dichroism to study interactions of carbosypeptidase A (Anson) and A/sub $\alpha+\beta$/ with substrates and inhibitors, 25:10401 (UCLA-12-801)
STRITTMATTER, P. A., Infrared emission from Be stars, 25:9018
STRNAD, J., Lever problem in special relativity, 25:9866
STROCK, W. G. Jr., Forest management plan, AEC Oak Ridge reservation: 1970--1975, 25:10356 (ORNL-TM-3175)
STROGONOV, A. A., Radioecological studies of the Mediterranean Sea, 25:8630
STROM, K. M., On the evolutionary status of stars above the horizontal branch in globular clusters, 25:8992
STROM, S. E., On the evolutionary status of stars above the horizontal branch in globular clusters, 25:8992
STUART, Bruce O., Studies of inhaled radon daughters, uranium ore dust, diesel exhaust, and cigarette smoke in dogs and hamsters, 25:8623 (BNWL-SA-3419)
STUBBE, P., Effect of electric fields on F-region behavior, 25:9315
STUHL, F., Kinetic isotope effects in the quenching of $O_2(b^1\Sigma/sub\ g/^+)$ by some deuterated compounds, 25:8249
STUMBUR, E. A., Reactivity measurements by pulse methods, 25:10309
STYRO, B. I., Altitude distribution of ^{238}U, ^{232}Th, and ^{239}Pu in atmospheric fallout, 25:8372
SUCKEWER, Szymon, Spectral measurements of plasma temperature in rod plasma injector, 25:9426
SUEOKA, Yoshitaka, Approach to the stability criterion for a nuclear reactor, 25:10316
SUESS, W., Microwave diagnostics of strong-current discharges with skin effect. II, 25:9424
SUGAHARA, Tsutomu, Radiation and carcinogenesis, 25:8611
SUGAR, R. L., Relativistic eikonal expansion, 25:9897
SUGAWARA, Masumi, Study of isobaric analogue state by (γ,p) reaction, 25:10053
SUGIMOTO, Daiichiro, Mixing between stellar envelope and core in advanced phases of evolution. II, 25:8972
SUH, Kiu S., Partially latent interaction in elementary particle formation, 25:9752
SUIT, Herman D., Afterloading vaginal irradiators, 25:8736
SUK, V., Bromopyrogallol red as colorimetric reagent. IV, 25:8212
SULLIVAN, A. H., Approach to a rem dosimeter using ionization chambers, 25:8562 (CERN/DI/HP-25)
SULLIVAN, J. J., Dosimetry of proton radiation fields in space with nuclear emulsions, 25:8682
SUMI, Naobumi, Approximate solution and measurement of the steady temperature distribution in a finite region with many circular holes, 25:8413
SUMNER, R. L., Measurement of the up-down asymmetries in the beta decay of polarized lambdas, 25:9626 (COO-1545-87)
SUNDERMEYER, Kurt, New vacuum trajectory for pion--nucleon scattering, 25:9785 (DESY-70/55)
SUNTA, C. M., Thermoluminescence spectrum of γ-irradiated natural CaF_2, 25:9548
SUPERATA, Michael A., Production of thin metallic single crystals, 25:8858
SURAMLISHVILI, G. I., Wave oscillations in weakly turbulent plasma, 25:9515
SUROV, N. S., Distribution of parameters in one- and two-phase subsonic plasma jets, 25:9434
SUSINI, A., Instrument for measuring rate of change of RF frequency in particle accelerators, 25:9905 (CERN-70-28)
SUSSKIND, Herbert, Combined hydroelectric pumped storage and nuclear power generation, 25:10109 (BNL-50238)
SUTTON, J., Radiolysis of 1 M aqueous ethanol solutions of potassium nitrate, 25:8301
SUZUKI, Fumio, Radiation and carcinogenesis, 25:8611
SUZUKI, Mahiko, Spectral-function sum rules for rho--w and rho--phi transitions, 25:9718
SVECHNIKOV, V. N., Phase diagram of the chromium--terbium system, 25:8889
SVRAKOFF, D., Some changes in the gingival connective tissue in acute radiation sickness, 25:8786
SWALLOW, E. C., Measurement of the up-down asymmetries in the beta decay of polarized lambdas, 25:9626 (COO-1545-87)
SWANSON, L. R., Model potential calculation of Raman tensor for Be, Mg, and Zn, 25:9598
SWANSON, William P., THEMI: Monte Carlo generation of electromagnetic events, 25:9705 (SLAC-123)
SWARTZ, H. M., Conformation of radioprotectant compounds. The crystal structures of 2-mercaptoethylamine hydrochloride and 3-mercaptopropylamine hydrochloride, 25:8268
SWIECA, Jorge Andre, Indefinite metric and stationary external interactions of quantized fields, 25:9864
Problems of stability for quantum fields in external time-dependent potentials, 25:9863
SWINTH, K. L., Solid state x-ray-alpha coincidence counter, 25:8465 (BNWL-SA-1514)
SYMONS, G. D., Angular correlation studies of the $^{42}Ca(\alpha,p\gamma)^{45}Sc$ reaction, 25:9996 (ANU-P-466)

XUM

SYNDER, Lewis E., Molecules in the interstellar medium. II, 25:9071
SYUZEV, V. N., Mechanism of gas release from ceramic nuclear fuels, 25:8958 (SRARI-P-73)
SZENDE, Gabriella, Calibration of gamma spectrometer, 25:8535

T

TABOR, W. H., Prog. rpt. on Oak Ridge Research Reactor, 7--9/70, 25:10270 (ORNL-TM-3256)
TACCONI, F. A., Dynamic behaviour of two-phase flow rods for nuclear reactor control, 25:10187
TADZHIKOV, M. M., Dosimetric evaluation of radiation effects in rats by air containing thoron, 25:8763
TAGAWA, Hiroaki, Thermodynamic properties of the actinide nitrides, 25:8941
TAKACS, J., Average cross-sections, 25:9923
TAKACS, S., Pinning of flux lines in superconducting niobium due to point defects, 25:9379
TAKADA, Akikazu, Strain and substrain differences in the recovery of thymus function after whole-body x-irradiation of mice, 25:8776
TAKADA, T., Electrical properties of V_8O_{15} single crystal, 25:9580
TAKADA, Yoshio, Breakdown of Pomeranchuk's conjecture and composite structure of hadrons, 25:9806
TAKADA, Yumiko, Strain and substrain differences in the recovery of thymus function after whole-body x-irradiation of mice, 25:8776
TAKAHASHI, S., Gas analysis of nuclear fuel elements, 25:10227
TAKAHASHI, Yasushi, Interaction of a gauge-independent spin-one field, 25:9854
TAKANO, Hideki, Accuracy of analytical treatments for resonance absorption in Doppler resonance regions, 25:10038
TAKASAKI, Minoru, Multiple scattering of protons and nitrogen ions on copper, 25:9163
TAKASHIMA, M., Effect of a magnetic field on thermal instability in a layer of Maxwell fluid, 25:9274
TAKESHIMA, Masaki, Design and project of radioactive treatment and disposal system in large capacity BWR nuclear power station, 25:8340
TAKEUTI, Yoitiro, Approximate solution and measurement of the steady temperature distribution in a finite region with many circular holes, 25:8413
TALBOT, Raymond J. Jr., Nonlinear pulsations of unstable massive main-sequence stars. I, 25:9039
TALLAN, N. M., Electrical properties and defect structure of ThO_2, 25:9577
TALMONT, Xavier L. R., Processes for simultaneously purifying and concentrating plutonium solutions, 25:8338
TAMURA, Kazushi, Propagation of Pc1 pulsations in F region, 25:9338
TANG, Yi-Noo, Prog. rpt. on high energy radioactive atoms resulting from nuclear transformations in systems of silicon-containing compounds, 2/70--1/71, 25:8310 (CRO-3898-2)
TANNER, James T., Neutron activation analysis program of the food and drug administration, 25:8227
TANNER, N. W., Proton capture gamma decay to excited states of ^{16}O, 25:9979
TANNOCK, Ian F., Age sensitivity of epithelial cells of mouse small intestine, 25:8785
TARABANOV, A. S., An experimental study of the thermal conductivity of high-porosity graphitic carbon, 25:8942
TARASOV, A. F., Variations in mean level of radio emission at 1.1 and 2.3 MHz, 25:9352
TARASOV, A. V., Cross section of anti Kd → KY_1Y_2, 25:9804 (JINR-P2-5231)
Processes of the type of double charge exchange at light nuclei, 25:9974 (JINR-P2-5286)
TARASOV, E. K., Momentum vector in a magnetic track spectrometer, 25:8561
TARKO, H., Impurity effects on annealing of radiation defects in p-type silicon, 25:9549
TARTAKOVSKII, V. K., Quasi-elastic knockout of nucleons from light nuclei by high energy electrons, 25:10058 (ITF-70-38)
TASSINARI, S. J., Determination of Ag, Cd, In, Sn, and Sb in Na solubility studies, 25:8198 (BNL-50271)
TAUSON, Peter O., Implantable circulatory support system, 25:8436
TAUTH, T., Method of calculation of trajectories of ions before injection into the proposed heavy-ion linear accelerator, 25:9911 (LYCEN-6949)
Parameters of ''Reflex''-type ion sources, 25:9912 (LYCEN-6953)
TAVENDALE, A. J., High-resolution nuclear radiation detectors from epitaxial n-GaAs, 25:8491
TAYLOR, A., Metallographic examination of sodium, 25:8845 (AERE-R-5483)
TAYLOR, Benjamin J., Scanner abundance studies. II, 25:8969
Scanner abundance studies. III, 25:9000
TAYLOR, G. N., Comparisons of simultaneous satellite and ground-based measurements of ionospheric parameters, 25:9308
Ionospheric electron concentration enhancement during a solar flare, 25:9333
TAYLOR, I. J., High speed pulse shape discriminator, 25:8507
Isobaric analog states in ^{24}Mg, ^{27}Al, and ^{28}Si, 25:10007
Pulse shape discrimination, 25:8506
TAYLOR, T. I., Preparation of ^{13}C by chemical exchange between amine carbamates and carbon dioxide, 25:8318 (CU-755-7, Sect.2)
Preparation of 99.5 percent ^{15}N by chemical exchange between oxides of nitrogen in a solvent carrier system, 25:8334
TAYLOR, W. H., Measurement of relative conversion ratio in particulate fuel, 25:10217
TAZZIOLI, F., Study of some problems of cavity resonators by means of finite differences, 25:9909 (LNF-70/17)
TELEGADAS, Kosta, Radioiodine levels in US public health service pasteurized milk network from 1963--1968 and their relationship to possible sources, 25:8629
TELL, B., Ion implantation of sodium, lithium, and neon in cadmium sulfide, 25:9561
TELLIER, Henry, Measurement and analysis of holmium total cross section for neutrons at energies between 0.005 and 1.7 keV, 25:10022 (CEA-N-1338)
TEMPER, E. M., Radiation induced defects in dielectric--semiconductor structures, 25:9566
TEPLIAKOV, V. A., Beam regulation in a 100-MeV linear accelerator, 25:9914 (NP-tr-1926)
TERENT'EV, V. P., Optimum neutron irradiation conditions for radioisotope production, 25:8308
TERNOVSKAYA, M. V., Measurements of fast-charged particles on Cosmos-137, 25:9354
TERZIAN, Yervant, Radio emission from small galactic nebulae, 25:9068
TESTER, John R., Effects of ionizing radiation on populations of Manitoba toads, Bufo hemiophrys, 25:8628
TESTUD, J., Gravity waves generated during magnetic substorms, 25:9293
TETEL'BAUM, S. D., Use of uranium hexafluoride in nuclear power installations, 25:10221
TEVEBAUGH, A. D., Guidelines for sodium fire prevention, detection, and control: report of the Ad Hoc Committee on sodium fires, 25:8827 (ANL-7691)
THENARD, Claude, Development of a clean shock tube for making spectroscopic measurements on a plasma, 25:9510
Intensities of spectral lines and background continuum of Ar plasma produced in a shock tube, 25:9423
THIEBERGER, P., Analog of variable moment for rotational states in even--even nuclei, 25:10084
THIELHEIM, K. O., Explicit solutions of half space problems in the two-group transport theory, 25:9619
THIRION, J. M., Excited states of ^{22}Ne, 25:10002
THOBE, Josef, Electrophoresis in a carrier-free buffer stream. I, 25:10414 (UCRL-Trans-1429)
THOMAS, C. C. Jr., Neutron activation analysis of inorganic constituents of airborne particulates, 25:8231
THOMAS, E. D., Bone marrow chimeras in man and animals, 25:8617
THOMAS, E. W., Formation of metastable hydrogen atoms by charge transfer, 25:9193 (ORO-2591-52)
Prog. rpt. on formation of excited hydrogen atoms by charge transfer and dissociation, 12/69--11/70, 25:9192 (ORO-2591-51)
THOMAS, G. R., Transient overpower irradiation of axially-restrained, zero-burnup, fast reactor fuel specimens, 25:10208 (GEAP-13562)
THOMAS, L. K., Thermal radiation and electronic density of states of W--Ta alloys, 25:9584
THOMASON, R. S., Neutron polarizations in the $^6Li(d,n)$ and $^7Li(d,n)$ reactions, 25:9984
THOME, P., Heat exchange unit for a nuclear reactor, 25:10204
THOMPSON, Barbara A., Determination of trace elements in glass by activation analysis using hydrated antimony pentoxide for sodium removal, 25:8223
THOMPSON, C. L., Neutron flux distribution resulting from fission source located at center of sphere of sodium, 25:9944 (ORNL-TM-3156)
THOMPSON, K. H., Relative biological effectiveness of heavy ions in producing mutations, tumors, and growth inhibition in the crucifer plant, arabidopsis, 25:8800
THOMPSON, Laird A., Rotational velocities in the Orion Nebula cluster, 25:8981
THOMPSON, M. A., Bubble chamber measurement of eta'(960) → $\gamma\gamma$ and eta'(960) → $\pi^0\pi^0$eta (eta → $3\pi^0$) decay rates, 25:9666
THOMPSON, R., Sodium purification and general handling facility, 25:8390 (AERE-R-5502)
THOMPSON, William F., Macromolecule synthesis and wall extensibility in relation to the mechanism of auxin-induced cell elongation, 25:10366 (RLO-2225-T-19-9)
THOMS, E., Radiation chemistry of alcohols. XV, 25:8300
THORNE, Kip S., Nonspherical gravitational collapse, 25:9155
THORNE, W. L., Development and results of an electrically heated seven-pin bundle assembly for thermal hydraulic testing in liquid metals, 25:10207 (BNWL-SA-3286)
THRANE, E. V., Ionospheric observations during annular solar eclipse of May 20, 1966. IV, 25:9312
Ionospheric observations during annular solar eclipse of

May 20, 1966. V, 25:9313
THUEMMLER, F., Dispersion fuel for high-flux reactors (UAl_3--Al), 25:8846 (KFK-1252)
Fabrication of ceramic materials by melting in an overpressure electric arc furnace, 25:8914
Relations between stereometric microstructure and properties of cermets and porous materials, 25:8944 (KFK-1236)
THURBER, David L., Prog. rpt. on geochemical studies on continental waters, annual, 10/70, 25:8346 (CU-2493-11)
TICHIN, V. G., Beam regulation in a 100-MeV linear accelerator, 25:9914 (NP-tr-1926)
TIETGE, J., Multipole analysis for the reactions $\gamma p \rightarrow K^+\Lambda$ and $\gamma p \rightarrow K^+\Sigma^0$, 25:9728
TIGHE, L. E., On-line computer system for a mass spectrometer, 25:8571 (AAEC/TM-568)
TIKHONIN, F. F., Experimental possibility of revealing the reaction $1^+ + 1^- \rightarrow \nu + \text{anti } \nu + \gamma$, 25:9627 (NP-18558)
TILBURY, Roy Sidney, Saline solution containing radioactive gas, 25:8309
TILLEY, D. R., Expanded vortex' states in superconducting films and surface sheath in inclined fields, 25:9375
Reactions $^{14}C + \alpha$, 25:9980
TIMOFEEV, A. V., Cyclotron heating of a plasma in a nonuniform magnetic field, 25:9404
TIMOSHCHUK, V. I., Radioecological studies of the Mediterranean Sea, 25:8630
TING, Chin-sen, Interaction of a magnetic impurity with electrons in metals and in superconductors, 25:9391
TING, Peter D., Studies of multiperipheral integral equations, 25:9758
TING, Robert Y., Predicting distribution of radionuclides in marine organisms, 25:8627
TINKHAM, M., Apparent universal behavior of fluctuation-induced diamagnetism in superconductors, 25:9369
TJIN A DJIE, H. R. E., Austern--Blair method for scattering of deuterons and alpha particles, 25:9991
TKACHEV, G. N., Measurements of the parameters of ionosphere by incoherent radiowave scattering, 25:9343
TOBIAS, C. W., Periodic phenomena in copper dissolution at constant current, 25:10404 (UCRL-19618)
Transfer processes in ECM, 25:10403 (UCRL-19615)
TOBUREN, L. H., Absolute cross sections, differential in energy and angle, for ejection of electrons from xenon by fast protons, 25:9191 (BNWL-SA-3631)
Anuglar and energy distributions of electrons from hydrogen ion breakup, 25:9190 (BNWL-SA-3498)
Conversion electron spectrum in decay of ^{195}Au, 25:10048
Electron distributions from hydrogen for 0.6, 1.0 and 1.5 MeV hydrogen ions, 25:9189 (BNWL-SA-3482)
TODA, I., Fast neutron study, 25:9995
TOEPFER, A. J., Ion heating in the dense plasma focus, 25:9401
TOET, D. Z., Cross sections and spin-density matrix elements in 5 GeV/c π^+ p four-pronged interactions, 25:9682
TOFE, Andrew John, Low energy fission of ^{232}Th, 25:10054
TOJYO, Isao, Influence of gamma-irradiation on the pollen formation of the moraceae, 25:8794 (NSJ-tr-158)
TOKUHARU, Yukuya, Effect of γ irradiation on dielectric constants of KH_2PO_4, 25:8275
TOLK, A., Accurate and precise titrimetric analysis of uranium in nuclear fuels, 25:8202 (RCN-126)
Determination of oxygen-to-uranium ratio in hyperstoichiometric uranium dioxide, 25:8203 (RCN-127)
Determination of oxygen-to-uranium ratio in hypostoichiometric uranium dioxide, 25:8204 (RCN-128)
TOLKACHEV, V. A., Influence of radiation dose and method of specimen preparation on the kinetics of radical accumulation in aniline, 25:8296
TOLSMA, L. D., Austern--Blair method for scattering of deuterons and alpha particles, 25:9991
TOMAS, E., Effect of K_3-vitamin and monoiodoacetic acid on serum coeruloplasmin activity, 25:8612
TOMEI, Alain, Two control schemes with dynamic constraints on a multivariable nonlinear system, 25:10185 (CEA-R-3588)
TOMINAGA, Hiroshi, Choice of activable tracer for spraying agricultural insecticides by helicopter, 25:8426 (NSJ-tr-155)
TOMLEY, Leslie J., Spectroscopic analysis of the silicon star HD 34452, 25:9056
TONG, L. S., Departure from nucleate boiling in rod bundles during pressure blowdown, 25:8418
TONOLINI, F., Sources of radiation and energy release in a thermal reactor, 25:10165 (CISE-R-233)
TOOLEY, J., Observation of the decay eta' $\rightarrow \gamma\gamma$, 25:9651 (COO-1764-111)
TORI, G., Lung scintiphotography with /sup 113m/In $Fe(OH)_3$ aggregates, 25:8721
TORIZUKA, Yoshiharu, Study of atomic nucleus by electron scattering, 25:10014
TOROPOVA, M. A., Determination of the boiling point of astatobenzene, 25:8269 (ANL-Trans-869)
Reaction with benzene of ^{128}I and ^{211}At formed from the noble gases during K-capture, 25:8284 (ANL-Trans-870)
TOTH, Z., Clinical value of liver function appraisal by means of ^{131}I-rose bengal. III, 25:8722
TOYA, R. E., Secondary disease mortality in rat-mouse radiation chimeras, 25:8619
TOYODA, Fumihiko, Cluster model and nonleptonic hyperon decays, 25:9739
Local duality in invariant amplitudes for πN scattering, 25:9796
TRADOWSKY, K., CAMAC: system of computer-controlled electronics, 25:8573 (KFK-1241)
TRASI, M. S., Determination of the reactor power response to a sinusoidal reactivity input by use of idempotent matrices, 25:10302 (BARC-502)
TRAUGER, D. B., Special develcpment problems of high-temperature gas-cooled reactor systems, 25:10166 (GA-10265)
TREDER, H.-J., Einstein--Bohr box experiment, 25:9154
TRENDELENBURG, E. A., Scientific research in space science at ESTEC, 25:9336
TRET'YAKOVA, S. P., Identification of elements 102 and 104 with the help of the collimation method, 25:10030 (KFK-tr-329)
TRICOT, R., Structural stability of austenitic Cr--Ni stainless steels to deformation and extremeley low temperature, 25:10357 (ORNL-tr-2314)
TRINDADE, A. R., Establishment of a general rule for a hollow-cathode arc discharge, 25:9431 (SC-T-70-4050)
Hollow-cathode discharges dependent on gas flow in arc operation, 25:9433 (SC-T-70-4053)
TRINDADE, Armando Rocha, New operation mode for a hollow-cathode arc discharge, 25:9432 (SC-T-70-4051)
TRIPATHY, Kishor C., Generalized wave equations. II, 25:9853
TRIPLETT, Larry L., RBE of fast neutrons in growth inhibition: evidence for a component requiring cell division, 25:8801
TROEIM, J., D-region sunrise auroral rocket flight, 25:9296
TROSHICHEV, O. A., Currents of quasi-captured particles and interaction with geomagnetic field, 25:9342
Currents of quasi-trapped particles, 25:9347
TROYON, F., Short wavelength instabilities in confinement of collision dominated plasma by rotating magnetic field, 25:9487 (LRP-42/70)
Theory of dynamic stabilization of Rayleigh--Taylor instability, 25:9488 (LRP-45/70)
TRUEMPER, J., Extensive air showers, 25:9253 (MPI-PAE/EXTRATERR-47)
TRUKHANOV, K. A., Effective protection of space ships, 25:9540
TRUSHKOV, N. P., Sorption of Sr and Ca cations on KU-2 type cation exchange resin, 25:8341
TRUTEN, V. I., Functional relationships for renormalizations in quantum electrodynamics, 25:9848
TSAGAKIS, E., Ionospheric observations during annular solar eclipse of May 20, 1966. IV, 25:9312
TSAI-CHU, Emission of light particles in the interactions produced by 26-GeV protons in nuclear emulsions, 25:9642
TSAP, T. T., Photospheric and chromospheric magnetic fields and the brightness of faculae and flocculi, 25:9095 (CSIRO-Trans-10258)
Photospheric magnetic fields and flocculi brightness, 25:9096 (CSIRO-Trans-10289)
TSENG, T. J., Configuration interaction combined with a correlation factor for two-electron atoms, 25:9242
TSEREN, Ch., Cross section of anti Kd $\rightarrow KY_1Y_2$, 25:9804 (JINR-P2-5231)
Processes of the type of double charge exchange at light nuclei, 25:9974 (JINR-P2-5286)
TSIPENYUK, Yu. M., Angular anisotropy of photofission of ^{239}Pu, 25:10024 (FEI-190)
TSUEI, C. C., Kondo temperature and unitarity limit in non-dilute magnetic amorphous alloys, 25:10347 (CALT-822-20)
TSUKADA, Hisashi, Fatigue strength of nuclear pressure vessel material ASTM A 302 B steel and its welded joints, 25:8868 (NSJ-tr-159)
TSVETKOV, V. P., Leptonic decays of vector mesons, 25:9766
TSVETKOV, Yu. D., Spatial distribution of radical during γ irradiation of methanol at 77°K, 25:8288
TSYTOVICH, V. N., Correlations of turbulent pulsations in plasma, 25:9475
Scattering of radiation within a spectral line emitted by turbulent plasma, 25:9481
TSYTSUGINA, V. G., Radioecological studies of the Mediterranean Sea, 25:8630
TUAN, S. F., Theoretical estimates of quark production cross sections at ultrahigh energies, 25:9811
TUAN, T. F., Asymptotic electron capture in hydrogen, 25:9211
TUCKER, T. C., Eigenvalues, radial expectation values, and potentials for free atoms from Z = 2 to 126 as calculated from relativistic Hartree--Fock--Slater atomic wave functions, 25:9168 (ORNL-4614)
TUGSAVUL, A., Determination of mercury and bromine in flour, 25:8588
TUKTAROV, N. S., Radiation amplification of caprolactam coloration and possibilities of application to high-current accelerators, 25:9552
TULINOV, V. F., Contribution of corpuscular radiation in ionizing D layer, 25:9339
TURCOTTE, Rheal Peter, X-ray studies of PrO--O system and structure of rare earth carbonates and formates, 25:8938
TURNER, B. E., Detection of interstellar cyanoacetylene,

25:9094
TURRICCHIA, A., Disposal of the low activity solid waste, 25:10131
TUTUBALIN, A. I., Electronic apparatus for rapidly identifying charged particles, 25:8530
TWIDELL, J. W., Structure of some trapped hold centers in CaF_2. II, 25:9546
TYAGI, Tuhi Ram, Aspects of electron content measurements from satellite radio beacon transmissions, 25:9294
TYKE, Ya., Reaction $^7Li(d,n)^8Be$, 25:9975 (JINR-P15-5143)
TYMINSKII, V. G., Mechanical quenching of the light of liquid scintillators, 25:8526
TYMPL, Milan, Possibility of luminescence of U/sub aq/$^{++}$ ion, 25:8267
TYUTIN, I. V., Anomalous properties of vector currents in exactly solvable field theory models, 25:9836
S matrix for Yang--Mills and gravitational fields, 25:9857
TZOAR, N., Electromagnetic instability of counterstreaming plasmas in a magnetic field, 25:9493

U

UCHIDA, T., Plasma containment in a combined mirror--multipole magnetic field, 25:9399
UEDA, Tomiko, Application of microwave spectroscopy to the self-exchange of deuterium in propylene-3-d_1 catalyzed by group VIII metals, 25:8258
UGLOW, Kenneth M., Analysis of DSB/FM telemetry system errors, 25:10371 (SC-CR-70-6092)
UHLENBUSCH, J., Behavior of free-burning electric arcs in transverse magnetic fields and gas flows, 25:9282
UI, Haruo, Boson Bogolyubov transformation and SU(1,1) group, 25:9822
Clebsch--Gordan formulas of SU(1,1) group, 25:9821
ULLAH, Nazakat, Relation between the transmission coefficient and the ratio of the average width to the average spacing, 25:10077
ULLALAND, S. L., Electron precipitation associated with sudden commencement of a geomagnetic storm, 25:9298
ULLMAIER, H., Pinning of flux lines in superconducting niobium due to point defects, 25:9379
UL'YANOV, M. I., Certain peculiarities of hematologic changes in the crush syndrome in irradiated animals, 25:8766
UNEZAWA, H., New approach to the Josephson effect, 25:9364
UNLAUF, E., Thermal conductivity of pure type II superconductors, 25:9392
UNLU, M. Yasar, Uptake of ^{203}Hg by Tapes decussatus L, 25:8625 (NP-18429)
UPHOFF, Delta E., Maternal modification of tissue antigenicity and the histocompatibility-2 (H-2) locus, 25:8618
UPTON, Edward K. L., Calibration of Hyades--Praesepe main sequence, 25:8982
USHANOV, A. I., Biomedical problems of space flight, 25:8755 (JPRS-51660)
USHKOVA, M. I., Use of the /sup 125m/Te isotope as a source of x-ray radiation, 25:8434
USOV, Yu. P., Shower spark chambers for detecting particles moving at small angles with respect to the beam being stopped, 25:8553
USPENSKII, L. N., Sensitivity of spherical neutron detectors in energy range from thermal to 10 MeV, 25:8522
USYNIN, G. B., Doppler effect and nuclear safety of a fast reactor, 25:10176

V

VAISENBERG, A. O., Direct production of electron--positron pairs by 2.94-GeV/c negative pions, 25:9661
VAL'DNER, O. A., 10-MeV linear electron accelerator designated as U-13, 25:9929
VALENTIN, Pierre, Intensities of spectral lines and background continuum of Ar plasma produced in a shock tube, 25:9423
VALENTINI, A. F., Degeneration of cells in mitosis induced by x radiation (20,000 to 100,000 R), 25:8751
Mitosis in in vitro cultured fibroblasts following x irradiation, 25:8752
VALVERDE, Nilo, Ion and electron motion in solid silver sulfide, silver selenide, and silver telluride, 25:10339 (ANL-Trans-868)
VAN ALTENA, W. F., Membership of intermediate-age open cluster NGC 2420, 25:9031
VAN BREDERODE, Robert Adrian, Properties of gels produced by reticulation of dilute aqueous solutions of poly(ethylene oxide) in ^{60}Co gamma radiation field, 25:8283
VAN BRUNT, R. J., Angular distribution of O- from dissociative electron attachment to O_2, 25:9221
VAN DE HULST, H. C., High-order scattering in diffuse reflection from a semi-infinite atmosphere, 25:9616
Reduction to H-functions in radiative transfer with a general anisotropic phase function, 25:9054
Spectrum of the anisotropic transfer equation, 25:9055
VANDENBERG, S. R., Status of pipe rupture study at General Electric Company. III, 25:8866 (GEAP-10205)
VAN DEN BERGH, S., Old open cluster NGC 7142, 25:9022
VAN DEN HEUVEL, E. P. J., Presence of metallic line stars in young clusters, 25:9051
VAN DE REE, J., Potential for the interaction of atoms and heavy polar molecules in thermal scattering, 25:9232
VAN DER KLEIN, C. A. M., Influence of physical lattice imperfections on a type II superconductor, 25:9376
VAN DER WEERD, J. C., Reaction mechanism in (p,pn) reactions, 25:10005
VAN ECK, J. H. M., Isotope encephalography: diagnosis of intracranial focal lesions, 25:8710 (NP-18560)
VAN HOOK, W. Alexander, Isotope separation by gas chromatography, 25:8333
VAN HORN, A., Study of I (1915) resonance in reaction $K^-p \to \Lambda\pi^0$, 25:9659 (UCRL-19789)
VANOLI, G., Some considerations on critical heat flux in rod clusters in annular dispersed vertical upward two-phase flow, 25:10215
VAN RENSBERGEN, Walter, Population of the 2^3S level of He in planetary nebulae, 25:9016
VARGEL, C., Aluminum alloys in seawater desalination installations, 25:10361 (URNL-tr-2413)
VASIL'EV, A. N., Criterion of algebraic closeness of the commutant of quantum field, 25:9844
VASIL'EV, L. G., Magnetohydrodynamics in marine engineering, 25:9266
VAVASSEUR, Camille, Noble-gas closed MHD loop fired with fossil fuels, 25:9264
VELGHE, A. G., Ha-emission objects in two selected regions of southern Milky Way, 25:9032
VELIKSON, B. A., Determination of $\pi\pi$ scattering phase shifts in reaction $\gamma p \to \pi\pi p$ at high energy, 25:9767
VELINOV, P., Electron density variations in the ionosphere, 25:9329
VELUSAMY, T., Polarization of Tycho's supernova remnant at 2.8 cm, 25:9073
VENERUSO, Anthony F., Realization of near-time-optimal feedback controllers, 25:10375 (SC-RR-70-544)
VENIKOV, N. I., Monochromatization system for the external beams of the 2.4-m isochronous cyclotron, 25:9926
VENNIK, J., Characteristic energy loss studies of V_2O_5 and V, 25:9583
VENTRICE, Carl A., Microwave propagation in presence of helical instability, 25:9530
VERESHCHAGIN, L. F., Question of high-pressure scale, 25:10352 (LA-tr-70-26)
VERESHCHINSKII, I. V., Determination of radiation yield of nitrite ions during irradiation of sodium nitrate solutions with small doses, 25:8297
VERGNAUD, Therese, Three-dimensional Monte-Carlo calculation (TRIPOLI code) of neutron spectra in lower shield of Phenix, 25:10193 (CEA-N-1359)
VERHAAR, B. J., Austern--Blair method for scattering of deuterons and alpha particles, 25:9991
VERHEUL-KLOMPMAKER, T. A., Accurate and precise titrimetric analysis of uranium in nuclear fuels, 25:8202 (RCN-126)
VERNOV, S. N., Measurements of fast-charged particles on Cosmos-137, 25:9354
VERNOV, Yu. S., Sum rules for the ratio of the π^+---p scattering amplitudes, 25:9789
VERRENGIA, F., Enzyme activities in rabbits after pan-irradiation, 25:8779
VERRI, G., Study of some problems of cavity resonators by means of finite differences, 25:9909 (LNF-70/17)
VERTUT, Jean, Improvements in protective closures, 25:8458
VERZEGNASSI, C., Interconnection between the Kroll--Ruderman theorem and the reliability of the Born approximation for the non-spin-flip p-wave photoproduction multipoles, 25:9724
VETYUKOV, V. N., Reliability of the evaporating channels of Beloyarsk power plant type reactors, 25:10106
VEVERE, I. Z., Rapid neutron activation method for aluminum determination in al coordination compounds, 25:8224
VIATTE, M., High-temperature embrittlement of binary Mg--Zr alloy by hydrogenation, 25:8874
VICKERS, Glenn T., Formation of giant cells and supergranules, 25:9112
VICKERY, B. J., Response of Savannah River guyed stack under wind and earthquake action, 25:10391 (TID-25618)
VIDAL, A., Model field theory in five dimensions, 25:9868
Wave equations in de-Sitter space, 25:9700
VIEHL, E., Cross-spectral-density sink frequency behavior in coupled core reactors, 25:10279
VINNIKOVA, A. N., Emissivity of carbides of Ta and Hf over range 1300 to 3000° K, 25:8930
VIRASORO, M. A., Formulation of dual theory in terms of functional integrations, 25:9901
VITTORIO, P. V., Effect of erythropoietin in combination with radioprotective agents on erythropoietic recovery and survival in irradiated mice, 25:8775
VITYAZEV, V. V., Expansion of planetary nebulas, 25:9013
VOEROES, Tibor, Excitation temperature functions of some spectrum lines of He, Ne, Ar, Kr, and Xe, 25:9172
VOEVODSKII, A. V., Liquid scintillators for large scintillator detectors, 25:8527
VOGEL, G. J., Engineering development of fluid-bed fluoride volatility processes. Part 16. A safety manual for the engineering-scale alpha facility, 25:8446 (ANL-7672)
VOINOV, E. M., Use of uranium hexafluoride in nuclear power installations, 25:10221

XUM

VOITOVETSKII, V. K., Resonant Bragg scattering of gamma rays by nuclei, 25:9596
VOLCHOK, H. L., Strontium-90 deposition in the Atlantic Ocean. III, 25:8368 (HASL-237, pp I.27-37)
VOLKOV, V. V., Infrared spectra and molecular properties of tetrahydroborates of metals of the $M(BH_4)_n$ type, 25:8263
VOLOSHIN, A. E., Spectrum of scattered laser radiation and the measurement of electron density in a pulsed plasma, 25:9409 (CTO-733)
VOLOSOV, V. I., Model experiment on diffusion of electrons in the magnetosphere, 25:9350
VON HARSDORF, J., State of instrumentation in nuclear medicine, 25:8500
VON SONNTAG, C., Gamma-radiolysis of 2-deoxy-D-ribose in aqueous solution, 25:8305
Radiation chemistry of alcohols. XV, 25:8300
VOROB'EV, V. A., Method for separating γ radiation dose rate of artificial and natural radioactive isotopes in ground, 25:8360
VOROB'EV, V. S., Nonequilibrium low-temperature plasma. III, 25:9435
VORONINA, S. M., Distribution of concentration of film moving along walls of pipe in presence of magnetic field, 25:9277
VOROTNIKOV, P. E., Empirical neutron transmission coefficients for heavy nuclei in energy region 0.05-2 MeV, 25:10020 (BNL-tr-379)
VOSSEN, P. G. T., Spark source mass spectrometric survey analysis of air pollution particulates, 25:8208
VOTINOV, S. N., Analysis of variation of deformation processes of construction materials after reactor irradiation. I, 25:8898 (SRARI-P-85)
VREEKSE, Simon A., Phase space analysis of reactor kinetics, 25:10311
VRILLON, Bernard, Autoclave valve, 25:8401
VUKALOVICH, M. P., Thermophysical properties of organic coolants, 25:8412

W

WAGNER, H., Comparison of lattice-parameter and resistivity change in electron-irradiated aluminum, 25:9564
WAKAIZUMI, Seiichi, Surface excitation model of hadron resonances, 25:9808
WAKAMATSU, Seiji, Numerical methods for solving one-point reactor kinetic equations, 25:10312
WALASEK, K., Derivation of a schroedinger type equation with damping for the dynamical system weakly coupled to a thermal bath, 25:9607
WALKER, G. E., Inelastic electron scattering and supermultiplets in the particle--hole model for ^{12}C, ^{16}O, ^{28}Si, ^{32}S, and ^{40}Ca, 25:10010
WALKER, James C. G., Transport properties of the ionospheric electron gas, 25:9302
WALKER, R. H., Na--Cs differential spin-exchange scattering, 25:9212
WALKER, W. D., Bubble chamber measurement of eta'(960) → γγ and eta'(960) → $\pi^0\pi^0$eta (eta → $3\pi^0$) decay rates, 25:9666
WALLERSTEIN, George, Spectroscopic analysis of the silicon star HD 34452, 25:9056
WALLIS, G., Higher-order temporal and spatial plasma wave echoes, 25:9534
WALSH, John R., Study of trace metals in fingernails and hair using neutron activation analysis, 25:8229
WALTER, Carl E., Conceptual design of a 2-Mw/sub t/ (375 kw/sub e/) nuclear-electric space power system, 25:10286
WALTER, J. F., Calculation of neutron detector response in a subcritical reactor, 25:10322
WALTER, P., Growing of structure-components in WC--TaC--Co hardmetal-alloys, 25:8877
WALTER, R. L., Neutron polarizations in the ^{6}LI(d,n) and ^{7}Li(d,n) reactions, 25:9984
WALTERS, G. P., Preliminary corrosion tests on some steam treated zirconium alloys, 25:8833 (AERE-M-1854)
WALTZ, W. R., Calculation of neutron detector response in a subcritical reactor, 25:10322
WAMBSGANSS, M. W., Vibration of a beam with motion-constraint stops, 25:10163 (ANL-7619)
WAND, R. H., Temperature and composition of ionosphere, 25:9316
WANG, George Shih-chang, Analysis of nuclear reactor equipment response to earthquake forces, 25:10248
WANG, R., Continuous series of metastable hexagonal close-packed solid solutions in the erbium--zirconium system, 25:8892
Isotope and ortho-para separations of the molecular hydrogens by adsorption at low temperatures, 25:8332
WARD, B. Q., Inoculated pack studies on low-dose irradiated marine products: shrimp, 25:8804 (TID-25556)
WARD, D., Thermal conduction in irreversible, Type-II superconductors, 25:9370
WARD, Donald R., RBE of fast neutrons in growth inhibition: evidence for a component requiring cell division, 25:8801
WARD, R., Expanded vortex' states in superconducting films and surface sheath in inclined fields, 25:9375
WASSON, O. A., Nonstatistical effects in reaction $^{163}Dy(n,\gamma)^{164}Dy$, 25:10047
WATANABE, Keiji, Two-pion exchange contribution to nucleon--nucleon scattering, 25:9807
WATERBURY, Glenn R., Controlled-potential coulometric and potentiometric titrations of uranium and plutonium in ceramic-type materials, 25:8200 (LA-4537)
WATKINS, C. D., Ionospheric electron concentration enhancement during a solar flare, 25:9333
WATSON, B. M., Recent developments at kuwait in the control of scale at elevated temperature, 25:10359 (ORNL-tr-2411)
WATSON, J. M., Measurement of the up-down asymmetries in the beta decay of polarized lambdas, 25:9626 (COO-1545-87)
WATSON, R. B., Systematic search for the lowest T = 2 state of ^{12}C using deuteron and ^{3}He induced reactions, 25:9972 (ANU-P-496)
WEAVER, Kelly Edward, Antiproton--neutron elastic cross section at 3.5 GeV/c, 25:9649
WEBB, R. C., Response of a mineral-oil based liquid scintillator to heavily ionizing particles, 25:8511
WEBB, T. G., Electron scattering by atomic hydrogen using a pseudo-state expansion. III, 25:9208
WEBER, H. J., (3,3) resonance and nucleon pole for NN → NNπ, 25:9819
Recurrence relation for Kostant's formula, 25:9820
WEDEMEYER, H., Fabrication of ceramic materials by melting in an overpressure electric arc furnace, 25:8914
WEEDMAN, D. W., Spectral observations of Markaryan galaxies with uv continuum. II, 25:9140
WEIGL, Josef, Effect of CCCP and UO_2^{++} on ion fluxes in roots, 25:8602
WEILNBOECK, W., Multipole analysis for the reactions γp → K+A and γp → K+Σ0, 25:9728
WEINBERG, Steven, Summing soft pions, 25:9783
WEINHOLD, Frank, Dickinson energy of H_2^+, 25:9178
WEISS, Harald H., Case study in technological innovation: food irradiation, 25:8813 (NP-18236)
WEISS, J. J., Nature of bleached color centers in irradiated alkaline ice, 25:8272
WEISZ, M., Behavior of cans and centering devices, 25:8857
WELTER, J.-M., Longitudinal magnetoresistance of neutron-irradiated copper, 25:9571
WENG, P. S., Radiation protection experience at the one-megawatt pool reactor THOR and its affiliated facilities, 25:10284
WENZL, H., Longitudinal magnetoresistance of neutron-irradiated copper, 25:9571
Thermal conductivity of pure type II superconductors, 25:9392
WERBIN, Harold, Prog. rpt. on photorepair of UV damage to DNA, 1/2/71, 25:8606 (ORO-3630-10)
WERLE, H., Physics investigations of steam-cooled fast reactor cores with a Pu-fueled central zone, 25:10258 (EURFNR-848)
WERNER, Gottfried, Electrophoresis in a carrier-free buffer stream. I, 25:10414 (UCRL-Trans-1429)
WERNER, Michael W., Molecular H in H I regions, 25:9088
WERTHAMER, N. R., Neutron scattering from phonons in solid helium, 25:9964
WESTLAKE, D. G., Metallic character of metal hydride, V_2H, 25:9592
WESTRUM, Edgar F. Jr., Prog. rpt. on low temperature chemical thermodynamics, annual, 11/69--11/70, 25:8260 (COO-1149-180)
WETTER, O., Isoelectric separation in protein chemistry, 25:10413 (UCRL-Trans-1428)
WHAN, R. E., Lattice expansion and strain in ion-bombarded GaAs and Si, 25:8964
WHEELER, Carlos V., Simple total-reflecting low-energy neutron spectrometer, 25:8536
WHEELER, David John, Nuclear reactors, 25:10225
WHIPPMAN, M. L., Bootstraps in local field theory, 25:9690 (NYU-2171-331)
WHITE, David, Isotope and ortho-para separations of the molecular hydrogens by adsorption at low temperatures, 25:8332
WHITE, Howard S., Finding events in a sea of bubbles, 25:8548 (UCRL-20126)
WHITE, Jerry D., Bacteria as specific binding agents for an isotopic assay of serum folate, 25:8809
WHITMAN, G. D., Time-dependent behavior of prestressed concrete pressure vessels, 25:10325 (ORNL-TM-3246)
WHITNEY, R. R., Electromagnetic structure of ^{3}He nucleus, 25:9965 (AD-710384)
WIEBICKE, H. J., Generalized DWBA model applied to $^{24}Mg(dp)^{25}Mg$ reaction at E/sub d/ = 13.5 MeV, 25:9897 (JINR-E4-5350)
WIEDNER, C. A., Construction of a multiwire proportional chamber, 25:8479 (JUL-CONF-4, pp 148-64)
WIESEMANN, K., Influence of a diaphragm on the electron distribution function in a gas-discharge plasma. I, 25:9471
WIGGINS, P. F., Construction materials for neutron capture-gamma-ray measurement assembly using ^{252}Cf, 25:8537
WILCOX, Ralph, Bounds for approximate solutions to operator differential equation Y(t) = M(t)Y(t), 25:10398 (TID-25627)
WILCOX, Ralph M., Truncation and preservation of moment properties for Fokker--Planck moment equations, 25:10387 (TID-25614)
WILDE, I. F., Fermion states of a boson field, 25:9850

XUM

WILDES, R. A., Effect of univalent cations on circular dichroism of pyruvate kinase, 25:10369 (RLO-2227-T-5-4)
WILHELM, J., Convergency problem in calculation of electron velocity distribution function in Lorentz plasma, 25:9473
Electron velocity distribution function in homogenous stationary Lorentz plasma in Ne, 25:9474
WILHELM, K., Electron precipitation associated with sudden commencement of a geomagnetic storm, 25:9298
WILHELM, Rolf, Experimental investigations on a toroidal screw pinch, 25:9489
WILKINSON, D. H., Finite nuclear size and radiative corrections in the construction and assessment of Kurie plots for allowed beta-decay, 25:10062 (RLO-1388-131)
WILL, F., Measurement of high surge current, 25:9505 (KFK-896)
WILLARD, Donald H., Studies of inhaled radon daughters, uranium ore dust, diesel exhaust, and cigarette smoke in dogs and hamsters, 25:8623 (BNWL-SA-3419)
WILLHOIT, Donald G., Dose and LET distributions in small-animal sized cylinders for a fission neutron spectrum, 25:8685
WILLIAMS, Clyde M., Digital computer data acquisition, display, and analysis system for the gamma camera, 25:8725
WILLIAMS, D. R., Photon activation analysis using electron linear accelerator at Harwell, 25:8216 (AERE-R-5363)
WILLIAMS, E. O., Model 50-600-75 Manganin Pulse Power Supply, 25:10381 (SCL-DR-70-130)
WILLIAMSON, A. R., Selection of a single antibody-forming cell clone and its propagation in syngeneic mice, 25:8769
WILLIS, M. S., Thermal diffusion column coefficients for the separation of N_2^{14}--$N^{14}N^{15}$ and O_2^{16}--$O^{16}O^{18}$, 25:8423 (MLM-1439(Rev.))
WILLMORE, A. P., Ionospheric observations during annular solar eclipse of May 20, 1966. II, 25:9310
WILSON, David J., Quantum vibrational transition probabilities in atom--diatomic molecule collisions. V, 25:9230
WILSON, James R., Numerical study of gravitational stellar collapse, 25:8997
WILSON, K. S. J., Measurement of LET spectra, 25:8492
WILSON, W. E., Anuglar and energy distributions of electrons from hydrogen ion breakup, 25:9190 (BNWL-SA-3498)
Electron distributions from hydrogen for 0.6, 1.0 and 1.5 MeV hydrogen ions, 25:9189 (BNWL-SA-3482)
Pulsed solid-state sources for microwave application, 25:10373 (SC-DR-70-698)
WIMBER, D. E., Meiosis in the grasshopper after x-rays, 25:8754
WINCHELL, Perrin, Cloud chemistry of fallout formation, 25:8362 (AD-707427)
WING, Robert F., Brightening of uv spectrum of carbon star HD 59643, 25:9001
WINKLER, G., Characteristics and uses of hexagonal ferrites, 25:10415 (UCRL-Trans-1431)
WINKLER, R., Convergency problem in calculation of electron velocity distribution function in Lorentz plasma, 25:9473
Electron velocity distribution function in homogenous stationary Lorentz plasma in Ne, 25:9474
WINNBERG, A., Observations of some OH sources in Cygnus, 25:9083
Search for OH 18-cm emission in the Cepheus IV association, 25:9015
WINSTON, R., Measurement of the up-down asymmetries in the beta decay of polarized lambdas, 25:9626 (COO-1545-87)
WIPFELDER, Rosemarie, Radioactive scleral shells in the treatment of conjunctival tumors, 25:8731
WIRFS, L. F., Total quality control concept for material balance measurements, 25:8448 (BNWL-SA-3336)
WIT, R., Regge cuts and asymptotic sum rules for πN forward scattering, 25:9800
WITHERS, H. Rodney, Age sensitivity of epithelial cells of mouse small intestine, 25:8785
WOJCIECHOWSKI, J., Accumulation of ^{85}Sr, 25:8597
WOLETZ, W., Modular program system for experimental programing for the PDP-9, 25:8572 (HMI-B-96)
WOLF, E., Evanescent waves and the electromagnetic field of a moving charged particle, 25:9613
Mutual neutron interchange through vacuum between boundary surfaces of reactor parts, 25:10290
Optimization of the cell dimensional parameters of an incore thermionic fuel element, 25:10226
WOLF, R., Influence of physical lattice imperfections on a type II superconductor, 25:9376
WOLFE, D. M., Measurement of the up-down asymmetries in the beta decay of polarized lambdas, 25:9626 (COO-1545-87)
WOLFE, J. H., Preliminary power spectra of the interplanetary plasma, 25:9102
WOLFE, W. A., Demountable magnetic lens, 25:9928
WOLFENDEN, Bryan, Instrumentation of nuclear reactors, 25:10191
WOLFF, Gerhard, Method for utilizing nuclear energy in the production of hydrogen, 25:10294
WOLFF, Sidney Carne, Spectroscopic analysis of the silicon star HD 34452, 25:9056
WOLFGANG, Hans, Method for utilizing nuclear energy in the production of hydrogen, 25:10294
WOLFSBERG, Max, Correction to the effect of anharmonicity on isotopic exchange equilibria, 25:8246
WONG, Alfred Y., General scheme of studying trapped particles in fusion devices, 25:9420
WONG, E., Energy levels of ^{45}Ti, 25:10003
WONG, Kam-yuen, Fast gas-phase isotopic exchange reactions in nitrogen oxides, 25:8255
WOOD, John L., Prog. rpt. on origin and fate of thiocyanate ion in metabolism, 5/54--10/70, 25:10363 (ORO-1637-21)
WOOD, L. E., Unitarity and fixed poles of weak amplitudes in a perturbation-theory model, 25:9898
WOODARD, Claude Lowell, Lattice parameters and thermal expansion coefficients of Al, Ag, and Mo, 25:8876
WOOLF, N. J., Infrared emission from Be stars, 25:9018
WOOLLAM, D. H. M., Teratogenic activity of x irradiation, 25:8703
WOOLLEY, R. G., Interaction of molecular multipoles with the electromagnetic field in the canonical formulation of noncovariant quantum electrodynamics, 25:9842
WORTLEY, G., Toxicity of pesticides labelled with radionuclides, 25:8600
WRENN, G. L., Comparisons of simultaneous satellite and ground-based measurements of ionospheric parameters, 25:9308
WRENN, R. L., Fatigue behavior of molybdenum, 25:8861 (AD-709580)
WRIGHT, B. E. G., Selection of a single antibody-forming cell clone and its propagation in syngeneic mice, 25:8769
WRIGHT, D. L., Nondestructive testing: new radiographic process, 25:8443
WRIGHT, P. J., Ultraviolet-light sensitive mutants of Aspergillus nidulans, 25:8640
WU, Alfred C. T., Studies in the Yang--Mills field, 25:9851
WUYTS, Jan, Population of the 2^3S level of He in planetary nebulae, 25:9016
WYANT, D. E., Hematopoietic recovery in irradiated dogs, 25:8774
WYNN, V. T., Measurement of the magnetic susceptibility of beryllium, 25:9578

Y

YABLOCHKIN, V. D., Biomedical problems of space flight, 25:8755 (JPRS-51660)
YAES, Robert J., Unitarization of the Veneziano amplitude, 25:9900
YAKOVLEV, S. G., Contribution of corpuscular radiation in ionizing D layer, 25:9339
YAKUBOV, I. T., Nonequilibrium low-temperature plasma. III, 25:9435
YAMADA, Takeshi, Gamma-ray leakage through a junction between lead and concrete walls, 25:10296 (NSJ-tr-157)
YAMAGISHI, Hideo, Nuclear accidents in nuclear installations, 25:8661 (JAERI-4052)
YAMAJI, Katsuhiro, Study on the radiation-induced chain crosslinking and crosslinking polymerization, 25:8276 (JAERI-Memo-4147)
YAMAMOTO, Osamu, Radiation-induced binding of phenylalanine and OH substituted derivatives, 25:8280
YAMAMURO, N., Fast neutron study, 25:9995
YAMASAKI, Tatsuo, Development of a device for measuring circumferential mechanical properties of cladding tubes, 25:8883
YAMASHITA, Nobuo, Conformation therapy technique on 6 MeV linear accelerator in treatment of the carcinoma of cervix uteri, 25:8740
YAMAUCHI, T., Fast neutron study, 25:9995
YAMAYA, S., Sintering and structure of TiC--Ni--Mo compacts, 25:8928 (UCRL-Trans-10505)
YAMAZAKI, Tetsuo, Multiple scattering of protons and nitrogen ions on copper, 25:9163
YANG, I. C., Radiocarbon in the southern oceans, 25:8381
YANG, Jae Choon, Fast neutron spectrum and flux in central thimble of TRIGA Mark-II reactor, 25:10277
YANG, T. P., Electromagnetic instability of counterstreaming plasmas in a magnetic field, 25:9493
YAOI, Y., Effect of uv-irradiated vesicular stomatitis virus on nucleic acid synthesis in chick embryo cells, 25:8806
YAROSHENKO, A. P., Dibaric particle in a constant electric field, 25:9729
YASUI, Masaru, Self-consistent band calculations for vanadium and chromium, 25:9597
YATABE, J. M., Development and results of an electrically heated seven-pin bundle assembly for thermal hydraulic testing in liquid metals, 25:10207 (BNWL-SA-3286)
YATSU, K., Plasma containment in a combined mirror--multipole magnetic field, 25:9399
YAZAWA, Kazuhiko, Multiple kink effect in graphite, 25:9586
YEARIAN, M. R., Electromagnetic structure of ^3He nucleus, 25:9965 (AD-710384)
YEATS, F. W., First British radioactive isotope powered thermoelectric generators, 25:8421 (AERE-M-1694)
YEH, Chung-yauw, Occurrence of spread F and geomagnetic activity over Taipei, Taiwan, 25:9290
YEN, W. L., A_2 meson production in K⁻d reactions, 25:9672
YIFTAH, S., Effect of errors in the delayed-neutron data on

fast reactor static and dynamic calculations, 25:10179
YILMAZ, Fatma, Three color photometry of galactic star clusters, 25:8993
YOSHIDA, Toshio, Effects of electron irradiation on conductivity in CdS, 25:9563
YOUMANS, Arthur H., Method and apparatus for neutron lifetime well logging using dual discrimination within one of two intervals, 25:8359
YOUNAN, I. S., Versatile and modular data acquisition system useful in nuclear experiments, 25:8483 (PH-1)
YOUNG, A. W., Radiocarbon in the southern oceans, 25:8381
YUDOVICH, M. V., Compton effect and power absorption by space charge, 25:9615
YUGO, Shigemi, Multiple kink effect in graphite, 25:9586
YUILL, W. A., Release of radioiodine from open pools, 25:8450 (IN-1449)
YUKHIMUK, A. K., Excitation of longitudinal oscillations of a magnetized plasma by a transverse electromagnetic wave, 25:9518
YULDASHEV, B. S., Integral equations of cascade kinematics, 25:9708
YUN, Suk Koo, CP violation in the neutral K system, 25:9828
YURCHENKO, E. I., Equilibrium and stability of plasma in closed magnetic traps without rotational transformation, 25:9491

Z

ZABOLITZKY, J. G., Short-range correlations in a Woods--Saxon shell model, 25:10071
ZAHN, J.-P., Instabilities of differential rotation, 25:8985
ZAITSEV, Yu. P., Radioecological studies of the Mediterranean Sea, 25:8630
ZAK, Radovan, Effects of hypertrophy and hypoxia on the turnover of myocardial components, 25:10336 (ACRH-1000-214)
ZAKHAROVA, R. P., Radiation amplification of caprolactam coloration and possibilities of application to high-current accelerators, 25:9552
ZALUTSKA, O. I., Ternary systems Gd--(Y, Tb, Dy, Ho, Er, Sc)--Al in region to 25 at. percent rare-earth metals, 25:8886
ZALUTSKII, I. I., Ternary systems Gd--(Y, Tb, Dy, Ho, Er, Sc)--Al in region to 25 at. percent rare-earth metals, 25:8886
ZAMECNIK, J., Functional changes in the vestibulocochlear analyzer due to irradiation, 25:8792
ZAMICK, L., Interaction of two nucleons in a nucleus, 25:10079
ZAMYATNIN, Yu. S., Measurement of energy spectra and average number anti ν of prompt fission neutrons, 25:10039
ZANASCHI, C., Instrument for measuring rate of change of RF frequency in particle accelerators, 25:9905 (CERN-70-28)
ZANGHI, Jean-Pierre, Diffusion coefficients of Ni--U system, 25:8865 (CEA-R-4066)
ZAPESOCHNYI, I. P., Transfer of excitation energy in ion--atom interaction, 25:9238
ZAVIDOVSKI, V. Ya., Mechanism of gas release from ceramic nuclear fuels, 25:8958 (SRARI-P-73)
ZAVILOPULO, A. N., Transfer of excitation energy in ion--atom interaction, 25:9238
ZBEREA, I., Formation and nature of twin crystals in U_3Si, 25:8946
ZEDELASHVILI, E. N., Products of anthracene transformation under (n,γ) irradiation, 25:8289
ZEISSIG, G. A., Minimum observable diameter of radio sources, 25:9084
ZELDOVIC, Ya. B., Gravitational instability of a two-component fluid: matter and radiation, 25:9157
ZEMACH, Charles, Methods for the Bethe--Salpeter equation. I, 25:9855
Methods for the Bethe--Salpeter equation. II, 25:9856
ZEMSKOVA, I. I., Mechanical quenching of the light of liquid scintillators, 25:8526
ZENKEVICH, P. R., Quasistochastic instability of the vibrations of particles in annular accelerators and storage rings, 25:9933
ZERWAS, P., Mass of the ninth pseudoscalar meson, 25:9779
ZESENKO, A. Ya., Radioecological studies of the Mediterranean Sea, 25:8630
ZETTWOOG, Pierre, Noble-gas closed MHD loop fired with fossil fuels, 25:9264
ZHARKOV, V. A., Optimum neutron irradiation conditions for radioisotope production, 25:8308
ZHELEZNYAKOV, V. V., Coherent mechanisms of emission and their application to pulsars. I, 25:9070
ZHILTSOVA, L. Ya., Degradation of the luminescence of plastic polystrene scintillators, 25:8582
Effect of natural lighting on plastic scintillators, 25:8528
Mechanical quenching of the light of liquid scintillators, 25:8526
ZHUKOVA, G. A., Radiation induced defects in dielectric--semiconductor structures, 25:9566
ZHURAVLEV, V. F., Recommendations concerning the maximum permissible tritium oxide concentrations in the atmosphere of industrial premises, 25:8678 (ORNL-tr-2403)
ZINKE, O. H., Snowplowing in a plasma rail gun, 25:9479
ZINOV'EV, G. M., Asymptotic properties of electron--proton scattering amplitude and sum rules for Schwinger term, 25:9701 (ITF-70-73)
Generalized Veneziano model, 25:9888 (ITF-70-78)
ZIPPER, W., Energies spread of Gaussian distributed beam in nuclear scattering experiments, 25:10086
ZNYSHEV, V. V., Natural circulation stability of heat transfer agent in one-loop system, 25:8414
ZOLLINGER, H., Stereochemistry of sigma-complex intermediate in sterically hindered electrophilic aromatic substitutions, 25:8242
ZOMBKOVSKII, S. M., Interaction $\pi^-\pi^-$ in the reaction $\pi^-p \to N^{*++}(1236)\pi^-\pi^-$ with impulse 4.47 GeV/c, 25:9655 (ITEF-767)
Reaction $\pi^-p \to rho^0\pi^-p$ with impulse 4.45 GeV/c, 25:9656 (ITEF-775)
Study of reaction $\pi^-p \to rho^0\pi^-p$ at 4.45 GeV/c, 25:9663
ZUBAREV, D. N., Derivation of a schroedinger type equation with damping for the dynamical system weakly coupled to a thermal bath, 25:9607
ZUBAREV, V. F., Ionization gauge for measured molecular flux densities in Ogra-II, 25:9430
ZUCKERMANN, M. J., Effect of localized spin fluctuations on the superconducting critical temperature of dilute alloys, 25:9374
ZUK, W. M., Angular correlation studies of the $^{42}Ca(\alpha,p_7)^{45}Sc$ reaction, 25:9996 (ANU-P-466)
Search for the 3446 keV level in ^{29}P via the $^{28}Si(p,\gamma)$ reaction, 25:10016 (ANU-P-503)
ZUPNIK, B. M., Chiral SU(2) x SU(2) dynamics for A_1, rho, and π mesons, 25:9781
ZURMUEHLE, R. W., Sensitivity of (^{3}He,t) reaction to final-state configurations, 25:10013
ZWALLY, H. Jay, Single-electron capture by C^{6+} in helium, neon, and argon below 40 keV, 25:9215
ZWICKER, Hartmut, Experimental investigations on a toroidal screw pinch, 25:9489
ZYGAN, H., Experimental investigation of the theoretical expressions for the Rydberg constant, 25:9246
ZYKOV, A. I., Determination of the critical current in a section with radial slots in the iris disk, 25:9907 (KFK-tr-335)

SUBJECT INDEX

Cross references are included in cumulative subject indexes and in *Subject Headings Used by the USAEC Division of Technical Information* (USAEC report TID-5001).

The reader is also referred to *Guide to Abstracting and Indexing for Nuclear Science Abstracts* (USAEC report TID-4576).

Most headings in the subject index are specific materials, things, and processes. The headings are followed by modifiers that describe the properties of, or processes applied to, the headings.

All index entries cite *NSA* volume and abstract numbers; volume number precedes the colon and the abstract number follows it. The designation (R) following the abstract number indicates a progress report; (P) indicates a patent; and (T) indicates a translation. Abstracts for reports other than progress reports carry no letter designation. Report numbers, where applicable, are included in parentheses after the abstract number of the citation. Published literature (journal article or book) can be identified by the absence of a report number.

Ideas presented in the original literature, rather than key words, have been indexed. The indexers have selected what seemed the most probable and logical place to look for typical information. Since it is not always possible to anticipate where a user would look for information, the cumulative indexes include numerous cross references. Consideration of synonymous or closely related terms will prove valuable.

Information is indexed for the greatest use to the greatest number of users. This requires that a topic be indexed to headings that most specifically describe it and not ordinarily to the headings that describe its ultimate use or to the general class headings that include the specific headings. For example, information on boiler design for the Fermi Fast Breeder Reactor would be indexed under the headings BOILERS and FERMI FAST BREEDER REACTOR but not necessarily under the headings REACTORS, FAST or REACTORS, BREEDER.

General or broad headings are reserved for general summaries, reviews, comprehensive reports, and similar literature.

Subject Heading Styles

Generally, the direct form of subject entry is used rather than inverted headings; e.g., AMINO ACIDS rather than ACIDS, AMINO; HELIUM ISOTOPES He-4 rather than HELIUM—ISOTOPES He-4 or HELIUM—He-4 ISOTOPES. Note, however, that in some cases parenthetic modifying terms or inverted headings such as NEUTRONS, FAST, are used where the alphabetical arrangement of a direct entry would cause information to be scattered. In addition, organic compounds are usually entered in the index in the inverted form to facilitate grouping like or related compounds with the parent compounds; e.g., BENZENE, BROMO- rather than BROMOBENZENE. In general, the nomenclature used is that of the subject indexes to *Chemical Abstracts*.

Alphabetization

Subject headings are alphabetized word by word. Parenthetic qualifiers, numbers, and Greek letters within subject headings are disregarded in alphabetizing unless there are two or more headings that are otherwise identical, in which case the qualifier, numerical progression, or spelled names for the Greek letters determine the order.

Examples:

M-Capture
  see ELECTRON CAPTURE
MAGNESIUM
MAGNESIUM ALLOYS AND SYSTEMS
MANGANESE FLUORIDES
MANGANESE FLUORIDES MnF_2
MESONS
MESONS (π)
MESONS (ρ)
1-PENTANOL
2-PENTANOL

Modifying Phrases

The modifiers appearing under a subject heading are written specifically to show the relation between the item being indexed and the heading. The modifier therefore contains a maximum of useful information. Although the modifier begins with the word judged to be of greatest use to the greatest number of users, there is still need for the searcher to consider all modifiers under the heading(s) of interest.

Modifiers usually form meaningful phrases when combined with the subject heading. Some are intended to be read following the subject heading, e.g., the entry HYDROGEN—sorption by charcoal should be read "hydrogen sorption by charcoal." As a result of placing the important word first, however, many modifiers must be rearranged for smooth reading, e.g., FORMALDEHYDE—yields in radiolysis of ethyl ether, effects of deuterium on, should be read "effects of deuterium on formaldehyde yields in radiolysis of ethyl ether" and URANIUM—crystal structure of, effect of cooling rate on allotropic transformations in, should be read "effect of cooling rate on allotropic transformations in crystal structure of uranium."

Special characters are added to modifiers in the fields of physics and reactor technology; if the modifier does not establish the experimental or theoretical character of a reference, a symbol (E), (T), or (E/T) is placed immediately after the modifying phrase and before the abstract number.

Physical States and Configurations of Materials

The specific physical state, if other than normal, or the geometric configuration of the material is included in the modifying phrase; e.g., information on liquid metals is indexed under the specific metal with "liquid" in the modifier and carbon crucibles is indexed under CARBON with "crucibles" appropriately placed in the modifier. The information on carbon crucibles is also indexed under CRUCIBLES.

Nomenclature of Inorganic Compounds

Inorganic compounds are indexed to subject headings in the direct form. Cations are listed in the order of increasing valence for polycationic salts of varying valence and in alphabetic order for polycationic salts in which all cations have the same valence; e.g., SODIUM ALUMINUM SILICATES and POTASSIUM SODIUM SULFATES. If more than one anionic species is presented in a compound, the anions are arranged alphabetically, e.g., BERYLLIUM FLUORIDE HYDROXIDES.

Nomenclature of Organic Compounds

Organic compounds are indexed by subject headings based on the indexes to *Chemical Abstracts* except in the area of enzymes, in which specific enzymes, named according to the 1964 recommendations of the International Union of Biochemistry, are used. In many cases nonproprietary names for drugs are used as subject headings, and cross references are made from the systematic chemical names. Subject headings for hormones appear in the inverted style at HORMONES.

Nomenclature of Life Sciences

Subject headings for plants are names of phyla with one exception: members of the Phylum Tracheophyta are indexed under class or subclass names. Scientific names (genus and species) are used as the initial, or file, word in the modifying phrase. Scientific names are omitted only when the name is not available in the literature or cannot be found in available references.

Subject headings for animals are the names of phyla with the following exceptions: (1) members of Phylum Arthropoda and Phylum Chordata are indexed under appropriate class name, and (2) common names are used for members of Class Mammalia.

Subject headings are entered for various classes of commodities, and specific products are identified in the file-word position of the modifier. In the following examples, approved subject headings are capitalized and typical modifier file words are listed in lower case.

Example 1	Example 2
CEREALS	MEATS
bread	beef
flour	fish
oats	mutton
rice	pork
rye	poultry
wheat	seafood

Diseases, pathological conditions, and in vitro studies of atypical cells and tissues are indexed under subject headings for the organism affected, under the appropriate anatomical structure of physiological phenomenon affected, and under the appropriate disease heading. Subject headings for diseases (defined as any deviation from the norm) are DISEASES; DISEASES, INFECTIOUS; DISEASES, NEOPLASTIC; DISEASES, PHYSIOLOGICAL; DISEASES, PLANT; and DISEASES, TRAUMATIC.

Diseases of mixed etiology are treated in the following manner: neoplastic diseases that are also classified as infectious or physiological are indexed under DISEASES, NEOPLASTIC; diseases in which a microorganism is the etiologic agent are classified under DISEASES, INFECTIOUS; physiological anomalies that are neither neoplastic nor infectious are indexed under DISEASES, PHYSIOLOGICAL; the acute radiation syndrome, nonspecific radiation injuries, trauma, and wounds or incisions inflicted mechanically are indexed under DISEASES, TRAUMATIC.

Specific diseases or pathological conditions are named in the file-word position of the modifier, in the author's terminology, and are set off from the remainder of the modifier by commas. Neoplasms are designated as benign or malignant in the file-word position when more specific information is not available.

Multicomponent Alloys and Other Systems

Multicomponent alloys and systems, except well-known trade names, are indexed under a subject heading for each component in the form "element systems" for nonmetals or "element alloys and systems" for metals. The modifier begins with element symbols for each component arranged alphabetically. In addition, if significance is placed on the base metal of the alloy, this is indicated by adding "-base" to the element symbol.

Example: A 1.5C, 12Cr, 0.25V, 0.8Mo, bal Fe alloy is indexed as

```
CARBON SYSTEMS
  C--Cr--Fe-base--Mo--V, ...
CHROMIUM ALLOYS AND SYSTEMS
  C--Cr--Fe-base--Mo--V,...
IRON ALLOYS AND SYSTEMS
  C--Cr--Fe-base--Mo--V, ...
MOLYBDENUM ALLOYS AND SYSTEMS
  C--Cr--Fe-base--Mo--V, ...
VANADIUM ALLOYS AND SYSTEMS
  C--Cr--Fe-base--Mo--V, ...
```

Well-known alloys, such as ZIRCALOY-2, are indexed under the trade name; cross references from each component of the alloy to the trade name appear in cumulative indexes.

Multicomponent systems in which nonmetallic elements are present in large percentage and which are commonly referred to as systems or mixtures are indexed in a manner similar to alloys.

Example: A tungsten–silicon preparation is indexed as

```
TUNGSTEN ALLOYS AND SYSTEMS
  Si--W, ...
SILICON SYSTEMS
  Si--W, ...
```

Multicompound systems and mixtures of inorganic compounds are indexed under the subject heading for each component compound; the modifiers begin with an alphabetical listing of compound formulas.

Example: A lead titanate–lead zirconate mixture is indexed as

```
LEAD TITANATES
  PbTiO3--PbZrO3
LEAD ZIRCONATES
  PbTiO3--PbZrO3
```

XUM

A mixed system of compounds and elements is indexed by a combined form of the preceding conventions; e.g., a dispersion of copper and alumina would be indexed as

ALUMINUM OXIDES
  Al_2O_3--Cu, ...
COPPER ALLOYS AND SYSTEMS
  Al_2O_3--Cu, ...

Mixtures of organic compounds are indexed under subject headings for each component of the mixture; the modifiers begin with an alphabetical listing of compound names.

Example:

ACETIC ACID
  acetic acid--BF_3, ...
BORON FLUORIDES
  acetic acid--BF_3, ...

Example:

BENZENE, CHLORO-
  bromophenol--chlorobenzene, ...
PHENOL, BROMO-
  bromophenol--chlorobenzene, ...

If modifiers for alloys and systems are included with other modifiers under the same subject heading, they are filed last.

Example:

CARBON SYSTEMS
  deposition on nuclear fuel particles
  molecular structure of
  neutron total cross section for
  sorptive properties for xenon
  Young's modulus for
  Al--C--Cr, superconductivity in
  B--C, phase studies for
  C--U--Zr, fabrication and physical properties of

Nomenclature of High Energy Physics

Information on particle-particle events is indexed under subject headings for the specific particles involved. The modifier file word *interactions* is followed by the specific interaction written in symbolic form. Particle nomenclature and symbols follow that of Rosenfeld, et al. *Data on Particles and Resonant States,* UCRL-8030 (latest revision). For consistency the incident particle is always written first. The mass (in MeV) of a resonance state is included in parentheses after the symbol to avoid ambiguity. Hyperfragments are indicated in modifiers as in the following examples: Λ-He^5, Σ-H^3, $\Lambda\Lambda$-Be^{10}. The superscript on the right indicates the total number of baryons in the composite system.

Examples:

MESONS (π^-)
  interactions $\pi^- + p \rightarrow \Lambda + K^+ + \pi^-$ at 6 GeV/c in hydrogen bubble chamber, $\Lambda K(1700)$ enhancement in, (E)
BARYONS, RESONANCE (N^*)
  production of $\Delta^{++}(1236)$ and $\Delta^0(1236)$ from $K^- + p \rightarrow K^- + p + \pi^+ + \pi^-$ interactions at 2.63 and 2.70 GeV/c, (E)
HYPERFRAGMENTS
  binding energy of $\Lambda\Lambda$-He^6, three-body α--Λ--Λ model for

Subject headings are also provided for specific models and theories.

Examples:

ELEMENTARY PARTICLE MODELS (TRIPLET)
  hadron total cross sections in quark, numerical analysis of
CURRENT ALGEBRA
  PCAC hypothesis for A_1 and rho dominance in $\pi \rightarrow e + \nu + \gamma$ decay
REGGE POLE THEORY
  predictions for polarization in $K^- + p \rightarrow$ anti $K^0 + n$, $\pi^- + p \rightarrow \pi^0 + n$, and $\pi^- + p \rightarrow$ eta + n interactions at high energies
SYMMETRY GROUPS
  $SU(2) \times SU(4)$ intermediate-coupling model for nucleon and hyperon isobars

Nomenclature of Reactor Technology

Subject headings for reactors are of three types:

(1) Specific reactors, e.g., ARGONNE RESEARCH REACTOR, SAXTON POWER REACTOR

(2) Reactors having a common physics or engineering characteristic, e.g., REACTORS, FAST; REACTORS, ORGANIC-COOLED; REACTORS, PRESSURIZED-WATER

(3) Reactors having a common purpose, e.g., REACTORS, POWER; REACTORS, RESEARCH

Information on specific reactors, type (1), is indexed under the one specific subject heading. Information on classes or types of reactors, types (2) (characteristics) and (3) (purpose), is indexed under all applicable headings. For example, information on a heavy-water-moderated organic-cooled power reactor is indexed under REACTORS, HEAVY WATER-MODERATED; REACTORS, ORGANIC-COOLED; and REACTORS, POWER.

Subject headings exist for selected reactor components, e.g., REACTOR FUEL ELEMENTS. When applicable, headings for components are indexed even though they may have been included in a modifier under a type (1) or (2) heading. The materials in reactor components are indexed when the information is peculiar to the material.

Modifier file words under reactor headings are of two primary types: one type expresses reactor characteristics, e.g., reactivity; the other, components, e.g., control rod. If no subject heading appears for a reactor component, the heading REACTORS is used, and the component is used as the modifier file word.

A

ACCELERATORS
auxiliaries for, hf superconducting waveguides and cavities for, 25:9396
particle vibrations in annular, quasistochastic instability of, 25:9933
phase oscillations in, with discontinuous acceleration, 25:9915(T) (SLAC-Trans-124)
use of high-current electron, for coloration enhancement of caprone, feasibility of, 25:9552
ACCIDENTS
bibliography on causes and consequences of radiation, in nuclear installations, 25:8661 (JAERI-4052)
control at Goodyear Atomic Corporation during 1969, progress report on programs for, 25:8692(R) (GAT-627)
iodine-131 release following, at La Hague UP 2 reprocessing plant, 25:8657 (CEA-R-4008)
radiation protection planning for, during radioisotope shipping in Italy, 25:8696
ACETALDEHYDE
yields from γ radiolysis of aqueous ethanol solutions as function of nitrate concentration, 25:8301
ACETIC ACID, [(CARBOXYMETHYLIMINO)BIS(ETHYLENENITRILO)]TETRA-
complexes with neptunium, thorium, or uranium, preparation and stability of, 25:8237 (KFK-1210)
radioprotective effects of, on rats against accumulation of transplutonium elements in bone, 25:8690 (CEA-CONF-1658)
ACETIC ACID, (ETHYLENEDINITRILO)TETRA-
complexes with neptunium, thorium, or uranium, preparation and stability of, 25:8237 (KFK-1210)
effects on calcium-45 efflux in myometrium of rats, 25:8601
ACETIC ACID, FLUORO-
sodium salt, radioprotective effects of, on survival of mice, x, 25:8700
ACETIC ACID, [(2-HYDROXYETHYL)IMINO]DI-
complexes with neptunium, thorium, or uranium, preparation and stability of, 25:8237 (KFK-1210)
ACETIC ACID, IODO-
effects on serum coeruloplasmin activity in rats, 25:8612
ACETIC ACID, NITRILOTRI-
complexes with neptunium, thorium, or uranium, preparation and stability of, 25:8237 (KFK-1210)
ACETIC ACID, VINYL ESTER, POLYMERS
development of strippable films of, for protection of surfaces against radioactive contamination, 25:8663
ACETYLENE
effects on γ-induced crosslinking of polyethylene, 25:8276 (JAERI-Memo-4147)
ion reactions in eV range with, mechanisms and cross sections for light emission in, (E), 25:9213
proton reactions at 15 to 150 keV with, cross sections for charge exchange in, (E), 25:9229
acetylene--SiH_4, ionization in mass spectrometer, reactions of products from, 25:8294
ACRIDINE, 3,6-BIS(DIMETHYLAMINO)-
radiation effects on binding of, with nucleoproteins of fibroblasts of mice, uv, 25:8770
radioprotective effects of, on transforming DNA in Bacillus subtilis, coliphages, and Escherichia coli, cesium-137 γ, 25:8707
ACTINIDE OXIDES
preparation of microspheres of, using sols or solutions, equipment and method for, 25:8916(P)
ACTINIDES
compounds, chemical thermodynamics of, 25:8260(R) (COO-1149-180)
neutron transmission coefficients at 0.05 to 2 MeV, empirical, (E), 25:10020(T) (BNL-tr-379)
ACTINOMYCIN
effects on human cells in vitro, 25:8632 (EUR-4526)
ACTIVATION ANALYSIS
cadmium filter for reactor neutron, 25:8226
euipment for neutron, remote and automatic control, 25:8579
separation processes for neutron, using selective ion exchange paper, 25:8221
uses by Food and Drug Administration, 25:8227
AEROSOLS
analysis of atmospheric, for inorganic pollutants by neutron activation, 25:8231
characteristics of radioactive, in atmosphere, effects of, on cloud dose calculations, 25:8668 (BNWL-SA-3424)
inhalation hazards to dogs and hamsters from diesel engine exhaust, in uranium mines, additive effects of radon decay products and uranium ore dusts on, in dogs and hamsters, 25:8623 (BNWL-SA-3419)
inhalation of plutonium-239-labeled, effects of concentration of, on lung clearance rate in rats, 25:8591 (CEA-CONF-1677)
research at JAERI during 1969 and 1970, progress report on, 25:8693(R) (JAERI-5025)
AET
effects on erythropoiesis and survival of γ-irradiated mice, effects of erythropoietin on, 25:8775
AGE
effects on living organisms in comparison with environment, radiation, and thermal energy, information theory for studying, 25:8742
AGRICULTURE
research and development in Puerto Rico, 1969, 25:8574(R) (PRNC-140)
use of nuclear techniques in research on, activities of joint FAO/IAEA, 25:8818
AIR
alpha-particle range at 0.2 to 2.0 MeV in, relation to energy, (E), 25:9162 (SC-RR-70-788)
analysis for trace elements by spark source mass spectrometry, 25:8208
content of diesel engine exhausts, radon decay products, and uranium ore dusts in uranium mine, relation of, to incidence of respiratory tract neoplasms in personnel, 25:8623 (BNWL-SA-3419)
effects on γ-radiation effects on collagen, 25:8307
gamma transport in, angular flux densities and exposure angular distributions for ^{60}Co, (T), 25:9539
heat transfer from fuel elements to, superposition method of determining temperature distribution in, 25:8409 (RD/B/N-1755)
proton range at 0.2 to 2.0 MeV in, relation to energy, (E), 25:9162 (SC-RR-70-788)
AIR SAMPLERS
design and operation of, for monitoring radioactivity in ground-level atmosphere at Nevada Test Site, 25:8393 (NVO-410-6)
AIRGLOW
production of $O(^1D)$ in night, by temperature-dependent dissociative recombination of O_2^+, (E/T), 25:9314
ALANINE, 3-(3,4-DIHYDROXYPHENYL)-
radioinduced binding to serum albumin, effects of acidity on γ, 25:8280
ALANINE, PHENYL-
radioinduced binding to serum albumin, effects of acidity on γ, 25:8280
ALARM SYSTEMS
design of criticality, for fuel reprocessing plant, 25:8486
ALBUMINS
radioinduced binding of phenylalanine and its derivatives to, effects of acidity on γ, 25:8280
ALGAE
analysis for cesium by thermal neutron activation and γ spectrometry, 25:8230
ALGORITHMS
derivation of feasible, for finding suboptimal chains, 25:10393 (TID-25620)
development for scheduling N tasks with M operations, 25:10383 (STAN-CS-70-165(App.2))
ALKENES
radioinduced polymerization of, on polyethylene powder, 25:8282(P)
ALKYL HALIDES
radiation effects on isomerization of, effects of temperature on, 25:8279
ALLOYS
Kondo temperature and unitarity limits in nondilute magnetic amorphous, 25:10347 (CALT-822-20)
properties and uses of superconducting, 25:9386
ALPHA PARTICLES
detection and measurement of, using gallium arsenide diodes, 25:8491
dose to human bones, effects of route of administration on plutonium-239, 25:8596(T) (LF-tr-41, pp 127-97)
dose to man following ingestion of radium-226, methods for calculating, 25:8669 (COO-2088-1)
dose to man, ICRP recommendations for maximum permissible radium-226, 25:8674(T) (LF-tr-41, pp 199-220)
dose to personnel in plutonium industry, maximum permissible plutonium-239, 25:8674(T) (LF-tr-41, pp 199-220)
effects on excitation of butanol and ethanol in presence of luminescing additives, 25:8274
effects on mutation rate and survival of Chlorella, 25:8755(T) (JPRS-51660)
effects on survival of HeLa cells following (n,α) reaction in cells, effects of boron-10 content on RBE for, 25:8745
effects on survival of HeLa cells in monolayer cultures, RBE for $^{10}B(n,\alpha)^7Li$, 25:8745
hazards to water supplies from polonium-210 migration in soils, 25:8593 (COO-1733-11)
range in air, nitrogen, and oxygen at 0.2 to 2.0 MeV, relation to energy, (E), 25:9162 (SC-RR-70-788)
reactions (α,2α) with beryllium-9, carbon-12, lithium-6, and oxygen-16 at 56 MeV, analysis using triangular graphs, (T), 25:9987
reactions (α,2α) with nuclei, polar and triangular diagrams for interpretation of, (T), 25:10059 (LYCEN-7039)
reactions (α,d) with calcium-42 at 26.5 MeV, deuteron spectra and angular distributions for, (E), 25:9966(R) (COO-1265-94)
reactions (α,f) with thorium-232 and uranium-238 at 20 to 29 MeV, delayed-neutron curves and fission-chain yields from, (E), 25:10056
reactions (α,n) with carbon-14 at 4.9 to 8.5 MeV, excitation function for, (E), 25:9980

reactions (α,nγ) with oxygen-18 at 5 to 16 MeV, γ spectra and angular distributions for, (E), 25:10002
reactions (α,pγ) with calcium-42 at 11 MeV, proton and gamma spectra and angular correlations from, (E), 25:9996 (ANU-P-466)
reactions (α,xnγ) with samarium-150 and -152 at 25 to 45 MeV, γ spectra from, (E), 25:9978(R) (ORO-3398-26)
reactions with copper and lead atoms, x-ray fluorescence yields from, (E), 25:9978(R) (ORO-3398-26)
reactions with silver at 85 MeV, spectra of light fragments from, (E), 25:9978(R) (ORO-3398-26)
reactions with Z = 26 to 50 atoms at 30 to 80 MeV, K-shell ionization cross sections for, (E), 25:9978(R) (ORO-3398-26)
scattering by carbon-12 at 35 MeV, α--γ angular correlations for inelastic, (E), 25:9978(R) (ORO-3398-26)
scattering by carbon-12, magnesium-24, nickel, nickel-58 and -60, titanium-48, cadmium, and cerium-140, validity of the Austern--Blair method for inelastic, (T), 25:9991
scattering by carbon-14 at 3.5 to 16.5 MeV, angular distributions for elastic, (E), 25:9980
scattering by nickel-58 at 26.5 MeV, angular distribution for elastic, (E), 25:9966(R) (COO-1265-94)

ALPHA SOURCES
activity in honey, 25:8665

ALUMINUM
abundance in iota Ori B, (E), 25:8995
abundance in L and H chondrites, (E), 25:8967
antideuteron reactions at 25 GeV/c, absorption cross sections for, (E), 25:9639
cracking in fuel cladding of, effects of embedded abrasive particles on, 25:8853 (ORNL-4600, pp 249)
crystal structure at 40 to 120°K, 25:8876
determination in air particulates by spark source mass spectrometry, 25:8208
determination in airborne particulates by neutron activation, 25:8231
determination in aluminum coordination compounds by neutron activation, 25:8224
determination in titanium and titanium dioxide by neutron activation, 25:8233
diffusion in, lattice-dynamical theory of isotope effects in, 25:9589
effects of additions of, on stress corrosion of chromium--iron--nickel alloys by boiling magnesium chloride solutions, 25:8834(R) (COO-2069-6)
effects on annealing of electron irradiation damage in p-type silicon, 25:9549
electron elastic scattering at 100 to 1300 keV by foils of, as function of foil thickness and incidence angle, single, plural, and multiple, (E), 25:9225
electron energy absorption profile of, thermoelastic response measurements of intense 1.5-MeV, 25:8569
positron elastic scattering at 100 to 1300 keV by foils of, as function of foil thickness and incidence angle, single, plural, and multiple, (E), 25:9225
preparation of dispersion-strengthened, using refractory oxide dispersoids, 25:8860(P)
radioinduced blistering of, correlation of hydrogen degassing with proton, 25:8905
radioinduced defects in, comparison of lattice-parameter and resistivity changes in annealing of 4.5°K electron, 25:9564
radioinduced defects in, low-temperature microscopic observations of annealing of 77°K neutron, 25:9542 (CEA-CONF-1681)
thermal expansion coefficients at 40 to 160°K, 25:8876

ALUMINUM ALLOYS AND SYSTEMS
book: Metallurgy and the Hot Working of Metals, 25:8894
corrosion properties in seawater at 20 to 120°C, 25:10361(T) (ORNL-tr-2413)
Al--Al_2O_3--U_3O_8, fabrication of aluminum-clad fuel plates of, for HFIR irradiation testing, 25:8956 (ORNL-4600, pp 235-48)
Al--C--Fe--Si--U-base, tensile properties of dilute, at 885 to 1150°F, 25:8867 (NLCO-1060)
Al--Ce--Ni, magnetic properties and phase diagram of CeNi/sub x/Al/sub 2-x/, 25:9576
Al--Co--Nb, phase diagram at 800°C, 25:8890
Al--Cr--Fe-base--Ni, corrosion by water containing trace chloride and oxygen at 200°C, stress, 25:8834(R) (COO-2069-6)
Al--Dy--Ni, magnetic properties and phase diagram of DyNi/sub x/Al/sub 2-x/, 25:9576
Al--Er--Ni, magnetic properties and phase diagram of ErNi/sub x/Al/sub 2-x/, 25:9576
Al--Fe--Nb, phase diagram at 800°C, 25:8890
Al--Gd--Ni, magnetic properties and phase diagram of GdNi/sub x/Al/sub 2-x/, 25:9576
Al--Ho--Ni, magnetic properties and phase diagram of HoNi/sub x/Al/sub 2-x/, 25:9576
Al--Lu--Ni, magnetic properties and phase diagram of LuNi/sub x/Al/sub 2-x/, 25:9576
Al--Mo--Ti-base--V, embrittlement by cadmium, effects of stress, temperature, and time on, 25:8879
Al--Nd, neodymium-145 Moessbauer spectrum in $NdAl_2$, 25:9594
Al--Nd--Ni, magnetic properties and phase diagram of NdNi/sub x/Al/sub 2-x/, 25:9576
Al--Ni--Pr, magnetic properties and phase diagram of PrNi/sub x/Al/sub2-x/, 25:9576
Al--Ni--Tb, magnetic properties and phase diagram of TbNi/sub x/Al/sub 2-x/, 25:9576
Al--Ni--Y, magnetic properties and phase diagram of ErNi/sub x/Al/sub 2-x/, 25:9576
Al--Ti-base--V, embrittlement by cadmium, effects of stress, temperature, and time on, 25:8879
Al--U, phase studies of, 25:8846 (KFK-1252)
Al--U, properties of intermetallic UAl_3 dispersion fuels of, electric, mechanical, and thermal, 25:8846 (KFK-1252)
Al--U_3O_8, fabrication of aluminum-clad fuel plates of, for HFIR irradiation testing, 25:8956 (ORNL-4600, pp 235-48)
Al--U_3O_8, grain structure and void content of fuel plates of, 25:8956 (ORNL-4600, pp 235-48)
Al-base--Dy--Gd, phase diagram at 500°C, 25:8886
Al-base--Er--Gd, phase diagram at 500°C, 25:8886
Al-base--Gd--Ho, phase diagram at 500°C, 25:8886
Al-base--Gd--Sc, phase diagram at 500°C, 25:8886
Al-base--Gd--Tb, phase diagram at 500°C, 25:8886
Al-base--Gd--Y, phase diagram at 500°C, 25:8886

ALUMINUM ISOTOPES Al-27
deuteron elastic and inelastic scattering at 20 MeV, angular distributions for, (E), 25:9966(R) (COO-1265-94)
deuteron reactions (d,He-3) at 20 MeV, angular distributions for, (E), 25:9966(R) (COO-1265-94)
deuteron reactions (d,Li-6) at 50 MeV, lithium-6 spectra and angular distributions for, (E), 25:9978(R) (ORO-3398-26)
energy levels from magnesium-26 (d,n) reactions, nuclear structure effects in gamma decay of isobaric analog, (E), 25:10007
helium-3 elastic scattering at 13 to 27 MeV, angular distributions for, (E/T), 25:9994
helium-3 reactions (He-3,t) at 18 MeV, differential cross sections from, (E/T), 25:10013
neutron scattering by polycrystalline, calculation of total coherent cross section for, (T), 25:9958
photon reactions (γ,π⁺) at 150 to 700 MeV, yields and cross sections for, (E), 25:9620 (LUNP-7007)

ALUMINUM OXIDES
effects of dispersions of, on properties of copper, 25:8873
fabrication of fine-grained and high-density, evaluation of methods for, 25:8937
mechanical properties of, review of effects of microstructure on, 25:8937
radiation effects on microstructure and swelling of polycrystalline, in-pile, 25:8954 (ORNL-4600, pp 210-15)
Al_2O_3--Ni, effects on deuterium exchange in propene, catalytic, 25:8258
Al--Al_2O_3--U_3O_8, fabrication of aluminum-clad fuel plates of, for HFIR irradiation testing, 25:8956 (ORNL-4600, pp 235-48)

AMERICIUM
separation from irradiated LMFBR fuels, solvent extraction processes for, 25:8316 (BNWL-CC-1939)

AMERICIUM ISOTOPES Am-241
distribution in organs of rats following inhalation and intramuscular injection, 25:8590 (CEA-CONF-1658)
neutron absorption resonance integrals at .025 eV, (E), 25:10019 (BNL-50242)

AMERICIUM ISOTOPES Am-242
neutron fission of, prompt neutron spectra and yield for thermal, (E), 25:10039

AMIDE POLYMERS
radioinduced coloration enhancement in caprone, fast-electron, 25:9552

AMIDES
effects on deuterium exchange between liquid ammonia and hydrogen, 25:8244

AMMONIA
proton reactions at 15 to 150 keV with, cross sections for charge exchange in, (E), 25:9229
NH_3--PH_3, radiolysis of, radical scavenging reactions in γ, 25:8299

AMMONIUM BROMIDES
effects on anodizing reactions of ammonium nitrate with zirconium in aqueous solutions, 25:8832(T) (AEC-tr-7204)

AMMONIUM CHLORIDES
complexes with carbon monoxide and cuprous chloride, carbon-13 exchange reactions with carbon monoxide and, 25:8339(P)
effects on anodizing reactions of ammonium nitrate with zirconium in aqueous solutions, 25:8832(T) (AEC-tr-7204)

AMMONIUM FLUORIDES
effects on anodizing reactions of ammonium nitrate with zirconium in aqueous solutions, 25:8832(T) (AEC-tr-7204)

AMMONIUM IODIDES
effects on anodizing reactions of ammonium nitrate with zirconium in aqueous solutions, 25:8832(T) (AEC-tr-7204)

AMMONIUM NITRATES
reactions with zirconium, effects of halides in aqueous solutions on anodizing, 25:8832(T) (AEC-tr-7204)

AMPHIBIA
Bufo hemiophrys, radiation effects on behavior and survival of, effects of hibernation on cesium-137, 25:8628
Rana pipiens, radiation effects on skin allografts in, effects of 5000 R dose on γ, 25:8620
Rana sp., radiosensitivity of hypothalamo-hypophysical neurosecretory system of, x, 25:8764
ANALYTICAL CHEMISTRY
instruments for, data processing system for, 25:8193 (UCRL-20132)
ANGIOSPERMIDAE
Arabidopsis thaliana, radioinduced growth inhibition, mutations, and tumors in seeds of, RBE for argon ion, carbon ion, helium ion, lithium ion, neon ion, and oxygen ion, 25:8800
Brassica sp., radiation effects on survival of plants of, γ and proton, 25:8755(T) (JPRS-51660)
grasses, iodine-131 content of, following accidental release at La Hague UP 2 plant, 25:8657 (CEA-R-4008)
Hordeum sp., radioinduced mutations in pollen of, strontium-90 β, 25:8648
Hordeum sp., radioinduced mutations in, γ, 25:8656
Morus alba, radiation effects on growth of flower buds, pollen grains, and pollen tetrads of, effects of dose on γ, 25:8794(T) (NSJ-tr-158)
Raphanus sp., radiation effects on survival of plants of, γ and proton, 25:8755(T) (JPRS-51660)
Tradescantia sp., radiation dosimetry for, monoenergetic neutron, 25:8677 (NYO-2740-7, pp 5-51)
Tradescantia sp., radiation effects on cell number and somatic aberrations in stamen hairs of, RBE for low energy and 0.43 MeV neutron, 25:8756 (NYO-2740-7, pp 154-217)
Triticum durum, radioinduced mutations in, for chlorophyll and spike variation, x, 25:8655
Triticum durum, mutations induced in, by diethyl sulfate and ethylmethanesulfonate, comparison of frequency of fast neutron, thermal neutron, and x-radioinduced mutations with, 25:8641
Triticum durum, radioinduced mutations in, for chlorophyll deficiency and morphological change, fast neutron, thermal neutron, and x, 25:8641
Tritium sp., radiation effects on growth of, RBE for neutron, γ, 25:8801
Vicia faba, radioinduced chromosome aberrations in roots of, effects of 5-azacytidine on x, 25:8639
Vicia faba, radioinduced chromosome aberrations in, effects of nitrosoguanidine on x, 25:8705
Zea sp., ion fluxes in roots of, effects of carbonylcyanide m-chlorophenylhydrazone and uranium oxide ions on chlorine and rubidium, 25:8602
ANILINE
radiolysis at 77 to 120°K, effects of dose and method of preparation on radical yields from electron pulse and γ, 25:8296
ANIMALS
plutonium-239 distribution in organs and tissues of, review of effects of administration route, age, and dose on, 25:8595(T) (LF-tr-41, pp 7-125)
radiation effects on primary virus infections in, review of x, 25:8699
radiation effects on small, effects of energy on microwave, 25:8790
radioinduced lung fibrosis in, following therapy for malignant tumors, pathology of, 25:8791
radioisotope transport in Mediterranean Sea, cesium-137, strontium-90, and uranium-238, 25:8630
virus infections in, review on effects of radiomimetic substances on primary, 25:8699
ANISOLE
radioinduced luminescence of solutions of, in butanol and methanol, α, β, and uv, 25:8274
ANNELIDA
Salmacina incrustans, radiation effects on morphogenesis of buds in, x, 25:8753
ANOXIA
radiation effects on, in bacteria, low energy electron, 25:8811
ANTARCTIC OCEAN
radium-226 content of, south of Australia, effects of calcium carbonate and calcium silicate on, (E), 25:8380
ANTHRACENE
electron channeling at 148 keV in monocrystals of, 25:9543
positron channeling at 247 keV in monocrystals of, 25:9543
radiolysis of crystals of, neutron, 25:8289
ANTIBODIES
production of G and M, in immunized, x-irradiated rabbits following stimulation by gamma globulin, 25:8621
radiation effects on formation of, in mammals, relation of radiosensitivity of lymph system to ionizing, 25:8762
radiation effects on, clone cells in mice following transfer, 25:8769
ANTIMONY
content of human lungs, methods for measurement of, using γ transmission scanning, 25:8726
determination in antimony--sodium alloys by dissolution, filtration, and colorimetry, 25:8198 (BNL-50271)
determination in titanium and titanium dioxide by neutron activation, 25:8233
determination of trace amounts of, in glass by neutron activation after sodium removal by hydrated antimony pentoxide, 25:8223
ANTIMONY ALLOYS AND SYSTEMS
Na--Sb, analysis of liquid, for antimony by dissolution, filtration, and colorimetry, 25:8198 (BNL-50271)
Nd--Sb, neodymium-145 Moessbauer spectrum in NdSb, 25:9594
ANTIMONY IONS
implantation into silicon at 20 keV, enhanced diffusion in high-temperature, 25:9569
ANTIMONY ISOTOPES Sb-121
energy levels from tin-120 proton resonances, spectroscopic factors, spin-parity assignments, and widths for isobaric analog, (E), 25:10044
neutron reactions with, Doppler effect and resonance parameters for 6.24 eV resonance in, (E), 25:10041
performance of activation detectors of, for neutron spectra measurements at 1 eV to 10 keV, 25:8481 (KFK-1233)
ANTIMONY ISOTOPES Sb-123
energy levels from tin-122 proton resonances, spectroscopic factors, spin-parity assignments, and widths for isobaric analog, (E), 25:10044
ANTIMONY ISOTOPES Sb-125
energy levels from tin-124 proton resonances, spectroscopic factors, spin-parity assignments, and widths for isobaric analog, (E), 25:10044
ANTIOXIDANTS
effects on storage life of γ-irradiated unleavened bread in India, 25:8819
ARCTIC REGION
electron concentration at 1000 km in polar, seasonal movement of ionization enhancement of, (E/T), 25:9317
universal time control in ionospheric winter F-region, theories of, (T), 25:9318
volcanic cycles and metallogeny of Novaya Zemlya, 25:10416(T) (UCRL-Trans-10504)
ARGON
abundance determination in 15 chondrites, (E), 25:8968
argon-ion reactions with, oscillations in charge-exchange cross sections for, (T), 25:9236
carbon-ion (C^{++}) reactions below 40 keV with, total cross sections for single-electron capture in, (E), 25:9215
diffusion of helium in, chromatographic determination of, 25:8424(R) (MLM-1768)
electric discharges in, effect of light irradiation on current pulses in electrodeless, 25:9449
electron elastic scattering at low energies by, effective cross sections for, (T), 25:9237
helium-atom reactions at 1.0 keV to 6.4 MeV with, Born cross sections for excitation in, (T), 25:9204
helium-atom reactions at 1.60 to 400 keV with, scaled cross sections for excitation in, (T), 25:9204
ion reactions in eV range with, mechanisms and cross sections for light emission in, (E), 25:9213
isotopic composition of, in 15 chondrites, (E), 25:8968
plasma jet of, effects of condensed phase on velocity and temperature distribution in subsonic, (E), 25:9434
plasma jets of, local thermodynamic equilibrium in, (E), 25:9454
plasma of cesium-seeded, current distribution in nonequilibrium, 25:9482
plasma of, electric conductivity enhancement by electric discharge in, (E), 25:9451
plasma of, electron density and temperature in shock tubes, 25:9418
plasma of, excitation temperature functions of spectra lines of, 25:9172
plasma of, magnetohydrodynamic properties in flowing, in cooled-wall channels, (E/T), 25:9281
plasma of, self-excited steady layers in column discharges, (T), 25:9465
plasma of, spectroscopic diagnostics in shock tubes, 25:9423
proton reactions at 4 to 26 keV with, total cross sections for formation of metastable hydrogen atoms by charge exchange in, (E), 25:9193 (ORO-2591-52)
proton reactions at 75 to 350 keV with, total cross sections for formation of fast excited hydrogen atoms by charge exchange in, (E), 25:9192(R) (ORO-2591-51)
reactions with oxygen molecules, dependence of vibrational transition probabilities on orientation angle in, (T), 25:9226
scattering by thallium fluoride at thermal energies, effects of asymmetric mass distribution on total cross section for, (T), 25:9232
thermodynamic properties of solid, as function of temperature, models for anharmonic, 25:8262 (UCRL-50903)
ARGON IONS
effects on Arabidopsis thaliana seeds, RBE for mutagenic and tumorigenic, 25:8800
effects on optical properties of gallium phosphide at 1.5 and 3 MeV, 25:9562
reactions with argon, oscillations in charge-exchange cross sections for, (T), 25:9236
reactions with gases in eV range, mechanisms and cross sections for light emission in, (E), 25:9213

XUM

scattering by argon ions at 77 and 300°K, intensity of, 25:8424(R) (MLM-1768)
ARGON ISOTOPES Ar-36
concentration by thermal diffusion, rates for, 25:8424(R) (MLM-1768)
mass hexadecapole moments of, Hartree--Fock--Bogolyubov calculations of, (T), 25:10008
ARGON ISOTOPES Ar-38
concentration by thermal diffusion, rates for, 25:8424(R) (MLM-1768)
mass hexadecapole moments of, Hartree--Fock--Bogolyubov calculations of, (T), 25:10008
ARGON ISOTOPES Ar-40
proton elastic scattering by, fine-structure analysis of isobaric analog resonances in, (T), 25:10073
ARGON ISOTOPES Ar-41
use as tracer for studying atmospheric dispersion of stack-released reactor effluents, 25:8363 (AECL-3731)
ARGON SYSTEMS
Ar--H, Stark broadening of resonance lines of neutral, 25:9171
Ar--H--He, plasma properties in dipole magnetic fields, 25:9414
ARIZONA
uranium deposits in Colorado plateau region of, geology and mineralogy of peneconcordant-type, 25:8377
uranium deposits near Grand Canyon, geology and mineralization of Orphan Mine, 25:8376
ARMY REACTORS (PM-3)
operation of 3A, summary of 1969--1970, 25:10297
ARSENIC
determination in air particulates by spark source mass spectrometry, 25:8208
determination in titanium and titanium dioxide by neutron activation, 25:8233
ASTATINE ISOTOPES At-211
reactions with benzene, yields from, 25:8284(T) (ANL-Trans-870)
ASTATINE ISOTOPES At-212
alpha decay of ground-state and isomeric, half-lives for, (E), 25:9966(R) (COO-1265-94)
ATLANTIC OCEAN
strontium-90 deposition at weather stations in, during 1963 to 1970, fallout, 25:8670(R) (HASL-237(App.))
strontium-90 deposition in, 1963 to 1970, relations with land deposition, 25:8368 (HASL-237, pp I.27-37)
ATMOSPHERE
book: Atmospheric Electricity. Vol. I. Fundamentals, Conductivity, Ions, 25:9286(T) (TT-67-51394/1)
cosmic-ray intensity variations in polar cap during Forbush decrease, Jan. 28, 1970, primary, (E), 25:9327
density variations at 300 and 505 km, 1967--1968 semiannual, (E), 25:9304
effluent dispersion in, argon-41 tracer studies of stack, 25:8363 (AECL-3731)
electric processes in, (T), 25:9286(T) (TT-67-51394/1)
fallout content of Ispra site, March to July 1970, 25:8370 (HASL-237, pp III.18-23)
fallout monitoring of, in Australia, Gibraltar, Hong Kong, and UK, Jan. to July 1970, 25:8364 (AERE-R-6556)
fallout scavenging from, by raindrops, chemical tracer studies of, 25:8365(R) (COO-1199-19)
gamma-ray omnidirectional intensities at balloon altitudes, 25:9305
iodine-129 release rates to, foliar contamination and specific activity methods for derivation of working limits for, 25:8681
iodine-131 content of ground-level, near ORNL reactors, comparison of calculated and measured data on, 25:8452 (ORNL-TM-3187)
lead isotope content of surface, at selected land and marine sites during 1963 to 1970, monthly averages of fallout stable, 25:8670(R) (HASL-237(App.))
plutonium-239 content of, in environs of plutonium industry, maximum permissible, 25:8674(T) (LF-tr-41, pp 199-220)
plutonium-239 distribution in Lithuanian, at 30 to 200 m altitude, 1966 to 1968, 25:8372
radiation monitoring in ground-level, at Nevada Test Site, development and operation of air samplers for, 25:8393 (NVO-410-6)
radiation monitoring of, in New Zealand during 1969, β, 25:8675(R) (NP-18529)
radioactive contamination of, in reactor fuel element plant during normal and high-risk operations, evaluation of biological and physical methods for control of, 25:8695
radioactive contamination of, near-nuclear power plants, effects of short-term releases on, 25:8371 (SZS-14/70 (pp 1-10))
radioactivity in Ispra site, from March to July 1970, gross beta, 25:8370 (HASL-237, pp III.18-23)
radioactivity in, from stack-released reactor effluents, accuracy of methods for calculating, 25:8668 (BNWL-SA-3424)
radioactivity monitoring in surface, at selected land and marine sites during 1963 to 1970, monthly averages of fallout gross γ, 25:8670(R) (HASL-237(App.))
radioactivity monitoring of, calibration and sensitivity of G--M, ionization, and scintillation detectors for krypton-85, 25:8467 (BRH/NERHL-70-4)
radioisotope content of surface, at selected land and marine sites during 1963 to 1970, monthly averages of fallout, 25:8670(R) (HASL-237(App.))
thorium-232 distribution in Lithuanian, at 30 to 200 m altitude, 1966 to 1968, 25:8372
tritium oxide of, of industrial, recommendations for maximum permissible, 25:8678(T) (ORNL-tr-2403)
uranium-238 distribution in Lithuanian, at 30 to 200 m altitude, 1966 to 1968, 25:8372
vapor exchange from, effects on tritium content in Crater Lake, Oregon, (E), 25:8347 (CU-2493-11, App.1)
ATMOSPHERES
analysis procedures for fuel element cover gas, in CANDU-type reactors, 25:10227
ATMOSPHERIC PRECIPITATION
effects on tritium content in Crater Lake, Oregon, (E), 25:8347 (CU-2493-11, App.1)
fallout monitoring of, in New Zealand during 1968 and 1969, total β, and content of strontium-89 and strontium-90, 25:8675(R) (NP-18529)
radioisotope content of, at worldwide sites during 1966 to 1970, plutonium-238, plutonium-239, and strontium-90, 25:8658 (HASL-237, pp II.1-16)
strontium-90 content of, over Atlantic Ocean, 1963 to 1970, 25:8368 (HASL-237, pp I.27-37)
ATOMIC CONSTANTS
Rydberg, experimental investigation of theoretical expressions for, 25:9246
ATOMIC ENERGY
development in Europe, review of ENEA activities during 1970, 25:10092(R) (NP-18600)
water uses in, 25:8326
ATOMIC ENERGY COMMISSION (USA)
programs for compensation of personnel for radiaton injuries, 25:8697
ATOMIC ENERGY, LEGAL ASPECTS
legislation related to compensation of personnel for radiation injuries in USA, 25:8697
regulations for shipping of fuel elements, review of East German, 25:8454 (SZS-14/70 (pp 11-21))
ATOMIC MODELS
energy levels of double-well potentials, (E), 25:9248
solutions for Thomas--Fermi--Dirac equation, convergence of series-expansion, 25:9250
ATOMIC STRUCTURE
calculations of, use of truncated multipolar expansion pair functions in, 25:9249
ATOMS
charged-particle reactions with, Born approximation expressions for differential ionization cross sections for, (E), 25:9195 (SC-RR-70-773)
electron elastic scattering by, use of local exchange potential in relativistic Hartree--Fock theory of, 25:9237
electron inelastic scattering at high energies by, linear-response theory of inelastic, 25:9217
electron scattering at intermediate energies by, (T), 25:9214
energy levels of, definition of quasi-stationary states, 25:9209
energy levels of, Hartree--Fock calculations of autoionization states, 25:9252
energy of ground-state two-electron, calculation using configuration-interaction wave functions and correlation factor, 25:9242
energy-density gradient in, effects of correlation correction on convergence in expansion of Thomas--Fermi, 25:9245
photon emission from system of N identical two-level, master-equation approach to spontaneous, 25:9244
photon reactions with subshells of Z = 2 to 54, ionization cross sections for, 25:9194 (SC-RR-70-721)
properties of Z = 2 to 126 calculated from relativistic Hartree--Fock--Slater wave functions, tables of, 25:9168 (ORNL-4614)
reactions with diatomic molecules, classical treatment of classically forbidden transitions in, 25:9227
reactions with diatomic molecules, dependence of vibrational transition probabilities on orientation angle in, (T), 25:9226
reactions with diatomic molecules, effects of mass and well depth on quantum vibrational transition probabilities in, (T), 25:9230
reactions with diatomic molecules, semiclassical treatment of transition probabilities for dissociation in, 25:9197
reactions with diatomic molecules, vibrational excitation in, (T), 25:9228
reactions with ions at low energies, method for measurement of excitation transfer in, 25:9238
reactions with molecules at thermal energies, effects of asymmetric mass distribution on, (T), 25:9232
wave functions for, construction using combination of gaussian and Slater-type orbitals, 25:9243
wave functions for, Hartree--Fock solutions and symmetry properties of self-consistent-field spin orbitals, 25:9247
AURORAL ZONE
conjugate point phenomena in, review of, (E/T), 25:9284(T) (JPRS-52023)
electric field intensity across ionospheric arc boundary, measurements of parallel and perpendicular, (E),

25:9303
electric field intensity in ionospheric, Langmuir-probe dc detector for, (E/T), 25:9301
radar echoes in southern, ssociation of x rays with diffuse and discrete, (E), 25:9320
x-ray emission in, associated with geomagnetic storm sudden commencement, July 27, 1966, (E), 25:9298
AUSTENITE
analysis for boron by neutron irradiation and alpha track autoradiography, 25:8235
AUSTRALIA
uranium reserves in, estimates of, 25:8373
AUTORADIOGRAPHY
literature published during 1969, documentation of quantitative α, 25:8584 (SZS-15/70)
methods using carbon-14 and tritium with overlaying emulsion layers for studies of labeling index in cells, 25:8589
AVES
Gallus sp., synthesis of nucleic acids in embryos of, following infection with ultraviolet-irradiated vesicular stomatitis virus, 25:8806
5-AZACYTIDINE
effects on x-radioinduced chromosome aberrations in Vicia faba, 25:8639

B

BACTERIOPHAGES
kappa, radioinduced mutations in, for clone formation, uv, 25:8653
lambda, radioinduced, in Escherichia coli mutants, uv, 25:8633 (NP-18483)
T3, radiation effects on transforming DNA in, protective effects of acridine orange against cesium-137 γ, 25:8707
T4, radiation damage to, repair replication of uv, 25:8636 (SU-326-P-7-X-22)
T7, induced inactivation of, by hydrogen atoms and radicals, 25:8808
T7, radioinduced inactivation of, electron and uv, 25:8808
BARIUM
abundance in eucrites, (E), 25:8966
abundance in meteorites and lunar samples, (E), 25:8965
determination in air particulates by spark source mass spectrometry, 25:8208
determination in titanium and titanium dioxide by neutron activation, 25:8233
BARIUM IONS
effects on calcium-45 efflux in myometrium of rats, 25:8601
BARIUM ISOTOPES Ba-138
electron reactions (e,e'p) with, proton spectra and excitation functions for, (E), 25:10053
photon reactions (γ,π⁺) at 150 to 700 MeV, yields and cross sections for, (E), 25:9620 (LUNP-7007)
BARIUM NITRITES
$Ba(NO_2)_2$--$BaSO_4$, radiolysis of crystals of, yields of nitrite radicals from γ, 25:8286
BARIUM SULFATES
sorptive properties for cerium, strontium, and zirconium from effluents from chemical decanning of reactor fuel elements, 25:8344(P)
$Ba(NO_2)_2$--$BaSO_4$, radiolysis of crystals of, yields of nitrite radicals from γ, 25:8286
BARIUM ZIRCONIUM SULFIDES
microstructure of, 25:8920
preparation and properties of, 25:8920
BARYONS
decay of, duality constraints on P-wave, (T), 25:9744
interactions with antibaryons, quark focusing principle for, 25:9760
interactions with baryons and mesons in quark model, breakdown of Pomerancuk conjecture for, (T), 25:9806
interactions with mesons, consistency conditions from duality for, (T), 25:9792
interactions with mesons, duality constraints on amplitudes for, 25:9799
Lagrangian model of chiral SU(3) x SU(3) with symmetry breaking in, 25:9794
mass differences and hyperon nonleptonic decay amplitudes in broken SU(3), relations between, 25:9830
matrix elements of, weak current--current quark Hamiltonian for octet behavior of, 25:9761
symmetry group SO(4,2) and three-dimensional canonical algebra for, relation between, 25:9832
BARYONS (ANTIPARTICLES)
interactions with baryons, quark focusing principle for, 25:9760
BARYONS, RESONANCE
decay of, review of spin and parity determination from, (T), 25:9774
parity and spin of, review of determination from particle production and decay, (T), 25:9774
production of aleph, in proton reactions with nuclei at 80 TeV in emulsions, (E), 25:9641
production of, review of spin and parity determination from, 25:9774
BARYONS, RESONANCE (N*)
decay of two- and three-baryon, quasi-nuclear model for, (T), 25:9803 (ITEF-759)
decay of, simple harmonic forces in nonrelativistic quark model for widths of, (T), 25:9788
interactions Δ + N, quasi-nuclear model for production of two- and three-baryon resonances in, (T), 25:9803 (ITEF-759)
mass and width of pπ⁻(1400) enhancement in K⁻ + n → K⁻ + π⁻ + p interactions at 12.6 GeV/c in bubble chamber, (E), 25:9658 (TID-25611)
production in e + p → e + N* interactions, simple harmonic forces in nonrelativistic quark model for, (T), 25:9788
production in γ + N → Δ(1236) + π interactions at 0.7 to 1 GeV, angular distribution asymmetry of π emission in, (T), 25:9798
production in γ + N → π + N interactions, simple harmonic forces in nonrelativistic quark model for, (T), 25:9788
production in p + p → p + N* interactions, surface excitation model for, (T), 25:9808
production of (2290) enhancement in π⁻ + p → π⁻ + p interactions at 1.71 to 5.53 GeV/c, scintillation counter spectrometer study of, (E), 25:9652 (COO-1764-112)
production of anti Δ⁻⁻(1236) in anti p + d → anti p + d(p + n) + π⁺ + π⁻ and anti p + d → anti p + d + π⁺ + π⁻ + π⁰ interactions at 7.0 GeV/c in bubble chamber, (E), 25:9636 (TID-25610)
production of d* enhancement in anti p + d → anti p + d(p + n) + π⁺ + π⁻ and anti p + d → p + d + π⁺ + π⁻ + π⁰ interactions at 7.0 GeV/c in bubble chamber, (E), 25:9636 (TID-25610)
production of Δ(1236) in e + p → e + p + π⁰ interactions, angular distributions and cross sections for, (E), 25:9625
production of Δ⁺⁺(1236) and Δ⁻(1236) in π⁺ + p → p + 2π⁺ + π⁻ and π⁺ + p → p(n) + 2π⁺ + π⁻ + π⁰(π⁺) interactions at 2.34 GeV/c, cross sections for, (E), 25:9662
production of Δ⁺⁺(1236) in π⁻ + p → p + π⁺ + 2π⁻ interactions at 4.47 GeV/c in hydrogen bubble chamber (E), 25:9655 (ITEF-767)
production of Δ⁺⁺(1236) with mesons in π⁺ + p interactions at 18.5 GeV/c, (E), 25:9677
production of nπ⁻π⁻(1627) enhancement in K⁻ + d → p + π⁺ + π⁻ + π⁻ + n + anti K⁰ interactions at 4.91 GeV/c, (E), 25:9671
production of P_{11}(1470) in γ + p → n + π⁺ interactions at 260 to 350 MeV, (E), 25:9623
production of pπ⁻(1400) enhancement in K⁻ + n → K⁻ + π⁻ + p interactions at 12.6 GeV/c in bubble chamber, (E), 25:9658 (TID-25611)
production of two- and three-baryon, in Δ + N interactions, quasi-nuclear model for, (T), 25:9803 (ITEF-759)
BARYONS, RESONANCE (Y*)
elasticity of Σ(2030) from K⁻ + n → K⁻ + n interactions at 1860 to 2150 MeV, (E), 25:9681
production of Σ(1910) in K⁻ + p → Λ + π⁰ interactions at 1.865 to 2.001 GeV in hydrogen bubble chamber, (E), 25:9659 (UCRL-19789)
properties of Σ(1910) from K⁻ + p → Λ + π⁰ interactions at 1.865 to 2.001 GeV in hydrogen bubble chamber, (E), 25:9659 (UCRL-19789)
BEAM SEPARATORS
operation of rf iris waveguide, in EH_{12} mode, 25:9939
BEAMS
kinetics of fermion, point process with multicoincidences in, (T), 25:9692
BEARINGS
design and development of liquid metal-lubricated, research program for, 25:8394(R) (NYO-3930-7)
BELGIUM
radioisotope content of human diet in, during 1968, cesium-137, and strontium-90, 25:8624 (EUR-4509)
BELOYARSK POWER REACTOR, UNIT 1
cooling system for, reliability of operation of, (T), 25:10106
BENZENE
carbon ion reactions with, at -196°C and 3 to 15,000 eV, yields from, 25:8311
proton reactions at 15 to 150 keV with, cross sections for charge exchange in, (E), 25:9229
reactions with astatine-211 and iodine-125, yields from, 25:8284(T) (ANL-Trans-870)
benzene--SiH_4, ionization in mass spectrometer, reactions of products from, 25:8294
BENZENE, ASTATO-
boiling point of, method for measuring, 25:8259(T) (ANL-Trans-869)
yields from reactions of benzene with astatine-211, 25:8284(T) (ANL-Trans-870)
BENZENE, IODO-
yields from reactions of benzene with iodine-125, 25:8284(T) (ANL-Trans-870)
BERYLLIUM
determination by neutron activation, automatic sample changer for, 25:8220 (Y-1744)
determination by photon activation in linac, 25:8225
effects of additions of, on stress corrosion of chromium--iron--nickel alloys by boiling magnesium chloride solutions, 25:8834(R) (COO-2069-6)

XUM

magnetic susceptibility of, total and electron-spin, (E), 25:9578
plasmon emission spectrum of electron-bombarded films of, 25:9554
Raman effect in crystals of, model potential calculation of first derivative of electronic polarizability for first-order, 25:9598
wave functions for, based on combination of gaussian and Slater-type orbitals, 25:9243
BERYLLIUM ALLOYS AND SYSTEMS
Be--Cr--Fe-base--Ni, corrosion by water containing trace chloride and oxygen at 200°C, stress, 25:8834(R) (COO-2069-6)
Be--Si--U, crystal structure of ordered solid solution of, 25:8947
Be--Si--U, phase studies of ordered solid solutions of, 25:8888
BERYLLIUM FLUORIDES
BeF_2--LiF, preparation and handling of molten, for use as MSRE coolant salt, 25:10211 (ORNL-4616)
BeF_2--LiF--NdF_3--ZrF_4, distillation of molten, removal of neodymium fluoride by low-pressure, (E), 25:10210 (ORNL-4434)
BeF_2--LiF--UF_4--ZrF_4, preparation and handling of molten, for use as MSRE fuel salt, 25:10211 (ORNL-4616)
BERYLLIUM IONS
photon reactions with Be^{2+}, calculation of resonances between first and second ionization thresholds in, using diagonalization method, 25:9239
BERYLLIUM ISOTOPES Be-8
alpha decay of, ionization detector system for spectra measurements in, 25:8513
energy level at 4.5 MeV from lithium-7 (d,n) reactions, (E), 25:9975 (JINR-P15-5143)
BERYLLIUM ISOTOPES Be-9
alpha reactions ($\alpha,2\alpha$) at 56 MeV, analysis using triangular graphs, (T), 25:9987
carbon-12 elastic scattering at 12 to 25 MeV, differential cross sections for, (E), 25:9988
carbon-12 reactions (C-12,C-13) at 12 and 15 MeV, differential cross sections for, (E), 25:9988
electron inelastic scattering by, energy spectra from, (E), 25:10014
energy levels of, neutron spectroscopic factors for, (E), 25:9988
helium-3 elastic scattering at 13 to 27 MeV, angular distributions for, (E/T), 25:9994
helium-3 reactions (He-3,2γ) at 1.67 to 1.76 MeV, excitation functions for, (E), 25:9972 (ANU-P-496)
neutron elastic scattering at 14.6 MeV, differential cross section angular distributions from, (E), 25:9995
oxygen-16 elastic scattering at 12 to 25 MeV, differential cross sections for, (E), 25:9988
oxygen-16 reactions (O-16,O-17) at 11 to 18 MeV, differential cross sections for, (E), 25:9988
triton reactions (t,n) at 1.10 MeV, angular distributions for, (E), 25:9976 (JINR-P15-5148)
BERYLLIUM NITRIDES
thermodynamic properties of Be_3N_2 at 20 to 315°K, thermal capacity measurements for determining, 25:8939
BERYLLIUM OXIDES
effects of dispersions of, on properties of copper, 25:8873
fabrication of fine-grained and high-density, evaluation of methods for, 25:8937
mechanical properties of, review of effects of microstructure on, 25:8937
radiation effects on modulus of rupture of polycrystalline, relations of heat treatment with fast neutron, 25:8959
BETA DECAY
Kurie plots for allowed, finite nuclear size and radiative corrections in the construction and assessment of, (T), 25:10062 (RLO-1388-131)
unique first-forbidden transitions in, (T), 25:10064
BETA PARTICLES
detection of low-level, miniature end-window ionization detector for, 25:8521
dosimetry in castings for implanted radioapplicators for therapy of epitheliomas, 25:8684
effects on excitation of butanol and ethanol in presence of luminescing additives, 25:8274
effects on heart function following scanning using iodine-131-labeled albumin macroaggregates, 25:8713 (UCLA-12-798)
emission following shutdown of thermal reactors, sources of, (T), 25:10165 (CISE-R-233)
emission from fission products, data tabulation of abundances and energies of, 25:10023 (CEA-N-1372)
BETA SOURCES
activity in honey, comparison of artificial and natural, 25:8665
dose distribution from contact tritium, 25:8437
monitoring of low-level, in gases internally-loaded G--M detector for, 25:8520
BETA SPECTROMETERS
detector for magnetic, position-sensitive proportional, 25:8472 (JUL-CONF-4, pp 22-9)
BETATRONS
beam intensity of 35-MeV, system for monitoring fluctuation of, 25:9936
BIBLIOGRAPHIES
on geology and hydrology of Nevada Test Site, 25:8355 (USGS-474-88)
on medical status of atomic bomb survivors and their offspring in Hiroshima and Nagasaki during 1969, 25:8741 (ABCC-TR-0-69)
on microscopic neutron data, supplement to CINDA 69, 25:9946 (TID-25165(Suppl.2))
on plutonium with appendix on transplutonium elements, index to 3rd quarter 1970, 25:8831
on plutonium with appendix on transplutonium elements, Oct., 1970, 25:8830
on production and industrial uses of radioisotopes, 25:8428 (ORNL-IIC-30(Pt.3))
on radiation accidents in nuclear installations, 25:8661 (JAERI-4052)
on tunneling, 25:8444 (ORNL-HUD-17)
on uses of metastable technetium-99 for scanning, 25:8712 (ORNL-TM-2091(Suppl.1))
BIG ROCK POINT POWER REACTOR
fuel elements for, technical specifications for instrumented type F, 25:10138 (DOCKET-50155-56)
fuel elements for, technical specifications for new centermelt, 25:10139 (DOCKET-50155-57)
BIOCHEMISTRY
research at AECL during 1970, progress report on, 25:8666(R) (AECL-3728)
BIOLOGICAL MATERIALS
analysis by neutron activation, 25:8227
radiation effects on, effects of dose on RBE for low energy fast neutron, 25:8756 (NYO-2740-7, pp 154-217)
BIOLOGICAL MODELS
development for predicting radioisotope transport in food chains of nuclear explosion-contaminated tropical ecosystems, 25:8626
BIOLOGICAL STRESS
effects of, induced by pressure, on x-radiosensitivity of dogs, 25:8766
BIOLOGY
research at AECL during 1970, progress report on, 25:8666(R) (AECL-3728)
BIOPHYSICS
research at Columbia Univ., July 1, 1970, 25:8676(R) (NYO-2740-7)
BIPHENYL
radioinduced luminescence of solutions of, in butanol and methanol, α, β, and uv, 25:8274
BISMUTH ALLOYS AND SYSTEMS
Bi--Pb, electron diffraction patterns at very low temperatures, 25:10410(T) (UCRL-Trans-1414)
BISMUTH ISOTOPES Bi-209
deuteron reactions (d,p) with, analysis using calculated form factors, (T), 25:10067
electron reactions (e,e'p) with, proton spectra and excitation functions for, (E), 25:10053
helium-3 fission at 22 to 34 MeV, delayed-neutron curves from, (E), 25:10056
neutron scattering by polycrystalline, calculation of total coherent cross section for, (T), 25:9958
photon reactions at 1 GeV, analysis of fission processes in, (E/T), 25:10037
proton reactions (p,n) and (p,np) at 24 to 30 MeV, ground-state studies by, (E/T), 25:10045
BISMUTH ISOTOPES Bi-214
content in man at various time intervals following ingestion of radium-226, methods for calculation of, 25:8669 (COO-2088-1)
BISMUTH TELLURIDES
properties for use in thermoelectric converters, 25:8421 (AERE-M-1594)
BLACK HOLES
mass of, concepts of irreducible, (T), 25:9153
production in nonspherical gravitational collapse, (T), 25:9155
transformations in, concepts of reversible and irreversible, (T), 25:9153
BLADDER
radiation dose to human, during intracavitary therapy of female gynecological carcinomas, γ, 25:8679 (SZS-6/70, pp 9-18)
BLOOD
analysis for iron-55, proportional detector for, 25:8466 (BNWL-SA-3624)
circulation in liver of swine, xenon-133 tracer study of in vitro, 25:8783
circulation in resting muscle, xenon-133 tracer study of effects of glucose and insulin on, 25:8586
radioisotope content of, of rats following inhalation and intramuscular injection of americium-241, curium-242, plutonium-238, and plutonium-239, 25:8590 (CEA-CONF-1658)
BLOOD CELLS
transplantation of hematopoietic, into irradiated recipients, review of factors affecting immune reactions following, 25:8616
BLOOD PLASMA
cortisol content of normal, double isotope derivative technique for measuring, 25:8585
tritium-labeled desacetyl-lanatoside C content of, of cardiopathic patients, 25:8724
BLOOD SERUM
radiation effects on coeruloplasmin activity in, of rats,

x, 25:8612
radiation effects on content of albumins and globulins in, of rabbits, microwave, 25:8784
radioinduced changes in lysozyme content of, in rabbits, uv, 25:8782
BLOWERS
development of helium, for gas cooled reactors, 25:10166 (GA-10265)
BOHUNICE POWER REACTOR, UNIT 1
pressure vessel for, pretightening procedures for flange joints on, (E/T), 25:10096 (ZJE-65)
pressure vessel for, radiation effects on mechanical properties of steel, 25:8900 (ZJE-90)
pressure vessel for, radiation effects on welds in steel, 25:8901 (ZJE-91)
BOILERS
design criteria for pressurized water reactor, analysis of aseismic, (E/T), 25:10248
development for gas cooled reactors, 25:10166 (GA-10265)
materials for steam, development of advanced, 25:8838 (ORNL-4600, pp 282-6)
BOILING
characteristics of departure from nucleate, in rod bundles during pressure blowdown, (E), 25:8418
heat transfer in pool, effects of bubble stabilization in vertically vibrating liquid column on, (E), 25:8419
heat transfer in sodium incipient pool, effects of inert gas partial pressure variations on, 25:8415
BONE MARROW
radiation effects on hematopoiesis in, of rats, effects of dose rate on, 25:8608
radioprotective effects of transplants of, on mice, effects of pre- and post-exposure splenectomy on x, 25:8706
transplantation into irradiated dogs, man, and monkeys, review of methods for, 25:8617
BONES
plutonium-239 content of, review of effects of administration route, age, and dose on, 25:8595(T) (LF-tr-41, pp 7-125)
radiation dose to, following different routes of administration of plutonium-239, maximum permissible, 25:8596(T) (LF-tr-41, pp 127-97)
radiation processing of human, for use in transplants, electron spin resonance study of paramagnetic species following γ, 25:8825
radioinduced fractures of human, following ingestion of radium-226, effects of dose and dose rate on, 25:8669 (COO-2088-1)
radioinduced lesions in human, following ingestion of radium-226, radiographic diagnosis of, 25:8669 (COO-2088-1)
radioinduced neoplasms in, of man, following ingestion of radium-226, effects of dose and dose rate on, 25:8669 (COO-2088-1)
radioisotope content of, of rats following inhalation and intramuscular injection of americium-241, curium-242, plutonium-238, and plutonium-239, 25:8590 (CEA-CONF-1658)
scanning of human, for diagnosis of non-union of fractures, use of strontum-85 for, 25:8720
strontium-85 accumulation in benign and malignant tumors of human, correlation of data with microscopic data, 25:8597
BOR-60 REACTOR
fuel element testing in, plans for, 25:8896(T) (BNWL-tr-57)
BORON
determination in air particulates by spark source mass spectrometry, 25:8208
determination in alloys and metals by neutron irradiation and alpha track autoradiography, 25:8235
effects on annealing of electron irradiation damage in p-type silicon, 25:9549
effects on creep in shielded metal-arc welds in stainless steel, 25:8849 (ORNL-4600, pp 142-6)
BORON CARBIDES
chemical composition of commercial-grade, 25:8912 (ORNL-4600, pp 167-74)
fabrication of agglomerated neutron moderators of, 25:8919(P)
microstructure of hot-pressed pellets of, 25:8912 (ORNL-4600, pp 167-74)
preparation of capsules of, for radiation testing, 25:8912 (ORNL-4600, pp 167-74)
BORON ISOTOPES B-10
deuteron reactions (d,2γ) at 2.66 to 2.84 MeV, excitation-function ratios from, (E), 25:9972 (ANU-P-496)
deuteron reactions (d,α) and (d,p) at 2.61 to 2.96 MeV, excitation-function ratios from, (E), 25:9972 (ANU-P-496)
helium-3 elastic scattering at 13 to 27 MeV, angular distributions for, (E/T), 25:9994
helium-3 elastic scattering at 14 MeV, optical-model analysis of angular distributions from, (E/T), 25:9993
helium-3 reactions (He-3,t) at 11 to 17 MeV, excitation functions and microscopic-model analysis of angular distributions from, (E/T), 25:9993
separation from boron-11 by chemical fractionation between boron trifluoride and its addition compounds, 25:8329
BORON ISOTOPES B-11
carbon-12 reactions (C-12,Li-7) at 72 to 100 MeV, energy spectra and angular distributions for, (E), 25:9986
energy levels from beryllium-9 (t,n) reactions, (E), 25:9976 (JINR-P15-5148)
helium-3 elastic scattering at 13 to 27 MeV, angular distributions for, (E/T), 25:9994
helium-3 elastic scattering at 14 MeV, optical-model analysis of angular distributions from, (E/T), 25:9993
helium-3 reactions (He-3,t) at 11 to 17 MeV, excitation functions and microscopic-model analysis of angular distributions from, (E/T), 25:9993
photon reactions (γ,π⁻) at 150 to 700 MeV, yields and cross sections for, (E), 25:9620 (LUNP-7007)
separation from boron-10 by chemical fractionation between boron trifluoride and its addition compounds, 25:8329
BORON NITRIDES
analysis for nitrogen, evaluation of chemical methods for, 25:8195 (AERE-R-6491)
BORON SYSTEMS
B--Mn--rare earths, crystal structure of $RMnB_4$, 25:8948
B--rare earths--V, crystal structure of RVB_4, 25:8948
BOSONS
field algebra for, fermion states in, 25:9850
field of spinless, model with nonlinear phi⁴ selfinteraction in two-dimensional space time for, (T), 25:9849
interactions in system of two neutral spinless, analytical properties of exactly solvable nonrelativistic two-channel, (T), 25:9772
interactions with spin-$^1/_2$ fermions, invariant-amplitude contributions of box diagrams in pseudoscalar, 25:9795
mass splitting of infinitely-degenerate, 25:9711
operators in SU(1,1) quasi-spin formalism, homogeneous canonical transformation of, 25:9822
properties of dense gas of, low-temperature, 25:9605
theory for, Hamiltonian implying exclusion principle in, (T), 25:9689 (LNF-70/22)
wave equations for spin-1, and -2, in de-Sitter space, (T), 25:9700
BOSONS, INTERMEDIATE-VECTOR
production of W pairs from γ + e interactions, cross sections for, (T), 25:9707
BRAIN
activity of, effects of training nervous processes on, 25:10411(T) (UCRL-Trans-1424)
radiation effects on content of albumins and globulins in, of rabbits, microwave, 25:8784
radiation effects on excitability of, of rats, effects of dose on proton and x, 25:8758(R) (UCB-34-P-82-10)
radiation effects on medulla oblongata tissue of, in rats, ultrastructural study of whole-body γ, 25:8787
radiation effects on, of cats, effects of, on spinal cords, x, 25:8771
radiosensitivity of hypothalamo-hypophysical neurosecretory system of amphibian, x, 25:8764
scanning for diagnosis of herpes hominis virus encephalitis in human, use of metastable technetium-99-labeled pertechnetate for, 25:8718
scanning for differential diagnosis of focal lesions in, evaluation of diagnostic results using iodine-131-labeled serum albumin, mercury-203-labeled neohydrin, or metastable technetium-99-labeled pertechnetates for, 25:8710 (NP-18560)
scanning of human, for diagnosis of cerebral abscesses, gammagraphic, 25:8714
scanning of human, use of radioisotope scanner in combination with digital computer for multiple view sectional, 25:8727
BREATH
tritium oxide content of expired, of ndustrial personnel, recommendations for maximum permissible, 25:8678(T) (ORNL-tr-2403)
BREMSSTRAHLUNG
dose to skin and whole-body of man following continuous exposure during one year to krypton-85 dispersed in atmosphere, calculation of, 25:8667 (BNWL-SA-3233)
reactions (γ,f) with plutonium-239, cross sections and angular anisotropy of, (E), 25:10024 (FEI-190)
reactions (γ,n) with fluorine-19, nitrogen-14, oxygen-16, and phosphorus-31 at 100 to 800 MeV, excitation functions for, (E/T), 25:9977 (LUNP-7009)
reactions (γ,p) with silicon-30 and 100 to 800 MeV, excitation functions for, (E/T), 25:9977 (LUNP-7009)
reactions with bismuth-209 and gold-197 at 1 GeV, analysis of fission processes in, (E/T), 25:10037
BROMINE
content of flour, neutron activation analysis for, 25:8588
determination in air particulates by spark source mass spectrometry, 25:8208
determination in airborne particulates by neutron activation, 25:8231
deuterium scattering by molecular, comparison of hydrogen scattering with, 25:8256
BROMINE ISOTOPES Br-79
effects on bromide center spectra in potassium iodide, 25:9585
BROMINE ISOTOPES Br-81
effects on bromide center spectra in potassium iodide,

XUM

25:9585
performance of activation detectors of, for neutron spectra measurements at 1 eV to 10 keV, 25:8481 (KFK-1233)
BROMINE ISOTOPES Br-82
toxicity of ethylene dibromide labeled with, to man following ingestion of contaminated flour, calculations for, 25:8600
BROMOPYROGALLOL RED
uses in colorimetric determination of hexavalent molybdenum, 25:8212
BROOKHAVEN ALTERNATING-GRADIENT SYNCHROTRON (AGS)
beam extraction for, ribbon effect in superconducting septum magnet for resonance, 25:9903 (BNL-15368)
BUBBLES
stabilization in vertically vibrating liquid column, effects on pool boiling heat transfer, (E), 25:8419
BUTANE, 1-BROMO-
radioinduced isomerization at 150 to 240°C, γ, 25:8279
BUTANEDIOL
yields from γ radiolysis of aqueous ethanol solutions as function of nitrate concentration, 25:8301
1-BUTANOL
radioinduced excitation in presence of luminescing additive, α, β, and uv, 25:8274

C

C-129 (NIOBIUM ALLOY)
microstructure of creep rupture specimens of, 25:8851 (ORNL-4600, pp 186-97)
CABLES
current flow model for superconducting transmission line, (T), 25:9377
response of multiconductor, to excitation at open break in shield, 25:10372 (SC-CR-70-6152)
CADMIUM
alpha inelastic scattering at 28 MeV, validity of the Austern--Blair method for, (T), 25:9991
determination in liquid cadmium--sodium alloys by dissolution, filtration, and EDTA titration, 25:8198 (BNL-50271)
effects on embrittlement of cadmium-coated aluminum--molybdenum--titanium--vanadium and aluminum--titanium--vanadium alloys, relations with stress, temperature, and time, 25:8879
properties as filter in activation analysis using reactor neutrons, 25:8226
quasi-particle creation in superconducting, ultrasonic attenuation by, (E/T), 25:9368
CADMIUM ALLOYS AND SYSTEMS
Cd--Na, analysis of liquid, for cadmium by dissolution, filtration, and EDTA titration, 25:8198 (BNL-50271)
CADMIUM ISOTOPES Cd-114
performance of activation detectors of, for neutron spectra measurements at 1 eV to 10 keV, 25:8481 (KFK-1233)
proton elastic scattering at 18.6 MeV, angular distributions for, (E), 25:9966(R) (COO-1265-94)
CADMIUM SULFIDES
ion implantations in, acceptor luminescence by sodium-, lithium-, and neon-, 25:9561
radiation effects on electric conductivity of single crystals of, low-temperature electron, 25:9563
CAFFEINE
effects on photoenzymatic repair in DNA of uv-irradiated Escherichia coli, 25:8649
radioprotective effects of, against mutagenesis and recombination inhibition in yeasts, uv, 25:8637
CALCIUM
abundance in atmospheres of sigma Boo, ν Her, and 41 Cyg, (E), 25:9014
abundance in L and H chondrites, (E), 25:8967
abundance in late G and K dwarfs in the solar neighborhood, (E), 25:8969
content of diet of goats, effects of, on calcium and phosphorus metabolism, 25:8592(R) (COO-1339-43)
content of milk in New York during 1954 to 1970, monthly and annual averages of fallout strontium 90 per gram in relation to, 25:8670(R) (HASL-237(App.))
determination in air particulates by spark source mass spectrometry, 25:8208
determination in titanium and titanium dioxide by neutron activation, 25:8233
effects on separation of strontium from water by ion exchange, 25:8341
CALCIUM CARBONATES
effects on radium-226 content in Antarctic Ocean south of Australia, (E), 25:8380
CALCIUM FLUORIDES
radioinduced thermoluminescence of natural-crystal, emission spectra of gamma, 25:9548
radioinduced trapped hole centers in yttrium- and lutetium-doped crystals of, ESR of x-, 25:9546
CALCIUM IONS
effects on calcium-45 efflux in myometrium of rats, 25:8601
CALCIUM ISOTOPES Ca-40
deuteron reactions (d,Li-6) at 50 MeV, lithium-6 spectra and angular distributions for, (E), 25:9978(R) (ORO-3398-26)
deuteron reactions (d,p) at 19 MeV, angular distributions for, (E), 25:9966(R) (COO-1265-94)
electron inelastic scattering by, energy spectra and form factors from, (E), 25:10014
electron inelastic scattering from, calculation of form factors using Serber--Yukawa residual interactions for, (T), 25:10010
energy levels from electron inelastic scattering with nucleon knockout at high energies, distorted wave analysis of nucleon momenta distributions in, (T), 25:9973 (ITF-70-42)
energy levels from electron inelastic scattering, wave functions for, (T), 25:10010
CALCIUM ISOTOPES Ca-42
alpha reactions (α,d) at 26.5 MeV, deuteron spectra and angular distributions for, (E), 25:9966(R) (COO-1265-94)
alpha reactions (α,pγ) at 11 MeV, proton and gamma spectra and angular correlations from, (E), 25:9996 (ANU-P-466)
CALCIUM ISOTOPES Ca-44
helium-3 reactions (He-3,t) at 29 MeV, angular distributions for, (E), 25:9966(R) (COO-1265-94)
CALCIUM ISOTOPES Ca-45
efflux in myometrium of rats, effects of barium ions, calcium ions, EDTA, and tetracaine on, 25:8601
transport in food chains of nuclear-explosion-contaminated estuarine and marine ecosystems in relation to daily ingestion by man, use of stable element content of fish and invertebrates for predicting, 25:8627
CALCIUM ISOTOPES Ca-47
metabolism in dairy cattle, effects of gestation, lactation, and parturition on, 25:8592(R) (COO-1339-43)
metabolism in goats, 25:8592(R) (COO-1339-43)
metabolism in rats, effects of estradiol on, 25:8592(R) (COO-1339-43)
use for scanning in diagnostic and metabolic studies, development of computer programs for, 25:8716
CALCIUM ISOTOPES Ca-48
proton elastic scattering by, fine-structure analysis of isobaric analog resonances in, (T), 25:10073
CALCIUM OXIDES
CaO--TiO_2, effects of electrode coating of, on mechanical properties of stainless steel welds, 25:8849 (ORNL-4600, pp 142-6)
CaO--ZrO_2, properties for use as high-temperature electric conductor or insulator, 25:8936
CALCIUM SILICATES
effects on radium-226 content in Antarctic Ocean south of Australia, (E), 25:8380
CALIFORNIUM ISOTOPES Cf-252
effectiveness as source of slow neutron beams for clinical radiography, 25:8709 (DP-1229)
fission of, delayed-neutron curves from spontaneous, (E), 25:10056
fission of, measurement of radiation dose distribution from, 25:8563 (NYO-2740-7, pp 52-110)
fission of, prompt neutron spectra and yield for spontaneous, (E), 25:10039
CALVERT CLIFFS POWER REACTOR, UNIT 1
auxiliary systems for, final safety analysis of, 25:10156 (DOCKET-50317-23)
buildings and structures for, final safety analysis of, 25:10155 (DOCKET-50317-22)
control systems for, final safety analysis of, 25:10155 (DOCKET-50317-22)
cooling system for, final safety analysis of, 25:10155 (DOCKET-50317-22)
electrical systems for, final safety analysis of, 25:10155 (DOCKET-50317-22)
engineered safeguards for, final safety analysis of, 25:10155 (DOCKET-50317-22)
instrumentation for, final safety analysis of, 25:10155 (DOCKET-50317-22)
operations aspects of, final safety analysis of, 25:10156 (DOCKET-50317-23)
quality assurance program for, safety analysis of, 25:10154 (DOCKET-50317-21)
radiation protection systems for, final safety analysis of, 25:10156 (DOCKET-50317-23)
radiation waste processing at, final safety analysis of, 25:10156 (DOCKET-50317-23)
site for, final safety analysis of, 25:10154 (DOCKET-50317-21)
steam and power conversion systems for, final safety analysis of, 25:10156 (DOCKET-50317-23)
technical specifications for, proposed complete, 25:10156 (DOCKET-50317-23)
CALVERT CLIFFS POWER REACTOR, UNIT 2
auxiliary systems for, final safety analysis of, 25:10156 (DOCKET-50317-23)
buildings and structures for, final safety analysis of, 25:10155 (DOCKET-50317-22)
control systems for, final safety analysis of, 25:10155 (DOCKET-50317-22)
cooling system for, final safety analysis of, 25:10155 (DOCKET-50317-22)
electrical systems for, final safety analysis of, 25:10155 (DOCKET-50317-22)

engineered safeguards for, final safety analysis of, 25:10155 (DOCKET-50317-22)
instrumentation for, final safety analysis of, 25:10155 (DOCKET-50317-22)
operations aspects of, final safety analysis of, 25:10156 (DOCKET-50317-23)
quality assurance program for, safety analysis of, 25:10154 (DOCKET-50317-21)
radiation protection systems for, final safety analysis of, 25:10156 (DOCKET-50317-23)
radiation waste processing at, final safety analysis of, 25:10156 (DOCKET-50317-23)
site for, final safety analysis of, 25:10154 (DOCKET-50317-21)
steam and power conversion systems for, final safety analysis of, 25:10156 (DOCKET-50317-23)
technical specifications for, proposed complete, 25:10156 (DOCKET-50317-23)

CANADA
deuterium content of surface waters in, economic importance to AECL of geographic and seasonal variations in, 25:8666(R) (AECL-3728)
uranium reserves in, estimates of, 25:8373

CANALS
construction using underground nuclear explosions, safety and technology of, 25:8388

CARBAMIC ACID, ETHYLNITROSO-, METHYL ESTER
effects on uv-irradiated Escherichia coli, effects of radiation dose with spectrum of mutagenic, 25:8642

CARBON
abundance in 15 Mon A, (E), 25:9042
abundance in iota Ori B, (E), 25:8995
analysis for cesium by thermal neutron activation and γ spectrometry, 25:8230
antideuteron reactions at 25 GeV/c, absorption cross sections for, (E), 25:9639
burning in stars, (T), 25:8987
crushing properties of pyrocarbon-coated particles of glassy, optical and photograhic methods for determination of, 25:8925 (EUR-4501)
deposition in helium cooled reactor cooling systems, kinetics of metal--gas reactions for, (E/T), 25:10195 (DP-Report-500)
determination in metals and ceramics by photon activation, 25:8216 (AERE-R-5363)
effects of additions of, on stress corrosion of chromium--iron--nickel alloys by boiling magnesium chloride solutions, 25:8834(R) (COO-2069-6)
effects on creep in shielded metal-arc welds in stainless steel, 25:8849 (ORNL-4600, pp 142-6)
electron energy losses at 25 keV in evaporated films of, spectra for loss range 20 to 400 MeV, (E), 25:9167
wave functions for, based on combination of gaussian and Slater-type orbitals, 25:9243

CARBON DIOXIDES
carbon-13 concentration by chemical exchange reactions between dibutylamine--triethylamine and, 25:8318 (CU-755-7, Sect.2)
carbon-13 concentration in chemical exchange reactions between dibutylamine--triethylamine and, 25:8320 (CU-755-7, Sect.6)
corrosive effects on graphite, performance of methane and carbon monoxide coolant additives on inhibiting, 25:10201(P)
effects on kinetics of oxidation of tungsten at 670 to 980°C, 25:8841
heat transfer from fuel elements to, superposition method of determining temperature distribution in, 25:8409 (RD/B/N-1755)
ion reactions in eV range with, mechanisms and cross sections for light emission in, (E), 25:9213
labeling with oxygen-15, 25:8711(R) (NYO-3937-2)
reactions with uranium carbide, oxidation, 25:8907 (CEA-Bib-183)

CARBON IONS
abundance in quasars, (E), 25:9074
effects on Arabidopsis thaliana seeds, RBE for mutagenic and tumorigenic, 25:8800
reactions with argon, helium, and neon below 40 keV of C^{++}, total cross sections for single-electron capture in, (E), 25:9215
reactions with benzene at -196°C and 3 to 15,000 eV, yields from, 25:8311

CARBON ISOTOPES
separation by gas chromatography, 25:8333

CARBON ISOTOPES C-11
production in cyclotrons by $^{10}B(d,n)^{11}C$ reaction, 25:8711(R) (NYO-3937-2)

CARBON ISOTOPES C-12
alpha inelastic scattering at 25.9 MeV, validity of the Austern--Blair method for, (T), 25:9991
alpha inelastic scattering at 35 MeV, α--γ angular correlations for, (E), 25:9978(R) (ORO-3398-26)
alpha reactions (α,2α) at 56 MeV, analysis using triangular graphs, (T), 25:9987
electron inelastic scattering by, energy spectra and form factors from, (E), 25:10014
electron inelastic scattering from, calculation of form factors using Serber--Yukawa residual interactions for, (T), 25:10010
energy levels from boron-10 (d,α), (d,p), and (d,2γ) reactions and beryllium-9 (He-3,2γ) reactions, partial widths for, (E), 25:9972 (ANU-P-496)
energy levels from electron inelastic scattering with nucleon knockout at high energies, distorted wave analysis of nucleon momenta distributions in, (T), 25:9973 (ITF-70-42)
energy levels from electron inelastic scattering, wave functions for, (T), 25:10010
helium-3 elastic scattering angular distributions at 13 to 27 MeV, (E/T), 25:9994
helium-3 inelastic scattering at 44 MeV, particle-γ angular correlations for, (E), 25:9978(R) (ORO-3398-26)
helium-3 inelastic scattering up to 30.6 MeV, excitation function for, (E), 25:9990
helium-3 reactions (He-3,d), (He-3,n), and (He-3,p) up to 30.6 MeV, excitation functions for, (E), 25:9989
helium-3 reactions (He-3,n) and (He-3,t) up to 30.6 MeV, excitation functions for, (E), 25:9990
helium-3 reactions (He-3,n) at 9.0 to 13.5 MeV, angular distributions for, (E), 25:9981
meson (π^-) absorption in 1s and 2p bound states, rates of, 25:9982
neon-20 reactions (Ne-20,O-16) at 72 to 100 MeV, energy spectra and angular distributions for, (E), 25:9986
neutron beam scattering by thick layers of, beam polarization and angular distribution from, (T), 25:9949
neutron elastic scattering at 14.6 MeV, optical-model analysis of differential cross sections for, (E/T), 25:9995
oxygen-16 reactions (O-16,C-12) at 72 to 100 MeV, energy spectra and angular distributions for, (E), 25:9986
proton elastic scattering at 1 GeV, differential cross section for, (T), 25:9983
reactions (C-12,4n) and (C-12,5n) with natural platinum at 82 MeV, gamma spectra from, (E), 25:10027 (JINR-E6-5379)
reactions (C-12,Be-9) with carbon-13 at 72 to 100 MeV, energy spectra and angular distributions for, (E), 25:9986
reactions (C-12,C-13) with beryllium-9 at 12 and 15 MeV, differential cross sections for, (E), 25:9988
reactions (C-12,Li-7) with boron-11 at 72 to 100 MeV, energy spectra and angular distributions for, (E), 25:9986
scattering by beryllium-9 at 12 to 25 MeV, differential cross sections for elastic, (E), 25:9988

CARBON ISOTOPES C-13
carbon-12 reactions (C-12,Be-9) at 72 to 100 MeV, energy spectra and angular distributions for, (E), 25:9986
concentration by carbon monoxide-to-methane conversion, rates for, 25:8424(R) (MLM-1768)
concentration by chemical exchange reactions between carbon dioxide and dibutylamine--triethylamine, 25:8320 (CU-755-7, Sect.6)
concentration by exchange reactions in amine carbamate--carbon dioxide systems, 25:8318 (CU-755-7, Sect.2)
concentration in carbamate--carbon dioxide by chemical exchange, rates for, 25:8424(R) (MLM-1768)
concentration in carbon monoxide by distillation, rates for, 25:8424(R) (MLM-1768)
concentration in carbon monoxide by exchange reactions with ammonium chloride--carbon monoxide--cuprous chloride complex, 25:8339(P)
concentration in methane by thermal diffusion, rates for, 25:8424(R) (MLM-1768)
concentration in products from photolysis of carbon monoxide, 25:8331
effects on ESR spectra and hyperfine coupling of diphenylmethyl and 9-fluorenyl radicals, 25:8252
energy levels of, neutron spectroscopic factors for, (E), 25:9988
helium-3 elastic scattering at 14 MeV, optical-model analysis of angular distributions from, (E/T), 25:9993
helium-3 reactions (He-3,t) at 14 MeV, microscopic-model analysis of angular distributions from, (E/T), 25:9993
oxygen-16 elastic scattering at 12 to 25 MeV, differential cross sections for, (E), 25:9988
oxygen-16 reactions (O-16,O-17) at 14 to 20 MeV, differential cross sections for, (E), 25:9988

CARBON ISOTOPES C-14
alpha elastic scattering at 3.5 to 16.5 MeV, angular distributions for, (E), 25:9980
alpha reactions (α,n) at 4.9 to 8.5 MeV, excitation function for, (E), 25:9980
content in southern oceans to 4000 m depths, 1968 and 1969, 25:8381
determination in animal tissues by liquid scintillation counting, 25:8213
toxicity of dieldrin, lindane, and malathion labeled with, to man following ingestion of contaminated flour, calculations for, 25:8600
use as tracer for studies of studies of diurnal variations in mitotic and labeling indexes, method for, 25:8589
use in isotope dilution technique for determining volume of milk in mammary glands of goats, 25:8587
use of nitroquinoline oxide-incorporated, for studying effects of carcinogens on colony formation, DNA, proteins, and RNA in HE cultured cells, 25:8746

XUM

CARBON MONOXIDES
carbon-13 concentration in, 25:8339(P)
complexes with ammonium chloride and cuprous chloride, carbon-13 exchange reactions with carbon monoxide and, 25:8339(P)
corrosion inhibition properties in carbon dioxide coolants, 25:10201(P)
effects on kinetics of oxidation of molybdenum and tungsten at 380 to 980°C, 25:8841
ion reactions in eV range with, mechanisms and cross sections for light emission in, (E), 25:9213
photolysis of, concentration of carbon-13 and oxygen-18 in products from, 25:8331
reactions with uranium carbide, oxidation, 25:8907 (CEA-Bib-183)
CARBON OXIDES
labeling with oxygen-15, 25:8711(R) (NYO-3937-2)
CARBON SYSTEMS
Al--C--Fe--Si--U-base, tensile properties of dilute, at 885 to 1150°F, 25:8867 (NLCO-1060)
C--Nb-base--V--Zr, preparation and properties of corrosion-resistant, for use in nuclear industry, 25:8856(P)
C--steel, failure of pipes of, effects of flaws on loads at, 25:8866 (GEAP-10205)
C--steel, fatigue of pipes of, cracking in low-cycle, 25:8866 (GEAP-10205)
C--steel, fatigue of, effects of BWR environments on low-cycle, 25:8866 (GEAP-10205)
C--steel, preparation for weldability testing, 25:8869 (ORNL-4600, pp 147-52)
C--UO_2, preparation of mixtures of, by reactions of sugar with uranyl nitrate in nitric acid, 25:8923
CARBONYL SULFIDE
photolysis of aqueous solutions of, yields of recoil sulfur from, 25:8312
CARBOXYPEPTIDASE A
conformations of, effects of temperature on, 25:10402 (UCLA-12-802)
interactions with inhibitors and substrates, circular dichroism study of, 25:10401 (UCLA-12-801)
CARDIAC PACEMAKERS
development of plutonium-238-fueled, French program for, 25:8430
heat sources for implantable, CEA program for design and testing of plutonium-238, 25:8425 (NP-18563)
CASCADE SHOWERS
development of initial stage of nuclear 100- to 1000-GeV, secondary interaction contribution to, (T), 25:9731
particle mass and energy distributions in, integral equations for, (T), 25:9708
CATS
radiation effects on spinal cord of, following exposure of brain stem, x, 25:8771
CATTLE
calcium-47 metabolism in, effects of gestation, lactation, and parturition on, 25:8592(R) (COO-1339-43)
CAVITY RESONATORS
mode frequencies of coupled, computer program for least squares fitting of ordered set of, 25:9902 (AECL-3669)
operating parameters of, finite difference equations for, 25:9909 (LNF-70/17)
performance of superconducting high-frequency, 25:9396
CELL DIVISION
radiation effects on rate of, of hematopoietic cells in rats, effects of dose rate on, 25:8608
radoinduced, in Oedogonium cardiacum, effects of dose rate on, 25:8644
CELLS
duplication of chromosome DNA of tumor, 25:8632 (EUR-4526)
elongation of plant, mechanisms in auxin induced, 25:10366 (RLO-2225-T-19-9)
radiation damage to human fibroblasts, repair replication of uv, 25:8636 (SU-326-P-7-X-22)
radiation effects on binding of acridine orange with nucleoproteins in fibroblast, of mice, uv, 25:8770
radiation effects on count of, in stamen hairs of Tradescantia, RBE for low energy and 0.43 MeV neutron, 25:8756 (NYO-2740-7, pp 154-217)
radiation effects on mitosis in, of kidneys of mice following inhalation of radon-220 and whole-body, 25:8763
radiation effects on morphology and physiology of, molecular mechanisms and techniques for demonstrating microbeam laser, ultraviolet, and visible, 25:8744
radiation effects on survival of, in intestinal epithelium of, effects of cell cycle stage on whole-body γ, 25:8785
radiosensitivity of transplants of murine ependymoma, in vivo, 25:8759
repair processes in mammalian, following γ-radioinduced double strand DNA breakage, strand rejoining mechanism for, 25:8605(R) (ORO-2832-85)
CELLS, CULTURED
carcinogenesis in, effects of carbon-14-labeled nitroquinoline oxide on, 25:8746
damage to DNA of mammalian, repair processes following carcinogenic quinoline, 4-nitro-, 1-oxide, 25:8611
mutations induced in Chinese hamster, by 5-bromodeoxyuridine and N-nitrosomethylurea, factors affecting expression of, 25:8638
radiation effects on antibody forming spleen, in mice, 25:8769
radiation effects on Chinese hamster and Vicia faba, comparison of OER and RBE for californium-252 mixed γ and neutron with radium γ, 25:8757 (NYO-2740-7, pp 218-56)
radiation effects on count of Sertoli, and spermatogonia of man, effects of dose on x, 25:8789(R) (NYO-4034-2)
radiation effects on DNA synthesis and mitosis in human cells, x, 25:8743
radiation effects on human, 25:8632 (EUR-4526)
radiation effects on mitosis rate in chicken fibroblast, effects of dose on x, 25:8752
radiation effects on survival of chicken fibroblast, effects of dose on x, 25:8751
radiation effects on survival of mammalian, in vivo, determination of survival curve for, 25:8777
radiation effects on survival of synchronized Chinese hamster, comparison of effects of aeration and hypoxia on californium-252 mixed γ and neutron, cobalt-60 γ, and x, 25:8757 (NYO-2740-7, pp 218-56)
radiation effects on survival of, effects of total dose as function of dose rate on recovery from, 25:8748
radioinduced damage to DNA in mammalian, repair processes following carcinogenic uv and x, 25:8611
radioinduced mutations in Chinese hamster, factors affecting expression of x, 25:8638
CELLS, HeLa
radiation effects on survival of, following (n,α) reaction in cells, effects of boron-10 content on RBE for α and recoil lithium ion, 25:8745
radiation effects on survival of, RBE of, 25:8745
radiosensitivity of, effects of oxygen content on protracted fast neutron, 25:8704
radiosensitivity of, effects of temperature on x, 25:8747
CELLULOSE
benzyl ether, radioinduced grafting of styrene on, γ, 25:8271
CERAMIC MATERIALS
analysis for carbon by photon activation, 25:8216 (AERE-R-5363)
conference on, Ronneby Brunn, Sweden, April 20 to 23, 1969, 25:8933
fabrication and properties of, review of, 25:8937
CEREALS
bread, radiation processing of unleavened, in India, effects of, on storage life, effects of antioxidants on, 25:8819
flour, bromine content, neutron activation analysis for determining, 25:8588
flour, contamination of, by radioisotope labeled pesticides, calculatons for toxicity of, to man, 25:8600
flour, mercury content of, neutron activation analysis for determining, 25:8588
flour, radiation processing of enriched, effects of, on vitamin content, 25:8816
radiation processing of, economic and legal aspects of, in USA during 1967, 25:8813 (NP-18236)
wheat, radiation processing of, effectiveness of γ, 25:8824
CEREBROSIDES
radiation effects on distribution of, in brain of developing rats, x, 25:8758(R) (UCB-34-P-82-10)
CERIUM
determination in titanium and titanium dioxide by neutron activation, 25:8233
effects on colorimetric determination of uranium in fuel reprocessing solutions, 25:8197 (BARC-510)
separation from effluents from chemical decanning of reactor fuel elements by sorption on barium sulfates, 25:8344(P)
CERIUM ALLOYS AND SYSTEMS
Al--Ce--Ni, magnetic properties and phase diagram of CeNi/sub x/Al/sub 2-x/, 25:9576
CERIUM ISOTOPES Ce-133
beta and electron-capture decay of, e--γ coincidence spectra from, (E), 25:10029 (JINR-P6-5200)
CERIUM ISOTOPES Ce-135
beta and electron-capture decay of, e--γ coincidence spectra from, (E), 25:10029 (JINR-P6-5200)
CERIUM ISOTOPES Ce-139
electron-capture decay of γ--γ coincidence spectra from, (E), 25:10029 (JINR-P6-5200)
CERIUM ISOTOPES Ce-140
alpha inelastic scattering at 25.9 MeV, validity of the Austern--Blair method for, (T), 25:9991
electron inelastic scattering at 50 and 60 MeV, energy spectra from, (E), 25:10046
energy levels from cerium-140 electron inelastic scattering at 50 and 60 MeV, radiation widths and spin--parity assignments for, (E), 25:10046
CERIUM ISOTOPES Ce-141
use in isotope dilution technique for determining volume of milk in mammary glands of goats, 25:8587
CERIUM ISOTOPES Ce-144
distribution in uranium dioxide fuels at high burnups, determination by gamma scanning, 25:8951(R) (GEAP-10217)

effects on blood, carcinogenesis, and life span of animals in comparison to plutonium-239, 25:8596(T) (LF-tr-41, pp 127-97)
CERIUM OXIDES
properties for use in dispersion strengthening of aluminum, 25:8860(P)
CeO_2--ThO_2, thermal conductivity of solid solutions of, at 25°C, 25:8932
CeO_2--ZrO_2, properties for use as high-temperature electric conductor or insulator, 25:8936
CERMETS
properties of, effects of stereometric microstructure on, 25:8944 (KFK-1236)
CERN SYNCHROTRON
beam injector for, magnetic field perturbation effects on, 25:9904 (CERN-70-24)
CESIUM
determination in algae, carbon, rocks, and seawater by thermal neutron activation and γ spectrometry, 25:8230
performance of activation detectors of, for neutron spectra measurements at 1 eV to 10 keV, 25:8481 (KFK-1233)
plasma of, Langmuir-probe measurements of electron energy distribution in positive column, (T), 25:9419
plasma of, Stark-broadening measurements for electron density, 25:9421
reactions with cesium and rubidium atoms, total cross sections for elastic scattering and spin exchange in, (T), 25:9202
scattering by potassium and sodium at 0.1 to 0.2 eV, differential cross sections for elastic and spin-exchange, (E), 25:9223
scattering by potassium and sodium at 0.1 to 0.2 eV, analysis of data on differential spin exchange in, (T), 25:9224
scattering by sodium, differential cross sections for spin exchange in, (T), 25:9212
separation from effluents from chemical decanning of reactor fuel elements by sorption on cobalt or nickel ferrocyanide, 25:8344(P)
CESIUM HYDROXIDES
radiation effects on ices of, γ, 25:8272
CESIUM ISOTOPES Cs-137
accumulation in Navicula seminulum, Plectonema boryanum, and Stigeoclonium lubricum, effects of temperature on, 25:8598
content in UK atmosphere and rainwater, Jan. to July 1970, 25:8364 (AERE-R-6556)
content of human diet in Chicago during July 1970, 25:8659 (HASL-237, pp III.14-17)
content of human diet in EURATOM countries during 1968, 25:8624 (EUR-4509)
content of milk in New Zealand during 1968, 25:8675(R) (NP-18529)
distribution in uranium dioxide fuels at high burnups, determination by gamma scanning, 25:8951(R) (GEAP-10217)
effects on behavior and survival of Manitoba toads, effects of hibernation on lethal, 25:8628
ratio to strontium 90 in tap water in New York City during 1965 to 1970, monthly and annual averages of fallout, 25:8670(R) (HASL-237(App.))
removal from rats, effectiveness of Prussian blue for, 25:8662(T) (UCRL-Trans-10488)
transport in Mediterranean Sea ecosystems, 25:8630
use for scanning in diagnostic and metabolic studies, development of computer programs for, 25:8716
use in preference to radium in radioapplicators for interstitial therapy of female gynecological carcinomas, 25:8730 (SZS-6/70, pp 28-35)
CHARGED-PARTICLE BEAMS
energy spread of Gaussian-distributed, in scattering by thin targets, (T), 25:10086
focusing by thin lenses with space charge, calculation of beam envelopes for, 25:9916 (UCRL-19313)
interactions with plasma, nonlinear theory for, 25:9466
interactions with plasma, spectral analysis of oscillations from, (E/T), 25:9535
scattering probability for fast test particles in plasma, (T), 25:9467
CHARGED PARTICLES
currents of quasi-trapped, and interaction with geomagnetic field, (T), 25:9342
currents of quasi-trapped, with discontinuities on day- and nightside of Earth, (T), 25:9347
detection of, response of mineral oil-based liquid scintillation detector for, 25:8511
diffusion in magnetosphere, simulation in trap with magnetic mirrors of, (E/T), 25:9350
effect of streams of, on ionospheric nighttime D region ionization at 90 to 95 km, (E/T), 25:9339
electromagnetic-wave scattering by beams of relativistic, (T), 25:9085
energy flux in radiation belts in 1966, fast, (E), 25:9354
intensity of Z greater than or equal to 1 and Z greater than or equal to 2, distribution by azimuth and zenith in equatorial ionosphere, (E), 25:9349
motion in homogeneous media, angular-spectrum representation of electromagnetic fields produced by, (T), 25:9613
reactions with atoms and ions, Born approximation expressions for differential ionization cross sections for, 25:9195 (SC-RR-70-773)
scattering at high energies, Bethe formula for Coulomb corrections to amplitude of, (T), 25:9704 (NP-18540)
CHEMICAL REACTIONS
conference on isotope effects in, Miami Beach, Fla., April 11, 1967, 25:8243
CHEMISTRY
research at AECL during 1970, progress report on, 25:8666(R) (AECL-3728)
CHIMERAS
radiation effects on immune reactions of bone marrow, in animals and man, review of, 25:8617
CHLORAMPHENICOL
radiosensitivity in relation to sterilization of ophthalmic ointments, 25:8826
CHLORINE
abundance in HD 34452, (E), 25:9056
determination in air particulates by spark source mass spectrometry, 25:8208
determination in airborne particulates by neutron activation, 25:8231
deuterium scattering by molecular, comparison of hydrogen scattering with, 25:8256
CHLORINE IONS
implantation into zinc telluride for p--n junction formation, 25:9560
transport in corn roots, effects of carbonylcyanide m-chlorophenylhydrazone and uranium oxide ions on, 25:8602
CHLORINE ISOTOPES Cl-35
effects on chloride center spectra in potassium iodide, 25:9585
neutron capture by, gamma spectra from thermal, (E), 25:10000 (PH-2)
neutron capture by, γ spectra from, (E), 25:10009
CHLORINE ISOTOPES Cl-36
binding energy, (E), 25:10000 (PH-2)
energy-level transitions from chlorine-35 neutron capture, (E), 25:10009
toxicity of DDT labeled with, to man following ingestion of contaminated flour, calculations for, 25:8600
CHLORINE ISOTOPES Cl-37
effects on chloride center spectra in potassium iodide, 25:9585
performance of activation detectors of, for neutron spectra measurements at 1 eV to 10 keV, 25:8481 (KFK-1233)
CHLORINE ISOTOPES Cl-38
reactions of recoil, with silicon compounds, 25:8310(R) (ORO-3898-2)
CHLOROPHYLL
radioinduced mutations of, in wheat seeds, x, 25:8655
CHLOROPHYTA
Chlamydomonas reinhardii, radiation effects on recovery of, effects of oxygen, effects of dose fractionation on, 25:8795
Chlorella sp., radiation effects on mutation rate and survival of, α, 25:8755(T) (JPRS-51660)
Oedogonium cardiacum, radiation effects on cell division and mitotic delay in, effects of dose rate on, 25:8644
Stigeoclonium lubricum, radioisotope accumulation by, effects of temperature on cesium-137, cobalt-57, iron-59, manganese-54, strontium-85, and zinc-65, 25:8598
CHROMIUM
abundance in HD 34452, (E), 25:9056
abundance in meteorites and lunar samples, (E), 25:8965
analysis for oxygen by inert gas fusion method, evaluation of bath materials for, 25:8194 (AECL-3743)
determination in air particulates by spark source mass spectrometry, 25:8208
determination in airborne particulates by neutron activation, 25:8231
determination in titanium and titanium dioxide by neutron activation, 25:8233
effects on colorimetric determination of uranium in fuel reprocessing solutions, 25:8197 (BARC-510)
electron band structure of, self-consistent calculations, 25:9597
CHROMIUM ALLOYS AND SYSTEMS
Al--Cr--Fe-base--Ni, corrosion by water containing trace chloride and oxygen at 200°C, stress, 25:8834(R) (COO-2069-6)
Be--Cr--Fe-base--Ni, corrosion by water containing trace chloride and oxygen at 200°C, stress, 25:8834(R) (COO-2069-6)
Cr--Fe--Ni, corrosion by water containing trace chloride and oxygen at 200°C, stress, 25:8834(R) (COO-2069-6)
Cr--Fe-base--Ni, corrosion by boiling aqueous magnesium chloride, effects of aluminum, beryllium, or carbon additions on stress, 25:8834(R) (COO-2069-6)
Cr--Fe-base--Ni--Pt, corrosion by water containing trace chloride and oxygen at 200°C, stress, 25:8834(R) (COO-2069-6)
Cr--Fe-base--Ni--Si, corrosion by water containing trace chloride and oxygen at 200°C, stress, 25:8834(R) (COO-2069-6)
Cr--Mo--Ni--stainless steel, analysis for molybdenum using mercaptosuccinic acid, spectrophotometric, 25:8210
Cr--Mo--steel, creep rupture of low-carbon ferritic, at

XUM

900 to 1100°F and 9 to 26 ksi, 25:8895 (BMI-1891, Sect.B)
Cr--Mo--steel, fatigue of pipes of, cracking in low-cycle, 25:8866 (GEAP-10205)
Cr--Mo--steel, preparation for weldability testing, 25:8869 (ORNL-4600, pp 147-52)
Cr--Mo--steel--V--W, analysis for molybdenum using mercaptosuccinic acid, spectrophotometric, 25:8210
Cr--N--Pu, phase studies of, 25:8910 (ORNL-4600, pp 41-56)
Cr--Nb--Ni-base, plastic deformation of precipitation-hardened, at 700°C, mechanisms of, 25:8884
Cr--Ni--stainless steel, analysis for molybdenum using mercaptosuccinic acid, spectrophotometric, 25:8210
Cr--Pt-base--Ti, properties for use as radioisotope fuel capsule material, 25:8850 (ORNL-4600, pp 181-5)
Cr--Tb, phase diagram of, 25:8889
CHROMIUM NITRIDES
analysis for nitrogen, evaluation of chemical methods for, 25:8195 (AERE-R-6491)
CHROMOSOMES
analysis of human karyotype of, using computer, 25:8632 (EUR-4526)
radiation effects on, of mice, effects of, on mutations for Rex gene, x, 25:8645
radioinduced aberrations of, in bone marrow cells of dogs, effects of dose on γ, 25:8755(T) (JPRS-51660)
radioinduced aberrations of, in coastal and interior Douglas fir, Sitka spruce, and western hemlock,, 25:8799
radioinduced aberrations of, in human lymphocytes in vitro, γ and x, 25:8788(T) (LIB/Trans-296)
radioinduced aberrations of, in mulberries, effects of dose on γ, 25:8794(T) (NSJ-tr-158)
radioinduced aberrations of, in Vicia faba, effects of 5-azacytidine on x, 25:8639
radioinduced aberrations of, in Vicia faba, effects of nitrosoguanidine on x, 25:8705
replication of DNA of, use of labeled precursors for determining, 25:8632 (EUR-4526)
CHROMOSPHERE
characteristics of small H-α plages, magnetic and spectral, (E), 25:9099
helium isotope abundances in, (E), 25:9103
magnetic fields in, (E), 25:9095(T) (CSIRO-Trans-10258)
radiative transfer in, (T), 25:9116
temperature structure of, (T), 25:9116
thermal conduction in, (T), 25:9116
velocity fields in magnetically disturbed regions of Hα, (E), 25:9106
CHRYSOPHYTA
Navicula seminulum, radioisotope accumulation by, effects of temperature on cesium-137, cobalt-57, iron-59, manganese-54, strontium-85, and zinc-65, 25:8598
CIRCADIAN CLOCK
effects on labeling and mitotic indexes of cells, autoradiographic technique for determining mechanisms of, 25:8589
CIRCUITS
transfer characteristics of, effects of component tolerances on, 25:10377(T) (SC-T-70-4048)
COATINGS
radioinduced production of aminoplast polymer, 25:8278(P)
COAXIAL CABLES
design for remote radiation detector, 25:8493(P)
COBALT
determination in air particulates by spark source mass spectrometry, 25:8208
determination in airborne particulates by neutron activation, 25:8231
determination in titanium and titanium dioxide by neutron activation, 25:8233
diffusion in, lattice-dynamical theory of isotope effects in, 25:9589
effects on colorimetric determination of uranium in fuel reprocessing solutions, 25:8197 (BARC-510)
COBALT ALLOYS AND SYSTEMS
Al--Co--Nb, phase diagram at 800°C, 25:8890
Co--Dy--Pr, magnetic properties and phase diagram of Pr/sub x/Dy/sub 1-x/Co_2, 25:9576
Co--Ho--Pr, magnetic properties and phase diagram of Pr/sub x/Ho/sub 1-x/Co_2, 25:9576
Co--Mo--steel--W, analysis for molybdenum using mercaptosuccinic acid, spectrophotometric, 25:8210
Co--Nd, neodymium-145 Moessbauer spectrum in $NdCo_2$, 25:9594
Co--TaC--WC, tensile properties of, effects of structure component growth on, 25:8877
Co--Th, crystal structure of intermetallic Th_2Co_7 in, 25:8893
COBALT FERROCYANIDES
sorptive properties for cesium from effluents from chemical decanning of reactor fuel elements, 25:8344(P)
COBALT ISOTOPES Co-57
accumulation in Navicula seminulum, Plectonema boryanum, and Stigeoclonium lubricum, effects of temperature on, 25:8598
preparation of Moessbauer source in copper, 25:9595
COBALT ISOTOPES Co-59
energy-level transitions from iron-59 beta decay, intensities of, (E), 25:10032(T) (ORNL-tr-2345)
COBALT ISOTOPES Co-60
use for scanning in diagnostic and metabolic studies, development of computer programs for, 25:8716
use in radioapplicators for interstitial therapy of female gynecological carcinomas, dose rate and dimensional advantages of, 25:8730 (SZS-6/70, pp 28-35)
COLLAGEN
radiation effects on dilute solutions of, in air and nitrogen, γ, 25:8307
COLLISION PROCESSES
formalism for resonance, definition of quasi-stationary states in, 25:9209
ionization in, Born approximation expressions for differential cross sections for, 25:9195 (SC-RR-70-773)
theory of rearrangement and scattering, separate treatment of open and closed channels in, 25:9220
COLORADO
uranium deposits in plateau region of, geology and mineralogy of peneconcordant-type, 25:8377
COMPOSITE MATERIALS
thermal conductivity of laminar, computer program for calculation of, 25:8961 (LA-4511)
COMPUTER PROGRAMS
ADSS, for reducing digitized seismic signal data, for CDC 6600, 25:8382 (UCRL-50939)
ANDYMG3, series of Monte Carlo programs for time-dependent transport of particles and photons in FORTRAN-IV, 25:9601 (LA-4539)
CONDOR 3, for two dimensional analysis of reactor lifetime, FORTRAN 4 for IBM 360/65, 25:10304 (EUR-4539)
CONVERT, for IBM-to-CDC program conversion, in FORTRAN for CDC 6600, 25:10350 (LA-4555)
development for analysis of radioisotope dosimetry and scanning in diagnosis and metabolic studies, 25:8716
DISPER, for least squares fitting of ordered set of mode frequencies from coupled rf cavities, 25:9902 (AECL-3669)
ELF, for calculating neutron propagation in cylinders and spheres by Monte-Carlo method, for IBM 360, 25:9941 (CEA-N-1361)
FMODEL, for evaluation of fuel cladding performance, 25:8911 (ORNL-4600, pp 65-80)
for analyzing spectra from Nuclear Data 50/50 Analyzer System, for PDP-8L, 25:8531 (MLM-1773)
for calculation of magnetic field in thick superconducting solenoid, 25:9393
for capital budgeting, user's manual for, 25:10337 (AECOP-621)
for determining radiation isodose around rectilinear probes in FORTRAN IV, 25:8683
FORGAD, for one dimensional few group finite difference reactor kinetics, FORTRAN 4 for CDC 6600, 25:10300 (AECL-3671(Add.1))
FREADN-1, for fast reactor excursion and accident dynamics analysis, FORTRAN IV for GE 635, 25:10241 (GEAP-13608)
ICON, for calculation of reactor fission product inventories, FORTRAN IV, 25:10236 (AERE-R-6242)
internal logic manual for controller, for Multiple Spectrometer Control System, 25:10343 (BNL-15437)
RELISH, for calculating ground-level radioactivity from accidental stack-release of ORNL reactor effluents, FORTRAN IV for IBM 360, 25:8452 (ORNL-TM-3187)
SAFE-CRACK, for nonlinear analysis of concrete structures, 25:8392 (GA-9994)
SNAP, for calculating two-dimensional neutron diffusion in various coordinate systems, in FORTRAN IV, 25:9947 (TRG-Report-1990)
SOLAN, for calculation of solid angles and angular acceptances for target--detector geometries, in FORTRAN, 25:9910 (LUSY-7007)
SPECTRAN, for high resolution spectrum analysis, user's manual for, 25:10353 (ORNL-4605)
SPECTRE, for dynamic response of cylindrical shells, 25:10380 (SCL-DR-70-108)
STAREL, for calculating ground-level radioactivity from stack-released reactor effluents at ORNL, FORTRAN IV for IBM 360, 25:8452 (ORNL-TM-3187)
TEPLO, for calculation of thermal conductivity of composites, FORTRAN IV for CDC 6600, 25:8961 (LA-4511)
THEMI, for incident beam energy from electron pairs from γ + p interactions using Monte Carlo method, in FORTRAN, 25:9705 (SLAC-123)
TRAXEN, for xenon spatial oscillation effects on reactor stability, FORTRAN for CDC-3300 and CDC-3600, 25:10306 (NP-18547)
VORTEX, for describing two-dimensional turbulent flow of incompressible inviscid homogeneous fluid, in ALGOL, FORTRAN, or USERCODE for KDF9, 25:8407 (CLM-R-106)
COMPUTERS
emulation of parallel and sequential, variable control microcomputer structure for, 25:10395 (TID-25623)
interfaces for, CAMAC modular, 25:8573 (KFK-1241)
parallel processing in, analysis of perfect shuffle for, 25:10382 (STAN-CS-70-158(App.5))
performance in combination with radioisotope scanners for multiple viewing and sectional scanning of brain,

25:8727
program routine for control of machine tool-path data, 25:8398 (Y-1750)
CONCRETES
analysis for cement by neutron activation of added traces, 25:8232(P)
development of backpacking, for Project Piledriver, 25:8962 (POR-4013)
development of epoxy grouting, for imbedding Project Piledriver instrumentation in surrounding rock, 25:8962 (POR-4013)
properties for use in shielding, 25:8960 (CEA-N-1355)
response of structures of, to strain, stress, and time varying loading, analytical method for analysis of, 25:8392 (GA-9994)
CONGO REPUBLIC
uranium reserves in, estimates of, 25:8373
CONNECTICUT YANKEE POWER REACTOR
administrative controls for, revised technical specifications for, 25:10140 (DOCKET-50213-88)
containment systems for, preliminary safety analysis of, 25:10142 (DOCKET-50213-91)
control systems for, preliminary safety analysis of, 25:10142 (DOCKET-50213-91)
emergency and auxiliary systems for, preliminary safety analysis of, 25:10142 (DOCKET-50213-91)
hazards analysis for, 25:10142 (DOCKET-50213-91)
instrumentation for, preliminary safety analysis of, 25:10142 (DOCKET-50213-91)
personnel for, training and responsibilities of, 25:10142 (DOCKET-50213-91)
pump flywheels for, ultrasonic inspection of main coolant, 25:10141 (DOCKET-50213-90)
shielding for, preliminary safety analysis of, 25:10142 (DOCKET-50213-91)
site for, preliminary safety analysis of, 25:10142 (DOCKET-50213-91)
steam and power conversion systems for, preliminary safety analysis of, 25:10142 (DOCKET-50213-91)
CONNECTIVE TISSUE
radiation effects on gingival, of rats, effects of cortisone and anabolic steroids on x, 25:8786
radiography of deuterated, 25:8709 (DP-1229)
CONTAINMENT SYSTEMS EXPERIMENT
spray systems for, effects of sodium hydroxide and sodium thiosulfate additives on fission product removal by, (E), 25:10256 (BNWL-1485)
CONTROL SYSTEMS
description of automatic, for short-lived isotope activation analysis, 25:8579
CONVERSION ELECTRONS
emission from fission products, data tabulation of abundances and energies of, 25:10023 (CEA-N-1372)
COPPER
alpha reactions at 30 to 80 MeV, K-shell ionization cross sections for, (E), 25:9978(R) (ORO-3398-26)
alpha reactions with, x-ray fluorescence yields from, (E), 25:9978(R) (ORO-3398-26)
analysis of high-purity, high-conductivity, for trace amounts of mercury by neutron activation, 25:8217 (MLM-1772)
antideuteron reactions at 25 GeV/c, absorption cross sections for, (E), 25:9639
determination in air particulates by spark source mass spectrometry, 25:8208
determination in airborne particulates by neutron activation, 25:8231
determination in human fingernails and hair by neutron activation and γ spectrometry, 25:8229
determination in titanium and titanium dioxide by neutron activation, 25:8233
determination of trace amounts of, in glass by neutron activation after sodium removal by hydrated antimony pentoxide, 25:8223
diffusion in, lattice-dynamical theory of isotope effects in, 25:9589
dissolution at constant electric currents, periodic phenomena in, 25:10404 (UCRL-19618)
electron elastic scattering at 100 to 1300 keV by foils of, as function of foil thickness and incidence angle, single, plural, and multiple, (E), 25:9225
electron energy absorption profile of, thermoelastic response measurements of intense 1.5-MeV, 25:8569
ion reactions at 40 keV to 1.1 MeV with, cross sections for L x-ray production in, as function of ion atomic number, (E), 25:9164
ion scattering by, mechanism of anisotropic, (E/T), 25:9556
nitrogen-ion multiple scattering at 1.28 and 2.29 MeV by, angular distributions and effective atomic numbers for, (E), 25:9163
positron annihilation at hexagonal zone face in, theory, 25:9606
positron elastic scattering at 100 to 1300 keV by foils of, as function of foil thickness and incidence angle, single, plural, and multiple, (E), 25:9225
properties of dispersion-hardened, 25:8873
proton multiple scattering at 0.407, 0.851, and 1.45 MeV by, angular distributions and effective atomic numbers for, (E), 25:9163
radiation effects on longitudinal magnetoresistance of, deviations from Kohler's rule in fast-neutron, 25:9571
radioinduced defects in beryllium-doped, fast neutron, 25:8902
COPPER ALLOYS AND SYSTEMS
book: Metallurgy and the Hot Working of Metals, 25:8894
Cu--Er, crystal structure of intermetallic ErCu, $ErCu_2$, and $ErCu_5$, 25:8887
Cu--Er, phase diagram of, 25:8887
COPPER CHLORIDES
complexes with ammonium chloride and carbon monoxide, carbon-13 exchange reactions with carbon monoxide and, 25:8339(P)
COPPER IONS
reactions with metals at 40 keV to 1.1 MeV, cross sections for L x-ray production in, as function of atomic number, (E), 25:9164
COPPER ISOTOPES Cu-63
performance of activation detectors of, for neutron spectra measurements at 1 eV to 10 keV, 25:8481 (KFK-1233)
COPPER ISOTOPES Cu-65
photon reactions (γ,π⁺) at 150 to 700 MeV, yields and cross sections for, (E), 25:9620 (LUNP-7007)
COPPER SULFATES
corrosive effects on welds in Type 304 stainless steel, 25:8848 (ORNL-4600, pp 131-41)
CORROSION LOOPS
operation of lithium-filled T-111 alloy, experience in, 25:8837 (ORNL-4600, pp 216-22)
COSMIC PARTICLES
acceleration of primary, by pulsars, (T), 25:9253 (MPI-PAE/EXTRATERR-47)
angular distribution of joint secondary π⁺, π⁻, and p spectra, thermodynamic model for, 25:9787
chemical composition of primary, (T), 25:9253 (MPI-PAE/EXTRATERR-47)
chemical composition of pulsar produced, (T), 25:9253 (MPI-PAE/EXTRATERR-47)
detection of narrow bundles of μ, spark chamber underground study of, (E), 25:9632
energy spectra of primary, (T), 25:9253 (MPI-PAE/EXTRATERR-47)
helium-3 flux in primary, (E), 25:9257
identification of heavy, incident on Apollo helmets, (E), 25:9255
isotropy at 10^{18} eV of primary, (T), 25:9253 (MPI-PAE/EXTRATERR-47)
meson (π) reactions with nuclei at 45 to 200 GeV in emulsions, 3π and 5π production in, (E), 25:9635 (INP-722)
proton interactions with protons at 90 to 800 GeV, spark-chamber--ionization-calorimeter study of charged-particle multiplicities in, (E), 25:9638
proton reactions with nuclei at 80 TeV in emulsions, aleph baryon production in, (E), 25:9641
COSMIC RADIATION
anisotropies in polar-cap solar, during 1969, (E), 25:9260
anisotropy of galactic, propagation-function dimensionality relation with fluctuation of, (T), 25:9258
detection of soft polar x, design and operation of satellite-borne proportional counters for, 25:8499
energy flux in radiation belts in 1966, fast, (E), 25:9354
intensity variations of primary, inside polar cap during Forbush decrease, Jan. 28, 1970, (E), 25:9327
intensity variations of solar, in Antarctica, (E/T), 25:9259
origin of diffuse gamma background, (T), 25:9254
propagation-function dimensionality relation with anisotropy fluctuation for galactic, 25:9258
radio wave intensity variations at 1.1 and 2.3 MHz, parameters affecting, (E/T), 25:9352
research program at European Space Research and Technology Centre, 25:9336
COSMIC RADIO SOURCES
detection of cyanoacetylene in Sgr B2, (E), 25:9094
detection of excited states of hydroxy in W3, (E), 25:9093
dimensions of, minimum observable diameter, (T), 25:9084
emission at very low temperatures in, free--free, (T), 25:9082
emission from, search for $H_2{}^{18}O$ 5625-MHz, (E), 25:9076
flux densities of seven compact, in HII regions, (E), 25:9077
hydrogen in direction of W49, optical depth and excitation temperature of, (E), 25:9069
identification of southern hemisphere, (E), 25:9067
methyl alcohol in Sgr A and Sgr B2, detection of, (E), 25:9060
positions of stars and galaxies in fields of southern hemisphere, (E), 25:9066
scintillation of, interplanetary, (T), 25:9084
spectra of OH sources in Cygnus, (E), 25:9083
spectral lines at 12.4 to 15.1 and 15.3 to 17.3 GHz, detection of strong, (E), 25:9058
COSMIC RAY TELESCOPES
design of scintillation, for measuring meson (μ) flux, 25:8556
COSMIC SHOWERS
detection of quarks in, (T), 25:9253 (MPI-PAE/EXTRATERR-

XUM

47)
distribution of, arrival direction, (T), 25:9253 (MPI-PAE/EXTRATERR-47)
momenta in, large transverse, (T), 25:9253 (MPI-PAE/EXTRATERR-47)
COSMIC X-RAY SOURCES
location of, relation to galactic x-ray background, (E/T), 25:9079
observations of, by satellite-borne lunar occultation technique, (E), 25:9065
Sco X-1, optical monitoring during 1967 to 1969, (E), 25:9086
Sco XR-1, distance to, (E/T), 25:9079
COSMOLOGY
Einstein equations in relativistic, complex oscillatory singularity in cosmological solutions of, (T), 25:9877
equivalence principle and geodesic De Broglie waves, (T), 25:9152
gravitational instability of fluid of radiation and matter, (T), 25:9157
helium abundance in big-bang, (T), 25:9156
properties of irradiated sets of linear topological space and convex bodies, 25:9614
universes in, action functional of general relativity as path length for closed empty, 25:9881
CRITICAL ASSEMBLIES
operation of ZPR-3, ZPR-6, ZPR-9 and ZPPR during November 1970, 25:10164(R) (ANL-7758)
physics parameters of plutonium fueled steam-cooled fast core mockup in SNEAK, (E/T), 25:10258 (EURFNR-848)
CROPS
improvement of agricultural, using radioinduced mutations, 25:8635 (STI/DOC-10/119)
polonium-210 uptake as oxide from soils by, transfer coefficients for calculating human dietary intake from, 25:8593 (COO-1733-11)
yield of agricultural, effects of seed irradiation on, 25:8813 (NP-18236)
CROSS SECTIONS
charge-exchange, for proton reactions with excited hydrogen atoms, quantal eight-state approximation for resonance, 25:9203
charge-exchange, for reactions of hydrogen ground-state and metastable atoms with iodine vapor at 0.2 to 2.5 eV, (E), 25:9218
electron-capture, for carbon ions (C^{4+}) in argon, helium, and neon below 40 keV, total single-, (E), 25:9215
excitation, for electron reactions with oxygen molecules at 0 to 1 eV, vibrational, (E), 25:9210
excitation, for helium 2^1P and 2^1S states by electron impact at 50 to 400 eV, (E), 25:9222
excitation, for helium-atom reactions with argon, krypton, and neon at 1.60 to 400 keV, scaled, (T), 25:9204
excitation, for helium-atom reactions with argon, helium, krypton, and neon at 1.0 keV to 6.4 MeV, Born, (T), 25:9204
excitation, for light emission in reactions of argon and nitrogen ions (N_2^+) with gases in eV range, (E), 25:9213
ionization, Born approximation expressions for differential, (T), 25:9195 (SC-RR-70-773)
ionization, for photon reactions with subshells of atoms having Z = 2 to 54, tabulation of, 25:9194 (SC-RR-70-721)
ionization, for proton reactions with xenon at 0.3 to 2.0 MeV, (E), 25:9191 (BNWL-SA-3631)
measurement of energy averaged, using Van de Graaff accelerators, 25:9923
photoelectric, for gamma reactions with uranium at 145, 192, 662, and 1250 keV, 25:9235
scattering, for alkali metal atoms by alkali metal atoms at 0.1 to 0.2 eV, differential elastic, (E), 25:9223
scattering, for alkali metal atoms by alkali metal atoms, total elastic, (T), 25:9202
scattering, for argon by thallium fluoride at thermal energies, effects of asymmetric mass distribution on total, (T), 25:9232
scattering, for electrons by helium at 50 to 400 eV, differential elastic, (E), 25:9222
spin-exchange, for cesium--sodium reactions, (T), 25:9212
spin-exchange, for reactions between alkali metal atoms at 0.1 to 0.2 eV, differential, (E), 25:9223
spin-exchange, for reactions between alkali metal atoms, total, (T), 25:9202
CRYOGENICS
equipment development for applications of superconductivity, 25:9397
CRYOSTATS
development for applications of superconductivity, 25:9397
CRYSTAL STRUCTURE
book: Metallurgy and the Hot Working of Metals, 25:8894
CRYSTALS
current carriers of conducting, in crossed electric and magnetic fields, distribution of, (T), 25:9608
ion scattering by, mechanism of anisotropic, (E/T), 25:9556
neutron coherent double scattering in plate, (T), 25:9963
CULTURE MEDIA
effects on xenon-irradiated Escherichia coli and Serratia marcescens, 25:8807
CURIUM
separation from irradiated LMFBR fuels, solvent extraction processes for, 25:8316 (BNWL-CC-1939)
CURIUM ISOTOPES Cm-242
alpha decay of, coincidence semiconductor detector system for measurement of x-ray-to-alpha ratio in, 25:8465 (BNWL-SA-1514)
distribution in organs of rats following inhalation and intramuscular injection, 25:8590 (CEA-CONF-1658)
CURIUM ISOTOPES Cm-244
alpha decay of, coincidence semiconductor detector system for measurement of x-ray-to-alpha ratio in, 25:8465 (BNWL-SA-1514)
fission of, prompt neutron spectra and yield for spontaneous, (E), 25:10039
CURIUM ISOTOPES Cm-245
neutron fission of, prompt neutron spectra and yield for thermal, (E), 25:10039
CURIUM OXIDES
compatibility of curium-244-enriched, with heat resisting capsule materials at 1250 to 1850°C, 25:8427(R) (ORNL-4639)
design and development of 2200-W curium-244-enriched heat sources of, 25:8427(R) (ORNL-4639)
diffusion of helium in, effects of temperature on, 25:8427(R) (ORNL-4639)
solubility and leach rates in water, 25:8427(R) (ORNL-4639)
Cm_2O_3--Gd_2O_3, diffusion of helium in, effects of temperature on, 25:8427(R) (ORNL-4639)
CURRENT ALGEBRA
classification of local Lie, 25:9754
decay $K^0 \rightarrow 2\nu + 2\gamma$ in, branching ratio for, 25:9738
field algebra in, classical Schwinger terms in, 25:9834 (RLO-1388-584)
Lie algebra in, classification of local, 25:9754
sigma-model in field-, nucleon source and πN coupling constant in, 25:9762
CYANOGEN
energy levels of, four new bound low-lying, (E), 25:9110
spectra of ionized, emission, (E), 25:9186
spectral lines in giant stars due to, strong absorption, (E), 25:9043
CYANOPHYTA
Plectonema boryanum, radioisotope accumulation by, effects of temperature on cesium-137, cobalt-57, iron-59, manganese-54, strontium-85, and zinc-65, 25:8558
CYANOPLATINATES
fluorescence of tetra-, 25:10378(T) (SC-T-70-4052)
CYCLOHEXANE, HEXACHLORO-
toxicity of carbon-14-labeled, to man following ingestion of contaminated flour, calculations for, 25:8600
CYCLOPHOSPHAMIDE
effects on primary virus infections in animals, review on, 25:8699
CYCLOTRONS
beam monochromator system for 100-MeV U-240, 25:9926
experimental facilities at Texas A and M variable-energy, development of, 25:9978(R) (ORO-3398-26)
operation of Texas A and M variable-energy, in period June 1, 1969 to June 1, 1970, 25:9978(R) (ORO-3398-26)
CYLINDERS
neutron propagation in, computer program using Monte-Carlo method for calculating, (T), 25:9941 (CEA-N-1361)
radiation dosimetry for uniform, comparison of unilateral and bilateral external γ, 25:8686
CYSTEAMINE
hydrochloride, crystal structure of, 25:8268

D

DATA ACQUISITION SYSTEMS
description of PDP-9 computer-based, for nuclear physics experiments, 25:8572 (HMI-B-96)
design of digital, for displacement measurements, 25:8397 (UCRL-72509)
operations of POPOP 4, 25:9942 (CTC-42)
DATA PROCESSING SYSTEMS
description of PDP-9 computer-based, for nuclear physics experiments, 25:8572 (HMI-B-96)
development for analytical chemistry laboratory, 25:8193 (UCRL-20132)
development of computer, for analysis of radioisotope scan data, 25:8711(R) (NYO-3937-2)
development of digital computer, for γ camera radioisotope scans, 25:8725
model for complex, microcomputer, 25:10394 (TID-25622)
DATA TABULATIONS
energy levels of A = 91 to 117 nuclei, spin--parity assignments for, (E), 25:10031 (ORNL-4627)
on radioisotope production and technology in West Germany, 25:8429(T) (ORNL-tr-2400)
photoionization cross sections for subshells of atoms having Z = 2 to 54, 25:9194 (SC-RR-70-721)
properties of atoms from Z = 2 to 126 calculated from relativistic Hartree--Fock--Slater wave functions, 25:9168 (ORNL-4614)

DECANOIC ACID, 17β-HYDROXYESTER-4-EN-3-ONE ESTER
effects on connective tissue of x-irradiated rats, 25:8786
DECONTAMINATION
films for radioactive surface, development of strippable plastic, 25:8663
methods for fabrics and materials in nuclear plants by washing, 25:8664(P)
DEOXYRIBONUCLEASE
role in excision repair of uv-irradiated DNA, 25:8636 (SU-326-P-7-X-22)
DESLANOSIDE
content of blood plasma of cardiopathic patients, tritium tracer study of effects of route of administration on, 25:8724
DEUTERIUM
content of surface waters in Canada, economic importance to AECL of geographic and seasonal variations in, 25:8666(R) (AECL-3728)
deuteron reactions (d,n) and (d,p) at 225 keV, energy spectra from, (E), 25:9968 (NP-18488)
effects on dissociation and ionization energies and photoelectron spectra of hydrofluoric acid, 25:8251
effects on ESR spectra of methyl radicals, 25:8257
effects on far infrared spectra of hydrochloric acid in nitrogen matrix, 25:8250
effects on intramolecular base catalysis in diazo coupling of 8-(2'-pyridyl)-2-naphthol, 25:8242
effects on quenching metastable oxygen compounds by acetylene, ethylene, propene, water, and hydrogen, 25:8249
effects on racemization of optically active carbon acids, 25:8253
effects on solvolysis of norbornyl brosylates, 25:8254
exchange between deuterated methylacetylene and water, mass-spectrometric equilibrium studies on, 25:8241 (CU-755-7, Sect.3)
exchange between liquid ammonia and hydrogen, catalytic effects of amides on, 25:8244
exchange reactions in optically active carbon acids, base-catalyzed, 25:8253
exchange reactions in propene catalyzed by Group eight metals, 25:8258
exchange with hydrogen in tissues, effects of, on neutron surface dose, 25:8709 (DP-1229)
ion reactions in eV range with molecular, mechanisms and cross sections for light emission in, (E), 25:9213
neutron reactions (n,2n) at 14.5 MeV, Monte Carlo simulation of cross sections from, (E/T), 25:9968 (NP-18488)
plasma of, electron temperature measurement using vacuum uv spectroscopy, 25:9407 (CEA-N-1391)
plasma of, ion heating in dense plasma focus, (E), 25:9401
plasma of, stability in toroidal screw pinch ISAR IV, (E), 25:9489
scattering by bromine and chlorine molecules, comparison of hydrogen scattering with, 25:8256
separation from hydrogen by thermal diffusion in trennschaukel, effects of chemical exchange between deuterium and hydrobromic acid on, 25:8422 (CU-755-7, Sect.5)
DEUTERIUM HYDRIDES
nuclear spin--spin coupling constant for molecule of, linked-cluster many-body perturbation calculation of, 25:9180
DEUTERONS
channeling energy losses at 20 to 28 keV in gold crystal foils, (E), 25:9555
interactions anti K + d → K + Y_1 + Y_2, cross sections for, (T), 25:9804 (JINR-P2-5231)
interactions anti p + d → anti p + d + π^+ + π^- + π^0 at 7.0 GeV/c in bubble chamber, anti Δ--(1236) and d* enhancement production and cross sections for, (E), 25:9636 (TID-25610)
interactions anti p + d → anti p + d(p + n) + π^+ + π^- at 7.0 GeV/c in bubble chamber, anti Δ--(1236) and d* enhancement production and cross sections for, (E), 25:9636 (TID-25610)
interactions anti p + d → K^- + d + anti Λ + π^0 at 7.0 GeV/c in bubble chamber, cross sections for, (E), 25:9636 (TID-25610)
interactions anti p + d → K^- + d(p + n) + Λ at 7.0 GeV/c in bubble chamber, cross sections for, (E), 25:9636 (TID-25610)
interactions K^- + d → p + π^+ + π^- + π^- + n + anti K^0 at 4.91 GeV/c, $n\pi^-\pi^-$(1627) enhancement in, (E), 25:9671
interactions K^+ + d at 0.36 to 0.72 GeV/c, total cross sections for, (E), 25:9673
interactions K^- + d at 0.36 to 0.72 GeV/c, total cross sections for, (E), 25:9673
interactions n + d at 700 to 2900 MeV/c, direct measurement of total cross sections for, (E), 25:9648
interactions p + d at 2.784 GeV/c, momentum spectra in, (E), 25:9634 (COO-1764-115)
interactions π^+ + d → 2p + π^+ + π^- + π^0 at 1.1 and 2.4 GeV/c in bubble chamber, eta and ω production in, (E), 25:9664
interactions π^+ + d → p + p + mγ (m = 2 to 6) at 2.15 GeV/c in bubble chamber, production and decay of X^0(1960) in, (E), 25:9666
interactions π^+ + d → p + p + π^+ + π^- + π^0 at 1.1 to 2.4 GeV/c, production and decay of eta and ω in, (E), 25:9675
interactions π^- + d at 5.53 GeV/c, momentum spectra in, (E), 25:9634 (COO-1764-115)
reactions (d,2γ) with boron-10 at 2.66 to 2.84 MeV, excitation-function ratios from, (E), 25:9972 (ANU-P-496)
reactions (d,α) and (d,p) with boron-10 at 2.61 and 2.96 MeV, excitation-function ratios from, (E), 25:9972 (ANU-P-496)
reactions (d,α) with titanium at 19 MeV, angular distributions for, (E), 25:9966(R) (COO-1265-94)
reactions (d,f) with thorium-232 at 11.5 MeV, fission-product yields and mass and charge distributions from, (E/T), 25:10054
reactions (d,f) with uranium-238 at 10.6 MeV, excitation functions and mass yield curves for, (E/T), 25:10052
reactions (d,He-3) with aluminum-27 at 20 MeV, angular distributions for, (E), 25:9966(R) (COO-1265-94)
reactions (d,He-3) with strontium-88 at 35 MeV, angular distributions for, (E), 25:9978(R) (ORO-3398-26)
reactions (d,He-3) with yttrium-89 at 30 to 40 MeV, angular distributions for, (E), 25:9978(R) (ORO-3398-26)
reactions (d,Li-6) with aluminum-27, calcium-40, magnesium-26, oxygen-16, and potassium-39 at 50 MeV, lithium-6 spectra and angular distributions for, (E), 25:9978(R) (ORO-3398-26)
reactions (d,n) and (d,p) with deuterium at 225 keV, energy spectra from, (E), 25:9968 (NP-18488)
reactions (d,n) with lithium-6 and -7 at 2.5 to 3.7 MeV, angular distributions of neutron polarization in, (E), 25:9984
reactions (d,n) with lithium-7 at 1.1 to 4 MeV, angular distributions and differential cross sections for, (E), 25:9975 (JINR-P15-5143)
reactions (d,n) with tritium at 220 keV, neutron spectra from, (E), 25:9968 (NP-18488)
reactions (d,n) with tritium, 14-MeV neutron source using, 25:9955
reactions (d,n) with tritium, differential neutron source strength from, 25:9957
reactions (d,p) with calcium-40 at 19 MeV, angular distributions for, (E), 25:9966(R) (COO-1265-94)
reactions (d,p) with iron-56, differential cross sections and residual nucleus orientation in, (E), 25:9998 (NP-18439)
reactions (d,p) with lead-206 and bismuth-209, analysis using calculated form factors, (T), 25:10067
reactions (d,p) with magnesium-24 at 13.5 MeV, generalized DWBA analysis of angular distributions from, (E/T), 25:9997 (JINR-E4-5350)
reactions (d,p) with nuclei in the lead region, realistic form factors for, (T), 25:10067
reactions (d,p) with titanium-50 at 18 MeV, angular distributions for, (E), 25:9966(R) (COO-1265-94)
scattering by aluminum-27 at 20 MeV, angular distributions for elastic and inelastic, (E), 25:9966(R) (COO-1265-94)
scattering by strontium-88 and yttrium-89 at 30 to 40 MeV, angular distributions for elastic, (E), 25:9978(R) (ORO-3398-26)
vertex function for, dispersion methods in charged scalar static model for, 25:9817
DEUTERONS (anti d)
reactions with aluminum, carbon, copper, lead, and lithium at 25 GeV/c, absorption cross sections for, (E), 25:9639
DEXTRAN
polymers, radiolysis of frozen aqueous suspensions of, 25:8298
radiation effects on molecules of cross-linked, intermolecular energy transfer at 77°K following x, 25:8613
DIAMONDS
ion bombardment damage in, x-ray diffraction study of lithium, 25:9557
DIBUTYLAMINE
dibutylamine--triethylamine, carbon-13 concentration by chemical exchange reactions between carbon dioxide and, 25:8318 (CU-755-7, Sect.2)
dibutylamine--triethylamine, carbon-13 concentration by chemical exchange reactions between carbon dioxide and, 25:8320 (CU-755-7, Sect.6)
DIDO REACTORS
rabbit facility for FRJ-2 (Juelich), design of hydraulic, 25:10274
safety rod circuits for HIFAR, design and operation manual for, 25:10252 (AAEC/M-9)
safety rod system for HIFAR, design and operation manual for, 25:10253 (AAEC/M-32)
DIELDRIN
toxicity of carbon-14 labeled, to man following ingestion of contaminated flour, calculations for, 25:8600
DIELECTRICS
dielectric--semiconductor, radioinduced electric charges in, 25:9566
DIET
cesium-137 content of human, in Chicago area during July 1970, measurements of, 25:8659 (HASL-237, pp III.14-17)

XUM

polonium-210 content of human, following uptake as oxide by crops from soils, transfer coefficients for calculating, 25:8593 (COO-1733-11)
radioisotope content of human, in EURATOM countries during 1968, cesium-137, and strontium-90, 25:8624 (EUR-4509)
strontium-90 content of human, in Chicago, New York City, and San Francisco from 1960 to 1970, 25:8658 (HASL-237, pp II.1-16)
strontium-90 content of human, in New York City and San Francisco from April to July 1970, 25:8658 (HASL-237, pp II.1-16)

DIFFERENTIAL EQUATIONS
Fokker--Planck moment, truncation and preservation of moment properties for, 25:10387 (TID-25614)
generalization of continued fractions and estimation of integrals, 25:10386 (TID-25613)
integration of, differential quadrature and long-term, 25:10389 (TID-25616)
minimum convolutions and Green's functions, 25:10385 (TID-25612)
solution to Y(t) = M(t)Y(t), bounds for approximate, 25:10398 (TID-25627)
solutions of nonlinear, asymptotic behavior of, 25:10417 (USCEE-344)

DIFFUSION
isotope effects in cubic metals, lattice-dynamical theory of, 25:9589

DIODES
radiation effects on, transient, 25:8581 (LYCEN-6933)

DISEASES
radioinduced, affecting heart of man following therapy, effects of cortisone on, 25:8708

DISEASES, INFECTIOUS
abscesses, radiodiagnosis of human cerebral, use of γ radiography for, 25:8714
cysts, radiodiagnosis of noncalcified hydatid, of Echinococcus in man using gold-198 scanning, 25:8719
encephalitis, radiodiagnosis of herpes hominis virus, in man, use of brain scanning with metastable technetium-99-labeled pertechnetate for, 25:8718

DISEASES, NEOPLASTIC
carcinomas, cell populations of ovarian, karyotype variability in, 25:8632 (EUR-4526)
carcinomas, induced in rats by 3,3-dimethyl-1-phenyl triazene, 25:10362(T) (ORNL-tr-2418)
carcinomas, radiotherapy of female genital, peritherapeutic dose and safety considerations during intracavitary radium γ, 25:8729 (SZS-6/70, pp 1-8)
carcinomas, radiotherapy of female gynecological, use of cesium-137 in preference to radium for interstitial γ, 25:8730 (SZS-6/70, pp 28-35)
carcinomas, radiotherapy of female gynecological, dose to bladder and rectum during intracavitary γ, 25:8679 (SZS-6/70, pp 9-18)
carcinomas, radiotherapy of human cervical, comparison between counter dual cobalt with linear accelerator and linear accelerator, 25:8740
epitheliomas, radiotherapy in man, dosimetry of iridium applicator castings for, 25:8684
Hodgkin's disease, radiotherapy of human, using high-energy x, 25:8734
Hodgkin's disease, radiotherapy of human, using high-energy x, 25:8735
leukemia, effects on x-irradiated mice, effects of triacetoneamine-N-oxyl on, 25:8701
leukemia, radiation effects on immune reactions to, following transplantation into allogenic mice, whole-body x, 25:8622
lymphomas, radiotherapy of human, high-energy x, 25:8734
lymphomas, radiotherapy of human, using high-energy x, 25:8735
malignant, incidence in uranium mine personnel, effects of inhalation of diesel engine exhausts, radon decay products, and uranium ore dusts on, additive effects of cigarette smoking on, 25:8623 (BNWL-SA-3419)
malignant, radiodiagnosis of gastric, use of metastable technetium-99 and scintillation counters for, 25:8723
malignant, radioinduced, in human bones following ingestion of radium-226, 25:8669 (COO-2088-1)
malignant, radiotherapy of human gynecological, methods for protection of patient during contact γ, 25:8688 (SZS-6/70)
malignant, radiotherapy of human intracavitary, using molded cobalt-60 afterloading sources for implant γ, 25:8738
malignant, radiotherapy of human skin, use of molded cobalt-60 afterloading sources for contact γ, 25:8738
malignant, radiotherapy of human uterus, design of radium-226 applicators for γ, 25:8736
malignant, radiotherapy of human uterus, design of variable-size afterloading radium-226 applicators for γ, 25:8736
malignant, radiotherapy of human, using iridium-192 wires for implant γ, 25:8737
malignant, radiotherapy of otorhinolaryngeal, in man, functional changes of vestibulocochlear analysor following, 25:8792
radioinduced, in swine, neutron, γ, and x, 25:8773
tumors, radiation effects on, of brain, experimental studies of x, 25:8759
tumors, radiotherapy of conjunctival, using phosphorus-32 in scleral shell applicators, 25:8731
tumors, radiotherapy of malignant, in animals and man, development of pulmonary fibrosis following, 25:8791
tumors, strontium-85 accumulation in benign and malignant, of human bone, correlation of data with microscopic data, 25:8597

DISEASES, PHYSIOLOGICAL
acidosis, metabolic, of in vitro swine liver cells, iodine-131 tracer study of, 25:8783
anomalies, radioinduced, in limbs of fetal mice, synergistic effects of synkavit on x, 25:8703
cirrhosis, radiodiagnosis of human liver, effectiveness of selenium-75-labeled selenomethionine scanning methods for, 25:8715
exophthalmos, radiotherapy of human endocrine, by thyroid ablation, iodine-131 β and γ, 25:8733
fibrosis, radioinduced pulmonary, in animals and man following therapy for malignant tumors, 25:8791
hypotension, arterial, in swine livers, xenon-133 tracer study of, 25:8783
pneumoconiosis, radiodiagnosis of antimony-induced, in human lungs, methods using γ transmission scanning for, 25:8726
radioinduced, in swine, neutron, γ, and x, 25:8773
secondary, radioinduced, in mice following transplantation of rat bone marrow, x, 25:8619

DISEASES, PLANTS
tumors, radioinduced, in Arabidopsis thaliana, RBE for heavy ion, 25:8800

DISEASES, TRAUMATIC
fractures, radiodiagnosis of non-union, in human bone, use of strontium-85 scanning for, 25:8720
fractures, radioinduced, in human bones following ingestion of radium-226, 25:8669 (COO-2088-1)
radiation injuries, diagnosis in personnel in relation to compensation, 25:8697
wounds, radiation effects on healing of, in mice, partial-body x, 25:8772

DISPERSION RELATIONS
nucleon anomalous magnetic moment in sidewise, 25:9702 (JINR-E2-5333)
scattering amplitude in, extrapolation of, 25:9895

DISSOLVERS
design for sheared clad ceramic fuels, 25:8445 (AERE-R-5104)

DISTILLATION APPARATUS
design of molecular, for sodium purification, 25:8390 (AERE-R-5502)

DNA NUCLEOTIDYLTRANSFERASE
radiation effects on activity of, effects of dose on x, 25:8610
role in excision repair of uv-irradiated DNA, 25:8636 (SU-326-P-7-X-22)

DOGS
radiation effects on blood pressure, leucocyte count, and respiration rate of, combined effects of biological stress on x, 25:8766
radiation effects on hematopoiesis in, comparison of x rays with neutrons and γ rays, 25:8774
radiation effects on immune reactions of, prior to bone marrow grafting, 25:8617
radiation effects on physiology of hematopoietic and nervous systems and reproductive capacity of, effects of dose on γ, 25:8755(T) (JPRS-51660)
respiratory tract of, additive effects of cigarette smoking on effects of chronic inhalation of diesel engine exhausts, radon decay products, and uranium ore dusts on, 25:8623 (BNWL-SA-3419)

DOORS
closure for, design of air-tight and soundproof, 25:8403(P)

DRESDEN POWER REACTOR, UNIT 1
radioactive effluents from, minimizing off-gas, 25:10136 (DOCKET-50010-75)

DRESDEN POWER REACTOR, UNIT 2
fuel elements for, safety analysis of gadolinium oxide (Gd_2O_3) containing, 25:10145 (DOCKET-50237-123)
operations incident of November 2, 1970, failure of standby diesel generator to start, 25:10120 (DOCKET-50237-125)
operations incident of September 24, 1970, safety analysis of spent radwaste demineralizer, 25:10119 (DOCKET-50237-124)

DRESDEN POWER REACTOR, UNIT 3
effluents from, effects on environment of chemical, radioactive and thermal, 25:10146 (DOCKET-50249-52)

DRUGS
analysis by neutron activation, 25:8227

DYSPROSIUM ALLOYS AND SYSTEMS
Al--Dy--Ni, magnetic properties and phase diagram of $DyNi_{2-x}Al_{2-x}$, 25:9576
Al-base--Dy--Gd, phase diagram at 500°C, 25:8886
Co--Dy--Pr, magnetic properties and phase diagram of $Pr_xDy_{1-x}Co_2$, 25:9576
Dy--Ni--Pr, magnetic properties and phase diagram of $Pr_xDy_{1-x}Ni_2$, 25:9576

DYSPROSIUM ISOTOPES Dy-163
neutron capture by, gamma spectra from, (E), 25:10047
neutron resonances in, correlations between partial radiative widths and reduced neutron widths in, (E), 25:10047

E

EARTH
magnetic fields in, origin of, (T), 25:9129
EARTHQUAKES
effects on 850-ft guyed stack, 25:10391 (TID-25618)
effects on soil interaction with reactor foundation structures, 25:10245 (ORO-3822-5)
ECOLOGY
book: Radioecological Studies of the Mediterranean Sea, 25:8630
ECOSYSTEMS
radioisotope transport in food chains of nuclear explosion-contaminated estuarine and marine, in relation to daily ingestion by man, use of stable element content of fish and invertebrates for predicting, 25:8627
radioisotope transport in food chains of nuclear explosion-contaminated tropical, ecological model for predicting, 25:8626
thermal effluent effects on, bibliography on, 25:10159 (ORNL-NSIC-81)
EDDY CURRENT TESTING
equipment for, design of coil for, 25:8440 (ORNL-4600, pp 266-70)
method for LMFBR components and materials, 25:8439 (ORNL-4600, pp 153-6)
ELECTRIC ARCS
initiation by ion bombardment, (E), 25:9442
ion temperature in hydrogen, Doppler measurement of, 25:9413(T) (SC-T-71-3001)
magnetic self-striction in low-pressure, Gvosdover effect in, 25:9441
operation of hollow-cathode, new mode for, 25:9432(T) (SC-T-70-4051)
properties of free-burning, in transverse magnetic fields and gas flow, (E/T), 25:9282
properties of hollow-cathode, (E/T), 25:9431(T) (SC-T-70-4050)
properties of hollow-cathode, gas flow in, (E/T), 25:9433(T) (SC-T-70-4053)
ELECTRIC CHARGES
Compton effect and energy absorption by, (T), 25:9615
energies of point, in polarized vacuum in Lorentz-invariant electrodynamics, field, 25:9867
ELECTRIC CONDUCTORS
current measurement in, methods for high surge, (E), 25:9505 (KFK-896)
ELECTRIC CONTROL SYSTEMS
design for automated electron beam welder, 25:8391 (EUR-4537)
reliability analysis of automatic, in emergency control switching system, 25:10108
ELECTRIC DISCHARGE
current distribution in pulse argon--cesium, with sectional electrodes, 25:9482
current pulses in lf electrodeless argon, effect of light irradiation on, 25:9449
electron distribution function in, effects of diaphragm on, (T), 25:9471
electron energy distribution in cesium, Langmuir-probe measurement of, (T), 25:9419
ion burst reflection from potential barrier of gridded energy analyzer in, (E), 25:9531
ion-pair production in, mean energy for, (E/T), 25:9161(T) (LA-tr-70-24)
ionization layers in argon column, self-excitation of, (T), 25:9465
ionization nonequilibrium in pulsed, during cooling of, (T), 25:9462
plasma conductivity enhancement by, supersonic argon, (E), 25:9451
plasma diagnostics in high-current with skin effect, microwave, 25:9428
plasma diagnostics in high-current with skin effect, microwave, 25:9424
plasma temperature measurement in, method for, (E/T), 25:9411 (ECRC/N-288)
plasma wave resonances in low-pressure, helicon, (T), 25:9512 (NP-18554)
striations in helium and neon, in longitudinal magnetic fields, (E), 25:9453
striations in hydrogen, microwave diagnostics of, 25:9425
wave disturbances in positive column, large-amplitude, (T), 25:9529
wave propagation in positive column, with finite-amplitude helical instability, (E), 25:9530
ELECTRIC FIELDS
current in ionospheric polar electrojets, plasma measurements for height-independent, (E), 25:9335
detection of dc vector ionospheric auroral zone, Langmuir probe operation for, (E/T), 25:9301
effects on ionospheric F-region diurnal behavior, (T), 25:9315
electron uniform acceleration in external, Maxwell electrodynamics for paradox of radiation from, (T), 25:9709
elementary particle mass in constant, (T), 25:9729
intensity across ionospheric auroral-arc boundary, measurements of parallel and perpendicular, (E), 25:9303
intensity in ionospheric equatorial and medium latitudes during twilight from barium cloud releases, (E), 25:9285 (MPI-PAE/EXTRATERR-49/70)
ELECTRIC GENERATORS
feasibility of homopolar, using superconducting field windings, 25:9394
ELECTRIC INSULATORS
design parameters for gas cleaned, for in-core instrumentation in gas cooled reactors, 25:10191(P)
ELECTRIC PROBES
performance of Langmuir, for electron energy distribution measurement in cesium discharges, (T), 25:9419
theory for diagnostics of argon discharge, large-sheath concept for continuum, 25:9429
use of plane, for plasma diagnostics in toroidal traps, 25:9410(T) (CTO-736)
ELECTRODES
arcing behavior of anode materials exposed to pulsed rf discharges, (E), 25:9442
ELECTRODYNAMICS
book: Lectures on Nonlinear Electrodynamics, 25:9869
electron uniform acceleration in external electric field in Maxwell, paradox of radiation from, 25:9709
ELECTROHYDRODYNAMIC GENERATORS
charged-particle size for, analysis of optimum, 25:9262
ELECTROJETS
electric fields in polar, plasma measurements for height-independent, (E), 25:9335
relation of equatorial, with ionospheric F2 anomaly and q-type sporadic-E layer, (E/T), 25:9291
structure of auroral, from measurements of field components, (E/T), 25:9334
ELECTROLYTES
radiation effects on distribution of, in brain of developing rats, x, 25:8758(R) (UCB-34-P-82-10)
ELECTROLYTIC CELLS
development for measurement of coolant flow induced vibrations in reactor fuel pins, 25:10271 (WHAN-FR-21)
ELECTROMAGNETIC FIELDS
fermions in external, formulation of relativistic quantum mechanics for spin-$^1/_2$, (T), 25:9841
Maxwell equations for, advanced and retarded solutions for, (T), 25:9835
Maxwell equations for, cylindrical wave solutions of, 25:9873
molecular multipole interactions with, canonical formulation of noncovariant quantum electrodynamics for, (T), 25:9842
plasma electron distribution function in arbitrary time-dependent, (T), 25:9470
properties of, produced by charged-particle motion in homogeneous media, angular-spectrum representation of, 25:9613
ELECTROMAGNETIC LENSES
charged-particle beam optics in thin, with space charge, 25:9916 (UCRL-19313)
design of demountable multipole, 25:9928(P)
performance of sextupole, with direct nonlinearity for slow beam extraction from synchrotron, 25:9913 (NP-18594)
ELECTROMAGNETIC WAVES
excitation at upper hybrid frequency in inhomogeneous plasma, harmonic, 25:9521
interactions with magnetized plasma, excitation of longitudinal oscillations in, (T), 25:9518
interactions with plasma in nonuniform magnetic fields, heating in, (T), 25:9404
scattering by beams of relativistic particles, (T), 25:9085
scattering by turbulent plasma, (T), 25:9481
scattering in infinite and semi-infinite media, (T), 25:9009
ELECTRON BEAMS
dosimetry of intense pulsed, thermoelastic response method for, 25:8569
interactions with mercury plasma, instabilities from slow, (E), 25:9447
interactions with neutral gas, turbulence from, (T), 25:9455 (AD-705265)
interactions with plasma, effect of collisions on instability in, (E/T), 25:9494
interactions with plasma, inhomogeneity effects on relaxation of ultrarelativistic, (T), 25:9472
interactions with plasma, nonlinear theory for electron oscillations in, (T), 25:9469
production of, solution of internal problem for laminar axisymmetric, (T), 25:9618
production of, theory for crossed-field and magnetron sources, 25:9617
properties between infinite plane gap electrodes, Monte Carlo calculation for, 25:9165
ELECTRON CAPTURE
measurement of ratios for, internal source scintillation spectrometer for, 25:8514
ELECTRON GAS
combination with Bloch pairs in many-body theory of nearly free electrons, 25:9606
heating of ionospheric E-layer, mechanism of, (E/T), 25:9341

XUM

radiative transfer in LTE atmosphere, Compton scatter source term for, 25:9440
ELECTRON MULTIPLIER TUBES
efficiency measurements for channel, electron source for, 25:8490
encapsulation of helical channel, for space flight applications, 25:8489
ELECTRON PAIRS
production in meson (π^-) reactions with nuclei at 2.94 GeV/c, direct, (E), 25:9661
ELECTRON-RING ACCELERATORS
development and research at Berkeley, 25:9917 (UCRL-20125)
electron--ion bunch diagnostics by bremsstrahlung in, 25:9908(T) (KFK-tr-337)
ELECTRON SOURCES
design of low-energy, for efficiency measurements of channel electron multipliers, 25:8490
theory for crossed-field and magnetron, internal problem solution in, 25:9617
theory for laminar axisymmetric powerful, solution of internal problem for, 25:9618
ELECTRONIC FILTERS
performance of low-order phase-locked loop, large signal, 25:10407 (UCRL-72390)
ELECTRONICS
book: Electronics for Nuclear Particle Analysis, 25:8488
ELECTRONS
acceleration in external electric field, Maxwell electrodynamics for paradox of radiation from uniform, (T), 25:9709
capture by nuclei in dense stars, effects on temperature, (T), 25:8973
channeling in silicon and anthracene monocrystals at 148 keV, 25:9543
detection at 10 to 100 keV, energy effects on resolution of surface-barrier silicon detector for, 25:8524
diffusion in magnetosphere, simulation in trap with magnetic mirrors of, (E/T), 25:9350
dose--depth profiles in plastic dosimeters, effects of trapped charge on, 25:8566
effects of fast, on coloration enhancement of caprone, 25:9552
effects of pulsed, on aniline at 83 and 120°K, 25:8296
effects on aluminum at 3 MeV and 4.5°K, comparison of lattice parameter and resistivity changes in annealing of, 25:9564
effects on beryllium films at 80 keV, plasmon emission in, 25:9554
effects on broadening of silicon lines, (E), 25:9187
effects on coliphage T7, inactivating, 25:8808
effects on electric conductivity of cadmium sulfide single crystals at 5 MeV, 25:9563
effects on iron and nickel at 1.5 and 3 MeV, dislocation loop nucleation in, 25:9541 (CEA-CONF-1680)
effects on lithium-doped silicon at 1 to 1.5 MeV, EPR study of defects induced in, 25:9558
effects on luminescence of copper-doped zinc sulfide, 25:8485
effects on lymphoid tissues in mice, RBE for whole-body, 25:8780
effects on mechanical properties and structure of modified Kapron fibers, 25:8270
effects on niobium at 3 MeV, superconducting flux pinning by point defects induced in, 25:9379
effects on oxygen enhancement ratios of bacteria, effects of surface or suspension location on fast, 25:8811
effects on p-type silicon at 1 Mev, impurity effects on annealing of, 25:9549
effects on polymerization of aminoplast film for coating particles, 25:8278(P)
effects on recovery of Chlamydomonas, effects of dose fractionation on, 25:8795
effects on silicon carbide single crystals, ESR of centers induced in, 25:9545
emission from Vela X, (T), 25:9256
energy absorption profiles in aluminum and copper at 1.5 MeV, thermoelastic response measurements of, 25:8569
energy distribution in thermionic converter, effects of excitation relaxation on, (T), 25:9267
energy flux at 120 to 178 km, soft, (E), 25:9345
energy flux in radiation belts in 1966, fast, (E), 25:9354
energy in quantum electrodynamics, renormalization functional relations for solution of self-, 25:9848
energy loss spectra in vanadium and vanadium pentoxide, characteristic, 25:9583
energy losses in carbon films and graphite single crystals at 25 keV, spectra for loss range 20 to 400 MeV, (E), 25:9167
energy of, quantum electrodynamics for finite value of self-, (T), 25:9867
extinction of trapped radiolytic, in alkaline ices at 77°K, thermal and photostimulated, 25:8287
gases of, transport coefficients of ionospheric, at 100 to 600 km, (E/T), 25:9302
interactions anti ν + e → anti ν + e, cross sections for, (T), 25:9746
interactions e + N, review of deep inelastic, (T), 25:9706 (SLAC-PUB-843)
interactions e + p → e + N^*, simple harmonic forces in nonrelativistic quark model for, (T), 25:9788
interactions e + p → e + p + π^0, angular distributions and cross sections for $\Delta(1236)$ production in, (E), 25:9625
interactions e + p, relation among asymptotic behavior of amplitude, spectral function of current commutator, and sum rules for Schwinger term for, 25:9701 (ITF-70-73)
interactions e + p, relation between p + p interactions at high energies and deep inelastic, 25:9805
interactions $e^+ + e^- \rightarrow e^+ + e^-$, S-matrix element for, 25:9740
interactions $e^+ + e^-$ at 0.7 x 2 to 1.2 x 2 GeV, spark chamber and scintillation counter study of Bhabha scattering and μ pair and hadron production in, (E), 25:9621 (NP-18581)
interactions γ + e, cross sections for W pair production in, (T), 25:9707
interactions in radiation field, polarization function for, 25:9867
interactions ν + e → e + ν, S-matrix element for, 25:9740
magnetic moment of, polarization function for calculation of anomalous, (T), 25:9867
mass of, formulas for relation with gravitational constant for, (T), 25:9878
mass renormalization in quantum electrodynamics, functional relations for, 25:9848
motion in solid silver selenide, silver sulfide, and silver telluride, 25:10339(T) (ANL-Trans-868)
propagation of cosmic-ray, (T), 25:9256
reactions (e,e'p) with barium-138, bismuth-209, lead-208, strontium-88, yttrium-89, and zirconium-90, proton spectra and excitation functions for, (E), 25:10053
reactions of hydrated, in pulse radiolysis of water at pH 7.0 to 12.7, 25:8291
reactions with diatomic molecules, model for vibrational excitation in, 25:9240
reactions with helium at 50 to 400 eV, differential cross sections for excitation of 2^1P and 2^1S states in, (E), 25:9222
reactions with helium at 500 eV, excitation of lowest singlet S and singlet P states in, (T), 25:9217
reactions with hydrogen atoms up to 54.4 eV, cross sections for excitation of 2s and 2p states in, (T), 25:9208
reactions with hydrogen atoms, calculation of phase shift and resonances for, using separate treatment of open and closed channels, 25:9220
reactions with hydrogen atoms, semi-empirical cross sections and rates for excitation and ionization in, 25:9184
reactions with mercury at 50 eV, angular correlation of photons emitted by excited atoms from, (E), 25:9206
reactions with nuclei with nucleon knockout at high energies, cross-section dependence on Woods--Saxon potential parameters, (T), 25:10058 (ITF-70-38)
reactions with oxygen molecules at 0 to 1 eV, vibrational excitation in, (E), 25:9210
reactions with oxygen molecules at 5.75 to 8.40 eV, angular distribution of oxygen ions (O^-) from dissociative electron attachment in, (E), 25:9221
scattering by aluminum, copper, lead, and silver foils at 100 to 1300 keV as function of foil thickness and incidence angle, single, plural, and multiple elastic, (E), 25:9225
scattering by argon and neon at low energies, effective cross sections for elastic, (T), 25:9237
scattering by atoms at high energies, linear-response theory of inelastic, 25:9217
scattering by atoms at intermediate energies, (T), 25:9214
scattering by atoms at low energies, use of local exchange potential in relativistic Hartree--Fock theory of elastic, 25:9237
scattering by calcium-40, carbon-12, oxygen-16, silicon-28, and sulfur-32, calculation of form factors for inelastic, (T), 25:10010
scattering by cerium-140 at 50 and 60 MeV, energy spectra from inelastic, (E), 25:10046
scattering by helium at 50 to 400 eV, differential cross sections for elastic, (E), 25:9222
scattering by helium-3, charge and magnetic form factors for high-energy, (E), 25:9965 (AD-710384)
scattering by nuclei with Z = 6 to 92, coefficients for adjustment of complex scattering factors for fast, (T), 25:10055
scattering by nuclei, spectra, form factors, and charge distributions from, (E), 25:10014
transition radiation from, nuclear resonance absorption of, (T), 25:9703 (JINR-P2-5042)
transport of, evaluation of Mott cross section and Goudsmit--Saunderson multiple-scattering distribution for, (T), 25:10087
wave function renormalization constants in quantum electrodynamics, functional relations for, 25:9848
ELECTROPHORESIS
method for carrier-free buffer stream, using continuous electrofocussing in natural pH, 25:10414(T) (UCRL-Trans-1429)
ELECTROSTATIC ANALYZERS
focusing properties of parallel plate, 25:8576

ELECTROSTATIC GENERATORS
design of proton, for crystal structure studies at 10 to 100 keV, 25:9918
ELEMENT 104
production using heavy ion reactions with collimation method identification, 25:10030(T) (KFK-tr-329)
ELEMENTARY PARTICLE MODELS
dual resonance model in extended particle model with quark--antiquark pairs, 25:9771
dual resonance, invariance properties of Lagrangian formulation of, 25:9696
dual resonance, off-shield functions of, 25:9695
dual resonance, review of, 25:9887 (ITF-70-43)
fireball, pionization in nucleon reactions with nuclei at 0.1 to 100 TeV in emulsions in, 25:9635 (INP-722)
multiperipheral, integral equation in, 25:9758
multiperipheral, magnitude of total cross sections for meson interactions at high energies, SU(n) symmetric, 25:9773
multiperipheral, production cross sections in, 25:9756
operator-droplet, field-theory realization of, 25:9860
sigma, summation of soft pseudoscalar π pairs in, 25:9782
tensor meson dominance, decoupling of f-exchange contribution from A amplitude in π + N interactions in, 25:9764 (DESY-70/58)
tensor meson dominance, meson decay widths and nucleon coupling constants for empirical test of, 25:9764 (DESY-70/58)
vector-dominance, photon propagator in, 25:9846
vector-meson dominance, Lorentz-invariant formulation of, 25:9723
Veneziano functions for mass spectra and angular distributions in anti N + N + K + anti K + π interactions at rest, four-point, 25:9765 (NP-18578)
Veneziano, 4-, 5-, and N-point functions in dual resonance model with nonlinear trajectories, 25:9884 (COO-1764-90)
Veneziano, 5-point function construction in dual resonance models with nonlinear trajectories, rules for, 25:9885 (COO-1764-98)
Veneziano, dual amplitudes with Regge cuts in, 25:9899
Veneziano, for amplitude with finite number of daughter Regge trajectories, generalized, 25:9888 (ITF-70-78)
Veneziano, for $K^+ + p \rightarrow K^+ + p + \omega$ interactions at 9 GeV/c, test of double-Regge behavior of generalized, 25:9797
Veneziano, functional integrals for N-particle amplitude in, 25:9901
Veneziano, $\gamma + N \rightarrow \pi + N$ cross sections in, (T), 25:9717
Veneziano, N-point function construction in dual resonance models with nonlinear trajectories, rules for, 25:9885 (COO-1764-98)
Veneziano, off-shell single-current amplitude in, 25:9725
Veneziano, potential-theory model for unitarization of amplitude in, 25:9900
Veneziano, prediction of rho'' daughter resonance contribution to amplitudes of $\pi^- + p \rightarrow \pi^- + \pi^+(\omega^0) + n(p)$ interactions from, (T), 25:9786
Veneziano, π + N charge-exchange polarization in, (T), 25:9793
ELEMENTARY PARTICLE MODELS (BOOTSTRAP)
formulation in local field theory, 25:9690 (NYO-2171-331)
hadron theory in, 25:9753
interactions $\pi + \pi$ and p + p in, derivation of Wu and Yang conjecture for cross sections of, 25:9809
multiperipheral Regge, properties of, 25:9757
ELEMENTARY PARTICLE MODELS (TRIPLET)
baryon and meson matrix elements in quark, weak current--current Hamiltonian for octet behavior of, 25:9761
hadron structure and dynamics in quark, 25:9759
meson (π) root-mean-square radius in nonrelativistic quark, 25:9788
meson resonances in nonrelativistic quark, nonstrange, 25:9788
N* decay in nonrelativistic quark, widths of, 25:9788
N* production in e + p + e + N* interactions in nonrelativistic quark, 25:9788
N* production in $\gamma + N \rightarrow \pi + N$ interactions in nonrelativistic quark, 25:9788
nucleon root-mean-square radius in nonrelativistic quark, 25:9788
quark focusing at hadronic vertices, 25:9760
ELEMENTARY PARTICLES
book: Intermediate Energy Nuclear Physics, 25:9694
book: Particles, Sources, and Fields, 25:9699
electromagnetic interactions of, constraints on scale-invariant function for, 25:9720
electroproduction of, constraints on scale-invariant function for, 25:9720
equations for spin-$^1/_2$ unequal-mass, quasipotential, (T), 25:9697
interactions of, helicity formalism for theorem on intuitive tests of parity conservation in two-body, (T), 25:9686 (COO-1764-100)
mass formulas in linear and nonlinear realization of chiral symmetry, effect of Kuo transformation on, 25:9825
mass in constant electric field, (T), 25:9729
mass of bound-state relativistic three-body system of, (T), 25:9688 (JINR-P2-5336)
mass splitting of infinitely-degenerate, 25:9711
motion of spinning, in general relativity theory, (T), 25:9874
production in multiperipheral model, cross sections for, 25:9756
production in partially latent quasidynamical strong interactions, (T), 25:9752
research at Minnesota Univ., Sept. 1969 to Aug. 1970, (E/T), 25:9685(R) (COO-1764-86)
spectrum-generating algebra for, finite-dimensional, 25:9698
strong interactions at high energies, representation for amplitude of relativistic, (T), 25:9749 (JINR-E2-5341)
strong interactions in quantum field theory, straight-line paths approximation for amplitudes of, 25:9751
strong interactions of, particle production from partially latent quasidynamical, (T), 25:9752
strong interactions of, total cross sections for, (E), 25:9640
strong interactions of, universal formulas for contributions of rho and sigma in, (T), 25:9750
theory for, Friedman, 25:9870 (JINR-P2-5289)
transport, Monte Carlo program for time-dependent, 25:9601 (LA-4539)
weak interactions of, definition of quasi-averages for negative four-fermion, (T), 25:9733 (ITF-70-52)
weak interactions of, historical review of, (E/T), 25:9735 (NYO-1932(2)-186)
weak interactions of, limiting relations for correlation averages for, (T), 25:9734 (ITF-70-53)
weak interactions of, mirror nuclei for determination of axial vector and vector coupling constants in, (T), 25:9742
weak interactions of, research at Pittsburgh Univ., Dec. 1969 to Dec. 1970, 25:9839(R) (NYO-3829-64)
weak interactions of, S-matrix elements of, 25:9740
ELEMENTARY PARTICLES (TRIPLET)
detection in cosmic air showers, (T), 25:9253 (MPI-PAE/EXTRATERR-47)
fusion reactions in quasars, (T), 25:9075
quark production in p + p interactions at ultrahigh energies, models for, (T), 25:9811
ELEMENTS
abundances of heavy, in peculiar A stars, (T), 25:8984
EMBRYOS
nucleic acid synthesis in chicken, following infection with ultraviolet-irradiated vesicular stomatitis virus, 25:8806
EMISSIVITY
equation for calculation of normal spectral, from electronic density of states, 25:9584
ENGINEERING
engineering materials list, 25:8396 (TID-4100(Suppl.61))
ENTROPY
oscillation to equilibrium in finite systems in contact with heat baths, 25:10365 (ORO-3895-9)
ENVIRONMENT
effects on living organisms in comparison with age, radiation, and thermal energy, information theory for studying, 25:8742
power plant effluent effects on, comparison of U.S. nuclear and fossil fuel, 25:10132 (BNWL-SA-3564)
radiation hazards to, surrounding Goodyear Atomic Corporation during 1969, progress report on programs and surveillance activities for controlling and reducing, 25:8692(R) (GAT-627)
radiation monitoring of, at JAERI during 1969 and 1970, results of routine, 25:8693(R) (JAERI-5025)
research program at ORNL on, 25:10354(R) (ORNL-4632)
ENZYMES
properties of, from thermomorphs and halophiles, 25:10368(R) (RLO-2227-T-5-2)
properties of, from thermomorphs and halophiles, 25:10367(R) (RLO-2227-T-5-1)
rate constants of, in Haemophilus influenza and yeast, measurement of uv, 25:8651
EPITHELIUM
radiation effects on survival of cells of, in intestine of mice, effects of cell cycle stage on whole-body γ, 25:8785
ERBIUM ALLOYS AND SYSTEMS
Al--Er--Ni, magnetic properties and phase diagram of ErNi/sub x/Al/sub 2-x/, 25:9576
Al-base--Er--Gd, phase diagram at 500°C, 25:8886
Cu--Er, crystal structure of intermetallic ErCu, $ErCu_2$, and $ErCu_4$, 25:8887
Cu--Er, phase diagram of, 25:8887
Er--Zr, solid solution formation in rapidly quenched, x-ray diffraction studies of metastable hcp, 25:8892
ERBIUM ISOTOPES Er-165
energy levels of, spin--parity assignments from superfluid model, (T), 25:10028 (JINR-P4-5228)
ERBIUM ISOTOPES Er-169
energy levels of, spin--parity assignments from superfluid model, (T), 25:10028 (JINR-P4-5228)
ERBIUM ISOTOPES Er-171
energy levels of, spin--parity assignments from superfluid model, (T), 25:10028 (JINR-P4-5228)
ERYTHROCYTES
labeling with oxygen-15, 25:8711(R) (NYO-3937-2)

XUM

radiation effects on rate of production of, in rats, effects of dose rate on, 25:8608
radioinduced changes in osmotic resistance of, in rabbits, uv, 25:8782
radiosensitivity of, effects of triacetoneamine-N-oxyl on, 25:8701
ERYTHROPOIESIS
radiation effects on, in mice injected with protective drugs, effects of erythropoietin on γ, 25:8775
ERYTHROPOIETIN
effects on erythropoietic recovery and survival of γ-irradiated mice injected with radioprotective drugs, 25:8775
ETHANE
radiolysis of, method for accumulating energy produced by, 25:8292(P)
yields from γ radiolysis of aqueous ethanol solutions as function of nitrate concentration, 25:8301
ETHANE, 1,1,1-TRICHLORO-2,2-BIS(p-CHLOROPHENYL)-
toxicity of chlorine-labeled, to man following ingestion of contaminated flour, calculations for, 25:8600
ETHANOL
effects on radiolysis of aqueous silver solutions and colloidal silver bromide, 25:8302
ETHYL SULFATES
effects on Triticum durum, mutagenic, 25:8641
ETHYLENE
yields from γ radiolysis of aqueous ethanol solutions as function of nitrate concentration, 25:8301
ethylene--SiH_4, ionization in mass spectrometer, reactions of products from, 25:8294
ETHYLENE, CHLORO-, POLYMERS
development of films of, for radioactive surface decontamination, 25:8663
use for fabrication of protective clothing for personnel, 25:8691
ETHYLENE, 1,2-DIBROMO-
toxicity of bromine-82 labeled, to man following ingestion of contaminated flour, calculations for, 25:8600
ETHYLENE GLYCOL
radiolysis of aqueous solutions of, yields from γ, 25:8300
ETHYLENE OXIDE
polymers, mechanical properties of gels of, produced by radioinduced reticulation, 25:8283
polymers, radioinduced production of gels from aqueous solutions of, γ, 25:8283
ETHYLENE POLYMERS
coating of powdered, with polymeric materials, 25:8282(P)
radiation effects on crosslinking of, effects of acetylene and fluorine on γ, 25:8276 (JAERI-Memo-4147)
radioinduced crosslinking of powdered, 25:8282(P)
radioinduced polymerization of olefin-unsaturated monomers on powder, 25:8282(P)
sorptive properties of modified powders of, for organic solvents and radioactive materials, 25:8282(P)
EUMYCOTA
Aspergillus nidulans, radioinduced mutations in, biochemical and genetic analysis of uv, 25:8640
Aspergillus nidulans, radioinduced mutations in, effects of pre-exposure treatment with 8-methoxypsoralen on uv, 25:8702
Fagus sylvatica, phosphorus-32 uptake by mycorrhiza of, effects of, on roots of Pinus, 25:8603
radiation effects on formation and dissociation of enzyme substrate-complexes in DNA of, uv, 25:8651
radiation effects on reproductive capacity of, used for food preparation, 25:8813 (NP-18236)
radiation effects on survival of, on fruits and vegetables, effects of dose on γ, 25:8813 (NP-18236)
Saccharomyces cerevisiae, frequency of mitotic recombination in mutants of, effects of delayed plating following treatment with nitrosoguanidine or nitrous acid on decrease of, 25:8797
Saccharomyces cerevisiae, radiation effects on budding cells of, genetic and physiological studies of x, 25:8798
Saccharomyces cerevisiae, radioinduced decrease in mitotic recombination frequency in mutants of, uv, 25:8797
Saccharomyces cerevisiae, radioinduced inactivation of mutants of, defective for dark repair, effects of liquid holding conditions on recovery from uv, 25:8797
Schizophyllum commune, radioinduced secondary mutations in, interactions with wild B/sub β/ alleles of x, 25:8643
Schizosaccharomyces pombe, radioinduced mutations and recombination inhibition in, protective effects of caffeine against uv, 25:8637
EUROPE
uranium enrichment in, economic and technical aspects of gaseous diffusion, nozzle, and ultracentrifugation methods for, 25:8435
EUROPIUM
abundance in HD 34452, (E), 25:9056
determination in titanium and titanium dioxide by neutron activation, 25:8233
EUROPIUM ISOTOPES Eu-152
use as tracer for measuring distribution of helicopter-sprayed agricultural insecticides, 25:8426(T) (NSJ-tr-155)
EUROPIUM OXIDES
Curie temperature of EuO films, effects of iron doping on, 25:9587
EXPERIMENTAL BREEDER REACTOR-II
instrumented subassembly system for, design and testing of prototype, 25:10171
kinetics for runs 25 to 30A, oscillator method and rod-drop method measurements of, 25:10173 (ANL-7542)
operation during November 1970, 25:10164(R) (ANL-7758)
protection system for, components hypothetical malfunction response testing of, 25:10228 (ANL-7665)
steam superheater in, tube baffle interaction from crossflow induced vibration in, (T), 25:10163 (ANL-7619)
EXPLODING WIRE PHENOMENA
use in hydro shock experiments, 25:8383 (AD-706767)
EXPLOSIONS
shock wave propagation through water from exploding wire, 25:8383 (AD-706767)
water waves from cratering, in shallow water, characteristics of, (E), 25:8386 (UCRL-50940)
EXPLOSIVES
emplacement of Project Piledriver, development of backpacking concretes for, 25:8962 (POR-4013)
ignition of laminar composite-type, computer program for studies of, 25:8961 (LA-4611)
EXPONENTIAL PILES
kinetics of heavy water moderated natural uranium fueled, calculational method for spatially dependent source, (E/T), 25:10307 (ORNL-TM-3136)
EYES
radiation effects on crystalline lenses of, neutrons, 25:8609
radiation effects on development of, in embryos of mice, x, 25:8646
radiation effects on retina of, of rabbits, use of electroretinogram for comparing toxic thermal neutron and x, 25:8761
radiation hazards to, of man, standards for protection against laser, 25:8694
radioinduced lesions in, protection against infrared, ionizing, laser, microwave, and uv, 25:8793
radioinduced opacifications of lens in, of mice, RBE for monoenergetic neutron, 25:8756 (NYO-2740-7, pp 154-217)
radiosensitivity of developing retinal tissues in, of monkey fetuses, effects of gestational age on x, 25:8757 (NYO-2740-7, pp 218-56)
radiotherapy of conjunctival neoplasms using phosphorus-32 in scleral shell applicators, 25:8731

F

FALLOUT
cloud chemistry and fractionation models for, 25:8362 (AD-707427)
effects of near ground-level nuclear explosion, on contamination of surface waters, (T), 25:8354 (HMI-B-86)
effects on organisms in river water following extreme reactor accident, 25:8660 (HMI-B-87)
monitoring at Ispra site, March to July 1970, 25:8370 (HASL-237, pp III.18-23)
monitoring at world sites from 1965 to 1970, data on, 25:8658 (HASL-237, pp II.1-16)
monitoring at worldwide sites, June to Sept. 1970, Health and Safety Laboratory Program for, 25:8367(R) (HASL-237)
monitoring in atmosphere in Australia, Gibraltar, Hong Kong, and UK, Jan. to July 1970, 25:8364 (AERE-R-6556)
monitoring in New Zealand during 1969, 25:8675(R) (NP-18529)
scavenging from atmosphere by raindrops, chemical tracer studies of, 25:8365(R) (COO-1199-19)
sources in relation to iodine-131 content of milk in USA during 1963 to 1968, 25:8629
FAST FLUX TEST FACILITY
design development requirements for, review of backup, 25:10266 (GEAP-5721)
design development requirements for, review of backup, 25:10265 (GEAP-5715)
design parameters for, review of conceptual backup, 25:10260 (GEAP-5552)
development of backup design for, December 1967 to February 1968, 25:10262(R) (GEAP-5641)
development of backup design for, June to August 1968, 25:10264(R) (GEAP-5684)
development of backup design for, March to May 1968, 25:10263(R) (GEAP-5650)
development of backup design for, May to August 1967, 25:10259(R) (GEAP-5550)
development of backup design for, September to November 1967, 25:10261(R) (GEAP-5614)
FAST TEST REACTOR
containment system for, conceptual backup design parameters for, 25:10260 (GEAP-5552)
containment system for, development of backup design, 25:10264(R) (GEAP-5684)
containment system for, development requirements for

backup design, 25:10266 (GEAP-5721)
control element drives for, development requirements for backup design, 25:10265 (GEAP-5715)
control elements for, development of backup design, 25:10263(R) (GEAP-5650)
control system for, development of backup design, 25:10264(R) (GEAP-5684)
cooling system for, conceptual backup design parameters for, 25:10260 (GEAP-5552)
cooling system for, development requirements for backup design, 25:10266 (GEAP-5721)
core for, conceptual backup design parameters for, 25:10260 (GEAP-5552)
core for, development requirements for backup design open lattice vertical, 25:10265 (GEAP-5715)
core structures for, development of backup design, 25:10263(R) (GEAP-5650)
core structures for, development of backup design, 25:10262(R) (GEAP-5641)
core structures for, development of backup design, 25:10264(R) (GEAP-5684)
cover gas system for, development requirements for backup design, 25:10266 (GEAP-5721)
emergency power system for, development requirements for backup design, 25:10266 (GEAP-5721)
engineered safeguards for, conceptual backup design parameters for, 25:10260 (GEAP-5552)
engineered safeguards for, development of backup design, 25:10263(R) (GEAP-5650)
engineered safeguards for, development of backup design, 25:10259(R) (GEAP-5550)
engineered safeguards for, development of backup design, 25:10261(R) (GEAP-5614)
experimental facilities for, conceptual backup design parameters for, 25:10260 (GEAP-5552)
experimental facilities for, development requirements for backup design, 25:10266 (GEAP-5721)
fuel assemblies for, cladding temperature variations and coolant mixing in seven-pin bundle, (E), 25:10207 (BNWL-SA-3286)
fuel elements for, development of backup design, 25:10263(R) (GEAP-5650)
fuel elements for, instrumentation requirements for driver, 25:10255 (BNWL-916)
fuel pins for, electric conductivity cell for measurement of coolant flow induced vibrations in, 25:10271 (WHAN-FR-21)
instrumentation for, development of backup design, 25:10259(R) (GEAP-5550)
instrumentation for, development requirements for backup design, 25:10265 (GEAP-5715)
instrumentation for, performance requirements for in-core, 25:10255 (BNWL-916)
loading facilities for, development of backup design, 25:10262(R) (GEAP-5641)
loading facilities for, development of backup design, 25:10259(R) (GEAP-5550)
loading facilities for, development of backup design, 25:10261(R) (GEAP-5614)
loading machine for, conceptual backup design parameters for, 25:10260 (GEAP-5552)
loading machine for, development requirements for backup design, 25:10265 (GEAP-5715)
neutron flux distribution for core-reflector interface of, comparison of design model calculations for, (T), 25:10272 (WHAN-FR-35)
physics measurements for backup design of, 25:10263(R) (GEAP-5650)
physics measurements for backup design of, 25:10261(R) (GEAP-5614)
physics measurements for backup design of, 25:10259(R) (GEAP-5550)
physics measurements for backup design of, 25:10262(R) (GEAP-5641)
physics measurements for backup design of, 25:10264(R) (GEAP-5684)
physics measurements for conceptual backup design of, 25:10260 (GEAP-5552)
power distribution for core--reflector interface of, comparison of design model calculations for, (T), 25:10272 (WHAN-FR-35)
pressure vessel for, development of backup design, 25:10262(R) (GEAP-5641)
pressure vessel for, development of backup design, 25:10261(R) (GEAP-5614)
pressure vessel for, development of backup design, 25:10264(R) (GEAP-5684)
pressure vessel for, development of backup design, 25:10259(R) (GEAP-5550)
pressure vessel for, development requirements for backup design, 25:10265 (GEAP-5715)
radioactive gas waste system for, development requirements for backup design, 25:10266 (GEAP-5721)
shielding for, conceptual backup design parameters for, 25:10260 (GEAP-5552)
shielding for, development of backup design, 25:10262(R) (GEAP-5641)
shielding for, development of backup design, 25:10261(R) (GEAP-5614)
shielding for, development of backup design, 25:10264(R) (GEAP-5684)
shielding for, development of backup design, 25:10259(R) (GEAP-5550)
shielding for, development of backup design, 25:10263(R) (GEAP-5650)
FECES
radioisotope content of, of rats following inhalation and intramuscular injection of americium-241, curium-242, plutonium-238, and plutonium-239, 25:8590 (CEA-CONF-1658)
FECUNDITY
radiation effects on, effects of dose rate, temperature, and chronic exosure on γ, 25:8750 (ORNL-4612)
FEDERAL REPUBLIC OF GERMANY
radioisotope content of human diet in, during 1968, cesium-137, and strontium-90, 25:8624 (EUR-4509)
FERMI FAST BREEDER REACTOR
operations history for August 1970, 25:10112 (DOCKET-50016-88)
FERMIONS
electrodynamics of, Schwinger terms in, 25:9852
equations for spin-$^1/_2$ unequal-mass, quasipotential, (T), 25:9697
field algebra for, 25:9850
interactions of, definition of quasi-averages for model systems with negative four-fermion, (T), 25:9687 (ITF-70-58-P)
interactions with linearized gravitational fields in general relativity theory, covariant Dirac equation for, (T), 25:9879
interactions with pseudoscalar bosons, invariant-amplitude contributions of box diagrams in spin-$^1/_2$, 25:9795
kinetics of beams of, point process with multicoincidences in, (T), 25:9692
Regge trajectory of, 25:9790
theory for spin-$^1/_2$, in external electromagnetic field, formulation of relativistic quantum mechanics in, (T), 25:9841
theory for, Hamiltonian implying exclusion principle in, (T), 25:9689 (LNF-70/22)
wave equations for spin-$^3/_2$, in de-Sitter space, (T), 25:9700
FERRATES
properties and uses of hexagonal, 25:10415(T) (UCRL-Trans-1431)
FERROMAGNETIC MATERIALS
Heisenberg model of impure, 25:10346(T) (BNL-tr-389)
FERTILIZERS
production of, cost analysis for dual purpose process heat and power reactor, 25:10293
FETUSES
radioinduced bone malformations in, of mice, synergistic effects of synkavit on x, 25:8703
radiosensitivity of developing retinal tissues in monkey, effects of gestational age on x, 25:8757 (NYO-2740-7, pp 218-56)
FIELD THEORY
coupling to gravitational fields, spherically symmetric initial solutions for, 25:9880
Einstein--Bohr box experiment, (T), 25:9154
models in, anomalous properties of vector currents in exactly solvable, 25:9836
Schwinger terms in local, 25:9834 (RLO-1388-584)
vector currents in exactly solvable models in, anomalous properties of, 25:9836
FILICINIDAE
Osmunda regalis, radioinduced synthesis of DNA in spores of, effects of light and dark growth conditions on x, 25:8614
FILMS
component redistribution in liquid binary mixture, moving along pipe wall in inhomogeneous magnetic field, (T), 25:9277
preparation of insulating thin, of thickness 10 to 50 A, 25:9385
preparation of superconducting thin, and dependence of properties on method of fabrication, 25:9385
FINS
heat transfer effects of internal, on performance of fast breeder reactor fuel elements, 25:10223
FIRES
control, detection, and prevention of sodium, guidelines for, 25:8827 (ANL-7691)
FISSION PRODUCTS
analysis procedures for gas, in CANDU-type reactor fuel elements, 25:10227
beta decay of, data tabulation of abundances and energies of beta particles and conversion electrons from, 25:10023 (CEA-N-1372)
beta spectra of plutonium-239, (E), 25:10036
content in operating reactors, ICON code for calculation of, 25:10236 (AERE-R-6242)
content of short-lived, in ground-level atmosphere in Australia, Gibraltar, Hong Kong, and UK, Nov. 1969 to Nov. 1970, 25:8364 (AERE-R-6556)
content of short-lived, in UK rainwater, Nov. 1969 to Nov. 1970, 25:8364 (AERE-R-6556)
decay activity in reactor fuels, optimization method for calculation of, 25:10308
decay in operating reactors, β and γ heating from, (T), 25:10299
diffusion of gaseous, from ceramic fuels, mechanisms of,

XUM

25:8958 (SRARI-P-73)
distribution in fallout, model for, 25:8362 (AD-707427)
distribution in gas cooled reactor cooling systems, 25:10244(R) (ORNL-TM-3212)
removal from molten fluoride mixtures, use of low-pressure distillation for, (E), 25:10210 (ORNL-4434)
removal from reactor containment systems, effectiveness of sprays for, (E), 25:10256 (BNWL-1485)
separation from irradiated LMFBR fuels, solvent extraction processes for, 25:8316 (BNWL-CC-1939)
yields from 11.2-MeV proton and 10.6-MeV deuteron fission of uranium-238, (E/T), 25:10052

FISSIONABLE MATERIAL
determination in reactor fuel elements and reactor fuels by activation and scintillation counting, 25:8215(P)

FLANGES
pretightening of large pressure vessel, procedures for, 25:10096 (ZJE-65)

FLOWMETERS
book: Electromagnetic Methods of Measuring the Parameters of MHD Processes, in Russian, 25:9273
design of electromagnetic, for liquids, 25:8400(P)

FLUID FLOW
book: Electromagnetic Methods of Measuring the Parameters of MHD Processes, in Russian, 25:9273
characteristics of incompressible inviscid homogeneous two-dimensional turbulent, VORTEX computer program for describing, 25:8407 (CLM-R-106)
heat transfer in forced laminar or turbulent, with exponential heat flux distribution, calculations for several flow geometries of, 25:8416
heat transfer in two-phase, in horizontal or vertical tubes, effects of tubing bends on, 25:8406 (CEA-CONF-1649)
magnetohydrodynamic channel, two-dimensional current distribution in, 25:9271
magnetohydrodynamic free convection in, for high and low Prandtl numbers, 25:9270
magnetohydrodynamic, effect of magnetic field on thermal instability in layer of Maxwell, (T), 25:9274
magnetohydrodynamic, effects of temperature dependence of transfer coefficients on flat-channel laminar, (T), 25:9276
magnetohydrodynamic, gas-ionizing shock waves in, (T), 25:9272
magnetohydrodynamic, hyperliptic flow past point source, 25:9269 (AD-706106)
magnetohydrodynamic, past moving plate in transverse magnetic field, (T), 25:9280
magnetohydrodynamic, stability of statically unstable heterogeneous shear flow, (T), 25:9279
temperature and void fraction distribution in, in heated channel with inlet subcooling, axial, (E/T), 25:8417

FLUORIDE VOLATILITY PROCESSES
operation of fluid-bed, safety manual for, 25:8446 (ANL-7672)

FLUORINE
determination in air particulates by spark source mass spectrometry, 25:8208
determination in uranium concentrates by volumetric titration using thorium nitrate, 25:8201 (LFEN-NI.-36-a)
effects on γ-induced crosslinking of polyethylene, 25:8276 (JAERI-Memo-4147)

FLUORINE ISOTOPES F-18
use for scanning in diagnostic and metabolic studies, development of computer programs for, 25:8716

FLUORINE ISOTOPES F-19
energy levels from oxygen-18 (He-3,d) reactions, spectroscopic factors for, (E), 25:9985
photon reactions (γ,n) at 100 to 800 MeV, excitation functions for, (E/T), 25:9977 (LUNP-7009)

FLUORINE ISOTOPES F-20
energy levels from oxygen-18 (He-3,p) reactions, spin assignments and branching and multipole mixing ratios for, (E), 25:10004

FLUORITES
radioinduced thermoluminescence of, emission spectra of gamma, 25:9548

FOOD
analysis by neutron activation, 25:8227
honey, radioactivity in, afferent radium α, 25:8665
honey, radioactivity in, comparison of artificial and natural β and γ, 25:8665
radiation processing of, activities of joint FAO/IAEA, 25:8818
radiation processing of, economic and legal aspects of, in USA during 1967, 25:8813 (NP-18236)
radiation processing of, training manual on technology and techniques for, 25:8814 (STI/DOC-10/114)
uranium content of, in Soviet Union, 25:8631

FOOD CHAINS
iodine-129 transport through, for use in deriving working limits for continuous release rates to atmosphere, 25:8681
radioisotope transport in, of nuclear explosion-contaminated estuarine and marine ecosystems in relation to daily ingestion by man, use of stable element content of fish and invertebrates for predicting, 25:8627
radioisotope transport in, of nuclear explosion-contaminated tropical ecosystems, ecological models for predicting, 25:8626

FOOD IRRADIATION FACILITIES
design and operation of production and research, training manual on, 25:8814 (STI/DOC-10/114)

FORMALDEHYDE
effects on uv-irradiated Escherichia coli, effects of radiation dose on spectrum of mutagenic, 25:8642

FORT CALHOUN POWER REACTOR, UNIT 1
design parameters of, revised and additional data on, 25:10151 (DOCKET-50285-39)
operations aspects of, revised and additional data on, 25:10151 (DOCKET-50285-39)

FOURIER TRANSFORMS
deconvolution using, statistical aspects of, 25:10351 (LA-4556)

FRANCE
radioisotope content of human diet in, during 1968, cesium-137 and strontium-90, 25:8624 (EUR-4509)
uranium reserves in, estimates of, 25:8373

FREE RADICALS
distribution of radiolytic, in methanol at 77°K, 25:8288

FRUCTOSEDIPHOSPHATE ALDOLASE
radiation effects on activity of, in rabbits, sublethal ionizing, 25:8779

FRUITS
grapes, radiation processing of, effects of, on storage life, γ, 25:8817
oranges, radiation effects on residue from Valencia, effects of, on methoxyl content, viscosity, and yield of pectins, 25:8823
radiation processing of, economic and legal aspects of, in USA during 1967, 25:8813 (NP-18236)

FUEL CAPSULES
materials for high-temperature, development and testing of, 25:8427(R) (ORNL-4639)
materials for radioisotope heat source, development of, 25:8850 (ORNL-4600, pp 181-5)
testing of curium-fueled, for leaks, 25:8427(R) (ORNL-4639)

FURNACES
design and operation of overpressure electric arc, for fabrication of ceramic materials, 25:8914
design of high-temperature, for compatibility testing, 25:8389 (AERE-M-1990)

FUSED SALTS
thermotransport in, isotope separation by, 25:8336
void fraction in reactor fuels, (E/T), 25:10177

G

GABON REPUBLIC
uranium reserves in, estimates of, 25:8373

GADOLINIUM ALLOYS AND SYSTEMS
Al--Gd--Ni, magnetic properties and phase diagram of GdNi/sub x/Al/sub 2-x/, 25:9576
Al-base--Dy--Gd, phase diagram at 500°C, 25:8886
Al-base--Er--Gd, phase diagram at 500°C, 25:8886
Al-base--Gd--Ho, phase diagram at 500°C, 25:8886
Al-base--Gd--Sc, phase diagram at 500°C, 25:8886
Al-base--Gd--Tb, phase diagram at 500°C, 25:8886
Al-base--Gd--Y, phase diagram at 500°C, 25:8886
Fe--Gd, crystal structure of intermetallic $(Gd_{2/3}2Fe_{1/3})Fe_{83}$, 25:8891

GADOLINIUM ISOTOPES Gd-152
energy-level scheme from terbium-152m decay, (E), 25:9978(R) (ORO-3398-26)

GADOLINIUM ISOTOPES Gd-156
beta decay of, conversion electron spectra and log ft value for, (E), 25:10034

GADOLINIUM OXIDES
diffusion of helium in, effects of temperature on, 25:8427(R) (ORNL-4639)
Ce_2O_3--Gd_2O_3, diffusion of helium in, effects of temperature on, 25:8427(R) (ORNL-4639)

GALAXIES
classification of clusters of, (E), 25:9125
detection of, in fields of southern hemisphere radio sources, (E), 25:9066
ejection of condensed plasmoids from nuclei of, (T), 25:9130
energy in groups and clusters of, (T), 25:9130
evolution of nuclei of, (T), 25:9130
evolution of two-dwarf emission-line, (E), 25:9126
expansion of clusters of, proposed test for, (T), 25:9133
hydrogen distribution in, (E), 25:9134
identification of Maffei 1 as member of Local Group, (E), 25:9148
kinematic of H II regions in NGC 4490-85, (E), 25:8994
luminosity of five elliptical, isophotes of, (E), 25:9139
luminosity of M31, (E/T), 25:9141
mass distribution in M33, (E), 25:9149
mass of M31, (E/T), 25:9141
model for M31, (E/T), 25:9141
properties of Sb and Sc, (E), 25:9137
radiation fields in nuclei of, (T), 25:9130
spectral classification of Markaryan, (E), 25:9140
spectral redshifts of 23 blue Haro, (E), 25:9128
spectral redshifts of 3C 390.3, two emission, (E),

25:9147
star formation in M31, rate of, (E), 25:9134
stellar content in nuclei of, with measured rotation curves, (E), 25:9137
stellar content of two dwarf emission-line, (E), 25:9126
stellar population model for M33, (E), 25:9149
structure of, spiral, (T), 25:9142
waves in disk, preference of trailing spiral, (T), 25:9138
GALLIUM
abundance in iota Ori B, (E), 25:8995
determination in titanium and titanium dioxide by neutron activation, 25:8233
determination of trace amounts of, in glass by neutron activation after sodium removal by hydrated antimony pentoxide, 25:8223
effects on annealing of electron irradiation damage in p-type silicon, 25:9549
preparation of thin single crystals of, development of mold for, 25:8858
GALLIUM ALLOYS AND SYSTEMS
Ga--V, superconductivity in intermetallic V_3Ga, pressure-enhanced, (E/T), 25:9372
GALLIUM ARSENIDES
performance of epitaxial n-type, as detector for alpha particles and gamma rays, 25:8491
radioinduced lattice expansion of, 400 keV xenon ion, 25:8964
GALLIUM PHOSPHIDES
ion implantation effects on optical properties of films and bulk, argon, 25:9562
GAMMA CAMERAS
development of, status of, 25:8500
image intensifier tubes for, 25:8497
operation of, 25:8497
GAMMA RADIATION
attenuation around rectilinear probe, computer calculation of, 25:8683
detection and discrimination in liquid scintillation detectors, 25:8506
detection and measurement of, using gallium arsenide diodes, 25:8491
detection of low-energy pulsed, from NP 0532, (E), 25:9062
detection of mineral deposit, by airborne sensors, uses in prospecting, 25:8378
detection of, relative photopeak efficiency of thallium-activated cesium iodide detector for, 25:8502
dose rates in soils from artificial and natural radioisotopes, method for distinguishing, 25:8360
dose to gonads, hands, and whole-body of medical personnel during preparation and application of γ emitters for interstitial therapy, 25:8689 (SZS-6/70, pp 19-27)
dose to human bladder and rectum during intracavitary therapy of female gynecological carcinomas, 25:8679 (SZS-6/70, pp 9-18)
dose to human bones, effects of route of administration plutonium-239, 25:8596(T) (LF-tr-41, pp 127-97)
dose to man following ingestion of radium-226, methods for calculating, 25:8669 (COO-2088-1)
dose to man, ICRP recommendations for maximum permissible radium-226, 25:8674(T) (LF-tr-41, pp 199-220)
dose to personnel in plutonium industry, maximum permissible plutonium-239, 25:8674(T) (LF-tr-41, pp 199-220)
dose to skin and whole-body of man following continuous exposure during one year to krypton-85 dispersed in atmosphere, calculation of, 25:8667 (BNWL-SA-3233)
dosimetry for uniform cylindrical phantoms, comparison of unilateral and bilateral external cobalt-60, 25:8686
dosimetry from radioisotopes deposited internally in man, counting geometry for, 25:8687
dosimetry of, response of lithium fluoride thermoluminescent dosimeters for, 25:8567
effects on alkaline ice at 77°K, extinction of trapped electrons and oxygen ions from, 25:8287
effects on ammonia--phosphine mixtures, 25:8299
effects on aniline at 77°K, 25:8296
effects on aqueous ethanol solutions of potassium nitrate, 25:8301
effects on aqueous sodium nitrate solutions, 25:8297
effects on aqueous solutions of 2-deoxyribose, yields from, 25:8305
effects on aqueous solutions of ethylene glycol, yields from, 25:8300
effects on bacterial spores in relation to sterilization of space craft, progress report on synergistic effects of low temperature on low dose rate inactivating, 25:8803(R) (TID-25468)
effects on barium sulfate crystals with nitrite ion impurities, 25:8286
effects on barley seeds, mutagenic, 25:8656
effects on binding of phenylalanine and its derivatives to serum albumin, 25:8280
effects on bleached color centers in alkaline ice, 25:8272
effects on chemical properties of lysozyme, effects of exposing dry solid state on cesium-137, 25:8604 (COO-690-41)
effects on chromosomes in bone marrow of dogs, effects of dose on aberrant, 25:8755(T) (JPRS-51660)
effects on chromosomes of lymphocytes in man, aberrant, 25:8788(T) (LIB/Trans-296)
effects on coastal Douglas fir, interior Douglas fir, Sitka spruce, and western hemlock, effects of, on cytogenetics, seed germination, and seedling growth in relation to sensitivity, 25:8799
effects on colloidal silver and silver bromide, 25:8302
effects on conditioned reflex response of nervous system in dogs, chronic low-dose, 25:8755(T) (JPRS-51660)
effects on count of leucocytes in peripheral blood of dogs, effects of dose on, 25:8755(T) (JPRS-51660)
effects on crosslinking of polyethylene, 25:8276 (JAERI-Memo-4147)
effects on cultured mammalian and plant cells, comparison of OER and RBE for californium-252 mixed neutron and, with radium, 25:8757 (NYO-2740-7, pp 218-56)
effects on dielectric constant of potassium acid phosphate at 70 to 150°K, 25:8275
effects on dilute solutions of collagen in air and nitrogen, 25:8307
effects on DNA in mammalian cells, existence of strand rejoining mechanism for cellular repair following, 25:8605(R) (ORO-2832-85)
effects on egg hatching and life spans of laboratory and natural snail populations, effects of dose rate, temperature, and chronic exposure on, 25:8750 (ORNL-4612)
effects on erythropoietic recovery and survival of mice, effects of erythropoietin on protective effects of drugs against, 25:8775
effects on germination of stored punjab red onions, 25:8815
effects on graft polymerization of methyl methacrylate on flaky glass, 25:8277(T) (NSJ-tr-160)
effects on grafting of styrene on benzyl cellulose, 25:8271
effects on growth of flower buds, pollen grains, and pollen tetrads of mulberries, 25:8794(T) (NSJ-tr-158)
effects on growth of spores of Clostridium botulinum Type E on fresh shrimp, effects of dose on, 25:8804 (TID-25556)
effects on heart function following scanning using iodine-131-labeled albumin macroaggregates, 25:8713 (UCLA-12-798)
effects on hematopoiesis in dogs, in comparison with neutrons and x rays, 25:8774
effects on hematopoiesis in rats, combined effects of reduced muscular activity and dose fractionation on, 25:8755(T) (JPRS-51660)
effects on hematopoietic colony formation in spleen of mice, effects of dexamethasone on, 25:8765
effects on hematopoietic colony formation in spleen of mice, effects of ACTH, cold exposure, and dexamethasone on, 25:8767
effects on heptane at low temperatures, effects of concentration of nitrous oxide and oxygen on kinetics of, 25:8281
effects on human bones used in transplants, electron spin resonance study of paramagnetic species following sterilizing cobalt-60, 25:8825
effects on iodomethane vapor and iodomethane--phosphine mixtures, yields of methane and hydrogen from, 25:8303
effects on isolated mammalian DNA in relation to incidence of double strand scissions, indirect mechanism for, 25:8605(R) (ORO-2832-85)
effects on isomerization of 1-bromobutane, 25:8279
effects on lithium-doped magnesia at 77°K, ESR of paramagnetic center induced in, 25:9544
effects on longevity, reproductive system, and fertility of female and male stable flies, 25:8822
effects on medulla oblongata tissue of brain of rats, ultrastructural study of whole-body, 25:8787
effects on methanol at 77°K, spatial distribution of radicals from, 25:8288
effects on mitotic recombination frequency in mutants of Saccharomyces cerevisiae, effects of delayed plating following exposure on, 25:8797
effects on natural calcium fluoride crystals, thermoluminescence emission spectra, 25:9548
effects on optical density of clear poly(methyl methacrylate), 25:8273
effects on p-type silicon, minority carrier lifetime study of recombination center annealing in, 25:9567
effects on p-type silicon, volume gradient of emf induced in, 25:9568
effects on populations of old-field mice, acute 500 R cobalt-60, 25:8760
effects on production of gels of polyethylene oxide in aqueous solutions, mechanical properties of products from, 25:8283
effects on rats, combined effects of reduced muscular activity and dose fractionation on excretion of calcium and chlorides in urine, 25:8755(T) (JPRS-51660)
effects on reproductive capacity of dogs, chronic low-dose, 25:8755(T) (JPRS-51660)
effects on resistance of steatite ceramics, 25:9551
effects on shelf life of shrimp, effects of blanching, moisture content, and sorbic acid on, 25:8820
effects on silicon at 1.25 MeV, defects induced in, 25:9572
effects on storage life and wholesomeness of cereals,

XUM

fruits, meats, seafood, and vegetables, economic aspects of, 25:8813 (NP-18236)
effects on storage life and wholesomeness of onions, potatoes, and wheat, 25:8824
effects on storage life of grapes, 25:8817
effects on storage life of unleavened bread in India, effects of antioxidants on, 25:8819
effects on survival and yield of corn, lettuce, radishes, squash, and tomatoes in comparison to effects of simulated radioactive fallout, chronic cesium-137, 25:8796
effects on survival of cabbage and radish plants, combined effects of protons on, 25:8755(T) (JPRS-51660)
effects on survival of epithelium cells in intestine of mice, effects of cell cycle stage on whole-body, 25:8785
effects on survival of Escherichia coli, effects of glucose on, 25:8812
effects on survival of mice, effects of temperature on, lethal, 25:8768
effects on survival of skin allografts in leopard frogs, effects of 5000 R dose on, 25:8620
effects on survival of synchronized cultures of Chinese hamster cells, comparison of effects of aeration and hypoxia on californium-252 mixed neutron and, 25:8757 (NYO-2740-7, pp 218-56)
effects on survival of synchronized cultures of Chinese hamster cells, comparison of effects of aeration and hypoxia on cobalt-60, 25:8757 (NYO-2740-7, pp 218-56)
effects on swine, pathological, 25:8773
effects on transforming DNA in Bacillus subtilis, bacteriophage T3, and Escherichia coli, protective effects of acridine orange against cesium-137, 25:8707
effects on tryptophyl groups of lysozyme, spectrography of, 25:8604 (COO-690-41)
effects on vitamin content of enriched flour, 25:8816
emission following shutdown of thermal reactors, sources of, (T), 25:10165 (CISE-R-233)
emission from Sun, (E/T), 25:9058 (MPI-PAE/EXTRATERR-48)
hazards to patients and personnel during intracavitary therapy of female genital carcinomas, reduction of radium, 25:8729 (SZS-6/70, pp 1-8)
hazards to water supplies from polonium-210 migration in soils, 25:8593 (COO-1733-11)
intensities at atmospheric balloon altitudes, omnidirectional, 25:9305
leakage through wall joints in shielding, (E/T), 25:10296(T) (NSJ-tr-157)
origin and diffusion of cosmic background, (T), 25:9254
production and transport in liquid nitrogen after fast neutron reactions, 25:9950
reactions with uranium at 145, 192, 662, and 1250 keV, K-shell x-ray production and photoelectric cross sections for, 25:9235
transport in air, angular flux densities and exposure angular distributions for ^{60}Co, (T), 25:9539
use for therapy of human cervical carcinomas, effectiveness of linear accelerator in comparison to counter dual linear accelerator and cobalt, 25:8740
uses in industry, development of new, 25:8432

GAMMA SOURCES
activity in honey, comparison of artificial and natural, 25:8665
design of variable-size radium-226, for use for implant therapy of neoplasms of human uterus, 25:8736
development of cobalt-60 afterloading molded, for use for therapy of intracavitary and skin neoplasms, 25:8738
development of iridium-192 afterloading wire, for use for implant therapy of neoplasms, 25:8737
preparation of Moessbauer ^{57}Co in copper, giving single-line spectrum, 25:9595

GAMMA SPECTROMETERS
calibration of thallium-activated sodium iodide scintillation, 25:8535
circuit for gain compensation for, 25:8540
design and performance of lithium-drifted germanium, 25:8541
fabrication of lithium-drifted germanium, 25:8463 (BLG-447)
resolution of lithium-drifted germanium, computer simulation analysis of effects of carrier trapping and electronic noise on, 25:8532 (UCRL-72481)
shielding for lithium-drifted germanium, with californium-252 source for neutron capture gamma spectroscopy, 25:8537
spectra analysis for, computer program for, 25:8531 (MLM-1773)

GARIGLIANO POWER REACTOR
maintenance during April to June 1970, 25:10126 (TID-25608)
neutron flux monitoring in, performance of in-core detectors for, 25:10107
operation during April to June 1970, 25:10126 (TID-25608)
waste disposal at, procedures for low activity solid, 25:10131

GAS CENTRIFUGES
design and operation of, for uranium enrichment in UK, 25:8431

GAS FLOW
calculation of transient, in underground natural gas reservoir containing nuclear explosion-created gas well, simplified model for, 25:8387 (UCRL-71868)
characteristics of quasi-developed turbulent, in strongly heated circular pipes, equations for predicting, 25:8420
magnetohydrodynamic, behavior of free-burning electric arcs in transverse magnetic fields and, (E/T), 25:9282
magnetohydrodynamic, properties of argon in cooled-wall channels, (E/T), 25:9281

GASEOUS DIFFUSION PLANTS
development for uranium enrichment in UK, 25:8431

GASEOUS DIFFUSION PROCESS
efficiency for isotope separation, effects of flow patterns on, 25:8438

GASES
book: Properties of Gases at High Temperatures, in Russian, 25:9444
droplet dispersion in flowing, design of mixing nozzle for producing, 25:8404(P)
electron transport in tissue-equivalent mixtures of, 25:8482 (NYO-2740-7, pp 112-53)
models of, stochastic operators in lattice, 25:10379(T) (SC-T-71-3000)
properties of dense charged Bose, low-temperature, 25:9605
properties of interplanetary, adiabatic relationship with, (T), 25:9115
proton multiple scattering by tissue-equivalent mixtures of, at 2.78 MeV, 25:8482 (NYO-2740-7, pp 112-53)
radioactivity measurements of, internally-loaded G--M detector for low-level beta, 25:8520
radiolysis of, equipment and experiments for pulse, 25:8285(R) (RPI-3821-5)
shock wave propagation in uniform magnetic field, magnetohydrodynamic pressure, (T), 25:9278
sorption by solids, effects of pressure on kinetics of, 25:10358(T) (ORNL-tr-2392)

GASTROINTESTINAL TRACT
radiosensitivity of human, relation of, to planning for therapy using high-energy ionizing radiations, 25:8739

GELATIN
effects on radiolysis of aqueous silver solutions and colloidal silver bromide, 25:8302

GENES
radioinduced mutations for Rex, in mice, x, 25:8645

GENETIC RECOMBINATION
frequency in mutants of Saccharomyces cerevisiae, effects of delayed plating following treatment with nitrosoguanidine or nitrous acid on decrease of, 25:8797
radiation effects on, in partially diploid derivatives of Escherichia coli, uv, 25:8634(R) (ORO-4024-1)
radioinduced decrease in frequency of, in mutants of Saccharomyces cerevisiae, uv, 25:8797
radioinduced, in yeast, protective effects of caffeine against uv, 25:8637

GENETICS
radiation effects on, of Drosophila melanogaster, neutron and x, 25:8756 (NYO-2740-7, pp 154-217)
research at AECL during 1970, progress report on, 25:8666(R) (AECL-3728)

GEOLOGY
bibliography on Nevada Test Site, 25:8355 (USGS-474-88)

GEOMAGNETIC FIELDS
activity in, correlation with ionospheric spread F occurrence, (E), 25:9290
conjugate point phenomena in auroral zone, review of, (E/T), 25:9284(T) (JPRS-52023)
current of quasi-trapped particles in, discontinuity, (T), 25:9347
origin, (T), 25:9129
perturbations of magnetospheric, associated with dynamic spectra of atmospheric whistlers, (E/T), 25:9346
pulsations at high latitudes, cooperative research on micro-, (E), 25:9326
pulsations in, relation of Pc2, -3, and -4, with intensity of ring current and location of plasmapause, (E/T), 25:9353
pulsations of, propagation through nighttime ionospheric F region of Pc1, (T), 25:9338
sudden commencements and sudden impulses in, correlation with magnetospheric boundary compressions, (E/T), 25:9332

GERMANIUM ALLOYS AND SYSTEMS
Ge--V, superconductivity in intermetallic V_3Ge, pressure-enhanced, (E/T), 25:9372
Ge--Zr-base, corrosion by steam at 300 to 600°C, factors affecting, 25:8833 (AERE-M-1854)

GERMANIUM ISOTOPES Ge-75
neutron capture by, determination of thermal cross section for second-order reaction products, (E), 25:10040

GERMANIUM SILICIDES
properties for use in thermoelectric converters, 25:8421 (AERE-M-1594)

GERMINATION
radiation effects on, of stored punjab red onions, γ, 25:8815

GLASS
analysis for trace elements by neutron activation after sodium removal by hydrated antimony pentoxide, 25:8223

radiation effects on subsequent polymerization of methyl methacrylate on flaky aluminosilicate, γ, 25:8277(T) (NSJ-tr-160)
GLOBULINS
effects on production of G and M antibodies in immunized, x-irradiated rabbits, serum gamma, 25:8621
radiation effects on activity of, in serum of rats, comparison of action of radiomimetics and x_n, 25:8612
GLOVE BOXES
design of vacuum, for sodium handling and purification, 25:8390 (AERE-R-5502)
vacuum system for, design for use in preparation of radiation targets, 25:8453 (ORNL-TM-3209)
GLUCOSE
effects on blood flow in resting muscle, combined effects of insulin on, xenon-133 tracer study of, 25:8586
effects on host-cell reactivation in Escherichia coli, 25:8812
GLUCOSE 6-PHOSPHATE DEHYDROGENASE
radiation effects on activity of, in rabbits, sublethal ionizing, 25:8779
GLYCINE
crystal structure of beta, electron diffraction determination of, 25:10405 (UCRL-20139)
GLYCINE, N-(CARBOXYMETHYL)-N'-(2-HYDROXYETHYL)-N,N'-ETHYLENEDI-
complexes with neptunium, thorium, or uranium, preparation and stability of, 25:8237 (KFK-1210)
GOATS
calcium metabolism in, effects of dietary calcium and phosphorus on, 25:8592(R) (COO-1339-43)
phosphorus metabolism in, effects of dietary calcium and phosphorus on, 25:8592(R) (COO-1339-43)
volume of milk in mammary glands of, determination using carbon-14-labeled polyethylene glycol and cerium-141, 25:8587
GOLD
compounds, gold-197 Moessbauer spectra in monovalent and trivalent, isomer shifts and quadrupole splittings in 4.2°K, 25:9593
determination by neutron activation or x-ray spectrographic and ion exchange methods, 25:8221
determination in airborne particulates by neutron activation, 25:8231
determination in human fingernails and hair by neutron activation and γ spectrometry, 25:8229
determination in titanium and titanium dioxide by neutron activation, 25:8233
determination of trace amounts of, in glass by neutron activation after sodium removal by hydrated antimony pentoxide, 25:8223
deuteron channeling energy losses at 20 to 28 keV in crystal foils of, (E), 25:9555
diffusion in, lattice-dynamical theory of isotope effects in, 25:9589
performance of activation detectors of, for neutron spectra measurements at 1 eV to 10 keV, 25:8481 (KFK-1233)
GOLD CHLORIDES
radiolysis of, formation of gold ions following pulse, 25:8306
GOLD IONS
yields of, following pulse radiolysis of gold chlorides, 25:8306
GOLD ISOTOPES Au-195
electron-capture decay of, branching ratios and conversion-electron spectra from, (E), 25:10048
GOLD ISOTOPES Au-197
electron elastic scattering by, charge distributions from, (E), 25:10014
Moessbauer spectra in gold(I) and (III) compounds at 4.2°K, isomer shifts and quadrupole splittings in, 25:9593
photon reactions at 1 GeV, analysis of fission processes in, (E/T), 25:10037
GOLD ISOTOPES Au-198
use for scanning human liver to detect noncalcified hydatid cysts, 25:8719
GONADS
radiation dose to, of medical personnel during preparation and application of γ emitters for interstitial therapy, γ, 25:8689 (SZS-6/70, pp 19-27)
GRANODIORITES
properties of Project Piledriver site, mechanical and physical, (E), 25:8962 (POR-4013)
GRAPHITE
arcing behavior of, exposed to pulsed rf discharge, (E), 25:9442
coating with niobium from vapor--gas mixture, mechanism of, 25:8917
corrosion of H327, by high temperature steam, (E), 25:10244(R) (ORNL-TM-3212)
corrosion of, inhibiting effects of methane and carbon monoxide coolant additives on carbon dioxide, 25:10201(P)
electric properties of, multiple kink effect of magnetic field on current--voltage characteristic, 25:9586
electron energy losses at 25 keV in single-crystal, spectra for loss range 20 to 400 MeV, (E), 25:9167
neutron spectra in, measurement of, 25:9956
oxidation of, inhibiting effects of phosphorus oxychloride on, 25:8906 (AERE-R-4857)
porosity of nuclear-grade, correlation with diffusion coefficients, 25:8924 (DP-Report-437)
thermal conductivity of high-porosity, at 500 to 2200°K, (E), 25:8942
GRAVITATION
constant of, formulas for relation of electron, neutron and proton masses with, (T), 25:9878
Einstein field equations with electromagnetic energy tensor in, cylindrical wave solutions of, 25:9873
Einstein theory of, expansion around Newtonian theory in flat and curved three-dimensional space, 25:9883
field equations for static axially symmetric shells and disks in general relativity, 25:9882
formalism for role in Friedman elementary particle theory, 25:9870 (JINR-P2-5289)
instability of fluid of matter and radiation, (T), 25:9157
GRAVITATIONAL COLLAPSE
black-hole production in nonspherical, (T), 25:9155
neutrino emission during stellar, (T), 25:8997
GRAVITATIONAL FIELDS
coupling to massless scalar fields, spherically symmetric initial solutions for, (T), 25:9880
fermion interactions with linearized, covariant Dirac equation for, (T), 25:9879
particle source of scalar--tensor, (T), 25:9880
quantization of, review of, (T), 25:9872
S-matrix formulation for, 25:9857
GRAVITATIONAL RADIATION
emission from galactic nuclei, (T), 25:9130
emission from neutron stars, angular momentum loss due to, (T), 25:9063
theory of, conserved quantities in, 25:9871
GRAVITY WAVES
generation of mid-latitude atmospheric, during magnetic substorms, (E/T), 25:9293
GROSSWELZHEIM SUPERHEAT REACTOR
design parameters for, 25:10172
fuel elements for, design problems for, 25:10172
operations history for, 25:10172
GROUND WATERS
flow into shallow lakes, natural radon tracer technique for measuring, 25:8350 (CU-2493-11, App.4)
particulate matter in, effects on radioisotopes transport through soils, (E/T), 25:8361
radioisotope transport by Hanford area, mathematical model for prediction of, 25:8345 (BNWL-SA-3494)
radon-222 content of Experimental Lakes Area, Ontario, 25:8352 (CU-2493-11, App.6)
GROUP THEORY
conformal group in, unitary representations of, 25:9823
Lie algebra in, representations of Gell-Mann--Dashen algebra with structure constants of arbitrary, 25:9824
representations of Gell-Mann--Dashen algebra with structure constants of arbitrary Lie algebra and O(3) symmetry in, 25:9824
GUANIDINE, 1-METHYL-3-NITRO-1-NITROSO-
effects on incidence of chromosome aberrations in x-irradiated Vicia faba, 25:8705
effects on yeast, effects of caffeine on mutagenic, 25:8637
GUANIDINE, NITROSO-
effects on mitotic recombination frequency in mutants of Saccharomyces cerevisiae, effects of delayed plating following exposure on, 25:8797
GYMNOSPERMIDAE
Picea sitchensis, radiation effects on cytogenetics, seed germination, and seedling growth in, γ, 25:8799
Pinus radiata, phosphorus-32 uptake by ectotrophic mycorrhiza on, 25:8603
Pseudotsuga menziesii, radiation effects on coastal, γ, 25:8799
Pseudotsuga menziesii, radiation effects on interior, effects of, on cytogenetics, seed germination, and seedling growth in relation to sensitivity, γ, 25:8799
Tsuga heterophylla, radiation effects on, effects of, on cytogenetics, seed germination, and seedling growth in relation to sensitivity, γ, 25:8799

H

H.B. ROBINSON POWER REACTOR, UNIT 2
operations incident of November 27, 1970, insertion failure of P-6 control rod assembly, 25:10123 (DOCKET-50261-49)
HI REGIONS
distribution in Carina, (E), 25:9146
distribution in M31, (E), 25:9134
molecular hydrogen density in, (T), 25:9088
molecular hydrogen formation on dust grains in, (T), 25:9087
temperatures of cold, kinetic, (E), 25:9132
HII REGIONS
comparison of extragalactic, to dwarf emission-line galaxies, (E), 25:9126
detection of faint, in NGC 4490-85, (E), 25:8994
detection of OH emission in Ceph IV association, (E), 25:9015
distances of, spectrophotometric, (E), 25:9145
distribution in M31, (E), 25:9134

XUM

dust--radiation instability in, (T), 25:8999
electron temperatures of, free--free Gaunt factor in, (T), 25:9081
flux densities of seven compact sources in, (E), 25:9077
identification of possible planetary nebulae as compact, (E), 25:8996
observations of faint extragalactic, (E), 25:9143
spectra of M17, M42, and IC 1795, shapes of radio recombination lines in, (E), 25:9080
velocities of, radial, (E), 25:9145

HADRONS
coupling constants of, causality function in four-fermion model with indefinite metric for, (T), 25:9741
coupling of, quark focusing principle for, 25:9760
coupling to π at low energies, S-matrix commutation with axial charge for universality of, (T), 25:9886 (DESY-70/57)
interaction vertex of, quark focusing, 25:9760
interactions at high energies in quantum field theory, straight-line paths approximation for amplitudes of, 25:9751
interactions in quark model, breakdown of Pomeranchuk conjecture for, (T), 25:9806
interactions of, chiral-symmetric coupling of soft π in, 25:9763
interactions of, eikonal Regge model for elastic, (T), 25:9776
interactions of, quark focusing and duality for, 25:9760
interactions of, surface excitation model for resonance production in, (T), 25:9808
interactions with hadrons at high energies, representation for amplitude of relativistic, (T), 25:9749 (JINR-E2-5341)
interactions with hadrons, particle production from partially latent quasidynamical, (T), 25:9752
interactions with hadrons, total cross sections for, (E), 25:9640
interactions with hadrons, universal formulas for contributions of rho and sigma in, (T), 25:9750
mass of, causality function in four-fermion model with indefinite metric for, (T), 25:9741
photoproduction of, Lorentz invariant formulation of vector-meson dominance in, 25:9723
production in $e^+ + e^-$ interactions at 0.7 x 2 to 1.2 x 2 GeV, spark chamber and scintillation counter study of, (E), 25:9621 (NP-18581)
structure and dynamics of, quark, 25:9759
theory for, fundamentalist and bootstrap, 25:9753
theory of, classification of local Lie algebra in, 25:9754

HAFNIUM
determination in titanium and titanium dioxide by neutron activation, 25:8233
effects on microstructure and postirradiation properties of Hastelloy N, 25:8870 (ORNL-4600, pp 271-81)

HAFNIUM ALLOYS AND SYSTEMS
Hf--Mo--Pt-base, properties for use as radioisotope fuel capsule material, 25:8850 (ORNL-4600, pp 181-5)
Hf--Pt-base, properties for use as radioisotope fuel capsule material, 25:8850 (ORNL-4600, pp 181-5)
Hf--Pt-base--W, properties for use as radioisotope fuel capsule material, 25:8850 (ORNL-4600, pp 181-5)
Hf--Pt-base--W, tensile properties at 25 to 1290°C, 25:8427(R) (ORNL-4639)
Hf--Ta, phase studies of, 25:8851 (ORNL-4600, pp 186-97)

HAFNIUM CARBIDES
emissivity at 1300 to 3000°K, integral normal, 25:8930
evaporation rates at 2800 to 3400°K, 25:8929

HAFNIUM ISOTOPES Hf-173
energy levels of, spin--parity assignments from superfluid model, (T), 25:10028 (JINR-P4-5228)

HAFNIUM ISOTOPES Hf-175
energy levels of, spin--parity assignments from superfluid model, (T), 25:10028 (JINR-P4-5228)

HAFNIUM OXIDES
properties for use in dispersion strengthening of aluminum, 25:8860(P)
reactions with rare earth oxides and yttrium oxide, study of phases formed during, 25:8935
HfO_2-base--Y_2O_3, preparation and properties of alkoxy-derived high-purity powdered, 25:8949
HfO_2-base--Y_2O_3, structure of alkoxy-derived high-purity powdered, 25:8949

HAIR
analysis of human, for copper, gold, manganese, sodium, and zinc by neutron activation and γ spectrometry, 25:8229

HALDEN BOILING REACTOR
control system for, development of on-line digital computer, 25:10125(R) (NP-18573)
fuel elements for, radiation testing of Zircaloy 2 clad uranium oxide (UO_2) pin type, 25:10125(R) (NP-18573)
instrumentation for, development of test, 25:10125(R) (NP-18573)
maintenance during 1969, 25:10125(R) (NP-18573)
operations during 1969, 25:10125(R) (NP-18573)

HALLAM POWER REACTOR
site for, environmental survey during November 1970, 25:10134 (DOCKET-1153-17)

HAMSTERS
respiratory tract of, effects of chronic inhalation of diesel engine exhausts, radon decay products, and uranium ore dusts on, 25:8623 (BNWL-SA-3419)

HANDS
radiation dose to, of medical personnel during preparation and application of γ emitters for interstitial therapy, γ, 25:8689 (SZS-6/70, pp 19-27)

HARBORS
construction using underground nuclear explosions, safety and technology of, 25:8388

HASTELLOY N
microstructure of, effects of hafnium, niobium, and titanium additions on, 25:8870 (ORNL-4600, pp 271-81)
radiation effects on creep rupture of, relations of hafnium, niobium, or titanium additions with neutron, 25:8870 (ORNL-4600, pp 271-81)

HEALTH PHYSICS
programs and services at Goodyear Atomic Corporation during 1969, progress report on, 25:8692(R) (GAT-627)
research and development in Puerto Rico, 1969, 25:8574(R) (PRNC-140)

HEART
component turnover in, effects of hypertrophy and hypoxia on, 25:10336 (ACRH-1000-214)
radiation effects on function of, following scanning using iodine-131-labeled albumin macroaggregates, β and γ, 25:8713 (UCLA-12-798)
radioinduced injuries to, in man following therapy, effects of cortisone on, 25:8708
scanning for blood circulation and muscle function using iodine-131-labeled albumin macroaggregates, 25:8713 (UCLA-12-798)

HEART, MECHANICAL
design of implantable radioisotope-fueled steam-driven, 25:8436(P)

HEAT EXCHANGERS
design parameters of module, for power reactors, 25:10204(P)
tubes for, design of plugs for defective, 25:10330(P)

HEAT PIPES
inspection of nickel, after operation at 600°C for 10,000 hrs with potassium working fluid, 25:8395 (ORNL-TM-3077)

HEAT-RESISTING ALLOYS AND METALS
reactions with platinum and tantalum in diffusion couples, metallography of phases from, 25:8851 (ORNL-4600, pp 186-97)
welds of, effects of composition on corrosion properties of, 25:8838 (ORNL-4600, pp 282-6)

HEAT TRANSFER
analysis in reactors, sigma method for hot channel and hot spot statistical, 25:10194 (CEA-R-3895)
calculations for axial temperature and void fraction distribution in heated channel with inlet subcooling, 25:8417
calculations for exponential heat flux distribution in forced laminar or turbulent flow in several flow geometries, 25:8416
calculations for internally heated finite region with many circular holes, 25:8413
calculations for temperature dependent thermal conductivity of materials cooled by convection, 25:10203
measurements for determining departure from nucleate boiling in rod bundles during pressure blowdown, 25:8418
measurements for two-phase fluid flow in horizontal or vertical tubes, effects of tubing bends on, 25:8406 (CEA-CONF-1649)
rate of pool boiling, effects of bubble stabilization in vertically vibrating liquid column on, (E), 25:8419
temperature distribution in forced convection, superposition method for determining, 25:8409 (RD/B/N-1755)

HEAT TRANSFER SYSTEMS
heat transfer medium circulation in one-loop, stability of natural, (T), 25:8414

HEATED EFFLUENTS
bibliography on effects of, 25:10159 (ORNL-NSIC-81)
discharge from nuclear power plants, management problems in, 25:10090 (CONF-700335-1)
release by U. S. power plants, potential environmental impact of, 25:10133 (BNWL-SA-3581)

HELIUM
abundance determination in 15 chondrites, (E), 25:8968
abundance in big-bang cosmology, (T), 25:9156
abundance in HD 34452, (E), 25:9056
abundance in iota Ori B, (E), 25:8995
abundance in late G and K dwarfs in the solar neighborhood, (E), 25:8969
abundance in M17, M42, and IC 1795, (E), 25:9080
abundance in quasars, (E), 25:9074
burning in globular cluster stars, (E), 25:8992
burning in rotating magnetic stars, flash, (T), 25:9027
burning in stars, (T), 25:8987
burning in stars, model of flash, (T), 25:9037
carbon-ion (C^{++}) reactions below 40 keV with, total cross sections for single-electron capture in, (E), 25:9215
detection of neutral, in continuous spectra of nebulae, (E), 25:9046
diffusion in argon, chromatographic determination of, 25:8424(R) (MLM-1768)
diffusion in curium-244 oxide--gadolinium oxide samples,

25:8427(R) (ORNL-4639)
diffusion in hydrogen, at 77 to 917°K, coefficients for, 25:8424(R) (MLM-1768)
diffusion in nitrogen at 1 atm, coefficient for, 25:8424(R) (MLM-1768)
diffusion in, coefficients for self-, 25:8424(R) (MLM-1768)
eigenvalue equation for, formulation and solution of perturbed generalized, 25:9185
electron elastic scattering at 50 to 400 eV by, differential cross sections for, (E), 25:9222
electron reactions at 50 to 400 eV with, differential cross sections for excitation of 2^1P and 2^1S states in, (E), 25:9222
electron reactions at 500 eV with, excitation of lowest singlet S and singlet P states in, (T), 25:9217
energy levels of, Hartree--Fock calculations of $2s^2\ ^1S$ state, 25:9252
energy levels of, population inversion in, 25:9170
energy of 1^1S and 2^3S states of, calculation using Feynman path integrals in imaginary time, 25:9177
energy of ground state of, calculation using configuration-interaction wave functions and correlation factor, 25:9242
intensity of nuclei of, distribution by azimuth and zenith at 300 to 450 km in equatorial ionosphere, (E), 25:9349
interactions between two and three atoms of, calculation of van der Waals, by numerical solution of Hartree--Fock equations, 25:9176
isotopic composition of, in 15 chondrites, (E), 25:8968
neutron scattering from phonons in solid, theory of inelastic coherent, (T), 25:9964
nitrogen-ion (N_2^+) reactions in eV range with, mechanisms and cross sections for light emission in, (E), 25:9213
photon reactions with, calculation of resonances between first and second ionization thresholds in, using diagonalization method, 25:9239
photon reactions with, evaluation of oscillator strength for ionization in, using dipole length and velocity formulations, 25:9205
plasma of, electron energy distribution functions and transport coefficients for, (T), 25:9464
plasma of, excitation temperature functions of spectra lines of, 25:9172
plasma of, microwave interferometric measurement of electron density in afterglow, 25:9417
plasma of, moving striations in longitudinal magnetic fields, (E), 25:9453
positron elastic scattering at low energies by, correlation effects on calculation of phase shifts for, 25:9196
production in π reactions with nuclei at 60 GeV/c in emulsions, (E), 25:9660
properties of ground-state, calculation using truncated multipolar expansion pair functions, 25:9249
properties of, literature survey on, 25:8261 (RISO-224)
proton reactions at 10 keV with, differential cross sections for formation of metastable hydrogen atoms by charge exchange in, (E), 25:9192(R) (ORO-2591-51)
proton reactions at 100 to 300 keV with, energy spectra of electrons ejected in, (E), 25:9241
proton reactions at 4 to 26 keV with, total cross sections for formation of metastable hydrogen atoms by charge exchange in, (E), 25:9193 (ORO-2591-52)
proton reactions at 75 to 350 keV with, total cross sections for formation of fast excited hydrogen atoms by charge exchange in, (E), 25:9192(R) (ORO-2591-51)
radioinduced production in nitride fuels by neutron reactions with nitrogen-14, 25:8957 (ORNL-4600, pp 250-1)
reactions with argon, helium, krypton, and neon at 1.0 keV to 6.4 MeV, Born cross sections for excitation in, (T), 25:9204
reactions with argon, krypton, and neon at 1.60 to 400 keV, scaled cross sections for excitation in, (T), 25:9204
spectra in planetary nebulae, population of 2^3S level in, (T), 25:9016
wave functions for 1^1S and 2^3S states of, calculation using Feynman path integrals in imaginary time, 25:9177
wave functions for, based on combination of gaussian and Slater-type orbitals, 25:9243

HELIUM IONS
effects on Arabidopsis thaliana seeds, RBE for mutagenic and tumorigenic, 25:8800
electron binding energy of He^-, determination from disintegration in electric fields, 25:9169
energy-level crossings in n = 3 term of He^+, in electric and magnetic fields, 25:9181
Lamb shift in He^+, 25:9161
Lamb shift in μ-mesic, (T), 25:9188
scattering by helium ions at 77 and 300°K, intensity of, 25:8424(R) (MLM-1768)
spectra of He^+, fine structure of hollow-cathode-excited 3204-A line in, 25:9182

HELIUM ISOTOPES He-3
abundance in chromosphere from solar-flare study, (E), 25:9103
electron scattering by, charge and magnetic form factors for high-energy, (E), 25:9965 (AD-710384)
flux in interplanetary space, (E), 25:9257
Lamb shift in μ-mesic ions of, (T), 25:9188
meson (π) interactions with, cross-section calculations using Glauber theory, (T), 25:9967 (JINR-P2-5335)
nucleon interactions with, cross-section calculations using Glauber theory, (T), 25:9967 (JINR-P2-5335)
reactions (He-3,2γ) with beryllium-9 at 1.67 to 1.76 MeV, excitation functions for, (E), 25:9972 (ANU-P-496)
reactions (He-3,d) with molybdenum-92 and sulfur-32 at 35 MeV, angular distributions for, (E), 25:9978(R) (ORO-3398-26)
reactions (He-3,d) with oxygen-18 at 16 MeV, angular distributions for, (E), 25:9985
reactions (He-3,d) with titanium-49 at 22 MeV, deuteron spectra and angular distributions for, (E), 25:9966(R) (COO-1265-94)
reactions (He-3,d), (He-3,n) and (He-3,p) with carbon-12 up to 30.6 MeV, excitation functions for, (E), 25:9989
reactions (He-3,f) with bismuth-209 at 22 to 34 MeV, delayed-neutron curves from, (E), 25:10056
reactions (He-3,f) with thorium-232 and uranium-238 at 22 to 34 MeV, delayed-neutron curves and fission-chain yields from, (E), 25:10056
reactions (He-3,n) and (He-3,t) with carbon-12 up to 30.6 MeV, excitation functions for, (E), 25:9990
reactions (He-3,n) with carbon-12 and oxygen-16 at 9.0 to 13.5 MeV, angular distributions for, (E), 25:9981
reactions (He-3,pγ) with oxygen-18 at 3.3 to 4.1 MeV, p-γ angular correlations from, (E), 25:10004
reactions (He-3,t) with aluminum-27 and sodium-23 at 18 MeV, differential cross sections from, (E/T), 25:10013
reactions (He-3,t) with boron-10 and -11 at 11 to 17 MeV, excitation functions and microscopic-model analysis of angular distributions from, (E/T), 25:9993
reactions (He-3,t) with calcium-44 at 29 MeV, angular distributions for, (E), 25:9966(R) (COO-1265-94)
reactions (He-3,t) with carbon-13 at 14 MeV, microscopic-model analysis of angular distributions from, (E/T), 25:9993
scattering by boron-10 and -11 and carbon-13 at 14 MeV, optical-model analysis of angular distributions from elastic, (E/T), 25:9993
scattering by carbon-12 at 44 MeV, particle-γ angular correlations for inelastic, (E), 25:9978(R) (ORO-3398-26)
scattering by carbon-12 up to 30.6 MeV, excitation function for inelastic, (E), 25:9990
scattering by helium-4 at 20 to 51 MeV, exchange effects in elastic, (E), 25:9966(R) (COO-1265-94)
scattering by helium-4 at 30 MeV, resonating-group calculation for elastic, (T), 25:9966(R) (COO-1265-94)
scattering by light nuclei, at 13 to 27 MeV, angular distributions from elastic, (E/T), 25:9994
scattering by magnesium-26 at 17.7 MeV, angular distributions for elastic and inelastic, (E), 25:9966(R) (COO-1265-94)
scattering by strontium-88 at 33.4 MeV, angular distribution for elastic, (E), 25:9978(R) (ORO-3398-26)
He-3--He-4, thermal diffusion in, 25:8424(R) (MLM-1768)

HELIUM ISOTOPES He-4
abundance in chromosphere from solar-flare study, (E), 25:9103
charge mobilities in superfluid, under pressure, (E), 25:9361
energy levels of, calculation of atomic, from polarization theory, 25:9173
flux in interplanetary space, (E), 25:9257
helium-3 elastic scattering at 20 to 51 MeV, exchange effects in, (E), 25:9966(R) (COO-1265-94)
helium-3 elastic scattering at 30 MeV, resonating group calculation for, (T), 25:9966(R) (COO-1265-94)
ion mobility in rotating superfluid, low-temperature trapped, (T), 25:9358
Lamb shift in μ-mesic ions of, (T), 25:9188
meson (K^-) elastic scattering at 115 to 160 MeV/c in helium bubble chamber, differential cross sections and scattering lengths for, (E/T), 25:9969
neutron beam scattering by thick layers of, beam polarization and angular distribution from, (T), 25:9949
quantized vortex lines in rotating superfluid, detection of single, (E), 25:9362
scattering by helium-4 at high energies, Coulomb effects in elastic, (T), 25:9715
sound in superfluid, third, (T), 25:9360
He-3--He-4, thermal diffusion in, 25:8424(R) (MLM-1768)

HELIUM SYSTEMS
Ar--H--He, plasma properties in dipole magnetic fields, 25:9414
He--Ne, electron energy distribution functions and transport coefficients for, (T), 25:9464

HEMATOLOGY
conference on, Munich, Germany, August 24 to 28, 1970, 25:8615

HEMATOPOIESIS
radiation effects on, in dogs, comparison of x rays with neutron and γ, 25:8774
radiation effects on, of rats, effects of dose rate on, 25:8608

HEMATOPOIETIC SYSTEM
radiation effects on function of, in dogs and rats, effects of dose on γ, 25:8755(T) (JPRS-51660)
radiation protection of, in dogs, effectiveness of shielding against protons, 25:8755(T) (JPRS-51660)
HEPTANE
radioinduced oxidation at low temperatures, effects of concentration of nitrous oxide and oxygen on kinetics of γ, 25:8281
HIBERNATION
effects on cesium-137 γ-irradiated Manitoba toads, 25:8628
HIGH-ENERGY PHYSICS
book: Intermediate Energy Nuclear Physics, 25:9694
book: Particles, Sources, and Fields, 25:9699
research at Minnesota Univ., Sept. 1969 to Aug. 1970, (E/T), 25:9685(R) (COO-1764-86)
research at Pittsburgh Univ., Dec. 1969 to Dec. 1970, 25:9839(R) (NYO-3829-64)
HIROSHIMA
atomic bombing of, bibliography on medical status of survivors and offspring during 1969, 25:8741 (ABCC-TR-0-69)
HISTONES
radioprotective effects of, on DNA components of nucleohistones in relation to single and double strand breakage, γ, 25:8605(R) (ORO-2832-85)
HODOSCOPES
data acquisition and control system for scintillation, Minsk-22 computer-based, 25:8560
HOLMIUM
magnetization in heating--cooling cycle, phase transformation in spontaneous, (E/T), 25:9579
HOLMIUM ALLOYS AND SYSTEMS
Al--Ho--Ni, magnetic properties and phase diagram of HoNi/sub x/Al/sub 2-x/, 25:9576
Al-base--Gd--Ho, phase diagram at 500°C, 25:8886
Co--Ho--Pr, magnetic properties and phase diagram of Pr/sub x/Ho/sub 1-x/Co_2, 25:9576
Ho--Ni--Pr, magnetic properties and phase diagram of Pr/sub x/Ho/sub 1-x/Ni_2, 25:9576
HOLMIUM ISOTOPES Ho-165
neutron total cross sections at 0.005 to 1.7 keV, transmission curves, strength functions, and level parameters from, (E), 25:10022 (CEA-N-1338)
HOLMIUM ISOTOPES Ho-166
beta decay of, beta--gamma angular correlations, form and shape factors, and log-ft values for, (T), 25:10050
HORMONES, ADRENAL
cortisol, content of normal blood plasma, use of double isotope derivative technique for measuring, 25:8585
cortisone, effects on connective tissue of x-irradiated rats, 25:8786
cortisone, use for treatment of radioinduced heart disease in man following therapy, 25:8708
dexamethasone, effects on hematopoietic colony formation in spleen of γ-irradiated mice, 25:8765
dexamethasone, effects on hematopoietic colony formation in spleen of γ-irradiated mice, 25:8767
hydrocortisone, effects on connective tissue of x-irradiated rats, 25:8786
hydrocortisone, radiosensitivity of acetate form of, in relation to sterilization of ophthalmic ointments, 25:8826
HORMONES, PANCREATIC
insulin, effects on blood flow in resting muscle, combined effects of glucose on, xenon-133 tracer study of, 25:8586
HORMONES, PITUITARY
adrenocorticotropin, effects on hematopoietic colony formation in spleen of γ-irradiated mice, 25:8767
HORMONES, SEX
estradiol, effects on metabolism of calcium-47 and strontium-85 in rats, 25:8592(R) (COO-1339-43)
estrogens, radioimmunoassay in plasma of cattle, 25:8592(R) (COO-1339-43)
HORMONES, THYROID
thyroxine, radiolysis of, effects of dose and energy on yields of iodine from x, 25:8304
triiodothyronine, radiolysis of, effects of dose and energy on yields of iodine from x, 25:8304
HOT CELLS
design and operation of Pakistan Institute of Nuclear Science, 25:8449 (CONF-691008-18)
development for studies on reprocessing thorium-containing fuels, 25:8324(T) (ORNL-tr-2406)
HUMIDITY
control of, system for precise low range, 25:10376 (SC-RR-70-775)
HYDRIDES
production process for porous metal, 25:10334(P)
HYDROBROMIC ACID
effects on thermal diffusion separation of deuterium from hydrogen by thermal diffusion in trennschaukel, 25:8422 (CU-755-7, Sect.5)
HYDROCARBONS
reactions with recoil silicon-31, 25:8310(R) (ORO-3898-2)
hydrocarbons--SiH_4, radiolysis of, mass spectrometric studies on reactions in, 25:8294
HYDROCHLORIC ACID
determination of free, in fuel reprocessing solutions, colorimetric, 25:8197 (BARC-510)
HYDROFLUORIC ACID
HF--HNO_3, corrosive effects on Type 304 stainless steel at 140°F, effects of thermally-induced sensitization on, 25:8834(R) (COO-2069-6)
HYDROGEN
abundance in quasars, (E), 25:9074
burning in stars, (T), 25:8987
density of molecular, in H I regions, (T), 25:9088
diffusion of helium in, at 77 to 917°K, cofficients for, 25:8424(R) (MLM-1768)
distribution in galaxy M33, (E), 25:9149
distribution of neutral, at 1000 to 3500 km, (T), 25:9344
distribution of, in direction of W49, (E), 25:9069
effects of interplanetary, on solar euv, (E/T), 25:9108
effects on broadening of silicon lines, (E), 25:9187
effects on coliphage T7, inactivating, 25:8808
effects on embrittlement of magnesium--zirconium alloy at high temperatures, relations with grain size, 25:8874
electron reactions up to 54.4 eV with atomic, cross sections for excitation of 2s and 2p states in, (T), 25:9208
electron reactions with atomic, calculation of phase shift and resonances for, using separate treatment of open and closed channels, 25:9220
electron reactions with atomic, semi-empirical cross sections and rates for excitation and ionization in, 25:9184
energy of atom of, calculation using O(2,1) algebra for relativistic and nonrelativistic cases, 25:9179
excitation potential of liquid, 25:9166
formation of molecular, on dust grains in H I regions, (T), 25:9087
hydrogen-ion (H_2^+) reactions at 0.6, 1.0, and 1.5 MeV with molecular, angular and energy distributions of electrons from, (E), 25:9189 (BNWL-SA-3482)
hydrogen-ion (H_2^+) reactions at 600 keV with molecular, angular and energy distributions of electrons from ion breakup in, (E), 25:9190 (BNWL-SA-3498)
intensity of Lyman-α, before and after solar eclipse, May 20, 1966, (E/T), 25:9309
ion reactions in eV range with molecular, mechanisms and cross sections for light emission in, (E), 25:9213
meson (μ^+) range in liquid, (T), 25:9166
photon reactions with ground-state atomic, electron spectra from, (E), 25:9200
photon reactions with molecular, electron spectra from, (E), 25:9199
plasma of, ion temperature measurement in arcs using thermal Doppler effect, 25:9413(T) (SC-T-71-3001)
plasma of, microwave diagnostics of striations in discharge, 25:9425
plasma of, shock-wave production and structure in colliding, (E/T), 25:9437
plasma of, temperature measurement method for discharge, (E/T), 25:9411 (ECRC/N-288)
positron reactions with atomic, generalized variational bounds and coupled-static approximation for, (T), 25:9216
production in endothermic system using nuclear reactor heat, system for, 25:10294(P)
production using heat from nuclear reactors, method for, 25:10292(P)
proton range in liquid, (T), 25:9166
proton reactions at 75 to 350 keV with molecular, total cross sections for formation of fast excited hydrogen atoms by charge exchange in, (E), 25:9192(R) (ORO-2591-51)
proton reactions with atomic, probability of charge exchange and excitation to 2s state in, (T), 25:9201
proton reactions with atomic, use of Faddeev equations and Coulomb T matrix in calculation of asymptotic amplitude for electron capture in, 25:9211
proton reactions with excited atoms of, quantal eight-state approximation for resonance charge exchange in, 25:9203
reactions with iodine vapor at 0.2 to 2.5 keV of ground-state and metastable (2S) atoms of, cross sections for proton production by charge exchange in, (E), 25:9218
scattering by bromine and chlorine molecules, comparison of deuterium scattering with, 25:8256
separation from deuterium by thermal diffusion in trennschaukel, effects of chemical exchange between deuterium and hydrobromic acid on, 25:8422 (CU-755-7, Sect.5)
spectral emission lines in 26 Be stars, widths of, (E), 25:9034
symmetry group SO(4,2) and three-dimensional canonical algebra for, relation between, 25:9832
wave functions for molecular, convergence properties of single-center, (T), 25:9251
yields from γ radiolysis of aqueous ethanol solutions as function of nitrate concentration, 25:8301
yields from γ radiolysis of heptane, effects of charged particles on production of, 25:8281
HYDROGEN IONS (H-)
energy of 1^1S and 2^3S states of, calculation using Feynman path integrals in imaginary time, 25:9177
polarizability of, variational calculation of electric dipole, 25:9174

properties of ground-state, calculation using truncated multipolar expansion pair functions, 25:9249
wave functions for 1^1S and 2^3S states of, calculation using Feynman path integrals in imaginary time, 25:9177
HYDROGEN IONS (H_2^+)
energy of 1s sigma state of, calculation using Pade-type variational wave function, 25:9175
energy of 1s sigma/sub g/ and 2p sigma/sub u/ states of, calculation using Dickinson's function, 25:9178
injection into magnetic mirror geometries at 4 MeV, accumulation in, 25:9506 (ORNL-TM-3207)
reactions with hydrogen molecules at 0.6, 1.0, and 1.5 MeV, angular and energy distributions of electrons from, (E), 25:9189 (BNWL-SA-3482)
reactions with hydrogen molecules at 600 keV, angular and energy distributions of electrons from ion breakup in, (E), 25:9190 (BNWL-SA-3498)
HYDROGEN ISOTOPES
separation by gas chromatography, 25:8333
separation by preferential adsorption at low temperatures, 25:8332
HYDROGEN OXIDES H_2O
concentration of hydrated ionized, at 80 to 100 km in D region, (E/T), 25:9288
HYDROGEN PEROXIDES
yields from γ radiolysis of aqueous ethanol solutions as function of nitrate concentration, 25:8301
HYDROGEN SYSTEMS
Ar--H, Stark broadening of resonance lines of neutral, 25:9171
Ar--H--He, plasma properties in dipole magnetic fields, 25:9414
H--Ne, Stark broadening of resonance lines of neutral, 25:9171
H--Ta, phase diagram of, 25:8885(T) (ANL-Trans-867)
HYDROLASES
DNA-pyrimidine dimer photomonomerase, purification of, from Baker's yeast, for photoreactivation studies, 25:8606(R) (ORO-3630-10)
HYDROLOGY
bibliography on Nevada Test Site, 25:8355 (USGS-474-88)
research program in, for determining sources of chemicals in Crater Lake and Lake Tahoe, 25:8348 (CU-2493-11, App.2)
research program in, for determining sources of chemicals in high-alkalinity closed basin lakes, 25:8349 (CU-2493-11, App.3)
HYDROMAGNETIC WAVES
propagation of geomagnetic Pc1, through nighttime ionospheric F region, (T), 25:9338
HYDROXYL (HO)
detection of excited states of, in W3, (E), 25:9093
radio emission from, from four sources in Cygnus, (E), 25:9083
radio emission from, in Ceph IV association, (E), 25:9015
spectra of vibrationally excited, magnetic resonance, (E), 25:8975
HYDROXYLAMINE
nitrate, production from hydroxylamine sulfate by cation exchange, evaluation of system for monitoring, 25:8199 (BNWL-CC-2502)
HYPERFRAGMENTS
decay Λ-H^6 → n + ^3H + π^+, (E), 25:9633
hyperon (Λ) binding energy in Λ-He^5, effect of hyperon (Σ) suppression on, 25:9815
production and decay from meson(π) and proton reactions with emulsion nuclei, (E), 25:9637
HYPERONS
decay amplitudes in broken SU(3), relations between baryon mass differences and nonleptonic, 25:9830
decay in cluster model, S- and P-wave nonleptonic, (T), 25:9739
production in anti K + d → K + Y_1 + Y_2 interactions, cross sections for, (T), 25:9804 (JINR-P2-5231)
production in partially latent quasidynamical anti K + N interactions, (T), 25:9752
HYPERONS (Λ)
binding energy in Λ-He^5, effect of hyperon (Σ) suppression on, 25:9815
coupling constant for πΣΛ using Adler consistency condition, 25:9812
decay Λ → p + e + ν, spark chamber and counter study of up-down asymmetries in, (E), 25:9626 (COO-1545-87)
interactions Λ + p at 1 to 5 GeV/c in hydrogen bubble chamber, elastic and total cross sections and final-state resonance production in, (E), 25:9631
interactions π + Λ, consistency conditions from duality for, (T), 25:9792
production in anti 1 + 1 → Λ^0 + anti Σ^0 interactions, differential cross sections, form factors, and polarizations in, (T), 25:9730
production in γ + p interactions at threshold to 2.0 GeV, multipole analysis of, (E/T), 25:9728
HYPERONS (anti Λ)
production in anti 1 + 1 → anti Λ^0 + Σ^0 interactions, differential cross sections, form factors, and polarizations in, (T), 25:9730
HYPERONS (Ω-)
decay in cluster model, S- and P-wave nonleptonic, (T), 25:9739
HYPERONS (Σ)
coupling constant for πΣΛ using Adler consistency condition, 25:9812
coupling constant for πΣΣ using Adler consistency condition, 25:9812
effects on hyperon (Λ) binding energy in Λ-He^5, 25:9815
interactions π + Σ, consistency conditions from duality for, 25:9792
HYPERONS (Σ^-)
decay Σ^- → n + π^-, duality constraints on, (T), 25:9744
HYPERONS (Σ^0)
decay Σ^0 → Λ^0 + e^+ + e^- in hydrogen bubble chamber, Λ^0 polarization for test of time reversal invariance in, (E), 25:9829
production in anti 1 + 1 → anti Λ^0 + Σ^0 interactions, differential cross sections, form factors, and polarizations in, (T), 25:9730
production in γ + p interactions at threshold to 2.0 GeV, multipole analysis of, (E/T), 25:9728
HYPERONS (anti Σ^0)
production in anti 1 + 1 → Λ^0 + anti Σ^0 interactions, differential cross sections, form factors, and polarizations in, (T), 25:9730
HYPOXIA
effects on γ-radiosensitivity of Chlamydomonas, 25:8795
effects on survival of californium-252 mixed γ and neutron, cobalt-60 γ, and x-irradiated synchronized cultures of Chinese hamster cells in comparison to effects of aeration, 25:8757 (NYO-2740-7, pp 218-56)

I

ICE
radiation effects on bleached color centers in alkaline, γ, 25:8272
radiolysis of alkaline, at 77°K, extinction of trapped electrons and oxygen ions in γ, 25:8287
radiolysis of, effects of charged groups on indirect action in x, 25:8298
IMMUNE REACTIONS
radiation effects on, in mice following transplantation of allogenic leukemia, whole-body x, 25:8622
radiation effects on, of animals following transplantation of hematopoietic cells, review of, 25:8616
radiation effects on, of hybrid mice following transplantation of bone marrow from parental strain, x, 25:8618
radiation effects on, of mice following transplantation of rat bone marrow, x, 25:8619
radioinduced suppression of, in man and animals prior to bone marrow grafting, 25:8617
IMPEDANCE BRIDGES
design for measurement of cold work effects in stainless steel, 25:8439 (ORNL-4600, pp 153-6)
IN-PILE LOOPS
emergency cooling requirements for heavy water cooled mixed carbide fuel irradiation, 25:10243 (NP-18535)
operation limits for heavy water cooled mixed carbide fuel irradiation, 25:10243 (NP-18535)
operation of sodium cooled Scarabee, safety of, 25:10254(T) (ANL-Trans-865)
INCOLOY 800
corrosion by steam at 595 to 650°C, 25:8838 (ORNL-4600, pp 282-6)
fatigue at 1000 to 1400°F, effects of hold times and strain on low-cycle, 25:8864 (BMI-1891, Sect.A)
tensile properties at 650°C, effects of aging at 500°C on, 25:8952 (ORNL-4600, pp 81-125)
welding of, testing filler metals for, 25:8854 (ORNL-4600, pp 252-65)
INCONEL 82
properties for use as filler metal in Incoloy 800 welding, 25:8854 (ORNL-4600, pp 252-65)
INCONEL 600
ductility of, effects of minor elements on, 25:8854 (ORNL-4600, pp 252-65)
fatigue of, effects of BWR environments on low-cycle, 25:8866 (GEAP-10205)
INCONEL 625
corrosion by steam at 595 to 650°C, 25:8838 (ORNL-4600, pp 282-6)
INDIA
power plants in, development of nuclear, 25:10098
INDIUM
determination in liquid indium--sodium alloys by dissolution, filtration, and ammonium hydroxide precipitation, 25:8198 (BNL-50271)
determination in titanium and titanium dioxide by neutron activation, 25:8233
performance of activation detectors of, for neutron spectra measurements at 1 eV to 10 keV, 25:8481 (KFK-1233)
preparation of thin single crystals of, development of mold for, 25:8858
superconducting critical field curve of, lead-alloying effects on, 25:9380
uses in neutron activation analysis of concrete for cement, 25:8232(P)

XUM

INDIUM ALLOYS AND SYSTEMS
In--Na, analysis of liquid, for indium by dissolution, filtration, and ammonium hydroxide precipitation, 25:8198 (BNL-50271)
In--Pb, electric conductivity and structure of liquid, correlation between, 25:8882
In--Sn, electric conductivity and structure of liquid, correlation between, 25:8882
In--Zn, electric conductivity and structure of liquid, correlation between, 25:8882
INDIUM ISOTOPES In-113
determination in animal tissues in presence of carbon-14 and tritium by liquid scintillation counting, 25:8213
use of iron hydroxide-incorporated metastable, for scintiphotography of human lungs, 25:8721
INDIUM ISOTOPES In-116
beta decay of, gamma spectra and log-ft value from, (E), 25:10049
INDOLE, 2-PHENYL-
radioinduced luminescence of solutions of, in butanol and methanol, α, β, and uv, 25:8274
INDUSTRIAL HYGIENE
programs and services at Goodyear Atomic Corporation during 1969, progress report on, 25:8692(R) (GAT-627)
INFORMATION CENTERS
operation of Nuclear Safety, during September and October 1970, 25:10244(R) (ORNL-TM-3212)
INFRARED RADIATION
effects on eyes, protection against pathological, 25:8793
INORGANIC COMPOUNDS
chemical thermodynamics of crystalline, 25:8260(R) (COO-1149-180)
INSECTA
Drosophila melanogaster, analysis of mutations controlling development in, 25:10399(R) (UCB-34-P-186-X-1)
Drosophila melanogaster, localization of heterochromatin in chromosomes of, 25:8632 (EUR-4526)
Drosophila melanogaster, radiation effects on genetics of, neutron and x, 25:8756 (NYO-2740-7, pp 154-217)
Drosophila sp., radiation dosimetry for, monoenergetic neutron, 25:8677 (NYO-2740-7, pp 5-51)
Goniaea sp., radiation effects on meiosis in, autoradiographic study of x, 25:8754
radiation effects on survival of, infesting cereals, fruits, and vegetables, effects of dose on γ, 25:8813 (NP-18236)
radiosterilization of, use of sterile male technique for, 25:8818
Sarcophaga peregrine, radiation effects on imago formation in, effects of dose and pupal exposure on strontium-90 β, 25:8749(T) (NSJ-tr-156)
Stomoxys calcitrans, radiation effects on longevity and reproduction in female and male, γ, 25:8822
INSECTICIDES
distribution of helicopter-sprayed, use of europium-152 for tracer measurements of, 25:8426(T) (NSJ-tr-155)
INSPECTION AND CONTROL
programs at Goodyear Atomic Corporation during 1969, progress report on, 25:8692(R) (GAT-627)
INSTRUMENTS
description of computer-controlled CAMAC modular, 25:8573 (KFK-1241)
development at Bhabe Atomic Research Center in 1969, 25:10017(R) (BARC-501)
development at PRNC, 1969, 25:8574(R) (PRNC-140)
development at Technische Hochschule in 1969, 25:10018(R) (BMBW-FBK-70-10)
emplacement in rock at Project Piledriver site, development of epoxy grout for, 25:8962 (POR-4013)
installation of pressure vessel, design of wall sealing arrangement for, 25:8402(P)
INTERFEROMETERS
performance of Fabry--Perot, for plasma diagnostics, 25:9408 (COO-1789-1)
INTERMETALLIC COMPOUNDS
properties and uses of superconducting, 25:9386
INTERSTELLAR MATERIAL
effects of passing clouds of, on stability disturbance of star clusters, (T), 25:9050
formation of molecular hydrogen on dust grains in H I regions, (T), 25:9088
formation of molecular hydrogen on dust grains in, (T), 25:9087
radio emission from molecules and free radicals in, (T), 25:9071
INTESTINES
radiation dose to rectal portion of human, during intracavitary therapy of female gynecological carcinomas, γ, 25:8679 (SZS-6/70, pp 9-18)
radiation effects on bioelectric properties and glucose transport in, of rats, combined effects of chronic bile diversion on x, 25:8607(R) (ORO-3882-3)
INVARIANCE PRINCIPLES
CP invariance in $K_2^0 \rightarrow \pi^+ + \pi^-$ decay, long-range field pulses as source of, (T), 25:9826 (NYO-2171-329)
CP violation in $K^0 \rightarrow 2\pi$ decay, review of, (T), 25:9828
CP violation in $K_2^0 \rightarrow 2\pi$ and $K_2^0 \rightarrow \pi + l + \nu$ decays, model with supplementary particles for test of, (T), 25:9827
parity conservation in two-body interactions, helicity formalism for theorem on intuitive tests of, (T), 25:9686 (COO-1764-100)
time reversal invariance test in Λ^0 polarization in $I^0 + \Lambda^0 + e^+ + e^-$ decay in hydrogen bubble chamber, (E), 25:9829
IODINE
determination in airborne particulates by neutron activation, 25:8231
hydrogen-atom reactions at 0.2 to 2.5 keV with vapor of, cross sections for proton production by charge exchange in, (E), 25:9218
production of radioactive, by decay of fallout tellurium oxide, 25:8362 (AD-707427)
removal of airborne, from reactor containment systems and fuel reprocessng off-gas streams, 25:8321(R) (IN-1363)
sorption on zeolites, 25:8321(R) (IN-1363)
yields from radiolysis of iodoamino acids, Auger effect in, 25:8304
IODINE IONS
reactions with xenon at 1.5 to 12 MeV, charge-state distributions from multiple ionization in, (E), 25:9219
IODINE ISOTOPES
production in deuteron and proton fission of thorium-232 at 11 MeV, yields of, (E/T), 25:10054
IODINE ISOTOPES I-125
effects on survival of Escherichia coli, mutagenic, 25:8654
reactions with benzene, yields from, 25:8284(T) (ANL-Trans-870)
use for scanning in diagnostic and metabolic studies, development of computer programs for, 25:8716
IODINE ISOTOPES I-129
release to atmosphere, derivation of working limits for continuous rates of, 25:8681
IODINE ISOTOPES I-131
content in ground-level atmosphere near ORNL reactors, comparison of calculated and measured data on, 25:8452 (ORNL-TM-3187)
content of grass and milk following accidental release of, at La Hague UP 2 plant, 25:8657 (CEA-R-4008)
content of milk in USA during 1963 to 1968, sources of, 25:8629
diffusion from open radioactive waste storage pools, method for prediction of, 25:8450 (IN-1449)
removal from reactor containment systems, effectiveness of sprays for, (E), 25:10256 (BNWL-1485)
sensitivity of rose bengal-incorporated, for liver function appraisal in comparison to sulfobromophthalein sodium, 25:8722
uptake and accumulation by thyroid of rats following intravenous injection in comparison to metastable technetium-99, 25:8599
use as tracer for in vitro study of liver cell function in swine livers, 25:8783
use for total thyroid ablation during therapy of human endocrine exophthalmos, 25:8733
use of albumin macroaggregate-incorporated, for scanning heart for function, 25:8713 (UCLA-12-798)
use of serum albumin-incorporated, for brain scanning, 25:8710 (NP-18560)
ION-ACOUSTIC WAVES
propagation in finite-geometry plasmas, dispersion relations for, 25:9525
ION BEAMS
interactions with hot-electron plasma, instabilities from, (E), 25:9450
profile of uniformly accelerated, approximation of Moak's integral for calculation of, 25:9925
ION EXCHANGE MATERIALS
effect of Sephadex derivatives on indirect action in frozen aqueous solutions, ESR study of, 25:8298
sorptive properties of KU-2 for strontium, effects of calcium on, 25:8341
sorptive properties of resin, for uranium in alkaline and acid suspensions, 25:8963
sorptive properties of zeolite, for iodine, 25:8321(R) (IN-1363)
ION SOURCES
beam extraction system for, optics of, 25:9922
performance of reflex-type, parameter relations for optimum, 25:9912 (LYCEN-6953)
IONIZATION
cross sections for, Born approximation expressions for differential, (T), 25:9195 (SC-RR-70-773)
IONOSPHERE
air density variations at 300 and 505 km in, 1967--1968 semiannual, (E), 25:9304
characteristics of Earth, Mars, and Venus, comparison of, (E/T), 25:9355
charged particle intensity of Z greater than or equal to 1 and Z greater than or equal to 2 at 300 to 450 km in equatorial, distribution by azimuth and zenith of, (E), 25:9349
cosmic radio-noise absorption measurements in, (E), 25:9337
D region, electron densities at 74 and 80 km from partial reflections observed during solar eclipse May 20, 1966, (E), 25:9312
D region, electron density and collision frequencies in, observed during solar eclipse, May 20, 1966, (E),

25:9311
D region, electron density increases in, during Oct. 21, 1968 solar flare, (E), 25:9300
D region, exponential model of calm, 25:9328
D region, ion composition at 80 to 100 km in, effect of energetic electron precipitation on hydrated hydrogen oxide positive, (E/T), 25:9288
D region, ionization at 90 to 95 km in nighttime, charged-particle contribution to, (E/T), 25:9339
D region, ionization in, by Lyman-α reactions with nitric oxide during solar eclipse, May 20, 1966, (E/T), 25:9309
D region, properties at 73 km in sunrise auroral, relation to 3180-A solar radiation occurrence, (E), 25:9296
D region, radio-wave absorption in, calculated and riometer measurements during solar maximum and minimum, (E/T), 25:9289
D region, relation of chemistry of, to radio propagation, (T), 25:9297
D region, solar x radiation absorption in, 25:9330
E region, heating of electron gas at high-altitude, by secondary electrons during solar eclipse, (E/T), 25:9341
E region, intensity of thermal sources heating, (E/T), 25:9340
E region, magnetic substorm-associated heat in auroral, generation of gravity waves by, (E/T), 25:9293
E region, meteor ionization due to ablating materials in, (E/T), 25:9307
E region, radio-wave absorption in, calculated and riometer measurements during solar maximum and minimum, (E/T), 25:9289
electric field intensity in equatorial and medium latitude, from barium cloud releases, (E), 25:9285 (MPI-PAE/EXTRATERR-49/70)
electrojets in, plasma measurements for height-independent electric fields in polar, (E), 25:9335
electrojets in, structure of auroral, (E/T), 25:9334
electron content and variations from Faraday radio transmission, geographical and geophysical aspects of, (E/T), 25:9294
electron content in mid- and high-latitude, associated with trough behavior, (E/T), 25:9287
electron density profile model for, using sums of E, F1, and F2 layers, (T), 25:9283 (AD-709888)
electron density variations in layers of, (T), 25:9329
electron enhancement during solar flares in sunlit, Feb. 20, 1970, (E), 25:9333
electron gases in, transport coefficients at 100 to 600 km, (E/T), 25:9302
electron impact ionization between regions of, rapid conjugate photo-, (E/T), 25:9127
electron temperature at 115 to 430 km in, Thomson scatter measurements of, (E), 25:9316
energy flux at 120 to 178 km, soft electron and uv, (E), 25:9345
F region, electric field and neutral wind effects on diurnal behavior of, (T), 25:9315
F region, ionization exchange with protonosphere, nighttime, (E), 25:9325
F region, propagation of geomagnetic Pc1 pulsations through, (T), 25:9338
F region, radio-wave absorption in, calculated and riometer measurements during solar maximum and minimum, (E/T), 25:9289
F region, traveling disturbances in, 25:9295
F region, true height profiles using 1 MHz nighttime ionograms, correction methods for, (E/T), 25:9319
F region, universal time control in winter Arctic, theories of, (T), 25:9318
F2 layer, critical frequency fo 1957 to 1960, associated with equatorial electrojet, anomalous, (E/T), 25:9291
F2 layer, electron density in mid-latitude topside northern hemisphere, seasonal anomaly of diurnal variations of, (E), 25:9322
intensity of Lyman-α before and during solar eclipse, May 20, 1966, (E/T), 25:9309
ion composition and temperature at 115 to 430 km in, Thomson scatter measurements above Arecibo, Puerto Rico, (E), 25:9316
observations during May 20, 1966 solar eclipse, positive-ion probe, (E/T), 25:9310
observations during May 20, 1966 solar eclipse, results of, (E/T), 25:9313
oscillations in, theory for quasi-periodic, (T), 25:9299
oxygen density at 70 to 85 km in, molecular, (E/T), 25:9309
ozone screening height of 58 km in, deduced from sunrise effects at vlf, (E/T), 25:9331
parameters of, incoherent radio wave scattering measurements for, (E), 25:9343
parameters of, simultaneous satellite and ground measurements of electron and positive-ion temperatures and plasma concentration, (E), 25:9308
polar peak at 1000 km in, attributed to solar plasma penetration at magnetospheric neutral point 80° geomagnetic latitude, (E/T), 25:9317
radio wave propagation below inhomogeneous isotropic, attenuation of elf and vlf, (E/T), 25:9292
radio-wave absorption in Antarctic, during 1969 austral winter, (E), 25:9324
radio-wave reflection from, irregular strength variations of diurnally-distributed, (T), 25:9323
research program at European Space Research and Technology Centre, 25:9336
sporadic E, irregularities at 100 km of q-type, associated with equatorial electrojet, (E/T), 25:9291
sporadic E, traveling disturbances in, 25:9295
spread F, occurrence of, correlation with geomagnetic activity over Taiwan, (E), 25:9290
x-ray spectral distribution of absorbed energy in, relation to black-body radiation law, (T), 25:9351

IONS
charged-particle reactions with, Born approximation expressions for differential ionization cross sections for, (E), 25:9195 (SC-RR-70-773)
electron emission, free--free, (T), 25:9082
energy of ground-state two-electron, calculation using configuration-interaction wave functions and correlation factor, 25:9242
motion in solid silver selenide, silver sulfide, and silver telluride, 25:10339(T) (ANL-Trans-868)
production at 75 km in, justification for solar x-ray contribution during solar eclipse May 20, 1966 to postive, (E/T), 25:9310
production in discharges, mean energy for pair, (E/T), 25:9161(T) (LA-tr-70-24)
reactions with atoms at low energies, method for measurement of excitation transfer in, 25:9238
reactions with copper at 40 keV to 1.1 MeV, cross sections for L x-ray production in, as function of atomic number, (E), 25:9164
reactions with molecules, ion-cyclotron-resonance method for measurement of collision and charge-exchange rates in, 25:9233
scattering by crystals, mechanism of anisotropic, (E/T), 25:9556

IRIDIUM
properties for use in curium-244 oxide cermets, 25:8427(R) (ORNL-4639)

IRIDIUM ISOTOPES Ir-191
performance of activation detectors of, for neutron spectra measurements at 1 eV to 10 keV, 25:8481 (KFK-1233)

IRIDIUM ISOTOPES Ir-192
beta and electron-capture decay of, gamma spectra and β and electron-capture intensities from, (E), 25:10032(T) (ORNL-tr-2345)
use for scanning in diagnostic and metabolic studies, development of computer programs for, 25:8716

IRON
abundance in HD 34452, (E), 25:9056
abundance in iota Ori B, (E), 25:8995
abundance in L and H chondrites, (E), 25:8967
abundance in late G and K dwarfs in the solar neighborhood, (E), 25:8969
alpha reactions at 30 to 80 MeV, K-shell ionization cross sections for, (E), 25:9978(R) (ORO-3398-26)
corrosion and passivation by aqueous sodium sulfate--sulfuric acid solutions, electrochemical study of effects of time on, 25:8834(R) (COO-2069-6)
determination in air particulates by spark source mass spectrometry, 25:8208
determination in airborne particulates by neutron activation, 25:8231
determination in titanium and titanium dioxide by neutron activation, 25:8233
diffusion in, lattice-dynamical theory of isotope effects in, 25:9589
effects on colorimetric determination of uranium in fuel reprocessing solutions, 25:8197 (BARC-510)
effects on magnetic properties of europium monoxide films, 25:9587
neutron propagation in, transport codes for, (E), 25:9536 (CEA-CONF-1669)
radiation damage in, ENDF/B calculations of cross section for neutron, 25:9573
radioinduced defects in, low-temperature microscopic observations of annealing of 77°K neutron, 25:9542 (CEA-CONF-1681)
radioinduced dislocation loops in, microscopic study of nucleation in electron, 25:9541 (CEA-CONF-1680)

IRON ALLOYS AND SYSTEMS
Al--C--Fe--Si--U-base, tensile properties of dilute, at 885 to 1150°F, 25:8867 (NLCO-1060)
Al--Cr--Fe-base--Ni, corrosion by water containing trace chloride and oxygen at 200°C, stress, 25:8834(R) (COO-2069-6)
Al--Fe--Nb, phase diagram at 800°C, 25:8850
Be--Cr--Fe-base--Ni, corrosion by water containing trace chloride and oxygen at 200°C, stress, 25:8834(R) (COO-2069-6)
Cr--Fe--Ni, corrosion by water containing trace chloride and oxygen at 200°C, stress, 25:8834(R) (COO-2069-6)
Cr--Fe-base--Ni, corrosion by boiling aqueous magnesium chloride, effects of aluminum, beryllium, or carbon additions on stress, 25:8834(R) (COO-2069-6)
Cr--Fe-base--Ni--Pt, corrosion by water containing trace chloride and oxygen at 200°C, stress, 25:8834(R) (COO-2069-6)
Cr--Fe-base--Ni--Si, corrosion by water containing trace chloride and oxygen at 200°C, stress, 25:8834(R) (COO-

2069-6)
Fe--Gd, crystal structure of intermetallic ($Gd_{2/3}2Fe_{1/3}$)Fe_3, 25:8891
Fe--Mo, analysis for molybdenum using mercaptosuccinic acid, spectrophotometric, 25:8210
Fe--Ni, corrosion by aqueous sulfuric acid at 25°C, effects of partial currents on, 25:8834(R) (COO-2069-6)
Fe-base--Ni, corrosion by water containing trace chloride and oxygen at 200°C, stress, 25:8834(R) (COO-2069-6)
IRON HYDROXIDES
sorptive properties for ruthenium from effluents from chemical decanning of reactor fuel elements, 25:8344(P)
IRON IONS
excitation rate of Fe XIV green coronal line, electron, (T), 25:9123
IRON ISOTOPES Fe-52
use for scanning in diagnostic and metabolic studies, development of computer programs for, 25:8716
IRON ISOTOPES Fe-55
determination in blood and other liquids, proportional detector for, 25:8466 (BNWL-SA-3624)
transport in food chains of nuclear-explosion-contaminated estuarine and marine ecosystems in relation to daily ingestion by man, use of stable element content of fish and invertebrates for predicting, 25:8627
IRON ISOTOPES Fe-56
deuteron reactions (d,p) with, differential cross sections and residual nucleus orientation for, (E), 25:9998 (NP-18439)
proton reactions (p,pn) at 17 MeV, mechanism of, (E), 25:10005
IRON ISOTOPES Fe-57
proton reactions (p,pn) at 17 MeV, mechanism of, (E), 25:10005
IRON ISOTOPES Fe-59
accumulation in Navicula seminulum, Plectonema boryanum, and Stigeoclonium lubricum, effects of temperature on, 25:8598
clearance from lungs of rats following inhalation, 25:8591 (CEA-CONF-1677)
transport in food chains of nuclear-explosion-contaminated estuarine and marine ecosystems in relation to daily ingestion by man, use of stable element content of fish and invertebrates for predicting, 25:8627
IRON OXIDES
diffusion in, mechanism for anion and cation, 25:8934
electric conductivity of, 25:8934
IRON SULFIDES
sorptive properties for ruthenium from effluents from chemical decanning of reactor fuel elements, 25:8344(P)
IRRADIATION FACILITIES
design and operation of gamma, for processing solid materials, 25:8432
design and operation of Pakistan Institute of Nuclear Science, 25:8449 (CONF-691008-18)
IRRADIATION TECHNIQUES
training manual on food, 25:8814 (STI/DOC-10/114)
use of inverted-Y, for therapy of human lymphomas using high-energy x, 25:8734
use of mantle, for therapy of human lymphomas using high-energy x, 25:8735
ISOTOPE EFFECTS
calculations of, approximation methods for, 25:8245
conference on, in chemical processes, Miami Beach, Fla., April 11, 1967, 25:8243
lattice-dynamical theory of, in diffusion in cubic metals, 25:9589
measurement in liquid metals, molten salts, and aqueous solutions, 25:8247
statistical theory of, gas chromatographic study on, 25:8333
ISOTOPE EXCHANGE
equilibrium constant for, approximation methods for prediction of, 25:8245
equilibrium constants for, correction to effect of anharmonicity on, 25:8246
ISOTOPE GENERATORS
design of closed, for preparation and containerization of radioisotopes, 25:8433(P)
ISOTOPE SEPARATION METHODS
development of adsorption, for gaseous isotopic mixtures, 25:8343(P)
development of electromigration, 25:8247
development of thermotransport, 25:8336
partition function ratios in, orthogonal polynomial analysis of, 25:8335
progress report on, Columbia University, Sept. 1970, 25:8317(R) (CU-755-7)
review on, 25:8328
ISOTOPES
electromigration in liquid metals, molten salts, and aqueous solutions, 25:8247
fractionation of, orthogonal polynomial analysis of, 25:8335
ITALY
radiation protection programs for human populations in event of accidents during radioisotope shipping in, 25:8696
radioisotope content of human diet in, during 1968, cesium-137, and strontium-90, 25:8624 (EUR-4509)

J

JAPAN
radiation monitoring activities at Atomic Energy Research Inst., Tokyo, during 1969 and 1970, 25:8673 (JAERI-Memo-4098)
JUPITER (PLANET)
radio emission from, polarization of decametric, (E), 25:9158
radio observations at 11.13 cm, (E), 25:9160

K

KETOSE-1-PHOSPHATE ALDOLASE
radiation effects on activity of, in rabbits, sublethal ionizing, 25:8779
KRYPTON
diffusion in, coefficients for self-, 25:8424(R) (MLM-1768)
helium-atom reactions at 1.0 keV to 6.4 MeV with, Born cross sections for excitation in, (T), 25:9204
helium-atom reactions at 1.60 to 400 keV with, scaled cross sections for excitation in, (T), 25:9204
nitrogen-ion (N_2^+) reactions in eV range with, mechanisms and cross sections for light emission in, (E), 25:9213
plasma of, excitation temperature functions of spectra lines of, 25:9172
proton reactions at 15 to 150 keV with, cross sections for charge exchange in, (E), 25:9229
thermodynamic properties of solid, as function of temperature, models for anharmonic, 25:8262 (UCRL-50903)
KRYPTON IONS
reactions with nitrogen molecules at 1 to 5 MeV, fluorescence efficiencies for excitation in, (E), 25:9234
KRYPTON ISOTOPES Kr-85
monitoring in atmosphere, calibration and sensitivity of G--M, ionization and scintillation detectors for, 25:8467 (BRH/NERHL-70-4)
production of pharmaceutical saline solution of, 25:8309(P)
release from West Valley Processing Plant, 25:8366 (DOCKET-50201-56)
KRYPTON ISOTOPES Kr-86
concentration by thermal diffusion, rates for, 25:8424(R) (MLM-1768)

L

LA CROSSE BOILING-WATER REACTOR
instrumentation for, safety analysis of automatic gain control system for, 25:10135 (DOCKET-1155-87)
operations history for October 1970, 25:10111 (DOCKET-1155-88)
operations history for September 1970, 25:10110 (DOCKET-1155-86)
LACTATE DEHYDROGENASE
radiation effects on activity of, in rabbits, sublethal ionizing, 25:8779
LAKES
chemical content and hydrology of dilute, Crater Lake and Lake Tahoe studies of, 25:8348 (CU-2493-11, App.2)
chemical content and hydrology of saline, Mono Lake, California studies of, 25:8349 (CU-2493-11, App.3)
groundwater flow into shallow, natural radon tracer technique for measuring, 25:8350 (CU-2493-11, App.4)
radon content of Cranberry and Sterling, in New York, measurement for groundwater flow studies, 25:8350 (CU-2493-11, App.4)
radon-222 content of small, in Experimental Lakes Area, Ontario, 25:8352 (CU-2493-11, App.6)
tritium content of Crater, in Oregon, effects of vapor exchange and precipitation on, (E), 25:8347 (CU-2493-11, App.1)
LAMINATES
thermal conductivity of, computer program for calculation of, 25:8961 (LA-4511)
LANTHANUM
determination in titanium and titanium dioxide by neutron activation, 25:8233
determination of trace amounts of, in glass by neutron activation after sodium removal by hydrated antimony pentoxide, 25:8223
performance of activation detectors of, for neutron spectra measurements at 1 eV to 10 keV, 25:8481 (KFK-1233)
LANTHANUM ALLOYS AND SYSTEMS
La--O--U, phase studies of, 25:8943 (KFK-1235)
LANTHANUM ISOTOPES La-133
energy levels at 97 and 130.7 keV from cerium-133 beta and electron-capture decay, lifetimes and spin--parity assignments of, (E), 25:10029 (JINR-P6-5200)

LANTHANUM ISOTOPES La-135
energy level at 119.4 keV from cerium-135 beta and electron-capture decay, lifetime of, (E), 25:10029 (JINR-P6-5200)
LANTHANUM ISOTOPES La-139
energy level at 165.8 keV from cerium-139 electron-capture decay, lifetime of, (E), 25:10029 (JINR-P6-5200)
LANTHANUM ZIRCONATES
formation of, kinetics of, 25:8935
LASER RADIATION
absorption by plasma, effect of oblique incidence on, (T), 25:9476
effects on eyes, protection against pathological, 25:8793
effects on morphology and physiology of cells, molecular mechanisms and techniques for demonstrating microbeam, 25:8744
hazards to eyes of man and personnel, standards for protection against, 25:8694
interactions with stationary plasma, heating in one-dimensional, (T), 25:9405
reactions with nickel, plasma beam production in, (E), 25:9484
scattering on plasma, magnetic field measurement from Thomson, (E), 25:9427
scattering on pulsed plasma, electron density determination from, (E), 25:9409(T) (CTO-733)
LASERS
performance for diagnostics of shock-produced xenon plasmas, 25:9422
use for xenon plasma production, electron density profiles in, (E), 25:9485
LEAD
alpha reactions with, x-ray fluorescence yields from, (E), 25:9978(R) (ORO-3398-26)
antideuteron reactions at 25 GeV/c, absorption cross sections for, (E), 25:9639
determination in air particulates by spark source mass spectrometry, 25:8208
diffusion in, lattice-dynamical theory of isotope effects in, 25:9589
electron elastic scattering at 100 to 1300 keV by foils of, as function of foil thickness and incidence angle, single, plural, and multiple, (E), 25:9225
neutron attenuation at 3 MeV, time response behavior of, (E/T), 25:9995
neutron spectra in, measurement of, 25:9956
positron elastic scattering at 100 to 1300 keV by foils of, as function of foil thickness and incidence angle, single, plural, and multiple, (E), 25:9225
superconducting intermediate state of, interphase boundary waves in, (E/T), 25:9363 (NYO-2150-64)
superconducting proximity effects in, acoustic surface wave study of, (E/T), 25:9378
superconducting transition temperature of thin films of, effect of strain on electrical resistance and, 25:9371
superconductivity tunneling in single-crystal films of, Fermi velocity from Tomasch oscillations in, 25:9373
LEAD ALLOYS AND SYSTEMS
thermal conduction in irreversible Type-II superconducting, (E/T), 25:9370
In--Pb, electric conductivity and structure of liquid, correlation between, 25:8882
LEAD ISOTOPES
energy levels of, calculation using particle-vibration coupling model, (T), 25:10043
LEAD ISOTOPES Pb-206
deuteron reactions (d,p) with, analysis using calculated form factors, (T), 25:10067
energy levels of, quasi-particle structure of ground state of pairing model of, (T), 25:10051
LEAD ISOTOPES Pb-207
energy levels of, properties of doublet, (E), 25:10033
LEAD ISOTOPES Pb-208
electron reactions (e,e'p) with, proton spectra and excitation functions for, (E), 25:10053
LEAD ISOTOPES Pb-210
proton reactions (p,d) with, analysis using calculated form factors, (T), 25:10067
relation of radon-222 daughter products to, corrections applying to model and conversion factor for, 25:8680
LEAD ISOTOPES Pb-214
content in man at various time intervals following ingestion of radium-226, methods for calculation of, 25:8669 (COO-2088-1)
LEAD TELLURIDES
properties for use in thermoelectric converters, 25:8421 (AERE-M-1594)
LEAK DETECTORS
performance of color changing, for water cooled and heavy water cooled reactor coolants, 25:10206(P)
LEAKS
detection of helium, from fuel elements, vacuum method for, 25:8461
LEPTONS
conservation law for, test for, (E), 25:9748
interactions $1^+ + 1^- \rightarrow \nu + \text{anti } \nu + \gamma$, detection of, (E), 25:9627 (NP-18558)
interactions anti 1 + 1 → Λ^0(anti Λ^0) + anti Σ^0(Σ^0), differential cross sections, form factors, and polarizations in, (T), 25:9730
self-energy from gravitational, weak, and electromagnetic interactions, 25:9714
LEPTONS (ANTIPARTICLES)
interactions anti 1 + 1 → Λ^0(anti Λ^0) + anti Σ^0(Σ^0), differential cross sections, form factors, and polarizations in, (T), 25:9730
LEUKOCYTES
properties and structure of polymorphonuclear, 25:10364(R) (ORO-3628-11)
radiation effects on count of, in peripheral blood of dogs, effects of dose on γ, 25:8755(T) (JPRS-51660)
radiation effects on relative counts of, in old-field mice, acute cobalt-60 γ, 25:8760
LEVEL INDICATORS
development of ultrasonic, for pressurized water systems, 25:10267 (IN-1442)
LIGASES
role in excision repair of uv-irradiated DNA, 25:8636 (SU-326-P-7-X-22)
LIGHT
effects on morphology and physiology of cells, molecular mechanisms and techniques for demonstrating microbeam, 25:8744
intensity of powerful coherent beams of, possibility of measurement of, 25:9615
reactions with matter, nonlinear effects in, 25:10406 (UCRL-20358)
LINEAR ACCELERATORS
beam current in slotted-iris-loaded section of Kharkov 2-GeV electron, critical, 25:9907(T) (KFK-tr-335)
beam extraction and focusing system for 360-MeV electron, 25:9927
beam injection in heavy-ion, ion trajectory calculation for, 25:9911 (LYCEN-6949)
beam power of electron, klystron modification for increased, 25:9938
beam regulation in 100-MeV proton, 25:9914(T) (NP-tr-1926)
development of 10-MeV electron U-13, 25:9929
development of superconducting, problems in, 25:9921
operation of high-current induction, high-frequency, 25:9937
use for radiotherapy for human cervical carcinomas in comparison with counter dual cobalt γ, 25:8740
LINEAR ENERGY TRANSFER
definition and applications of, ICRU, 25:8671 (ICRU-16)
distribution in tissue equivalent small animal phantoms in relation to fission neutron spectrum, 25:8685
spectra measurements using Rossi tissue-equivalent proportional detector, for neutrons, 25:8492
LIQUID FLOW
component redistribution in binary mixture film moving along pipe wall in inhomogeneous magnetic field, (T), 25:9277
LIQUID METAL FAST BREEDER REACTOR
cladding for, effects of fabrication variables on defects in stainless steel, 25:8847 (ORNL-4600, pp 126-30)
components and materials for, nondestructive testing of, 25:8439 (ORNL-4600, pp 153-6)
components for, development of welding methods for, 25:8848 (ORNL-4600, pp 131-41)
components for, performance of shielded metal-arc method for welding of, 25:8849 (ORNL-4600, pp 142-6)
development at Argonne National Laboratory, November 1970, 25:10164(R) (ANL-7758)
dynamics of, space--time effects on, (T), 25:10180
fuel assemblies for, cladding temperature variations and coolant mixing in seven-pin bundle, (E), 25:10207 (BNWL-SA-3286)
fuel element for, radioinduced helium production in, 25:8957 (ORNL-4600, pp 250-1)
fuel elements for, comparison of computer programs and calculation models for calculation of performance of pin type, 25:10212 (TID-25590)
fuel elements for, design and development of, 25:8911 (ORNL-4600, pp 65-80)
fuel elements for, effects of power cycling on performance of, 25:8835 (ORNL-4600, pp 57-64)
fuel elements for, Failed-Fuel Mockup facility for testing, 25:10244(R) (ORNL-TM-3212)
fuel elements for, failure threshold of zero burnup Type 316 stainless steel clad plutonium oxide (PuO_2)--uranium oxide (UO_2) pin type, 25:10208 (GEAP-13562)
fuel for, solvent extraction processes for reprocessing of, 25:8316 (BNWL-CC-1939)
fuels for, development of nitride, 25:8910 (ORNL-4600, pp 41-56)
materials for, development of, 25:8863(R) (BMI-1891)
reliability of components of, fault trees and malfunction catalog of, 25:10237 (BAW-1344)
safety system for 1000 MW(e), fault trees and malfunction catalog for, 25:10237 (BAW-1344)
LIQUIDS
analysis for iron-55, proportional detector for, 25:8466 (BNWL-SA-3624)
bubble stabilization in vertically vibrating column of, effects on pool boiling heat transfer, (E), 25:8419
LITHIUM
antideuteron reactions at 25 GeV/c, absorption cross sections for, (E), 25:9639
corrosive effects on T-111 alloy at high temperatures,

XUM

25:8837 (ORNL-4600, pp 216-22)
radioinduced defects in silicon doped with, EPR study of electron, 25:9558
LITHIUM FLUORIDES
radiation effects on lattice parameter of single crystals of, annealing of neutron, 25:9565
thermoluminescence correlation with optical absorption for dosimetry-grade, for various heat treatments, 25:9574
BeF_2--LiF, preparation and handling of molten, for use as MSRE coolant salt, 25:10211 (ORNL-4616)
BeF_2--LiF--NdF_3--ZrF_4, distillation of molten, removal of neodymium fluoride by low-pressure, (E), 25:10210 (ORNL-4434)
BeF_2--LiF--UF_4--ZrF_4, preparation and handling of molten, for use as MSRE fuel salt, 25:10211 (ORNL-4616)
LITHIUM IONS
effects on Arabidopsis thaliana seeds, RBE for mutagenic and tumorigenic, 25:8800
effects on diamonds at 40 keV, 25:9557
effects on survival of HeLa cells following (n,α) reaction in cells, effects of boron-10 content on RBE for recoil, 25:8745
implantation into cadmium sulfide, acceptor luminescence induced by, 25:9561
photon reactions with Li^+, calculation of resonances between first and second ionization thresholds in, using diagonalization method, 25:9239
properties of ground-state Li^+, calculation using truncated multipolar expansion pair functions, 25:9249
LITHIUM ISOTOPES Li-6
alpha reactions (α,2α) at 56 MeV, analysis using triangular graphs, (T), 25:9987
deuteron reactions (d,n) at 2.5 to 3.7 MeV, angular distribution of neutron polarization in, (E), 25:9984
separation from lithium-7 by extraction chromatography, 25:8330
LITHIUM ISOTOPES Li-7
deuteron reactions (d,n) at 1.1 to 4 MeV, angular distributions and differential cross sections for, (E), 25:9975 (JINR-P15-5143)
deuteron reactions (d,n) at 2.5 to 3.7 MeV, angular distribution of neutron polarization in, (E), 25:9984
separation from lithium-6 by extraction chromatography, 25:8330
LIVER
cell function and distribution of blood flow in swine, iodine-131 and xenon-133 tracer studies of in vitro, 25:8783
plutonium-239 content of, review of effects of administration route, age, and dose on, 25:8595(T) (LF-tr-41, pp 7-125)
radiation effects on, of mice, effects of simultaneous eruption of Ascaris suum larvae on x, 25:8781
radioisotope content of, of rats following inhalation and intramuscular injection of americium-241, curium-242, plutonium-238, and plutonium-239, 25:8590 (CEA-CONF-1658)
scanning of human, evaluation of methods for selenium-75 labeled selenomethionine, 25:8715
scanning of human, to detect noncalcified hydatid cysts, use of gold-198 for, 25:8719
LOW TEMPERATURE PHYSICS
research at Technische Hochschule in 1969, 25:10018(R) (BMBW-FBK-70-10)
LUNAR MATERIALS
element abundances in, barium, chromium, magnesium, and neodymium, (E), 25:8965
LUNGS
plutonium-239 clearance from, of rats, 25:8590 (CEA-CONF-1658)
plutonium-239 content of, review of effects of administration route, age, and dose on, 25:8595(T) (LF-tr-41, pp 7-125)
radiation effects on relative weights of, in old-field mice, acute cobalt-60 γ, 25:8760
radiation effects on, of mice following exposure of thorax, x, 25:8778
radiation effects on, of mice, effects of simultaneous eruption of Ascaris suum larvae on x, 25:8781
radioinduced fibrosis in, of animals and man following therapy for malignant tumors, 25:8791
radioisotope clearance in rats, iron-59 and plutonium-239, 25:8591 (CEA-CONF-1677)
scanning of human, for measurement of antimony content, γ transmission methods for, 25:8726
scintiphotography of human, using metastable indium-113-labeled iron hydroxide, 25:8721
shielding of patient, during therapy using high-energy x, 25:8735
LUTETIUM ALLOYS AND SYSTEMS
Al--Lu--Ni, magnetic properties and phase diagram of LuNi/sub x/Al/sub 2-x/, 25:9576
LYMPH NODES
radiation effects on, in mice, RBE for whole-body electron, 25:8780
LYMPH SYSTEM
radiosensitivity of, in mammals, relation of, to antibody formation, ionizing, 25:8762
LYMPHOCYTES
radiation effects on count of, in old-field mice, acute cobalt-60 γ, 25:8760
radiation effects on synthesis of DNA in human, effects of low dose on x, 25:8647
LYSOZYME
radiation effects on chemical properties of, effects of exposing dry solid state on γ, 25:8604 (COO-690-41)

M

M-252 (NICKEL ALLOY)
analysis for molybdenum using mercaptosuccinic acid, spectrophotometric, 25:8210
MACHINE TOOLS
tool-path data for numerically-controlled, computer routine for adjusting or compensating, 25:8398 (Y-1750)
MACHINING
transfer processes in electrochemical, 25:10403 (UCRL-19615)
MAGNESIUM
abundance in Iota Ori B, (E), 25:8995
abundance in L and H chondrites, (E), 25:8967
abundance in late G and K dwarfs in the solar neighborhood, (E), 25:8969
abundance in meteorites and lunar samples, (E), 25:8965
determination in air particulates by spark source mass spectrometry, 25:8208
radioinduced defects in, low-temperature microscopic observations of annealing of 77°K neutron, 25:9542 (CEA-CONF-1681)
Raman effect in crystals of, model potential calculation of first derivative of electronic polarizability for first-order, 25:9598
MAGNESIUM ALLOYS AND SYSTEMS
book: Metallurgy and the Hot Working of Metals, 25:8894
Bi--Mg, electric resistance and transparency of films of, 25:10344(T) (BNL-tr-386)
KBr-base--Mg, optical absorption and electric conductivity of diffused crystals of, 25:9570
Mg--Sb, electric resistance and transparency of films of, 25:10344(T) (BNL-tr-386)
Mg--Sb, preparation and properties of variable composition films of, 25:10345(T) (BNL-tr-387)
Mg--Sn, electric resistance and transparency of films of, 25:10344(T) (BNL-tr-386)
Mg--Zr, embrittlement by hydrogen at high temperatures, effects of grain size on, 25:8874
Mg--Zr, use in cladding plugs for plutonium-loaded fuel elements, 25:8857
MAGNESIUM CHLORIDES
corrosive effects on chromium--iron--nickel alloys at 154°C, effects of aluminum, beryllium or carbon additions on stress, 25:8834(R) (COO-2069-6)
corrosive effects on Type 304 stainless steel at 154°C, effects of partial currents on, 25:8834(R) (COO-2069-6)
MAGNESIUM HYDRIDES
spectra in sunspots, absorption, (E), 25:9101
MAGNESIUM ISOTOPES Mg-24
abundance in Sun, (E), 25:9101
alpha inelastic scattering at 25.9 MeV, validity of the Austern--Blair method for, (T), 25:9991
deuteron reactions (d,p) at 13.5 MeV, generalized DWBA analysis of angular distributions from, (E/T), 25:9997 (JINR-E4-5350)
energy levels from sodium-23 (d,n) reactions, nuclear structure effects in gamma decay of isobaric analog, (E), 25:10007
helium-3 elastic scattering at 13 to 27 MeV, angular distributions for, (E/T), 25:9994
mass hexadecapole moments of, Hartree--Fock--Bogolyubov calculations of, (T), 25:10008
MAGNESIUM ISOTOPES Mg-25
abundance in Sun, (E), 25:9101
helium-3 elastic scattering at 13 to 27 MeV, angular distributions for, (E/T), 25:9994
MAGNESIUM ISOTOPES Mg-26
abundance in Sun, (E), 25:9101
deuteron reactions (d,Li-6) at 50 MeV, lithium-6 spectra and angular distributions for, (E), 25:9978(R) (ORO-3398-26)
energy levels from aluminum-27 (d,He-3) reactions, spectroscopic factors for, (E), 25:9966(R) (COO-1265-94)
helium-3 elastic and inelastic scattering at 17.7 MeV, angular distributions for, (E), 25:9966(R) (COO-1265-94)
helium-3 elastic scattering at 13 to 27 MeV, angular distributions for, (E/T), 25:9994
mass hexadecapole moments of, Hartree--Fock--Bogolyubov calculations of, (T), 25:10008
MAGNESIUM ISOTOPES Mg-28
mass hexadecapole moments of, Hartree--Fock--Bogolyubov calculations of, (T), 25:10008
MAGNESIUM OXIDES
effects of dispersions of, on properties of copper, 25:8873
fabrication of fine-grained and high-density, evaluation of methods for, 25:8937
mechanical properties of, review of effects of microstructure on, 25:8937

XUM

properties for use as high-temperature insulator, 25:8936
radiation effects on microstructure and swelling of monocrystalline, in-pile, 25:8954 (ORNL-4600, pp 210-15)
radioinduced paramagnetic center in lithium-doped, ESR of gamma, 25:9544
spectral identification of, in large sunspot, (E), 25:9100
MAGNET COILS
design of helical, for stellarator-type configurations, 25:9509
energy storage and liberation by superconducting, 25:9395
MAGNETIC FIELDS
effects of inhomogeneous, on component distribution in binary mixture in liquid film moving along pipe wall, (T), 25:9277
effects on pressure shock propagation in gas, (T), 25:9278
effects on statically unstable heterogeneous shear flow, (T), 25:9279
interaction with ring current of quasi-captured particles producing main phase of magnetic storm, magnetospheric, (T), 25:9342
origin of astrophysical, (T), 25:9129
production of galactic, (T), 25:9136
production of galactic, (T), 25:9135
MAGNETIC MIRROR MACHINES
performance of multi-MeV H_2^+ injection--accumulation experiment, 25:9506 (ORNL-TM-3207)
plasma confinement in, with octupole magnetic fields, (E), 25:9399
plasma distribution and end losses from, effect of co-ordinate space phenomena on, (T), 25:9406
MAGNETIC MIRRORS
plasma electric conductivity in, effect of electron collisions on, (T), 25:9480
MAGNETIC PROBES
performance for high surge current measurements, (E), 25:9505 (KFK-896)
MAGNETIC STORMS
gravity wave generation during sub-, mid-latitude atmospheric, (E/T), 25:9293
main phase of, produced by interaction between ring current of quasi-captured particles and magnetospheric magnetic field, (T), 25:9342
sudden commencement of July 27, 1966, electron precipitation-associated x-ray observations during, (E), 25:9298
MAGNETOHYDRODYNAMIC GENERATORS
book: Applied Magnetohydrodynamics, In Russian, 25:9275
book: Magnetohydrodynamics in Marine Engineering, 25:9266
electric potential distribution between electrodes of Faraday tube with supersonic current of ionized argon, 25:9263
high temperatures from combustion of natural fuel in, methods for obtaining, 25:9261
performance of electrodeless inductive, for plasma acceleration or power generation, 25:9439
performance of noble-gas closed loop, fired with fossil fuels, (E/T), 25:9264
performance optimization for multiterminal Hall-type, (T), 25:9265
working fluid for, use of uranium fluoride (UF_6), 25:10221
MAGNETOHYDRODYNAMICS
book: Applied Magnetohydrodynamics, In Russian, 25:9275
book: Electromagnetic Methods of Measuring the Parameters of MHD Processes, in Russian, 25:9273
book: Magnetohydrodynamics in Marine Engineering, 25:9266
MAGNETOSPHERE
boundary compression of, correlation with geomagnetic bay onsets, (E/T), 25:9332
electron diffusion in, simulation in trap with magnetic mirrors of, (E/T), 25:9350
geomagnetic field perturbations in, associated with dynamic spectra of atmospheric whistlers, (E/T), 25:9346
ionization exchange of protonosphere with nighttime F region, (E), 25:9325
plasma flow past Earth, interplanetary, (E/T), 25:9348
ring current of quasi-captured particles in high-latitude, distribution of, (T), 25:9342
whistler propagation between conjugate hemispheres in, walking-trace, (E), 25:9325
MAGNETOTAIL
propagation of primary low-energy cosmic radiation in, McMurdo Station-launched balloon data on, (E), 25:9327
MAGNETS
design of 70-kOe pulsed, for 25-liter bubble chamber, 25:8555
field leakage at surface of superconducting septum, effect of ribbon layers on, 25:9903 (BNL-15368)
magnetic field calculations for thick superconducting solenoid, computer program for, 25:9393
MALATHION
toxicity of carbon-14, phosphorus-32, sulfur-35, or tritium labeled, to man following ingestion of contaminated flour, calculations for, 25:8600
MAMMALIA
radiation effects on antibody formation in, ionizing, 25:8762
MAN
cortisol content of normal blood plasma of, double isotope derivative technique for measuring, 25:8585
medical status of atomic bomb survivors and offspring in Hiroshima and Nagasaki during 1969, bibliography on, 25:8741 (ABCC-TR-0-69)
radiation dose to bladder and rectum of, during intracavitary therapy of female gynecological carcinomas, γ, 25:8679 (SZS-6/70, pp 9-18)
radiation dose to skin and whole-body of, following continuous exposure during one year to krypton-85 dispersed in atmosphere, combined Bremsstrahlung and γ, 25:8667 (BNWL-SA-3233)
radiation dosimetry in, following internal deposition of radioisotopes, counting geometry for, 25:8687
radiation effects on count of germ cells in testes of, effects of dose on x, 25:8789(R) (NYO-4034-2)
radiation effects on function of vestibulocochlear analysor of, following cancer therapy in otorhinolaryngeal area, 25:8792
radiation effects on immune reactions of, prior to bone marrow grafting, 25:8617
radiation effects on reproductive capacity of, following ingestion of radium-226, 25:8669 (COO-2088-1)
radiation hazards to eyes of, standards for protection against laser, 25:8694
radiation injuries to heart of, following therapy, cortisone treatment of auto-immune mechanism of, 25:8708
radiation protection guidelines for use of radioisotopes for diagnostic studies on, 25:8717
radiation protection methods for, during contact γ radiotherapy of gynecological neoplasms, 25:8688 (SZS-6/70)
radiation protection standards for, in Italy, 25:8698
radioinduced aberrations of chromosomes in lymphocytes in, γ and x, 25:8788(T) (LIB/Trans-296)
radioinduced lung fibrosis in, following therapy for malignant tumors, pathology of, 25:8791
radioinduced suppression of ovulation in, effects of age on dose of ionizing, 25:8732
radioisotope ingestion by, from nuclear explosion-contaminated estuarine and marine food chains, use of stable element content of fish and invertebrates for predicting, 25:8627
radiosensitivity of gastrointestinal tract and interstitial tissues in, relation of, to planning for therapy using high-energy ionizing radiations, 25:8739
radiotherapy of endocrine exophthalmos in, effectiveness of thyroid ablation by iodine-131 for β and γ, 25:8733
radiotherapy of female genital carcinomas in, peritherapeutic dose and safety considerations during intracavitary radium γ, 25:8729 (SZS-6/70, pp 1-8)
radiotherapy of lymphomas in, method using high-energy x, 25:8734
radiotherapy of lymphomas in, method using high-energy x, 25:8735
strontium-85 accumulation in benign and malignant bone tumors of, correlation of data with microscopic data, 25:8597
strontium-90 uptake by, in EURATOM countries during 1968, 25:8624 (EUR-4509)
toxicity of radioisotope-labeled pesticides in, following ingestion of contaminated flour, calculations for, 25:8600
MANGANESE
abundance in L and H chondrites, (E), 25:8967
determination in air particulates by spark source mass spectrometry, 25:8208
determination in airborne particulates by neutron activation, 25:8231
determination in human fingernails and hair by neutron activation and γ spectrometry, 25:8229
determination in mandibular rat incisors following intraperitoneal injection of manganese chloride, by thermal neutron activation and scintillation counting, 25:8222
determination in titanium and titanium dioxide by neutron activation, 25:8233
determination of trace amounts of, in glass by neutron activation after sodium removal by hydrated antimony pentoxide, 25:8223
effects on colorimetric determination of uranium in fuel reprocessing solutions, 25:8197 (BARC-510)
performance of activation detectors of, for neutron spectra measurements at 1 eV to 10 keV, 25:8481 (KFK-1233)
MANGANESE ALLOYS AND SYSTEMS
B--Mn--rare earths, crystal structure of $RMnB_4$, 25:8948
C--Mn--P, radial distribution function for amorphous, 25:10348 (CALT-822-21)
MANGANESE ISOTOPES Mn-54
accumulation in Navicula seminulum, Plectonema boryanum, and Stigeoclonium lubricum, effects of temperature on, 25:8598
transport in food chains of nuclear-explosion-contaminated estuarine and marine ecosystems in relation to daily ingestion by man, use of stable

XUM

element content of fish and invertebrates for predicting, 25:8627
MANGANESE OXIDES
diffusion in, mechanism for anion and cation, 25:8934
electric conductivity of, 25:8934
MANY BODY PROBLEM
gauge fields in, (T), 25:9357
theory of nearly free electrons, use for positron annihilation in periodic field, 25:9606
MARS (PLANET)
ionosphere of, comparison with Earth and Venus inospheres, (E/T>, 25:9355
MASS SPECTROMETERS
data acquisition and control system for, on-line PDP-8L computer, 25:8571 (AAEC/TM-568)
detectors for, position-sensitive spark and multiwire proportional, 25:8476 (JUL-CONF-4, pp 71-120)
ion optical properties of three-sector, with energy dispersion, 25:8578
MATERIALS TESTING
equipment and method for circumferential mechanical properties of fuel cladding tubes, 25:8883
equipment for high-temperature compatibility testing in argon atmosphere, 25:8389 (AERE-M-1990)
method for simulating structural response of circular cylindrical shells to nuclear explosions, acceptable imperfections in impulse load inputs for, (T), 25:8441 (SC-RR-70-600)
MATHEMATICAL PHYSICS
properties of irradiated sets of linear topological space and convex bodies, 25:9614
research at Pittsburgh Univ., Dec. 1969 to Dec. 1970, 25:9839(R) (NYO-3829-64)
Schroedinger equation with damping for system weakly coupled to thermal bath, 25:9607
MATHEMATICS
approximation techniques in discrete dynamic programming, 25:10396 (TID-25624)
approximation techniques in discrete dynamic programming, 25:10397 (TID-25625)
difference equations with two-point boundary conditions, one sweep numerical method for vector-matrix, 25:10384 (TID-25609)
dimensionality reduction by approximation, 25:10418 (USCEE-350)
functional equations in theory of dynamic programming, 25:10388 (TID-25615)
realization of near-time-optimal feedback controllers, 25:10375 (SC-RR-70-544)
solution of optimal control problems by dynamic programming, method for reducing dimensionality in, 25:10419 (USCEE-377)
system identification using splines with unknown end points, 25:10390 (TID-25617)
MEATS
radiation processing of, economic and legal aspects of, in USA during 1967, 25:8813 (NP-18236)
seafood, radiation processing of fresh shrimp, effects of, on storage life and wholesomeness, γ, 25:8804 (TID-25556)
seafood, radiation processing of shrimp, effects of blanching, moisture content, and sorbic acid on γ, 25:8820
MECHANICAL DRIVES
description of sample-positioning, for scrap uranium analysis, 25:8447(R) (BHO-65-1)
MECHANICS
book: Formulations of Classical and Quantum Dynamical Theory, 25:9840
MEDICAL PERSONNEL
radiation dose to gonads, hands, and whole-body of, during preparation and application of γ emitters for interstitial therapy, γ, 25:8689 (SZS-6/70, pp 19-27)
radiation protection methods for, during preparation and application of γ emitters for interstitial therapy, 25:8689 (SZS-6/70, pp 19-27)
radiation protection programs for x-ray technicians, 25:8690
MEDICINE
programs and services of medical division at Goodyear Atomic Corporation during 1969, progress report on, 25:8692(R) (GAT-627)
MEDITERRANEAN SEA
book: Radioecological Studies of the Mediterranean Sea, 25:8630
MEIOSIS
radiation effects on chiasma frequency in, in grasshoppers, effects of temperature on x, 25:8754
MEMORY DEVICES
cycle-allocation disciplines for multiaccess, 25:10408 (UCRL-72648)
MERCURY
content of flour, neutron activation analysis for, 25:8588
determination by neutron activation, 25:8227
determination in airborne particulates by neutron activation, 25:8231
determination of trace amounts of, in copper by neutron activation, 25:8217 (MLM-1772)
electron reactions at 50 eV with, angular correlation of photons emitted by excited atoms from, (E), 25:9206
plasma of, instabilities from slow electron beam interactions, (E), 25:9447
MERCURY ACETATES, PHENYL-
toxicity of mercury-203-labeled, to man following ingestion of contaminated flour, calculations for, 25:8600
MERCURY ISOTOPES Hg-203
content of muscles and visceral organs of molluscs following uptake from food and seawater, 25:8625 (NP-18429)
toxicity of phenylmercuric acetate-incorporated, to man following ingestion of contaminated flour, calculations for, 25:8600
use of neohydrin-incorporated, for brain scanning, 25:8710 (NP-18560)
MESIC ATOMS
Lamb shift in ionized helium μ-, (R), 25:9188
meson (π)--nucleus scattering lengths from, (E/T), 25:9791
MESONS
decay of, empirical test of tensor meson dominance from widths of, (T), 25:9764 (DESY-70/58)
field theory for vector, equivalent formulations of, 25:9858
interactions in system of two neutral spinless, analytical properties of exactly solvable nonrelativistic two-channel, (T), 25:9772
interactions of, duality and factorization of amplitudes for, 25:9896
interactions with baryons in quark model, breakdown of Pomeranchuk conjecture for, (T), 25:9806
interactions with baryons, consistency conditions from duality for, (T), 25:9792
interactions with baryons, duality constraints on amplitudes for, 25:9799
interactions with baryons, quark focusing principle for, 25:9760
interactions with mesons at high energies, SU(n) symmetric multiperipheral model for magnitude of total cross sections for, (T), 25:9773
interactions with mesons, dual resonance and extended particle models for, (T), 25:9771
mass formula in Lagrangian model of chiral SU(3) x SU(3) with symmetry breaking, 25:9794
mass of ninth pseudoscalar, from sum rules for spin-zero spectral functions, 25:9779
mass spectra of low-lying, predictions from duality in baryon--antibaryon interactions for narrow states in, 25:9768
matrix elements of, weak current--current quark Hamiltonian for octet behavior of, 25:9761
production of excess of light, in relation to Dalitz pairs from proton reactions with nuclei at 26 GeV in emulsions, (E), 25:9642
spectra of, duality and factorization constraints on, 25:9896
symmetry group SU(2) x SU(2) for pseudoscalar, Schwinger terms in current model of chiral, 25:9833
theory for, Hamiltonian implying exclusion principle in, (T), 25:9689 (LNF-70/22)
MESONS (eta)
decay eta → π⁺ + π⁻ + γ in chiral Lagrangian model, 25:9780
decay eta⁰ → π⁰ + γ + γ in chiral Lagrangian model, 25:9780
production and decay in π⁺ + d → p + p + π⁺ + π⁻ + π⁰ interactions at 1.1 to 2.4 GeV/c, (E), 25:9675
production in γ + p → eta + p interactions at 4 and 6 GeV, Veneziano model for, (T), 25:9712
production in π⁺ + d → 2p + π⁺ + π⁻ + π⁰ interactions at 1.1 and 2.4 GeV/c in bubble chamber, (E), 25:9664
production in π⁺ + p interactions at 18.5 GeV/c, energy dependence of cross sections for, (E), 25:9677
production of eta⁰ in π⁺ + p → p + 2π⁺ + π⁻ and π⁺ + p → p(n) + 2π⁺ + π⁻ + π⁰(π⁺) interactions at 2.34 GeV/c, cross sections for, (E), 25:9662
MESONS (f)
exchange of f⁰(1260) in t-channel of π + N interactions, (T), 25:9802
production of f⁰ in π⁻ + p → n + π⁺ + π⁻ backward interactions at 2 to 6 GeV/c, spark chamber study of differential cross sections and density matrix elements for, (E), 25:9654 (COO-1764-114)
production of f⁰ in π⁺ + p interactions at 18.5 GeV/c, energy dependence of cross sections for, (E), 25:9677
MESONS (K)
decay K → 3π, π scattering lengths from ratio of total probabilities for, (T), 25:9736
decay K → π + π + l + ν, current algebra and chiral symmetry for axial-vector form factors of, 25:9743
decay of, phenomenological Lagrangian models for soft-pion limit and ΔI = 1/2 rule for nonleptonic, (T), 25:9732 (BNL-50260)
interactions anti K + d → K + Y_1 + Y_2, cross sections for, (T), 25:9804 (JINR-P2-5231)
interactions anti K + N, hyperon production in partially latent quasidynamical, (T), 25:9752
interactions K + π, symmetry-breaking corrections to, 25:9743
interactions K + π, two-parameter effective-range formula for scalar form factor of, 25:9777
reactions with light nuclei, cross sections for double

charge-exchange, (T), 25:9974 (JINR-P2-5286)
MESONS (K⁻)
interactions K⁻ + d → p + π⁺ + π⁻ + π⁻ + n + anti K⁰ at 4.91 GeV/c, nπ⁻π⁻(1627) enhancement in, (E), 25:9671
interactions K⁻ + d at 0.36 to 0.72 GeV/c, total cross sections for, (E), 25:9673
interactions K⁻ + n → K⁻ + n at 1860 to 2150 MeV, elasticity of Σ(2030) from partial-wave analyses of, (E), 25:9681
interactions K⁻ + n → K⁻ + π⁻ + p at 12.6 GeV/c in bubble chamber, pπ⁻(1400) enhancement, cross section for K⁻ + π⁻ → K⁻ + π⁻ interactions, and cross sections for, (E), 25:9658 (TID-25611)
interactions K⁻ + n → Λ⁰ + A_2^- at 4.48 GeV/c, spin and parity of A_2 from production and decay in, (E), 25:9672
interactions K⁻ + n → Σ⁰ + A_2^- at 4.48 GeV/c, spin and parity of A_2 from production and decay in, (E), 25:9672
interactions K⁻ + p → K⁻ + p at 0.98 to 1.34 GeV, anti KN partial-wave amplitudes from, (E/T), 25:9667
interactions K⁻ + p → K⁻ + p at 3.55 to 6.9 GeV/c, spark chamber study of differential cross sections for, (E), 25:9684
interactions K⁻ + p → Λ + π⁰ at 1.865 to 2.001 GeV in hydrogen bubble chamber, properties of Σ(1910) from, (E), 25:9659 (UCRL-19789)
interactions K⁻ + p → p + K⁻ + M⁰(953) at 3.9 and 4.6 GeV/c in hydrogen bubble chamber, mass and width of M(953) in, (E), 25:9683
interactions K⁻ + p at 0.36 to 0.72 GeV/c, total cross sections for, (E), 25:9673
interactions K⁻ + p, eikonal Regge model for elastic, 25:9755
interactions K⁻ + π⁻ → K⁻ + π⁻, K⁻ + n → K⁻ + π⁻ + p interactions at 12.6 GeV/c in bubble chamber for determining cross sections of, (E), 25:9658 (TID-25611)
reactions with neon at rest in bubble chamber, conversion electron pairs from nuclei excitation in, (E), 25:10012
scattering by helium-4 at 115 to 160 MeV/c in helium bubble chamber, differential cross sections and scattering lengths for elastic, (E/T), 25:9969
MESONS (K⁰)
decay K⁰ → 2π + 2γ in current algebra, branching ratio for, 25:9738
decay K⁰ → 2π, review of CP violation in, (T), 25:9828
decay K_2^0 → 2π, model with supplementary particles for K_2^0--K_1^0 interference for test of CP violation in, (T), 25:9827
decay K_2^0 → π + l + ν, model with supplementary particles for charge asymmetry for test of CP violation in, (T), 25:9827
decay K_2^0 → π + μ + ν at 3 to 12 GeV/c, wire spark chamber spectrometer study of form factors for, (E), 25:9629 (UCLA-1054)
decay K_2^0 → π⁺ + π⁻ + π⁰, matrix element constant from wire chamber magnetic spectrometer study of, (E), 25:9628 (UCLA-1052)
decay K_2^0 → π⁺ + π⁻ + π⁰, parametrization of π⁰ spectrum in, (E), 25:9630
decay K_2^0 → π⁺ + π⁻ decay, long-range field pulses as source of CP invariance in, (T), 25:9826 (NYO-2171-329)
mass difference (K_1^0 - K_2^0), time dependence of anti K⁰ + p interactions in hydrogen bubble chamber for determining, (E), 25:9631
mass difference (K_2^0 - K_1^0) from weak interaction S-matrix, 25:9740
mass shift of K_1^0, multichannel N/D formalism for, (T), 25:9778
regeneration K_2^0 → K_1^0 at high energies, design and performance of magnetic spark chamber spectrometer for studying, 25:8544 (JINR-P1-5361)
MESONS (anti K⁰)
interactions anti K⁰ + p in hydrogen bubble chamber, K_1^0 - K_2^0 mass difference determination from time dependence of, (E), 25:9631
MESONS (K⁺)
decay K⁺ → π + π + e + ν, form factors and rate of, 25:9747
decay K⁺ → π⁺ + γ + γ in axial-vector dominance model, π⁺ spectra and branching ratio for, (T), 25:9745
interactions K⁺ + d at 0.36 to 0.72 GeV/c, total cross sections for, (E), 25:9673
interactions K⁺ + p → K⁺ + p + ω at 9 GeV/c, test of double-Regge behavior of generalized Veneziano model for, 25:9797
interactions K⁺ + p → K⁺ + p at 3.55 to 6.9 GeV/c spark chamber study of differential cross sections for, (E), 25:9684
interactions K⁺ + p → K⁺(K⁰) + π⁻(π⁰) + π⁺ + p at 10 GeV/c, low-mass enhancements in Kππ spectrum from, (E), 25:9679
interactions K⁺ + p at 0.36 to 0.72 GeV/c, total cross sections for, (E), 25:9673
interactions K⁺ + p, eikonal Regge model for elastic, 25:9755
MESONS (μ)
decay μ → e + ν + ν, determination from neutrino bubble chamber exposures, (E), 25:9748
detection of narrow bundles of cosmic, spark chamber underground study of, (E), 25:9632
flux measurements of cosmic, scintillation telescope detector for, 25:8556
MESONS (μ⁻)
production of μ⁻--μ⁺ pairs in e⁺ + e⁻ interactions at 0.7 x 2 to 1.2 x 2 GeV, spark chamber and scintillation counter study of, (E), 25:9621 (NP-18581)
MESONS (μ⁺)
production of μ⁻--μ⁺ pairs in e⁺ + e⁻ interactions at 0.7 x 2 to 1.2 x 2 GeV, spark chamber and scintillation counter study of, (E), 25:9621 (NP-18581)
range in liquid hydrogen, (T), 25:9166
MESONS (ω)
decay ω → 2π relative to ω → 3π, branching ratio for, (T), 25:9718
decay ω → 3π in chiral Lagrangian model, 25:9780
decay ω → e⁺ + e⁻(+γ) radiative corrections for, (T), 25:9766
decay ω → μ⁺ + μ⁻(+γ) radiative corrections for, (T), 25:9766
electromagnetic transition rho → ω, spectral-function sum rules for, 25:9718
interference effect of rho--ω in anti p + p → π⁺ + π⁺ + π⁻ + π⁻ interactions at 1.63 to 2.20 GeV/c, (E), 25:9647
production and decay in π⁺ + d → p + p + π⁺ + π⁻ + π⁰ interactions at 1.1 to 2.4 GeV/c, (E), 25:9675
production in γ + N interactions at high energies, SU(3) quark model for, (T), 25:9713
production in π⁺ + d → 2p + π⁺ + π⁻ + π⁰ interactions at 1.1 and 2.4 GeV/c in bubble chamber, (E), 25:9664
production in π⁺ + p interactions at 18.5 GeV/c, energy dependence of cross sections for, (E), 25:9677
production of ω⁰ in π⁺ + p → p + p + 2π⁺ + π⁻ and π⁺ + p → p(n) + 2π⁺ + π⁻ + π⁰(π⁺) interactions at 2.34 GeV/c, cross sections for, (E), 25:9662
MESONS (phi)
decay phi → e⁺ + e⁻(+γ), radiative corrections for, (T), 25:9766
decay phi → μ⁺ + μ⁻(+γ), radiative corrections for, (T), 25:9766
electromagnetic transition rho → phi, spectral-function sum rules for, 25:9718
production in γ + N interactions at high energies, SU(3) quark model for, (T), 25:9713
production in γ + p → phi + p interactions, Cheng--Wu picture for, (T), 25:9716
MESONS (π)
coupling constant for πN in current-field algebra, 25:9762
coupling constant for πΣΛ using Adler consistency condition, 25:9812
coupling constant for πΣΣ using Adler consistency condition, 25:9812
coupling of soft-, in hadron interactions, chiral-symmetric, 25:9783
coupling to hadrons at low energies, S-matrix commutation with axial charge for universality of, (T), 25:9886 (DESY-70/57)
dynamics of A_1rhoπ system, chiral SU(2) x SU(2), 25:9781
emission of soft-, in hadron processes, effects of, 25:9782
exchange contribution to N + N scattering, two-body, 25:9807
interactions K + π, symmetry-breaking corrections to, 25:9743
interactions K + π, two-parameter effective-range formula for scalar form factor of, 25:9777
interactions of, research at Houston Univ., 1970, (E), 25:9657(R) (ORO-3948-2)
interactions of, scattering length determination from total probabilities for K → 3π decay, (T), 25:9736
interactions π + Λ, consistency conditions from duality for, (T), 25:9792
interactions π + N at low and intermediate energies, local duality in invariant amplitudes for, 25:9796
interactions π + N in Veneziano model, polarization in charge-exchange, 25:9793
interactions π + N, consistency conditions from duality for, (T), 25:9792
interactions π + N, direct-channel Regge poles for finite-energy sum rules for amplitudes of, 25:9801
interactions π + N, epsilon(700) and f^0(1260) exchange in t-channel of, (T), 25:9802
interactions π + N, model of fermion trajectory for, 25:9790
interactions π + N, Regge cuts and asymptotic sum rules for amplitudes of forward, 25:9800
interactions π + N, scattering lengths for, (E/T), 25:9791
interactions π + N, tensor meson dominance for decoupling of f-exchange contribution from A amplitude in, (T), 25:9764 (DESY-70/58)
interactions π + N, vacuum trajectory for, (T), 25:9785 (DESY-70/55)
interactions π + π → π + π, chiral SU(2) x SU(2) Lagrangian for, 25:9781
interactions π + π, bootstrap model for derivation of Wu and Yang conjecture for cross sections of, (T),

XUM

25:9809
interactions $\pi + \pi$, $\gamma + p \to 2\pi + p$ interactions at high energies for determination of phase shifts for, (T), 25:9767
interactions $\pi + \pi$, hard-pion current algebra for I = 0 s-wave phase shifts for, 25:9775
interactions $\pi + \pi$, phase shifts from $\pi^- + p \to \pi + \pi + N$ interactions at 2.77 GeV/c, (E/T), 25:9670
interactions $\pi + \pi$, restriction from crossing symmetry and unitarity on amplitudes for, 25:9784
interactions $\pi + \pi$, S-wave scattering length from $\pi^- + p \to \pi^0 + \pi^0 + n$ interactions at 378 MeV for, (E), 25:9668
interactions $\pi + \pi$, two-parameter effective-range formula for scalar form factor of, 25:9777
interactions $\pi + I$, consistency conditions from duality for, 25:9792
interactions rho + $\pi \to$ rho + π, chiral SU(2) x SU(2) Lagrangian for, 25:9781
interactions with helium-3 and tritium, cross-section calculations using Glauber theory, (T), 25:9967 (JINR-P2-5335)
production in $\gamma + N \to \Delta(1236) + \pi$ interactions at 0.7 to 1 GeV, angular distribution asymmetry of, (T), 25:9798
production in $\gamma + N \to N + \pi$ interactions, chiral Lagrangian formalism for, 25:9726
production in $\gamma + N \to \pi + N$ interactions, simple harmonic forces in nonrelativistic quark model for N^* production in, (T), 25:9788
production in $\gamma + N$ interactions at low energies, Kroll--Ruderman theorem and Born approximation for p-wave multipoles in, 25:9724
production in $\gamma + p$ and $\gamma + n$ interactions, fits to differential cross sections for, 25:9727
radius of, simple harmonic forces in nonrelativistic quark model for root-mean-square, (T), 25:9788
reactions with emulsion nuclei at high energies, mass distribution and decays of hyperfragments produced in, (E), 25:9637
reactions with light nuclei, cross sections for double charge-exchange, (T), 25:9974 (JINR-P2-5286)
reactions with nuclei at 45 to 200 GeV in emulsions, 3π and 5π production in, (E), 25:9635 (INP-722)
reactions with nuclei at 60 GeV in emulsions, helium production in, (E), 25:9660
scattering by nuclei, scattering lengths for, (E/T), 25:9791

MESONS (π^-)
absorption by nuclei, short-range nucleon--nucleon correlations from shell-model description of, 25:9982
absorption rate for 1s and 2p bound states in carbon-12, 25:9982
absorption rate for 1s and 2p bound states in oxygen-18, 25:9982
absorption rate for 1s and 2p bound states in oxygen-16, 25:9982
interactions $K^- + \pi^- \to K^- + \pi^-$, $K^- + n \to K^- + \pi^- + p$ interactions at 12.6 GeV/c in bubble chamber for determining cross sections of, (E), 25:9658 (TID-25611)
interactions $\pi^- + d$ at 5.53 GeV/c, momentum spectra in, (E), 25:9634 (COO-1764-115)
interactions $\pi^- + p \to 2\pi^- + \pi^+ + p$ at 5.0 to 7.5 GeV/c in bubble chamber, coherence of isoscalar and isovector exchange amplitudes for A_2^- production in, (E), 25:9650 (COO-1195-202)
interactions $\pi^- + p \to n + 2\gamma$ at 3.65 GeV/c, spark chamber and scintillation counter study of eta' production in, (E), 25:9651 (COO-1764-111)
interactions $\pi^- + p \to n + \pi^+ + \pi^-$ at 2 to 6 GeV/c, spark chamber study of differential cross sections and density matrix elements for rho and f^0 production in backward, (E), 25:9654 (COO-1764-114)
interactions $\pi^- + p \to p + \pi^+ + 2\pi^-$ at 4.47 GeV/c in hydrogen bubble chamber $\Delta^{++}(1236)$ production and $\pi^+ + p$ virtual scattering and $\pi^- + \pi^-$ scattering cross sections and angular distributions in, (E), 25:9655 (ITEF-767)
interactions $\pi^- + p \to p + \pi^-$ + neutral boson state at 8 GeV/c, search for higher-mass resonances in, (E), 25:9676
interactions $\pi^- + p \to p + \pi^+ + \pi^- + \pi^-$ + neutral boson state at 8 GeV/c, search for higher-mass resonances in, (E), 25:9676
interactions $\pi^- + p \to \pi + \pi + N$ at 2.77 GeV/c, $\pi\pi$ phase shifts from, (E/T), 25:9670
interactions $\pi^- + p \to \pi^0 + n$ at 2 to 6 GeV/c, differential cross sections for backward, (E), 25:9674
interactions $\pi^- + p \to \pi^0 + n$ at 2 to 6 GeV/c, differential cross sections, isospin, u- and s-channel amplitudes and phase for backward, (E), 25:9653 (COO-1764-113)
interactions $\pi^- + p \to \pi^0 + n$ in Veneziano model, polarization in, 25:9793
interactions $\pi^- + p \to \pi^0 + \pi^0 + n$ at 378 MeV, S-wave $\pi + \pi$ scattering length from, (E), 25:9668
interactions $\pi^- + p \to \pi^- + p$ at 1.71 to 5.53 GeV/c, scintillation counter spectrometer study of (2290) enhancement in differential cross sections for, (E), 25:9652 (COO-1764-112)
interactions $\pi^- + p \to \pi^- + p$ at 2.85 to 6.9 GeV/c, spark chamber study of angular distributions for, (E), 25:9684
interactions $\pi^- + p \to \pi^- + \pi^+ + n$ at 2.77 GeV/c, elastic cross section for $\pi^+ + \pi^-$ interactions from, (E/T), 25:9669
interactions $\pi^- + p \to \pi^+ + \pi^- + n$, resonance approximation for rho production in, 25:9894
interactions $\pi^- + p \to \pi^- + \pi^+(\pi^0) + n(p)$, Veneziano model prediction of rho'' daughter resonance contribution to amplitudes of, (T), 25:9786
interactions $\pi^- + p \to rho^0 + \pi^- + p$ at 4.45 GeV/c in hydrogen bubble chamber, differential cross sections and mass distributions for, (E), 25:9663
interactions $\pi^- + p \to rho^0 + \pi^- + p$ at 4.45 GeV/c in hydrogen bubble chamber, mass distributions for, (E), 25:9656 (ITEF-775)
interactions $\pi^- + p$, eikonal Regge model for elastic, 25:9755
interactions $\pi^- + p$, sum rules for amplitude ratio of $\pi^+ + p$ interactions to, (T), 25:9789
interactions $\pi^+ + \pi^-$ from $\pi^- + p \to \pi^- + \pi^+ + n$ interactions at 2.77 GeV/c, cross sections for elastic, (E/T), 25:9669
interactions $\pi^- + \pi^-$ in $\pi^- + p \to p + \pi^+ + 2\pi^-$ interactions at 4.47 GeV/c in hydrogen bubble chamber, cross sections and angular distributions for, (E), 25:9655 (ITEF-767)
interactions $\pi^+ + \pi^-$, analytic structure of off-mass-shell S-wave amplitude of, (T), 25:9763 (COO-1428-239)
production in $\gamma + N$ interactions, off-shell single-current amplitude in Veneziano model for, 25:9725
production in photon reactions (γ,π^-) with boron-11 at 150 to 700 MeV, yields and cross sections for, (E), 25:9620 (LUNP-7007)
production of $\pi^+ - \pi^-$ pairs in $\pi^- + p \to n + \pi^+ + \pi^-$ backward interactions at 2 to 6 GeV/c, spark chamber study of differential cross sections and density matrix elements for, (E), 25:9654 (COO-1764-114)
reactions with nuclei at 2.94 GeV/c, direct production of electron pairs in, (E), 25:9661
reactions with nuclei, rho'' daughter resonance detection in, (T), 25:9786

MESONS (π^0)
decay of cosmic, gamma background from, (T), 25:9254
lifetime measurement of, shower spark chamber for, 25:8553

MESONS (π^+)
interactions $\pi^+ + d \to 2p + \pi^+ + \pi^- + \pi^0$ at 1.1 and 2.4 GeV/c in bubble chamber, eta and ω production in, (E), 25:9664
interactions $\pi^+ + d \to p + p + m\pi$ (m = 2 to 6) at 2.15 GeV/c in bubble chamber, production and decay of $X^0(1960)$ in, (E), 25:9666
interactions $\pi^+ + d \to p + p + \pi^+ + \pi^- + \pi^0$ at 1.1 to 2.4 GeV/c, production and decay of eta and ω in, (E), 25:9675
interactions $\pi^+ + p \to 2\pi^+ + \pi^- + p$ at 7.0 to 8.5 GeV/c in bubble chamber, coherence of isoscalar and isovector exchange amplitudes for A_2^+ production in, (E), 25:9650 (COO-1195-202)
interactions $\pi^+ + p \to \Delta^{++} + A_2^0$ at 5 GeV/c, cross sections and spin-density matrix elements, (E), 25:9682
interactions $\pi^+ + p \to \Delta^{++} + eta^0$ at 5 GeV/c, cross sections and spin-density matrix elements for, (E), 25:9682
interactions $\pi^+ + p \to \Delta^{++} + f^0$ at 5 GeV/c, cross sections and spin-density matrix elements for, (E), 25:9682
interactions $\pi^+ + p \to \Delta^{++} + \omega^0$ at 5 GeV/c, cross sections and spin-density matrix elements for, (E), 25:9682
interactions $\pi^+ + p \to \Delta^{++} + rho^0$ at 5 GeV/c, cross sections and spin-density matrix elements for, (E), 25:9682
interactions $\pi^+ + p \to p + 2\pi^+ + \pi^-$ 2.34 GeV/c, resonance production cross sections in, (E), 25:9662
interactions $\pi^+ + p \to p + A_2^+$ at 5 GeV/c, cross sections and spin-density matrix elements for, (E), 25:9682
interactions $\pi^+ + p \to p + B^+$ at 5 GeV/c, cross sections and spin-density matrix elements for, (E), 25:9682
interactions $\pi^+ + p \to p + rho^+$ at 5.2 GeV/c, differential cross section for backward rho^+ production in, (E), 25:9665
interactions $\pi^+ + p \to p(n) + 2\pi^+ + \pi^- + \pi^0(\pi^+)$ at 2.34 GeV/c, resonance production cross sections in, (E), 25:9662
interactions $\pi^+ + p \to \pi^+ + p$ at 2.85 to 6.9 GeV/c, spark chamber study of angular distributions for, (E), 25:9684
interactions $\pi^+ + p$ at 0.82 to 2.74 GeV/c, polarization and differential cross section for elastic, (E), 25:9680
interactions $\pi^+ + p$ at 18.5 GeV/c, cross sections for production of rho^0, f^0, g^0, eta^0, ω^0, and $\Delta^{++}(1236)$ in, (E), 25:9677
interactions $\pi^+ + p$ at 8 GeV/c, density matrix elements and spin population resonance parameters in, (E/T), 25:9678
interactions $\pi^+ + p$ in $\pi^- + p \to p + \pi^+ + 2\pi^-$ interactions at 4.47 GeV/c in hydrogen bubble chamber, virtual, (E), 25:9655 (ITEF-767)
interactions $\pi^+ + p$, eikonal Regge model for elastic, 25:9755

interactions π^+ + p, sum rules for amplitude ratio of π^- + p interactions to, (T), 25:9789
interactions π^+ + π^- from π^- + p → π^- + π^+ + n interactions at 2.77 GeV/c, cross sections for elastic, (E/T), 25:9669
interactions π^+ + π^-, analytic structure of off-mass-shell S-wave amplitude of, (T), 25:9763 (COO-1428-239)
production in γ + N interactions, off-shell single-current amplitude in Veneziano model for, 25:9725
production in γ + p → n + π^+ interactions at 260 to 350 MeV, absolute differential cross sections for, (E), 25:9623
production in γ + p → π^+ + n interactions at small momentum transfers, cross section asymmetry for, (E), 25:9624
production in photon reactions (γ,π^+) with nuclei at 150 to 700 MeV, yields and cross sections for, (E), 25:9620 (LUNP-7007)
production of π^+--π^- pairs in π^- + p → n + π^+ + π^- backward interactions at 2 to 6 GeV/c, spark chamber study of differential cross sections and density matrix elements for, (E), 25:9654 (COO-1764-114)
reactions with nuclei, rho'' daughter resonance detection in, (T), 25:9786

MESONS (rho)
contribution of rho'' to amplitudes of π^- + p → π^- + $\pi^+(\pi^0)$ + n(p) interactions, Veneziano model prediction of, (T), 25:9786
contributions to strong interactions, universal formulas for, (T), 25:9750
decay rho^0 → e^+ + e^-(+γ), radiative corrections for, (T), 25:9766
decay rho^0 → μ^-(+γ), radiative corrections for, (T), 25:9766
dynamics of A_1rhoπ system, chiral SU(2) x SU(2), 25:9781
electromagnetic transition rho → ω, spectral-function sum rules for, 25:9718
electromagnetic transition rho → phi, spectral-function sum rules for, 25:9718
interactions rho + π → rho + π, chiral SU(2) x SU(2) Lagrangian for, 25:9781
interference effect of rho--ω in anti p + p → π^+ + π^+ + π^- + π^- interactions at 1.63 to 2.20 GeV/c, (E), 25:9647
mass splitting (rho^+ - rho^0), spectral-function sum rule for, 25:9718
production in γ + N interactions at high energies, SU(3) quark model for, (T), 25:9713
production in γ + p → rho^0 + p interactions, Cheng--Wu picture for, (T), 25:9716
production in π^- + p → π^+ + π^- + n interactions, resonance approximations for, 25:9894
production of rho'' daughter resonance in π^- and π^+ reactions with nuclei, detection of, (T), 25:9786
production of rho^0 in π^- + p → n + π^+ + π^- backward interactions at 2 to 6 GeV/c, spark chamber study of differential cross sections and density matrix elements for, (E), 25:9654 (COO-1764-114)
production of rho^0 in π^+ + p → p + 2π^+ + π^- and π^+ + p → p(n) + 2π^+ + π^- + $\pi^0(\pi^+)$ interactions at 2.34 GeV/c, cross sections for, (E), 25:9662
production of rho^0 in π^- + p → rho^0 + π^- + p interactions at 4.45 GeV/c in hydrogen bubble chamber, mass distributions for, (E), 25:9656 (ITEF-775)
production of rho^0 in π^+ + p interactions at 18.5 GeV/c, energy dependence of cross sections for, (E), 25:9677

MESONS (X^0)
decay rates of X^0 → γ + γ and X^0 → π^0 + π^0 + eta from π^+ + d interactions at 2.15 GeV/c, (E), 25:9666
decay X^0 → π^0 + γ + γ in chiral Lagrangian model, 25:9780
decay X^0 → π^+ + π^- + γ in chiral Lagrangian model, 25:9780
mass from sum rules for spin-zero spectral function, 25:9779

MESONS, RESONANCE
contributions of sigma to strong interactions, universal formulas for, (T), 25:9750
coupling constant for epsilonN, broken scale invariance for, 25:9762
decay A_1 → rho + π and A_1 → 3π, chiral SU(2) x SU(2) Lagrangian for, 25:9781
decay A_2 → eta^0 + π^- relative to A_2 → (rho + π)$^-$ from production in π^- + p interactions at 8 GeV/c, (E), 25:9676
decay delta → 2γ in SU(3)-symmetric limit, 25:9719
decay epsilon → 2γ in SU(3)-symmetric limit, model for, 25:9719
decay eta' → 2γ, spark chamber study of branching ratio and partial width of, (E), 25:9651 (COO-1764-111)
decay M^0(953) → eta(γ) + π^+ + π^- in hydrogen bubble chamber, branching ratio for, (E), 25:9683
decay of, review of spin and parity determination from, (T), 25:9774
dynamics of A_1rhoπ system, chiral SU(2) x SU(2), 25:9781
exchange of epsilon(700) in t-channel of π + N interactions, (T), 25:9802
mass and width of M^0(953) in K^- + p → K^- + p + M^0(953) interactions at 3.9 and 4.6 GeV/c in hydrogen bubble chamber, (E), 25:9683
model for nonstrange, simple harmonic forces in nonrelativistic quark, (T), 25:9788
parity and spin of A_2 from production and decay in K^- + n → $A^0(I^0)$ + A_2^- interactions at 4.48 GeV/c, 25:9672
parity and spin of, review of determination from particle production and decay, (T), 25:9774
production of A_2^- in π^- + p → 2π^- + π^+ + p interactions at 5.0 to 7.5 GeV/c in bubble chamber, coherence of isoscalar and isovector exchange amplitudes for, (E), 25:9650 (COO-1195-202)
production of A_2^+ in π^+ + p → 2π^+ + π^- + p interactions at 7.0 to 8.5 GeV/c in bubble chamber, coherence of isoscalar and isovector exchange amplitudes for, (E), 25:9650 (COO-1195-202)
production of doubly charged, in anti p + p → π^+ + π^+ + π^- + π^- + nπ^0 interactions at 1.6 to 2.2 GeV/c, upper limits for cross sections for, (E), 25:9643
production of eta' in π^- + p → n + 2γ interactions at 3.65 GeV/c, spark chamber and scintillation counter study of, (E), 25:9651 (COO-1764-111)
production of g^0 in π^+ + p interactions at 18.5 GeV/c, energy dependence of cross sections for, (E), 25:9677
production of higher-mass resonances in π^- + p interactions at 8 GeV/c, (E), 25:9676
production of low-mass enhancements in Kππ spectrum from K^+ + p → $K^+(K^0)$ + $\pi^-(\pi^0)$ + π^+ + p interactions at 10 GeV/c, (E), 25:9679
production of M^0(953) in K^- + p → K^- + p + M^0(953) at 3.9 and 4.6 GeV/c in hydrogen bubble chamber, (E), 25:9683
production of, review of spin and parity determination from, 25:9774
splitting of A_2 in classification of low-lying meson spectra, 25:9768

MESOXALONITRILE
m-chlorophenylhydrazone of, effects on ion fluxes in corn roots, 25:8602

METALLURGICAL EQUIPMENT
design for determination of low-temperature mechanical properties of alloys and metals, 25:8881
development for measuring mechanical properties of cladding tubes, 25:8883

METALS
abundance in late G and K dwarfs in the solar neighborhood, (E), 25:8969
abundance in open cluster NGC 6791, (E), 25:9000
analysis for boron by neutron irradiation and alpha track autoradiography, 25:8235
analysis for carbon and oxygen by photon activation, 25:8216 (AERE-R-5363)
analysis for nitrogen by vacuum melt extraction, 25:8205
coating of sheets of, radioinduced polymerization of aminoplast films for, 25:8278(P)
copper-ion reactions at 40 keV to 1.1 MeV with, cross sections for L x-ray production in, as function of atomic number, (E), 25:9164
emissivity calculation from electronic density of states, normal spectral, 25:9584
magnetic impurity interactions with electrons in, (T), 25:9391
plasticity of bcc, dynamic micro-, 25:10349 (CONF-700545-1)
radiation effects on embrittlement of bcc and fcc, neutron, 25:8898 (SRARI-P-85)
thermotransport in liquid, isotope separation by, 25:8336

METEORITES
composition of L and H chondrites, (E), 25:8967
composition of Stannern and Nuevo Laredo, (E), 25:8966
element abundances in, barium, chromium, magnesium, and neodymium, (E), 25:8965
rare gases in chondrites, abundance and isotopic composition of, (E), 25:8968

METEOROLOGY
research at AECL during 1970, progress report on, 25:8666(R) (AECL-3728)

METEORS
ionization due to ablating materials in ionospheric E region, (E/T), 25:9307

METHACRYLIC ACID, METHYL ESTER
polymerization of, mechanisms of chain crosslinking in, 25:8276 (JAERI-Memo-4147)
radiation effects on subsequent polymerization on aluminosilicate glass, γ, 25:8277(T) (NSJ-tr-160)

METHACRYLIC ACID, METHYL ESTER, POLYMERS
radiation effects on optical density of, γ, 25:8273

METHANE
combustion in MHD generator, methods for obtaining high temperatures in, 25:9261
corrosion inhibition properties in carbon dioxide coolants, 25:10201(P)
effects on kinetics of oxidation of tungsten at 670 to 980°C, 25:8841
ion reactions in eV range with, mechanisms and cross sections for light emission in, (E), 25:9213
reactions between ions and molecules of, ion-cyclotron-resonance measurements of collision and charge-exchange rates in, 25:9233
yields from γ radiolysis of aqueous ethanol solutions as function of nitrate concentration, 25:8301
methane--SiH_4, ionization in mass spectrometer, reactions of products from, 25:8294

METHANE, DICHLORODIFLUORO-
use for simulating forced convection burnout in water,

XUM

25:8410
METHANE, IODO-
radiolysis of, methane and hydrogen yields as function of pressure from γ, 25:8303
reactions with reactor containment spray solutions, effects of sodium thiosulfate on rate of, (E), 25:10244(R) (ORNL-TM-3212)
removal from reactor containment systems, effectiveness of sprays for, (E), 25:10256 (BNWL-1485)
iodomethane--PH_3, radiolysis of vapor-phase, yields of methane and hydrogen from γ, 25:8303
METHANESULFONIC ACID, ETHYL ESTER
effects on Triticum durum, mutagenic, 25:8641
METHANOL
radio emission from, detection in Sagittarius of, (E), 25:9060
radioinduced excitation in presence of luminescing additive, α, β, and uv, 25:8274
radiolysis at 77°K, spatial distribution of radicals from γ, 25:8288
METHIONINE, N-ACETYL-
radiation effects on positron annihilation in, x, 25:8269
8-METHOXYPSORALEN
effects on incidence of mutations in uv-irradiated Aspergillus nidulans, effects of time of treatment on, 25:8702
METHYL RED
reactions of, square wave dissociation field effect apparatus for kinetic studies on, 25:8240
METROLOGY
quantum theory of, 25:9612
MICE
epidermal cell mitotic and labeling indexes in hairless, modified autoradiographic technique for studying diurnal variations in, 25:8589
radiation dosimetry for, monoenergetic neutron, 25:8677 (NYO-2740-7, pp 5-51)
radiation effects on chromosomes of, effects of, on mutations for Rex gene, x, 25:8645
radiation effects on erythropoietic recovery and survival of, effects of erythropoietin on protective effects of drugs against γ, 25:8775
radiation effects on eye development in embryos of, x, 25:8646
radiation effects on hematopoietic colony formation in spleen of, effects of ACTH, cold exposure, and dexamethasone on γ, 25:8767
radiation effects on hematopoietic colony formation in spleen of, effects of dexamethasone on γ, 25:8765
radiation effects on immune reactions and survival of, following transplantation of bone marrow from parental strain, x, 25:8618
radiation effects on immune reactions of, following transplantation of rat bone marrow, x, 25:8619
radiation effects on immune reactions to allogenic leukemia transplants in, whole-body x, 25:8622
radiation effects on liver and lungs of, effects of simultaneous eruption of Ascaris suum larvae on x, 25:8781
radiation effects on lungs of, following exposure of thorax, x, 25:8778
radiation effects on lymphoid tissue in, RBE for whole-body electron, 25:8780
radiation effects on mitosis in kidney cells of, following radon-220 inhalation, 25:8763
radiation effects on Peromyscus polionotus, under field conditions, acute sublethal γ, 25:8760
radiation effects on survival of epithelium cells in intestine of, effects of cell cycle stage on whole-body γ, 25:8785
radiation effects on survival of, effects of pre- and post-exposure splenectomy on protective effects of bone marrow transplants against x, 25:8706
radiation effects on thymus function in, effects of strain on recovery from whole-body x, 25:8776
radiation effects on transfer of antibody-forming clone in, 25:8769
radiation effects on, effects of, on mechanism of wound healing, partial-body x, 25:8772
radiation effects on, effects of, on mitosis in kidney cells, whole-body, 25:8763
radiation effects on, protective effects of sodium fluoroacetate against x, 25:8700
radioinduced bone malformations in fetuses of, synergistic effects of synkavit on x, 25:8703
radioinduced inactivation of Scrapie virus in, effects of wave length on monochromatic uv, 25:8805
radioinduced lens opacification in, RBE for monoenergetic neutron, 25:8756 (NYO-2740-7, pp 154-217)
radiosensitivity of leukemic, effects of triacetoneamine-N-oxyl on x, 25:8701
radiosensitivity of, effects of temperature on γ, 25:8768
MICHIGAN, LAKE
mass balance in, effects of thermal effluents on, 25:10340 (ANL-ES-1)
MICROTOMES
performance for preparation of sodium metallograhic specimens, 25:8845 (AERE-R-5483)
MICROWAVE OSCILLATORS
performance of solid-state, 25:10373 (SC-DR-70-698)
MICROWAVES
effects on animals and plants, pathological, 25:8790
effects on content of albumins and globulins in blood serum and brain tissues of rabbits, effects of dose on, 25:8784
effects on eyes, protection against pathological, 25:8793
propagation in positive column plasma, with finite-amplitude helical instability, (E), 25:9530
scattering by 1f oscillations in theta-pinch plasma, (E/T), 25:9520
scattering on helium afterglow plasma, electron density measurement from, 25:9417
use for cooking by man, hazards evaluation, 25:8790
use for diagnostics of cold collisionless plasma, 25:9408 (COO-1789-1)
use for diagnostics of high-current discharges with skin effect, 25:9424
use for diagnostics of striations in hydrogen discharges, 25:9425
use for in-core temperature and neutron flux measurements, 25:10326 (RT/FI-(70)7)
use for plasma diagnostics in high-current discharges, 25:9428
MILITARY PERSONNEL
radiation hazards to eyes of, standards for protection against laser, 25:8694
MILK
iodine-131 content of, following accidental release at La Hague UP 2 plant, 25:8657 (CEA-R-4008)
iodine-131 content of, in USA during 1963 to 1968, sources of, 25:8629
radioisotope content of, in New Zealand during 1968, cesium-137 and strontium-90, 25:8675(R) (NP-18529)
strontium-90 content of, from Ispra environs during March to July 1970, 25:8370 (HASL-237, pp III.18-23)
strontium-90 content of, in EURATOM countries during 1968, 25:8624 (EUR-4609)
strontium-90 content of, per gram calcium in New York during 1954 to 1970, monthly and annual averages of fallout, 25:8670(R) (HASL-237(App.))
volume in mammary glands of goats, determination using carbon-14-labeled polyethylene glycol and cerium-141, 25:8587
MILKY WAY
cosmic-ray propagation in, (T), 25:9256
hydrogen distribution in Carina, neutral, (E), 25:9140
magnetic field of, generation of, (T), 25:9135
magnetic field of, generation of, (T), 25:9136
magnetic fields in, origin of, (T), 25:9129
photometry of 45 H-α emission objects in southern, (E), 25:9032
photometry of halo of, in selected area 57, (E), 25:9144
rotation of, effects of accuracy of stellar distances in estimates of, (T), 25:9150
rotation of, from H II regions, (E), 25:9145
rotation of, use of Population-I Cepheids for determining, (E/T), 25:9151
star distribution in southern, OB, (E), 25:9026
structure of, spiral, (E), 25:9146
structure of, spiral, (T), 25:9142
x-ray background in, relation to discrete sources, (E/T), 25:9079
MILLSTONE POINT POWER REACTOR, UNIT 1
operations incident of December 23, 1970, condenser vacuum decrease due to cracked seal weld, 25:10121 (DOCKET-50245-49)
operations incident of December 23, 1970, select control rod drive malfunction, 25:10121 (DOCKET-50245-49)
operations incident of December 31, 1970, failure of D.C. emergency lube oil pump during test start of gas turbine generator, 25:10122 (DOCKET-50245-50)
MINERAL DEPOSITS
prospecting for, development of airborne remote-sensing methods for, 25:8378
MINERALS
determination in rocks from Project Gasbuggy holes GB-1 and GB-3, petrographic, 25:8385 (PNE-G-69)
MINING
hazards of uranium, to personnel, relation of inhalation of diesel engine exhausts, radon decay products, and uranium ore dusts to, 25:8623 (BNWL-SA-3419)
MITOSIS
cell count during, modified autoradiographic technique for diurnal variation in, 25:8589
radiation effects on rate of, in cultured chicken fibroblasts, effects of dose on x, 25:8752
radiation effects on rate of, in cultured chicken fibroblasts, relation to survival, x, 25:8751
radiation effects on, in cultured human cells, x, 25:8743
radioinduced delay of, in Oedogonium cardiacum, effects of dose rate on, 25:8644
MOESSBAUER EFFECT
Bragg scattering at high reflection orders in tin-119 dioxide, 25:9596
source for, preparation and properties of cobalt-57--copper, 25:9595
MOISTURE GAGES
design of neutron radiometric, for soils, 25:8570

MOLECULES
atom reactions with diatomic, classical treatment of classically forbidden transitions in, 25:9227
atom reactions with diatomic, dependence of vibrational transition probabilities on orientation angle in, (T), 25:9226
atom reactions with diatomic, effects of mass and well depth on quantum vibrational transition probabilities in, (T), 25:9230
atom reactions with diatomic, semiclassical treatment of transition probabilities for dissociation in, 25:9197
atom reactions with diatomic, vibrational excitation in, (T), 25:9228
atom reactions with heavy polar, at thermal energies, effects of asymmetric mass distribution on, (T), 25:9232
electron reactions with diatomic, model for vibrational excitation in, 25:9240
energy levels of, definition of quasi-stationary states, 25:9209
interactions with electromagnetic field, in canonical formulation of noncovariant quantum electrodynamics, (T), 25:9842
ion reactions with, ion-cyclotron-resonance method for measurement of collision and charge-exchange rates in, 25:9233
radiation effects on aggregation of, of lysozyme, effects of ionic strength and pH on γ, 25:8604 (COO-690-41)
radio emission from interstellar, (T), 25:9071
wave functions for, construction using combination of gaussian and Slater-type orbitals, 25:9243
wave functions for, convergence properties of single-center, (T), 25:9251
MOLLUSCA
Physa heterostropha, radiation effects on egg hatching and life spans of laboratory and natural populations of, effects of dose rate and temperature on γ, 25:8750 (ORNL-4612)
Tapes decussatus, mercury-203 content of muscles and visceral organs of, following uptake from food and seawater, 25:8625 (NP-18429)
MOLTEN SALT REACTOR EXPERIMENT
core for, fluid dynamic and heat transfer characteristics of, (E), 25:10196 (ORNL-TM-3229)
dynamic characteristics of uranium-233 fueled and uranium-235 fueled, (T), 25:10183
fuel salt for, measurement of void fraction in, (E/T), 25:10177
fuel salt reprocessing for, use of low-pressure distillation in, (E), 25:10210 (ORNL-4434)
fueling of, preparation and handling of salt mixtures for, 25:10211 (ORNL-4616)
neutron flux-to-pressure frequency response for, (E/T), 25:10177
neutron flux-to-pressure frequency response for, (T), 25:10178
reactivity to power frequency response of, techniques for determination of, (E/T), 25:10182
MOLYBDENUM
analysis for oxygen by inert gas fusion method, evaluation of bath materials for, 25:8194 (AECL-3743)
compatibility of fuel capsules of, with curium-244 oxide at 1250 to 1850°C, 25:8427(R) (ORNL-4639)
crystal structure to 180°K, 25:8876
determination by anodic stripping at constant current using hanging mercury drop electrode, 25:8206
determination in air particulates by spark source mass spectrometry, 25:8208
determination in airborne particulates by neutron activation, 25:8231
determination in high alloy steel using mercaptosuccinic acid, spectrophotometric, 25:8210
determination in titanium and titanium dioxide by neutron activation, 25:8233
determination of hexavalent, using Bromopyrogallol Red, colorimetric, 25:8212
effects on properties of molybdenum--nickel--titanium carbide alloy, 25:8928(T) (UCRL-Trans-10505)
fatigue behavior of arc-cast polycrystalline, 25:8861 (AD-709580)
mechanical properties at 20 to 239°K, design of device for determining low-temperature, 25:8881
oxidation at 380 to 755°C, effects of carbon monoxide on kinetics of, 25:8841
properties for use in curium-244 oxide cermets, 25:8427(R) (ORNL-4639)
quasi-particle creation in superconducting, ultrasonic attenuation by, (E/T), 25:9368
radiation effects on mechanical properties of, fast neutron, 25:8952 (ORNL-4600, pp 81-125)
reduction of, voltammetric studies of, 25:8211
thermal expansion coefficients at 30 to 170°K, 25:8876
MOLYBDENUM ALLOYS AND SYSTEMS
Cr--Mo--Ni--stainless steel, analysis for molybdenum using mercaptosuccinic acid, spectrophotometric, 25:8210
Al--Mo--Ti-base--V, embrittlement by cadmium, effects of stress, temperature, and time on, 25:8879
Co--Mo--steel--W, analysis for molybdenum using mercaptosuccinic acid, spectrophotometric, 25:8210
Cr--Mo--steel, creep rupture of low-carbon ferritic, at 900 to 1100°F and 9 to 26 ksi, 25:8895 (BMI-1891, Sect.B)
Cr--Mo--steel, fatigue of pipes of, cracking in low-cycle, 25:8866 (GEAP-10205)
Cr--Mo--steel, preparation for weldability testing, 25:8869 (ORNL-4600, pp 147-52)
Cr--Mo--steel--V--W, analysis for molybdenum using mercaptosuccinic acid, spectrophotometric, 25:8210
Fe--Mo, analysis for molybdenum using mercaptosuccinic acid, spectrophotometric, 25:8210
Hf--Mo--Pt-base, properties for use as radioisotope fuel capsule material, 25:8850 (ORNL-4600, pp 181-5)
Mo--Ni--TiC-base, properties for use as cutting tools, effects of molybdenum content on, 25:8928(T) (UCRL-Trans-10505)
Mo--Pt-base, tensile properties at 25 to 1093°C, 25:8427(R) (ORNL-4639)
Mo--Pt-base--Ti, tensile properties at 25 to 1290°C, 25:8427(R) (ORNL-4639)
Mo--Re, radiation effects on mechanical properties of, fast neutron, 25:8952 (ORNL-4600, pp 81-125)
Mo--Re--W-base, creep of arc-melted, at 1200 to 2200°C, effects of stress on, 25:8852 (ORNL-4600, pp 198-209)
Mo--V-base, corrosion by sodium at 600°C, effects of oxygen on, 25:8836 (ORNL-4600, pp 157-66)
Mo-base--Ti, radiation effects on mechanical properties of, fast neutron, 25:8952 (ORNL-4600, pp 81-125)
MOLYBDENUM FLUORIDES
MoF_6--UF_6, phase equilibrium studies at 2,600 torr, 25:8264
MOLYBDENUM ISOTOPES Mo-91
beta and electron-capture decay of, gamma spectra, log-ft values, and branching ratios from, (E), 25:10057
energy-level transitions from molybdenum-92 (γ,n) reactions at 20 to 22 MeV, gamma spectra from, (E), 25:10057
MOLYBDENUM ISOTOPES Mo-92
helium-3 reactions (He-3,d) at 35 MeV, angular distributions for, (E), 25:9978(R) (ORO-3398-26)
MOLYBDENUM ISOTOPES Mo-95
proton reactions (p,pn) at 17 MeV, mechanism of, (E), 25:10005
MOLYBDENUM ISOTOPES Mo-98
performance of activation detectors of, for neutron spectra measurements at 1 eV to 10 keV, 25:8481 (KFK-1233)
MOLYBDENUM ISOTOPES Mo-99
yields from alpha and helium-3 fission of bismuth-209, thorium-232, and uranium-238 at 20 to 34 MeV, (E), 25:10056
MOLYBDENUM NITRIDES
analysis for nitrogen, evaluation of chemical methods for, 25:8195 (AERE-R-6491)
MONKEYS
radiation effects on immune reactions of, prior to bone marrow grafting, 25:8617
radiosensitivity of developing retinal tissues in fetuses of, effects of gestational age on x, 25:8757 (NYO-2740-7, pp 218-56)
MOON
electromagnetic sounding using the solar wind, (T), 25:9159
MUSCLES
blood circulation in resting, effects of glucose and insulin on, xenon-133 tracer study of, 25:8586
radioisotope content of, of rats following inhalation and intramuscular injection of americium-241, curium-242, plutonium-238, and plutonium-239, 25:8590 (CEA-CONF-1658)
MUTAGENS
effects on plants, use of, for mutation breeding, 25:8635 (STI/DOC-10/119)
MUTATIONS
induced in cultured Chinese hamster cells by 5-bromodeoxyuridine and N-nitrosomethylurea, factors affecting expression of, 25:8638
induced in cultured Chinese hamster cells, factors affecting, 25:8638
induced in durum wheat by diethyl sulfate and ethylmethanesulfonate, comparison of frequency of, 25:8641
radioinduced, for crop improvement, 25:8818
radioinduced, in Arabidopsis thaliana, RBE for heavy ion, 25:8800
radioinduced, in Aspergillus nidulans, biochemical and genetic analysis of uv, 25:8640
radioinduced, in Aspergillus nidulans, effects of pre-exposure treatment with 8-methoxypsoralen on uv, 25:8702
radioinduced, in barley seeds for culm length and early ripening, γ, 25:8656
radioinduced, in cultured Chinese hamster cells, factors affecting expression of x, 25:8638
radioinduced, in durum wheat for chlorophyll deficiency and morphological change, comparison of frequency of fast neutron, thermal neutron, and x, 25:8641
radioinduced, in Escherichia coli for auxotrophy, combined effects of formaldehyde or nitrosomethylurethan on spectrum of uv, 25:8642
radioinduced, in Escherichia coli, classification and properties of uv, 25:8633 (NP-18483)
radioinduced, in Escherichia coli, iodine-125 γ, 25:8654

XUM

radioinduced, in Escherichia coli, repair replication of uv, 25:8636 (SU-326-P-7-X-22)
radioinduced, in phage kappa, for clone formation, uv, 25:8653
radioinduced, in plants, use of, for crop improvement, 25:8635 (STI/DOC-10/119)
radioinduced, in pollen of barley, strontium-90, 25:8648
radioinduced, in Schizophyllum commune, interactions with wild B/sub β/ alleles of x, 25:8643
radioinduced, in wheat seeds for chlorophyll and spike variation, x, 25:8655
radioinduced, in yeast, protective effects of caffeine against uv, 25:8637
radiosensitive, effects on recombination in partially diploid derivatives of Escherichia coli, 25:8634(R) (ORO-4024-1)
MUTSU REACTOR
shielding for, γ-ray leakage through joints between walls of, (E/T), 25:10296(T) (NSJ-tr-157)
MYELIN
radiation effects on formation of, in brain of developing rats, x, 25:8758(R) (UCB-34-P-82-10)
MZFR (SIEMENS REACTOR)
experimental facilities of, operation limits and emergency cooling requirements for heavy water cooled mixed carbide fuel irradiation loop, 25:10243 (NP-18535)

N

NAGASAKI
atomic bombing of, bibliography on medical status of survivors and offspring during 1969, 25:8741 (ABCC-TR-0-69)
NAILS
analysis of human, for copper, gold, manganese, sodium, and zinc by neutron activation and γ spectrometry, 25:8229
1,4-NAPHTHALENEDIOL, 2-METHYL-
bis(dihydrogenphosphate) tetrasodium salt, effects on incidence of bone malformations in fetuses of x-irradiated mice, 25:8703
NAPHTHOL
radioinduced luminescence of solutions of, in butanol and methanol, α, β, and uv, 25:8274
NATURAL GAS
production stimulation by Project Gasbuggy, numerical model for simulating transient gas flow in underground reservoir following, 25:8387 (UCRL-71868)
production stimulation using underground nuclear explosions, safety and technology of, 25:8388
reactions in Gasbuggy chimney, 25:8384 (PNE-G-68)
NEBULAE
brightness of Southern Coalsack, surface, (E), 25:9131
cooling rates for gaseous, (T), 25:8974
electron temperatures in Orion, (E), 25:9028
nitrogen abundance in Orion, (E), 25:9028
radio emission from ninety small galactic, (E), 25:9068
spectra of gaseous, emission, (T), 25:8974
spectra of Orion, [S II] doublet in, (E), 25:9020
spectra of Orion, Hα/[N II] ratio in, (E), 25:9028
spectra of Orion, neutral helium in, (E), 25:9046
NEMATODA
Ascaris suum, effects on liver and lungs of x-irradiated mice, 25:8781
NEODYMIUM
abundance in meteorites and lunar samples, (E), 25:8965
neodymium-145 Moessbauer spectrum in, 25:9594
NEODYMIUM ALLOYS AND SYSTEMS
magnetic hyperfine fields at neodymium nuclei in magnetically ordered, 25:9594
Al--Nd, neodymium-145 Moessbauer spectrum in $NdAl_2$, 25:9594
Al--Nd--Ni, magnetic properties and phase diagram of NdNi/sub x/Al/sub 2-x/, 25:9576
Co--Nd, neodymium-145 Moessbauer spectrum in $NdCo_2$, 25:9594
Nd--Sb, neodymium-145 Moessbauer spectrum in NdSb, 25:9594
NEODYMIUM BORIDES
neodymium-145 Moessbauer spectrum in, 25:9594
NEODYMIUM CHLORIDES
neodymium-145 Moessbauer spectrum in, 25:9594
NEODYMIUM FLUORIDES
neodymium-145 Moessbauer spectrum in, 25:9594
removal from fused salts by low pressure distillation, (E), 25:10210 (ORNL-4434)
BeF_2--LiF--NdF_3--ZrF_4, distillation of molten, removal of neodymium fluoride by low-pressure, (E), 25:10210 (ORNL-4434)
NEODYMIUM HAFNATES
formation of, kinetics of, 25:8935
NEODYMIUM IODIDES
neodymium-145 Moessbauer spectrum in, 25:9594
NEODYMIUM ISOTOPES Nd-142
proton reactions (p,d) with, angular distributions for, (E), 25:9978(R) (ORO-3398-26)
NEODYMIUM ISOTOPES Nd-145
nuclear properties of 72.5-keV level of, from Moessbauer effect in yttrium chloride and neodymium compounds, 25:9594
NEODYMIUM OXIDES
neodymium-145 Moessbauer spectrum in, 25:9594
NEON
abundance determination in 15 chondrites, (E), 25:8968
abundance in HD 34452, (E), 25:9056
abundance in O-type stars, (E), 25:9042
carbon-ion (C^{6+}) reactions below 40 keV with, total cross sections for single-electron capture in, (E), 25:9215
electron elastic scattering at low energies by, effective cross sections for, (T), 25:9237
helium-atom reactions at 1.0 keV to 6.4 MeV with, Born cross sections for excitation in, (T), 25:9204
helium-atom reactions at 1.60 to 400 keV with, scaled cross sections for excitation in, (T), 25:9204
isotopic composition of, in 15 chondrites, (E), 25:8968
meson (K^-) reactions at rest in bubble chamber, conversion electron pairs from nuclei excitation in, (E), 25:10012
nitrogen-ion (N_2^+) reactions in eV range with, mechanisms and cross sections for light emission in, (E), 25:9213
plasma of, electron energy distribution functions and transport coefficients for, (T), 25:9464
plasma of, electron velocity distribution function for homogeneous Lorentz, (T), 25:9474
plasma of, electron velocity distribution function for Lorentz, (T), 25:9473
plasma of, excitation temperature functions of spectra lines of, 25:9172
plasma of, moving striations in longitudinal magnetic fields, (E), 25:9453
thermodynamic properties of solid, as function of temperature, models for anharmonic, 25:8262 (UCRL-50903)
wave functions for, based on combination of gaussian and Slater-type orbitals, 25:9243
NEON IONS
effects on Arabidopsis thaliana seeds, RBE for mutagenic and tumorigenic, 25:8800
implantation into cadmium sulfide, acceptor luminescence induced by, 25:9561
reactions with nitrogen molecules at 1 to 5 MeV, fluorescence efficiencies for excitation in, (E), 25:9234
scattering by neon ions at 77 and 300°K, intensity of, 25:8424(R) (MLM-1768)
NEON ISOTOPES Ne-18
energy levels from neon-20 (p,t) reactions, (E), 25:10006
energy levels from oxygen-16 (He-3,n) reactions, spins and parities of, (E), 25:9981
NEON ISOTOPES Ne-20
concentration by thermal diffusion, rates for, 25:8424(R) (MLM-1768)
mass hexadecapole moments of, Hartree--Fock--Bogolyubov calculations of, (T), 25:10008
proton reactions (p,t) at 50 MeV, differential cross sections for, (E), 25:10006
reactions (Ne-20,O-16) with carbon-12 at 72 to 100 MeV, energy spectra and angular distributions for, (E), 25:9986
NEON ISOTOPES Ne-21
concentration by thermal diffusion, rates for, 25:8424(R) (MLM-1768)
NEON ISOTOPES Ne-22
energy levels from oxygen-18 alpha resonances, spin-parity assignments for, (E), 25:10002
mass hexadecapole moments of, Hartree--Fock--Bogolyubov calculations of, (T), 25:10008
proton elastic scattering by, fine-structure analysis of isobaric analog resonances in, (T), 25:10073
NEON ISOTOPES Ne-24
mass hexadecapole moments of, Hartree--Fock--Bogolyubov calculations of, (T), 25:10008
NEON SYSTEMS
H--Ne, Stark broadening of resonance lines of neutral, 25:9171
He--Ne, electron energy distribution functions and transport coefficients for, (T), 25:9464
NEPTUNIUM
complexes with pyridineacetic acids and alpha-aminopolyacetic acids, preparation and stability of, 25:8237 (KFK-1210)
separation from irradiated LMFBR fuels, solvent extraction processes for, 25:8316 (BNWL-CC-1939)
NEPTUNIUM ISOTOPES Np-237
alpha decay of, coincidence semiconductor detector system for measurement of x-ray-to-alpha ratio in, 25:8465 (BNWL-SA-1514)
determination in fuel reprocessing solutions, 25:8324(T) (ORNL-tr-2406)
neutron absorption resonance integrals at .025 eV, (E), 25:10019 (BNL-50242)
NERVOUS SYSTEM
radiation effects on conditioned reflex response of, in dogs, chronic low-dose γ, 25:8755(T) (JPRS-51660)
radiation effects on function of vestibulocochlear analyser of, in man following therapy of cancer, 25:8792
NETHERLANDS
radioisotope content of human diet in, during 1968,

cesium-137, and strontium-90, 25:8624 (EUR-4509)
NEUTRINOS
electric charge of, dependence on mass for upper limit for, (T), 25:9737
emission from neutron-rich matter in supernovae, (T), 25:8998
emission from stars undergoing gravitational collapse, (T), 25:8997
interactions in bubble chambers, determination of neutral particles in μ decay from, (E), 25:9748
magnetic and monopole moments of massless, upper limits for, (T), 25:9737
production of ν--anti ν pairs in solar interior, electromagnetic, (T), 25:9737
NEUTRINOS (ANTI ν)
detection of, use of helium-3 counters for, 25:8550
production of ν--anti ν pairs in solar interior, electromagnetic, (T), 25:9737
NEUTRINOS (ν/sub e/)
interactions ν + e → e + ν, S-matrix element for, 25:9740
NEUTRINOS (anti ν/sub e/)
energy spectra from uranium-235 fission products, (T), 25:9746
interactions anti ν + e → anti ν + e, cross sections for, (T), 25:9746
NEUTRON BEAMS
energy spread of Gaussian-distributed, in scattering by thin targets, (T), 25:10086
polarization from scattering by thick layers of carbon-12, helium-4, and oxygen-16, (T), 25:9949
scattering by thick layers of carbon-12, helium-4, and oxygen-16, beam polarization and angular distribution from, (T), 25:9949
NEUTRON CAPTURE THERAPY
dosimetry for, fast, 25:8677 (NYO-2740-7, pp 5-51)
NEUTRON CROSS SECTIONS
information on, POPOP 4 data library for, 25:9942 (CTC-42)
measurement at Rensselaer Polytechnic Institute during April through June 1970, 25:9945(R) (RPI-328-190)
supplement to CINDA 69, 25:9946 (TID-25165(Suppl.2))
NEUTRON SOURCES
calibration of 10 Ci Pu-Be, 25:8677 (NYO-2740-7, pp 5-51)
characteristics of tritium (d,n), 25:9955
description of 14-MeV, for uranium analysis in scrap recovery plant, 25:8447(R) (BHO-65-1)
design of intense, using electron linear accelerator with fast reactor modules, for time-of-flight beam experiments, 25:9954
design of tritium (d,n), for calibration of detectors, 25:9940 (BARC-499)
intensity of tritium (d,n), differential, 25:9957
shielding materials for californium-252, for neutron capture gamma spectroscopy, 25:8537
NEUTRON SPECTROMETERS
design of total-reflecting cold, for reactor beam holes, 25:8536
performance of rotating-crystal time-of-flight thermal, with phased chopper, 25:8533
pulse discriminator for liquid scintillation time-of-flight, design and performance of, 25:8507
NEUTRON STARS
angular momentum loss in, due to gravitational radiation, (T), 25:9063
formation in supernovae, (T), 25:8998
models of static configurations, (T), 25:9008
NEUTRONS
absorption by plutonium-239, uranium-235, and uranium-238 in Doppler resonance regions, shielding factors for, (T), 25:10038
absorption in Doppler resonance regions, accuracy of analytical treatments for resonance, 25:10038
attenuation in shielding materials, (E/T), 25:9948
capture by chlorine-35, γ spectra from, (E), 25:10009
capture by dysprosium-163, correlations between partial radiative widths and reduced neutron widths in, (E), 25:10047
capture by dysprosium-163, gamma spectra from, (E), 25:10047
decay n → p + e + ν, limiting relations for correlation averages for, (T), 25:9734 (ITF-70-53)
detection and discrimination in liquid scintillation detectors, 25:8506
detection at thermal energies to 10 MeV, sensitivity of spherical polyethylene-moderated scintillation detectors for, 25:8522
detection of pulse shape discriminator system with stilbene scintillation detector for gamma discrimination for, 25:8525
detection of, energy response of air-filled parallel plate cavity for, 25:8677 (NYO-2740-7, pp 5-51)
detection of, position-sensitive array of boron trifluoride proportional detectors for, 25:8473 (JUL-CONF-4, pp 30-47)
diffusion in two-dimensional media, computer program for calculating, (T), 25:9947 (TRG-Report-1990)
distribution in graphite moderated water cooled coupled core reactors, cross spectral density sink frequency for, (E/T), 25:10278
distribution in graphite moderated water cooled coupled core reactors, cross spectral density sink frequency for, (T), 25:10275
distribution in graphite moderated water cooled coupled core reactors, cross spectral density sink frequency for, (E/T), 25:10279
dosimetry applications, instrumentation, and techniques, research on, 25:8677 (NYO-2740-7, pp 5-51)
dosimetry for Drosophila, mice, and Tradescantia, monoenergetic, 25:8677 (NYO-2740-7, pp 5-51)
dosimetry of californium-252, design and performance of ionization chambers for, 25:8677 (NYO-2740-7, pp 5-51)
effects on anthracene crystals, 25:8289
effects on cell number and somatic aberrations in Tradescantia stamen hairs, RBE for low energy and 0.43 MeV, 25:8756 (NYO-2740-7, pp 154-217)
effects on chemical and mechanical properties of Czechoslovakia reactor pressure vessel steels, 25:8899 (ZJE-89)
effects on creep rupture of Hastelloy N, relations with refractory metal additions, 25:8870 (ORNL-4600, pp 271-81)
effects on cultured mammalian and plant cells, comparison of OER and RBE for californium-252 mixed γ and, with radium, 25:8757 (NYO-2740-7, pp 218-56)
effects on dielectric--semiconductor structures, 25:9566
effects on Drosophila melanogaster, genetic, 25:8756 (NYO-2740-7, pp 154-217)
effects on embrittlement of bcc and fcc metals, 25:8898 (SRARI-P-85)
effects on embrittlement of Type 22K steel, (E), 25:8903
effects on hematopoiesis in dogs, in comparison with x and γ rays, 25:8774
effects on lattice parameter of lithium fluoride single crystals, annealing of, 25:9565
effects on lens opacification in mice, RBE for monoenergetic, 25:8756 (NYO-2740-7, pp 154-217)
effects on mechanical properties of pressure vessel steel, 25:8900 (ZJE-90)
effects on mechanical properties of uranium oxide (UO_2) and Zircaloy 2, 25:10125(R) (NP-18573)
effects on potassium chloride, yields of recoil sulfur-35 from, 25:8312
effects on silicon carbide single crystals, ESR of centers induced in, 25:9545
effects on solids, ENDF/B calculations of primary-recoil spectra and damage cross sections for, 25:9573
effects on survival of synchronized cultures of Chinese hamster cells, comparison of effects of aeration and hypoxia on californium-252 mixed γ and, 25:8757 (NYO-2740-7, pp 218-56)
effects on swine, pathological, 25:8773
effects on various elements of the eye, injurious, 25:8609
effects on welds in steel pressure vessels, 25:8901 (ZJE-91)
emission from fission of plutonium-239, -240, -241, uranium-233, -235, 25:10025 (INDC(NDS)-19/N)
emission from pulsars, (T), 25:9253 (MPI-PAE/EXTRATERR-47)
emission from Sun, (E/T), 25:9098 (MPI-PAE/EXTRATERR-48)
flux distribution in convergatron type research reactor, (T), 25:10285
flux distribution in power reactors, hybrid computer solution of space--time, 25:10303 (CEA-CONF-1684)
flux distributions in reactors, generalized multiple collision probabilities for calculation of, (T), 25:10313
flux measurements in reactor cores, microwave technique for, 25:10326 (RT/FI-(70)7)
flux-to-pressure frequency response for molten salt reactors, (E/T), 25:10177
flux-to-pressure frequency response for molten salt reactors, (T), 25:10178
interactions anti p + n → anti p + n at 3.5 GeV/c in bubble chamber, differential and total cross sections for, (E), 25:9649
interactions anti p + n → π^- + π^- + π^+, dual formula for hole structure in Dalitz plot for, 25:9770
interactions anti p + n, theory of linearly rising trajectories for annihilation, 25:9769
interactions γ + n → n + π^0, low-energy theorems for, 25:9721
interactions γ + n → p + π^-, low-energy theorems for, 25:9721
interactions γ + n → π^- + p in Veneziano model, cross sections for, 25:9717
interactions γ + n, fits to differential cross sections for π production in, 25:9727
interactions K^- + n → K^- + n at 1860 to 2150 MeV, elasticity of Σ(2030) from partial-wave analyses of, (E), 25:9681
interactions K^- + n → K^- + π^- + p at 12.6 GeV/c in bubble chamber, $p\pi^-$(1400) enhancement, cross section for K^- + π^- → K^- + π^- interactions, and cross sections for, (E), 25:9658 (TID-25611)
interactions K^- + n → Λ^0 + A_2^- at 4.48 GeV/c, spin and parity of A_2 from production and decay in, (E), 25:9672
interactions K^- + n → Σ^0 + A_2^- at 4.48 GeV/c, spin and parity of A_2 from production and decay in, (E), 25:9672

XUM

interactions n + d at 700 to 2900 MeV/c, direct measurement of total cross sections for, (E), 25:9648
interactions n + n, comprehensive analysis of p + p interactions below 30 MeV for scattering length for, (T), 25:9814
interactions n + p at 700 to 2900 MeV/c, direct measurement of total cross sections for, (E), 25:9648
mass of, formulas for relation with gravitational constant for, (T), 25:9878
monitoring of, polyethylene-moderated boron trifluoride proportional detector system using self-auditing circuits for, 25:8501
propagation in cylinders and spheres, computer program using Monte-Carlo method for calculating, (T), 25:9941 (CEA-N-1361)
propagation in media with isotropic scattering, transverse, (T), 25:9961
propagation through large thickness of iron, transport codes for, (E), 25:9536 (CEA-CONF-1669)
reactions for secondary γ radiation yield, POPOP 4 data library for, 25:9942 (CTC-42)
reactions with holmium-165 at 0.005 to 1.7 keV, total cross sections, transmission curves, strength functions, and level parameters from, (E), 25:10022 (CEA-N-1338)
reactions with nuclei, (E/T), 25:9948
reactions with plutonium-240 at less than 1 MeV, cross sections and resonance parameters for, (E), 25:10021 (CEA-N-1273)
resonance capture of, calculation of material dependent correction factor for mean chord length for, (T), 25:10310
scattering by aluminum-27 and bismuth-209, calculations of cross sections for total coherent, (T), 25:9958
scattering from phonons in solid helium, theory of inelastic coherent, (T), 25:9964
scattering in plate crystal, coherent double, (T), 25:9963
spectra in nonmultiplying materials, measurement of, 25:9956
spectra measurements at 1 eV to 10 keV, performance of multifoil activation detectors for, 25:8481 (KFK-1233)
thermalization of, scattering moments, infinite-medium Green's functions, and solutions to Boltzmann transport equation in, (T), 25:9962
thermalization studies on, 25:9943(R) (GA-10223)
transmission coefficients for heavy nuclei at 0.05 to 2 MeV, empirical, (E), 25:10020(T) (BNL-tr-379)
transport in slabs, criticality for energy-dependent, (T), 25:9960
transport of, application of Chandrasekhar's method to, 25:9951
transport of, Green's function approach for boundary-value problems in, (T), 25:9952
transport theory for, linear integral equations for H-functions in, 25:9953

NEUTRONS, COLD
scattering by tungsten-186, amplitudes for coherent elastic, (E), 25:10026 (JINR-E3-5371)

NEUTRONS, DELAYED
detection for analysis of uranium scrap, detector array arrangement for, 25:8447(R) (BHO-65-1)
effects on reactivity during fuel density oscillations in reactors, (T), 25:10305 (IAE-1955)
groups from alpha and helium-3 fission of bismuth-209, thorium-232, and uranium-238 and spontaneous fission of californium-252, half-lives of, (E), 25:10056

NEUTRONS, EPITHERMAL
reactions with antimony-121, Doppler effect and resonance parameters for 6.24 eV resonance in, (E), 25:10041
spectra in water moderated lattices, analytical two-group formalism for, (E/T), 25:10320 (AE-405)

NEUTRONS, FAST
attenuation in lead at 3 MeV, time response behavior of, (E/T), 25:9995
detection at 40 to 400 MeV, efficiency of large liquid scintillation detector for, 25:8512
detection of, large-volume mineral oil-based liquid scintillation detector for, 25:8547 (PURC-4159-13)
dose from criticality accidents, performance of activation detectors for measuring, 25:10181
dosimetry for therapy, 25:8677 (NYO-2740-7, pp 5-51)
dosimetry of, low-temperature p--n junction silicon detector for, 25:8565(P)
effects on biological materials, effects of dose on RBE for low energy, 25:8756 (NYO-2740-7, pp 154-217)
effects on ceramic electric insulators, 25:8954 (ORNL-4600, pp 210-15)
effects on creep rupture of Type 304 stainless steel at 600°C, 25:8897 (ORNL-TM-3169)
effects on creep rupture of Type 304 stainless steel, 25:8952 (ORNL-4600, pp 81-125)
effects on defect formation in beryllium-doped copper, 25:8902
effects on dislocation pinning in sodium chloride single crystals, 25:9547
effects on encapsulated plutonium dioxide--uranium dioxide fuels, 25:8909 (ORNL-4600, pp 3-40)
effects on growth of γ-irradiated wheat seedlings, RBE for, 25:8801
effects on magnetoresistance of copper, 25:9571
effects on mechanical properties of molybdenum, 25:8952 (ORNL-4600, pp 81-125)
effects on mechanical properties of molybdenum--rhenium alloy, 25:8952 (ORNL-4600, pp 81-125)
effects on mechanical properties of molybdenum--titanium alloy, 25:8952 (ORNL-4600, pp 81-125)
effects on metals at 77°K, low-temperature microscopic observations of annealing of defects induced in, 25:9542 (CEA-CONF-1681)
effects on modulus of rupture of polycrystalline beryllium oxide, relations with heat treatment, 25:8959
effects on refractory metal carbides, 25:8957 (ORNL-4600, pp 250-1)
effects on silicon, defects induced in, 25:9572
effects on stainless steel fuel element cladding, 25:8896(T) (BNWL-tr-57)
effects on survival of HeLa cells, effects of oxygen content on, during protracted exposure using californium-252 source, 25:8704
effects on tensile properties of Incoloy 800 at 650°C, 25:8952 (ORNL-4600, pp 81-125)
effects on Triticum durum, mutagenic, 25:8641
effects on void structure in Nickel 270, 25:8952 (ORNL-4600, pp 81-125)
energy transfer of, Rossi detector measurement of spectra of linear, 25:8492
flux in central thimble of TRIGA Mark 2 reactor, 25:10277
flux measurements of, response of cadmium-shielded paraffin-moderated indium activation detectors for, 25:8495
flux measurements of, spectra analysis of stilbene scintillation detectors for, 25:8509
production in tritium (d,n) reactions at 220 keV, spectra and absolute energies of, (E), 25:9968 (NP-18488)
pulse decay and distribution in reactor moderators, effects of inelastic scattering on, (T), 25:10315
reactions (n,2n) with deuterium at 14.5 MeV, Monte Carlo simulation of cross sections from, (E/T), 25:9968 (NP-18488)
reactions (n,α) with boron-10 in HeLa cells, RBE for α particles and lithium ion recoil in relation to cell survival following, 25:8745
reactions with liquid nitrogen, secondary gamma production and transport after, (E/T), 25:9950
scattering by beryllium-9 and carbon-12 at 14.6 MeV, angular distributions from elastic, (E), 25:9995
scattering by yttrium-89 at 4.19 to 8.56 MeV, differential cross sections for elastic and inelastic, (E), 25:9999 (ORNL-4552)
spectra in central thimble of TRIGA Mark 2 reactor, 25:10277

NEUTRONS, FISSION
dosimetry in tissue equivalent small animal phantoms in relation to LET, Monte Carlo sampling method for, 25:8685
effects on survival of HeLa cells, effects of boron-10 concentration on RBE for, 25:8745
flux distribution in sodium sphere, from point source at center, 25:9944 (ORNL-TM-3156)

NEUTRONS, THERMAL
absorption resonance integrals for americium-241 and neptunium-237, (E), 25:10019 (BNL-50242)
capture by chlorine-35, gamma spectra from, (E), 25:10000 (PH-2)
capture by germanium-75, osmium-190, and platinum-196, determination of cross sections from second-order reaction products, (E), 25:10040
diffusion in water, calculation models for, (T), 25:10301 (AEEW-R-701)
dose to body surface, role of hydrogen-deuterium exchange and surface dose in, 25:8709 (DP-1229)
dosimetry of, response of lithium fluoride thermoluminescent dosimeters for, 25:8567
effects on encapsulated plutonium dioxide--uranium dioxide fuels, 25:8909 (ORNL-4600, pp 3-40)
effects on retina of rabbits, use of electroretinogram for estimating RBE of toxic, 25:8761
effects on Triticum durum, mutagenic, 25:8641
flux distribution in boiling reactor, effects of steam voids on, (E/T), 25:10175
flux in research reactors, design requirements for high, 25:10268(T) (LA-4399-TR)
flux variations in lattice cell arrays, effects of fuel element bowing on, (T), 25:10319
pulse decay and distribution in water and heavy water, Monte Carlo analysis of time dependent, (T), 25:10314
reaction rates in lattice cell arrays, effects of fuel element bowing on, (T), 25:10319
reactions (n,α) with boron-10 in HeLa cells, RBE for α particles and lithium ion recoil in relation to cell survival following, 25:8745
reactions (n,f) with americium-242, curium-245, plutonium-238, thorium-229, and uranium-235, prompt neutron spectra and yields from, (E), 25:10039

NEVADA TEST SITE
bibliography on geology and hydrology of, 25:8355 (USGS-474-88)
radiation monitoring of ground-level atmosphere at, development and operation of air sampler for, 25:8393 (NVO-410-6)

NEW MEXICO
uranium deposits in Colorado plateau region of, geology and mineralogy of peneconcordant-type, 25:8377
NEW YORK
cesium-137 ratio to strontium-90 in tap water of New York City, during 1965 to 1970, monthly and annual averages of fallout, 25:8670(R) (HASL-237(App.))
strontium 90 content of milk per gram calcium in, during 1954 to 1970, monthly and annual averages of fallout, 25:8670(R) (HASL-237(App.))
strontium 90 content of tap water in New York City, during 1954 to 1970, monthly and annual averages of fallout, 25:8670(R) (HASL-237(App.))
strontium 90 ratio to cesium 137 in tap water in New York City, during 1965 to 1970, monthly and annual averages of fallout, 25:8670(R) (HASL-237(App.))
NEW ZEALAND
radiation protection programs of, during 1969, 25:8675(R) (NP-18529)
NICKEL
alpha inelastic scattering at 25.9 MeV, validity of the Austern--Blair method for, (T), 25:9991
alpha reactions at 30 to 80 MeV, K-shell ionization cross sections for, (E), 25:9978(R) (ORO-3398-26)
corrosion of heat pipes of, by potassium working fluid, (E), 25:8395 (ORNL-TM-3077)
determination in air particulates by spark source mass spectrometry, 25:8208
determination in airborne particulates by neutron activation, 25:8231
determination in titanium and titanium dioxide by neutron activation, 25:8233
diffusion in, lattice-dynamical theory of isotope effects in, 25:9589
effects on colorimetric determination of uranium in fuel reprocessing solutions, 25:8197 (BARC-510)
effects on deuterium exchange in propene, catalytic, 25:8258
plasma of, production by laser irradiation of solid target, (E), 25:9484
radiation effects on void structure in high-purity, fast neutron, 25:8952 (ORNL-4600, pp 81-125)
radiation effects on, ENDF/B primary-recoil spectra in different neutron spectra, 25:9573
radioinduced defects in, low-temperature microscopic observations of annealing of 77°K neutron, 25:9542 (CEA-CONF-1681)
radioinduced dislocation loops in, microscopic study of nucleation in electron, 25:9541 (CEA-CONF-1680)
solvent properties for uranium at 975 to 1075°C, 25:8865 (CEA-R-4066)
spectra of, oscillator strengths in, (E), 25:9117
NICKEL ALLOYS AND SYSTEMS
Al_2O_3--Ni, effects on deuterium exchange in propene, catalytic, 25:8258
Al--Ce--Ni, magnetic properties and phase diagram of CeNi/sub x/Al/sub 2-x/, 25:9576
Al--Cr--Fe-base--Ni, corrosion by water containing trace chloride and oxygen at 200°C, stress, 25:8834(R) (COO-2069-6)
Al--Dy--Ni, magnetic properties and phase diagram of DyNi/sub x/Al/sub 2-x/, 25:9576
Al--Er--Ni, magnetic properties and phase diagram of ErNi/sub x/Al/sub 2-x/, 25:9576
Al--Gd--Ni, magnetic properties and phase diagram of GdNi/sub x/Al/sub 2-x/, 25:9576
Al--Ho--Ni, magnetic properties and phase diagram of HoNi/sub x/Al/sub 2-x/, 25:9576
Al--Lu--Ni, magnetic properties and phase diagram of LuNi/sub x/Al/sub 2-x/, 25:9576
Al--Nd--Ni, magnetic properties and phase diagram of NdNi/sub x/Al/sub 2-x/, 25:9576
Al--Ni--Pr, magnetic properties and phase diagram of PrNi/sub x/Al/sub2-x/, 25:9576
Al--Ni--Tb, magnetic properties and phase diagram of TbNi/sub x/Al/sub 2-x/, 25:9576
Al--Ni--Y, magnetic properties and phase diagram of ErNi/sub x/Al/sub 2-x/, 25:9576
Be--Cr--Fe-base--Ni, corrosion by water containing trace chloride and oxygen at 200°C, stress, 25:8834(R) (COO-2069-6)
Cr--Fe--Ni, corrosion by water containing trace chloride and oxygen at 200°C, stress, 25:8834(R) (COO-2069-6)
Cr--Fe-base--Ni, corrosion by boiling aqueous magnesium chloride, effects of aluminum, beryllium, or carbon additions on stress, 25:8834(R) (COO-2069-6)
Cr--Fe-base--Ni--Pt, corrosion by water containing trace chloride and oxygen at 200°C, stress, 25:8834(R) (COO-2069-6)
Cr--Fe-base--Ni--Si, corrosion by water containing trace chloride and oxygen at 200°C, stress, 25:8834(R) (COO-2069-6)
Cr--Mo--Ni--stainless steel, analysis for molybdenum using mercaptosuccinic acid, spectrophotometric, 25:8210
Cr--Nb--Ni-base, plastic deformation of precipitation-hardened, at 700°C, mechanisms of, 25:8884
Cr--Ni--stainless steel, analysis for molybdenum using mercaptosuccinic acid, spectrophotometric, 25:8210
Dy--Ni--Pr, magnetic properties and phase diagram of Pr/sub x/Dy/sub 1-x/Ni_2, 25:9576
Fe--Ni, corrosion by aqueous sulfuric acid at 25°C, effects of partial currents on, 25:8834(R) (COO-2069-6)
Fe-base--Ni, corrosion by water containing trace chloride and oxygen at 200°C, stress, 25:8834(R) (COO-2069-6)
Ho--Ni--Pr, magnetic properties and phase diagram of Pr/sub x/Ho/sub 1-x/Ni_2, 25:9576
Mo--Ni--TiC-base, properties for use as cutting tools, effects of molybdenum content on, 25:8928(T) (UCRL-Trans-10505)
NICKEL FERROCYANIDES
sorptive properties for cesium from effluents from chemical decanning of reactor fuel elements, 25:8344(P)
NICKEL ISOTOPES
energy levels of, quasi-particle structure of ground state of pairing model of, (T), 25:10051
NICKEL ISOTOPES Ni-58
alpha elastic scattering at 26.5 MeV, angular distribution for, (E), 25:9966(R) (COO-1265-94)
alpha inelastic scattering at 18.0 to 52.0 MeV, validity of the Austern--Blair method for, (T), 25:9991
electron inelastic scattering by, energy spectra and form factors from, (E), 25:10014
NICKEL ISOTOPES Ni-60
alpha inelastic scattering at 11.9 to 18 MeV, validity of the Austern--Blair method for, (T), 25:9991
electron inelastic scattering by, energy spectra and form factors from, (E), 25:10014
proton reactions (p,pn) at 17 MeV, mechanism of, (E), 25:10005
NICKEL ISOTOPES Ni-61
proton reactions (p,pn) at 17 MeV, mechanism of, (E), 25:10005
NICKEL ISOTOPES Ni-64
proton reactions (p,pn) at 17 MeV, mechanism of, (E), 25:10005
NIGER
uranium reserves in, estimates of, 25:8373
NIOBIUM
alpha reactions at 30 to 80 MeV, K-shell ionization cross sections for, (E), 25:9978(R) (ORO-3398-26)
analysis for oxygen by inert gas fusion method, evaluation of bath materials for, 25:8194 (AECL-3743)
compatibility of fuel capsules of, with curium-244 oxide at 1250 to 1850°C, 25:8427(R) (ORNL-4639)
deposition on graphite from vapor--gas mixture, mechanism of, 25:8917
effects on microstructure and postirradiation properties of Hastelloy N, 25:8870 (ORNL-4600, pp 271-81)
Fermi surface of single crystals of, de Haas--van Alphen study of, 25:9575
mechanical properties at 20 to 239°K, design of device for determining low-temperature, 25:8881
radiation effects on, ENDF/B primary-recoil spectra in different neutron spectra, 25:9573
superconducting flux pinning by point defects in electron-irradiated, 25:9379
superconductivity of, effect of physical lattice imperfections on, (E), 25:9376
thermal conductivity of pure superconducting, (E/T), 25:9392
yield behavior of single crystals of, effects of impurities on, 25:8880
NIOBIUM ALLOYS AND SYSTEMS
Al--Co--Nb, phase diagram at 800°C, 25:8890
Al--Fe--Nb, phase diagram at 800°C, 25:8890
C--Nb-base--V--Zr, preparation and properties of corrosion-resistant, for use in nuclear industry, 25:8856(P)
Cr--Nb--Ni-base, plastic deformation of precipitation-hardened, at 700°C, mechanisms of, 25:8884
Nb--U-base, explosive properties of, following immersion in nitric acid, 25:8840 (RFP-1575)
Nb-base--Zr, compatibility of fuel capsules of, with curium-244 oxide at 1250°C, 25:8427(R) (ORNL-4639)
NIOBIUM CARBIDES
evaporation rates at 2800 to 3400°K, 25:8929
NIOBIUM CHLORIDES
reduction by hydrogen for niobium deposition on graphite, mechanism of, 25:8917
NIOBIUM ISOTOPES Nb-91
energy-level transitions from isomeric molybdenum-91 beta and electron-capture decay, (E), 25:10057
NIOBIUM ISOTOPES Nb-95
separation from fission products by solvent extraction using dioctyl phosphate, 25:8214
NIOBIUM NITRIDES
analysis for nitrogen, evaluation of chemical methods for, 25:8195 (AERE-R-6491)
NITRIC ACID
determination of free, in fuel reprocessing solutions, colorimetric, 25:8197 (BARC-510)
reactions with niobium--uranium alloys, explosive, 25:8840 (RFP-1575)
reactions with sugar and uranyl nitrate to form carbon--uranium dioxide mixtures, 25:8923
HF--HNO_3, corrosive effects on Type 304 stainless steel at 140°F, effects of thermally-induced sensitization on, 25:8834(R) (COO-2069-6)
NITRITES
yields from γ radiolysis of aqueous ethanol solutions as

XUM

function of nitrate concentration, 25:8301
yields from radiolysis of aqueous solutions of sodium nitrate, 25:8297
NITROGEN
abundance in iota Ori B, (E), 25:8995
abundance in late G and K dwarfs in the solar neighborhood, (E), 25:8969
abundance in Orion Nebula, (E), 25:9028
alpha-particle range at 0.2 to 2.0 MeV in, relation to energy, (E), 25:9162 (SC-RR-70-788)
determination in metals by vacuum melt extraction, 25:8205
determination in nitrides, evaluation of chemical methods for, 25:8195 (AERE-R-6491)
diffusion of helium in, at 1 atm, coefficient for, 25:8424(R) (MLM-1768)
effects on γ-radiation effects on collagen, 25:8307
effects on kinetics of oxidation of tungsten at 670 to 980°C, 25:8841
ion reactions at 1 to 5 MeV with molecular, fluorescence efficiencies for excitation in positive-, (E), 25:9234
ion reactions in eV range with molecular, mechanisms and cross sections for light emission in, (E), 25:9213
neutron reactions with liquid, secondary gamma production and transport after, (E/T), 25:9950
nitrogen-ion (N_2^+) reactions with molecular, ion-cyclotron-resonance measurements of collision and charge-exchange rates in, 25:9233
photon reactions with ground-state atomic, electron spectra from, (E), 25:9200
proton range at 0.2 to 2.0 MeV in, relation to energy, (E), 25:9162 (SC-RR-70-788)
proton reactions at 4 to 26 keV with molecular, total cross sections for formation of metastable hydrogen atoms by charge exchange in, (E), 25:9193 (ORO-2591-52)
proton reactions at 75 to 350 keV with molecular, total cross sections for formation of fast excited hydrogen atoms by charge exchange in, (E), 25:9192(R) (ORO-2591-51)
reactions with liquid tin--uranium alloys, kinetics and thermodynamics of uranium nitride formation in, 25:8325(R) (SU-326-P-28-X-2)
NITROGEN IONS
scattering by copper at 1.28 and 2.29 MeV, angular distributions and effective atomic numbers for multiple, (E), 25:9163
NITROGEN IONS (N^+)
reactions with nitrogen molecules at 1 to 5 MeV, fluorescence efficiencies for excitation in, (E), 25:9234
NITROGEN IONS (N_2^+)
reactions with gases in eV range, mechanisms and cross sections for light emission in, (E), 25:9213
reactions with nitrogen molecules at 1 to 5 MeV, fluorescence efficiencies for excitation in, (E), 25:9234
reactions with nitrogen molecules, ion-cyclotron-resonance measurements of collision and charge-exchange rates in, 25:9233
NITROGEN ISOTOPES
concentration by gaseous diffusion, effects of cross-flow on efficiency of, 25:8438
NITROGEN ISOTOPES N-13
half-life of, (E), 25:9989
production in cyclotrons by $^{12}C(d,n)^{13}N$ reaction, 25:8711(R) (NYO-3937-2)
NITROGEN ISOTOPES N-14
photon reactions (γ,n) at 100 to 800 MeV, excitation functions for, (E/T), 25:9977 (LUNP-7009)
separation of molecular, from molecular nitrogen ($^{14}N^{15}N$) by thermal diffusion, column coefficients for, 25:8423 (MLM-1439(Rev.))
NITROGEN ISOTOPES N-15
concentration in nitric oxide by low-temperature gas chromatography, 25:8319 (CU-755-7, Sect.4)
concentration in nitrogen oxides by chemical exchange, 25:8334
exchange reactions in oxynitrogen compounds, approximation methods for predictions of, 25:8245
exchange with nitrogen-14 in nitrogen dioxide, 25:8255
proton reactions (p,γ) at 4.1 to 12.8 MeV, gamma spectra from, (E), 25:9979
separation of molecular ($^{14}N^{15}N$), from nitrogen-14 by thermal diffusion, column coefficients for, 25:8423 (MLM-1439(Rev.))
NITROGEN OXIDES
effects on x-radiosensitivity of spores of Bacillus megaterium, 25:8810
NITROGEN OXIDES NO
abundance of positive ionized, at 115 to 430 km in ionosphere, Thomson scatter measurements of, (E), 25:9316
ion reactions in eV range with, mechanisms and cross sections for light emission in, (E), 25:9213
separation of isotopic isomers of, by low-temperature gas chromatography, 25:8319 (CU-755-7, Sect.4)
NO--N_2O_3, nitrogen-15 concentration in, by chemical exchange, 25:8334
NITROGEN OXIDES N_2O
effects on γ-radioinduced oxidation of heptane at low temperatures, kinetics of, 25:8281
ion reactions in eV range with, mechanisms and cross sections for light emission in, (E), 25:9213
NITROGEN OXIDES N_2O_3
NO--N_2O_3, nitrogen-15 concentration in, by chemical exchange, 25:8334
NITROGEN SYSTEMS
Cr--N--Pu, phase studies of, 25:8910 (ORNL-4600, pp 41-56)
N--Th, phase diagram for, 25:8927 (ORNL-4503(Vol.2))
NITROUS ACID
effects on mitotic recombination frequency in mutants of Saccharomyces cerevisiae, effects of delayed plating following exposure on, 25:8797
effects on uv-radiosensitive mutants of Aspergillus nidulans, sensitivity to lethal, 25:8640
NOBELIUM
production using heavy ion reactions with collimation method identification, 25:10030(T) (KFK-tr-329)
NOVAE
light curves for CP Lac, v476 Cyg, and DQ Her, (E/T), 25:9010
light emission from, sources of pre-maximum, (T), 25:9010
NOZZLES
design of mixing, to produce water droplet dispersion in flowing gases, 25:8404(P)
stresses in reactor pressure vessel, effects of attachment configuration on, (E), 25:10244(R) (ORNL-TM-3212)
NUCLEAR EMULSIONS
meson (π) reactions at 60 GeV/c in, helium production in, (E), 25:9660
meson (π) reactions at high energies, mass distribution and decays of hyperfragments produced in, (E), 25:9637
meson (π) reactions with nuclei at 45 to 200 GeV in, 3π and 5π production in, (E), 25:9635 (INP-722)
nucleon reactions with nuclei at 0.1 to 100 TeV in, angular distributions, pionization, and fireballs in, (E), 25:9635 (INP-722)
proton reactions at high energies, mass distributions and decays of hyperfragments produced in, (E), 25:9637
proton reactions with nuclei at 26 GeV in, emission of excess of light mesons in relation to Dalitz pairs in, (E), 25:9642
proton reactions with nuclei at 80 TeV in, aleph baryon production in, (E), 25:9641
NUCLEAR ENGINEERING
research and development in Puerto Rico, 1969, 25:8574(R) (PRNC-140)
NUCLEAR EXPLOSIONS
effects on circular cylindrical shells, acceptable imperfections in impulse loads for simulation testing of, (T), 25:8441 (SC-RR-70-600)
NUCLEAR EXPLOSIONS, ATMOSPHERIC
effects on fallout content of atmosphere and rainwater in Australia, Gibraltar, Hong Kong, and UK, Jan. to July 1970, 25:8364 (AERE-R-6556)
effects on strontium-90 content in stratosphere of Chinese and French, comparison of Streak model-computed and measured data on, 25:8369 (HASL-237, pp I.38-62)
fallout from near ground-level, effects on contamination of surface waters, (T), 25:8354 (HMI-B-86)
NUCLEAR EXPLOSIONS, UNDERGROUND
effects of Jorum Event, on surface fractures and faults in Pahute Mesa area, 25:8356 (USGS-474-92)
NUCLEAR MAGNETIC RESONANCE
uses in well logging, 25:8358(P)
NUCLEAR MATTER
energy gap in, calculation using velocity-dependent nucleon--nucleon potential, (T), 25:10066
ground-state properties of alpha, analysis using variational method, (T), 25:10070
theory of, application to finite nuclei, (T), 25:10080
NUCLEAR MODELS
collective, classical analog of variable-moment-of-inertia formulas for rotational energy levels in even--even nuclei, (T), 25:10084
collective, dipole strengths, γ-absorption cross sections, energy levels, and potential-energy surfaces for giant resonance in, (T), 25:10083
Fermi gas, rearrangement of Goldstone linked-cluster expansion for, (T), 25:10075
shell, construction of E2 effective operators for, 25:10072
shell, energy levels from Morse-type potential well, (T), 25:10085
shell, five-dimensional quasispin toward a complete classification of the isospin characteristics of states in the seniority scheme, 25:10078
shell, short-range correlations in Woods--Saxon potential for, (T), 25:10071
NUCLEAR PHYSICS
book: Intermediate Energy Nuclear Physics, 25:9694
research at Bhaba Atomic Research Center in 1969, 25:10017(R) (BARC-501)
research at Chalk River Nuclear Laboratories April 1 to June 30, 1970, 25:9970(R) (AECL-3668)
research at Minnesota Univ., Sept. 1969 to Aug. 1970, (T), 25:9685(R) (COO-1764-86)
research at Technische Hochschule in 1969, 25:10018(R) (BMBW-FBK-70-10)

XUM

NUCLEAR POWER
development in Europe, review of ENEA activities during 1970, 25:10092(R) (NP-18600)
NUCLEAR POWER PLANTS
book: Optimization of Parameters for Nuclear Power Plants, in Romanian, 25:10130
construction in Taiwan, planning studies for, 25:10089 (CONF-691020-3)
construction of, review of U. S. industry progress and commitments on, 25:10088 (CONF-690967-1)
design parameters for, techniques for optimization of, 25:10130
development in Europe, review of ENEA activities during 1970, 25:10092(R) (NP-18600)
development in Germany, 25:10105
development in India of, 25:10098
development in Pakistan of, 25:10098
development in Spain, predictions for 1970 to 2000, 25:10104
development in U. S., survey of, 25:10102
economics of multipurpose, for provision of thermal energy to urban areas, 25:10094 (ORNL-HUD-14)
economics of U. S., in combination with hydroelectric pumped storage, (T), 25:10109 (BNL-50238)
effluents from U.S., environmental effects of radioactive and thermal, 25:10132 (BNWL-SA-3564)
krypton-85 release by, calculations of skin and whole-body dose to man from, 25:8667 (BNWL-SA-3233)
radioactive effluents from, dosage to man from, 25:10159 (ORNL-NSIC-81)
radioactive effluents from, effects of reactor operations on, 25:10162
radioactive effluents from, effects of short-term releases on annual atmospheric burden from, 25:8371 (SZS-14/70 (pp 1-10))
radioactive effluents from, permissible activity rates for atmosphere exhausted, 25:10161
radioactivity release rates for development of standards for, 25:10161
thermal effluents from U. S., potential environmental impact of, 25:10133 (BNWL-SA-3581)
thermal effluents from, bibliography on effects of, 25:10159 (ORNL-NSIC-81)
thermal effluents from, management of, 25:10090 (CONF-700335-1)
NUCLEAR REACTIONS
analysis of (α,2α), polar and triangular diagrams for, (T), 25:10059 (LYCEN-7039)
nucleon quasi-elastic knockout in high-energy electron-induced, (T), 25:10058 (ITF-70-38)
resonance scattering, exactly soluble three-body model of, 25:9890
resonances in, fine-structure analysis of isobaric analog, 25:10073
scattering by thin targets, energy spread of Gaussian-distributed beam in, (T), 25:10086
theory for, differential equation method for nonrelativistic Feynman amplitude in, 25:10065
NUCLEAR REACTIONS (DIRECT)
realistic form factors for (d,p) and (p,d), in the lead region, (T), 25:10067
theory of one- and two-particle transfer, Green's function derivation of, (T), 25:10082
NUCLEAR STRUCTURE
Coulomb-induced ΔT = 1 admixture in ground states, 25:10061 (NYO-2171-330)
five-dimensional quasispin toward a complete classification of the isospin characteristics of shell-model states in the seniority scheme, 25:10078
vibrations in nuclei, bootstrap theory of, (T), 25:10063 (RLO-1925-46)
NUCLEAR THEORY
applications of t-matrix perturbation theory, 25:10068
Coulomb-induced ΔT = 1 admixture in ground states, 25:10061 (NYO-2171-330)
energy-level width and spacing and transmission coefficients in, relation between, 25:10077
ground-state wave function in, derivation using RPA summing of perturbation theory diagrams, 25:10076
Hartree--Bogoliubov, application to neutron--proton pairing, 25:10060 (NP-18538)
nucleon--nucleon interactions in, ultrahigh-intensity accelerator study of, 25:9810
nucleon--nucleon potential in, calculation of oscillator matrix elements from phase shift data, 25:10074
nucleon--nucleon potentials from microscopic-model analysis of (He-3,t) reactions with light nuclei, strength parameters of effective, 25:9993
NUCLEI
algorithms for problem of two centers in quantum mechanics, (T), 25:9600 (JINR-P4-5040)
alpha reactions (α,2α) with, polar and triangular diagrams for interpretation of, (T), 25:10059 (LYCEN-7039)
beta transitions of mirror, determination of axial vector and vector coupling constants in weak interactions from superallowed, (T), 25:9742
electron capture by, in dense stars, (T), 25:8973
electron reactions with nucleon knockout at high energies with, cross-section dependence on Woods--Saxon potential parameters, (T), 25:10058 (ITF-70-38)
electron scattering by Z = 6 to 92, coefficients for adjustment of complex scattering factors for fast, (T), 25:10055
energy levels from independent-particle model using Morse-type potential well, (T), 25:10085
energy levels of A = 91 to 117, spin--parity assignments for, (E), 25:10031 (ORNL-4627)
energy levels of even--even, classical analog of variable-moment-of-inertia formulas for rotational, (T), 25:10084
energy levels of nonmagic, method for calculation of giant dipole resonance, (T), 25:10069
energy levels of, energy widths of quasistationary, (T), 25:10081
energy-level width and spacing and transmission coefficients in, relation between, 25:10077
mass hexadecapole moments of 2s, 1d shell, Hartree--Fock--Bogolyubov calculations of, (T), 25:10008
meson (K) double charge-exchange reactions with light, cross sections for, (T), 25:9974 (JINR-P2-5286)
meson (π) double charge-exchange reactions with light, cross sections for, (T), 25:9974 (JINR-P2-5286)
meson (π) reactions at 60 GeV/c in emulsions, helium production in, (E), 25:9660
meson (π) reactions with nuclei at 45 to 200 GeV in emulsions, 3π and 5π production in, (E), 25:9635 (INP-722)
meson (π) scattering by, scattering lengths for, (E/T), 25:9791
meson (π⁻) absorption by, short-range nucleon--nucleon correlations from shell-model description of, 25:9582
meson (π⁻) and (π⁺) reactions with, rho'' daughter resonance detection in (T), 25:9786
meson (π⁻) reactions at 2.94 GeV/c, direct production of electron pairs in, (E), 25:9661
neutron reactions with, (E/T), 25:9948
nucleon interactions in 2s--1d shell of, core-polarization corrections to, (T), 25:10079
nucleon reactions at 0.1 to 100 TeV in emulsions, angular distributions, pionization and fireballs in, (E), 25:9635 (INP-722)
proton reactions at 26 GeV in emulsions, emission of excess of light mesons in relation to Dalitz pairs in, (E), 25:9642
proton reactions at 80 TeV in emulsions, aleph baryon production in, (E), 25:9641
transition radiation absorption by, resonance, (T), 25:9703 (JINR-P2-5042)
vibrations in, bootstrap theory of, (T), 25:10063 (RLO-1925-46)
NUCLEIC ACID
plutonium binding with, in bones and liver, 25:8595(T) (LF-tr-41, pp 7-125)
synthesis in chicken embryos following infection by ultraviolet-irradiated vesicular stomatitis virus, 25:8806
NUCLEIC ACID, DEOXYRIBO-
carcinogen damage to, of mammalian cultured cells, repair processes following quinoline, 4-nitro-,1-oxide, 25:8611
duplication of chromosome, in tumor cells, 25:8632 (EUR-4526)
radiation damage to, of Escherichia coli, model for excision repair of, 25:8636 (SU-326-P-7-X-22)
radiation effects of synthesis of, in human lymphocytes, low dose x, 25:8647
radiation effects on formation and dissociation of enzyme substrate-complexes in, of Haemophilus influenza and yeasts, rate constants for, 25:8651
radiation effects on synthesis of, in cultured human cells, x, 25:8743
radiation effects on synthesis of, in eyes β, 25:8609
radiation effects on synthesis of, in human spermatogonia and spermatocytes, x, 25:8789(R) (NYO-4034-2)
radiation effects on template properties of, effects of dose on x, 25:8610
radiation effects on transforming, in Bacillus subtilis, bacteriophage T3, and Escherichia coli, protective effects of acridine orange against cesium-137 γ, 25:8707
radiation effects on, in Haemophilus influenzae, determination of repair rate of uv, 25:8650
radiation effects on, of Escherichia coli, analysis of photoenzymatic repair of, uv, 25:8652
radiation effects on, role of DNA-pyrimidine dimer photomonomerase in photoreactivation of uv, 25:8606(R) (ORO-3630-10)
radioinduced damage to, in cultured mammalian cells, repair processes following carcinogenic uv and x, 25:8611
radioinduced double strand breakage in, of mammalian cells, existence of strand rejoining mechanism for cellular repair following γ, 25:8605(R) (ORO-2832-85)
radioinduced double strand scissions in isolated mammalian, indirect mechanism for γ, 25:8605(R) (ORO-2832-85)
radioinduced lesions in, of Escherichia coli, effects of photoenzymatic repair inhibition by caffeine of uv, 25:8649
radioinduced photoproducts in, of Escherichia coli, uv, 25:8633 (NP-18483)
radioinduced synthesis of, in fern spores, effects of

XUM

dose fractionation on x, 25:8614
synthesis in cell cultures after exposure to carbon-14-labeled nitroquinoline oxide, 25:8746
synthesis of, modified autoradiographic technique for diurnal variation of cell count during, 25:8589
NUCLEIC ACID, RIBO-
effects on, carcinogenic carbon-14-labeled quinoline, 4-nitro-,1-oxide incorporation into HE cultured cells, 25:8746
metabolism in Tetrahymena, regulatory role of histones in, 25:10400 (UCLA-12-788)
NUCLEOGENESIS
helium abundance in big-bang, (T), 25:9156
processes of stellar, (T), 25:8987
NUCLEONS
coupling constant for epsilonN, broken scale invariance for, 25:9762
coupling constant for πN in current-field algebra, 25:9762
coupling constants of, empirical test of tensor meson dominance from, (T), 25:9764 (DESY-70/58)
form factor of, threshold expansion for radius of, 25:9722
form factors of, effect of soft pseudoscalar π exchange on, 25:9782
interactions anti K + N, hyperon production in partially latent quasidynamical, (T), 25:9752
interactions anti N + N → K + anti K + π at rest, four-point Veneziano functions for mass spectra and angular distributions in, (T), 25:9765 (NP-18578)
interactions anti N + N, theory of linearly rising trajectories for annihilation, 25:9769
interactions Δ + N, quasi-nuclear model for production of two- and three-baryon resonances in, (T), 25:9803 (ITEF-759)
interactions e + N, review of deep inelastic, (T), 25:9706 (SLAC-PUB-843)
interactions γ + N → Δ(1236) + π at 0.7 to 1 GeV, angular distribution asymmetry of π emission in, (T), 25:9798
interactions γ + N → N + π, chiral Lagrangians formalism for, 25:9726
interactions γ + N → π + N, simple harmonic forces in nonrelativistic quark model for N* production in, (T), 25:9788
interactions γ + N at high energies in SU(3) quark model, vector meson production in, (T), 25:9713
interactions γ + N at low energies, Kroll--Ruderman theorem and Born approximation for p-wave multipoles for π production in, 25:9724
interactions γ + N in Veneziano model, off-shell single-current amplitude for charged π production in, 25:9725
interactions in 2s--1d shell, core-polarization corrections to, (T), 25:10079
interactions N + N, nuclear and particle theory from ultrahigh-intensity accelerator study of, 25:9810
interactions N + N, two-pion-exchange contribution to, 25:9807
interactions of two, dispersion methods in charged scalar static model for, 25:9817
interactions π + N at low and intermediate energies, local duality in invariant amplitudes for, 25:9796
interactions π + N in Veneziano model, polarization in charge-exchange, 25:9793
interactions π + N, consistency conditions from duality for, (T), 25:9792
interactions π + N, direct-channel Regge poles for finite-energy sum rules for amplitudes of, 25:9801
interactions π + N, epsilon(700) and f°(1260) exchange in t-channel of, (T), 25:9802
interactions π + N, model of fermion trajectory for, 25:9790
interactions π + N, Regge cuts and asymptotic sum rules for amplitudes of forward, 25:9800
interactions π + N, scattering lengths for, (E/T), 25:9791
interactions π + N, tensor meson dominance for decoupling of f-exchange contribution from A amplitude in, (T), 25:9764 (DESY-70/58)
interactions π + N, vacuum trajectory for, (T), 25:9785 (DESY-70/55)
interactions with helium-3 and tritium, cross-section calculations using Glauber theory, (T), 25:9967 (JINR-P2-5335)
magnetic moment of, sidewise dispersion relations for anomalous, (T), 25:9702 (JINR-E2-5333)
magnetic moments in chiral Lagrangian formalism, non-minimal currents for, 25:9726
radius of, simple harmonic forces in nonrelativistic quark model for root-mean-square, (T), 25:9788
reactions with nuclei at 0.1 to 100 TeV in emulsions, angular distributions, pionization, and fireballs in, (E), 25:9635 (INP-722)
NUCLEONS (anti N)
interactions anti N + N → K + anti K + π at rest, four-point Veneziano functions for mass spectra and angular distributions in, (T), 25:9765 (NP-18578)
interactions anti N + N, theory of linearly rising trajectories for annihilation, 25:9769
NUCLEOPROTEINS
radiation effects on binding of, with acridine orange in fibroblasts of mice, uv, 25:8770

O

OAK RIDGE AREA (TENN.)
forest management plan for, 25:10356 (ORNL-TM-3175)
OCONEE POWER REACTOR, UNIT 1
buildings and structures for, safety analysis of instrumentation for, 25:10149 (DOCKET-50269-31)
cooling system piping for, dye penetrant tests for cladding of elbows and straight sections of, 25:10149 (DOCKET-50269-31)
operation of, notice of proposed issuance of license for, 25:10148 (DOCKET-50269-30)
safety evaluation of, Division of Reactor Licensing, 25:10150 (DOCKET-50269-32)
OCONEE POWER REACTOR, UNIT 2
buildings and structures for, safety analysis of instrumentation for, 25:10149 (DOCKET-50269-31)
cooling system piping for, dye penetrant tests for cladding of elbows and straight sections of, 25:10149 (DOCKET-50269-31)
OCONEE POWER REACTOR, UNIT 3
buildings and structures for, safety analysis of instrumentation for, 25:10149 (DOCKET-50269-31)
cooling system piping for, dye penetrant tests for cladding of elbows and straight sections of, 25:10149 (DOCKET-50269-31)
OGRA DEVICES
plasma density measurement in Ogra II, ionization gage for molecular, 25:9430
ORGANIC COMPOUNDS
chemical thermodynamics of crystalline, 25:8260(R) (COO-1149-160)
sorption by modified polyethylene powder, 25:8282(P)
ORGANIC COMPOUNDS, SULFO-
radiolysis of, mass-spectrometric studies on, 25:8290
ORGANISMS
radiation effects on living, in comparison with age, environment, and thermal energy, information theory for studying, 25:8742
ORGANS
radiation effects on weight of, of old-field mice, acute cobalt-60 γ, 25:8760
ORNL HIGH-FLUX ISOTOPE REACTOR
fuel elements for, radiation effects on channel spacings and configuration of, 25:8956 (ORNL-4600, pp 235-48)
ORNL RESEARCH REACTOR
maintenance during July to September 1970, 25:10270(R) (ORNL-TM-3256)
operations during July to September 1970, 25:10270(R) (ORNL-TM-3256)
OSCILLATORS
performance of superconducting high-frequency, 25:9396
OSMIUM ISOTOPES Os-190
neutron capture by, determination of thermal cross section for second-order reaction products, (E), 25:10040
OSMIUM ISOTOPES Os-192
energy levels from iridium-192 beta and electron-capture decay, (E), 25:10032(T) (ORNL-tr-2345)
energy-level transitions from iridium-192 beta and electron-capture decay, intensities of, (E), 25:10032(T) (ORNL-tr-2345)
OVARIES
radioinduced suppression of ovulation by, in human females, effects of age on dose of ionizing, 25:8732
OXADIAZOLE, DIPHENYL-
radioinduced luminescence of solutions of, in butanol and methanol, α, β, and uv, 25:8274
OXAZOLE, 2,2'-p-PHENYLENEBIS[5-PHENYL-
effects on luminescence degradation in uv-irradiated polystyrene scintillators activated with, 25:8582
OXAZOLE, TRIPHENYL-
radioinduced luminescence of solutions of, in butanol and methanol, α, β, and uv, 25:8274
OXYGEN
abundance in iota Ori B, (E), 25:8995
activity in plutonium dioxide--uranium dioxide fuels at 1700 to 2250°C, 25:8926(R) (GEAP-12133)
alpha-particle range at 0.2 to 2.0 MeV in, relation to energy, (E), 25:9162 (SC-RR-70-788)
argon-atom reactions with molecular, dependence of vibrational transition probabilities on orientation angle in, (T), 25:9226
burning in stars, (T), 25:8987
density at 70 to 85 km in ionosphere, molecular, (E/T), 25:9309
determination by indirect neutron or triton activation using lithium-6, 25:8218 (NP-18592)
determination in metals by inert gas fusion method, evaluation of bath materials for, 25:8194 (AECL-3743)
determination in metals by photon activation, 25:8216 (AERE-R-5363)
determination of abundance of, relative to uranium in hypostoichiometric uranium dioxide, revised gas chromatography method for, 25:8204 (RCN-128)
determination of abundance of, relative to uranium in hyperstoichiometric uranium dioxide, titrimetric, 25:8203 (RCN-127)

XUM

diffusion in plutonium dioxide--uranium dioxide, effects of thermal gradients on, 25:8926(R) (GEAP-12133)
effects of D-region atomic, on radio-wave propagation, (E/T), 25:9297
effects on γ-radioinduced oxidation of heptane at low temperatures, kinetics of, 25:8281
effects on neutron-radiosensitivity of HeLa cells, during protracted exposure to californium-252 source, 25:8704
effects on radioinduced defects in lithium-doped silicon, 25:9558
electron reactions at 0 to 1 eV with molecular, vibrational excitation in, (E), 25:9210
electron reactions at 5.75 to 8.40 eV with, angular distribution of oxygen ions (O^-) from dissociative electron attachment in, (E), 25:9221
ion reactions in eV range with molecular, mechanisms and cross sections for light emission in, (E), 25:9213
photon reactions with ground-state atomic, electron spectra from, (E), 25:9200
production of night airglow O(^{1}D), by temperature-dependent dissociative recombination of O_2^+, (E/T), 25:9314
proton range at 0.2 to 2.0 MeV in, relation to energy, (E), 25:9162 (SC-RR-70-788)
proton reactions at 4 to 26 keV with molecular, total cross sections for formation of metastable hydrogen atoms by charge exchange in, (E), 25:9193 (ORO-2591-52)
radiolysis of aqueous solutions of, intermediate states in, 25:8293
radiolysis of aqueous solutions of, monomolecular reactions in, 25:8295
radioprotective effects of, effects of fractionation on γ, 25:8795
reactions with molybdenum and tungsten at 380 to 980°C, effects of carbon dioxide, carbon monoxide, methane, and nitrogen of kinetics of oxidation, 25:8841
reactions with uranium carbide, kinetics of, 25:8907 (CEA-Bib-183)
spectra of metastable molecules of, deuterium isotope effects in quenching of, 25:8249

OXYGEN IONS
effects on Arabidopsis thaliana seeds, RBE for mutagenic and tumorigenic, 25:8800
energy of ground-state O^{6+}, calculation using configuration-interaction wave functions and correlation factor, 25:9242
implantation in silicon at 220 keV, localized vibrational modes and divacancy absorption spectra induced in, 25:9550
relation of D-region molecular, on radio propagation, (E/T), 25:9297

OXYGEN IONS (O^+)
abundance at 115 to 430 km in ionosphere, Thomson scatter measurements of, (E), 25:9316
reactions with nitrogen molecules at 1 to 5 MeV, fluorescence efficiencies for excitation in, (E), 25:9234

OXYGEN IONS (O^-)
extinction of trapped radiolytic, in alkaline ices at 77°K, thermal and photostimulated, 25:8287

OXYGEN IONS (O_2^+)
abundance at 115 to 430 km in ionosphere, Thomson scatter measurements of, (E), 25:9316
dissociative recombination in night airglow, yield of O(^{1}D) from, (E/T), 25:9314
reactions with nitrogen molecules at 1 to 5 MeV, fluorescence efficiencies for excitation in, (E), 25:9234

OXYGEN ISOTOPES O-14
energy levels from carbon-12 (He-3,n) reactions, spins and parities of, (E), 25:9981
half-life of, (E), 25:9989

OXYGEN ISOTOPES O-15
incorporation in carbon oxides, erythrocytes, and water for use for positron scanning, 25:8711(R) (NYO-3937-2)
production in cyclotrons by ^{14}N(d,n)^{15}O reaction, 25:8711(R) (NYO-3937-2)

OXYGEN ISOTOPES O-16
alpha reactions (α,2α) at 56 MeV, analysis using triangular graphs, (T), 25:9987
deuteron reactions (d,Li-6) at 50 MeV, lithium-6 spectra and angular distributions for, (E), 25:9978(R) (ORO-3398-26)
electron inelastic scattering by, energy spectra from, (E), 25:10014
electron inelastic scattering from, calculation of form factors using Serber--Yukawa residual interactions for, (T), 25:10010
energy levels from electron inelastic scattering with nucleon knockout at high energies, distorted wave analysis of nucleon momenta distributions in, (T), 25:9973 (ITF-70-42)
energy levels from electron inelastic scattering, wave functions for, (T), 25:10010
energy levels from many-nucleon transfer reactions, (E), 25:9986
energy levels from nitrogen-15 (p,γ) reactions, (E), 25:9979
helium-3 reactions (He-3,n) at 9.0 to 13.5 MeV, angular distributions for, (E), 25:9981
meson (π⁻) absorption in 1s and 2p bound states, rates of, 25:9982
neutron beam scattering by thick layers of, beam polarization and angular distribution from, (T), 25:9949
photon reactions (γ,n) at 100 to 800 MeV, excitation functions for, (E/T), 25:9977 (LUNP-7009)
reactions (O-16,C-12) with carbon-12 at 72 to 100 MeV, energy spectra and angular distributions for, (E), 25:9986
reactions (O-16,O-17) with beryllium-9 and carbon-13 at 11 to 20 MeV, differential cross sections for, (E), 25:9988
scattering by beryllium-9 and carbon-13 at 12 to 25 MeV, differential cross sections for elastic, (E), 25:9988
separation of molecular, from molecular oxygen ($^{16}O^{18}O$) by thermal diffusion, column coefficients for, 25:8423 (MLM-1439(Rev.))

OXYGEN ISOTOPES O-17
energy levels of, neutron spectroscopic factors for, (E), 25:9988

OXYGEN ISOTOPES O-18
alpha reactions (2α,2n) in stars, (T), 25:9037
alpha reactions (α,nγ) at 5 to 16 MeV, γ spectra and angular distributions from, (E), 25:10002
concentration in nitric oxide by low-temperature gas chromatography, 25:8319 (CU-755-7, Sect.4)
concentration in products from photolysis of carbon monoxide, 25:8331
energy levels from carbon-14 (α,n) reactions and alpha elastic scattering, spins and parities of resonance, (E), 25:9980
energy levels of, shell-model calculations using realistic one-boson exchange potentials, (T), 25:9992
exchange between water and ATP in presence of myosin, 25:8248
exchange reactions in oxynitrogen compounds, approximation methods for predictions of, 25:8245
exchange with oxygen-16 in nitrogen dioxide, kinetic studies on, 25:8255
helium-3 reactions (He-3,d) at 16 MeV, angular distributions for, (E), 25:9985
helium-3 reactions (He-3,pγ) at 3.3 to 4.1 MeV, p-γ angular correlations from, (E), 25:10004
meson (π⁻) absorption in 1s and 2p bound states, rates of, 25:9982
radio-wave emission from water vapor containing, in cosmic sources, (E), 25:9076
separation of molecular ($^{16}O^{18}O$), from oxygen-16 by thermal diffusion, column coefficients for, 25:8423 (MLM-1439(Rev.))

OXYGEN SYSTEMS
La--O--U, phase studies of, 25:8943 (KFK-1235)
O--PrO, phases and structure in nonstoichiometric regions of, at high temperatures, 25:8938
O--Pu, phase studies of high-temperature oxygen equilibrium in, 25:8945

OYSTER CREEK POWER REACTOR, UNIT 1
control system for, revised technical specifications for control rod withdrawal prohibit function of startup, 25:10144 (DOCKET-50219-119)
operations incident of December 18, 1970, malfunction of vacuum breaker block valves during surveillance test, 25:10118 (DOCKET-50219-117)
power level for, safety analysis of 1930 MW(t), 25:10143 (DOCKET-50219-118)

OZONE
abundance in sunrise auroral D region at 40 km, (E), 25:9296
effects of D-region, on radio-wave propagation, (E/T), 25:9297
screening height in ionosphere, deduction from sunrise effects at vlf, (E/T), 25:9331

P

PAHUTE MESA AREA (NEV.)
geologic faults and surface fractures in, effects of Jorum Event on, 25:8356 (USGS-474-92)
geology of, revised lithographic data from Drill Hole No. 1 on, 25:8357 (USGS-474-96)

PAKISTAN
power plants in, development of nuclear, 25:10098

PALLADIUM
alpha reactions at 30 to 80 MeV, K-shell ionization cross sections for, (E), 25:9978(R) (ORO-3398-26)
effects on deuterium exchange in propene, catalytic, 25:8258

PALLADIUM ISOTOPES Pd-105
proton reactions (p,pn) at 17 MeV, mechanism of, (E), 25:10005

PALLADIUM ISOTOPES Pd-106
energy levels from palladium-108 (p,t) reactions, (E), 25:9966(R) (COO-1265-94)

PALLADIUM ISOTOPES Pd-108
performance of activation detectors of, for neutron spectra measurements at 1 eV to 10 keV, 25:8481 (KFK-1233)
proton reactions (p,t) at 19 MeV, angular distributions for, (E), 25:9966(R) (COO-1265-94)

XUM

PARTICLE TRACKS
analysis of bubble chamber, DAPR system at LRL for, 25:8548 (UCRL-20126)
analysis of bubble chamber, distribution function for Coulomb multiple scattering effects for, 25:8559
analysis of bubble chamber, least squares and maximum probability methods for, 25:8558
analysis of bubble chamber, review on measuring devices for, 25:8554
analysis of magnetic spectrometer spark chamber, momentum, 25:8561
replication of heavy cosmic, in Apollo helmets, (E), 25:9255
PARTICLES
motion of spinning, in general relativity theory, (T), 25:9874
PEACH BOTTOM POWER REACTOR, UNIT 1
operations history for November 1970, 25:10114 (DOCKET-50171-75)
operations incident of December 28, 1970, malfunction of helium monitoring moisture detectors, 25:10115 (DOCKET-50171-76)
PECTINS
content of methoxyls, viscosity, and yield of, from irradiated residue of Valencia oranges, 25:8823
PERSONNEL
inhalation hazards to uranium mining, testing in dogs and hamsters, 25:8623 (BNWL-SA-3419)
radiation dose and dose rate to skeleton in radium dial, following ingestion of radium-226, computer calculations of, 25:8669 (COO-2088-1)
radiation dose to, in plutonium industry, ICRP recommendations for maximum permissible plutonium-239 α and γ, 25:8674(T) (LF-tr-41, pp 199-220)
radiation hazards to, at Goodyear Atomic Corporation during 1969, progress report on programs and services or controlling and reducing, 25:8692(R) (GAT-627)
radiation injuries in USA, legislation related to, compensation for, 25:8697
radiation injuries of nuclear energy, accidental, 25:8661 (JAERI-4052)
radiation monitoring of, at JAERI during 1969 and 1970, results of routine, 25:8693(R) (JAERI-5025)
radiation monitoring programs for, in New Zealand, 25:8675(R) (NP-18529)
radiation protection of, against radioisotope inhalation or ingestion, design of plastic ventilated suit for, 25:8691
radioinduced bone lesions in radium dial, following ingestion of radium-226, radiographic diagnosis of, 25:8669 (COO-2088-1)
tritium oxide content in expired air and urine of industrial, recommendations for maximum permissible, 25:8678(T) (ORNL-tr-2403)
PERTURBATION THEORY
applications of t-matrix, 25:10068
Pade approximation to vacuum expectation value of exponential operators, 25:9847
scattering amplitudes in, unitarity and fixed poles of weak, 25:9898
tetrahedron graphs in, duality of nonplanar, 25:9693
PESTICIDES
residue in relation to environmental contamination, conference on use of nuclear techniques to study, 25:8583 (STI/PUB-252)
PHANTOMS
radiation dosimetry for uniform cylindrical, comparison of unilateral and bilateral external γ, 25:8686
radiation dosimetry in tissue equivalent small animal, in relation to LET, Monte Carlo sampling method for, 25:8685
PHASE DIAGRAMS
book: Metallurgy and the Hot Working of Metals, 25:8894
PHENIX FAST REACTOR
shielding of, TRIPOLI code calculation of neutron spectra in lower, 25:10193 (CEA-N-1359)
PHOSPHINE
iodomethane--PH_3, radiolysis of vapor-phase, yields of methane and hydrogen from γ, 25:8303
NH_3--PH_3, radiolysis of, radical scavenging reactions in γ, 25:8299
PHOSPHORIC ACID, DIOCTYL ESTER
solvent properties for niobium and zirconium, 25:8214
PHOSPHORIC ACID, TRIBUTYL ESTER
solvent properties for plutonium, 25:8338(P)
PHOSPHORS
luminescence degradation in activated plastic, uv, 25:8582
PHOSPHORUS
abundance in iota Ori B, (E), 25:8995
abundance in L and H chondrites, (E), 25:8967
content of diet of goats, effects of, on calcium and phosphorus metabolism, 25:8592(R) (COO-1339-43)
determination in air particulates by spark source mass spectrometry, 25:8208
effects on creep in shielded metal-arc welds in stainless steel, 25:8849 (ORNL-4600, pp 142-6)
PHOSPHORUS ISOTOPES P-29
energy level at 3.446 MeV from silicon-28 (p,γ) reactions, (E), 25:10016 (ANU-P-503)
PHOSPHORUS ISOTOPES P-31
photon reactions (γ,n) at 100 to 800 MeV, excitation functions for, (E/T), 25:9977 (LUNP-7009)
PHOSPHORUS ISOTOPES P-32
toxicity of malathion labeled with, to man following ingestion of contaminated flour, calculations for, 25:8600
transport in food chains of nuclear-explosion-contaminated estuarine and marine ecosystems in relation to daily ingestion by man, use of stable element content of fish and invertebrates for predicting, 25:8627
uptake by Fogus mycorrhiza on Pinus, effects of temperature on, 25:8603
use in radioapplicators for therapy of conjunctival neoplasms, 25:8731
PHOSPHORYL CHLORIDES
effects on inhibition of graphite oxidation, 25:8906 (AERE-R-4857)
PHOTOCONDUCTIVITY
measurement at high frequencies in photosynthesizing systems, 25:10412(T) (UCRL-Trans-1427)
PHOTOGRAPHY
uses of aerial, for mineral prospecting, 25:8378
uses of aerial, in uranium prospecting, 25:8375
PHOTONS
coincidence counting in emission from quasi--monochromatic source, 25:8518
effects on aqueous solutions of carbonyl sulfides, yields of recoil sulfur-35 from, 25:8312
interactions γ + e, cross sections for W pair production in, (T), 25:9707
interactions γ + N $\rightarrow$ Δ(1236) + π at 0.7 to 1 GeV, angular distribution asymmetry of π emission in, (T), 25:9798
interactions γ + N $\rightarrow$ N + π, chiral Lagrangians formalism for, 25:9726
interactions γ + n $\rightarrow$ n + π^0, low-energy theorems for, 25:9721
interactions γ + n $\rightarrow$ p + π^-, low-energy theorems for, 25:9721
interactions γ + N $\rightarrow$ π + N, simple harmonic forces in nonrelativistic quark model for N* production in, (T), 25:9788
interactions γ + n $\rightarrow$ π^- + p in Veneziano model, cross sections for, 25:9717
interactions γ + N at high energies in SU(3) quark model, vector meson production in, (T), 25:9713
interactions γ + N at low energies, Kroll--Ruderman theorem and Born approximation for p-wave multipoles for π production in, 25:9724
interactions γ + N in Veneziano model, off-shell single-current amplitude for charged π production in, 25:9725
interactions γ + n, fits to differential cross sections for π production in, 25:9727
interactions γ + p $\rightarrow$ 2π + p at high energies, determination of $\pi\pi$ scattering phase shifts from, (T), 25:9767
interactions γ + p $\rightarrow$ Δ^{++} + π^- below 5.8 GeV, density matrix elements and spin population resonance parameters in, (E/T), 25:9678
interactions γ + p $\rightarrow$ eta + p at 4 and 6 GeV, Veneziano model for, (T), 25:9712
interactions γ + p $\rightarrow$ K^+ + Λ at threshold to 2.0 GeV, multipole analysis of, (E/T), 25:9728
interactions γ + p $\rightarrow$ K^+ + Σ^0 at threshold to 2.0 GeV, multipole analysis of, (E/T), 25:9728
interactions γ + p $\rightarrow$ n + π^+ at 260 to 350 MeV, absolute differential cross sections and P_{11}(1470) production in, (E), 25:9623
interactions γ + p $\rightarrow$ n + π^+, low-energy theorems for, 25:9721
interactions γ + p $\rightarrow$ p + π^0, low-energy theorems for, 25:9721
interactions γ + p $\rightarrow$ p + rho^0 below 5.8 GeV, density matrix elements and spin population resonance parameters in, (E/T), 25:9678
interactions γ + p $\rightarrow$ phi + p, Cheng--Wu picture for, (T), 25:9716
interactions γ + p $\rightarrow$ π^+ + n at 3.4 GeV at small momentum transfers, cross section asymmetry for, (E), 25:9624
interactions γ + p $\rightarrow$ π^+ + n in Veneziano model, cross sections for, 25:9717
interactions γ + p $\rightarrow$ rho^0 + p, Cheng--Wu picture for, (T), 25:9716
interactions γ + p, computer program using Monte Carlo method for determining incident beam energy spectrum from electron pairs from, (T), 25:9705 (SLAC-123)
interactions γ + p, fits to differential cross sections for π production in, 25:9727
interactions with hadrons, Lorentz invariant formulation of vector-meson dominance in, 25:9723
polarization measurements of, sensitivity of rectangular lithium-drifted silicon detector for, 25:8508
production in quark fusion, (T), 25:9075
propagator in rho-dominance model, 25:9846
reactions (γ,π^-) with boron-11 at 150 to 700 MeV, yields and cross sections for, (E), 25:9620 (LUNP-7007)
reactions (γ,π^+) with nuclei at 150 to 700 MeV, yields and cross sections for, (E), 25:9620 (LUNP-7007)
reactions with helium and helium-like ions, calculation of resonances between first and second ionization thresholds in, using diagonalization method, 25:9239
reactions with helium, evaluation of oscillator strength

for ionization in, using dipole length and velocity formulations, 25:9205
scattering by arbitrary-spin targets, low-energy theorems for Compton, (T), 25:9710
transport, Monte Carlo program for time-dependent, 25:9601 (LA-4539)
wave function renormalization constants in quantum electrodynamics, functional relations for, 25:9848
PHOTOSPHERE
brightness of faculae and flocculi in, (E), 25:9095(T) (CSIRO-Trans-10258)
brightness of flocculi in, (E), 25:9096(T) (CSIRO-Trans-10289)
cell formation in, giant, (T), 25:9112
characteristics of small H-α plages, magnetic and spectral, (E), 25:9099
granule formation in, super-, (T), 25:9112
magnetic fields in, (E), 25:9096(T) (CSIRO-Trans-10289)
magnetic fields in, (E), 25:9095(T) (CSIRO-Trans-10258)
spectra of, identification of silicon hydride ion in, (E), 25:9120
spectral-line profiles of, numerical experiments on, (E), 25:9119
PHYSICS
research at ANL Jan. through March 1970, 25:10015(R) (ANL-7699)
research at ANL Oct. through Dec. 1969, 25:9971(R) (ANL-7698)
PICOLINIC ACID
1-oxide, complexes with neptunium, thorium, or uranium, preparation and stability of, 25:8237 (KFK-1210)
complexes with neptunium, thorium, or uranium, preparation and stability of, 25:8237 (KFK-1210)
PINCH DEVICES
plasma instabilities in toroidal screw pinch ISAR IV, (E), 25:9489
PINCH EFFECT
microwave scattering by lf plasma oscillations in theta-, (E/T), 25:9520
plasma instability in helically symmetric theta-, high β, (T), 25:9498
plasma instability in rotating theta, finite Larmor radius equations for, 25:9497
radiations from theta-, enhanced far-ir, (E), 25:9448
shock wave formation in collisionless plasmas in theta, (E), 25:9452
stabilization of corrugated theta, with long-wave perturbations with m = 1, 25:9501
PIPES
closure device for ends of, design for handling radioactive materials, 25:8458(P)
design parameters of spaced in-core reactor, with multiple injection nozzles, 25:10200(P)
failure of reactor, probability analysis for, 25:8866 (GEAP-10205)
gas flow in strongly heated circular, method for characterizing quasi-developed turbulent, (T), 25:8420
stresses in internally pressurized out-of-round, method for calculation of, 25:8871 (ORNL-TM-3244)
PITUITARY GLAND
control of anterior, by hypothalamus, 25:10392(R) (TID-25619)
PLANETARY NEBULAE
dust--radiation instability in, (T), 25:8999
expansion of envelopes of, (T), 25:9013
identification of YM 29 as, (E), 25:9047
matter emission from, (T), 25:9013
morphology and kinematic study of NGC 6720 and NGC 6853, (E), 25:9048
radio observations of, at 2 cm, (E), 25:8996
spectra of, neutral helium in, (E), 25:9046
spectra of, population of 2^3S level of helium in, (T), 25:9016
PLANETS
magnetic fields in, origin of, (T), 25:9129
plasma flow past, interplanetary, (E/T), 25:9348
PLANTS
polonium-210 content of foliage of greenhouse, role of fallout as primary source for, 25:8593 (COO-1733-11)
radiation effects on small, effects of energy on microwave, 25:8790
radioisotope transport in Mediterranean Sea, cesium-137, strontium-90, and uranium-238, 25:8630
PLASMA
book: Properties of Gases at High Temperatures, in Russian, 25:9444
boundary problems in, finite-difference solutions for, 25:9460
charged-particle beam interactions with, nonlinear theory for, 25:9466
charged-particle beam interactions with, spectral analysis of oscillations from, (E/T), 25:9535
charged-particle beam scattering probability in, fast test, (T), 25:9467
charged-particle orbits in two electrostatic waves of arbitrary amplitude, (T), 25:9477
conductivity enhancement of supersonic argon, in electric discharges, (E), 25:9451
conductivity of magnetically confined, with low electric fields, (E/T), 25:9443
conductivity of nonequilibrium, hf, (T), 25:9463
conductivity of trapped, effect of electron collisions on electric, (T), 25:9480
confinement in combined mirror and octupole magnetic fields, (E), 25:9399
confinement in fusion devices, echo studies of, 25:9420
confinement in magnetic mirrors, effect of co-ordinate space phenomena on end losses, (T), 25:9406
confinement in rotating magnetic fields, short-wavelength instabilities in, (T), 25:9487 (LRP-42/70)
confinement in time changing toroidal octupole magnetic field, motion in, (E/T), 25:9402
current distribution in nonequilibrium, in argon--cesium pulse discharge with sectional electrodes, 25:9482
currents in stellarator-confined, from oscillation of helical winding currents, (T), 25:9511
diagnostics in Ogra II, ionization gage for molecular flux density, 25:9430
diagnostics in shock tubes, electron temperature and density, 25:9418
diagnostics in toroidal magnetic traps, using plane probe, 25:9410(T) (CTO-736)
diagnostics of argon discharge, continuum probe theory for, 25:9429
diagnostics of cesium, Stark-broadening measurements for electron density, 25:9421
diagnostics of cold collisionless, using microwaves and Fabry--Perot interferometers, 25:9408 (COO-1789-1)
diagnostics of deuterium, vacuum uv spectroscopy of electron temperature, 25:9407 (CEA-N-1391)
diagnostics of discharge, temperature, (E/T), 25:9411 (ECRC/N-288)
diagnostics of helium afterglow, using microwave interferometers, 25:9417
diagnostics of high-current discharges with skin effect, microwave, 25:9424
diagnostics of hydrogen arc, ion temperature using Doppler effect, 25:9413(T) (SC-T-71-3001)
diagnostics of laser-produced xenon, electron density, (E), 25:9485
diagnostics of low-pressure cesium discharge, Langmuir-probe measurement of electron energy distribution, (T), 25:9419
diagnostics of rare gas, excitation temperature functions for, 25:9172
diagnostics of shock-produced argon, spectroscopic, 25:9423
diagnostics of shock-produced xenon, spectroscopy and laser interferometry, 25:9422
diagnostics of striations in hydrogen discharge, microwave, 25:9425
diagnostics of strong-current discharges with skin effect, using microwaves, 25:9428
diagnostics of trapped particles in fusion devices, using echo phenomena, 25:9420
diagnostics of, aperture effects in parameter determination by scattering method, (T), 25:9415
diagnostics using laser scattering, electron density, (E), 25:9409(T) (CTO-733)
diagnostics using Thomson scattering of laser light, magnetic field, (E), 25:9427
diffusion equation for, numerical solution of, 25:9468
diffusion in toroidal systems, classical, (T), 25:9400
electric discharges in argon columns, self-excited steady layers in, (T), 25:9465
electric discharges in helium and neon, moving striations in, (E), 25:9453
electric discharges in, ionization nonequilibrium during cooling of pulsed, (T), 25:9462
electric discharges in, pseudowave reflection from potential barrier of gridded energy analyzer in, (E), 25:9531
electron beam interactions with mercury, instabilities from slow, (E), 25:9447
electron beam interactions with neutral gas, turbulence from, (T), 25:9455 (AD-705265)
electron beam interactions with, effect of collisions on instability in, (E/T), 25:9494
electron beam interactions with, inhomogeneity effects on relaxation of ultrarelativistic, (T), 25:9472
electron beam interactions with, nonlinear theory for electron oscillations in, (T), 25:9469
electron density in nonequilibrium, (T), 25:9435
electron distribution function for discharge, effects of diaphragm on, (T), 25:9471
electron distribution function in arbitrary time-dependent electromagnetic fields, (T), 25:9470
electron energy distribution in thermionic, effects of excitation relaxation on, (T), 25:9267
electron velocity distribution function for homogeneous Lorentz, (T), 25:9474
electron velocity distribution function for Lorentz, convergency problem in, (T), 25:9473
equilibrium and stability in closed magnetic traps without rotational transformation, (T), 25:9491
equilibrium and stability in toroidal fields, effects of hf electric fields on, 25:9499
flow of interplanetary, past Earth and planets, (E/T), 25:9348
flow of rarefied, past charged bodies, far-wake structure in, 25:9478
heating by cyclotron waves in nonuniform magnetic fields, (T), 25:9404

XUM

heating by cyclotron waves in nonuniform magnetic fields, (T), 25:9403
heating by laser-irradiation of stationary, one-dimensional, (T), 25:9405
heating in dense plasma focus, ion, (E), 25:9401
heating in Helios, near cyclotron frequency, 25:9398(R) (ORO-3895-15)
injection of 4-MeV H_2^+ ions in magnetic mirrors, accumulation in, 25:9506 (ORNL-TM-3207)
ion beam interactions with hot-electron, instabilities from, (E), 25:9450
ionization degree in nonequilibrium, equation for, 25:9435
kinetic theory of turbulent pulsations in, correlation functions for, 25:9475
kinetic theory of, numerical solution of diffusion equation, 25:9468
kinetics of, elliptic boundary-value solutions for, 25:9456 (JUL-663-PP)
laser beam scattering on, effect of oblique incidence on absorption, (T), 25:9476
motion of injected, in time-changing toroidal octupole magnetic fields, (E/T), 25:9402
oscillations in beam--plasma system, spectral analysis of, (E/T), 25:9535
oscillations in bounded magnetized, longitudinal, (E), 25:9532
oscillations in weakly turbulent, phase velocity of, (T), 25:9515
production by laser irradiation of solid nickel targets, (E), 25:9484
production in electromagnetic shock tubes, precursor ionization, 25:9486
production of quiescent, with T/sub i/ > T/sub e/ in magnetic fields, (E), 25:9483
properties of flowing argon, in channels with cooled walls in transverse magnetic fields, 25:9281
radiations from theta-pinch, enhanced far-ir, (E), 25:9448
radiations from, noise suppression techniques for macroparticle models, 25:9457 (UCRL-72604)
research in Helios Q device, Sept. 1970, 25:9398(R) (ORO-3895-15)
shock formation and structure in colliding, collisionless electrostatic, (E/T), 25:9437
shock wave formation in collisionless, magnetic-piston, (E), 25:9452
shock wave interactions with, electron density behind, (E/T), 25:9446
shock wave propagation in collisionless magnetized, (T), 25:9461
shock wave structure in electromagnetic shock tubes, (E/T), 25:9445
simulation by computer, modifications to oscillations, fluctuations, and collisions in, 25:9459 (UCRL-72635)
simulation of collisionless, noise suppression techniques for macroparticle models, 25:9457 (UCRL-72604)
simulation of, formulation of self-consistent 2- and $2^1/_2$-dimensional electromagnetic and relativistic, 25:9458 (UCRL-72613)
spectra of neutral argon and neon, Stark broadening of resonance lines of, 25:9171
spectra of, clean shock tube development for, 25:9510
stability and equilibrium in closed magnetic traps without rotational equilibrium, (T), 25:9491
stability and equilibrium of toroidal, effect of hf electric fields on, 25:9499
stability in rotating magnetic fields, short-wavelength, (T), 25:9487 (LRP-42/70)
stability in toroidal configurations, growth rate of kink, (T), 25:9492
stability in toroidal screw pinch ISAR IV, (E), 25:9489
stability in toroidal systems, trapped-particle effects on drift-wave, (T), 25:9490
stability in uniform magnetic fields, velocity-shear and low-frequency, (T), 25:9496
stability of cold and warm electron beams in, effect of collisions on, (E/T), 25:9494
stability of counterstreaming, electromagnetic, (T), 25:9493
stability of high β, in helically symmetric theta pinch, (T), 25:9498
stability of multicomponent, electrostatic, (T), 25:9500
stability of rotating theta pinch, finite Larmor radius equations for, 25:9497
stability of, amplitde limitation of collisional drift, (T), 25:9495
stability of, collision effects on Rayleigh--Taylor, (T), 25:9502
stabilization of corrugated theta pinch, with long-wave perturbations with m = 1, 25:9501
stabilization of electron waves in, quasi-linear calculation with allowance for spontaneous emission, (T), 25:9524
stabilization of Rayleigh--Taylor instabilities in, (T), 25:9488 (LRP-45/70)
thermonuclear reactions in, emission spectra from, (T), 25:9504 (FOA-4-4438)
transport coefficients for helium and neon, electron energy distribution, (T), 25:9464
transport toward hoops in single-ring dc device, 25:9503(R) (COO-1726-70)
wave coupling in, ion-, (E/T), 25:9513
wave disturbances in positive column, large-amplitude, (T), 25:9529
wave echoes in, higher-order temporal and spatial, (T), 25:9534
wave echoes in, theory for spatial, 25:9519
wave excitation at upper hybrid frequency in inhomogeneous, harmonic, 25:9521
wave excitation in cold nonuniform magnetized, harmonic, (T), 25:9523
wave excitation in magnetized, by transverse electromagnetic waves, (T), 25:9518
wave interactions in bounded magneto-, nonlinear, (T), 25:9514
wave interactions in hot electron, three extraordinary, (T), 25:9528
wave propagation in binary mixtures, kinetic theory of, (T), 25:9533
wave propagation in finite geometry, dispersion relations for ion--acoustic, 25:9525
wave propagation in one-component, kinetic theory of, (T), 25:9527
wave propagation in positive column, with finite-amplitude helical instability, (E), 25:9530
wave propagation in Q devices, ion--acoustic, (E/T), 25:9522
wave propagation in relativistic, dispersion relation for longitudinal, (T), 25:9516
wave propagation in uniform infinite, with weak beam, (T), 25:9526
wave propagation in weakly turbulent, correlation functions for, 25:9475
wave reflection from potential barrier of gridded energy analyzer in discharge, ion-, (E), 25:9531
wave resonances in low-pressure discharges, helicon, (T), 25:9512 (NP-18554)
wave scattering by lf oscillations in theta-pinch, micro-, (E/T), 25:9520
wave scattering in turbulent, electromagnetic-, (T), 25:9481
wave stabilization in, quasi-linear calculation with allowance for spontaneous emission, (T), 25:9524
wave--particle beam interactions in, hydromagnetic, (T), 25:9455 (AD-705265)
waves in, amplitude limitation of collisional drift, (T), 25:9495
waves in, analog device for computing dispersion relations for electron, 25:9517

PLASMA ACCELERATORS
feasibility of Hall-current and self-magnetic, 25:9438
feasibility of, with inductive MPD converters, 25:9439
ion heating in dense plasma focus, (E), 25:9401
jet fine structure in focus, using x-ray pinhole cameras, 25:9412(T) (LA-tr-70-25)
jet temperature in Rod Plasma Injector, spectra measurement of, 25:9426
snowplowing in rail-type gun, (T), 25:9479

PLASMA JETS
conductivity enhancement of supersonic argon, in electric discharges, (E), 25:9451
diagnostics in focus device, fine structure measurement using x-ray pinhole cameras, 25:9412(T) (LA-tr-70-25)
diagnostics in RPI, spectra measurement of temperature, 25:9426
diagnostics of pulse, spectroscopic methods for charged-particle density, 25:9416
diagnostics of three-component, in dipole magnetic fields, 25:9414
temperature distribution in one- and two-phase subsonic, effects of condensed phase on, (E), 25:9434
thermodynamic equilibrium in argon, local, (E), 25:9454
velocity distribution in one- and two-phase subsonic, effects of condensed phase on, (E), 25:9434

PLASMAPAUSE
location of, relation with Pc2, -3, and -4 geomagnetic field pulsations, (E/T), 25:9353
monitoring of, worldwide technique for, (E), 25:9325

PLASTICS
cosmic-particle track identification in Apollo helmets, (E), 25:9255
electron dose--depth profiles in dosimeters, effects of trapped charge on, 25:8566
molding into parts, defects related to, 25:10341 (BDX-613-166)

PLATES
fluid flow past moving infinite flat, in transverse magnetic field, (T), 25:9280
neutron coherent double scattering in crystalline, (T), 25:9963
neutron propagation in, transverse, (T), 25:9961
neutron transport in, criticality for energy-dependent, (T), 25:9960

PLATINUM
carbon-12 reactions (C-12,4n) and (C-12,5n) at 82 MeV with natural, gamma spectra from, (E), 25:10027 (JINR-E6-5379)
effects on deuterium exchange in propene, catalytic, 25:8258
effects on thermal diffusion separation of deuterium from hydrogen by thermal diffusion in trennschaukel, 25:8422 (CU-755-7, Sect.5)

reactions with refractory metals in diffusion couples, metallography of phases from, 25:8851 (ORNL-4600, pp 186-97)

PLATINUM ALLOYS AND SYSTEMS
Cr--Fe-base--Ni--Pt, corrosion by water containing trace chloride and oxygen at 200°C, stress, 25:8834(R) (COO-2069-6)
Cr--Pt-base--Ti, properties for use as radioisotppe fuel capsule material, 25:8850 (ORNL-4600, pp 181-5)
Hf--Mo--Pt-base, properties for use as radioisotope fuel capsule material, 25:8850 (ORNL-4600, pp 181-5)
Hf--Pt-base, properties for use as radioisotope fuel capsule material, 25:8850 (ORNL-4600, pp 181-5)
Hf--Pt-base--W, properties for use as radioisotope fuel capsule material, 25:8850 (ORNL-4600, pp 181-5)
Hf--Pt-base--W, tensile properties at 25 to 1290°C, 25:8427(R) (ORNL-4639)
Mo--Pt-base, tensile properties at 25 to 1093°C, 25:8427(R) (ORNL-4639)
Mo--Pt-base--Ti, tensile properties at 25 to 1290°C, 25:8427(R) (ORNL-4639)
Pt-base--Rh, tensile properties at 1093 to 1290°C, 25:8427(R) (ORNL-4639)

PLATINUM ISOTOPES Pt-192
energy levels from iridium-192 beta decay, (E), 25:10032(T) (ORNL-tr-2345)
energy-level transitions from iridium-192 beta decay, intensities of, (E), 25:10032(T) (ORNL-tr-2345)

PLATINUM ISOTOPES Pt-195
energy levels from gold-195 electron-capture decay, skin--parity assignments for, (E), 25:10048
energy-level transitions from gold-195 electron-capture decay, conversion coefficients, multipolarities, and L-subshell ratios for, (E), 25:10048
proton reactions (p,pn) at 17 MeV, mechanism of, (E), 25:10005

PLATINUM ISOTOPES Pt-196
neutron capture by, determination of thermal cross section for second-order reaction products, (E), 25:10040

PLATINUM ISOTOPES Pt-198
performance of activation detectors of, for neutron spectra measurements at 1 eV to 10 keV, 25:8481 (KFK-1233)

PLATYHELMINTHES
Echinococcus granulosus, detection of noncalcified cysts of, in man using gold-198, 25:8719

PLOWSHARE PROJECT
analysis of rock samples from Project Gasbuggy holes GB-1 and GB-3 in, data tabulation on petrographic, 25:8385 (PNE-G-69)
gas composition in Project Gasbuggy chimney in, model for, 25:8384 (PNE-G-68)
natural gas production stimulation in Project Gasbuggy, numerical model for simulating transient gas flow in underground reservoir following, 25:8387 (UCRL-71868)
technology development in, review of, 25:8388
water waves from cratering explosions in shallow water in, characteristics of, 25:8386 (UCRL-50940)

PLUTONIUM
bibliography on, index to 3rd quarter 1970 of, 25:8831
bibliography on, Oct., 1970, 25:8830
chemical properties of, 25:8238(T) (LF-tr-41, pp 3-5)
determination in plutonium carbide--uranium carbide, plutonium dioxide--uranium dioxide, and plutonium nitride--uranium nitride fuels by controlled-potential coulometric and potentiometric titrations, 25:8200 (LA-4537)
development of pressurized water reactor, using fuel cycle, 25:10222
diffusion from clad fuel elements, use of aluminum or graphite barrier for prevention of, 25:8857
disproportionation of tetravalent and pentavalent, effects of presence of hexavalent plutonium on, 25:8239 (MLM-1744)
production by pyrochemical reduction of plutonium dioxide using calcium, 25:8236 (ARH-SA-72)
purification of acidic solutions of, 25:8338(P)
radioinduced contraction of β- and delta-, at 4.2°K, self-, 25:8904
separation from acidic solutions by solvent extraction using TBP, 25:8338(P)
separation from irradiated LMFBR fuels, solvent extraction processes for, 25:8316 (BNWL-CC-1939)
use in pressurized water reactor fuels, (E/T), 25:10213(R) (WCAP-3385-25)

PLUTONIUM ALLOYS AND SYSTEMS
Cr--N--Pu, phase studies of, 25:8910 (ORNL-4600, pp 41-56)
O--Pu, phase studies of high-temperature oxygen equilibrium in, 25:8945

PLUTONIUM CARBIDES
PuC--UC, analysis for plutonium and uranium by controlled-potential coulometric and potentiometric titrations, 25:8200 (LA-4537)

PLUTONIUM ISOTOPES Pu-238
alpha decay of, coincidence semiconductor detector system for measurement of x-ray-to-alpha ratio in, 25:8465 (BNWL-SA-1514)
content of atmospheric precipitation and worldwide HASL sites from 1966 to 1970, 25:8658 (HASL-237, pp II.1-16)
deposition at world sites from 1965 to 1970, measurements of, 25:8658 (HASL-237, pp II.1-16)
design and testing of sealed heat sources of, for implantable cardiac pacemakers, CEA program for, 25:8425 (NP-18563)
determination in fuel reprocessing solutions, 25:8324(T) (ORNL-tr-2406)
distribution in organs of rats following inhalation and intramuscular injection, 25:8590 (CEA-CONF-1658)
neutron fission of, prompt neutron spectra and yield for thermal, $\bar{\nu}$(E), 25:10039
use as heat source in French cardiac pacemaker program, 25:8430

PLUTONIUM ISOTOPES Pu-239
alpha decay of, coincidence semiconductor detector system for measurement of x-ray-to-alpha ratio in, 25:8465 (BNWL-SA-1514)
clearance from lungs of rats, effects of aerosol concentration on rate of, 25:8591 (CEA-CONF-1677)
content of air and water in environs of plutonium industry, maximum permissible, 25:8674(T) (LF-tr-41, pp 199-220)
content of atmospheric precipitation and worldwide HASL sites from 1966 to 1970, 25:8658 (HASL-237, pp II.1-16)
determination in fuel reprocessing solutions, 25:8324(T) (ORNL-tr-2406)
distribution in Lithuania atmosphere at 30 to 200 m altitude, 1966 to 1968, 25:8372
distribution in organs and tissues, review of effects of administration route, age, and dose on, 25:8595(T) (LF-tr-41, pp 7-125)
distribution in organs of rats following inhalation and intramuscular injection, 25:8590 (CEA-CONF-1658)
effects on animals, review of toxic, 25:8594(T) (LF-tr-41)
effects on hematopoiesis, life span, and pathology of animals, review of effects of administration route on, 25:8596(T) (LF-tr-41, pp 127-97)
effects on human bones, carcinogenic α and γ, 25:8674(T) (LF-tr-41, pp 199-220)
fission of, energy-dependent neutron yield for, 25:10025 (INDC(NDS)-19/N)
neutron absorption in Doppler resonance regions, shielding factors for, (T), 25:10038
nuclear properties of, 25:8238(T) (LF-tr-41, pp 3-5)
photofission of, cross sections and angular anisotropy of, (E), 25:10024 (FEI-190)

PLUTONIUM ISOTOPES Pu-240
alpha decay of, coincidence semiconductor detector system for measurement of x-ray-to-alpha ratio in, 25:8465 (BNWL-SA-1514)
determination in fuel reprocessing solutions, 25:8324(T) (ORNL-tr-2406)
fission of, energy-dependent neutron yield for, 25:10025 (INDC(NDS)-19/N)
neutron reactions at less than 1 MeV, cross sections and resonance parameters for, (E), 25:10021 (CEA-N-1273)

PLUTONIUM ISOTOPES Pu-241
fission of, energy-dependent neutron yield for, 25:10025 (INDC(NDS)-19/N)

PLUTONIUM NITRIDES
thermodynamic properties of, 25:8941
PuN--UN, analysis for plutonium and uranium by controlled-potential coulometric and potentiometric titrations, 25:8200 (LA-4537)
PuN--UN, preparation and fabrication of fuel pins of, methods for, 25:8910 (ORNL-4600, pp 41-56)
PuN--UN, properties of fuel pellets of, chemical and microstructural, 25:8910 (ORNL-4600, pp 41-56)

PLUTONIUM OXIDES PuO_2
preparation of sols of, methods for, 25:8909 (ORNL-4600, pp 3-40)
reduction to metal using calcium, pyrochemical, 25:8236 (ARH-SA-72)
PuO_2--UO_2, analysis for plutonium and uranium by controlled-potential coulometric and potentiometric titrations, 25:8200 (LA-4537)
PuO_2--UO_2, diffusion of oxygen in, effects of thermal gradients on, 25:8926(R) (GEAP-12133)
PuO_2--UO_2, fabrication of fuel pins of, by Sphere-Pac loading of microspheres, 25:8909 (ORNL-4600, pp 3-40)
PuO_2--UO_2, microstructure of microspheres of, 25:8909 (ORNL-4600, pp 3-40)
PuO_2--UO_2, oxygen activity in fuels of, at 1700 to 2250°C, 25:8926(R) (GEAP-12133)
PuO_2--UO_2, oxygen-to-metal ratio in, precision and source of variation in, 25:8909 (ORNL-4600, pp 3-40)
PuO_2--UO_2, performance of fuel pins of stainless steel-clad, effects of power cycling on, 25:8835 (ORNL-4600, pp 57-64)
PuO_2--UO_2, preparation of dense microspheres of, methods for, 25:8909 (ORNL-4600, pp 3-40)
PuO_2--UO_2, radiation effects on burnup, microstructure, and mechanical properties of fuels of, in-pile, (E), 25:10213(R) (WCAP-3385-25)
PuO_2--UO_2, radiation effects on encapsulated fuels of, fast and thermal neutron, 25:8909 (ORNL-4600, pp 3-40)
PuO_2--UO_2, radiation effects on grain size in Sphere-Pac fuel Pins of, in-pile, 25:8911 (ORNL-4600, pp 65-80)
PuO_2--UO_2, radiation effects on metal distribution in

XUM

Sphere-Pac fuels of, in-pile, 25:8911 (ORNL-4600, pp 65-80)
PuO_2--UO_2, radiation effects on microstructure of, relations of preparation method with in-pile, 25:8955 (ORNL-4600, pp 225-34)
PuO_2--UO_2, reactions with sodium in failed fuel elements at high temperatures, effects of oxygen-to-metal ratio on, 25:8926(R) (GEAP-12133)
POINT BEACH POWER REACTOR, UNIT 1
operations incident of December 9, 1970, improper service water outlet valve lineup for radioactive waste discharge, 25:10124 (DOCKET-50266-37)
POLLEN
radiation effects on formation of, of mulberries, effects of dose on γ, 25:8794(T) (NSJ-tr-158)
radioinduced mutations in, of barley, strontium-90 β, 25:8648
POLONIUM ISOTOPES Po-202
energy level from platinum-194 (C-12,4n) and platinum-195 (C-12,5n) reactions, lifetime for 8^+, (E), 25:10027 (JINR-E6-5379)
energy-level transitions from platinum-194 (C-12,4n) and platinum-195 (C-12,5n) reactions, probabilities for E2, (E), 25:10027 (JINR-E6-5379)
POLONIUM ISOTOPES Po-204
energy level from platinum-194 (C-12,2n) and platinum-195 (C-12,3n) reactions, lifetime for 8^+, (E), 25:10027 (JINR-E6-5379)
energy-level transitions from platinum-194 (C-12,2n) and platinum-195 (C-12,3n) reactions, probabilities for E2, (E), 25:10027 (JINR-E6-5379)
POLONIUM ISOTOPES Po-210
content of cigarette smoke, 25:8623 (BNWL-SA-3419)
content of greenhouse soil and vegetation, role of fallout as primary source for, 25:8593 (COO-1733-11)
decay of, in-beam measurement of internal conversion electrons from, (E), 25:9978(R) (ORO-3398-26)
effects on blood, carcinogenesis, and life span of animals in comparison to plutonium-239, 25:8596(T) (LF-tr-41, pp 127-97)
energy levels from bismuth-209 (He-3,d) reactions, (E), 25:9966(R) (COO-1265-94)
migration in soils, hazards to water supplies from, 25:8593 (COO-1733-11)
sorption as oxide by agricultural top soils in relation to silt content and soil pH, distribution coefficients for, 25:8593 (COO-1733-11)
uptake as oxide from soils by crops, transfer coefficients for calculating human dietary intake from, 25:8593 (COO-1733-11)
POLONIUM ISOTOPES Po-211
alpha decay of ground-state and isomeric, half-lives for, (E), 25:9966(R) (COO-1265-94)
POLYMERS
deposition on polyethylene powder, 25:8282(P)
radioinduced formation of, in lysozyme, 25:8604 (COO-650-41)
POROUS MATERIALS
properties of, effects of stereometric microstructure on, 25:8944 (KFK-1236)
POSITRON CAMERAS
development for scanning using carbon-11, nitrogen-13, or oxygen-15 as tracers for, 25:8711(R) (NYO-3937-2)
POSITRONIUM
reactions with protons, generalized variational bounds and coupled-static approximation for, (T), 25:9216
POSITRONS
annihilation in periodic field, many-body theory of nearly free electrons, 25:9606
channeling in silicon and anthracene monocrystals at 247 keV, 25:9543
interactions $e^+ + e^- + e^+ + e^-$, S-matrix element for, 25:9740
interactions $e^+ + e^-$ at 0.7 x 2 to 1.2 x 2 GeV, spark chamber and scintillation counter study of Bhabha scattering and μ pair and hadron production in, (E), 25:9621 (NP-18581)
radiation effects on annihilation of, in acetylmethionine, 25:8269
reactions with hydrogen atoms, generalized variational bounds and coupled-static approximation for, (T), 25:9216
scattering by aluminum, copper, lead, and silver foils at 100 to 1300 keV as function of foil thickness and incidence angle, single, plural, and multiple elastic, (E), 25:9225
scattering by helium at low energies, correlation effects on calculation of phase shifts for elastic, 25:9196
POTASSIUM
abundance in L and H chondrites, (E), 25:8967
corrosive effects of working fluid of, on nickel heat pipe, (E), 25:8395 (ORNL-TM-3077)
determination in air particulates by spark source mass spectrometry, 25:8208
determination in airborne particulates by neutron activation, 25:8231
determination in titanium and titanium dioxide by neutron activation, 25:8233
flow in tubes, pressure drop in two-phase upward, 25:8405 (BNL-13957)
reactions between atoms of, total cross sections for elastic scattering and spin exchange in, (T), 25:9202
scattering by cesium, potassium, and rubidium at 0.1 to 0.2 eV, analysis of data on differential spin exchange in, (T), 25:9224
scattering by cesium, potassium, and rubidium at 0.1 to 0.2 eV, differential cross sections for elastic and spin-exchange, (E), 25:9223
POTASSIUM ACID PHOSPHATES
radiation effects on dielectric constant of, at 70 to 150°K, γ, 25:8275
POTASSIUM BROMIDES
F-center spectra of, isotope splitting of, (E/T), 25:9585
KBr-base--Mg, optical absorption and electric conductivity of diffused crystals of, 25:9570
POTASSIUM CHLORIDES
radiation effects on, reactions of recoil sulfur-35 from neutron, 25:8312
radioinduced color centers in pure and doped crystals of, role of motion of holes, anion vacancies, and excitations in x, 25:9553
POTASSIUM HYDROXIDES
radiation effects on ices of, γ, 25:8272
POTASSIUM IODIDES
F-center spectra of, isotope splitting of, (E/T), 25:9585
POTASSIUM ISOTOPES K-39
deuteron reactions (d,Li-6) at 50 MeV, lithium-6 spectra and angular distributions for, (E), 25:9978(R) (ORO-3398-26)
effects on F-center spectra of potassium bromide and iodide, 25:9585
POTASSIUM ISOTOPES K-41
effects on F-center spectra of potassium bromide and iodide, 25:9585
photon reactions (γ,π^+) at 150 to 700 MeV, yields and cross sections for, (E), 25:9620 (LUNP-7007)
POTASSIUM NITRATES
effects on radiolysis of aqueous silver solutions, 25:8302
radiolysis of aqueous ethanol solutions of, γ, 25:8301
POWER PLANTS
combustion products for thermoelectric, with open-cycle MHD generator, production of high-temperature, 25:9261
economics of U. S. hydroelectric pumped storage, in combination with nuclear power plants, 25:10109 (BNL-50238)
feasibility of noble-gas closed-loop MHD, fired with fossil fuels, economic and technical, (E/T), 25:9264
POWER SUPPLIES
design of pulse, for piezoresistive gages, 25:10381 (SCL-DR-70-130)
PRASEODYMIUM ALLOYS AND SYSTEMS
Al--Ni--Pr, magnetic properties and phase diagram of PrNi/sub x/Al/sub2-x/, 25:9576
Co--Dy--Pr, magnetic properties and phase diagram of Pr/sub x/Dy/sub 1-x/Co_2, 25:9576
Co--Ho--Pr, magnetic properties and phase diagram of Pr/sub x/Ho/sub 1-x/Co_2, 25:9576
Dy--Ni--Pr, magnetic properties and phase diagram of Pr/sub x/Dy/sub 1-x/Ni_2, 25:9576
Ho--Ni--Pr, magnetic properties and phase diagram of Pr/sub x/Ho/sub 1-x/Ni_2, 25:9576
PRASEODYMIUM ISOTOPES Pr-141
proton reactions (p,d) with, angular distributions for, (E), 25:9978(R) (ORO-3398-26)
PRASEODYMIUM ISOTOPES Pr-144
distribution in uranium dioxide fuels at high burnups, determination by gamma scanning, 25:8951(R) (GEAP-10217)
PRASEODYMIUM OXIDES
properties for use in dispersion strengthening of aluminum, 25:8860(P)
O--PrO_x phases and structure in nonstoichiometric regions of, at high temperatures, 25:8938
PREAMPLIFIERS
design of fast current, for neutron collimation for surface-barrier detector, 25:8519
PRESSURE
scales for high and very high, validity of, 25:10352(T) (LA-tr-70-26)
PRESSURE VESSELS
closures for graphite moderated gas cooled reactor prestressed concrete, use of prestressing tendons for securing heat exchanger access, 25:10198(P)
design of concrete, for reactor core and pressure suppression containment, 25:10169(P)
design requirements of steel, for boiling and pressurized water reactors, 25:10197
development of prestressed concrete, for gas cooled reactors, 25:10166 (GA-10265)
flange joints for large, pretightening procedures for, (E/T), 25:10096 (ZJE-65)
performance of prestressed concrete, model testing for long-term, (E), 25:10325 (ORNL-TM-3246)
radiation effects on chemical and mechanical properties of steels for Czechoslovakia reactor, 25:8899 (ZJE-89)
radiation effects on mechanical properties of steel, neutron, 25:8900 (ZJE-90)
radiation effects on welds in steel, neutron, 25:8901 (ZJE-91)
response to loading of prestressed concrete, analytical

method for analysis of ultimate, 25:8392 (GA-9994)
seals for wall probe penetrations in, design of hermetic, 25:8402(P)
standards for reactor prestressed concrete, summary of French, 25:10160(T) (ORNL-tr-2402)
stress concentrations in nozzles of, effects of attachment configuration on, (E), 25:10244(R) (ORNL-TM-3212)
PROCESS EQUIPMENT
duct closure for, design of, 25:8458(P)
PROPANE
radiolysis of, method for accumulating energy produced by, 25:8292(P)
2-PROPANETHIOL, 1-AMINO-
hydrochloride, crystal structure of, 25:8268
PROPENE
deuterium exchange reactions in, catalyzed by Group eight metals, 25:8258
PROPIOLONITRILE
microwave emission from, in Sgr B2, (E), 25:9094
PROPULSION
conference on space-vehicle, 10th international, Rome, Italy, 3/70, 25:10420
feasibility of plasma, using inductive MPD converters, 25:9439
feasibility of plasma, using self-magnetic and Hall-current devices, 25:9438
PROPYNE
deuterium exchange between water and deuterated, mass-spectrometric equilibrium studies on, 25:8241 (CU-755-7, Sect.3)
PROSPECTING
equipment and method for geophysical, using neutron well logging with pulse height discrimination, 25:8359(P)
PROTACTINIUM
determination in fuel reprocessing solutions, 25:8324(T) (ORNL-tr-2406)
PROTECTIVE CLOTHING
design of plastic ventilated suit for protection of personnel against radioisotope inhalation or ingestion, 25:8691
PROTECTIVE OINTMENTS
radiosterilization of ophthalmic, in relation to radiosensitivity of chloramphenicol and hydrocortisone acetate moieties, 25:8826
PROTEINS
binding to carcinogenic carbon-14-labeled nitroquinone oxide in cell cultures, 25:8746
chemistry of, isoelectric separation in, 25:10413(T) (UCRL-Trans-1428)
plutonium binding with, in bones and liver, 25:8595(T) (LF-tr-41, pp 7-125)
PROTONS
dosimetry during space flight, use of nuclear emulsions to determine, 25:8682
effects on excitability of brain of rats, effects of dose on, 25:8758(R) (UCB-34-P-82-10)
effects on hematopoietic system in dogs, effectiveness of body shielding for protection against, 25:8755(T) (JPRS-51660)
effects on silicon--silica structures at 50 keV, electric charges induced in, 25:9566
effects on surface blistering in aluminum at 100 keV, correlation with hydrogen degassing, 25:8905
effects on survival of cabbage and radish plants, combined effects of γ on, 25:8755(T) (JPRS-51660)
energy flux in radiation belts in 1966, fast, (E), 25:9354
flux in interplanetary space, (E), 25:9257
interactions anti p + p → anti n + n at 1.8 GeV/c, differential cross sections for, (E), 25:9644
interactions anti p + p → anti p + p at 3.55 GeV/c, spark chamber study of differential cross sections for, (E), 25:9684
interactions anti p + p → anti p + p eikonal Regge model for, (T), 25:9776
interactions anti p + p → $K^+ + K^-$ in liquid-propane bubble chamber, fraction of annihilation, (E), 25:9645
interactions anti p + p → $K^+ + K^-$ in liquid-propane bubble chamber, fraction of annihilation, (E), 25:9645
interactions anti p + p → $\pi^+ + \pi^+ + \pi^- + \pi^- + n\pi^0$ at 1.6 to 2.2 GeV/c, upper limits for production cross sections for, (E), 25:9643
interactions anti p + p → $\pi^+ + \pi^+ + \pi^- + \pi^-$ at 1.63 to 2.20 GeV/c, rho--ω interference in, (E), 25:9647
interactions anti p + p → $\pi^+ + \pi^-$ in liquid-propane bubble chamber, fraction of annihilation, (E), 25:9645
interactions anti p + p at 49.4 to 181 MeV, anti p polarization from elastic, (E), 25:9646
interactions anti p + p at high energies, Regge-pole model for elastic, (T), 25:9813
interactions anti p + p, eikonal Regge model for elastic, 25:9755
interactions anti p + p, theory of linearly rising trajectories for annihilation, 25:9769
interactions e + p → e + N^*, simple harmonic forces in nonrelativistic quark model for, (T), 25:9788
interactions e + p → e + p + π^0, angular distributions and cross sections for $\Delta(1236)$ production in, (E), 25:9625
interactions e + p, relation among asymptotic behavior of amplitude, spectral function of current commutator, and sum rules for Schwinger term for, 25:9701 (ITF-70-73)
interactions e + p, relation between p + p interactions at high energies and deep inelastic, 25:9805
interactions γ + p → 2π + p at high energies, determination of $\pi\pi$ scattering phase shifts from, (T), 25:9767
interactions γ + p → $\Delta^{++} + \pi^-$ below 5.8 GeV, density matrix elements and spin population resonance parameters in, (E/T), 25:9678
interactions γ + p → eta + p at 4 and 6 GeV, Veneziano model for, (T), 25:9712
interactions γ + p → $K^+ + \Lambda$ at threshold to 2.0 GeV, multipole analysis of, (E/T), 25:9728
interactions γ + p → $K^+ + \Sigma^0$ at threshold to 2.0 GeV, multipole analysis of, (E/T), 25:9728
interactions γ + p → n + π^+ at 260 to 350 MeV, absolute differential cross sections and $P_{11}(1470)$ production in, (E), 25:9623
interactions γ + p → n + π^+, low-energy theorems for, 25:9721
interactions γ + p → p + π^0, low-energy theorems for, 25:9721
interactions γ + p → p + rho^0 below 5.8 GeV, density matrix elements and spin population resonance parameters in, (E/T), 25:9678
interactions γ + p → phi + p, Cheng--Wu picture for, (T), 25:9716
interactions γ + p → π^+ + n at 3.4 GeV at small momentum transfers, cross section asymmetry for, (E), 25:9624
interactions γ + p → π^+ + n in Veneziano model, cross sections for, 25:9717
interactions γ + p → rho^0 + p, Cheng--Wu picture for, (T), 25:9716
interactions γ + p, computer program using Monte Carlo method for determining incident beam energy spectrum from electron pairs from, (T), 25:9705 (SLAC-123)
interactions γ + p, fits to differential cross sections for π production in, 25:9727
interactions K^+ + p → K^+ + p + ω at 9 GeV/c, test of double-Regge behavior of generalized Veneziano model for, 25:9797
interactions K^- + p → K^- + p at 0.98 to 1.34 GeV, anti KN partial-wave amplitudes from, (E/T), 25:9667
interactions K^+ + p → K^+ + p at 3.55 to 6.9 GeV/c spark chamber study of differential cross sections for, (E), 25:9684
interactions K^- + p → K^- + p at 3.55 to 6.9 GeV/c, spark chamber study of differential cross sections for, (E), 25:9684
interactions K^+ + p → $K^+(K^0)$ + $\pi^-(\pi^0)$ + π^+ + p at 10 GeV/c, low-mass enhancements in K$\pi\pi$ spectrum from, (E), 25:9679
interactions K^- + p → Λ + π^0 at 1.865 to 2.001 GeV in hydrogen bubble chamber, properties of $\Sigma(1910)$ from, (E), 25:9659 (UCRL-19789)
interactions K^- + p → p + K^- + $M^0(953)$ at 3.9 and 4.6 GeV/c in hydrogen bubble chamber, mass and width of M(953) in, (E), 25:9683
interactions K^+ + p at 0.36 to 0.72 GeV/c, total cross sections for, (E), 25:9673
interactions K^- + p at 0.36 to 0.72 GeV/c, total cross sections for, (E), 25:9673
interactions K^+ + p, eikonal Regge model for elastic, 25:9755
interactions K^- + p, eikonal Regge model for elastic, 25:9755
interactions Λ + p at 1 to 5 GeV/c in hydrogen bubble chamber, elastic and total cross sections and final-state resonance production in, (E), 25:9631
interactions n + p at 700 to 2900 MeV/c, direct measurement of total cross sections for, (E), 25:9648
interactions p + d at 2.784 GeV/c, momentum spectra in, (E), 25:9634 (COO-1764-115)
interactions p + p → p + N^*, surface excitation model for, (T), 25:9808
interactions p + p → p + p + π^0 at low and moderate energies, differential cross sections for, 25:9819
interactions p + p → π + particle at high energy, O(3,1) analysis of single-particle spectra in, 25:9816
interactions p + p at 20 and 300 GeV/c, thermodynamic model for angular distribution of π^- production in, 25:9787
interactions p + p at 90 to 800 GeV, spark-chamber--ionization-calorimeter study of charged-particle multiplicities in, (E), 25:9638
interactions p + p at high energies, Regge-pole model for elastic, (T), 25:9813
interactions p + p at high energies, relation between deep inelastic e + p interactions and inelastic, 25:9805
interactions p + p at ultrahigh energies, models for quark production cross sections from, (T), 25:9811
interactions p + p below 30 MeV, two-parameter description of ^3P phase shifts for n + n scattering length from comprehensive analysis of, (T), 25:9814
interactions p + p, bootstrap model for derivation of Wu and Yang conjecture for cross sections of, (T), 25:9809
interactions p + p, eikonal Regge model for elastic, 25:9755
interactions p + p, two-particle symmetry group for phase

XUM

shift of elastic, 25:9818
interactions π^- + p → $2\pi^-$ + π^+ + p at 5.0 to 7.5 GeV/c in bubble chamber, coherence of isoscalar and isovector exchange amplitudes for A_2^- production in, (E), 25:9650 (COO-1195-202)
interactions π^+ + p → $2\pi^+$ + π^- + p at 7.0 to 8.5 GeV/c in bubble chamber, coherence of isoscalar and isovector exchange amplitudes for A_2^+ production in, (E), 25:9650 (COO-1195-202)
interactions π^+ + p → Δ^{++} + A_2^0 at 5 GeV/c, cross sections and spin-density matrix elements, (E), 25:9682
interactions π^+ + p → Δ^{++} + eta^0 at 5 GeV/c, cross sections and spin-density matrix elements for, (E), 25:9682
interactions π^+ + p → Δ^{++} + f^0 at 5 GeV/c, cross sections and spin-density matrix elements for, (E), 25:9682
interactions π^+ + p → Δ^{++} + ω^0 at 5 GeV/c, cross sections and spin-density matrix elements for, (E), 25:9682
interactions π^+ + p → Δ^{++} + rho^0 at 5 GeV/c, cross sections and spin-density matrix elements for, (E), 25:9682
interactions π^- + p → n + 2γ at 3.65 GeV/c, spark chamber and scintillation counter study of eta' production in, (E), 25:9651 (COO-1764-111)
interactions π^- + p → n + π^+ + π^- at 2 to 6 GeV/c, spark chamber study of differential cross sections and density matrix elements for rho and f^0 production in backward, (E), 25:9654 (COO-1764-114)
interactions π^+ + p → p + $2\pi^+$ + π^- 2.34 GeV/c, resonance production cross sections in, (E), 25:9662
interactions π^+ + p → p + A_2^+ at 5 GeV/c, cross sections and spin-density matrix elements for, (E), 25:9682
interactions π^+ + p → p + B^+ at 5 GeV/c, cross sections and spin-density matrix elements for, (E), 25:9682
interactions π^- + p → p + π^+ + $2\pi^-$ at 4.47 GeV/c in hydrogen bubble chamber Δ^{++}(1236) production and π^+ + p virtual scattering and π^- + π^- scattering cross sections and angular distributions in, (E), 25:9655 (ITEF-767)
interactions π^- + p → p + π^- + neutral boson state at 8 GeV/c, search for higher-mass resonances in, (E), 25:9676
interactions π^- + p → p + π^+ + π^- + π^- + neutral boson state at 8 GeV/c, search for higher-mass resonances in, (E), 25:9676
interactions π^+ + p → p + rho^+ at 5.2 GeV/c, differential cross section for backward rho^+ production in, (E), 25:9665
interactions π^+ + p → p(n) + $2\pi^+$ + π^- + $\pi^0(\pi^+)$ at 2.34 GeV/c, resonance production cross sections in, (E), 25:9662
interactions π^- + p → π + π + N at 2.77 GeV/c, $\pi\pi$ phase shifts from, (E/T), 25:9670
interactions π^- + p → π^0 + n at 2 to 6 GeV/c, differential cross sections for backward, (E), 25:9674
interactions π^- + p → π^0 + n at 2 to 6 GeV/c, differential cross sections, isospin, u- and s-channel amplitudes and phase for backward, (E), 25:9653 (COO-1764-113)
interactions π^- + p → π^0 + n in Veneziano model, polarization in, 25:9793
interactions π^- + p → π^0 + π^0 + n at 378 MeV, S-wave π + π scattering length from, (E), 25:9668
interactions π^- + p → π^- + p at 1.71 to 5.53 GeV/c, scintillation counter spectrometer study of (2290) enhancement in differential cross sections for, (E), 25:9652 (COO-1764-112)
interactions π^+ + p → π^+ + p at 2.85 to 6.9 GeV/c, spark chamber study of angular distributions for, (E), 25:9684
interactions π^- + p → π^- + p at 2.85 to 6.9 GeV/c, spark chamber study of angular distributions for, (E), 25:9684
interactions π^- + p → π^- + π^+ + n at 2.77 GeV/c, elastic cross section for π^+ + π^- interactions from, (E/T), 25:9669
interactions π^- + p → π^+ + π^- + n, resonance approximation for rho production in, 25:9894
interactions π^- + p → π^- + $\pi^+(\omega^0)$ + n(p), Veneziano model prediction of rho'' daughter resonance contribution to amplitudes of, (T), 25:9786
interactions π^- + p → rho^0 + π^- + p at 4.45 GeV/c in hydrogen bubble chamber, differential cross sections and mass distributions for, (E), 25:9663
interactions π^- + p → rho^0 + π^- + p at 4.45 GeV/c in hydrogen bubble chamber, mass distributions for, (E), 25:9656 (ITEF-775)
interactions π^+ + p at 0.82 to 2.74 GeV/c, polarization and differential cross section for elastic, (E), 25:9680
interactions π^+ + p at 18.5 GeV/c, cross sections for production of rho^0, f^0, g^0, eta^0, ω^0, and Δ^{++}(1236) in, (E), 25:9677
interactions π^+ + p at 8 GeV/c, density matrix elements and spin population resonance parameters in, (E/T), 25:9678
interactions π^+ + p in π^- + p → p + π^+ + $2\pi^-$ interactions at 4.47 GeV/c in hydrogen bubble chamber, virtual, (E), 25:9655 (ITEF-767)
interactions π^+ + p, eikonal Regge model for elastic, 25:9755
interactions π^- + p, eikonal Regge model for elastic, 25:9755
interactions π^+ + p, sum rules for amplitude ratio of π^- + p interactions to, (T), 25:9789
interactions π^- + p, sum rules for amplitude ratio of π^+ + p interactions to, (T), 25:9789
magnetic moment of, measurement using omegatron, (E), 25:9622
magnetic moment of, polarization function for calculation of anomalous, (T), 25:9867
mass of, formulas for relation with gravitational constant for, (T), 25:9878
range in air, nitrogen, and oxygen at 0.2 to 2.0 MeV, relation to energy, (E), 25:9162 (SC-RR-70-788)
range in liquid hydrogen, (T), 25:9166
reactions (p,d) with lead-210, analysis using calculated form factors, (T), 25:10067
reactions (p,d) with neodymium-142, praseodymium-141, and samarium-144, angular distribution for, (E), 25:9978(R) (ORO-3398-26)
reactions (p,d) with nuclei in the lead region, realistic form factors for, (T), 25:10067
reactions (p,f) with thorium-232 at 11.3 MeV, fission-product yields and mass and charge distributions from, (E/T), 25:10054
reactions (p,f) with uranium-238 at 11.2 MeV, excitation functions and mass yield curves for, (E/T), 25:10052
reactions (p,γ) with nitrogen-15 at 4.1 to 12.8 MeV, gamma spectra from, (E), 25:9979
reactions (p,n) and (p,np) with bismuth-209 at 24 to 30 MeV, ground-state studies by, (E/T), 25:10045
reactions (p,n) with scandium-45 at 2.8 to 5.6 MeV, neutron and γ spectra and angular distributions for, (E), 25:10003
reactions (p,pn) with nuclei at 17 MeV, mechanism of, (E), 25:10005
reactions (p,t) with neon-20 at 50 MeV, differential cross sections for, (E), 25:10006
reactions (p,t) with palladium-108 and silver-109 at 19 MeV, angular distributions for, (E), 25:9966(R) (COO-1265-94)
reactions (p,t) with samarium-144, angular distributions and Q-value for, (E), 25:9978(R) (ORO-3398-26)
reactions with acetylene, ammonia, benzene, krypton, and xenon at 15 to 150 keV, cross sections for charge exchange in, (E), 25:9229
reactions with argon, helium, hydrogen, and nitrogen at 75 to 350 keV, total cross sections for formation of fast excited hydrogen atoms by charge exchange in, (E), 25:9192(R) (ORO-2591-51)
reactions with argon, helium, nitrogen, and oxygen gases at 4 to 26 keV, total cross sections for formation of metastable hydrogen atoms by charge exchange in, (E), 25:9193 (ORO-2591-52)
reactions with emulsion nuclei at high energies, mass distribution and decays of hyperfragments produced in, (E), 25:9637
reactions with helium at 10 keV, differential cross sections for formation of metastable hydrogen atoms by charge exchange in, (E), 25:9192(R) (ORO-2591-51)
reactions with helium at 100 to 300 keV, energy spectra of electrons ejected in, (E), 25:9241
reactions with hydrogen atoms, probability of charge exchange and excitation to 2s state in, (T), 25:9201
reactions with hydrogen atoms, use of Faddeev equations and Coulomb T matrix in calculation of asymptotic amplitude for electron capture in, 25:9211
reactions with hydrogen excited atoms, quantal eight-state approximation for resonance charge exchange in, 25:9203
reactions with nitrogen molecules at 1 to 5 MeV, fluorescence efficiencies for excitation in, (E), 25:9234
reactions with nuclei at 26 GeV in emulsions, emission of excess of light mesons in relation to Dalitz pairs in, (E), 25:9642
reactions with nuclei at 80 TeV in emulsions, aleph baryon production in, (E), 25:9641
reactions with positronium, generalized variational bounds and coupled-static approximation for, (T), 25:9216
reactions with xenon at 0.3 to 2.0 MeV, angular and energy distributions of electrons from, (E), 25:9191 (BNWL-SA-3631)
scattering by argon-40, calcium-48, and neon-22, fine-structure analysis of isobaric analog resonances in elastic, (T), 25:10073
scattering by cadmium-114, zinc-68, and zirconium-90 at 18.6 MeV, angular distributions for elastic, (E), 25:9966(R) (COO-1265-94)
scattering by carbon-12 at 1 GeV, differential cross section for elastic, (T), 25:9983
scattering by copper at 0.407, 0.851, and 1.45 MeV, angular distributions and effective atomic numbers for multiple, (E), 25:9163
scattering by samarium-144 at 30 MeV, optical model analysis of elastic, (E), 25:9978(R) (ORO-3398-26)
scattering by strontium-88 at 8.5 to 12 MeV, excitation functions for elastic and inelastic, (E), 25:10011
scattering by tin-120, -122, and -124 at 9.85 to 10.90 MeV, angular distributions and polarization for

elastic, (E), 25:10044
scattering by tissue-equivalent gas mixtures at 2.78 MeV, measurement of multiple, 25:8482 (NYO-2740-7, pp 112-53)
scattering by ytterbium-176 at 19 MeV, angular distributions for elastic and inelastic, (E), 25:9966(R) (COO-1265-94)
spectra of, in solar wind, (E), 25:9102
PROTONS (anti p)
interactions anti p + d → anti p + d + π^+ + π^- + π^0 at 7.0 GeV/c in bubble chamber, anti Δ^{--}(1236) and d^* enhancement production and cross sections for, (E), 25:9636 (TID-25610)
interactions anti p + d → anti p + d(p + n) + π^+ + π^- at 7.0 GeV/c in bubble chamber, anti Δ^{--}(1236) and d^* enhancement production and cross sections for, (E), 25:9636 (TID-25610)
interactions anti p + d → K^- + d(p + n) + Λ at 7.0 GeV/c in bubble chamber, cross sections for, (E), 25:9636 (TID-25610)
interactions anti p + n → anti p + n at 3.5 GeV/c in bubble chamber, differential and total cross sections for, (E), 25:9649
interactions anti p + n → π^- + π^- + π^+, dual formula for hole structure in Dalitz plot for, 25:9770
interactions anti p + n, theory of linearly rising trajectories for annihilation, 25:9769
interactions anti p + p → anti n + n at 1.8 GeV/c, differential cross sections for, (E), 25:9644
interactions anti p + p → anti p + p at 3.55 GeV/c, spark chamber study of differential cross sections for, (E), 25:9684
interactions anti p + p → anti p + p eikonal Regge model for, (T), 25:9776
interactions anti p + p → π^+ + π^+ + π^- + π^- + $n\pi^0$ at 1.6 to 2.2 GeV/c, upper limits for production cross sections for, (E), 25:9643
interactions anti p + p → π^+ + π^+ + π^- + π^- at 1.63 to 2.20 GeV/c, rho--ω interference in, (E), 25:9647
interactions anti p + p → π^+ + π^- in liquid-propane bubble chamber, fraction of annihilation, (E), 25:9645
interactions anti p + p at 49.4 to 181 MeV, anti p polarization from elastic, (E), 25:9646
interactions anti p + p at high energies, Regge-pole model for elastic, (T), 25:9813
interactions anti p + p, eikonal Regge model for elastic, 25:9755
interactions anti p + p, theory of linearly rising trajectories for annihilation, 25:9769
PROTOZOA
Amoeba sp., function of Golgi apparatus in, 25:10338(T) (ANL-Trans-866)
Tetrahymena pyriformis, radiation damage to, repair replication of uv, 25:8636 (SU-326-P-7-X-22)
PRUSSIAN BLUE
effectiveness for removal of cesium-137 from rats, 25:8662(T) (UCRL-Trans-10488)
preparation of colloidally-soluble, methods for, 25:8662(T) (UCRL-Trans-10488)
PUERTO RICO
nuclear power plants in, programming for optimum economics of, 25:10291 (TID-25630)
PULSARS
angular momentum loss in, due to gravitational radiation, (T), 25:9063
cosmic-particle acceleration by, (T), 25:9253 (MPI-PAE/EXTRATERR-47)
CP 0328, drifting of spectral features of, (E), 25:9059
CP 0834, drifting of spectral features of, (E), 25:9059
CP 1133, drifting of spectral features of, (E), 25:9059
CP 1919, drifting of spectral features of, (E), 25:9059
detection of, optical, (E), 25:9090
electron emission from Vela X, high-energy, (T), 25:9256
emission mechanisms for, antenna, (T), 25:9070
luminosity of, secular decrease of optical and x-ray, (E), 25:9092
neutron emission from, (T), 25:9253 (MPI-PAE/EXTRATERR-47)
NP 0532, accurate timing of light flashes during 1969--1970 season, (E), 25:9089
NP 0532, decrease of optical luminosity of, (E), 25:9092
NP 0532, detection of low-energy pulsed γ rays from, (E), 25:9062
NP 0532, optical and x-ray bursts from, (T), 25:9072
optical pulses from fifteen, limits for, (E), 25:9061
PSR 0833, luminosity of, (E), 25:9092
PSR 1237 + 25, correlated subpulse structure in, (E), 25:9064
pulse characteristics of, (T), 25:9072
scintillation of, interstellar, (T), 25:9072
scintillations at 2388 MHz, interstellar, (E), 25:9091
PULSE ANALYZERS
dead time correction for measuring half-life of short-lived radioisotopes, 25:8515
PULSE DISCRIMINATORS
circuit analysis for proportional detectors, 25:8516
design and performance of high speed, 25:8507
performance for neutron--gamma discrimination in liquid scintillation detectors, 25:8506
PULSE GENERATORS (ELECTRONICS)
design for stabilizing nuclear spectrometer circuit, 25:8542
design of digital rf burst, for NMR relaxation measurements, 25:8575
design of high-voltage, for deflector plates for beam injection system for ITEP 7-GeV synchrotron, 25:9932
design of high-voltage, for deflector plates for beam injection system for ITEP 7-GeV synchrotron, 25:9931
design of sawtooth current, for studying superconductivity, 25:8580
PULSE SHAPERS
design with zero regeneration time for elimination of pulse pile-up, 25:8545 (JINR-P13-5377)
PUMPS
bearings for high-capacity sodium, development of sodium-lubricated, 25:8394(R) (NYO-3930-7)
design criteria for pressurized water reactor, analysis of aseismic, (E/T), 25:10248
design of screw-type, for transferring wastes in phosphate glass process, engineering drawings for, 25:8457
PUPAE
radioinduced inhibition of imago formation in, of Sarcophaga, effects of dose on strontium-90 β, 25:8749(T) (NSJ-tr-156)
PYRUVATE KINASE
dichroism of, effects of univalent cations on circular, 25:10369 (RLO-2227-T-5-4)

Q

Q DEVICES
design and operation of, 25:9522
plasma instabilities in, edge oscillation in, (T), 25:9496
research on Helios, Sept. 1970, 25:9398(R) (ORO-3895-15)
QUALITY CONTROL
methods for improving accuracy of material balance accounting systems, 25:8448 (BNWL-SA-3336)
QUANTUM ELECTRODYNAMICS
book: Lectures on Nonlinear Electrodynamics, 25:9869
divergences in, renormalization functional relations for, 25:9848
electron mass renormalization in, functional relations for, 25:9848
electron self-energy in, renormalization functional relations for solution for, 25:9848
electron wave function renormalization constants in, functional relations for, 25:9848
field energies of point charges in polarized vacuum in Lorentz-invariant, 25:9867
fields in, functional method for solutions of Klein--Gordon and Dirac equations in external, 25:9845
formulation of Lorentz-invariant, finite field energies of point charges in polarized vacuum in, 25:9867
formulation of noncovariant, molecular multipole interaction with electromagnetic field in canonical, 25:9842
gauge invariance and renormalized transition probability in, 25:9859
photon wave function renormalization constants in, functional relations for, 25:9848
renormalization in, consequences of, 25:9861
scattering amplitudes in, operator-droplet model for, 25:9860
Schwinger terms in fermion, 25:9852
self-consistency in, renormalization functional relations for, 25:9848
QUANTUM FIELD THEORY
Bethe--Salpeter equation for, N/D method for, 25:9856
Bethe--Salpeter equation in, spectral functions and expansion in spherical harmonics of, 25:9855
book: Formulations of Classical and Quantum Dynamical Theory, 25:9840
book: Particles, Sources, and Fields, 25:9699
bootstrap formulation in local, 25:9690 (NYO-2171-331)
boson states in two-dimensional, C^* algebra for, 25:9850
charge operators in general, rigged Hilbert space formalism for, 25:9838 (NYO-3829-60)
commutators in axiomatic, equal-time, 25:9837 (ITF-70-57)
fermion states in two-dimensional, C^* algebra for, 25:9850
field commutant in, criterion of algebraic closeness of, 25:9844
field equation in SL(2,C) x D x O(3), mass spectra and wave functions from, 25:9853
field interaction in, Hamiltonian for gauge-independent spin-one, 25:9854
field interactions with external time-dependent potentials, 25:9863
field interactions with strong external stationary field, indefinite metric for, 25:9864
field products in, logarithmic behavior in short-distance, 25:9865
formulations of massive vector, equivalent, 25:9858
model of lambda$(\text{phi}^4)_2$, without cutoffs, 25:9849
research at Pittsburgh Univ., Dec. 1969 to Dec. 1970, 25:9839(R) (NYO-3829-64)
sum rules in axiomatic, validiy of Gell-Mann--Fubini, 25:9837 (ITF-70-57)

XUM

Thirring model of, energy--momentum tensors and scale invariance in, 25:9862
Ward identities in axiomatic, validity of normal, 25:9837 (ITF-70-57)
Yang--Mills field in, S-matrix formulation for, 25:9857
Yang--Mills field, cancellation between longitudinal and scalar components in interactions of massless, 25:9851
QUANTUM MECHANICS
algorithms for calculation of eigenvalues of two-center problem in, (T), 25:9600 (JINR-P4-5040)
book: Formulations of Classical and Quantum Dynamical Theory, 25:9840
eigenfrequencies of wave equation for finite domain, distribution of, 25:9604
formulation of relativistic, for spin-$^1/_2$ fermions in external electromagnetic field, 25:9841
measurement problem in, insolubility of, 25:9612
measurements in, theory for, 25:9603
research at Pittsburgh Univ., Dec. 1969 to Dec. 1970, 25:9839(R) (NYO-3829-64)
Schroedinger equation with damping for system weakly coupled to thermal bath, 25:9607
Schroedinger equation, reduction of potential of, according to scattering data, 25:9610
transformations applied to Dirac equation, nonrelativistic, (T), 25:9599 (JINR-P2-5314)
vacuum expectation values of exponential operators in, 25:9847
QUASARS
atmosphere of PHL 5200, formation of resonance lines in, (T), 25:9044
carbon ion abundance in, (E), 25:9074
helium abundance in, (E), 25:9074
hydrogen abundance in, (E), 25:9074
identification of southern hemisphere, (E), 25:9067
mass loss from nuclei of, (T), 25:9130
models for, slow rotation of relativistic polytropic, (T), 25:9078
quark fusion in, (T), 25:9075
radiation fields in nuclei of, (T), 25:9130
spectra of, mechanism for high-frequency radio, (T), 25:9085
spectral classification of Markaryan galaxies as, (E), 25:9140
spectrophotometry of, (E), 25:9074
QUINOLINE, 4-NITRO-, 1-OXIDE
effects of carbon-14-labeled, on colony formation, DNA, proteins, and RNA of cultured cells, 25:8746
effects on DNA in cultured mammalian cells, repair processes following carcinogenic, 25:8611

R

RABBITS
radiation effects on activity of glycolytic enzymes of, sublethal ionizing, 25:8779
radiation effects on antibody production in immunized, following stimulation by G and M gamma globulins, x, 25:8621
radiation effects on content of albumins and globulins in blood serum and brain tissues of, microwave, 25:8784
radiation effects on lysozyme content of blood serum and osmotic resistance of erythrocytes in, whole-body uv, 25:8782
radiation effects on retina of, use of electroretinogram for comparing toxic thermal neutron and x, 25:8761
RADIATION
dosimetry for radioisotope uses in medical diagnosis and metabolic studies, computer program for, 25:8716
effects of pulsed, on gold chloride solutions, 25:8306
effects on activity of glycolytic enzymes of rabbits, sublethal ionizing, 25:8779
effects on aqueous solutions of oxygen, 25:8295
effects on aqueous solutions of oxygen, 25:8293
effects on cell division and mitotic delay in Oedogonium cardiacum, effects of dose rate on, 25:8644
effects on chloramphenicol and hydrocortisone acetate in relation to sterilization of ophthalmic ointments, 25:8826
effects on cultured cells, effects of total dose as function of dose rate on recovery from lethal, 25:8748
effects on diodes and bipolar transistors, transient, 25:8581 (LYCEN-6933)
effects on ethane or propane, method for accumulating energy produced by, 25:8292(P)
effects on eyes, protection against pathological ionizing, 25:8793
effects on function of vestibulocochlear analysor in man following cancer therapy, 25:8792
effects on hematopoiesis in rats, effects of dose rate on, 25:8608
effects on human gastrointestinal tract and interstitial tissues during therapy, high-energy ionizing, 25:8739
effects on immune reactions of animals following transplantation of hematopoietic cells, review of, 25:8616
effects on immune reactions of dogs, man, and monkeys prior to bone marrow grafting, 25:8617
effects on living organisms, in comparison with age, environment, and thermal energy, information theory for studying, 25:8742
effects on lymph system in mammals, relation of, to antibody formation, ionizing, 25:8762
effects on mitosis in kidney cells of mice, whole-body, 25:8763
effects on organic sulfides, mass-spectrometric studies on, 25:8290
effects on ovulation by man, effects of age on dose required for suppression of, ionizing, 25:8732
effects on personnel, legislation related to compensation for injuries caused by, in USA, 25:8697
effects on plants, use of mutagenic, for crop improvement, 25:8635 (STI/DOC-10/119)
effects on residue from Valencia oranges, effects of, on methoxyl content, viscosity, and yield of pectins, 25:8823
effects on sodium chloride crystals, anion-vacancy processes occurring after F-light bleaching of, 25:9559
effects on storage life of mushrooms, ionizing, 25:8821(P)
effects on survival of mammalian tissue in vivo, determination of survival curve for, 25:8777
effects on tissues of potatoes, determination of histological, 25:8802
effects on transfer of antibody-forming clone cells in mice, 25:8769
hazards to personnel and surrounding environs at Goodyear Atomic Corporation during 1969, progress report on programs for controlling and reducing, 25:8692(R) (GAT-627)
transport in infinite and semi-infinite media, (T), 25:9009
use for therapy of malignant tumors in animals and man, pathology of lung fibrosis following, 25:8791
RADIATION CHEMISTRY
equipment and experiment development for pulse radiolysis, 25:8285(R) (RPI-3821-5)
RADIATION DETECTORS
book: Electronics for Nuclear Particle Analysis, 25:8488
cables for remote, design of coaxial, 25:8493(P)
calibration of, 14-MeV neutron source for, 25:9940 (BARC-499)
conference on position--sensitive, 25:8469 (JUL-CONF-4)
data acquisition system for pulse-type, development of modular, 25:8483 (PH-1)
dead time correction for multichannel analyzer for measuring half-life of short-lived radioisotopes, 25:8515
development for area, environmental, and personnel monitoring at AECL during 1970, 25:8666(R) (AECL-3728)
development for radiological protection during radiotherapy, survey on, 25:8487
geometry calculations for target--, computer program for solid angle and angular acceptance, 25:9910 (LUSY-7007)
response to material changes in subcritical reactors, use of few-group diffusion theory for prediction of, (E/T), 25:10322
uses of position-sensitive, for simultaneous determination of several parameters of particles, 25:8475 (JUL-CONF-4, pp 59-70)
windows for, for spectroscopy, 25:8534(P)
RADIATION DETECTORS, ACTIVATION
performance of indium and sulfur, for measuring criticality accident fast neutron dose, 25:10181
performance of various, for neutron spectra measurements at 1 eV to 10 keV, 25:8481 (KFK-1233)
response of cadmium-shielded paraffin-moderated indium, for fast neutron flux measurements, 25:8495
RADIATION DETECTORS, BUBBLE CHAMBER
magnet for 25-liter, 70-kOe pulsed, 25:8555
particle tracks in, DAPR system at LRL for analysis of, 25:8548 (UCRL-20126)
particle tracks in, distribution function for Coulomb multiple scattering effects for analysis of, 25:8559
particle tracks in, least squares and maximum probability methods for determining kinematic parameters of, 25:8558
particle tracks in, review on measuring devices for analysis of, 25:8554
resolution of 1- to 2-meter, Monte Carlo study of, 25:8549 (UR-875-324)
RADIATION DETECTORS, CLOUD CHAMBER
design and operation of discharge--condensation, 25:8551
RADIATION DETECTORS, FISSION CHAMBER
description of neutron source-monitoring, 25:8447(R) (BHO-65-1)
design with alarm system for criticality detection at fuel reprocessing plant, 25:8486
RADIATION DETECTORS, GEIGER-MUELLER
calibration for environmental monitoring of krypton-85, 25:8467 (BRH/NERHL-70-4)
design of internally-loaded, for measuring low-level beta activity of gases, 25:8520
sensitivity for environmental monitoring of krypton-85, 25:8467 (BRH/NERHL-70-4)
RADIATION DETECTORS, IONIZATION CHAMBER
calibration for environmental monitoring of krypton-85, 25:8467 (BRH/NERHL-70-4)
design and performance for californium-252 neutron dosimetry, 25:8677 (NYO-2740-7, pp 5-51)

design of gridded, for spectra measurements in alpha decay of beryllium-8, 25:8513
design of miniature end-window, for low-level beta detection, 25:8521
design of tissue-equivalent, for rem dose rate measurements, 25:8562 (CERN/DI/HP-29)
development for dosimetry, 25:8482 (NYO-2740-7, pp 112-53)
electron transport in tissue-equivalent, 25:8482 (NYO-2740-7, pp 112-53)
performance for detection of 5 to 150 kV x rays, 25:8672 (ICRU-17)
sensitivity for environmental monitoring of krypton-85, 25:8467 (BRH/NERHL-70-4)

RADIATION DETECTORS, PROPORTIONAL
calibration of Rossi tissue-equivalent, for LET spectra measurements, 25:8492
circuit for multiwire, design of threshold and delay, 25:8468 (CEAL-1054)
circuit for polyethylene-moderated boron trifluoride, self-auditing, 25:8501
circuit for telescope, for charged particle identification, 25:8530
circuits for position-sensitive, analog division, 25:8471 (JUL-CONF-4, pp 11-21)
description for delayed neutron detection in uranium scrap analysis, 25:8447(R) (BHO-65-1)
description of position-sensitive, for use with magnetic spectrographs, 25:8476 (JUL-CONF-4, pp 71-120)
design and operation of satellite-borne, for measurement of soft solar x rays, 25:8499
design for determination of iron-55 in blood and other liquids, 25:8466 (BNWL-SA-3624)
design of end-window variable geometry, for x ray detection, 25:8510
design of position-sensitive multiwire, for use with split-pole magnetic spectrograph, 25:8478 (JUL-CONF-4, pp 141-7)
design of position-sensitive multiwire, for use wth magnetic spectrograph, 25:8479 (JUL-CONF-4, pp 148-64)
development and research on wall-less, 25:8563 (NYO-2740-7, pp 52-110)
development of position-sensitive, 25:8470 (JUL-CONF-4, pp 1-10)
development of position-sensitive multiwire, 25:8477 (JUL-CONF-4, pp 121-40)
performance of position-sensitive array of boron trifluoride, for neutron detection, 25:8473 (JUL-CONF-4, pp 30-47)
performance of position-sensitive, for use in magnetic beta spectrometer, 25:8472 (JUL-CONF-4, pp 22-9)
pulse shape discrimination systems for, theory of, 25:8516
resolution of argon--methane, energy dependence of pulse-height, 25:8505
use of helium-3, for antineutrino and collapsing star detection, 25:8550

RADIATION DETECTORS, SCINTILLATION
calibration for environmental monitoring of krypton-85, 25:8467 (BRH/NERHL-70-4)
calibration of thallium-activated sodium iodide, for gamma spectroscopy, 25:8535
circuit for telescope, for charged particle identification, 25:8530
design and performance of internal source, for measurement of electron capture ratios, 25:8514
design and performance of large-volume mineral oil-based liquid, for neutron detection, 25:8547 (PURC-4159-13)
efficiency of large liquid, for neutron detection at 40 to 400 MeV, 25:8512
efficiency of NE213 from neutrons of 2 to 14.5 MeV, absolute, (E), 25:9968 (NP-18488)
efficiency of thallium-activated cesium iodide, relative photopeak, 25:8502
light output and scintillation time of polystyrene-based plastic, effects of natural light on, 25:8528
performance for partial- or whole-body measurements of γ from radioisotopes deposited in human body, evaluation of counting geometry for, 25:8687
performance of petroleum-based liquid, 25:8527
properties of europium-activated lithium-6 iodide, at low temperatures, 25:8529
pulse shape discriminator for neutron--gamma discrimination in NE213 liquid, 25:8507
pulse shape discriminator system for stilbene, for neutron and gamma discrimination, 25:8525
pulse shape discriminators for neutron--gamma discrimination in liquid, performance of, 25:8506
quenching of toluene-base liquid, with copper and iron powder, 25:8526
response of mineral oil-based liquid, to ionizing particles, 25:8511
sensitivity for environmental monitoring of krypton-85, 25:8467 (BRH/NERHL-70-4)
sensitivity of spherical polyethylene-moderated, for neutrons from thermal to 10 MeV, 25:8522
solvents for liquid, comparison of pulse shape discrimination capabilities of, 25:8504
spectra analysis for stilbene, for fast neutron flux measurements, 25:8509
use of liquid, for nuclear spectroscopy, review on, 25:8539

RADIATION DETECTORS, SEMICONDUCTOR
circuits for position-sensitive, analog division, 25:8471 (JUL-CONF-4, pp 11-21)
design and performance of coincidence system for measurement of x-ray-to-alpha ratios in alpha decay of transuranic elements, 25:8465 (BNWL-SA-1514)
preamplifier for surface-barrier, for neutron collimation, current, 25:8519
resolution of gallium-arsenide, for alpha particles and gamma rays, 25:8491

RADIATION DETECTORS, SEMICONDUCTOR (GERMANIUM)
description of scanning-type, for determining fuel element burnup, 25:8951(R) (GEAP-10217)
design and performance of lithium-drifted, for gamma spectroscopy, 25:8541
fabrication by ion implantation, 25:8484(P)
fabrication of lithium-drifted, for gamma spectroscopy, 25:8463 (BLG-447)
shielding for lithium-drifted, with californium-252 source for neutron capture gamma spectroscopy, 25:8537

RADIATION DETECTORS, SEMICONDUCTOR (SILICON)
characteristics of, 25:8523
design and performance of lithium-drifted, 25:8546 (LYCEN-6847)
design and performance of position-sensitive, for use with magnetic charged-particle spectrometer, 25:8474 (JUL-CONF-4, pp 48-58)
design of low-temperature p--n junction, for fast neutron dosimetry, 25:8565(P)
design of thin-window surface-barrier, 25:8498(P)
fabrication and performance of small diffused, for medical and biological uses, 25:8464 (BMBW-FBK-70-15)
fabrication by ion implantation, 25:8484(P)
fabrication of lithium-drifted, 25:8546 (LYCEN-6847)
performance for γ transmission scanning, for measurement of antimony content of human lungs using iodine-125 source, 25:8726
resolution of surface-barrier, for electron detection at 10 to 100 keV, energy dependence of, 25:8524
sensitivity of rectangular lithium-drifted, for polarization measurements of photons, 25:8508
time resolution of telescope surface-barrier, 25:8517

RADIATION DETECTORS, SPARK CHAMBER
description of position-sensitive, for use with magnetic spectrographs, 25:8476 (JUL-CONF-4, pp 71-120)
design and performance of magnetic, for $K_2^0 + K_1^0$ regeneration studies at high energies, 25:8544 (JINR-P1-5361)
design of position-sensitive multiwire, for use with split-pole magnetic spectrograph, 25:8478 (JUL-CONF-4, pp 141-7)
design of small-angle shower, for internal synchrotron targets, 25:8553
development and uses of position-sensitive, with ferrite core memory, 25:8480 (JUL-CONF-4, pp 165-71)
efficiency at lower limit of ionization, measurement of, 25:8557
operation and performance of wire, with magnetostrictive readout, 25:8552
particle track information storage in streamer, high-voltage pulsing method for, 25:8543 (DESY-70/60)
particle tracks in magnetic spectrometer, calculation of momentum vectors for, 25:8561

RADIATION DOSE
calculations of absorbed and exposure, applications of LET for, 25:8671 (ICRU-16)
calculations of absorbed and rate of, in human radium dial painters at various time intervals following ingestion of radium-226, computer methods using decay scheme data for, 25:8669 (COO-2088-1)

RADIATION DOSIMETERS
charge trapping effects on electron dose--depth profiles in plastic, 25:8566
development for radiological protection during radiotherapy, survey on, 25:8487

RADIATION DOSIMETERS, CHEMICAL
errors in ferrous sulfate, 25:8564
performance for use for 5 to 150 kV x rays, 25:8672 (ICRU-17)

RADIATION DOSIMETERS, COLORIMETRIC
calibration of clear Perspex HX, 25:8568

RADIATION DOSIMETERS, THERMOLUMINESCENT
annealing of lithium fluoride, optical absorption correlation for pre- and post-irradiation, 25:9574
performance of TLD-100 lithium fluoride, for mixed radiations, 25:8567

RADIATION DOSIMETRY
method for intense electron pulses, thermoelastic response, 25:8569
research at Columbia Univ., July 1, 1970, 25:8676(R) (NYO-2740-7)
research at JAERI during 1969 and 1970, progress report on, 25:8693(R) (JAERI-5025)
theory of micro-, developments in, 25:8563 (NYO-2740-7, pp 52-110)

RADIATION MONITORING
equipment for ground-level, in Nevada Test Site atmosphere, development and operation of air sampling, 25:8393 (NVO-410-6)
methods for nuclear energy installations following accidents, 25:8661 (JAERI-4052)

XUM

programs at Atomic Energy Research Inst., Tokyo, during 1969 and 1970, 25:8673 (JAERI-Memo-4098)
programs at JAERI during 1969 and 1970, results of routine area, environmental, and personnel, 25:8693(R) (JAERI-5025)
programs in New Zealand during 1969, 25:8675(R) (NP-18529)
research at JAERI during 1969 and 1970, progress report on environmental, 25:8693(R) (JAERI-5025)
RADIATION PROTECTION
methods during contact γ radiotherapy of gynecological neoplasms, 25:8688 (SZS-6/70)
methods for medical personnel during preparation and application of γ emitters for interstitial therapy, 25:8689 (SZS-6/70, pp 19-27)
problems from release of radioactive effluents from power reactors, 25:10162
programs at JAERI during 1969 and 1970, progress report on, 25:8693(R) (JAERI-5025)
programs for dental and medical x-ray personnel, 25:8690
programs for nuclear installations, 25:8661 (JAERI-4052)
programs for protection of human populations in Italy in event of accidents during shipping of radioisotopes, 25:8696
standards for maximum permissible concentration of radioisotopes in body of man in Italy, 25:8698
RADIATION RATE METERS
design with noise suppression, 25:8503
RADIATION TARGET CANS
design for radioisotope production, 25:8429(T) (ORNL-tr-2400)
design for studies of oxide fuel reactions with stainless steel cladding, 25:8835 (ORNL-4600, pp 57-64)
operating safety of single-walled NaK cooled capsules for irradiation of high-power fuel pins, 25:10257(T) (EURFNR-764)
RADIATION TARGET CHAMBERS
design of gaseous, scattering spectra line shape calculations for, 25:9924
RADIATION TARGETS
design for radioisotope production, 25:8429(T) (ORNL-tr-2400)
geometry calculations for detector--, computer program for solid angle and angular acceptance, 25:9910 (LUSY-7007)
preparation of radioisotope, design of vacuum glove box for, 25:8453 (ORNL-TM-3209)
RADICALS
effects on coliphage T7, inactivating, 25:8808
RADIO ASTRONOMY
radiation from molecules in interstellar space, (T), 25:9071
RADIO GALAXIES
identification of southern hemisphere, (E), 25:9067
RADIO WAVES
absorption in Antarctic ionosphere during 1969 austral winter, (E), 25:9324
absorption in ionosphere of cosmic background, (E), 25:9337
absorption in ionosphere of cosmic, calculated and riometer measurements during solar maximum and minimum, (E/T), 25:9289
absorption of mid-frequency, irregular strength variations of diurnally-distributed, (T), 25:9323
correlation of auroral radar echoes and x rays in southern auroral zone, (E), 25:9320
emission from ninety small galactic nebulae, (E), 25:9068
intensity variation at 1.1 and 2.3 MHz of cosmic, parameters affecting, (E/T), 25:9352
polarization of Jovian decametric, (E), 25:9158
propagation below inhomogeneous isotropic ionospheres, attenuation of elf and vlf, (E/T), 25:9292
propagation from satellites of, Faraday rotation determination for ionospheric electron content and variations, (E/T), 25:9294
propagation in high-latitude D region, seasonal-dependent chemical changes of, (E/T), 25:9297
propagation of vlf, effects of Mar. 18 and Sept. 11, 1969 annular solar eclipses on phase deviations of, (E), 25:9105
scattering of incoherent, for measurements of ionospheric parameters, (E), 25:9343
RADIOACTIVE CONTAMINATION
control of airborne, at reactor fuel element fabrication plant during normal and high-risk operations, evaluation of biological and physical methods for, 25:8695
removal from linens and materials in nuclear plants by washing, 25:8664(P)
RADIOACTIVE MATERIALS
processing of plutonium-containing, safety manual for operation of fluoride volatility process for, 25:8446 (ANL-7672)
release from nuclear power plants, effects on annual atmospheric burden, 25:8371 (SZS-14/70 (pp 1-10))
sorption by modified polyethylene powder, 25:8282(P)
transfer system for, design of duct closure for, 25:8458(P)
RADIOACTIVE WASTE
analysis for ruthenium, spectrographic, 25:8196 (BARC-504)
diffusion of iodine-131 from liquid, stored in open pools, method for prediction of, 25:8450 (IN-1449)
disposal of low activity solid, procedures at nuclear power plants for, 25:10131
disposal of ORNL reactor-produced gaseous, method for calculating ground-level contamination from stack, 25:8452 (ORNL-TM-3187)
disposal of solid, in salt deposits, National Academy of Sciences recommendations for, 25:8455 (TID-25576)
management at Pakistan Institute of Nuclear Science, equipment and methods for, 25:8449 (CONF-691008-18)
processing and disposal of, at BWR nuclear power station, 25:8340
processing of high-level, from fuel reprocessing, 25:8324(T) (ORNL-tr-2406)
pump for concentrated, design of screw-type, 25:8457
shipping of solidified high-level, design and safety evaluation of containers for, 25:8451 (ORNL-TM-2971)
treatment at JAERI during 1969 and 1970, progress report on routine, 25:8693(R) (JAERI-5025)
treatment of liquid, at JAERI during 1969 and 1970, research on, 25:8693(R) (JAERI-5025)
RADIOACTIVITY
calculation of ground-level atmospheric, from near reactor stacks at ORNL, methods for, 25:8452 (ORNL-TM-3187)
monitoring in surface atmosphere at selected land and marine sites during 1963 to 1970, monthly averages of fallout gross γ, 25:8670(R) (HASL-237(App.))
RADIOAPPLICATORS
design of variable-size afterloading radium-226, for use for γ implant therapy of neoplasms of human uterus, 25:8736
performance of welded radium cell, for intracavitary therapy of female genital carcinomas, 25:8729 (SZS-6/70, pp 1-8)
preparation and application of γ-emitting, for interstitial therapy, methods for protection of medical personnel during, 25:8689 (SZS-6/70, pp 19-27)
preparation of requirement for isodose curve deformation in, 25:8730 (SZS-6/70, pp 28-35)
radiation dosimetry of, castings for iridium, 25:8684
use for interstitial therapy of female gynecological carcinomas, preference for cesium-137 over radium in, 25:8730 (SZS-6/70, pp 28-35)
use of lead scleral shell, with phosphorus-32 for therapy of conjunctival neoplasms, 25:8731
RADIOBIOLOGY
research and development in Puerto Rico, 1969, 25:8574(R) (PRNC-140)
research at Columbia Univ., July 1, 1970, 25:8676(R) (NYO-2740-7)
RADIOCHEMICAL PROCESSING PLANTS
criticality alarm system for, 25:8486
design and operation of Pakistan Institute of Nuclear Science, for reprocessing spent fuels, 25:8449 (CONF-691008-18)
design for recovery of uranium from scrap, 25:8447(R) (BHD-65-1)
design of JUPITER, for reprocessing thorium-containing fuels, 25:8324(T) (ORNL-tr-2406)
equipment for fuel handling in, design of hydraulic lifting, 25:8445 (AERE-R-5104)
iodine-131 release at La Hague UP 2, content of grass and milk following accidental, 25:8657 (CEA-R-4008)
off-gas streams from, iodine removal from, 25:8321(R) (IN-1363)
operation of Eurochemic, developments in, 25:8327
RADIOGRAPHY, BIOMEDICAL
imaging system for, contrast perception in, 25:8496
methods using slow neutrons with deuteration of tissues, evaluation of clinical applications of, 25:8709 (DP-1229)
radiation protection programs for dental and medical personnel during, 25:8690
RADIOGRAPHY, INDUSTRIAL
equipment and method for neutron, in resonance region, 25:8442
equipment for reading radiographs from, development of closed-circuit television, 25:8440 (ORNL-4600, pp 266-70)
equipment for, design and operation of, 25:8443
imaging system for, contrast perception in, 25:8496
RADIOISOTOPE SCANNERS
development of computer data analysis system for use with hybrid, 25:8711(R) (NYO-3937-2)
development of, status of, 25:8500
images from, contrast perception in, 25:8496
operating parameters of ratemeter controlled, with color display, 25:8494
performance in combination with digital computer for multiple viewing and sectional scanning of brain, 25:8727
RADIOISOTOPE SCANNING
analysis by computer, program for, 25:8716
data acquisition, analysis, and display systems for, using γ cameras, development of digital computer for, 25:8725
radiation protection guidelines for patients during, 25:8717
review of literature, results, and techniques for

differential diagnosis of focal brain lesions using, 25:8710 (NP-18560)
RADIOISOTOPES
bibliography on production and industrial uses of, 25:8428 (ORNL-IIC-30(Pt.3))
content of bone-seeking, in air and water in environs of plutonium industry, 25:8674(T) (LF-tr-41, pp 199-220)
content of human body, standards for in Italy for maximum permissible, 25:8698
content of surface atmosphere at selected land and marine sites during 1963 to 1970, monthly averages of fallout, 25:8670(R) (HASL-237(App.))
decay in solids, chemical effects from, 25:8313
decay in solids, chemical effects from, 25:8314
effects of artificial and natural, on gamma dose rates in soils, method for distinguishing, 25:8360
half-life measurements of short-lived, automatic dead time correction for, 25:8515
half-life measurements of, use of liquid scintillation detectors for, 25:8539
preparation of solutions of daughter, from parent radioisotopes, design of closed system for, 25:8433(P)
production at Pakistan Institute of Nuclear Science, equipment and methods for, 25:8449 (CONF-691008-18)
production in West Germany, methods and status of, 25:8429(T) (ORNL-tr-2400)
production of, optimum irradiation conditions for, 25:8308
transport by Hanford area ground waters, mathematical model for predicting, 25:8345 (BNWL-SA-3494)
transport in food chains of nuclear explosion-contaminated tropical ecosystems, ecological models for predicting, 25:8626
transport in food chains of nuclear explosion-contaminated estuarine and marine ecosystems in relation to daily ingestion by man, use of stable element content of fish and invertebrates for predicting, 25:8627
transport through soils, effects of fine particulate matter in ground waters on, (E/T), 25:8361
use as tracers for medical studies, guidelines for protection of patients during, 25:8717
use in radiomicrobiologic assay for serum folate in Lactobacillus casei, methods for, 25:8809
RADIOMETRIC TESTING
method for measuring thickness of fuel element cladding, 25:8440 (ORNL-4600, pp 266-70)
RADIOTHERAPY
directory of high-energy centers for, in 1970, worldwide, 25:8728 (STI/PUB-251)
methods for human lymphomas using inverted-γ x-ray exposure, 25:8734
methods for human lymphomas using mantle x-ray exposure, 25:8735
research and development in Puerto Rico, 1969, 25:8574(R) (PRNC-140)
RADIUM
transport in Antarctic Ocean south of Australia, mechanisms of, (E/T), 25:8380
use for intracavitary therapy of female genital carcinomas, peritherapeutic dose and safety considerations during γ, 25:8729 (SZS-6/70, pp 1-8)
use for scanning in diagnostic and metabolic studies, development of computer programs for, 25:8716
RADIUM ISOTOPES Ra-226
content in Antarctic Ocean south of Australia, effects of calcium carbonate and calcium silicate on, (E), 25:8380
effects on blood, carcinogenesis, and life span of animals in comparison to plutonium-239, 25:8596(T) (LF-tr-41, pp 127-97)
use as tracer in hydrological studies of gas exchange and vertical mixing, 25:8352 (CU-2493-11, App.6)
RADON
content in Cranberry and Sterling Lakes, New York, measurements for groundwater flow studies, 25:8350 (CU-2493-11, App.4)
content of decay products of, in uranium mine air, effects of, on respiratory tract pathology, additive effects of diesel engine exhausts and uranium ore dusts on, in dogs and hamsters, 25:8623 (BNWL-SA-3419)
use for scanning in diagnostic and metabolic studies, development of computer programs for, 25:8716
use of natural, in tracer technique for measuring groundwater flow into lakes, 25:8350 (CU-2493-11, App.4)
RADON ISOTOPES Rn-220
effects on mitosis in kidney cells of mice following inhalation, 25:8763
RADON ISOTOPES Rn-222
content in groundwaters, streams, and small lakes in Experimental Lakes Area, Ontario, (E), 25:8352 (CU-2493-11, App.6)
content in man at various time intervals following ingestion of radium-226, methods for calculation of, 25:8669 (COO-2088-1)
decay products of, dosimetry following inhalation in relation to lead-210 body burden, conversion factors in model for estimating, 25:8680
RAINWATER
electric charge and size of drops of, effects on atmospheric scavenging efficiency for fallout, (E), 25:8365(R) (COO-1199-19)
fallout monitoring of UK, Jan. to July 1970, 25:8364 (AERE-R-6556)
fallout scavenging from atmosphere by, chemical tracer studies of, 25:8365(R) (COO-1199-19)
fission product content of UK, Nov. 1969 to Nov. 1970, 25:8364 (AERE-R-6556)
tritium content of UK, Jan. 1969 to June 1970, 25:8364 (AERE-R-6556)
RARE EARTH ALLOYS AND SYSTEMS
B--Mn--rare earths, crystal structure of $RMnB_4$, 25:8948
B--rare earths--V, crystal structure of RVB_4, 25:8948
RARE EARTH CARBONATES
structure at high temperatures, 25:8938
RARE EARTH FORMATES
structure at high temperatures, 25:8938
RARE EARTH ISOTOPES
production in deuteron and proton fission of thorium-232 at 11 MeV, yields of, (E/T), 25:10054
RARE EARTH OXIDES
preparation of microspheres of, using sols or solutions, equipment and method for, 25:8916(P)
reactions with hafnium dioxide, study of phases formed during, 25:8935
rare earth oxide--ZrO_2, properties for use as high-temperature electric conductor or insulator, 25:8936
rare earth oxides--ZrO_2, formation of solid solutions of, kinetics of, 25:8935
RARE EARTHS
abundance in eucrites, (E), 25:8966
compounds, chemical thermodynamics of, 25:8260(R) (COO-1149-180)
determination in airborne particulates by neutron activation, 25:8231
determination in uranium or zirconium by optical fluorescence spectroscopy, phosphors for, 25:8207
RARE GASES
effects of void-trapped, on incipient boiling superheat in sodium, 25:8415
reactions with sodium atoms, impact-parameter calculation of cross sections for fine-structure transitions in, 25:9207
RATS
calcium-45 efflux in myometrium of, effects of external calcium concentration on, 25:8601
calcium-47 metabolism in, effects of estradiol on, 25:8592(R) (COO-1339-43)
radiation effects on biochemistry of developing brain of, 25:8758(R) (UCB-34-P-82-10)
radiation effects on bioelectric properties and glucose transport in intestine of, combined effects of chronic bile diversion on x, 25:8607(R) (ORO-3882-3)
radiation effects on coeruloplasmin activity in blood serum of, comparison of K_3-vitamin and monoiodoacetic acid effects with x, 25:8612
radiation effects on connective tissue of, effects of cortisone and anabolic steroids on x, 25:8786
radiation effects on hematopoiesis and excretion of calcium and chlorides in urine of, combined effects of reduced muscular activity and dose fractionation on γ, 25:8755(T) (JPRS-51660)
radiation effects on hematopoiesis in, effects of dose rate on, 25:8608
radiation effects on medulla oblongata tissue in brain of, ultrastructural study of whole-body γ, 25:8787
radioisotope clearance from lungs of, effects of aerosol concentration on rate of iron-59 and plutonium-239, 25:8591 (CEA-CONF-1677)
radioisotope distribution in organs of, following inhalation and intramuscular injection of americium-241, curium-242, plutonium-238, and plutonium-239, 25:8590 (CEA-CONF-1658)
strontium-85 metabolism in, effects of estradiol on, 25:8592(R) (COO-1339-43)
technetium-99 uptake and accumulation by thyroid of, following intravenous injection in comparison to iodine-131, metastable, 25:8599
REACTIVITY
calculation during fuel density oscillations, effects of delayed neutrons on, (T), 25:10305 (IAE-1955)
calculation of fast reactor, effects of delayed neutron data errors on, (T), 25:10179
calculations for liquid metal cooled fast breeder reactors, space--time effects on, (T), 25:10180
measurement of boiling reactor, effects of steam voids on, (E/T), 25:10175
measurement of reserve, double over-compensation method for, (E/T), 25:10321
measurement of subcritical, pulsed neutron methods for, (T), 25:10309
measurements of heavy water moderated power reactor, comparison of spectral analysis and maximum likelihood methods for, (E/T), 25:10091 (NP-18595)
REACTOR CONTAINMENT STRUCTURES
thermal insulation for liquid sodium cooled, description of liquid sodium, 25:10199(P)
transient effects on dry well, analytical model for pressure and temperature, (E/T), 25:10232
REACTOR CONTAINMENT SYSTEMS
blast energy absorption by, core vessel top shield

XUM

assembly for, 25:10247(P)
design with means for using primary coolant as emergency core coolant, 25:10231(P)
fission product removal from, effects of sodium hydroxide and sodium thiosulfate additives on sprays for, (E), 25:10256 (BNWL-1485)
iodine removal from, by sorption on zeolites, 25:8321(R) (IN-1363)
spray systems for, effectiveness of fission product removal by, (E), 25:10244(R) (ORNL-TM-3212)
REACTOR CONTROL ELEMENTS
drives for water cooled, description of dual interconnected hydraulic pistons, 25:10188(P)
fission gas venting capillary valve for liquid metal cooled rod type, 25:10189
guide tubes for boiling water cooled, description of removable, 25:10218(P)
materials for, development status of, 25:8828 (BNWL-SA-3426)
REACTOR CONTROL SYSTEMS
book: Control of Nuclear Power Reactors, in Russian, 25:10190
development of on-line digital computer, 25:10125(R) (NP-18573)
development of two phase flow rods for automatic, 25:10187
REACTOR COOLANTS
book: Thermophysical Properties of Organic Coolants (In Russian), 25:8412
circulation in one-loop system, stability of natural, (T), 25:8414
properties of organic, physical and thermal, 25:8412
REACTOR EXPERIMENTAL FACILITIES
rabbit facility for FRJ-2 (Juelich), design of hydraulic, 25:10274
REACTOR FUEL ELEMENTS
analysis for fissionable material by activation and scintillation counting, 25:8215(P)
assemblies of parallel rod-type, characteristics of departure from nuclear boiling during pressure blowdown in, (E), 25:8418
assemblies of vertical rod-type, method for predicting burnout in, 25:8408 (CONF-660675-1)
bowing in lattice cell arrays, neutron flux and reaction rate variations from, (T), 25:10319
cladding for, chemical and radiation effects on rupture of Zircaloy, (E), 25:10244(R) (ORNL-TM-3212)
cladding for, development status of, 25:8828 (BNWL-SA-3426)
cladding for, effects of coolant loss accidents on embrittlement of Zircaloy, (E), 25:10244(R) (ORNL-TM-3212)
cladding for, effects of embedded abrasive particles on failure of aluminum, 25:8853 (ORNL-4600, pp 249)
cladding for, radiation scattering method for measuring thickness of, 25:8956 (ORNL-4600, pp 235-48)
cladding for, review of research on failure of Zircaloy, 25:8839 (ORNL-TM-3188)
cladding for, testing of Type 316 stainless steel, 25:8911 (ORNL-4600, pp 65-80)
critical heat flux for water--steam cooled cluster arranged, 25:10215
decanning of, decontamination of effluents from chemical, 25:8344(P)
design of cermet plate-type, for irradiation testing in HFIR, 25:8956 (ORNL-4600, pp 235-48)
design parameters for bottom loading, with independent support, 25:10333(P)
design parameters for series connected thermionic, optimum, 25:10226
design parameters of water cooled partitioned cylinder shaped central void, 25:10219(P)
design parameters of water cooled zirconium alloy clad pyrolytic graphite coated particle type, 25:10220(P)
development of prototype, for heavy water moderated and cooled thorium breeder reactor, (E/T), 25:10209 (JUL-654-RG)
development of thermal water cooled and fast breeder, 25:10101
diffusion of plutonium from clad, use of aluminum or graphite barrier for prevention of, 25:8857
fabrication of potassium--sodium bonded pin-type nitride, using stainless steel cladding, 25:8910 (ORNL-4600, pp 41-56)
failure of sodium cooled, facility for mockup testing of, 25:10244(R) (ORNL-TM-3212)
failure threshold of zero burnup liquid sodium cooled Type 316 stainless steel clad plutonium oxide (PuO_2)--uranium oxide (UO_2) pin type, 25:10208 (GEAP-13562)
fission product content in irradiated, ICON code for calculation of, 25:10236 (AERE-R-6242)
gas analysis procedures for zirconium alloy clad uranium oxide (UO_2), cover and fission, 25:10227
guide tubes for boiling water cooled, description of removable, 25:10218(P)
handling of sheared clad, in reprocessing plant, design of hydraulic equipment for, 25:8445 (AERE-R-5104)
heat transfer coefficient of metal clad ceramic, balanced oscillator method for in-pile measurement of gap conductance, (E/T), 25:10323(T) (EURFNR-774)
heat transfer to carbon dioxide and air from, superposition method of determining temperature distribution in, 25:8409 (RD/B/N-1755)
performance of fast breeder, effects of internal fins on heat transfer, (T), 25:10223
performance of SA-1 rod-type, at high burnups, 25:8951(R) (GEAP-10217)
properties of plutonium oxide (PuO_2)--uranium oxide (UO_2), radiation effects on burnup, microstructure, and mechanical, in-pile, (E), 25:10213(R) (WCAP-3385-25)
radiation effects on dimensions of SA-1 rod-type, at high burnups, 25:8951(R) (GEAP-10217)
radiation testing of Zircaloy 2 clad uranium oxide (UO_2) pin type, 25:10125(R) (NP-18573)
reprocessing of, design and operation of Pakistan Institute of Nuclear Science facilities for, 25:8449 (CONF-691008-18)
shipping of, review of East German regulations for, 25:8454 (SZS-14/70 (pp 11-21))
spacers for power, description of continuous ring, 25:10224(P)
spacers for, design of helical tangential spring, 25:10332(P)
support grids for, effects of rod ovality and diameter change on dimple spacing of, (T), 25:10167 (WAPD-TM-714)
temperature distribution in, effects of surface coolant blockage on, 25:10244(R) (ORNL-TM-3212)
testing for fast reactors, methods for, 25:8896(T) (BNWL-tr-57)
thermal conductivity of metal clad ceramic, balanced oscillator method for in-pile measurement of, (E/T), 25:10323(T) (EURFNR-774)
thermal conductivity of, error analysis for balanced oscillator method measurements of in-pile, 25:10324(T) (EURFNR-775)
welding of rod-type, in vacuum, electron-beam method for, 25:8461
REACTOR FUELS
activity of, optimization method for calculation of fission product decay, 25:10308
analysis for fissionable material by activation and scintillation counting, 25:8215(P)
analysis for uranium, accurate and precise titrimetric method for, 25:8202 (RCN-126)
burnup analysis by determination of zirconium-95, 25:8214
cladding for, equipment and method for measuring tensile strength of, 25:8883
conversion ratio for gas cooled particle type, measurement of relative, 25:10217
cost analysis for water cooled power reactors, 25:10100
cycles for power, economic optimization of, (T), 25:10233 (BNWL-SA-3605)
cycles for predicted development in U.S. during 1970 to 2020, 25:10095 (WASH-1098)
development at Argonne National Laboratory, November 1970, 25:10164(R) (ANL-7758)
development of coated particle, for gas cooled reactors, 25:10166 (GA-10265)
development of, research program for, 25:8829(R) (ORNL-4600)
diffusion of fission gases from ceramic, mechanisms of, 25:8958 (SRARI-P-73)
economics of, systematic seven-page guide for calculating, 25:10216
materials for, development status of, 25:8828 (BNWL-SA-3426)
preparation of ceramic, advantages of sol-gel methods for, 25:8915
production of pellet-type, vacuum methods for, 25:8461
production of stable hypostoichiometric oxide, 25:8921(P)
reprocessing of graphite-matrix, fluidized-bed combustion process for, 25:8322 (IN-1423)
reprocessing of LMFBR, solvent extraction processes for, 25:8316 (BNWL-CC-1939)
reprocessing of molten salts by low-pressure distillation, removal of lanthanide fission products by, (E), 25:10210 (ORNL-4434)
reprocessing of thorium-containing, development of processes for, 25:8324(T) (ORNL-tr-2406)
reprocessing of thorium-containing, flowsheets for KFA--TBP 23/25 process for, 25:8324(T) (ORNL-tr-2406)
reprocessing of, in-line colorimetric determination of uranium in solutions from, 25:8197 (BARC-510)
reprocessing of, jet grinders for particle-size control in fluidized-bed denitrator in, 25:8323 (IN-1439)
reprocessing of, nitride forming reactions in liquid uranium alloys for, 25:8325(R) (SU-326-P-28-X-2)
reprocessing of, pilot plant for nonaqueous, 25:8342
supplies in European Communities, commission report on, 25:10327
REACTOR LOADING MACHINES
design parameters of double prehension, for water cooled reactors, 25:10329(P)
design parameters with movable shaft, 25:10331(P)
development of gas cooled, 25:10166 (GA-10265)
winches for, design of, 25:8460
REACTOR MODERATORS
materials for, development status of, 25:8828 (BNWL-SA-3426)
neutron pulse decay and distribution in, effects of

inelastic scattering on fast, (T), 25:10315
production process for porous metal hydride particles with capacity for controlled absorption and release of hydrogen, 25:10334(P)
REACTOR SAFETY
development at Argonne National Laboratory, November 1970, 25:10164(R) (ANL-7758)
research and development program during September and October 1970, 25:10244(R) (ORNL-TM-3212)
REACTOR SAFETY EXPERIMENTS
coolant level indicator for LOFT, development of ultrasonic, 25:10267 (IN-1442)
operation of TREAT during November 1970, 25:10164(R) (ANL-7758)
REACTOR SIMULATORS
performance of digital computer display system, for phase space analysis of reactor kinetics, 25:10311
program for xenon spatial oscillation effects on stability, 25:10306 (NP-18547)
use of digital computer, for automatic control characteristics of liquid sodium cooled fast reactors, 25:10186 (KFK-1179)
use of hybrid computer, for coolant temperature control schemes for liquid metal cooled reactors, 25:10185 (CEA-R-3988)
REACTORS
accidents in, biological significance of radioactive fallout contamination of river water following extreme, 25:8660 (HMI-B-87)
components of, heat transfer characteristics of convectively cooled temperature dependent thermal conductivity, (T), 25:10203
cooling system for, design of channel closure valve for, 25:8401(P)
cooling systems for, sigma method for hot channel and hot spot statistical analysis in, 25:10194 (CEA-R-3895)
criticality accidents in, performance of activation detectors for measuring fast neutron dose from, 25:10181
fission product content in operating, ICON code for calculation of, 25:10236 (AERE-R-6242)
fission product decay heating in, (T), 25:10299
heat transfer in, method for calculation and measurement of, 25:8413
kinetics equations for, numerical methods for solution of one-point, 25:10312
kinetics for, CONDOR 3 computer program for lifetime, 25:10304 (EUR-4539)
kinetics for, FORGAD computer program for, 25:10300 (AECL-3671(Add.1))
kinetics of, calculation of material dependent correction factor for mean chord length for, (T), 25:10310
kinetics of, performance of digital computer display system for phase space analysis of, 25:10311
kinetics of, transport theory analysis of, 25:10317
lattice cell reaction rates in, effects of fuel element bowing on, (T), 25:10319
neutron flux distributions in, generalized multiple collision probabilities for calculation of, (T), 25:10313
neutron flux in, effects of fuel element bowing on, (T), 25:10319
neutron flux measurements in, microwave technique for in-core, 25:10326 (RT/FI-(70)7)
physics constants and parameters for, (E/T), 25:9948
power response to reactivity inputs, use of idempotent matrices for determination of, 25:10302 (BARC-502)
pressure vessels for, model testing for long-term performance of prestressed concrete, (E), 25:10325 (ORNL-TM-3246)
reactivity during fuel density oscillations in, effects of delayed neutrons on, (T), 25:10305 (IAE-1955)
reactivity measurement in subcritical, pulsed neutron methods for, (T), 25:10309
reactivity of subcritical, double over-compensation method for determination of reserve, (E/T), 25:10321
shielding calculations for, (E/T), 25:9948
stability of, simplified method for calculating, (T), 25:10316
structures for, effects of earthquakes on soil interaction with foundation, 25:10245 (ORO-3822-5)
temperature measurements in, microwave technique for in-core, 25:10326 (RT/FI-(70)7)
thermal insulation for, description of laminated metal, 25:10335(P)
transfer function of subcritical zero-power, calculational method for spatially dependent source, 25:10307 (ORNL-TM-3136)
REACTORS, BOILING
containment sprays for, analysis of iodine removal, 25:10238(R) (BMI-1890)
control rod drives for, description of dual interconnected hydraulic piston, 25:10188(P)
coolant loss accident conditions in, computer simulation of, 25:10238(R) (BMI-1890)
cooling system for, description of spaced in-core ducts with multiple injection nozzles, 25:10200(P)
core for, description of parallel arranged removable guide tubes in, 25:10218(P)
core physics for, effects of steam voids on, (E/T), 25:10175
emergency core cooling system for, computer for simulation of, 25:10238(R) (BMI-1890)
performance of heavy water pressure tube type, effects of water coolant on, (T), 25:10205
pressure vessels for, materials properties and design requirements for steel, 25:10197
REACTORS, BREEDER
core for fast, with unclad fuel elements of uniform enrichment, 25:10170(P)
fuel element supports for, effects of fuel element ovality and diameter change on dimple spacing of, (T), 25:10167 (WAPD-TM-714)
fuel elements for fast, development of, 25:10101
fuel elements for fast, effects of internal fins on power of, (T), 25:10223
fuel elements for heavy water moderated and cooled thorium, development of prototype, (E/T), 25:10209 (JUL-654-RG)
REACTORS, CANDU-TYPE
fuel elements for, cover and fission gas analysis procedures for, 25:10227
REACTORS, FAST
containment structure for liquid sodium cooled, description of liquid sodium thermal insulation for, 25:10199(P)
control characteristics for Na 2, effects of correct dead time simulation on automatic, 25:10186 (KFK-1179)
control elements for liquid metal cooled breeder, description of gas venting capillary valve for rod type, 25:10189
core disassembly accidents in, FREADM-1 code for dynamics of, 25:10241 (GEAP-13608)
core for breeder, with unclad fuel elements of uniform enrichment, 25:10170(P)
development in U. S., survey of, 25:10102
development in U.S.S.R. of, problems related to, 25:10099
development prediction in U.S. during 1970 to 2020, systems analysis for optimum economic, 25:10095 (WASH-1098)
Doppler effect in, effects of neutron flux variations and fuel heterogeneity on, (T), 25:10176
fuel elements for breeder, development of, 25:10101
fuel elements for breeder, effects of internal fins on power of, (T), 25:10223
kinetics of symmetrically reflected, validity of point model for subcritical, 25:10307 (ORNL-TM-3136)
physics calculations for, effects of delayed neutron data errors on, (T), 25:10179
physics characteristics of, Rensselaer Polytechnic Institute studies on, (E/T), 25:9945(R) (RPI-328-190)
physics parameters of steam cooled, mockup measurements on, (E/T), 25:10258 (EURFNR-848)
safety of, effects of negative Doppler coefficient on, (T), 25:10176
REACTORS, FRANCE
pressure vessels for, standards for prestressed concrete, 25:10160(T) (ORNL-tr-2402)
REACTORS, GAS-COOLED
blowers for high temperature, development of helium, 25:10166 (GA-10265)
boiler for high temperature, development of, 25:10166 (GA-10265)
coolant additives for graphite moderated, corrosion inhibiting effects of methane and carbon monoxide, 25:10201(P)
cooling systems for high temperature, kinetics of carbon deposition reactions in, (E/T), 25:10195 (DP-Report-500)
cooling systems for, analysis of fission products in, 25:10244(R) (ORNL-TM-3212)
cooling systems for, description of double cooling passage, 25:10202(P)
core access for, description of top closure with dual purpose fuel loading and control element standpipes, 25:10225(P)
core configuration for, with parallel prismoidal columns of moderator material containing fuel, 25:10168(P)
core design with double coolant channels, 25:10202(P)
design of helium cooled, for producing hydrogen gas in endothermic system, 25:10294(P)
development in U. S., survey of, 25:10102
development prediction in U.S. during 1970 to 2020, systems analysis for optimum economic, 25:10095 (WASH-1098)
fuels for high temperature, development of coated particle, 25:10166 (GA-10265)
fuels for, measurement of relative conversion ratio for particle type, 25:10217
instrumentation for graphite moderated, description of gas cleaned electrical insulators for in-core, 25:10191(P)
loading machines for high temperature, development of, 25:10166 (GA-10265)
loading of, system of standpipes and guides for, 25:10230(P)
performance of heavy water pressure tube type, effects of carbon dioxide coolant on, (T), 25:10205
pressure vessel for graphite moderated, use of prestressing tendons for securing heat exchanger access closures in prestressed concrete, 25:10198(P)
pressure vessel for high temperature, development of

XUM

prestressed concrete, 25:10166 (GA-10265)
turbine for, design parameters of closed cycle carbon dioxide gas, 25:10250(P)
turbine for, design parameters of closed cycle carbon dioxide gas, 25:10249(P)
turbines for, part load performance of direct cycle gas, (T), 25:10251

REACTORS, GERMANY
development of power, 25:10105
development of power, problems related to, 25:10097

REACTORS, GRAPHITE-MODERATED
coolant additives for gas cooled, corrosion inhibiting effects of methane and carbon monoxide, 25:10201(P)
cooling systems for high temperature, kinetics of carbon deposition reactions in, (E/T), 25:10195 (DP-Report-500)
instrumentation for gas cooled, description of gas cleaned electrical insulators for in-core, 25:10191(P)
physics calculations for water cooled coupled core, cross spectral density sink frequency for, (E/T), 25:10279
physics calculations for water cooled coupled core, cross spectral density sink frequency for, (T), 25:10275
physics calculations for water cooled coupled core, cross spectral density sink frequency for, (E/T), 25:10278
pressure vessel for gas cooled, use of prestressing tendons for securing heat exchanger access closures in prestressed concrete, 25:10198(P)

REACTORS, HEAVY WATER-MODERATED
coolant leak detector for, description of color changing, 25:10206(P)
coolants for pressure tube type, nuclear properties of carbon dioxide, heavy water, and light water, (T), 25:10205
development prediction in U.S. during 1970 to 2020, systems analysis for optimum economic, 25:10095 (WASH-1098)
fuel elements for heavy water cooled thorium breeder, development of prototype, (E/T), 25:10209 (JUL-654-RG)
neutron spectra in uranium oxide (UO_2) fueled, analytical two-group formalism for epithermal, (E/T), 25:10320 (AE-405)
physics characteristics of highly enriched, analytical procedures for, (E/T), 25:10318
power excursions in natural uranium fueled pressure tube type, model for self-limiting, (T), 25:10281
shielding of, SABINE code calculations of neutron flux in iron--water, 25:10192 (CEA-N-1354)

REACTORS, LIQUID METAL-COOLED
containment structure for fast, description of liquid sodium thermal insulation for, 25:10199(P)
control characteristics for Na 2, effects of correct dead time simulation on automatic, 25:10186 (KFK-1179)
control elements for fast breeder, description of gas venting capillary valve for rod type, 25:10189
control schemes for, analysis of coolant temperature, (E/T), 25:10185 (CEA-R-3988)
coolant flow in, design of electromagnetic flowmeter for measurement of, 25:8400(P)
development in U. S., survey of, 25:10102
standards for, development of engineering, 25:10244(R) (ORNL-TM-3212)

REACTORS, MARITIME
protection from ship accidents, review of procedures for, 25:10295(T) (JPRS-51939)

REACTORS, MOLTEN-SALT
development in U. S., survey of, 25:10102

REACTORS, ORGANIC-COOLED
power excursions in natural uranium fueled pressure tube type, model for self-limiting, (T), 25:10281

REACTORS, POWER
components of, fabrication facilities in Spain for, 25:10103
control system for CIRENE, development of two phase flow rods for automatic, 25:10187
control systems for, design and operation of, 25:10190
cooling system for pressurized water, analysis of earthquake resistant design criteria for components of, (E/T), 25:10248
cost analysis in Pakistan for dual purpose process heat, for fertilizer production, 25:10293
design parameters of 300 kW(t), for use for research submarine propulsion and working power, 25:10298
development in Germany, 25:10105
development in Germany of, problems related to, 25:10097
development in Spain, predictions for 1970 to 2000, 25:10104
development in U. S., survey of, 25:10102
development predictions in U.S. during 1970 to 2020, systems analysis for optimum economic, 25:10095 (WASH-1098)
economics for water cooled dual purpose process heat, for urban heating and power, 25:10094 (ORNL-HUD-14)
economics in Puerto Rico for industrial applications of process heat, programming for optimum, 25:10291 (TID-25630)
fuel cycle for water cooled, cost analysis of, 25:10100
fuel cycles for U. S., effects of uranium supply on, 25:10214
fuel cycles for, economic optimization of, (T), 25:10233 (BNWL-SA-3605)
fuel elements for CIRENE, critical heat flux in cluster arranged, 25:10215
fuel elements for thermionic, optimum design parameters for series connected, 25:10226
fuel elements for, description of continuous ring spacer for, 25:10224(P)
fuel for, use of uranium fluoride (UF_4), 25:10221
heat exchanger module for, description of, 25:10204(P)
loading scheme for pressurized water, calculation of optimum, (T), 25:10184
neutron flux distribution in, hybrid computer solution of space--time, 25:10303 (CEA-CONF-1684)
pressure vessels for, French standards for prestressed concrete, 25:10160(T) (ORNL-tr-2402)
pressure vessels with integral pressure suppression chamber, description of, 25:10169(P)
shield assembly for, blast energy absorber structure for top, 25:10247(P)
stability of, digital simulation of xenon spatial oscillation effects on, 25:10306 (NP-18547)
turbine for, design parameters of closed cycle carbon dioxide gas, 25:10250(P)
turbine for, design parameters of closed cycle carbon dioxide gas, 25:10249(P)
turbines for, part load performance of direct cycle gas, (T), 25:10251

REACTORS, PRESSURIZED-WATER
containment sprays for, analysis of iodine removal, 25:10238(R) (BMI-1890)
containment vessels for, effects of post-accident pressure and temperature transients on, (E/T), 25:10232
control rod drives for, description of dual interconnected hydraulic piston, 25:10188(P)
coolant loss accident conditions in, computer simulation of, 25:10238(R) (BMI-1890)
coolant loss accidents in, pressure and temperature transients from, (E/T), 25:10232
coolant loss accidents in, RELAP3 code predictions of transient pressures and residual water following, (E/T), 25:10242 (IN-1444)
cooling system for power, analysis of earthquake resistant design criteria for components of, (E/T), 25:10248
economics in U.S.S.R. of, 25:10099
emergency core cooling system for, computer for simulation of, 25:10238(R) (BMI-1890)
emergency core cooling system for, use of lost primary coolant in, 25:10231(P)
emergency core cooling systems for, heat transfer capabilities of bottom flooding, (E), 25:10229 (WCAP-7544)
fuel cycle for, development of plutonium, 25:10222
fuel elements for, effects of coolant loss accidents on Zircaloy cladding of, 25:10244(R) (ORNL-TM-3212)
fuels for, utilization of plutonium in, (E/T), 25:10213(R) (WCAP-3385-25)
loading scheme for power, calculation of optimum, (T), 25:10184
pressure vessels for, materials properties and design requirements for steel, 25:10197

REACTORS, PROCESS HEAT
cost analysis in Pakistan for dual purpose power, for fertilizer production, 25:10293
design of helium cooled, for producing hydrogen gas in endothermic system, 25:10294(P)
economics for water cooled dual purpose power, for urban heating and power, 25:10094 (ORNL-HUD-14)
economics in Puerto Rico for industrial applications of power, programming for optimum, 25:10291 (TID-25630)
use for production of hydrogen, 25:10292(P)

REACTORS, RESEARCH
design parameters of University of Missouri Research Reactor, 25:10273
fuel elements in TRIGA, detection and location of failed, (E), 25:10283
fuel elements of FR-2, balanced oscillator method measurements of in-pile thermal conductivity for, 25:10324(T) (EURFNR-775)
in-pile loop for CABRI, design and safety of Scarabee, 25:10254(T) (ANL-Trans-865)
kinetics of convergatron flux trap, analysis of multigroup point, (T), 25:10285
neutron flux for, design requirements for high thermal, 25:10268(T) (LA-4399-TR)
neutron flux in central thimble of TRIGA Mark 2, measurement of fast, 25:10277
neutron spectra in central thimble of TRIGA Mark 2, measurement of fast, 25:10277
operation of THOR, review of radiation exposure incidents during, 25:10284
operation of U.S.S.R. SM-2, design requirements for high thermal neutron flux, 25:10268(T) (LA-4399-TR)
operations for University of Missouri Research Reactor, review of, 25:10273
physics measurements for FMRB, cross spectral density sink frequency, (E/T), 25:10279
power excursions in natural uranium fueled pressure tube type, model for self-limiting, (T), 25:10281
pulsing of Illinois University TRIGA, method for fast, (E/T), 25:10282
radiation effects testing of fuels in FR-2, safety analysis of single-walled NaK cooled capsules for,

25:10257(T) (EURFNR-764)
safety of FMRB, effects of coupled core installation on, 25:10269 (NP-18496)
REACTORS, ROCKET
costs for, comparison of chemical propelled vehicles with deep space operation, 25:10287
REACTORS, SUPERHEATING
physics parameters of steam cooled fast, mockup measurements on, (E/T), 25:10258 (EURFNR-848)
REACTORS, SWIMMING-POOL
cooling system with means for trapping failed fuel particles, description of, 25:10276(P)
design and operation of Pakistan Institute of Nuclear Science, 25:8449 (CONF-691008-18)
design parameters for, with independent cooling system, 25:10280(P)
REACTORS, THERMAL
dynamics of, comparison of methods for analysis of, (E/T), 25:10174 (LFEN-109-B)
kinetics of, comparison of methods for analysis of, (E/T), 25:10174 (LFEN-109-B)
shutdown of, radiation and energy release sources following, (T), 25:10165 (CISE-R-233)
REACTORS, U.S.S.R.
development of fast and pressurized water, 25:10099
REACTORS, WATER-COOLED
construction of, review of U. S. industry progress and commitments on, 25:10088 (CONF-690967-1)
coolant leak detector for, description of color changing, 25:10206(P)
coolant loss accidents in, transient core heatup during blowdown phase of, (E), 25:10246
development in U. S., survey of, 25:10102
development predictions in U.S. during 1970 to 2020, systems analysis for optimum economic, 25:10095 (WASH-1098)
economics for dual purpose process heat and power, for urban heating and power, 25:10094 (ORNL-HUD-14)
fuel cycle for power, cost analysis of, 25:10100
fuel elements for, description of partitioned cylinder shaped central void, 25:10219(P)
fuel elements for, description of zirconium alloy clad pyrolytic graphite coated particle type, 25:10220(P)
fuel elements for, development of, 25:10101
fuel elements for, effects of coolant loss accidents on Zircaloy cladding of, 25:10244(R) (ORNL-TM-3212)
loading machine for, design parameters of double prehension, 25:10329(P)
physics calculations for graphite moderated coupled core, cross spectral density sink frequency for, (E/T), 25:10278
physics calculations for graphite moderated coupled core, cross spectral density sink frequency for, (T), 25:10275
physics calculations for graphite moderated coupled core, cross spectral density sink frequency for, (E/T), 25:10279
standards for, development of engineering, 25:10244(R) (ORNL-TM-3212)
REACTORS, WATER-MODERATED
moderator for, thermal neutron diffusion in, (T), 25:10301 (AEEW-R-701)
neutron detector response to material changes in subcritical, use of few-group diffusion theory for prediction of, (E/T), 25:10322
neutron spectra in uranium oxide (UO_2) fueled, analytical two-group formalism for epithermal, (E/T), 25:10320 (AE-405)
piping failure in, probability analysis for, 25:8866 (GEAP-10205)
shielding of, SABINE code calculations of neutron flux in iron--water, 25:10192 (CEA-N-1354)
RECOILS
reactions in solids, chemical effects from, 25:8313
reactions in solids, chemical effects from, 25:8314
REFRACTORY MATERIALS
arcing behavior of, exposed to pulsed rf discharge, (E), 25:9442
REGGE POLE THEORY
daughter trajectories in amplitude from generalized Veneziano model, 25:9888 (ITF-70-78)
dual resonance model with nonlinear trajectories in, 4-, 5-, and N-point functions and loop diagrams in, 25:9884 (COO-1764-90)
dual resonance models in, review of, 25:9887 (ITF-70-43)
dual resonance models with nonlinear trajectories in, rules for Veneziano N-point function construction in, 25:9885 (COO-1764-98)
dual resonance models with nonlinear trajectories in, rules for Veneziano 5-point function construction in, 25:9885 (COO-1764-98)
dual resonance theory with nonlinear trajectories, loop diagrams in, 25:9691 (RLO-1388-592)
eikonal model for elastic scattering in, 25:9776
fermion trajectory in, 25:9790
multiperipheral bootstrap in, properties of, 25:9757
residues in scattering amplitudes, Gribov--Pomeranchuk pole in, 25:9893
scattering amplitude with cuts in, dual, 25:9899
trajectory for π + N interactions, vacuum, 25:9785
(DESY-70/55)
RELATIVE BIOLOGICAL EFFECTIVENESS
values for 15 MeV electrons in relation to effects on lymphoid tissues, 25:8780
values for argon ions, carbon ions, helium ions, lithium ions, neon ions, and oxygen ions in relation to growth inhibition, mutagenesis, and tumorigenesis in Arabidopsis thaliana seeds, 25:8800
values for α particles and recoil lithium ions in relation to survival of HeLa cells following (n,α) reaction in cells, effects of boron-10 content on, 25:8745
values for neutrons, 25:8756 (NYO-2740-7, pp 154-217)
values for neutrons in γ-irradiated wheat leaves, 25:8801
RELATIVITY THEORY
action functional as path length in general, for closed empty universes, 25:9881
Cauchy problem for nonlinear Boltzmann equation in special, 25:9843
Einstein equations in, complex oscillatory singularity in cosmological solutions of, 25:9877
Einstein field equations with electromagnetic energy tensor in general, cylindrical wave solutions of, 25:9873
Einstein--Bohr box experiment, (T), 25:9154
elementary particle motion in general, 25:9874
elementary particles in general, Friedman theory for, 25:9870 (JINR-P2-5289)
extended bodies in general, moments of energy--momentum tensor and charge--current vector for, 25:9875
fermion interactions with linearized gravitational fields in general, covariant Dirac equation for, 25:9879
field interactions in flat space--time of special, model in five dimensions for, 25:9868
gravitational field of static axially symmetric shells and disks in general, 25:9882
masses with arbitrary baryon number in Treder tetrad theory in general, static equilibrium states of spherically symmetric, 25:9876
models of static configurations of large masses, (T), 25:9008
Newtonian electrodynamics from general, (T), 25:9052
particle motion in general, 25:9874
quantization of general, review of, 25:9872
superspace in general, 25:9872
torque in special, 25:9866
REMOTE-HANDLING EQUIPMENT
design of hydraulic rabbit, for reactor experimental facilities, 25:10274
REPUBLIC OF CHINA
nuclear power plant construction in, planning studies for, 25:10089 (CONF-691020-3)
RESINS
radioinduced polymerization of coatings of aminoplast, on substrates, 25:8278(P)
RHEINSBERG POWER REACTOR
core cooling following failure of main power supply, reliability of auxiliary power supply for, (T), 25:10093(T) (NP-tr-1928)
emergency control switching system for, reliability analysis of automatic, 25:10108
RHENIUM
compatibility of fuel capsules of, with curium-244 oxide at 1250 to 1850°C, 25:8427(R) (ORNL-4639)
emittance at 1200 to 2800°K, total hemispherical, 25:8878
RHENIUM ALLOYS AND SYSTEMS
Mo--Re, radiation effects on mechanical properties of, fast neutron, 25:8952 (ORNL-4600, pp 81-125)
Mo--Re--W-base, creep of arc-melted, at 1200 to 2200°C, effects of stress on, 25:8852 (ORNL-4600, pp 198-209)
Re--W-base, compatibility of fuel capsules of, with curium-244 oxide at 1250 to 1800°C, 25:8427(R) (ORNL-4639)
Re--W-base, creep at 1800°C and 1000 psi, effects of low-pressure oxygen on, 25:8852 (ORNL-4600, pp 198-209)
Re--W-base, creep of arc-melted, at 1200 to 2200°C, effects of stress on, 25:8852 (ORNL-4600, pp 198-209)
Re--W-base, preparation by vapor deposition from reduced hexafluoride vapors, development of method for, 25:8852 (ORNL-4600, pp 198-209)
RHENIUM FLUORIDES
ReF_6--WF_6, reduction for production of rhenium--tungsten alloys by vapor deposition, development of method for, 25:8852 (ORNL-4600, pp 198-209)
RHENIUM ISOTOPES Re-187
performance of activation detectors of, for neutron spectra measurements at 1 eV to 10 keV, 25:8481 (KFK-1233)
RHODIUM
alpha reactions at 30 to 80 MeV, K-shell ionization cross sections for, (E), 25:9978(R) (ORO-3398-26)
effects on colorimetric determination of uranium in fuel reprocessing solutions, 25:8197 (BARC-510)
effects on deuterium exchange in propene, catalytic, 25:8258
properties for use in curium-244 oxide cermets, 25:8427(R) (ORNL-4639)
RHODIUM ALLOYS AND SYSTEMS
Pt-base--Rh, tensile properties at 1093 to 1290°C, 25:8427(R) (ORNL-4639)

XUM

RIBOSE, 2-DEOXY-
radiolysis of aqueous solutions of, yields from γ, 25:8305
RICHLAND AREA (WASH.)
waste disposal at, mathematical model for predicting ground water contamination from, 25:8345 (BNWL-SA-3494)
RING CURRENT
effect on magnetospheric magnetic field, (T), 25:9342
intensity of, relation with Pc2, -3, and -4 geomagnetic field pulsations, (E/T), 25:9353
RNA NUCLEOTIDYLTRANSFERASE
radiation effects on activity of, effects of dose on x, 25:8610
ROCKET REACTORS (NERVA)
structures for, effects of launch and mission requirements on stress limits of, 25:10289
ROCKETS
research program at European Space Research and Technology Centre on sounding, 25:9336
ROCKS
analysis by neutron activation and autoradiography, 25:8234
analysis for cesium and tantalum by thermal neutron activation and γ spectrometry, 25:8230
analysis for uranium by neutron activation, 25:8219 (PH-3)
analysis of Project Gasbuggy holes GB-1 and GB-3, data tabulation on petrographic, 25:8385 (PNE-G-69)
crystal structure of, autoradiographic studies on, 25:8234
lithology of Pahute Mesa Drill Hole No. 1, revised data on, 25:8357 (USGS-474-96)
ROOTS
ion fluxes in corn, effects of carbonylcyanide m-chlorophenylhydrazone and uranium oxide ions on chlorine and rubidium, 25:8602
ROSE BENGAL
sensitivity of iodine-131-labeled, for liver function appraisal in comparison to sulfobromophthalein sodium, 25:8722
ROVER REACTORS
fuel for, fluidized-bed burner for reprocessing of, 25:8322 (IN-1423)
RUBIDIUM
reactions with cesium and rubidium atoms, total cross sections for elastic scattering and spin exchange in, (T), 25:9202
scattering by potassium and sodium at 0.1 to 0.2 eV, analysis of data on differential spin exchange in, (T), 25:9224
scattering by potassium and sodium at 0.1 to 0.2 eV, differential cross sections for elastic and spin-exchange, (E), 25:9223
RUBIDIUM IONS
transport in corn roots, effects of carbonylcyanide m-chlorophenylhydrazone and uranium oxide ions on, 25:8602
RUTHENIUM
determination by atomic absorption spectrophotometry, 25:8209
determination in iron oxide-coated silicious waste materials, spectrographic, 25:8196 (BARC-504)
effects on colorimetric determination of uranium in fuel reprocessing solutions, 25:8197 (BARC-510)
separation from effluents from chemical decanning of reactor fuel elements by sorption on ferrous hydroxide or sulfide, 25:8344(P)
RUTHENIUM ISOTOPES Ru-106
distribution in uranium dioxide fuels at high burnups, determination by gamma scanning, 25:8951(R) (GEAP-10217)

S

S-816 (COBALT ALLOY)
analysis for molybdenum using mercaptosuccinic acid, spectrophotometric, 25:8210
S-MATRIX
amplitude for weak interactions, 25:9740
commutation with axial charge, Adler self-consistency condition and universality of π coupling to hadrons at low energies from, 25:9886 (DESY-70/57)
formulation for gravitational fields, 25:9857
formulation for Yang--Mills field, 25:9857
SAFETY
programs and services of safety department at Goodyear Atomic Corporation during 1969, progress report on, 25:8692(R) (GAT-627)
SALT DEPOSITS
radioactive waste disposal in, National Academy of Sciences recommendations for solid, 25:8455 (TID-25576)
SALTS
effects on reactions of hydrated electrons in pulse radiolysis of water, 25:8291
SAMARIUM
determination in titanium and titanium dioxide by neutron activation, 25:8233
SAMARIUM ISOTOPES Sm-144
proton elastic scattering at 30 MeV, optical model analysis of, (E), 25:9978(R) (ORO-3398-26)
proton reactions (p,d) with, angular distributions for, (E), 25:9978(R) (ORO-3398-26)
proton reactions (p,t) with, angular distributions and Q-value for, (E), 25:9978(R) (ORO-3398-26)
SAMARIUM ISOTOPES Sm-148
energy levels from samarium-150 (p,t) reactions, (E), 25:9966(R) (COO-1265-94)
SAMARIUM ISOTOPES Sm-150
alpha reactions (α,xnγ) at 25 and 30 MeV, γ spectra from, (E), 25:9978(R) (ORO-3398-26)
proton reactions (p,t) at 19 MeV, triton spectra from, (E), 25:9966(R) (COO-1265-94)
SAMARIUM ISOTOPES Sm-151
energy level at 167 keV, g-factor for, (E), 25:10035
energy-level transitions in, multipolarities for, (E), 25:10035
SAMARIUM ISOTOPES Sm-152
alpha reactions (α,xnγ) at 40 and 45 MeV, γ spectra from, (E), 25:9978(R) (ORO-3398-26)
energy levels from samarium-154 (p,t) reactions, (E), 25:9966(R) (COO-1265-94)
performance of activation detectors of, for neutron spectra measurements at 1 eV to 10 keV, 25:8481 (KFK-1233)
SAMARIUM ISOTOPES Sm-154
proton reactions (p,t) at 19 MeV, triton spectra from, (E), 25:9966(R) (COO-1265-94)
SAN ONOFRE POWER REACTOR, UNIT 1
operations history for December 1970, 25:10117 (DOCKET-50206-102)
operations history for November 1970, 25:10116 (DOCKET-50206-100)
SAPPHIRES
radiation effects on microstructure and swelling of synthetic, in-pile, 25:8954 (ORNL-4600, pp 210-15)
SATELLITES
cosmic x-ray observation with, lunar occultation technique for, (E), 25:9065
research program at European Space Research and Technology Centre, 25:9336
SAXTON POWER REACTOR
control elements for, revised scram test schedule for, 25:10137 (DOCKET-50146-67)
fuel elements for, authorization for 4000 MWd Core 3 operation before midlife inspection of, 25:10137 (DOCKET-50146-67)
fuels for Core II of, burnup of plutonium oxide (PuO_2)--uranium oxide (UO_2), (E/T), 25:10213(R) (WCAP-3385-25)
operation during July to September 1970, summary of Core III, 25:10213(R) (WCAP-3385-25)
SCALERS
development of modular, for radiation detectors, 25:8483 (PH-1)
SCANDIUM
abundance in eucrites, (E), 25:8966
hydrolysis of, square wave dissociation field effect apparatus for kinetic studies on, 25:8240
magnetic properties of, incipient antiferro-, 25:9591
performance of activation detectors of, for neutron spectra measurements at 1 eV to 10 keV, 25:8481 (KFK-1233)
superconductivity in, search for, 25:9591
SCANDIUM ALLOYS AND SYSTEMS
Al-base--Gd--Sc, phase diagram at 500°C, 25:8886
SCANDIUM ISOTOPES Sc-44
energy levels from scandium-45 (α,d) reactions, spectroscopic factors for, (E), 25:9966(R) (COO-1265-94)
SCANDIUM ISOTOPES Sc-45
energy levels from calcium-42 (α,pγ) reactions, spin assignments for, (E), 25:9996 (ANU-P-466)
energy levels from titanium-46 (d,He-3) reactions, spectroscopic factors for, (E), 25:9966(R) (COO-1265-94)
energy-level transitions from calcium-42 (α,pγ) reactions, multipole mixing ratios for, (E), 25:9996 (ANU-P-466)
proton reactions (p,n) at 2,8 to 5.6 MeV, neutron and γ spectra and angular distributions for, (E), 25:10003
SCANDIUM ISOTOPES Sc-46
transport in food chains of nuclear-explosion-contaminated estuarine and marine ecosystems in relation to daily ingestion by man, use of stable element content of fish and invertebrates for predicting, 25:8627
SCANDIUM ISOTOPES Sc-47
energy levels from titanium-48 (d,He-3) reactions, spectroscopic factors for, (E), 25:9966(R) (COO-1265-94)
SCATTERING
amplitudes in dual-symmetric theory, functional integrals for N-particle Veneziano, 25:9901
amplitudes in perturbation-theory model, unitarity and fixed poles of weak, 25:9898
amplitudes of high-energy, representation for relativistic, 25:9749 (JINR-E2-5341)
amplitudes of, direct-channel Regge poles for finite-energy sum rules for, 25:9801
amplitudes of, relativistic eikonal expansion of, 25:9897

amplitudes of, S-matrix commutation with axial charge for Adler zeros of, 25:9886 (DESY-70/57)
amplitudes of, two-particle symmetry model for partial-wave, 25:9818
amplitudes with finite number of daughter Regge trajectories in, generalized Veneziano model for, 25:9888 (ITF-70-78)
amplitudes with Regge cuts in Veneziano model, dual, 25:9899
average angle of, in energy-dependent problems, (T), 25:9959
formalism for resonahce, definition of quasi-stationary states in, 25:9209
parameters in, K harmonics for, 25:9889 (JINR-P4-5366)
phase shifts in elastic potential, Pade and Fredholm approximants for S-wave, 25:9892
potential, Pade and Fredholm approximants for S-wave phase shifts in elastic, 25:9892
potential, resonance approximations for, 25:9894
potential-theory model of, unitarization of Veneziano amplitude in, 25:9900
resonance, exactly soluble three-body model of, 25:9890
S-matrix for inelastic, WKB method for calculation of, 25:9198
theory of two-body, including exchange reactions and excitation in internal states, classical, 25:9231
theory of, correspondence between classical observable and semiclassical S-matrix in, 25:9228
three-body problem with local potentials, model Hamiltonian for, 25:9891
time delay in, K harmonics for, 25:9889 (JINR-P4-5366)
wave functions for inelastic, WKB method for calculation of, 25:9198
SCHIZOMYCOTA
Bacillus megaterium, radiosensitivity of spores of, effects of nitrous oxide on, 25:8810
Bacillus subtilis, radiation effects on transforming DNA in, protective effects of acridine orange against cesium-137 γ, 25:8707
Clostridium botulinum, radiation effects on growth of spores of Type E, on fresh shrimp, γ, 25:8804 (TID-25556)
Escherichia coli, radiation damage to DNA of, model for excision repair of, 25:8636 (SU-326-P-7-X-22)
Escherichia coli, radiation effects on DNA of, analysis of photoenzymatic repair of, uv, 25:8652
Escherichia coli, radiation effects on genetic recombination in partially diploid derivatives of, uv, 25:8634(R) (ORO-4024-1)
Escherichia coli, radiation effects on survival of, iodine-125 γ, 25:8654
Escherichia coli, radiation effects on survival of, effects of sodium fluorescein and culture medium on xenon, 25:8807
Escherichia coli, radiation effects on transforming DNA in, protective effects of acridine orange against cesium-137 γ, 25:8707
Escherichia coli, radioinduced lesions in DNA of, effects of photoenzymatic repair inhibition by caffeine on uv, 25:8649
Escherichia coli, radioinduced mutations in, for auxotrophy, combined effects of formaldehyde with nitrosomethylurethan on spectrum of uv, 25:8642
Escherichia coli, radiosensitive mutants of, review of properties of uv, 25:8633 (NP-18483)
Escherichia coli, radiosensitivity of, effects of glucose on, γ, 25:8812
Ferrobacillus ferrooxidans, use in leaching of uranium ores, 25:8337
Haemophilus influenza, radiation effects on formation and dissociation of enzyme substrate-complexes in DNA of, uv, 25:8651
Haemophilus influenzae, radiation effects on photolysis of DNA in, determination of repair rate of uv, 25:8650
Lactobacillus casei, assay for serum folate in, methods for radioisotope, 25:8809
Micrococcus lysodeikticus, lytic effects of lysozyme on, 25:8604 (COO-690-41)
Mycoplasma sp., radiation damage to, repair replication of uv, 25:8636 (SU-326-P-7-X-22)
radioinduced inactivation of spores of, in relation to sterilization of space craft, progress report on synergistic effects of low temperature on low dose rate γ, 25:8803(R) (TID-25468)
radiosensitivity of anoxic, effects of triacetoneamine-N-oxyl on, 25:8701
Serratia marcescens, radiation effects on survival of, effects of sodium fluorescein and culture medium on xenon, 25:8807
Shigella flexneri, radiation effects on OER of, effects of anoxia on, 25:8811
SCINTILLATION CAMERAS
images from, contrast perception in, 25:8496
SEALS AND GLANDS
design for through-wall pressure vessel probe mounts, 25:8402(P)
design for tightly closing apertures, 25:8403(P)
SEAWATER
analysis for cesium by thermal neutron activation and γ spectrometry, 25:8230
carbon-14 content of southern oceans to 4000 m depths, 1968 and 1969, 25:8381
corrosive effects on materials at temperatures to 150°C, 25:10360(T) (ORNL-tr-2412)
desalination of, use of acrylic polymers, acid, and calcium carbonate precipitation in control of scale formation at high temperatures in, 25:10359(T) (ORNL-tr-2411)
mercury-203 content of, in comparison to content of molluscs, 25:8625 (NP-18429)
SEED
radiation effects on germination of, in coastal and interior Douglas fir, Sitka spruce, and western hemlock, γ, 25:8799
radiation effects on, of agricultural plants, effects on crop yield from, 25:8813 (NP-18236)
radioinduced mutations in, of wheat, x, 25:8655
SEISMIC WAVES
measurements of, ADSS computer program for reducing digitized data from, 25:8382 (UCRL-50939)
SEISMOLOGY
research at Bhaba Atomic Research Center in 1969, 25:10017(R) (BARC-501)
SELENIUM
determination by neutron activation, 25:8227
SELENIUM ISOTOPES Se-72
energy levels from germanium-70 (α,2n) reactions, collective, (E), 25:10001
SELENIUM ISOTOPES Se-74
energy levels from germanium-72 (α,2n) reactions, collective, (E), 25:10001
SELENIUM ISOTOPES Se-75
effectiveness of selenomethionine-incorporated, for diagnosis of human liver cirrhosis, evaluation of biphasic scanning methods for, 25:8715
SELENIUM ISOTOPES Se-76
energy levels from germanium-74 (α,2n) reactions, collective, (E), 25:10001
SELENIUM ISOTOPES Se-78
energy levels from germanium-76 (α,2n) reactions, collective, (E), 25:10001
SELENIUM ISOTOPES Se-80
performance of activation detectors of, for neutron spectra measurements at 1 eV to 10 keV, 25:8481 (KFK-1233)
SELENIUM SYSTEMS
Se--Zr-base, corrosion by steam at 300 to 600°C, factors affecting, 25:8833 (AERE-M-1854)
SEMICONDUCTORS
book: Methods of Investigation of Thermoelectric Properties of Semiconductors, in Russian, 25:9590
dielectric--semiconductor, radioinduced electric charges in, 25:9566
SENA POWER REACTOR
fuel inventory for August 1970, 25:10128 (TID-25629)
fuel inventory for September 1970, 25:10127 (TID-25628)
maintenance during August 1970, 25:10128 (TID-25629)
maintenance during September 1970, 25:10127 (TID-25628)
operations during August 1970, 25:10128 (TID-25629)
operations during September 1970, 25:10127 (TID-25628)
SEPARATORS
improvement of film-type, by use of inhomogeneous magnetic field, (T), 25:9277
SERPUKHOV SYNCHROTRON
magnetic field topography in open and closed units of electromagnet in, 25:9906 (IFVE-SKU-69-95)
SEYFERT GALAXIES
mass loss from nuclei of, (T), 25:9130
spectral classification of Markaryan galaxies as, (E), 25:9140
SF MATERIALS ACCOUNTING
accuracy of, total quality control method for improving, 25:8448 (BNWL-SA-3336)
methods for uranium analysis in scrap recovery plant, 25:8447(R) (BHO-65-1)
SHELLS (GEOMETRY)
response of circular cylindrical, to nuclear explosions, acceptable imperfections in impulsive loads for simulation testing of structural, (T), 25:8441 (SC-RR-70-600)
SHIELDED CONTAINERS
design and safety of, for shipping solidified high-level radioactive wastes, calculations for, 25:8451 (ORNL-TM-2971)
design for irradiated fuels, 25:8456(P)
SHIELDING
access holes in reactor, description of top closure for, 25:10225(P)
book: Effective Protection of Space Ships, 25:9540
calculation of, (T), 25:9948
calculations for, comparison of Monte Carlo and discrete ordinate one-dimensional transport codes in, (E), 25:9536 (CEA-CONF-1669)
description of uranium scrap recovery plant, 25:8447(R) (BHO-65-1)
effectiveness of body, for protection of hematopoietic system in dogs against protons, 25:8755(T) (JPRS-51660)
gamma radiation leakage through right-angle wall joints in reactor, (E/T), 25:10296(T) (NSJ-tr-157)
neutron flux in iron--water layer, SABINE code calculations of, 25:10192 (CEA-N-1354)
radiation standards subcommittee report, 25:9538 (ORNL-

XUM

TM-3251)
SHIPPING
radiation protection programs for human population in event of accidents during radioisotope, in Italy, 25:8696
SHIPPINGPORT PRESSURIZED-WATER REACTOR
operation during October 25, 1969, to January 23, 1970, 25:10129(R) (WAPD-MRP-131)
SHIPS
book: Magnetohydrodynamics in Marine Engineering, 25:9266
operation of nuclear, reactor protection procedures for safe, 25:10295(T) (JPRS-51939)
SHOCK TUBES
design for plasma spectra studies, 25:9510
electron density behind shock front in magnetohydrodynamic, (E/T), 25:9446
plasma diagnostics in, electron temperature and density, 25:9418
plasma diagnostics in, using fast-response spectrometers, 25:9423
plasma production in electromagnetic, precursor ionization, 25:9486
shock wave structure in electromagnetic, in flowing gas, (E/T), 25:9445
SHOCK WAVES
current behind piston-driven, calculation of, 25:9436
magnetic field induction by piston-driven, calculation of, 25:9436
production and structure in colliding plasmas, collisionless electrostatic, (E/T), 25:9437
production in collisionless plasmas, in strong theta pinch, (E), 25:9452
propagation in gas in uniform magnetic field of pressure, magnetohydrodynamic, (T), 25:9278
propagation in solar wind, (T), 25:9107
propagation in warm collisionless magnetoplasma, (T), 25:9461
propagation of chromospheric flare-induced, distribution in solar wind of, (E/T), 25:9356
properties and uses of, 25:10409 (UCRL-72770)
structure in flowing gas in electromagnetic shock tubes, (E/T), 25:9445
structure of MHD gas-ionizing, (T), 25:9272
SILANE
reactions of substituted, with recoil silicon-31 and tritium, 25:8310(R) (ORO-3898-2)
reactions with recoil silicon-31 and tritium, 25:8310(R) (ORO-3898-2)
acetylene--SiH_4, ionization in mass spectrometer, reactions of products from, 25:8294
benzene--SiH_4, ionization in mass spectrometer, reactions of products from, 25:8294
ethylene--SiH_4, ionization in mass spectrometer, reactions of products from, 25:8294
hydrocarbons--SiH_4, radiolysis of, mass spectrometric studies on reactions in, 25:8294
methane--SiH_4, ionization in mass spectrometer, reactions of products from, 25:8294
SILICON
abundance in HD 34452, (E), 25:9056
abundance in iota Ori B, (E), 25:8995
abundance in L and H chondrites, (E), 25:8967
compounds, reactions with recoil chlorine-38, 25:8310(R) (ORO-3898-2)
determination in air particulates by spark source mass spectrometry, 25:8208
effects on creep in shielded metal-arc welds in stainless steel, 25:8849 (ORNL-4600, pp 142-6)
electron channeling at 148 keV in monocrystals of, 25:9543
ion implantation in single crystals of, enhanced diffusion in high-temperature antimony, 25:9569
oxygen-ion implantation at 220 keV in, localized vibrational modes and divacancy absorption spectra, 25:9550
positron channeling at 247 keV in monocrystals of, 25:9543
radioinduced defects in lithium-doped single crystals of, EPR study of electron, 25:9558
radioinduced defects in p-type, impurity effects on annealing of electron, 25:9549
radioinduced defects in p-type, minority carrier lifetime study of recombination center annealing in gamma, 25:9567
radioinduced defects in single crystals of, x-ray topograhic study of gamma and fast-neutron, 25:9572
radioinduced emf in p-type, volume-gradient gamma, 25:9568
radioinduced lattice expansion of, 400 keV xenon ion, 25:8964
spectral broadening of lines of, by electrons and hydrogen atoms, (E), 25:9187
SILICON CARBIDES
radioinduced centers in 3C and 6H single crystals of, ESR of electron and neutron, 25:9545
SILICON HYDRIDES
detection of ionized, in photospheric spectrum, (E), 25:9120
SILICON ISOTOPES Si-28
electron inelastic scattering from, calculation of form factors using Serber--Yukawa residual interactions for, (T), 25:10010
energy levels from aluminum-27 (d,n) reactions, nuclear structure effects in isobaric analog, (E), 25:10007
energy levels from electron inelastic scattering, wave functions for, (T), 25:10010
mass hexadecapole moments of, Hartree--Fock--Bogolyubov calculations of, (T), 25:10008
SILICON ISOTOPES Si-30
mass hexadecapole moments of, Hartree--Fock--Bogolyubov calculations of, (T), 25:10008
photon reactions (γ,p) at 100 to 800 MeV, excitation functions for, (E/T), 25:9977 (LUNP-7009)
SILICON ISOTOPES Si-31
reactions of recoil, with hydrocarbons and silanes, 25:8310(R) (ORO-3898-2)
SILICON ISOTOPES Si-32
mass hexadecapole moments of, Hartree--Fock--Bogolyubov calculations of, (T), 25:10008
SILICON OXIDES
effects of dispersions of, on properties of copper, 25:8873
properties for use in dispersion strengthening of aluminum, 25:8860(P)
Si--SiO_2, radioinduced electric charges in dielectric-semiconductor structures, proton, 25:9566
SILICON SYSTEMS
Al--C--Fe--Si--U-base, tensile properties of dilute, at 885 to 1150°F, 25:8867 (NLCO-1060)
Be--Si--U, crystal structure of ordered solid solution of, 25:8947
Be--Si--U, phase studies of ordered solid solutions of, 25:8888
Cr--Fe-base--Ni--Si, corrosion by water containing trace chloride and oxygen at 200°C, stress, 25:8834(R) (COO-2069-6)
Si--SiO_2, radioinduced electric charges in dielectric-semiconductor structures, proton, 25:9566
SILTS
effects of fine suspended, in ground waters, on radioisotope transport through soils, (E/T), 25:8361
SILVER
alpha reactions at 30 to 80 MeV, K-shell ionization cross sections for, (E), 25:9978(R) (ORO-3398-26)
alpha reactions at 85 MeV, spectra of light fragments from, (E), 25:9978(R) (ORO-3398-26)
crystal structure at 40 to 180°K, 25:8876
determination in airborne particulates by neutron activation, 25:8231
determination in liquid silver--sodium alloys by dissolution, filtration, and potassium thiocyanate titration, 25:8198 (BNL-50271)
determination in titanium and titanium dioxide by neutron activation, 25:8233
diffusion in, lattice-dynamical theory of isotope effects in, 25:9589
electron elastic scattering at 100 to 1300 keV by foils of, as function of foil thickness and incidence angle, single, plural, and multiple, (E), 25:9225
positron elastic scattering at 100 to 1300 keV by foils of, as function of foil thickness and incidence angle, single, plural, and multiple, (E), 25:9225
radioinduced production and solubilization of colloidal, effects of organic solutes and nitrates on γ, 25:8302
thermal expansion coefficients at 50 to 160°K, 25:8876
SILVER ALLOYS AND SYSTEMS
Ag--Na, analysis of liquid, for silver by dissolution, filtration, and potassium thiocyanate titration, 25:8198 (BNL-50271)
SILVER BROMIDES
radiolysis of colloidal, effect of organic solutes on γ, 25:8302
SILVER ISOTOPES Ag-107
energy levels from silver-109 (p,t) reactions, (E), 25:9966(R) (COO-1265-94)
SILVER ISOTOPES Ag-109
proton reactions (p,t) at 19 MeV, angular distributions for, (E), 25:9966(R) (COO-1265-94)
SILVER NITRATES
radiolysis of aqueous gelatin-containing solutions of, γ, 25:8302
SKIN
plutonium-239 content of, review of effects of administration route, age, and dose on, 25:8595(T) (LF-tr-41, pp 7-125)
radiation effects on allografts of, in leopard frogs, effects of 5000 R dose on γ, 25:8620
SMOKES
polonium-210 content of tobacco, relation of, to content of tissues following inhalation by dogs, 25:8623 (BNWL-SA-3419)
SODIUM
abundance in late G and K dwarfs in the solar neighborhood, (E), 25:8969
bearings for use in liquid, design and development of, 25:8394(R) (NYO-3930-7)
boiling of, effects of inert gas partial pressure variations on incipient, 25:8415
combustion of, guidelines for control, detection, and prevention of, 25:8827 (ANL-7691)
corrosive effects on refractory alloys at high temperatures, 25:8836 (ORNL-4600, pp 157-66)

determination in air particulates by spark source mass spectrometry, 25:8208
determination in airborne particulates by neutron activation, 25:8231
determination in human fingernails and hair by neutron activation and γ spectrometry, 25:8229
determination in titanium and titanium dioxide by neutron activation, 25:8233
diffusion in, lattice-dynamical theory of isotope effects in, 25:9569
effects on oxidation of Type 304L stainless steel at 760°C, 25:8836 (ORNL-4600, pp 157-66)
handling and purification of, design of facility for, 25:8390 (AERE-R-5502)
neutron flux distribution in sphere of, from fission source at center, 25:9944 (ORNL-TM-3156)
performance of activation detectors of, for neutron spectra measurements at 1 eV to 10 keV, 25:8481 (KFK-1233)
preparation of metallographic specimens of, uses of microtomes in, 25:8845 (AERE-R-5483)
reactions between atoms of, total cross sections for elastic scattering and spin exchange in, (T), 25:9202
reactions with plutonium dioxide--uranium dioxide fuels at high temperatures, effects of oxygen-to-metal ratio on, 25:8926(R) (GEAP-12133)
reactions with rare gas atoms, impact-parameter calculation of cross sections for fine-structure transitions in, 25:9207
scattering by cesium, differential cross sections for spin exchange in, (T), 25:9212
scattering by cesium, potassium, and rubidium at 0.1 to 0.2 eV, analysis of data on differential spin exchange in, (T), 25:9224
scattering by cesium, potassium, and rubidium at 0.1 to 0.2 eV, differential cross sections for elastic and spin-exchange, (E), 25:9223

SODIUM ALLOYS AND SYSTEMS
Ag--Na, analysis of liquid, for silver by dissolution, filtration, and potassium thiocyanate titration, 25:8196 (BNL-50271)
Cd--Na, analysis of liquid, for cadmium by dissolution, filtration, and EDTA titration, 25:8198 (BNL-50271)
In--Na, analysis of liquid, for indium by dissolution, filtration, and ammonium hydroxide precipitation, 25:8198 (BNL-50271)
Na--Sb, analysis of liquid, for antimony by dissolution, filtration, and colorimetry, 25:8198 (BNL-50271)
Na--Sn, analysis of liquid, for tin by dissolution, filtration, and colorimetry, 25:8198 (BNL-50271)

SODIUM BOROHYDRIDES
phase studies on, 25:8263
spectra of, ir, 25:8263

SODIUM CHLORIDES
anion-vacancy processes occurring after F-light bleaching or irradiation of crystals of, study of thermally activated, 25:9559
radiation effects on dislocation pinning in single crystals of, internal friction and Young's modulus study of fast-neutron, 25:9547

SODIUM HYDROXIDES
radiation effects on ices of, γ, 25:8272
spray additives of, effects on fission product removal from containment systems of, 25:10256 (BNWL-1485)

SODIUM IONS
implantation into cadmium sulfide, acceptor luminescence induced by, 25:9561

SODIUM ISOTOPES Na-20
alpha decay of, α spectra from β-delayed, (E), 25:9978(R) (ORO-3398-26)

SODIUM ISOTOPES Na-23
helium-3 reactions (He-3,t) at 18 MeV, DWBA analysis of differential cross sections from, (E/T), 25:10013

SODIUM NITRATES
radiolysis of aqueous solutions of, yields of nitrites from γ, 25:8297

SODIUM SULFATES
H_2SO_4--Na_2SO_4, corrosive and passivating effects on iron, electrochemical studies of, 25:8834(R) (COO-2069-6)

SODIUM THIOSULFATES
effects of spray additives of, on fission product removal from containment systems of, 25:10256 (BNWL-1485)
effects on methyl iodide reaction rate with reactor containment spray solutions, (E), 25:10244(R) (ORNL-TM-3212)

SOIL MECHANICS
interactions with reactor structure foundations, effects of earthquakes on, 25:10245 (ORO-3822-5)

SOILS
gamma dose rates in, from artificial and natural radioisotopes, method for distinguishing, 25:8360
polonium-210 content of greenhouse, role of fallout as primary source for, 25:8593 (COO-1733-11)
polonium-210 migration in, hazards to water supplies from, 25:8593 (COO-1733-11)
polonium-210 sorption as oxide by agricultural top, in relation to silt content and soil pH, distribution coefficients for, 25:8593 (COO-1733-11)
polonium-210 uptake as oxide by crops from, transfer coefficients for calculating human dietary intake from, 25:8593 (COO-1733-11)
radioisotope transport through Hanford area, mathematical model for prediction of, 25:8345 (BNWL-SA-3494)
radioisotope transport through, effects of fine particulate matter in ground waters on, (E/T), 25:8361
research at AECL during 1970, progress report on, 25:8666(R) (AECL-3728)
strontium-90 content of Rocky Flats, Colorado, from atmospheric nuclear explosion fallout, measurement of, 25:8353 (HASL-237, pp I.11-26)
water content of, neutron radiometric gage for measurement of, 25:8570

SOL-GEL PROCESS
advantages for preparation of ceramic nuclear fuels, 25:8915

SOLAR CORONA
properties of, from study of solar wind, (T), 25:9107
spectra of, electron excitation rate for 5303-A line in, (T), 25:9123

SOLAR FLARES
effect on electron enhancement in sunlit ionosphere, Feb. 20, 1970, (E), 25:9333
effects on D-region electron density, Oct. 21, 1968, (E), 25:9300
effects on solar wind, (T), 25:9107
helium isotope abundances in, (E), 25:9103
shock waves from chromospheric, propagation of, (E/T), 25:9356

SOLAR GRANULES
formation of giant, (T), 25:9112

SOLAR RADIATION
absorption of hard x, in ionospheric D region, 25:9330
relation of 3180-A, to D-region properties at 73 km in sunrise auroral ionosphere, (E), 25:9296

SOLAR RADIO BURSTS
detection at all frequencies, simultaneous observations at Earth and on spacecraft, (E/T), 25:9124
relation of millimeter, to gradual rise of soft x-ray emission, (E/T), 25:9121

SOLAR WIND
composition of, (T), 25:9107
discontinuities in, correlation with anisotropic plasma and magnetic field, (T), 25:9306
dynamics of, (T), 25:9107
electron temperature in two-component, (T), 25:9114
interactions with Moon, electromagnetic sounding, (T), 25:9159
proton density in, power spectra of, (E), 25:9102
shock wave propagation in, distribution of chromospheric flare-induced, (E/T), 25:9356

SOLAR X-RAY BURSTS
relation to millimeter radio bursts, (E/T), 25:9121

SOLID STATE PHYSICS
research at Bhaba Atomic Research Center in 1969, 25:10017(R) (BARC-501)
research at Chalk River Nuclear Laboratories April 1 to June 30, 1970, 25:9970(R) (AECL-3668)
research at Technische Hochschule in 1969, 25:10018(R) (BMBW-FBK-70-10)

SOLIDS
radiation effects on, reactions of recoils from, 25:8314
radiation effects on, reactions of recoils from, 25:8313

SORBIC ACID
effects on shelf life of γ-irradiated shrimp, 25:8820

SOUTHWEST EXPERIMENTAL FAST OXIDE REACTOR
cover gas monitoring system for, failed fuel operation specifications for, 25:10240 (DOCKET-50231-63)
fuel elements for, operation restrictions for guinea pig, 25:10239 (DOCKET-50231-61)
operations history for August to October 1970, 25:10235 (DOCKET-50231-64)
operations incident of December 12, 1970, malfunction of emergency electrical system circuit breaker, 25:10234 (DOCKET-50231-62)

SOVIET UNION
uranium content of foods in, 25:8631

SPACE
properties of gases in interplanetary, adiabatic relationship with, (T), 25:9115
research program at European Space Research and Technology Centre, 25:9336

SPACE FLIGHT
effects on physiology of animals and plants, 25:8755(T) (JPRS-51660)
radiation dosimetry during Apollo VI and VII, use of nuclear emulsions for proton, 25:8682

SPACE VEHICLES
book: Effective Protection of Space Ships, 25:9540
conference on propulsion of, 10th international, Rome, Italy, 3/70, 25:10420
materials for, performance of, 25:10288
propulsion systems for deep, comparison of operation costs for chemical and nuclear, 25:10287
radiation flux mapping of OPE-model, containing radioisotopic thermoelectric generator, 25:9537 (N-70-34007)
radiosterilization of, progress report on projects related to low temperature, low dose rate γ, 25:8803(R) (TID-25468)
stress analysis for, 25:10288
stress limits of nuclear propelled, effects of launch and mission requirements on, 25:10289

XUM

SPAIN
nuclear power plants in, development during 1970 to 2000 of, 25:10104
power reactor component fabrication facilities in, 25:10103
SPECTROMETERS
circuits for nuclear, pulse generator for stabilizing, 25:8542
detector for magnetic charged-particle, position-sensitive semiconductor, 25:8474 (JUL-CONF-4, pp 48-58)
detector for magnetic, position-sensitive multiwire proportional, 25:8479 (JUL-CONF-4, pp 148-64)
detectors for magnetic, position-sensitive spark and multiwire proportional, 25:8476 (JUL-CONF-4, pp 71-120)
detectors for split-pole magnetic, multiwire spark and proportional, 25:8478 (JUL-CONF-4, pp 141-7)
windows for, design of, 25:8534(P)
SPECTROSCOPY
book: Developments in Applied Spectroscopy, 25:8538
SPERMATOGENESIS
radiation effects on uptake of tritium-labeled thymidine by human and rat, autoradiography of x, 25:8789(R) (NYO-4034-2)
SPHERES
neutron propagation in, computer program using Monte-Carlo method for calculating, (T), 25:9941 (CEA-N-1361)
SPINAL CORD
radiation effects on, of animals, following exposure of brain stem, x, 25:8771
SPLEEN
radiation effects on hematopoietic colony formation in, of mice, effects of ACTH, cold exposure, and dexamethasone on γ, 25:8767
radiation effects on hematopoietic colony formation in, of mice, effects of dexamethasone on γ, 25:8765
radiation effects on lymphoid tissue in, of mice, RBE for whole-body electrons, 25:8780
removal from mice, effects of, on x-radioprotective effects of bone marrow transplants, pre- and post-exposure, 25:8706
SPORES
radiation effects on growth of Clostridium botulinum Type E, on fresh shrimp, γ, 25:8804 (TID-25556)
radiosensitivity of Bacillus megaterium, effects of concentration of hydroxyl radicals on x, 25:8810
SPRAYS
performance for removal of fission products from reactor containment, effects of sodium hydroxide and sodium thiosulfate additives on, (E), 25:10256 (BNWL-1485)
STABLE ISOTOPES
content in surface atmosphere at selected land and marine sites during 1963 to 1970, monthly averages of fallout, 25:8670(R) (HASL-237(App.))
separation and purification of, research program on, 25:8424(R) (MLM-1768)
STACK DISPOSAL
effluents from reactor, argon-41 tracer studies of atmospheric dispersion of, 25:8363 (AECL-3731)
radiation doses from, accuracy of methods for calculating, 25:8668 (BNWL-SA-3424)
radioactive contamination of atmosphere by nuclear power plant, effects of short-term releases on, 25:8371 (SZS-14/70 (pp 1-10))
radioactive gas release from power reactor, effects of reactor operation on, 25:10162
radioactivity release from ORNL reactor, methods for calculating, 25:8452 (ORNL-TM-3187)
STAINLESS STEEL
book: Metallurgy and the Hot Working of Metals, 25:8894
corrosion by boiling aqueous magnesium chloride, effects of partial currents on, 25:8834(R) (COO-2069-6)
corrosion by hydrofluoric acid--nitric acid solutions at 140°F, effects of thermally-induced sensitization on, 25:8834(R) (COO-2069-6)
corrosion by sulfuric acid at 140°F, effects of thermally-induced sensitization on, 25:8834(R) (COO-2069-6)
corrosion of Type 304, by steam at 525 to 650°C, 25:8838 (ORNL-4600, pp 282-6)
corrosion of welds in Type 304, by copper sulfate, test specimen preparation for studies of, 25:8848 (ORNL-4600, pp 131-41)
creep in welds in, effects of boron, carbon, phosphorus, silicon, and sulfur on, 25:8849 (ORNL-4600, pp 142-6)
defects in tubes of Type 316, effects of fabrication variables on, 25:8847 (ORNL-4600, pp 126-30)
fatigue of pipes of Type 304, cracking in low-cycle, 25:8866 (GEAP-10205)
fatigue of Type 304, at 1200°F, effects of hold times and strain on, 25:8864 (BMI-1891, Sect.A)
fatigue of Type 304, effects of BWR environments on low-cycle, 25:8866 (GEAP-10205)
hardening of Type 316, methods for shock, 25:8895 (BMI-1891, Sect.B)
mass transfer to vanadium at 600 to 700°C by sodium, 25:8836 (ORNL-4600, pp 157-66)
mechanical properties at 20 to 239°K, design of device for determining low-temperature, 25:8881
mechanical properties of welds in, effects of lime--titanium dioxide electrode coating on, 25:8849 (ORNL-4600, pp 142-6)
microstructure of Type 316, effects of thermomechanical treatments on, 25:8952 (ORNL-4600, pp 81-125)
microstructure of, effects of cold working on, 25:8854 (ORNL-4600, pp 252-65)
oxidation of Type 304L, at 760°C, effects of sodium on, 25:8836 (ORNL-4600, pp 157-66)
plastic deformation of austenitic, at very low temperatures, 25:10357(T) (ORNL-tr-2314)
properties for use in internal reactor components, review of, 25:8828 (BNWL-SA-3426)
properties of Type 316, physical and tensile, 25:8911 (ORNL-4600, pp 65-80)
properties of welds of, effects of ferritic and martensitic secondary phases on, 25:8854 (ORNL-4600, pp 252-65)
radiation effects on creep rupture of Type 304, at 600°C, fast neutron, 25:8897 (ORNL-TM-3169)
radiation effects on creep rupture of Type 304, fast neutron, 25:8952 (ORNL-4600, pp 81-125)
radiation effects on fuel element cladding of, fast neutron, 25:8896(T) (BNWL-tr-57)
radiation effects on tensile properties of Types 347 and 348, in-pile, 25:8895 (BMI-1891, Sect.B)
solvent properties for transition metal $M_{23}C_6$-phase in Type 316, at 750 to 1100°C, 25:8875
welding of Type 304, performance of submerged-arc method for, 25:8848 (ORNL-4600, pp 131-41)
Cr--Mo--Ni--stainless steel, analysis for molybdenum using mercaptosuccinic acid, spectrophotometric, 25:8210
Cr--Ni--stainless steel, analysis for molybdenum using mercaptosuccinic acid, spectrophotometric, 25:8210
STANDARDS
development of water cooled and liquid metal cooled reactor engineering, 25:10244(R) (ORNL-TM-3212)
STAR CLUSTERS
age of NGC 7142, 25:9022
color--magnitude diagram of NGC 7142, (E), 25:9022
distance of NGC 2236, (E), 25:9024
distance to Hyades, (E), 25:8982
distance to Praesepe, (E), 25:8982
distances of NGC 7226, NGC 7245, IC 1442, and Be 94, (E), 25:8993
distribution functions of, (T), 25:8971
metal abundance in NGC 6791, (E), 25:9000
models for globular, (T), 25:8971
photometry of NGC 7226, NGC 7245, IC 1442, and Be 94, three-color, (E), 25:8993
photometry of RR Lyrae variables in NGC 6171, (E), 25:8970
stability disturbance by passing interstellar clouds, (T), 25:9050
star membership of open cluster NGC 2420, (E), 25:9031
stars in M7 and NGC 7160, metallic-line, (E), 25:9051
stellar evolution in M2, M10, M13, M15, and NGC 6712, above horizontal branch, (E), 25:8992
velocities in Orion Nebula, rotational, (E), 25:8981
STARS
abundance analysis of iota Ori B, (E), 25:8995
atmospheres of, Chandrasekhar's X and Y functions for, (T), 25:9045
atmospheres of, curves-of-growth for expanding, (T), 25:9012
atmospheres of, formation of resonance lines in extended and expanding, (T), 25:9044
atmospheres of, radiative transfer with general anisotropic phase function in, 25:9054
atmospheres of, spectrum of anisotropic transfer equation for, (T), 25:9055
book: Binary Star Systems with Atmospheres of zeta Aurigae Eclipsing Type, in Russian, 25:8983
carbon abundance in 15 Mon A, (E), 25:9042
color of P Cyg, (E), 25:9036
color--magnitude diagrams for, in NGC 2420, (E), 25:9031
colors of main-sequence, UBVr, (E/T), 25:8988
convection in A and F, (E/T), 25:8989
detection of collapsing, use of helium-3 counters for, 25:8550
detection of infrared, in Cygnus, (E), 25:8991
detection of metallic-line, in M7 and NGC 7160, (E), 25:9051
detection of OH emission in Ceph IV association, (E), 25:9015
detection of, in fields of southern hemisphere radio sources, (E), 25:9066
distance separations for 23 visual double, (E), 25:9053
distances of Population-I Cepheid, use in determining galactic rotation, (E/T), 25:9151
distances to, effects on estimates of galactic rotation, (T), 25:9150
distribution in galaxy M33, (E), 25:9149
distribution of late B-type, (E), 25:8976
distribution of OB, in southern Milky Way, (E), 25:9026
dynamics of triple systems, effects of different masses on, (T), 25:9007
element abundances in peculiar A, (T), 25:8984
encounter phenomena in triple, (T), 25:8979
envelope models for A-Type, (T), 25:9019
envelopes of Wolf--Rayet components of close binary,

asymmetries, (T), 25:9004
evolution above horizontal branch in M2, M10, M13, M15, and NGC 6712, (E), 25:8992
evolution of 0.6-solar-mass, (T), 25:8978
evolution of Cepheids, (E/T), 25:8977
evolution of cores of, with initial mass 10 and 3 solar masses, (T), 25:8972
evolution of growing carbon cores of, (T), 25:9006
evolution of Population II, early, (T), 25:9041
evolution of unstable massive main-sequence, (T), 25:9039
evolution of, models for pre-supernova, (T), 25:9038
formation from grain-enriched gases, (T), 25:8999
formation in M31, (E), 25:9134
gas jets in close binary, trajectories of, (T), 25:9011
helium flash in, r-process in hydrodynamical model of, (T), 25:9037
infrared emission from Be, (E), 25:9018
kinematics of late B-type, (E), 25:8976
luminosities of OB, from Hβ indices, (E), 25:9049
luminosities of young disk-population red, (E), 25:9002
luminosity of P Cyg, (E), 25:9036
magnetic fields in, origin of, (T), 25:9129
mass accretion in white-dwarf, effects on pulsational stability, (T), 25:9040
mass loss from T Tauri, (E), 25:9029
mass loss rates for vibrationally unstable very massive main-sequence, (T), 25:9023
mass losses in close-binary, (T), 25:9033
metal abundances in late G and K dwarf, in the solar neighborhood, (E), 25:8969
model for calculating elements of close-binary, 25:8980
model for HD 173650, oblique rotator, (E/T), 25:9021
models for uniformly rotating main-sequence, (T), 25:9030
models for, slow rotation of relativistic polytropic, (T), 25:9078
models of, presupernova, (T), 25:9006
motion in close-binary, apsidal, (T), 25:9033
motion test for late-type, apsidal-, (T), 25:9005
neon abundance in O-type, (E), 25:9042
neutrino emission during gravitational collapse, (T), 25:8997
nucleosynthesis in, processes for, (T), 25:8987
parameters of stellar ring 274, (E), 25:9036
photometry of H-α emission, in southern Milky Way, (E), 25:9032
photometry of RR Lyrae variable, in NGC 6171, (E), 25:8970
position angles for 23 visual double, (E), 25:9053
pulsational stability of, effects of mass accretion on, (T), 25:9040
pulsations of unstable massive main-sequence, nonlinear, (T), 25:9039
radio spectrum of infrared, hydroxyl, (E), 25:8975
rotation effects in main-sequence, (T), 25:9030
rotation of, instabilities of differential, (T), 25:8985
spectra of 26 Be, widths of emission lines in, (E), 25:9034
spectra of giant, with strong cyanogen absorption, (E), 25:9043
spectra of HD 218393, radial velocities and line profile in, (E), 25:9017
spectra of HD 43818, variations in, (E), 25:9025
spectra of HD 59643, brightening of ultraviolet, (E), 25:9001
spectra of K line in γ Boo and three other A-type, (E), 25:9035
spectra of sigma Boo, ν Her, and 41 Cyg, (E), 25:9014
spectra of six O-type, (E), 25:9042
spectral analysis of HD 34452, model-atmosphere, (E), 25:9056
spectral parameters of technetium-containing, (E), 25:9057
spectrograms of CH Cygni, (E), 25:8990
spectrophotometric studies of nine Of, (E), 25:8986
spectrophotometry of F, (E), 25:9014
structure of atmospheres of binary, with atmospheres of zeta Aurigae eclipsing type, 25:8983
temperature of dense, effects of electron capture on, (T), 25:8973
temperatures of young disk-population red, (E), 25:9002
thermal behavior of rotating magnetic, (T), 25:9027
vacuum surrounding massive rotating Newtonian, (T), 25:9052
velocities in Orion Nebula cluster of 26 O6--A7, rotational, (E), 25:8981
velocities in short-period A-type binary, rotational, 25:9003

STEAM
corrosive effects on H327 graphite, (E), 25:10244(R) (ORNL-TM-3212)
corrosive effects on Incoloy 800 and Inconel 625 at 595 to 650°C, 25:8838 (ORNL-4600, pp 282-6)
corrosive effects on Type 304 stainless steel at 595 to 650°C, 25:8838 (ORNL-4600, pp 282-6)
corrosive effects on zirconium and zirconium alloys at 300 to 600°C, 25:8833 (AERE-M-1854)
mixing with water to produce dispersion of droplets in flowing gases, design of nozzle for, 25:8404(P)
H_2O--steam, flow in bleed piping of nuclear power plant turbine, stability of, (E), 25:8411

STEAM POWER PLANTS
effluents from U.S., environmental effects of gaseous and thermal, 25:10132 (BNWL-SA-3564)
thermal effluents from, management of, 25:10090 (CONF-700335-1)

STEATITES
radiation effects on electric conductivity of, gamma, 25:9551

STEEL
analysis for nitrogen by vacuum melt extraction, 25:8205
analysis of high alloy, for molybdenum using mercaptosuccinic acid, spectrophotometric, 25:8210
book: Metallurgy and the Hot Working of Metals, 25:8894
fatigue of Type A302B, analysis of failure modes in, 25:8868(T) (NSJ-tr-159)
fracture toughness of A533 pressure vessel plate, (E), 25:10244(R) (ORNL-TM-3212)
fracture toughness of heavy-section Type A533B, effects of crack initiation mode, environment, and precrack stresses on, 25:8872 (WCAP-7579)
hydrogenation by sulfuric acid electrolyte at 290°C, effects of Tryion B protective coating on, 25:8842
mechanical properties of pressure vessel, 25:10197
preparation of heavy-section notch specimens of Type A533B, methods for, 25:8872 (WCAP-7579)
preparation of Sandvik Type HT8X6, for weldability testing, 25:8869 (ORNL-4600, pp 147-52)
radiation effects on chemical and mechanical properties of reactor pressure vessel, neutron, 25:8899 (ZJE-89)
radiation effects on embrittlement of Type 22K, neutron, 25:8903
radiation effects on mechanical properties of pressure vessel, neutron, 25:8900 (ZJE-90)
radiation effects on tensile properties of welds in pressure vessel, neutron, 25:8901 (ZJE-91)
C--steel, failure of pipes of, effects of flaws on loads at, 25:8866 (GEAP-10205)
C--steel, fatigue of pipes of, cracking in low-cycle, 25:8866 (GEAP-10205)
C--steel, fatigue of, effects of BWR environments on low-cycle, 25:8866 (GEAP-10205)
C--steel, preparation for weldability testing, 25:8869 (ORNL-4600, pp 147-52)
Co--Mo--steel--W, analysis for molybdenum using mercaptosuccinic acid, spectrophotometric, 25:8210
Cr--Mo--steel, creep rupture of low-carbon ferritic, at 900 to 1100°F and 9 to 26 ksi, 25:8895 (BMI-1891, Sect.B)
Cr--Mo--steel, fatigue of pipes of, cracking in low-cycle, 25:8866 (GEAP-10205)
Cr--Mo--steel, preparation for weldability testing, 25:8869 (ORNL-4600, pp 147-52)
Cr--Mo--steel--V--W, analysis for molybdenum using mercaptosuccinic acid, spectrophotometric, 25:8210

STELLARATORS
magnet coil design for, helical, 25:9509
magnet coil windings for, current induction in plasma from current oscillations in helical, (T), 25:9511
magnetic field calculations for l = 2 helical windings, 25:9508
plasma diagnostics in L-1, using plane electrostatic probes, 25:9410(T) (CTO-736)

STEROIDS
effects on primary virus infections in animals, review on, 25:8699

STOMACH
scanning in dogs and man, use of metastable technetium-99 for, 25:8723

STORAGE RINGS
description of Orsay electron--positron, 25:9919
particle vibrations in, quasistochastic instability of, 25:9933

STRATOSPHERE
strontium-90 content of, following Chinese and French atmospheric nuclear tests, comparison of Streak model-computed and measured data for, 25:8369 (HASL-237, pp I.38-62)

STRONTIUM
abundance in eucrites, (E), 25:8966
abundance in HD 34452, (E), 25:9056
determination in air particulates by spark source mass spectrometry, 25:8208
determination in mandibular rat incisors following intraperitoneal injection of strontium nitrate, by thermal neutron activation and scintillation counting, 25:8222
separation from effluents from chemical decanning of reactor fuel elements by sorption on barium sulfate, 25:8344(P)
separation from water by ion exchange, effect of calcium on, 25:8341

STRONTIUM ISOTOPES Sr-85
accumulation in Navicula seminulum, Plectonema boryanum, and Stigeoclonium lubricum, effects of temperature on, 25:8598
metabolism in rats, effects of estradiol on, 25:8592(R) (COO-1339-43)
uptake by benign and malignant human bone tumors, correlation of data with microscopic data, 25:8597
use for bone scanning for diagnosis of non-union of fractures, 25:8720

XUM

use for scanning in diagnostic and metabolic studies, development of computer programs for, 25:8716
STRONTIUM ISOTOPES Sr-87
use for scanning in diagnostic and metabolic studies, development of computer programs for, 25:8716
STRONTIUM ISOTOPES Sr-88
deuteron elastic scattering at 30 to 40 MeV, angular distributions for, (E), 25:9978(R) (ORO-3398-26)
deuteron reactions (d,He-3) at 35 MeV, angular distributions for, (E), 25:9978(R) (ORO-3398-26)
electron reactions (e,e'p) with, proton spectra and excitation functions for, (E), 25:10053
helium-3 elastic scattering at 33.4 MeV, angular distribution for, (E), 25:9978(R) (ORO-3398-26)
photon reactions (γ,π*) at 150 to 700 MeV, yields and cross sections for, (E), 25:9620 (LUNP-7007)
proton elastic and inelastic scattering at 8.5 to 12 MeV, excitation functions for, (E), 25:10011
STRONTIUM ISOTOPES Sr-89
deposition and ratio to strontium-90 at selected worldwide land sites during 1956 to 1970, monthly averages of fallout, 25:8670(R) (HASL-237(App.))
energy levels from proton scattering by strontium-88, analog, (E), 25:10011
transport in food chains of nuclear-explosion-contaminated estuarine and marine ecosystems in relation to daily ingestion by man, use of stable element content of fish and invertebrates for predicting, 25:8627
STRONTIUM ISOTOPES Sr-90
content and distribution in stratosphere following Chinese and French atmospheric nuclear explosions, comparison of Streak model-computed and measured data for, 25:6369 (HASL-237, pp I.38-62)
content in milk from Ispra environs during March to July 1970, 25:8370 (HASL-237, pp III.18-23)
content in soils at Rocky Flats, Colorado from fallout, 25:8353 (HASL-237, pp I.11-26)
content in UK atmosphere and rainwater, Jan. to July 1970, 25:8364 (AERE-R-6556)
content of atmospheric precipitation and worldwide HASL sites from 1966 to 1970, 25:8658 (HASL-237, pp II.1-16)
content of human diet in Chicago, New York City, and San Francisco from 1960 to 1970, 25:8658 (HASL-237, pp II.1-16)
content of human diets in New York City and San Francisco from April to July 1970, 25:8658 (HASL-237, pp II.1-16)
content of milk and rainwater in New Zealand during 1968 and 1969, 25:8675(R) (NP-18529)
content of milk and total human diet in EURATOM countries during 1968, relation of, to uptake by man, 25:8624 (EUR-4509)
content of milk per gram calcium in New York during 1954 to 1970, monthly and annual averages of fallout, 25:8670(R) (HASL-237(App.))
content of tap water in New York City during 1954 to 1970, monthly and annual averages of fallout, 25:8670(R) (HASL-237(App.))
deposition and ratio to strontium-89 at selected worldwide land sites during 1956 to 1970, monthly averages of fallout, 25:8670(R) (HASL-237(App.))
deposition at Atlantic Ocean weather stations during 1963 to 1970, fallout, 25:8670(R) (HASL-237(App.))
deposition in Atlantic Ocean, 1963 to 1970, relations with land deposition, 25:8368 (HASL-237, pp I.27-37)
deposition of, estimate to 1970 of cumulative worldwide, 25:8364 (AERE-R-6556)
effects on blood, carcinogenesis, and life span of animals in comparison to plutonium-239, 25:8596(T) (LF-tr-41, pp 127-97)
effects on imago formation in Sarcophaga, effects of dose and pupal exposure on, 25:8749(T) (NSJ-tr-156)
effects on pollen of barley, mutagenic, 25:8648
ratio to cesium 137 in tap water in New York City during 1965 to 1970, monthly and annual averages of fallout, 25:8670(R) (HASL-237(App.))
transport in Mediterranean Sea ecosystems, 25:8630
STRUCTURAL BEAMS
vibration dynamics of force excited, effects of motion constraint stops on, (T), 25:10163 (ANL-7619)
STRUCTURES
response to loading of two-dimensional concrete, nonlinear quasi-static analysis of, 25:8392 (GA-9994)
STYRENE
radioinduced grafting on benzyl cellulose, γ, 25:8271
STYRENE POLYMERS
radioinduced luminescence degradation in activated, uv, 25:8582
SUBMARINE REACTORS
design parameters of 300 kW(t) research, for propulsion and working power, 25:10298
SUCCINIC ACID, MERCAPTO-
uses in spectrophotometric determination of molybdenum in high alloy steel, 25:8210
SUGARS
reactions with nitric acid and uranyl nitrate to form carbon--uranium dioxide mixtures, 25:8923
SULFOBROMOPHTHALEIN SODIUM
use for liver function appraisal in comparison to iodine-131-labeled rose bengal, 25:8722
SULFUR
abundance in iota Ori B, (E), 25:8995
determination in air particulates by spark source mass spectrometry, 25:8208
effects on creep in shielded metal-arc welds in stainless steel, 25:8849 (ORNL-4600, pp 142-6)
SULFUR ISOTOPES S-32
electron inelastic scattering from, calculation of form factors using Serber--Yukawa residual interactions for, (T), 25:10010
energy levels from electron inelastic scattering, wave functions for, (T), 25:10010
helium-3 reactions (He-3,d) at 35 MeV, angular distributions for, (E), 25:9978(R) (ORO-3398-26)
mass hexadecapole moments of, Hartree--Fock--Bogolyubov calculations of, (T), 25:10008
SULFUR ISOTOPES S-34
mass hexadecapole moments of, Hartree--Fock--Bogolyubov calculations of, (T), 25:10008
SULFUR ISOTOPES S-35
reactions of recoil, from neutron-irradiated potassium chloride in aqueous solutions, 25:8312
reactions of recoil, from photolysis of carbonyl sulfides in aqueous solutions, 25:8312
toxicity of malathion-incorporated, to man following ingestion of contaminated flour, calculations for, 25:8600
use in double isotope tracer technique for measuring cortisol content of blood plasma, 25:8585
SULFUR ISOTOPES S-36
mass hexadecapole moments of, Hartree--Fock--Bogolyubov calculations of, (T), 25:10008
SULFURIC ACID
corrosive effects on iron--nickel alloys, effects of partial currents on, 25:8834(R) (COO-2069-6)
corrosive effects on Type 304 stainless steel at 140°F, effects of thermally-induced sensitization on, 25:8834(R) (COO-2069-6)
reactions with steel in electrolytic cells, effects of Tryion B protective coating on hydrogenation, 25:8842
H_2SO_4--Na_2SO_4, corrosive and passivating effects on iron, electrochemical studies of, 25:8834(R) (COO-2069-6)
SUN
eclipse of, effect of May 20, 1966, on ionosphere, Lyman-α intensities, positive-ion density, and electron density, (E/T), 25:9313
eclipse of, effect on D-region electron densities at 74 and 80 km during May 20, 1966, (E), 25:9312
eclipse of, effect on electron densities and collision frequencies in D region during May 20, 1966, (E), 25:9311
eclipse of, effect on ionospheric intensity of Lyman-α and D-region ionization during May 20, 1966, (E/T), 25:9309
eclipse of, effect on ionospheric ionization at 75 km during May 20, 1966, (E/T), 25:9310
eclipses of Mar. 18 and Sept. 11, 1969, effects on vlf phase transmissions, (E), 25:9105
gamma-ray emission from, (E/T), 25:9098 (MPI-PAE/EXTRATERR-48)
magnesium isotope abundances in, from sunspot absorption spectra, (E), 25:9101
magnetic field of, (T), 25:9122
magnetic fields in, origin of, (T), 25:9129
motion of, with respect to Population-I Cepheids, (E/T), 25:9151
neutrino pair production in interior of, (T), 25:9737
neutron emission from, (E/T), 25:9098 (MPI-PAE/EXTRATERR-48)
oblateness of, temperature variation and, (E/T), 25:9113
spectra of, observation of Zeeman effect in, (T), 25:9122
spectra of, polarization at the limb of continuum, (E/T), 25:9109
temperature of atmosphere of, differential rotation, meridional velocities, and pole--equator differences in, (T), 25:9111
turbulence in, micro-, (T), 25:8988
ultraviolet Lyman-α scattering during radiation period of, (E/T), 25:9108
x radiation from, data from Vela V and VI for Sept. 1, 1969 to Jan. 1, 1970, (E), 25:9097 (LA-4454(Vol.2))
x-ray emission from, six-minute periodicity during, (E), 25:9104
SUNSPOTS
distribution of, east--west asymmetry in, (E/T), 25:9118
filament motions in, (E), 25:9106
spectra of, identification of lines of magnesium oxide in, (E), 25:9100
SUPERCONDUCTIVITY
Josephson effect in, theory and applications of, 25:9384
SUPERCONDUCTORS
conference on superconducting materials, Aussois, France, 3/69, 25:9381
critical temperature of dilute alloys, effect of localized spin fluctuations on, (T), 25:9374
diamagnetism in, behavior of fluctuation-induced, (T), 25:9369
electric properties of, sawtooth current generator for studying, 25:8580

fabrication of thin films of, and effect on properties, 25:9385
Josephson effect in, boson approach to, (T), 25:9364
magnetic impurity interactions with electrons in, (T), 25:9391
order parameter fluctuations in, onset of surface superconductivity due to, 25:9388
properties of alloy and compound, 25:9386
properties of excitonic insulator, 25:9367
proximity effects in, acoustic surface wave study of, (E/T), 25:9378
thermal conduction in irreversible, Type-II, (E/T), 25:9370
thermal conductivity of pure Type-II, (E/T), 25:9392
thermodynamics of, and microscopic theory, 25:9382
transition temperature and critical fields of, magnetic effects on, 25:9383
tunneling in single crystal and polycrystalline thin films, (E/T), 25:9390
ultrasonic attenuation in, by quasi-particle creation, (E/T), 25:9368
ultrasound absorption in intermediate state of, effect of magnetic field on, 25:9365
use in magnet coils for energy storage and liberation, 25:9395
use of alloy and compound, 25:9386
uses in high-frequency electronic equipment, 25:9396
uses of, cryogenic devices for, 25:9397
uses of, in electric generator field windings, 25:9394
vortex states in films and surface sheath in inclined fields, (E/T), 25:9375
vortex trapping in, mechanism of, 25:9387

SUPERFLUIDITY
gauge fields in, (T), 25:9357
vortex motion in, 25:9359

SUPERNOVA REMNANTS
radio polarization of Tycho's, at 2.8 cm, (E), 25:9073

SUPERNOVAE
light curves for, (T), 25:9038
model for, featuring heavy-element reimplosion, (T), 25:8998
models for, evolutionary, (T), 25:9006
models of pre-supernova evolution, (T), 25:9038
neutron-star formation in, (T), 25:8998

SURFACE WATERS
contamination by fallout from near ground-level nuclear explosions, method for estimating, 25:8354 (HMI-B-86)
contamination of urban environment, Project Ross geochemical research program for studying, 25:8351 (CU-2493-11, App.5)
deuterium content of, in Canada, economic importance to AECL of geographic and seasonal variations in, 25:8666(R) (AECL-3728)
geochemistry of, research program on, 25:8346(R) (CU-2493-11)
radioisotope contamination of, following extreme reactor accident, biological significance of fallout, 25:8660 (HMI-B-87)
radon-222 content of Experimental Lakes Area, Ontario, 25:8352 (CU-2493-11, App.6)

SWEDISH REACTORS (R-3)
dynamics of, comparison of spectral analysis and maximum likelihood methods for, (E/T), 25:10091 (NP-18595)

SWINE
radioinduced pathological conditions in, neutron, γ, and x, 25:8773
strontium retention in, 25:8592(R) (COO-1339-43)

SYMMETRY GROUPS
O(3), structure constants of, representations of Gell-Mann--Dashen algebra with, 25:9824
Lie algebra, finite-dimensional spectrum-generating, 25:9698
O(2,1) formulation for relativistic and nonrelativistic hydrogen atom, 25:9179
SO(4,2) and three-dimensional canonical algebra for, 25:9832
SU(1,1) quasi-spin formalism for boson Bogolyubov transformation, 25:9822
SU(1,1), Clebsch--Gordon formulas for, 25:9821
SU(2) x SU(2) chiral, for pseudoscalar mesons, Schwinger terms in current models of, 25:9833
SU(2) x SU(2) chiral, Lagrangian for A_1, π, and rho dynamics in, 25:9781
SU(3) x SU(3) breaking, determination of Lagrangian in, 25:9831
SU(I + 1), recurrence relation for Kostant formula for, 25:9820
SU(n) symmetric multiperipheral model for magnitude of total cross sections for meson interactions at high energies, 25:9773
SW(3), Kuo transformation in linear and nonlinear chiral, 25:9825
two-particle, for partial-wave amplitudes, 25:9818

SYMMETRY GROUPS SU(3)
baryon mass differences and nonleptonic decay amplitudes in broken, relations between, 25:9830

SYNCHROCYCLOTRONS
design conversion of Saxonburg, into heavy ion isochronous cyclotron, 25:9920
radiofrequency system of CERN, instrument for measuring rate of change of frequency of, 25:9905 (CERN-70-28)

SYNCHROTRONS
beam extraction from, sextupole lenses with direct nonlinearity for slow, 25:9913 (NP-18594)
beam injection system for ITEP 7-GeV proton, pulse generator for deflector plates for, 25:9932
beam injection system for ITEP 7-GeV proton, pulse generator for deflector plates for, 25:9931
betatron and closed-orbit oscillations in, magnetic field perturbation effects on, 25:9904 (CERN-70-24)
bremsstrahlung spectrum from, measurement of constancy of maximum energy of, 25:9935
particle instability at high frequency accelerating fields, 25:9934

SYSTEMS FOR NUCLEAR AUXILIARY POWER (SNAP)
design parameters for 375 kW(e) heat pipe cooled reactor, conceptual, 25:10286
neutron exchange between boundary surfaces of leakage controlled reactor parts, (E/T), 25:10290
power distribution in reflector controlled SER, (E/T), 25:10290
reactivity variations in reflector controlled SER, (E/T), 25:10290

T

T-111 (TANTALUM ALLOY)
compatibility of fuel capsules of, with curium-244 oxide at 1250 to 1850°C, 25:8427(R) (ORNL-4639)
compatibility with thulium-170 oxide at 1600°C, 25:8427(R) (ORNL-4639)
corrosion and failure of lithium-filled loops of, analysis of, 25:8837 (ORNL-4600, pp 216-22)
fabrication of fuel capsule end caps of, by extrusion, 25:8427(R) (ORNL-4639)
fabrication of fuel capsules of, by back extrusion, 25:8850 (ORNL-4600, pp 181-5)
radiation effect on uranium nitride fuel cladding of, 25:8953 (ORNL-4600, pp 177-80)

TANTALUM
compatibility of fuel capsules of, with curium-244 oxide at 1250 to 1850°C, 25:8427(R) (ORNL-4639)
determination in rocks by thermal neutron activation and γ spectrometry, 25:8230
emissivity of, calculation of normal spectral, 25:9584
reactions with refractory metals in diffusion couples, metallography of phases from, 25:8851 (ORNL-4600, pp 186-97)

TANTALUM ALLOYS AND SYSTEMS
H--Ta, phase diagram of, 25:8885(T) (ANL-Trans-867)
Hf--Ta, phase studies of, 25:8851 (ORNL-4600, pp 186-97)
Ta--W, emissivity of, calculation of normal spectral, 25:9584
Ta--Zr, physical properties of age-hardening, 25:8851 (ORNL-4600, pp 186-97)
Ta-base--W, compatibility of fuel capsules of, with curium-244 oxide at 1250 to 1850°C, 25:8427(R) (ORNL-4639)
Ta-base--W, compatibility with thulium-170 oxide at 1600°C, 25:8427(R) (ORNL-4639)
Ta-base--W, fabrication of fuel capsules of, by back extrusion, 25:8850 (ORNL-4600, pp 181-5)
Ta-base--W, fabrication of fuel capsules of, by extrusion, 25:8427(R) (ORNL-4639)

TANTALUM BORIDES
phase studies of TaB and TaB_2, 25:8912 (ORNL-4600, pp 167-74)

TANTALUM CARBIDES
emissivity at 1300 to 3000°K, integral normal, 25:8930
evaporation rates at 2800 to 3400°K, 25:8929
Co--TaC--WC, tensile properties of, effects of structure component growth on, 25:8877

TANTALUM NITRIDES
analysis for nitrogen, evaluation of chemical methods for, 25:8195 (AERE-R-6491)

TANTALUM OXIDES
structure of perovskite-type phase in cubic, electron-diffraction study of, 25:8950

TECHNETIUM
spectral absorption lines in stars due to, (E), 25:9057

TECHNETIUM ISOTOPES Tc-99
uptake and accumulaton of metastable, by thyroid of rats following intravenous injection in comparison to iodine-131, 25:8599
use for scanning in diagnostic and metabolic studies, development of computer programs for, 25:8716
use of metastable, for scanning, bibliography on, 25:8712 (ORNL-TM-2091(Suppl.1))
use of metastable, for stomach scanning in dogs and man, 25:8723
use of pertechnetate-incorporated metastable, for brain scanning, 25:8710 (NP-18560)
use of pertechnetate-incorporated metastable, for brain scanning for diagnosis of herpes hominis virus encephalitis, 25:8718

TEETH
analysis of mandibular rat incisors for manganese and strontium following intraperitoneal injections, by thermal neutron activation and scintillation counting, 25:8222

TELEMETERING SYSTEMS
development survey of AM frequency division multiplex,

XUM

25:10374 (SC-M-70-684)
error analysis for DSB/FM, 25:10371 (SC-CR-70-6092)
TELEVISION EQUIPMENT
use in radiographic equipment for inspection of reactor materials, 25:8440 (ORNL-4600, pp 266-70)
TELLURIUM ISOTOPES Te-122
energy levels of, description using proton-quadrupole vibrator coupling, (T), 25:10042
TELLURIUM ISOTOPES Te-124
energy levels of, description using proton-quadrupole vibrator coupling, (T), 25:10042
TELLURIUM ISOTOPES Te-125
properties of metastable, for x-ray source used in fluorescent analyses, 25:8434
TELLURIUM ISOTOPES Te-126
energy levels of, description using proton-quadrupole vibrator coupling, (T), 25:10042
TELLURIUM ISOTOPES Te-128
energy levels of, description using proton-quadrupole vibrator coupling, (T), 25:10042
TELLURIUM ISOTOPES Te-130
energy levels of, description using proton-quadrupole vibrator coupling, (T), 25:10042
TELLURIUM OXIDES
decay of fallout fission product, release of iodine from, 25:8362 (AD-707427)
TEMPERATURE
distribution along axis of heated channel with inlet subcooling, (E/T), 25:8417
distribution of steady-state, in internally heated finite region with many circular holes, (E/T), 25:8413
measurement and regulation of at 1 to 15°K, 25:9397
TERBIUM ALLOYS AND SYSTEMS
Al--Ni--Tb, magnetic properties and phase diagram of TbNi/sub x/Al/sub 2-x/, 25:9576
Al-base--Gd--Tb, phase diagram at 500°C, 25:8886
Cr--Tb, phase diagram of, 25:8889
TERBIUM ISOTOPES Tb-152
beta and electron-capture decay of isomeric, γ energies from, (E), 25:9978(R) (ORO-3398-26)
TERBIUM ISOTOPES Tb-156
energy levels from gadolinium-156 decay, (E), 25:10034
TERBIUM OXIDES
terbium (Tb^{++}) EPR in polycrystalline, analysis of line shapes from, (E/T), 25:9582
TERPHENYL
effects on luminescence degradation in uv-irradiated polystyrene scintillators activated with, 25:8582
TESTES
radiation effects on count of germ cells in human, effects of dose on x, 25:8789(R) (NYO-4034-2)
TETRACAINE
effects on calcium-45 efflux in myometrium of rats, 25:8601
TEXTILES
radiation effects on mechanical properties and structure of modified Kapron, electron, 25:8270
THALLIUM FLUORIDES
argon-atom scattering at thermal energies by, effects of asymmetric mass distribution on total cross section for, (T), 25:9232
THALLIUM ISOTOPES Tl-197
electron-capture decay of, in-beam measurement of internal conversion electrons from, (E), 25:9978(R) (ORO-3398-26)
THALLIUM ISOTOPES Tl-207
energy levels of, properties of doublet, (E), 25:10033
THERMAL INSULATION
design parameters for laminated metal, for reactor cores, 25:10335(P)
design parameters for liquid sodium cooled fast reactor containment structures, 25:10199(P)
THERMAL RADIATION
effects on living organisms in comparison with age, environment, and radiation, information theory for studying, 25:8742
THERMIONIC CONVERTERS
book: Plasma Thermionic Energy Conversion, in Russian, 25:9268
electron energy distribution in, effects of excitation relaxation on, (T), 25:9267
fuel elements for in-reactor, optimum design parameters for series connected, 25:10226
THERMOELECTRIC CONVERTERS
efficiency of strontium-90-fueled Ripple I and II, 25:8421 (AERE-M-1594)
radiation flux mapping problems of spacecraft containing radioisotopic, 25:9537 (N-70-34007)
THERMOELECTRIC PROPERTIES
book: Methods of Investigation of Thermoelectric Properties of Semiconductors, in Russian, 25:9590
THERMONUCLEAR REACTIONS
spectra from, calculations for emission, (T), 25:9504 (FOA-4-4438)
tabulation of resonance, for CTR use, 25:9507 (ORNL-TM-3233(Rev.))
THERMONUCLEAR REACTORS
development of levitated octupole, research on, 25:9503(R) (COO-1726-70)
magnetic field calculations for Torsatron, 25:9508
plasma anomalous resistivity in toroidal, at low electric fields, (E/T), 25:9443
plasma confinement in octupole, with magnetic mirrors, 25:9399
plasma diagnostics in toroidal, using plane probes, 25:9410(T) (CTO-736)
plasma diagnostics in, echo studies of trapped-particle, 25:9420
plasma diffusion in toroidal systems, classical, (T), 25:9400
plasma drift-wave instabilities in toroidal, trapped-particle effect on, (T), 25:9490
plasma equilibrium and stability in closed, without rotational transformation, (T), 25:9491
plasma equilibrium and stability in toroidal, effect of hf electric fields on, 25:9499
plasma injection and motion in time-changing toroidal octupole, (E/T), 25:9402
plasma kink instability in toroidal, growth rate of, (T), 25:9492
plasma transport toward hoops of single-ring dc device, 25:9503(R) (COO-1726-70)
THERMOSPHERE
energy dissipation of gravity waves during magnetic substorms, (E/T), 25:9293
hydrogen at 1000 to 3500 km in, distribution of neutral, (T), 25:9344
ultraviolet radiation at 1000 to 3500 km in, distribution of solar dispersed Lyman-α, (E), 25:9344
whistler propagation in low-latitude upper, ion reflections and shape changes of downward, 25:9321
THIOCYANATES
metabolism in mammals, reaction mechanisms for, 25:10363(R) (ORO-1637-21)
THORAX
radiation effects on, of mice, effects of, on lungs, x, 25:8778
THOREX PROCESS
flowsheet development for, 25:8324(T) (ORNL-tr-2406)
THORIUM
abundance in eucrites, (E), 25:8966
complexes with pyridineacetic acids and alpha-aminopolyacetic acids, preparation and stability of, 25:8237 (KFK-1210)
determination in fuel reprocessing solutions, 25:8324(T) (ORNL-tr-2406)
determination in titanium and titanium dioxide by neutron activation, 25:8233
hydrolysis of, square wave dissociation field effect apparatus for kinetic studies on, 25:8240
THORIUM ALLOYS AND SYSTEMS
Co--Th, crystal structure of intermetallic Th_2Co_7 in, 25:8893
N--Th, phase diagram for, 25:8927 (ORNL-4503(Vol.2))
Th--U, superconductivity and normal-state properties of, (E/T), 25:9389
THORIUM BOROHYDRIDES
phase studies on, 25:8263
spectra of, ir, 25:8263
THORIUM CARBIDES
production of spherical particles of, from salt solutions, 25:8922(P)
THORIUM ISOTOPES Th-229
neutron fission of, prompt neutron spectra and yield for thermal, (E), 25:10039
THORIUM ISOTOPES Th-232
alpha fission at 20 to 29 MeV, delayed-neutron curves and fission-chain yields from, (E), 25:10056
deuteron fission at 11.5 MeV, fission-product yields and mass and charge distributions from, (E/T), 25:10054
distribution in Lithuania atmosphere at 30 to 200 m altitude, 1966 to 1968, 25:8372
helium-3 fission at 22 to 34 MeV, delayed-neutron curves and fission-chain yields from, (E), 25:10056
proton fission at 11.3 MeV, fission-product yields and mass and charge distributions from, (E/T), 25:10054
THORIUM NITRATES
uses in volumetric titration of fluorine, 25:8201 (LFEN-NI.-36-a)
THORIUM NITRIDES
preparation by consumable electrode method in overpressure electric arc furnace, 25:8914
properties of, data manual on chemical, mechanical, and physical, 25:8927 (ORNL-4503(Vol.2))
thermodynamic properties of, 25:8941
THORIUM OXIDES
production of spherical particles of, from salt solutions, 25:8922(P)
sorptive properties for water at 25 to 500°C, 25:8266
THORIUM OXIDES ThO_2
defect structure of high-purity polycrystalline, 25:9577
effects of dispersions of, on properties of copper, 25:8873
electric properties of high-purity polycrystalline, at 1000 to 1600°C, effects of oxygen partial pressure on, 25:9577
CeO_2--ThO_2, thermal conductivity of solid solutions of, at 25°C, 25:8932
ThO_2--UO_2, thermal conductivity solid solutions of, at 100 and 500°C, 25:8932
THREE MILE ISLAND POWER REACTOR, UNIT 1
cooling system for, safety analysis of flow tubes of, 25:10152 (DOCKET-50289-30)

operation of, license application for, 25:10153 (DOCKET-50289-31)
owners of, financial statements of, 25:10153 (DOCKET-50289-31)
THREE MILE ISLAND POWER REACTOR, UNIT 2
containment structure for, safety analysis of tendon anchorage for prestressed concrete, 25:10157 (DOCKET-50320-20)
THULIUM
energy-level transitions in, observation of K x rays from $2s/sub\ 1/2/--1s/sub\ 1/2/$, 25:9183
THULIUM OXIDES
compatibility with heat resisting capsule materials at 1600 to 2000°C, 25:8427(R) (ORNL-4639)
THYMIDINE
radiation effects on uptake of tritium-labeled, by spermatogonia of man and rats, x, 25:8789(R) (NYO-4034-2)
THYMUS GLAND
radiation effects on function of, in mice, effects of strain on recovery from from whole-body x, 25:8776
THYROID GLAND
radioinduced ablation of human, for therapy of endocrine exophthalmos, iodine-131 β and γ, 25:8735
technetium-99 uptake and accumulation by, of rats following intravenous injection in comparison to iodine-131, metastable, 25:8599
THYRONINE, DIIODO-
radiolysis of, effects of dose and energy on yields of iodine from x, 25:8304
TIN
alpha reactions at 35 to 80 MeV, K-shell ionization cross sections for, (E), 25:9978(R) (ORO-3398-26)
determination in air particulates by spark source mass spectrometry, 25:8208
determination in liquid sodium--tin alloys by dissolution, filtration, and colorimetry, 25:8198 (BNL-50271)
determination in titanium and titanium dioxide by neutron activation, 25:8233
superconducting intermediate state in, effect of magnetic field on ultrasound absorption in, 25:9365
superconducting tunneling in single-crystal and polycrystalline thin films of, (E/T), 25:9390
TIN ALLOYS AND SYSTEMS
In--Sn, electric conductivity and structure of liquid, correlation between, 25:8882
Na--Sn, analysis of liquid, for tin by dissolution, filtration, and colorimetry, 25:8198 (BNL-50271)
Sn--U, reactions of liquid, with nitrogen, thermodynamics and kinetics of uranium nitride formation in, 25:8325(R) (SU-326-P-28-X-2)
TIN ISOTOPES Sn-116
energy-level transitions from indium-116 beta decay, branching ratios, intensities, and multipolarities for, (E), 25:10049
TIN ISOTOPES Sn-117
proton reactions (p,pn) at 17 MeV, mechanism of, (E), 25:10005
TIN ISOTOPES Sn-119
Moessbauer effect in dioxide of, Bragg scattering at high reflection orders, 25:9596
proton reactions (p,pn) at 17 MeV, mechanism of, (E), 25:10005
TIN ISOTOPES Sn-120
proton elastic scattering at 9.85 to 10.90 MeV, angular distribution and polarization for, (E), 25:10044
proton reactions (p,pn) at 17 MeV, mechanism of, (E), 25:10005
TIN ISOTOPES Sn-122
proton elastic scattering at 9.85 to 10.90 MeV, angular distribution and polarization for, (E), 25:10044
TIN ISOTOPES Sn-124
proton elastic scattering at 9.85 to 10.90 MeV, angular distribution and polarization for, (E), 25:10044
TIN OXIDES
tin-119 Moessbauer effect in, Bragg scattering at high reflection orders, 25:9596
TISSUES
analysis of animal, for carbon-14 and tritium by liquid scintillation counting, 25:8213
analysis of animal, for indium-113m in presence of carbon-14 and tritium by liquid scintillation counting, 25:8213
radiation dose to, LET for proton, 25:8682
radiation effects on, of potatoes following processing, determination of, 25:8802
radiosensitivity of human interstitial, relation of, to planning for therapy using high-energy ionizing radiations, 25:8739
TITANIUM
abundance in eucrites, (E), 25:8966
abundance in HD 34452, (E), 25:9056
abundance in L and H chondrites, (E), 25:8967
analysis for trace impurities by neutron activation, 25:8233
determination in air particulates by spark source mass spectrometry, 25:8208
deuteron reactions (d,α) at 19 MeV, angular distributions for, (E), 25:9966(R) (COO-1265-94)
effects on microstructure and postirradiation properties of Hastelloy N, 25:8870 (ORNL-4600, pp 271-81)
TITANIUM ALLOYS AND SYSTEMS
book: Metallurgy and the Hot Working of Metals, 25:8894
Al--Mo--Ti-base--V, embrittlement by cadmium, effects of stress, temperature, and time on, 25:8879
Al--Ti-base--V, embrittlement by cadmium, effects of stress, temperature, and time on, 25:8879
Cr--Pt-base--Ti, properties for use as radioisotope fuel capsule material, 25:8850 (ORNL-4600, pp 181-5)
Mo--Pt-base--Ti, tensile properties at 25 to 1290°C, 25:8427(R) (ORNL-4639)
Mo-base--Ti, radiation effects on mechanical properties of, fast neutron, 25:8952 (ORNL-4600, pp 81-125)
Ti--V, thermodynamic properties of, 25:8862 (AD-709957)
TITANIUM CARBIDES
evaporation rates at 2800 to 3400°K, 25:8929
Mo--Ni--TiC-base, properties for use as cutting tools, effects of molybdenum content on, 25:8928(T) (UCRL-Trans-10505)
TITANIUM ISOTOPES Ti-45
energy levels from scandium-45 (p,n) reactions, spin-parity assignments for, (E), 25:10003
TITANIUM ISOTOPES Ti-48
alpha inelastic scattering at 52 MeV, validity of the Austern--Blair method for, (T), 25:9991
TITANIUM ISOTOPES Ti-49
helium-3 reactions (He-3,d) at 22 MeV, deuteron spectra and angular distributions for, (E), 25:9966(R) (COO-1265-94)
TITANIUM ISOTOPES Ti-50
deuteron reactions (d,p) at 18 MeV, angular distributions for, (E), 25:9966(R) (COO-1265-94)
TITANIUM NITRIDES
analysis for nitrogen, evaluation of chemical methods for, 25:8195 (AERE-R-6491)
TITANIUM OXIDES
analysis for trace impurities by neutron activation, 25:8233
diffusion in, mechanism for anion and cation, 25:8934
electric conductivity of, 25:8934
properties for use in dispersion strengthening of aluminum, 25:8860(P)
CaO--TiO_2, effects of electrode coating of, on mechanical properties of stainless steel welds, 25:8849 (ORNL-4600, pp 142-6)
TOBACCO (the commodity)
smoke from, chemical composition of, 25:10355(R) (ORNL-4642)
TRACER TECHNIQUES
evaluation of radioactive, for measuring distribution of helicopter-sprayed agricultural insecticides, 25:8426(T) (NSJ-tr-155)
use of argon-41, for studying atmospheric dispersion of stack-released reactor effluents, 25:8363 (AECL-3731)
use of radium-226, for hydrological studies of gas exchange and vertical mixing, 25:8352 (CU-2493-11, App.6)
TRANSDUCERS
design for fuel capsules for studies of cladding--fuel reactions, 25:8835 (ORNL-4600, pp 57-64)
development and testing of proximity and pressure, for operation in high-temperature liquid sodium, 25:8394(R) (NYO-3930-7)
performance of displacement, in digital data acquisition system, 25:8397 (UCRL-72509)
TRANSISTORS
radiation effects on bipolar, transient, 25:8581 (LYCEN-6930)
TRANSITION METAL CARBIDES
radiation effects on, fast neutron, 25:8957 (ORNL-4600, pp 250-1)
solubility of $M_{23}C_6$, in Type 316 stainless steel at 750 to 1100°C, 25:8875
TRANSITION METAL NITRIDES
crack formation in Type X6CrMo$_4$, metallographic studies of, 25:8940
TRANSITION RADIATION
absorption by nuclei in thin plates, resonance, (T), 25:9703 (JINR-P2-5042)
TRANSPORT THEORY
Boltzmann equation in, Cauchy problem for nonlinear, 25:9843
Boltzmann-type equations in radiation, solution of, 25:9611
book: Nuclear Reactor Theory, 25:10317
discrete ordinates quadrature over unit sphere, 25:9602 (LA-4554)
equation of, cone of radiation in solution of kinetic, 25:9609
equations in, spectrum of anisotropic transfer, 25:9055
radiative transfer, linear integral equations for H-functions in, 25:9953
radiative, reduction to H functions in, 25:9054
scattering angle in energy-dependent problems in, sensitivity of average of cosine of, 25:9959
scattering in diffuse reflection from semi-infinite atmospheres, high-order, (T), 25:9616
solutions of half-space problems in two-group, explicit, 25:9619
TRANSURANIUM ELEMENTS
alpha decay of, coincidence semiconductor detector system for measurement of x-ray-to-alpha ratio in, 25:8465

XUM

(BNWL-SA-1514)
bibliography on, index to 3rd quarter 1970 of, 25:8831
bibliography on, Oct., 1970, 25:8830
TRIAMCINOLONE ACETONIDE
use for therapy of dysthyroid infiltration in man, 25:8733
TRIETHYLAMINE
dibutylamine--triethylamine, carbon-13 concentration by chemical exchange reactions between carbon dioxide and, 25:8320 (CU-755-7, Sect.6)
dibutylamine--triethylamine, carbon-13 concentration by chemical exchange reactions between carbon dioxide and, 25:8318 (CU-755-7, Sect.2)
TRITIUM
beta particles from, dose distribution of, 25:8437
content in Crater Lake, Oregon, effects of vapor exchange and precipitation on, (E), 25:8347 (CU-2493-11, App.1)
content in UK rainwater, Jan. 1969 to June 1970, 25:8364 (AERE-R-6556)
determination in animal tissues by liquid scintillation counting, 25:8213
deuteron reactions (d,n) at 220 keV, neutron spectra from, (E), 25:9968 (NP-18488)
deuteron reactions (d,n) with, 14-MeV neutron source using, 25:9955
deuteron reactions (d,n) with, differential neutron source strength from, 25:9957
distribution in Zircaloy cladding at high burnups, 25:8951(R) (GEAP-10217)
meson (π) interactions with, cross-section calculations using Glauber theory, (T), 25:9967 (JINR-P2-5335)
nucleon interactions with, cross-section calculations using Glauber theory, (T), 25:9967 (JINR-P2-5335)
reactions of recoil, with silanes, 25:8310(R) (ORO-3898-2)
toxicity of malathion-incorporated to man following ingestion of contaminated flour, calculations for, 25:8600
use as tracer for studies of studies of diurnal variations in mitotic and labeling indexes, method for, 25:8589
use for studying effects of route of administration on deslanoside concentrations in cardiopathic patients, 25:8724
use in double isotope tracer technique for measuring cortisol content of blood plasma, 25:8585
TRITONS
reaction (t,n) with beryllium-9 at 1.10 MeV, angular distributions for, (E), 25:9976 (JINR-P15-5148)
TSURUGA POWER REACTOR
turbine for, design of auxiliary equipment for, 25:8399
TUBES
alignment of fuel element guide, for reactor reloading, 25:10230(P)
design parameters of removable guide, for reactor refueling, 25:10218(P)
plugs for defective heat exchanger, design of, 25:10330(P)
tensile properties of, equipment and method for measuring circumferential, 25:8883
TUNGSTEN
compatibility of fuel capsules of, with curium-244 oxide at 1250 to 1850°C, 25:8427(R) (ORNL-4639)
compatibility with thulium-170 oxide at 1600°C, 25:8427(R) (ORNL-4639)
creep of vapor deposited, at 1200 to 2200°C, effects of stress on, 25:8852 (ORNL-4600, pp 198-209)
deposition on substrates by plasma spraying, 25:8855
determination in titanium and titanium dioxide by neutron activation, 25:8233
effects of dispersions of, on properties of copper, 25:8873
emissivity of, calculation of normal spectral, 25:9584
oxidation at 670 to 980°C, effects of carbon dioxide, carbon monoxide, methane, and nitrogen on kinetics of, 25:8841
production of [100] crystal oriented, by tungsten hexachloride vapor reduction, 25:8852 (ORNL-4600, pp 198-209)
production of sheets of, development of vapor deposition method for, 25:8852 (ORNL-4600, pp 198-209)
properties for use in curium-244 oxide cermets, 25:8427(R) (ORNL-4639)
properties of welds in vapor-deposited, 25:8852 (ORNL-4600, pp 198-209)
surface oxidation of, field emission and electron microscopic study of needle crystals formed by, 25:8843
TUNGSTEN ALLOYS AND SYSTEMS
Co--Mo--steel--W, analysis for molybdenum using mercaptosuccinic acid, spectrophotometric, 25:8210
Cr--Mo--steel--V--W, analysis for molybdenum using mercaptosuccinic acid, spectrophotometric, 25:8210
Hf--Pt-base--W, properties for use as radioisotope fuel capsule material, 25:8850 (ORNL-4600, pp 181-5)
Hf--Pt-base--W, tensile properties at 25 to 1290°C, 25:8427(R) (ORNL-4639)
Mo--Re--W-base, creep of arc-melted, at 1200 to 2200°C, effects of stress on, 25:8852 (ORNL-4600, pp 198-209)
Re--W-base, compatibility of fuel capsules of, with curium-244 oxide at 1250 to 1800°C, 25:8427(R) (ORNL-4639)
Re--W-base, creep at 1800°C and 1000 psi, effects of low-pressure oxygen on, 25:8852 (ORNL-4600, pp 198-209)
Re--W-base, creep of arc-melted, at 1200 to 2200°C, effects of stress on, 25:8852 (ORNL-4600, pp 198-209)
Re--W-base, preparation by vapor deposition from reduced hexafluoride vapors, development of method for, 25:8852 (ORNL-4600, pp 198-209)
Ta--W, emissivity of, calculation of normal spectral, 25:9584
Ta-base--W, compatibility of fuel capsules of, with curium-244 oxide at 1250 to 1850°C, 25:8427(R) (ORNL-4639)
Ta-base--W, compatibility with thulium-170 oxide at 1600°C, 25:8427(R) (ORNL-4639)
Ta-base--W, fabrication of fuel capsules of, by back extrusion, 25:8850 (ORNL-4600, pp 181-5)
Ta-base--W, fabrication of fuel capsules of, by extrusion, 25:8427(R) (ORNL-4639)
TUNGSTEN CARBIDES
Co--TaC--WC, tensile properties of, effects of structure component growth on, 25:8877
TUNGSTEN CHLORIDES
reduction for vapor deposition of [100] crystal oriented tungsten, development of method for, 25:8852 (ORNL-4600, pp 198-209)
TUNGSTEN FLUORIDES
ReF_6--WF_6, reduction for production of rhenium--tungsten alloys by vapor deposition, development of method for, 25:8852 (ORNL-4600, pp 198-209)
UF_6--WF_6, phase equilibrium studies at 2,600 torr, 25:8265
TUNGSTEN ISOTOPES W-186
neutron elastic scattering at 0.0004 eV, amplitudes for coherent, (E), 25:10026 (JINR-E3-5371)
performance of activation detectors of, for neutron spectra measurements at 1 eV to 10 keV, 25:8481 (KFK-1233)
TUNGSTEN OXIDES
growth of small crystals in drops formed on needle crystals of, 25:8859
structure of needle crystals grown on tungsten, field emission and electron microscopic study of, 25:8843
TUNNELS
construction of, bibliography on, 25:8444 (ORNL-HUD-17)
TURBINES
design parameters for closed cycle carbon dioxide gas, 25:10249(P)
design parameters for closed cycle carbon dioxide gas, 25:10250(P)
equipment for Tsuruga nuclear power plant, design of auxiliary, 25:8399
performance of direct cycle gas, part load, (T), 25:10251
steam--water flow in bleed piping of nuclear power plant, stability of, (E), 25:8411
TURKEY POINT POWER REACTOR, UNIT 3
containment dome for, construction and testing of, 25:10147 (DOCKET-50250-37)
TYROSINE
radioinduced binding to serum albumin, effects of acidity on γ, 25:8280
TZM (MOLYBDENUM ALLOY)
compatibility of fuel capsules of, with curium-244 oxide at 1250 to 1850°C, 25:8427(R) (ORNL-4639)
compatibility with thulium-170 oxide at 1600°C, 25:8427(R) (ORNL-4639)
tensile properties at 1093 to 1290°C, 25:8427(R) (ORNL-4639)

U

UDIMET 500
analysis for molybdenum using mercaptosuccinic acid, spectrophotometric, 25:8210
ULTRASONIC TESTING
method for LMFBR components and materials, 25:8439 (ORNL-4600, pp 153-6)
method for reactor materials, 25:8440 (ORNL-4600, pp 266-70)
ULTRAVIOLET RADIATION
distribution of solar dispersed Lyman-α, at 1000 to 3500, (E), 25:9344
effect of sudden increases of fluxes of, on electron density in sunlit ionosphere, Feb. 20, 1970, (E), 25:9333
effects on Aspergillus nidulans, biochemical and genetic analysis of mutagenic, 25:8640
effects on Aspergillus nidulans, effects of pre-exposure treatment with 8-methoxypsoralen on lethal and mutagenic, 25:8702
effects on clone formation in phage kappa, 25:8653
effects on coliphage T7, inactivating, 25:8808
effects on DNA in cultured mammalian cells, repair processes following, carcinogenic, 25:8611
effects on DNA of Escherichia coli, analysis of photoenzymatic repair of, 25:8652
effects on DNA of Escherichia coli, effects of photoenzymatic repair inhibition by caffeine on, 25:8649
effects on DNA of Escherichia coli, model for excision

XUM

repair of, 25:8636 (SU-326-P-7-X-22)
effects on DNA, role of DNA-pyrimidine dimer photomonomerase in photoreactivation of, 25:8606(R) (ORO-3630-10)
effects on enzyme-substrate binding in DNA in Haemophilus influenza and yeast, rate constants for, 25:8651
effects on Escherichia coli, combined effects of formaldehyde or nitrosomethylurethan with spectrum of mutagenic, 25:8642
effects on Escherichia coli, review of mutagenic, 25:8633 (NP-18483)
effects on excitation of butanol and ethanol in presence of luminescing additives, 25:8274
effects on eyes, protection against pathological, 25:8793
effects on frequency of gene conversion in Escherichia coli, mutagenic, 25:8634(R) (ORO-4024-1)
effects on genetic recombination in partially diploid derivatives of Escherichia coli, 25:8634(R) (ORO-4024-1)
effects on lysozyme content of blood serum and osmotic resistance of erythrocytes in rabbits, effects of whole-body dose on uv, 25:8782
effects on mitotic recombination frequency in mutants of Saccharomyces cerevisiae, 25:8797
effects on morphology and physiology of cells, molecular mechanisms and techniques for demonstrating microbeam, 25:8744
effects on photolysis of DNA in Haemophilus influenzae, determination of repair rate of, 25:8650
effects on polymerization of aminoplast film for coating particles, 25:8278(P)
effects on Scrapie virus following injection into mice, effects of wave length on inactivating monochromatic, 25:8805
effects on uptake of acridine orange by fibroblasts of mice, effect of nucleoproteins on, 25:8770
effects on vesicular stomatitis virus, effects of, on synthesis of RNA and DNA in chick embryos following infection, 25:8806
effects on yeast cell mutants defective for dark repair, effects of liquid holding conditions on recovery from inactivating, 25:8797
effects on yeasts, protective effects of caffeine against, 25:8637
energy flux at 120 to 178 km, solar Lyman-α, (E), 25:9345
intensity of solar extreme, effects of interplanetary hydrogen on, (E/T), 25:9108
reactions with hydrogen molecules, electron spectra from, (E), 25:9199
reactions with hydrogen, nitrogen, and oxygen ground-state atoms, electron spectra from, (E), 25:9200

UNITED KINGDOM
radiation monitoring of atmosphere and rainwater in, to July 1970, 25:8364 (AERE-R-6556)
uranium enrichment in, development of gas centrifuge and gaseous diffusion facilities for, 25:8431

UNIVERSE
expansion of, role of cosmological zero-point fluctuation of metric in slowed-down, (T), 25:9152
quantization of closed, superspace and finite-dimensional models in review of, (T), 25:9872

URANIUM
abundance in eucrites, (E), 25:8966
analysis for rare earths by optical fluorescence spectroscopy, phosphors for, 25:8207
complexes with pyridineacetic acids and alpha-aminopolyacetic acids, preparation and stability of, 25:8237 (KFK-1210)
content of food in Soviet Union, 25:8631
determination in fuel reprocessing solutions, in-line colorimetric, 25:8197 (BARC-510)
determination in geological samples by neutron activation, 25:8219 (PH-3)
determination in reactor fuels, accurate and precise titrimetric method for, 25:8202 (RCN-126)
determination in scrap, description of radiometric equipment and method for, 25:8447(R) (BHD-65-1)
determination in titanium and titanium dioxide by neutron activation, 25:8233
determination of abundance of, relative to oxygen in hyperstoichiometric uranium dioxide, titrimetric, 25:8203 (RCN-127)
determination of abundance of, relative to oxygen in hypostoicniometric uranium dioxide, revised gas chromatography method for, 25:8204 (RCN-128)
enrichment in European Community, economic and technical aspects of gaseous diffusion, nozzle, and ultracentrifugation methods for, 25:8435
enrichment in UK, development of gas centrifuge and gaseous diffusion facilities for, 25:8431
luminescence of tetravalent, in aqueous solutions, 25:8267
mechanical properties at 20 to 239°K, design of device for determining low-temperature, 25:8881
mining in western U. S., summary of 1969 activities on, 25:10328
photon reactions at 145, 192, 662, and 1250 keV with, K-shell x-ray production and photoelectric cross sections for, 25:9235
processing of reactor fuels containing, at Eurochemic plant, 25:8327
separation from acid and alkaline suspensions, properties of ion exchange resins for, 25:8963
separation from irradiated LMFBR fuels, solvent extraction processes for, 25:8316 (BNWL-CC-1939)
separation from spent Rover fuels, fluidized-bed combustion process for, 25:8322 (IN-1423)
solubility in nickel at 975 to 1075°C, 25:8865 (CEA-R-4066)
supply of, effects on U. S. power reactor fuel cycles of, 25:10214
determination in plutonium carbide--uranium carbide, plutonium dioxide--uranium dioxide, and plutonium nitride--uranium nitride fuels by controlled-potential coulometric and potentiometric titrations, 25:8200 (LA-4537)

URANIUM ALLOYS AND SYSTEMS
Al--C--Fe--Si--U-base, tensile properties of dilute, at 885 to 1150°F, 25:8867 (NLCO-1060)
Al--U, phase studies of, 25:8846 (KFK-1252)
Al--U, properties of intermetallic UAl_3 dispersion fuels of, electric, mechanical, and thermal, 25:8846 (KFK-1252)
Be--Si--U, crystal structure of ordered solid solution of, 25:8947
Be--Si--U, phase studies of ordered solid solutions of, 25:8888
La--O--U, phase studies of, 25:8943 (KFK-1235)
Nb--U-base, explosive properties of, following immersion in nitric acid, 25:8840 (RFP-1575)
Sn--U, reactions of liquid, with nitrogen, thermodynamics and kinetics of uranium nitride formation in, 25:8326(R) (SU-326-P-28-X-2)
Th--U, superconductivity and normal-state properties of, (E/T), 25:9389

URANIUM BOROHYDRIDES
phase studies on, 25:8263
spectra of, ir, 25:8263

URANIUM CARBIDES
crushing properties of pyrocarbon-coated particles of, optical and photographic methods for determination of, 25:8925 (EUR-4501)
oxidation in gaseous environments, kinetics of, 25:8907 (CEA-Bib-183)
production of spherical particles of, from salt solutions, 25:8922(P)
PuC--UC, analysis for plutonium and uranium by controlled-potential coulometric and potentiometric titrations, 25:8200 (LA-4537)
UC--UN, preparation by consumable electrode method in overpressure electric arc furnace, 25:8914
UC--UO, preparation by consumable electrode method in overpressure electric arc furnace, 25:8914

URANIUM CONCENTRATES
analysis for fluorine by volumetric titration using thorium nitrate, 25:8201 (LFEN-NI.-36-a)

URANIUM DEPOSITS
geology and mineralization of Orphan Mine, Grand Canyon, Arizona, 25:8376
geology and mineralogy of Colorado Plateau peneconcordant-type, 25:8377
geology and mineralogy of Heaths Peak, Carbon County, Wyoming, 25:8379
geology and mineralogy of Wyoming roll-type, 25:8377
prospecting for, methods of financing small operations in, 25:8374
prospecting for, photogeological methods for, 25:8375

URANIUM FLUORIDES UF_4
BeF_2--LiF--UF_4--ZrF_4, preparation and handling of molten, for use as MSRE fuel salt, 25:10211 (ORNL-4616)

URANIUM FLUORIDES UF_6
preparation in nonaqueous fuel reprocessing pilot plant, 25:8342
use for MHD generator working fluid, 25:10221
use for reactor fuels, 25:10221
MoF_6--UF_6, phase equilibrium studies at 2,600 torr, 25:8264
UF_6--WF_6, phase equilibrium studies at 2,600 torr, 25:8265

URANIUM ISOTOPES U-232
effects on blood, carcinogenesis, and life span of animals in comparison to plutonium-239, 25:8596(T) (LF-tr-41, pp 127-97)

URANIUM ISOTOPES U-233
effects on blood, carcinogenesis, and life span of animals in comparison to plutonium-239, 25:8596(T) (LF-tr-41, pp 127-97)
fission of, energy-dependent neutron yield for, 25:10025 (INDC(NDS)-19/N)

URANIUM ISOTOPES U-235
fission of, energy-dependent neutron yield for, 25:10025 (INDC(NDS)-19/N)
fission products of, energy spectra of electron antineutrinos from, (T), 25:9746
neutron absorption in Doppler resonance regions, shielding factors for, (T), 25:10038
neutron fission of, prompt neutron spectra and yield for thermal, (E), 25:10039

URANIUM ISOTOPES U-238
alpha fission at 20 to 29 MeV, delayed-neutron curves and fission-chain yields from, (E), 25:10056

XUM

deuteron fission at 10.6 MeV, excitation functions and mass yield curves for, (E/T), 25:10052
distribution in Lithuania atmosphere at 30 to 200 m altitude, 1966 to 1968, 25:8372
helium-3 fission at 22 to 34 MeV, delayed-neutron curves and fission-chain yields from, (E), 25:10056
neutron absorption in Doppler resonance regions, shielding factors for, (T), 25:10038
proton fission at 11.2 MeV, excitation functions and mass yield curves for, (E/T), 25:10052
transport in Mediterranean Sea ecosystems, 25:8630

URANIUM NITRIDES
fabrication of pellets of, by cold pressing and sintering, 25:8913(T) (ORNL-tr-2365)
preparation by consumable electrode method in overpressure electric arc furnace, 25:8914
production by nitrogen reactions with liquid tin--uranium alloys, thermodynamics and kinetics of, 25:8325(R) (SU-326-P-28-X-2)
radiation effects on T-111-clad fuel pins of, in-pile, 25:8953 (ORNL-4600, pp 177-80)
thermodynamic properties of, 25:8941
PuN--UN, analysis for plutonium and uranium by controlled-potential coulometric and potentiometric titrations, 25:8200 (LA-4537)
PuN--UN, preparation and fabrication of fuel pins of, methods for, 25:8910 (ORNL-4600, pp 41-56)
PuN--UN, properties of fuel pellets of, chemical and microstructural, 25:8910 (ORNL-4600, pp 41-56)
UC--UN, preparation by consumable electrode method in overpressure electric arc furnace, 25:8914

URANIUM ORES
concentration by water leaching, ue of bacteria in, 25:8357
inhalation of dusts of, effects on respiratory tract pathology in dogs and hamsters, 25:8623 (BNWL-SA-3419)

URANIUM OXIDES
effects on ion fluxes in corn roots, 25:8602
production of spherical particles of, from salt solutions, 25:8922(P)

URANIUM OXIDES UO
UC--UO, preparation by consumable electrode method in overpressure electric arc furnace, 25:8914

URANIUM OXIDES UO_2
analysis of hyperstoichiometric, for oxygen/uranium, titrimetric, 25:8203 (RCN-127)
analysis of hypostoichiometric, for oxygen/uranium, revised gas chromatography method for, 25:8204 (RCN-128)
crushing properties of pyrocarbon-coated particles of, optical and photographic methods for determination of, 25:8925 (EUR-4501)
diffusion in, mechanism for anion and cation, 25:8934
electric conductivity at 1100 to 1700°C, 25:8908 (BARC-507)
electric conductivity of, 25:8934
microstructure at 1100 to 1700°C, 25:8908 (BARC-507)
properties for use in dispersion strengthening of aluminum, 25:8860(P)
radiation effects on mechanical properties of, neutron, 25:10125(R) (NP-18573)
radiation effects on thermal diffusivity of, in-pile, 25:8965 (ORNL-4600, pp 225-34)
radiation effects on Zircaloy-clad fuels of, at high burnups, 25:8951(R) (GEAP-10217)
reactions with sodium oxide at 450 to 520°C, exotherms of, 25:8926(R) (GEAP-12133)
C--UO_2, preparation of mixtures of, by reactions of sugar with uranyl nitrate in nitric acid, 25:8923
PuO_2--UO_2, analysis for plutonium and uranium by controlled-potential coulometric and potentiometric titrations, 25:8200 (LA-4537)
PuO_2--UO_2, diffusion of oxygen in, effects of thermal gradients on, 25:8926(R) (GEAP-12133)
PuC_2--UO_2, fabrication of fuel pins of, by Sphere-Pac loading of microspheres, 25:8909 (ORNL-4600, pp 3-40)
PuO_2--UO_2, microstructure of microspheres of, 25:8909 (ORNL-4600, pp 3-40)
PuO_2--UO_2, oxygen activity in fuels of, at 1700 to 2250°C, 25:8926(R) (GEAP-12133)
PuO_2--UO_2, oxygen-to-metal ratio in, precision and source of variation in, 25:8909 (ORNL-4600, pp 3-40)
PuO_2--UO_2, performance of fuel pins of stainless steel-clad, effects of power cycling on, 25:8835 (ORNL-4600, pp 57-64)
PuO_2--UO_2, preparation of dense microspheres of, methods for, 25:8909 (ORNL-4600, pp 3-40)
PuO_2--UO_2, radiation effects on burnup, microstructure, and mechanical properties of fuels of, in-pile, (E), 25:10213(R) (WCAP-3385-25)
PuO_2--UO_2, radiation effects on encapsulated fuels of, fast and thermal neutron, 25:8909 (ORNL-4600, pp 3-40)
PuO_2--UO_2, radiation effects on grain size in Sphere-Pac fuel pins of, in-pile, 25:8911 (ORNL-4600, pp 65-80)
PuO_2--UO_2, radiation effects on metal distribution in Sphere-Pac fuels of, in-pile, 25:8911 (ORNL-4600, pp 65-80)
PuO_2--UO_2, radiation effects on microstructure of, relations of preparation method with in-pile, 25:8955 (ORNL-4600, pp 225-34)
PuO_2--UO_2, reactions with sodium in failed fuel elements at high temperatures, effects of oxygen-to-metal ratio on, 25:8926(R) (GEAP-12133)
ThO_2--UO_2, thermal conductivity solid solutions of, at 100 and 500°C, 25:8932

URANIUM OXIDES UO_3
production by denitration of uranyl nitrate in fluidized bed, jet grinders for particle-size control in, 25:8323 (IN-1439)

URANIUM OXIDES U_3O_8
properties of, standards for burned and high-fired, 25:8956 (ORNL-4600, pp 235-48)
separation from uranium ores by bacteria-aided water leaching, 25:8337
Al--Al_2O_3--U_3O_8, fabrication of aluminum-clad fuel plates of, for HFIR irradiation testing, 25:8956 (ORNL-4600, pp 235-48)
Al--U_3O_8, fabrication of aluminum-clad fuel plates of, for HFIR irradiation testing, 25:8956 (ORNL-4600, pp 235-48)
Al--U_3O_8, grain structure and void content of fuel plates of, 25:8956 (ORNL-4600, pp 235-48)

URANIUM RESERVES
estimates for noncommunist countries, 25:8373

URANIUM SILICIDES
formation of bicrystals in, above 700°C, study of, 25:8946

URANYL COMPOUNDS
hydrolysis of, square wave dissociation field effect apparatus for kinetic studies on, 25:8240

URANYL NITRATES
criticality of enriched, in intersecting pipe, model for calculating, 25:8459
denitration in fluidized bed, jet grinders for particle-size control in, 25:8323 (IN-1439)
reactions with nitric acid and sugar to form carbon--uranium dioxide mixtures, 25:8923

UREA, 1-METHYL-1-NITROSO-
effects on cultured Chinese hamster cells, factors affecting expression of mutagenic, 25:8638

URETHAN POLYMERS
production of foams of, equipment and methods for, 25:10342 (BDX-613-252)

URIDINE, 5-BROMO-2'-DEOXY-
effects on cultured Chinese hamster cells, factors affecting expression of mutagenic, 25:8638

URINE
radioisotope content of, of rats following inhalation and intramuscular injection of americium-241, curium-242, plutonium-238, and plutonium-239, 25:8590 (CEA-CONF-1658)
tritium oxide content of, of industrial personnel, recommendations for maximum permissible, 25:8678(T) (ORNL-tr-2403)

UTAH
uranium deposits in plateau region of, geology and mineralogy of peneconcordant-type, 25:8377

UTERUS
calcium-45 efflux in myometrium of, of rats, effects of external calcium concentrations on, 25:8601

V

VACCINES
radioinduced attenuation of, for control of animal parasites, 25:8818

VACUUM GAGES
performance of ionization, for molecular plasma density measurement in Ogra II, 25:9430

VACUUM SYSTEMS
operation of all-metal ultrahigh, effects of evaporation on, 25:8462

VACUUM TECHNIQUES
uses in nuclear installations, review of, 25:8461

VALVES
design of autoclave-type, for closing ends of vertical reactor coolant channels, 25:8401(P)
design parameters for capillary, for venting fission gases from liquid metal cooled control elements, 25:10189

VAN ALLEN RADIATION BELTS
charged-particle flux in 1966 in inner and outer, fast, (E), 25:9354
currents of quasi-trapped particles with discontinuities on the daytime and nighttime sides of the Earth, (T), 25:9347

VAN DE GRAAFF ACCELERATORS
control system for voltage conditioning of, automatic, 25:9930
development and operation for radiological research, 25:8482 (NYO-2740-7, pp 112-53)
experimental facilities at University of Minnesota tandem, development of, 25:9966(R) (COO-1265-94)
experimental facility and method for measurement of energy averaged cross sections, 25:9923
operation of University of Minnesota tandem, 25:9966(R) (COO-1265-94)

VANADIUM
compatibility of fuel capsules of, with curium-244 oxide at 1250 to 1850°C, 25:8427(R) (ORNL-4639)
creep at 600°C and 12000 psi stress, effects of low-pressure nitrogen on, 25:8836 (ORNL-4600, pp 157-66)

XUM

determination at nanogram levels by neutron activation and radiochemical separation, 25:8228
determination by neutron activation, 25:8227
determination in air particulates by spark source mass spectrometry, 25:8208
determination in airborne particulates by neutron activation, 25:8231
determination in titanium and titanium dioxide by neutron activation, 25:8233
electron band structure of, self-consistent calculations, 25:9597
electron chracteristic energy loss spectra of, band structure and plasmons from, 25:9583
mass transfer to stainless steel at 600 to 700°C by sodium, 25:8836 (ORNL-4600, pp 157-66)
superconducting flux-flow noise spectrum in foils of, 25:9366

VANADIUM ALLOYS AND SYSTEMS
Al--Mo--Ti-base--V, embrittlement by cadmium, effects of stress, temperature, and time on, 25:8879
Al--Ti-base--V, embrittlement by cadmium, effects of stress, temperature, and time on, 25:8879
B--rare earths--V, crystal structure of RVB_4, 25:8948
C--Nb-base--V--Zr, preparation and properties of corrosion-resistant, for use in nuclear industry, 25:8856(P)
Cr--Mo--steel--V--W, analysis for molybdenum using mercaptosuccinic acid, spectrophotometric, 25:8210
Ga--V, superconductivity in intermetallic V_3Ga, pressure-enhanced, (E/T), 25:9372
Ge--V, superconductivity in intermetallic V_3Ge, pressure-enhanced, (E/T), 25:9372
Mo--V-base, corrosion by sodium at 600°C, effects of oxygen on, 25:8836 (ORNL-4600, pp 157-66)
Ti--V, thermodynamic properties of, 25:8862 (AD-709957)
V-base--Zr, corrosion by sodium at 600°C, effects of oxygen on, 25:8836 (ORNL-4600, pp 157-66)

VANADIUM HYDRIDES
electric conductivity of V_2H down to 4.2°K, 25:9592

VANADIUM ISOTOPES V-50
energy levels from titanium-49 (He-3,d) reactions, (E), 25:9966(R) (COO-1265-94)

VANADIUM ISOTOPES V-51
photon reactions (γ,π^+) at 150 to 700 MeV, yields and cross sections for, (E), 25:9620 (LUNP-7007)

VANADIUM NITRIDES
analysis for nitrogen, evaluation of chemical methods for, 25:8195 (AERE-R-6491)

VANADIUM OXIDES
electric properties of pure V_2O_5 single crystals, (E/T), 25:9581
electric properties of V_6O_{13} single crystals, metal-to-semiconductor phase transition in, (E), 25:9580
electron characteristic energy loss spectra of V_2O_5, band structure and plasmons from, 25:9583

VANADIUM SILICIDES
superconductivity in, pressure-enhanced, (E/T), 25:9372

VEGETABLES
corn, radiation effects on survival and yield of, in comparison to effects of simulated radioactive fallout, chronic cesium-137, 25:8796
lettuce, radiation effects on survival and yield of, in comparison to effects of simulated radioactive fallout, chronic cesium-137, 25:8796
mushrooms, radiation processing of, and their growing soil, patent for process for, 25:8821(P)
onions, radiation processing of punjab red, effects of, on germination, γ, 25:8815
onions, radiation processing of, effectiveness of γ, 25:8824
potatoes, radiation processing of, effectiveness of γ, 25:8824
potatoes, radiation processing of, identification of irradiated tissues by, 25:8802
radiation processing of, economic and legal aspects of, in USA during 1967, 25:8813 (NP-18236)
radishes, radiation effects on survival and yield of, in comparison to effects of simulated radioactive fallout, chronic cesium-137, 25:8796
squash, radiation effects on survival and yield of, in comparison to effects of simulated radioactive fallout, chronic cesium-137, 25:8796
tomatoes, radiation effects on survival and yield of, in comparison to effects of simulated radioactive fallout, chronic cesium-137, 25:8796

VENTILATION
control of, design of duct closure for, 25:8403(P)

VENUS (PLANET)
ionosphere of, comparison with Earth and Mars ionospheres, (E/T), 25:9355

VIBRATIONS
dynamics of force excited beams, effects of motion constraint stops on, 25:10163 (ANL-7619)
measurement of liquid flow induced, development of electric conductivity cell for, 25:10271 (WHAN-FR-21)

VIRUSES
infection in animals, effects of radiomimetic substances and x radiation on primary, 25:8699
Scrapie, radioinduced inactivation of, following injection in mice, effects of wave length on monochromatic uv, 25:8805
vesicular stomatitis, radiation effects on, effects of, on DNA synthesis in chicken embryos, 25:8606

VITAMIN B GROUP
folic acid, assay in Lactobacillus casei, methods for radioisotope, 25:8809
niacin, radiation effects on content of, in enriched flour, 25:8816
riboflavin, radiation effects on content of, in enriched flour, 25:8816
thiamine, radiation effects on content of, in enriched flour, 25:8816

VITAMIN K GROUP
K3, effects on serum coeruloplasmin activity in rats, 25:8612

VOID FRACTION
distribution along axis of heated channel with inlet subcooling, (E/T), 25:8417

VOLTMETERS
calibration of Kerr cell, development and analysis of methods for, 25:10370 (SC-CR-69-3266)

W

WASPALOY
analysis for molybdenum using mercaptosuccinic acid, spectrophotometric, 25:8210

WATER
boiling of high-pressure, in rod bundles during pressure blowdown, characteristics of departure from nucleate, (E), 25:8418
corrosive effects of trace chloride- and oxygen-containing, on chromium-iron-nickel alloys at 200°C, 25:8834(R) (COO-2069-6)
deuterium exchange between deuterated methylacetylene and, mass-spectrometric equilibrium studies on, 25:8241 (CU-755-7, Sect.3)
effects on shelf life of γ-irradiated shrimp, 25:8820
flow of boiling, in vertical rod bundles, method for predicting burnout conditions for, 25:8408 (CONF-660675-1)
heat transfer to, Freon 12 model for burnout in forced convective, 25:8410
labeling with oxygen-15, 25:8711(R) (NYO-3937-2)
mixing with steam to produce dispersion of droplets in flowing gases, design of nozzle for, 25:8404(P)
neutron diffusion in, calculation models for thermal, (T), 25:10301 (AEEW-R-701)
neutron pulse decay and distribution in, Monte Carlo analysis of time dependent thermal, (T), 25:10314
plutonium-239 content of, in environs of plutonium industry, maximum permissible, 25:8674(T) (LF-tr-41, pp 199-220)
radio-wave emission from oxygen-18 enriched, in cosmic sources, (E), 25:9076
radiolysis at pH 7.0 to 12.7, effects of salts on reactions of hydrated electrons in pulse, 25:8291
radiolysis of oxygen-containing, intermediate states in, 25:8293
radiolysis of oxygen-containing, monomolecular reactions in, 25:8295
separation of strontium from, by ion exchange, effects of calcium on, 25:8341
shock wave propagation through, from exploding wires, 25:8383 (AD-706767)
solvent properties for curium-244 oxide, 25:8427(R) (ORNL-4639)
uses in nuclear industry, 25:8326
H_2O--steam, flow in bleed piping of nuclear power plant turbine, stability of, (E), 25:8411

WATER-d_2
effects on number of cells in colony, 25:8632 (EUR-4526)
effects on slow neutron radiograph in animal tissues, 25:8709 (DP-1229)
neutron pulse decay and distribution in, Monte Carlo analysis of time dependent thermal, (T), 25:10314
production of, evaluation of various processes for, 25:8328
production of, review on processes for, 25:8315 (AAEC/TM-562)
toxicity to rats, 25:8709 (DP-1229)

WATER-t
content in atmosphere of industrial premises and expired air and urine of personnel, recommendations for maximum permissible, 25:8678(T) (ORNL-tr-2403)

WATER SUPPLIES
cesium-137 ratio to strontium-90 in, of New York City during 1965 to 1970, monthly and annual averages of fallout, 25:8670(R) (HASL-237(App.))
radiation hazards to, from polonium-210 migration in soils, α and γ, 25:8593 (COO-1733-11)
radioisotope contamination of, following extreme reactor accident, biological significance of fallout, 25:8660 (HMI-B-87)
strontium 90 ratio to cesium 137 in, of New York City during 1965 to 1970, monthly and annual averages of fallout, 25:8670(R) (HASL-237(App.))
strontium-90 content of, in New York City during 1954 to 1970, monthly and annual averages of fallout, 25:8670(R) (HASL-237(App.))

WATER VAPOR
reactions with uranium carbide, oxidation, 25:8907 (CEA-

XUM

Bib-183)
sorption by thorium oxide at 25 to 500°C, 25:8266
WATER WAVES
characteristics of cratering explosion-generated, in shallow water, analysis of data on, 25:8386 (UCRL-50940)
WATERFORD POWER REACTOR, UNIT 3
construction of, permit application for, 25:10158 (DOCKET-50382-1)
operation of, license application for, 25:10158 (DOCKET-50382-1)
owners of, financial statements of, 25:10158 (DOCKET-50382-1)
WATERFORD POWER REACTOR, UNIT 4
construction of, permit application for, 25:10158 (DOCKET-50382-1)
operation of, license application for, 25:10158 (DOCKET-50382-1)
owners of, financial statements of, 25:10158 (DOCKET-50382-1)
WELDING
equipment for electron beam, design of programmer for automated, 25:8391 (EUR-4537)
performance of shielded metal-arc, for fabrication of LMFBR stainless steel components, 25:8849 (ORNL-4600, pp 142-6)
WELL LOGGING
equipment and method for neutron, using pulse height discrimination, 25:8359(P)
method for quantitative, using nuclear magnetic resonance, 25:8358(P)
WEST VALLEY PROCESSING PLANT
krypton-85 release from, 25:8366 (DOCKET-50201-56)
WHISTLERS
propagation in low-latitude thermosphere, ion reflections and shape changes of downward, (E), 25:9321
propagation of walking-trace, between conjugate hemispheres, (E), 25:9325
spectra of, associated with magnetospheric geomagnetic disturbances, dynamic, (E/T), 25:9346
WIND
effect of neutral, on ionospheric F-region diurnal behavior, (T), 25:9315
effects on 850-ft guyed stack, 25:10391 (TID-25618)
effects on ground-level contamination from stack-released reactor effluents at ORNL, methods for calculating, 25:8452 (ORNL-TM-3187)
WINDOWS
closure for, design of air-tight and soundproof, 25:8403(P)
WIRES
current flow model for superconducting transmission line, (T), 25:9377
WYOMING
uranium deposits at Heaths Peak, Carbon County, geology and mineralogy of, 25:8379
uranium deposits in, geology and mineralogy of roll-type, 25:8377

X

X RADIATION
absorption of hard solar, in ionospheric D region, 25:9330
detection in southern auroral zone, association with diffuse and discrete auroral radar echoes, (E), 25:9320
detection of soft solar 44- to 55-A, design and operation of satellite-borne proportional counters for, 25:8499
detection of, end-window variable geometry proportional detector for, 25:8510
dosimetry for therapy, high-energy, 25:8735
dosimetry for therapy, high-energy, 25:8734
dosimetry of 5 to 150 kV, methods for, 25:8672 (ICRU-17)
dosimetry of, response of lithium fluoride thermoluminescent dosimeters for, 25:8567
effect of sudden increases of fluxes of, on electron density in sunlit ionosphere, Feb. 20, 1970, (E), 25:9333
effects on bioelectric properties and glucose transport in intestine of rats, combined effects of chronic bile diversion on, 25:8607(R) (ORO-3882-3)
effects on blood pressure, leucocyte count, and respiration rate of dogs, effects of biological stress induced by pressure on, 25:8766
effects on cell damage in spores of Bacillus megaterium, effects of nitrous oxide on, 25:8810
effects on chromosomes of lymphocytes in man, aberrant, 25:8788(T) (LIB/Trans-296)
effects on chromosomes of mice, effects of, on mutations for Rex gene, 25:8645
effects on chromosomes of Vicia faba, combined effects of post-exposure treatment with 5-azacytidine on aberrant, 25:8639
effects on chromosomes of Vicia faba, effects of nitrosoguanidine on aberrant, 25:8705
effects on connective tissue of rats, effects of cortisone and anabolic steroids on, 25:8786
effects on count of germ cells in human testes, effects of dose on in vitro, 25:8789(R) (NYO-4034-2)
effects on cultured Chinese hamster cells, factors affecting expression of mutagenic, 25:8638
effects on development of retinal tissues in fetuses of monkeys, effects of gestational age on, 25:8757 (NYO-2740-7, pp 218-56)
effects on development, electrical activity, and neurochemical activity of brain of rats, 25:8758(R) (UCB-34-P-82-10)
effects on DNA in cultured mammalian cells, repair processes following, carcinogenic, 25:8611
effects on DNA synthesis in human lymphocytes, effects of low dose range on, 25:8647
effects on doped calcium fluoride, ESR of trapped hole centers induced in, 25:9546
effects on Drosophila melanogaster, genetic, 25:8756 (NYO-2740-7, pp 154-217)
effects on excitability of brain of rats, effects of dose on, 25:8758(R) (UCB-34-P-82-10)
effects on eye development in embryos of mice, 25:8646
effects on fetuses of mice, synergistic effects of synkavit on teratogenic, 25:8703
effects on frozen aqueous solutions, effects of Sephadex, 25:8298
effects on HeLa S3 cells, effects of temperature on, 25:8747
effects on hematopoiesis in dogs, in comparison with mixed neutrons and γ rays, 25:8774
effects on hypothalamo-hypophysical neurosecretory system in amphibia, 25:8764
effects on immune reactions and survival of hybrid mice following transplantation of bone marrow from parental strain, 25:8618
effects on immune reactions of mice following transplantation of rat bone marrow, effects of age and dose of donor cells and sex on, 25:8619
effects on immune reactions to transplants of allogenic leukemia in mice, whole-body, 25:8622
effects on iodoamino acids, 25:8304
effects on leukemic mice, effects of triacetoneamine-N-oxyl on, 25:8701
effects on liver and lungs of mice, effects of simultaneous eruption of Ascaris suum larvae on, 25:8781
effects on meiosis in grasshoppers, tritium tracer study of effects of temperature on, 25:8754
effects on mice, effects of pre- and post-exposure splenectomy on protective effects of bone marrow transplants against lethal, 25:8706
effects on mice, effects of, on mechanism of wound healing, partial-body, 25:8772
effects on mitosis in WI-38 diploid strain of cultured human cells, 25:8743
effects on mitosis rate in cultured chicken fibroblasts, effects of dose on, 25:8752
effects on morphogenesis of buds in Salmacina incrustans, 25:8753
effects on positron annihilation in acetylmethionine, 25:8269
effects on potassium bromide crystals containing diffused magnesium, 25:9570
effects on potassium chloride crystals with and without dopants, role of motion of holes, anion vacancies, and excitons in coloration, 25:9553
effects on primary mutant of Schizophyllum commune, mutagenic, 25:8643
effects on primary virus infections in animals, review on, 25:8699
effects on production of gamma G and M antibodies following stimulation by serum gamma globulin in immunized rabbits, 25:8621
effects on retina of rabbits, use of electroretinogram for comparing with toxic effects of thermal neutrons, 25:8761
effects on Saccharomyces cerevisiae budding cells, genetic and physiological studies of, 25:8798
effects on Sephadex molecules, intermolecular energy transfer at 77°K following, 25:8613
effects on serum coeruloplasmin activity in rats, 25:8612
effects on spinal cord of animals, following exposure of brain stem, inhibitory, 25:8771
effects on survival in spores of ferns, lethal, 25:8614
effects on survival of cells of subcutaneously transplantable ependymomas in mice, 25:8759
effects on survival of cultured chicken fibroblasts, effects of dose on, 25:8751
effects on survival of mice, protective effects of sodium fluoroacetate against 700 to 1000 R, 25:8700
effects on survival of synchronized cultures of Chinese hamster cells, comparison of effects of aeration and hypoxia on, 25:8757 (NYO-2740-7, pp 218-56)
effects on swine, pathological, 25:8773
effects on template properties of DNA, effects of dose on, 25:8610
effects on thymus function in mice, effects of strain on recovery from whole-body, 25:8776
effects on Triticum durum, mutagenic, 25:8641
effects on ultrastructure of lungs of mice following exposure of thorax, 25:8778
effects on wheat seeds, mutagenic, 25:8655
emission from Sun, data from Vela V and VI for Sept. 1, 1969 to Jan. 1, 1970, (E), 25:9097 (LA-4454(Vol.2))

XUM

emission from Sun, six-minute periodicity during, (E), 25:9104
emission in auroral zone associated with geomagnetic storm sudden commencement, July 27, 1966, (E), 25:9298
ionization at 75 km in ionosphere by solar, observations during solar eclipse May 20, 1966, (E/T), 25:9310
relation of cosmic background, to discrete sources, (E/T), 25:9079
spectral distribution of absorbed energy of ionospheric, relation to black-body radiation law, (T), 25:9351

X-RAY-ABSORPTION ANALYSIS
source for, properties of metastable tellurium-125, 25:8434

X-RAY CAMERAS
design for diffraction analysis of radioactive powders, 25:8577(P)
use of pinhole, for fine-structure measurements of plasma focus, 25:9412(T) (LA-tr-70-25)

X-RAY-DIFFRACTION ANALYSIS
camera for, for radioactive powders, 25:8577(P)

X-RAY FLUORESCENCE ANALYSIS
source for, properties of metastable tellurium-125, 25:8434

X-RAY SOURCES
performance of metastable tellurium-125, for fluorescent x-ray analyses, 25:8434

X-RAY SPECTROSCOPY
separation processes for, using selective ion exchange paper, 25:8221

XENON
effects on power oscillations in reactors, digital simulation of spatial, 25:10306 (NP-18547)
effects on survival of Escherichia coli and Serratia marcescens, effects of sodium fluorescein and culture medium on, 25:8807
iodine-ion reactions at 1.5 to 12 MeV with, charge-state distributions from multiple ionization in, (E), 25:9219
plasma of, electron density profile measurement of laser-produced, (E), 25:9485
plasma of, excitation temperature functions of spectra lines of, 25:9172
plasma of, spectroscopy and laser interferometric measurements of shock-produced, 25:9422
proton reactions at 0.3 to 2.0 MeV, with, angular and energy distributions of electrons from, (E), 25:9191 (BNWL-SA-3631)
proton reactions at 15 to 150 keV with, cross sections for charge exchange in, (E), 25:9229
thermodynamic properties of solid, as function of temperature, models for anharmonic, 25:8262 (UCRL-50903)

XENON IONS
effects on lattice expansion and strain in silicon and gallium arsenide at 400 keV, 25:8564

XENON ISOTOPES Xe-124
concentration by thermal diffusion, rates for, 25:8424(R) (MLM-1768)

XENON ISOTOPES Xe-131
concentration by thermal diffusion, rates for, 25:8424(R) (MLM-1768)

XENON ISOTOPES Xe-133
production of pharmaceutical saline solution of, 25:8309(P)
use as tracer for in vitro study of blood flow in swine livers, 25:8783

p-XYLENE
radioinduced luminescence of solutions of, in butanol and methanol, α, β, and uv, 25:8274

Y

YANKEE POWER REACTOR
operations history for November 1970, 25:10113 (DOCKET-50029-141)

YTTERBIUM
phase transition in high-purity, first-order magnetic, 25:9588

YTTERBIUM ISOTOPES Yb-167
energy levels of, spin--parity assignments from superfluid model, (T), 25:10028 (JINR-P4-5228)

YTTERBIUM ISOTOPES Yb-176
proton elastic and inelastic scattering at 19 MeV, angular distributions for, (E), 25:9966(R) (COO-1265-94)

YTTRIUM
abundance in eucrites, (E), 25:8966

YTTRIUM ALLOYS AND SYSTEMS
Al--Ni--Y, magnetic properties and phase diagram of ErNi/sub x/Al/sub 2-x/, 25:9576
Al-base--Gd--Y, phase diagram at 500°C, 25:8886

YTTRIUM CHLORIDES
neodymium-145 Moessbauer hyperfine structure in $YCl_3 \cdot 6H_2O$, 25:9594

YTTRIUM ISOTOPES Y-89
deuteron elastic scattering at 30 to 40 MeV, angular distributions for, (E), 25:9978(R) (ORO-3398-26)
deuteron reactions (d,He-3) at 30 to 40 MeV, angular distributions for, (E), 25:9978(R) (ORO-3398-26)
electron reactions (e,e'p) with, proton spectra and excitation functions for, (E), 25:10053
neutron elastic and inelastic scattering at 4.19 to 8.56 MeV, differential cross sections for, (E), 25:9999 (ORNL-4552)

YTTRIUM OXIDES
radiation effects on microstructure and swelling of polycrystalline, in-pile, 25:8954 (ORNL-4600, pp 210-15)
reactions with hafnium dioxide, study of phases formed during, 25:8935
HfO_2-base--Y_2O_3, preparation and properties of alkoxy-derived high-purity powdered, 25:8949
HfO_2-base--Y_2O_3, structure of alkoxy-derived high-purity powdered, 25:8949
Y_2O_3--ZrO_2, properties for use as high-temperature electric conductor or insulator, 25:8936

Z

ZINC
determination in air particulates by spark source mass spectrometry, 25:8208
determination in airborne particulates by neutron activation, 25:8231
determination in human fingernails and hair by neutron activation and γ spectrometry, 25:8229
determination in titanium and titanium dioxide by neutron activation, 25:8233
Raman effect in crystals of, model potential calculation of first derivative of electronic polarizability for first-order, 25:9598
reactions with zinc ions at low energies, transfer of excitation energy in, (E), 25:9238

ZINC ALLOYS AND SYSTEMS
In--Zn, electric conductivity and structure of liquid, correlation between, 25:8882

ZINC IONS
reactions with zinc atoms at low energies, transfer of excitation energy in, (E), 25:9238

ZINC ISOTOPES Zn-64
performance of activation detectors of, for neutron spectra measurements at 1 eV to 10 keV, 25:8481 (KFK-1233)

ZINC ISOTOPES Zn-65
accumulation in Navicula seminulum, Plectonema boryanum, and Stigeoclonium lubricum, effects of temperature on, 25:8598
transport in food chains of nuclear-explosion-contaminated estuarine and marine ecosystems in relation to daily ingestion by man, use of stable element content of fish and invertebrates for predicting, 25:8627

ZINC ISOTOPES Zn-68
proton elastic scattering at 18.6 MeV, angular distributions for, (E), 25:9966(R) (COO-1265-94)

ZINC SULFIDES
radiation effects on luminescence of copper-doped, electron, 25:8485

ZINC TELLURIDES
ion implantation for p--n junction formation in, chlorine, 25:9560

ZIRCALOY
deformation and failure of tubes of, at high temperatures, review of research on, 25:8839 (ORNL-TM-3188)
embrittlement of cladding of, review of research on, 25:8839 (ORNL-TM-3188)
embrittlement of, effects of reactor coolant loss accidents on, (E), 25:10244(R) (ORNL-TM-3212)
radiation effects on ductility of (E), 25:10244(R) (ORNL-TM-3212)

ZIRCALOY-2
corrosion by steam at 300 to 600°C, factors affecting, 25:8833 (AERE-M-1854)
radiation effects on mechanical properties of, neutron, 25:10125(R) (NP-18573)
tritium distribution in fuel cladding of, at high fuel burnups, 25:8951(R) (GEAP-10217)
welding of tubes of, methods for homogenizing joints in, 25:8844 (AERE-M-1561)

ZIRCONIUM
abundance in eucrites, (E), 25:8966
alpha reactions at 30 to 80 MeV, K-shell ionization cross sections for, (E), 25:9978(R) (ORO-3398-26)
analysis for oxygen by inert gas fusion method, evaluation of bath materials for, 25:8194 (AECL-3743)
analysis for rare earths by optical fluorescence spectroscopy, phosphors for, 25:8207
compatibility of fuel capsules of, with curium-244 oxide at 1250 to 1650°C, 25:8427(R) (ORNL-4639)
corrosion by steam at 300 to 600°C, factors affecting, 25:8833 (AERE-M-1854)
determination in air particulates by spark source mass spectrometry, 25:8208
mechanical properties at 20 to 239°K, design of device for determining low-temperature, 25:8881
passivation of electropolished, effects of halides in aqueous ammonium nitrate on, 25:8832(T) (AEC-tr-7204)
production of reactor-grade, vacuum methods for, 25:8461
separation from effluents from chemical decanning of reactor fuel elements by sorption on barium sulfates,

XUM

25:8344(P)
ZIRCONIUM ALLOYS AND SYSTEMS
properties for use in internal reactor components, review of, 25:8828 (BNWL-SA-3426)
C--Nb-base--V--Zr, preparation and properties of corrosion-resistant, for use in nuclear industry, 25:8856(P)
Er--Zr, solid solution formation in rapidly quenched, x-ray diffraction studies of metastable hcp, 25:8852
Ge--Zr-base, corrosion by steam at 300 to 600°C, factors affecting, 25:8833 (AERE-M-1854)
Mg--Zr, embrittlement by hydrogen at high temperatures, effects of grain size on, 25:8874
Mg--Zr, use in cladding plugs for plutonium-loaded fuel elements, 25:8857
Nb-base--Zr, compatibility of fuel capsules of, with curium-244 oxide at 1250°C, 25:8427(R) (ORNL-4639)
Se--Zr-base, corrosion by steam at 300 to 600°C, factors affecting, 25:8833 (AERE-M-1854)
Ta--Zr, physical properties of age-hardening, 25:8851 (ORNL-4600, pp 186-97)
V-base--Zr, corrosion by sodium at 600°C, effects of oxygen on, 25:8836 (ORNL-4600, pp 157-66)
ZIRCONIUM BOROHYDRIDES
phase studies on, 25:8263
spectra of, ir, 25:8263
ZIRCONIUM CARBIDES
emissivity of pyrolytic, at 1200 to 2900°K, integrated hemispherical, 25:8931
evaporation rates at 2800 to 3400°K, 25:8929
ZIRCONIUM FLUORIDES
BeF_2--LiF--NdF_3--ZrF_4, distillation of molten, removal of neodymium fluoride by low-pressure, (E), 25:10210 (ORNL-4434)
BeF_2--LiF--UF_4--ZrF_4, preparation and handling of molten, for use as MSRE fuel salt, 25:10211 (ORNL-4616)
ZIRCONIUM ISOTOPES Zr-90
electron reactions (e,e'p) with, proton spectra and excitation functions for, (E), 25:10053
proton elastic scattering at 18.6 MeV, angular distributions for, (E), 25:9966(R) (COO-1265-94)
ZIRCONIUM ISOTOPES Zr-91
proton reactions (p,pn) at 17 MeV, mechanism of, (E), 25:10005
ZIRCONIUM ISOTOPES Zr-95
determination as measure of fuel burnup, 25:8214
distribution in uranium dioxide fuels at high burnups, determination by gamma scanning, 25:8951(R) (GEAP-10217)
separation from fission products by solvent extraction using dioctyl phosphate, 25:8214
ZIRCONIUM NITRIDES
analysis for nitrogen, evaluation of chemical methods for, 25:8195 (AERE-R-6491)
ZIRCONIUM OXIDES
diffusion in, mechanism for anion and cation, 25:8934
electric conductivity of, 25:8934
preparation of stabilized, using lime and rare earth oxides, 25:8918(P)
properties for use in dispersion strengthening of aluminum, 25:8869(P)
CaO--ZrO_2, properties for use as high-temperature electric conductor or insulator, 25:8936
CeO_2--ZrO_2, properties for use as high-temperature electric conductor or insulator, 25:8936
rare earth oxide--ZrO_2, properties for use as high-temperature electric conductor or insulator, 25:8936
rare earth oxides--ZrO_2, formation of solid solutions of, kinetics of, 25:8935
Y_2O_3--ZrO_2, properties for use as high-temperature electric conductor or insulator, 25:8936

XUM

REPORT NUMBER INDEX

Reports, conference papers and proceedings, numbered translations, and patents are included in this index. Each item is listed by report number; this is followed by the abstract number and a brief notation regarding public availability. The index entries show which reports are on file in the institutions listed on the back of the front cover (Dep.), which reports have been published in open-literature journals (journal citation), and which reports can be purchased (source and price). Whenever a report is identified by more than one number, the availability is given under the primary number, and a cross reference is given under the secondary report number.

The report number codes apply to USAEC reports unless designated otherwise. Non-USAEC reports are identified by parenthetical notes after the report codes; e.g., (non-AEC), (British), (Canadian), (French). The note (Misc.) identifies the codes used for both USAEC and non-USAEC reports. Patents are listed under the heading "PATENTS"; the country of origin is included in parentheses.

A comprehensive list of both USAEC and non-USAEC report codes is contained in the latest revision of TID-85, *Report Number Series Used by the Division of Technical Information in Cataloging Reports.* This information is also included in the Cumulative Report Number Index (issued annually).

Availability of USAEC Reports

All USAEC Reports abstracted in *Nuclear Science Abstracts* are available through one or more of the following sources:

(1) University and public libraries in the United States. A list of these organizations appears on the inside front cover of each issue of *NSA*.

(2) NCR Microcard Editions in Microcard and micronegative form. Orders and inquiries should be sent to: Order Processing Department, 365 South Oak Street, West Salem, Wisconsin 54669.

(3) National Technical Information Service, U. S. Department of Commerce, Springfield, Virginia 22151.

(4) Superintendent of Documents, U. S. Government Printing Office, Washington, D. C. 20402.

(5) National Cash Register Co., P. O. Box 3111, Oak Ridge, Tenn. 37830, in micronegative form. Purchase details available on request.

Availability of Non-USAEC Reports

U. S. Reports. Reports of U. S. Government agencies are available to the public from the National Technical Information Service (NTIS). If specific availability is not shown, inquiries may be directed to NTIS.

Non-U. S. Reports. Reports of atomic energy organizations of other countries are available from NTIS for U. S. sale only. Specific availability in the country of origin is shown, when known, at the report number entry. Otherwise, inquiries should be made to the organizations listed below:

AUSTRALIA

Australian Atomic Energy Commission Research Establishment. Available upon request from the Library, Australian Atomic Research Establishment, Private Mail Bag, Sutherland, New South Wales, Australia.

BELGIUM

Centre d'Étude de l'Energie Nucléaire. Available upon request to individuals and organizations from the Centre d'Etude de l'Energie Nucléaire (C.E.N.), Studiecentrum voor Kernenergie (S.C.K.), Technical Information Dept., MOL-DONK (Belgium).

CERN

CERN European Organization for Nuclear Research. Available without charge from CERN European Organization for Nuclear Research, Geneva 23, Switzerland. Copies are deposited in libraries throughout the world.

FRANCE

Commissariat à l'Energie Atomique. Inquiries for reports numbered 1-2199 should be addressed to Service Central de Documentation du C.E.A., Centre d'Etudes Nucléaires de Saclay, Boîte postale n° 2, 91. GIF-sur-YVETTE, FRANCE. Reports numbered 2200 and above are available from La Documentation Française, 31 quai Voltaire, 75, PARIS (7e), FRANCE.

Service Central de Protection contre les Rayonnements Ionisants. Copies are available from Ministère de la Santé Publique, Service Central de Protection contre les Rayonnements Ionisants, B.P. n° 78 Le Vesinet (France) Telex 25667.

GERMANY

Deutsches Elektronen-Synchrotron DESY. Copies are available from Deutsches Elektronen-Synchrotron DESY, Dokumentation, 2000 Hamburg 52, Notkestieg 1, Germany.

Gesellschaft für Kernforschung mbH (KFK). Copies are available from Gesellschaft für Kernforschung mbH, 75 Karlsruhe, Postfach 947, Germany. Copies are also deposited in many national nuclear centers in the world.

Kernforschungsanlage. Copies may be ordered from Zentralbibliothek der Kernforschungsanlage Jülich, Jülich, Bundesrepublik Deutschland.

Hahn-Meitner-Institute für Kernforschung. Available without charge from Hahn-Meitner-Institute für Kernforschung Ber-

XUM

lin, Bibliothek, Glienicker Strasse 100, 1 Berlin 39, Germany. Copies are deposited in many national nuclear centers in the world.

Johann-Wolfgang-Goethe Universität, Frankfurt Am Main, Institut für Kernphysik, (IKF). Copies are available from Gmelin Institut, 40–42 Varrentrappstrasse, Frankfurt (Main), West Germany.

ISRAEL

Israel Atomic Energy Commission. Available without charge from Israel Atomic Energy Commission, Soreq Nuclear Research Centre, Yavne, Israel.

ITALY

Centro Informazioni Studi Esperienze (CISE). For sale at CISE Press Office, Casella Postale 3986, Milano, Italy. Copies are deposited in the libraries of various nuclear centers in Italy and abroad.

Comitato Nazionale per l'Energia Nucleare. Copies are available from Comitato Nazionale per l'Energia Nucleare, Divisione Affari Internazionali e Studi Economici, Ufficio Pubblicazioni, Via Belisario, 15, Roma, Italy.

JAPAN

Japan Atomic Energy Research Institute (JAERI). Available from the Staff Supply Cooperative of Japan Atomic Energy Research Institute (JAERI), Tokai-mura, Naka-gun, Ibaraki-ken, Japan. Copies are deposited in depositories in Tokyo, Nagoya, and Osaka.

Nagoya University. Copies are available from Research Information Center, Institute of Plasma Physics, Nagoya University, Nagoya, Japan.

University of Tokyo. Available free of charge from Institute for Nuclear Study, University of Tokyo, Tanashi-Machi, Kitatama-gun, Tokyo, Japan.

NETHERLANDS

Reactor Centrum Nederland. For sale by Reactor Centrum Nederland, 112 Scheveningseweg, 's-Gravenhage, The Netherlands. Copies are deposited in university libraries in Holland and in many national nuclear centers in the world.

NEW ZEALAND

Institute of Nuclear Sciences. Copies are available from Librarian, N. Z. Institute of Nuclear Sciences, D.S.I.R., Private Bag, Lower Hutt, New Zealand. Copies are deposited in other countries.

PAKISTAN

Atomic Energy Center. Copies are available from Atomic Energy Center, P. O. Box 658, Lahore, (West Pakistan).

POLAND

Reports of the Polish nuclear institutes are published by the Nuclear Energy Information Center of the Government Commissioner for Use of Nuclear Energy. Copies are available free of charge from Nuclear Energy Information Center, Palace of Culture and Science, Warsaw, Poland.

SPAIN

Junta de Energia Nuclear. "JEN" reports are available without charge from Servicio de Documentation, Junta de Energia Nuclear, Ciudad Universitaria, Madrid (3), España.

SWITZERLAND

Eidgenössisches Institut für Reaktorforschung. "EIR" reports are available from Eidgenössisches Institut für Reaktorforschung, c/o Bibliothek, 5303 Würenlingen/Switzerland.

TURKEY

Turkish Atomic Energy Commission. Copies are available free of charge from T.A.E.C., Çekmece Nuclear Research Center, P. O. Box 1, Airport, Istanbul, Turkey.

Conferences

Published conference proceedings as well as individual unpublished papers from conferences are included in this index. A CONF number is assigned to the conference if published proceedings are received and also if only a single paper is received. The base number used is year-month-sequence. Thus, the number CONF-650101 indicates that the conference was held in 1965, in January, and that this was the first January 1965 conference so received. This number would be assigned to complete published proceedings. If individual papers are received, the base number is extended to include a paper number, e.g., CONF-650101-1. As additional papers are received, they will be assigned consecutive numbers in the series, CONF-650101-1, CONF-650101-2, etc. This numbering system ensures that all papers received from a conference will be associated with that conference in this index.

If published proceedings are received after the receipt of individual papers, the complete proceedings will be abstracted and the abstract number will appear in this index with the base CONF number.

Abbreviations Used in Availability Column

AECL	Reports of the Atomic Energy of Canada Limited are for sale by the Scientific Document Distribution Office, Atomic Energy of Canada Limited, Chalk River, Ontario, Canada.
CFSTI	See NTIS
DENM	Reports of the Atomic Energy Commission Research Establishment, Riso, are available on exchange from the Library, Danish Atomic Energy Commission, Riso, Roskilde, Denmark. Also for sale at the price shown from Jul. Gjellerup, Booksellers, 87 Sölvgade, Kobenhavn K., Denmark. Reports of Danatom are available on loan from Research Establishment, Riso, Roskilde, Denmark. Copies are available from Danatom, Aurehojvej 2, Hellerup, Denmark.
Dep.	AEC reports so designated are maintained in the organizations listed on the inside front cover of *NSA*. Prior to July 1, 1965, reports were deposited either in printed copy form or in microform. After that time, all reports have been in the form of micronegatives. Reports from other countries so designated are available in the United States at the organizations listed on the inside front cover of *NSA*.

XUM

DTIE — Available from the U. S. Atomic Energy Commission, Division of Technical Information Extension, P. O. Box 62, Oak Ridge, Tennessee 37830. (Conference papers are available on loan only.)

EM — Blueprints of AEC engineering drawings are available from NTIS, U. S. Department of Commerce, Springfield, Virginia 22151. Current prices of the CAPE-packages may be obtained from this address. TID-4100, available from the Division of Technical Information Extension, P. O. Box 62, Oak Ridge, Tennessee 37830, contains information on all the CAPE-packages for sale.

EUR — For sale by Centrale de vente des publications des Communautés européennes 37, rue Glesener-Luxembourg.

GPO — For sale by the Superintendent of Documents, Government Printing Office, Washington, D. C. 20402.

IAEA — Available from the International Atomic Energy Agency, Vienna, Austria, and from its sales agencies in various countries throughout the world. A list of these agencies is found in each STI/DOC and STI/PUB publication.

NORW — Reports from Forsvarets Forskningsinstitutt are available from Norwegian Defense Research Establishment, Library, P. O. Box 25, Kjeller, Norway.
"KR" reports are available on an exchange basis from the Library, Institutt for Atomenergi, Box 40, Kjeller, Norway.
Reports of the Norwegian Reactor School are available from the Library, Institutt for Atomenergi, P. O. Box 40, Kjeller, Norway.

NRC — For sale by the National Research Council of Canada, Ottawa, Ontario, Canada.

NTIS — For sale by the National Technical Information Service (NTIS), U. S. Department of Commerce, Springfield, Virginia 22151 at the following prices for eye legible copy:

1–300 pages	$3.00
301–600 pages	$6.00
601–900 pages	$9.00

Documents over 900 pages have special prices which may be obtained from NTIS. Microfiche copy of each separately bound document can be purchased for $0.95.

Reports issued by organizations outside the United States will be sold by NTIS *only to purchasers within the United States.*
Purchasers outside the United States may acquire such reports from the sources described elsewhere in these columns.

OECD — Available from O. E. C. D., Publications 2, rue, André-Pascal, 75 Paris 16e, France, and from its sales agencies in various countries throughout the world. A list of these agencies is found in each OECD publication.

SWED — "AE" reports are for sale from Aktiebolaget Atomenergi, Library Section, Box 43041, Stockholm 43, Sweden. Microcopy of these reports is available from the International Documentation Center, Turnba, Sweden.
Reports of the VDDIT-series may be obtained from Aktiebolaget Atomenergi, Information Office, Scientific and Technical Information, Box 43041, Stockholm 43, Sweden.
Other series are not generally available to the public. Organizations in the Atomic Energy field may obtain copies from Aktiebolaget Atomenergi.

UK — United Kingdom Atomic Energy Authority reports generally may be purchased from Her Majesty's Stationery Office, P. O. Box 569, London S.E.1. Copies of many UKAEA reports (particularly earlier ones) may be purchased in microcopy form from Micro Methods Ltd., East Ardsley, Wakefield, Yorkshire, England. Copies of UKAEA reports are deposited with the National Lending Library for Science and Technology and 10 public libraries in England; with the USAEC and (through USAEC) with NTIS; and in most national nuclear centers throughout the world. In the USA, UKAEA reports are available on a subscription basis, by subject category, from UNIPUB, Inc., P. O. Box 433, New York, N. Y. 10016, USA.

UN — Mail orders should be directed to the Sales Section, Room 1059, United Nations Headquarters, New York, New York 10017.

ZAED — Available from Zentralstelle für Atomkernenergie Dokumentation, 6000 Frankfurt/Main 90, P. O. Box 901069, Westendstr. 21, West Germany

XUM

Report No.	Abstract No.	Availability
AAEC/M-	(Australian)	
9	25-10252	Dep. NTIS (U. S. Sales Only), 12p.
32	25-10253	Dep. NTIS (U. S. Sales Only), 16p.
AAEC/TM-	(Australian)	
562	25-8315	Dep. NTIS (U. S. Sales Only), 62p.
568	25-8571	Dep. NTIS (U. S. Sales Only), 23p.
ABCC-TR-		
0-69	25-8741	Dep. NTIS, 7p.
ACNP-	(Misc.)	
70503.2	25-10135	See DOCKET-1155-87
ACRH-		
1000-214	25-10336	Dep. NTIS, 28p.
AD-	(Misc.)	
705265	25-9455	NTIS, 10p.
706106	25-9269	NTIS, 97p.
706767	25-8383	NTIS, 17p.
707427	25-8362	NTIS, 65p.
709280	25-8861	NTIS, 27p.
709888	25-9283	NTIS, 39p.
709957	25-8862	NTIS, 51p.
710384	25-9965	NTIS, 15p.
AE-	(Non-AEC)	
405	25-10320	Dep. NTIS (U. S. Sales Only), 23p.
AEC-tr-		
7204	25-8832	Dep. NTIS
AECL-	(Canadian)	
3668	25-9970	Dep. NTIS (U. S. Sales Only). AECL $2.50, 123p.
3669	25-9902	Dep. NTIS (U. S. Sales Only). AECL $1.00, 37p.
3671(Add.1)	25-10300	Dep. NTIS (U. S. Sales Only). AECL $1.00, 24p.
3728	25-8666	Dep. NTIS (U. S. Sales Only). AECL $1.50, 52p.
3731	25-8363	Dep. NTIS (U. S. Sales Only). AECL $0.50, 21p.
3745	25-8194	Dep. NTIS (U. S. Sales Only). AECL $0.50, 16p.
AECOP-		
621	25-10337	Dep. NTIS, 30p.
AEEW-R-	(British)	
701	25-10301	Dep. NTIS (U. S. Sales Only). UK 6s. 6d, 31p.
AERE-M-	(British)	
1561	25-8844	Dep. NTIS (U. S. Sales Only), 31p.
1594	25-8421	Dep. NTIS (U. S. Sales Only), 11p.
1854	25-8833	Dep. NTIS (U. S. Sales Only), 4p.
1990	25-8389	Dep. NTIS (U. S. Sales Only), 8p.
AERE-R-	(British)	
4857	25-8906	Dep. NTIS (U. S. Sales Only), 29p.
5104	25-8445	Dep. NTIS (U. S. Sales Only), 36p.
5363	25-8216	Dep. NTIS (U. S. Sales Only), 26p.
5483	25-8845	Dep. NTIS (U. S. Sales Only), 16p.
5502	25-8390	Dep. NTIS (U. S. Sales Only), 10p.
6242	25-10236	Dep. NTIS (U. S. Sales Only). UK 5s. 6d, 38p.
6491	25-8195	Dep. NTIS (U. S. Sales Only). UK 2s. 6d, 14p.
6556	25-8364	Dep. NTIS (U. S. Sales Only). UK 8s, 53p.
AFML-TR-	(Non-AEC)	
70-119(Pt. 1)	25-8662	See AD-709957
AFOSR-	(Misc.)	
70-444-TR	25-9455	See AD-705265
70-527-TR	25-9269	See AD-706106
ANL-		
7542	25-10173	Dep. NTIS, 73p.
7619	25-10163	Dep. NTIS, 44p.
7665	25-10228	Dep. NTIS, 91p.
7672	25-8446	Dep. NTIS, 91p.
7691	25-8827	Dep. NTIS, 166p.
7698	25-9971	Dep. CFSTI, 44p.
7699	25-10015	Dep. NTIS, 47p.
7758	25-10164	Dep. NTIS, 129p.
ANL-ES-		
1	25-10340	Dep. NTIS, 24p.
ANL-Trans-		
865	25-10254	Dep. NTIS
866	25-10338	Dep. NTIS
867	25-8885	Dep. NTIS
868	25-10339	Dep. NTIS
869	25-8259	Dep. NTIS
870	25-8284	Dep. NTIS
ANU-P-	(Australian)	
466	25-9996	Dep. CFSTI (U. S. Sales Only), 32p.
496	25-9972	Dep. CFSTI (U. S. Sales Only), 8p.
503	25-10016	Dep. CFSTI (U. S. Sales Only), 9p.
ARH-SA-		
72	25-8236	Dep. NTIS, 18p.
BARC-	(Non-AEC)	
499	25-9940	Dep. NTIS (U. S. Sales Only), 21p.
501	25-10017	Dep. CFSTI (U. S. Sales Only), 112p.
502	25-10302	Dep. NTIS (U. S. Sales Only), 7p.
504	25-8196	Dep. NTIS (U. S. Sales Only), 7p.
507	25-8908	Dep. NTIS (U. S. Sales Only), 16p.
510	25-8197	Dep. NTIS (U. S. Sales Only), 44p.
BAW-	(Misc.)	
1344	25-10237	Dep. NTIS, 67p.
BDX-		
613-166	25-10341	Dep. NTIS, 18p.
613-252	25-10342	Dep. NTIS, 6p.
BHO-		
65-1	25-8447	Dep. NTIS, 16p.
BLG-	(Belgian)	
447	25-8463	Dep. NTIS (U. S. Sales Only), 27p.
BLWT-		
5-68	25-10391	See TID-25618
BMBW-FBK-	(West German)	
70-10	25-10018	Dep. NTIS (U. S. Sales Only), 187p.
70-15	25-8464	Dep. NTIS (U. S. Sales Only), 57p.
BMI-	(Misc.)	
1890	25-10238	Dep. NTIS, 36p.
1891	25-8863	Dep. NTIS, 12p.
BNL-		
13957	25-8405	Dep. NTIS, 11p.
15368	25-9903	Dep. NTIS, 4p.
15437	25-10343	Dep. NTIS, 115p.
50238	25-10109	Dep. NTIS, 83p.
50242	25-10019	Dep. NTIS, 14p.
50260	25-9732	Dep. NTIS, 62p.
50271	25-8198	Dep. NTIS, 15p.
BNL-tr-		
379	25-10020	Dep. NTIS
386	25-10344	Dep. NTIS
387	25-10345	Dep. NTIS
389	25-10346	Dep. NTIS
BNWL-		
916	25-10255	Dep. NTIS, 136p.
1485	25-10256	Dep. NTIS, 147p.
BNWL-CC-		
1939	25-8316	Dep. NTIS, 31p.
2502	25-8199	Dep. NTIS, 19p.
BNWL-SA-		
1514	25-8465	Dep. NTIS, 21p.
3233	25-8667	Dep. NTIS, 16p.
3286	25-10207	Dep. NTIS, 22p.
3336	25-8448	Dep. NTIS, 18p.
3419	25-8623	Dep. NTIS, 24p.
3424	25-8668	Dep. NTIS, 13p.
3426	25-8828	Dep. NTIS, 30p.
3482	25-9189	Dep. NTIS, 14p.
3494	25-8345	Dep. NTIS, 24p.
3498	25-9190	Dep. NTIS, 14p.
3564	25-10132	Dep. NTIS, 16p.
3581	25-10133	Dep. NTIS, 31p.
3605	25-10233	Dep. NTIS, 14p.
3624	25-8466	Dep. NTIS, 11p.
3631	25-9191	Dep. NTIS, 18p.
BNWL-tr-		
57	25-8896	Dep. NTIS
BRH/NERHL-	(Non-AEC)	
70-4	25-8467	NTIS, 37p.
CALT-		
822-20	25-10347	Dep. NTIS, 11p.
822-21	25-10348	Dep. NTIS, 14p.
CAPE-		
2040	25-8457	EM
CEA-Bib-	(French)	
163	25-8907	Dep. NTIS (U. S. Sales Only), 19p.
CEA-CONF-	(French)	
1645	25-8406	Dep. NTIS (U. S. Sales Only), 11p.

XUM

Report No.	Abstract No.	Availability
1658	25-8590	Dep. NTIS (U. S. Sales Only), 8p.
1669	25-9536	Dep. NTIS (U. S. Sales Only), 17p.
1677	25-8591	Dep. NTIS (U. S. Sales Only), 7p.
1680	25-9541	Dep. NTIS (U. S. Sales Only), 2p.
1681	25-9542	Dep. NTIS (U. S. Sales Only), 2p.
1684	25-10303	Dep. NTIS (U. S. Sales Only), 43p.
CEA-N-	(French)	
1273	25-10021	Dep. CFSTI (U. S. Sales Only), 51p.
1338	25-10022	Dep. NTIS (U. S. Sales Only), 20p.
1354	25-10192	Dep. NTIS (U. S. Sales Only), 31p.
1358	25-8960	Dep. NTIS (U. S. Sales Only), 10p.
1359	25-10193	Dep. NTIS (U. S. Sales Only), 40p.
1361	25-9941	Dep. NTIS (U. S. Sales Only), 35p.
1372	25-10023	Dep. NTIS (U. S. Sales Only), 26p.
1391	25-9407	Dep. NTIS (U. S. Sales Only), 37p.
CEA-R-	(French)	
3895	25-10194	Dep. NTIS (U. S. Sales Only), 69p.
3988	25-10185	Dep. NTIS (U. S. Sales Only), 89p.
4008	25-8657	Dep. NTIS (U. S. Sales Only), 45p.
4066	25-8865	Dep. NTIS (U. S. Sales Only), 79p.
CEAL-		
1054	25-8468	Dep. NTIS, 10p.
CERN-	(European Organization for Nuclear Research)	
70-24	25-9904	Dep. NTIS (U. S. Sales Only), 141p.
70-28	25-9905	Dep. NTIS (U. S. Sales Only), 22p.
CERN/DI/HP-	(European Organization for Nuclear Research)	
29	25-8562	Dep. NTIS (U. S. Sales Only), 11p.
CISE-R-	(Italian)	
233	25-10165	Dep. NTIS (U. S. Sales Only), 38p.
CLM-R-	(British)	
106	25-8407	Dep. NTIS (U. S. Sales Only). UK 5s 6d, 41p.
CONF-640109-	(Symposium on Neutron Dosimetry for Radiological Purposes, London, England, Jan. 24, 1964)	
1	25-8562	See CERN/DI/HP-29
CONF-660318-	(Dragon Contractors' Research and Development Symposium, Harwell, England, March 1966)	
11	25-8924	See DP-Report-437
CONF-660675-	(Symposium on Boiling Crisis in Two-Phase Flow Systems, Ispra, Italy, June 14-17, 1966)	
1	25-8408	Dep. NTIS (U. S. Sales Only), 72p.
CONF-670341-	(Conference on Gas-Metal Reactions in Environments Containing CO_2, London, England, March 1967)	
1	25-10195	See DP-Report-500
CONF-670460-	(Conference on Isotope Effects in Chemical Processes, Miami Beach, Fla., Apr. 11, 1967)	
	25-8243	Advan. Chem. Ser.; No. 89, 1-278(1969)
CONF-680560-	(7th National Meeting on Society for Applied Spectroscopy, Chicago, Ill., May 13-17, 1968)	
	25-8538	New York; Plenum Publishing Corporation (1969). 348p. $15.00
CONF-681228-	(Panel on Nuclear Techniques for Studying Pesticide Residue Problems, Vienna, Austria, Dec. 16-20, 1968)	
	25-8583	See STI/PUB-252
CONF-690343-	(Conference on Superconducting Materials, Aussois, France, Mar. 10-12, 1969)	
	25-9381	Rev. Phys. Appl.; 4: 543-91(Dec 1969)
CONF-690415-	(10th Structures, Structural Dynamics and Material Conference, New Orleans, La., Apr. 16, 1969)	
	25-10288	New York; American Society of Mechanical Engineers (1969). 476p. $22.00
CONF-690432-	(5th International Conference on Science of Ceramics, Ronneby Brunn, Sweden, Apr. 20-23, 1969)	
	25-8933	Goteborg; Swedish Institute for Silicate Research (1970). 588p. Pound 5.8.9
CONF-690722-	(Symposium on Position Sensitive Detectors in Nuclear Physics, Julich, Germany, June 8-9, 1969)	
	25-8469	See JUL-CONF-4
CONF-690811-	(7th International Conference on High Energy Accelerators, Moscow, U.S.S.R., Aug. 28-Sept. 2, 1969)	
17	25-9916	See UCRL-19313
CONF-690967-	(Joint Power Conference, Charlotte, N.C., Sept. 21-25, 1969)	
1	25-10088	
CONF-691008-	(Symposium on Radiation Safety Problems in the Design and Operation of ''Hot'' Facilities, Saclay, France, Oct. 13-17, 1969)	
18	25-8449	Dep. NTIS (U. S. Sales Only), 24p.
CONF-691020-	(Symposium on Nuclear Energy Costs and Economic Development, Istanbul, Turkey, Oct. 20-24, 1969)	
3	25-10089	Dep. NTIS (U. S. Sales Only), 9p.
CONF-700216-	(73rd National Western Mining Conference and Exhibition, Denver, Colo., Feb. 13-19, 1970)	
	25-10328	Denver; Colorado Mining Association (1970). 143p. $5.00
CONF-700318-	(10th International Technical-Scientific Meeting on Space, Rome, Italy, Mar. 9-11, 1970)	
	25-10420	Roma; XVII Rassegna Internazionale Elettronica Nucleare e Teleradiocinematografica (1970). 528p
CONF-700335-	(Conference on the International and Interstate Regulation of Water Pollution, New York, N.Y., Mar. 12, 1970)	
1	25-10090	Dep. NTIS, 10p.
CONF-700541-	(11th Annual Meeting of the Institute of Nuclear Materials Management, Gatlinburg, Tenn., May 25-27, 1970)	
2	25-8448	See BNWL-SA-3336
CONF-700545-	(3rd International Symposium on Pure Materials in Science and Technology, Dresden, East Germany, May 4-8, 1970)	
1	25-10349	Dep. NTIS, 47p.
CONF-700623-	(International Conference on Bubble Chamber Technology, Argonne, Ill., June 10-12, 1970)	
2	25-8549	See UR-875-324
CONF-700631-	(2nd Meeting of the Seas Symbolic Mathematical Computation Project, Darmstadt, Germany, June 1970)	
1	25-9456	See JUL-663-PP
CONF-700708-	(6th Interamerican Seminar on Cosmic Rays, La Paz, Bolivia, July 19-24, 1970)	
2	25-9253	See MPI-PAE/EXTRATERR-47
3	25-9635	See INP-722
CONF-700709-	(International Powder Metallurgy Conference, New York, N.Y., July 12-16, 1970)	
1	25-8944	See KFK-1236
CONF-700710-	(Conference on Special Topics in Quantum Field Theory, St. Louis, Mo., July 27-31, 1970)	
1	25-9838	See NYO-3829-60
CONF-700805-	(4th International Heat Transfer Conference, Versailles, France, Aug. 29-Sept. 5, 1970)	
4	25-8406	See CEA-CONF-1649
CONF-700806-	(15th International Conference on High Energy Physics, Kiev, U.S.S.R., Aug. 26-Sept. 4, 1970)	
29	25-9870	See JINR-P2-5289
53	25-9659	See UCRL-19789
54	25-9626	See COO-1545-87
CONF-700809-	(7th International Congress on Electron Microscopy, Grenoble, France, Aug. 30-Sept. 5, 1970)	
3	25-9542	See CEA-CONF-1681
4	25-9541	See CEA-CONF-1680
CONF-700810-	(Symposium on Environmental Aspects of Nuclear Power Stations, New York, N.Y., Aug. 10-14, 1970)	
52	25-8667	See BNWL-SA-3233
CONF-700820-	(13th International Congress of Hematology, Munich, Germany, Aug. 24-28, 1970)	
	25-8615	Munich; J. F. Lehmanns Verlag (1970). 176p
CONF-700823-	(1st International Symposium on Genetics of Industrial Microorganisms, Prague,	

XUM

Report No.	Abstract No.	Availability
		Czechoslovakia, Aug. 23-28, 1970)
1	25-8636	See SU-326-P-7-X-22
CONF-700827-		(18th Annual Specialty Conference, Minneapolis, Minn., Aug. 19-21, 1970)
1	25-8345	See BNWL-SA-3494
CONF-700828-		(4th International Heat Transfer Conference, Paris, France, Aug. 31-Sept. 5, 1970)
1	25-8405	See BNL-13957
CONF-700904-		(Conference on Power Reactor Systems and Components, Williamsburg, Va., Sept. 1-3, 1970)
1	25-10166	See GA-10265
CONF-700926-		(3rd International Symposium on Fresh Water from the Sea, Dubrovnik, Yugoslavia, Sept. 13-17, 1970)
2	25-10360	See ORNL-tr-2412
3	25-10359	See ORNL-tr-2411
4	25-10361	See ORNL-tr-2413
CONF-700929-		(Proton Linear Accelerator Conference, Batavia, Ill., Sept. 28-Oct. 2, 1970)
3	25-9917	See UCRL-20125
CONF-700930-		(Seminar on Radiation Protection Problems Relating to Transuranium Elements, Karlsruhe, Germany, Sept. 21-25, 1970)
1	25-8590	See CEA-CONF-1658
CONF-700931-		(3rd International Symposium on Inhaled Particles, London, England, Sept. 21-23, 1970)
1	25-8591	See CEA-CONF-1677
3	25-8623	See BNWL-SA-3419
CONF-700934-		(2nd International Conference on the Science of Materials, Tremezzo, Italy, Sept. 13-25, 1970)
1	25-8828	See BNWL-SA-3426
CONF-700936-		(Symposium on Cardiac Hypertrophy, Bratislava, Czechoslovakia, Sept. 13-16, 1970)
1	25-10336	See ACRH-1000-214
CONF-701007-		(Meeting on Concretes Used in Nuclear Reactors, Berlin, Germany, Oct. 5-9, 1970)
2	25-10325	See ORNL-TM-3246
CONF-701015-		(Symposium on Future Extraction and Selection in Pattern Recognition, Argonne, Ill., Oct. 5-7, 1970)
1	25-8548	See UCRL-20126
CONF-701016-		(Symposium on Fundamental Aspects of Electrochemical Machining, Atlantic City, N.J., Oct. 4-9, 1970)
1	25-10404	See UCRL-19618
2	25-10403	See UCRL-19615
CONF-701018-		(23rd Gaseous Electronics Conference, Hartford, Conn., Oct. 21-23, 1970)
1	25-9189	See BNWL-SA-3482
CONF-701019-		(CREST Meeting on Reactivity Effects in Large Power Reactors, Ispra, Italy, Oct. 28-30, 1970)
2	25-10303	See CEA-CONF-1684
CONF-701020-		(Monte Carlo Seminar Workshop, Oak Ridge, Tenn., Oct. 5-7, 1970)
1	25-9536	See CEA-CONF-1669
CONF-701021-		(Thermal Power Generation Conference, Pullman, Wash., Oct. 13, 1970)
1	25-10132	See BNWL-SA-3564
CONF-701022-		(Regional Meeting of the AIChE, Richland, Wash., Oct. 23, 1970)
1	25-10233	See BNWL-SA-3605
CONF-701023-		(Symposium on The Use of Nuclear Techniques in The Measurement and Control of Environmental Pollution, Salzburg, Austria, Oct. 26-30, 1970)
2	25-8363	See AECL-3731
CONF-701024-		(UMR-Mervin J. Kelly Communications Conference, St. Louis, Mo., Oct. 5-7, 1970)
1	25-10407	See UCRL-72390
CONF-701026-		(Conference of the Physics of Opto-Electronic Materials, General Motors Research Symposium, Warren, Mich., Oct. 5-6, 1970)
1	25-10406	See UCRL-20358
CONF-701103-		(63rd National Meeting of the American Institute of Chemical Engineers, Chicago, Ill., Nov. 29--Dec. 3, 1970)
6	25-8236	See ARH-SA-72
CONF-701106-		(5th Annual Midyear Topical Symposium on Health Physics Aspects of Nuclear Facility Siting, Idaho Falls, Idaho, Nov. 3-6, 1970)
2	25-8668	See BNWL-SA-3424
CONF-701108-		(Meeting of the Division of Particles and Fields of the American Physical Society, Austin, Tex., Nov. 5-6, 1970)
1	25-9650	See COO-1195-202
3	25-9706	See SLAC-PUB-843
CONF-701109-		(IEEE Nuclear Science Symposium, New York, N.Y., Nov. 4-6, 1970)
1	25-8532	See UCRL-72481
4	25-8466	See BNWL-SA-3624
5	25-8465	See BNWL-SA-1514
CONF-701110-		(ASME Winter Annual Meeting, New York, N.Y., Nov. 30-Dec. 3, 1970)
2	25-10207	See BNWL-SA-3286
CONF-701111-		(Electron and Atomic Physics Division Meeting, Seattle, Wash., Nov. 23-25, 1970)
1	25-9191	See BNWL-SA-3631
3	25-9190	See BNWL-SA-3498
CONF-701113-		(4th Conference on Numerical Simulation of Plasmas, Washington, D.C., Nov. 2-3, 1970)
1	25-9457	See UCRL-72604
2	25-9459	See UCRL-72635
3	25-9458	See UCRL-72613
CONF-701114-		(Meeting on Division of Plasma Physics, Washington, D.C., Nov. 4-7, 1970)
1	25-9506	See ORNL-TM-3207
CONF-710101-		(International Conference on Systems, Networks, and Computers, Oaxtepec, Mexico, Jan. 19-21, 1971)
1	25-10408	See UCRL-72648
COO-		
690-41	25-8604	Dep. NTIS, 168p.
881-291	25-9666	Phys. Lett.; 33B: 505-8(7 Dec 1970)
1149-180	25-8260	Dep. NTIS, 31p.
1195-202	25-9650	Dep. NTIS, 11p.
1199-19	25-8365	Dep. NTIS, 40p.
1265-94	25-9966	Dep. NTIS, 184p.
1339-43	25-8592	Dep. NTIS, 21p.
1428-239	25-9763	Dep. NTIS, 8p.
1545-87	25-9626	Dep. NTIS, 16p.
1686-11	25-8812	Int. J. Radiat. Biol.; 18: 159-72(1970)
1726-70	25-9503	Dep. NTIS, 24p.
1733-11	25-8593	Dep. NTIS, 142p.
1764-86	25-9685	Dep. NTIS, 55p.
1764-90	25-9884	Dep. NTIS, 51p.
1764-98	25-9885	Dep. NTIS, 11p.
1764-100	25-9686	Dep. NTIS, 15p.
1764-111	25-9651	Dep. NTIS, 9p.
1764-112	25-9652	Dep. NTIS, 23p.
1764-113	25-9653	Dep. NTIS, 50p.
1764-114	25-9654	Dep. NTIS, 9p.
1764-115	25-9634	Dep. NTIS, 10p.
1789-1	25-9408	Dep. NTIS, 12p.
2069-6	25-8834	Dep. NTIS, 62p.
2068-1	25-8669	Dep. NTIS, 99p.
CSIRO-Trans-		(Australian)
10258	25-9095	Dep. NTIS (U. S. Sales Only)
10289	25-9096	Dep. NTIS (U. S. Sales Only)
CTC-		
42	25-9942	Dep. CFSTI, 88p.
CTO-		(Non-AEC)
733	25-9409	Dep. NTIS (U. S. Sales Only)
736	25-9410	Dep. NTIS (U. S. Sales Only)
CU-		(Misc.)
755-7	25-8317	Dep. NTIS, 268p.
2493-11	25-8346	Dep. NTIS, 282p.
DESY-		(German)
69/29	25-9915	For translation see SLAC-Trans-124
70/55	25-9785	Dep. NTIS (U. S. Sales Only), 24p.
70/57	25-9886	Dep. NTIS (U. S. Sales Only), 21p.
70/58	25-9764	Dep. NTIS (U. S. Sales Only), 7p.
70/60	25-8543	Dep. NTIS (U. S. Sales Only), 13p.
DOCKET-1153-		(Hallam Nuclear Power Facility) (AEC)
17	25-10134	Dep. NTIS, 3p.
DOCKET-1155-		(LaCrosse Boiling Water Reactor) (AEC)
86	25-10110	Dep. NTIS, 37p.

XUM

Report No.	Abstract No.	Availability
87	25-10135	Dep. NTIS, 20p.
88	25-10111	Dep. NTIS, 27p.
DOCKET-50010-	(Dresden Nuclear Power Station; See also DOCKET-50237 and DOCKET-50249) (Non-AEC)	
75	25-10136	Dep. NTIS, 1p.
DOCKET-50016-	(Enrico Fermi Atomic Power Plant) (Non-AEC)	
88	25-10112	Dep. NTIS, 15p.
DOCKET-50029-	(Yankee Atomic Electric Co.) (Non-AEC)	
141	25-10113	Dep. NTIS, 16p.
DOCKET-50146-	(Saxton Nuclear Experimental Corporation) (Non-AEC)	
67	25-10137	Dep. NTIS, 2p.
DOCKET-50155-	(Big Rock Point Reactor) (Misc.)	
56	25-10138	Dep. NTIS, 10p.
57	25-10139	Dep. NTIS, 32p.
DOCKET-50171-	(Peach Bottom Atomic Power Station; See also DOCKET-50277 and DOCKET-50278) (Non-AEC)	
75	25-10114	Dep. NTIS, 11p.
76	25-10115	Dep. NTIS, 9p.
DOCKET-50201-	(West Valley Reprocessing Plant--Formerly Spent Fuel Processing Plant) (Misc.)	
56	25-8366	Dep. NTIS, 3p.
DOCKET-50206-	(San Onofre Nuclear Generating Station) (Misc.)	
100	25-10116	Dep. NTIS, 7p.
102	25-10117	Dep. NTIS, 5p.
DOCKET-50213-	(Connecticut Yankee Atomic Power Plant) (Misc.)	
88	25-10140	Dep. NTIS, 15p.
90	25-10141	Dep. NTIS, 4p.
91	25-10142	Dep. NTIS, 337p.
DOCKET-50219-	(Oyster Creek Nuclear Power Plant) (Non-AEC)	
117	25-10118	Dep. NTIS, 2p.
118	25-10143	Dep. NTIS, 144p.
119	25-10144	Dep. NTIS, 2p.
DOCKET-50231-	(Southwest Experimental Fast Oxide Reactor) (Non-AEC)	
61	25-10239	Dep. NTIS, 4p.
62	25-10234	Dep. NTIS, 3p.
63	25-10240	Dep. NTIS, 17p.
64	25-10235	Dep. NTIS, 28p.
DOCKET-50237-	(Dresden Nuclear Power Station, See also DOCKET-50249) (Non-AEC)	
123	25-10145	Dep. NTIS, 2p.
124	25-10119	Dep. NTIS, 2p.
125	25-10120	Dep. NTIS, 2p.
DOCKET-50245-	(Millstone Point Nuclear Power Station) (Non-AEC)	
49	25-10121	Dep. NTIS, 2p.
50	25-10122	Dep. NTIS, 1p.
DOCKET-50249-	(Dresden Nuclear Power Station; See also DOCKET-50237) (Non-AEC)	
52	25-10146	Dep. NTIS, 184p.
DOCKET-50250-	(Turkey Point, See also DOCKET-50251) (Non-AEC)	
37	25-10147	Dep. NTIS, 107p.
DOCKET-50261-	(H. B. Robinson) (Non-AEC)	
49	25-10123	Dep. NTIS, 19p.
DOCKET-50266-	(Point Beach Nuclear Plant) (Non-AEC)	
37	25-10124	Dep. NTIS, 2p.
DOCKET-50269-	(Oconee Nuclear Station, See also DOCKET-50270, and DOCKET-50287) (Non-AEC)	
30	25-10148	Dep. NTIS, 14p.
31	25-10149	Dep. NTIS, 109p.
32	25-10150	Dep. NTIS, 114p.
DOCKET-50270-	(Oconee Nuclear Station, See also DOCKET-50269, and DOCKET-50287) (Non-AEC)	
30	25-10149	See DOCKET-50269-31
DOCKET-50285-	(Fort Calhoun Station) (Non-AEC)	
39	25-10151	Dep. NTIS, 107p.
DOCKET-50287-	(Oconee Nuclear Station; see also DOCKET-50269 and DOCKET-50270) (Non-AEC)	
27	25-10149	See DOCKET-50269-31
DOCKET-50289-	(Three Mile Island Nuclear Station) (Non-AEC)	
30	25-10152	Dep. NTIS, 1p.
31	25-10153	Dep. NTIS, 28p.
DOCKET-50317-	(Calvert Cliffs Nuclear Power Plant, See also DOCKET-50318) (Non-AEC)	
21	25-10154	Dep. NTIS, 369p.
22	25-10155	Dep. NTIS, 506p.
23	25-10156	Dep. NTIS, 502p.
DOCKET-50318-	(Calvert Cliffs Nuclear Power Plant, See also DOCKET-50317) (Non-AEC)	
21	25-10154	See DOCKET-50317-21
22	25-10155	See DOCKET-50317-22
23	25-10156	See DOCKET-50317-23
DOCKET-50320-	(Oyster Creek Nuclear Power Plant, See also DOCKET-50219) (Non-AEC)	
20	25-10157	Dep. NTIS, 195p.
DOCKET-50382-	(Louisiana Power and Light Plant) (Non-AEC) (See also DOCKET-50383)	
1	25-10158	Dep. NTIS, 38p.
DOCKET-50383-	(Louisiana Power and Light Plant) (Non-AEC) (See also DOCKET-50382)	
1	25-10158	See DOCKET-50382-1
DP-		
1229	25-8709	Dep. CFSTI, 21p.
DP-Report-	(British)	
437	25-8924	Dep. NTIS, 20p.
500	25-10195	Dep. NTIS, 39p.
DPC-		
851-16	25-10110	See DOCKET-1155-86
851-17	25-10111	See DOCKET-1155-88
EANDC(E)-	(European-American Nuclear Data Committee)	
126-AL	25-10021	See CEA-N-1273
ECRC/N-	(British)	
288	25-9411	Dep. NTIS (U. S. Sales Only), 13p.
EUR-	(European Atomic Energy Community)	
3708	25-10186	See KFK-1179
3969	25-10258	See EURFNR-848
4501	25-8925	Dep. NTIS (U. S. Sales Only). EUR FF 4.45, 22p.
4509	25-8624	Dep. NTIS (U. S. Sales Only). EUR DM 6,20, 66p.
4526	25-8632	Dep. NTIS (U. S. Sales Only). EUR Lit. 500,-, 20p.
4537	25-8391	Dep. NTIS (U. S. Sales Only). EUR FF 6,65, 44p.
4539	25-10304	Dep. NTIS (U. S. Sales Only). EUR Fr.F 13.80, 82p.
EURFNR-	(European Atomic Energy Community)	
764	25-10257	Dep. NTIS
774	25-10323	Dep. NTIS
775	25-10324	Dep. NTIS
848	25-10258	Dep. NTIS (U. S. Sales Only), 70p.
FEI-	(Russian)	
190	25-10024	Dep. NTIS (U. S. Sales Only), 15p.
FOA-	(Swedish)	
4-4438	25-9504	Dep. NTIS (U. S. Sales Only), 100p.
GA-	(Misc.)	
9945	25-8362	See AD-707427
9994	25-8352	Dep. NTIS, 131p.
10223	25-9943	Dep. CFSTI, 18p.
10265	25-10166	Dep. NTIS, 42p.
GAT-		
627	25-8692	Dep. NTIS, 48p.
GEAP-	(Misc.)	
5550	25-10259	Dep. NTIS, 46p.
5552	25-10260	Dep. NTIS, 166p.
5614	25-10261	Dep. NTIS, 128p.
5641	25-10262	Dep. NTIS, 97p.
5650	25-10263	Dep. NTIS, 130p.
5684	25-10264	Dep. NTIS, 146p.
5715	25-10265	Dep. NTIS, 14p.
5721	25-10266	Dep. NTIS, 122p.
10205	25-8866	Dep. NTIS, 72p.
10217	25-8951	Dep. NTIS, 52p.
12133	25-8926	Dep. NTIS, 12p.
13562	25-10208	Dep. NTIS, 92p.
13608	25-10241	Dep. NTIS, 236p.
HASL-		
237	25-8367	Dep. CFSTI, 117p.
237(App.)	25-8670	Dep. CFSTI, 400p.
HEPL-	(Misc.)	
635	25-9965	See AD-710384
HIT-		
439	25-9537	See N-70-34007
HMI-B-	(German)	

XUM

Report No.	Abstract No.	Availability
86	25-8354	Dep. NTIS (U. S. Sales Only), 42p.
87	25-8660	Dep. NTIS (U. S. Sales Only), 61p.
96	25-8572	Dep. NTIS (U. S. Sales Only), 82p.
IAE-	(Russian)	
1693	25-10268	For translation see LA-4399-TR
1955	25-10305	Dep. NTIS (U. S. Sales Only), 23p.
2015	25-9412	For translation see LA-tr-70-25
ICRU-	(Non-AEC)	
16	25-8671	ICRU Publications, Washington, D. C
17	25-8672	ICRU Publications, Washington, D. C. $2.50
IFVE-SKU-	(Russian)	
69-95	25-9906	Dep. NTIS (U. S. Sales Only), 23p.
IN-		
1363	25-8321	Dep. NTIS, 39p.
1428	25-8322	Dep. NTIS, 38p.
1439	25-8323	Dep. NTIS, 26p.
1442	25-10267	Dep. NTIS, 14p.
1444	25-10242	Dep. NTIS, 21p.
1445	25-8450	Dep. NTIS, 14p.
INDC(NDS)-	(International Atomic Energy Agency)	
19/N	25-10025	Dep. CFSTI (U. S. Sales Only), 63p.
INP-	(Polish)	
722	25-9635	Dep. NTIS (U. S. Sales Only), 50p.
IPST-Cat.-	(Russian)	
1995	25-9286	See TT-67-51394/1
ITEF-	(Russian)	
759	25-9803	Dep. NTIS (U. S. Sales Only), 32p.
767	25-9655	Dep. NTIS (U. S. Sales Only), 28p.
775	25-9656	Dep. NTIS (U. S. Sales Only), 16p.
ITF-	(Russian)	
70-38	25-10058	Dep. NTIS (U. S. Sales Only), 17p.
70-42	25-9973	Dep. NTIS (U. S. Sales Only), 25p.
70-43	25-9887	Dep. NTIS (U. S. Sales Only), 51p.
70-52	25-9733	Dep. NTIS (U. S. Sales Only), 20p.
70-53	25-9734	Dep. NTIS (U. S. Sales Only), 16p.
70-57	25-9837	Dep. NTIS (U. S. Sales Only), 17p.
70-58-P	25-9687	Dep. NTIS (U. S. Sales Only), 20p.
70-73	25-9701	Dep. NTIS (U. S. Sales Only), 6p.
70-78	25-9888	Dep. NTIS (U. S. Sales Only), 8p.
JAERI-	(Japanese)	
4052	25-8661	Dep. NTIS (U. S. Sales Only), 203p.
5025	25-8693	Dep. NTIS (U. S. Sales Only), 111p.
JAERI-Memo-	(Japanese)	
4098	25-8673	Dep. NTIS (U. S. Sales Only), 81p.
4147	25-8276	Dep. NTIS (U. S. Sales Only), 118p.
JHU-	(Misc.)	
7009(Rev.)	25-9636	See TID-25610
7013(Rev.)	25-9658	See TID-25611
7016(Rev.)	25-9629	See UCLA-1054
7018(Rev.)	25-9628	See UCLA-1052
JINR-	(Russian)	
E2-5333	25-9702	Dep. NTIS (U. S. Sales Only), 15p.
E2-5341	25-9749	Dep. NTIS (U. S. Sales Only), 36p.
E3-5371	25-10026	Dep. NTIS (U. S. Sales Only), 11p.
E4-5350	25-9997	Dep. NTIS (U. S. Sales Only), 28p.
E6-5379	25-10027	Dep. NTIS (U. S. Sales Only), 11p.
P1-5361	25-8544	Dep. NTIS (U. S. Sales Only), 24p.
P2-5042	25-9703	Dep. NTIS (U. S. Sales Only), 11p.
P2-5231	25-9804	Dep. NTIS (U. S. Sales Only), 9p.
P2-5286	25-9974	Dep. NTIS (U. S. Sales Only), 14p.
P2-5289	25-9870	Dep. CFSTI (U. S. Sales Only), 31p.
P2-5314	25-9599	Dep. NTIS (U. S. Sales Only), 5p.
P2-5335	25-9967	Dep. NTIS (U. S. Sales Only), 9p.
P2-5336	25-9688	Dep. NTIS (U. S. Sales Only), 14p.
P4-5040	25-9600	Dep. NTIS (U. S. Sales Only), 42p.
P4-5228	25-10028	Dep. NTIS (U. S. Sales Only), 14p.
P4-5366	25-9889	Dep. NTIS (U. S. Sales Only), 16p.
P6-5200	25-10029	Dep. CFSTI (U. S. Sales Only), 16p.
P7-4797	25-10030	For translation see KFK-tr-329
P9-4850	25-9908	For translation see KFK-tr-337
P13-5377	25-8545	Dep. NTIS (U. S. Sales Only), 12p.
P15-5143	25-9970	Dep. CFSTI (U. S. Sales Only), 17p.
P15-5148	25-9976	Dep. CFSTI (U. S. Sales Only), 8p.
JPRS-	(Non-AEC)	
51660	25-8755	NTIS
51939	25-10295	NTIS
52023	25-9284	NTIS
JUL-	(German)	
654-RG	25-10209	Dep. NTIS (U. S. Sales Only), 144p.
663-PP	25-9456	Dep. NTIS (U. S. Sales Only), 35p.
JUL-CONF-	(German)	
4	25-8469	
KFK-	(German)	
898	25-9505	Dep. NTIS (U. S. Sales Only), 20p.

Report No.	Abstract No.	Availability
1049	25-8913	For translation see ORNL-tr-2365
1125	25-10323	For translation see EURFNR-774
1140	25-10324	For translation see EURFNR-775
1143	25-10257	For translation see EURFNR-764
1179	25-10186	Dep. NTIS (U. S. Sales Only), 63p.
1210	25-8237	Dep. NTIS (U. S. Sales Only), 45p.
1233	25-8481	Dep. NTIS (U. S. Sales Only), 103p.
1235	25-8943	Dep. NTIS (U. S. Sales Only), 74p.
1236	25-8944	Dep. NTIS (U. S. Sales Only), 15p.
1241	25-8573	Dep. NTIS (U. S. Sales Only), 32p.
1252	25-8846	Dep. NTIS (U. S. Sales Only), 83p.
1266	25-10258	See EURFNR-848
KFK-tr-	(German)	
329	25-10030	Dep. CFSTI (U. S. Sales Only)
335	25-9907	Dep. CFSTI (U. S. Sales Only)
337	25-9908	Dep. CFSTI (U. S. Sales Only)
KHFTI-	(Russian)	
69-25	25-9907	For translation see KFK-tr-335
LA-		
4399-TR	25-10268	Dep. NTIS
4454(Vol.2)	25-9097	Dep. NTIS, 124p.
4511	25-8961	Dep. NTIS, 44p.
4537	25-8200	Dep. NTIS, 19p.
4539	25-9601	Dep. NTIS, 21p.
4554	25-9602	Dep. NTIS, 16p.
4555	25-10350	Dep. NTIS, 9p.
4556	25-10351	Dep. NTIS, 37p.
LA-tr-		
70-24	25-9161	Dep. NTIS
70-25	25-9412	Dep. NTIS
70-26	25-10352	Dep. NTIS
LF-tr-		
41	25-8594	Dep. NTIS
LFEN-	(Portuguese)	
109-B	25-10174	Dep. NTIS (U. S. Sales Only), 171p.
LFEN-NI.-	(Portuguese)	
36-a	25-8201	Dep. NTIS (U. S. Sales Only), 20p.
LIB/Trans-	(Australian)	
296	25-8788	Dep. NTIS (U. S. Sales Only)
LNF-	(Italian)	
70/17	25-9909	Dep. CFSTI (U. S. Sales Only), 13p.
70/22	25-9689	Dep. CFSTI (U. S. Sales Only), 10p.
LRP-	(Swiss)	
42/70	25-9487	Dep. NTIS (U. S. Sales Only), 14p.
45/70	25-9488	Dep. NTIS (U. S. Sales Only), 15p.
LUNP-	(Swedish)	
7007	25-9620	Dep. NTIS (U. S. Sales Only), 31p.
7009	25-9977	Dep. NTIS (U. S. Sales Only), 34p.
LUSY-	(Swedish)	
7007	25-9910	Dep. NTIS (U. S. Sales Only), 75p.
LYCEM-	(French)	
6847	25-8546	Dep. NTIS (U. S. Sales Only), 23p.
6933	25-8581	Dep. NTIS (U. S. Sales Only), 107p.
6949	25-9911	Dep. NTIS (U. S. Sales Only), 13p.
6953	25-9912	Dep. NTIS (U. S. Sales Only), 15p.
7039	25-10059	Dep. NTIS (U. S. Sales Only), 63p.
MF-	(Misc.)	
61	25-9269	See AD-706106
MIAPH-TP-	(Non-AEC)	
69-23	25-10365	See ORO-3895-9
MLM-		
1439(Rev.)	25-8423	Dep. NTIS, 127p.
1744	25-8239	Dep. NTIS, 47p.
1768	25-8424	Dep. NTIS, 35p.
1772	25-8217	Dep. NTIS, 12p.
1773	25-8531	Dep. NTIS, 19p.
MPI-PAE/ EXTRATERR-	(European Organization for Nuclear Research)	
47	25-9253	Dep. NTIS (U. S. Sales Only), 24p.
48	25-9048	Dep. NTIS (U. S. Sales Only), 24p.
49/70	25-9285	Dep. NTIS (U. S. Sales Only), 19p.
MTI-	(Misc.)	
70-TR-61	25-8394	See NYU-3930-7
N-	(Misc.)	
70-34007	25-9537	NTIS, 26p.
NASA-CR-	(Misc.)	
109876	25-9537	See N-70-34007
NLCO-		

Report No.	Abstract No.	Availability
1060	25-8867	Dep. NTIS, 9p.
NP-	(AEC File No. for Non-AEC Reports)	
18104	25-9948	Moscow; Atomizdat (1967). 540p
18236	25-8813	CFSTI, 80p.
18372	25-9410	For translation see CTO-736
18429	25-8625	Dep. CFSTI (U. S. Sales Only), 27p.
18439	25-9998	Dep. CFSTI (U. S. Sales Only), 87p.
18483	25-8633	Dep. NTIS (U. S. Sales Only), 99p.
18486	25-9968	Dep. NTIS (U. S. Sales Only), 70p.
18498	25-10269	Dep. NTIS (U. S. Sales Only), 55p.
18512	25-9869	Copenhagen; Nordisk Institut for Teoretisk Atomfysik (1970). 153p
18529	25-8675	Dep. NTIS (U. S. Sales Only), 41p.
18535	25-10243	Dep. NTIS (U. S. Sales Only), 68p.
18538	25-10060	Dep. NTIS (U. S. Sales Only), 107p.
18540	25-9704	Dep. NTIS (U. S. Sales Only), 16p.
18547	25-10306	Dep. NTIS (U. S. Sales Only), 117p.
18554	25-9512	Dep. NTIS (U. S. Sales Only), 117p.
18558	25-9627	Dep. NTIS (U. S. Sales Only), 11p.
18560	25-8710	Dep. NTIS (U. S. Sales Only), 262p.
18563	25-8425	Dep. NTIS (U. S. Sales Only), 55p.
18573	25-10125	Dep. NTIS (U. S. Sales Only), 165p.
18578	25-9765	Dep. NTIS (U. S. Sales Only), 32p.
18581	25-9621	Dep. NTIS (U. S. Sales Only), 54p.
18592	25-8218	Dep. NTIS (U. S. Sales Only), 153p.
18594	25-9913	Dep. NTIS (U. S. Sales Only), 10p.
18595	25-10091	Dep. NTIS (U. S. Sales Only), 33p.
18600	25-10092	Dep. NTIS (U. S. Sales Only), 117p.
NP-tr-	(AEC File No. for Non-AEC Translations)	
1926	25-9914	Dep. CFSTI (U. S. Sales Only)
1928	25-10095	Kernenergie; 13: 279-83(1970)
NRL-AR-	(New Zealand)	
20	25-8675	See NP-18529
NSJ-tr-	(Japanese)	
155	25-8426	Dep. NTIS (U. S. Sales Only)
156	25-8749	Dep. NTIS (U. S. Sales Only)
157	25-10296	Dep. NTIS (U. S. Sales Only)
158	25-8794	Dep. NTIS (U. S. Sales Only)
159	25-8868	Dep. NTIS (U. S. Sales Only)
160	25-8277	Dep. NTIS (U. S. Sales Only)
NTS-		
220	25-8355	See USGS-474-88
NVO-		
410-6	25-8393	Dep. NTIS, 8p.
NYO-		
1932(2)-186	25-9735	Dep. NTIS, 16p.
2150-64	25-9363	Dep. NTIS, 36p.
2171-329	25-9826	Dep. NTIS, 6p.
2171-330	25-10061	Dep. NTIS, 8p.
2171-331	25-9690	Dep. NTIS, 22p.
2740-7	25-8676	Dep. CFSTI, 263p.
3270-44	25-10116	See DOCKET-50206-100
3270-45	25-10117	See DOCKET-50206-102
3829-60	25-9838	Dep. NTIS, 19p.
3829-64	25-9839	Dep. NTIS, 22p.
3930-7	25-8394	Dep. NTIS, 32p.
3937-2	25-8711	Dep. NTIS, 20p.
4034-2	25-8789	Dep. NTIS, 28p.
ORNL-		
4434	25-10210	Dep. NTIS, 52p.
4503(Vol.2)	25-8927	Dep. NTIS, 13p.
4552	25-9999	Dep. NTIS, 52p.
4600	25-8829	Dep. NTIS, 296p.
4605	25-10353	Dep. NTIS, 20p.
4612	25-8760	Dep. NTIS, 71p.
4614	25-9168	Dep. NTIS, 267p.
4616	25-10211	Dep. NTIS, 41p.
4627	25-10031	Dep. NTIS, 283p.
4632	25-10354	Dep. NTIS, 128p.
4639	25-8427	Dep. NTIS, 28p.
4642	25-10355	Dep. NTIS, 207p.
ORNL-HUD-		
14	25-10094	Dep. NTIS, 195p.
17	25-8444	Dep. NTIS, 263p.
ORNL-IIC-		
30(Pt.3)	25-8428	Dep. NTIS, 49p.
ORNL-NSIC-		
81	25-10159	Dep. NTIS, 165p.
ORNL-TM-		
2091(Suppl. 1)	25-8712	Dep. NTIS, 25p.
2971	25-8451	Dep. NTIS, 28p.
3077	25-8395	Dep. NTIS, 62p.
3136	25-10307	Dep. NTIS, 91p.
3156	25-9944	Dep. NTIS, 26p.
3169	25-8897	Dep. NTIS, 23p.
3175	25-10356	Dep. NTIS, 28p.

Report No.	Abstract No.	Availability
3187	25-8452	Dep. NTIS, 171p.
3188	25-8839	Dep. NTIS, 34p.
3207	25-9506	Dep. NTIS, 21p.
3209	25-8453	Dep. NTIS, 11p.
3212	25-10244	Dep. NTIS, 142p.
3229	25-10196	Dep. NTIS, 36p.
3233(Rev.)	25-9507	Dep. NTIS, 6p.
3244	25-8871	Dep. NTIS, 70p.
3246	25-10325	Dep. NTIS, 25p.
3251	25-9538	Dep. NTIS, 17p.
3256	25-10270	Dep. NTIS, 52p.
ORNL-tr-		
2314	25-10357	Dep. NTIS
2345	25-10032	Dep. NTIS
2365	25-8913	Dep. NTIS
2392	25-10358	Dep. NTIS
2400	25-8429	Dep. NTIS
2402	25-10160	Dep. NTIS
2403	25-8678	Dep. NTIS
2406	25-8324	Dep. NTIS
2411	25-10359	Dep. NTIS
2412	25-10360	Dep. NTIS
2413	25-10361	Dep. NTIS
2418	25-10362	Dep. NTIS
ORO-		
1637-21	25-10363	Dep. NTIS, 15p.
2591-51	25-9192	Dep. NTIS, 29p.
2591-52	25-9193	Dep. NTIS, 19p.
2832-85	25-8605	Dep. NTIS, 111p.
3106-27	25-8299	Radiat. Res.; 44: 296-304(Nov 1970)
3106-28	25-8303	Radiat. Res.; 44: 305-12(Nov 1970)
3398-26	25-9978	Dep. CFSTI, 162p.
3628-11	25-10364	Dep. NTIS, 11p.
3630-10	25-8606	Dep. NTIS, 19p.
3822-5	25-10245	Dep. NTIS, 201p.
3882-3	25-8607	Dep. CFSTI, 12p.
3895-9	25-10365	Dep. NTIS, 15p.
3895-15	25-9398	Dep. NTIS, 56p.
3898-2	25-8310	Dep. NTIS, 60p.
3948-2	25-9657	Dep. NTIS, 25p.
4024-1	25-8634	Dep. CFSTI, 5p.
PATENTS	(British)	
1,208,480	25-8664	
1,208,673	25-8403	
1,209,932	25-8402	
1,209,953	25-10188	
1,210,127	25-10219	
1,210,212	25-10330	
1,210,787	25-10198	
1,210,938	25-8309	
1,211,011	25-10201	
1,211,526	25-10170	
1,211,528	25-8458	
1,211,561	25-10191	
1,211,816	25-8344	
1,211,886	25-10334	
1,211,954	25-10225	
1,212,299	25-10231	
1,212,458	25-10230	
1,212,480	25-10247	
1,212,696	25-10168	
1,213,397	25-10218	
1,213,425	25-10220	
1,213,426	25-8916	
1,213,873	25-8282	
1,213,961	25-8232	
1,214,314	25-10200	
1,214,372	25-8404	
1,214,439	25-10199	
PATENTS	(Canadian)	
850,004	25-10206	
854,399	25-10224	
855,320	25-9928	
PATENTS	(French)	
1,566,809	25-10333	
1,568,883	25-8919	
1,569,635	25-8918	
1,569,732	25-10204	
1,569,898	25-8456	
1,570,300	25-10250	
1,570,301	25-10249	
1,570,724	25-10329	
1,571,841	25-8484	
1,570,956	25-8215	
1,571,230	25-8921	
1,571,496	25-10332	
1,572,233	25-10292	
1,572,234	25-8292	
1,572,687	25-10202	
1,573,413	25-8856	
1,573,792	25-10169	
1,573,897	25-8660	
1,575,858	25-10280	
1,575,859	25-10276	
1,576,367	25-8498	
1,589,148	25-10335	
1,589,435	25-8577	

XUM

Report No.	Abstract No.	Availability
1,589,447	25-8401	
1,589,456	25-8400	
1,589,495	25-8534	
1,589,905	25-8493	
2,000,788	25-10331	
PATENTS	(U. S.)	
3,527,645	25-8821	
3,527,946	25-8565	
3,528,000	25-8358	
3,532,885	25-8359	
3,533,220	25-8343	
3,533,757	25-8338	
3,534,409	25-8436	
3,535,079	25-8339	
3,535,082	25-10294	
3,535,085	25-8433	
3,535,148	25-8278	
3,535,264	25-8922	
PH-	(Swedish)	
1	25-8483	Dep. NTIS (U. S. Sales Only), 10p.
2	25-10000	Dep. NTIS (U. S. Sales Only), 21p.
3	25-8219	Dep. NTIS (U. S. Sales Only), 10p.
PNE-G-		
68	25-8384	Dep. NTIS, 37p.
69	25-8385	Dep. NTIS, 76p.
POR-	(Misc.)	
4013	25-8962	Dep. NTIS, 241p.
PR-B-	(Canadian)	
86	25-8666	See AECL-3728
PR-P-	(Canadian)	
86	25-9970	See AECL-3668
PRDC-EF-		
84	25-10112	See DOCKET-50016-88
PRNC-		
140	25-8574	Dep. CFSTI, 157p.
PURC-		
4159-13	25-8547	Dep. NTIS, 21p.
RCN-	(Dutch)	
126	25-8202	Dep. NTIS (U. S. Sales Only), 11p.
127	25-8203	Dep. NTIS (U. S. Sales Only), 14p.
128	25-8204	Dep. NTIS (U. S. Sales Only), 10p.
RD/B/N-	(British)	
1755	25-8409	Dep. NTIS (U. S. Sales Only), 43p.
RFP-		
1575	25-8840	Dep. NTIS, 5p.
RISO-	(Danish)	
224	25-8261	Dep. NTIS (U. S. Sales Only), 42p.
RLO-		
1388-131	25-10062	Dep. NTIS, 13p.
1388-584	25-9834	Dep. NTIS, 11p.
1388-592	25-9691	Dep. NTIS, 32p.
1928-46	25-10063	Dep. NTIS, 132p.
2228-T-19-9	25-10366	Dep. NTIS, 20p.
2227-T-5-1	25-10367	Dep. NTIS, 14p.
2227-T-5-2	25-10368	Dep. NTIS, 11p.
2227-T-5-4	25-10369	Dep. NTIS, 12p.
RPI-	(Misc.)	
328-190	25-9945	Dep. CFSTI, 104p.
3821-5	25-8285	Dep. NTIS, 26p.
RT/FI-	(Italian)	
(70)7	25-10326	Dep. NTIS (U. S. Sales Only), 32p.
RT/PROT-	(Italian)	
(69)6	25-8687	G. Fis. Sanit. Prot. Radiaz.; 12: 200-13(Jul-Sep 1968)
(69)14	25-8695	G. Fis. Sanit. Prot. Radiaz.; 12: No. 2, 80-97(Apr-Jun 1968)
S-	(Misc.)	
349	25-8408	See CONF-660675-1
SC-CR-		
69-3266	25-10370	Dep. NTIS, 97p.
70-6092	25-10371	Dep. NTIS, 112p.
70-6152	25-10372	Dep. NTIS, 35p.
SC-DR-		
70-698	25-10373	Dep. NTIS, 52p.
SC-M-		
70-684	25-10374	Dep. NTIS, 102p.
SC-RR-		
70-544	25-10375	Dep. NTIS, 175p.
70-600	25-8441	Dep. NTIS, 72p.
70-721	25-9194	Dep. NTIS, 79p.
70-773	25-9195	Dep. NTIS, 22p.
70-775	25-10376	Dep. NTIS, 26p.
70-788	25-9162	Dep. NTIS, 22p.
SC-T-		
70-4048	25-10377	Dep. NTIS
70-4050	25-9431	Dep. NTIS
70-4051	25-9432	Dep. NTIS
70-4052	25-10378	Dep. NTIS
70-4053	25-9433	Dep. NTIS
71-3000	25-10379	Dep. NTIS
71-3001	25-9415	Dep. NTIS
SCL-DR-		
70-108	25-10380	Dep. NTIS, 186p.
70-130	25-10381	Dep. NTIS, 32p.
SLAC-		
123	25-9705	Dep. NTIS, 13p.
SLAC-PUB-		
843	25-9706	Dep. NTIS, 22p.
SLAC-Trans-		
124	25-9915	Dep. NTIS
SM-	(Misc.)	
125/60	25-8449	See CONF-691008-18
126/43	25-10089	See CONF-691020-3
SRARI-P-	(Russian)	
73	25-8958	Dep. NTIS (U. S. Sales Only), 28p.
85	25-8598	Dep. NTIS (U. S. Sales Only), 30p.
STAN-CS-		
70-158(App. 5)	25-10382	Dep. NTIS, 36p.
70-165(App. 2)	25-10383	Dep. NTIS, 34p.
STI/DOC-	(International Atomic Energy Agency)	
10/114	25-8814	IAEA $4.00
10/119	25-8635	IAEA $6.00
STI/PUB-	(International Atomic Energy Agency)	
251	25-8728	IAEA $5.00
252	25-8583	IAEA $3.00
SU-	(Misc.)	
326-P-28-X-2	25-8325	Dep. NTIS, 13p.
326-P-7-X-22	25-8636	Dep. NTIS, 23p.
SZS-	(German)	
6/70	25-8688	Dep. NTIS (U. S. Sales Only), 35p.
14/70 (pp 1-10)	25-8371	Dep. NTIS (U. S. Sales Only)
14/70 (pp 11-21)	25-8454	Dep. NTIS (U. S. Sales Only)
15/70	25-8584	Dep. NTIS (U. S. Sales Only), 21p.
TID-		
4100(Suppl. 61)	25-8396	DTIE Free
25165 (Suppl.2)	25-9946	DTIE Free
25468	25-8803	Dep. CFSTI, 75p.
25556	25-8804	Dep. NTIS, 43p.
25576	25-8455	Dep. GPO $0.35
25590	25-10212	Dep. NTIS, 56p.
25606	25-10317	New York; Van Nostrand Reinhold Company (1970). 635p. $24.50
25608	25-10126	Dep. NTIS, 19p.
25609	25-10384	Dep. NTIS, 16p.
25610	25-9636	Dep. NTIS, 45p.
25611	25-9658	Dep. NTIS, 27p.
25612	25-10385	Dep. NTIS, 4p.
25613	25-10386	Dep. NTIS, 5p.
25614	25-10387	Dep. NTIS, 14p.
25615	25-10388	Dep. NTIS, 5p.
25616	25-10389	Dep. NTIS, 5p.
25617	25-10390	Dep. NTIS, 11p.
25618	25-10391	Dep. NTIS, 144p.
25619	25-10392	Dep. NTIS, 26p.
25620	25-10393	Dep. NTIS, 67p.
25622	25-10394	Dep. NTIS, 50p.
25623	25-10395	Dep. NTIS, 65p.
25624	25-10396	Dep. NTIS, 28p.
25625	25-10397	Dep. NTIS, 21p.
25627	25-10398	Dep. NTIS, 32p.
25628	25-10127	Dep. NTIS, 17p.
25629	25-10128	Dep. NTIS, 15p.
25630	25-10291	Dep. NTIS, 239p.
TRG-Report-	(British)	
1990	25-9947	Dep. NTIS (U. S. Sales Only). UK 10s, 76p.

Report No.	Abstract No.	Availability
TT-	(Misc.)	
67-51394/1	25-9286	NTIS
UCB-		
34-P-82-10	25-8758	Dep. CFSTI, 25p.
34-P-186-X-1	25-10399	Dep. NTIS, 8p.
UCLA-		
12-788	25-10400	Dep. CFSTI, 28p.
12-798	25-8713	Dep. NTIS, 41p.
12-801	25-10401	Dep. NTIS, 36p.
12-802	25-10402	Dep. NTIS, 41p.
1052	25-9628	Dep. NTIS, 12p.
1054	25-9629	Dep. NTIS, 12p.
UCRL-		
19313	25-9916	Dep. NTIS, 57p.
19615	25-10403	Dep. NTIS, 28p.
19618	25-10404	Dep. NTIS, 17p.
19789	25-9659	Dep. NTIS, 16p.
20125	25-9917	Dep. NTIS, 12p.
20126	25-8548	Dep. NTIS, 26p.
20132	25-8193	Dep. NTIS, 9p.
20139	25-10405	Dep. NTIS, 147p.
20358	25-10406	Dep. NTIS, 30p.
50903	25-8262	Dep. NTIS, 57p.
50939	25-8382	Dep. NTIS, 46p.
50940	25-8386	Dep. NTIS, 7p.
71868	25-8387	Dep. NTIS, 47p.
72390	25-10407	Dep. NTIS, 5p.
72481	25-8532	Dep. NTIS, 8p.
72509	25-8397	Dep. NTIS, 6p.
72604	25-9457	Dep. NTIS, 20p.
72613	25-9458	Dep. NTIS, 16p.
72635	25-9459	Dep. NTIS, 34p.
72648	25-10408	Dep. NTIS, 5p.
72770	25-10409	Dep. NTIS, 12p.
UCRL-Trans-		
1414	25-10410	Dep. NTIS
1424	25-10411	Dep. NTIS
1427	25-10412	Dep. NTIS
1428	25-10413	Dep. NTIS
1429	25-10414	Dep. NTIS
1431	25-10415	Dep. NTIS
10488	25-8662	Dep. NTIS
10504	25-10416	Dep. NTIS
10505	25-8928	Dep. NTIS

Report No.	Abstract No.	Availability
UNC-	(Misc.)	
5266	25-8447	See BHO-65-1
UR-		
875-324	25-8549	Dep. NTIS, 41p.
USCEE-	(Non-AEC)	
344	25-10417	Dep. NTIS, 4p.
350	25-10418	Dep. NTIS, 18p.
377	25-10419	Dep. NTIS, 15p.
USGS-		
474-88	25-8355	Dep. NTIS, 67p.
474-92	25-8356	Dep. NTIS, 10p.
474-96	25-8357	Dep. NTIS, 8p.
WAPD-MRP-		
131	25-10129	Dep. NTIS, 26p.
WAPD-TM-	(Misc.)	
714	25-10167	Dep. NTIS, 13p.
WASH-		
1098	25-10095	GPO $2.00
WCAP-	(Misc.)	
3385-25	25-10213	Dep. NTIS, 26p.
7544	25-10229	Dep. NTIS, 226p.
7579	25-8872	Dep. NTIS, 31p.
WHAN-FR-		
21	25-10271	Dep. NTIS, 42p.
36	25-10272	Dep. NTIS, 20p.
WT-	(Misc.)	
4013	25-8962	See POR-4013
WW-TM-	(Non-AEC)	
70-3	25-9283	See AD-709888
Y-		
1744	25-8220	Dep. NTIS, 15p.
1750	25-8398	Dep. NTIS, 17p.
ZFK-RCH-	(German)	
1	25-8429	For translation see ORNL-tr-2400
ZJE-	(Czechslovakian)	
65	25-10096	Dep. NTIS (U. S. Sales Only), 34p.
89	25-8899	Dep. NTIS (U. S. Sales Only), 16p.
90	25-8900	Dep. NTIS (U. S. Sales Only), 30p.
91	25-8901	Dep. NTIS (U. S. Sales Only), 30p.

☆U. S. GOVERNMENT PRINTING OFFICE: 1971—436-211/19

XUM

UNITED STATES
ATOMIC ENERGY COMMISSION
P. O. BOX 62
OAK RIDGE, TENNESSEE 37830

GO\

OFFICIAL BUSINESS

POSTAGE AND FEES PAID
U. S. ATOMIC ENERGY COMMISSION

POSTAGE AND FEES PAID
U. S. GOVERNMENT PRINTING OFFICE

UNIVERSITY MICROFILMS 1
ATTN MRS. MARLENE HURST
MANAGER, PUBLISHER RELATIONS
ANN ARBOR MICHIGAN 48106

AEC SYMPOSIUM SERIES

Available from the National Technical Information Service, U. S. Department of Commerce, Springfield, Virginia 22151

1 **Progress in Medical Radioisotope Scanning** (TID-7673), Oak Ridge Institute of Nuclear Studies, 1963, $6.00
2 **Reactor Kinetics and Control** (TID-7662), The University of Arizona, 1964, $6.00
3 **Dynamic Clinical Studies with Radioisotopes** (TID-7678), Oak Ridge Institute of Nuclear Studies, 1964, $6.00
4 **Noise Analysis in Nuclear Systems** (TID-7679), University of Florida, 1964, $6.00
5 **Radioactive Fallout from Nuclear Weapons Tests** (CONF-765), U. S. Atomic Energy Commission, 1965, $6.00
6 **Radioactive Pharmaceuticals** (CONF-651111), Oak Ridge Institute of Nuclear Studies, 1966, $6.00
7 **Neutron Dynamics and Control** (CONF-650413), The University of Arizona, 1966, $6.00
8 **Luminescence Dosimetry** (CONF-650637), Stanford University, 1967, $6.00
9 **Neutron Noise, Waves, and Pulse Propagation** (CONF-660206), University of Florida, 1967, $6.00
10 **Use of Computers in Analysis of Experimental Data and the Control of Nuclear Facilities** (CONF-660527), Argonne National Laboratory, 1967, $6.00
11 **Compartments, Pools, and Spaces in Medical Physiology** (CONF-661010), Oak Ridge Associated Universities, 1967, $6.00
12 **Thorium Fuel Cycle** (CONF-660524), Oak Ridge National Laboratory, 1968, $6.00
13 **Radioisotopes in Medicine: In Vitro Studies** (CONF-671111), Oak Ridge Associated Universities, 1968, $6.00
14 **Abundant Nuclear Energy** (CONF-680810), Oak Ridge Associated Universities, 1969, $6.00
15 **Fast Burst Reactors** (CONF-690102), The University of New Mexico, 1969, $9.00
16 **Biological Implications of the Nuclear Age** (CONF-690303), Lawrence Radiation Laboratory, 1969, $6.00
17 **Radiation Biology of the Fetal and Juvenile Mammal** (CONF-690501), Pacific Northwest Laboratory, 1969, $9.00
18 **Inhalation Carcinogenesis** (CONF-691001), Oak Ridge National Laboratory, 1970, $6.00
19 **Myeloproliferative Disorders of Animals and Man** (CONF-680529), Pacific Northwest Laboratory, 1970, $9.00
20 **Medical Radionuclides: Radiation Dose and Effects** (CONF-691212), Oak Ridge Associated Universities, 1970, $6.00
21 **Morphology of Experimental Respiratory Carcinogenesis** (CONF-700501), Oak Ridge National Laboratory, 1970, $6.00
22 **Precipitation Scavenging (1970)** (CONF-700601), Pacific Northwest Laboratory, 1970, $6.00

XUM

XUM